

Leonard Barolli  
Olivier Terzo *Editors*

# Complex, Intelligent, and Software Intensive Systems

Proceedings of the 11th International  
Conference on Complex, Intelligent,  
and Software Intensive Systems  
(CISIS-2017)

# **Advances in Intelligent Systems and Computing**

Volume 611

## **Series editor**

Janusz Kacprzyk, Polish Academy of Sciences, Warsaw, Poland  
e-mail: [kacprzyk@ibspan.waw.pl](mailto:kacprzyk@ibspan.waw.pl)

### *About this Series*

The series “Advances in Intelligent Systems and Computing” contains publications on theory, applications, and design methods of Intelligent Systems and Intelligent Computing. Virtually all disciplines such as engineering, natural sciences, computer and information science, ICT, economics, business, e-commerce, environment, healthcare, life science are covered. The list of topics spans all the areas of modern intelligent systems and computing.

The publications within “Advances in Intelligent Systems and Computing” are primarily textbooks and proceedings of important conferences, symposia and congresses. They cover significant recent developments in the field, both of a foundational and applicable character. An important characteristic feature of the series is the short publication time and world-wide distribution. This permits a rapid and broad dissemination of research results.

### *Advisory Board*

#### Chairman

Nikhil R. Pal, Indian Statistical Institute, Kolkata, India

e-mail: [nikhil@isical.ac.in](mailto:nikhil@isical.ac.in)

#### Members

Rafael Bello Perez, Universidad Central “Marta Abreu” de Las Villas, Santa Clara, Cuba

e-mail: [rbellop@uclv.edu.cu](mailto:rbellop@uclv.edu.cu)

Emilio S. Corchado, University of Salamanca, Salamanca, Spain

e-mail: [escorchado@usal.es](mailto:escorchado@usal.es)

Hani Hagrass, University of Essex, Colchester, UK

e-mail: [hani@essex.ac.uk](mailto:hani@essex.ac.uk)

László T. Kóczy, Széchenyi István University, Győr, Hungary

e-mail: [koczy@sze.hu](mailto:koczy@sze.hu)

Vladik Kreinovich, University of Texas at El Paso, El Paso, USA

e-mail: [vladik@utep.edu](mailto:vladik@utep.edu)

Chin-Teng Lin, National Chiao Tung University, Hsinchu, Taiwan

e-mail: [ctlin@mail.nctu.edu.tw](mailto:ctlin@mail.nctu.edu.tw)

Jie Lu, University of Technology, Sydney, Australia

e-mail: [Jie.Lu@uts.edu.au](mailto:Jie.Lu@uts.edu.au)

Patricia Melin, Tijuana Institute of Technology, Tijuana, Mexico

e-mail: [epmelin@hafsamx.org](mailto:epmelin@hafsamx.org)

Nadia Nedjah, State University of Rio de Janeiro, Rio de Janeiro, Brazil

e-mail: [nadia@eng.uerj.br](mailto:nadia@eng.uerj.br)

Ngoc Thanh Nguyen, Wroclaw University of Technology, Wroclaw, Poland

e-mail: [Ngoc-Thanh.Nguyen@pwr.edu.pl](mailto:Ngoc-Thanh.Nguyen@pwr.edu.pl)

Jun Wang, The Chinese University of Hong Kong, Shatin, Hong Kong

e-mail: [jwang@mae.cuhk.edu.hk](mailto:jwang@mae.cuhk.edu.hk)

More information about this series at <http://www.springer.com/series/11156>

Leonard Barolli · Olivier Terzo  
Editors

# Complex, Intelligent, and Software Intensive Systems

Proceedings of the 11th International  
Conference on Complex, Intelligent,  
and Software Intensive Systems (CISIS-2017)

 Springer

*Editors*

Leonard Barolli  
Department of Information  
and Communication Engineering,  
Faculty of Information Engineering  
Fukuoka Institute of Technology  
Fukuoka  
Japan

Olivier Terzo  
Istituto Superiore Mario Boella  
Turin  
Italy

ISSN 2194-5357                      ISSN 2194-5365 (electronic)  
Advances in Intelligent Systems and Computing  
ISBN 978-3-319-61565-3            ISBN 978-3-319-61566-0 (eBook)  
DOI 10.1007/978-3-319-61566-0

Library of Congress Control Number: 2017943076

© Springer International Publishing AG 2018

This work is subject to copyright. All rights are reserved by the Publisher, whether the whole or part of the material is concerned, specifically the rights of translation, reprinting, reuse of illustrations, recitation, broadcasting, reproduction on microfilms or in any other physical way, and transmission or information storage and retrieval, electronic adaptation, computer software, or by similar or dissimilar methodology now known or hereafter developed.

The use of general descriptive names, registered names, trademarks, service marks, etc. in this publication does not imply, even in the absence of a specific statement, that such names are exempt from the relevant protective laws and regulations and therefore free for general use.

The publisher, the authors and the editors are safe to assume that the advice and information in this book are believed to be true and accurate at the date of publication. Neither the publisher nor the authors or the editors give a warranty, express or implied, with respect to the material contained herein or for any errors or omissions that may have been made. The publisher remains neutral with regard to jurisdictional claims in published maps and institutional affiliations.

Printed on acid-free paper

This Springer imprint is published by Springer Nature  
The registered company is Springer International Publishing AG  
The registered company address is: Gewerbestrasse 11, 6330 Cham, Switzerland

# Welcome Message of CISIS-2017 International Conference Organizers

Welcome to the 11th International Conference on Complex, Intelligent, and Software Intensive Systems (CISIS-2017), which will be held from July 10 to 12, 2017, at Istituto Superiore Mario Boella (ISMB), Torino, Italy, in conjunction with the 11th International Conference on Innovative Mobile and Internet Services in Ubiquitous Computing (IMIS-2017).

The aim of the conference is to deliver a platform of scientific interaction between the three interwoven challenging areas of research and development of future ICT-enabled applications: software-intensive systems, complex systems, and intelligent systems.

Software-intensive systems are systems, which heavily interact with other systems, sensors, actuators, devices, other software systems, and users. More and more domains are involved with software-intensive systems, e.g., automotive, telecommunication systems, embedded systems in general, industrial automation systems, and business applications. Moreover, the outcome of Web services delivers a new platform for enabling software-intensive systems. The conference is thus focused on tools, practically relevant and theoretical foundations for engineering software-intensive systems.

Complex systems research is focused on the overall understanding of systems rather than its components. Complex systems are very much characterized by the changing environments in which they act by their multiple internal and external interactions. They evolve and adapt through internal and external dynamic interactions.

The development of intelligent systems and agents, which is each time more characterized by the use of ontologies, and their logical foundations build a fruitful impulse for both software-intensive systems and complex systems. Recent research in the field of intelligent systems, robotics, neuroscience, artificial intelligence, and cognitive sciences is very important factor for the future development and innovation of software-intensive and complex systems.

The CISIS-2017 is aiming at delivering a forum for in-depth scientific discussions among the three communities. The papers included in the proceedings cover all aspects of theory, design, and application of complex systems, intelligent systems, and software-intensive systems. The conference received 170 papers and accepted 43 papers (about 25% acceptance rate), which were selected after a careful review process.

We are very proud and honored to have 2 distinguished keynote talks by Dr. Sven Helmer, Free University of Bozen-Bolzano, Italy, and Dr. Patrick Demichel, Hewlett Packard, France, who will present their recent work and will give new insights and ideas to the conference participants.

The organization of an International Conference requires the support and help of many people. A lot of people have helped and worked hard to produce a successful CISIS-2017 technical program and conference proceedings. First, we would like to thank all the authors for submitting their papers, the program committee members, and the reviewers who carried out the most difficult work by carefully evaluating the submitted papers.

We are grateful to Honorary Co-Chairs Prof. Makoto Takizawa, Hosei University, Japan, and Dr. Paolo Mulassano, Istituto Superiore Mario Boella, Italy, for their guidance and advices.

This year in conjunction with CISIS-2017 we have 8 International Workshops that complemented CISIS-2017 program with contributions for specific topics. We would like to thank the Workshop Co-Chairs and all workshops' organizers for organizing these workshops.

We thank Shinji Sakamoto, Donald Elmazi, and Yi Liu, Fukuoka Institute of Technology, Japan, as Web Administrators for their excellent and timely work.

Finally, we would like to thank the local arrangement team of ISMB for their support and good local arrangement for the conference.

We hope you will enjoy the conference and have a great time in Torino, Italy.

## **CISIS-2017 International Conference Organizers**

### **CISIS-2017 General Co-chairs**

Leonard Barolli	Fukuoka Institute of Technology (FIT), Japan
Olivier Terzo	Istituto Superiore Mario Boella, Italy

### **CISIS-2017 Program Committee Co-chairs**

Lorenzo Mossuca	Istituto Superiore Mario Boella, Italy
Beniamino Di Martino	Università degli Studi della Campania Luigi Vanvitelli, Italy
Paolo Giaccone	Politecnico di Torino, Italy

# Welcome Message from CISIS-2017 Workshops Co-chairs

Welcome to the Workshops of the 11th International Conference on Complex, Intelligent, and Software Intensive Systems (CISIS-2017), which will be held from July 10 to 12, 2017, at Istituto Superiore Mario Boella (ISMB), Torino, Italy.

We are pleased that for this edition of CISIS International Conference we have 8 International Workshops. Some of these workshops are in 7th, 8th, 9th, and 10th editions. The objective was to complement as much as possible the main theme of CISIS 2017 with specific topics of different workshops in order to cover topics from the three challenging areas of ICT-enabled applications: software-intensive systems, complex systems, and intelligent systems.

The list of workshops is as follows.

1. The 11th International Workshop on Engineering Complex Distributed Systems (**ECDS-2017**)
2. The 10th International Workshop on Engineering Parallel and Multi-Core Systems (**ePaMus-2017**)
3. The 10th International Workshop on Intelligent Informatics and Natural Inspired Computing (**IINIC-2017**)
4. The 8th International Workshop on Frontiers on Complex, Intelligent, and Software Intensive Systems (**FCISIS-2017**)
5. The 8th International Workshop on Virtual Environment and Network-Oriented Applications (**VENOA 2017**)
6. The 7th Semantic Web/Cloud Information and Services Discovery and Management (**SWISM-2017**)



7. The 7th International Workshop on Intelligent Computing In Large-Scale Systems (**ICLS-2017**)
8. The 4th International Workshop on Energy-Aware Systems, Communications and Security (**EASyCoSe-2017**)

These workshops bring to the researchers conducting research in specific themes the opportunity to learn from this rich multi-disciplinary experience. The Workshop Co-Chairs would like to thank CISIS-2017 International Conference Organizers for their help and support. We are grateful to the workshops' organizers for their great efforts and hard work in proposing the workshops, selecting the papers, and the interesting programs and for the arrangements of the workshops during the conference days. We are grateful to Shinji Sakamoto, Donald Elmazi, and Yi Liu, Fukuoka Institute of Technology, Japan, for their excellent work and support as Web Administrators. We would like to give special thanks to the Local Organization Team of ISMB, Torino, Italy.

We hope you enjoy the workshops' program and proceedings.

## **Workshops Co-chairs of CISIS-2017 International Conference**

Makoto Ikeda	Fukuoka Institute of Technology, Japan
Farookh Hussain	University Technology Sidney, Australia
Giuseppe Caragnano	Istituto Superiore Mario Boella, Italy

## **CISIS-2017 Organizing Committee**

### **Honorary Chairs**

Makoto Takizawa	Hosei University, Japan
Paolo Mulassano	Istituto Superiore Mario Boella, Italy

### **General Co-chairs**

Leonard Barolli	Fukuoka Institute of Technology, Japan
Olivier Terzo	Istituto Superiore Mario Boella, Italy

**Program Committee Co-chairs**

Lorenzo Mossucca	Istituto Superiore Mario Boella, Italy
Beniamino Di Martino	Università degli Studi della Campania Luigi Vanvitelli, Italy
Paolo Giaccone	Politecnico di Torino, Italy

**Workshop Co-chairs**

Makoto Ikeda	Fukuoka Institute of Technology, Japan
Farookh Hussain	University Technology Sidney, Australia
Giuseppe Caragnano	Istituto Superiore Mario Boella, Italy

**International Advisory Board**

Yoshitaka Shibata	Iwate Prefectural University, Japan
David Taniar	Monash University, Australia
Minoru Uehara	Toyo University, Japan
Arjan Duresi	IUPUI, USA
Giuseppe Vecchi	Politecnico di Torino, Italy
Flora Amato	University of Naples, Italy

**Award Co-chairs**

Santi Caballé	Open University of Catalonia, Spain
Hiroshi Shigeno	Keio University, Japan

**International Liaison Co-chairs**

Fumiaki Sato	Toho University, Japan
Wenny Rahayu	La Trobe University, Australia
Lorenzo Mossucca	Istituto Superiore Mario Boella, Italy

**Publicity Co-chairs**

Hui-Huang Hsu	Tamkang University, Taiwan
Markus Aleksy	ABB AG Corporate Research Center, Germany
Akio Koyama	Yamagata University, Japan
Fabrizio Bertone	Istituto Superiore Mario Boella, Italy
Mariapia Martino	Politecnico di Torino, Italy

**Local Arrangement Co-chairs**

Klodiana Goga	Istituto Superiore Mario Boella, Italy
Cristiana D'Alberto	Istituto Superiore Mario Boella, Italy

**Web Administrator Chairs**

Shinji Sakamoto	Fukuoka Institute of Technology, Japan
Donald Elmazi	Fukuoka Institute of Technology, Japan
Yi Liu	Fukuoka Institute of Technology, Japan

**Track Areas and PC Members****1. Database and Data Mining Applications****Track Co-chairs**

Kin Fun Li	University of Victoria, Canada
Silvia Chiusano	Politecnico di Torino, Italy
Pavel Krömer	Technical University of Ostrava, Czech Republic

**PC Members**

Antonio Attanasio	Istituto Superiore Mario Boella Italy
Tibebe Beshah	Addis Ababa University, Ethiopia
Jana Heckenbergerova	University of Pardubice, Czech Republic
Konrad Jackowski	Wroclaw University of Technology, Poland
Petr Musílek	University of Alberta, Canada
Aleš Zamuda	University of Maribor, Slovenia
Tania Cerquitelli	Politecnico di Torino, Italy
Elisa Quintarelli	Politecnico di Milano, Italy
Genoveva Vargas-Solar	French Council of Scientific Research, LIG-LAFMIA, France
Xiaolan Sha	Sky, UK
Deepali Arora	University of Victoria, Canada
Kosuke Takano	Kanagawa Institute of Technology, Japan
Masahiro Ito	Toshiba Lab, Japan
Watheq ElKharashi	Ain Shams University, Egypt
Martine Wedlake	IBM, USA

## 2. Artificial Intelligence and Bio-inspired Computing

### Track Co-chairs

Mikhael Simonov	ISMB, Turin, Italy
Hai Dong	Royal Melbourne Institute of Technology, Australia
Salvatore Vitabile	University of Palermo, Italy

### PC Members

Kit Yan Chan	Curtin University, Australia
Shang-Pin Ma	National Taiwan Ocean University, Taiwan
Sajib Mistry	RMIT University, Australia
Klodiana Goga	Istituto Superiore Mario Boella, Italy
Le Sun	Victoria University, Australia
Vincenzo Conti	University of Enna Kore, Italy
Minoru Uehara	Toyo University, Japan
Philip Moore	Lanzhou University, China
Mauro Migliardi	University of Padua, Italy
Dario Bonino	Istituto Superiore Mario Boella, Italy
Andrea Tettamanzi	University of Nice, France
Cornelius Weber	Hamburg University, Germany
Tim Niesen	German Research Center for Artificial Intelligence (DFKI), Germany
Rocco Raso	German Research Center for Artificial Intelligence (DFKI), Germany
Fulvio Corno	Politecnico di Torino, Italy

## 3. Multimedia and E-learning Systems

### Track Co-chairs

Santi Caballe	Open University of Catalonia, Spain
Yoshinari Nomura	Okayama University, Japan
Weiwei Chen	Google, USA

### PC Members

Kaoru Sugita	Fukuoka Institute of Technology, Japan
Yoshiaki Kasahara	Kyushu University, Japan
Shunsuke Mihara	Lockon Inc., Japan

Shunsuke Oshima	Kumamoto National College of Technology, Japan
Yuuichi Teranishi	NICT, Japan
Jordi Conesa	Open University of Catalonia, Spain
Soumya Barnejee	Institut National des Sciences Appliquées, France
David Bañeres	Open University of Catalonia, Spain
Nicola Capuano	University of Salerno, Italy
Nestor Mora	Open University of Catalonia, Spain
Jorge Moneo	University of San Jorge, Spain
David Gañán	Open University of Catalonia, Spain
Isabel Guitart	Open University of Catalonia, Spain
Michalis Feidakis	University of the Aegean, Greece
Modesta Pousada	Open University of Catalonia, Spain
Kazunori Ueda	Kochi University of Technology, Japan

## 4. Next-Generation Wireless Networks

### Track Co-chairs

Yunfei Chen	University of Warwick, UK
Evjola Spaho	Polytechnic University of Tirana, Albania
Sriram Chellappan	Missouri University of Science and Technology, USA

### PC Members

Elis Kulla	Okayama University of Science, Japan
Santi Caballé	Open University of Catalonia, Spain
Admir Barolli	Aleksander Moisiu University, Albania
Omer Wagar	University of Engineering and Technology, Poland
Zhibin Xie	Jiangsu University of Science and Technology, China
Jun Wang	Nanjing University of Post and Telecommunication, China

## 5. Semantic Web, Web Services, and Data Integration

### Track Co-chairs

Muhammad Younas	Oxford Brookes University, UK
Antonio Messina	Istituto di Calcolo e Reti ad Alte Prestazioni CNR, Italy
Natalia Kryvinska	Comenius University in Bratislava, Slovakia

### PC Members

Fabrizio Bertone	Istituto Superiore Mario Boella, Italy
Pietro Storniolo	Istituto di Calcolo e Reti ad Alte Prestazioni CNR, Italy
Agnese Augello	Istituto di Calcolo e Reti ad Alte Prestazioni CNR, Italy
Arianna Pipitone	University of Palermo, Italy
Cristian Lai	CRS4 Center for Advanced Studies, Research and Development in Sardinia, Italy
Christine Bauer	University of Vienna, Austria
Ivan Demydov	Lviv Polytechnic National University, Ukraine
Ciprian Dobre	Politehnica University of Bucharest, Romania
Christophe Feltus	University of Namur, Belgium
Michal Gregus	Comenius University in Bratislava, Slovakia
Christine Strauss	University of Vienna, Austria
Tor-Morten Grønli	Westerdals, Norway
George Ghinea	Brunel University London, UK
Irfan Awan	University of Bradford, UK

## 6. Autonomic Computing and Communication

### Track Co-chairs

Ciprian Dobre	University Politehnica of Bucharest, Romania
Salvatore Venticinquè	Università degli Studi della Campania Luigi Vanvitelli, Italy
Gregorio Martinez	University of Murcia, Spain

### PC Members

Alba Amato	Istituto di Calcolo e Reti ad Alte Prestazioni— Italian National Research Center (CNR), Italy
Francesco Moscato	Università degli Studi della Campania Luigi Vanvitelli, Italy

Florin Fortis	West University of Timisoara, Romania
Luca Pilosu	Istituto Superiore Mario Boella, Italy
Geir Horn	University of Oslo, Norway
Constandinos X. Mavromoustakis	University of Nicosia, Cyprus
Radu Tudoran	European Research Center, Huawei Technologies Duesseldorf GmbH, Germany
Luis Javier Garcia Villalba	Universidad Complutense de Madrid, Spain
Manuel Gil Perez	University of Murcia, Spain

## 7. Security and Trusted Computing

### Track Co-chairs

Hiroaki Kikuchi	Meiji University, Japan
Omar Khadeer Hussain	University of New South Wales Canberra, Australia
Rajat Saxena	Indian Institute of Technology Indore, India

### PC Members

Saqib Ali	Sultan Qaboos University, Oman
Zia Rehman	COMSATS Institute of Information Technology (CIIT), Pakistan
Morteza Saberi	UNSW Canberra, Australia
Sazia Parvin	UNSW Canberra, Australia
Farookh Hussain	University of Technology, Sydney, Australia
Walayat Hussain	University of Technology, Sydney, Australia
Sabu Thampi	Indian Institute of Information Technology and Management-Kerala (IIITM-K), Technopark Campus, India
Sun Jingtao	National Institute of Informatics, Japan
Antoine Perréard	Graduate School in Computer Science and Mathematics Engineering, France
Anitta Patience Namanya	University of Bradford, UK
Smita Rai	Uttarakhand Board of Technical Education Roorkee, India
Abhishek Saxena	American Tower Corporation Limited, India

## 8. Optimization and Modeling of Complex Systems

### Track Co-chairs

Hiroyuki Fujioka	Fukuoka Institute of Technology, Japan
Alfredo Cuzzocrea	University of Trieste, Italy
Zahoor Khan	Higher Colleges of Technology, UAE

### PC Members

Takuya Tajima	Fukuoka Institute of Technology, Japan
Jing Fu	Fukuoka Institute of Technology, Japan
Kaoru Fujioka	Fukuoka Women's University, Japan
Osvaldo Gervasi	University of Perugia, Italy
Rim Moussa	University of Carthage, Tunisia
Walter Ukovich	University of Trieste, Italy
Florin Pop	University Politehnica of Bucharest, Romania
Umar Qasim	University of Alberta, Canada
Nadeem Javaid	COMSATS IIT, Pakistan
Muhammad Imran	King Saud University, Saudi Arabia

## 9. P2P, Grid and Scalable Computing

### Track Co-chairs

Harold Castro	Universidad de Los Andes, Colombia
Javid Taheri	Karlstad University, Sweden
Hamid R. Arabnia	University of Georgia, USA

### PC Members

Lorenzo Mossuca	Istituto Superiore Mario Boella, Italy
Cesar Diaz	Universidad Jorge Tadeo Lozano, Colombia
Marcelo Naiouf	Universidad de la Plata, Argentina
Michel Riveill	University Nice Sophia Antipolis, France
Carlos Barrios	Universidad Industrial de Santander, Colombia
Andreas Kassler	Karlstad University, Sweden
Dzmitry KliazovIich	University of Luxembourg, Luxembourg
Mohamad Reza Hoseiny	University of Sydney, Australia
David Sol	Technological Institute of Monterrey, Mexico
Saeed Bastani	University of Lund, Sweden



## 10. Cloud Computing Services and Orchestration Tools

### Track Co-chairs

Olivier Terzo	ISMB, Italy
Khalid Mohiuddin	King Khalid University, Saudi Arabia
Salvatore Distefano	Politecnico di Milano, Milan, Italy

### PC Members

Rustem Dautov	Kazan Federal University, Russia
Giovanni Merlino	University of Messina, Italy
Francesco Longo	University of Messina, Italy
Dario Bruneo	University of Messina, Italy
Nik Bessis	Edge Hill University, UK
MingXue Wang	Ericsson, Ireland
Luciano Gaido	Istituto Nazionale di Fisica Nucleare (INFN), Italy
Giacinto Donvito	Istituto Nazionale di Fisica Nucleare (INFN), Italy
Andrea Tosatto	Open-Xchange, Germany

## 11. FPGA Heterogeneous Architecture

### Track Co-chairs

Fujio Kurokawa	Nagasaki University, Japan
Eto Haruhi	Nagasaki University, Japan
Antonio Portero Trujillo	IT4Innovations, Czech Republic
Jan Martinovic	IT4Innovations, Czech Republic

### PC Members

Yuichiro Shibata	Nagasaki University, Japan
Masaharu Tanaka	Nagasaki University, Japan
Hidenori Maruta	Nagasaki University, Japan
Alberto Scionti	Istituto Superiore Mario Boella, Italy
Zhibin Yu	Shenzhen Institutes of Advanced Technology, China
Julio Sahuquillo	Universitat Politecnica de Valencia, Spain
Dimitrios Soudris	Technical University of Athens (NTUA), Greece

Màrius Montón  
Sunil Shukla  
David Castells

IoT Partners, Spain  
IBM T.J. Watson Research Center, USA  
Autonomous University of Barcelona, Spain

## 12. Fog Computing

### Track Co-chairs

Rodrigo Calheiros  
Paolo Giaccone

Western Sydney University, Australia  
Politecnico di Torino, Italy

### PC Members

Pietro Ruiu  
Guilherme Rodrigues

Istituto Superiore Mario Boella, Italy  
Federal Institute of Education, Science and  
Technology Sul Rio-Grandense, Brazil  
Farroupilha Federal Institute of Education,  
Science and Technology, Brazil

Fabio Rossi

University of Louisiana Lafayette, USA  
University of Tasmania, Australia  
University of Melbourne, Australia  
University of Melbourne, Australia  
PwC, Australia  
University of Luxemburg, Luxemburg

Mohsen Amini Salehi  
Saurabh Garg  
Masud Moshtaghi  
Adel Nadjaran Toosi  
Amir Vahid Dastjerdi  
Claudio Fiandrino

### CISIS-2017 Reviewers

Ali Khan Zahoor  
Barolli Admir  
Barolli Leonard  
Bessis Nik  
Bista Bhed  
Caballé Santi  
Castiglione Aniello  
Chellappan Sriram  
Chen Hsing-Chung  
Chen Xiaofeng  
Conti Vincenzo  
Cui Baojiang  
Di Martino Beniamino  
Durrezi Arjan

Enokido Tomoya  
Ficco Massimo  
Fiore Ugo  
Fujioka Hiroyuki  
Fun Li Kin  
Gentile Antonio  
Gotoh Yusuke  
Hussain Farookh  
Hussain Omar  
Javaid Nadeem  
Jeong Joshua  
Ikeda Makoto  
Ishida Tomoyuki  
Kikuchi Hiroaki

Kolici Vladi  
Koyama Akio  
Kulla Elis  
Lee Kyungroul  
Loia Vincenzo  
Matsuo Keita  
Migliardi Mauro  
Koyama Akio  
Kryvinska Natalia  
Nishide Ryo  
Nishino Hiroaki  
Oda Tetsuya  
Ogiela Lidia  
Ogiela Marek  
Palmieri Francesco  
Paruchuri Vamsi Krishna  
Rahayu Wenny  
Rawat Danda  
Rho Seungmin  
Shibata Yoshitaka

Sato Fumiaki  
Spaho Evjola  
Suganuma Takuo  
Sugita Kaoru  
Takizawa Makoto  
Taniar David  
Terzo Olivier  
Tokuyasu Tatsushi  
Uchida Noriki  
Uehara Minoru  
Uda Ryuya  
Venticinque Salvatore  
Vitabile Salvatore  
Waluyo Agustinus Borgy  
Wang Xu An  
Woungang Isaac  
Xhafa Fatos  
Yim Kangbin  
Younas Muhammad

# Welcome Message from ECDS-2017 International Workshop Co-chairs

It is our great pleasure to welcome you to the 11th International Workshop on Engineering Complex Distributed Systems (ECDS-2017), which will be held in conjunction with the 11th International Conference on Complex, Intelligent, and Software Intensive Systems (CISIS-2017) from July 10 to 12, 2017, at Istituto Superiore Mario Boella (ISMB), Torino, Italy.

In the past, this field included technology concerns related to middleware solutions, dealing with the heterogeneity of the miscellaneous hardware and software environments and computing infrastructure. These technologies have been used to address the integration of existing legacy applications and improve the interoperability between applications across enterprises. The advances in wireless communication and pervasive computing extend this traditional wired area of distributed systems and make new advanced application possible. The complexity of today's applications requires additional approaches to be able to realize an enterprise application time- and cost-saving. This includes the ability to model business processes, business policies, and event-oriented aspects of large systems and express these models through design solutions to address the complexity of enterprise applications and ease software design efforts. In addition, the engineering of complex distributed systems also requires a good understanding of the problem areas of concern for information systems and business administration, such as process management, supply chain management, security issues, and electronic business. These topics need to be addressed in order to deal with the complexity of today's increasingly dynamic, mobile, cross-organizational, and cross-jurisdictional systems.

In this workshop, various aspects of the design and implementation of distributed systems will be discussed. The scope of the presented papers ranges from engineering approaches and techniques to applications.

This workshop would not have been possible without the help of many people. First of all, we would like to thank all the authors for submitting their papers to our workshop. We also like to thank the Program Committee Chair, program committee members, and additional reviewers, who carefully evaluated the submitted papers.

We hope that you find the ECDS-2017 program inspiring and that the workshop provides you with the opportunity to interact, share ideas with, and learn from other

distributed systems researchers from around the world. We also encourage you to continue to participate in future ECDS workshops, to increase its visibility, and to interest others in contributing to this growing community.

## **ECDS 2017 Workshop Co-chairs**

Leonard Barolli	Fukuoka Institute of Technology, Japan
Makoto Takizawa	Hosei University, Japan

## **ECDS-2017 Organizing Committee**

### **Workshop Co-chairs**

Leonard Barolli	Fukuoka Institute of Technology (FIT), Japan
Makoto Takizawa	Hosei University, Japan

### **PC Chair**

Takahiro Uchiya	Nagoya Institute of Technology, Japan
-----------------	---------------------------------------

### **Program Committee Members**

Markus Aleksy	ABB Corporate Research, Germany
Irfan Awan	University of Bradford, UK
Bhed Bahadur Bista	Iwate Prefectural University, Japan
Arjan Duresi	Indiana University Purdue University at Indianapolis, USA
Tomoya Enokido	Rissho University, Japan
Ralf Gitzel	ABB Corporate Research, Germany
Hui-Huang Hsu	Tamkang University, Taiwan
Axel Korthaus	Queensland University of Technology, Australia
Akio Koyama	Yamagata University, Japan
Thomas Preuss	University of Brandenburg, Germany
Nobuyoshi Sato	Iwate Prefectural University, Japan
Takuo Suganuma	Tohoku University, Japan
Kaoru Sugita	Fukuoka Institute of Technology, Japan
David Taniar	Monash University, Australia
Minoru Uehara	Toyo University, Japan
Marten van Sinderen	University of Twente, The Netherlands
Fatos Xhafa	Technical University of Catalonia, Spain
Muhammad Younas	Oxford Brookes University, UK
Maciej Zygmunt	ABB Corporate Research, Poland
Stefan Kuhlins	Heilbronn University, Germany

# **Welcome Message from ePaMuS-2017 International Workshop Chair**

Welcome to the 10th International Workshop on Engineering Parallel and Multi-Core Systems (ePaMuS-2017), which will be held in conjunction with the 11th International Conference on Complex, Intelligent, and Software Intensive Systems (CISIS-2017) from July 10 to 12, 2017, at Istituto Superiore Mario Boella (ISMB), Torino, Italy.

The need for increase in computational power has led to the multi-core era. Multi-core processors are becoming all pervasive, and nowadays, the multi-core processors are found not only in computers (servers, PCs, and laptops) but also in mobile and many other devices. The multi-core systems thus increase the computational power yet achieving this is not straightforward. In order to take advantage of multi-core systems, it is necessary to fully exploit their parallel computing nature. Additionally, as the number of cores that can be packed into a chip is increasing, advanced parallel software approaches are needed to bridge the gap between the potential and real performance of multi-core systems and applications.

This workshop aims to bring together researchers and developers from the fields of parallel computing, multi-core systems, and software engineering to contribute and discuss on the latest findings in parallel programming techniques, hardware architectures, and parallel software platforms for multi-core systems.

Many people were involved in this workshop. We would like to thank all the PC members and authors for their contribution to make this workshop a successful event.

We would like to wish you fruitful discussions during the workshop and a pleasant stay in Torino, Italy.

## **ePaMuS-2017 Workshop Chair**

Leonard Barolli

Fukuoka Institute of Technology, Japan

## ePaMuS-2017 Organizing Committee

### Workshop Chair

Leonard Barolli

Fukuoka Institute of Technology, Japan

### Program Committee Members

Markus Aleksy	ABB, Germany
Victor Bacu	Technical University of Cluj-Napoca, Romania
Arquimedes Canedo	IBM Research Lab, Japan
Dirceu Cavendish	UCLA, USA
Antonio Gentile	University of Palermo, Italy
Laurent Choy	Total E&P, France
Ciprian Dobre	University Politehnica of Bucharest, Romania
Horacio Gonzalez-Vélez	Robert Gordon University, UK
Dorian Gorgan	Technical University of Cluj-Napoca, Romania
Fabrice Huet	University of Nice, INRIA-CNRS, France
Gul N. Khan	Ryerson University, Canada
Kin Fun Li	University of Victoria, Canada
Beniamino Di Martino	Università degli Studi della Campania Luigi Vanvitelli, Italy
Edward David Moreno	UFS—Federal University of Sergipe, Brazil
Dana Petcu	West University of Timisoara, Romania
Florin Pop	University Politehnica of Bucharest, Romania
Ivan Rodero	The State University of New Jersey, USA
Mudar Sarem	HUST University, China
Fadi Sibai	Saudi Aramco, KSA, UEA
Albert Zomaya	University of Sidney, Australia

# **Message from IINIC-2017 International Workshop Organizers**

Advanced information processing technologies have the potential to significantly accelerate research in different fields. In particular, techniques from artificial intelligence, machine learning, and data mining can assist researchers in the discovery of new knowledge for next-generation applications. This workshop aims to attract state-of-the-art solutions and novel attempts in this direction.

The 10th International Workshop on Intelligent Informatics and Natural Inspired Computing (IINIC-2017) will provide a platform for researchers to meet and exchange their thoughts. IINIC-2017 will be held in conjunction with the 11th International Conference on Complex, Intelligent, and Software Intensive Systems (CISIS-2017) from July 10 to 12, 2017, at Istituto Superiore Mario Boella (ISMB), Torino, Italy.

Many people contributed to the success of IINIC-2017. We wish to thank the program committee members for their great effort. We also would like to express our gratitude to the main organizers of CISIS-2017 for their excellent work in organizing the conference. We would like to thank and congratulate all the contributing authors for their support to the workshop.

## **IINIC-2017 Workshop Co-chairs**

Hui-Huang Hsu  
Leonard Barolli

Tamkang University, Taiwan  
Fukuoka Institute of Technology, Japan

## **IINIC-2017 Organizing Committee**

### **Workshop Co-chairs**

Hui-Huang Hsu  
Leonard Barolli

Tamkang University, Taiwan  
Fukuoka Institute of Technology, Japan



**Program Committee Members**

Tun-Wen Pai	National Taiwan Ocean University, Taiwan
Oliver Ray	University of Bristol, UK
Oda Tetsuya	Fukuoka Institute of Technology, Japan
Elis Kulla	Okayama University of Science, Japan
Salvatore Vitabile	University of Palermo, Italy
Omar Khadeer Hussain	University of New South Wales Canberra, Australia
Takuo Suganuma	Tohoku University, Japan
Makoto Ikeda	Fukuoka Institute of Technology, Japan
Fatos Xhafa	Technical University of Catalonia, Spain
Santi Caballé	Open University of Catalonia, Spain
Farookh Hussain	University of Technology Sydney, Australia
Takahiro Uchiya	Nagoya Institute of Technology, Japan

# Message from FCISIS-2017 International Workshop Organizers

It is our great pleasure to welcome you for the 8th International Workshop on Frontiers on Complex, Intelligent, and Software Intensive Systems (FCISIS-2017). The workshop will be held in conjunction with the 11th International Conference on Complex, Intelligent, and Software Intensive Systems (CISIS-2017) from July 10 to 12, 2017, at Istituto Superiore Mario Boella (ISMB), Torino, Italy.

The objective of FCISIS workshop is to foster the discussion in a rich interdisciplinary context of the three challenging areas of ICT-enabled applications: software-intensive systems, complex systems, and intelligent systems. FCISIS-2017 is conceived in terms of special papers, which were also carefully selected, from the organizers.

We would like to thank all participants of the workshop for submitting their research works and for their participation and look forward to meet you again in forthcoming editions of the workshop.

## FCISIS-2017 Workshop Chair

Leonard Barolli

Fukuoka Institute of Technology, Japan

## FCISIS-2017 Organizing Committee

### Workshop Co-chairs

Leonard Barolli

Fukuoka Institute of Technology, Japan

### Program Committee Members

Tatsushi Tokuyasu

Fukuoka Institute of Technology, Japan

Makoto Ikeda

Fukuoka Institute of Technology, Japan

Tomoya Enokido	Rissho University, Japan
Farookh Hussain	University Technology Sydney, Australia
Nik Bessis	Edge Hill University, UK
Hiroaki Kikuchi	Meiji University, Japan
Akio Koyama	Yamagata University, Japan
Keita Matsuo	Fukuoka Institute of Technology, Japan
Hiroaki Nishino	Oita University, Japan
Tetsuya Shigeyasu	Hiroshima International University, Japan
Makoto Takizawa	Hosei University, Japan
Salvatore Vitabile	University of Palermo, Italy
Admir Barolli	Aleksander Moisiu University of Durrresi, Albania
Elis Kulla	Okayama University of Science, Japan
Evjola Spaho	Polytechnic University of Tirana, Albania
Noriki Uchida	Fukuoka Institute of Technology, Japan
Hiroshi Maeda	Fukuoka Institute of Technology, Japan

# Message from VENOA-2017 International Workshop Organizers

Welcome to the 9th International Workshop on Virtual Environment and Network-Oriented Applications (VENOA-2017), which will be held in conjunction with the 11th International Conference on Complex, Intelligent, and Software Intensive Systems (CISIS-2017) at Istituto Superiore Mario Boella (ISMB), Torino, Italy, from July 10 to 12, 2017.

The past eight workshops were very successful, and many high-quality papers were presented and published in these workshops. We are pleased to announce the continuation of this workshop for serving as a forum for the exchange of information and ideas in the field of 3D computer graphics, virtual reality (VR), augmented reality (AR), mobile communications, IoT, and Web and network applications. We again received many unique and high-quality paper submissions in this workshop. We strictly follow the CISIS review procedures and finally selected excellent papers for publication and presentation. The program shows a variety of research activities with high relevance to the scope of the workshop.

This workshop cannot be organized without hard and excellent work of CISIS-2017 conference organizers. We would like to express our sincere appreciation to VENOA-2017 program committee members and reviewers for their cooperation in completing their efforts under a very tight schedule. We also give our special thanks to all authors for their valuable contributions. We hope that these papers will have significant impacts and stimulate future research activities.

## VENOA-2017 Workshop Co-chairs

Yong-Moo Kwon  
Hiroaki Nishino

Korea Institute of Science and Technology, Korea  
Oita University, Japan

## VENOA-2017 Organizing Committee

### Workshop Co-chairs

Yong-Moo Kwon	Korea Institute of Science and Technology, Korea
Hiroaki Nishino	Oita University, Japan

### Program Committee Members

Minoru Ikebe	Oita University, Japan
Eiji Aoki	Institute for Hypernetwork Society, Japan
Byungrae Cha	Gwangju Institute of Science and Technology, Korea
Makoto Fujimura	Nagasaki University, Japan
Nobuo Funabiki	Okayama University, Japan
Ken'ichi Furuya	Oita University, Japan
Nobukazu Iguchi	Kinki University, Japan
Tsuneo Kagawa	Oita University, Japan
Laehyun Kim	Korea Institute of Science and Technology, Korea
JongWon Kim	Gwangju Institute of Science and Technology, Korea
Byung-Gook Lee	Dongseo University, Korea
Jong Weon Lee	Sejong University, Korea
Yukikazu Murakami	Kagawa National College of Technology, Japan
Makoto Nakashima	Oita University, Japan
Dahlan Nariman	Ritsumeikan Asia Pacific University, Japan
Satoshi Ohtake	Oita University, Japan
Yoshihiro Okada	Kyushu University, Japan
Yoshitaka Sakurai	Meiji University, Japan
Shinji Sugawara	Chiba Institute of Technology, Japan
Shigeto Tajima	Osaka University, Japan
Kenzi Watanabe	Hiroshima University, Japan
Kazuyuki Yoshida	Oita University, Japan

# Message from SWISM-2017 International Workshop Organizers

Welcome to the 7th International Workshop on Semantic Web/Cloud Information and Services Discovery and Management (SWISM-2017), which is held in conjunction with the 11th International Conference on Complex, Intelligent, and Software Intensive Systems (CISIS-2017) at Istituto Superiore Mario Boella (ISMB), Torino, Italy, from July 10 to 12, 2017.

SWISM-2017 will bring together scientists, engineers, computer users, and students to exchange and share their experiences, new ideas, and research results about all aspects (theory, applications, and tools) of intelligent and semantic methods applied to Web and cloud-based systems and to discuss the practical challenges encountered and the solutions adopted.

The program of SWISM-2017 includes papers related to information retrieval, ontologies, intelligent agents, intelligent techniques for management, and programming of cloud services and business processes. The program for the conference is the result of excellent work of reviewers and program committee members. We hope you will find the final program enriching and stimulating.

We believe that all of papers and topics will provide novel ideas, new theoretical and experimental results, work in progress and state-of-the-art techniques, and stimulate the future research activities in this area.

Papers collected in this international workshop were carefully reviewed by at least 3 reviewers. According to the review results, the program committee members selected high-quality papers to be presented in this workshop.

We would like to express our sincere appreciation to all program committee members for their cooperation. We are thankful to General Co-Chairs, Honorary Chairs, Program Committee Co-Chairs, and Workshops Co-Chairs of CISIS-2017 for excellent conference organization. It was a great pleasure working with them.

We are grateful to all authors for their valuable contributions and attendees who contributed to the success of the program with their papers and speeches on their research results, and with their attending the conference.

We hope you will enjoy the workshop and conference and have a great time in Torino.

## **SWISM-2017 Workshop Co-chairs**

Beniamino Di Martino	Università degli Studi della Campania Luigi Vanvitelli, Italy
Salvatore Venticinque	Università degli Studi della Campania Luigi Vanvitelli, Italy
Antonio Esposito	Università degli Studi della Campania Luigi Vanvitelli, Italy

## **SWISM-2017 Organizing Committee**

### **Workshop Co-chairs**

Beniamino Di Martino	Università degli Studi della Campania Luigi Vanvitelli, Italy
Salvatore Venticinque	Università degli Studi della Campania Luigi Vanvitelli, Italy
Antonio Esposito	Università degli Studi della Campania Luigi Vanvitelli, Italy

### **Program Committee Members**

Omer Rana	University of Cardiff, UK
Siegfried Benkner	University of Vienna, Austria
Marios Dikaiakos	University of Cyprus, Cyprus
Dieter Kranzmueller	University Ludwig Maximilian of Munich, Germany
Antonino Mazzeo	University Federico II of Naples, Italy
Domenico Talia	University of Calabria, Italy
Rocco Aversa	Università degli Studi della Campania Luigi Vanvitelli, Italy
Thomas Fahringer	University of Innsbruck, Austria
Vincenzo Loia	University of Salerno, Italy

# **Message from ICLS-2017 International Workshop Chair**

Welcome to the 7th edition of Intelligent Computing in Large-Scale Systems (ILCS-2017) International Workshop organized in conjunction with the 11th International Conference on Complex, Intelligent, and Software Intensive Systems (CISIS-2017) at Istituto Superiore Mario Boella (ISMB), Torino, Italy, from July 10 to 12, 2017.

Intelligent computing is usually defined as advanced computing methods and techniques based on classical computational intelligence, artificial intelligence, and intelligent agents. Large-scale distributed systems, such as grids, peer-to-peer and ad hoc networks, constellations, and clouds, enable the aggregation and sharing of geographically distributed resources from different organization with distinct owners, administrators, and policies.

With the advent of large-scale distributed systems, where efficient inter-domain operation is one of the most important features, it is arguably required to investigate novel methods and techniques to enable secure access to data and resources, efficient scheduling, self-adaptation, decentralization, and self-organization. The concept of intelligent computing in large-scale systems brings together results from both areas with a positive impact on the development of new efficient data and information systems.

The aim of ICLS workshop is to gather innovative academic and industrial researchers related to all aspects of intelligent computing in large-scale distributed systems, ranging from conceptual and theoretical developments to advanced technologies and innovative applications and tools.

I would like to thank all authors for submitting their research works to the workshop and the reviewers for their time and constructive feedback to authors.

I do hope all of you enjoy ICLS-2017 and will join again the next workshop edition.

## **ICLS-2017 International Workshop Chair**

Leonard Barolli

Fukuoka Institute of Technology, Japan



## **ICLS-2017 Organizing Committee**

### **Workshop Chair**

Leonard Barolli

Fukuoka Institute of Technology, Japan

### **Program Committee Members**

Tomoya Enokido

Rissho University, Japan

Kin Fun Li

University of Victoria, Canada

Giovanni Morana

Catania University, Italy

Richard Hill

University of Derby, UK

Makoto Ikeda

Fukuoka Institute of Technology, Japan

Philip Moore

Lanzhou University, China

Hiroaki Nishino

Oita University, Japan

Evjola Spaho

Polytechnic University of Tirana, Albania

Makoto Takizawa

Hosei University, Japan

Olivier Terzo

ISMB, Italy

Salvatore Vitabile

University of Palermo, Italy

Muhammad Younas

Oxford Brookes, UK

# **Welcome Message from EASyCoSe-2017 International Workshop Co-chairs**

Welcome to the 4th International Workshop on Energy-Aware Systems, Communications and Security (EASyCoSe-2017). The workshop is held in conjunction with the 11th International Conference on Complex, Intelligent, and Software Intensive Systems (CISIS-2017) at Istituto Superiore Mario Boella (ISMB), Torino, Italy, from July 10 to 12, 2017.

The main goal of this workshop is to bring together researchers and practitioners, from both the industrial and academic communities, who are interested in addressing issues and challenges related to optimizing computing and networking system power consumption, energy efficient systems, and energy-related issues. The papers included in the proceedings present novel ideas regarding several hot topics in state-of-the-art ICT and security arena, mainly concerning energy-aware decision making, enhanced access control, and energy-related attacks.

For organizing an international event, the support and help of many people are needed. First, we would like to thank all authors for submitting and presenting their papers. We also greatly appreciated the support from program committee members and reviewers who carried out the most difficult work of carefully evaluating the submitted papers.

We would also like to give our special thanks to Prof. Leonard Barolli, General Co-Chair of the CISIS-2017, for his strong encouragement and guidance.

We hope all of you will enjoy EASyCoSe-2017 and find this a productive opportunity to exchange ideas with many researchers.

## **EASyCoSe-2017 WorkShop Co-chairs**

Mauro Migliardi  
Francesco Palmieri

University of Padua, Italy  
University of Salerno, Italy

## **EASyCoSe-2017 Organizing Committee**

### **Workshop Chairs**

Mauro Migliardi	University of Padua, Italy
Francesco Palmieri	University of Salerno, Italy

### **Program Committee**

Davide Careglio	Universitat Politècnica de Catalunya, Spain
Aniello Castiglione	University of Salerno, Italy
Bruno Carpentieri	University of Salerno, Italy
Fred Chong	University of California Santa Barbara, USA
Massimo Ficco	Università degli Studi della Campania Luigi Vanvitelli, Italy
Ugo Fiore	Federico II University of Naples, Italy
Fang-Yie Leu	Tunghai University, Taiwan (ROC)
Mauro Iacono	Università degli Studi della Campania Luigi Vanvitelli, Italy
Alessio Merlo	University of Genoa, Italy
Sergio Ricciardi	Universitat Politècnica de Catalunya, Spain
Matthew Sorrell	University of Adelaide, Australia
Vaidy Sunderam	Emory University, USA

# **CISIS-2017 Keynote Talks**

# Raspberries on the Edge

Sven Helmer

Free University of Bozen-Bolzano, Bolzano, Italy

**Abstract.** With the advent of the Internet of Things (IoT), billions of new devices will join the data networks, many of them generating data streams originating from sensors or other sources. Instead of pushing all these data to centralized (cloud) servers, it makes a lot of sense to preprocess, analyze, and aggregate it on-site. This is the central idea of edge computing, reducing storage requirements for central servers, lowering the network load, and also decreasing reaction times for time-critical applications. Deploying the necessary infrastructure for edge computing is already a challenge in well-developed, urbanized settings, and it is even harder to do so in harsh environments located in rural and remote areas. Platforms based on small single-board computers, such as Raspberry Pis, could ameliorate this situation by providing a solution with low costs and power consumption. In this keynote, we look at some of the challenges faced by edge computing in general and also explore particular low-resource scenarios.

# The Future of IT Technologies

Patrick Demichel

Hewlett Packard, Paris, France

**Abstract.** Our society and industry are facing a large number of MegaTrends. The IIoT, “Intelligent Internet of Things,” and machine learning are some of the most promising. At the same time, we observe many signs that we are reaching some fundamental limits of our old technologies and infrastructures. Our laboratories demonstrated a decade ago that we have no choice but to implement a radical and holistic transformation, if we expect to reach the Exascale frontier at a reasonable power envelop. We anticipated also a set of news problems, such as edge computing and its requirements in term of security. This large research program called “The Machine” is now entering its final development phase with a group of partners grouped in a consortium named “gen-Z.” We will explore what are the fundamental bricks enabling this historical evolution of our architectures. We will also consider some implications on how we could solve our most challenging problems in a short future, with a huge potentiality for the IIoT, Exascale, and ML ecosystems.

# Contents

## **The 11th International Conference on Complex, Intelligent, and Software Intensive Systems (CISIS-2017)**

<b>A Delay-Aware Fuzzy-Based System for Selection of IoT Devices in Opportunistic Networks</b> . . . . .	3
Miralda Cuka, Donald Elmazi, Tetsuya Oda, Elis Kulla, Makoto Ikeda, and Leonard Barolli	
<b>A GA-Based Simulation System for WMNs: Performance Analysis for Different WMN Architectures Considering Weibull Distribution, HWMP and TCP Protocols</b> . . . . .	14
Admir Barolli, Tetsuya Oda, Makoto Ikeda, Keita Matsuo, Leonard Barolli, and Makoto Takizawa	
<b>Performance Evaluation of a Vegetable Recognition System Using Caffe and Chainer</b> . . . . .	24
Makoto Ikeda, Yuki Sakai, Tetsuya Oda, and Leonard Barolli	
<b>Energy-Efficient Quorum Selection Algorithm for Distributed Object-Based Systems</b> . . . . .	31
Tomoya Enokido, Dilawaer Duolikun, and Makoto Takizawa	
<b>Selection of Actor Nodes in Wireless Sensor and Actor Networks: A Fuzzy-Based System Considering Packet Error Rate as a New Parameter</b> . . . . .	43
Donald Elmazi, Miralda Cuka, Tetsuya Oda, Elis Kulla, Makoto Ikeda, and Leonard Barolli	
<b>A Fuzzy-Based Approach for Improving Team Collaboration in MobilePeerDroid Mobile System</b> . . . . .	56
Yi Liu, Kosuke Ozero, Keita Matsuo, Makoto Ikeda, and Leonard Barolli	

**Energy-Aware Dynamic Migration of Virtual Machines in a Server Cluster** . . . . . 70  
 Dilawaer Duolikun, Ryo Watanabe, Tomoya Enokido, and Makoto Takizawa

**Flexible Synchronization Protocol to Prevent Illegal Information Flow in Peer-to-Peer Publish/Subscribe Systems.** . . . . . 82  
 Shigenari Nakamura, Lidia Ogiela, Tomoya Enokido, and Makoto Takizawa

**An Energy-Efficient Migration Algorithm of Virtual Machines in Server Clusters** . . . . . 94  
 Ryo Watanabe, Dilawaer Duolikun, Tomoya Enokido, and Makoto Takizawa

**Using the Web of Data in Semantic Sensor Networks** . . . . . 106  
 Cristian Lai, Antonio Pintus, and Alberto Serra

**A Communication Method for Wireless Mesh Networks Suitable to IoT Communication Environment.** . . . . . 117  
 Kyohei Kishi, Hiroyuki Suzuki, and Akio Koyama

**Influences of ILS Localizer Signal over Complicated Terrain** . . . . . 128  
 Junichi Honda, Hirohisa Tajima, and Hisashi Yokoyama

**Evaluation of Never Die Network System for Disaster Prevention Based on Cognitive Wireless Technologys.** . . . . . 139  
 Goshi Sato, Noriki Uchida, Norio Shiratori, and Yoshitaka Shiabat

**Monitoring Health of Large Scale Software Systems Using Drift Detection Techniques** . . . . . 152  
 L.H.C. Prabodha, W.R.R. Vithanage, L.T. Ranaweera, D.M.M.A.I.B. Dissanayake, and S. Ranathunga

**An Efficient Scheduling of Electrical Appliance in Micro Grid Based on Heuristic Techniques** . . . . . 164  
 Sardar Mehboob Hussain, Ayesha Zafar, Rabiya Khalid, Samia Abid, Umar Qasim, Zahoor Ali Khan, and Nadeem Javaid

**Personal Data in Cyber Systems Security** . . . . . 174  
 Marek R. Ogiela and Lidia Ogiela

**Performance Measurement of Energy Management Controller Using Heuristic Techniques** . . . . . 181  
 Adnan Ahmed, Awais Manzoor, Asif Khan, Adnan Zeb, Hussain Ahmad Madni, Umar Qasim, Zahoor Ali Khan, and Nadeem Javaid



**Managing Energy in Smart Homes Using Binary Particle Swarm Optimization** . . . . . 189  
 Samia Abid, Ayesha Zafar, Rabiya Khalid, Sakeena Javaid, Umar Qasim, Zahoor Ali Khan, and Nadeem Javaid

**Single Hop Selection Based Forwarding in WDFAD-DBR for Under Water Wireless Sensor Networks** . . . . . 197  
 Zaheer Ahmad, Arshad Sher, Saba Gull, Farwa Ahmed, Umar Qasim, Zahoor Ali Khan, and Nadeem Javaid

**A Framework for Ranking of Software Design Patterns** . . . . . 205  
 Shahid Hussain, Jacky Keung, and Arif Ali Khan

**Real-Time Body Gestures Recognition Using Training Set Constrained Reduction** . . . . . 216  
 Fabrizio Milazzo, Vito Gentile, Antonio Gentile, and Salvatore Sorce

**Towards Better Population Sizing for Differential Evolution Through Active Population Analysis with Complex Network** . . . . . 225  
 Adam Viktorin, Roman Senkerik, Michal Pluhacek, and Tomas Kadavy

**WORDY: A Semi-automatic Methodology Aimed at the Creation of Neologisms Based on a Semantic Network and Blending Devices** . . . . . 236  
 Daniele Schicchi and Giovanni Pilato

**Conveying Audience Emotions Through Humanoid Robot Gestures to an Orchestra During a Live Musical Exhibition** . . . . . 249  
 Marcello Giardina, Salvatore Tramonte, Vito Gentile, Samuele Vinanzi, Antonio Chella, Salvatore Sorce, and Rosario Sorbello

**A Kernel Support Vector Machine Based Technique for Crohn’s Disease Classification in Human Patients** . . . . . 262  
 Albert Comelli, Maria Chiara Terranova, Laura Scopelliti, Sergio Salerno, Federico Midiri, Giuseppe Lo Re, Giovanni Petrucci, and Salvatore Vitabile

**On the Design of a System to Predict Student’s Success** . . . . . 274  
 David Bañeres and Montse Serra

**DoppioGioco. Playing with the Audience in an Interactive Storytelling Platform** . . . . . 287  
 Rossana Damiano, Vincenzo Lombardo, and Antonio Pizzo

**BioGrakn: A Knowledge Graph-Based Semantic Database for Biomedical Sciences** . . . . . 299  
 Antonio Messina, Haikal Pribadi, Jo Stichbury, Michelangelo Bucci, Szymon Klarman, and Alfonso Urso

<b>Security Infrastructure for Service Oriented Architectures at the Tactical Edge</b> . . . . .	310
Vasileios Gkioulos and Stephen D. Wolthusen	
<b>An Application Using a BLE Beacon Model Combined with Fully Autonomous Wheelchair Control.</b> . . . . .	323
Shugo Miyamoto, Takamasa Koshizen, Takanari Matsumoto, Hiroaki Kawase, Makoto Higuchi, Yasuo Torimoto, Koji Uno, and Fumiaki Sato	
<b>UnipaBCI a Novel General Software Framework for Brain Computer Interface.</b> . . . . .	336
Salvatore Tramonte, Rosario Sorbello, Marcello Giardina, and Antonio Chella	
<b>XML-VM: An XML-Based Grid Computing Middleware.</b> . . . . .	349
Alfredo Cuzzocrea, Enzo Mumolo, Marco Tessarotto, Giorgio Mario Grasso, and Danilo Amendola	
<b>Intelligent Sensor Data Fusion for Supporting Advanced Smart Health Processes</b> . . . . .	361
Alfredo Cuzzocrea, Fernando Ferri, and Patrizia Grifoni	
<b>Hardware Design of a Smart Meter Communication Interface for Smart Grids.</b> . . . . .	371
William Richard Kintzel, Mauro Marcelo Mattos, and Altamir Rosani Borges	
<b>Performance Analysis of WRF Simulations in a Public Cloud and HPC Environment.</b> . . . . .	384
Klodiana Goga, Antonio Parodi, Pietro Ruiu, and Olivier Terzo	
<b>HyperLoom Possibilities for Executing Scientific Workflows on the Cloud</b> . . . . .	397
Vojtech Cima, Stanislav Böhm, Jan Martinovič, Jiří Dvorský, Thomas J. Ashby, and Vladimir Chupakhin	
<b>A Scalable and Low-Power FPGA-Aware Network-on-Chip Architecture.</b> . . . . .	407
Somnath Mazumdar, Alberto Scionti, Antoni Portero, Jan Martinovič, and Olivier Terzo	
<b>Design of a Control System Card for Frequency Inverter in FPGA</b> . . . . .	421
Horacio Matsuura, Mauro Marcelo Mattos, and Luiz Henrique Meyer	
<b>Ising-Model Optimizer with Parallel-Trial Bit-Sieve Engine</b> . . . . .	432
Satoshi Matsubara, Hirotaka Tamura, Motomu Takatsu, Danny Yoo, Behraz Vatankhahghadim, Hironobu Yamasaki, Toshiyuki Miyazawa, Sanroku Tsukamoto, Yasuhiro Watanabe, Kazuya Takemoto, and Ali Sheikholeslami	

**An FPGA Based Heterogeneous Redundant Control System Using Controller Virtualization** . . . . . 439  
 Masaharu Tanaka, Haruhi Eto, Nobumasa Matsui, and Fujio Kurokawa

**Power Performance Analysis of FPGA-Based Particle Filtering for Realtime Object Tracking** . . . . . 451  
 Akane Tahara, Yoshiki Hayashida, Theint Theint Thu, Yuichiro Shibata, and Kiyoshi Oguri

**HLS-Based FPGA Acceleration of Building-Cube Stencil Computation** . . . . . 463  
 Rie Soejima, Yuichiro Shibata, and Kiyoshi Oguri

**Enriching Remote Control Applications with Fog Computing.** . . . . . 475  
 Claudio Fiandrino, Paolo Giaccone, Ahsan Mahmood, and Luca Maioli

**The 11th International Workshop on Engineering Complex Distributed Systems (ECDS-2017)**

**Dynamic MAC Protocol Designed for UAV Collision Avoidance System** . . . . . 489  
 Xiao Ou Song

**A Method for Estimating the Camera Parameters Based on Vanishing Points** . . . . . 499  
 Wan Fang, Li HaiNing, Jin HuaZhong, Lei GuangBo, and Ruan Ou

**Research and Construction of the Full-Service IP High-Speed Intelligent Bearer Network for the Digital Oil Field.** . . . . . 508  
 Xian Zhang, YuMin Feng, and XiaoHui Song

**Verification Using Multi-agent Simulation for Evacuation Guidance with Robots.** . . . . . 516  
 Ryuta Sugie, Takahiro Uchiya, and Ichi Takumi

**Development Support Mechanism for Deep Learning Agent on DASH Agent Framework.** . . . . . 526  
 Kento Watanabe, Takahiro Uchiya, Ichi Takumi, and Tetsuo Kinoshita

**The 10th International Workshop on Engineering Parallel and Multi-Core Systems (ePaMus-2017)**

**A Bayes Classifier-Based OVFD Algorithm for Massive Stream Data Mining on Big Data Platform** . . . . . 537  
 Liangde Li, Peng Li, He Xu, and Fangzhou Chen

<b>Congestion Aware Routing for On-Chip Communication in NoC Systems</b> . . . . .	547
Gul N. Khan and Stephen Chui	
<b>Data Locality Aware Algorithm for Task Execution on Distributed, Cloud Based Environments</b> . . . . .	557
Mihai Bica and Dorian Gorgan	
<b>Asynchronous Page-Rank Computation in Spark</b> . . . . .	567
Chao Li, JianXia Chen, Zhi Yang, and WuYan Chen	
<b>The 10th International Workshop on Intelligent Informatics and Natural Inspired Computing (IINIC- 2017)</b>	
<b>Energy-Aware Routing in A4SDN</b> . . . . .	577
G. Cammarata, A. Di Stefano, G. Morana, and D. Zito	
<b>Energy Optimization Algorithm Based on Data Density Correlation in Wireless Sensor Network</b> . . . . .	589
Jiang Wanyuan, Li Peng, Xu He, and Nie Huqing	
<b>Design and Implementation of Urban Vehicle Positioning System Based on RFID, GPS and LBS</b> . . . . .	599
Cong Qian, He Xu, Peng Li, and Yizhuo Wang	
<b>Radio Spectrum Management for Cognitive Radio Based on Fuzzy Neural Methodology</b> . . . . .	609
Hang Yang, Yuan Liang, Jingcheng Miao, and Dongmei Zhao	
<b>Optimized Energy Efficient Routing Using Dynamic Clustering in Wireless Sensor Networks</b> . . . . .	617
M.Z. Siddiqi, N. Ilyas, A. Aziz, H. Kiran, S. Arif, J. Tahir, U. Qasim, Z.A. Khan, and N. Javaid	
<b>Quantitative Deliberation Model and the Method of Consensus Building</b> . . . . .	627
Xuan Li, Caiquan Xiong, Jiabao Guo, and Gang Liu	
<b>The 8th International Workshop on Frontiers on Complex, Intelligent and Software Intensive Systems (FCISIS-2017)</b>	
<b>Distinguishing Property for Full Round KECCAK-<math>f</math> Permutation</b> . . . . .	639
Maolin Li and Lu Cheng	
<b>Optimal Control of Carrier-Based Aircraft Steam Launching Valve</b> . . . . .	647
Chengtao Cai, Yujia Cui, and Yanhua Liang	
<b>Design and Implementation of Food Safety Traceability System Based on RFID Technology</b> . . . . .	657
Jie Ding, He Xu, Peng Li, and Runyu Xie	

**PaEffExtr: A Method to Extract Effect Statements Automatically from Patents** . . . . . 667  
 Na Deng, Xu Chen, Ou Ruan, Chunzhi Wang, Zhiwei Ye, and Jingbai Tian

**An Efficient Data Aggregation Scheme in Privacy-Preserving Smart Grid Communications with a High Practicability** . . . . . 677  
 Bofeng Pan, Peng Zeng, and Kim-Kwang Raymond Choo

**A Hot Area Mobility Model for Ad Hoc Networks Based on Mining Real Traces of Human** . . . . . 689  
 Lingyun Jiang, Fan He, Zhiqiang Zou, Zhengyuan Wang, and Lijuan Sun

**The 8th International Workshop on Virtual Environment and Network-Oriented Applications (VENOA 2017)**

**A Parameter Optimization Tool and Its Application to Throughput Estimation Model for Wireless LAN** . . . . . 701  
 Nobuo Funabiki, Chihiro Taniguchi, Kyaw Soe Lwin, Khin Khin Zaw, and Wen-Chung Kao

**Virtual IP Network Practice System with Software Agent** . . . . . 711  
 Nobukazu Iguchi

**Creating Learning Materials by Learners Themselves Using Partial Bookmarking for Web Curation** . . . . . 721  
 Takehiro Nagatomo, Takahiro Tachibana, Keizo Sato, and Makoto Nakashima

**Autonomous Decentralized System for Knowledge Refinement of Contents Published over Networks** . . . . . 732  
 Takuma Horiuchi and Shinji Sugawara

**A Device Status Visualization System Based on Mobile Markerless AR Technology** . . . . . 743  
 Toshiyuki Haramaki and Hiroaki Nishino

**A Color Scheme Explorer Based on a Practical Color Design Framework** . . . . . 752  
 Satoru Miura and Hiroaki Nishino

**Performance Testing of Mass Distributed Abyss Storage Prototype for SMB** . . . . . 762  
 ByungRae Cha, YoonSeok Cha, Sun Park, and JongWon Kim

**3D Model Generation of Cattle Using Multiple Depth-Maps for ICT Agriculture** . . . . . 768  
 Naoto Maki, Shohei Nakamura, Shigeru Takano, and Yoshihiro Okada

**The Ubiquitous Greenhouse for Technology Education in Junior High School** . . . . . 778  
 Kazuaki Yoshihara, Kiko Fujimori, and Kenzi Watanabe

**Log Data Visualization and Analysis for Supporting Medical Image Diagnosis** . . . . . 785  
 Tsuneo Kagawa, Shuichi Tanoue, and Hiroaki Nishino

**Study on Data Utilization of Regional Industry in Cross-Cutting and Systematic Regional Community Networks** . . . . . 795  
 Eiji Aoki, Zenjiro Oba, and Ritsuko Watanabe

**Photo Alive!: Elderly Oriented Social Communication Service** . . . . . 805  
 Masooma Zehra Syeda, Meeree Park, and Yong-Moo Kwon

**Realizing Diverse Services Over Hyper-converged Boxes with SmartX Automation Framework** . . . . . 817  
 JongWon Kim

**The 7th Semantic Web/Cloud Information and Services Discovery and Management (SWISM-2017)**

**A Target Driven Approach Supporting Data Diversified Generation in IoT Applications** . . . . . 825  
 Flora Amato, Beniamino Di Martino, Fiammetta Marulli, Antonino Mazzeo, and Francesco Moscato

**Smart Communities of Intelligent Software Agents for Collaborating and Semantically Interoperable Micro-Grids** . . . . . 834  
 Rocco Aversa, Beniamino Di Martino, Geir Horn, Svein Hallsteinsen, Salvatore Venticinquè, and Shanshan Jiang

**A Simulation Approach for the Optimization of Solar Powered Smart Migro-Grids** . . . . . 844  
 Alba Amato, Rocco Aversa, Beniamino Di Martino, Marco Scialdone, and Salvatore Venticinquè

**A Security Metric Catalogue for Cloud Applications** . . . . . 854  
 Valentina Casola, Alessandra De Benedictis, Massimiliano Rak, and Umberto Villano

**Providing Sensor Services by Data Correlation: The #SmartME Approach** . . . . . 864  
 Nidhi Kushwaha, Giovanni Merlino, Longo Francesco, Bruneo Dario, Antonio Puliafito, and O.P. Vyas

**A Fuzzy Prolog and Ontology Driven Framework for Medical Diagnosis Using IoT Devices** . . . . . 875  
 Beniamino Di Martino, Antonio Esposito, Salvatore Liguori, Francesco Ospedale, Salvatore Augusto Maisto, and Stefania Nacchia

**Plug’n’play IoT Devices: An Approach for Dynamic Data Acquisition from Unknown Heterogeneous Devices** . . . . . 885  
 Argyro Mavrogiorgou, Athanasios Kiourtis, and Dimosthenis Kyriazis

**Automatising Mashup of Cloud Services with QoS Requirements** . . . . . 896  
 Claudia Di Napoli, Luca Sabatucci, and Massimo Cosentino

**Towards Osmotic Computing: Looking at Basic Principles and Technologies.** . . . . . 906  
 Massimo Villari, Antonio Celesti, and Maria Fazio

**Towards the Integration of a HPC Build System in the Cloud Ecosystem** . . . . . 916  
 Ioan Drăgan, Teodora Selea, and Teodor-Florin Fortiș

**The 7th International Workshop on Intelligent Computing In Large-Scale Systems (ICLS-2017)**

**On Context-Aware Evidence-Based Data Driven Development of Diagnostic Scales for Depression** . . . . . 929  
 Philip Moore and Hai Van Pham

**Simulation of Upward Underwater Image Distortion Correction** . . . . . 943  
 Chengtao Cai, Jia Zheng, and Yanhua Liang

**Survey of Big Data Platform Based on Cloud Computing Container Technology** . . . . . 954  
 Wei Liu, Weibei Fan, Peng Li, and Liangde Li

**A Planner for Supporting Countermeasures in Large Scale Cyber Attacks** . . . . . 964  
 Flora Amato and Francesco Moscato

**Randomizing Greedy Ensemble Outlier Detection with GRASP** . . . . . 974  
 Lediona Nishani and Marenglen Biba

**The 4th International WorkShop on Energy-Aware Systems, Communications and Security (EASyCoSe-2017)**

**Energy Efficient System for Environment Observation** . . . . . 987  
 Giorgio Giordanengo, Luca Pilosu, Lorenzo Mossucca, Flavio Renga, Simone Ciccia, Olivier Terzo, Giuseppe Vecchi, Vincenzo Romano, and Ingrid Hunstad

**Balancing Demand and Supply of Energy for Smart Homes.** . . . . . 1000  
 Saqib Kazmi, Hafiz Majid Hussain, Asif Khan, Manzoor Ahmad, Umar Qasim, Zahoor Ali Khan, and Nadeem Javaid

**EENET: Energy Efficient Detection of NETwork Changes  
Using a Wireless Sensor Network** . . . . . 1009  
Walter Balzano, Aniello Murano, and Fabio Vitale

**Reducing the Impact of Traffic Sanitization on Latency Sensitive  
Applications**. . . . . 1019  
Mauro Migliardi, Alessio Merlo, and Sherenaz Al-Haj Baddar

**Design and Deployment of Identity Recognition Systems**. . . . . 1027  
Carlo Ferrari and Michele Moro

**The Safety of Your Own App with App Inventor** . . . . . 1037  
Paolo Musmarra

**Author Index**. . . . . 1045



**The 11th International Conference  
on Complex, Intelligent, and Software  
Intensive Systems (CISIS-2017)**

# A Delay-Aware Fuzzy-Based System for Selection of IoT Devices in Opportunistic Networks

Miralda Cuka<sup>1</sup>(✉), Donald Elmazi<sup>1</sup>, Tetsuya Oda<sup>2</sup>, Elis Kulla<sup>2</sup>, Makoto Ikeda<sup>3</sup>,  
and Leonard Barolli<sup>3</sup>

<sup>1</sup> Graduate School of Engineering, Fukuoka Institute of Technology (FIT),  
3-30-1 Wajiro-Higashi, Fukuoka, Higashi-Ku 811-0295, Japan  
mcuka91@gmail.com, donald.elmazi@gmail.com

<sup>2</sup> Department of Information and Computer Engineering, Okayama University  
of Science, 1-1 Ridai-cho, Okayama, Kita-Ku 700-0005, Japan  
oda.tetsuya.fit@gmail.com, kulla@ice.ous.ac.jp

<sup>3</sup> Department of Information and Communication Engineering, Fukuoka Institute  
of Technology (FIT), 3-30-1 Wajiro-Higashi, Fukuoka, Higashi-Ku 811-0295, Japan  
makoto.ikd@acm.org, barolli@fit.ac.jp

**Abstract.** The opportunistic networks are the variants of Delay Tolerant Networks (DTNs). These networks can be useful for routing in places where there are few base stations and connected routes for long distances. In an opportunistic network, when nodes move away or turn off their power to conserve energy, links may be disrupted or shut down periodically. These events result in intermittent connectivity. When there is no path existing between the source and the destination, the network partition occurs. Therefore, nodes need to communicate with each other via opportunistic contacts through store-carry-forward operation. In this work, we consider the IoT device selection problem in opportunistic networks. We propose a delay-aware fuzzy-based system consisting of three input parameters. The output parameter is IoT device selection decision. We evaluate the performance of the proposed system by simulations. The simulation results show that the proposed system makes a proper selection decision of IoT-devices in opportunistic networks.

## 1 Introduction

The Internet is dramatically evolving and creating various connectivity methodologies. The Internet of Things (IoT) is one of those methodologies which transform current Internet communication to Machine-to-Machine (M2M) basis. Hence, IoT can seamlessly connect the real world and cyberspace via physical objects that embed with various types of intelligent sensors. A large number of Internet-connected machines will generate and exchange an enormous amount of data that make daily life more convenient, help to make a tough decision and provide beneficial services. The IoT probably becomes one of the most popular networking concepts that has the potential to bring out many benefits [1].

Opportunistic Networks are the variants of Delay Tolerant Networks (DTNs). It is a class of networks that has emerged as an active research subject in the recent times. Owing to the transient and un-connected nature of the nodes, routing becomes a challenging task in these networks. Sparse connectivity, no infrastructure and limited resources further complicate the situation. Hence, the challenges for routing in opportunistic networks is very different from the traditional wireless networks. However, their utility and potential for scalability makes them a huge success. These networks can be useful for routing in places where one is not likely to find base stations and connected routes for long distances [2].

The Fuzzy Logic (FL) is unique approach that is able to simultaneously handle numerical data and linguistic knowledge. It is a nonlinear mapping of an input data (feature) vector into a scalar output. Fuzzy set theory and FL establish the specifics of the nonlinear mapping.

In this paper, we propose and implement a simulation system for selection of IoT devices in opportunistic networks. The system is based on fuzzy logic and considers three parameters for IoT device selection. We show the simulation results for different values of parameters.

The remainder of the paper is organized as follows. In the Sect. 2, we present a brief introduction of IoT. In Sect. 3, we describe the basics of opportunistic networks including research challenges and architecture. In Sect. 4, we introduce the proposed system model and its implementation. Simulation results are shown in Sect. 5. Finally, conclusions and future work are given in Sect. 6.

## 2 IoT

### 2.1 IoT Architecture

The typical IoT architecture can be divided into five layers as shown in Fig. 1. Each layer is briefly described below.

**Perception Layer:** The perception layer is similar to physical layer in OSI model which consists of the different types of sensor devices and environmental elements. This layer generally deals with identification and collection of specific information by each type of sensor devices. The gathered information can be location, wind speed, vibration, pH level, humidity, amount of dust in the air and so on. The gathered information is transmitted through Network layer toward central information processing system.

**Network Layer:** The Network layer plays an important role in securely transfers and keeps the sensitive information confidential from sensor devices to the central information processing system through 3G, 4G, UMTS, WiFi, WiMAX, RFID, Infrared and Satellite dependent on the type of sensors devices. Thus, this layer is mainly responsible for transferring the information from Perception layer to upper layer.

**Middleware Layer:** The devices in the IoT system may generate various type of services when they are connected and communicated with others. Middleware

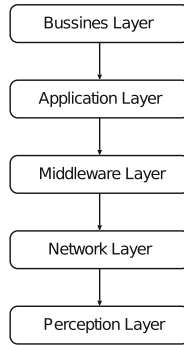


**Fig. 1.** IoT architecture layers

layer has two essential functions, including service management and store the lower layer information into the database. Moreover, this layer has capability to retrieve, process, compute information, and then automatically decide based on the computational results.

**Application Layer:** Application layer is responsible for inclusive applications management based on the processed information in the Middleware layer. The IoT applications can be smart postal, smart heath, smart car, smart glasses, smart home, smart independent living, smart transportation, etc.

**Business Layer:** This layer functions cover the whole IoT applications and services management. It can create practically graphs, business models, flow chart and executive report based on the amount of accurate data received from lower layer and effective data analysis process. Based on the good analysis results, it will help the functional managers or executives to make more accurate decisions about the business strategies and roadmaps.

## 2.2 IoT Protocols

In following we will briefly describe about the most frequently used protocols for Machine-to-Machine (M2M) communication.

The Message Queue Telemetry Transport (MQTT) is a Client Server publishes or subscribes messaging transport protocol. It is light weight, open, simple and designed so as to be easy to implement. The protocol runs over TCP/IP or over other network protocol that provided ordered, lossless, bi-directional connections. The MQTT features include use of the publish/subscribe message pattern which provides one-to-many message distribution, a messaging transport that is agnostic to the content of the payload. Furthermore, the MQTT protocol has not only minimized transport overhead and protocol exchange to reduce network traffic but also has an extraordinary mechanism to notify interested parties when an abnormal disconnection occur as well.

The Constraint Application Protocol (CoAP) is a specialized web transfer protocol for use with constrained nodes and constrained networks. The nodes

often have 8-bit microcontroller with small amounts of ROM and RAM, while constrained network often have high packet error rate and typical throughput is 10 kbps. This protocol designed for M2M application such as smart city and building automation. The CoAP provides a request and response interaction model between application end points, support build-in discovery services and resources, and includes key concepts of the Web such as URIs and Internet media types. CoAP is designed to friendly interface with HTTP for integration with the Web while meeting specialized requirements such as multicast support, very low overhead and simplicity for constrained environments.

### 3 Opportunistic Networks

#### 3.1 Opportunistic Networks Challenges

In an opportunistic network, when nodes move away or turn off their power to conserve energy, links may be disrupted or shut down periodically. These events result in intermittent connectivity. When there is no path existing between the source and the destination, the network partition occurs. Therefore, nodes need to communicate with each other via opportunistic contacts through store-carry-forward operation. In this section, we consider two specific challenges in an opportunistic network: the contact opportunity and the node storage.

- *Contact Opportunity*: Due to the node mobility or the dynamics of wireless channel, a node can make contact with other nodes at an unpredicted time. Since contacts between nodes are hardly predictable, they must be exploited opportunistically for exchanging messages between some nodes that can move between remote fragments of the network. The routing methods for opportunistic networks can be classified based on characteristics of participants' movement patterns. The patterns are classified according to two independent properties: their inherent structure and their adaptiveness to the demand in the network. Other approaches proposed message ferries to provide communication service for nodes in the deployment areas. In addition, the contact capacity needs to be considered [3,4].
- *Node Storage*: As described above, to avoid dropping packets, the intermediate nodes are required to have enough storage to store all messages for an unpredictable period of time until next contact occurs. In other words, the required storage space increases as a function of the number of messages in the network. Therefore, the routing and replication strategies must take the storage constraint into consideration [5].

#### 3.2 Opportunistic Networks Architectures

In an opportunistic network, a network is typically separated into several network partitions called regions. Traditional applications are not suitable for this kind of environment because they normally assume that the end-to-end connection must exist from the source to the destination.

The opportunistic network enables the devices in different regions to inter-connect by operating message in a store-carry-forward fashion. The intermediate nodes implement the store-carry-forward message switching mechanism by overlaying a new protocol layer, called the bundle layer, on top of heterogeneous region-specific lower layers.

In an opportunistic network, each node is an entity with a bundle layer which can act as a host, a router or a gateway. When the node acts as a router, the bundle layer can store, carry and forward the entire bundles (or bundle fragments) between the nodes in the same region. On the other hand, the bundle layer of gateway is used to transfer messages across different regions. A gateway can forward bundles between two or more regions and may optionally be a host, so it must have persistent storage and support custody transfers.

## 4 Proposed System

### 4.1 System Parameters

Based on Opportunistic Networks characteristics and challenges, we consider the following parameters for implementation of our proposed system.

**IoT Device Speed (IDS):** There are different types of IoT devices in opportunistic networks scenarios such as: mobile phone terminals, computers, cars, trains, planes, robots and so on. Considering that high speed IoT devices can transfer the information faster, they will be selected with high probability.

**IoT Device Waiting Time for sending data (IDWT):** Considering network congestion some IoT devices wait longer and some wait less for sending data. The IoT devices that have been waiting longer have a high possibility to be selected.

**IoT Device Remaining Energy (IDRE):** The IoT devices in opportunistic networks are active and can perform tasks and exchange data in different ways from each other. Consequently, some IoT devices may have a lot of remaining power and other may have very little, when an event occurs.

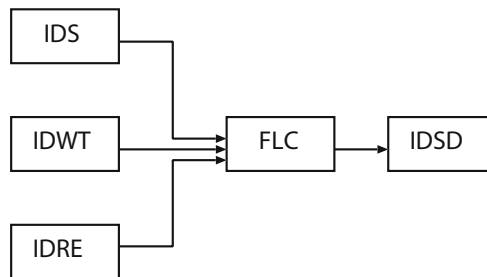


**Fig. 2.** Proposed system model.

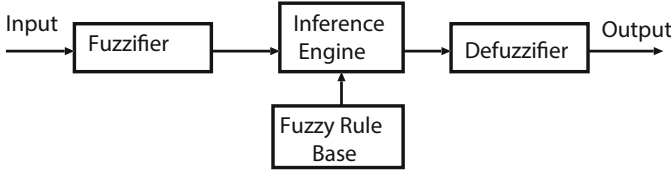


**Fig. 3.** FLC structure.

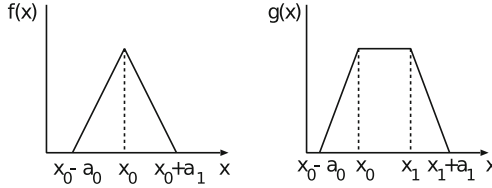


**Fig. 4.** Triangular and trapezoidal membership functions.

**IoT Device Selection Decision (IDSD):** The proposed system considers the following levels for IoT device selection:

- Very Low Selection Possibility (VLSP) - The IoT device will have very low probability to be selected.
- Low Selection Possibility (LSP) - There might be other IoT devices which can do the job better.
- Middle Selection Possibility (MSP) - The IoT device is ready to be assigned a task, but is not the “chosen” one.
- High Selection Possibility (HSP) - The IoT device takes responsibility of completing the task.
- Very High Selection Possibility (VHSP) - The IoT device has almost all required information and potential to be selected and then allocated in an appropriate position to carry out a job.

## 4.2 System Implementation

Fuzzy sets and fuzzy logic have been developed to manage vagueness and uncertainty in a reasoning process of an intelligent system such as a knowledge based

**Table 1.** Parameters and their term sets for FLC.

Parameters	Term sets
IoT Device Speed (IDS)	Slow (Sl), Medium (Md), Fast (Fa)
IoT Device Waiting Time (IDWT)	Low (Lo), Medium (Me), High (Hi)
IoT Device Remaining Energy (IDRE)	Low (Lw), Medium (Md), High (Hg)
IoT Device Selection Decision (IDSD)	VLSP, LSP, MSP, HSP, VHSP

system, an expert system or a logic control system [6–19]. In this work, we use fuzzy logic to implement the proposed system.

The structure of the proposed system is shown in Fig. 2. It consists of one Fuzzy Logic Controller (FLC), which is the main part of our system and its basic elements are shown in Fig. 3. They are the fuzzifier, inference engine, Fuzzy Rule Base (FRB) and defuzzifier.

As shown in Fig. 4, we use triangular and trapezoidal membership functions for FLC, because they are suitable for real-time operation [20]. The  $x_0$  in  $f(x)$  is the center of triangular function,  $x_0(x_1)$  in  $g(x)$  is the left (right) edge of trapezoidal function, and  $a_0(a_1)$  is the left (right) width of the triangular or trapezoidal function. We explain in details the design of FLC in following.

We use three input parameters for FLC:

- IoT Device Speed (IDS);
- IoT Device Waiting Time (IDWT);
- IoT Device Remaining Energy (IDRE).

The term sets for each input linguistic parameter are defined respectively as shown in Table 1.

$$\begin{aligned} T(IDS) &= \{Slow(Sl), Medium(Md), Fast(Fa)\} \\ T(IDWT) &= \{Low(Lo), Medium(Me), High(Hi)\} \\ T(IDRE) &= \{Low(Lw), Medium(Md), High(Hg)\} \end{aligned}$$

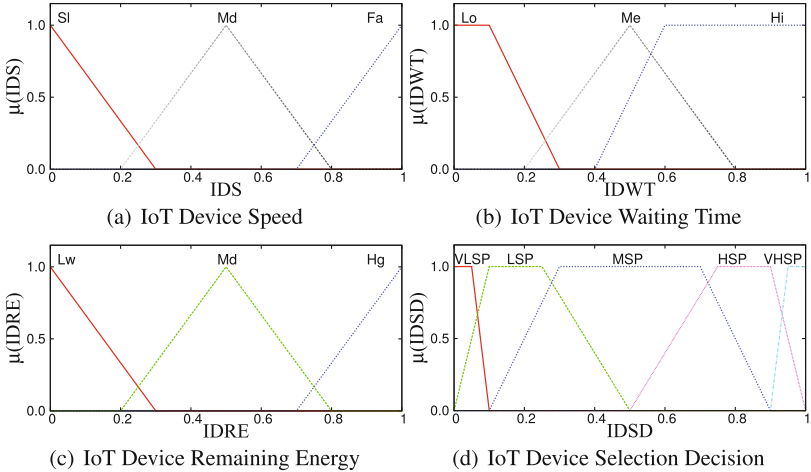


**Fig. 5.** Fuzzy membership functions.



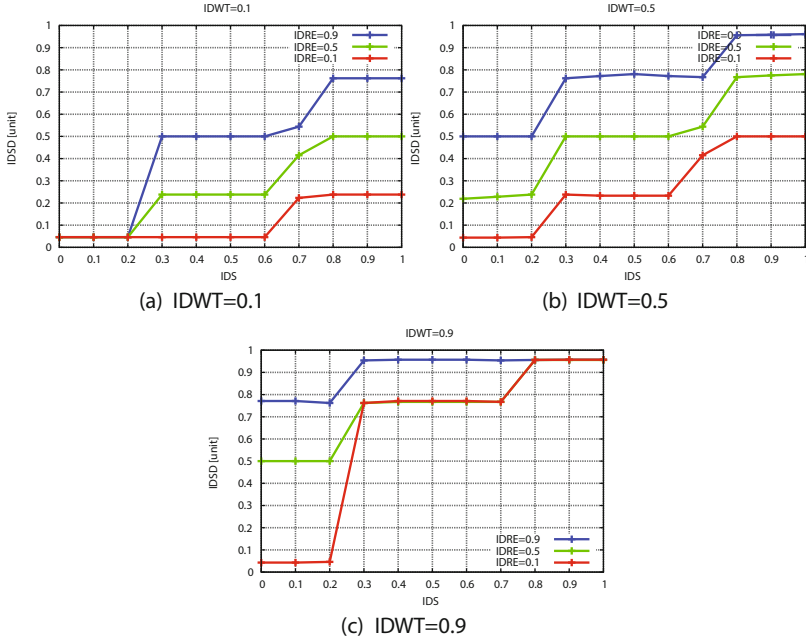


**Fig. 6.** Results for different values of IDWT.

The membership functions for input parameters of FLC are defined as:

$$\begin{aligned}
 \mu_{Sl}(IDS) &= f(IDS; Sl_0, Lo_1, Sl_{w0}, Sl_{w1}) \\
 \mu_{Md}(IDS) &= f(IDS; Md_0, Md_{w0}, Md_{w1}) \\
 \mu_{Fa}(IDS) &= f(IDS; Fa_0, Hi_1, Fa_{w0}, Fa_{w1}) \\
 \mu_{Lo}(IDWT) &= g(IDWT; Lo_0, Lo_1, Lo_{w0}, Lo_{w1}) \\
 \mu_{Me}(IDWT) &= f(IDWT; Me_0, Me_{w0}, Me_{w1}) \\
 \mu_{Hi}(IDWT) &= g(IDWT; Hi_0, Hi_1, Hi_{w0}, Hi_{w1}) \\
 \mu_{Lw}(IDRE) &= f(IDRE; Lw_0, Lw_1, Lw_{w0}, Lw_{w1}) \\
 \mu_{Md}(IDRE) &= f(IDRE; Md_0, Md_{w0}, Md_{w1}) \\
 \mu_{Hg}(IDRE) &= f(IDRE; Hg_0, Hg_1, Hg_{w0}, Hg_{w1})
 \end{aligned}$$

The small letters  $w0$  and  $w1$  mean left width and right width, respectively.

The output linguistic parameter is the Actor Node Selection Decision (IDSD). We define the term set of IDSD as:

$$\{ \text{Very Low Selection Possibility (VLSP)}, \\
 \text{Low Selection Possibility (LSP)}, \\
 \text{Middle Selection Possibility (MSP)}, \\
 \text{High Selection Possibility (HSP)}, \\
 \text{Very High Selection Possibility (VHSP)} \}.$$

The membership functions for the output parameter  $IDSD$  are defined as:

$$\begin{aligned}\mu_{VLSP}(IDSD) &= g(IDSD; VLSP_0, VLSP_1, VLSP_{w0}, VLSP_{w1}) \\ \mu_{LSP}(IDSD) &= g(IDSD; LSP_0, LSP_1, LSP_{w0}, LSP_{w1}) \\ \mu_{MSP}(IDSD) &= g(IDSD; MSP_0, MSP_1, MSP_{w0}, MSP_{w1}) \\ \mu_{HSP}(IDSD) &= g(IDSD; HSP_0, HSP_1, HSP_{w0}, HSP_{w1}) \\ \mu_{VHSP}(IDSD) &= g(IDSD; VHSP_0, VHSP_1, VHSP_{w0}, VHSP_{w1}).\end{aligned}$$

The membership functions are shown in Fig. 5 and the Fuzzy Rule Base (FRB) is shown in Table 2. The FRB forms a fuzzy set of dimensions  $|T(IDS)| \times$

**Table 2.** FRB of proposed fuzzy-based system.

No	IDS	IDWT	IDRE	IDSD
1	Sl	Lo	Lw	VLSP
2	Sl	Lo	Md	VLSP
3	Sl	Lo	Hg	MSP
4	Sl	Me	Lw	VLSP
5	Sl	Me	Md	LSP
6	Sl	Me	Hg	VLSP
7	Sl	Hi	Lw	VLSP
8	Sl	Hi	Md	MSP
9	Sl	Hi	Hg	HSP
10	Md	Lo	Lw	VLSP
11	Md	Lo	Md	LSP
12	Md	Lo	Hg	HSP
13	Md	Me	Lw	LSP
14	Md	Me	Md	MSP
15	Md	Me	Hg	HSP
16	Md	Hi	Lw	MSP
17	Md	Hi	Md	HSP
18	Md	Hi	Hg	VHSP
19	Fa	Lo	Lw	LSP
20	Fa	Lo	Md	MSP
21	Fa	Lo	Hg	VHSP
22	Fa	Me	Lw	MSP
23	Fa	Me	Md	HSP
24	Fa	Me	Hg	VHSP
25	Fa	Hi	Lw	HSP
26	Fa	Hi	Md	VHSP
27	Fa	Hi	Hg	VHSP

$|T(IDWT)| \times |T(IDRE)|$ , where  $|T(x)|$  is the number of terms on  $T(x)$ . The FRB has 27 rules. The control rules have the form: IF “conditions” THEN “control action”.

## 5 Simulation Results

We present the simulation results in Fig. 6. In Fig. 6(a) is shown the relation between IDSD and IDS for different IDRE values. The IDWT is considered 0.1. We see that when the speed is increased, the possibility of the present IoT device to be selected for carrying out a job is increased. By increasing the IDRE value, the IDSD is also increased. This means that the IoT device with higher remaining energy will be selected. The value of IDSD is increased faster when the IDS is from 0.2 to 0.8.

In Fig. 6(b) and (c) we increase the IDWT value to 0.5 and 0.9, respectively. We see that with the increase of the IDWT parameter, the possibility of a IoT device to be selected is increased.

## 6 Conclusions and Future Work

In this paper, we proposed and implemented a fuzzy-based simulation system for selection of IoT devices in opportunistic networks. We considered three parameters to select an IoT device to carry out a required task.

We evaluated the proposed system by some simulation results. The simulation results show that when the speed is increased, the possibility of IoT device to be selected for carrying out a job is increased. By increasing the IDRE value, the IDSD is also increased.

In the future work, we will consider also other parameters for IoT device selection in opportunistic networks and make extensive simulations to evaluate the proposed system.

## References

1. Kraijak, S., Tuwanut, P.: A survey on internet of things architecture, protocols, possible applications, security, privacy, real-world implementation and future trends. In: IEEE 16th International Conference on Communication Technology (ICCT), pp. 26–31. IEEE (2015)
2. Dhurandher, S.K., Sharma, D.K., Woungang, I., Bhati, S.: HBPR: history based prediction for routing in infrastructure-less opportunistic networks. In: IEEE 27th International Conference on Advanced Information Networking and Applications (AINA), pp. 931–936. IEEE (2013)
3. Akbas, M., Turgut, D.: APAWSAN: actor positioning for aerial wireless sensor and actor networks. In: IEEE 36th Conference on Local Computer Networks (LCN), pp. 563–570, October 2011
4. Akbas, M., Brust, M., Turgut, D.: Local positioning for environmental monitoring in wireless sensor and actor networks. In: IEEE 35th Conference on Local Computer Networks (LCN), pp. 806–813, October 2010

5. Melodia, T., Pompili, D., Gungor, V., Akyildiz, I.: Communication and coordination in wireless sensor and actor networks. *IEEE Trans. Mob. Comput.* **6**(10), 1126–1129 (2007)
6. Inaba, T., Sakamoto, S., Kolicic, V., Mino, G., Barolli, L.: A CAC scheme based on fuzzy logic for cellular networks considering security and priority parameters. In: *The 9th International Conference on Broadband and Wireless Computing, Communication and Applications (BWCCA-2014)*, pp. 340–346 (2014)
7. Spaho, E., Sakamoto, S., Barolli, L., Xhafa, F., Barolli, V., Iwashige, J.: A fuzzy-based system for peer reliability in JXTA-Overlay P2P considering number of interactions. In: *The 16th International Conference on Network-Based Information Systems (NBIS-2013)*, pp. 156–161 (2013)
8. Matsuo, K., Elmazi, D., Liu, Y., Sakamoto, S., Mino, G., Barolli, L.: FACS-MP: a fuzzy admission control system with many priorities for wireless cellular networks and its performance evaluation. *J. High Speed Netw.* **21**(1), 1–14 (2015)
9. Grabisch, M.: The application of fuzzy integrals in multicriteria decision making. *Eur. J. Oper. Res.* **89**(3), 445–456 (1996)
10. Inaba, T., Elmazi, D., Liu, Y., Sakamoto, S., Barolli, L., Uchida, K.: Integrating wireless cellular and ad-hoc networks using fuzzy logic considering node mobility and security. In: *The 29th IEEE International Conference on Advanced Information Networking and Applications Workshops (WAINA-2015)*, pp. 54–60 (2015)
11. Kulla, E., Mino, G., Sakamoto, S., Ikeda, M., Caballé, S., Barolli, L.: FBMIS: a fuzzy-based multi-interface system for cellular and ad hoc networks. In: *International Conference on Advanced Information Networking and Applications (AINA-2014)*, pp. 180–185 (2014)
12. Elmazi, D., Kulla, E., Oda, T., Spaho, E., Sakamoto, S., Barolli, L.: A comparison study of two fuzzy-based systems for selection of actor node in wireless sensor actor networks. *J. Ambient Intell. Humanized Comput.* **6**(5), 635–645 (2015)
13. Zadeh, L.: Fuzzy logic, neural networks, and soft computing. *ACM Commun.* **37**, 77–84 (1994)
14. Spaho, E., Sakamoto, S., Barolli, L., Xhafa, F., Ikeda, M.: Trustworthiness in P2P: performance behaviour of two fuzzy-based systems for JXTA-Overlay platform. *Soft Comput.* **18**(9), 1783–1793 (2014)
15. Inaba, T., Sakamoto, S., Kulla, E., Caballe, S., Ikeda, M., Barolli, L.: An integrated system for wireless cellular and ad-hoc networks using fuzzy logic. In: *International Conference on Intelligent Networking and Collaborative Systems (INCoS-2014)*, pp. 157–162 (2014)
16. Matsuo, K., Elmazi, D., Liu, Y., Sakamoto, S., Barolli, L.: A multi-modal simulation system for wireless sensor networks: a comparison study considering stationary and mobile sink and event. *J. Ambient Intell. Humanized Comput.* **6**(4), 519–529 (2015)
17. Kolicic, V., Inaba, T., Lala, A., Mino, G., Sakamoto, S., Barolli, L.: A fuzzy-based CAC scheme for cellular networks considering security. In: *International Conference on Network-Based Information Systems (NBIS-2014)*, pp. 368–373 (2014)
18. Liu, Y., Sakamoto, S., Matsuo, K., Ikeda, M., Barolli, L., Xhafa, F.: A comparison study for two fuzzy-based systems: improving reliability and security of JXTA-Overlay P2P platform. *Soft Comput.* **20**(7), 2677–2687 (2016)
19. Matsuo, K., Elmazi, D., Liu, Y., Sakamoto, S., Mino, G., Barolli, L.: FACS-MP: a fuzzy admission control system with many priorities for wireless cellular networks and its performance evaluation. *J. High Speed Netw.* **21**(1), 1–14 (2015)
20. Mendel, J.M.: Fuzzy logic systems for engineering: a tutorial. *Proc. of the IEEE* **83**(3), 345–377 (1995)

# A GA-Based Simulation System for WMNs: Performance Analysis for Different WMN Architectures Considering Weibull Distribution, HWMP and TCP Protocols

Admir Barolli<sup>1</sup>(✉), Tetsuya Oda<sup>2</sup>, Makoto Ikeda<sup>3</sup>, Keita Matsuo<sup>3</sup>,  
Leonard Barolli<sup>3</sup>, and Makoto Takizawa<sup>4</sup>

<sup>1</sup> Department of Information Technology, Aleksander Moisiu University of Durres,  
L.1, Rruga e Currilave, Durres, Albania

[admir.barolli@gmail.com](mailto:admir.barolli@gmail.com)

<sup>2</sup> Department of Information and Computer Engineering,  
Okayama University of Science (OUS),

1-1 Ridaicho, Kita-ku, Okayama 700-0005, Japan

[oda.tetsuya.fit@gmail.com](mailto:oda.tetsuya.fit@gmail.com)

<sup>3</sup> Department of Information and Communication Engineering,  
Fukuoka Institute of Technology (FIT),

3-30-1 Wajiro-Higashi, Higashi-Ku, Fukuoka 811-0295, Japan

[makoto.ikd@acm.org](mailto:makoto.ikd@acm.org), [{kt-matsuo,barolli}@fit.ac.jp](mailto:{kt-matsuo,barolli}@fit.ac.jp)

<sup>4</sup> Hosei University, 3-7-2, Kajino-Machi, Koganei-Shi, Tokyo 184-8584, Japan

[makoto.takizawa@computer.org](mailto:makoto.takizawa@computer.org)

**Abstract.** In our previous work, we implemented WMN-GA system which is based on Genetic Algorithms (GAs) and used it for node placement problem in WMNs. In this paper, we evaluate the performance of Weibull distribution of mesh clients for two WMN architectures considering PDR, throughput, delay, fairness index and energy metrics. For simulations, we used ns-3, Hybrid Wireless Mesh Protocol (HWMP) and TCP. We compare the performance of both architectures. The simulation results show that the PDR for both WMN architectures is almost the same. The throughput of I/B WMN is a little bit higher than Hybrid WMN. The delay of Hybrid WMN is lower than I/B WMN. The fairness index and the remaining energy for both WMN architectures are almost the same.

## 1 Introduction

Wireless Mesh Networks (WMNs) [1] can be seen as a special type of wireless ad-hoc networks. WMNs are based on mesh topology, in which every node (representing a server) is connected through wireless links to one or more nodes, enabling thus the information transmission in more than one path. The path redundancy is a robust feature of mesh topology. Compared to other topologies, mesh topology does not need a central node, allowing networks based on

it to be self-healing. These characteristics of networks with mesh topology make them very reliable and robust networks to potential server node failures.

There are a number of application scenarios for which the use of WMNs is a very good alternative to offer connectivity at a low cost. It should also be mentioned that there are applications of WMNs which are not supported directly by other types of wireless networks such as cellular networks, ad hoc networks, wireless sensor networks and standard IEEE 802.11 networks. There are many applications of WMNs in Neighboring Community Networks, Corporate Networks, Metropolitan Area Networks, Transportation Systems, Automatic Control Buildings, Medical and Health Systems, Surveillance and so on.

The main issue of WMNs is to achieve network connectivity and stability as well as QoS in terms of user coverage. This problem is very closely related to the family of node placement problems in WMNs [2–5], among them, the mesh router mesh nodes placement. We consider the version of the mesh router nodes placement problem in which we are given a grid area where to deploy a number of mesh router nodes and a number of mesh client nodes of fixed positions (of an arbitrary distribution) in the grid area. The objective is to find a location assignment for the mesh routers to the cells of the grid area that maximizes the network connectivity and client coverage.

As node placement problems are known to be computationally hard to solve for most of the formulations [6, 7], Genetic Algorithms (GAs) has been recently investigated as an effective resolution method.

In our previous work [8, 9], we considered the version of the mesh router nodes placement problem in which we are given a grid area where to deploy a number of mesh router nodes and a number of mesh client nodes of fixed positions (of an arbitrary distribution) in the grid area. We used WMN-GA system to optimize the location of mesh routers the network connectivity.

In this work, we use the topology generated by WMN-GA system and evaluate by simulations the performance of Weibull distribution of mesh clients considering two architectures of WMNs by sending multiple Constant Bit Rate (CBR) flow in the network. For simulations, we use ns-3, Hybrid Wireless Mesh Protocol (HWMP) and TCP. As evaluation metrics we considered PDR, throughput, delay, fairness index and energy.

The structure of the paper is as follows. In Sect. 2, we make an explanation of architectures of WMNs. In Sect. 3, we make an overview of HWMP routing protocol. In Sect. 4, we show the description and design of the simulation system. In Sect. 5, we show the simulation results. Finally, conclusions and future work are given in Sect. 6.

## 2 Architectures of WMNs

In this section, we describe the architectures of WMN. The architecture of the nodes in WMNs [10–16] can be classified according to the functionalities they offer as follows:

**Infrastructure/Backbone WMNs:** This type of architecture (also known as infrastructure meshing) is the most used and consists of a grid of mesh routers which are connected to different clients. Moreover, routers have gateway functionality thus allowing Internet access for clients. This architecture enables integration with other existing wireless networks and is widely used in neighboring communities.

**Client WMNs:** Client meshing architecture provides a communications network based on peer-to-peer over client devices (there is no the role of mesh router). In this case we have a network of mesh nodes which provide routing functionality and configuration as well as end-user applications, so that when a packet is sent from one node to another, the packet will jump from node to node in the mesh of nodes to reach the destination.

**Hybrid WMNs:** This architecture combines the two previous ones, so that mesh clients are able to access the network through mesh routers as well as through direct connection with other mesh clients. Benefiting from the advantages of the two architectures, Hybrid WMNs can connect to other networks (Internet, Wi-Fi, and sensor networks) and enhance the connectivity and coverage due to the fact that mesh clients can act as mesh routers.

### 3 Overview of HWMP Routing Protocol

Hybrid Wireless Mesh Protocol (HWMP) defined in IEEE 802.11s, is a basic routing protocol for a wireless mesh network. It is based on AODV [17] and tree-based routing. It relies on peer link management protocol by which each mesh point discovers and tracks neighboring nodes. If any of these are connected to a wired backhaul, there is no need for HWMP, which selects paths from those assembled by compiling all mesh point peers into one composite map.

HWMP protocol is hybrid, because it supports two kinds of path selection protocols. Although these protocols are very similar to routing protocols, but bear in mind, that in case of IEEE 802.11s these use MAC addresses for “routing”, instead of IP addresses. Therefore, we use the term “path” instead of “route” and thus “path selection” instead of “routing”.

HWMP is intended to displace proprietary protocols used by vendors like Meraki for the same purpose, permitting peer participation by open source router firmware.

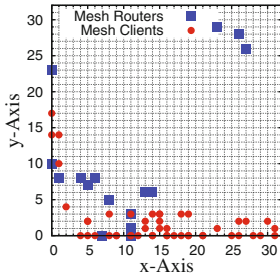
## 4 Simulation System Description and Design

### 4.1 Positioning of Mesh Routers by WMN-GA System

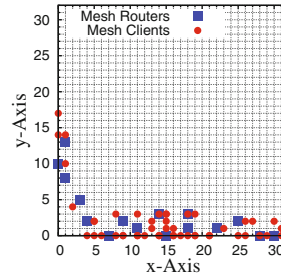
We use WMN-GA system for node placement problem in WMNs. A bi-objective optimization is used to solve this problem by first maximizing the number of connected routers in the network and then the client coverage. The input parameters of WMN-GA system are shown in Table 1. In Fig. 1, we show the location of mesh

**Table 1.** Input parameters of WMN-GA system.

Parameters	Values
Number of clients	48
Number of routers	16, 20, 24, 28, 32
Grid width	32 units
Grid height	32 units
Independent runs	10
Number of generations	200
Population size	64
Selection method	Linear ranking
Crossover rate	80%
Mutate method	Single
Mutate rate	20%
Distribution of clients	Weibull



(a) Number of generations: 1 (12, 17)



(b) Number of generations: 200 (16, 47)

**Fig. 1.** Location of mesh routers and clients for exponential distribution;  $(m, n)$ :  $m$  is SGC,  $n$  is NCMC.

routers and clients for first generations and the optimized topologies generated by WMN-GA system for Weibull distribution.

In Fig. 2 are shown the simulation results of Size of Giant Component (SGC) vs. number of generations. After few generations, all routers are connected with each other.

Then, we optimize the position of routers in order to cover as many mesh clients as possible. The simulation results of SGC and Number of Covered Mesh Clients (NCMC) are shown in Table 2.

## 4.2 Simulation Description

We conduct simulations using ns-3 simulator. The simulations in ns-3 are done for number of generations 1 and 200. The area size is considered  $640 \text{ [m]} \times 640 \text{ [m]}$



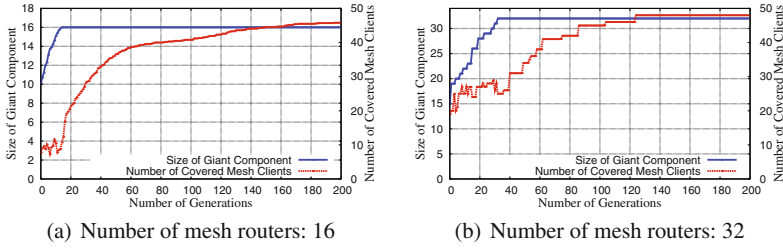


**Fig. 2.** SGC and NCMC vs. number of generations for exponential distribution.

**Table 2.** Evaluation of WMN-GA system.

Number of mesh routers	Weibull distribution	
	SGC	NCMC
16	16	47
20	20	48
24	24	48
28	28	48
32	32	48

(or 32 units  $\times$  32 units) and the number of mesh routers is from 16 to 32. We used HWMP routing protocol and sent multiple CBR flows over TCP. The pairs source-destination are the same for all simulation scenarios. Log-distance path loss model and constant speed delay model are used for the simulation and other parameters are shown in Table 3.

### 4.3 NS-3

The ns-3 simulator [18] is developed and distributed completely in the C++ programming language, because it better facilitated the inclusion of C-based implementation code. The ns-3 architecture is similar to Linux computers, with internal interface and application interfaces such as network interfaces, device drivers and sockets. The goals of ns-3 are set very high: to create a new network simulator aligned with modern research needs and develop it in an open source community. Users of ns-3 are free to write their simulation scripts as either C++ *main()* programs or Python programs. The ns-3's low-level API is oriented towards the power-user but more accessible "helper" APIs are overlaid on top of the low-level API.

In order to achieve scalability of a very large number of simulated network elements, the ns-3 simulation tools also support distributed simulation. The ns-3 support standardized output formats for trace data, such as the pcap format used by network packet analyzing tools such as tcpdump, and a standardized input format such as importing mobility trace files from ns-2 [19].

**Table 3.** Simulation parameters for ns-3.

Parameters	Values
Area size	640 [m] × 640 [m]
Number of mesh routers	24
Distributions of mesh clients	Weibull
Number of mesh clients	48
MAC	IEEE 802.11s
Propagation loss model	Log-distance path loss model
Propagation delay model	Constant speed model
Routing protocol	HWMP
Transport protocol	TCP
Application type	CBR
Packet size	1024 [Bytes]
Number of source nodes	10
Number of destination nodes	1
Transmission energy	17.4 [mJ]
Receiving energy	19.7 [mJ]
Simulation time	600 [s]

The ns-3 simulator is equipped with *Pyviz* visualizer, which has been integrated into mainline ns-3, starting with version 3.10. It can be most useful for debugging purposes, i.e. to figure out if mobility models are what you expect, where packets are being dropped. It is mostly written in Python and it works both with Python and pure C++ simulations. The function of ns-3 visualizer is more powerful than network animator (*nam*) of ns-2 simulator.

The ns-3 simulator has models for all network elements that comprise a computer network. For example, network devices represent the physical device that connects a node to the communication channel. This might be a simple Ethernet network interface card or a more complex wireless IEEE 802.11 device.

The ns-3 is intended as an eventual replacement for popular ns-2 simulator. The ns-3's wifi models a wireless network interface controller based on the IEEE 802.11 standard [20]. The ns-3 provides models for these aspects of 802.11:

1. Basic 802.11 DCF with infrastructure and ad hoc modes.
2. 802.11a, 802.11b, 802.11g and 802.11s physical layers.
3. QoS-based EDCA and queueing extensions of 802.11e.
4. Various propagation loss models including Nakagami, Rayleigh, Friis, LogDistance, FixedRss, and so on.
5. Two propagation delay models, a distance-based and random model.
6. Various rate control algorithms including Aarf, Arf, Cara, Onoe, Rraa, ConstantRate, and Minstrel.

## 5 Simulation Results

In this section, we present the simulation results. For evaluation, we used the PDR, throughput, delay, fairness index and energy metrics. We analyze and compare the simulation results of I/B WMN and Hybrid WMN architectures considering Weibull distribution.

In Fig. 3, we show the simulation results for PDR metric. The simulation results show that the PDR for both WMN architectures is almost the same. In Fig. 4, we show the simulation results of throughput metric. The throughput of I/B WMN is a little bit higher than Hybrid WMN.

In Fig. 5, the delay of Hybrid WMN is lower than I/B WMN. In Fig. 6, we show the fairness index. The fairness index for both WMN architectures is almost the same. In Fig. 7, we show the remaining energy for both WMN architectures. We can see that the remaining energy for both architectures is almost the same.

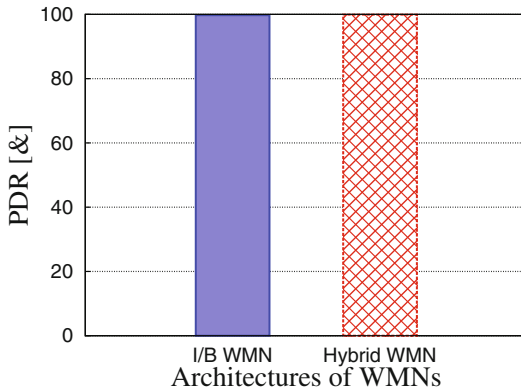


**Fig. 3.** Results of average PDR.

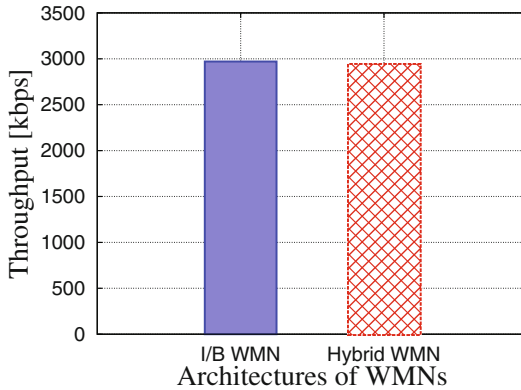


**Fig. 4.** Results of average throughput.

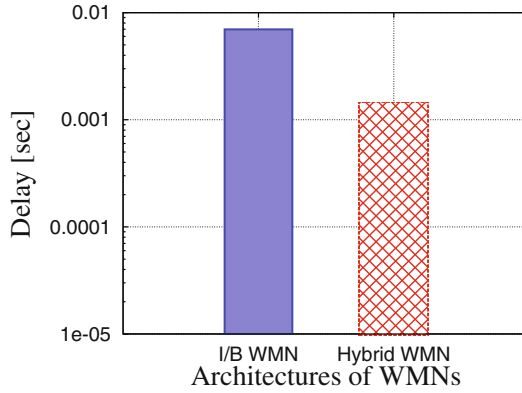


**Fig. 5.** Results of average delay.

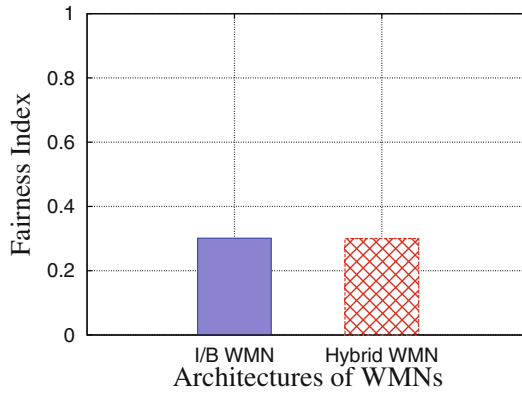


**Fig. 6.** Results of fairness index.

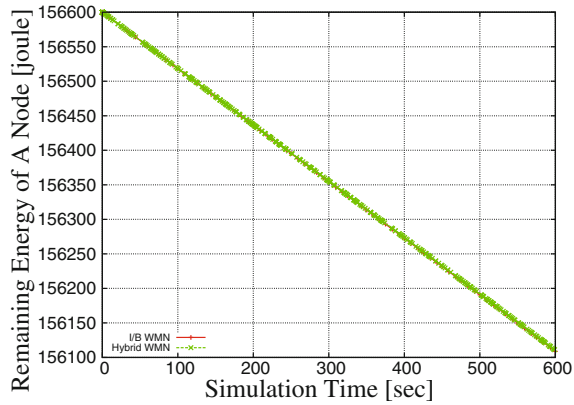


**Fig. 7.** Results of remaining energies.

## 6 Conclusions

In this paper, we evaluated by simulations the performance of the WMN architectures considering PDR, throughput, delay, fairness index and energy metrics. The topologies of WMNs are generated using WMN-GA system. The clients are distributed in the grid area using Weibull distribution.

We carried out the simulations using ns-3 simulator and HWMP. We transmitted multiple CBR flows over TCP. For simulations, we considered log-distance path loss model and constant speed delay model. From simulations, we found the following results.

- The PDR for both WMN architectures are almost the same.
- The throughput of I/B WMN is a little bit higher than Hybrid WMN.
- The delay of Hybrid WMN is lower than I/B WMN.
- The fairness index and remaining energy for both WMN architectures are almost the same.

In this work, we consider HWMP and TCP protocols. In the future work, we would like to make extensive simulations for different density of mesh clients and grid sizes.

## References

1. Akyildiz, I.F., Wang, X., Wang, W.: Wireless mesh networks: a survey. *Comput. Netw.* **47**(4), 445–487 (2005)
2. Franklin, A., Murthy, C.: Node placement algorithm for deployment of two-tier wireless mesh networks. In: *IEEE GLOBECOM 2007*, pp. 4823–4827 (2007)
3. Muthaiah, S.N., Rosenberg, C.: Single gateway placement in wireless mesh networks. In: *Proceedings of 8th International IEEE Symposium on Computer Networks*, Turkey, pp. 4754–4759 (2008)
4. Tang, M.: Gateways placement in backbone wireless mesh networks. *Int. J. Commun. Netw. Syst. Sci.* **2**(1), 45–50 (2009)
5. Vanhatupa, T., Hännikäinen, M., Hämäläinen, T.D.: Genetic algorithm to optimize node placement and configuration for WLAN planning. In: *Proceedings of 4th International Symposium on Wireless Communication Systems*, pp. 612–616 (2007)
6. Lim, A., Rodrigues, B., Wang, F., Xua, Zh.:  $k$ -center problems with minimum coverage. *Theor. Comput. Sci.* **332**(1–3), 1–17 (2005)
7. Wang, J., Xie, B., Cai, K., Agrawal, D.P.: Efficient mesh router placement in wireless mesh networks, In: *MASS*, Pisa, Italy, pp. 9–11 (2007)
8. Oda, T., Barolli, A., Xhafa, F., Barolli, L., Ikeda, M., Takizawa, M.: WMN-GA: a simulation system for WMNs and its evaluation considering selection operators. *J. Ambient Intell. Humanized Comput. (JAIHC)* **4**(3), 323–330 (2013). Springer
9. Ikeda, M., Oda, T., Kulla, E., Hiyama, M., Barolli, L., Younas, M.: Performance evaluation of WMN considering number of connections using NS-3 simulator. In: *The Third International Workshop on Methods, Analysis and Protocols for Wireless Communication (MAPWC 2012)*, Victoria, Canada, pp. 498–502, 12–14 November 2012

10. Xhafa, F., Sanchez, C., Barolli, L.: Locals search algorithms for efficient router nodes placement in wireless mesh networks. In: International Conference on Network-Based Information Systems (NBiS), pp. 572–579 (2009)
11. Oda, T., Barolli, A., Spaho, E., Barolli, L., Xhafa, F.: Analysis of mesh router placement in wireless mesh networks using friedman test. In: Proceedings of the 28th IEEE International Conference on Advanced Information Networking and Applications (IEEE AINA), Victoria, Canada, pp. 289–296, May 2014
12. Oda, T., Sakamoto, S., Barolli, A., Ikeda, M., Barolli, L., Xhafa, F.: A GA-based simulation system for WMNs: performance analysis for different WMN architectures considering TCP. In: 2014 Eighth International Conference on Broadband and Wireless Computing, Communication and Applications (BWCCA), Guangzhou, China, pp. 120–126, November 2014
13. Oda, T., Barolli, A., Spaho, E., Xhafa, F., Barolli, L., Takizawa, M.: Evaluation of WMN-GA for different mutation operators. *Int. J. Space Based Situated Comput. (IJSSC)* **2**(3), 149–157 (2012). Inderscience
14. Oda, T., Sakamoto, S., Barolli, A., Spaho, E., Barolli, L., Xhafa, F.: Effect of different grid shapes in wireless mesh network genetic algorithm system. *Int. J. Web Grid Serv. (IJWGS)* **10**(4), 371–395 (2014). Inderscience
15. Oda, T., Barolli, A., Spaho, E., Barolli, L., Xhafa, F., Younas, M.: Effects of population size for location-aware node placement in WMNs: evaluation by a genetic algorithm based approach. *Pers. Ubiquit. Comput. (PUC)* **18**(2), 261–269 (2014). Springer
16. Lala, A., Kolici, V., Oda, T., Barolli, L., Barolli, A., Xhafa, F.: A web interface for wireless mesh networks based on heuristic algorithms: optimization and analysis for different scenarios. *Int. J. Web Grid Serv. (IJWGS)* **11**(3), 327–346 (2015). Inderscience
17. Perkins, C., Belding-Royer, E., Das, S.: Ad hoc On-demand Distance Vector (AODV) Routing, IETF RFC 3561, July 2003
18. ns-3. <https://www.nsnam.org/>
19. The Network Simulator-ns-2. <http://www.isi.edu/nsnam/ns/>
20. IEEE 802.11, Wireless LAN Medium Access Control (MAC) and Physical Layer (PHY) Specifications, IEEE Computer Society Std., June 2007. <http://standards.ieee.org/getieee802/download/802.11-2007.pdf>

# Performance Evaluation of a Vegetable Recognition System Using Caffe and Chainer

Makoto Ikeda<sup>1</sup>(✉), Yuki Sakai<sup>2</sup>, Tetsuya Oda<sup>3</sup>, and Leonard Barolli<sup>1</sup>

<sup>1</sup> Department of Information and Communication Engineering, Fukuoka Institute of Technology, 3-30-1 Wajiro-higashi, Higashi-ku, Fukuoka 811-0295, Japan  
makoto.ikd@acm.org, barolli@fit.ac.jp

<sup>2</sup> Graduate School of Engineering, Fukuoka Institute of Technology, 3-30-1 Wajiro-higashi, Higashi-ku, Fukuoka 811-0295, Japan  
mgm15004@bene.fit.ac.jp

<sup>3</sup> Department of Information and Computer Engineering, Okayama University of Science, 1-1 Ridai-cho, Kita-ku, Okayama 700-0005, Japan  
oda@ice.ous.ac.jp

**Abstract.** Deep neural network has a deep hierarchy that connect multiple internal layers for feature detection and recognition learning. In our previous work, we proposed a vegetable recognition system which was based on Caffe framework. In this paper, we evaluate the performance of learning accuracy and loss for vegetable category recognition system which is based on Caffe and Chainer frameworks. We evaluate the performance of recognition rate for different categories of vegetables with different pixel sizes.

**Keywords:** Deep neural network · Vegetable recognition · Caffe · Chainer

## 1 Introduction

In recent years, machine learning has driven advances within many technology in an effort to modernize and develop a more intelligent and reliable-based information system [26, 27]. It has been rapidly bringing technological changes in our daily lives to improve our life and be more comfortable [8, 18, 28].

iOS 10 considers intelligent suggestions system based on deep learning using current location, calendar availability, contact information, recent addresses, and more. *Siri* will quickly grow into the role of an AI or a bot. Technologies to detect a specific object in images are expected to further expand to wide range of applications [3, 5, 7, 11, 15, 19, 25, 30].

In [22], we proposed a vegetable category recognition system considering Deep Neural Network (DNN). The image data used for Caffe framework was set to eight kinds of vegetables. For evaluation, three different learning iterations were used.

In [21], we proposed a *VegeShop* tool, which is mobile application to sell and buy the vegetables for seller and buyer. It provides dynamic detection of camera

features and controls. We implemented VegeShop also in website. Buyer uses VegeShop tool or VegeShop website to purchase vegetables. The user interface serves as e-commerce system for sellers and buyers in Android mobile device. The system can be accessed ubiquitously from anywhere. Moreover, our system can be applied also for other category recognition.

In this paper, we evaluate the performance of learning accuracy and loss for vegetable category recognition system which is based on Caffe and Chainer frameworks. Moreover, we evaluate the performance of recognition rate for different categories of vegetables with different pixel sizes.

The structure of the paper is as follows. In Sect. 2, Neural Networks are introduced. The proposed system design is shown in Sect. 3. In Sect. 4, we show the evaluation results. Finally, conclusions and future work are given in Sect. 5.

## 2 Neural Networks

Brain is a collection of a large number of nerve cells called neurons. Neurons receive signals through synapses located on the dendrites or membrane of the neuron. When the signals received are strong enough, the neuron is activated and emits a signal through the axon. The learning and identification of pattern are determined by the intensity of signal changes.

The complexity of real neurons is highly abstracted, but Artificial Neural Network (ANN) [12, 23, 29] has a biologically-inspired programming paradigm, which enables a computer to learn from observational data [6, 10]. The models inspired by ANN are Convolutional Neural Network (CNN), recurrent neural network, deep belief network and deep boltzmann machine.

### 2.1 Deep Neural Network (DNN)

Deep Learning also called DNN has a deep hierarchy that connect multiple internal layers for feature detection and representation learning. Representation learning is to learn how to express the extracting essential information from observation data in the real world. Feature extraction so far needs trial and error by artificially operations, however, Deep Learning uses a pixel level of the image as input value, and acquire the characteristic that is most suitable by learning, and identify it [9, 16]. The simplest kind of neural network is a single-layer perceptron network, which consists of a single layer of output, the inputs are fed directly to the outputs. In this way it can be considered the simplest kind of feed-forward network. It has become easy to learn by adopting the back propagation in a multi-layer neural network. In this work, we use CNN to recognize vegetable category.

### 2.2 Convolutional Neural Network (CNN)

Learning method in a CNN uses the back propagation model like an conventional multi-layer perceptron. Then, in order to update the weighting filter and coupling



coefficient, CNN uses stochastic gradient descent. In this way, CNN recognize the optimized feature by using the convolutional and pooling operations [14, 17, 20, 24]. For the task of category recognition, Rectified Linear Units (ReLU) is used in CNN to speed up training.

CNN has been successfully applied to object recognition. The network consists of a set of layers each of which contains one or more planes. Each unit in a plane receives input from a small neighborhood in the planes of the previous layer.

### 3 Vegetable Recognition System

The structure of our proposed object detection and tracking system is shown in Fig. 1. The image processing part of the system runs on Ubuntu Linux (CPU: Intel Core i3 3.3 GHz, GPU: GeForce GTX1060 6 GB, RAM: 12 GB) equipped with Caffe and Chainer.

Caffe is a deep learning framework made with expression, speed, and modularity in mind. It is developed by the Berkeley Vision and Learning Center (BVLC), as well as community contributors and is popular for computer vision [13]. It is easy to compose models from existing layers, but relatively difficult to add new layers or optimizers [4].

Chainer is a flexible framework for neural networks. Most existing deep learning frameworks are based on the define-and-run scheme. Since the network is statically defined before any forward/backward computation, all the logic must be embedded into the network architecture as data. Chainer stores the history of computation instead of programming logic. This strategy enables us to fully leverage the power of programming logic in Python [2].

Monitoring system is composed of sensors and wireless camera. These devices are connected with Raspberry Pi. In addition, proposed VegeShop tool [21] provides the monitoring function. The monitoring system runs Linux Raspbian [1] with kernel 2.6. All experiments have been performed in indoor environment, within our departmental floor of size roughly 20 m.

Based on object detection characteristics and challenges, we consider the recognition ratio which is computed by the Caffe and Chainer frameworks.

For seller and buyer, we proposed a VegeShop tool, which is mobile application to sell and buy the vegetables [21]. It provides dynamic detection of camera features and controls. The image data store in cloud storage (dropbox). We can manage the files from any Android mobile devices or computer that are connected to the Internet. Using our system after recognition procedure, we see a list of vegetables in Android mobile device. In this way, seller can easily selects the vegetable name, price and other details using the mobile application. Finally, VegeShop tool uploads the data of vegetable on database of our system.

### 4 Evaluation Results

Here, we evaluate the performance of learning accuracy and loss by Caffe and Chainer frameworks. The loss shows the number of errors that the system did

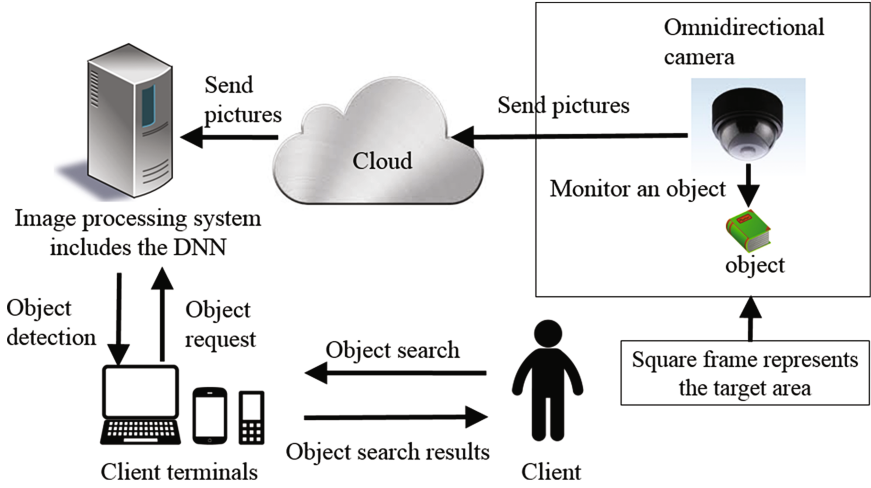


Fig. 1. Enhanced object detection and tracking system.

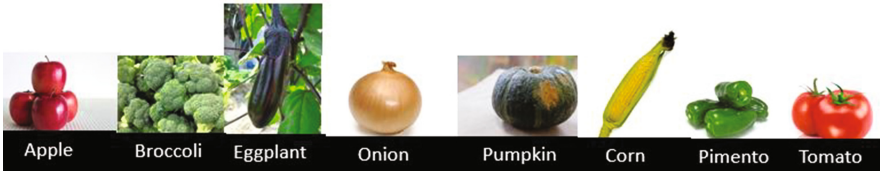


Fig. 2. Vegetables use for testing.

not recognize the vegetables. The number of learning iterations are 4,500 (fixed). For the evaluation, we used image data of eight categories of vegetables (see Fig. 2). We prepared totally 7,200 image data (nine hundreds image data for each vegetable) for different pixel sizes  $32 \times 32$  or  $256 \times 256$ .

While for evaluating the performance of recognition rate by different DNN frameworks, we used totally eighty image data (ten image data for each vegetable).

In Figs. 3 and 4 are shown the results of learning accuracy and loss for different DNN frameworks. From these results, we observed that the results of Caffe are higher than Chainer. For both DNN frameworks, when pixel sizes is  $256 \times 256$ , the results of accuracy is increased rapidly with the increase of iterations.

In Fig. 5(a) are shown the results of recognition rates for different vegetables. We observed that the results of tomato are low compared with other vegetables. Moreover, we noticed that the difference of performance is big, even if when pixel size is  $256 \times 256$ . For five categories of vegetables, when pixel sizes is  $256 \times 256$  with Caffe framework, the results of recognition rate are higher than other cases.

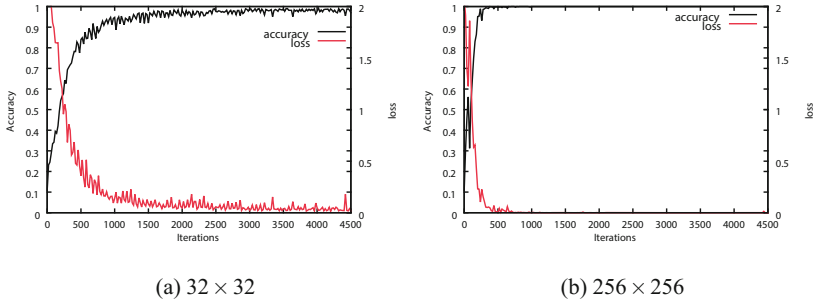


**Fig. 3.** Results of accuracy and loss for Caffe framework.

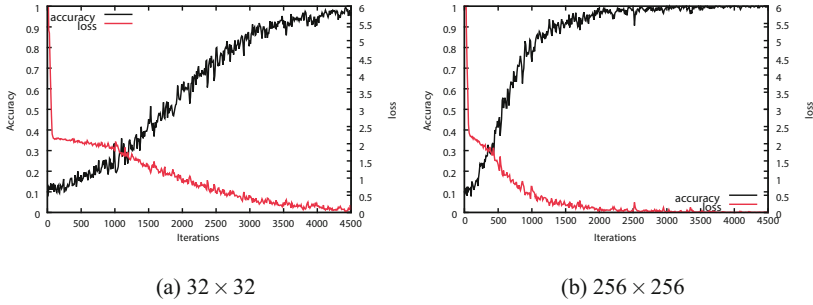


**Fig. 4.** Results of accuracy and loss for Chainer framework.

In Fig. 5(b) are shown the results of mean recognition rate considering different pixel sizes for each DNN framework. For Caffe framework, we observed that the difference of the performance is big.

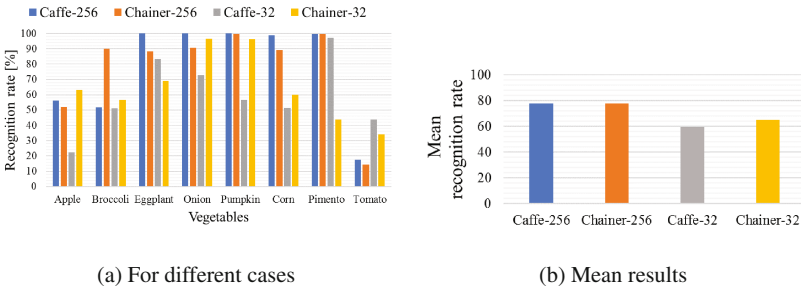


**Fig. 5.** Results of recognition rates.

## 5 Conclusions

In this paper, we evaluated the performance of learning accuracy and loss for vegetable category recognition system which is based on Caffe and Chainer frameworks. Moreover, we evaluated the performance of recognition rate for different categories of vegetables with different pixel sizes. In the future work, we would like to improve the proposed system to recognize vegetables with similar colors and patterns.

## References

1. Raspbian website. <https://www.raspbian.org/>
2. Chainer - a flexible framework of neural networks (2015). <http://docs.chainer.org/en/stable/index.html>
3. Aapo, H.: Fast and robust fixed-point algorithms for independent component analysis. *IEEE Trans. Neural Netw.* **10**(3), 626–634 (1999)
4. Abadi, M., Barham, P., Chen, J., Chen, Z., Davis, A., Dean, J., et. al.: TensorFlow: A system for large-scale machine learning. In: 12th USENIX Symposium on Operating Systems Design and Implementation (OSDI-2016), pp. 265–283, November 2016
5. Azad, P., Asfour, T., Dillmann, R.: Combining harris interest points and the sift descriptor for fast scale-invariant object recognition. In: Proceeding of the IEEE/RSJ International Conference on Intelligent Robots and Systems (IROS-2009), pp. 4275–4280, October 2009
6. Cun, Y.L.: Generalization and network design strategies. Technical Report CRG-TR-89-4, Department of Computer Science, University of Toronto, June 1989
7. Fujiyoshi, H.: Gradient-based feature extraction: Sift and hog. Technical report, IEICE, August 2007
8. Gentile, A., Santangelo, A., Sorce, S., Vitabile, S.: Human-to-human interfaces: emerging trends and challenges. *Int. J. Space-Based Situated Comput.* **1**(1), 3–17 (2011)
9. Hinton, G.E., Osindero, S., Teh, Y.W.: A fast learning algorithm for deep belief nets. *Neural Comput.* **18**(7), 1527–1554 (2006)
10. Hinton, G.E., Salakhutdinov, R.: Reducing the dimensionality of data with neural networks. *Science* **313**(5786), 504–507 (2006)
11. Huang, L.J., Liu, Q.H., Tang, J., Li, P.: Scratch line detection and restoration based on sobel operator. *Int. J. Grid Util. Comput.* **6**(2), 67–73 (2015)
12. Jain, A.K., Mao, J., Mohiuddin, K.M.: Artificial neural networks: a tutorial. *Computer* **29**(3), 31–44 (1996)
13. Jia, Y., Shelhamer, E., Donahue, J., Karayev, S., Long, J., Girshick, R., Guadarrama, S., Darrell, T.: Caffe: Convolutional architecture for fast feature embedding (2014). arXiv preprint [arXiv:1408.5093](https://arxiv.org/abs/1408.5093)
14. Kang, L., Kumar, J., Ye, P., Li, Y., Doermann, D.: Convolutional neural networks for document image classification. In: Proceedings of 22nd International Conference on Pattern Recognition 2014 (ICPR-2014), pp. 3168–3172, August 2014
15. Karahan, S., Karaoz, A., Ozdemir, O.F., Gul, A.G., Uludag, U.: On identification from periocular region utilizing sift and surf. In: Proceedings of the 22-nd European Signal Processing Conference (EUSIPCO-2014), pp. 1392–1396, September 2014

16. Le, Q.V.: Building high-level features using large scale unsupervised learning. In: Proceedings of IEEE International Conference on Acoustics, Speech and Signal Processing 2013 (ICASSP-2013), pp. 8595–8598, May 2013
17. Lee, H., Grosse, R., Ranganath, R., Ng, A.Y.: Convolutional deep belief networks for scalable unsupervised learning of hierarchical representations. In: Proceedings of the 26th Annual International Conference on Machine Learning, pp. 609–616, June 2009
18. Moore, P., Thomas, A., Tadros, G., Xhafa, F., Barolli, L.: Detection of the onset of agitation in patients with dementia: real-time monitoring and the application of big-data solutions. *Int. J. Space-Based Situated Comput.* **3**(3), 136–154 (2013)
19. Nakano, T., Kida, T.: Two dimensional pattern matching for jpeg images. Technical report, IEICE, December 2008
20. Sainath, T.N., Kingsbury, B., Mohamed, A.R., Dahl, G.E., Saon, G., Soltau, H., Beran, T., Aravkin, A.Y., Ramabhadran, B.: Improvements to deep convolutional neural networks for LVCSR. In: Proceedings of IEEE Workshop on Automatic Speech Recognition and Understanding 2013 (ASRU-2013), pp. 315–320, December 2013
21. Sakai, Y., Oda, T., Ikeda, M., Barolli, L.: VegeShop Tool: A tool for vegetable recognition using DNN. In: Proceedings of the 11th International Conference on Broad-Band Wireless Computing, Communication and Applications (BWCCA-2016), pp. 683–691, November 2016
22. Sakai, Y., Oda, T., Ikeda, M., Barolli, L.: A vegetable category recognition system using deep neural network. In: Proceedings of the 10th International Conference on Innovative Mobile and Internet Services in Ubiquitous Computing (IMIS-2016), PP. 189–192, July 2016
23. Sikora, R., Sikora, J., Cardelli, E., Chady, T.: Artificial neural network application for material evaluation by electromagnetic methods. In: Proceedings of International Joint Conference on Neural Networks (IJCNN-1999), vol. 6, pp. 4027–4032, July 1999
24. Takaki, S., Yamagishi, J.: Deep auto-encoder based low-dimensional feature extraction using FFT spectral envelopes in statistical parametric speech synthesis. IEICE Technical Report 2015-SLP-109(18), 1–6, November 2015
25. Tola, E., Lepetit, V., Fua, P.: A fast local descriptor for dense matching. In: Proceedings of the IEEE Conference on Computer Vision and Pattern Recognition (CVPR-2008), pp. 1–8, June 2008
26. Tsugawa, S., Ohsaki, H.: Community structure and interaction locality in social networks. *IPSJ J.* **56**(6) (2015)
27. Ueda, K., Tamai, M., Yasumoto, K.: A system for daily living activities recognition based on multiple sensing data in a smart home. In: Proceedings of the Multimedia, Distributed, Cooperative, and Mobile Symposium (DICOMO-2014), pp. 1884–1891, July 2014
28. Ueki, M.: Human-centric computing to effort. *Transactions of the Japan Society of Mechanical Engineers* (2013)
29. Uhrig, R.E.: Introduction to artificial neural networks. In: Proceedings of the IEEE 21st International Conference on Industrial Electronics, Control, and Instrumentation (IECON-1995), vol. 1, pp. 33–37, November 1995
30. Uijlings, J.R.R., Smeulders, A.W.M., Scha, R.J.H.: Real-time visual concept classification. *IEEE Trans. Multimedia* **12**(7), 665–681 (2010)

# Energy-Efficient Quorum Selection Algorithm for Distributed Object-Based Systems

Tomoya Enokido<sup>1</sup>(✉), Dilawaer Duolikun<sup>2</sup>, and Makoto Takizawa<sup>2</sup>

<sup>1</sup> Faculty of Business Administration, Ritssho University, Tokyo, Japan  
eno@ris.ac.jp

<sup>2</sup> Department of Advanced Sciences, Faculty of Science and Engineering,  
Hosei University, Tokyo, Japan  
dilewerdolkun@gmail.com, makoto.takizawa@computer.org

**Abstract.** Distributed applications are composed of multiple objects and each object is replicated in order to increase reliability, availability, and performance. On the other hand, the larger amount of electric energy is consumed in a system since multiple replicas of each object are manipulated on multiple servers. In this paper, the energy efficient quorum selection (EEQS) algorithm is proposed to construct a quorum for each method issued by a transaction in the quorum based locking protocol so that the total electric energy consumption of servers to perform methods can be reduced. We show the total energy consumption of servers, the average execution time of each transaction, and the number of aborted transactions can be reduced in the EEQS algorithm compared with the random algorithm in the evaluation.

**Keywords:** Energy-aware information systems · Quorum-based locking protocol · Object-based systems · EEQS algorithm · Data management

## 1 Introduction

In object-based systems [1,5], applications manipulate objects distributed on multiple servers. Each object is a unit of computation resource like a file and is an encapsulation of data and methods to manipulate the data in the object. A transaction is an atomic sequence of methods [3] to manipulate objects. A collection of conflicting transactions are required to be serializable [4] to keep objects consistent. In order to provide reliable application services [2], each object is replicated on multiple servers. Replicas of each object have to be mutually consistent. In the two-phase locking (2PL) protocol [3], one of the replicas of an object for a *read* method and all the replicas for a *write* method are locked before manipulating the object to keep the replicas mutually consistent, i.e. *read-one-write-all* scheme. However, the 2PL protocol is not efficient in write-dominated application, since all the replicas have to be locked for every write method. On the other hand, numbers  $nQ^r$  and  $nQ^w$  of replicas of an object are locked in the quorum-based protocol [5,6] for *read* and *write* methods, respectively.

Subsets of replicas locked for read and write methods are referred to as *read* and *write quorums*, respectively. The quorum numbers  $nQ^r$  and  $nQ^w$  have to be “ $nQ^r + nQ^w > N$ ” where  $N$  is the total number of replicas. Here, the more number of write methods are issued, the smaller number of write quorum can be taken. As a result, the overhead to perform write methods can be reduced. On the other hand, since methods issued to each object are performed on multiple replicas, the total amount of electric energy consumed in a system is larger than non-replication systems. It is critical to not only realize the fault-tolerant application service but also reduce the total energy consumption of an object-based system as discuss in the Green computing [7, 8].

In this paper, an *energy efficient quorum selection (EEQS)* algorithm is proposed to construct a quorum for each method issued by a transaction in the quorum based locking protocol so that the total electric energy consumption of servers to perform methods can be reduced. We evaluate the EEQS algorithm in terms of the total energy consumption of servers, the average execution time of each transaction, and the number of aborted transactions compared with the random algorithm. The evaluation results show the total energy consumption of servers, the average execution time of each transaction, and the number of aborted transactions in the EEQS algorithm can be maximumly reduced to 31%, 40%, and 65% of the random algorithm, respectively.

In Sect. 2, we discuss the data access model and power consumption model of a server. In Sect. 3, we discuss the EEQS algorithm. In Sect. 4, we evaluate the EEQS algorithm compared with random algorithm.

## 2 System Model

### 2.1 Objects and Transactions

A system is composed of multiple servers  $s_1, \dots, s_n$  ( $n \geq 1$ ) interconnected in reliable networks. That is, messages can be delivered to their destinations in the sending order and without message loss. Let  $S$  be a cluster of servers  $s_1, \dots, s_n$  ( $n \geq 1$ ). Let  $O$  be a set of objects  $o_1, \dots, o_m$  ( $m \geq 1$ ) [1]. Each object  $o_h$  is a unit of computation resource like a file and is an encapsulation of data and methods to manipulate the data in the object  $o_h$ . In this paper, we assume each object  $o_h$  supports *read* ( $r$ ) and *write* ( $w$ ) methods for manipulating data in the object  $o_h$ . Let  $op(o_h)$  be a state obtained by performing a method  $op$  ( $\in \{r, w\}$ ) on an object  $o_h$ . A pair of methods  $op_1$  and  $op_2$  on an object  $o_h$  are *compatible* if and only if (iff)  $op_1 \circ op_2(o_h) = op_2 \circ op_1(o_h)$ . Otherwise, a method  $op_1$  *conflicts* with another method  $op_2$ . For example, a pair of read methods  $r_1$  and  $r_2$  are compatible on an object  $o_h$ . On the other hand, a write method conflicts with read and write methods on an object  $o_h$ .

Each object  $o_h$  is replicated on multiple servers to make the system more reliable and available. Let  $R(o_h)$  be a set of replicas  $o_h^1, \dots, o_h^l$  ( $l \geq 1$ ) [2] of an object  $o_h$ . Let  $nR(o_h)$  be the total number of replicas of an object  $o_h$ , i.e.  $nR(o_h) = |R(o_h)|$ . Replicas of each object  $o_h$  are distributed on multiple servers in a server cluster  $S$ . Let  $S_h$  be a subset of servers which hold a replica of an object

$o_h$  in a server cluster  $S$  ( $S_h \subseteq S$ ). For example, a server cluster  $S$  is composed of five servers  $s_1, \dots, s_5$  as shown in Fig. 1. There are three objects  $o_1, o_2$ , and  $o_3$ . There are three replicas of each object  $o_h$ , i.e.  $nR(o_h) = 3$  ( $h = 1, \dots, 3$ ). Here,  $S_1 = \{s_1, s_2, s_5\}$  since replicas  $o_1^1, o_1^2$ , and  $o_1^3$  of the object  $o_1$  are stored in the servers  $s_1, s_2$ , and  $s_5$ .

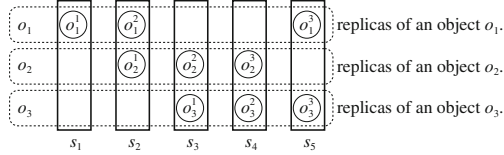


**Fig. 1.** A server cluster  $S$  and objects.

A *transaction* is an atomic sequence of methods [3]. A transaction  $T_i$  is initiated in a client  $cl_i$  and issues  $r$  and  $w$  methods to manipulate replicas of objects. Multiple conflicting transactions are required to be *serializable* [3,4] to keep object mutually consistent. Let  $\mathbf{T}$  be a set of  $\{T_1, \dots, T_k\}$  ( $k \geq 1$ ) of transactions. Let  $H$  be a schedule of the transactions in  $\mathbf{T}$ , i.e. a sequence of methods performed in  $\mathbf{T}$ . A transaction  $T_i$  *precedes* another transaction  $T_j$  ( $T_i \rightarrow_H T_j$ ) in a schedule  $H$  iff a method  $op_i$  from the transaction  $T_i$  is performed before a method  $op_j$  from the transaction  $T_j$  and  $op_i$  conflicts with  $op_j$ . A schedule  $H$  is serializable iff the precedent relation  $\rightarrow_H$  is acyclic.

## 2.2 Quorum-Based Locking Protocol

In this paper, multiple conflicting transactions are serialized by using the *quorum-based locking* protocol [5,6]. Let  $Q_h^{op}$  ( $op \in \{r, w\}$ ) be a subset of replicas of an object  $o_h$  to be locked by a method  $op$ , named a *quorum* of the method  $op$  on the object  $o_h$  ( $Q_h^{op} \subseteq R(o_h)$ ). Let  $nQ_h^{op}$  be the *quorum number* of a method  $op$  on a object  $o_h$ , i.e.  $nQ_h^{op} = |Q_h^{op}|$ . The quorums have to satisfy the following constraints: (1)  $Q_h^r \subseteq R(o_h)$ ,  $Q_h^w \subseteq R(o_h)$ , and  $Q_h^r \cup Q_h^w = R(o_h)$ . (2)  $nQ_h^r + nQ_h^w > nR(o_h)$ , i.e.  $Q_h^r \cap Q_h^w \neq \phi$ . (3)  $nQ_h^w > nR(o_h)/2$ . Let  $\mu(op)$  be a *lock mode* of a method  $op$  ( $\in \{r, w\}$ ). If  $op_1$  is compatible with  $op_2$  on an object  $o_h$ , the lock mode  $\mu(op_1)$  is compatible with  $\mu(op_2)$ . Otherwise, a lock mode  $\mu(op_1)$  conflicts with another lock mode  $\mu(op_2)$ .

A transaction  $T_i$  locks replicas of an object  $o_h$  by using the following quorum-based locking protocol [5] before manipulating the replicas with a method  $op$ .

### [Quorum-based locking protocol]

1. A quorum  $Q_h^{op}$  for a method  $op$  is constructed by selecting  $nQ_h^{op}$  replicas in a set  $R(o_h)$  of replicas.
2. If every replica in a quorum  $Q_h^{op}$  can be locked by a lock mode  $\mu(op)$ , the replicas in the quorum  $Q_h^{op}$  are manipulated by the method  $op$ .



3. When the transaction  $T_i$  commits or aborts, the locks on the replicas in the quorum  $Q_h^{op}$  are released.

Each replica  $o_h^q$  has a *version number*  $v_h^q$ . Suppose a transaction  $T_i$  reads an object  $o_h$ . The transaction  $T_i$  selects  $nQ_h^r$  replicas in the set  $R(o_h)$ , i.e. *read* ( $r$ ) quorum  $Q_h^r$ . If every replica in the  $r$ -quorum  $Q_h^r$  can be locked by a lock mode  $\mu(r)$ , the transaction  $T_i$  reads data in a replica  $o_h^q$  whose version number  $v_h^q$  is the maximum in the  $r$ -quorum  $Q_h^r$ . Every  $r$ -quorum surely includes at least one newest replica since  $nQ_h^r + nQ_h^w > nR(o_h)$ . Next, suppose a transaction  $T_i$  writes data in an object  $o_h$ . The transaction  $T_i$  selects  $nQ_h^w$  replicas in the set  $R(o_h)$ , i.e. *write* ( $w$ ) quorum  $Q_h^w$ . If every replica in the  $w$ -quorum  $Q_h^w$  can be locked by a lock mode  $\mu(w)$ , the transaction  $T_i$  writes data in a replica  $o_h^q$  whose version number  $v_h^q$  is maximum in the  $w$ -quorum  $Q_h^w$  and the version number  $v_h^q$  of the replica  $o_h^q$  is incremented by one. The updated data and version number  $v_h^q$  of the replica  $o_h^q$  are sent to every other replica in the  $w$ -quorum  $Q_h^w$ . Then, data and version number of each replica in the  $w$ -quorum  $Q_h^w$  are replaced with the newest values. When a transaction  $T_i$  commits or aborts, the locks on every replica in a quorum  $Q_h^{op}$  ( $op \in \{r, w\}$ ) are released.

### 2.3 Data Access Model

Methods which are being performed and already terminate are *current* and *previous* at time  $\tau$ , respectively. Let  $RP_t(\tau)$  and  $WP_t(\tau)$  be sets of current *read* ( $r$ ) and *write* ( $w$ ) methods on a server  $s_t$  at time  $\tau$ , respectively. Let  $P_t(\tau)$  be a set of current  $r$  and  $w$  methods on a server  $s_t$  at time  $\tau$ , i.e.  $P_t(\tau) = RP_t(\tau) \cup WP_t(\tau)$ . Let  $r_{ti}(o_h^q)$  and  $w_{ti}(o_h^q)$  be methods issued by a transaction  $T_i$  to read and write data in a replica  $o_h^q$  on a server  $s_t$ , respectively. By each method  $r_{ti}(o_h^q)$  in a set  $RP_t(\tau)$ , data is read in a replica  $o_h^q$  at rate  $RR_{ti}(\tau)$  [B/sec] at time  $\tau$ . By each method  $w_{ti}(o_h^q)$  in a set  $WP_t(\tau)$ , data is written in a replica  $o_h^q$  at rate  $WR_{ti}(\tau)$  [B/sec] at time  $\tau$ . Let  $maxRR_t$  and  $maxWR_t$  be the maximum read and write rates [B/sec] of  $r$  and  $w$  methods on a server  $s_t$ , respectively. The read rate  $RR_{ti}(\tau) (\leq maxRR_t)$  and write rate  $WR_{ti}(\tau) (\leq maxWR_t)$  are given as follows:

$$RR_{ti}(\tau) = fr_t(\tau) \cdot maxRR_t. \quad WR_{ti}(\tau) = fw_t(\tau) \cdot maxWR_t. \quad (1)$$

Here,  $fr_t(\tau)$  and  $fw_t(\tau)$  are degradation ratios.  $0 \leq fr_t(\tau) \leq 1$  and  $0 \leq fw_t(\tau) \leq 1$ . The degradation ratios  $fr_t(\tau)$  and  $fw_t(\tau)$  are given as follows:

$$fr_t(\tau) = \frac{1}{|RP_t(\tau)| + rw_t \cdot |WP_t(\tau)|}. \quad fw_t(\tau) = \frac{1}{wr_t \cdot |RP_t(\tau)| + |WP_t(\tau)|}. \quad (2)$$

Here,  $0 \leq rw_t \leq 1$  and  $0 \leq wr_t \leq 1$ .

The *read laxity*  $lr_{ti}(\tau)$  [B] and *write laxity*  $lw_{ti}(\tau)$  [B] of methods  $r_{ti}(o_h^q)$  and  $w_{ti}(o_h^q)$  show how much amount of data are read and written in a replica  $o_h^q$  by the methods  $r_{ti}(o_h^q)$  and  $w_{ti}(o_h^q)$  at time  $\tau$ , respectively. Suppose that methods  $r_{ti}(o_h^q)$  and  $w_{ti}(o_h^q)$  start on a server  $s_t$  at time  $st_{ti}$ , respectively. At time  $st_{ti}$ ,

the read laxity  $lr_{ti}(\tau) = rb_h^q [B]$  where  $rb_h^q$  is the size of data in a replica  $o_h^q$ . The write laxity  $lw_{ti}(\tau) = wb_h^q [B]$  where  $wb_h^q$  is the size of data to be written in a replica  $o_h^q$ . The read laxity  $lr_{ti}(\tau)$  and write laxity  $lw_{ti}(\tau)$  at time  $\tau$  are given as  $lr_{ti}(\tau) = rb_h^q - \sum_{\tau=st_{ti}}^{\tau} RR_{ti}(\tau)$  and  $lw_{ti}(\tau) = wb_h^q - \sum_{\tau=st_{ti}}^{\tau} WR_{ti}(\tau)$ , respectively.

## 2.4 Power Consumption Model of a Server

Let  $E_t(\tau)$  be the electric power [W] of a server  $s_t$  at time  $\tau$ .  $maxE_t$  and  $minE_t$  show the maximum and minimum electric power [W] of the server  $s_t$ , respectively. The *power consumption model for a storage server (PCS model)* [7] to perform storage and computation process are proposed. In this paper, we assume only  $r$  and  $w$  methods are performed on a server  $s_t$ . According to the PCS model, the electric power  $E_t(\tau)$  [W] of a server  $s_t$  to perform multiple  $r$  and  $w$  methods at time  $\tau$  is given as follows:

$$E_t(\tau) = \begin{cases} WE_t & \text{if } |WP_t(\tau)| \geq 1 \text{ and } |RP_t(\tau)| = 0. \\ WRE_t(\alpha) & \text{if } |WP_t(\tau)| \geq 1 \text{ and } |RP_t(\tau)| \geq 1. \\ RE_t & \text{if } |WP_t(\tau)| = 0 \text{ and } |RP_t(\tau)| \geq 1. \\ minE_t & \text{if } |WP_t(\tau)| = |RP_t(\tau)| = 0. \end{cases} \quad (3)$$

A server  $s_t$  consumes the minimum electric power  $minE_t$  [W] if no method is performed on the server  $s_t$ , i.e. the electric power in the idle state of the server  $s_t$ . The server  $s_t$  consumes the electric power  $RE_t$  [W] if  $|WP_t(\tau)| = 0$  and  $|RP_t(\tau)| \geq 1$ , i.e. only and at least one  $r$  method is performed on the server  $s_t$ . The server  $s_t$  consumes the electric power  $WE_t$  [W] if  $|WP_t(\tau)| \geq 1$  and  $|RP_t(\tau)| = 0$ , i.e. only and at least one  $w$  method is performed on the server  $s_t$ . The server  $s_t$  consumes the electric power  $WRE_t(\alpha)$  [W] =  $\alpha \cdot RE_t + (1 - \alpha) \cdot WE_t$  [W] where  $\alpha = |RP_t(\tau)| / (|RP_t(\tau)| + |WP_t(\tau)|)$  if  $|WP_t(\tau)| \geq 1$  and  $|RP_t(\tau)| \geq 1$ , i.e. both at least one  $r$  method and at least one  $w$  method are concurrently performed. Here,  $minE_t \leq RE_t \leq WRE_t(\alpha) \leq WE_t \leq maxE_t$ .

The total energy consumption  $TE_t(\tau_1, \tau_2)$  [J] of a server  $s_t$  from time  $\tau_1$  to  $\tau_2$  is  $\sum_{\tau=\tau_1}^{\tau_2} E_t(\tau)$ . The processing power  $PE_t(\tau)$  [W] of a server  $s_t$  at time  $\tau$  is  $E_t(\tau) - minE_t$ . The total processing energy consumption  $TPE_t(\tau_1, \tau_2)$  of a server  $s_t$  from time  $\tau_1$  to  $\tau_2$  is given as  $TPE_t(\tau_1, \tau_2) = \sum_{\tau=\tau_1}^{\tau_2} PE_t(\tau)$ . The total processing energy consumption laxity  $tpecl_t(\tau)$  shows how much electric energy a server  $s_t$  has to consume to perform every current  $r$  and  $w$  methods on the server  $s_t$  at time  $\tau$ . The total processing energy consumption laxity  $tpecl_t(\tau)$  of a server  $s_t$  at time  $\tau$  is obtained by the following **TPECL** <sub>$t$</sub>  procedure:

```

TPECL $t$ ( $\tau$ ) {
  if  $RP_t(\tau) = \phi$  and  $WP_t(\tau) = \phi$ , return(0);
  laxity =  $E_t(\tau) - minE_t$ ; /*  $PE_t(\tau)$  of a server  $s_t$  at time  $\tau$  */
  for each  $r$ -method  $r_{ti}(o_h^q)$  in  $RP_t(\tau)$ , {
     $lr_{ti}(\tau + 1) = lr_{ti}(\tau) - RR_{ti}$ ;
    if  $lr_{ti}(\tau + 1) = 0$ ,  $RP_t(\tau + 1) = RP_t(\tau) - \{r_{ti}(o_h^q)\}$ ;
  }
}

```

```

}
for each  $w$ -method  $w_{ti}(o_h^q)$  in  $WP_t(\tau)$ , {
   $lw_{ti}(\tau + 1) = lw_{ti}(\tau) - WR_{ti}$ ;
  if  $lw_{ti}(\tau + 1) = 0$ ,  $WP_t(\tau + 1) = WP_t(\tau) - \{w_{ti}(o_h^q)\}$ ;
}
return( $laxity + TPECL_t(\tau + 1)$ );
}

```

In the  $TPECL_t$  procedure, each time  $\tau$  data is read in a replica  $o_h^q$  by a method  $r_{ti}(o_h^q)$ , the read laxity  $lr_{ti}(\tau)$  of the method  $r_{ti}(o_h^q)$  is decremented by read rate  $RR_{ti}$ . Similarly, the write laxity  $lw_{ti}(\tau)$  of a method  $w_{ti}(o_h^q)$  is decremented by write rate  $WR_{ti}$  each time  $\tau$  data is written in a replica  $o_h^q$  by the method  $w_{ti}(o_h^q)$ . If the read laxity  $lr_{ti}(\tau + 1)$  and write laxity  $lw_{ti}(\tau + 1)$  get 0, every data is read and written in the replica  $o_h^q$  by the methods  $r_{ti}(o_h^q)$  and  $w_{ti}(o_h^q)$ , respectively, and the methods terminate at time  $\tau$ .

### 3 Quorum Selection Algorithm

We propose an *energy-efficient quorum selection (EEQS)* algorithm to select replicas to be members of a quorum of each method in the quorum-based locking protocol so that the total energy consumption of a server cluster  $S$  to perform read and write methods can be reduced. Suppose a transaction  $T_i$  issues a method  $op$  ( $op = \{r, w\}$ ) to manipulate an object  $o_h$  at time  $\tau$ . Each transaction  $T_i$  selects a subset  $S_h^{op} (\subseteq S_h)$  of  $nQ_h^{op}$  servers in a subset  $S_h$  by following  $EEQS$  procedure:

```

EEQS( $op, o_h, \tau$ ) { /*  $op \in \{r, w\}$  */
   $S_h^{op} = \phi$ ;
  while ( $nQ_h^{op} > 0$ ) {
    for each server  $s_t$  in  $S_h$ , {
      if  $op = r$ ,  $RP_t(\tau) = RP_t(\tau) \cup \{op\}$ ;
      else  $WP_t(\tau) = WP_t(\tau) \cup \{op\}$ ; /*  $op = w$  */
       $TPE_t(\tau) = TPECL_t(\tau)$ ;
    }
     $server =$  a server  $s_t$  where  $TPE_t(\tau)$  is the minimum;
     $S_h^{op} = S_h^{op} \cup \{server\}$ ;  $S_h = S_h - \{server\}$ ;  $nQ_h^{op} = nQ_h^{op} - 1$ ;
  }
  return( $S_h^{op}$ );
}

```

Suppose a server cluster  $S$  is composed of five servers  $s_1, \dots, s_5$  and replicas of three objects  $o_1, o_2$ , and  $o_3$  are distributed on multiple servers in the server cluster  $S$  as shown in Fig. 1, i.e.  $S_1 = \{s_1, s_2, s_5\}$ ,  $S_2 = \{s_2, s_3, s_4\}$ , and  $S_3 = \{s_3, s_4, s_5\}$ . Every server  $s_t$  ( $t = 1, \dots, 5$ ) follows the same data access model and power consumption model as shown in Table 1. The size of data in every object  $o_h$  ( $h = 1, \dots, 3$ ) is 80 [MB]. There are three replicas for each object  $o_h$ , i.e.  $nR(o_h) = 3$ . The quorum numbers  $nQ_h^w$  and  $nQ_h^r$  for every object  $o_h$  are two, i.e.  $nQ_h^w = nQ_h^r = 2$ .

**Table 1.** Homogeneous cluster  $S$ 

Server $s_t$	$maxRR_t$	$maxWR_t$	$rw_t$	$wr_t$	$minE_t$	$WE_t$	$RE_t$
$s_t$	80 [MB/sec]	45 [MB/sec]	0.5	0.5	39 [W]	53 [W]	43 [W]

At time  $\tau_0$ , a pair of replicas  $o_1^1$  and  $o_1^3$  stored in the servers  $s_1$  and  $s_5$  are being locked by a transaction  $T_1$  with a lock mode  $\mu(w)$  and a pair of write methods  $w_{11}(o_1^1)$  and  $w_{51}(o_1^3)$  are being performed on the servers  $s_1$  and  $s_5$ , respectively, as shown in Fig. 2. Let  $T_i.Q_h^{op}$  be a quorum to perform a method  $op$  issued by a transaction  $T_i$ . Let  $T_i.S_h^{op}$  be a subset of servers which hold replicas in a quorum  $T_i.Q_h^{op}$  constructed by a transaction  $T_i$ . The  $w$ -quorum  $T_1.Q_1^w$  is  $\{o_1^1, o_1^3\}$  since the quorum number  $nQ_1^w = 2$ . The subset  $T_1.S_1^w$  is  $\{s_1, s_5\}$  since a pair of replicas  $o_1^1$  and  $o_1^3$  are stored in the servers  $s_1$  and  $s_5$ , respectively. A pair of write laxities  $lw_{11}(\tau_0)$  and  $lw_{51}(\tau_0)$  are 45 [MB], respectively, at time  $\tau_0$ .

Suppose a transaction  $T_2$  issues a write method to the object  $o_3$  at time  $\tau_0$ . The size of data to be written in the object  $o_3$  by the write method issued by the transaction  $T_2$  is 45 [MB], i.e. the write laxity  $lw_{t2}(\tau_0) = 45$  [MB]. Here,  $R(o_3) = \{o_3^1, o_3^2, o_3^3\}$  and  $S_3 = \{s_3, s_4, s_5\}$  as shown in Fig. 1. First, the transaction  $T_2$  constructs a  $w$ -quorum  $T_2.Q_3^w$  by the procedure **EEQS**( $w, o_3, \tau_0$ ). Suppose a write method  $w_{32}(o_3^1)$  is issued to a replica  $o_3^1$  stored in the server  $s_3$  at time  $\tau_0$ . No method is performed on the server  $s_3$  at time  $\tau_0$ . Hence,  $WP_3(\tau_0) = WP_3(\tau_0) \cup \{w_{32}(o_3^1)\} = \{w_{32}(o_3^1)\}$ . Since only one write method  $w_{32}(o_3^1)$  is performed on the server  $s_3$  at time  $\tau_0$ , the degradation ratio  $fw_3(\tau_0)$  is  $1/(wr_3 \cdot |RP_3(\tau_0)| + |WP_3(\tau_0)|) = 1/(0.5 \cdot 0 + 1) = 1$  and the write method  $w_{32}(o_3^1)$  is performed on the server  $s_3$  at write rate  $WR_{32}(\tau_0) = fw_3(\tau_0) \cdot maxWR_3 = 1 \cdot 45 = 45$  [MB/sec]. Hence, the write laxity  $lw_{32}(\tau_1)$  gets 0 since  $lw_{32}(\tau_0) - WR_{32}(\tau_0) = 45$  [MB] - 45 [MB] = 0 at time  $\tau_1$ . Here, the write method  $w_{32}(o_3^1)$  terminates at time  $\tau_1$  and no method is performed after time  $\tau_1$ . Similarly, if a write method  $w_{42}(o_3^2)$  is issued to a replica  $o_3^2$  stored in the server  $s_4$  at time  $\tau_0$  as shown in Fig. 2, the write method  $w_{42}(o_3^2)$  terminates at time  $\tau_1$  since no method is performed on the server  $s_4$  at time  $\tau_0$ . Suppose a write method  $w_{52}(o_3^3)$  is issued to a replica  $o_3^3$  stored in the server  $s_5$  at time  $\tau_0$ . Here, a pair of write methods  $w_{51}(o_1^3)$  and  $w_{52}(o_3^3)$  are concurrently performed on the server  $s_5$  at time  $\tau_0$ , i.e.  $WP_5(\tau_0) = \{w_{51}(o_1^3), w_{52}(o_3^3)\}$  and  $|WP_5(\tau_0)| = 2$ . Here, the degradation ratio  $fw_5(\tau_0)$  is  $1/(wr_5 \cdot |RP_5(\tau_0)| + |WP_5(\tau_0)|) = 1/(0.5 \cdot 0 + 2) = 0.5$ . A pair of the write methods  $w_{51}(o_1^3)$  and  $w_{52}(o_3^3)$  are concurrently performed on the server  $s_5$  at write rate  $WR_{51}(\tau_0) = WR_{52}(\tau_0) = fw_5(\tau_0) \cdot maxWR_5 = 0.5 \cdot 45 = 22.5$  [MB/sec], respectively. Hence, the write laxity  $lw_{51}(\tau_1)$  is 22.5 [MB/sec] at time  $\tau_1$  since  $lw_{51}(\tau_0) - WR_{51}(\tau_0) = 45$  [MB] - 22.5 [MB] = 22.5 [MB]. Similarly, the write laxity  $lw_{52}(\tau_1)$  is 22.5 [MB] at time  $\tau_1$ . At time  $\tau_1$ , a pair of the write methods  $w_{51}(o_1^3)$  and  $w_{52}(o_3^3)$  are still concurrently performed on the server  $s_5$  at write rate 22.5 [MB/sec]. The write laxity  $lw_{51}(\tau_2)$  gets 0 at time  $\tau_2$  since  $lw_{51}(\tau_1) - WR_{51}(\tau_1) = 22.5$  [MB] - 22.5 [MB] = 0. Similarly, the write laxity  $lw_{52}(\tau_2)$  gets 0 at time  $\tau_1$ . Here, a pair of write methods  $w_{51}(o_1^3)$  and  $w_{52}(o_3^3)$  terminate at time  $\tau_2$ .

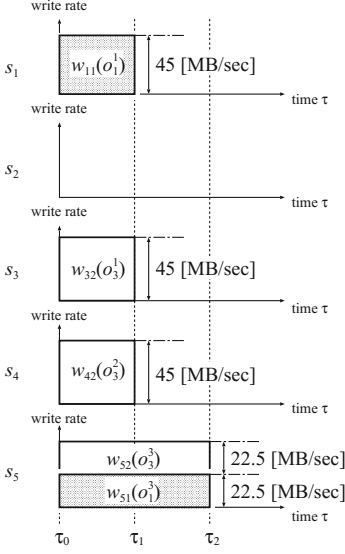


**Fig. 2.** Example of method execution.

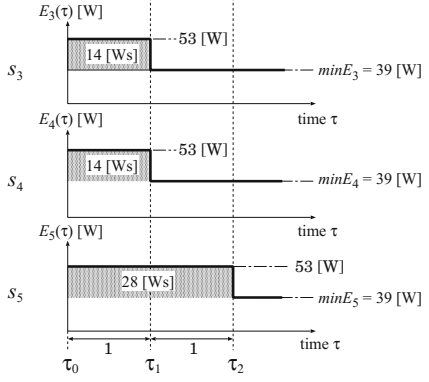


**Fig. 3.** Total processing energy consumption laxity [J].

Figure 3 shows the electric power [W] of the servers  $s_3$ ,  $s_4$ , and  $s_5$  to perform the write methods as shown in Fig. 2. The electric power  $E_t(\tau)$  [W] of a server  $s_t$  at time  $\tau$  is given in formula (3). At time  $\tau_0$  to  $\tau_1$ , only the write method  $w_{32}(o_3^1)$  is performed on the server  $s_3$ , i.e.  $|WR_3(\tau_0)| = 1$  and  $|RP_3(\tau_0)| = 0$ . Hence, the electric power consumption  $E_3(\tau_0) = WE_3 = 53$  [W]. Similarly,  $E_4(\tau_0) = WE_4 = 53$  [W] in the server  $s_4$ . In the server  $s_5$ , only a pair of write methods  $w_{51}(o_1^3)$  and  $w_{52}(o_3^3)$  are performed, i.e.  $|WR_5(\tau_0)| = 2$  and  $|RP_5(\tau_0)| = 0$ . Hence, the electric power consumption  $E_5(\tau_0) = WE_5 = 53$  [W]. The total processing power consumption  $TPE_3(\tau_0, \tau_1)$  is  $E_3(\tau_0) - \min E_3 = 53 - 39 = 14$  [W]. Similarly,  $TPE_4(\tau_0, \tau_1)$  and  $TPE_5(\tau_0, \tau_1)$  are 14 [W], respectively. At time  $\tau_1$  to  $\tau_2$ , a pair of write methods  $w_{51}(o_1^3)$  and  $w_{52}(o_3^3)$  are performed on the server  $s_5$ , i.e.  $|WR_5(\tau_1)| = 2$  and  $|RP_5(\tau_1)| = 0$ . Hence,  $E_5(\tau_1) = WE_5 = 53$  [W] and  $TPE_5(\tau_1, \tau_2) = 53 - 39 = 14$  [W].

The hatched area shows the total processing energy consumption laxity  $tpecl_t(\tau_0)$  [J] of each server  $s_t$  ( $t = \{3, 4, 5\}$ ) where the write method  $w_{t2}(o_3)$  issued by the transaction  $T_2$  is performed on the server  $s_t$  at time  $\tau_0$ . Here,  $tpecl_3(\tau_0) = TPE_3(\tau_0, \tau_1) = 14$  [J].  $tpecl_4(\tau_0) = TPE_4(\tau_0, \tau_1) = 14$  [J].  $tpecl_5(\tau_0) = TPE_5(\tau_0, \tau_1) + TPE_5(\tau_1, \tau_2) = 14 + 14 = 28$  [J]. Here, a  $w$ -quorum  $T_2.Q_3^w$  is constructed by a pair of replicas  $o_3^1$  and  $o_3^2$  stored in the servers  $s_3$  and  $s_4$  since  $nQ_3^w = 2$  and  $tpecl_3(\tau_0) = tpecl_4(\tau_0) < tpecl_5(\tau_0)$ , i.e.  $T_2.Q_3^w = \{o_3^1, o_3^2\}$  and  $T_2.S_3^w = \{s_3, s_4\}$ .

## 4 Evaluation

### 4.1 Environment

We evaluate the EEQS algorithm in terms of the total energy consumption of a server cluster  $S$ , the average execution time of each transaction, and the average number of aborted transactions compared with the random algorithm. In the random algorithm, a quorum for each method is randomly selected. In this evaluation, a homogeneous server cluster  $S$  which is composed of ten homogeneous servers  $s_1, \dots, s_{10}$  ( $n = 10$ ) is considered. In the server cluster  $S$ , every server  $s_t$  ( $t = 1, \dots, 10$ ) follows the same data access model and power consumption model as shown in Table 1. Parameters of each server  $s_t$  are given based on the experimentations [7]. There are fifty objects  $o_1, \dots, o_{50}$  in a system, i.e.  $O = \{o_1, \dots, o_{50}\}$ . The size of data in each object  $o_h$  is randomly selected between 50 and 100 [MB]. Each object  $o_h$  supports *read* ( $r$ ) and *write* ( $w$ ) methods. The total number of replicas for every object is five, i.e.  $nR(o_h) = 5$  and  $R(o_h) = \{o_h^1, \dots, o_h^5\}$  ( $h = 1, \dots, 50$ ). Replicas of each object are randomly distributed on five servers in the server cluster  $S$ . The quorum number  $nQ_h^w$  of a  $w$  method on every object  $o_h$  is three, i.e.  $nQ_h^w = 3$ . The quorum number  $nQ_h^r$  of a  $r$  method on every object  $o_h$  is three,  $nQ_h^r = 3$ .

The number  $m$  of transactions are issues to manipulate objects in a system. Each transaction issues three methods randomly selected from one-hundred methods on the fifty objects. By each  $r$  and  $w$  method issued by a transaction  $T_i$  to a replica  $o_h^q$  of an object  $o_h$ , the total amount of data of the replica  $o_h^q$  are fully read and written, respectively. The starting time of each transaction  $T_i$  is randomly selected in a unit of one second between 1 and 360 [sec].

### 4.2 Average Execution Time of Each Transaction

We evaluate the EEQS algorithm in terms of the average execution time [sec] of each transaction. Let  $ET_i$  be the execution time [sec] of a transaction  $T_i$  where the transaction  $T_i$  commits. For example, suppose a transaction  $T_i$  starts at time  $st_i$  and commits at time  $et_i$ . Here, the execution time  $ET_i$  of the transaction  $T_i$  is  $et_i - st_i$  [sec]. The execution time  $ET_i$  for each transaction  $T_i$  is measured ten times for each total number  $m$  of transactions ( $0 \leq m \leq 500$ ). Let  $ET_i^{tm}$  be the execution time  $ET_i$  obtained in  $tm$ -th simulation. The average execution time  $AET$  [sec] of each transaction for each total number  $m$  of transactions is  $\sum_{tm=1}^{10} \sum_{i=1}^m ET_i^{tm} / (m \cdot 10)$ .

Figure 4 shows the average execution time  $AET$  [sec] in the server cluster  $S$  to perform the total number  $m$  of transaction in the EEQS and random algorithms. In the EEQS and random algorithms, the average execution time  $AET$  increases as the total number  $m$  of transactions increases since more number of transactions are concurrently performed. For  $0 < m \leq 500$ , the average execution time  $AET$  can be more shorter in the EEQS algorithm than the random algorithm. This means that the data access resources in the server cluster  $S$  can be more efficiently utilized in the EEQS algorithm than the random algorithm.

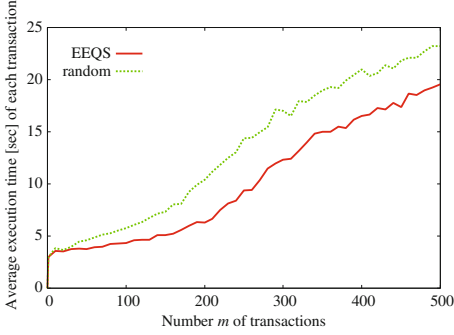


**Fig. 4.** Average execution time  $AET$  [sec] of each transaction.

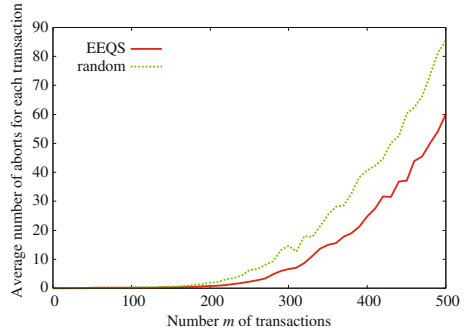


**Fig. 5.** Average number of aborts for each transaction

### 4.3 Average Number of Aborted Transaction Instances

If a transaction  $T_i$  could not lock every replica in an  $r$ -quorum  $Q_h^r$  and  $w$ -quorum  $Q_h^w$ , the transaction  $T_i$  aborts. Then, the transaction  $T_i$  is restarted after  $\delta$  time units. The time units  $\delta$  [sec] is randomly selected between twenty and thirty seconds in this evaluation. Every transaction  $T_i$  is restarted until the transaction  $T_i$  commits. Each execution of a transaction is referred to as transaction *instance*. We measure how many number of transaction instances are aborted until each transaction commits. Let  $AT_i$  be the number of aborted instances of a transaction  $T_i$ . The number of aborted instances  $AT_i$  for each transaction  $T_i$  is measured ten times for each total number  $m$  of transactions ( $0 \leq m \leq 500$ ). Let  $AT_i^{tm}$  be the number of aborted transaction instances  $AT_i$  obtained in  $tm$ th simulation. The average number of aborted instances  $AAT$  of each transaction for each total number  $m$  of transactions is  $\sum_{tm=1}^{10} \sum_{i=1}^m AT_i^{tm} / (m \cdot 10)$ .

Figure 5 shows the average number of aborted transaction instances  $AAT$  in the server cluster  $S$  to perform the total number  $m$  of transactions in the EEQS and random algorithms. In the EEQS and random algorithms, the average number of aborted transaction instances  $AAT$  increases as the total number  $m$  of transactions increases. The more number of transactions are concurrently performed, the more number of transactions cannot lock replicas. Hence, the number of aborted transactions instance increases in the EEQS and random algorithms. For  $0 < m \leq 500$ , the average number of aborted instances  $AAT$  of each transaction can be more reduced in the EEQS algorithm than the random algorithm. The data access resources in the server cluster  $S$  can be more efficiently utilized in the EEQS algorithm than the random algorithm. Hence, the average execution time of each transaction can be shorter in the EEQS algorithm than the random algorithm. As a result, the number of aborted transactions can be more reduced in the EEQS algorithm than the random algorithm since the number of transaction to be concurrently performed can be reduced.

#### 4.4 Average Total Energy Consumption of a Server Cluster

We evaluate the EEQS algorithm in terms of the average total energy consumption [J] of the homogeneous server cluster  $S$  to perform the number  $m$  of transactions. Let  $TEC_{tm}$  be the total energy consumption [J] to perform the number  $m$  of transactions ( $0 \leq m \leq 500$ ) in the server cluster  $S$  obtained in the  $tm$ -th simulation. The total energy consumption  $TEC_{tm}$  is measured ten times for each number  $m$  of transactions. Then, the average total energy consumption  $ATEC$  [J] of the server cluster  $S$  is calculated as  $\sum_{tm=1}^{10} TEC_{tm}/10$  for each number  $m$  of transactions.

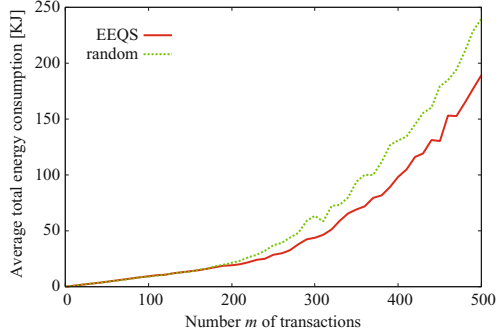


**Fig. 6.** Average total energy consumption (ATEC) [KJ].

Figure 6 shows the average total energy consumption  $ATEC$  of the server cluster  $S$  to perform the number  $m$  of transactions in the EEQS and random algorithms. In the EEQS and random algorithms, the average total energy consumption  $ATEC$  of the server cluster  $S$  increases as the number  $m$  of transactions increases. For  $0 \leq m \leq 500$ , the average total energy consumption  $ATEC$  of the server cluster  $S$  can be more reduced in the EEQS algorithm than the random algorithm. In the EEQS algorithm, each time a transaction  $T_i$  issues a method  $op \in \{r, w\}$  to an object  $o_h$ , the transaction  $T_i$  selects a subset  $nS_h^{op}$  ( $\subseteq S_h$ ) of  $nQ_h^{op}$  servers which hold a replica  $o_h^q$  of the object  $o_h$  so that the total processing energy consumption laxity of a server cluster  $S$  is the minimum. In addition, the average execution time and the number of aborted instances of each transaction can be more reduced in the EEQS algorithm than the random algorithm. As a result, the average total energy consumption  $ATEC$  of the server cluster  $S$  to perform the number  $m$  of transactions can be more reduced in the EEQS algorithm than the random algorithm.

Following the evaluation, the total energy consumption of a server cluster, the average execution time of each transaction, and the number of aborted transactions in the EEQS algorithm can be maximumly reduced to 31%, 40%, and 65% of the random algorithm, respectively. Hence, the EEQS algorithm is more useful than the random algorithm.



## 5 Concluding Remarks

In this paper, we newly proposed the EEQS algorithm to select a quorum for each method issued by a transaction in the quorum based locking protocol so that the total energy consumption of a server cluster to perform methods issued by transactions can be reduced. We evaluated the EEQS algorithm in terms of the total energy consumption of a server cluster, the average execution time of each transaction, and the number of aborted transactions compared with the random algorithm. The evaluation results show the average total energy consumption of a server cluster, the average execution time of each transaction, and the average number of aborted transaction instances can be more reduced in the EEQS algorithm than the random algorithm. Hence, the EEQS algorithm is more useful than the random algorithm.

## References

1. Object Management Group Inc.: Common object request broker architecture (CORBA) specification, version 3.3, part 1 - interfaces (2012). <http://www.omg.org/spec/CORBA/3.3/Interfaces/PDF>
2. Schneider, F.B.: Replication Management Using the State-Machine Approach. Distributed Systems. ACM Press, New York (1993)
3. Bernstein, P.A., Hadzilacos, V., Goodman, N.: Concurrency Control and Recovery in Database Systems. Addison-Wesley, Boston (1987)
4. Gray, J.N.: Notes on data base operating systems. In: Bayer, R., Graham, R.M., Seegmüller, G. (eds.) Operating Systems. LNCS, vol. 60, pp. 393–481. Springer, Heidelberg (1978)
5. Tanaka, K., Hasegawa, K., Takizawa, M.: Quorum-based replication in object-based systems. *J. Inf. Sci. Eng.* **16**(3), 317–331 (2000)
6. Garcia-Molina, H., Barbara, D.: How to assign votes in a distributed system. *J. ACM* **32**(4), 814–860 (1985)
7. Sawada, A., Kataoka, H., Duolikun, D., Enokido, T., Takizawa, M.: Energy-aware clusters of servers for storage and computation applications. In: Proceedings of the 30th IEEE International Conference on Advanced Information Networking and Applications (AINA-2016), pp. 400–407 (2016)
8. Natural Resources Defense Council (NRDC): Data center efficiency assessment - scaling up energy efficiency across the data center industry: Evaluating key drivers and barriers (2014). <http://www.nrdc.org/energy/files/data-center-efficiency-assessment-IP.pdf>

# Selection of Actor Nodes in Wireless Sensor and Actor Networks: A Fuzzy-Based System Considering Packet Error Rate as a New Parameter

Donald Elmazi<sup>1</sup>(✉), Miralda Cuka<sup>1</sup>, Tetsuya Oda<sup>2</sup>, Elis Kulla<sup>2</sup>, Makoto Ikeda<sup>3</sup>,  
and Leonard Barolli<sup>3</sup>

<sup>1</sup> Graduate School of Engineering, Fukuoka Institute of Technology (FIT),  
3-30-1 Wajiro-Higashi, Higashi-Ku, Fukuoka 811-0295, Japan  
donald.elmazi@gmail.com, mcuka91@gmail.com

<sup>2</sup> Department of Information and Computer Engineering, Okayama University  
of Science, 1-1 Ridai-cho, Kita-Ku, Okayama 700-0005, Japan  
oda.tetsuya.fit@gmail.com, kulla@ice.ous.ac.jp

<sup>3</sup> Department of Information and Communication Engineering, Fukuoka Institute  
of Technology (FIT), 3-30-1 Wajiro-Higashi, Higashi-Ku, Fukuoka 811-0295, Japan  
makoto.ikd@acm.org, barolli@fit.ac.jp

**Abstract.** In Wireless Sensor and Actor Networks (WSANs), sensors and actors collaborate together to get the information about the physical environment and perform appropriate actions. In order to provide effective sensing and acting, a distributed local coordination mechanism is necessary among sensors and actors. The degree of errors encountered during data transmission over a communication is different. The higher the error rate, the less reliable the connection or data transfer will be. In this work, we consider the actor node selection problem and propose a fuzzy-based system that based on data provided by sensors and actors selects an appropriate actor node. We use 4 input parameters. Different from our previous work, we consider also the Packet Error Rate (PER) parameter. The output parameter is Actor Selection Decision (ASD). The simulation results show that the proposed system makes a proper selection of actor nodes.

## 1 Introduction

Wireless Sensor Networks (WSNs) can be defined as a collection of wireless self-configuring programmable multi-hop tiny devices, which can bind to each other in an arbitrary manner, without the aid of any centralized administration, thereby dynamically sending the sensed data to the intended recipient about the monitored phenomenon. WSNs are comprised of multiple sensors which are connected to each other in order to perform collaborative or cooperative functions. These nodes are typically connected as a multi-hop mesh network [1–3].

Wireless Sensor and Actor Networks (WSANs), have emerged as a variation of WSNs. WSANs are capable of monitoring physical phenomena, processing sensed data, making decisions based on the sensed data and completing appropriate tasks when needed. WSAN devices deployed in the environment are sensors able to sense environmental data, actors able to react by affecting the environment or have both functions integrated [4]. For example, in the case of a fire, sensors relay the exact origin and intensity of the fire to actors so that they can extinguish it before spreading in the whole building or in a more complex scenario, to save people who may be trapped by fire [5].

Unlike WSNs, where the sensor nodes tend to communicate all the sensed data to the sink by sensor-sensor communication, in WSANs, two new communication types may take place. They are called sensor-actor and actor-actor communications. Sensed data is sent to the actors in the network through sensor-actor communication. After the actors analyse the data, they communicate with each other in order to assign and complete tasks. To provide effective operation of WSAN, it is very important that sensors and actors coordinate in what are called sensor-actor and actor-actor coordination. Coordination is not only important during task conduction, but also during network's self-improvement operations, i.e. connectivity restoration [6,7], reliable service [8], Quality of Service (QoS) [9,10] and so on.

Sensor-Actor (SA) coordination defines the way sensors communicate with actors, which actor is accessed by each sensor and which route should data packets follow to reach it. Among other challenges, when designing SA coordination, care must be taken in considering energy minimization because sensors, which have limited energy supplies, are the most active nodes in this process. On the other hand, Actor-Actor (AA) coordination helps actors to choose which actor will lead performing the task (actor selection), how many actors should perform and how they will perform. Actor selection is not a trivial task, because it needs to be solved in real time, considering different factors. It becomes more complicated when the actors are moving, due to dynamic topology of the network.

In this paper, different from our previous work [11], we propose and implement a simulation system which considers also the Packet Error Rate (PER) parameter. The system is based on fuzzy logic and considers four input parameters for actor selection. We show the simulation results for different values of parameters.

The remainder of the paper is organized as follows. In Sect. 2, we describe the basics of WSANs including research challenges and architecture. In Sect. 3, we describe the system model and its implementation. Simulation results are shown in Sect. 4. Finally, conclusions and future work are given in Sect. 5.

## 2 WSAN

### 2.1 WSAN Challenges

Some of the key challenges in WSAN are related to the presence of actors and their functionalities.

- *Deployment and Positioning*: At the moment of node deployment, algorithms must consider to optimize the number of sensors and actors and their initial positions based on applications [12, 13].
- *Architecture*: When important data has to be transmitted (an event occurred), sensors may transmit their data back to the sink, which will control the actors' tasks from distance or transmit their data to actors, which can perform actions independently from the sink node [14].
- *Real-Time*: There are a lot of applications that have strict real-time requirements. In order to fulfill them, real-time limitations must be clearly defined for each application and system [15].
- *Coordination*: In order to provide effective sensing and acting, a distributed local coordination mechanism is necessary among sensors and actors [14].
- *Power Management*: WSAAN protocols should be designed with minimized energy consumption for both sensors and actors [16].
- *Mobility*: Protocols developed for WSAANs should support the mobility of nodes [7, 17], where dynamic topology changes, unstable routes and network isolations are present.
- *Scalability*: Smart Cities are emerging fast and WSAAN, as a key technology will continue to grow together with cities. In order to keep the functionality of WSAAN applicable, scalability should be considered when designing WSAAN protocols and algorithms [13, 17].

## 2.2 WSAAN Architecture

A WSAAN is shown in Fig. 1. The main functionality of WSAANs is to make actors perform appropriate actions in the environment, based on the data sensed from sensors and actors. When important data has to be transmitted (an event occurred), sensors may transmit their data back to the sink, which will control the actors' tasks from distance, or transmit their data to actors, which can perform actions independently from the sink node. Here, the former scheme is called Semi-Automated Architecture and the latter one Fully-Automated Architecture

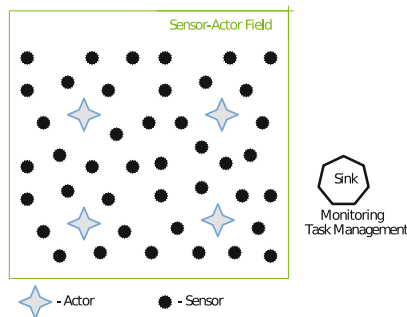


Fig. 1. Wireless sensor actor network (WSAAN).

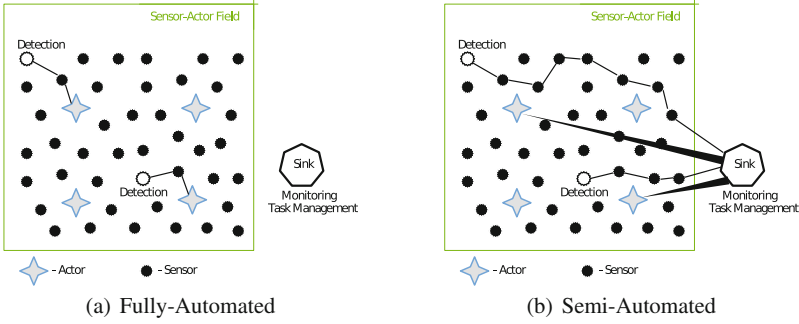


Fig. 2. WSN architectures.

(see Fig. 2). Obviously, both architectures can be used in different applications. In the Fully-Automated Architecture are needed new sophisticated algorithms in order to provide appropriate coordination between nodes of WSN. On the other hand, it has advantages, such as *low latency*, *low energy consumption*, *long network lifetime* [4], *higher local position accuracy*, *higher reliability* and so on.

### 3 Proposed System Model

#### 3.1 Problem Description

After data has been sensed from sensors, they are collected to the sink for semi-automated architecture or spread to the actors for fully-automated architecture. Then a task is assigned to actors. In general, one or more actors take responsibility and perform appropriate actions. Different actors may be chosen for acting, depending on their characteristics and conditions. For example, if an intervention is required in a building, a flying robot can go there faster and easier. While, if a kid is inside a room in fire, it is better to send a small robot. The issue here is which of the actors will be selected to respond to critical data collected from the field (actor selection).

If WSN uses semi-automated architecture, the sinks are used to collect data and control the actors. They may be supplied with detailed information about actors characteristics (size, ability etc.). If fully-automated architecture is being used, the collected data are processed only by actors, so they first have to decide whether they have the proper ability and right conditions to perform. Soon after that, actors coordinate with each-other, to decide more complicated procedures like acting multiple actors, or choosing the most appropriate one from several candidates. In this work, we propose a fuzzy-based system in order to select an appropriate actor node for a required task.

#### 3.2 System Parameters

Based on WSN characteristics and challenges, we consider the following parameters for implementation of our proposed system.

**Job Type (JT):** A sensed event may be triggered by various causes, such as when water level passed a certain height of the dam. Similarly, for solving a problem, actors need to perform actions of different types. Actions may be classified regarding time duration, complexity, working force required etc., and then assign a priority to them, which will guide actors to make their decisions. In our system, JT is defined by three levels of difficulty. The hardest the task, the more likely an actor is to be selected.

**Distance to Event (DE):** The number of actors in a WSN is smaller than the number of sensors. Thus, when an actor is called for action near an event, the distance from the actor to the event is different for different actors and events. Depending on three distance levels, our system takes decisions on the availability of the actor node.

**Remaining Energy (RE):** As actors are active in the monitored field, they perform tasks and exchange data in different ways from each other. Consequently, also based on their characteristics, some actors may have a lot of power remaining and other may have very little, when an event occurs. We consider three levels of RP for actor selection.

**Packet Error Rate (PER):** The number of packets that the nodes exchange with each other is high. The degree of errors that occurs during data transmission over a communication connection can be high or low. If the PER for an actor is low, this actor node can be selected to do the task.

**Actor Selection Decision (ASD):** Our system is able to decide the willingness of an actor to be assigned a certain task at a certain time. The actors respond in five different levels, which can be interpreted as:

- Very Low Selection Possibility (VLSP) - It is not worth assigning the task to this actor.
- Low Selection Possibility (LSP) - There might be other actors which can do the job better.
- Middle Selection Possibility (MSP) - The Actor is ready to be assigned a task, but is not the “chosen” one.
- High Selection Possibility (HSP) - The actor takes responsibility of completing the task.
- Very High Selection Possibility (VHSP) - Actor has almost all required information and potential and takes full responsibility.

### 3.3 System Implementation

Fuzzy sets and fuzzy logic have been developed to manage vagueness and uncertainty in a reasoning process of an intelligent system such as a knowledge based system, an expert system or a logic control system [18–31]. In this work, we use fuzzy logic to implement the proposed system.

The structure of the proposed system is shown in Fig. 3. It consists of one Fuzzy Logic Controller (FLC), which is the main part of our system and its basic

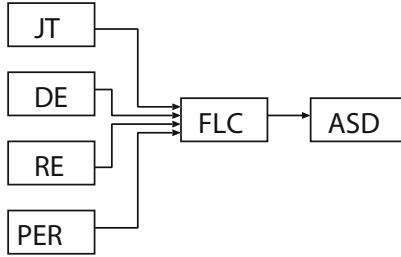


**Fig. 3.** Proposed system.

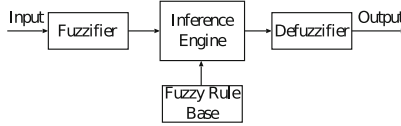


**Fig. 4.** FLC structure.

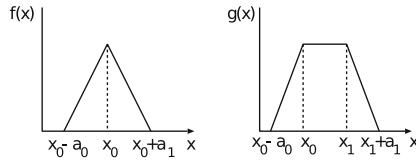


**Fig. 5.** Triangular and trapezoidal membership functions.

elements are shown in Fig. 4. They are the fuzzifier, inference engine, Fuzzy Rule Base (FRB) and defuzzifier.

As shown in Fig. 5, we use triangular and trapezoidal membership functions for FLC, because they are suitable for real-time operation [32]. The  $x_0$  in  $f(x)$  is the center of triangular function,  $x_0(x_1)$  in  $g(x)$  is the left (right) edge of trapezoidal function, and  $a_0(a_1)$  is the left (right) width of the triangular or trapezoidal function. We explain in details the design of FLC in following.

### 3.4 Description of FLC

We use four input parameters for FLC:

- Job Type (JT);
- Distance to Event (DE);
- Remaining Energy (RE);
- Packet Error Rate (PER).

The term sets for each input linguistic parameter are defined respectively as shown in Table 1.

The output linguistic parameter is the Actor Selection Decision (ASD).

**Table 1.** Parameters and their term sets for FLC.

Parameters	Term Sets
Job Type (JT)	Easy (Ea), Moderate (Mo), Hard (Hd)
Distance to Event (DE)	Near (Ne), Middle (Mi), Far (Fa)
Remaining Energy (RE)	Low (Lo), Medium (Me), High (Hi)
Packet Error Rate (PER)	Low (Lw), Medium (Md), High (Hg)
Actor Selection Decision (ASD)	VLSP, LSP, MSP, HSP, VHSP

The membership functions are shown in Fig. 6 and the Fuzzy Rule Base (FRB) is shown in Table 2. The FRB forms a fuzzy set of dimensions  $|T(JT)| \times |T(DE)| \times |T(RE)| \times |T(PER)|$ , where  $|T(x)|$  is the number of terms on  $T(x)$ . The FRB has 81 rules. The control rules have the form: IF “conditions” THEN “control action”.

### 4 Simulation Results

We present the simulation results in Figs. 7, 8 and 9. From results, we found that as JT becomes difficult, the ASD becomes higher, because actors are programmed for different jobs. As we can see, the performance is constant from 0 to

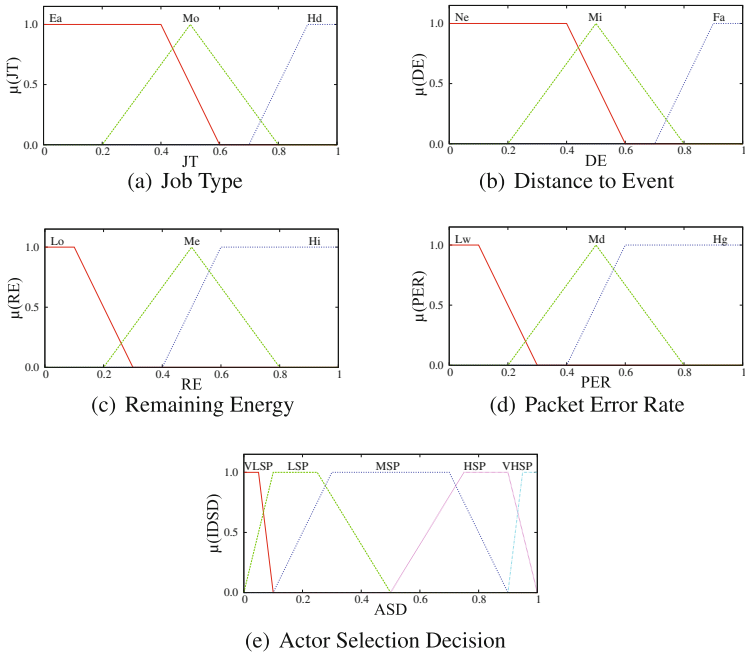


**Fig. 6.** Fuzzy membership functions.



**Table 2.** FRB of proposed fuzzy-based system.

No	JT	DE	RE	PER	ASD	No	JT	DE	RE	PER	ASD
1	Ea	Ne	Lo	Lw	VHSP	41	Mo	Mi	Me	Md	LSP
2	Ea	Ne	Lo	Md	HSP	42	Mo	Mi	Me	Hg	LSP
3	Ea	Ne	Lo	Hg	MSP	43	Mo	Mi	Hi	Lw	VHSP
4	Ea	Ne	Me	Lw	VHSP	44	Mo	Mi	Hi	Md	HSP
5	Ea	Ne	Me	Md	VHSP	45	Mo	Mi	Hi	Hg	MSP
6	Ea	Ne	Me	Hg	HSP	46	Mo	Fa	Lo	Lw	MSP
7	Ea	Ne	Hi	Lw	VHSP	47	Mo	Fa	Lo	Md	VLSP
8	Ea	Ne	Hi	Md	VHSP	48	Mo	Fa	Lo	Hg	VLSP
9	Ea	Ne	Hi	Hg	VHSP	49	Mo	Fa	Me	Lw	MSP
10	Ea	Mi	Lo	Lw	HSP	50	Mo	Fa	Me	Md	LSP
11	Ea	Mi	Lo	Md	MSP	51	Mo	Fa	Me	Hg	VLSP
12	Ea	Mi	Lo	Hg	LSP	52	Mo	Fa	Hi	Lw	HSP
13	Ea	Mi	Me	Lw	HSP	53	Mo	Fa	Hi	Md	MSP
14	Ea	Mi	Me	Md	MSP	54	Mo	Fa	Hi	Hg	LSP
15	Ea	Mi	Me	Hg	LSP	55	Hd	Ne	Lo	Lw	MSP
16	Ea	Mi	Hi	Lw	VHSP	56	Hd	Ne	Lo	Md	LSP
17	Ea	Mi	Hi	Md	HSP	57	Hd	Ne	Lo	Hg	VLSP
18	Ea	Mi	Hi	Hg	HSP	58	Hd	Ne	Me	Lw	HSP
19	Ea	Fa	Lo	Lw	MSP	59	Hd	Ne	Me	Md	MSP
20	Ea	Fa	Lo	Md	LSP	60	Hd	Ne	Me	Hg	LSP
21	Ea	Fa	Lo	Hg	VLSP	61	Hd	Ne	Hi	Lw	VHSP
22	Ea	Fa	Me	Lw	HSP	62	Hd	Ne	Hi	Md	HSP
23	Ea	Fa	Me	Md	MSP	63	Hd	Ne	Hi	Hg	MSP
24	Ea	Fa	Me	Hg	LSP	64	Hd	Mi	Lo	Lw	LSP
25	Ea	Fa	Hi	Lw	VHSP	65	Hd	Mi	Lo	Md	VLSP
26	Ea	Fa	Hi	Md	HSP	66	Hd	Mi	Lo	Hg	VLSP
27	Ea	Fa	Hi	Hg	MSP	67	Hd	Mi	Me	Lw	LSP
28	Mo	Ne	Lo	Lw	VHSP	68	Hd	Mi	Me	Md	VLSP
29	Mo	Ne	Lo	Md	MSP	69	Hd	Mi	Me	Hg	VLSP
30	Mo	Ne	Lo	Hg	MSP	70	Hd	Mi	Hi	Lw	HSP
31	Mo	Ne	Me	Lw	VHSP	71	Hd	Mi	Hi	Md	LSP
32	Mo	Ne	Me	Md	HSP	72	Hd	Mi	Hi	Hg	LSP
33	Mo	Ne	Me	Hg	MSP	73	Hd	Fa	Lo	Lw	VLSP
34	Mo	Ne	Hi	Lw	VHSP	74	Hd	Fa	Lo	Md	VLSP
35	Mo	Ne	Hi	Md	VHSP	75	Hd	Fa	Lo	Hg	VLSP
36	Mo	Ne	Hi	Hg	HSP	76	Hd	Fa	Me	Lw	LSP
37	Mo	Mi	Lo	Lw	MSP	77	Hd	Fa	Me	Md	VLSP
38	Mo	Mi	Lo	Md	LSP	78	Hd	Fa	Me	Hg	VLSP
39	Mo	Mi	Lo	Hg	VLSP	79	Hd	Fa	Hi	Lw	MSP
40	Mo	Mi	Me	Lw	HSP	80	Hd	Fa	Hi	Md	LSP
						81	Hd	Fa	Hi	Hg	VLSP

0.7 unit and after that is decreased for different values of RE. When we increase the PER parameter, the ASD is decreased.

In Fig. 8, we can see that the performance is lower than in Fig. 7, because the DE is increased. Furthermore in Fig. 9, we can see that the performance is the lowest because DE and PER are increased much more.

The DE defines the distance of the actor from the job place, so when DE is small, the ASD is higher. The actors closest to the job place use less energy to reach the job position. When RE is increased, the ASD is increased. However, when PER is increased the ASD is decreased and the actor node is not selected for the required job.

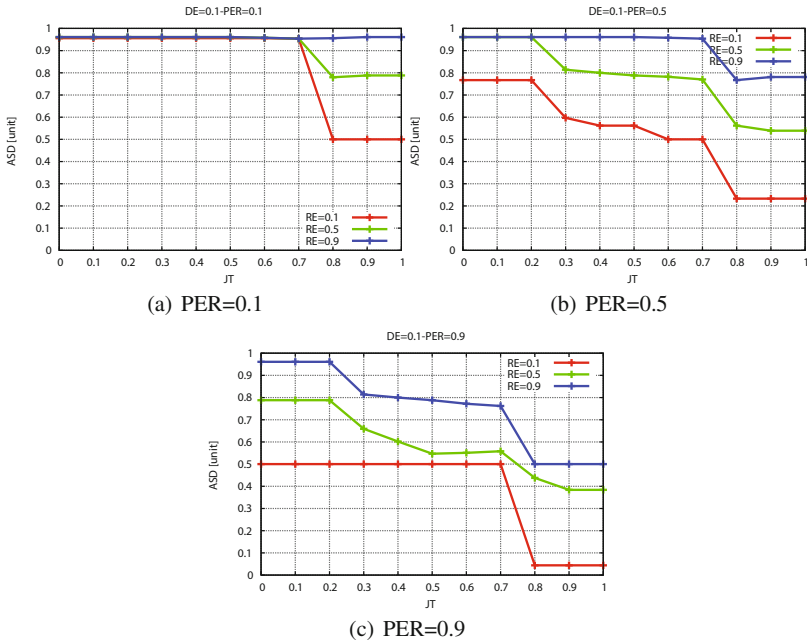


Fig. 7. Results for DE = 0.1.

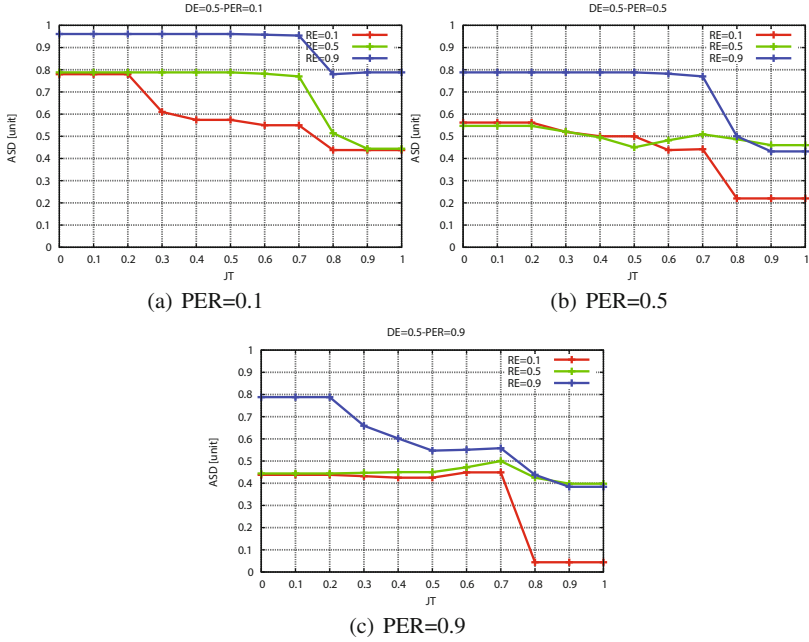


Fig. 8. Results for  $DE = 0.5$ .

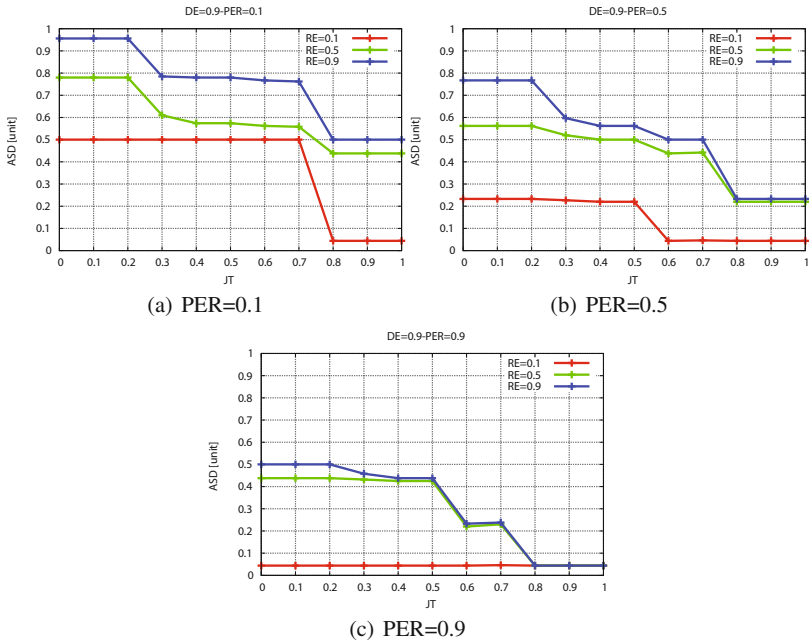


Fig. 9. Results for  $DE = 0.9$ .

## 5 Conclusions and Future Work

In this paper, we proposed and implemented a fuzzy-based simulation system for WSN, which takes into account four input parameters (including PER) and decides the actor selection for a required task in the network. From simulation results, we conclude as follows.

- When JT and RE parameters are increased, the ASD parameter is increased, so the probability that the system selects an actor node for the job is high.
- When DE and PER parameters are increased, the ASD parameter is decreased, so the probability that an actor node is selected for the required task is low.

In the future work, we will consider also other parameters for actor selection and make extensive simulations to evaluate the proposed system.

## References

1. Akyildiz, I., Su, W., Sankarasubramaniam, Y., Cayirci, E.: Wireless sensor networks: a survey. *Comput. Netw.* **38**(4), 393–422 (2002). (Elsevier)
2. Atassi, A., Sayegh, N., Elhajj, I., Chehab, A., Kayassi, A.: Decentralised malicious node detection in WSN. *Int. J. Space-Based Situated Comput.* **4**(1), 12–25 (2014)
3. Boyinbode, O., Le, H., Takizawa, M.: A survey on clustering algorithms for wireless sensor networks. *Int. J. Space-Based Situated Comput.* **1**(2/3), 130–136 (2011)
4. Akyildiz, I.F., Kasimoglu, I.H.: Wireless sensor and actor networks: Research challenges. *Ad Hoc Netw. J.* (Elsevier) **2**(4), 351–367 (2004)
5. Bahrepour, M., Meratnia, N., Poel, M., Taghikhaki, Z., Havinga, P.J.: Use of wireless sensor networks for distributed event detection in disaster management applications. *Int. J. Space-Based Situated Comput.* **2**(1), 58–69 (2012)
6. Haider, N., Imran, M., Saad, N., Zakariya, M.: Performance analysis of reactive connectivity restoration algorithms for wireless sensor and actor networks. In: *IEEE 11th Malaysia International Conference on Communications (MICC-2013)*, pp. 490–495, November 2013
7. Abbasi, A., Younis, M., Akkaya, K.: Movement-assisted connectivity restoration in wireless sensor and actor networks. *IEEE Trans. Parallel Distrib. Syst.* **20**(9), 1366–1379 (2009)
8. Li, X., Liang, X., Lu, R., He, S., Chen, J., Shen, X.: Toward reliable actor services in wireless sensor and actor networks. In: *IEEE 8th International Conference on Mobile Ad hoc and Sensor Systems (MASS-2011)*, pp. 351–360, October 2011
9. Akkaya, K., Younis, M.: Cola: A coverage and latency aware actor placement for wireless sensor and actor networks. In: *IEEE 64th Conference on Vehicular Technology (VTC-2006) Fall*, pp. 1–5, September 2006
10. Kakarla, J., Majhi, B.: A new optimal delay and energy efficient coordination algorithm for WSN. In: *IEEE International Conference on Advanced Networks and Telecommunications Systems (ANTS-2013)*, pp. 1–6, December 2013
11. Elmazi, D., Spaho, E., Kulla, E., Oda, T., Ikeda, M., Barolli, L.: Selection of actor nodes in wireless sensor and actor networks considering as a new parameter actor congestion situation. In: *19th International Conference on Network-Based Information Systems (NBIS-2016)*, pp. 29–36 (2016)

12. Akbas, M., Turgut, D.: APAWSAN: Actor positioning for aerial wireless sensor and actor networks. In: IEEE 36th Conference on Local Computer Networks (LCN-2011), pp. 563–570, October 2011
13. Akbas, M., Brust, M., Turgut, D.: Local positioning for environmental monitoring in wireless sensor and actor networks. In: IEEE 35th Conference on Local Computer Networks (LCN-2010), pp. 806–813, October 2010
14. Melodia, T., Pompili, D., Gungor, V., Akyildiz, I.: Communication and coordination in wireless sensor and actor networks. *IEEE Trans. Mobile Comput.* **6**(10), 1126–1129 (2007)
15. Gungor, V., Akan, O., Akyildiz, I.: A real-time and reliable transport ( $RT^2$ ) protocol for wireless sensor and actor networks. *IEEE/ACM Trans. Netw.* **16**(2), 359–370 (2008)
16. Selvaradjou, K., Handigol, N., Franklin, A., Murthy, C.: Energy-efficient directional routing between partitioned actors in wireless sensor and actor networks. *IET Commun.* **4**(1), 102–115 (2010)
17. Nakayama, H., Fadlullah, Z., Ansari, N., Kato, N.: A novel scheme for wsan sink mobility based on clustering and set packing techniques. *IEEE Trans. Autom. Control* **56**(10), 2381–2389 (2011)
18. Inaba, T., Sakamoto, S., Kolici, V., Mino, G., Barolli, L.: A CAC scheme based on fuzzy logic for cellular networks considering security and priority parameters. In: The 9-th International Conference on Broadband and Wireless Computing, Communication and Applications (BWCCA-2014), pp. 340–346 (2014)
19. Spaho, E., Sakamoto, S., Barolli, L., Xhafa, F., Barolli, V., Iwashige, J.: A fuzzy-based system for peer reliability in JXTA-overlay P2P considering number of interactions. In: The 16th International Conference on Network-Based Information Systems (NBIS-2013), pp. 156–161 (2013)
20. Matsuo, K., Elmazi, D., Liu, Y., Sakamoto, S., Mino, G., Barolli, L.: FACS-MP: A fuzzy admission control system with many priorities for wireless cellular networks and its performance evaluation. *J. High Speed Netw.* **21**(1), 1–14 (2015)
21. Grabisch, M.: The application of fuzzy integrals in multicriteria decision making. *Eur. J. Oper. Res.* **89**(3), 445–456 (1996)
22. Inaba, T., Elmazi, D., Liu, Y., Sakamoto, S., Barolli, L., Uchida, K.: Integrating wireless cellular and ad-hoc networks using fuzzy logic considering node mobility and security. In: The 29th IEEE International Conference on Advanced Information Networking and Applications Workshops (WAINA-2015), pp. 54–60 (2015)
23. Kulla, E., Mino, G., Sakamoto, S., Ikeda, M., Caballé, S., Barolli, L.: FBMIS: A fuzzy-based multi-interface system for cellular and ad hoc networks. In: IEEE International Conference on Advanced Information Networking and Applications (AINA-2014), pp. 180–185 (2014)
24. Elmazi, D., Kulla, E., Oda, T., Spaho, E., Sakamoto, S., Barolli, L.: A comparison study of two fuzzy-based systems for selection of actor node in wireless sensor actor networks. *J. Ambient Intell. Humanized Comput.* **6**(5), 635–645 (2015)
25. Zadeh, L.: Fuzzy logic, neural networks, and soft computing. *ACM Commun.* **37**(3), 77–84 (1994)
26. Spaho, E., Sakamoto, S., Barolli, L., Xhafa, F., Ikeda, M.: Trustworthiness in P2P: performance behaviour of two fuzzy-based systems for JXTA-overlay platform. *Soft Comput.* **18**(9), 1783–1793 (2014)
27. Inaba, T., Sakamoto, S., Kulla, E., Caballe, S., Ikeda, M., Barolli, L.: An integrated system for wireless cellular and ad-hoc networks using fuzzy logic. In: International Conference on Intelligent Networking and Collaborative Systems (INCoS-2014), pp. 157–162 (2014)

28. Matsuo, K., Elmazi, D., Liu, Y., Sakamoto, S., Barolli, L.: A multi-modal simulation system for wireless sensor networks: a comparison study considering stationary and mobile sink and event. *J. Ambient Intell. Humanized Comput.* **6**(4), 519–529 (2015)
29. Kolicic, V., Inaba, T., Lala, A., Mino, G., Sakamoto, S., Barolli, L.: A fuzzy-based CAC scheme for cellular networks considering security. In: *International Conference on Network-Based Information Systems (NBIS-2014)*, pp. 368–373 (2014)
30. Liu, Y., Sakamoto, S., Matsuo, K., Ikeda, M., Barolli, L., Xhafa, F.: A comparison study for two fuzzy-based systems: improving reliability and security of JXTA-overlay P2P Platform. *Soft Comput.* **20**(7), 2677–2687 (2015)
31. Matsuo, K., Elmazi, D., Liu, Y., Sakamoto, S., Mino, G., Barolli, L.: FACS-MP: A fuzzy admission control system with many priorities for wireless cellular networks and its performance evaluation. *J. High Speed Netw.* **21**(1), 1–14 (2015)
32. Mendel, J.M.: Fuzzy logic systems for engineering: a tutorial. *Proc. IEEE* **83**(3), 345–377 (1995)

# A Fuzzy-Based Approach for Improving Team Collaboration in MobilePeerDroid Mobile System

Yi Liu<sup>1</sup>(✉), Kosuke Ozera<sup>1</sup>, Keita Matsuo<sup>2</sup>, Makoto Ikeda<sup>2</sup>,  
and Leonard Barolli<sup>2</sup>

<sup>1</sup> Graduate School of Engineering, Fukuoka Institute of Technology (FIT),  
3-30-1 Wajiro-Higashi, Higashi-ku, Fukuoka 811-0295, Japan  
ryuui1010@gmail.com, kosuke.o.fit@gmail.com

<sup>2</sup> Department of Information and Communication Engineering,  
Fukuoka Institute of Technology (FIT),  
3-30-1 Wajiro-Higashi, Higashi-ku, Fukuoka 811-0295, Japan  
kt-matsuo@fit.ac.jp, makoto.ikd@acm.org, barolli@fit.ac.jp

**Abstract.** Mobile computing has many application domains. One important domain is that of mobile applications supporting collaborative work, such as, eLearning and eHealth. In this work we present a distributed event-based awareness approach for P2P groupware systems. Unlike centralized approaches, several issues arise and need to be addressed for awareness in P2P groupware systems, due to their large-scale, dynamic and heterogenous nature. In such applications, a team of people collaborate online using smartphones to accomplish a common goal, such as a project development in e-Business. Often, however, the members of the team has to take decision or solve conflicts in project development (such as delays, changes in project schedule, task assignment, etc.) and therefore members have to vote. Voting can be done in many ways, and in most works in the literature consider majority voting, in which every member of the team accounts on for a vote. In this work, we consider a more realistic case where a vote does not account equal for every member, but accounts on according to member's active involvement and reliability in the groupwork. We present a voting model, that we call qualified voting, in which every member has a voting score according to four parameters. Then, we use fuzzy based model to compute a voting score for the member. This model will be to implemented in MobilePeerDroid system to give more realistic view of the collaborative activity and better decisions for the groupwork, while encouraging peers to increase their reliability in order to increase their voting score.

## 1 Introduction

Peer to Peer technologies has been among most disruptive technologies after Internet. Indeed, the emergence of the P2P technologies changed drastically the concepts, paradigms and protocols of sharing and communication in large scale distributed systems. As pointed out since early 2000 years [1–5], the nature of the sharing

and the direct communication among peers in the system, being these machines or people, makes possible to overcome the limitations of the flat communications through email, newsgroups and other forum-based communication forms.

The usefulness of P2P technologies on one hand has been shown for the development of stand alone applications. On the other hand, P2P technologies, paradigms and protocols have penetrated other large scale distributed systems such as Mobile Ad hoc Networks (MANETs), Groupware systems, Mobile Systems to achieve efficient sharing, communication, coordination, replication, awareness and synchronization. In fact, for every new form of Internet-based distributed systems, we are seeing how P2P concepts and paradigms again play an important role to enhance the efficiency and effectiveness of such systems or to enhance information sharing and online collaborative activities of groups of people. We briefly introduce below some common application scenarios that can benefit from P2P communications.

With the fast development in mobile technologies we are witnessing how the mobile devices are widely used for supporting collaborative team work. Indeed, by using mobile devices (such as PDAs, smartphones, etc.) members of a team can not only be geographically distributed, they can also be supported on the move, when network connection can change over time. In this paper, we propose a fuzzy-based system for qualified voting in P2P mobile collaborative team.

Fuzzy Logic (FL) is the logic underlying modes of reasoning which are approximate rather than exact. The importance of FL derives from the fact that most modes of human reasoning and especially common sense reasoning are approximate in nature [6]. FL uses linguistic variables to describe the control parameters. By using relatively simple linguistic expressions it is possible to describe and grasp very complex problems. A very important property of the linguistic variables is the capability of describing imprecise parameters.

The concept of a fuzzy set deals with the representation of classes whose boundaries are not determined. It uses a characteristic function, taking values usually in the interval  $[0, 1]$ . The fuzzy sets are used for representing linguistic labels. This can be viewed as expressing an uncertainty about the clear-cut meaning of the label. But important point is that the valuation set is supposed to be common to the various linguistic labels that are involved in the given problem.

The fuzzy set theory uses the membership function to encode a preference among the possible interpretations of the corresponding label. A fuzzy set can be defined by exemplification, ranking elements according to their typicality with respect to the concept underlying the fuzzy set [7].

In this paper, we propose a fuzzy-based peer voting score system for MobilePeerDroid system considering four parameters: Number of Activities the Member Participates (NAMP), Number of Activities the Member has Successfully Finished (NAMESF), Number of Available Team Members (NATM), Number of Activities the Member Failures (NAMF) to decide the Voting Score (VS). We evaluated the proposed system by simulations. The simulation results show that with increasing of NAMP, NAMESF, and NATM, the VS is increasing, but with increasing of NAMF, the VS is decreased. Thus, the proposed system can choose reliable peers with good voting score in P2P mobile collaborative team.



The structure of this paper is as follows. In Sect. 2, we introduce the scenarios of collaborative teamwork. In Sect. 3, we introduce the vote weights and voting score. In Sect. 4, we introduce FL used for control. In Sect. 5, we present the proposed fuzzy-based system. In Sect. 6, we discuss the simulation results. Finally, conclusions and future work are given in Sect. 7.

## 2 Scenarios of Collaborative Teamwork

In this section, we describe and analyse some main scenarios of collaborative teamwork for which P2P technologies can support efficient system design.

### 2.1 Collaborative Teamwork and Virtual Campuses

Collaborative work through virtual teams is a significant way of collaborating in modern businesses, online learning, etc. [8]. Collaboration in virtual teams requires efficient sharing of information (both data sharing among the group members as well as sharing of group processes) and efficient communication among members of the team. Additionally, coordination and interaction are crucial for accomplishing common tasks through a shared workspace environment. P2P systems can enable fully decentralized collaborative systems by efficiently supporting different forms of collaboration [9]. One such form is using P2P networks, with super-peer structure as show in Fig. 1.

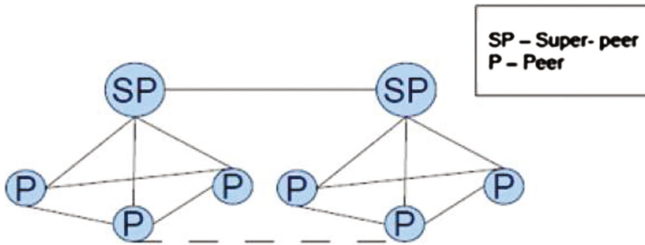


Fig. 1. Super-peer P2P group network.

During the last two decades, online learning has become very popular and there is a widespread of virtual campuses or combinations of face-to-face with semi-open teaching and learning. Virtual campuses are now looking at ways to effectively support learners, especially for online courses implemented as PBL-Project Based Learning or SBL Scenario Based Learning there is an increasing need to develop mobile applications that support these online groupwork learning paradigms [10]. In such setting, P2P technologies offer interesting solutions for (a) decentralizing the virtual campuses, which tend to grow and get further centralized with the increase of number of students enrolled, new degrees, and increase in academic activity; (b) in taking advantage of resources of students and

developing volunteerbased computing systems as part of virtual campuses and (c) alleviating the communication burden for efficient collaborative teamwork. The use of P2P libraries such as JXTA have been investigated to design P2P middleware for P2P eLearning applications. Also, the use of P2P technologies in such setting is used for P2P video synchronization in a collaborative virtual environment [11]. Recently, virtual campuses are also introducing social networking among their students to enhance the learning activities through social support and scaffolding. Again the P2P solutions are sought in this context [12] in combination with social networking features to enhance especially the interaction among learners sharing similar objectives and interest or accomplishing a common project.

## 2.2 Mobile Ad Hoc Networks (MANETs)

Mobile ad-hoc networks are among most interesting infrastructureless network of mobile devices connected by wireless having self-configuring properties [13]. The lack of fixed infrastructure and of a centralized administration makes the building and operation in MANETS challenging. P2P networks and mobile ad hoc networks (MANETs) follow the same idea of creating a network without a central entity. All nodes (peers) must collaborate together to make possible the proper functioning of the network by forwarding information on behalf of others in the network [14]. P2P and MANETs share many key characteristics such as self-organization and decentralization due to the common nature of their distributed components. Both MANETs and P2P networks follow a P2P paradigm characterized by the lack of a central node or peer acting as a managing server, all participants having therefore to collaborate in order for the whole system to work. A key issue in both networks is the process of discovering the requested data or route efficiently in a decentralized manner. Recently, new P2P applications which uses wireless communication and integrates mobile devices such as PDA and mobile phones is emerging. Several P2P-based protocols can be used for MANETs such as Mobile P2P Protocol (MPP), which is based on Dynamic Source Routing (DSR), JXTA protocols, and MANET Anonymous Peer-to-peer Communication Protocol (MAPCP), which serves as an efficient anonymous communication protocol for P2P applications over MANET.

## 3 Vote Weights

### 3.1 Votes with Embedded Weight

The weights can be included in voting bulletins distributed to voters, which would then be copied into the votes sent to Counters. But this approach requires a strong assumption: the voters' application must be trusted not to forge weights. Since the voters' application may be tampered in some scenarios, namely when "voting anywhere" is considered, the voters' side cannot be trusted to give the correct input for the system when weights are considered.

The simple copy/paste of weights could be strengthened by adding a cleartext value of the weight when submitting a blinded vote digest for getting a signature from an Administrator. Then, the weight, checked and signed by all the required Administrators, could be added to the final vote submitted to Counters. A bit commitment value should also be added to the weight to prevent stolen, signed weights, to be used by other voters. The drawback of this approach is that protocol messages from voters to Administrators and from voters to Counters would increase in size, namely would double in size. This collides with the requirement of keeping the performance of system close to the performance of the initial version of REVS (Robust Electronic Voting System [15]).

### 3.2 Voting Score

Score voting (sometimes called range voting) is a single-winner voting system where voters rate candidates on a scale. The candidate with the highest rating wins. For comparison, consider ratings systems from site like: Internet Movie Database, Amazon, Yelp, and Hot or Not. Variations of score voting can use a score-style ballot to elect multiple candidates simultaneously.

Simplified forms of score voting automatically give skipped candidates the lowest possible score for the ballot they were skipped. Other forms have those ballots not affect the candidate's rating at all. Those forms not affecting the candidates rating frequently make use of quotas. Quotas demand a minimum proportion of voters rate that candidate in some way before that candidate is eligible to win [16].

## 4 Application of Fuzzy Logic for Control

The ability of fuzzy sets and possibility theory to model gradual properties or soft constraints whose satisfaction is matter of degree, as well as information pervaded with imprecision and uncertainty, makes them useful in a great variety of applications.

The most popular area of application is Fuzzy Control (FC), since the appearance, especially in Japan, of industrial applications in domestic appliances, process control, and automotive systems, among many other fields.

### 4.1 FC

In the FC systems, expert knowledge is encoded in the form of fuzzy rules, which describe recommended actions for different classes of situations represented by fuzzy sets.

In fact, any kind of control law can be modeled by the FC methodology, provided that this law is expressible in terms of "if ... then ..." rules, just like in the case of expert systems. However, FL diverges from the standard expert system approach by providing an interpolation mechanism from several rules. In the contents of complex processes, it may turn out to be more practical to get knowledge from an expert operator than to calculate an optimal control, due to modeling costs or because a model is out of reach.

## 4.2 Linguistic Variables

A concept that plays a central role in the application of FL is that of a linguistic variable. The linguistic variables may be viewed as a form of data compression. One linguistic variable may represent many numerical variables. It is suggestive to refer to this form of data compression as granulation [17].

The same effect can be achieved by conventional quantization, but in the case of quantization, the values are intervals, whereas in the case of granulation the values are overlapping fuzzy sets. The advantages of granulation over quantization are as follows:

- it is more general;
- it mimics the way in which humans interpret linguistic values;
- the transition from one linguistic value to a contiguous linguistic value is gradual rather than abrupt, resulting in continuity and robustness.

## 4.3 FC Rules

FC describes the algorithm for process control as a fuzzy relation between information about the conditions of the process to be controlled,  $x$  and  $y$ , and the output for the process  $z$ . The control algorithm is given in “if ... then ...” expression, such as:

- If  $x$  is small and  $y$  is big, then  $z$  is medium;
- If  $x$  is big and  $y$  is medium, then  $z$  is big.

These rules are called *FC rules*. The “if” clause of the rules is called the antecedent and the “then” clause is called consequent. In general, variables  $x$  and  $y$  are called the input and  $z$  the output. The “small” and “big” are fuzzy values for  $x$  and  $y$ , and they are expressed by fuzzy sets.

Fuzzy controllers are constructed of groups of these FC rules, and when an actual input is given, the output is calculated by means of fuzzy inference.

## 4.4 Control Knowledge Base

There are two main tasks in designing the control knowledge base. First, a set of linguistic variables must be selected which describe the values of the main control parameters of the process. Both the input and output parameters must be linguistically defined in this stage using proper term sets. The selection of the level of granularity of a term set for an input variable or an output variable plays an important role in the smoothness of control. Second, a control knowledge base must be developed which uses the above linguistic description of the input and output parameters. Four methods [18–21] have been suggested for doing this:

- expert’s experience and knowledge;
- modelling the operator’s control action;
- modelling a process;
- self organization.

Among the above methods, the first one is the most widely used. In the modeling of the human expert operator’s knowledge, fuzzy rules of the form “If Error is small and Change-in-error is small then the Force is small” have been used in several studies [22, 23]. This method is effective when expert human operators can express the heuristics or the knowledge that they use in controlling a process in terms of rules of the above form.

#### 4.5 Defuzzification Methods

The defuzzification operation produces a non-FC action that best represent the membership function of an inferred FC action. Several defuzzification methods have been suggested in literature. Among them, four methods which have been applied most often are:

- Tsukamoto’s Defuzzification Method;
- The Center of Area (COA) Method;
- The Mean of Maximum (MOM) Method;
- Defuzzification when Output of Rules are Function of Their Inputs.

### 5 Proposed Fuzzy-Based Peer Voting Score System

The P2P group-based model considered is that of a superpeer model. In this model, the P2P network is fragmented into several disjoint peergroups (see Fig. 2). The peers of each peergroup are connected to a single superpeer. There is frequent local communication between peers in a peergroup, and less frequent global communication between superpeers.

To complete a certain task in P2P mobile collaborative team work, peers often have to interact with unknown peers. Thus, it is important that group members must select reliable peers to interact.

In [24], we already proposed a system with three parameters. In this work, we consider four parameters: Numbers of Activities the Member Participates (NAMP), Number of Activities the Member has Successfully Finished (NAMSF), Number of Available Team Members (NATM), Number of Activities the Member Failures (NAMF) to decide the Voting Score (VS). The structure of this system called Fuzzy-based Vote System (FVS) is shown in Fig. 3. These four parameters are fuzzified using fuzzy system, and based on the decision of fuzzy system a voting score is calculated. The membership functions for our system are shown in Fig. 4. In Table 1, we show the Fuzzy Rule Base (FRB) of our proposed system, which consists of 81 rules.

The input parameters for FVS are: NAMP, NAMSF, NATM, NAMF and the output linguistic parameter is VS. The term sets of *NAMP*, *NAMSF*, *NATM* and *NAMF* are defined respectively as:

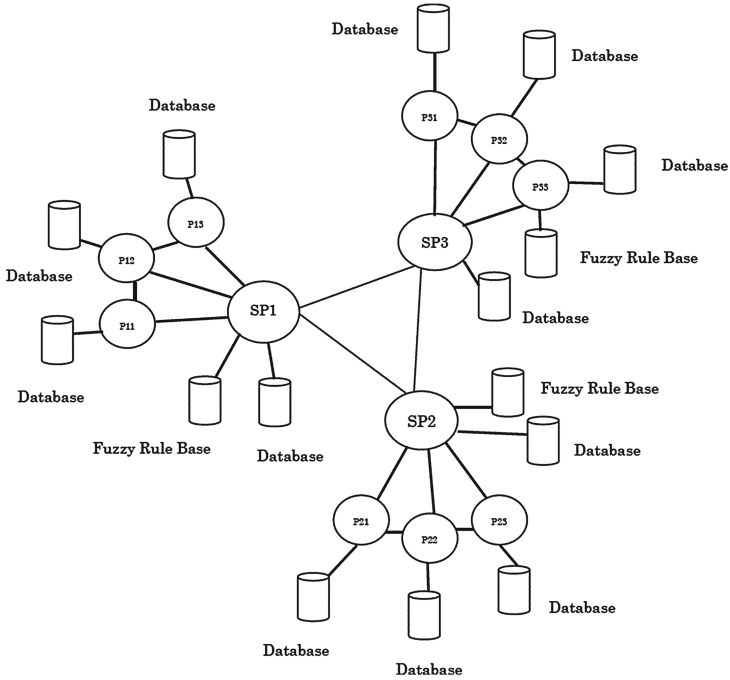


Fig. 2. P2P group-based model.

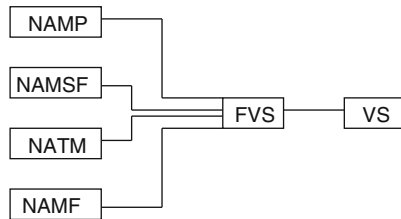
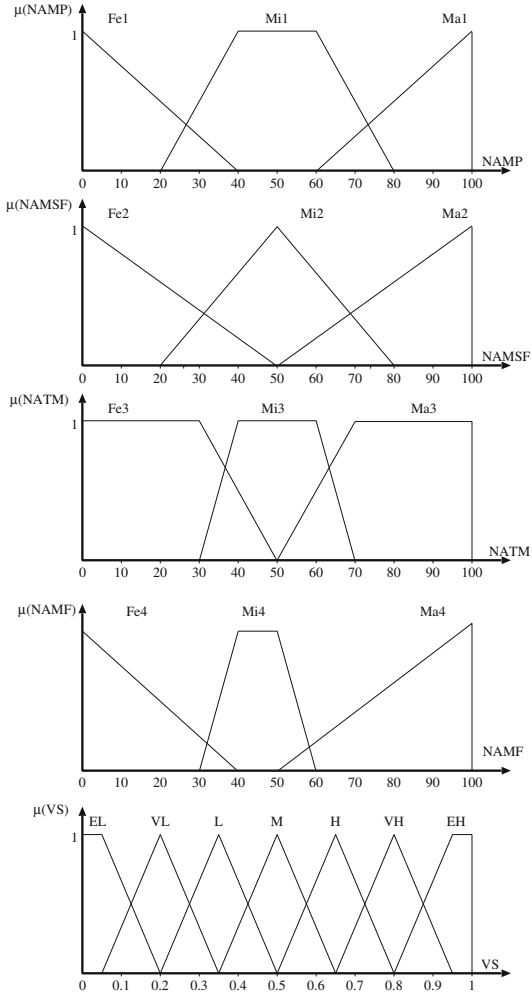


Fig. 3. Proposed of structure.

$$\begin{aligned}
 NAMP &= \{Few1, Middle1, Many1\} \\
 &= \{Fe1, Mi1, Ma1\}; \\
 NAMSF &= \{Few2, Middle2, Many2\} \\
 &= \{Fe2, Mi2, Ma2\}; \\
 NATM &= \{Few3, Middle3, Many3\} \\
 &= \{Fe3, Mi3, Ma3\}; \\
 NAMF &= \{Few4, Middle4, Many4\} \\
 &= \{Fe4, Mi4, Ma4\}.
 \end{aligned}$$



**Fig. 4.** Membership functions.

and the term set for the output  $VS$  is defined as:

$$VS = \begin{pmatrix} \textit{Extremely Low} \\ \textit{Very Low} \\ \textit{Low} \\ \textit{Middle} \\ \textit{High} \\ \textit{Very High} \\ \textit{Extremely High} \end{pmatrix} = \begin{pmatrix} EL \\ VL \\ L \\ M \\ H \\ VH \\ EH \end{pmatrix}$$

Table 1. FRB.

Rule	NAMP	NAMSF	NATM	NAMF	VS	Rule	NAMP	NAMSF	NATM	NAMF	VS
1	Fe1	Fe2	Fe3	Fe4	VL	41	Mi1	Mi2	Mi3	Mi4	M
2	Fe1	Fe2	Fe3	Mi4	EL	42	Mi1	Mi2	Mi3	Ma4	VL
3	Fe1	Fe2	Fe3	Ma4	EL	43	Mi1	Mi2	Ma3	Fe4	EH
4	Fe1	Fe2	Mi3	Fe4	L	44	Mi1	Mi2	Ma3	Mi4	VH
5	Fe1	Fe2	Mi3	Mi4	VL	45	Mi1	Mi2	Ma3	Ma4	L
6	Fe1	Fe2	Mi3	Ma4	EL	46	Mi1	Ma2	Fe3	Fe4	VH
7	Fe1	Fe2	Ma3	Fe4	H	47	Mi1	Ma2	Fe3	Mi4	L
8	Fe1	Fe2	Ma3	Mi4	L	48	Mi1	Ma2	Fe3	Ma4	VL
9	Fe1	Fe2	Ma3	Ma4	EL	49	Mi1	Ma2	Mi3	Fe4	EH
10	Fe1	Mi2	Fe3	Fe4	L	50	Mi1	Ma2	Mi3	Mi4	H
11	Fe1	Mi2	Fe3	Mi4	EL	51	Mi1	Ma2	Mi3	Ma4	L
12	Fe1	Mi2	Fe3	Ma4	EL	52	Mi1	Ma2	Ma3	Fe4	EH
13	Fe1	Mi2	Mi3	Fe4	M	53	Mi1	Ma2	Ma3	Mi4	VH
14	Fe1	Mi2	Mi3	Mi4	VL	54	Mi1	Ma2	Ma3	Ma4	H
15	Fe1	Mi2	Mi3	Ma4	EL	55	Ma1	Fe2	Fe3	Fe4	H
16	Fe1	Mi2	Ma3	Fe4	VH	56	Ma1	Fe2	Fe3	Mi4	L
17	Fe1	Mi2	Ma3	Mi4	M	57	Ma1	Fe2	Fe3	Ma4	EL
18	Fe1	Mi2	Ma3	Ma4	VL	58	Ma1	Fe2	Mi3	Fe4	VH
19	Fe1	Ma2	Fe3	Fe4	M	59	Ma1	Fe2	Mi3	Mi4	M
20	Fe1	Ma2	Fe3	Mi4	VL	60	Ma1	Fe2	Mi3	Ma4	VL
21	Fe1	Ma2	Fe3	Ma4	EL	61	Ma1	Fe2	Ma3	Fe4	EH
22	Fe1	Ma2	Mi3	Fe4	VH	62	Ma1	Fe2	Ma3	Mi4	VH
23	Fe1	Ma2	Mi3	Mi4	L	63	Ma1	Fe2	Ma3	Ma4	M
24	Fe1	Ma2	Mi3	Ma4	VL	64	Ma1	Mi2	Fe3	Fe4	VH
25	Fe1	Ma2	Ma3	Fe4	EH	65	Ma1	Mi2	Fe3	Mi4	M
26	Fe1	Ma2	Ma3	Mi4	H	66	Ma1	Mi2	Fe3	Ma4	VL
27	Fe1	Ma2	Ma3	Ma4	L	67	Ma1	Mi2	Mi3	Fe4	EH
28	Mi1	Fe2	Fe3	Fe4	L	68	Ma1	Mi2	Mi3	Mi4	VH
29	Mi1	Fe2	Fe3	Mi4	VL	69	Ma1	Mi2	Mi3	Ma4	L
30	Mi1	Fe2	Fe3	Ma4	EL	70	Ma1	Mi2	Ma3	Fe4	EH
31	Mi1	Fe2	Mi3	Fe4	H	71	Ma1	Mi2	Ma3	Mi4	EH
32	Mi1	Fe2	Mi3	Mi4	L	72	Ma1	Mi2	Ma3	Ma4	H
33	Mi1	Fe2	Mi3	Ma4	EL	73	Ma1	Ma2	Fe3	Fe4	EH
34	Mi1	Fe2	Ma3	Fe4	VH	74	Ma1	Ma2	Fe3	Mi4	H
35	Mi1	Fe2	Ma3	Mi4	M	75	Ma1	Ma2	Fe3	Ma4	L
36	Mi1	Fe2	Ma3	Ma4	VL	76	Ma1	Ma2	Mi3	Fe4	EH
37	Mi1	Mi2	Fe3	Fe4	M	77	Ma1	Ma2	Mi3	Mi4	VH
38	Mi1	Mi2	Fe3	Mi4	VL	78	Ma1	Ma2	Mi3	Ma4	H
39	Mi1	Mi2	Fe3	Ma4	EL	79	Ma1	Ma2	Ma3	Fe4	EH
40	Mi1	Mi2	Mi3	Fe4	VH	80	Ma1	Ma2	Ma3	Mi4	EH
						81	Ma1	Ma2	Ma3	Ma4	VH



## 6 Simulation Results

In this section, we present the simulation results for our proposed system. In our system, we decided the number of term sets by carrying out many simulations. These simulation results were carried out in MATLAB.

From Fig. 5 to Fig. 7, we show the relation between NAMP, NAMSF, NATM, NAMF and VS. In this simulation, we consider the NATM as a constant parameter.

In Fig. 5, we consider the NAMF value 0 unit. We change the NATM value from 0 to 100 units. When the NATM increases, the VS is increased. Also, when the NAMSF and NAMP increase, the VS is increased.

In Figs. 6 and 7, we increase the NAMF values to 50 and 100 units, respectively. We see that, when the NAMF increases, the VS is decreased.

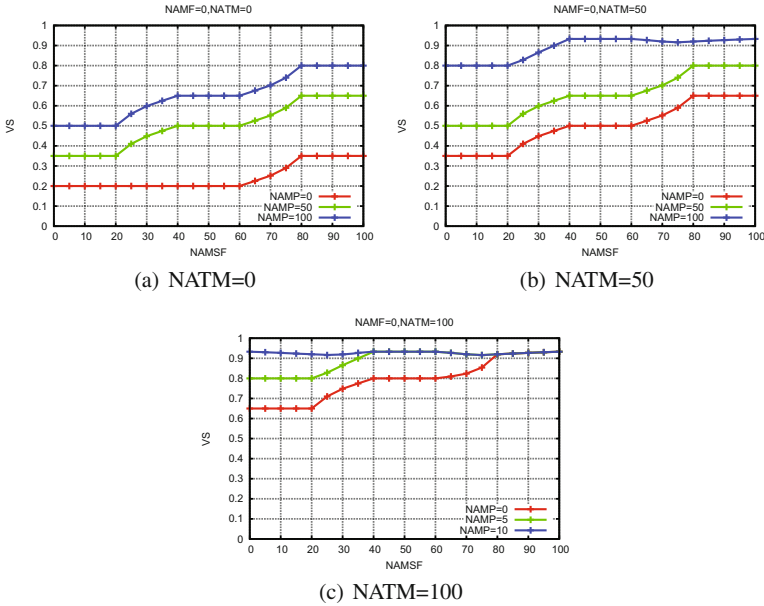


Fig. 5. Voting score for different NATM when NAMF = 0.

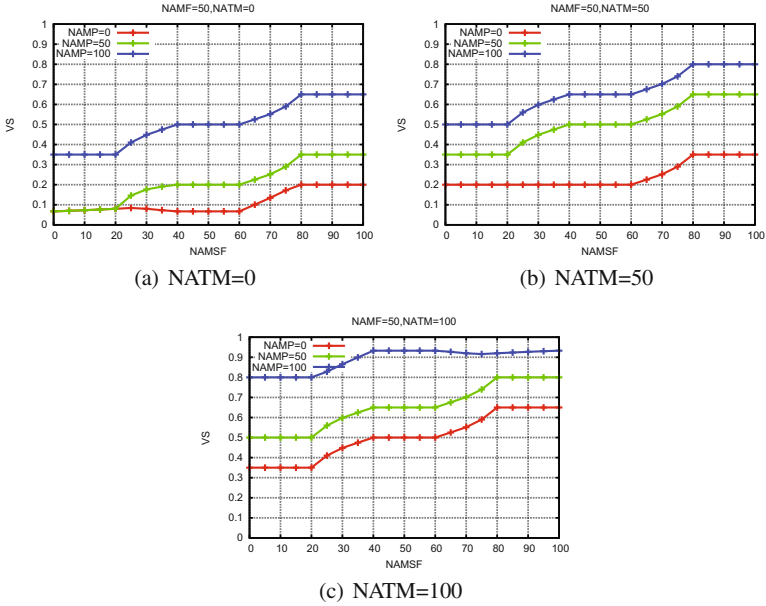


Fig. 6. Voting score for different NATM when NAMF = 50.

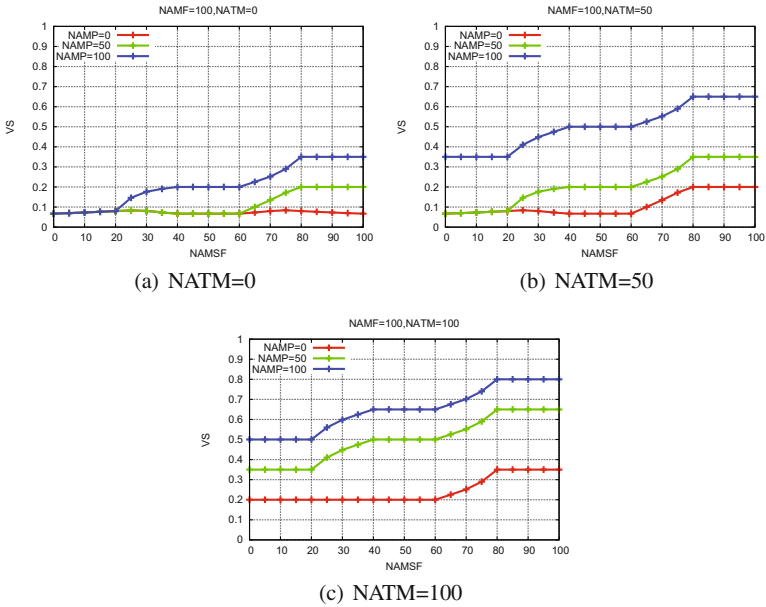


Fig. 7. Voting score for different NATM when NAMF = 100.

## 7 Conclusions and Future Work

In this paper, we proposed a fuzzy-based system to decide the VS. We took into consideration four parameters: NAMP, NAMSF, NATM and NAMF. We evaluated the performance of proposed system by computer simulations. From the simulations results, we conclude as follows.

- When NAMP, NAMSF and NATM are high, the voting score is high.
- With increasing of NAMF, the VS is decreased.
- The proposed system can choose reliable peers with good voting score in P2P mobile collaborative team.

In the future, we would like to make extensive simulations to evaluate the proposed systems and compare the performance with other systems.

## References

1. Oram, A. (ed.): *Peer-to-Peer: Harnessing the power of disruptive technologies*. O'Reilly and Associates, CA (2001)
2. Sula, A., Spaho, E., Matsuo, K., Barolli, L., Xhafa, F., Miho, R.: A new system for supporting children with autism spectrum disorder based on IoT and P2P technology. *Int. J. Space-Based Situated Comput.* **4**(1), 55–64 (2014). doi:[10.1504/IJSSC.2014.060688](https://doi.org/10.1504/IJSSC.2014.060688)
3. Di Stefano, A., Morana, G., Zito, D.: QoS-aware services composition in P2PGrid environments. *Int. J. Grid Util. Comput.* **2**(2), 139–147 (2011). doi:[10.1504/IJGUC.2011.040601](https://doi.org/10.1504/IJGUC.2011.040601)
4. Sawamura, S., Barolli, A., Aikebaier, A., Takizawa, M., Enokido, T.: Design and evaluation of algorithms for obtaining objective trustworthiness on acquaintances in P2P overlay networks. *Int. J. Grid Util. Comput.* **2**(3), 196–203 (2011). doi:[10.1504/IJGUC.2011](https://doi.org/10.1504/IJGUC.2011)
5. Higashino, M., Hayakawa, T., Takahashi, K., Kawamura, T., Sugahara, K.: Management of streaming multimedia content using mobile agent technology on pure P2P-based distributed e-learning system. *Int. J. Grid Util. Comput.* **5**(3), 198–204 (2014). doi:[10.1504/IJGUC.2014.062928](https://doi.org/10.1504/IJGUC.2014.062928)
6. Inaba, T., Obukata, R., Sakamoto, S., Oda, T., Ikeda, M., Barolli, L.: Performance evaluation of a QoS-aware fuzzy-based CAC for LAN access. *Int. J. Space-Based Situated Comput.* **6**(4), 228–238 (2016). doi:[10.1504/IJSSC.2016.082768](https://doi.org/10.1504/IJSSC.2016.082768)
7. Terano, T., Asai, K., Sugeno, M.: *Fuzzy Systems Theory And Its Applications*. Academic Press INC. Harcourt Brace Jovanovich Publishers (1992)
8. Mori, T., Nakashima, M., Ito, T.: SpACCE: a sophisticated ad hoc cloud computing environment built by server migration to facilitate distributed collaboration. *Int. J. Space-Based Situated Comput.* **2**(4), 230–239 (2011). doi:[10.1504/IJSSC.2012.050000](https://doi.org/10.1504/IJSSC.2012.050000)
9. Xhafa, F., Poulouvassilis, A.: Requirements for distributed event-based awareness in P2P groupware systems. In: *Proceedings of AINA 2010*, pp. 220–225 (2010)
10. Xhafa, F., Barolli, L., Caballé, S., Fernandez, R.: Supporting scenario-based online learning with P2P group-based systems. In: *Proceedings of NBiS 2010*, pp. 173–180, September 2010

11. Gupta, S., Kaiser, G.: P2P video synchronization in a collaborative virtual environment. In: Proceedings of the 4th International Conference on Advances in Web-Based Learning (ICWL 2005), pp. 86–98 (2005)
12. Martnez-Alemn, A.M., Wartman, K.L.: Online Social Networking on Campus Understanding What Matters in Student Culture. Taylor and Francis, Routledge (2008)
13. Puzar, M., Plagemann, T.: Data sharing in mobile ad-hoc networks - a study of replication and performance in the MIDAS data space. *Int. J. Space-Based Situated Comput.* **1**(1), 18–29 (2011). doi:[10.1504/IJSSC.2011.040340](https://doi.org/10.1504/IJSSC.2011.040340)
14. Spaho, E., Kulla, E., Xhafa, F., Barolli, L.: P2P solutions to efficient mobile peer collaboration in MANETs. In: Proceedings of 3PGCIC 2012, pp. 379–383, November 2012
15. Joaquim, R., Zùquete, A., Ferreira, P.: REVS robust electronic voting system. *IADIS Int. J. WWW/Internet* **1**(2), 47–63 (2003)
16. <https://electology.org/score-voting>
17. Kandel, A.: *Fuzzy Expert Systems*. CRC Press, Boca Raton (1992)
18. Zimmermann, H.J.: *Fuzzy Set Theory and Its Applications*. Kluwer Academic Publishers, Dordrecht (1991). Second Revised Edition
19. McNeill, F.M., Thro, E.: *Fuzzy Logic a Practical Approach*. Academic Press Inc., Boston (1994)
20. Zadeh, L.A., Kacprzyk, J.: *Fuzzy Logic for the Management of Uncertainty*. Wiley, Chichester (1992)
21. Procyk, T.J., Mamdani, E.H.: A linguistic self-organizing process controller. *Automatica* **15**(1), 15–30 (1979)
22. Klir, G.J., Folger, T.A.: *Fuzzy Sets, Uncertainty, and Information*. Prentice Hall, Englewood Cliffs (1988)
23. Munakata, T., Jani, Y.: Fuzzy systems: an overview. *Commun. of ACM* **37**(3), 69–76 (1994)
24. Liu, Y., Oda, T., Matsuo, K., Barolli, L., Xhafa, F.: A fuzzy-based system for qualified voting in P2P mobile collaborative team. In: Proceedings of BWCCA-2016, pp. 175–186, November 2016.

# Energy-Aware Dynamic Migration of Virtual Machines in a Server Cluster

Dilawaer Duolikun<sup>1</sup>(✉), Ryo Watanabe<sup>1</sup>, Tomoya Enokido<sup>2</sup>,  
and Makoto Takizawa<sup>1</sup>

<sup>1</sup> Hosei University, Tokyo, Japan  
dilewerdolkun@gmail.com, ryo.watanabe.4h@stu.hosei.ac.jp,  
makoto.takizawa@computer.org

<sup>2</sup> Rissho University, Tokyo, Japan  
eno@ris.ac.jp

**Abstract.** Virtual machines are now widely used to support applications with virtual computation service in server clusters. Here, a virtual machine can migrate from a host server to a guest server while processes are being performed. In this paper, we discuss a virtual machine migration approach to reducing the electric energy consumption of servers. In our previous studies, virtual machines are fixed in a cluster. In this paper, we consider a cluster where virtual machines are dynamically created and dropped. We propose a dynamic virtual machine migration (DVMM) algorithm to reduce the total electric energy consumption of servers. We evaluate the DVMM algorithm and show the total electric energy consumption and active time of servers and the average execution time of processes can be reduced compared with other non-migration algorithms.

## 1 Introduction

Huge amount of electric energy is consumed by servers in scalable clusters like cloud computing systems [12, 17]. We have to reduce the electric energy consumed by servers [1] to realize eco society [2]. In order to discuss how to reduce the electric energy consumption of servers in a cluster, we first need a power consumption model which shows how much electric power a server consumes to perform application processes. Types of power consumption models of a server to perform computation, communication, and storage types of processes are proposed in our previous studies [13–16, 18, 19, 26–28]. In order to reduce the electric energy consumption, types of server selection algorithms [6, 14–16, 19, 20, 22–24] are proposed. Here, each time a client issues a request to a cluster, a host server is selected to perform a request process so that the total electric energy consumption of the servers can be reduced. On the other hand, a process migration approach is also discussed where processes migrate to more energy-efficient servers [4–6, 8].

A cluster provides applications with virtual computation service by using virtual machines like KVM [3] and VMware [1]. Applications processes can be performed on a virtual machine without being conscious of what servers support what computation resources in a cluster. Furthermore, a virtual machine on a host

server can migrate to a guest server while processes are being performed on the virtual machine like live migration [3, 31]. In our previous studies [7, 9–11, 29, 30], types of energy-efficient migration algorithms are proposed, where a virtual machine migrates from a host server to a more energy-efficient guest server. Here, a set of virtual machines are fixed in a cluster. In this paper, we consider a cluster where virtual machines are dynamically created and dropped depending on number of processes to be performed. We newly propose a dynamic virtual machine migration (DVMM) algorithm. Here, if a request process is issued to a cluster, a host server is first selected. Then, a virtual machine is newly created or selected in existing virtual machines and the process is performed on the virtual machine. Each virtual machine migrates from the host server to a guest server if processes on the virtual machine can be more energy-efficiently performed on the guest server. We evaluate the DVMM algorithm compared with the non-dynamic virtual machine migration EAMV [11] and non-migration algorithms. We show the total electric energy of servers can be reduced by the DVMM algorithm in the evaluation.

In Sect. 2, we present a model of virtual machines. In Sect. 3, we discuss power consumption and computation models of a server. In Sect. 4, we discuss how to estimate the expected electric energy of servers. In Sect. 5, we propose the DVMM algorithm. In Sect. 6, we evaluate the DVMM algorithm.

## 2 System Model

A cluster  $S$  is composed of servers  $s_1, \dots, s_m$  ( $m \geq 1$ ). Each server  $s_t$  is equipped with a set  $CP_t$  of  $np_t$  ( $\geq 1$ ) homogeneous CPUs,  $cp_{t0}, \dots, cp_{t,np_t-1}$ . Each CPU  $cp_{tk}$  is composed of  $cc_t$  ( $\geq 1$ ) homogeneous cores  $c_{tk0}, \dots, c_{tk,cc_t-1}$ . Each core  $c_{tki}$  supports a set  $\{th_{tki0}, \dots, th_{tki,ct_t-1}\}$  of  $ct_t$  ( $\geq 1$ ) homogeneous threads. ( $\geq 1$ ). A server  $s_t$  thus supports processes with the total number  $nt_t = np_t \cdot cc_t \cdot ct_t$  of threads on  $nc_t (= np_t \cdot cc_t)$  cores. Each process is at a time allocated to one thread [25]. A thread is *active* if at least one process is performed, otherwise *idle*. A server is *active* if at least one thread is active, otherwise *idle*. In this paper, a *process* means a computation type of an application process to be performed on a server, which uses CPU.

A cluster  $S$  supports applications with a virtual machines. Each virtual machine  $vm_h$  is supported with threads of a server  $s_t$ . Here,  $s_t$  is a *host* server of the virtual machine  $vm_h$  and  $vm_h$  is a *resident* virtual machine of the server  $s_t$ .  $VM_t(\tau)$  shows a set of resident virtual machines on a host server  $s_t$  and  $HS_h(\tau)$  denotes a host server of a virtual machine  $vm_h$  at time  $\tau$ . A process  $p_i$  on a virtual machine  $vm_h$  is a *resident* process of the virtual machine  $vm_h$ .  $VCP_h(\tau)$  shows a set of resident processes of a virtual machine  $vm_h$  at time  $\tau$ . A virtual machine  $vm_h$  is *active* at time  $\tau$  if  $|VCP_t(\tau)| > 0$ , i.e. at least one process is performed, otherwise *idle*. Time an active virtual machine gets idle is referred to as *idled* time.  $CP_t(\tau)$  is a set of all the resident processes performed on virtual machines of a server  $s_t$  at time  $\tau$ , i.e.  $CP_t(\tau) = \cup_{VM_h \in SVM_t(\tau)} VCP_h(\tau)$ . A server  $s_t$  where at least one virtual machine resides, i.e.  $VM_t(\tau) > 0$  is a

hosting server. A virtual machine  $vm_h$  on a host server  $s_t$  can migrate to a guest server  $s_u$  while resident processes are performed.

### 3 Power Consumption and Computation Models

#### 3.1 MLPCM Model

The electric power consumption  $E_t(\tau)$  [W] of a server  $s_t$  to perform computation processes at time  $\tau$  is given in the MLPCM (Multi-Level Power Consumption with Multiple CPUs) model [20] as follows:

$$E_t(\tau) = \min E_t + ap_t \cdot bE_t + ac_t \cdot cE_t + at_t \cdot tE_t. \quad (1)$$

Here,  $ap_t$  ( $\leq np_t$ ),  $ac_t$  ( $\leq nc_t$ ), and  $at_t$  ( $\leq nt_t$ ) are numbers of active CPUs, cores, and threads of a server  $s_t$ .

In Linux operating systems, processes are allocated to  $nt_t$  ( $\geq 1$ ) threads in the round-robin (RR) algorithm [25]. The electric power consumption  $CE_t(n)$  [W] of a server  $s_t$  to concurrently perform  $n$  ( $= |CP_t(\tau)|$ ) ( $\geq 1$ ) processes at time  $\tau$  is given in the MLPCM model [20] as follows:

$$CE_t(n) = \begin{cases} \min E_t & \text{if } n = 0. \\ \min E_t + n \cdot (bE_t + cE_t + tE_t) & \text{if } 1 \leq n \leq np_t. \\ \min E_t + np_t \cdot bE_t + n \cdot (cE_t + tE_t) & \text{if } np_t < n \leq nc_t. \\ \min E_t + np_t \cdot bE_t + nc_t \cdot cE_t + n \cdot tE_t & \text{if } nc_t < n \leq nt_t. \\ \max E_t = \min E_t + np_t \cdot bE_t + nc_t \cdot cE_t + nt_t \cdot tE_t & \text{if } n > nt_t. \end{cases} \quad (2)$$

Here, if  $n > nt_t$ , a server  $s_t$  consumes the maximum electric power  $\max E_t = \min E_t + np_t \cdot bE_t + nc_t \cdot cE_t + nt_t \cdot tE_t$ . For  $n_1 < n_2 \leq nt_t$ ,  $CE_t(n_1) < CE_t(n_2)$ .  $CE_t(n_1) = CE_t(n_2) = \max E_t$  for  $nt_t \leq n_1 < n_2$ . Even if no process is performed, a server  $s_t$  consumes the minimum electric power  $\min E_t$ . In this paper, we assume  $E_t(\tau) = CE_t(|CP_t(\tau)|)$  for each server  $s_t$ .

#### 3.2 MLC Model

The computation model of a server shows how long it takes to perform each process on the server. It takes  $T_{ti}$  time units [tu] to perform a process  $p_i$  on a thread of a server  $s_t$ . If only a process  $p_i$  is exclusively performed on a server  $s_t$  without any other process, the execution time  $T_{ti}$  of the process  $p_i$  is minimum,  $T_{ti} = \min T_{ti}$ . In a cluster  $S$  of servers  $s_1, \dots, s_m$  ( $m \geq 1$ ),  $\min T_i$  shows a minimum one of  $\min T_{1i}, \dots, \min T_{mi}$ . That is,  $\min T_i = \min T_{fi}$  on the fastest thread which is on a server  $s_f$  in the cluster  $S$ . Here, the server  $s_f$  is *fastest*. We assume one virtual computation step [vs] is performed on a thread of the fastest server  $s_f$  for one time unit [tu]. This means, the maximum computation rate  $\max CRT_f$  of a thread of a fastest server  $s_f$  is assumed to be one [vs/tu]. Here, the maximum computation rate  $\max CRT$  in the cluster  $S$  is  $\max CRT_f$  ( $= 1$ ). On another server  $s_t$ ,  $\max CRT_t \leq \max CRT_f$ . The total number  $VC_i$  of

virtual computation steps of a process  $p_i$  is defined to be  $minT_i$  [tu]  $\cdot$   $maxCRT_f$  [vs/tu] =  $minT_i$  [vs] where a server  $s_f$  is the fastest. The maximum computation rate  $maxCR_{ti}$  of a process  $p_i$  on a server  $s_t$  is  $VC_i/minT_{ti}$  [vs/tu] ( $\leq 1$ ). On a fastest server  $s_f$ ,  $maxCR_{fi} = maxCRT_f = maxCRT = 1$ . For every pair of processes  $p_i$  and  $p_j$  on a server  $s_t$ ,  $maxCR_{ti} = maxCR_{tj} = maxCRT_t$  ( $\leq 1$ ) [18]. The computation rate  $CR_t(\tau)$  of a server  $s_t$  at time  $\tau$  is  $at_t \cdot maxCRT_t$  where  $at_t$  ( $\leq nt_t$ ) is the number of active threads. The maximum computation rate  $maxCR_t$  of a server  $s_t$  is  $nt_t \cdot maxCRT_t$ . The computation rate  $NPR_t(n)$  [vs/tu] of a server  $s_t$  to perform  $n$  processes is given from the computation rate  $CR_t(\tau)$  as follows:

$$NPR_t(n) = \begin{cases} n \cdot maxCRT_t & \text{if } n \leq nt_t. \\ maxCR_t (= nt_t \cdot maxCRT_t) & \text{if } n > nt_t. \end{cases} \quad (3)$$

Here, each process  $p_i$  is performed at rate  $NPR_{ti}(n) = NPR_t(n)/n$ .

**[Multi-level computation (MLC) model]** [19]. The computation rate  $CR_{ti}(\tau)$  [vs/sec] of a process  $p_i$  on a server  $s_t$  at time  $\tau$  is  $NPR_{ti}(|CP_t(\tau)|)$ .

Suppose a process  $p_i$  on a server  $s_t$  starts at time  $st$  and ends at time  $et$ . Here,  $\sum_{\tau=st}^{et} CR_{ti}(\tau) = VC_i$  [vs]. At time  $\tau$  a process  $p_i$  starts on a server  $s_t$ , the computation laxity  $plc_i(\tau)$  of a process  $p_i$  is  $VC_i$ . At each time  $\tau$ , the laxity  $plc_i(\tau)$  is decremented by the computation rate  $CR_{ti}(\tau)$ . The process  $p_i$  terminates if  $plc_i(\tau) \leq 0$ .

## 4 Estimation Model

Processes issued by clients are performed on virtual machines in a clusters  $S$ . It is not easy to estimate the idled time of each virtual machine on each server  $s_t$  [7,9–11]. In this paper, we propose a simple estimation model. We assume each process  $p_i$  has the same amount of virtual computation steps,  $VC_i = VC$  as discussed in paper [21]. We also assume that every process finishes the half  $VC_i/2 = VC/2$  of the total virtual computation steps and assume  $VC = 1$ . Here, suppose  $n$  processes are currently performed on a server  $s_t$ . The total amount of computation to be performed by the  $n$  processes is  $n/2$ . If  $k$  new processes start, the amount of virtual computation of the  $k$  processes is  $k$ . Hence, totally  $(n/2 + k)$  virtual computation steps are considered to be performed on the server  $s_t$ . The computation rate of the server  $s_t$  is  $NPR_t(n+k)$ . It takes  $(n/2 + k)/NPR_t(n+k)$  time units [tu] to perform  $n$  current processes and  $k$  new processes. Hence, the expected termination time  $MET_t(n, k)$  [tu] of each server  $s_t$  to perform  $n$  current processes and  $k$  ( $\geq 0$ ) new processes is given as follows:

$$MET_t(n, k) = (n/2 + k)/NPR_t(n+k). \quad (4)$$

Here, the server  $s_t$  consumes the electric power  $CE_t(n+k)$  [W] to concurrently perform  $(n+k)$  processes. Hence, the expected electric energy



$MEE_t(n, k)$  [Wtu] is considered to be consumed by a server  $s_t$  to perform  $n$  current processes and  $k$  new processes as follows:

$$MEE_t(n, k) = MET_t(n, k) \cdot CE_t(n+k) = (n/2+k) \cdot CE_t(n+k) / NPR_t(n+k). \quad (5)$$

In the estimation model, only the number  $n (= |CP_t(\tau)|)$  of current processes performed is used to estimate the electric energy consumption of a server  $s_t$ .

## 5 A Virtual Machine Migration (VMM) Algorithm

### 5.1 Virtual Machine Selection

We newly propose a *dynamic virtual machine migration (DVMM)* algorithm in this paper. Here, virtual machines are dynamically created and dropped while the number of virtual machines is fixed in our previous algorithms [7, 9–11, 29, 30].

Let  $VM$  be a set of virtual machines in a cluster  $S$  of servers  $s_1, \dots, s_m$  ( $m \geq 1$ ). Initially,  $VM = \phi$ , i.e. there is no virtual machine in the cluster  $S$ .  $VM_t$  shows a set of resident virtual machines on each server  $s_t$ . Initially,  $VM_t = \phi$  for every server  $s_t$ .

First, a process  $p_i$  is issued to a cluster  $S$  at time  $\tau$ . Here, we assume  $n_t (= |CP_t(\tau)| \geq 0)$  processes are concurrently performed on each server  $s_t$ . Let  $nv_h$  be the number  $|VCP_h(\tau)|$  of resident processes on each virtual machine  $vm_h$ . One server  $s_t$  is selected in the cluster  $S$  and then a virtual machine  $vm_h$  is created on the server  $s_t$  as follows:

#### [VM selection (VMS)]

1. Select a server  $s_t$  whose expected electric energy consumption  $MEE_t(n_t, 1)$  is minimum in the cluster  $S$ .
2. Select a virtual machine  $vm_h$  whose  $nv_h$  is minimum in the server  $s_t$ .
3. If  $nv_h > maxNVM_t$ , create a virtual machine  $vm_h$  on the server  $s_t$ , i.e.  $VM_t = VM_t \cup \{vm_h\}$ .
4. Perform the process  $p_i$  on the virtual machine  $vm_h$ .

As discussed [29, 30], the average execution time of processes is independent of the number of virtual machines and just depends on the number of the processes on a host server. Hence, a server  $s_t$  is first selected, whose expected electric energy consumption  $MEE_t(n_t, 1)$  is minimum to perform  $n_t$  current processes and one new process  $p_i$  in the VM selection algorithm. A new virtual machine  $vm_h$  is created to perform a new process on a selected server  $s_t$  if there is no virtual machine on the server  $s_t$ . Processes are issued to the virtual machine  $vm_h$ . If the number  $nv_h$  of processes on the virtual machine  $vm_h$  is larger than  $maxNVM_t$ , i.e.  $nv_h > maxNVM_t$ , a new virtual machine  $vm_h$  is created on the server  $s_t$  and the new process  $p_i$  is performed on the virtual machine  $vm_h$ . If there are multiple resident virtual machines on a server  $s_t$ , a resident virtual machine  $vm_h$  is selected, whose  $nv_h$  is minimum. If  $nv_h > maxNVM_t$ , a new virtual machine

$vm_h$  is created where the process  $p_i$  is performed. Otherwise, the process  $p_i$  is performed on the virtual machine  $vm_h$ .

As a resident process terminates on a virtual machine  $vm_h$ , the number  $nv_h$  of resident processes decreases. If a virtual machine  $vm_h$  gets idle, i.e.  $nv_h = 0$ , the virtual machine  $vm_h$  is dropped on a host server  $s_t$  as follows:

### [VM drop]

1. A process  $p_i$  terminates on a virtual machine  $vm_h$  of a host server  $s_t$ .
2. If the virtual machine  $vm_h$  is idle, i.e. no process is performed, the virtual machine  $vm_h$  is dropped,  $VM_t = VM_t - \{vm_h\}$ ;

If a new process is issued to a cluster  $S$ , a virtual machine  $vm_h$  is created on a server. If a virtual machine  $vm_h$  gets idle, the virtual machine  $vm_h$  is dropped. Thus, virtual machines are dynamically created and dropped depending on the number of processes performed in cluster  $S$ .

## 5.2 Virtual Machine Migration

Each server  $s_t$  is periodically checked if an active virtual machine  $vm_h$  on the server  $s_t$  is to migrate to another server.

[VM migration (VMM)]. The following procedure is periodically performed for each server  $s_t$ :

1. Obtain the expected electric energy consumption  $EE_u$  and expected termination time  $ET_u$  of every server  $s_u$  to perform only  $n_u$  current processes ( $u = 1, \dots, m$ );

$$EE_u = MEE_u(n_u, 0); ET_u = MET_u(n_u, 0);$$

2. Select a virtual machine  $vm_h$  in the set  $VM_t$ , where  $nv_{th}$  ( $= |VCP_h(\tau)|$ ) ( $> 0$ ) is minimum in the host server  $s_t$ . The expected electric energy  $NE_t$  and termination time  $NT_t$  of the server  $s_t$  to perform every process after the virtual machine  $vm_h$  migrates to another server are obtained as follows:

$$NE_t = MEE_t(n_t - nv_{th}, 0); NT_t = MET_t(n_t - nv_{th}, 0);$$

3. Obtain the expected electric energy consumption  $NE_{tu}$  and expected termination time  $NT_{tu}$  of each server  $s_u$  ( $\neq s_t$ ) to perform not only the  $n_u$  current processes but also  $nv_{th}$  processes on the virtual machine  $vm_h$ ;

$$NE_{tu} = MEE_u(n_u + nv_{th}, 0); NT_{tu} = MET_u(n_u + nv_{th}, 0);$$

4. Select a server  $s_u$  where  $EE_t + EE_u > NE_t + NE_{tu}$  and  $NE_{tu}$  is minimum;
5. Migrate the virtual machine  $mv_h$  from the host server  $s_t$  to the guest server  $s_u$  if  $s_u$  is found.

For each server  $s_t$ , the steps in the VM migration algorithm are performed. At step 1, the expected electric energy  $EE_u$  and expected termination time  $ET_u$  of each server  $s_u$  are obtained where only  $n_u$  current processes are performed, i.e. no resident virtual machine migrates. At step 2, one resident virtual machine  $vm_h$  is selected on the server  $s_t$ , where the minimum number  $nv_{th}$  of processes are performed. The expected electric energy consumption  $EE_t$  of the server  $s_t$  is obtained by the estimation procedure  $MEE_t(n_t - nv_{th}, 0)$ , where the virtual machine  $vm_h$  migrates from a server  $s_t$  to another server. That is,  $nv_{th}$  processes leave the server  $s_t$ . Next, the virtual machine  $vm_h$  migrates to another server  $s_u$ . Here,  $nv_{th}$  processes carried by the virtual machine  $vm_h$  are performed on the server  $s_u$  in addition to  $n_u$  current processes. Hence, the expected electric energy consumption  $NE_{tu}$  of the server  $s_u$  is  $MEE_t(n_u + nv_{th}, 0)$ . For the server  $s_t$ , the expected electric energy consumption  $NE_{tu}$  of each server  $s_u$  ( $\neq s_t$ ) is obtained. We find a server  $s_u$  where the total electric energy consumption of the servers  $s_t$  and  $s_u$  can be reduced, i.e.  $EE_t + EE_u > NE_t + NE_{tu}$  and  $NE_{tu}$  is minimum. Then, the virtual machine  $vm_h$  migrates from the server  $s_t$  to the server  $s_u$ .

## 6 Evaluation

We evaluate the DVMM algorithm in terms of the total electric energy consumption  $TEE$  [Wtu] and total active time  $TAT$  [tu] of servers and the average execution time  $AET$  [tu] of processes compared with the migration type EAMV algorithm [11] the non-migration random (RD) and round robin (RR) algorithms. In the RD algorithm, one virtual machine  $vm_h$  is randomly selected. In the RR algorithm, a virtual machine  $vm_h$  is selected after a virtual machine  $vm_{h-1}$ . In the RD and RR algorithms, every virtual machine  $vm_h$  does not migrate. In the EAMV algorithm, the number  $v$  of virtual machines are fixed where  $v = 8$ . In the DVMM algorithm, virtual machines are dynamically created and dropped. In the EAMV and DVMM algorithms, a virtual machine  $vm_h$  is selected and migrates to an energy-efficient guest server. In the evaluation,  $maxNVM$  is 5.

There are  $m$  heterogeneous servers  $s_1, \dots, s_m$  in a cluster  $S$ . The electric power consumption parameters like  $minE_t$  and  $maxE_t$  [W] and the performance parameters like  $maxCRT_t$  of each server  $s_t$  are randomly taken as shown in Table 1. Initially, there is no virtual machine in the cluster  $S$ .

The number  $n(\geq 1)$  of processes  $p_1, \dots, p_n$  are randomly issued to the cluster  $S$ . In the simulation, one time unit [tu] is assumed to be 100 [msec]. In each process configuration  $PF_{ng}$ , the minimum execution time  $minT_i$  of each process  $p_i$  is randomly taken from 5 to 10 [tu], i.e. 0.5 to 1.0 [sec]. The amount  $VS_i$  [vs] of virtual computation steps of each process  $p_i$  is  $minT_i$  as discussed in this paper. The start time  $stime_i$  of each process  $p_i$  is randomly taken from 0 to  $xtime - 1$ . The simulation time  $xtime$  is 1,000 [tu] (= 100 [sec]). The simulation is time-based. We randomly generate four process configurations  $PF_{n1}, \dots, PF_{n4}$  of the processes  $p_1, \dots, p_n$ .

Four server configurations  $SF_1, \dots, SF_4$  of the servers  $s_1, \dots, s_m$  ( $m = 4$ ) are randomly generated. In each server configuration  $SF_k$ , the parameters of each

server  $s_t$  are randomly taken. For each combination of the configurations  $SF_k$  and  $PF_{ng}$ , the electric energy consumption  $EE_t$  and active time  $AT_t$  of each server  $s_t$  and the execution time  $ET_i$  of each process  $p_i$  are obtained.

Figure 1 shows the total electric energy  $TEE = EE_1 + \dots + EE_4$  [J] of the servers  $s_1, \dots, s_4$  for number  $n$  of processes. As shown in Fig. 1, the total electric energy consumption  $TEE$  of the DVMM algorithm is smaller than the other non-migration RD and RR algorithms. For example, only 40% of the electric energy of the RD and RR algorithm is consumed in the DVMM and EAMV algorithms for  $n \geq 800$ . In the DVMM and EAMV algorithms, a virtual machine on a host server migrates to another guest server if the host server is expected to consume more electric energy to perform processes. Hence, the total electric energy consumption  $TEE$  of the clusters can be reduced in the DVMM algorithm compared with the non-migration algorithms. The servers consume smaller electric energy in the DVMM algorithm than the EAMV algorithm.

Figure 2 shows the total active time  $AT$  [tu] of the four servers for the number  $n$  of processes. The active time of a server  $s_t$  means time when the server  $s_t$  is active, i.e. at least one process is performed on the server  $s_t$ . The total active

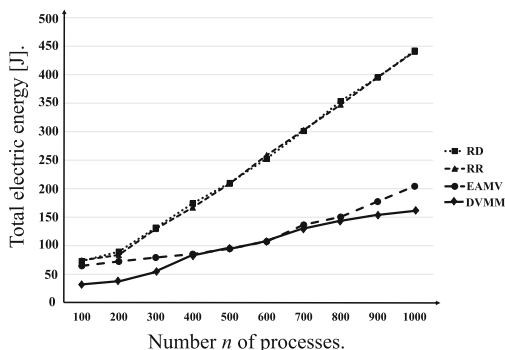


Fig. 1. Total electric energy consumption ( $m = 4$ ).

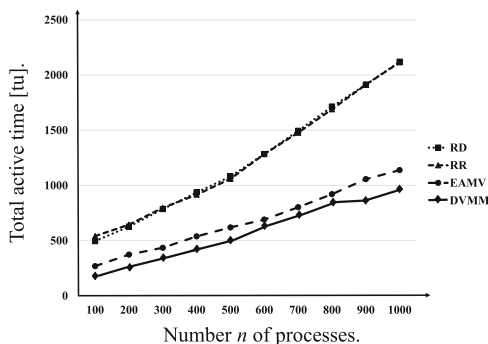
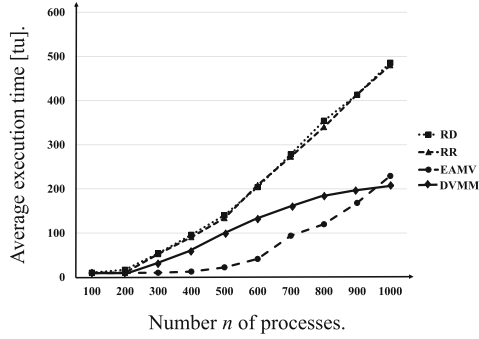


Fig. 2. Total active time of servers ( $m = 4$ ).



**Fig. 3.** Average execution time of processes ( $m = 4$ ).

**Table 1.** Parameters.

Parameters	Values
$m$	Number of servers $s_1, \dots, s_m$ ( $\geq 1$ )
$np_t$	Number of CPUs ( $\leq 2$ )
$cc_t$	Number of cores ( $1 \sim 8$ )/CPU
$ct_t$	Threads/Core ( $= 2$ )
$nt_t$	Number of threads ( $= 2 \cdot np_t \cdot cc_t$ )
$maxCRT_t$	$0.5 \sim 1$ [vs/tu]
$maxCR_t$	$nt_t \cdot maxCRT_t$ [vs/tu]
$minE_t$	$80 \sim 100$ [W]
$maxE_t$	$100 \sim 200$ [W]
$bE_t$	$(maxE_t - minE_t)/(4 \cdot np_t)$ [W]
$cE_t$	$5 \cdot (maxE_t - minE_t)/(8 \cdot np_t \cdot nc_t)$ [W]
$tE_t$	$(maxE_t - minE_t)/(8 \cdot nt_t)$ [W]
$n$	Number of processes $p_1, \dots, p_n$ ( $n \geq 1$ )
$minT_i$	Minimum computation time of a process $p_i$ ( $5 \sim 10$ [tu])
$VS_i$	$5 \sim 10$ [vs] ( $VS_i = minT_i$ )
$stime_i$	Starting time of $p_i$ ( $0 \leq st_i < xtime - 1$ )
$xtime$	Simulation time ( $= 200$ [tu] $= 20$ [sec])
$v$	Number of virtual machines $VM_1, \dots, VM_v$ ( $v = 8$ )

time of the  $m$  servers in the DVMM algorithm is shorter than the EAMV and non-migration algorithms. For example, the total active time  $AT$  of the servers of the DVMM algorithm is half of the RR and RD algorithms and 10% shorter than the EAMV algorithm. This means, the servers are more lightly loaded in the DVMM algorithm than the other algorithms.

Figure 3 shows the average execution time  $AET$  [tu] of the number  $n$  of processes on the four servers.  $AET = (et_1 + \dots + et_n)/n$  for number  $n$  of processes  $p_1, \dots, p_n$ . The average execution time  $AET$  of the processes in the DVMM algorithm is shorter than the RD and RR algorithms but the longer than the EAMV algorithm. In the simulation, the average minimum execution time ( $= (minT_1 + \dots + minT_n)/n$ ) of the processes is 7.5 [tu] as shown in Table 1. In the DVMM algorithm, the  $AET$  of the  $n$  processes is shorter than 10 [tu] for  $n \leq 300$  and 11 [tu] for  $n = 200$ . On the other hand, the  $AET$  of the  $n$  processes is about 50 and 100 [tu] in the RD and RR algorithms for  $n = 300$  and  $n = 400$ , respectively. By migrating virtual machines, the average execution time  $AET$  of the processes can be thus reduced in the DVMM algorithm compared with the non-migration algorithms.

## 7 Concluding Remarks

In this paper, the electric energy consumption of servers in a cluster is tried to be reduced by migrating virtual machines from host servers to guest servers. In this paper, virtual machines are dynamically created and dropped depending on the number of processes. We newly proposed the dynamic virtual machine migration (DVMM) algorithm. Here, a host server is first selected if a new process is issued to a cluster. Then, a virtual machine is created on the host server if the minimum number of resident processes on the virtual machines is larger. Then, the process is performed on the virtual machine. Furthermore, each server is periodically checked. If there is a guest server which is expected to consume smaller electric energy, a virtual machine migrates from the host server to the guest server. We evaluated the DVMM algorithm and showed the total electric energy consumption and the active time of servers can be reduced.

**Acknowledgment.** This work was supported by JSPS KAKENHI grant number 15H02695.

## References

1. An american company that provides cloud and virtualization software and services (vmware, inc.). <https://en.wikipedia.org/wiki/VMware>
2. COP 21, 2015 united nations climate change conference (2015). [https://en.wikipedia.org/wiki/2015\\_United\\_Nations\\_Climate\\_Change\\_Conference](https://en.wikipedia.org/wiki/2015_United_Nations_Climate_Change_Conference)
3. A virtualization infrastructure for the Linux Kernel (kernel-based virtual machine). [https://en.wikipedia.org/wiki/Kernel-based\\_Virtual\\_Machine](https://en.wikipedia.org/wiki/Kernel-based_Virtual_Machine)
4. Duolikun, D., Aikebaier, A., Enokido, T., Takizawa, M.: Power consumption models for migrating processes in a server cluster. In: Proceedings of the 17th International Conference on Network-Based Information Systems (NBIS-2014), pp. 155–162 (2014)
5. Duolikun, D., Enokido, T., Takizawa, M.: Asynchronous migration of process replicas in a cluster. In: Proceedings of IEEE the 29th International Conference on Advanced Information Networking and Applications (AINA-2015), pp. 271–278 (2015)

6. Duolikun, D., Enokido, T., Takizawa, M.: Energy-efficient replication and migration of processes in a cluster. In: Proceedings of the 9th International Conference on Complex, Intelligent and Software Intensive Systems (CISIS-2015), pp. 118–125 (2015)
7. Duolikun, D., Enokido, T., Takizawa, M.: An energy-aware algorithm to migrate virtual machines in a server cluster. Accepted at Int. J. Space-Based Situated Comput. (2017)
8. Duolikun, D., Nakamura, S., Enokido, T., Takizawa, M.: An energy-efficient process migration approach to reducing electric energy consumption in a cluster of servers. Int. J. Commun. Netw. Distrib. Syst. **15**(4), 400–420 (2015)
9. Duolikun, D., Nakamura, S., Watanabe, R., Enokido, T., Takizawa, M.: Energy-aware migration of virtual machines in a cluster. In: Proceedings of the 11th International Conference on Broadband and Wireless Computing, Communication and Applications (BWCCA-2016), pp. 21–32 (2016)
10. Duolikun, D., Watanabe, R., Enokido, T., Takizawa, M.: A model for migration of virtual machines to reduce electric energy consumption. In: Proceedings of the 10th International Conference on Complex, Intelligent and Software Intensive Systems (CISIS-2016), pp. 160–166 (2016)
11. Duolikun, D., Watanabe, R., Enokido, T., Takizawa, M.: A model for migration of virtual machines to reduce electric energy consumption. In: Proceedings of the 19th International Conference on Network-Based Information Systems (NBIS-2016), pp. 50–57 (2016)
12. Elnozahy, E.N., Kistler, M., Rajamony, R.: Energy-efficient server clusters. Power-Aware Comput. Syst. **2325**, 179–197 (2003)
13. Enokido, T., Aikebaier, A., Deen, M., Takizawa, M.: Power consumption-based server selection algorithms for communication-based systems. In: Proceedings of the 13th International Conference on Network-Based Information Systems (NBIS-2010), pp. 201–208 (2010)
14. Enokido, T., Aikebaier, A., Takizawa, M.: A model for reducing power consumption in peer-to-peer systems. IEEE Syst. J. **4**(2), 221–229 (2010)
15. Enokido, T., Aikebaier, A., Takizawa, M.: Process allocation algorithms for saving power consumption in peer-to-peer systems. IEEE Trans. Ind. Electron. **58**(6), 2097–2105 (2011)
16. Enokido, T., Aikebaier, A., Takizawa, M.: An extended simple power consumption model for selecting a server to perform computation type processes in digital ecosystems. IEEE Trans. Ind. Inf. **10**(2), 1627–1636 (2014)
17. Ghemawat, S., Gobiuff, H., Leung, S.T.: The Google file system. In: Proceedings of ACM the 19th Symposium on Operating System Principle (SOPI 2003), pp. 29–43 (2003)
18. Kataoka, H., Duolikun, D., Enokido, T., Takizawa, M.: Multi-level computation and power consumption models. In: Proceedings of the 18th International Conference on Network-Based Information Systems (NBIS-2015), pp. 40–47 (2015)
19. Kataoka, H., Duolikun, D., Enokido, T., Takizawa, M.: Power consumption and computation models of a server with a multi-core CPU and experiments. In: Proceedings of IEEE the 29th International Conference on Advanced Information Networking and Applications Workshops (WAINA-2015), pp. 217–223 (2015)
20. Kataoka, H., Duolikun, D., Enokido, T., Takizawa, M.: Energy-aware server selection algorithm in a scalable cluster. In: Proceedings of IEEE the 30th International Conference on Advanced Information Networking and Applications (AINA-2016), pp. 565–572 (2016)

21. Kataoka, H., Duolikun, D., Enokido, T., Takizawa, M.: Simple energy-aware algorithms for selecting a server in a scalable cluster. In: Proceedings of IEEE the 31st International Conference on Advanced Information Networking and Applications Workshops (WAINA-2017), pp. 146–153 (2017)
22. Kataoka, H., Sawada, A., Duolikun, D., Enokido, T., Takizawa, M.: Simple energy-efficient server selection algorithm in a scalable cluster. In: Proceedings of the 11th International Conference on Broadband and Wireless Computing, Communication and Applications (BWCCA-2016), pp. 45–46 (2016)
23. Lynar, T.M., Herbert, R.D., Chivers, S., Chivers, W.J.: Resource allocation to conserve energy in distributed computing. *Int. J. Grid Util. Comput.* **2**(1), 1–10 (2011)
24. Lynar, T.M., Simon, Herbert, R.D., Chivers, W.J.: Reducing energy consumption in distributed computing through economic resource allocation. *Int. J. Grid Util. Comput.* **4**(4), 231–241 (2013)
25. Negus, C., Boronczyk, T.: *CentOS Bible*, 1st edn. Wiley, Hoboken (2009)
26. Sawada, A., Kataoka, H., Duolikun, D., Enokido, T., Takizawa, M.: Energy-aware clusters of servers for storage and computation applications. In: Proceedings of IEEE the 30th International Conference on Advanced Information Networking and Applications (AINA-2016), pp. 400–407 (2016)
27. Sawada, A., Kataoka, H., Duolikun, D., Enokido, T., Takizawa, M.: Energy-aware server selection algorithms for storage and computation processes. In: Proceedings of the 11th International Conference on Broadband and Wireless Computing, Communication and Applications (BWCCA-2016), pp. 45–56 (2016)
28. Sawada, A., Kataoka, H., Duolikun, D., Enokido, T., Takizawa, M.: Selection algorithms to select energy-efficient servers for storage and computation processes. In: Proceedings of the 19th International Conference on Network-Based Information Systems (NBIS-2016), pp. 218–225 (2016)
29. Watanabe, R., Duolikun, D., Enokido, T., Takizawa, M.: An eco model of process migration with virtual machines in clusters. In: Proceedings of the 18th International Conference on Network-Based Information Systems (NBIS-2016), pp. 292–297 (2016)
30. Watanabe, R., Duolikun, D., Enokido, T., Takizawa, M.: Energy-aware virtual machine migration models in a scalable cluster of servers. In: Proceedings of IEEE the 31st International Conference on Advanced Information Networking and Applications (AINA-2017), pp. 85–92 (2017)
31. Xilong, Q., Peng, X.: An energy-efficient virtual machine scheduler based on CPU share-reclaiming policy. *Int. J. Grid Util. Comput.* **6**(2), 113–120 (2015)



# Flexible Synchronization Protocol to Prevent Illegal Information Flow in Peer-to-Peer Publish/Subscribe Systems

Shigenari Nakamura<sup>1</sup>(✉), Lidia Ogiela<sup>2</sup>, Tomoya Enokido<sup>3</sup>,  
and Makoto Takizawa<sup>1</sup>

<sup>1</sup> Hosei University, Tokyo, Japan  
nakamura.shigenari@gmail.com, makoto.takizawa@computer.org

<sup>2</sup> AGH University of Science and Technology, Krakow, Poland  
logiela@agh.edu.pl

<sup>3</sup> Rissho University, Tokyo, Japan  
eno@ris.ac.jp

**Abstract.** In the peer-to-peer type of topic-based publish/subscribe (P2PPS) model, each peer (process) can publish event messages and event messages are notified to target peers with no centralized coordinator. Some information of a peer may flow to target peers by publishing an event message. Here, a target peer recognizes an event message to be related with topics which are in a publication of the event message and the peer subscribes. On the other hand, the peer forgets topics which are in a publication of the event message but not in a set of topics which the peer subscribes. We have to prevent illegal information flow to occur by flowing the forgotten topics. In this paper, we newly propose a flexible synchronization (FS) protocol and a relevance concept of topics to prevent illegal information flow to be caused by the forgotten topics. In the FS protocol, even if an event message carries forgotten topics, a peer accepts the event message if the forgotten topics are related with the subscription topics. In the evaluation, the number of illegal information flows decreases in the FS protocol.

## 1 Introduction

A distributed system is composed of peer processes (peers) which are cooperating with one another by exchanging messages in networks. In distributed systems, information in objects flow to other objects by transactions manipulating the objects. If a peer can read data of an object, which the peer is not allowed to read, by accessing to another object, illegal information flow occur. Types of synchronization protocols [6–17] are proposed based on the role-based access control (RBAC) model [5] to prevent illegal information flow among objects. On the other hand, context-based systems like publish/subscribe (PS) systems [1, 2, 4, 25] are getting important in various applications. In this paper, we consider a peer-to-peer (P2P) model of topic-based PS system [24] (P2PPS model) [22, 23]

where each peer can play both publisher and subscriber roles and there is no centralized coordinator. This means, event messages from multiple peers are delivered to a destination peer independently of one another.

In the *topic-based access control* (TBAC) model of PS systems [18], a peer manipulates topics in publish (*pb*) and subscribe (*sb*) operations. An access rule  $\langle p_i, t, op \rangle$  means that a peer  $p_i$  is allowed to manipulate a topic  $t$  in an operation  $op$ .  $p_i.P$  shows the publication of a peer  $p_i$ , which is a subset of topics granted to the peer  $p_i$ .  $p_i.S$  indicates the subscription of a peer  $p_i$  which is also a subset of topics granted to the peer  $p_i$ . An event message  $e$  published by a peer  $p_i$  is notified to a target peer  $p_j$  if the subscription  $p_j.S$  includes at least one common topic with the publication  $e.P$ . Here, the topics which are in the publication  $e.P$  but not in the subscription  $p_j.S$  are *forgotten* topics of a target peer  $p_j$ . Suppose the peer  $p_i$  publishes the event message  $e_2$  after receiving another event message  $e_1$  from other peer. Here, the event message  $e_2$  may include *hidden* topics which are in the subscription  $p_i.S$  of the publisher peer  $p_i$  but not in the publication  $e_2.P$  of  $e_2$ . This means, the event message  $e_2$  may bring event messages related with the hidden topics to the target peer  $p_j$ . Hidden or forgotten topics of an event message for a peer are *implicit* topics. Thus, the target peer  $p_j$  receives an event message regarding some topics which the peer  $p_j$  is not allowed to subscribe. Here, an illegal information flow from the peer  $p_i$  to the peer  $p_j$  occurs.

In our previous studies, the subscription-based synchronization (SBS) [18], subscription initialization SBS (SI-SBS) [19], topic-based synchronization (TBS) [20], and SI-TBS [20] protocols are proposed based on the TBAC model to prevent illegal information flow of the hidden topics. In the every protocol, the notification of an event message which may cause illegal information flow is banned at each target peer. In the SBS and SI-SBS protocols, it is checked whether or not the notification may cause illegal information flow in terms of access rights of each peer. In the TBS and SI-TBS protocols, it is checked whether or not the notification may cause illegal information flow in terms of only topics which each peer really manipulates. However, the SBS, SI-SBS, TBS, and SI-TBS protocols do not prevent the illegal information flow to occur by the forgotten topics.

In this paper, we newly propose a *flexible synchronization* (*FS*) protocol and a relevance concept of topics to prevent illegal information flow of forgotten topics. In the FS protocol, if an event message with the forgotten topics is notified to a target peer, the peer does not ban the notification and rather includes the forgotten topics in the subscription if the forgotten topics are related with topics in which the peer is interested. Even if a peer knows only a part of topics in a system, the peer can newly obtain topics in the subscription, which are related with topics which the peer subscribes. We evaluate the FS protocol in terms of the number of illegal information flows. In the evaluation, the number of illegal information flows decreases as the number of event messages published increases in the FS protocol.

In Sect. 2, we discuss the information flow relation among peers in the TBAC model. In Sect. 3, we propose the FS protocol and the relevance concept of topics to prevent illegal information flow of the forgotten topics to occur. In Sect. 4, we evaluate the FS protocol.

## 2 Information Flow in TBAC Model

### 2.1 TBAC Model

In this paper, we consider a peer-to-peer (P2P) model of a publish/subscribe (PS) system [1, 2, 4, 25] (P2PPS model) [22, 23] which includes a set  $P$  of peer processes (peers)  $p_1, \dots, p_{pn}$  ( $pn \geq 1$ ) with no centralized coordinator. Each peer  $p_i$  can play both publisher and subscriber roles and a pair of event messages published by different peers are independently delivered to every common target peer in the P2PPS model. In this paper, we consider a topic-based PS system [24]. Let  $T$  be a set  $\{t_1, \dots, t_{tn}\}$  ( $tn \geq 1$ ) of all topics in a system. A peer  $p_i$  publishes an event message  $e$  with publication  $e.P (\subseteq T)$ . A peer  $p_i$  specifies the subscription  $p_i.S (\subseteq T)$ , which shows topics in which the peer  $p_i$  is interested. An event message  $e$  is notified to a peer  $p_i$  if the publication  $e.P$  and the subscription  $p_i.S$  include at least one common topic, i.e.  $e.P \cap p_i.S \neq \phi$ . Here,  $p_i$  is a *target* peer of the event message  $e$ .

In the *topic-based access control* (TBAC) model [18], an access rule  $\langle p_i, t, op \rangle$  means that a peer  $p_i$  is allowed to manipulate a topic  $t$  in an operation  $op$ . Here,  $op$  shows a publish ( $pb$ ) or subscribe ( $sb$ ) operation. Let  $A$  be a set of access rules authorized in the system. An access right is specified in a pair  $\langle t, op \rangle$  of a topic  $t$  and an operation  $op$ . A peer  $p_i$  is allowed to publish an event message  $e$  with publication  $e.P (\subseteq T)$  only if the peer  $p_i$  is granted a publication right  $\langle t, pb \rangle$  for every topic  $t$  in the publication  $e.P$ . The subscription  $p_i.S (\subseteq T)$  of a peer  $p_i$  is a subset of topics on which the peer  $p_i$  is allowed to subscribe an event message, i.e.  $\{t \mid \langle p_i, t, sb \rangle \in A\}$ . If a peer  $p_i$  is a target peer of an event message  $e$ , topics which are in the publication  $e.P$  but not in the subscription  $p_i.S$  are *forgotten* topics  $e.F$  of the event message  $e$ . Here, a target peer  $p_i$  recognizes an event message  $e$  with respect to topics in the intersection of  $e.P$  and  $p_i.S$  but forgets the forgotten topics.

Figure 1 shows the TBAC model. Suppose there are three peers  $p_i, p_j$ , and  $p_k$ . Here, the peer  $p_j$  is allowed to publish an event message  $e_1$  on a topic  $t_1$  since  $p_j$  is granted an access right  $\langle t_1, pb \rangle$ . The peer  $p_i$  is allowed to receive the event message  $e_1$  which is related with the topic  $t_1$  since  $p_i$  is granted an access right  $\langle t_1, sb \rangle$ . However, the peer  $p_j$  is not allowed to receive an event message which is related with the topic  $t_2$  and  $t_3$  published by the peer  $p_i$  since  $p_j$  is not granted an access rights  $\langle t_2, sb \rangle$  and  $\langle t_3, sb \rangle$ . The peer  $p_k$  is allowed to receive an event message  $e_2$  published by the peer  $p_i$  which is granted access rights  $\langle t_2, pb \rangle$  and  $\langle t_3, pb \rangle$  since  $p_k$  is granted an access right  $\langle t_2, sb \rangle$ . Here, the topic  $t_3$  which is related with the event message  $e_2$  but the peer  $p_k$  is not allowed to subscribe is forgotten topic.

### 2.2 Information Flow Relations

Suppose a peer  $p_i$  publishes an event message  $e_2$  with a publication  $e.P (\subseteq p_i.P)$  after receiving another event message  $e_1$ . Here, the event message  $e_2$  might carry data in the event message  $e_1$  which is characterized by topics  $e_1.P$ . Some topics

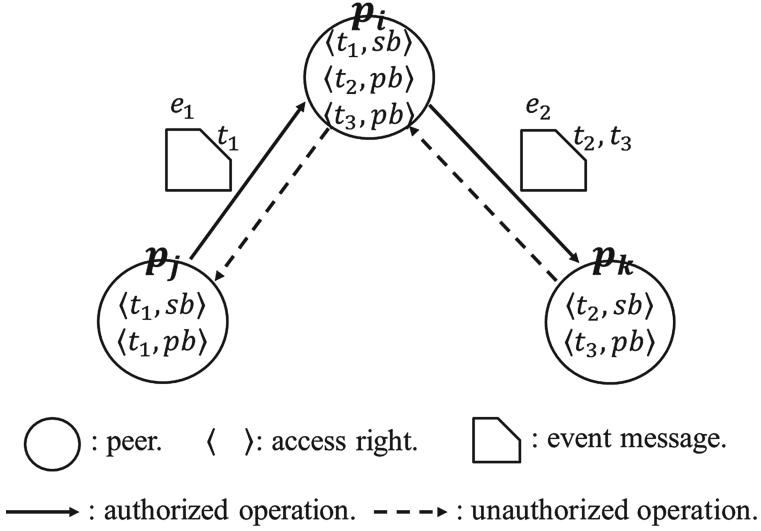


Fig. 1. TBAC model

in  $e_1.P$  which are not in  $e_2.P$  are hidden topics which a target peer of  $e_2$  does not know. Let  $e.H$  be a set of *hidden* topics of an event message  $e$  with respect to the target peer  $p_j$ . Hidden topics may be related with an event message  $e$  but are not included in the publication  $e.P$ , i.e.  $\{t \mid t \in p_i.S \text{ but } t \notin e.P\}$ . Here, even if a target peer  $p_j$  receives an event message  $e$ , the peer  $p_j$  does not recognize the event message  $e$  might be related with the hidden topics. Topics which are in the publication  $e.P$  but not in the subscription  $p_j.S$ , i.e.  $\{t \mid t \in e.P \text{ but } t \notin p_j.S\}$ , are *forgotten* topics  $e.F$  ( $= e.P - p_j.S$ ) of the event message  $e$  with respect to the target peer  $p_j$ . A target peer  $p_j$  recognizes an event message  $e$  to be related with topics in  $e.P \cap p_j.S$  but forgets the event message  $e$  is related with the topics in  $e.F$ .

If an event message  $e$  is notified to a target peer  $p_i$ , the event message  $e$  is related with topics in the subscription  $p_i.S$ . Furthermore, the event message  $e$  is related with not only forgotten topics  $e.F$  in the publication  $e.P$  but also hidden topics  $e.H$  which the event message  $e$  does not bring to the peer  $p_i$ . *Implicit* topics of a peer  $p_i$  are hidden or forgotten topics of event messages which the peer  $p_i$  receives.

Let  $p_i.I$  indicate a set of implicit topics of a peer  $p_i$ .  $p_i.I$  is manipulated as follows:

1.  $p_i.I$  is initially  $\phi$ .
2. Each time a peer  $p_i$  receives an event message  $e$ ,  $p_i.I = p_i.I \cup (e.H - p_i.S) \cup e.F$ ;
3. Let  $e.P$  be a set of publication topics of an event message  $e$ ,  $e.F$  be  $p_i.S - e.P$ , and  $e.H$  be  $p_i.I - e.P$ . Then, the peer  $p_i$  publishes an event message  $e$ .

Thus, implicit topics are accumulated in the peer  $p_i$  each time the peer  $p_i$  receives an event message.

First, the information flow relation ( $\rightarrow$ ) among peers is defined as follows [18,19]:

**[Definition]** A peer  $p_i$  *flows* to a peer  $p_j$  ( $p_i \rightarrow p_j$ ) iff (if and only if)  $p_i.P \cap p_j.S \neq \phi$ .

The information flow relation  $p_i \rightarrow p_j$  means an event message published by a peer  $p_i$  is allowed to be notified to a peer  $p_j$ . A pair of peers  $p_i$  and  $p_j$  are *equivalent* ( $p_i \leftrightarrow p_j$ ) iff  $p_i \rightarrow p_j$  and  $p_j \rightarrow p_i$ . A peer  $p_i$  is *compatible* with a peer  $p_j$  ( $p_i \rightarrow p_j$ ) iff the peer  $p_i$  does not flow to the peer  $p_j$ , i.e.  $p_i \not\rightarrow p_j$ . There is no information flow relation among the peers  $p_i$  and  $p_j$  if  $p_i \rightarrow p_j$ . A pair of peers  $p_i$  and  $p_j$  are compatible with each other ( $p_i \rightleftharpoons p_j$ ) iff  $p_i \rightarrow p_j$  and  $p_j \rightarrow p_i$ .

**[Definition]** [18,19]

1. A peer  $p_i$  *legally flows* to a peer  $p_j$  ( $p_i \Rightarrow p_j$ ) iff one of the following conditions holds:
  - a.  $p_i.S \neq \phi$ ,  $p_i \rightarrow p_j$ , and  $p_i.S \subseteq p_j.S$ .
  - b. For some peer  $p_k$ ,  $p_i \Rightarrow p_k$  and  $p_k \Rightarrow p_j$ .
2. A pair of peers  $p_i$  and  $p_j$  are *legally equivalent* with each other ( $p_i \Leftrightarrow p_j$ ) iff  $p_i \Rightarrow p_j$  and  $p_j \Rightarrow p_i$ .
3. A peer  $p_i$  *illegally flows* to a peer  $p_j$  ( $p_i \mapsto p_j$ ) iff  $p_i \rightarrow p_j$  but  $p_i \not\Rightarrow p_j$ .

The legal information flow relation  $\Rightarrow$  is transitive but not symmetric. If a peer  $p_i$  flows to a peer  $p_j$  ( $p_i \rightarrow p_j$ ), i.e.  $p_i.P \cap p_j.S \neq \phi$ , an event message published by the peer  $p_i$  can be notified to the peer  $p_j$ . Otherwise, no information from the peer  $p_i$  flow into the peer  $p_j$ . The condition " $p_i.S \subseteq p_j.S$ " means that every topic in the subscription  $p_i.S$  is also in the subscription  $p_j.S$ . This means, an event message  $e$  from the peer  $p_i$  to the peer  $p_j$  is related with no hidden topic for the peer  $p_j$ , i.e.  $e.H = \phi$ . It is noted  $p_i.S = p_j.S$  if  $p_i \Leftrightarrow p_j$ . For a pair of peers  $p_i$  and  $p_j$ , if  $p_i \Rightarrow p_j$  and  $p_i.S \neq p_j.S$ , the legal information flow relation  $p_j \Rightarrow p_i$  does not hold. This means, the legal information flow relation  $\Rightarrow$  is acyclic. On the other hand, the illegal information flow relation  $\mapsto$  is not transitive, differently from the transitive legal flow relation  $\Rightarrow$ . Even if  $p_i \mapsto p_j$  and  $p_j \mapsto p_k$ ,  $p_i \Rightarrow p_k$  may hold.

Suppose there are three peers  $p_i$ ,  $p_j$ , and  $p_k$  and three topics  $t_1$ ,  $t_2$ , and  $t_3$ ,  $T = \{t_1, t_2, t_3\}$  in a system. We also suppose a peer  $p_i$  is granted a pair of access rights  $\langle t_2, pb \rangle$  and  $\langle t_1, sb \rangle$ , i.e. the publication  $p_i.P (= \{t_2\})$  and subscription  $p_i.S (= \{t_1\})$ , another peer  $p_j$  is granted access rights  $\langle t_1, pb \rangle$ ,  $\langle t_1, sb \rangle$ , and  $\langle t_2, sb \rangle$ , i.e.  $p_j.P (= \{t_1\})$  and  $p_j.S (= \{t_1, t_2\})$ , and the other peer  $p_k$  is granted access rights  $\langle t_3, pb \rangle$ ,  $\langle t_1, sb \rangle$ , and  $\langle t_3, sb \rangle$ , i.e.  $p_k.P (= \{t_3\})$  and  $p_k.S (= \{t_1, t_3\})$ . First, the peer  $p_i$  publishes an event message  $e_1$  with publication  $e_1.P = \{t_2\}$  ( $\subseteq p_i.P$ ). Here, the peer  $p_i$  flows to the peer  $p_j$  ( $p_i \rightarrow p_j$ ) since  $p_i.P (= \{t_2\}) \cap p_j.S (= \{t_1, t_2\}) \neq \phi$ .  $p_i \Rightarrow p_j$  since  $p_i.S \neq \phi$ ,  $p_i \rightarrow p_j$ , and  $p_i.S (= \{t_1\}) \subseteq p_j.S (= \{t_1, t_2\})$ . Hence, the event message  $e_1$  is notified to the peer  $p_j$ .

Next, suppose a peer  $p_j$  publishes an event message  $e_2$  with publication  $e_2.P = \{t_1\}$  ( $\subseteq p_j.P$ ). Here,  $p_j \rightarrow p_k$  since  $p_j.P (= \{t_1\}) \cap p_k.S (= \{t_1, t_3\}) \neq \phi$ . However,

the peer  $p_j$  illegally flows to the peer  $p_k$  ( $p_j \mapsto p_k$ ) since  $p_j.S (= \{t_1, t_2\}) \not\subseteq p_k.S (= \{t_1, t_3\})$ . This means, an event message on the topic  $t_2$  which the peer  $p_k$  is not allowed to subscribe can be notified to the peer  $p_k$ . Here, event information illegally flows to the peer  $p_k$  from the peer  $p_j$ .

### 3 Synchronization Protocols

#### 3.1 Protocols for the Hidden Topics

We discuss protocols based on the TBAC model to prevent illegal information flow of the hidden topics among peers to be caused by publication and notification of event messages. There are two ways, subscription-based synchronization (SBS) [18] and topic-based synchronization (TBS) [20], to check whether or not illegal information flow to occur when an event message is notified to a target peer. A peer  $p_i$  includes topics in the publication  $p_i.P$  and subscription  $p_i.S$ . A peer  $p_i$  is associated with subsets  $p_i.PP$  and  $p_i.PS$  of the topics granted for publication and subscription, respectively. Here,  $p_i.PP$  and  $p_i.PS$  are referred to as publication and subscription *purposes* [3] of a peer  $p_i$ , respectively. This means, a peer  $p_i$  is allowed to issue a publication operation  $pb$  on a topic  $t$  only if  $t \in p_i.PP$  and to issue a subscription operation  $sb$  on a topic  $t$  only if  $t \in p_i.PS$ .

In the SBS way, it is checked whether or not the notification may cause illegal information flow in terms of access rights of each peer. If a peer  $p_i$  publishes an event message  $e$  with the publication  $e.P$ , a peer  $p_j$  manipulates the subscription  $p_j.S$  on receipt of the event message  $e$  as follows:

1. If  $p_i.S \Rightarrow p_j.PS$ , the event message  $e$  is notified to the peer  $p_j$  and  $p_j.S = p_i.PS \cup p_j.S$ ;
2. Otherwise, the notification of the event message  $e$  is banned at the peer  $p_j$ .

In the TBS way, it is checked whether or not the notification may cause illegal information flow in terms of only topics which each peer really manipulates. If a peer  $p_i$  publishes an event message  $e$  with the publication  $e.P$ , a peer  $p_j$  manipulates the subscription  $p_j.S$  as follows:

1. If  $p_i.S \Rightarrow p_j.PS$ , the event message  $e$  is notified to a peer  $p_j$ ;
  - a. if  $p_i.S \neq \phi$ ,  $p_j.S = p_i.S \cup p_j.S$ ;
  - b. if  $p_i.S = \phi$ ,  $p_j.S = (p_j.PS \cap e.P) \cup p_j.S$ ;
2. Otherwise, the notification is banned at the peer  $p_j$ .

In the SBS and TBS protocols, the notifications which may cause illegal information flow are banned at the target peers. To more reduce the number of notifications banned, we discuss the subscription initialization (SI) approach [19]. In the SI approach, if a notification from a peer  $p_i$  to a peer  $p_j$  is banned, the subscription  $p_i.S$  is initialized with some probability. We consider an initialization parameter  $\alpha$  to allow a peer  $p_i$  to initialize its subscription  $p_i.S$ . If the ratio of the number of notifications banned to the total number of notifications in one publication is equal to or more than  $\alpha$ , the subscription  $p_i.S$  is initialized. We evaluate the SBS, SI-SBS, TBS, and SI-TBS protocols in terms of the number of notifications banned [21].

### 3.2 Flexible Synchronization (FS) Protocol for the Forgotten Topics

In the SBS, SI-SBS, TBS, and SI-TBS protocols, illegal information flow to be caused by forgotten topics are not considered. However, illegal information flow of forgotten topics also occurs in a P2PPS system. In this paper, we propose a new flexible synchronization (FS) protocol to prevent illegal information flow of the forgotten topics.

In the FS protocol, notifications which may cause illegal information flow of forgotten topics are banned. Since P2PPS systems are open and scalable, each peer  $p_i$  may not know about every topic in the system. This means, there might be topics which a peer  $p_i$  does not know but may interest  $p_i$ . These topics might be brought to the peer by forgotten topics of event messages. In this paper, we discuss how to include forgotten topics of interest to the peer  $p_i$ . We newly introduce a *relevance* concept of topics which shows how much a pair of topics are related. In this paper, topics are ordered. This means, topics are classified. Suppose there are three topics  $t_i$ ,  $t_j$ , and  $t_k$ . If  $|i - j| < |i - k|$ , the topic  $t_j$  is more related with the topic  $t_i$  than the topic  $t_k$ . We assume the relevance  $RbT_{kl}$  ( $0 \leq RbT_{kl} \leq 1$ ) between a  $k$ th topic  $t_k$  and an  $l$ th topic  $t_l$  is given as follows:

$$RbT_{kl} = e^{-\{(l-k)^2/(2 \times 3^2)\}}. \quad (1)$$

Here, which topics each peer includes in its publication and subscription purposes are decided based on the relevance concept. The purpose of each peer is composed of topics which are related with one another. Publication of each event message is also composed of topics related to the topics in the publication purpose. On receipt of an event message  $e$ , a peer  $p_i$  accepts the event message  $e$  even if the event message  $e$  includes forgotten topics  $e.F$  if some forgotten topics are related with topics in which  $p_i$  is interested. The number of topics which each peer is allowed to subscribe increases as the number of event messages which each peer receives increases. That is, each peer  $p_i$  learns other topics which  $p_i$  should subscribe by receiving event messages and subscribes the topics which the peer cannot subscribe at first. We assume there is a main topic in the subscription purpose of each peer  $p_i$ . The main topic  $t_k$  of a peer  $p_i$  means that the peer  $p_i$  mainly subscribes the topic  $t_k$ .

**[Flexible Synchronization (FS) Protocol].** A peer  $p_i$  publishes an event message  $e$  with the publication  $e.P$  to a peer  $p_j$  whose main topic is  $t_k$ .

1. If  $e.P \subseteq p_j.PS$ , the event message  $e$  is notified to a peer  $p_j$ ;
2. If  $e.P \not\subseteq p_j.PS$ ,  $e.F \neq \phi$ , and  $BWT(e, p_j, k) \leq AWT(e, p_j, k)$ , the event message  $e$  is notified to a peer  $p_j$ . Each topic  $t_l$  ( $\{t_l \mid t_l \in e.F\}$ ) is added to  $p_j.PS$  with probability  $RbT_{kl}$ .
3. Otherwise, the notification is banned at a peer  $p_j$ .

Let  $AWT(e, p_j, k)$  be a total weight of topics in the publication  $e.P$  and subscription purpose  $p_j.PS$  of a peer  $p_j$  ( $\{t_m \mid t_m \in e.P \cap p_j.PS\}$ ) for acceptance. The total weight  $AWT(e, p_j, k)$  is given as follows:

$$AWT(e, p_j, k) = \sum_{t_m \in e.P \cap p_j.PS} RbT_{km}. \quad (2)$$

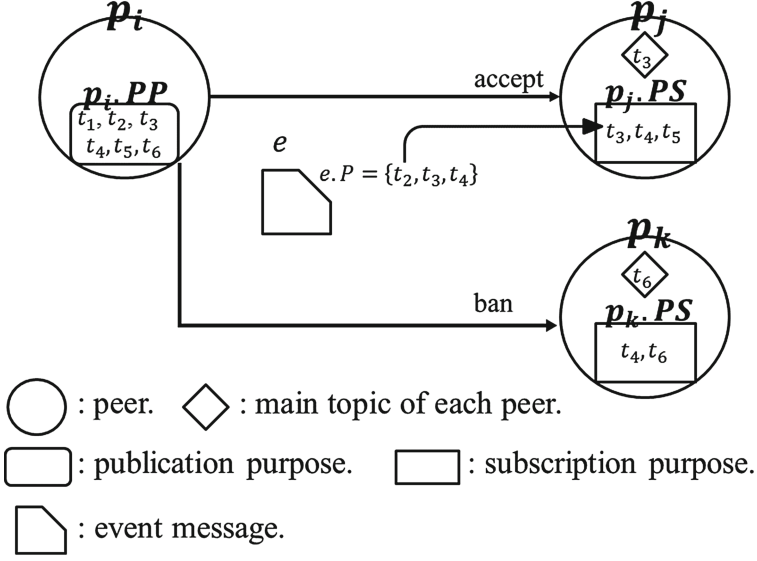


Fig. 2. FS protocol

Let  $BWT(e, p_j, k)$  be a total weight of topics ( $\{t_l \mid t_l \in e.F\}$ ) for ban. The total weight  $BWT(e, p_j, k)$  is given as follows:

$$BWT(e, p_j, k) = \sum_{t_l \in e.F} (1 - RbT_{kl}). \quad (3)$$

Suppose there are three peers  $p_i$ ,  $p_j$ , and  $p_k$  as shown in Fig. 2. Here, the publication purpose  $p_i.PS$  of the peer  $p_i$  includes six topics  $t_1$  to  $t_6$ . First, the peer  $p_i$  publishes an event message  $e$  with publication  $e.P$  which is composed of topics  $t_2$ ,  $t_3$ , and  $t_4$  to the target peers. The peer  $p_j$  receives the event message  $e$  since  $e.P \cap p_j.PS (= \{t_3, t_4\}) \neq \phi$ . Here, the total weight for acceptance  $AWT(e, p_j, 3)$  is about 1.95 ( $= RbT_{33} + RbT_{34} = 1 + 0.95$ ). The total weight for ban  $BWT(e, p_j, 3)$  is about 0.05 ( $= 1 - RbT_{32}$ ). Since  $BWT(e, p_j, 3) < AWT(e, p_j, 3)$ , the peer  $p_j$  accepts the event message  $e$ . The forgotten topic  $t_2$  is added to the subscription purpose  $p_j.PS$  with probability  $RbT_{32} (= 0.95)$ . On the other hand, the peer  $p_k$  also receives the event message  $e$  since  $e.P \cap p_k.PS (= \{t_4\}) \neq \phi$ . Here, the total weight for acceptance  $AWT(e, p_k, 6)$  is about 0.8 ( $= RbT_{64}$ ). The total weight for ban  $BWT(e, p_k, 6)$  is about 0.98 ( $= (1 - RbT_{62}) + (1 - RbT_{63}) = 0.59 + 0.39$ ). Since  $BWT(e, p_k, 6) > AWT(e, p_k, 6)$ , the notification from the peer  $p_i$  is banned at the peer  $p_k$ .

## 4 Evaluation

We evaluate the FS protocol on a topic set  $T = \{t_1, \dots, t_{tn}\}$  ( $tn \geq 1$ ) and a peer set  $P = \{p_1, \dots, p_{pn}\}$  ( $pn \geq 1$ ) in terms of number of illegal information flows.



In the FS protocol, the subscription purpose  $p_i.PS$  of the target peer  $p_i$  is updated each time an event message is notified to the peer  $p_i$ . If an event message is illegally notified to a peer  $p_i$ , the notification of the event message is banned. We assume an event message can be reliably broadcast to every target peer.

Publish ( $pb$ ) and subscribe ( $sb$ ) operations are supported on each topic. Each peer  $p_i$  is granted a publication purpose  $p_i.PP$  and a subscription purpose  $p_i.PS$  which are composed of topics which are related with one another. In the evaluation, each subscription purpose  $p_i.PS$  is generated based on the relevance of topics. The relevance between a  $k$ th topic and an  $l$ th topic is obtained by the formula (1). First, a topic  $t_k$  is randomly selected and included in the purpose  $p_i.PS$  as a topic which the peer  $p_i$  mainly subscribes. Then, each  $t_n$  of the other topics ( $\{t_n \mid t_n \in T - t_k\}$ ) are included in the purpose  $p_i.PS$  with the probability  $RbT_{kn}$ . Each publication purpose  $p_i.PP$  is also generated like subscription purpose.

In the evaluation, we consider fifty peers ( $pn = 50$ ) and twenty topics ( $tn = 20$ ). A collection  $P$  of  $pn$  peers  $p_1, \dots, p_{pn}$  are randomly generated on  $tn$  topics  $t_1, \dots, t_{tn}$ , i.e.  $P = \{p_1, \dots, p_{50}\}$  and  $T = \{t_1, \dots, t_{20}\}$ . The number  $en$  of event messages are exchanged between peers on the topic set  $T$  in the FS protocol. We randomly create a peer set  $P$  on the topic set  $T$  seven hundred times for each  $en$ . First, one peer  $p_i$  is randomly selected in the peer set  $P$ . Then, the peer  $p_i$  publishes an event message  $e$  with the publication  $e.P$  which is composed of some topics randomly selected in the publication purpose  $p_i.PP$  to every target peer  $p_j$ . If the peer  $p_j$  can subscribe all the topics in  $e.P$ , the notification is notified to the peer  $p_j$ . Even if the peer  $p_j$  is not allowed to subscribe all the topics in  $e.P$ , i.e.  $e.F \neq \phi$ , and all the topics in  $e.F$  are strongly related with a topic which the peer  $p_j$  mainly subscribes, the notification is also notified to the peer  $p_j$  and some topics in  $e.F$  are added to the subscription purpose  $p_j.PS$ . Here, all the topics in  $e.F$  are strongly related with a main topic  $t_k$  of the peer  $p_j$  means every topic  $t_l$  in  $e.F$  is added to the purpose  $p_j.PS$  with probability  $RbT_{kl}$ . Otherwise, the notification is banned. These steps are iterated  $en$  times. For a given peer set  $P$ ,  $en$  event messages are published seven hundreds times in the FS protocol. Then, we calculate the average ratio of the number of illegal information flows for each  $en$  in the FS protocol.

Figure 3 shows the ratio of the number of illegal information flows of the forgotten topics occurring to the total number of information flows for the number of event messages published. If no information flow control is performed, about 80% of information flows are illegal for one to five hundred event messages as the dotted line. On the other hand, in the FS protocol, the number of illegal information flows decreases as the number  $en$  of event messages increases. For example, about 32% of information flows are illegal for fifty event messages ( $en = 50$ ), but about 20% are for five hundred event messages ( $en = 500$ ).

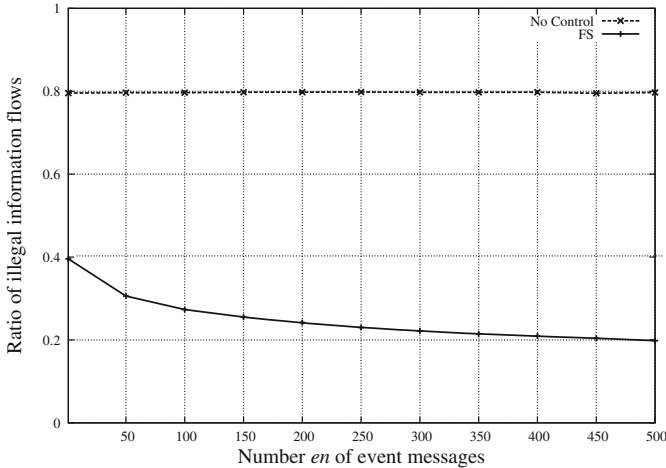


**Fig. 3.** Ratio of the illegal information flows of the forgotten topics.

## 5 Concluding Remarks

In this paper, we newly proposed the flexible synchronization (FS) protocol to prevent illegal information flow of forgotten topics in a P2PPS model based on the topic-based access control (TBAC) model. In our previous studies, the SBS, SI-SBS, TBS, and SI-TBS protocols are proposed to prevent illegal information flow of hidden topics. However, the illegal information flow of forgotten topics are not considered. In the FS protocol, the notifications which may cause illegal information flow of forgotten topics are banned. In this paper, we newly proposed the relevance concept of topics. Even if an event message carries forgotten topics, a peer accepts the event message if the forgotten topics are related with topics in the subscription purpose of the peer. Then, the forgotten topics are added to the subscription purpose of the peer. Thus, even if a peer does not know every topic in a system, the peer obtains new topics which interest the peer through notifications of event messages. The more number of event messages are published, the more number of topics each peer can subscribe. We evaluated the FS protocol in terms of number of illegal information flows occurring. In the evaluation, the number of illegal information flows decreases as the number of event messages published increases in the FS protocol.

**Acknowledgment.** This work was supported by JSPS KAKENHI grant number 15H0295.

## References

1. Google alert. <http://www.google.com/alerts>
2. Blanco, R., Alencar, P.: Event models in distributed event based systems. In: Principles and Applications of Distributed Event-Based Systems, pp. 19–42 (2010)

3. Enokido, T., Takizawa, M.: Purpose-based information flow control for cyber engineering. *IEEE Trans. Ind. Electron.* **58**(6), 2216–2225 (2011)
4. Eugster, P.T., Felber, P.A., Guerraoui, R., Kermarrec, A.M.: The many faces of publish/subscribe. *ACM Comput. Surv.* **35**(2), 114–131 (2003)
5. Ferraiolo, D.F., Kuhn, D.R., Chandramouli, R.: *Role-based Access Controls*, 2nd edn. Artech, Boston (2007)
6. Nakamura, S., Duolikun, D., Aikebaier, A., Enokido, T., Takizawa, M.: Read-write abortion (rwa) based synchronization protocols to prevent illegal information flow. In: *Proceedings of the 17th International Conference on Network-Based Information Systems (NBIS-2014)*, pp. 120–127 (2014)
7. Nakamura, S., Duolikun, D., Aikebaier, A., Enokido, T., Takizawa, M.: Role-based information flow control models. In: *Proceedings of IEEE the 28th International Conference on Advanced Information Networking and Applications (AINA-2014)*, pp. 1140–1147 (2014)
8. Nakamura, S., Duolikun, D., Aikebaier, A., Enokido, T., Takizawa, M.: Synchronization protocols to prevent illegal information flow in role-based access control systems. In: *Proceedings of the 8th International Conference on Complex, Intelligent, and Software Intensive Systems (CISIS-2014)*, pp. 279–286 (2014)
9. Nakamura, S., Duolikun, D., Enokido, T., Takizawa, M.: A flexible read-write abortion protocol to prevent illegal information flow. In: *Proceedings of IEEE the 29th International Conference on Advanced Information Networking and Applications (AINA-2015)*, pp. 155–162 (2015)
10. Nakamura, S., Duolikun, D., Enokido, T., Takizawa, M.: A flexible read-write abortion protocol to prevent illegal information flow among objects. *J. Mobile Multimedia* **11**(3&4), 263–280 (2015)
11. Nakamura, S., Duolikun, D., Enokido, T., Takizawa, M.: A flexible read-write abortion protocol with sensitivity of objects to prevent illegal information flow. In: *Proceedings of the 9th International Conference on Complex, Intelligent, and Software Intensive Systems (CISIS-2015)*, pp. 289–296 (2015)
12. Nakamura, S., Duolikun, D., Enokido, T., Takizawa, M.: A flexible read-write abortion protocol with sensitivity of roles. In: *Proceedings of the 18th International Conference on Network-Based Information Systems (NBIS-2015)*, pp. 132–139 (2015)
13. Nakamura, S., Duolikun, D., Enokido, T., Takizawa, M.: Role safety in a flexible read-write abortion protocol. In: *Proceedings of the 10th International Conference on Broadband and Wireless Computing, Communication and Applications (BWCCA-2015)*, pp. 333–340 (2015)
14. Nakamura, S., Duolikun, D., Enokido, T., Takizawa, M.: A write abortion-based protocol in role-based access control systems. *Int. J. Adapt. Innovative Syst.* **2**(2), 142–160 (2015)
15. Nakamura, S., Duolikun, D., Enokido, T., Takizawa, M.: Influential abortion probability in a flexible read-write abortion protocol. In: *Proceedings of IEEE the 30th International Conference on Advanced Information Networking and Applications (AINA-2016)*, pp. 1–8 (2016)
16. Nakamura, S., Duolikun, D., Enokido, T., Takizawa, M.: A read-write abortion (RWA) protocol to prevent illegal information flow in role-based access control systems. *Int. J. Space-Based Situated Comput.* **6**(1), 43–53 (2016)
17. Nakamura, S., Duolikun, D., Takizawa, M.: Read-abortion (RA) based synchronization protocols to prevent illegal information flow. *J. Comput. Syst. Sci.* **81**(8), 1441–1451 (2015)

18. Nakamura, S., Enokido, T., Takizawa, M.: Information flow control models in peer-to-peer publish/subscribe systems. In: Proceedings of the 10th International Conference on Complex, Intelligent, and Software Intensive Systems (CISIS-2016), pp. 167–174 (2016)
19. Nakamura, S., Enokido, T., Takizawa, M.: Subscription initialization (SI) protocol to prevent illegal information flow in peer-to-peer publish/subscribe systems. In: Proceedings of the 19th International Conference on Network-Based Information Systems (NBIS-2016), pp. 42–49 (2016)
20. Nakamura, S., Enokido, T., Takizawa, M.: Topic-based synchronization (TBS) protocols to prevent illegal information flow in peer-to-peer publish/subscribe systems. In: Proceedings of the 11th International Conference on Broadband and Wireless Computing, Communication and Applications (BWCCA-2016), pp. 57–68 (2016)
21. Nakamura, S., Ogiela, L., Enokido, T., Takizawa, M.: Evaluation of protocols to prevent illegal information flow in peer-to-peer publish/subscribe systems. In: Proc. of IEEE the 31st International Conference on Advanced Information Networking and Applications (AINA-2017), pp. 631–638 (2017)
22. Nakayama, H., Duolikun, D., Enokido, T., Takizawa, M.: Selective delivery of event messages in peer-to-peer topic-based publish/subscribe systems. In: Proceedings of the 18th International Conference on Network-Based Information Systems (NBIS-2015), pp. 379–386 (2015)
23. Nakayama, H., Duolikun, D., Enokido, T., Takizawa, M.: Reduction of unnecessarily ordered event messages in peer-to-peer model of topic-based publish/subscribe systems. In: Proceedings of IEEE the 30th International Conference on Advanced Information Networking and Applications (AINA-2016), pp. 1160–1167 (2016)
24. Setty, V., van Steen, M., Vitenberg, R., Voulgaris, S.: Poldercast: Fast, robust, and scalable architecture for P2P topic-based pub/sub. In: Proceedings of ACM/IFIP/USENIX 13th International Conference on Middleware (Middleware 2012), pp. 271–291 (2012)
25. Tarkoma, S.: Publish/Subscribe System: Design and Principles, 1st edn. Wiley, Hoboken (2012)

# An Energy-Efficient Migration Algorithm of Virtual Machines in Server Clusters

Ryo Watanabe<sup>1</sup>(✉), Dilawaer Duolikun<sup>1</sup>, Tomoya Enokido<sup>2</sup>,  
and Makoto Takizawa<sup>1</sup>

<sup>1</sup> Hosei University, Tokyo, Japan  
ryo.watanabe.4h@stu.hosei.ac.jp, dilewerdolkun@gmail.com,  
makoto.takizawa@computer.org

<sup>2</sup> Rissho University, Tokyo, Japan  
eno@ris.ac.jp

**Abstract.** Virtual machines are now widely used to support applications with virtual service on computation resources. Furthermore, a virtual machine can migrate from a host server to a guest server while processes are being performed. In this paper, we propose a Simple Energy-aware Migration (SEAM) algorithm to migrate a virtual machine to another energy-efficient server in order to reduce the electric energy consumption. Here, the amount of computation to be performed by processes on a virtual machine is simply estimated only by using the number of the processes. We show the total electric energy consumption of the servers can be reduced in the SEAM algorithm compared with non-migration algorithms in the evaluation.

## 1 Introduction

We have to reduce the electric energy consumption of servers in clusters like cloud computing systems [1] in order to realize eco society [3]. There are approaches to reducing the electric energy consumption of servers [5, 9, 10, 12–14, 16, 17]. Energy-efficient hardware components like CPUs [2] are developed in the hardware-oriented approach. On the other hand, in our macro-level approach [9–11], we try to reduce the total electric energy consumed by servers to perform application processes issued by a cluster. In our approach, one energy-efficient server is selected to perform a process in types of algorithms [8, 11, 15]. In another migration approach [6, 7], a process on a host server migrates to an energy-efficient guest server which is expected to consume smaller electric energy than the host server. Cloud computing systems support applications with virtual computation service by using virtual machines [4]. A virtual machine can migrate from a host server to another guest server while processes are being performed on the virtual machine, i.e. live migration [4]. In our previous studies [6, 7], if a process is issued to a cluster, a virtual machine is selected to perform the process by estimating the termination time of each process currently performed and the electric energy consumption of each server. Then, if a host server is expected to consume more electric energy, a virtual machine migrates to another guest

server. However, it is not easy to collect information of processes like computation laxites and virtual machines on each server. It also takes time to do the estimation by using the information of processes and virtual machines.

In papers [20, 21], the simple virtual machine migration (SVM) and modified SVM (MSVM) algorithms are proposed where the idled time of each virtual machine is simply estimated without considering the termination time of each process. Here, we assume every current process  $p_i$  on a virtual machine finishes the half of total amount  $VC_i$  of computation. The total amount computation of a virtual machine is given as the summation of  $VC_i$  of each resident process  $p_i$  on the virtual machine. It is not easy to get the amount  $VC_i$  of computation of each process  $p_i$ . In this paper, we assume every process  $p_i$  has the same amount of computation. In this paper, we newly propose a simple method to estimate the termination time of processes. The idled time of each virtual machine is simply estimated only by using just the number of processes on each virtual machine. We also propose a *Simple Energy-Aware Migration (SEAM)* algorithm to energy-efficiently migrate virtual machine by using the simple estimation model in this paper.

We evaluate the SEAM algorithm compared with other non-migration algorithms. The SEAM algorithm is computationally simple. We show the electric energy consumption of servers can be reduced in the migration algorithm.

In Sect. 2, we present a system model. In Sect. 3, we present the power consumption and computation models. In Sect. 4, we discuss how to simply estimate the electric energy consumption of each server. In Sect. 5, we propose the SEAM algorithm. In Sect. 6, we evaluate the SEAM algorithm.

## 2 System Model

A cluster  $S$  is composed of servers  $s_1, \dots, s_m$  ( $m \geq 1$ ) and supports applications on clients with virtual computation service on computation resources by using virtual machines  $vm_1, \dots, vm_v$  ( $v \geq 1$ ) like KVM [4]. Here, applications can use computation resources like CPUs and storages in a cluster without being conscious of which servers support what computation resources. If a client issues a request to the cluster  $S$ , one virtual machine  $vm_h$  is selected, where a process  $p_i$  to handle the request is created and performed. Here, the process  $p_i$  is a *resident* process of the virtual machine  $vm_h$ . A virtual machine  $vm_h$  is *active* if at least one process is performed, else *idle*. An active server  $s_t$  is one where there is at least one active resident virtual machine. A server which hosts at least one resident virtual machine is a *hosting* server, otherwise *free*.  $VCP_h(\tau)$  indicates a set of resident processes on the virtual machine  $vm_h$  at time  $\tau$ . Time when a virtual machine  $vm_h$  gets idle is *idled* time. Time when an idle virtual machine gets active is *activated* time. A virtual machine  $vm_h$  on a host server  $s_t$  is a *resident* one on the host server  $s_t$ .  $VM_t(\tau)$  denotes a set of resident virtual machines on a server  $s_t$  at time  $\tau$ . A virtual machine  $vm_h$  can migrate from a host server  $s_t$  to another guest server  $s_u$  while processes are being performed without suspending the processes i.e. live migration [4].

### 3 Power Consumption and Computation Models

#### 3.1 MLPCM Model

In this paper, a process means a computation type of application process where CPU resource is used. A server  $s_t$  is composed of  $np_t$  ( $\geq 1$ ) homogeneous CPUs. Each CPU  $cp_{tk}$  is composed of  $cc_t$  ( $\geq 1$ ) homogeneous cores. There are  $nc_t$  ( $= np_t \cdot cc_t$ ) cores in the server  $s_t$ . Each core  $c_{tkh}$  supports the same number  $ct_t$  ( $\leq 2$ ) of threads. The total number  $nt_t$  of homogeneous threads on a server  $s_t$  is  $np_t \cdot cc_t \cdot ct_t$ . An *active* thread is a thread where at least one process is performed. An *active* core, CPU, and server are ones where at least one thread is active. Let  $CP_t(\tau)$  be a set of processes performed on a server  $s_t$  at time  $\tau$ .

The electric power consumption of a server  $s_t$  is  $minE_t + ap_t \cdot bE_t + ac_t \cdot cE_t + at_t \cdot tE_t$  where  $ap_t$  ( $\leq np_t$ ),  $ac_t$  ( $\leq nc_t$ ), and  $at_t$  ( $\leq nt_t$ ) are number of active CPUs, cores, and threads, respectively. The electric power consumption  $NE_t(n)$  [W] of a server  $s_t$  to concurrently perform  $n$  processes at time  $\tau$  is given in the MLPCM model as follows [15, 16]:

$$NE_t(n) = \begin{cases} minE_t & \text{if } n = 0. \\ minE_t + n \cdot (bE_t + cE_t + tE_t) & \text{if } 0 \leq n \leq np_t. \\ minE_t + np_t \cdot bE_t + n \cdot (cE_t + tE_t) & \text{if } np_t < n \leq nc_t. \\ minE_t + np_t \cdot bE_t + nc_t \cdot cE_t + n \cdot tE_t & \text{if } nc_t < n \leq nt_t. \\ maxE_t = minE_t + np_t \cdot bE_t + nc_t \cdot cE_t + nt_t \cdot tE_t & \text{if } n > nt_t. \end{cases} \quad (1)$$

The electric power consumption  $E_t(\tau)$  [W] of a server  $s_t$  where  $n$  ( $= |CP_t(\tau)|$ ) processes are performed at time  $\tau$  is assumed to be  $NE_t(n)$ . Even if  $n \geq nt_t$ , a server  $s_t$  consumes the maximum electric power  $NE_t(n) = maxE_t$ . An idle server  $s_t$  consumes  $NE_t(0) = minE_t$ . For example, in a server DL360p Gen8 of two Intel CPUs Xeon E5-2667 v2 [2],  $minE_t = 126.1$ ,  $bE_t = 30$ ,  $cE_t = 5.6$ ,  $tE_t = 0.6$ ,  $maxE_t = 301.1$  [W],  $np_t = 2$ ,  $nc_t = 16$ , and  $nt_t = 32$ .

#### 3.2 MLCM Model

Each process  $p_i$  is at a time performed on a thread of a host server  $s_t$ . It takes  $T_{ti}$  time units [tu] to perform a process  $p_i$  on a thread of a server  $s_t$ . If only a process  $p_i$  is performed on a server  $s_t$  without any other process, the execution time  $T_{ti}$  of the process  $p_i$  is minimum  $minT_{ti}$ . In a cluster  $S$  of servers  $s_1, \dots, s_m$  ( $m \geq 1$ ),  $minT_i$  shows a minimum one in a set  $\{minT_{1i}, \dots, minT_{mi}\}$ . If  $minT_{fi} = minT_i$ , a thread of a server  $s_f$  is *fastest* in a cluster  $S$ . A server  $s_f$  with a fastest thread is *fastest*.

We assume one virtual computation step [vs] is performed on a thread of a fastest server  $s_f$  for one time unit [tu]. Here, the maximum computation rate  $maxCRT_f$  of a thread of a fastest server  $s_f$  is one,  $maxCRT_f = 1$ [vs/tu]. The total number  $VC_i$  of virtual computation steps of a process  $p_i$  is defined to be  $minT_i$  [tu]  $\cdot maxCRT_f$  [vs/tu]  $= minT_i$  [vs]. The maximum computation rate  $maxCR_{ti}$  of a process  $p_i$  on a server  $s_t$  is  $VC_i/minT_{ti}$  [vs/tu] ( $\leq 1$ ). For a fastest

server  $s_f$ ,  $maxCR_{f_i} = VC_i/minT_{f_i} = VC_i/minT_i = 1$  [vs/tu]. On a thread of a server  $s_t$ ,  $maxCR_{t_i} = maxCR_{t_j} = maxCRT_t$ [vs/tu] for every pair of processes  $p_i$  and  $p_j$ .

The computation rate  $CR_t(\tau)$  of a server  $s_t$  of time  $\tau$  is  $at_t \cdot maxCRT_t$  where  $at_t (\leq nt_t = np_t \cdot cc_t \cdot ct_t)$  threads are active. The maximum computation rate  $maxCR_t$  [vs/tu] ( $\leq 1$ ) of a server  $s_t$  is the summation of maximum computation rates of  $nt_t$  threads, i.e.  $maxCR_t = nt_t \cdot maxCRT_t$ . As presented here,  $at_t = n$  if  $n \leq nt_t$  and  $at_t = nt_t$  if  $n > nt_t$  where  $n = |CP_t(\tau)|$ . The computation rate  $NCR_t(n)$  is equally allocated to each current process  $p_i$  at each time  $\tau$ . Suppose a process  $p_i$  starts on a server  $s_t$  at time  $\tau$ . That is,  $NCR_{t_i}(n) = NCR_{t_j}(n)$  for every pair of processes  $p_i$  and  $p_j$  on a server  $s_t$ . The computation rate  $NCR_t(n)$  [vs/tu] of a server  $s_t$  to concurrently perform  $n$  processes is given according to the computation rate  $CR_t(\tau)$  as follows:

$$NCR_t(n) = \begin{cases} n \cdot maxCRT_t & \text{if } n \leq nt_t. \\ maxCR_t & \text{if } n > nt_t. \end{cases} \quad (2)$$

The computation rate  $NCR_{t_i}(n)$  of each process  $p_i$  performed with  $(n - 1)$  processes on a server  $s_t$  is  $NCR_t(n)/n$ :

$$NCR_{t_i}(n) = \begin{cases} maxCRT_t & \text{if } n \leq nt_t. \\ maxCR_t/n & \text{if } n > nt_t. \end{cases} \quad (3)$$

If a process  $p_i$  starts at time  $st$  and ends at time  $et$ . Here,  $\sum_{\tau=st}^{et} CR_{t_i}(\tau) = VC_i$  [vs] ( $= maxCRT_f \cdot minT_i$ ) where  $s_f$  is the fastest server.  $VC_i$  shows the total amount of computation to be performed by a process  $p_i$ . The computation laxity  $lc_{t_i}(\tau)$  [vs] is the number of virtual computation steps [vs] to be performed in the process  $p_i$  on a server  $s_t$  after time  $\tau$ . At time  $\tau$  a process  $p_i$  starts,  $lc_{t_i}(\tau) = VC_i$ . Then, the laxity  $lc_{t_i}(\tau)$  is decremented by the computation rate  $CR_{t_i}(\tau)$ , i.e.  $lc_{t_i}(\tau + 1) = lc_{t_i}(\tau) - CR_{t_i}(\tau)$ . If  $lc_{t_i}(\tau + 1) \leq 0$ , the process  $p_i$  terminates at time  $\tau$ .

## 4 Estimation Model

A client issues a request process  $p_i$  to a set  $VM$  of virtual machines  $vm_1, \dots, vm_v$  ( $v \geq 1$ ) in a cluster  $S$  of servers  $s_1, \dots, s_m$ . First, one host virtual machine  $vm_h$  in the set  $VM$  is selected to perform the process  $p_i$ . Furthermore, each virtual machine  $vm_h$  can migrate from a host server  $s_t$  to a guest server  $s_u$  [4]. It is not easy to estimate the termination time of each current process  $p_i$  on every virtual machine  $vm_h$  of a server  $s_t$  by using the computation laxity  $lc_{t_i}(\tau)$  and the computation rate  $NCR_{t_i}(n)$  as discussed in papers [6, 7, 15–17, 19]. Here,  $n = |CP_t(\tau)|$ . In well-formed applications, only fixed types of processes are issued in a cluster. Here, we can get the total amount of  $VC_i$  of virtual computation steps of each process  $p_i$ . We assume each current process  $p_i$  ( $\in VCP_h(\tau)$ ) on a virtual machine  $vm_h$  finishes the half of the total computation  $VC_i$  by time  $\tau$ . Here, the total virtual computation steps  $slc_t(\tau) = \sum_{p_i \in CP_t(\tau)} VC_i/2$  have to



be performed on a server  $s_t$  at time  $\tau$ . The expected termination time  $ET_t$  [tu] of a server  $s_t$  is given as follows:

$$ET_t = slc_t(\tau)/NCR_t(n). \quad (4)$$

This means, it is expected to take  $ET_t$  [tu] to perform every current resident process on a host server  $s_t$ . The expected electric energy consumption  $EE_t$  [J] of a server  $s_t$  to perform  $n$  processes at time  $\tau$  is obtained by multiplying the execution time  $ET_t$  [tu] by the electric power consumption  $NE_t(n)$  [J/tu] to be given as follows:

$$\begin{aligned} EE_t &= ET_t \cdot NE_t(n) \\ &= (CE_t(n)/NCR_t(n)) \cdot slc_t(\tau). \end{aligned} \quad (5)$$

Here,  $NE_t(n)/NCR_t(n)$  [J/vs] indicates the electric energy consumption of a server  $s_t$  to perform one virtual computation step.

Next, suppose one new process  $p_i$  starts on a server  $s_t$  at time  $\tau$ . The expected termination time  $NET_t$  and expected electric energy  $NEE_t$  of a server  $s_t$  to perform both  $n$  current processes and the new process  $p_i$  is given as follows:

$$NET_t = (slc_t(\tau) + VC_i)/NCR_t(n+1). \quad (6)$$

$$\begin{aligned} NEE_t &= NET_t \cdot NE_t(n+1) \\ &= (slc_t(\tau) + VC_i) \cdot NE_t(n+1)/NCR_t(n+1). \end{aligned} \quad (7)$$

It is difficult to obtain the total amount  $VC_i$  of virtual computation steps of each process  $p_i$  in types of applications. Hence, we assume  $VC_i$  to be a constant,  $VC = 1$ . The simplified server laxity  $sslc_h(\tau)$  of a server  $s_t$  is just defined to be the half of the number  $n$  of current processes, i.e.  $sslc_t(\tau) = n \cdot VC/2 = n/2$ .

Suppose  $n$  processes are performed on a server  $s_t$  and  $k$  new processes are issued to the server  $s_t$ . Here, the total amount of computation to perform  $n$  current processes is  $n/2$ . The total computation to perform  $k$  new processes is  $k$ . Here, totally  $(n/2 + k)$  computation has to be performed on the server  $s_t$ . The computation rate of the server  $s_t$  is  $NCR_t(n+k)$  since  $(n+k)$  processes are concurrently performed. The expected termination time  $SET_t(n, k)$  of a server  $s_t$  to perform  $n$  current processes and  $k$  new processes is given as follows:

$$SET_t(n, k) = (n/2 + k)/NCR_t(n+k). \quad (8)$$

The expected electric energy consumption  $SEE_t(n, k)$  of a server  $s_t$  to perform  $n$  current processes and  $k$  new processes is give as follows:

$$\begin{aligned} SEE_t(n, k) &= SET_t(n, k) \cdot NE_t(n+k) \\ &= (n/2 + k) \cdot NE_t(n+k)/NCR_t(n+k). \end{aligned} \quad (9)$$

## 5 Energy-Efficient Migration of Virtual Machines

### 5.1 VM Selection (VMS) Algorithm

First, suppose a client issues a process  $p_i$  to a cluster  $S$  of servers  $s_1, \dots, s_m$  with a set of virtual machines  $vm_1, \dots, vm_v$  at time  $\tau$ . Variables  $n_t$  and  $nv_h$  show the numbers  $|CP_t(\tau)|$  and  $|VCP_h(\tau)|$  of processes performed on each server  $s_t$  and virtual machine  $vm_h$ , respectively, at time  $\tau$ . As discussed in the SGEA algorithm [18], not only a host server of a new process  $p_i$  but also the other servers consume electric energy. Here, let  $NT_t$  and  $NE_t$  be  $SET_t(n_t, 1)$  and  $SEE_t(n_t, 1)$ , respectively, where a new process is assumed to be performed and  $NT_t$  and  $NE_t$  be  $SET_u(n_t, 0)$  and  $SEE_u(n_t, 0)$ , respectively, where only current processes are performed for each server  $s_t$ .

The expected electric energy consumption  $NSEE_{tu}$  of a server  $s_u$  ( $\neq s_t$ ) for a host server  $s_t$  is calculated as follow:

$$NSEE_{tu} = \begin{cases} NE_u + (NT_t - NT_u) \cdot minE_u & \text{if } NT_t \geq NT_u. \\ NE_u \cdot NT_u / NT_t & \text{if } NT_t < NT_u. \end{cases} \quad (10)$$

The expected total electric energy consumption  $SGEE_t$  for a host server  $s_t$  is  $NE_t + \sum_{u=1, \dots, m(\neq t)} NSEE_{tu}$ .

A virtual machine  $vm_h$  is first selected for the process  $p_i$  by the following VM selection algorithm:

[**VM selection**]. A client issues a process  $p_i$  at time  $\tau$ .

1. **select** a host server  $s_t$  for the process  $p_i$ , whose expected total electric energy consumption  $SGEE_t$  is minimum.
2. **select** a virtual machine  $vm_h$  on the selected host server  $s_t$  where the number  $nv_h$  of resident processes is minimum.
3. **perform** the process  $p_i$  on the virtual machine  $vm_h$  of the host server  $s_t$ .

If a process  $p_i$  is issued to a virtual machine  $vm_h$  on a server  $s_t$ , the expected termination time  $ET_t = SET_t(n_t, 1)$  to finish both the process  $p_i$  and every current process is given as  $(n_t/2+1)/NCR_t(n_t+1)$ . The server  $s_t$  is considered to consume the electric power  $NE_t(n_t+1)$  [W] to perform the  $n_t$  current processes and the process  $p_i$ . Here, the expected electric energy  $EE_t = SEE_t(n_t, 1)$  to be consumed by a server  $s_t$  to perform the new process  $p_i$  in addition to  $n_t$  current processes is  $(NE_t(n_t+1)/NCR_t(n_t+1)) \cdot (n_t/2+1)$  [J]. The processes on the server  $s_t$  are expected to terminate by time  $ET_t (= SET_t(n_t, 1))$ . For each server  $s_u$  ( $\neq s_t$ ), the expected electric energy  $NSEE_u$  is calculated by formula 10. A server  $s_t$  whose expected total electric energy  $SGEE_t$  is minimum is selected as a host server of the process  $p_i$ .

Then, a virtual machine  $vm_h$  where the minimum number of processes are performed is selected on the selected server  $s_t$ .

## 5.2 VM Migration (VMM) Algorithm

Each hosting server  $s_t$  where there is at least one resident virtual machine is periodically checked. If migration conditions are satisfied on a hosting server  $s_t$  at time  $\tau$ , one active resident virtual machine  $vm_h$  on the server  $s_t$  is selected to migrate to another server  $s_u$  which is more energy-efficient. Variables  $n_t$  and  $nv_h$  show the numbers  $|CP_t(\tau)|$  and  $|VCP_h(\tau)|$  of processes, respectively, on a server  $s_t$  and a virtual machine  $vm_h$  at time  $\tau$ .

### [VMM algorithm]

```

 $X$  = a set of hosting servers which host virtual machines in a cluster  $S$ ;
for each hosting server  $s_t$  in  $X$ ,  $EE_t = SEE_t(n_t, 0)$ ;
while ( $|X| > 0$ )
{
  select a server  $s_t$  in  $X$  where  $EE_t$  is largest;
  select an active virtual machine  $vm_h$  on  $s_t$  where  $nv_h$  is minimum;
   $NEE_t = SEE_t(n_t - nv_h, 0)$ ;
  for each hosting server  $s_u$  ( $\neq s_t$  in  $X$ ) in  $S$ ,  $NEE_u = SEE_u(n_u + nv_h, 0)$ ;
  select a server  $s_u$  where  $(EE_t + EE_u) - (NEE_t + NEE_u) > 0$  and  $NEE_u$ 
is smallest;
  if  $s_u$  is found, {
    migrate  $vm_h$  from  $s_t$  to  $s_u$ ;
     $SVM_t(\tau) = SVM_t(\tau) - \{vm_h\}$ ;  $SVM_u(\tau) = SVM_u(\tau) \cup \{vm_h\}$ ;
    if  $s_u$  is in  $X$ ,  $X = X - \{s_u\}$ ;
  }; /* if end */
   $X = X - \{s_t\}$ ;
}; /* while  $X$  end */

```

First, the expected electric energy consumption  $EE_t$  of each hosting server  $s_t$  to perform every current process is obtained where  $EE_t = SEE_t(n_t, 0)$ .  $X$  is a set of hosting servers in the cluster  $S$ . A server  $s_t$  whose expected electric energy consumption  $EE_t$  is largest is selected in the set  $X$ . Here,  $nv_h$  processes are performed on each virtual machine  $vm_h$ . A virtual machine  $vm_h$  is then selected on the selected server  $s_t$ . The expected electric energy consumption  $NEE_t$  of the server  $s_t$  is obtained where the virtual machine  $vm_h$  leaves, i.e.  $NEE_t = SEE_t(n_t - nv_h, 0)$ . The expected electric energy  $NEE_u$  of every other server  $s_u$  is obtained, where  $nv_h$  processes on the virtual machine  $vm_h$  restart, i.e.  $NEE_u = SEE_u(n_u + nv_h, 0)$ . If  $(EE_t + EE_u) > (NEE_t + NEE_u)$ , the virtual machine  $vm_h$  can migrate from the host server  $s_t$  to the server  $s_u$  since the total electric energy to be consumed by both the servers  $s_t$  and  $s_u$  can be reduced. A server  $s_u$  with smallest  $NEE_u$  is selected in cluster  $S$ . Then, the virtual machine  $vm_h$  migrates from the server  $s_t$  to the server  $s_u$ . If a server  $s_u$  is selected as a guest server of the host server  $s_t$ , the server  $s_u$  is then not taken as a host server, i.e.  $s_u$  is removed from the set  $X$ . The host server  $s_t$  is also removed from the set  $X$ . If  $X$  gets empty, the VMM algorithm terminates.

## 6 Evaluation

We consider a cluster  $S$  of four real servers DSLab2, DSLab1, Sunny, and Atria ( $m = 4$ ) denoted by  $s_1, s_2, s_3$ , and  $s_4$ , respectively, in our laboratory and four virtual machines  $VM_1, \dots, VM_8$  ( $v = 8$ ). Initially, each server  $s_t$  hosts two virtual machines.  $s_1$  and  $s_2$  are equipped with two and one Intel Xeon E5-2667 v2 CPU, respectively. Sunny and Atria are equipped with one Intel Xeon E5-2620 and Intel Corei7-6700K CPU, respectively. The performance parameters like maximum thread computation rate  $maxCRT_t$  and electric energy parameters like minimum power consumption  $minE_t$  of each server  $s_t$  are shown in Table 1. For example, the server  $s_1$  supports totally 32 threads and  $s_3$  supports eight threads. The threads of the servers  $s_1$  and  $s_2$  are the fastest, i.e. maximum thread computation rate is 1.

**Table 1.** Parameters of servers.

Parameters	DSLAb2 ( $s_1$ )	DSLAb1 ( $s_2$ )	Sunny ( $s_3$ )	Atira ( $s_4$ )
$np_t$	2	1	1	1
$nc_t$	8	8	6	4
$nt_t$	32	16	12	8
$maxCRT_t$ [vs/tu]	1.0	1.0	0.5	0.7
$maxCR_t$ [vs/tu]	32	16	6	5.6
$minE_t$ [W]	126.1	126.1	87.2	41.3
$maxE_t$ [W]	301.1	207.3	131.2	89.5
$bE_t$ [W]	30	30	16	15
$cE_t$ [W]	5.6	5.6	3.6	4.7
$tE_t$ [W]	0.8	0.8	0.9	1.1

In the simulation, the total electric energy consumption  $EE_t$  and active time  $AT_t$  of each server  $s_t$  is obtained. Active time  $AT_t$  of a server  $s_t$  is time when the server  $s_t$  is active, i.e. at least one process is performed. The total active time  $AT_t$  of each server  $s_t$  is also obtained.

There are  $n$  ( $> 0$ ) processes  $p_1, \dots, p_n$ . The starting time  $stime_i$  of each process  $p_i$  is randomly taken from time 0 to  $xtime - 1$ . Here,  $xtime$  is 1,000 time units [tu]. In fact, one time unit [tu] shows 100 [msec] [17]. The minimum execution time  $minT_i$  is randomly taken from 5 to 10 [tu]. The amount  $VC_i$  of computation steps of each process  $p_i$  is 5 to 10 [vs]. The parameters of each process  $p_i$  are shown in Table 2. Each process  $p_i$  starts at time  $stime_i$  and terminates at time  $etime_i$ . The termination time  $etime_i$  is obtained in the simulation. The execution time  $T_i$  of a process  $p_i$  is  $etime_i - stime_i + 1$  [tu]. The simulation ends at time  $etime$  when every process terminates, i.e.  $etime = max(etime_1, \dots, etime_n)$ . For each server  $s_t$ , the electric energy consumption  $EE_t$  is calculated as  $\sum_{\tau=0}^{etime} E_t(\tau)$ .

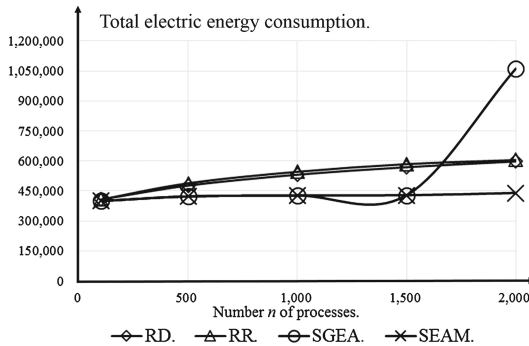
**Table 2.** Parameters of processes.

Parameters	Values
$n$	Number of processes $p_1, \dots, p_n$ ( $\geq 0$ ).
$minT_i$ [tu]	Minimum computation time of a process $p_i$ .
$VC_i$ [vs]	$5 \sim 10$ ( $VC_i = minT_i$ ).
$st_i$ [tu]	starting time of $p_i$ ( $0 \leq st_i < xtime - 1$ ).
$xtime$ [tu]	simulation time (= 1,000 (= 100[sec])).

We consider the random (RD), round robin (RR), SGEA [18], and SEAM algorithms. In the RD and RR algorithms, virtual machines do not migrate and stay on host servers. In the SGEA algorithm, a server  $s_t$  whose total electric energy consumption  $SGEE_t$  is minimum is first selected. Then, a resident virtual machine  $vm_h$  on server  $s_t$  where minimum number of processes are performed is selected to perform the process. Virtual machines do not migrate. In the SEAM algorithm, virtual machines migrate to more energy efficient servers.

Figure 1 shows the total electric energy consumption  $TEE$  [J] of the four servers in the cluster  $S$  for number  $n$  of processes.  $TEE = EE_1 + \dots + EE_4$ . The total electric energy consumption  $TEE$  of the servers  $s_1, \dots, s_4$  can be reduced in the SEAM algorithm compared with the non-migration RD and RR algorithms. The total electric energy consumption  $TEE$  of the SEAM algorithm is almost the same as the SGEA algorithm for  $n \leq 1,500$ . For  $n > 1,500$ , the SEAM algorithm supports the smallest electric energy consumption than the SGEA algorithm.

Figure 2 shows the total active time  $TAT$  [tu] of the four servers.  $TAT = AT_1 + \dots + AT_4$  where  $AT_t$ . The total active time  $TAT$  of the servers in the SEAM algorithm is shorter than the SGEA, RD, and RR algorithms. For example, the total active time  $TAT$  of the SEAM algorithm is about one fourth of the RD and RR algorithms for  $n = 1,500$ . This means, servers are less loaded in the

**Fig. 1.** Total electric energy consumption ( $m = 4, v = 8$ ).

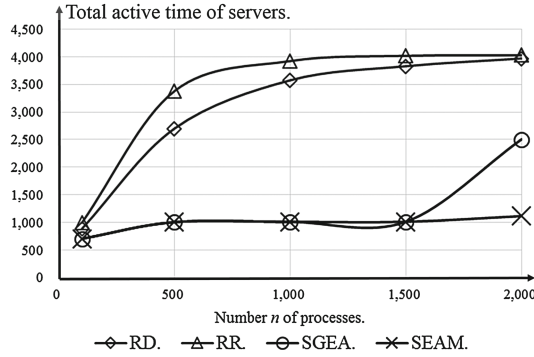


Fig. 2. Total active time ( $m = 4, v = 8$ ).

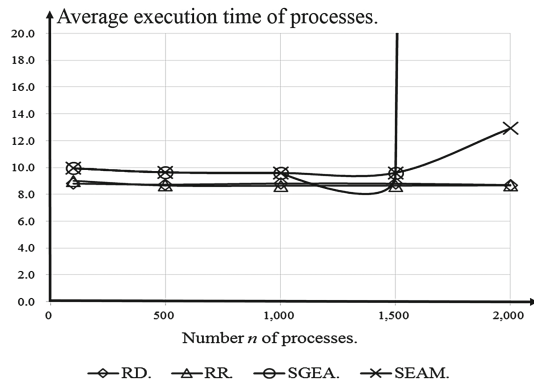


Fig. 3. Average execution time ( $m = 4, v = 8$ ).

SEAM algorithm than the non-migration RD and RR algorithms. Because each virtual machine migrates from a host server to a less loaded server if the host server is overloaded.

Figure 3 shows the average execution time  $AET$  [tu] of the  $n$  processes.  $AET = (T_1 + \dots + T_n)/n$ . The average execution time  $AET$  of the SEAM algorithm is longer than the non-migration RD and RR algorithms. It takes longer time to perform each process in the SEAM algorithm. We have to reduce the average execution time  $AET$  of the processes in the SEAM algorithm. We have to improve the SEAM algorithm so that the average execution time of the processes can be shorter than the non-migration RD and RR algorithms.

## 7 Concluding Remarks

It is critical to discuss how to reduce the electric energy consumed by servers in a cluster to realize eco-society [3]. Here, a virtual machine on a host server migrates to a guest server which is expected to consume smaller electric energy

while processes are being performed. In this paper, we newly proposed the SEAM algorithm where virtual machines migrate to more energy efficient servers. Here, the total amount of computation to be done by resident processes of each virtual machine is simply estimated only by using the number of resident processes on each virtual machine. In the evaluation, we showed the total electric energy consumption and active time of servers in the SEAM algorithm can be more reduced than non-migration algorithms. For example, the total electric energy consumption is reduced to 25% and 75% of the non-migration random (RD) and round-robin (RR) algorithms, respectively. On the other hand, the average execution time of the processes of the SEAM algorithm is longer than the non-migration algorithms.

**Acknowledgment.** This work was supported by JSPS KAKENHI grant number 15H0295.

## References

1. Google, google green. <http://www.google.com/green/>
2. Intel xeon processor 5600 series: The next generation of intelligent server processors white paper. <http://www.intel.com/content/www/us/en/processors/xeon/xeon-processor-e5-family.html>
3. United nations climate change conference (COP21). <https://en.wikipedia.org/wiki/2015>
4. A virtualization infrastructure for the Linux Kernel (kernel-based virtual machine).[https://en.wikipedia.org/wiki/Kernel-based\\_Virtual\\_Machine](https://en.wikipedia.org/wiki/Kernel-based_Virtual_Machine)
5. Duolikun, D., Enokido, T., Takizawa, M.: Power consumption models for migrating processes in a cluster. In: Proceedings of International Conference on Complex, Intelligent, and Software Intensive Systems (NBIS-2014), pp. 15–22 (2014)
6. Duolikun, D., Enokido, T., Takizawa, M.: Asynchronous migration of process replica in a cluster. In: Proceedings of IEEE the 29th International Conference on Advanced Information Networking and Applications (AINA-2015), pp. 271–278 (2015)
7. Duolikun, D., Enokido, T., Takizawa, M.: Asynchronous migration of process replica in a cluster. In: Proceedings of the 9th International Conference on Complex, Intelligent, and Software Intensive Systems (CISIS-2015), pp. 118–125 (2015)
8. Enokido, T., Takizawa, M.: Energy-efficient delay time-based process allocation algorithm for heterogeneous server clusters. In: Proceedings of IEEE the 29th International Conference on Advanced Information Networking and Applications (AINA-2015), pp. 279–286 (2015)
9. Enokido, T., Aikebaier, A., Takizawa, M.: A model for reducing power consumption in peer-to-peer systems. *IEEE Syst. J.* **4**(2), 221–229 (2010)
10. Enokido, T., Aikebaier, A., Takizawa, M.: An integrated power consumption model for communication and transaction based applications. In: Proceedings of IEEE the 25th International Conference on Advanced Information Networking and Applications (AINA-2011), pp. 627–636 (2011)
11. Enokido, T., Aikebaier, A., Takizawa, M.: Process allocation algorithms for saving power consumption in peer-to-peer systems. *IEEE Trans. Ind. Electron.* **58**(6), 2097–2105 (2011)

12. Enokido, T., Aikebaier, A., Takizawa, M.: Evaluation of the extended improved redundant power consumption laxity-based (eirpclub) algorithm. In: Proceedings of IEEE the 28th International Conference on Advanced Information Networking and Applications (AINA-2014), pp. 940–947 (2014)
13. Enokido, T., Aikebaier, A., Takizawa, M.: An extended simple power consumption model for selecting a server to perform computation type processes in digital ecosystems. *IEEE Trans. Ind. Inf.* **10**(2), 1627–1636 (2014)
14. Enokido, T., Takizawa, M.: Power consumption and computation models of virtual machines to perform computation type application processes. In: Proceedings of the 9th International Conference on Complex, Intelligent, and Software Intensive Systems (CISIS-2015), pp. 126–133 (2015)
15. Kataoka, H., Duolikun, D., Enokido, T., Takizawa, M.: Evaluation of energy-aware server selection algorithm. In: Proceedings of the 9th International Conference on Complex, Intelligent, and Software Intensive Systems (CISIS-2015), pp. 318–325 (2015)
16. Kataoka, H., Duolikun, D., Enokido, T., Takizawa, M.: Multi-level computation and power consumption models. In: Proceedings of the 18th International Conference on Network-Based Information Systems (NBIS-2015), pp. 40–47 (2015)
17. Kataoka, H., Duolikun, D., Enokido, T., Takizawa, M.: Power consumption and computation models of a server with a multi-core CPU and experiments. In: Proceedings of IEEE the 29th International Conference on Advanced Information Networking and Applications Workshops (WAINA-2015), pp. 217–223 (2015)
18. Kataoka, H., Duolikun, D., Enokido, T., Takizawa, M.: Simple energy-aware algorithms for selecting a server in a scalable cluster. In: Proceedings of IEEE the 31st International Conference on Advanced Information Networking and Applications Workshops (WAINA-2017), pp. 146–153 (2017)
19. Sawada, A., Kataoka, H., Duolikun, D., Enokido, T., Takizawa, M.: Energy-aware clusters of servers for storage and computation applications. In: Proceedings of IEEE the 30th International Conference on Advanced Information Networking and Applications (AINA-2016), pp. 400–407 (2016)
20. Watanabe, R., Duolikun, D., Enokido, T., Takizawa, M.: An energy-efficient migration model of processes with virtual machine in a server cluster. In: Proceedings of the 11th International Conference on Broadband and Wireless Computing, Communication and Applications (BWCCA-2016), pp. 33–44 (2016)
21. Watanabe, R., Duolikun, D., Enokido, T., Takizawa, M.: Energy-aware virtual machine migration models in a scalable cluster of servers. In: Proceedings of IEEE the 31st International Conference on Advanced Information Networking and Applications (AINA-2017), pp. 85–92 (2017)



# Using the Web of Data in Semantic Sensor Networks

Cristian Lai<sup>1</sup>(✉), Antonio Pintus<sup>2</sup>, and Alberto Serra<sup>1</sup>

<sup>1</sup> CRS4, Center for Advanced Studies, Research and Development in Sardinia,  
Ed. 2 Loc. Piscina Manna, 09010 Pula, CA, Italy

{cristian.lai,alserra}@crs4.it

<sup>2</sup> VIVOCHA S.p.A., Via Rockefeller, 43, 09126 Cagliari, CA, Italy  
apintus@vivocha.com

**Abstract.** In this paper we investigated new methods of effectively performing data modelling for making Internet of Things information accessible to humans and machines. In the current era of technology, we need efficient methods and solutions able to structure, annotate, share and make sense of the IoT data. We assumed that *Things* are basically active participants in information processes by exchanging data and information “sensed” about the environment. Semantics provide unambiguous machine-interpretable descriptions for data related to *Things*. In our methodology we proposed to encode sensor and observation data annotations through Semantic Web technologies and to embed them within devices. Moreover, we transformed such annotations to semantic descriptions, by using the cloud-based ThingSpeak middleware. The obtained descriptions are expected to compound a shared RDF Knowledge Base, useful to improve integration and communication processes between different networks.

**Keywords:** Internet of Things · Ontology, Knowledge Base · Information retrieval · Sensor network · Semantic sensor network

## 1 Introduction

During the recent years the amount of information is growing exponentially. Not only the one on the Web, but also the one provided by distributed Sensor Networks. Sensor Networks are crucial parts of the Internet of Things (IoT). The IoT will play a key role in the next generation of information production and management, networking and communication developing. Nowadays, it is possible to utilise wide networks with multiple sensors or in general *Things*. *Things* are basically active participants in information processes by exchanging data and information “sensed” regarding the environment. However, the heterogeneous nature of the *Things* makes interoperability among them a challenging issue. There is a lack of integration and communication between different networks. A specific issue basically concerns how to manage information obtained

from raw data. This paper shows that semantic technologies, based on machine-interpretable representation formalisms, applied to Sensor Networks, appear as a promise for describing *Things*, sharing and integrating information and inferring new knowledge together with other intelligent processing techniques. This research investigates new methods of effectively performing data modelling, new methods for making IoT information accessible to humans and machines in order to efficiently deal both information management and retrieval processes. Today, we need efficient methods and solutions able to structure, annotate, share and make sense of the IoT data. *Things* need to be interconnected and to communicate autonomously. Providing unambiguous data description enables automated information communication and interaction. Semantics can provide unambiguous machine-interpretable descriptions regarding what data represents, where it originates from, how it can be related to its surroundings and who is providing it. Data can be used as singular as well as plural context based knowledge in different application domains. Moreover, data needs to be exchanged among *Things* and other users on the Internet. Data originating from a device or a human can be combined with other data to create different abstractions of the environment. Semantics can support this integration and it allows to move toward the concept of Semantic Sensor Networks.

In this paper we also explain how to integrate IoT devices and the cloud-based ThingSpeak<sup>1</sup> platform, which is an open source Internet of Things application and API (application programming interface) for storing and retrieving data from Things using HTTP. The ThingSpeak API allows for numeric data processing such as time scaling, averaging, median summing, and rounding and it is used as a middleware to manage all the low-level network operations, data collection and real-time data annotation/transformation. The solution proposed might be useful for several real life IoT applications such as Smart Home applications, IoT agriculture with weather management and eHealth where semantics combined with the Internet of Things can be a good approach for supporting other technologies for learning and improving the quality of life for children with autism spectrum disorder (ASD) [10].

Data collected from devices represents various tangible as well as intangible objects, e.g., temperature, humidity, light, GPS position. Data may have different meanings according to the environment and the related devices, even though the data type. The integration of devices' data requires the definition of standard schemes. The effective annotation and description of devices, observation and measurement data, are included in the fundamental steps to the construction of Semantic Sensor Networks. In our methodology, we propose to encode sensor and observation data annotations through Semantic Web technologies and to embed them within devices. Moreover, we propose to transform such annotations to semantic descriptions through ThingSpeak platform. Such descriptions will compound a shared RDF Knowledge Base. We fix our attention on sensing

---

<sup>1</sup> <https://thingspeak.com/>.

stations based on Arduino<sup>2</sup> microcontrollers. Key contributions of this paper include:

- Definition of a meta-modelling formalism for annotating things and raw data;
- Use of the ThingSpeak IoT platform to transform semantic annotations to semantic descriptions using Semantic Web formats, compounding a shared RDF Knowledge Base;
- Definition of innovative techniques for integrating information in Semantic Sensor Networks.

The remainder of this paper is organised as follows: Sect. 2 briefly introduces related ontologies and some technologies useful in this research; Sect. 3 introduces the proposed methodology; Sect. 4 illustrates the transformation process; and Sect. 5 provides conclusions.

## 2 State of the Art

Sensors are typically locked into closed systems. To unlock valuable sensor data from closed systems, a service infrastructure is proposed in [9] in order to connect sensors to the Internet and publish their output in well-understood, machineprocessable formats on the Web thus making them accessible and usable at large scale under controlled access. In this work, authors focus on publishing sensor-related data on the Web would help to find relevant information by directly accessing sensor data, i.e., by directly observing the real world, integrated with related information from the Web. They provide vocabularies to integrate descriptions of sensors and things with the LOD cloud. Anyway, they neglect the embedding aspects within devices, that need to be investigated in order to obtain self contained elements in the IoT. In [11] a middleware based approach allows applications to communicate with a middleware that intermediates to the things. The middleware is responsible to collect metadata from the things, store it, process it when necessary and respond to clients' requests. All the metadata declarations are collected in a single continuous block inside the device's firmware. This approach does not allow to adapt metadata declarations that are strongly constrained within devices. A rule based approach should extend a middleware with flexible mechanisms necessary to contextualize the information provided by devices. In the literature, there are several state-of-art addressing sensor. In [4] Compton et al., provides a survey of the semantic specification of sensors. Issues still remain unresolved about the correct structure and scope of sensor ontology. No current ontology is able to completely express all the properties required for semantic sensor networks. Anyway, in literature there is a set of ontologies, which allow representing real-world devices. In [7], the authors provide a review of existing ontologies which can be used according to our objectives. In this study, we are inspired mainly by these ontologies and we briefly analysed the SSN and CF ontologies. We assume that Linked Open Data provides

---

<sup>2</sup> <https://www.arduino.cc/>.

the proper technologies to publish sensor data encoded to JSON-LD notation. The SSN [3] ontology is a work provided by the W3C Semantic Sensor Network Incubator Group. It can describe sensors, sensing, the measurement capabilities of sensors, the observations that result from sensing, and deployments in which sensors are used. The ontology covers large parts of the SensorML [2] and O&M [5] standards, omitting calibrations, process descriptions and data types, not necessarily to be sensor specific. It consists of 41 concepts and 39 object properties, directly inheriting from 11 DUL<sup>3</sup> concepts and 14 DUL object properties. Significant to the ontology is the concept of sensor (*ssn:Sensor*) and observation (*ssn:Observation*). The ontology is limited only to high-level concepts in order to enhance modularity and reusability. The Climate and Forecast (CF) Ontology<sup>4</sup> represents standard names for use with climate and forecast data in the atmosphere, surface and ocean domains. It was designed mainly to address data types such as numerical weather prediction model outputs and climatology data. The CF conventions are also applicable to many classes of observational data, and have been adopted by a number of groups for such applications. Specific descriptors can be appropriately used to represent units, standard names, measures, etc. Linked Sensor Data is an approach to represent and publish sensor descriptions as well as observations on the Web using the Linked Open Data best practices [1]. With the help of the Linked Open Data approach, it is possible to relate different resources on the Web. LOD is based on four best practices [13] of publishing data as linked data, which include using URI's as names for things, using HTTP URI's to enable people to look up those names, providing useful RDF information related to URI's that are looked up by machine or people and linking the URI's to other URI's. JSON-LD [12] provides a simple serialisation format for Linked Data based on JSON. This format is inspired by an entity-centric approach instead of the triple-centric approach used for other common LOD serialisation formats. JSON-LD is 100% compatible with JSON and represents a generic serialisation format used also to implement concrete Web APIs [8].

### 3 Methodology

Our methodology proposes a two-step process. The **first step** focuses on sensors and observations data annotations, encoded through Semantic Web technologies. Semantic annotations are embedded within sensing stations based on Arduino microcontrollers. Sensing stations are basically devices that provide a small piece of information about their features; they are able to announce themselves in the network and declare what they observe. This information is minimised, in order to relieve sensors from details keeping information representation very small. The **second step** provides enriched semantic descriptions thanks to the idea of Linked Sensor Data [1,6], which facilitates in publishing

<sup>3</sup> <http://www.loa.istc.cnr.it/ontologies/DUL.owl>.

<sup>4</sup> <http://www.w3.org/2005/Incubator/ssn/ssnx/cf/cf-property>.

and using enriched sensor data with the help of the Linked Open Data<sup>5</sup> principles. Resources are enriched and associated to each other as well as to other type of virtual and/or real world objects through semantic links. The second step is based on the ThingSpeak platform, and it is automated starting from the annotations provided by devices. Obviously, devices are directly connected to ThingSpeak through its web API. For the **first step**, we consider some devices in order to easily drive the modelling and design of the basic set of sensing capabilities. We identify a set of basic components called *Things*, that can be shared within a sensor network and then used jointly (e.g., temperature and humidity sensor). For the **second step**, we divert our attention to the semantic meta-formalisms necessary to annotate a general set of sensor networks components. Although aspects such as detailed measures features and units, are not tackled by the existing SSN ontology, still we think that it is best to start from there. The set of things, features, constraints and data are required to combine the SSN ontology and other ontologies. The set of resulting ontologies is used to model an interconnected eco-system of devices, following the paradigm of Linked Open Data. This approach allows to create a distributed RDF Knowledge Base integrating the various annotations first embedded within sensors and then transformed into enriched descriptions through the ThingSpeak middleware. We basically focus our attention on sensor network components such as “stations”, “sensors” and “observations”.

## 4 Semantic Annotations and Descriptions

As per our vision, semantic *Things* need to be shared, processed and interpreted. Combining different ontologies makes possible an interoperable process for users that share and use the same ontologies. Even though existing ontologies can be referenced, different semantic annotations and descriptions can be supported providing links to other ontologies and Knowledge Bases. Semantic annotations and descriptions are used to represent devices and real-world objects. Delivering sensor data as Linked Sensor Data enables discovery, access, query and interpretation of sensor data. *Things* become context-aware, and are able to configure themselves and exchange information as well as show intelligent/cognitive behaviour. Common frameworks are essential for describing as well as representing the data and making it accessible and processable across different domains.

### 4.1 SSN Knowledge Base

To address our purposes we use state-of-art ontologies while giving due consideration to the specific concepts and properties. As a result, we build the Semantic Sensor Network Knowledge Base containing all the semantic descriptions.

---

<sup>5</sup> <http://linkeddata.org>.

## 4.2 Embedding Semantics Annotations Within Devices

To implement our methodology, we apply the proposed technique to real-world devices. We generate semantic annotations, the so called *snippets*. Snippets are plain JSON objects and are embedded directly within devices. A JSON object is an unordered collection of zero or more key/value pairs, where a key is a string and a value can be a string, a number, a boolean, null, an object or an array. Objects provide information concerning the sensing providers and the kind of sensing measures. We address two different cases: (i) *sensing features*; (ii) *sensing data*. In case of *sensing features*, a snippet is composed of an individual and an observed property. The individual identifies the specific sensor, while the observed property refers to the measure. Individuals become mainly from state-of-art ontologies (SSN and CF), but in many cases we need to define our specific individuals. As a common convention we use specific namespaces inherited from state-of-art ontologies, whereas the base namespace is defined as “:”.

The following examples show the snippets for sensing features related to two different sensors, temperature and luminosity.

Snippet 1: temperature sensor

```
{"whois": "sensor_Temperature_1",
 "observes": "cf-property:air_temperature"}
```

Snippet 2: luminosity sensor

```
{"whois": "sensor_Luminosity_1",
 "observes": "luminosity"}
```

Each of these two snippets is composed of two key/value pairs. The *whois* key identifies the sensor, while the *observes* value addresses the observed property. Since we didn't find (in SSN and CF) a suitable individual addressing luminosity, we defined the individual “:luminosity” in our Knowledge Base.

Considering *sensing (measured) data*, a snippet is composed of an observed property and an observed value.

Snippet 3: luminosity observation

```
{"what": ":luminosity",
 "observedData": "50"}
```

Snippet 4: temperature observation

```
{"what": "cf-property:air_temperature",
 "observedData": "22"}
```

The *what* key identifies the observed property, while the *observedData* key addresses the observed value.

## 4.3 From Semantic Annotations to Descriptions

The embedded semantic annotations become semantic descriptions encoded through the JSON-LD notation. Starting from the “Snippet 1”, a sensor of temperature is described as follows.

## Description 1: temperature sensor

```

{"@id": ":sensor_Temperature_1",
"@type": "ssn:Sensor",
"dbpedia-owl:thumbnail": { "@id":
  "http://mydomain.com/images/img10.jpg" },
"rdfs:label": [
  { "@language": "it", "@value":
    "Temperatura" },
  { "@language": "en", "@value":
    "Temperature" }
],
"ssn:observes": { "@id":
  "cf-property:air_temperature" },
"ssn:onPlatform": { "@id": ":station_1" } }

```

It is a new entry (individual) for our RDF Knowledge Base. The snippet's *whois* value becomes the description *@id* (the identifier for this individual: *:sensor\_Temperature\_1*). The *observes* value is related to the individual *:sensor\_Temperature\_1* through the *ssn:observes* property. The other information is provided by the ThingSpeak middleware (described in Sect. 4.3). Through the *rdfs:label* property, we provide a label in several languages. This sensor is installed on the devices specified by the *ssn:onPlatform* property.

The following is the description related to the sensing measure, related to the “Snippet 2”:

## Description 2: temperature observation

```

{"@id": ":temperatureObservation_1",
"@type": "ssn:Observation",
"ssn:observationResult": {
  "@type": "ssn:SensorOutput",
  "ssn:hasValue": {
    "qudt:numericValue": {
      "@type": "xsd:double",
      "@value": "22.0"
    },
    "qudt:unit": {
      "@id": "qudt:degreeCelsius"
    }
  }
},
"ssn:observationResultTime": {
  "time:inXSDDatetime": {
    "@type": "xsd:dateTime",
    "@value": "2016-01-24T12:30:35"
  }
},
"ssn:observedBy": ":sensor_Temperature_1"
}

```

The observed data is transformed into a “ssnd:observedResult”, enriched with the unit of measure (“qudt:unit”). In this case the property belongs to the QUDT (quantities, Units, Dimensions and Data Types) ontology<sup>6</sup>.

In addition we can define the description related to a station and we can insert it directly in the Knowledge Base.

```

Description 3: a station
{
  "@id": ":station_1",
  "dbpedia-owl:city": {
    "@id": "dbpedia-it:Pula_(Italia)"
  },
  "rdfs:label": [
    { "@language": "it", "@value":
      "Stazione di rilevamento Edificio 1" },
    { "@language": "en", "@value":
      "Station Building 1" }
  ],
  "geo:lat": "38.991",
  "geo:long": "8.937",
  "rdf:type": {
    "@id": "ssn:Station"
  }
}

```

This description provides a short information (“rdfs:label”), gps coordinates (“geo:lat” and “geo:long”) and the location (“dbpedia-owl:city”). Further information can be reached following the link “dbpedia-it:Pula\_(Italia)” through the DBPedia knowledge base<sup>7</sup>.

**The ThingSpeak Middleware.** The proposed methodology, and the dynamic as well as scalable Semantic Sensor Network, are based on the ThingSpeak platform. The ThingSpeak workspace allows to quickly prototype and deploy the whole system, focusing on the semantic aspects of research and delegating to ThingSpeak all the low-level, networking operations. The ThingSpeak platform allows simplifying the connection, and the resulting collection of data of an heterogeneous range of devices, applications and general data sources. Also, it facilitates the interconnection of *Things* as Channels, letting them communicate with ease. Thanks to its API, devices able to use the HTTP protocol can be connected. When a *Thing* (device) is created and receives data, it is possible to write and set rules to manage specific *React* conditions. Rules can express filters on data as well as transformations. The integrated rule-based engine embedded in the platform allows transforming data coming from heterogeneous things in real-time: from raw measurements and packets to structured Linked Data, in compliance with Semantic Web standards of W3C. The ThingSpeak platform plays a key role in our methodology. It provides a comfortable way to automatically transform semantic annotations to descriptions. Figure 1 summarises the

<sup>6</sup> <http://www.qudt.org/>.

<sup>7</sup> <http://it.dbpedia.org>.



entire annotations to descriptions transformation process in case of a sensing features announcement: (1) the sensing station/device produces a snippet containing the announcement (semantic annotation) and sends it to ThingSpeak via HTTP; (2) ThingSpeak platform is instructed about how to on-the-fly transform the received annotation to a correspondent semantic description. This transformation takes place thanks to a rule interpreted by ThingSpeak as the snippet is produced by the sensing station; (3) the resulting description is then stored in our RDF Knowledge Base. All the communications make use of the platform APIs. In case of sensing data the process is equivalent.

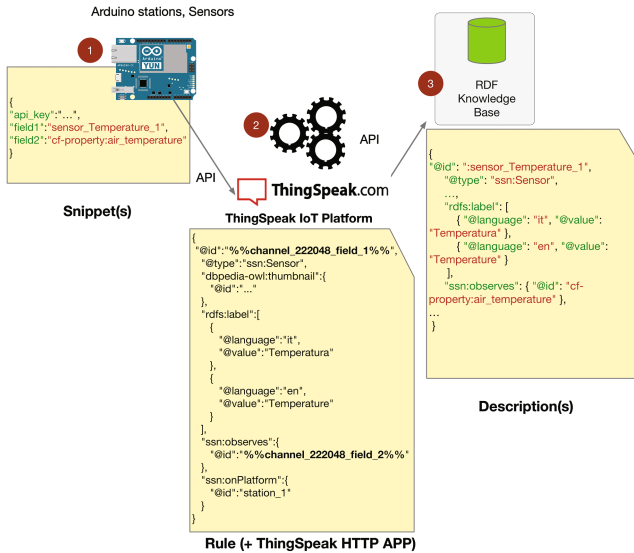


**Fig. 1.** The transformation process from semantic annotations to semantic descriptions, using the ThingSpeak IoT platform.

Let’s briefly dissert about how the rule works in our system. A ThingSpeak rule is a text-based data template, applied to incoming data generated by a connected *Thing* called *Channel* to another component called *ThingHTTP*. A *ThingHTTP* is a *ThingSpeak app*<sup>8</sup> that simplify device communication with web services and API without having to implement the protocol on the device level. The *ThingHTTP* app is connected by the *React* component triggered by a *channel*. Templates can be used in the *ThingHTTP* body to access data from the React. The real power of the ThingSpeak rule system is that the template can contain regular code snippets, which dynamically contribute to define the transformation to apply to data. The following is the rule used to transform the annotated snippet to a corresponding semantic description (as in Fig. 1):

<sup>8</sup> <https://thingspeak.com/apps>.

## A semantic transformation Rule

```

{
  "@id": "%channel_222048_field_1%",
  "@type": "ssn:Sensor",
  "dbpedia-owl:thumbnail": {
    "@id": "http://..."
  },
  "rdfs:label": [
    {
      "@language": "it",
      "@value": "Temperatura"
    },
    {
      "@language": "en",
      "@value": "Temperature"
    }
  ],
  "ssn:observes": {
    "@id": "%channel_222048_field_2%"
  },
  "ssn:onPlatform": {
    "@id": "station_1"
  }
}

```

Generally, the *ThingHTTP* code snippets embedded in rules must be contained inside a `%% %%` pair. In our case, the code `%channel_222048_field_1%` simply selects the *field\_1* key from the snippet coming from the sensor (*whois* key) at *channel\_222048* in order to complete the desired *@id* semantic description, following the rule template and using the selected value. Figure 1 shows the result: a description is then stored in the RDF Knowledge Base. This is a really simple case, although it perfectly fits to our requirements. For example, more complex rules could dynamically assign different thumbnail images based on a condition or, for a measurement, it could transform a temperature to generate semantic descriptions including different scales and units (e.g., Celsius, Fahrenheit, ...). A rule is an extremely powerful and flexible mechanism and, once written, it is applied to every data produced by a particular *Thing*.

## 5 Conclusions

In the world of IoT, Sensor Networks are able to collect wide range of heterogeneous data for monitoring environmental phenomenon. Assuming that *Things* are active participants in information processes, we use semantic technologies for providing unambiguous data modelling, describing *Things*, sharing and integrating information. In this paper we discussed how to benefit from Semantic Web technologies in Semantic Sensor Networks. In our approach, devices are active part of heterogeneous networks, thanks to their ability to announce themselves and to provide sensing data. Data originating from devices will be part of the

world of Linked Sensor Data, through distributed RDF Knowledge Bases. To move from devices to Knowledge Bases we adopted the ThingSpeak open source cloud-based IoT platform.

## References

1. Barnaghi, P., Presser, M.: Publishing linked sensor data. In: The 3rd International workshop on Semantic Sensor Networks 2010 (SSN10) in Conjunction with the 9th International Semantic Web Conference (ISWC 2010) (2010)
2. Botts, M., Robin, A.: OpenGIS sensor model language (SensorML) implementation specification. Technical report, Open Geospatial Consortium (2007)
3. Compton, M., Barnaghi, P., Bermudez, L., Garca-Castro, R., Corcho, O., Cox, S., Graybeal, J., Hauswirth, M., Henson, C., Herzog, A., Huang, V., Janowicz, K., Kelsey, W.D., Phuoc, D.L., Lefort, L., Leggieri, M., Neuhaus, H., Nikolov, A., Page, K., Passant, A., Sheth, A., Taylor, K.: The SSN ontology of the W3C semantic sensor network incubator group. *Web Semant. Sci. Serv. Agents World Wide Web* **17**, 25–32 (2012)
4. Compton, M., Henson, C., Lefort, L., Neuhaus, H., Sheth, A.: A survey of the semantic specification of sensors. In: 2nd International Semantic Sensor Networks Workshop (2009)
5. Cox, S.: Observations and Measurements - Part 1 - Observation Schema (OGC 07-022r1). OpenGIS Implementation Standard, December 2007
6. Keßler, C., Janowicz, K.: Linking sensor data - why, to what, and how? In: Taylor, K., Ayyagari, A., Roure, D.D. (eds.) *Proceedings of the 3rd International Workshop on Semantic Sensor Networks, SSN 2010, Shanghai, China, 7 November 2010*, vol. 668 of *CEUR Workshop Proceedings*. CEUR-WS.org (2010)
7. Kolchin, M., Klimov, N., Andreev, A., Shilin, I., Garayzuev, D., Mouromtsev, D., Zakoldaev, D.: Ontologies for web of things: a pragmatic review. In: Klinov, P., Mouromtsev, D. (eds.) *KESW 2015*. *CCIS*, vol. 518, pp. 102–116. Springer, Cham (2015). doi:[10.1007/978-3-319-24543-0\\_8](https://doi.org/10.1007/978-3-319-24543-0_8)
8. Lanthaler, M.: Creating 3rd generation web apis with hydra. In: Carr, L., Laender, A.H.F., Lóscio, B.F., King, I., Fontoura, M., Vrandecic, D., Aroyo, L., de Oliveira, J.P.M., Lima, F., Wilde, E. (eds.) *22nd International World Wide Web Conference, WWW 2013, Rio de Janeiro, Brazil, 13–17 May 2013, Companion Volume*, pp. 35–38. *International World Wide Web Conferences Steering Committee/ACM* (2013)
9. Pfisterer, D., et al.: PITFIRE: toward a semantic web of things, n. *IEEE Commun. Mag.* **49**(11), 40–48 (2011)
10. Sula, A., Spaho, E., Matsuo, K., Barolli, L., Xhafa, F., Miho, R.: A new system for supporting children with autism spectrum disorder based on IoT and P2P technology. *Int. J. Space-Based Situated Comput.* **4**, 55–64 (2014). IEEE
11. Fortuna, C., et al.: Metadata management for the web of things: a practical perspective. In: *Proceedings of the Third International Workshop on the Web of Things*. ACM (2012)
12. Sporny, M.L.M., Kellogg, G.: JSON-LD 1.0 - A JSON-based Serialization for Linked Data (2013). <http://www.w3.org/TR/json-ld>
13. Tim, B.-L.: Linked data (2006). <http://www.w3.org/DesignIssues/LinkedData.html>

# A Communication Method for Wireless Mesh Networks Suitable to IoT Communication Environment

Kyohei Kishi, Hiroyuki Suzuki, and Akio Koyama<sup>(✉)</sup>

Department of Informatics, Graduate School of Science and Engineering,  
Yamagata University, 4-3-16 Jonan, Yonezawa, Yamagata 992-8510, Japan  
tym93449@st.yamagata-u.ac.jp,  
{shiroyuki, akoyama}@yz.yamagata-u.ac.jp

**Abstract.** Recently, Wireless Mesh Networks (WMN) are widespread as extension technology of Wireless LAN (WLAN) area. WMN can provide low cost and wide area WLAN by connecting Access Points (AP) of WLAN to mesh shape. Meanwhile, a research of Internet of Things (IoT) is doing actively. The IoT is a technology which connects various things to the Internet, and collects and analyzes information of the things or controls the things. In order to realize IoT, the communication environments to the Internet have to prepare. So, it is considered to provide the communication environment widely by using WMN. However, what is worried in case of assuming IoT is an increase in network traffic. This becomes a cause of degrade of network performance. In this paper, we propose a packet integration method and a route reconstruction method to avoid degradation of network performance with increasing network traffic. In packet integration method, by dynamically deciding a waiting time for the packet integration, the packet integration is performed efficiently, and increasing of network traffic is suppressed. In the route reconstruction method, a destination node monitors a packet delay and throughput, and if the route characteristic becomes bad, the route is reconstructed. The simulation results showed that the proposed method has better performance than the conventional method.

## 1 Introduction

Recently, by spreading of mobile nodes like laptop PCs, smart phones and tablet PCs, use of Wireless LAN (WLAN) is increasing [1]. Since communication area of WLAN provided by one Access Point (AP) is narrow, use of Wireless Mesh Networks (WMN) which can offer WLAN area widely is wide spread. Generally, in the case of providing WLAN area widely, installing of plural APs is needed. However, since normal AP connections are wired connection, a construction is needed. In WMN, since connections among APs are wireless, a construction is not needed. Therefore, WMN can offer a large WLAN area cheaply.

A communication of WMN is performed by multi-hop communication which relays packets at plural APs, and connected to the Internet via GW. This is normal use of WMN. Therefore, network performance is great effect by routing protocol which decides communication route because plural APs relay the packets at communication.

As routing protocol of WMN, a Hybrid Wireless Mesh Protocol (HWMP) which combines Radio Metric Ad-hoc On-demand Distance Vector (RM-AODV) of reactive type and Radio Metric Optimized Link State Routing (RM-OLSR) of proactive type is standardized [2, 3, 4]. In route construction of RM-AODV of HWMP, the route construction is performed at a source node when data is generated, and the communication is performed at same route while the flow is continue. However, even though a route characteristic is degrade by other data flow in the network, the communication is continue. So, it is considered that a method which detects route degradation and performs route reconstruction flexibly is effective.

Meanwhile, recently, the research of Internet of Things (IoT) is doing actively in both fields of industry and academic [5]. IoT is a research that various things in the world are connected to Internet and by collecting and analyzing information of these things, and these results are used by various application efficiently. By using WMN which is extension technology of WLAN, to use WMN to IoT is useful because it provides communication area widely with low cost. However, in IoT environment, it is considered that the traffic in the network increases with increasing of connected nodes. Moreover, IoT traffics are considered to small size because they include a lot of sensor and tag data. For instance, in Zigbee which is standard of sensor network, maximum packet size is 127 byte including header [6]. Therefore, it is considered that the communication overhead becomes large by generating small size packets.

In this research, as show in Fig. 1, we suppose the network structure where WMN is backbone network, and sensor networks, ad-hoc networks and tag networks are connected to AP of WMN. When these networks carry the traffics of IoT, following problems are considered. As mentioned before, the first problem, is that the network traffic increase with increase of connected nodes. As the result, data dropping rate and delay may increase by occurring of network congestions. The second problem is that the route situations between source and destination nodes may become worse than at the time of route constructing by increasing of traffics.

In this paper, we propose a packet integration method for WMN supposing IoT environment. The proposed method aims to avoid network congestion with increasing network traffic and increase packet arrival rate and decrease delay. This method also aim to reduce overhead which occurs with network load and sending packets, by integrating plural packets gathered to an AP. Since this method can avoid increasing network traffic, the packet arrival rate can increase and delay can decrease. Moreover, we also propose a route reconstruction method which detects deterioration of route characteristic and reconstruct the route. This method detects deterioration of the route by monitoring packet delay and throughput at the destination node. When the destination node detects deterioration of the route, the destination node sends reconstruction message to the source node. After receiving the reconstruction message at the source node, the source node reconstructs the route.

The structure of this paper is as follows. In Sect. 2, we introduce related works. In Sect. 3, we explain the proposed method. In Sect. 4, we discuss performance evaluation. Finally, some conclusions are given in Sect. 5.

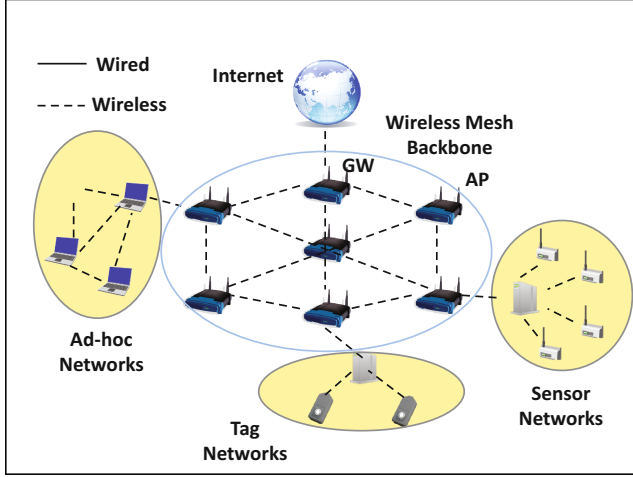


Fig. 1. A supposed network structure.

## 2 Related Works

### 2.1 Hybrid Wireless Mesh Protocol

A Hybrid Wireless Mesh Protocol (HWMP) which is hybrid protocol combined with proactive type and reactive type was proposed as a routing protocol for WMN [4].

#### (a) Metric

The HWMP adopts Airtime as a routing metric. The Airtime is transmission delay of a frame between APs. An Eq. (1) shows a value  $C_a$  (Cost of Airtime) of Airtime.

$$C_a = \left[ O_{ca} + O_p + \frac{B_t}{r} \right] \frac{1}{1 - e_f} \quad (1)$$

In the Eq. (1),  $O_{ca}$  is channel overhead,  $O_p$  is protocol overhead,  $B_t$  is the number of bits of a test frame.  $r$  and  $e_f$  are transmission rate and frame error rate. The transmission rate and frame error rate are measured by test frames.

Since the Airtime is link metric, in the route selection,  $\text{Airtime}_{\text{path}}$  which is summation of the Airtime between APs is used. The route of smallest  $\text{Airtime}_{\text{path}}$  is selected in the route selection.

#### (b) Route construction by Reactive type

In this section, we describe a route construction method by reactive type in HWMP. The route construction used two control packets called Path Request (PREQ) and Path Reply (PREP).

- (1) Route search
  - i. When a data sending request occurs at a source node, the node which does not have a route to the destination node searches a route to the destination node for a route construction. To do so, firstly, the source node broadcasts PREQ.
  - ii. Relay nodes which receive PREQ calculate Airtime of a link and this value is added to a metric field of PREQ. Concurrently, the node increments a hop count of PREQ and decrement a TTL of PREQ. Furthermore, the relay nodes update own routing table based on information in PREQ. Then, the relay nodes rebroadcast PREQ. This process is repeated until PREQ arrives at a destination node.
  - iii. When the destination node receives the PREQ, a route reply is performed.
- (2) Route reply
  - i. The destination node generates a PREP including the searched route and sends the PREP to the source node by unicast.
  - ii. Relay nodes of the PREP calculates the Airtime and update the routing table.
  - iii. After the source node receives PREP, the source node sends a data packet based on the route in PREP.

## 2.2 Packet Filling Method

Packet filling method supposes to perform real-time communication like Voice over IP (VoIP) between nodes under APs in WMN [7]. This method realizes a packet transmission with low packet loss and low packet transmission delay by bundling up the relatively small packets which are communicated between APs. This method focused on two problems. One is congestion with increasing the number of packets. Other one is overhead of IEEE802.11 protocol.

In the experiments, performance was measured by increasing the number of sessions from one to five. Here, the session means one unidirectional communication.

The conditions of experiments in this work are as follows.

- A packet size is 200 octets.
- A transmission duration is 20 ms.
- The number of transmission packets is 5000.

The experimental results show that the packet transmission delay of unicast communication in 5 session was over 350 ms. Meanwhile, transmission delay of the packet filling method was about 20 ms. Regarding packet error rate, unicast communication was over 7%. Meanwhile, error rate of the packet filling method was less than 1%. From the results, it showed that the packet filling method is effective for short data size packet like VoIP application. In this experiments, packet waiting time of the packet filling method was static.

## 2.3 Problems of Related Works

Not only HWMP, conventional reactive type routing protocols construct the route by using routing metric. After that, the route characteristics may change by new flows or other reasons. However, conventional reactive type routing protocols continue use same route. If the route characteristics became bad, it is considered that to reconstruct new route is better. However, conventional routing protocols cannot adapt these situations. This is first problem.

Meanwhile, in the packet filling method, appropriate packet waiting time for the packet filling were not considered. In this method, the performance may big change by packet waiting time. If waiting time is short, the number of filling packet becomes few. Meanwhile, if the waiting time is long, packet transmission delay becomes long. Therefore, it is necessary to derive an expression for an appropriate packet waiting time. This is second problem.

## 3 Proposed Method

### 3.1 Outline

The proposed method supposes WMN in IoT environment and HWMP as routing protocol. To solve the problems in related works, we aim reducing network traffic by packet integration and avoiding deterioration of route characteristic by route reconstruction.

As a method to solve the problems, we propose two methods. First method aims reducing network traffic by integration of small packets with same destination. Second method suppresses deterioration of route characteristic by monitoring route characteristics at the destination node. In this method, when the destination node detects deterioration of route characteristics, the destination node requests the route reconstruction to the source node. By this process, as the source node search new route with good characteristic, deterioration of route characteristic may avoid.

### 3.2 Packet Integration Method

As mentioned outline, it is considered that large amounts of small size packets are generated on the networks in IoT environment. Even the small size packet, in the communication, the header and trailer are needs and overhead like protocol processing also occurs. To reduce these overheads, it is considered that to integrate of small size packets with same destination to one packet is good. By this operation, reducing of network traffic is expected. Because increasing of network traffic may occur congestion and prevent flow of other packets on the network, reducing of network traffic is expected to avoid congestion. As the result, improve packet arrival rate and reduces delay.

There is a thing to consider at integration of plural packets. It is the sending timing of integrated packets. Two threshold are set for this. One is the threshold of a packet size and other one is the threshold of waiting time for integrated packets.



Regarding the integrated packet size, in this research, we set 1500 octets as Maximum Transmission Unit (MTU). We decided this length to prevent occurring a fragment of frame at datalink layer.

In the IoT environment, it is necessary to consider packets generated by sensor devices. In a communication standard of Zigbee which is famous protocol of sensor networks, a packet size is 127 octets including a header. From this length, we assume networks in which a large number of packets of 100 octets are generated in this research. Moreover, the threshold of packet size after integration sets 1400 octets which are not over MTU (1500 octets). This is because MTU includes header length. From this, it is possible to integrate 14 packet maximum.

Next threshold is threshold of waiting time for integration packets. The reason which sets this threshold is that if an integrating node waits until the threshold of packet size, it is possible to become long waiting time. To avoid this situation, the threshold of waiting time for integration packets is set.

From relation of waiting time and throughput, the waiting time ( $W$ ) is expressed to Eq. (2).

$$W[s] = \frac{P[bit]}{T[bps]} \quad (2)$$

where,  $T$  is the throughput of receiving packets at the integration node and  $P$  is the integrated data amounts. Therefore, the waiting time of integration until threshold of packet size is expressed to Eq. (3).

$$W[s] = \frac{11200[bit]}{T} \quad (3)$$

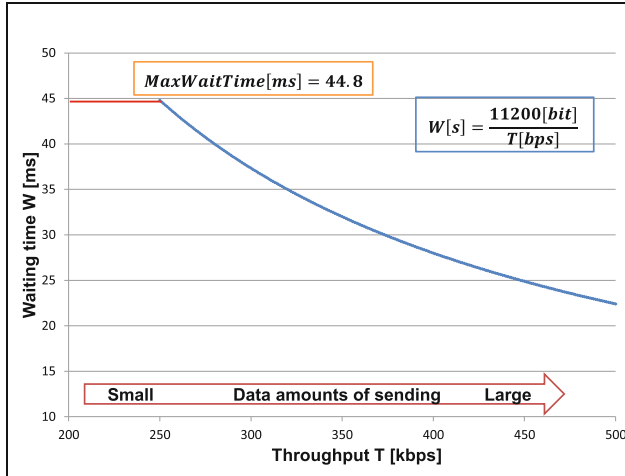
11200 bit is a value obtained by converting 1400 octets into a bit. The waiting time is decided by Eq. (3).

Figure 2 shows a graph of relation of the waiting time and throughput. In Fig. 2, when the throughput is small, the waiting time becomes very large. Therefore, we set maximum waiting time. Because transmission rate of sensor nodes in Zigbee is 250 kbps, the maximum waiting time sets 44.8 ms. This value is obtained by Eq. (3) by inputting 250 kbps to throughput.

### 3.3 Route Reconstruction Method

A route has to construct before sending dataflow. The dataflow continues to use the constructed route. However, it is considered to deteriorate the using route because another new dataflow occurred. Normally, even if the current using route is deteriorated, the route continues use if the route is not broken. But, using the deteriorated route is not effective. Therefore, in the proposed method, when the destination node detected route deterioration, the source node reconstructs a new route.

In the route reconstruction, it is necessary to judge whether the current route is deteriorate or not. So, setting of judgement criteria of the route deterioration is needed.



**Fig. 2.** Relation between waiting time and throughput.

The route characteristics can be judged by data arrival rate, throughput and delay at the destination node. Basically, since data arrival rate and throughput are proportional relation, in the route reconstruction, we only measure throughput and delay of data flow and compared them with past throughput and delay for judgement of route deterioration. For getting of delay of a data packet, sending time at the source node is added to in the packet header. By using this time, delay is calculated by difference of receiving time and sending time.

In throughput, confirmation duration for deterioration is set and the deterioration is calculated by received data amounts in this duration. The Eq. (4) shows condition equation for deterioration judgement.

$$PD \times 1.2 < D \ \&\& \ PT \times 0.8 > T \quad (4)$$

where, PD and D means an average delay of past and current, and PT and T means throughput of past and current. 1.2 and 0.8 are weight values for delay and throughput. By using the weighted values, useless route reconstruction can be avoided. Because a lot of control packets flow by frequently route reconstruction, this may interfere with other packet communications and may cause degradation of network performance.

The procedure of route reconstruction is explained by using Fig. 3.

- i. In the interval A, when the destination node received a data packet, it records delay and throughput per source nodes.
- ii. After passing a constant time (2 s), average delay and throughput in the interval A are calculated.
- iii. Delay and throughput in the interval B are recorded similar to procedure i.
- iv. Average delay and throughput of the interval A and B are compared.

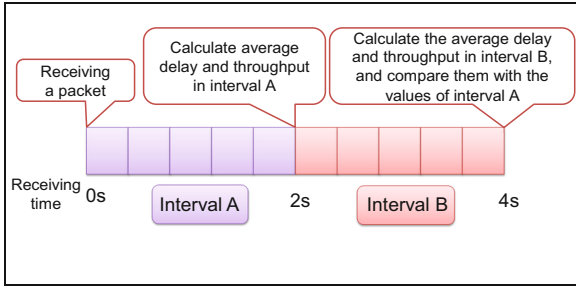


Fig. 3. Judgement of route deterioration.

- v. If condition Eq. (4) is satisfied, in this case the destination node judges route deterioration and it sends a request packet for route reconstruction.
- vi. When the source node receives the request packet, it performs route reconstruction. The route reconstruction procedure is same as HWMP route construction procedure.

## 4 Performance Evaluation

### 4.1 Evaluation Way

Performance evaluation was performed by simulation. The simulator is Network Simulator 3 (NS3) [8]. Table 1 shows simulation conditions and Fig. 4 shows network topology. Comparison protocol is HWMP which mentioned in Sect. 2. As network topology, APs are located as grid shape of  $5 \times 5$ . Source nodes are increased from two to six, so load is gradually added to the network. Here, a source node sends one flow. Source nodes are selected randomly for each simulation. Note that distance between source nodes and destination node (Gateway) is over 2 hops. The simulation was performed at ten times and these average values are drawn to the graph. The destination node is a gateway which is a center node. Table 2 shows contents of generated flows.

Table 1. Simulation conditions.

Simulation time	100 [s]
Distance between adjacent nodes	100 [m]
Number of flows	2–6
Number of source nodes	2–6
Packet transmission rate	Average 250 kbps, VBR
Number of simulations	10 times for each
Interval of Judgement of route deterioration	2 [s]
Threshold of integrated packet size	1400 [octets]

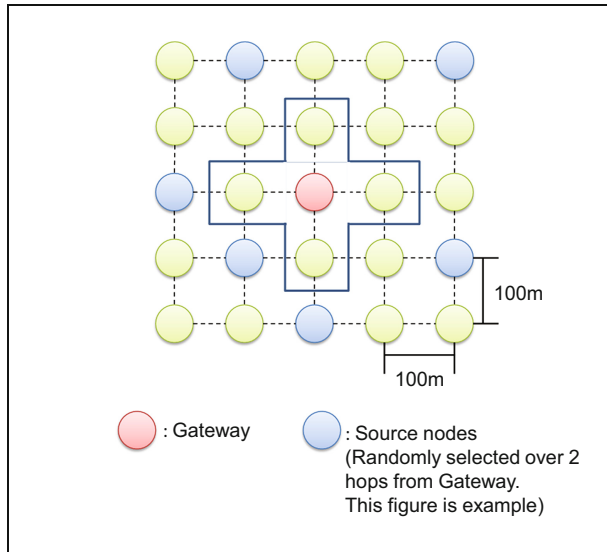


**Fig. 4.** Network topology.

**Table 2.** Contents of generated flows.

The number of total flows	The number of flows for 100 octet packets	The number of flows for 1024 octet packets
2	1	1
3	2	1
4	2	2
5	3	2
6	3	3

## 4.2 Simulation Results and Considerations

The results of packet arrival rate and average delay for HWMP and the proposed method are shown in Figs. 5 and 6, respectively.

As shown in Figs. 5 and 6, the proposed method has better performance than HWMP both characteristics of packet arrival rate and average delay. The packet arrival rate of the proposed method improved about 10% in average than HWMP and the average delay of the proposed method improved about 90% in average than HWMP.

The reason of the improvement of characteristics is that the packet drop rate was reduced because the number of packets which flows network was suppressed by the packet integration method. Furthermore, it is considered that due to the reduction of network traffic, the unused bandwidth increased, so the route reconstruction method was also worked effectively. From these results, we found that in congested networks suppressing network traffic leads to improvement in performance. Moreover, it is considered that the route reconstruction method prevents degradation of the route.

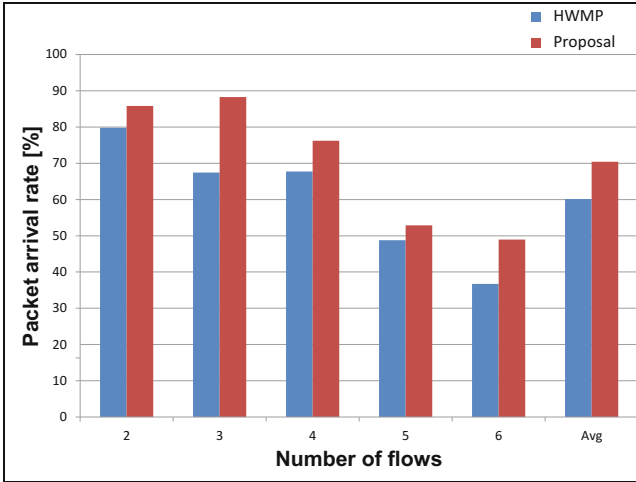


Fig. 5. Packet arrival rate.

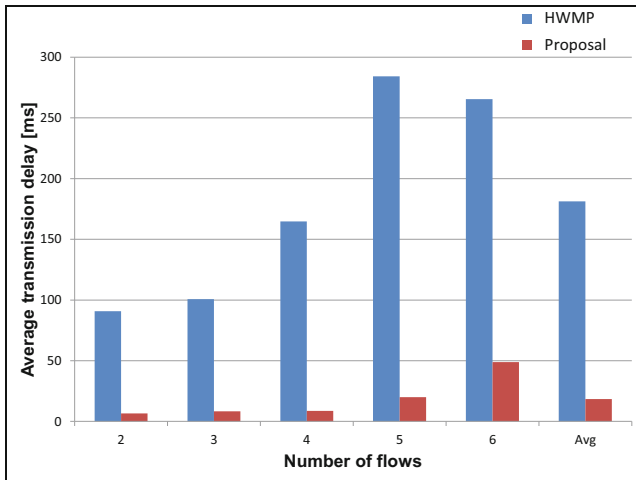


Fig. 6. Average transmission delay per a packet.

## 5 Conclusions

In this paper, as a communication method for WMN which suitable to an IoT communication environment, we proposed the packet integration method by dynamic waiting time and the route reconstruction method which detects route degradation and performs route reconstruction. From the performance evaluation results, the packet arrival rate of the proposed method improved about 10% in average than the conventional method and average transmission delay of the proposed method improved

about 90% in average than the conventional method. From the results of the packet integration method, we showed that the proposed method is effective in the environment where a lot of small size packets are generated. Furthermore, from the results of the route reconstruction method, we showed that the route characteristics improved by reacting quickly for the route degradation.

As the future works, we would like to adopt machine learning to the waiting time of the packet integration method and degradation judgement of route reconstruction method.

## References

1. Ministry of Internal Affairs of Japan, Survey on Communications Usage Trends in 2015. [http://www.soumu.go.jp/johotsusintokei/statistics/data/160722\\_1.pdf](http://www.soumu.go.jp/johotsusintokei/statistics/data/160722_1.pdf)
2. Yang, Y., Wang, J., Kravets, R.: Designing routing metrics for mesh networks. In: Proceedings of IEEE Workshop on Wireless Mesh Networks, pp. 1–9 (2005)
3. Perlins, C.E., B-Royer, E.M., Das, S.R.: Ad hoc on-demand distance vector (AODV) routing. IETF RFC3561 (2003)
4. IEEE P802.11s/D1.07: Hybrid Wireless Mesh Protocol (HWMP) (2007)
5. Cisco Systems IoT Incubation Lab: Impact of Internet of Everything, Impress R&D, Tokyo (2013)
6. Baronti, P., Pillai, P., Chook, V.W.C., Chessa, S., Gotta, A., Fun Hu, Y.: Wireless sensor networks: a survey on the state of the art and the 802.15.4 and ZigBee standards. *Comput. Commun.* **30**, 1655–1695 (2007)
7. Itaya, S., Hasegawa, J., Davis, P., Kadowaki, N., Obana, S.: proposal efficient transmission method for wireless mesh network. *Tech. R. IEICE* **106**(44), 115–118 (2006)
8. NS-3 network simulator official website. <http://www.nsnam.org/>

# Influences of ILS Localizer Signal over Complicated Terrain

Junichi Honda<sup>1</sup>(✉), Hirohisa Tajima<sup>1</sup>, and Hisashi Yokoyama<sup>2</sup>

<sup>1</sup> Surveillance and Communications Department,  
Electronic Navigation Research Institute (ENRI), National Institute of Maritime,  
Port and Aviation Technology, Chofu, Tokyo 182-0012, Japan

j-honda@enri.go.jp

<sup>2</sup> Japan Aviation Consultant D&T Co., Ltd. (ACDT),  
Niiza, Saitama Prefecture 352-0031, Japan

**Abstract.** This paper is concerned with a numerical simulation of Instrument Landing System (ILS) Localizer (LOC). LOC provides the guidance in the horizontal position of an aircraft for the runway center line. The radiation from LOC antenna generates the composite field which is amplitude modulated by a 90 Hz and a 150 Hz tone. The performance of the LOC is given by the difference in the depth of the modulation (DDM) along the runway centerline. However, their signals are influenced by the scattered waves if the LOC antenna is located over the complicated ground condition. In this paper, we consider the influences of the scattered waves caused by the complicated terrain, from a view point of the numerical simulation by the ray-tracing method (RTM). Firstly the basic principle of the LOC is introduced. Next, the simplified RTM is discussed. Finally, we show some numerical examples for field intensity distribution and DDM. We discuss how the scattered waves influence the performance of LOC.

## 1 Introduction

An Instrument Landing System (ILS) plays an important role in safety aircraft landing to an airport. It mainly consists of Localizer (LOC), Glide Path (GP) and Maker (MK) [1]. Among them, the LOC provides the guidance in the horizontal position of the aircraft for the runway centerline [1]. The radiation from the LOC antenna consisting of log-periodic dipole antenna (LPDA), forms the composite field pattern by the amplitude modulation of a 90 Hz and a 150 Hz. The specification of the LOC is provided by the difference of the depth of the modulation (DDM). When the aircraft moves along runway center line, DDM becomes zero, resulting in no movement of the cross point indicator [2]. The value of DDM is also regulated by International Civil Aviation Organization (ICAO) [1], and the quality of the LOC is classified into three categories (CAT I, CAT II and CAT III). The LOC specification shall be satisfied with the category corresponding to runway visual range. However, when large aircraft, fixed structures and complicated terrain exist within the coverage of LOC radiation, multipath

interferences will impact the LOC course and path structure. Therefore, it is very important to investigate the multipath environment for maintaining the LOC quality.

Focusing on the LOC system, multipath interferences from fixed objects and aircraft have been studied, and many research papers have been reported so far [3–8]. On the other hands, numerical simulations for 2D terrain profile have been investigated for GP [9–11]. Therefore, little has been reported on the multipath interferences from complicated 3D terrains. In this paper, we discuss the multipath interferences if the LOC is located on the non-flat ground.

In general, multipath interferences from buildings such as hanger were discussed from a view point of numerical method using some techniques that are the Helmholtz wave equation [4], the Method of Moment (MoM), the Physical Optics (PO) [6] and so on. Considering the numerical accuracy, MoM is one of the best solution. However, it requires much computer memory and computation time. In this paper, we employ the simplified ray-tracing method (RTM) [12] for searching rays between a source and a receiver, and computing electromagnetic fields. We have applied this method to the radar cross section and analysis of propagation characteristics on an airport surface [12–14]. The RTM generally requires much computation time to treat complicated electromagnetic environment. However, the proposed method enables to rapidly compute electromagnetic field by simplifying the ray searching algorithm.

Firstly, we review the basic principle of LOC. Next, the simplified RTM is introduced. The idea is based on the discrete ray tracing method (DRTM) which was used for analyzing EM field along random rough surface [15]. The numerical method consists of the discretization of the terrain profile and simplified ray searching. It should be noted that each face constituting 3D terrain model is larger than the wavelength because the RTM is a high frequency approximation as well as PO. Finally, field intensities along landing course and DDM are shown as numerical results. We discuss how the scattered waves from complicated terrain influence to the ILS signals.

## 2 ILS Localizer

This section describes the basic principle of LOC. The LOC antenna generally consists of 14 or 24 LPDAs in Japan. The LOC antenna emits a carrier wave and sideband waves which are amplitude modulated by 90 and 150 Hz [1]. Figure 1 shows an image figure of the radiation of LOC antenna. Sideband waves emit to be a symmetric beam pattern for runway centerline. The receiver unit loaded on an aircraft determines the approach course by using the DDM. There is a two-frequency LOC system which uses two carrier frequencies, in order to manage the high category airport and to prevent multipath interferences.

### 2.1 Radiation Pattern of LOC Antenna

The LOC operates from 108 MHz to 112 MHz. The antenna configuration is shown in Fig. 2. The length  $d_n$  between LPDAs is determined by the wavelength  $\lambda$ .



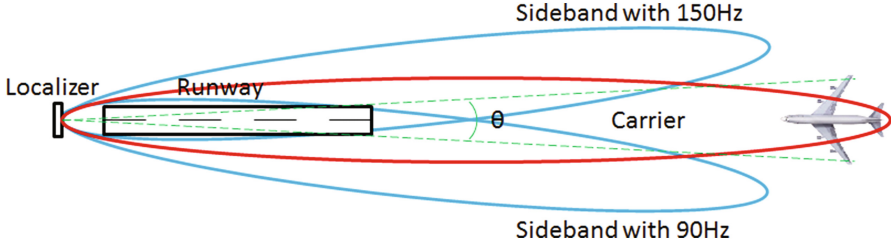


**Fig. 1.** Image figure of the radiation of LOC antenna.

The length between LPDAs is generally selected to be  $d = 0.6\lambda$ . Each LPDA has different power feed to generate optimized beam pattern corresponding to an airport. Electric field of each antenna is given by

$$E_i^{car} = \frac{\sqrt{P_{car}} \cdot k_m^{car}}{\sqrt{\sum_{m=1}^M k_m^{car2}}} \tag{1}$$

$$E_i^{sb} = \frac{\sqrt{P_{sb}} \cdot k_m^{sb}}{\sqrt{\sum_{m=1}^M k_m^{sb2}}} \tag{2}$$

where  $E^{car}$  and  $E^{sb}$  are electric fields of carrier wave (car) and sideband wave (sb), respectively.  $P_{car}$  is the input power of carrier wave, and  $P_{sb}$  is the input power of sideband waves. They are supplied from a transmitter unit. Variables  $k^{car}$  and  $k^{sb}$  are each antenna feed, respectively. The number of antenna ( $M$ ) is selected to be 12 which means that the number of LPDAs is totally 24. Power feeds of 12 LPDAs of left group are same as those of right group.

Radiation pattern is generated by the combination of all LPDAs. The electric field intensity of CAR at far field is given by

$$E_r^{car} = \sum_{n=1}^N E_i^{car} D(\theta) \frac{e^{-j\kappa r_n}}{r_n} \tag{3}$$

where  $D(\theta)$  is the directivity of LPDA. Wavenumber  $\kappa$  is given by  $2\pi/\lambda$ , and  $r$  is the propagation length from a source to a receiver. Electric field of CAR is expressed as the sum of radiated fields.

On the other hand, the electric field intensity of SB is given by

$$E_r^{sb} = \sum_{n=1}^{N/2} \left( E_i^{sb} D(\theta_n^R) \frac{e^{-j\kappa r_n^R}}{r_n^R} - E_i^{sb} D(\theta_n^L) \frac{e^{-j\kappa r_n^L}}{r_n^L} \right) \tag{4}$$

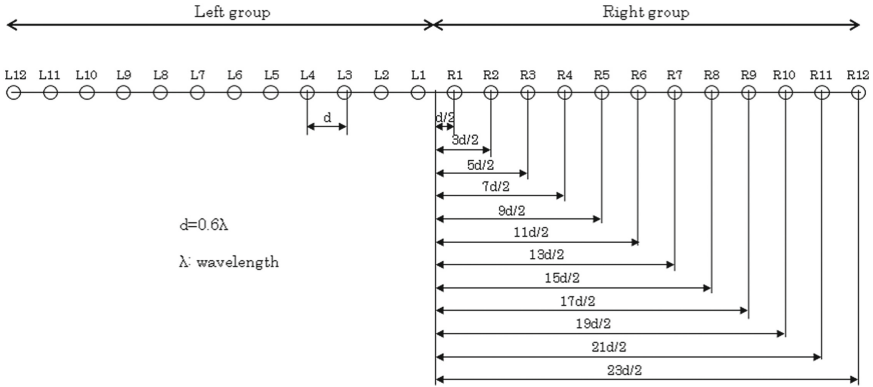


Fig. 2. LOC antenna configuration.

where suffixes  $R$  and  $L$  correspond to right group and left group. Electric field of SB is expressed by the subtraction of radiated fields from right and left groups as shown in Fig. 2.

Figure 3 shows an example of LOC radiation patterns. This figure shows relative received powers in dB. A solid curve is carrier wave and a dotted curve is sideband wave.

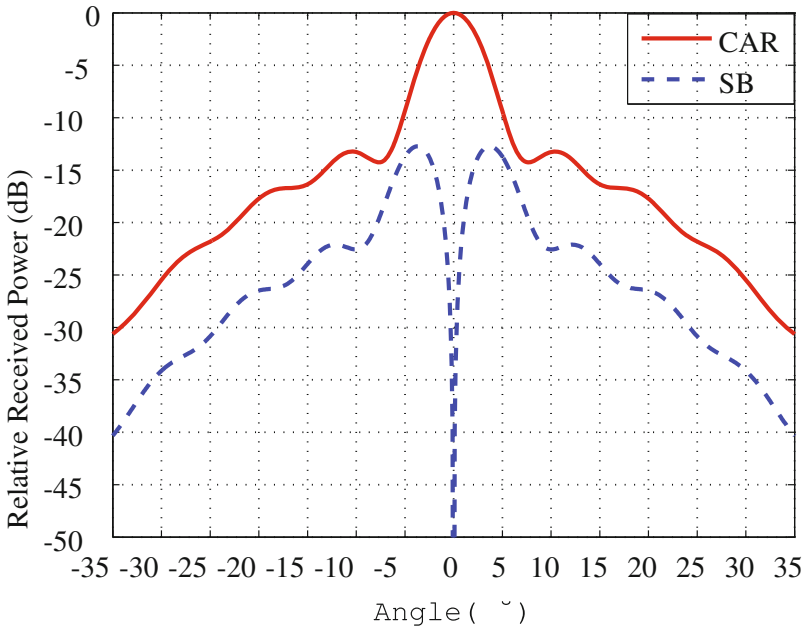


Fig. 3. An example of LOC radiation pattern.

### 2.2 DDM

The specification of LOC is defined by the DDM. Its value must be less than 0.155 (=150  $\mu$ A) which is regulated by ICAO [1]. The value of DDM is computed by

$$DDM = M_{90} - M_{150} \tag{5}$$

where  $M_{90}$  and  $M_{150}$  are the depth of modulation of 90 Hz and 150 Hz signals, respectively. In general, the value of DDM becomes zero when the aircraft moves along the runway center line. However, the occurrence of the multipath interference of LOC signal causes the degrading of the system quality. They are dependent on the total environment around LOC antenna. Each airport has an operation method suites the category (CAT I, II or III), and the deviation of DDM shall be satisfied with the category in operation. Figure 4 shows the DDM limitation for each CAT.

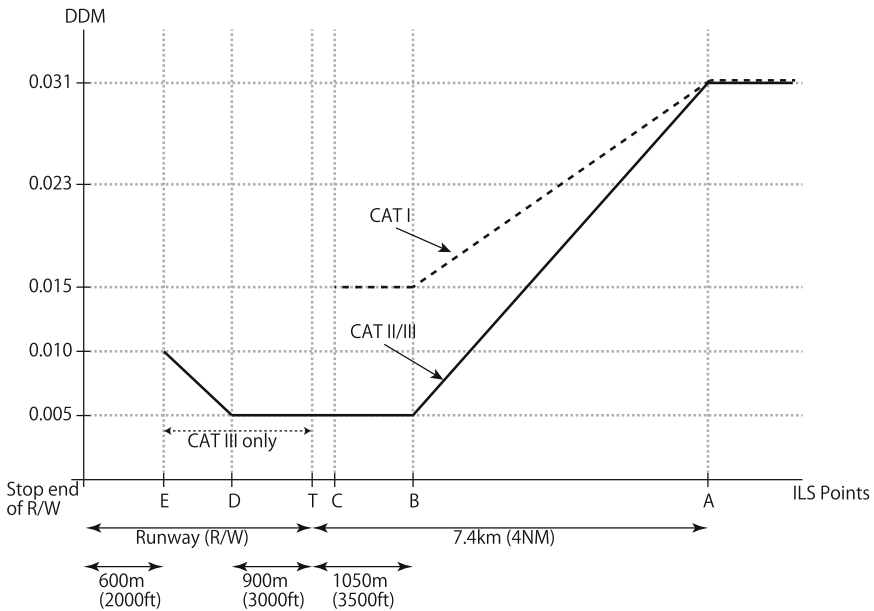


Fig. 4. Classification of category.

### 3 Numerical Method

In this study, the RTM is employed to compute scattered fields because it treats relatively large analytical region in comparison with other methods [16]. The RTM firstly searches rays from a source to a receiver, and secondly compute electromagnetic fields based on the ray data. Computation time of searching rays depends on the propagation environment. In general, the searching rays

dominate about 90% in the total computation time. Since our target is the large analytical region, the simplified RTM is applied [12]. In this section, the principle of the proposed simplified RTM is described.

There are two steps in the proposed method. Firstly, we discretize scattering objects in terms of representative points as follows [13]:

$$\mathbf{p}_{mn}^i = (x_{mn}^i, y_{mn}^i, z_{mn}^i) \quad (6)$$

$$(i = 1, 2, \dots, I, \quad m = 1, 2, \dots, M, \quad n = 1, 2, \dots, N)$$

where  $i$  is the number of obstacles,  $m$  is the number of faces and  $n$  is the number of representative points constituting the face. This is very important to rapidly compute electromagnetic fields and to maintain the field accuracy. It should be noted that the sizes of each face must be larger than the wavelength [16]. Therefore, the small parts of obstacles are ignored if they are smaller than the wavelength. A unit normal vector of each face is also needed. It is given by

$$\mathbf{n}_m^i = \frac{\mathbf{a}_m^{i(1)} \times \mathbf{a}_m^{i(2)}}{|\mathbf{a}_m^{i(1)} \times \mathbf{a}_m^{i(2)}|} \quad (7)$$

where  $a^{(1)}$  and  $a^{(2)}$  are adjacent vector expressions of each face. Position and normal vectors are enough information for searching rays. Figure 5 shows discretized faces, and allocation of position and normal vectors.

Secondly, we simplify the procedure of ray searching. First, a representative point at each face is selected. In this paper, the representative point is located at the center of each face. Next, we determine whether each representative point and

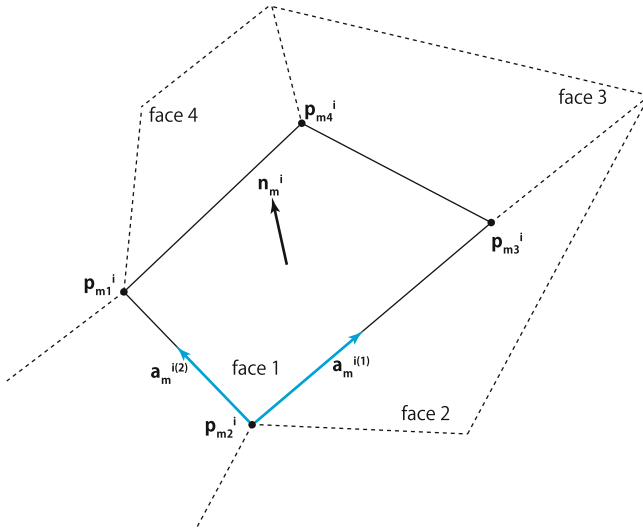


Fig. 5. Discretized faces.

source/receiver are in line-of-sight (LOS) with each other. If the representative point is in LOS for both source and receiver, the method generates initial rays by connecting from the source to the receiver via representative points. However, they are not real rays. In order to obtain more accurate rays, those rays are modified by using the imaging method [15]. Figure 6 illustrates the concept of the ray searching above complicated terrain.

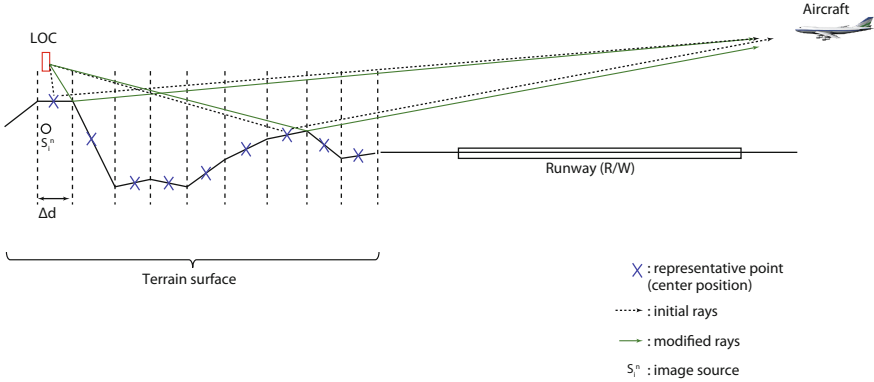


Fig. 6. Ray searching.

Electromagnetic fields are computed based on the ray data. Electric field at the receiver side is given by

$$E = \sum_{n=1}^N \left[ \prod_{m=1}^{M_n^i} (D_{nm}^i) \cdot \prod_{k=1}^{M_n^s} (D_{nk}^s) \cdot E_0 \right] \frac{e^{-j\kappa r_n}}{r_n} \quad (8)$$

where  $\mathbf{E}_0$  is the electric vector of the  $n$ -th ray at the first reflection or diffraction point,  $N$  is the total number of rays,  $M_n^i$  is the number of times of image diffraction, and  $M_n^s$  is the number of times of source diffraction. The distance of the  $n$ -th ray from the source to the receiver is given by

$$r_n = \sum_{k=0}^{k=M_n^i+M_n^s} r_{nk} \quad (n = 1, 2, \dots, N) \quad (9)$$

where  $r_{nk}$  is the  $k$ -th distance from one reflection or diffraction point to the next one. Diffraction is divided into two parts, that is, source diffraction and image diffraction [15]. They are given for the field continuity. Details are discussed in reference [16].

## 4 Numerical Example

Some numerical examples are shown in this section. In this paper, we select the one-frequency LOC system which has a carrier frequency. Carrier frequency

$f = 100$  MHz and input power of CAR  $P_i = 10$  W are selected as parameters. Figure 7 shows the geometry of the problem. Runway (R/W) is 3000 m with a small slope. Terrain surface between LOC and the R/W end is random surfaces which consist of 50 m meshes. Roughness data is given by the uniform distribution except for runway area. The LOC is located at 350 m behind the runway end, and its height is 8 m. It should be noted that this is not real environment. Figure 8 shows an example of ray distribution between the source and the receiver. It is shown that many scattered waves arrive at the receiver side. Electric fields are computed by such ray information.

Figures 9 and 10 show the field distribution in 3D where the receiver is located at 6 m height. In this figure, we disregarded the multiple reflection and diffractions. The unit is expressed in dB. Figure 9 is carrier wave, and Fig. 10 is sideband wave. It is demonstrated that the radiation forms are distorted by the scattered

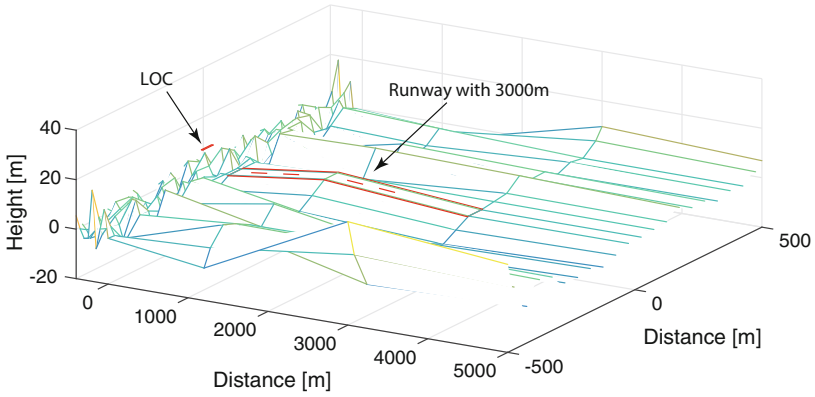


Fig. 7. Geometry of the problem.

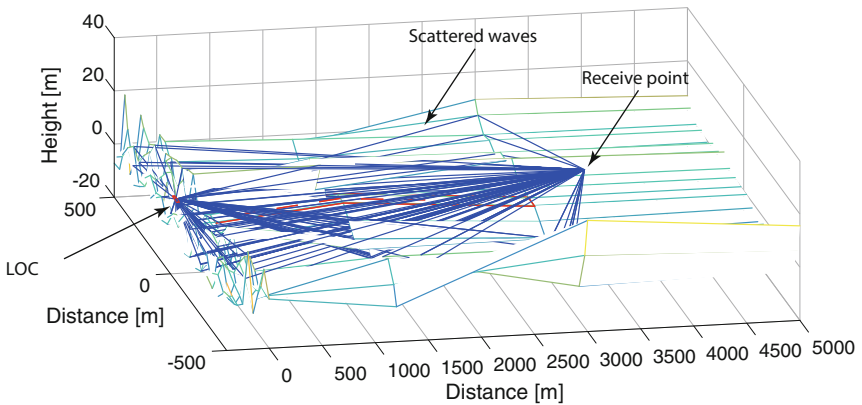


Fig. 8. An example of ray distribution.

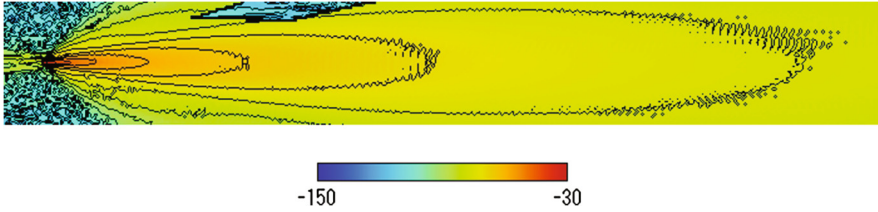


Fig. 9. Field distribution (carrier).

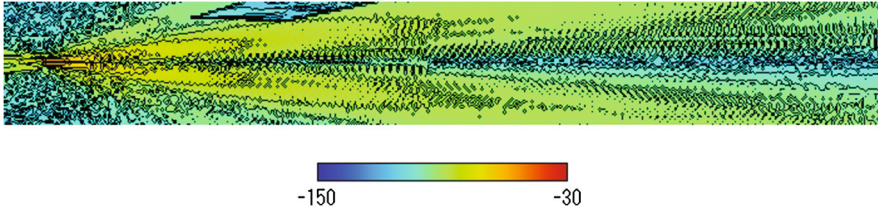


Fig. 10. Field distribution (sideband).

waves from the complicated terrain. Sideband waves are especially influenced by unneeded waves.

Finally, we show the value of DDM along runway center line. Figure 11 shows field intensity along runway center line. Red and blue lines are carrier and sideband waves, respectively. Field intensity of sideband wave along runway center line becomes generally zero. However, it is shown in this figure that the scattered waves penetrate to the approach course. This would be the cause that the DDM is dis-

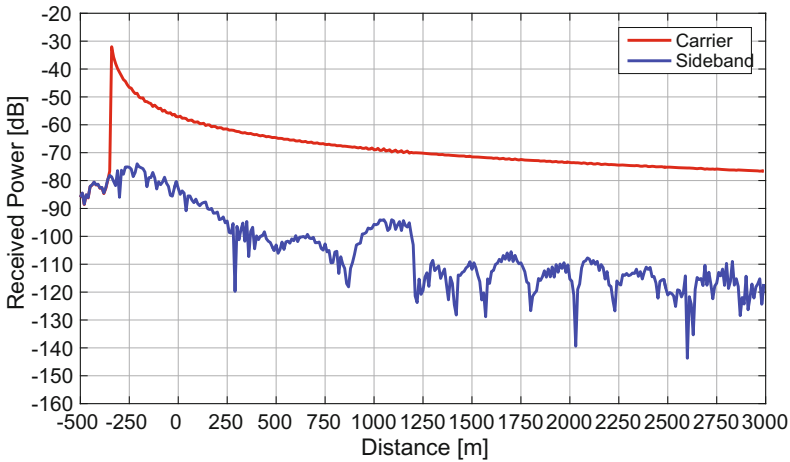
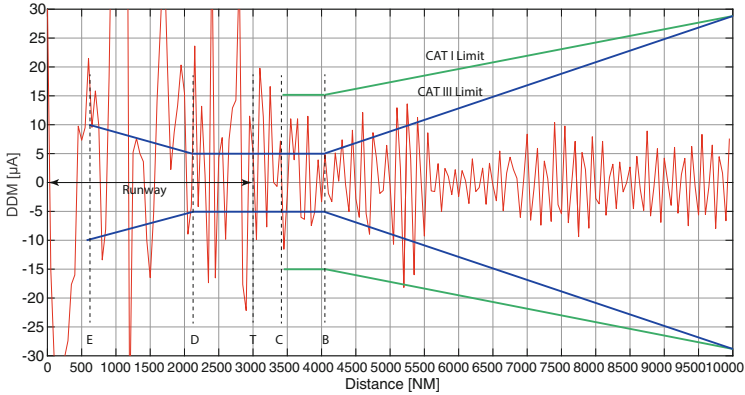


Fig. 11. Filed intensity along runway center line.



**Fig. 12.** Estimated DDM.

torted. Figure 12 shows the value of DDM estimated by the result of Fig. 11. In this figure, the ICAO limitation is also indicated. It is demonstrated that the DDM is strongly influenced by the scattered wave. It is also found that this result does not satisfy with the ICAO CAT III limitation, and the values satisfy with only CAT I limitation. The values, however, are actually smoothed since we disregarded the filter depending on the target speed.

In this paper, we found that the scattered waves caused by the complicated terrain impact on the LOC signals, resulting in the degrading LOC quality. In order to prevent those phenomenon, the counter poise or other techniques would be expected to be used for covering the terrain surfaces. However, we also need to confirm numerical accuracy.

## 5 Conclusion

In this paper, we discussed the influences of multipath interferences caused by 3D terrain model to LOC. Firstly, the principle of LOC was reviewed. Next, the simplified RTM was shown to treat the large analytical region and to rapidly compute electromagnetic fields. They are achieved by discretizing the scattering object and simplifying ray searching. Finally, some numerical results were shown. 3D terrain profile was generated by the uniform random unit. It has been shown that many diffracted rays arrive at receiver side. We have found that the scattered waves of sideband penetrate to the approach course. It has been found that the DDM was distorted by scattered waves. In order to prevent this problem, we need some techniques to cover the terrain.

This paper is the first approach to analyze multipath environment which causes the degradation of LOC signals. This paper presented the concept of the analytical method. We need to confirm the numerical accuracy of the proposed method. We would like to also compare the numerical result with the experimental result. They will be our future works.



**Acknowledgment.** The work was supported in part by a Grant-in-Aid for Young Scientists (B) (16K18072) from Japan Society for Promotion of Science.

## References

1. ICAO (International Civil Aviation Organization): Aeronautical Telecommunications, Annex 10, vol. 1, 6th edn. (2006)
2. Chin, G., Jordan, L., Kahn, D., Morin, S.: Instrument landing system performance prediction. In: IEEE MTT-S International Microwave Symposium, pp. 346–348, May 1975
3. Redlich, R.W., Gorman, J.T.: Disturbance of ILS localizer signals by reflections from large hangers. *IEEE Trans. Aerosp. Electron. Syst.* **AES-5**, 1001–1002 (1969)
4. Shin, S.L.: ILS localizer multipath analysis. *IEEE Trans. Aerosp. Electron. Syst.* **AES-7**(1), 54–60 (1971)
5. Thain, A., Estienne, J-P., Robert, J., Peres, G., Cambon, G., Evain, L., Splitz, B.: A solution for ILS disturbance due to a building. In: Proceedings of the 6th European Conference on Antenna and Propagation (EuCAP), pp. 2392–2395, March 2012
6. Thain, A., Estienne, J.P., Peres, G., Spitz, B., Evain, L., Kumar, M.: Comparisons of different approaches for ILS simulation. In: Proceedings of the 4th European Conference on Antenna and Propagation (EuCAP), Barcelona, Spain, pp. 1–5, April 2010
7. Geise, R., Schueuer, J., Thiele, L., Notte, K., Beckers, T., Enders, A.: A slotted waveguide setup as scaled instrument-landing-system for measuring scattering of an A380 and large objects. In: Proceedings of the Fourth European Conference on Antenna and Propagation (EuCAP 2010), Barcelona, Spain, pp. 227–231, April 2010
8. Greving, G., Biermann, W.D.: Theoretical aspect and numerical solution of scattered from objects under grazing angle incidence - the A380 and the aircraft tailfin. In: Proceedings of the 37th European Microwave Conference, Munich, Germany, pp. 1369–1372, October 2007
9. Godfrey, J., et al.: Terrain modeling using the half-plane geometry with applications to ILS glide slope antenna. *IEEE Trans. Antennas Propag.* **24**, 370–378 (1976)
10. Luebbers, R., Ungvichian, V., Mitchell, L.: GTD terrain reflection model applied to ILS glide slope. *IEEE Trans. Aerosp. Electron. Syst.* **18**, 11–20 (1982)
11. Walton, E.K.: Effect of wet snow on the null-reference ILS system. *IEEE Trans. Aerosp. Electron. Syst.* **29**, 1030–1035 (1993)
12. Honda, J., Otsuyama, T.: An estimation algorithm of scattered powers caused by a moving aircraft. *IEICE Commun. Express* **2**(11), 490–495 (2013)
13. Honda, J., Otsuyama, T.: Estimation of target detection rate in aircraft surveillance system. In: Proceedings of the 17th International Conference on Network-Based Information Systems (NBIS 2014), Salerno, Italy, pp. 561–565, September 2014
14. Honda, J., Otsuyama, T.: Rapid computation algorithm for radio wave propagation characteristics on airport surface. In: Proceedings of the Eighth International Conference on Complex Intelligent and Software Intensive Systems (CISIS 2014), Birmingham, United Kingdom, pp. 302–306, July 2014
15. Honda, J., Uchida, K., Yoon, K.Y.: Estimation of radio communication distance along random rough surface. *IEICE Trans. Electron.* **E93-C**(1), 39–45 (2010)
16. Takematsu, M., Uchida, K., Honda, J.: Method for reduction of field computation time for discrete ray tracing method. *IEICE Trans. Electron.* **E97-C**(3), 198–206 (2014)

# Evaluation of Never Die Network System for Disaster Prevention Based on Cognitive Wireless Technologys

Goshi Sato<sup>1</sup>, Noriki Uchida<sup>2</sup>, Norio Shiratori<sup>3</sup>,  
and Yoshitaka Shiabat<sup>1(✉)</sup>

<sup>1</sup> Iwate Prefectural University, 152-52 Sugo, Takizawa, Iwate 020-0693, Japan  
sato\_g@ipu-office.iwate-pu.ac.jp,

shibata@iwate-pu.ac.jp

<sup>2</sup> Fukuoka Institute of Technology,  
3-30-1 Wajiro-Higashi-Ku, Fukuoka 811-0295, Japan  
n-uchida@fit.ac.jp

<sup>3</sup> Waseda University, 1-104, Totsuka, Shinjuku, Tokyo 169-0071, Japan  
norio@shiratori.riec.tohoku.ac.jp

**Abstract.** We developed a Never Die Network (NDN) system that is a new network system to achieve both the Network Capability in the normal and Network Connectivity in disaster based on the experience of Great East Japan Earthquake. In this paper, we propose a method for the system to autonomously derive the optimum packet flow by measuring the communication state such as throughput and packet loss in a system such as to considering multiple different access networks. We prepared a test bed that implements a prototype system, and evaluated based on a disaster scenario.

## 1 Introduction

By large tsunami disaster caused by the Great East Japan Earthquake that occurred in 2011, following problems occur in the affected areas of information and communication systems [1].

- Failure or congestion in the wired communication network and a mobile communication network
- Unknown radio waves available around
- Failure recovery work flame by the network administrator absence
- Occurs of information isolated region
- Failure revelation of emergency communication equipment that is not used everyday
- Failure of power supply equipment, low battery

To solve these problems, a network system having the following characteristics has been required.

- Physically redundant hardware configuration
- Available communication radio waves the system itself is detected

- Understand the changes in the network performance due to congestion, etc.
- The provision of Internet connections by automatic network configuration changes
- Dynamic expansion of the network provides coverage
- And both Network Connectivity under Network Capacity and disaster situation at the time of normal
- Autonomous power supply

	FTH	WiMAX	Cellular	Satellite	WiFi
Connection	Wired Internet Connection	Wireless Internet Connection	Wireless (Wide area) Internet Connection	Wireless (Outdoor area) Internet Connection	Wireless Local Network
Speed	High Speed	20~75Mbps	128Kbps~20Mbps	Low Speed	High Speed
Weak point	Not resistant to disaster	narrow available area	Easy to congestion	High Delay (RTT500~1000ms)	short communication distance (Possible distance improvement in directional antenna)
vs. Disaster	×	△	△	○	○

Fig. 1. Comparison of various types of information communication systems

In addition, in the Great East Japan Earthquake, actually satellite IP communication systems and mobile phone network wireless LAN, a plurality of different communication network such as an ad-hoc network is introduced into the affected areas, it was a great effect on the temporary restoration of the network [2]. However, in those network systems that are utilized in the event of a disaster, as shown in Fig. 1, and found to have strong and weak points, respectively, it is considered to be not available in some situations.

Therefore, instead of the network systems, such as relying on certain single information communication unit only, a network system such as utilizing a plurality of different information communication unit redundantly is considered to be effective.

We therefore, a plurality of different information and communication means is integrated management, it is possible to continue to flexibly follow the ever-changing situation in the event of a disaster, there is a network system that combines the Network Capability during normal time of Network Connectivity and disaster Never Dies network system.

## 2 Purpose

The purpose is to develop Never Die Network (NDN) system based on lessons earthquake using cognitive radio technology and SDN technologies in order to enable communication even under any circumstances of the disaster. NDN system can accommodate a plurality of different Internet access network based on the experience of the Great East Japan Earthquake. Housing access network either wired or wireless. Moreover, the environment surrounding the network to change from moment to

moment, it is necessary to follow them network performance and such as throughput and packet loss rate in the affected areas, such as failure and cutting. Therefore, in this research will be monitored by the rapid and minimal packet by cognitive radio technology in the network performance and status of all of the housing access network. Then, we propose a rapid and efficient data flow control will be implemented using SDN techniques in order to avoid a decrease in network performance due to the physical failure or congestion, etc. Development requirements of NDN system is as follows.

- Equipped with a plurality of different information and communication equipment
- To implement the detection capabilities of each network performance by cognitive radio technology
- To implement a mechanism to automatically avoid the physical failure or congestion or the like by using the SDN technology
- To implement a mechanism to extend the network range using the ad-hoc communication technology
- The achieve both Network Capacity of the normal and Network Connectivity under disaster situation
- Autonomous power supply

### 3 System Architecture

The system configuration of NDN System is shown in Fig. 2. The system consists of three elements including NDN switches, mobile NDN switch, and NDN controller.

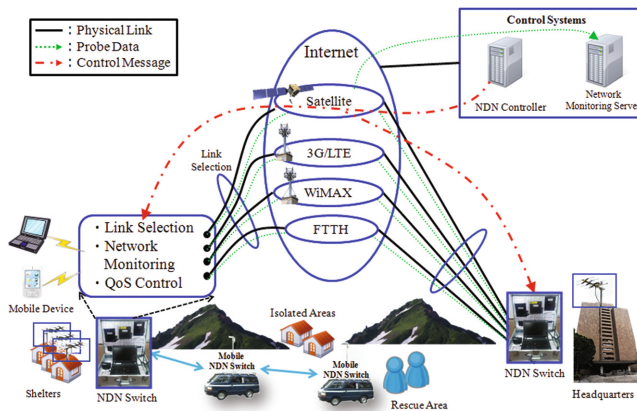


Fig. 2. System configuration

NDN switch acts as a fixed Internet gateway and placed at the important base such as shelter and disaster response headquarters. A plurality of different access networks are available, such as 3G/LTE and WiMAX and FTTH and satellite communications to accommodate the SDN techniques. The network monitor periodically network

performance for each access network by cognitive radio technology and feeds back the result to the packet flow. Also NDN System includes a self-power that can be supplied independently.

Mobile NDN switch is different from the NDN switch as an Internet gateway. The main function of Mobile NDN switch is to provide a network connection between the information isolated areas such as rescue operations location and gateway NDN switch and to build a multi-hop network to a remote location by the ad hoc communication technology. It should be noted that the description of the mobile NDN switch is omitted in this paper.

NDN controller is connected always all of the NDN switches via a satellite communication network and to grasp the failure of network devices by receiving a feedback of network performance monitoring results. Based on feedback of the NDN controller issues the appropriate control instructions to all of the NDN switches.

## 4 Problems to Be Solved for the NDN System

Preceding NDN systems, it is necessary to perform the dynamic switching based on the monitoring result by network users while using the network to constantly monitor the state of a plurality of different internet access networks. In this chapter, we will be clear the problems to be solved in order to NDN system realization including Network Measurement Problems, Link Switching Problem and Communication Priority Problem.

With Network Measurement Problems, NDN system comprising a plurality of different access networks is always measures the state of each Internet access networks available in order to follow the state of communication such as the ever-changing disaster area throughput and packet loss rate and delay time. If the measurement packet amount is increased, there is a problem that inhibits the communication from the network user to be transferred on the NDN system. Because it means that measuring the change in network performance on the network system. Thus, lightweight and fast network performance measurement method is required that is considering a communication session through the NDN on the system.

With Link Switching Problem, Network environment surrounding the disaster area to change dynamically. In addition, the application requests to the disaster information network is constantly changing, as shown in Fig. 3.

NDN system requires the ability to select the best Internet access network. By understanding the disaster area of network status. In addition, it is necessary to respond to changes in the application requirements of the network users.

With Communication Priority Problem, Under accident conditions, temporary communication systems such as mobile communications vehicle is assumed that down by very many communication request occurs against capable of providing network capacity. However, there is a communication should be processed with priority in the disaster situation, for example, local governments between communication and medical facilities between communication. NDN system must to execute the priority processing to recognize the priority of the communication packet and the offloading packet based on the traffic.

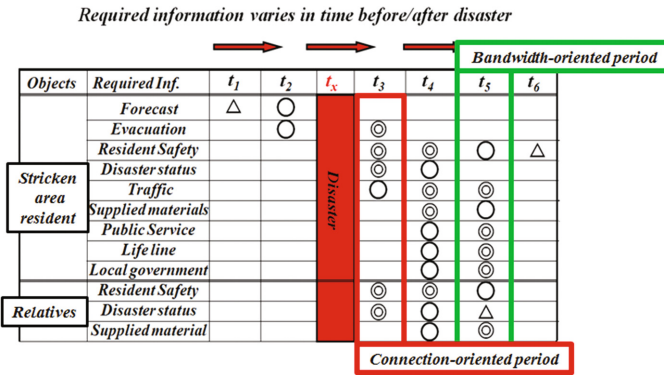


Fig. 3. The application requests to the disaster information network

## 5 The Proposed Method

### 5.1 The Network Performance Measurement Method in NDN

The system performs the measurement monitoring network performance in order to detect a change of network performance. The target measurements are as follows.

- throughput
- average delay time
- packet loss rate

With monitoring the network throughput, two methods including passive and active methods are existed [3]. In passive methods, the throughput is calculated by implementing the monitoring function at all of the routers which the packets pass through. In active method, on the other hand, probe packets are transmitted between the end-to-end terminals [4]. In passive method, the monitoring functions have to be installed on the all of the routers where packets pass through. This is very difficult because Internet is huge and managed by different organizations. Therefore, by this reason, in our system, the active method is applied. Furthermore, there are two active methods including available bandwidth measuring method such as iperf and packet train method such as pathchirp and pathquik [5, 6]. In the available bandwidth measuring method, a large number of packets are inserted. While in the packet train method, only limited number of the probe packets are used in a limited period. For this reason, the packet train method is applied in our system.

Transmitted and received time stamps are expressed  $T_s$ , and  $T_r$ . The packet transmission interval is expressed as  $T_i$ , the total number of transmitted packets is  $n$ . These are used to calculate network performance by the following equations.

- The average delay time ( $D$ )

$$D = \frac{\sum (T_r - T_s)}{n} \tag{1}$$

- The packet loss rate (*PLR*)

$$PLR = 1 - \frac{n'}{n} \quad (2)$$

( $n'$ : The number of UDP packets successfully received)

## 5.2 Link Selection Method

To the problem of degraded network performance due to congestion and so on, in this research, we solve by link switching based on network performance. In the proposed method, to detect the performance degradation of the network by monitoring on a throughput, delay, and packet loss. For example, in this figure, because there is congestion in WiMAX and high delay satellite, and requirement of low latency, 3G is selected.

First, the measurement results are smoothed by this formula.

$$n_i = am_i + bm_{i-1} + cm_{i-2} \quad (3)$$

Where  $a$ ,  $b$ ,  $c$  are the weight of moving average.  $m$  is the measurement results for each time. Then, smoothing values are normalized by this formula.

$$S_i = \begin{cases} (1 - \frac{n_i - l_i}{u_i - l_i}) * 10 & (l_i < n_i < u_i) \\ 1 & (n_i \geq u_i) \\ 9 & (n_i \leq l_i) \end{cases} \quad (4)$$

$$S_i = \left( \frac{n_i - l_i}{u_{max} - l_i} \right) * 10$$

Where  $n$  is the smoothed value,  $l$  is the minimum value, and  $u$  is the maximum value in monitoring history. Finally, it will be evaluated using the normalized value by this formula.

$$P_i = xn_{throughput} + yn_{packet\ loss\ rate} + zn_{delay} \quad (5)$$

Where  $x$ ,  $y$ ,  $z$  are the weight of the network policy.

## 6 Prototype and Performance Evaluation

In order to demonstrate and evaluate dynamic link select function, we build a prototype system by OpenFlowSwitch device. On each site, we set the OpenFlowSwitch equipped with a variety of wireless access devices for this system. Wireless access networks to be used in the present prototype system are Satellite with ave. 1.3 Mbps in down speed, 3G/LTE with ave. 3.5 Mbps in down speed and FTTH with ave. 25 Mbps in down speed.

We were prepared two evaluation environment. Environment 1 simply switch between the three Internet access network (Fig. 4). Environment 2 is switched using the function of the NDN system (Fig. 5). We evaluated the end-to-end throughput and packet loss as network performance based on the disaster occurrence scenario. The scenario is as follows: Initially all three access networks including satellite network with Ave. 1.29 Mbps throughput, 3G/LTE network with Ave. 3.5 Mbps and FTTH with Ave. 25.01 Mbps are alive and the FTTH link is selected. Then a disaster occurred after 10 s. FTTH network stopped due to cable failure. Then link of the FTTH network is automatically switched to the 3G/LTE network. After 20 s is elapsed, 3G/LTE network is congested and the network link is automatically switched from 3G/LTE to satellite network.

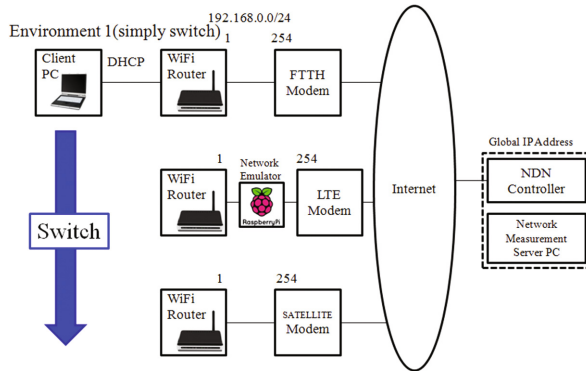


Fig. 4. Evaluation Environment 1

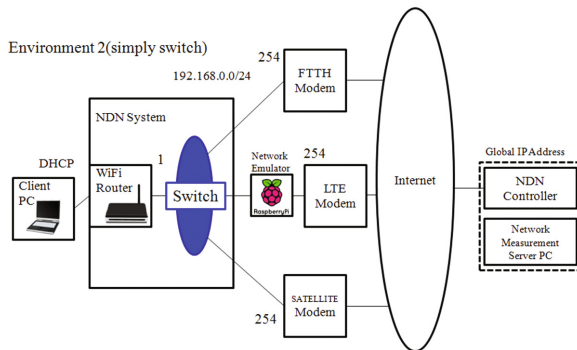


Fig. 5. Evaluation Environment 2

We measured the end-to-end network throughput. The result of end-to-end throughput is shown in Figs. 6 and 7. After 10 s from the starting time, the end-to-end throughput suddenly decreased from Ave. 25 Mbps throughput to Ave. 3.5 Mbps by satellite link. After 20 s–30 s, the network link was switched to 3G/LTE network with



Ave. 1.29 Mbps. Environment 1 performs simple switching without performing measurement. So environment 1 had continued to use the congested network. On the other hand, environmental 2 can detect a change in network performance by using the function of NDN system. So it was possible to carry out a rapid switching. Thus, even though the disaster occurred and all of the networks were failed, the satellite network could be always alive and maintained the communication link to the Internet and realized Never-Die Network.

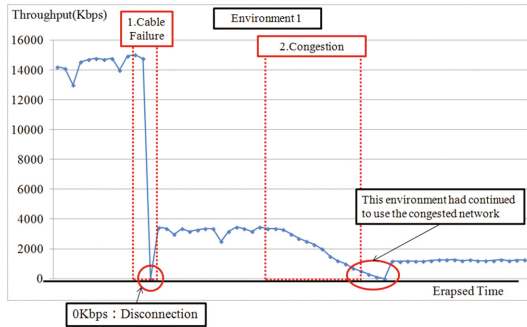


Fig. 6. Performance monitoring result in Environment 1

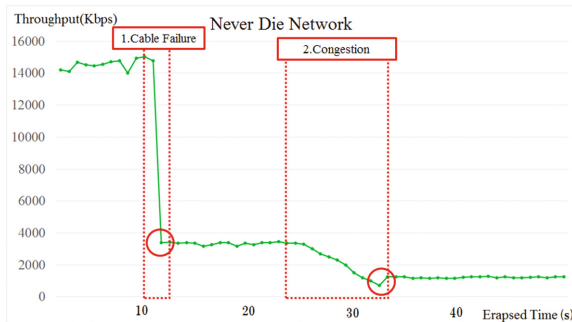


Fig. 7. Performance monitoring result in Environment 2

Next, the communication experiment is to evaluate the network performance provided by the mobile NDN system. Experiments were performed with straight road in the Mt. Iwate. This road there is no obstacle between the 1200 m, it was selected as the field of the wireless communication experiment. Communication experiments are carried out between mobile NDN system with the two vehicles, place the mobile communications vehicle equipped with a mobile NDN system, attach the equipment to the antenna pole, keep extending the antenna pole as much as possible (Fig. 11). Then, by moving the other mobile communication car by 100 m, to collect data by measuring the performance. Wireless bridge that is connected to the mobile NDN system was selected the following three types, 5 GHzFWA, 2.4 GHz (IEEE802.11b), 2.4 GHz (IEEE802.11b/g).

We measured the throughput and delay time in each wireless bridge. In addition, we measured the throughput and latency of the network which the mobile NDN system was constructed. Furthermore we have prepared to verify it is possible to switch in response to the performance request to the network, two types of performance requirements, throughput oriented  $x, y, z (7,1,1)$  and the delay time oriented  $x, y, z (1,7,1)$ . Raspberry Pi for network measurement is connected to the wireless bridge. Raspberry Pi is constantly measuring the network performance of each wireless bridge, and notifies the measurement result to the NDN controller.

By using these mechanisms, it is possible to perform dynamically switched based on the measurement results of the network performance. Moreover, by considering the performance requirements when the switching determination, it is possible to switch in response to the request. We evaluate the functionality of the proposed system by measuring the performance of the NDN system. The results of this experiment are shown below.

Network performance measurement results for each wireless bridge is shown in Figs. 8 and 9. Bridge 1 has a high throughput has a delay time is 100 ms or higher. In addition it became unable to communicate in the 200 m point because of the omni-directional antenna equipment. Bridge 2 for utilizing IEEE802.11b, throughput is lower than the bridge 1, the delay time is about 50 ms. In addition, it was possible connection to 600 m for the planar antenna equipment. Bridge 3 has a lower throughput due to the speed limit, but the delay time is the smallest. Further, the communication distance is longer than 1 km, due to the integrated antenna of high power.

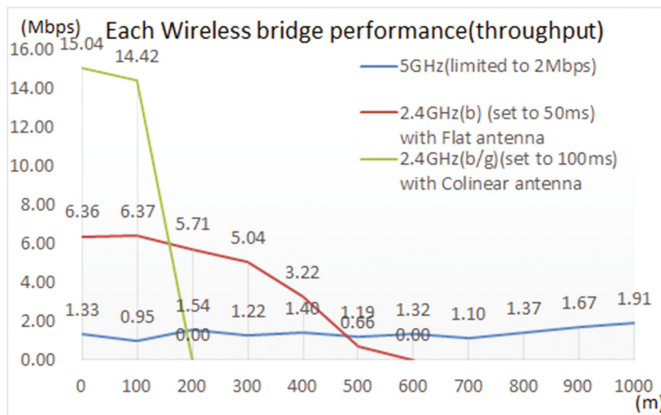
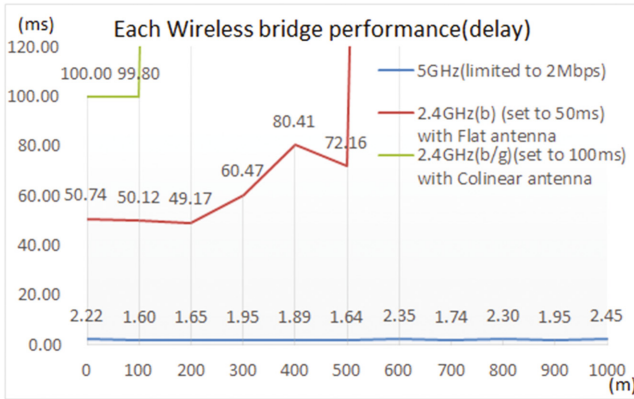
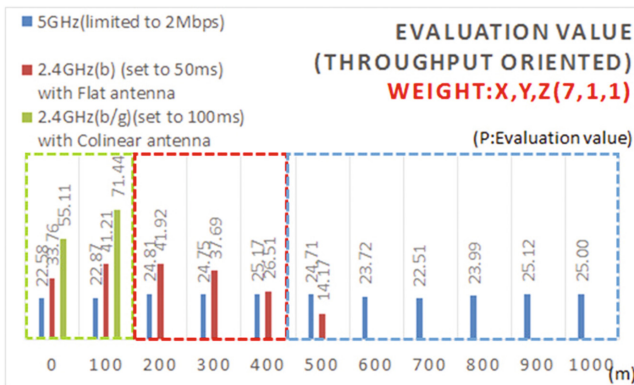


Fig. 8. Changes in the throughput of each wireless bridge

If the priority to throughput (Fig. 10), the performance measurement results of NDN system, shown in Figs. 11 and 12. In the 100 m point, the most high-speed bridge 3 has been selected as the route. In the 200 m point, bridge 3 link down due to communication distance limit of omni-directional antenna, switched to the bridge 2. Then, the bridge 2 is able to communicate by the plane antenna to the 500 m point. But gradually reduced by throughput distance away, it was switched to the bridge 1 in the



**Fig. 9.** Changes in the delay time in each wireless bridge



**Fig. 10.** Calculation results of the evaluation value at each point (throughput-oriented)

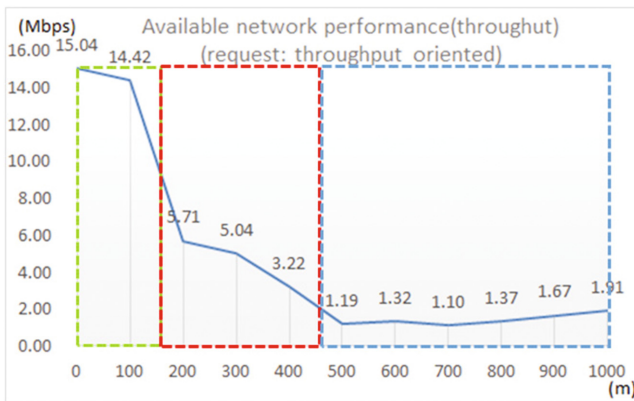


**Fig. 11.** Change in the measured throughput from the client terminal (throughput-oriented)

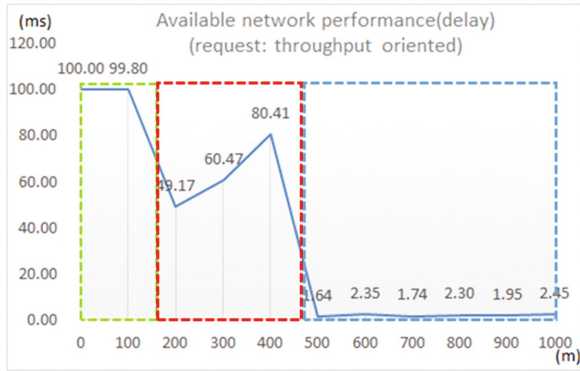


Fig. 12. Change in the measured delay time from the client terminal (throughput-oriented)

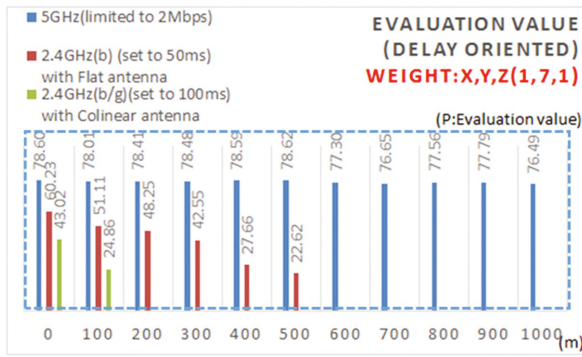


Fig. 13. Calculation results of the evaluation value at each point (delay-oriented (x,y,z:1,7,1))

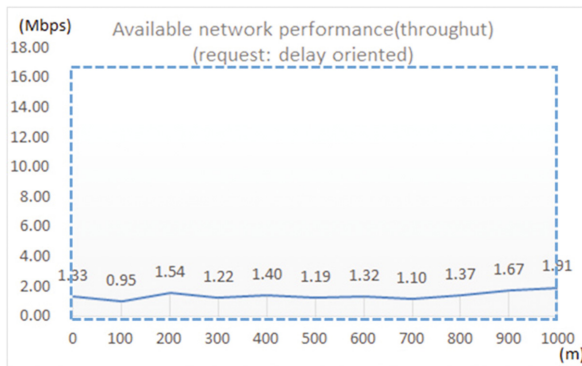
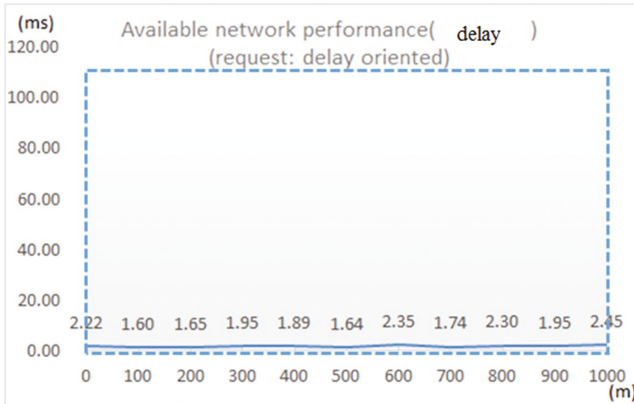


Fig. 14. Change in the measured throughput from the client terminal (delay-oriented)



**Fig. 15.** Change in the measured delay time from the client terminal (delay-oriented)

500 m point. This is because the evaluation value of the bridge 2 in the 500 m point evaluation value of the bridge 1 is exceeded (see 500 m point in Fig. 13).

In the case of the delay time oriented, performance measurement results of the NDN system is as shown in Figs. 14 and 15. As shown in figures, at all points, the bridge 1 is selected. This is due to the delay time of bridge 2 and bridge 3 is large, the evaluation value is reduced in the delay time-oriented requirements. Thus, using the present system, it has been demonstrated possible to select a network matching the requirements by giving a request for a network as a weight.

## 7 Conclusion and Discussion

In this study, we have implemented a cognitive radio system using the SDN technology. Cognitive radio device is equipped with FTTH, 3G/LTE mobile telephone network, a satellite communication network. Currently, we are running the prototype system by placing the three based in cognitive radio device. Furthermore, we constructed a test bed environment to evaluate the performance and functionality of the system. In addition, we demonstrated the link switching based on the measured value of the network performance using the test bed and showed the availability of NDN system.

In the future, we are planning to implement the following evaluation experiment on the test bed including Evaluation of the measurement time and amount of data on network performance measurement, Evaluation of communication inhibition rate by the network performance measurement method that considers the communication session, Evaluation of the network capabilities by the access network switching method based on network performance measured value and the application request.

**Acknowledgements.** The research was supported by SCOPE (Strategic Information and Communications R&D Promotion Programme) Grant Number 142302010 by Ministry of Internal Affairs and Communications in Japan.

## References

1. Shibata, Y., Uchida, N., Shiratori, N.: Analysis and proposal of disaster information network from experience of the great East Japan earthquake. *IEEE Commun. Mag.* **52**, 44–48 (2014). Japan Police Department, “The Great East Japan Disaster. <http://www.npa.go.jp/archive/keibi/biki/index.htm>
2. Ali, A.A., Michaut, F., Lepage, F.: CRAN, end-to-end available bandwidth measurement tools: a comparative evaluation of performances. In: *IPS-MoMe* (2006)
3. Gerber, A., Pang, J., Spatscheck, O., Venkataraman, S.: AT&T labs, speed testing without speed tests: estimating achievable download speed from passive measurements. In: *IMC 2010*, 1–3 November 2010
4. Ribeiro, V.J., Riedi, R.H., Baraniuk, R.G.: pathChirp: efficient available bandwidth estimation for network paths. Presented at *Passive and Active Monitoring Workshop (PAM 2003)*, San Diego, CA, US, 6–8 April 2003
5. Oshiba, T., Nakajima, K.: Quick end-to-end available bandwidth estimation for QoS of real-time multimedia communication. In: *Computers and Communications (ISCC)* (2010). Service Platforms Res. Labs., NEC Corp., Japan
6. Satty, T.L., et al.: How to make a decision: the analytic hierarchy process. *Eur. J. Oper. Res.* **48**, 9–26 (1990)
7. Uchida, N.: Min-max based AHP method for route selection in cognitive wireless network. In: *Proceedings of the 2010 13th International Conference on Network-Based Information Systems, NBIS 2010*, pp. 22–27 (2010)
8. Uchida, N., Takahata, K., Shibata, Y.: Disaster information system from communication traffic analysis and connectivity (quick report from Japan Earthquake and Tsunami on March 11th, 2011). In: *The 14th International Conference on Network-Based Information Systems (NBIS 2011)*, Tirana, Albania, pp. 279–285, September 2011
9. Open Networking Foundation, Intro to OpenFlow. <https://www.opennetworking.org/standards/intro-to-openflow>
10. Uchida, N., Sato, G., Shibata, Y., et al.: Selective routing protocol for cognitive wireless networks based on user’s policy. In: *The 12th International Workshop on Multimedia Network Systems and Applications (MNSA 2010)*, pp. 112–117, June 2010

# Monitoring Health of Large Scale Software Systems Using Drift Detection Techniques

L.H.C. Prabodha<sup>(✉)</sup>, W.R.R. Vithanage, L.T. Ranaweera,  
D.M.M.A.I.B. Dissanayake, and S. Ranathunga

Department of Computer, Science and Engineering, University of Moratuwa,  
Katubedda, Moratuwa, Sri Lanka  
{chamilprabodha.12,ruchindra.12,lochana.12,amitha.12,  
surangika}@cse.mrt.ac.lk

**Abstract.** Anomaly detection in large-scale software systems is important to guarantee smooth operation of the system. Upon detection of an anomaly, it is vital to identify the root cause behind the anomaly to decipher actionable information and prevent future incidents. Isolation of root causes becomes inherently difficult as the number of components and parameters in each component increase. This paper discusses successful application of three drift detection techniques, namely meta algorithm, fixed cumulative window model and Page-Hinckley test to identify the parameters that correlate to system abnormalities in a large scale complex software system. Out of these, change detection meta algorithm produced the best result.

## 1 Introduction

Statistical information related to the health of a software system can be accessed through various system specific parameters that are either logged to a file system or produced as data streams. In order to determine the root cause of a system anomaly, it is vital to identify the parameters generating the abnormal behaviour. This helps to prevent similar situations in the future. This is a difficult task to be carried out under manual inspection since there are many components and parameters in complex system that need to be monitored. Moreover, though machine learning techniques allow the system health to be determined using system specific parameters, they cannot be directly used to identify changes in parameters that relate to a system anomaly.

The number and type of parameters of a software system depend on its sub-components and their complexity. Identifying specific parameters that correspond to anomalies in software systems is explored in areas of feature selection, root cause analysis and monitoring and control of software systems. Feature selection techniques such as correlation based feature selection and principle component analysis provide a reduced set of parameters, which are closely related to abnormalities [8, 13]. The domain of root cause analysis discusses techniques such as clustering [3, 11], dynamic dependency models [2], extended Kalman filters [21], dynamic invariants detection [9] and Complex Event Processing (CEP) [7].

Drift detection techniques provide a memory efficient solution to identify the changes present in data on real time basis. Moreover, drift detection techniques have reasonable delay times in detecting changes compared to other techniques [17]. As in dynamic dependency models, and clustering, drift detection is not limited to identifying only the components that show abnormalities. Unlike CEP, drift detection techniques do not require hand-crafted rules.

Research carried out in the domain of drift detection has produced several techniques to identify drifts in data streams [1, 5, 12, 15, 18, 20]. These techniques have been applied in domains such as production systems [16] and industrial boiler systems [14]. However, drift detection has not been used to identify parameters that indicate poor health of large scale software systems.

This research proposes a method of root cause analysis of abnormal situations in complex systems, using drift detection techniques. In particular, this research applies drift detection techniques to data streams produced by a large-scale trading system to detect drifts in parameters of the system components, in order to identify parameters that show abnormal variations during system anomalies.

The dataset used in this research is synthesized to reflect four error scenarios in the trading system: file I/O error, connection error, processing error, and component health, for two complete days. Data corresponds to three components of the system, each containing 150 parameters in average. This research evaluates the results produced by three drift detection techniques: change detection meta algorithm, fixed cumulative window model and Page-Hinckley test.

The rest of the paper is organized as follows. Next section discusses related work in the domain of root cause analysis. In Sect. 2.3, techniques and methodology employed in this research are presented. Section 3 presents the evaluation and results. Finally, Sect. 4 concludes the paper.

## 2 Related Work

### 2.1 Root Cause Analysis

Correlation based feature selection and principle component analysis as feature selection techniques produce a reduced set of parameters, which correlates to abnormalities in software systems [8, 13]. Thus reduced parameters can be monitored closely under anomalous conditions of a system.

Clustering techniques and statistical tests have been used by Chen et al. [3] for root cause analysis of large scale internet services. Julisch [11] employs clustering techniques to form clusters of alarms for root cause analysis in the domain of intrusion detection. In distributed software systems, components and the dependencies have been modelled through dynamic dependency graphs [2]. System components are represented by nodes, and the dependencies among the components are represented by weighted edges.

In terms of identifying the changing parameters in software systems, a solution presented by Zheng et al. [21] based on extended Kalman filters monitors comparatively few parameters in the system. Research by Hangal and Lamb [9]



employs dynamic invariant detection for root cause analysis and focuses on identifying the faults in source code in software systems rather than the causes of faults of a system in execution. Since the components are distributed in most of the large software systems, faults in source code can occur anywhere in the system. Hence this approach has limitations with respect to large software systems.

As presented by Grell and Nano [7], CEP allows monitoring of parameters and identifying those that caused a particular fault in software systems real-time.

Clustering and dynamic dependency models identify only the components in software system that correlate to the anomalies of the system. The focus on the parameters that cause abnormal conditions is not highlighted in these techniques. Furthermore, techniques such as extended Kalman filters and dynamic invariant detection focus only on few parameters of software systems. CEP techniques require manual generation of the queries that detect the changes in parameter values.

## 2.2 Drift Detection

Drift detection is known as identifying the changes in statistical properties of parameters [6]. When the data streams become complex with the existence of a large number of parameters, drift detection techniques provide a memory efficient solution to identify the changes in parameters. The domain of drift detection consists of several drift detection techniques such as very fast decision tree learner, concept-adapting very fast decision tree learner, drift detection method (DDM), change detection meta algorithm (CDMA), fixed cumulative window model (FCWM), Jensen-Shannon distance, adaptive windowing, and Page-Hinckley test.

Decision tree learning has been used by Domingos and Hulten [4] to detect changes in webserver request data. Decision tree induction can be used to learn from high speed data streams. Though this approach is robust to low memory, it consists of the underlying assumption that data distribution is static throughout the data stream. To address the computational costs of the aforementioned approach, Hulten et al. [10] proposed concept-adapting very fast decision tree learner, which improves the previous work by changing the internal statistics of the model in order to avoid the need to learn the model for every new example.

CDMA was proposed by Kifer et al. [12] with the assumption that data is generated independently. Furthermore above research makes no assumption of the nature of probability distribution that generates the data and uses a fixed window and a sliding window for the comparison of inbound data. It is observed that the presence of negative values in data does not affect the computations used in this technique.

DDM proposed by Gama et al. [5] identifies drifts based on Bernoulli trials and approximation of binomial distribution to normal distribution. This research produces experimental results using a perceptron, a neural network, and a decision tree, which are learned under concept drift. This technique uses less memory since it does not require any data structure to detect drifts.

FCWM by Sebastio et al. [18] consists of a method where concept drift detection is addressed by monitoring probability distributions. Two windows,

a reference window and a current window are compared through the probability distributions using Kullback-Leibler divergence in order to detect drifts. Here the reference window consists of the past data while the current window consists of more recent data instances. Since fixed cumulative window uses data structures for the comparison of probability distributions, it tends to consume more memory and time comparatively. However the algorithm produces reasonable delay times in drift detection [17].

Jensen-Shannon distance is employed by Sez et al. [20] by combining the statistical process control algorithm of Gama et al. [5] and Kullback-Leibler divergence. Sez et al. [20] used Jensen-Shannon distance that eventually uses Kullback-Leibler divergence to create the distance metric. While using base 2 logarithm to calculate Kullback-Leibler divergence, the Jensen-Shannon distance is bounded between zero and one [20]. Since the threshold value space is reduced, defining a threshold value is fairly easier than other techniques.

Rather than using a fixed window model, Bifet and Gavalda [1] propose a solution that uses adapting windows to detect changes in time varying data streams. Adaptive windowing algorithm maintains a variable window, which consists of binary or real number values. The proposed algorithm adaptively grows the window length when the data stream is stationary and shrinks when the stream is subjected to change. Since adaptive windowing uses data structures to detect drifts, it is not memory efficient to apply this technique to complex systems that consist many components and parameters. For prediction of mass flow in broiler systems, adaptive windowing has been used to identify the drifts [16].

Page-Hinckley test is a sequential analysis technique developed to efficiently detect changes in normal behaviour of data [15]. The algorithm computes a cumulative variable, which is defined as the cumulative difference between the past data values and the average up to current instance. Alerts of changes are produced whenever the difference between current cumulative variable value and minimum cumulative variable value exceeds a predefined threshold. Page-Hinckley test detects changes in the average of a Gaussian signal [14]. Though Page-Hinckley test tends to produce relatively high false alarms, it is efficient in time and memory as the algorithm does not employ data structures to detect drifts. In a research conducted by Mouss et al. [14] Page-Hinckley test is used to detect faults appear in pasteurization system of argoalimentry production system.

As discussed above, each drift detection technique has its pros and cons. In particular, fixed cumulative window model and Page-Hinckley test perform better than other drift detection techniques in terms of delay in drift detection [17]. Unlike in other techniques, Jensen-Shannon distance is able to reduce the space of the distance threshold by producing distances in the range zero and one [18].

### 2.3 Techniques and Methodology

The target system of this research is a trading system with multiple distributed components. For simplicity, we focus only on a subsystem which represent significant part of the operation. Out of the drift detection techniques discussed in Sect. 2, in this research, three drift detection techniques: CDMA developed by

Kifer et al. [12], fixed cumulative window model [18], and Page-Hinckley test [15] are applied to determine the changing statistics of the selected trading system.

CDMA allows comparison of two windows using various distance metrics. Fixed cumulative window model maps the distance to a range between zero and one. Page-Hinckley test employs a cumulative summation of data points rather than the distance between two data windows. Since Page-Hinckley test does not use any data structures during computations, it is more memory efficient. In terms of delay in detecting changes, fixed cumulative window model and Page-Hinckley test produce reasonable delay times [17].

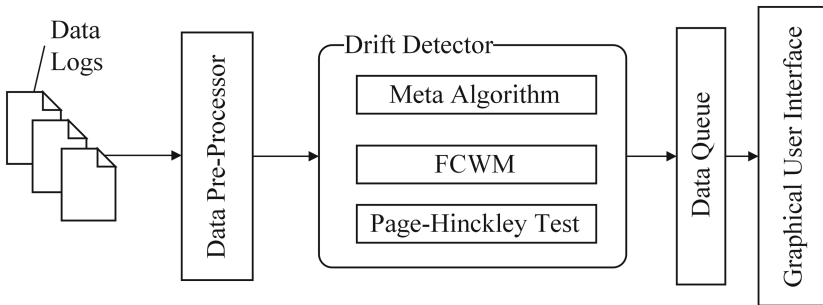
Number of components comprising the aforementioned subsystem considered in this research are as follows; Native Gateway - 2, Sequencer - 1 and Matching Engine - 1. Data streams produced by these components are n-dimensional, comprising of n attributes and values. Average value for n is 150 for the considered subsystem. Furthermore, each instance of data includes a timestamp followed by a component name, attribute name and attribute values. Every component produces a burst of data instances with a time granularity of one second.

Table 1 shows the structure of a stat line produced by a component. Data filtering component in our framework produces: <Nov 23 2016 14:07:35, 0, 0, 434, 455, 2, 14995, 1, 1, 0, 0, 0> as a parameter vector corresponding to the data shown in Table 1.

**Table 1.** The structure of a stat line

Timestamp	Component name	Stat name	Attributes and values
Nov 23 2016 14:07:35	Native Gateway	Native Real Time Partition 1 Sequencer	Total = 0, Rate = 0, Last Seq = 434
Nov 23 2016 14:07:35	Native Gateway	Native Real Time Partition 1 Distribution Server	Total = 455, Rate = 2, Last Seq = 14995

As shown in Fig. 1, our framework consists of a data pre-processor that buffers the bursts of data and filters relevant values to produce a parameter vector. These parameter vectors are sent to the drift detector component to detect changes in each parameter.



**Fig. 1.** Drift detection framework

Drift detector can make use of one of the three drift detection techniques: Page-Hinckley test, fixed cumulative window model and the CDMA. A selected drift detection technique is applied parallel on each parameter, which is monitored by the techniques mentioned above. Data filter component inserts ‘-1’ to the parameter vector if an attribute is not present in the data stream. Otherwise data filter component inserts the respective value of an attribute.

Each of the above drift detection techniques requires two predefined parameters: window size and threshold value. Increasing window size would neglect spikes in data streams and capture changes that last longer. However, this produces the risk of increase in false negative rate by not detecting changes corresponding to the actual fault. Similarly, decreasing the window size introduces the problem of high false positive rate. When the threshold value is larger, the algorithms produce few false positives. However this may result in not detecting some of the changes in data distribution [6, 12, 17].

## 2.4 Change Detection Meta Algorithm

This algorithm produces alerts whenever there are mismatches between the statistical properties in data windows. Kifer et al. [12] use two windows, a reference window and a sliding window to compare the statistical properties of data within each window. L1 norm is used as the distance metric for the comparison of two windows in change detection algorithm. In this research, the same algorithm is used with L2 norm as the distance metric. This algorithm is more robust to the ‘-1’ values in the parameter vector since the distance is calculated using L2 norm. The effect of negative values does not affect the algorithm.

## 2.5 Fixed Cumulative Window Model

Fixed cumulative window model uses probability distributions of two windows prior to any comparison between the windows. We obtain the distributions from the histograms, which are generated from the data in each window. One of the main problems encountered when learning histograms from data is deciding the number of bins or intervals. In past research, there are several methods for defining the number of bins in histogram such as Sturges rule, Scotts rule, and Freedman and Diaconiss rule [18, 19]. Sturges rule is only valid for moderate number of observed data points. Scotts rule employs Guassing density as a reference standard. For this research we employ Freedman and Diaconiss rule, which is  $k = 2(IQ)n^{-1/3}$  where  $k$  is the number of bins,  $IQ$  is the interquartile range and  $n$  is the number of data points. Since Diaconiss rule does not rely on reference standards and is not bound to the number of data point observations, it allows to generate an approximation of distribution of a given data window.

## 2.6 Page Hinkley Test

Page-Hinckley test is a sequential analysis technique used to detect changes in data streams [15]. The algorithm computes a cumulative variable, which is

defined as the cumulative difference between the past data values and the average up to current instance. It is observed that a time window of 24 instances gives the minimum delay in detected changes. Therefore we used 24 instances of past data points to calculate the cumulative variable. Alerts of change are produced whenever the difference between current cumulative variable value and minimum cumulative variable value exceeds a predefined threshold. However, when the cumulative variable is calculated, the ‘-1’ values affect the final cumulative sum. A possible solution for this problem is to take the absolute cumulative sum. However this does not guarantee to detect changes in values near ‘-1’.

### 3 Evaluation

#### 3.1 Dataset Generation

With the inherent nature of trading systems being highly available, extremely few occurrences of anomalies is observed in production environments. Therefore, data corresponding to abnormal operation is generated through a set of fault tolerance (FT) tests executed in an iterative manner to get multiple occurrences of faults. FT tests reflects four types of errors that could arise in the software components: file I/O error, connection error, processing error, and component status error. File I/O error is simulated for the Sequencer component while other error types are simulated for Matching Engine and Native Gateway components.

- File I/O error Related to anomalous behaviour in operations related to file input-output operations, this error is simulated by freezing I/O threads in software components.
- Connection error Related to connections between components in terms of TCP communication, this error is simulated by connection disruptions.
- Processing error Related to issues in processing, this error is simulated by freezing processing thread in software components for a specified time.
- Component status error Related to component health, this error is simulated by killing software components.

Each FT test is executed in 100 iterations within two days. In order to tag data corresponding to anomalies, timestamps before and after executing each iteration of fault scenario are recorded. The time of the subsystem is synchronized using network time protocol to prevent timestamp mismatches. However, it is assumed that the internal delay between recording of timestamp and actual execution of scenario is less than one second granularity of the data stream generated. Drift detector monitors each component’s parameters in the considered subsystem and detects changing parameters between the execution and termination of a fault scenario.

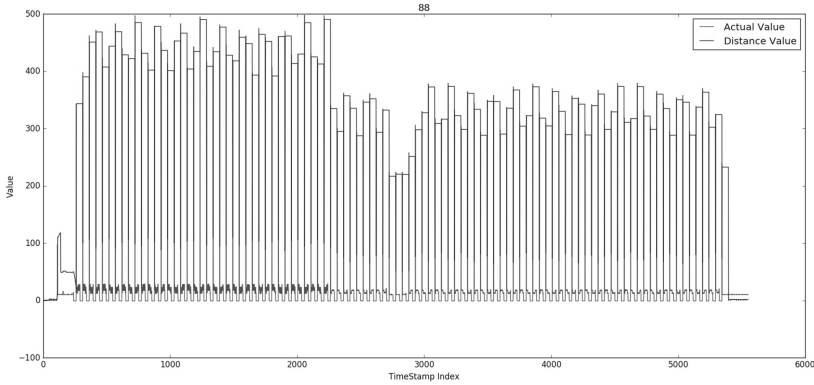
#### 3.2 Experimental Results

Table 2 relates to the evaluation of the results of drift detection for the parameters of two components: Sequencer and Native Gateway using precision, recall

**Table 2.** Precision, recall and F-score of components and their parameters under meta algorithm

Sequencer				Native Gateway			
Variable	Precision	Recall	F-score	Variable	Precision	Recall	F-score
46	100	95	97.44	0	90	99	94.29
48	97.44	38	54.68	8	89.29	100	94.34
49	97.44	38	54.68	20	92.59	100	96.15
50	97.44	38	54.68	21	96.08	98	97.03
54	100	100	100	22	96.08	98	97.03
69	97.44	38	54.68	23	96.04	97	96.52
76	95.24	100	97.56	27	91.59	98	94.69
77	95.24	100	97.56	31	93.07	94	93.53
78	95.24	100	97.56	52	94.34	100	97.09
79	100	99	99.50	53	94.34	100	97.09
80	100	99	99.50	55	99.01	100	99.50
81	100	99	99.50	56	99.01	100	99.50
82	95.24	100	97.56	57	94.34	100	97.09
83	100	99	99.50				
84	100	98	98.99				
85	100	98	98.99				
86	100	98	98.99				
87	100	98	98.99				
88	100	100	100				
89	100	98	98.99				
90	97.09	100	98.52				
91	98.04	99.00	99.01				

and F-Score metrics. Sequencer and Native Gateway consist of 109 and 78 parameters respectively. Table 2 shows the parameters of above components that show variation during system anomaly. The data used for evaluation is labelled as anomalous and normal using automated scripts. The timestamp is recorded by the automated scripts when data is labelled. This timestamp is used to identify the actual anomalous time period for a particular error scenario. Results produced by drift detection are evaluated against the labels produced by the automated scripts using above evaluation metrics. In Sequencer, four out of 22 detected parameters produce very low recall values due to the fact that the values corresponding to these parameters producing different variations. CDMA performs well for the components Sequencer and Native Gateway. However, fixed cumulative window model and Page-Hinckley test are not able to detect variations in parameters of Native Gateway due to the effect of ‘-1’ present in the

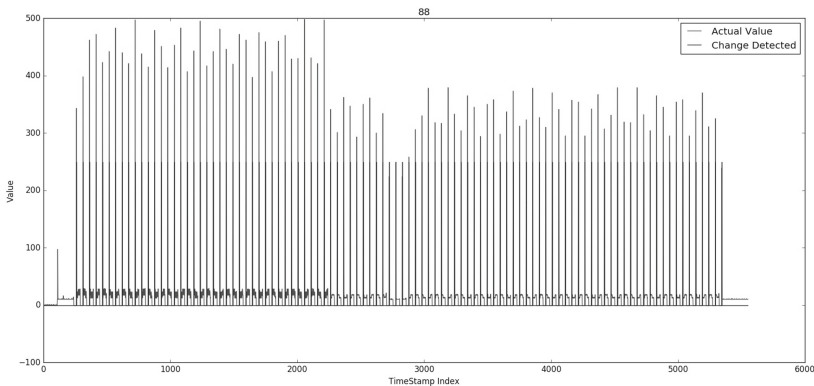


**Fig. 2.** Actual value and the distance between the fixed window and sliding window of Disk: Written Rate attribute of sequencer component

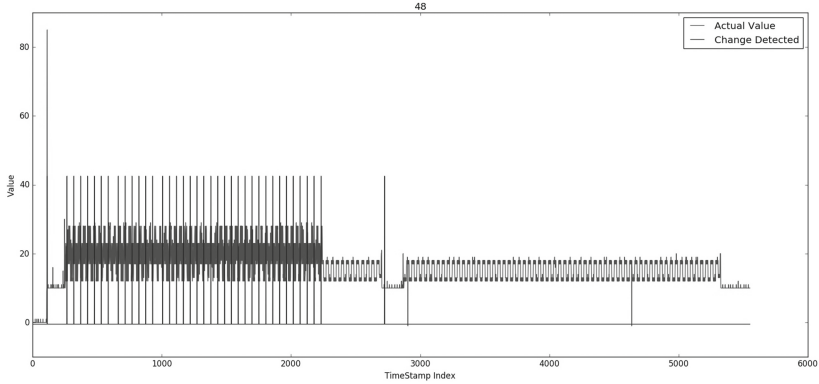
parameter vectors while calculating distance metrics. For the Sequencer component, fixed cumulative model and Page-Hinckley test produce results similar to CDMA.

Figure 2 shows the variation of distance value and the actual value of Disk: Written Rate attribute (denoted as attribute 88 in Table 2) of sequencer against the time under CDMA. Among the statistics related to the sequencer component, Disk: Written Rate attribute is expected to produce significant changes as the file I/O thread of sequencer component is terminated. Disk: Written Rate attribute depicts changes in value at the same time as a fault occurs.

Figure 3 shows the change points in values of Disk: Written Rate attribute and the detected changes, which was produced by CDMA. It is evident that the CDMA is capable of identifying changing points in parameter values.



**Fig. 3.** Detected change points of Disk: Written Rate attribute of Sequencer using change detection meta algorithm



**Fig. 4.** Detected changes of Message Queue from Sequencer to Disk Handler: Rate attribute of Sequencer under change detection meta algorithm

The four parameters representing low recall values exhibit a higher amount of false negatives. Due to the fixed threshold value of the drift detector, the low variations in data are not detected correctly. As shown in Fig. 4, change in variations of Message Queue from Sequencer to Disk Handler: Rate attribute (denoted as attribute 48 in Table 2) are not detected by the drift detector component since the difference between the fixed window and the sliding window is below the predefined drift detection threshold value. Therefore the parameters demonstrating low variations are expected to produce poor recall values. However, for rest of the parameters, CDMA produces better precision and recall and the relevant changes corresponding to system faults are successfully captured by the drift detector.

## 4 Conclusion

This research employs three drift detection techniques to identify root causes of anomalies that can arise in components of a pre-defined subsystem of a large scale trading system. Through drift detection, each parameter is monitored, and changes of parameters are detected during an abnormal condition occurring in the system. These changing parameters are identified as root causes of the anomaly.

The techniques used in this research require configuration of parameters such as threshold value and window sizes. Window size is configured with the same value for every parameter. However, configuring threshold value requires prior observation of data distributions. This research lacks the ability to automatically configure parameters of the drift detector component and expects to employ more dynamic solution for drift detection in future work. When recording the timestamps of statistics, this research assumes the internal delays of component are less than a second. If the delays are larger the detected drifts may not



correspond to the correct anomaly. The research can be extended to utilize other adaptive algorithms such as adaptive windowing to develop a dynamic solution.

## References

1. Bifet, A., Gavaldà, R.: Learning from time-changing data with adaptive windowing. In: *SDM*, vol. 7, pp. 443–448. SIAM (2007)
2. Brown, A., Kar, G., Keller, A.: An active approach to characterizing dynamic dependencies for problem determination in a distributed environment. In: *Proceedings of 2001 IEEE/IFIP International Symposium on Integrated Network Management*, pp. 377–390. IEEE (2001)
3. Chen, M.Y., Kiciman, E., Fratkin, E., Fox, A., Brewer, E.: Pinpoint: problem determination in large, dynamic internet services. In: *Proceedings of the International Conference on Dependable Systems and Networks, DSN 2002*, pp. 595–604. IEEE (2002)
4. Domingos, P., Hulten, G.: Mining high-speed data streams. In: *Proceedings of the Sixth ACM SIGKDD International Conference on Knowledge Discovery and Data Mining*, pp. 71–80. ACM (2000)
5. Gama, J., Medas, P., Castillo, G., Rodrigues, P.: *Learning with Drift Detection*. Springer, Heidelberg (2004)
6. Gama, J., Iobait, I., Bifet, A., Pechenizkiy, M., Bouchachia, A.: A survey on concept drift adaptation. *ACM Comput. Surv. (CSUR)* **46**(4), 44 (2014)
7. Grell, S., Nano, O.: Experimenting with complex event processing for large scale Internet services monitoring. In: *Proceedings of iCEP* (2008)
8. Hall, M.A.: *Correlation-based feature selection for machine learning*. Ph.D. thesis, The University of Waikato (1999)
9. Hangal, S., Lam, M.S.: Tracking down software bugs using automatic anomaly detection. In: *Proceedings of the 24th International Conference on Software Engineering*, pp. 291–301. ACM (2002)
10. Hulten, G., Spencer, L., Domingos, P.: Mining time-changing data streams. In: *Proceedings of the Seventh ACM SIGKDD International Conference on Knowledge Discovery and Data Mining*, pp. 97–106. ACM (2001)
11. Julisch, K.: Clustering intrusion detection alarms to support root cause analysis. *ACM Trans. Inf. Syst. Secur. (TISSEC)* **6**(4), 443–471 (2003)
12. Kifer, D., Ben-David, S., Gehrke, J.: Detecting change in data streams. In: *Proceedings of the Thirtieth International Conference on Very Large Data Bases*, vol. 30 (2004)
13. Lakhina, S., Joseph, S., Verma, B.: Feature reduction using principal component analysis for effective anomaly based intrusion detection on NSL-KDD (2010)
14. Mouss, H., Mouss, D., Mouss, N., Sefouhi, L.: Test of page-hinckley, an approach for fault detection in an agro-alimentary production system. In: *5th Asian Control Conference*, vol. 2, pp. 815–818. IEEE (2004)
15. Page, E.: Continuous inspection schemes. *Biometrika* **41**(1/2), 100–115 (1954)
16. Pechenizkiy, M., Bakker, J., Iobait, I., Ivannikov, A., Krkkinen, T.: Online mass flow prediction in CFB boilers with explicit detection of sudden concept drift. *ACM SIGKDD Explor. Newsletter* **11**(2), 109–116 (2010)
17. Sebastiao, R., Gama, J.: A study on change detection methods. In: *Progress in Artificial Intelligence, 14th Portuguese Conference on Artificial Intelligence, EPIA*, pp. 12–15 (2009)

18. Sebastiao, R., Gama, J.: Change detection in learning histograms from data streams. In: Portuguese Conference on Artificial Intelligence, pp. 112–123. Springer, Heidelberg (2007)
19. Sebastiao, R., Gama, J., Rodrigues, P.P., Bernardes, J.: Monitoring incremental histogram distribution for change detection in data streams. In: Knowledge Discovery from Sensor Data, pp. 25–42. Springer, Heidelberg (2010)
20. Sez, C., Rodrigues, P.P., Gama, J., Robles, M., Garca-Gmez, J.M.: Probabilistic change detection and visualization methods for the assessment of temporal stability in biomedical data quality. *Data Min. Knowl. Discov.* **29**(4), 950–975 (2015)
21. Zheng, T., Yang, J., Woodside, M., Litoiu, M., Iszlai, G.: Tracking time-varying parameters in software systems with extended kalman filters. In: Proceedings of the 2005 Conference of the Centre for Advanced Studies on Collaborative Research, pp. 334–345. IBM Press (2005)

# An Efficient Scheduling of Electrical Appliance in Micro Grid Based on Heuristic Techniques

Sardar Mehboob Hussain<sup>1</sup>, Ayesha Zafar<sup>1</sup>, Rabiya Khalid<sup>1</sup>, Samia Abid<sup>1</sup>, Umar Qasim<sup>2</sup>, Zahoor Ali Khan<sup>3</sup>, and Nadeem Javaid<sup>1</sup>(✉)

<sup>1</sup> COMSATS Institute of Information Technology, Islamabad 44000, Pakistan  
nadeemjavaidqau@gmail.com

<sup>2</sup> Cameron Library, University of Alberta, Edmonton, AB T6G 2J8, Canada

<sup>3</sup> Computer Information Science, Higher Colleges of Technology,  
Fujairah 4114, United Arab Emirates  
<http://www.njavaid.com>

**Abstract.** Unlike existing centralized grids, smart grids (SGs) have the ability to reduce fossil fuel combustion and carbon emissions up to a significant mark. Smart homes and smart building are becoming more attractable due to low energy consumption and high comfort. Different demand side management (DSM) programs have been proposed to involve users in decision making process of SGs. Power consumption pattern of shiftable home appliances is modified in response of some rebates to achieve certain benefits. In this paper, an energy management model is proposed using genetic algorithm (GA), teaching learning based optimization (TLBO), enhanced differential evolution (EDE) algorithm and our novel proposed EDTLA. The main objectives include: daily electricity bill minimization, peak to average ratio reduction and user comfort maximization. Simulation results validate the performance and applicability of our proposed model.

## 1 Introduction

Integration of advanced information and communication technology (ICT) into the traditional power grid forms smart grid (SG) [1]. Two important properties of SG are integration of renewable energy sources (RESs) and demand side management (DSM).

An emerging type of distributed generation network, called micro grid (MG), is perceived as medium voltage or low voltage power system with small distributed generation, controllable distributed loads and on site energy storage. MG works in both, grid connected and islanded modes. Major objectives of SG include reduced electricity bill, reduced peak to average ratio (PAR), maximized user comfort and balanced power consumption. In order to achieve aforementioned objectives, various DSM techniques have been proposed in literature.

In this paper, we propose a state of the art energy management model (EMM) under DSM for a residential complex of 30 homes. We use four heuristic techniques to optimally schedule home appliances to minimize daily electricity cost,

peak to average ratio (PAR) and maximize user comfort. One of our major contributions is that, we propose a novel hybrid algorithm which outperforms genetic algorithm (GA), teaching learning based optimization (TLBO) and enhanced differential evolution (EDE) algorithm in terms of cost minimization and PAR reduction. Remainder of the paper is organised as follows. Section 2 comprises of recent related work. Section 3 depicts the detail description of proposed model. Simulation findings and results are discussed in Sect. 4. Lastly, in Sect. 5, concluding remarks are presented followed by future directions.

## 2 Related Work

Scheduling problems are usually perceived as optimization problems and solved using different optimization techniques. In order to optimally schedule home tasks in residential MG, several methods have been proposed in literature. Some of the recent approaches are discussed hereunder.

An active controller is proposed in [2] to optimally integrate heating and cooling system in MG. The research improves reliability of MG and minimizes cost of MG, size of RESs and imported energy from grid. Several smart homes are considered and stability of MG is analysed. The main purpose of this study is to minimize peak load and consumption cost.

In [3], authors propose a SG equipped with 100% RESs to satisfy electricity and heating demands. Battery storage system (BSS) is used to deal with the fluctuating behavior of RESs. Combined heat and power (CHPs) plants and district heating and cooling system are introduced, which are responsible for providing heating and cooling loads to households and other commercial buildings.

Large scale integration of RESs into the power system requires cooperative interaction among active distribution networks (ADNs) of MG. A cooperative interaction between AD system (ADS) connected to multiple grids and energy system is formulated in [4] and dynamic energy management strategy is proposed. A bi-level and twofold optimization problem is formulated. A hybrid algorithm of rough set theory-hierarchical and non-dominated sorting GA (NSGA) is considered for optimization problem.

In [5], real time energy storage management for RE integration in MG is considered. Authors use off-line algorithm for optimization and propose a novel sliding window based on-line algorithm. The main objectives of research are to minimize the cost of power purchased from grid and maximize the penetration of RESs in MG.

In [6], joint operation of energy storage and load scheduling with RESs is considered in residential area domain. Electricity demand, starting times of appliances, length of operation times of appliances and RE generation are considered as stochastic and intermittent. The stochastic nature of problem is solved by modifying Lyapunov optimization technique.

In [7], an energy control system is proposed in a smart home of residential domain. Different types of appliances are scheduled according to given time frame. The optimization problem is solved using linear programming.

The major objective was to reduce electricity bill. A trade-off between cost and discomfort is also calculated using Taguchi loss function.

Participation of different DSM strategies in home energy management system (HEMS) is analysed in [8]. The use of different incentive based algorithmic techniques in DSM are analysed and their impact is elaborated. However, PAR and discomfort of users are not tackled in this study, which are important parameters of HEMS.

The load scheduling and power trading problems in residential area of MG with large share of RE are discussed in [9]. An approximate dynamic programming is used for appliance scheduling and a game theoretic approach is used for power trading among different users.

In [10], authors use RTP signal in DSM programs to reduce daily electricity bill and PAR. A new load scheduling learning algorithm is proposed which schedules appliances after learning from a series of actions. The change in load scheduling, power demand and pricing signal are modeled as Markov decision process.

### 3 System Model

Our system model comprises of a smart building of 30 homes in a MG scenario shown in Fig. 1. Each home is equipped with 12 smart appliances, which are to

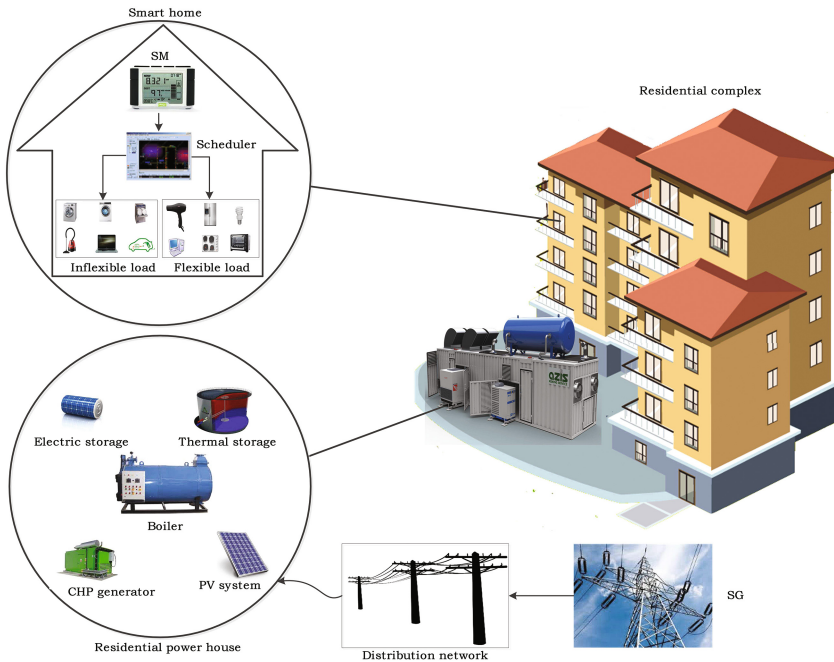


Fig. 1. Smart residential complex

be scheduled within given time window, as shown in Table 1. All appliances must not start before the earliest starting time and finish respective working hours prior to finishing time horizon. Start and end times of appliances are assumed to be provided by users, whereas, other parametric values are based on [11], and listed in Table 1. A time interval of half hour is considered, because minimum of one hour operation time for home appliances seems impractical. Since, some home appliances like coffee maker and toaster work for less than one hour a day.

**Table 1.** Parameters of appliances

Task	Power (kW)	Earliest starting time (h)	Latest finishing time (h)	Time window length (h)	Duration (h)
Dish washer	1.5	9	17	8	2
Cloth washer	1.5	9	12	3	1.5
Spin dryer	2.5	13	18	5	1
Cooker hob	3	8	9	0.5	0.5
Cooker oven	5	18	19	0.5	0.5
Microwave	1.7	8	9	0.5	0.5
Lighting	0.84	18	24	6	6
Laptop	0.1	18	24	6	2
Desktop	0.3	18	24	6	3
Cleaner	1.2	9	17	8	0.5
Fridge	0.3	0	24	-	24
Electric car	3.5	18	8	14	3

### 3.1 Load Categorization

In view of daily power consumption pattern, appliances are categorised in two groups, i.e. flexible loads and inflexible loads, as described below.

1. Inflexible appliances: Typically, inflexible loads include fridge, fan and light etc., which are considered as must run loads and can not be shifted to later hours. These appliances usually do not participate in demand response.
2. Flexible appliances: Flexible loads are also known as shiftable or burst loads. Flexible appliances include dish washer, washing machine, spin dryer, etc. Power consumption pattern of burst appliances can be altered to later hours in response of some incentives.

### 3.2 Energy Consumption Model

Each consumer in smart building has two sets of appliances, as discussed earlier, i.e.  $F$  and  $I$ . The set of flexible appliances  $F = \{a_1, a_2, a_3, \dots, a_f\}$  and the set of inflexible appliances  $I = \{b_1, b_2, b_3, \dots, b_i\}$  over a scheduling horizon of  $T = \{1, 2, 3, 4, 5, \dots, 48\}$ . The hourly electricity demand of a single appliance is given as:

$$E_{a,t} = E_{a,t_1} + E_{a,t_2} + E_{a,t_3}, \dots, + E_{a,t_{48}} \quad (1)$$

where  $E_{a,t_1} + E_{a,t_2} + E_{a,t_3}, \dots, + E_{a,t_{48}}$  denote electricity demand of each appliance in respective time slot. The daily electricity consumption of both types of appliances (flexible and inflexible) is given by Eqs. (2) and (3) respectively.

$$E^a = \sum_{t=1}^{48} \left( \sum_{f=1}^F E_t^a \right) = \{E_{t_1}^a + E_{t_2}^a + \dots + E_{t_{48}}^a\} \quad \forall f \in F \quad (2)$$

$$E^b = \sum_{t=1}^{48} \left( \sum_{i=1}^I E_t^b \right) = \{E_{t_1}^b + E_{t_2}^b + \dots + E_{t_{48}}^b\} \quad \forall i \in I \quad (3)$$

where  $E_{t_1}^a, E_{t_2}^a, \dots, E_{t_{48}}^a$  denote the power consumption of flexible appliances and  $E_{t_1}^b, E_{t_2}^b, \dots, E_{t_{48}}^b$  represent the power consumption of inflexible appliances at time  $t$ . The total daily power consumption  $E^{sum}$  is given as,

$$E^{sum} = \sum_{t=1}^{48} \left( \sum_{f=1}^F E_{t,f \in F}^a + \sum_{i=1}^I E_{t,i \in I}^b \right) \quad (4)$$

### 3.3 PAR

The basic aim behind balancing the PAR is to maintain the equilibria of demand and supply between utility and consumers. In our proposed system model, PAR is defined as the ratio between peak load over average load in a given time frame and is symbolized as  $\psi$ . Mathematically PAR can be written as:

$$\psi = \frac{\max(E_t)}{\frac{1}{T} \sum_{t=1}^{48} E_t} \quad (5)$$

### 3.4 Waiting Time

Inflexible appliances are supposed to run with highest priority and without any delay, so these appliances do not have any concern with waiting time or delay. Flexible tasks play crucial role in optimization by altering power consumption behavior. Let  $\alpha_a$  and  $\beta_a$  are start and end times of flexible appliance  $a$ , such that  $\alpha_a \leq \beta_a$  within the given time window. In our model, we consider waiting time as discomfort. The more the waiting time is, lesser the comfort is. We denote  $\xi_a$  as working duration and  $\sigma_a$  as actual start time of appliance  $a$ .  $\sigma_a$  has a value not less than  $\alpha_a$  but less than or equal to  $\beta_a - \alpha_a$  given as:

$$\sigma_a \in [\alpha_a, \beta_a - \xi_a] \quad (6)$$

### 3.5 Objective Function

The objective is to minimize consumption cost and PAR. In the objective function given below, both involved parties, i.e. consumer and utility, are considered in order to maintain balance between demand and supply. Electricity cost depends on pricing signal announced by utility company and appliances' power consumption pattern. We have no control over pricing signal however, we minimize the cost by altering power consumption pattern of appliances.

$$\min \sum_{t=1}^{48} \left( \varphi_1 \cdot \sum_{i=1}^{30} \sum_{k=1}^{12} \left( E_t^{sum} \times E_t^p \right) + \varphi_2 \cdot \psi \right) \quad (7)$$

where  $E_t^{sum}$  is total power consumption at time  $t$ ,  $E_t^p$  is price of electricity at time  $t$  announced by utility,  $\varphi_1$  and  $\varphi_2$  are weights of two objectives with the value of 0.5 each.

## 4 Simulations and Discussion

In this section, we present simulation findings and comparatively evaluate the working of GA, TLBO, EDE and our novel proposed EDTLA under RTP environment. RTP signal is taken from [11], which is assumed to be known ahead, so that users can make informed decisions. The performance measuring parameters include: electricity demand, electricity consumption cost, PAR and user discomfort, each of which are discussed hereunder.

### 4.1 Electricity Demand

The energy consumption pattern of all appliances under four different techniques is shown in Fig. 2. GA schedules most of the appliances either in early morning or before evening while remaining within the limits of provided time window. The daily power requirement profile of all appliances under TLBO remains flat throughout the day. This is why TLBO performs well in cost and PAR. TLBO has relatively small power demand during high price hours as compared to other cases.

EDE mimics the behaviour of GA particularly in morning hours and later, unlike GA, EDE has flattened curve during the rest of the day. Peak power demand in any time interval is 150 kWh, which is better than both, GA and TLBO. Our proposed technique results in flat behaviour during the whole day. EDTLA neither schedules appliances in high price hour nor creates peak in low price hours. From the above results, it can be seen that EDTLA has more appropriate and flat demand curve among all algorithms.

### 4.2 Electricity Cost

Figure 3 shows comparison of hourly power consumption cost under aforementioned techniques. EDE shows some spikes, however, their impact on total cost



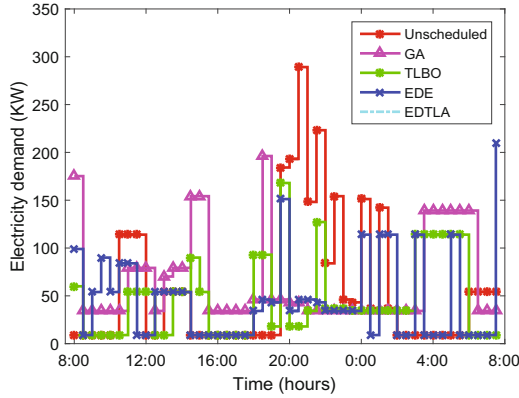


**Fig. 2.** Hourly electricity demand under four techniques.

is negligible because these spikes last for one or a couple of low price time intervals. On the other hand, TLBO has a flat curve during the whole day because it utilizes low price hours. EDE does not schedule appliances during time slots 10–20 which in result, creates peak later in time slots with high price. Due to which, EDE has highest total electricity cost among four techniques, as can be seen in Fig. 4. GA and EDE have comparable cost of consumption, however, GA performs slightly better. Our proposed EDTLA shows flat behavior of power consumption throughout the day, so, its power consumption cost is minimum among all algorithms. Total electricity bill for one day is 135.88 \$, 116.37 \$, 89.47 \$, 118.66 \$ and 82.14 \$ in case of unscheduled, GA, TLBO, EDE and EDTLA respectively.

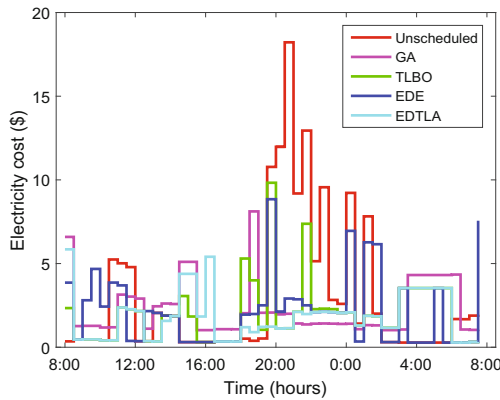


**Fig. 3.** Hourly electricity cost of residential building.

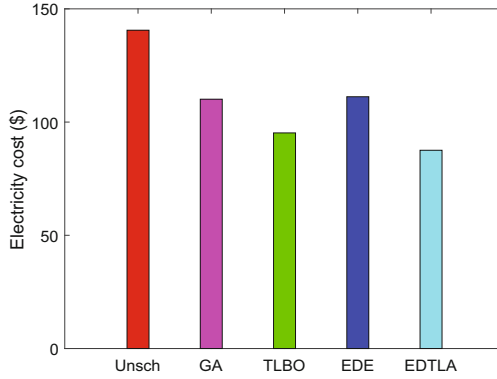


**Fig. 4.** Daily electricity bill of building.

### 4.3 PAR

Performance of four different heuristic techniques assessed in terms of PAR is shown in Fig. 5. It is clear that scheduling with GA, TLBO, EDE and EDTLA leads towards low PAR as compared to unscheduled case. EDE has highest PAR among scheduling algorithms, because it creates several small peaks in low price hours, as also shown in Fig. 2. This is mainly due to unavailability of threshold on power consumption. GA creates a mediocre peak, so it shows moderate PAR. TLBO has flat pattern during the whole day except interval 20, so its PAR is minimum among all algorithms, which is approximately 3.6. Whilst, our proposed algorithm further decreases the PAR and achieves 5% more efficient results as compared to TLBO.

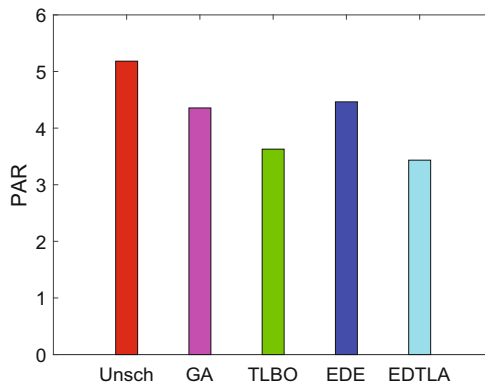


**Fig. 5.** PAR under four heuristic techniques.

#### 4.4 User Discomfort

User discomfort is calculated in terms of time delay of appliances from the earliest starting time window. Figure 6 shows the waiting time of all appliances under four different heuristic techniques. It can be clearly seen that EDE has minimum delay which means least discomfort, however, at the cost of huge electricity bill, as depicted in Fig. 4. GA and TLBO have comparable waiting time. EDTLA has more waiting time than TLBO algorithm, which is mainly due to convergence towards global optimal solution. TLBO schedules appliances sharply as it finds minimum price time slot, however, our proposed technique first completely searches and then schedules according to the price signal and given time window. In unscheduled case, appliances run whenever they are required, regardless of cost and grid stability concerns, so user discomfort is not calculated in unscheduled case.

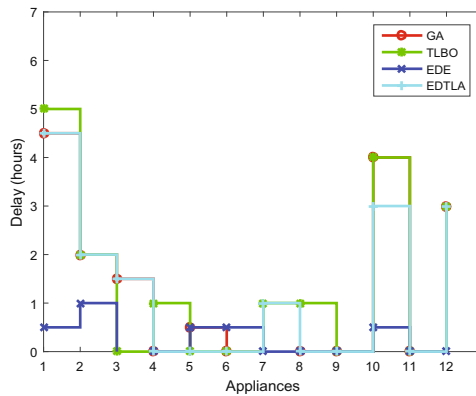


Fig. 6. User discomfort in terms of delay.

## 5 Conclusion

In this paper, we propose an EMM to optimally schedule home tasks in order to lower electricity bill, reduce PAR and maximize user comfort in a MG scenario. The existing heuristic based techniques, i.e. GA, TLBO and EDE are used in this study and a novel hybrid algorithm is proposed. It is concluded that each algorithm has capability to achieve aforementioned objectives under similar scenario, however, trade-offs between different objectives also exist. Simulation results prove the applicability and validity of our newly proposed hybrid algorithm, which outperforms the existing techniques in terms of cost and PAR reduction. The proposed model is generic and can be enhanced by adding other homes, building and daily electricity tasks. The future work may include power trading among multiple homes, MGs and EVs under large share of RESs.

## References

1. Lo, C.-H., Ansari, N.: The progressive smart grid system from both power and communications aspects. *IEEE Commun. Surv. Tutorials* **14**(3), 799–821 (2012)
2. Samadi, P., Wong, V.W.S., Schober, R.: Load scheduling and power trading in systems with high penetration of renewable energy resources. *IEEE Trans. Smart Grid* **7**(4), 1802–1812 (2016)
3. Hakimi, S.M., Moghaddas-Tafreshi, S.M.: Optimal planning of a smart microgrid including demand response and intermittent renewable energy resources. *IEEE Transactions on Smart Grid* **5**(6), 2889–2900 (2014)
4. García, J.A.M., Mena, A.J.G.: Optimal distributed generation location and size using a modified teaching-learning based optimization algorithm. *Int. J. Electr. Power Energy Syst.* **50**, 65–75 (2013)
5. Mathiesen, B.V., et al.: Smart energy systems for coherent 100% renewable energy and transport solutions. *Appl. Energy* **145**, 139–154 (2015)
6. Lv, T., Ai, Q.: Interactive energy management of networked microgrids-based active distribution system considering large-scale integration of renewable energy resources. *Appl. Energy* **163**, 408–422 (2016)
7. Rahbar, K., Jie, X., Zhang, R.: Real-time energy storage management for renewable integration in microgrid: an off-line optimization approach. *IEEE Trans. Smart Grid* **6**(1), 124–134 (2015)
8. Zhang, Y., et al.: Day-ahead smart grid cooperative distributed energy scheduling with renewable and storage integration. *IEEE Trans. Sustain. Energy* **7**(4), 1739–1748 (2016)
9. Chapman, A.C., Verbič, G., Hill, D.J.: Algorithmic and strategic aspects to integrating demand-side aggregation and energy management methods. *IEEE Trans. Smart Grid* **7**(6), 2748–2760 (2016)
10. Shirazi, E., Jadid, S.: Optimal residential appliance scheduling under dynamic pricing scheme via HEMDAS. *Energy Build.* **93**, 40–49 (2015)
11. Zhang, D., et al.: Economic and environmental scheduling of smart homes with microgrid: DER operation and electrical tasks. *Energy Convers. Manage.* **110**, 113–124 (2016)

# Personal Data in Cyber Systems Security

Marek R. Ogiela<sup>1(✉)</sup> and Lidia Ogiela<sup>2</sup>

<sup>1</sup> Faculty of Electrical Engineering, Automatics, Computer Science and Biomedical Engineering, AGH University of Science and Technology, 30 Mickiewicza Ave., 30-059 Krakow, Poland  
mogiela@agh.edu.pl

<sup>2</sup> Cryptography and Cognitive Informatics Research Group, AGH University of Science and Technology, 30 Mickiewicza Ave., 30-059 Krakow, Poland  
logiela@agh.edu.pl

**Abstract.** In this paper will be presented the ways of using personal information for security purposes and applications. In particular several different approaches will be described, which present application of personal biometric features, as well as behavioral patterns characteristic for particular users. Both behavioral and biometrics pattern can be extracted thanks to the application of new generation cognitive information systems. Obtained personal feature vectors, can be used in many security application, as well as in personalized cryptographic protocols. Such solutions will be described in this paper.

## 1 Introduction

In modern security solutions and cryptographic protocols an important role plays application of personal, individual characteristics or specific behavioral features. In many applications we need to develop secure protocols, which allow in particular cases to be assigned to each user of security protocols. Such requirements may be fulfilled by using some specific and very unique personal features in creation of secure cryptographic procedure. Involving personal features or specific patterns into security algorithms, finally allow to provide required security level, but also to determine particular user when it will be necessary to reveal such information. In this paper will be described selected cryptographic solutions, which are based on using personal features or behavioral patterns. Such solutions may be created due to the application of the latest cognitive computation technologies and systems, as well as some biologically-inspired approaches. Also the application of such technologies may be very broad for example for securing strategic or classified data, intelligent and secure transmission, information and services management in distributed infrastructures or in the Cloud environment and many others [1–3]. In near future such technologies may play important role in ambient world infrastructure or pervasive and ubiquitous computing [4–6].

The main goal of this paper will be presentation of several security techniques and cryptographic procedures, which are based on cognitive computation or bio-inspired approaches. Presented solutions will be based on evaluation of the personal features or very unique personal characteristics, which next can be involved into the encryption process [6, 7]. Such solutions are very promising for development of modern

cryptography, and may allow to extend existing cryptographic methodologies towards a new branch of cognitive cryptography [8, 9].

In particular in this paper will be presented approaches of using cognitive and personal information for creation of strong encryption keys, as well as behavioral authentication protocols.

## 2 Extraction of Personal Patterns for Security Purposes

For security application it is possible to use both standard biometric patterns as well as nonstandard personal features including behavioral characteristics. For extraction standard biometrics it is possible to use simple devices dedicated for acquiring such type of information. From our point of view more interesting is acquisition of nonstandard personal features and behavioral patterns, which may be applicable for security purposes. Conducted research showed that for such purposes are very useful cognitive information systems [5, 10].

Cognitive information systems try to imitate the brain functions and are based on one of the known model of human visual perception, named knowledge based perception [4, 11]. In this perception model cognitive resonance processes are performed to deeply analyze observed situation or patterns, and to allow understand its semantic meaning.

Based on such model we tried to develop several different classes of cognitive information systems [4, 12]. Among them we could also define systems dedicated to visual data interpretation, which may be applicable for security purposes, and for extraction nonstandard personal features or characteristics.

Using cognitive information systems we tried to show some new opportunities for its application for personal information extraction, and using them in new security protocols and cryptographic procedures. The most common application may be connected with generation of strong cryptographic keys or creation of a special kind of behavioral lock using movement patterns. It is worth underline that creation of such cryptographic solutions is inspired by biological models and finally allows to create a new branch called cognitive cryptography defined in [7, 12].

Cognitive cryptography combine techniques which guarantee data confidentiality with personal information extracted from biometric patterns, and usually is connected with application of cognitive information systems.

Related security area to cognitive cryptography, which also may use cognitive information systems, is personalized cryptography [12]. In personalized cryptography encryption process can be personalized and dependent on individual information associated with a specific person. To extract such information it is necessary to have a cognitive system, which will analyze personal patterns and extract certain unique characteristics, which may be used in cryptographic procedure.

The most important areas of application of cognitive systems for security purposes include:

- Threshold algorithms for secret sharing using personal data.
- Information management protocols, which use biological models.

- Visual cryptography with an individual perception threshold set for a particular user.
- Multi-secret steganography, and digital watermarking depending on personal feature [2].

### 3 Biometric and Cognitive Keys for Cryptographic Protocols

Application of cognitive information systems allow to create a very large personal information records, which contain different personal features and individual characteristics. Such personal data can be used for creation of advanced crypto-biometric security solutions.

One of the possible application may be connected with secret sharing applications, where we can apply biometric threshold schemes [2].

Such threshold schemes allow to generate personalized shadows, which may be associated with particular person. It allows not only to restore the original information, but also to determine, who the owner of particular secret shares is.

In biometric threshold schemes we can use both standard as well as non-standard personal information [11, 12], and the general methodology of application personal features for threshold procedure is following:

- Very unique or biometric features of particular person should be collected.
- Selected features should be converted into the form of feature vector.
- Secret information can be splitted using one of threshold schemes, according key included in feature vector.
- Generated shares can be distributed between trusted persons.

The second important areas of application of cognitive keys are connected with using various biologically inspired approaches in security applications.

The most important example of such solutions may include DNA cryptography, and linguistic threshold schemes [8, 9]. In linguistic thresholds schemes thanks to the application of formal grammars, it is possible to encode bit blocks of information with different length, what may be very important while performing hierarchical secret sharing and management procedures.

### 4 Behavioral Features for Security Applications

For security applications we can consider not only biometric information registered for particular person, but also some specific behavioral patterns connected with gesture or movement activities.

Having motion sensors or simple devices, which allow trace finger or hand movements we can use them for extraction of specific motion patterns for security purposes. The simplest solution is using hand or finger movements for personal authentication procedures, during which we can extract very specific personal features, which next may be used for cryptographic solutions and authentication protocols. Such simple gesture or movement allow to create special kind of behavioral lock or cryptographic procedure. In general finger motion analysis seems to be most natural and easiest, so it may be

focused on tracing a fingertip positions during making particular gesture for security or authentication procedures. Analysis of simple gestures has many advantages like noninvasive data acquisition, possibility of analysis of determined or fixed movement patterns, considering the motion dynamics and acceleration, and of course real-time analysis and feature extraction.

For security applications we should consider only complex gesture or movements, which will be sufficient for obtaining the distinctive features of particular user. For this purpose we can analyze movements performed using one or more fingertips or, if necessary, for other parts of analyzed hand (Fig. 1).

## Hand or finger movements as behavioral keys



**Fig. 1.** Palm or hand movement patterns as behavioral keys.

For extraction of personal movement features we can use any motion sensor, which is able to register hand position changes during the time. As a result of such analysis we should create a personal feature vector containing very specific parameters about analyzed motion like direction, velocity or acceleration.

The first stage in such analysis is connected with creation of learning set, containing particular number of well described motion patterns. The second stage allow to classify a new pattern by comparing it with elements stored in learning set. Such comparison is made by calculation the distance or similarity factor between new registered signal and signals stored in learning set. Base of feature vector and classification function it is possible to determine the type of hand or finger movement. Having personal features encoded in the feature vector, it is possible to use them in different security applications.

The simplest application may be connected with direct personal authentication, based on finger movements recognized as biometric pattern. Another may be connected with using unique personal features, as individual parameters for cryptographic protocols like secret splitting, biometric key generation, multi secret steganography, fuzzy vault etc. The security of such application is strongly depended on complexity of



analyzed movements. So the better cryptographic solution may be constructed, when we consider more complicated or very specific gestures.

### 5 Visual Perception Features for Security Applications

Beside behavioral features it is also possible to consider some individual perception capabilities for security purposes. Such perception features may be very important in visual cryptography, where it is possible to establish different visual perception threshold for a given person or participants of protocol.

Looking on the images or visual secret parts very often we can notice different objects or information (Fig. 2).



Fig. 2. Different perception of observed objects.

In such cases adding additional visual parts it is possible to receive more information, which finally allow to recognize original image. In such procedure it is possible to

#### Information shared and restored with a different number of shares

Fig. 3. Visual secret recognition possibilities with different visual perception thresholds.

establish individual restoring threshold for particular persons. Such threshold will allow to read details of the picture for this person, but for others will not be sufficient. In practical solutions perception threshold may depends on personal eye sensitivity, but also should be dependent on some expectation about the content of restored images or previous experiences.

An example of such situation is presented in Fig. 3, where we split the picture of well know film star, and try to reconstruct it by adding particular shares. For people without any expectation about the content of such image, it is necessary to collect the total number of secret shares to fully reveal it. But for persons who know this person or have some additional knowledge it is possible to early recognize the content of this picture.

## 6 Conclusions

In this paper we presented different possibilities of using personal features and unique parameters for security application and cryptography. Such personal information may be used in creation of personal cryptographic keys, but also for secret sharing procedures and multi-secret steganography algorithms. Besides biometric parameters, some behavioral features may also be used in advanced cryptographic protocols and application. Extraction of personal or behavioral characteristics is possible thanks to the application of cognitive information systems, which allow extract unique parameters from nonstandard personal patterns or specific human body movements. Application of such specific and unique parameters proved that personal features, and cognitive systems can be used in development of advanced cryptography procedures for strong key generation, secret management, visual cryptography, and creation of behavioral lock.

**Acknowledgments.** This work has been supported by the AGH University of Science and Technology research Grant No 11.11.120.329.

## References

1. Cox, I.J., Miller, M.L., Bloom, J., Fridrich, J., Kalker, J.: *Digital Watermarking and Steganography*. Morgan Kaufmann Publishers, Burlington (2008)
2. Jin, Z., Teoh, A.B.J., Goi, B.-M., Tay, Y.-H.: Biometric cryptosystems: a new biometric key binding and its implementation for fingerprint minutiae-based representation. *Pattern Recogn.* **56**, 50–62 (2016)
3. Ogiela, L.: Computational intelligence in cognitive healthcare information systems. *Stud. Comput. Intell.* **309**, 347–369 (2010)
4. Ogiela, L.: Cognitive informatics in image semantics description, identification and automatic pattern understanding. *Neurocomputing* **122**, 58–69 (2013)
5. Ogiela, L., Ogiela, M.R.: Beginnings of cognitive science. In: *Advances in Cognitive Information Systems. Cognitive Systems Monographs*, vol. 17, pp. 1–18 (2012)

6. Ogiela, L., Ogiela, M.R.: Data mining and semantic inference in cognitive systems. In: Xhafa, F., Barolli, L., Palmieri, F., et al. (eds.) 2014 International Conference on Intelligent Networking and Collaborative Systems (IEEE INCoS 2014) Salerno, Italy, pp. 257–261, 10–12 September 2014
7. Ogiela, L., Ogiela, M.R.: Management Information Systems. LNEE, vol. 331, pp. 449–456. Springer, Heidelberg (2015)
8. Ogiela, M.R., Ogiela, U.: Linguistic approach to cryptographic data sharing. In: FGCN 2008 – The 2nd International Conference on Future Generation Communication and Networking, Hainan Island, China, vol. 1, pp. 377–380, 13–15 December 2008
9. Ogiela, M.R., Ogiela, U.: Security of linguistic threshold schemes in multimedia systems. *Stud. Comput. Intell.* **226**, 13–20 (2009)
10. Ogiela, M.R., Ogiela, U.: Shadow Generation Protocol in Linguistic Threshold Schemes. *CCIS*, vol. 58, pp. 35–42. Springer, Heidelberg (2009)
11. Ogiela, M.R., Ogiela, U.: Grammar Encoding in DNA-Like Secret Sharing Infrastructure. *LNCS*, vol. 6059, pp. 175–182. Springer, Heidelberg (2010)
12. Ogiela, M.R., Ogiela, U.: Secure Information Management Using Linguistic Threshold Approach. *Advanced Information and Knowledge Processing*. Springer, London (2014)

# Performance Measurement of Energy Management Controller Using Heuristic Techniques

Adnan Ahmed<sup>1</sup>, Awais Manzoor<sup>1</sup>, Asif Khan<sup>1</sup>, Adnan Zeb<sup>1</sup>,  
Hussain Ahmad Madni<sup>1</sup>, Umar Qasim<sup>2</sup>, Zahoor Ali Khan<sup>3</sup>,  
and Nadeem Javaid<sup>1</sup>(✉)

<sup>1</sup> COMSATS Institute of Information Technology, Islamabad 44000, Pakistan  
[nadeemjavaidqau@gmail.com](mailto:nadeemjavaidqau@gmail.com)

<sup>2</sup> Cameron Library, University of Alberta, Edmonton T6G 2J8, Canada

<sup>3</sup> Computer Information Science, Higher Colleges of Technology, Fujairah 4114,  
United Arab Emirates  
<http://www.njavaid.com>

**Abstract.** A smart grid is a modernized form of the traditional grid. Smart grid benefits both, consumer and energy services provider. Demand side management is one of the key component of smart grid to fulfill consumers electricity demands in an efficient manner. It helps consumers to manage their load in an effective way to reduce their electricity bill. In this paper, we design a home energy management controller based on three heuristic techniques: teaching learning based optimization, binary particle swarm optimization and enhanced differential evaluation. The major objective of designing this controller is to minimize consumers electricity bill while maximizing consumers satisfaction. Simulation results show that TLBO achieved maximum user satisfaction at minimum cost and peak to average ratio. A tradeoff analysis between user satisfaction and energy consumption cost is demonstrated in simulation results.

## 1 Introduction

Traditional electricity power systems are complex systems serving us over an extensive period of time. Traditional grid fails to fulfill the increasing demand of highly efficient and reliable energy. The flow of information between provider and consumer is unidirectional from producer to consumer. In the traditional grid, power outage and lack of fault detection are two major drawbacks. To overcome these problems the concept of smart grid (SG) was introduced.

SG is an advanced form of the traditional grid. It incorporates the information and communication technology, which provides two-way communication between the consumer and supplier. This two-way communication plays a vital role to intelligently monitor the services of the system. SG has better self-management, self-healing, and real-time monitoring abilities.

In the era of SG, demand side management (DSM) plays a significant role to achieve a balanced load. Customer participation is an important aspect to implement DSM successfully. DSM efficiently manages the load, instead of presurizing the more power generation. However, it is necessary to examine the behavior of the consumer to predict the habitual consumption pattern.

DSM design demand response (DR) programs which helps consumers to reduce peaks power demand in on-peak hours. DR programs include incentive based and price based DR. In the incentive-based scheme, money is paid back to the consumer for the time that is utilized to shut down the appliances during on-peak hours. However, for this purpose, there must be an agreement between the consumer and utility. According to this agreement, an administrator has some degree of control to directly disconnect, reduce or schedule appliances to save cost [1]. In price-based scheme consumer are offered with time-varying prices according to their power consumption. So consumer adjusts their appliances according to the schedule from on-peak hours to an off-peak hour [2]. Electricity prices change dynamically according to time (day, Week or month). As every consumer wants to consume more electricity at the lower price, so price-based schemes play an important role to motivate the consumers to shift electricity load towards off-peak hours.

In this paper, we applied three heuristic algorithms: teaching learning based optimization (TLBO), binary particle swarm optimization (BPSO), enhanced differential evolution (EDE) to solve the load scheduling problems. We choose these algorithms due to their self-organization, self-optimization, self-protection and self-healing [3]. These algorithms are tested with the simulative consideration of a home energy management system (HEMS) under day ahead real time pricing (DA-RTP) environment. Simulation results show that aforementioned algorithms are capable of reducing cost and PAR in comparison to the unscheduled load, however, there is a trade-off between cost and user satisfaction.

The rest of the paper is organized as follows. Section 2 describes the related work, the problem description is in Sect. 3. Simulation results discuss in Sect. 4, and finally, Sect. 5 provides a Conclusion.

## 2 Related Work and Motivation

In the literature, many DSM based load scheduling techniques are presented to reduce the electricity bill and PAR. HEM system is an important feature in residential scheduling. Substantial work has been carried out in literature for designing of HEMS.

Ahmed et al. in [4] focused on the DSM for plug-in hybrid electric vehicle (PHEV) charging at low voltage transformer. The main objective is to flatten the electricity load curve and fulfilled the consumers requirement for their PHEV to be charged with in time. Convex programming technique is used to solve load management problem. Simulation results show that proposed algorithm efficiently flatten the power load curve.

A distributed algorithm is used to manage sparse load shifting in DSM [5]. Authors make the contribution in the three forms: firstly, remodel the DSM

to improve sparsity. Secondly, developed a bidirectional framework to seek the Nash equilibrium and the third is, Newton method used to accelerate the convergence of co-ordination updates on the supply side. Distributed algorithm basic objective is to schedule the home appliances and increased the user comfort, by implementing the sparse load shifting technique. Simulation results show that sparse pattern helped to increase the user comfort significantly.

Mitra et al. used Load shifting technique to reduce the cost and minimize the peak demand. Time slots are considered in hour wise manner. Starting from the first hour of the day to the last hour of the day [6]. Authors used modified form of the particle swarm optimization (PSO) for DSM. PSO algorithm is used to reduce the utility cost and minimize the peak demand. It is based on heuristics and it is able to adapt itself according to the problem. This algorithm is implemented on three area loads of SG, which are industrial, commercial and residential. Simulation result shows that significant saving was made in the utility bills.

Main objective of authors is to minimize the power utilization during the peak hours. This problem efficiently solved by using the evolutionary algorithm. Load is divided into three services area industrial, residential and commercial. Use of electricity in peak hours vary in every services area. The authors in [7] used genetic algorithm (GA) in DSM and benefited with an overall reduction of 21.91%. However, author did not consider the user comfort. Authors in [8] proposed a scheduling model for appliances, in this scenario dynamic pricing scheme is used. In this scheme, an optimization model proposed that minimize the cost for the consumer. Different pricing function is being used in this model to make it more realistic. Consumer comfort issue and welfare are also incorporate in this model. However, PAR is not considered in this model.

Electricity consumption cost is minimized by scheduling the appliances [11]. Twenty-four appliances are considered to schedule their energy consumption and load using different heuristic techniques. These heuristic techniques include WDO, BPSO, and GA. All these techniques are implemented in Matlab. Each technique performance is evaluated and compared. The result shows that performance of BPSO is the best as compared to GA and WDO. However, user comfort is not considered in this work.

### 3 Problem Description

In SG, energy optimization and cost reduction are two difficult tasks due to randomness in energy consumption pattern. In HEMS, all the appliances are scheduled in such a way that consumer will pay the minimum cost. HEMS plays an important role in minimizing the cost while maximizing the user comfort level.

DSM deal with the activities that modify the electricity consumption in order to minimize the energy consumption cost and offer more economic benefit. Ahmed et al. in [4] focused on user comfort and energy consumption threshold. Authors redesigned the EMS and improved it efficiently by shifting the load.

Appliance scheduling implemented by using an activity on off control mechanism. A tradeoff analysis between comfort, and appliances delay is considered. User comfort and energy consumption are major achievements of this work. However, the cost factor is not taken into consideration.

Nash equilibrium is used to find globally minimizes the total energy consumption cost and PAR. In [9] Authors showed contribution in three forms, remodel the DSM, and find nash equilibrium in the DSM and fast gradient method is used for demand-side optimization. Nikaido-Isoda function based relaxation algorithm is used to find out the nash equilibrium. However, proposed scheme is not deal with the flexibility of power usage pattern and human behavior. In [10] a DSM method implemented by using integer linear programming technique. The proposed model minimize the PAR and increase the user comfort.

Many strategies had been proposed to tackle aforementioned problems, However in [11] minimize the power load during on-peak hours and efficiently distribute that load during off-peak hours by using optimization techniques. An evolutionary technique GA is used to solve load distribution problem. Results show that the power utilization during on-peak hour effectively distributes in off peak hour. However, authors are not considered the user comfort.

In [12] heuristic algorithms (BPSO, TLBO, EDE) are flexible for specified constraints are easy to implement and have less computational complexity. In this work, we used three different optimization algorithms; TLBO, BPSO, EDE to solve the appliance scheduling problem. These algorithms are chosen due to their decentralized control system, self-optimization, self-protection and self-organization. These algorithms are implemented with Simulative consideration of HEMS in DA-RTP environment.

## 4 Simulation Results and Discussion

In this section, we investigate the performance of our presented model. We measure the performance of each algorithm and choose the best one with respect to cost and waiting time. For this purpose, we consider three different type of appliances and apply EDE, TLBO, and BPSO to achieve our objectives. We assume that electricity prices are between the 5 to 20 dollars/kwh. The detailed comparison is provided below.

### 4.1 Clothes Dryer

We consider the cloth dryer for scheduling due to its higher flexibility to shift its operation onto next time slot. Figures 1 and 2 shows the performance of cloth dryer in term of cost and average waiting time respectively. Simulation results for cloth dryer are summarized in Table 1. We conclude from simulation results that there is a tradeoff between cost and waiting time. In the case of TLBO cost is minimum, however, we sacrifice for user comfort satisfaction. It totally depends upon consumer that he want to save cost or affords delay.

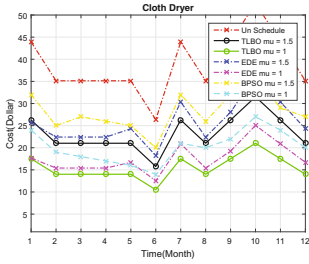


**Fig. 1.** Cloth dryer energy consumption cost

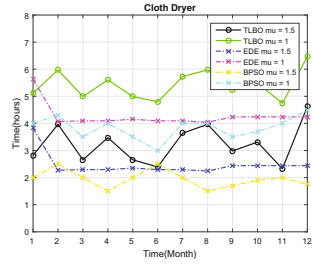


**Fig. 2.** Cloth dryer average waiting time

**Table 1.** Cloth dryer performance

Technique name	Priority	Average cost (\$)	Reduction in cost	Average delay in hours
TLBO	1.5	278	40%	3.25
	1.0	186	60%	5.50
EDE	1.5	313	33%	2.50
	1.0	216	53%	4.26
BPSO	1.5	337	27%	2.00
	1.0	242	48%	4.00

**4.2 Dishwasher**

A dishwasher is an ideal appliance for DSM due to short duty cycle and high energy consumption and peak demand. Figures 3 and 4 shows the average cost and average waiting time for each month. Simulation results are summarized in Table 2. Two time factor is used for dishwasher, large time factor means higher

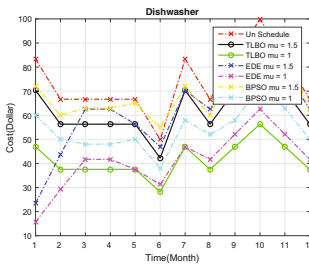


**Fig. 3.** Dishwasher energy consumption cost

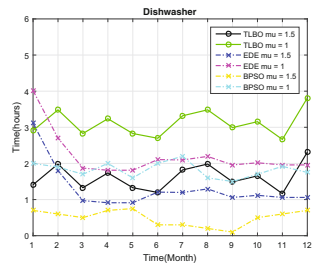


**Fig. 4.** Dishwasher average waiting time



**Table 2.** Dishwasher performance

Technique name	Priority	Average cost (\$)	Reduction in cost	Average delay in hours
TLBO	1.5	746	15.52%	1.75
	1.0	500	43%	3.25
EDE	1.5	755	14%	1.50
	1.0	530	40%	2.25
BPSO	1.5	836	05%	1.00
	1.0	647	27%	2.00

priority and it is lead to shorter time factor appliances. We use three heuristic techniques to find out the best time schedule for a dishwasher at minimum cost. If we saw the simulation result comparatively than TLBO is showed maximum delay, Its basic reason is that there is a tradeoff between the cost and user satisfaction and we will try to find an equilibrium position.

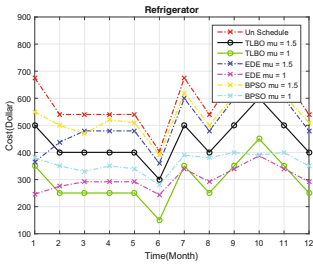


**Fig. 5.** Refrigerator energy consumption cost

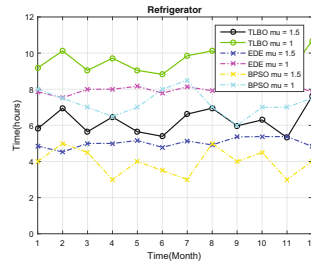


**Fig. 6.** Refrigerator average waiting time

**Table 3.** Refrigerator performance

Technique name	Priority	Average cost (\$)	Reduction in cost	Average delay in hours
TLBO	1.5	5304	26%	6.22
	1.0	3504	51%	8.52
EDE	1.5	6296	12%	5.00
	1.0	3718	48%	7.50
BPSO	1.5	5650	21%	4.00
	1.0	4340	39%	6.8

### 4.3 Refrigerator

Simulation result for refrigerator execution cost and waiting time are shown in Figs. 5 and 6 respectively. By comparing these results we find that the best performance is showed by TLBO as compared to EDE and BPSO with respect to cost, but in TLBO delay time is not minimum as compared to the other heuristic techniques. Its basic reason is that there is a tradeoff between the cost and delay time.

## 5 Conclusion

In this paper, a real-time appliance scheduling scheme is presented for DSM. Three home appliances with different duty cycles and time sensitivities are considered. Our primary objective is to schedule smart appliances in such a way that consumer pay minimum consumption cost at maximum satisfaction level. For this purpose, we have applied three optimization techniques: TLBO, EDE, and BPSO to measure their performance for different parameters. Extensive simulations are conducted to determine the best optimization technique in term of cost minimization and user satisfaction maximization. Results show that TLBO performs best amongst all other techniques due to its low complexity, real-time and distributed characteristics. TLBO successfully achieved maximum user satisfaction while minimizing users electric bill.

## References

1. Ghazvini, M.A.F., Soares, J., Abrishambaf, O., Castro, R., Vale, Z.: Demand response implementation in smart households. *Energy Buildings* (2017)
2. Iqbal, Z., Javaid, N., Khan, M.R., Ahmed, I., Khan, Z.A., Qasim, U.: Cost and load reduction using heuristic algorithms in smart grid. In: 2016 30th International Conference on Advanced Information Networking and Applications Workshops (WAINA), pp. 24–30. IEEE (2016)
3. Gupta, I., Anandini, G.N., Gupta, M.: An hour wise device scheduling approach for demand side management in smart grid using particle swarm optimization. In: 2016 National Power Systems Conference (NPSC), pp. 1–6. IEEE (2016)
4. Ahmed, N., Levorato, M., Li, G.-P.: Residential consumer-centric demand side management. *IEEE Trans, Smart Grid* (2017)
5. Li, C., Yu, X., Yu, W., Chen, G., Wang, J.: Efficient computation for sparse load shifting in demand side management. *IEEE Trans. Smart Grid* **8**(1), 250–261 (2017)
6. Mitra, K., Dutta, G.: Electricity consumption scheduling with energy storage, home-based renewable energy production and a customized dynamic pricing scheme. No. Wp. 1. Indian Institute of Management Ahmedabad, Research and Publication Department (2016)., November 2016
7. Bharathi, C., Rekha, D., Vijayakumar, V.: Genetic algorithm based demand side management for smart grid. *Wirel. Pers. Commun.* **93**(2), 481–502 (2017)
8. Arif, A., Javed, F., Arshad, N.: Integrating renewables economic dispatch with demand side management in micro-grids: a genetic algorithm-based approach. *Energy Effi.* **7**(2), 271–284 (2014)

9. Su, W., Huang, A.Q.: Proposing a electricity market framework for the Energy Internet. In: 2013 IEEE Power and Energy Society General Meeting (PES), pp. 1–5. IEEE (2013)
10. Qayyum, F. A., Naeem, M., Khwaja, A.s., Anpalagan, A., Guan, L., Venkatesh, B.: Appliance scheduling optimization in smart home networks. IEEE , pp. 2176-2190 (2015). Access 3
11. Priya, E.B., Sathish Kumar, K.: A survey on residential demand side management architecture, approaches, optimization models and methods. *Renew. Sustain. Energy Rev.* 59, 342–351 (2016)
12. Bozchalui, M.C., Hashmi, S.A., Hassen, H., Cañáizares, C.A., Bhattacharya, K.: Optimal operation of residential energy hubs in smart grids. *IEEE Trans. Smart Grid* 3(4), 1755–1766 (2012)

# Managing Energy in Smart Homes Using Binary Particle Swarm Optimization

Samia Abid<sup>1</sup>, Ayesha Zafar<sup>1</sup>, Rabiya Khalid<sup>1</sup>, Sakeena Javaid<sup>1</sup>, Umar Qasim<sup>2</sup>, Zahoor Ali Khan<sup>3</sup>, and Nadeem Javaid<sup>1</sup>✉

<sup>1</sup> COMSATS Institute of Information Technology, Islamabad 44000, Pakistan  
nadeemjavaidqau@gmail.com

<http://www.njavaid.com>

<sup>2</sup> Cameron Library, University of Alberta, Edmonton, AB T6G 2J8, Canada

<sup>3</sup> Computer Information Science, Higher Colleges of Technology,  
Fujairah 4114, United Arab Emirates

**Abstract.** The greenhouse gas emission is increasing around the globe. In order to reduce its emission factor, the concept of microgrid is introduced, which integrates renewable energy sources. The microgrid has a point of common coupling which helps to exchange power with utility during different times of a day to meet load demand. Based on all the system constraints, an energy management strategy is proposed in this research work, which helps to minimize the power consumption peak and operating cost of microgrid. For this purpose the appliances of each smart home in the residential area and distributed generator of microgrid are scheduled using binary particle swarm optimization to economically meet the consumer demand considering the desired objectives. For this purpose, proposed strategy is employed for the economic energy management of homes and microgrid. Significance of the proposed strategy is proved through performing simulations.

## 1 Introduction

About 80% of people around the world have access to electricity. Due to immense use of electricity, power system consequently has to tackle challenges like depletion of reserves of non-renewable sources and generating energy from non-renewable sources. Generating electricity from these sources is a major cause of environmental pollution [1]. In fact 25% of greenhouse gas emission around the globe is due to generating electricity from non-renewable sources like: oils, burning coals and natural gas [2].

To prevail this dilemma an energy management strategy is required which employs renewable sources. For this purpose it is essential to develop distributed generators (DGs) for the generation of electricity through renewable sources. Numerous renewable energy sources (RES) have been developed in the past which extract energy from natural sources and convert into electricity like: photovoltaic (PV) panels, wind turbines (WTs) and hydro systems etc. However, the energy generated by these sources is intermittent which lacks in reliability.

To provide a highly reliable energy generation, several types of energy generation sources are currently available. Such mechanisms include micro turbine (MT), fuel cell (FC), WT, PV and hydro systems. Still, these DGs cannot be connected directly to the upstream utility grid.

To establish a connection between utility and these sources the concept of microgrid is introduced. A microgrid integrates several DGs, multiple loads and energy storage systems (ESSs) to provide a stable service in a limited area. In grid-connected mode it works in connection with the main grid. To establish a connection between microgrid and main grid point of common coupling (PCC) is used.

On the other hand, a smart home is a very necessary unit of microgrid. Since early nineties the concept of smart homes has been evolved. The usage of electricity is rapidly increasing in every smart home. With the increase of electricity usage, the need to improve the overall efficiency of electrical grids is also increasing. Hence, energy efficiency is becoming a more challenging task for smart homes [3]. In this paper, we propose an energy management strategy for both smart homes and microgrid. We consider microgrid as a local electricity provision network to fulfil the demand coming from a residential area. The residential area comprises of ten smart home. First we focus on implementing a demand side management (DSM) strategy for shaving consumption peak of each home in the considered area. Then based on load we schedule the energy resources of microgrid in an economical way which further helps to reduce the operational cost. For scheduling of appliances and DGs, a swarm intelligent technique, binary particle swarm optimization (BPSO) is used. This technique helps to find the best schedule for each appliance and each DG according to the desired objectives. Results show that the proposed strategy is more feasible and it effectively achieves the required goals.

The rest of this paper is organized as follows. Section 2 presents a literature review. Section 3 illustrates the problem statement and proposed solution and Sect. 4 presents binary particle swarm optimization. Section 5 presents the results and simulations. Finally, Sect. 6 concludes the overall work.

## 2 Literature Review

A lot of research has been conducted for the optimal scheduling of microgrid. An energy management strategy is one of the essential points to optimize generation pattern of microgrid in either grid-connected or islanded mode. In [4], a multi-objective energy management system is proposed for microgrid. It aims at minimizing pollutant emission and operating cost. This work introduced a load model of electric vehicles (EVs) under two modes: coordinated and autonomous mode. For energy management, an improved PSO is proposed in this work. The improved PSO introduces variable inertia weight factor and penalty factors.

Zhang *et al.* [5] presented a day ahead scheduling model for microgrid which considers a transmission network. This work aims at minimizing the total generation and operating cost of distributed energy resources (DERs) in a microgrid with the consideration of power flow constraints. For this purpose, a hybrid technique

harmony search algorithm with differential evolution is proposed in this work. To increase the search ability of this techniques, authors have made some modifications in the working of control parameters. To prove the effectiveness of the proposed technique it is compared with other hybrid heuristic techniques.

Muhammad *et al.* [6] proposed an energy management architecture which integrated RES. They also present opportunistic scheduling algorithms in real-time scheduling pricing environment. They formulate the problem through optimal stopping rule. Moreover, different users are classified and based on energy demand of each user the energy management architecture assigns priority to each user.

Lingfeng *et al.* [7] proposed a multi-agent control system for smart building. The main objective of this work is to minimize the power consumption without compromising user comfort. For this purpose, the proposed system consists of four types of agents: switch, central coordinator, local control and load agents. The mentioned agents cooperate with each other to achieve the desired objectives.

### 3 Problem Statement and Proposed Solution

To achieve the desired objectives in energy management of a microgrid, a strategy is needed. A lot of research has been conducted on such strategies which focus on minimizing the operating cost. The operating cost involves the maintenance cost of DERs, fuel cost and the cost of electricity bought from the utility. In [8], an expert energy management system is proposed for microgrid. It aims at minimizing the operating cost as well as the net emission of energy resources. However, the load demand considered in this research work is not balanced. In this work, ESS was charged by buying electricity from utility during low peak hours and utilizing the stored energy in high peak hours. Also, authors did not consider the case when grid's condition is jeopardized. Lin *et al.* in [9], also proposed an energy management strategy for microgrid using enhanced bee colony optimization technique. They aim at minimizing the operating cost of microgrid. However, the load demand curve considered in this work has more load on high peak hours as compared to the load on low peak hours. This means that no DSM strategy has been implemented at consumers' end, which needs to be considered. Furthermore, in [10], a mixed integer linear programming (MILP) model is proposed for the scheduling of energy consumption at user premises using microgrid system. The objective of this research work is to minimize the operating cost of DERs. Although, they did not consider the integration of RESs which would further help in the reduction of their desired objective.

Taking the above mentioned limitations under consideration, the main focus of our research work is on energy management of microgrid. A microgrid is considered as a local energy provision source to fulfil the load demand of the residential area. It constitutes different DERs i.e. MT, FC, PV panel, WTs and an ESS. Moreover, the microgrid is connected to the traditional power grid to meet the load demand. We consider a residential area which consists of ten smart homes. The appliances of each home have been categorized as fixed and shift-able appliances.

The energy consumption pattern of each home depends on the type of electrical appliances, living habits of residents and the types of household. In order to reduce electricity cost, energy consumers reduce the consumption of energy on high peak hour (when electricity price is high) and fulfil the load requirement on low peak hours (when electricity price is low). For this purpose, we have used a swarm intelligence technique, BPSO, which helps to schedule the home appliances from high peak to low peak hours. Moreover, the DGs of microgrid have also been scheduled using the same technique which helps to turn on the generators according to the load demand considering the economical criteria. In the proposed strategy, we charge the ESS from surplus energy of different generators and RES and discharge the required power when the power generated by fuel based DGs and RESs is insufficient to meet the load demand. At first, the load demand of the energy consumer is satisfied through microgrid, in case, if the microgrid does not have sufficient power supply then rest of the consumer demand is fulfilled through buying electricity from utility. When the amount of energy generated by microgrid exceeds the load demand of consumer then excessive power will be used to charge the ESS. If surplus power is still available then it will be sold back to the utility. Motive of the proposed energy management system is to find optimal set points of home appliances at user premises and to adjust the set points of DGs and ESS with respect to the economical criteria. In Eq. 1, a generalized formulation to shave the power consumption peak is given as follow: A DSM strategy for residential area is achieved through shaving the peak power consumption and shifting load to hours where load demand satisfies the below mentioned threshold.

$$x_1 = \min \sum_{t=1}^T \max L_D(t) \quad (1)$$

Equation 1 represents the objective function which is to minimize the maximum load demand at each time interval 't'. Where,  $L_D(t)$  is the load demand of the consumer at time 't'.

$$x_2 = \min \sum_{t=1}^T \left\{ \sum_{i=1}^{N_G} [sv_i(t) \cdot P_{gen,i}(B_{gen,i}(t) + M_{c,i})] + S_{gen,i} \cdot sv_i \right. \\ \left. + \sum_{j=1}^{N_{ES}} [P_{st,j}(t) \cdot B_{st,j}(t)] + P_u(t) \cdot B_u(t) \right\} \quad (2)$$

Equation 2 represents the function to minimize the operational cost of microgrid. In this equation  $sv_i$  represents the ON/OFF state of DG sources,  $P_{gen,i}$ ,  $P_{st,j}$  and  $P_u$  represent the power generated by the generators, ESS and power exchanged with utility, respectively. Whereas,  $B_{gen,i}$ ,  $B_{st,i}$ ,  $B_u$  represent the bids of generators, ESS and utility.  $M_{c,i}$  is the maintenance cost of DGs and  $S_{gen,i}$  is the start up and shut down cost of DGs.

## 4 BPSO

PSO was first described by James Kennedy and Russel C. Eberhart in 1997. It helps to find optimal solutions of problems continuous in nature. However, this technique cannot be applied to discrete optimization problems directly. Aiming at discrete problems, authors extended the PSO to BPSO in 1997 [11]. Basically BPSO is a swarm intelligence optimization techniques which mimics the behaviour of flock of birds flying together to achieve a specific objective. Each bird or particle in the flock represents a solution to the problem. Initially, in BPSO based energy management system, basic parameters are initialized. The position vector represents the set of possible solutions to the problem. Each row in the position matrix represents a candidate solution. Firstly, velocity of the particle is updated using Eq. 3 which is used in conventional PSO [12]:

$$v_{ij}(t+1) = v_i(t) + c_1(p_{best} - x_i(t)) + c_2(p_g - x_i(t)) \quad (3)$$

The major difference between PSO and BPSO is that, in BPSO, velocity of the particle is updated with respect to the probability of the particle to be 0 or 1. For this purpose, velocity of the particle is bound with the range  $\{0, 1\}$ . To map all continuous number to the specified range sigmoidal function is used as:

$$v_{ij}(t+1) = \frac{1}{1 + e^{-v_{ij}(t+1)}} \quad (4)$$

With respect to Eq. 4 the position of particle is updated. Each bit of the updated velocity vector is compared with a randomly generated number  $r \in \{0, 1\}$ . If the value of  $r$  is less than the specific bit of velocity than the position 1 will be allocated to the respected bit of position vector else 0 will be put in that bit. The updated position vector is evaluated on the base of fitness function and this process continues until the fitness criteria is not met. Finally, Gbest values is returned by the scheduler.

## 5 Results and Discussions

For the application of proposed strategy, we have considered a residential area and a low voltage microgrid. The residential area consists of ten homes as discussed earlier, each home has fixed and shift-able appliances. Residential users change their consumption pattern according to the electricity price rate of current time. The microgrid considered in this work consist of a set of DERs which includes: a MT, a FC, a PV, two WTs and an ESS. In this work we have evaluated the performance of proposed strategy in two modes: grid-connected mode, islanded mode. It is important to mention that, in this study, we have considered a period of one day which is further divided into the time intervals of one hour. The real life experimental data for PV and WT is obtained from [13] and [8] respectively.

Figure 1 illustrates the hourly scheduled and unscheduled load demands of a residential area. We have used BPSO technique which helps to schedule the



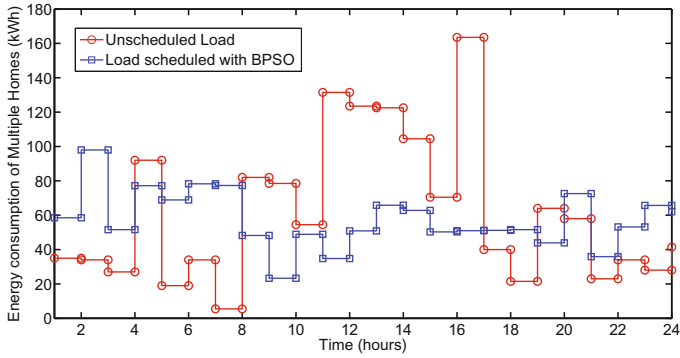


**Fig. 1.** Load demand of residential area

**Table 1.** Load in grid-connected mode (kWh)

Hour	Scheduled load	Microgrid supply	ESS	$P_u$
1	58.5000	92.0266	-16.6667	-16.8599
2	98.0000	92.1600	5.8400	0
3	51.6000	32.3200	10.8267	8.4533
4	77.2000	62.3466	0	14.8534
5	68.9000	95.3600	-16.6667	-9.7933
6	78.3000	92.3466	-14.0466	0
7	77.3000	89.4666	-12.1666	0
8	48.2000	29.2200	13.5000	5.4800
9	23.3000	29.8966	-6.5966	0
10	48.9000	28.3000	13.5000	7.1000
11	34.8000	31.0834	3.7166	0
12	50.9000	30.0934	18.7599	2.0467
13	65.8000	63.9834	0	1.8166
14	62.9000	89.9934	-16.6667	-10.5267
15	50.3000	37.6134	12.6866	0
16	51.0000	37.3766	3.9801	9.6433
17	51.2000	33.3934	0	17.8066
18	51.6000	38.3666	0	13.2334
19	43.9000	35.0666	0	8.8334
20	72.6000	67.8934	0	4.7066
21	35.9000	38.0800	-2.1800	0
22	53.2000	38.2134	2.1800	12.8066
23	65.7000	99.8666	-16.6667	-17.4999
24	62.0000	98.2934	-16.6667	-19.6267

load at user premises. As shown in this figure, hours from 9 am–5 pm are high peak hours because of more use of electricity in the defined time. Hence, most of the load on high peak hours has been shifted to low-peak hours where electricity price is low. This strategy helps to shave power consumption peaks and helps to get a uniformly distributed load demand of consumer in a day.

According to the scheduled load demand, we have scheduled DERs of microgrid using the same technique used for load scheduling. The scheduling procedure is done in such a way to minimize total operating cost of DERs while creating a balance between demand and supply. While scheduling in grid-connected mode, RES are given more priority to turn on because of their environment friendly nature and less bid costs. Table 1 demonstrates that, if consumer’s demand at a specific time interval is less than the power supplied by microgrid than ESS will be charged by the surplus power considering its constraints. If surplus power is more than the per hour charge rate of ESS, the remaining power will be sold back to the grid. Whereas, when power supplied by microgrid is less than the consumer demand, the required load demand will be fulfilled through the energy stored in ESS. However, if the required power is greater than the discharge rate of ESS, then remaining load will be fulfilled through buying energy from utility. Here, it is very important to note that in column  $P_u$  negative values indicate surplus power sold back to the utility grid, whereas positive values show the energy bought from utility to meet load demand. Table 2 represents the total operating cost of microgrid’s DG sources.

**Table 2.** Total Operating Cost

Modes	Utility	Grid-connected mode
Operating cost (cents/kWh)	36277	30985

## 6 Conclusion

In this paper, an energy management strategy is proposed using BPSO, to make a balance between demand and supply. For this purpose, a residential area is considered which consists of ten homes and load of each home is scheduled. The microgrid integrates fuel based generators, RES and ESS. Our objective is to reduce operating cost or DERs and to minimize the operational cost of DERs in a microgrid. Moreover, we have also minimized the use of power from utility grid it enables to reduce peak to average ratio. To achieve our objectives, we have calculated operating cost of DERs by fulfilling load demand in grid-connected mode. The results conclude that the operating cost is significantly reduced as compared to the cost of fulfilling consumer demand through utility.

## References

1. Tayab, U.B., Roslan, M.A.B., Hwai, L.J., Kashif, M.: A review of droop control techniques for microgrid. *Renew. Sustain. Energy Rev.* **76**, 717–727 (2017)
2. Global Greenhouse Gas Emissions Data? 6 April 2017. <https://www.epa.gov/ghgemissions/global-greenhouse-gas-emissions-data>
3. Zhou, B., Li, W., Chan, K.W., Cao, Y., Kuang, Y., Liu, X., Wang, X.: Smart home energy management systems: concept, configurations, and scheduling strategies. *Renew. Sustain. Energy Rev.* **61**, 30–40 (2016)
4. Liu, H., Ji, Y., Zhuang, H., Hongbin, W.: Multi-objective dynamic economic dispatch of microgrid systems including vehicle-to-grid. *Energies* **8**(5), 4476–4495 (2015)
5. Zhang, J., Yihong, W., Guo, Y., Wang, B., Wang, H., Liu, H.: A hybrid harmony search algorithm with differential evolution for day-ahead scheduling problem of a microgrid with consideration of power flow constraints. *Appl. Energy* **183**, 791–804 (2016)
6. Rasheed, M.B., Javaid, N., Ahmad, A., Awais, M., Khan, Z.A., Qasim, U., Alrajeh, N.: Priority and delay constrained demand side management in real-time price environment with renewable energy source. *Int. J. Energ. Res.* **40**(14), 2002–2021 (2016)
7. Wang, L., Wang, Z., Yang, R.: Intelligent multiagent control system for energy and comfort management in smart and sustainable buildings. *IEEE Trans. Smart Grid* **3**(2), 605–617 (2012)
8. Motevasel, M., Seifi, A.R.: Expert energy management of a micro-grid considering wind energy uncertainty. *Energy. Convers. Manage.* **83**, 58–72 (2014)
9. Lin, W.-M., Chia-Sheng, T., Tsai, M.-T.: Energy management strategy for microgrids by using enhanced bee colony optimization. *Energies* **9**(1), 5 (2015)
10. Zhang, D., Evangelisti, S., Lettieri, P., Papageorgiou, L.G.: Economic and environmental scheduling of smart homes with microgrid: DER operation and electrical tasks. *Energy. Convers. Manage.* **110**, 113–124 (2016)
11. Valle, D.Y., Venayagamoorthy, G.K., Mohagheghi, S., Hernandez, J.-C., Harley, R.G.: Particle swarm optimization: basic concepts, variants and applications in power systems. *IEEE Trans. Evol. Comput.* **12**(2), 171–195 (2008)
12. Beheshti, Z., Shamsuddin, S.M., Hasan, S.: Memetic binary particle swarm optimization for discrete optimization problems. *Inf. Sci.* **299**, 58–84 (2015)
13. Chen, C., Duan, S., Cai, T., Liu, B., Gangwei, H.: Smart energy management system for optimal microgrid economic operation. *IET Renew. Power Gener.* **5**(3), 258–267 (2011)

# Single Hop Selection Based Forwarding in WDFAD-DBR for Under Water Wireless Sensor Networks

Zaheer Ahmad<sup>1</sup>, Arshad Sher<sup>1</sup>, Saba Gull<sup>1</sup>, Farwa Ahmed<sup>1</sup>, Umar Qasim<sup>2</sup>, Zahoor Ali Khan<sup>3</sup>, and Nadeem Javaid<sup>1</sup>(✉)

<sup>1</sup> COMSATS Institute of Information Technology, Islamabad 44000, Pakistan  
nadeemjavaidqau@gmail.com

<sup>2</sup> Cameron Library, University of Alberta, Edmonton T6G 2J8, Canada

<sup>3</sup> Computer Information Science, Higher Colleges of Technology,  
Fujairah 4114, United Arab Emirates  
<http://www.njavaid.com>

**Abstract.** The design of routing protocols for Underwater Wireless Sensor Networks (UWSNs) holds many challenges, due to long propagation, high mobility, limited bandwidth and multi path routing. As a consequence of the occurrence of the void hole, and uneven distribution of nodes in the network, the selection of next forwarding in one hop or even two hops may result in failure of forwarding in indigenous sparse deployment region. In order to reduce the probability of occurrence of void hole this protocol presents Single Hop Selection based Forwarding WDFAD-DBR (SHSF-WDFAD-DBR), which selects at least two optimal forwarder nodes in the communication range to reduce the probability of occurrence of void hole and it also avoids the backward transmissions. In addition the mechanism of forwarding area division and neighbor node prediction mechanism is proposed to reduce the energy consumption caused by duplicate packets and neighbor request. Finally the simulations are conducted to verify the efficiency and legitimacy of SHSF-WDFAD-DBR with respect to Packet Delivery Ratio (PDR) and energy tax.

## 1 Introduction

As an encouraging solution to aquatic conservational monitoring and consideration, UWSNs have appealed significant attention recently from both academia and industry. UWSNs are deployed in acoustic atmosphere to enable applications like oceanographic data gathering, offshore assessment, disaster avoidance, supported navigation, circulated tactical surveillance and mine reconnaissance [1]. The subsurface environment of UWSNs are quite diverse and complex in many traits with that of terrestrial wireless sensor networks. The main difference between terrestrial wireless sensor networks and underwater wireless sensor networks is the communication channel and high-frequency, as radio signals attenuate rapidly in underwater. So acoustic communication appears as a better

choice for UWSNs [2]. The underwater acoustic communication has few limitations for instance, high propagation delay, high bit error rate and low bandwidth. In under water acoustic networks nodes move freely due to ocean current which causes to provide a dynamic configuration in network [3]. That is why the UWSNs are considered a three dimensional networks, however terrestrial wireless sensor networks are always considered a two dimensional networks. The acoustic networks are much more partially related with terrestrial networks, because the underwater sensor nodes often cost much more than terrestrial sensor networks. In acoustic communication the sensor nodes need to be left in underwater for many days or even longer time without any power resource. Besides all this due to high manufacturing area and cost with maximum monitored area the UWSNs has become the major factor in the design and implementation process.

Due to above mentioned constraints and challenges, the terrestrial and ad hoc routing schemes cannot be applied in UWSNs. Therefore designing a reliable, energy efficient routing protocol which not only reduces the end-to-end delay but also enhances the network life time has become one of the primary factor in UWSNs research area in the deep ocean.

Motivated by all above considerations, this routing scheme proposes an efficient routing protocol for underwater acoustic sensor networks for deep Ocean. This protocol avoids the void hole in local sparse region and suppresses duplicate packets and reduces extra cost communication. Which improves the reliability of network, minimizes energy expenditure but it also minimizes the end-to-end delay.

**Contributions:** We propose a novel and efficient routing protocol called single hop selection based forwarding WDFAD-DBR which makes routing decisions on the bases of minimum depth, maximum residual energy and, the selection of at least two Potential Forwarder Nodes (PFNs) in the communication range. Second we divide the transmission range with depth threshold, auxiliary and primary forwarding area, and the selection of optimal nodes to forward the packet on basis of minimum holding time in the transmission range causes to suppress the packets holding the packet below the forwarder node. Third to handle the mobility of nodes this protocol predicts the neighbor nodes movement like WDFAD-DBR. Finally we perform the simulation results to conclude the effectiveness of SHSF-WDFAD-DBR.

## 2 Related Work

This section reviews some related work on the routing protocol in UWSNs and review the limitations and advantages of the previous existing schemes. In UWSNs routing protocols are divided into three types, location based, depth based and location free routing. In depth based DBR, EEDBR, Hydro Cast and WDFAD-DBR are few routing protocols, whereas the location based VBF and HH-VBF are the few routing protocols and location free routing protocols are divided into clustering. The FBR is used to reduce the unnecessary flooding, nodes steadily increases the forwarding area by calculating the flooding angle and transmission

power level on the bases of pre-regulated angle and power. Nodes send maximum RTS in the sparse network, which causes to increase the maximum energy consumption and end-to-end delay by the exchange of RTS and CTS, though the protocol provides high data delivery ratio, but it consumes maximum energy due to many attempts of transmitting a packet in under water sparse network [4]. In DFR the base angle is calculated on the bases of network density and link quality and the current angle of node is determined by itself from source node to destination node. The node forwards the packet if the node lies in the communication range of base angle otherwise it discards the packet directly. However the use of constant power level in the entire network consumes the maximum energy, more over in sparse network distribution the eligible nodes cannot be found when void hole occur [5]. In vector based forwarding (VBF) the transmission range of packet is determined by virtual pipeline from source node to destination node. VBF protocol conserves energy by restricting the packet transmission direction and range of forwarding, due to limited packet pipeline transmission and radius, the forwarding nodes cannot be found in sparse region. Which causes a void hole, however the radius threshold has huge influence on network performance [6]. To discuss the above mentioned issues of VBF the HH-VBF protocol is proposed which hop by hop changes the direction of forwarding pipeline in the entire network. This scheme helps to forward the packet according to the current topology information of the network, though the network performance is little improved by dynamically changing the direction of pipeline, but has low performance in sparse distribution due to the constant pipeline radius [7].

In [8] the authors proposed a depth based routing protocol (DBR), in which the data is transmitted on the basis of lower depth to sink using greedy approach in the next hop. But this scheme not focuses on the occurrence of void hole, thus the packet delivery ratio is decreased, whereas the EEDBR forwards the packets on the bases of residual energy and depth and calculates the holding time when receive packet, but it also not focuses on the occurrence of void hole [9]. In Hydro Cast protocol the data forwarding packet is same as DBR, and the mechanism for avoiding void hole and channel interference is used to improve the network performance [10]. Whereas the few typical routing protocols used for beacon based routing like H2-DAB [11] and REBAR [12]. These schemes are not providing any location information which causes to reduce the hardware cost for node position. The sink node dynamically assign a separate address to each node in H2-DAB on the basis of hop count, where as to increase the reliability of H2-DAB, 2H-ACK uses two hops acknowledgement mechanism instead of one hop forwarding. The H2-DAB and 2HACK horizontal layering is used with the use of multi-sink scenario. REBAR uses concentric layers, whereas horizontal layers are used to balance energy consumption to increase the life time of the network. This scheme contains few problems like, if the updating information is too maximum the layering information could be stolen and the nodes may move to the other layers by water current.

In [13] clustering schemes are proposed based on two phases: set up phase and communication phase. The set up phase is used to select the cluster heads according to their residual energy, where as in communication phase member

nodes sense and collect their data and send it the corresponding cluster heads. Then the aggregated data is transmitted to the sink through multi hop, which adds an extra burden on the network and causes end-to-end delay. Therefore cluster routing is not adequate for UWSNs in time-critical application.

### 3 Network Architecture

SHSF-WDFAD-DBR uses a multi-sink network architecture, which is composed of anchored nodes, relay nodes and sink nodes as shown in Fig.1. Anchored nodes are static at the bottom of the ocean which sense, collect and forwards data to the relay nodes. Relay nodes are deployed randomly inside the specific dimension with different depths which not only sense their own data but it also forwards the received data. Sink nodes are the destination nodes which are equipped with both radio and acoustic modems, as the acoustic modems are used for under-water communication, and radio modems are used for land communication. Anchored and relay nodes are used to forward data to the sink through multi path relaying between source nodes to destination.

Sink nodes are located at the surface of the water which send and receive data through satellite with radio link, as the sinks are directly connected to each other through radio links. We assume that, if packet is received by one sink that is considered to be received by all sinks and the packet is successfully transmitted to the satellite, and satellite delivers it to the control station.

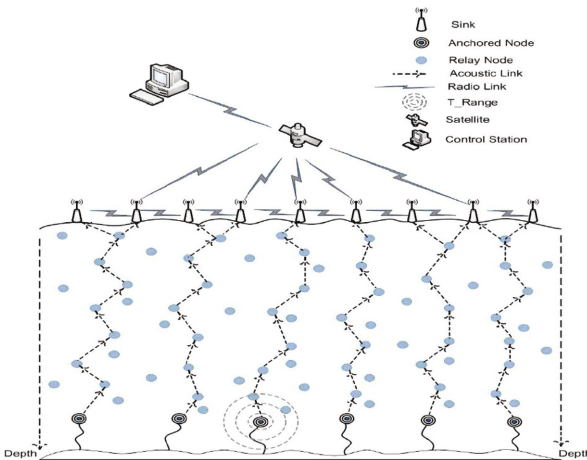


Fig. 1. Network architecture

### 3.1 Computing Holding Time and Data Communication Phase

When source node broadcast a packet the receivers in the transmission range receives the packet. As it can be seen from Fig. 2 node S broadcast the packet and it is received by A, B, C, D and H in case of considering no collision and bit error rate. S1, S2 and S3 are the transmission ranges of nodes S, A and B respectively. As few nodes are within the transmission range of node A and B. It can be seen from Fig. 2 that node S broadcast the packet equipped with PFNs IDs and holding time information, upon receiving this data packet by other nodes in the communication range directly discarded except PFNs. If node A has at least two PFNs in the communication range, then node A forwards the data packet. In this scenario the nodes lying below node A suppresses their packet transmission. But if node A has no PFNs in its communication range, then node B has to hold the packet till to the reception of beacon message. Either this message is forwarded by node A or by node S. As it can be seen from Fig. 2 that node B lies in the communication range, so node B receives the beacon message from node A. If node B lies out side the communication range then node A forwards the beacon message to node S and then beacon is forwarded to node B. This causes to minimize the energy consumption of network. Because node B already contains the data packet. In this way this scheme enhances the life time of network. In this way we can avoid the backward transmission of data packet, and reduces the probability of void hole in advance.

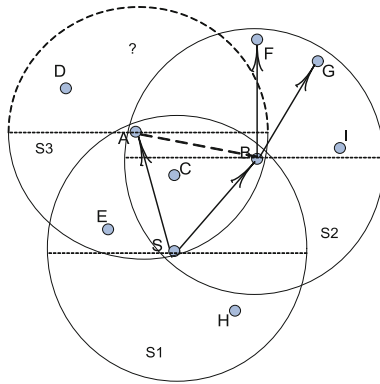


Fig. 2. Holding time of a packet

## 4 Performance Parameters

To evaluate the performance of SHSF-WDFAD-DBR we use the following four metrics, PDR (Packet delivery ratio) and Energy tax.



### 4.1 PDR Comparison

In Fig. 3 it can be observed that with the increase of number of nodes the PDR of SHSF-WDFAD-DBR, Intar and WDFAD-DBR is increases. When network is sparse the chances of void hole probability is maximum and minimum packets are delivered to the destination. But in dense network with the increase of number of nodes maximum packets are delivered to the sink. Figure 3 expresses that the performance of SHSF-WDFAD-DBR is comparatively better than that of Intar and WDFAD-DBR in sparse distribution as well as the dense distribution. WDFAD-DBR and Intar does not provide the better PDR because it does not avoid the void hole probability in term of selection of two hops and consideration of end-to-end path selection in Intar.

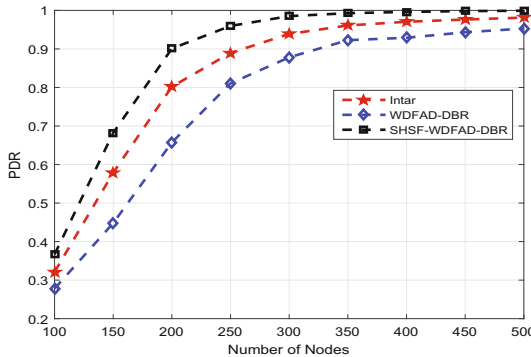
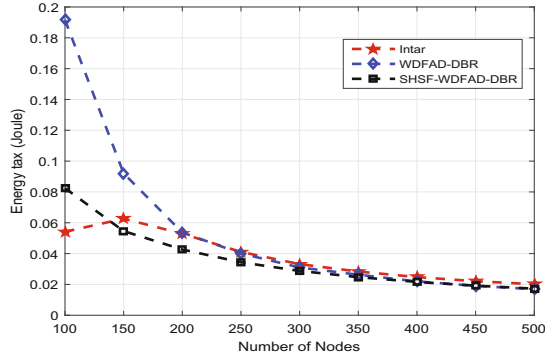


Fig. 3. PDR with increasing node density for comparing schemes

SHSF-WDFAD-DBR shows an increase tendency with the increase of average number of neighbors per node which causes to increase the PDR of SHSF-WDFAD-DBR. More over the channel interference is not considered by the WDFAD-DBR and Intar at maximum node densities, but SHSF-WDFAD reduces the channel interference through control messages which increases the PDR of SHSF-WDFAD-DBR. Because the maximum packets are delivered from the auxiliary and primary forwarding area, this is the reason the PDR is comparatively better than that of compare schemes. The overall accumulative PDR of SHSF-WDFAD-DBR to WDFAD-DBR is 13.1% high and accumulative PDR to Intar is 5.7% which shows comparatively very high PDR relatively to compare schemes.

### 4.2 Energy Tax Comparison

As expected the energy tax increases with the increase of number of nodes. The node density causes collision probability at receiver side without adopting any mechanism of suppression and packet duplication. Because collision probability



**Fig. 4.** Energy tax with increasing node density for comparing schemes

increases the energy tax. In the sparse network minimum packets are delivered to sink and probability of occurring of void hole is maximum, but comparatively to dense network maximum packets are delivered to sink with the increase of number of nodes which reduces the probability of void hole. It also spends unnecessary energy due to increase of number of packets. It can be seen from Fig. 4 that energy tax of SHSF-WDFAD-DBR is less than of WDFAD-DBR because of selection of two hops data transmission in WDFAD-DBR and the occurrence of probability of void holes in sparse network is higher than in dense network. This causes in failure of forwarding packets.

In addition the SHSF-WDFAD-DBR considers the one hop selection based forwarding with two selective PFNs, which minimizes the energy tax through the mechanism of packet suppression. As the number of duplicate packet transmission is avoided in SHSF-WDFAD-DBR through control message mechanism and piggy backing approach. The backward transmissions are avoided in the proposed scheme which effectively reduces the energy consumption. The depth threshold and forwarding area division also reduces the energy expenditure. This is the reason that energy tax in SHSF-WDFAD-DBR is comparatively less than WDFAD-DBR and Intar.

In addition the Intar establishes the communication path through HELLO message initialization from source node to sink node but it causes to spends maximum energy. As it can be seen from Fig. 4 Intar and WDFAD-DBR have high energy expenditure than SHSF-WDFAD-DBR. The total accumulative energy tax of SHSF-WDFAD-DBR is 16.63% less than that of WDFAD-DBR, where as the total accumulative energy tax to Intar is 16.66%. Which comparatively shows a less energy tax due to restriction of packet duplication, packet suppression and one hop selection based forwarding in SHSF-WDFAD-DBR.

## 5 Conclusion

In 3D under acoustic networks, due to large deployment regions, cost and expensive manufacturing network has become high dynamic, which results into a void

hole in local sparse region. In this paper we proposed and evaluated the data routing for UWSNs. SHSF-WDFAD-DBR provides a novel based topology information to avoid the void hole with the selection of two optimal forwarder nodes. This protocol avoids the backward transmission of packet in case of occurrence of void hole, and the communication area division significantly improves the network performance. Thus it reduces the energy effectively. The simulation results showed that the performance of SHSF-WDFAD-DBR is improved in terms of delivery ratio and energy consumption with compared schemes.

## References

1. Ali, T., Jung, L.T., Ameer, S.: Flooding control by using angle based cone for UWSNs. In: 2012 International Symposium on Telecommunication Technologies (ISTT), pp. 112–117. IEEE, November 2012
2. Hwang, D., Kim, D.: DFR: directional flooding-based routing protocol for underwater sensor networks. In: OCEANS 2008, pp. 1–7. IEEE, September 2008
3. Xie, P., Cui, J.H., Lao, L.: VBF: vector-based forwarding protocol for underwater sensor networks. In: International Conference on Research in Networking, pp. 1216–1221. Springer, Berlin Heidelberg, May 2006
4. Nicolaou, N., See, A., Xie, P., Cui, J.H., Maggiorini, D.: Improving the robustness of location-based routing for underwater sensor networks. In: OCEANS 2007-Europe, pp. 1–6. IEEE, June 2007
5. Yan, H., Shi, Z.J., Cui, J.H.: DBR: depth-based routing for underwater sensor networks. In: International Conference on Research in Networking, pp. 72–86. Springer, Berlin Heidelberg, May 2008
6. Wahid, A., Kim, D.: An energy efficient localization-free routing protocol for underwater wireless sensor networks. *Int. J. Distrib. Sens. Netw.* **8**(4), 307246 (2012)
7. Uichin, L., Wang, P., Noh, Y.: Pressure routing for underwater sensor networks. In: Proceedings of the IEEE, INFOCOM (2010)
8. Ayaz, M., Abdullah, A.: Hop-by-hop dynamic addressing based (H2-DAB) routing protocol for underwater wireless sensor networks. In: 2009 International Conference on Information and Multimedia Technology, ICIMT 2009, pp. 436–441. IEEE, December 2009
9. Ayaz, M., Abdullah, A., Faye, I.: Hop-by-hop reliable data deliveries for underwater wireless sensor networks. In: 2010 International Conference on Broadband, Wireless Computing, Communication and Applications (BWCCA), pp. 363–368. IEEE, November 2010
10. Gopi, S., Govindan, K., Chander, D., Desai, U.B., Merchant, S.N.: E-PULRP: energy optimized path unaware layered routing protocol for underwater sensor networks. *IEEE Trans. Wirel. Commun.* **9**(11), 3391–3401 (2010)
11. Chen, J., Wu, X., Chen, G.: REBAR: a reliable and energy balanced routing algorithm for UWSNs. In: 2008 Seventh International Conference on Grid and Cooperative Computing, GCC 2008, pp. 349–355. IEEE, October 2008
12. Yu, H., Yao, N., Wang, T., Li, G., Gao, Z., Tan, G.: Weighting depth and forwarding area division DBR routing protocol for UASNs. *Ad Hoc Netw.* **37**, 256–282 (2016)
13. Domingo, M.C.: A distributed energy-aware routing protocol for underwater wireless sensor networks. *Wirel. Pers. Commun.* **57**(4), 607–627 (2011)

# A Framework for Ranking of Software Design Patterns

Shahid Hussain<sup>(✉)</sup>, Jacky Keung, and Arif Ali Khan

Department of Computer Science,  
City University of Hong Kong, Kowloon Tong, Hong Kong  
{Shussain7-c, aliakhan2-c}@my.cityu.edu.hk,  
Jacky.Keung@cityu.edu.hk

**Abstract.** Several software design patterns have been familiarized either in canonical or as variant solutions in order to solve a problem. Novice designers mostly adopt patterns without considering their ground reality and relevancy with design problems, which may cause to increase the development and maintenance efforts. In order to realize the ground reality and to automate the selection process, the existing automated systems for the selection of design patterns either need formal specification or precise learning through training the numerous classifiers. In order to address this issue, we propose an approach on the base of a supervised learning technique named ‘Learning to Rank’, to rank the design patterns with respect to text similarity with the description of the given design problems. Subsequently, we also propose an evaluation model in order to assess the effectiveness of the proposed approach. We evaluate the effectiveness of the proposed approach in the context of several design pattern collections and relevant design problems. The promising experimental results indicate the applicability of the proposed approach.

## 1 Introduction

In software development life cycle, software design is considered as a most challenging task as compared to other activities. An architecture-based design method is one of main category which can be realized during the evolution process. In this category, different software architectural styles (presented through design components and their relationship) are applied and can be considered as coordination tools among the activities of the software development life cycle. For example, it provides a bridge between satisfactions of system’s critical requirements to implementation [1]. The most common architecture-based design method is Attribute Driven Design (ADD) which incorporates the different architectural strategies and patterns to fulfill the quality attributes. In the working procedure of ADD, a software developer selects an architectural style and chooses the desired quality attributes included in the software system. Subsequently, software developers use the description of design requirements related to selected architectural component and employed software design patterns [2]. Over many years, based on their experiences, software developers have encapsulated and suggested the proven solutions to satisfy the recurring design problems. Subsequently, the experience-based solutions are organized and realizes as a standardized form for

design patterns. For example, the canonical solution of Composite GoF (Gang-of-Four) design pattern is the result of formulating the recurring structural and compound design problems related to the composition of objects from its nesting and building tree structures [3].

The employment of design patterns in software development is considered as an alternative approach to software refactoring to address the declined quality of the software system. Besides, other advantages to employ the design patterns are; to maintain consistency between design and implementation, enabling the relationship between developers, increase reusability and software modularization [3]. However, due to the existence of an alternative solution of spoiled patterns [4], the challengeable design patterns [5], and interdisciplinary design patterns [6], it is so difficult for a novice designer to find appropriate design pattern(s) and determine its applicability in order to solve a design problem. Since design patterns are formulated on the base of software developer’s experience, consequently, a designer with no or little experience with design patterns have concerns how to find the best one.

In order to address this issue, we propose an approach to rank the design patterns on the base of their text similarity with given design problem(s). The proposed approach is formulated through a supervised learning task named ‘Learning to Rank’ which can help to rank the design patterns on their ground truth. The current efforts to automate the design pattern selection process can be divided into three approaches named UML-Based [7–9], Ontology-Based [10–12] and Text categorization based approach [13–15].

Subsequently, for the effective results of automated systems which based on Text categorization approach, there is need of an ample training sample size or separate classifiers for each pattern class in order to solve the multi-class problem [16]. However, it is not easy in the existence of complex and interdisciplinary design pattern

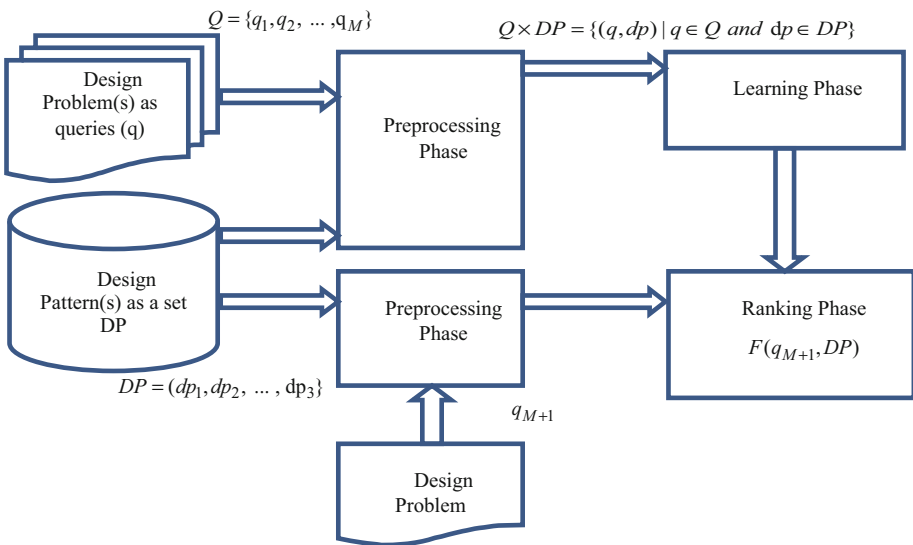


Fig. 1. Overview of proposed approach

collection, where numerous classifiers will be required to make effective learning for each pattern class [5, 7]. In this study, we consider design pattern(s) selection as information retrieval problem [13–15] and proposed an approach to rank the design pattern(s) for given design problem(s) using a supervised learning task named ‘Learning to Rank’. There are numerous list-wise ranking algorithms (Coordinate Ascent, AdaRank and LambdaMART) and, point-wise and pair-wise (RankNet, MART and RankBoost) have been applied in the domain of information retrieval applications [17]. However, in this paper; we incorporate only LambdaMART [18] in the proposed approach. The LambdaMART has been applied to combine the strengths of the boosted tree classification and LambdaRank (which is described through neural network models). The framework of the proposed approach is shown in the Fig. 1.

## 2 Related Work

In 1977, Alexander, the father of patterns describe a roadmap to capture the design knowledge and present through a collection of patterns in order to help the architects and engineers. According to Alexander, a pattern can be described in three sections context, a problem description (we used this section in the preprocessing phase of proposed approach, described in Sect. 4.1) and a corresponding solution. However, the building components of each section vary which depend on the developer’s experience and knowledge in the response of handling design problems. For example, in the domain of object-oriented development Gamma et al. [3] present 23 design patterns and classified them into three groups named Creational, Structural and Behavioral. Subsequently, we summarized the researcher’s efforts made to automate the selection of design patterns which are UML-Based, Ontology-Based and Text categorization based approaches.

D-K Kim and C.E. Khawand depict an approach to select the design pattern by specifying its problem domain. They reported that problem domain of design patterns can help to describe the known problems in the context. The authors used Role-Based Modeling Language (RBML) as UML based pattern specification language to describe the Meta-model to formalize the design patterns [7]. Hasso and Carlson consider the problem description part of design patterns; perform semantic analysis of sentences, and on the base of words meaning which suggest the classification of design patterns. In their study, the authors perform semantic analysis using linguistic theory and consider the meaning of verbs for the classification of design patterns [10].

S.M.H. Hasheminejad and S. Galileo [13], and S. Hussain et al. [14, 15] consider the design pattern selection as an information retrieval problem, used the text categorization approach, and present the automated method to select the design pattern with respect to the degree of similarity between the description of design problems and problem definitions of the retrieved design patterns.

In both studies, the authors consider the classification and selection of design patterns with respect to the given design problem as a problem of information retrieval and used text categorization approach. Subsequently, the common objective of both studies is to obtain promising results with respect to ground truth. However, for the precise learning, either there is need of enough sample size or numerous classifiers to

overcome the multi class problem. Recently, a new machine learning technique ‘Learning to Rank’ has been applied in different information retrieval related application such as web search. The ‘Learning to Rank’ is a supervised learning technique which is used for the creation of the ranking model  $f(q, d)$  to retrieve document  $d$  with respect to query  $q$ . In our study, we consider the design pattern selection as information retrieval problem and proposed an approach based on ‘Learning to Rank’ to select the appropriate design pattern(s) for given design problem(s).

### 3 Brief Description of Text Categorization

The text categorization approach is performed either through supervised or unsupervised learning techniques. The former techniques use class labels assigned to documents and latter techniques use attributes of the data and dis(similarity) measures to automate their learning. Text preprocessing is mandatory for the text categorization and should be performed before the learning process [11]. The Preprocessing, indexing and feature selection are the main steps which are performed during the text preprocessing. In the preprocessing step, two activities are performed to transform documents into strings. The first activity is to remove stop words that are more frequent words and carry no information, such as Preposition, Conjunction, and Pronouns. The second activity is word stemming, which is performed to make a group of words that have same conceptual meaning. Subsequently, the numbers of words in the documents collection are reduced. Porter’s stemmer is a well-recognized stemming algorithm [19], used to transform English words into their stem iteratively through a set of rules. Subsequently, in indexing step, Vector Space Model (VSM) is used as well-known indexing method to describe the documents. In VSM, each document is described by a vector of words. Commonly, a document collection is described through a word-by-document matrix  $D$ , where each entry refers to the word’s occurrence in the document.

$$D = (W_{wd}) \quad (1)$$

In the Eq. 1,  $W_{wd}$  is the weight of word  $w$  in document  $d$ . There are many ways to determine the weight  $W_{wd}$  of word  $w$  in document  $d$ . For example, Binary, Term Frequency (TF), Term Frequency Inverse Document Frequency (TFIDF), Term Frequency Collection (TFC), Length Term Collection (LTC), and Entropy are commonly used weighting methods in text categorization [11]. The term weighting schemes are used to improve the performance and remove the noise from the documents. Finally, In feature selection step, different techniques are used to remove the features, however, computational time and classification accuracy are the main issues related to the discriminative power of each technique [16].

## 4 Overview of Proposed Approach

The rapid development of software design patterns leads to an increase in the amount of its electronic documentation worldwide. Therefore, there is a need to organize these patterns in order to reduce the time required to a novice designer to select the appropriate design pattern(s). This situation motivate us to consider this issue (design pattern organization and selection problem) as an information retrieval problem and use the text categorization approach to rank the design pattern with respect to text relevance with design problems. Though this issue is addressed by [13–15] in their study, however, in the case of complex and interdisciplinary design pattern collections where numerous classifiers are required to make supervised learning for each pattern class or need of a global filter-based feature method to construct a more representative feature set to overcome the multi-class problem.

We look out the capacity of automated text categorization in different domains and use in the proposed approach for two purposes, (1) to rank the design patterns with respect to the text relevancy with design problem(s) description and (2) automatically retrieve a more appropriate design pattern(s) for a given real design problem. The ranking tasks are performed by using local  $f(q, d)$  and global  $F(q, D)$  ranking models. These ranking are created to rank the set of documents  $D$  with respect to user's query  $q$ . The existing approaches BM25 model and LMIR (Language Model for IR) are implemented to rank the documents by creating  $f(q, d)$  without training, however, in order to achieve our objective, we employ a machine learning technique named 'Learning to Rank' to construct a ranking model for the selection of more appropriate design pattern(s) for a given design problem. As a supervised learning technique, 'Learning to Rank' require training and testing data. We incorporate a widely used list-wise ranking algorithm named LambdaMART in the proposed approach. Subsequently, we formulate the proposed approach in three phases Preprocessing, Learning (on training data) and Ranking (on testing data).

### 4.1 Preprocessing

The first phase of the proposed approach is preprocessing which applied to problem description of all design patterns of a desired collection and description of the given design problem. The sequence of preprocessing activities is depicted in Fig. 2.

The first two activities are performed to remove the stop words and words stemming consecutively. There are several text mining tools like JPreText (A simple Text

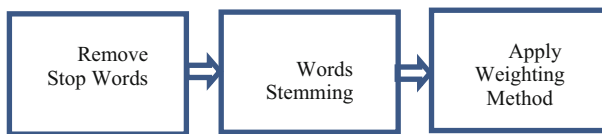


Fig. 2. Preprocessing activities



Preprocessing Tool)<sup>1</sup> and their APIs<sup>2</sup> (Application Programming Interfaces) are available to perform these tasks. The problem description part of each design pattern and design problem description is presented in the form of a feature vector. Subsequently, a Vector Space Model (VSM) includes non-repeated terms of all documents is created. The structure of Vector Space Model (VSM) with for N design pattern and a design problem with M non-repeated terms. Finally, in the last activity, one of weighting schemes (Sect. 3) is applied to the vector space model.

## 4.2 Learning Phase

In the domain of information retrieval, three approaches of ‘Learning to Rank’ are followed in order to overcome the corresponding problem. In the learning phase of proposed approach, we analyzed the list-wise ranking algorithm named LambdaMART due to the existence of design patterns either as variant or a spoiled form of canonical solution and ranking them with respect to text relevancy with the given design problem. Subsequently, LambdaMART satisfied the properties (a) consistency, (b) soundness, (c) convexity and computational efficiency regarding the Loss function point of view. Usually, two tasks are performed in the learning phase. The first task is performed to conduct learning on the pairwise (Problem-Pattern) preference and construct a training set which includes design patterns, design problems and their relevance levels. There are several ways to describe the relevance levels between design patterns and design problem, such as use of similarity measures [20] or use of labels to grade the patterns associated with the design problem. In this study, we assumed the latter approach in order to evaluate the pattern relevance with respect to a design problem. The formalization of training set for learning is shown as follow:

We assume that  $Q$  is design problem set (that is  $\{q_1, q_2, \dots, q_M\}$ ), where  $q$  referred to a design problem),  $DP$  is the pattern set (that is  $\{dp_1, dp_2, \dots, dp_N\}$ , where  $dp$  referred to a design pattern), and  $L$  is the label set (that is  $\{1, 2, \dots, l\}$ ) denotes different grades. The label set  $L = \{l_{1,1}, l_{1,2}, \dots, l_{1,N}\}$  and  $DP = \{dp_{1,1}, dp_{1,2}, \dots, dp_{1,N}\}$  pattern set are created with respect to the association with a given design problem  $q_1$  and are ordered  $l \succ l-1 \succ l-2 \succ \dots \succ 1$  accordingly. Where  $\succ$  depicts the order relation. Subsequently, a feature vector  $v_{i,j} = \phi(q_i, dp_{i,j})$ ,  $i = 1, 2, \dots, m$ ;  $j = 1, 2, \dots, n$  is created from each problem-pattern pair  $(q_i, dp_{i,j})$  where  $\phi$  referred as feature function for a problem-pattern pair. Finally, the training dataset is created according to Eq. 2.

$$Training\ Set = \{(q_i, DP_i), L_i\}_{i=1}^M \quad (2)$$

The second task is performed to construct a local ranking model  $f(q, dp)$  in order to assign score to a problem-pattern pair  $(q, dp)$  and global ranking model  $F(q, DP)$  to assign a list of scores to problem-patterns pairs  $(q, DP)$ . We assume that  $F(\cdot)$  is mapping function which maps a list of feature vectors  $V = \{v_1, v_2, \dots, v_3\}$  to list of grades.

<sup>1</sup> <http://sites.labc.icmc.usp.br/torch/msd2011/jpretext/>.

<sup>2</sup> <http://www.opencalais.com/opencalais-demo/>.

The design problem and its associated documents form a group which is represented through i.i.d. data, while members of each group have no i.i.d [16].

### 4.3 Ranking Phase

In the ranking phase of proposed approach, we define the ranking list that is permutation  $\pi_i \in \Pi_i$  for a given design problem  $q$  and relevant patterns  $DP_i$ . Where  $\Pi_i$  referred to the list of permutations  $\pi_i$  on  $P_i$  to present the position (or rank) of a pattern. For example, the position of the  $j^{\text{th}}$  pattern can be represented as  $\pi_i(j)$ . The testing dataset consist of a new design problem  $q_{M+1}$  and the associated patterns  $DP_{M+1}$ , shown in Eq. 3.

$$\text{Testing Dataset} = \{(q_{M+1}, DP_{M+1})\} \quad (3)$$

Subsequently, we create the feature  $v_{M+1}$  and used the ranking model (Sect. 4.2) to assign the grades to the patterns  $DP_{M+1}$  and output the ranking list  $\pi_{M+1}$  in sorted form.

### 4.4 Design Pattern Groups

In the domain of software engineering, some groups of experts have categorized the design patterns on the base their intent, motivation, and applicability. In this study, we consider two well-known design pattern collections in order to evaluate our proposed approach.

#### A. Gang-of-Four (GoF) Design Pattern Collection

The GoF collection includes 23 object-oriented design patterns which are divided into three groups named Creational, Structural, and Behavioral. This case study includes 1465 non-repeated words of all 23 design patterns after removing the stop words and words stemming [3].

#### B. Douglass Design Pattern Collection

The Douglass collection includes 34 real time systems relevant design patterns which are divided into five categories named Concurrency, Safety, and Reliability, Distribution, Memory, and Resource. This case study includes 1271 non-repeated words of all 34 design patterns after removing the stop words and words stemming [21].

### 4.5 Design Pattern Groups

Subsequently, we consider 20 real design problems from different resources [4, 22, 23] in order to evaluate the effectiveness of proposed approach; however, we mention the description of only one design problem due to space limitation.

- Design Problem

“An arithmetic expression consists of an operand, an operator (+ − ∗ /), and another operand. The operand can be a number, or another arithmetic expression. Thus, 2 + 3 and (2 + 3) + (4 ∗ 6) are both valid expressions.”

## 5 Evaluation Model for Proposed Approach

In the text categorization approach, Precision and Recall for the learners can be estimated using micro-averaging or macro-averaging equations, however, the precision of micro-averaging (used in this study) is better than macro-averaging. In order to select the best weighting method for ranking algorithms used in the proposed approach, the effect of each method such as Binary, TFIDF, TFC, LTC and Entropy on ranking algorithm is computed in term of Precision, Recall and F-measure [11]. Subsequently, weighting method with highest F-measure is chosen for the ranking algorithm.

$$P = \frac{\sum_{c=1}^N TP_c}{\sum_{c=1}^N (TP_c + FP_c)}, \quad \text{Micro - Averaging} \quad (4)$$

$$R = \frac{\sum_{c=1}^N TP_c}{\sum_{c=1}^N (TP_c + FN_c)}, \quad \text{Micro - Averaging} \quad (5)$$

$$F = \frac{2 \times P \times R}{(P + R)} \quad (6)$$

In the Eqs. 4 and 5, N is the number of design pattern classes decided to evaluate the performance of learning techniques used in the proposed approach. For example, in the case of GoF design pattern collection N is 3 (Sect. 4.3). The term TP is the number of design problems which are correctly identified for each design pattern class, FP is the number of design problems which are incorrectly identified for each design pattern class, and FN is the number of design problems which are missed from each corresponding design pattern class. The values of P, R, and F are computed using Eqs. 4–6 respectively.

Usually, the performance of ranking models is evaluated through a comparison between their computed ranking lists (computed permutations) and the ranking list given on the ground truth. There are numerous widely used performance measures in the domain of Information Retrieval (IR). For example, Mean Average Precision (MAP), Kendall’s Tau, Discounted Cumulative Gain (DCG), and Normalized Discounted Cumulative Gain (NDCG). However, in this study, we used NDCG measure to evaluate the performance of the ranking function created through LambdaMART used in the proposed approach. The Normalized Discounted Cumulative Gain (NDCG) is an improved form of DCG, which can be computed through the Eq. 7.

$$NDCG(k) = G_{\max,i}^{-1}(k) \sum_{j:\pi_i(j) \leq k} G(j)D(\pi_i(j)) \quad (7)$$

Where  $G(\cdot)$  and  $D(\cdot)$  referred as gain function and position discount function of pattern  $DP_{i,j}$  in  $\pi_i$ . The summation is computed over the top  $k$  positions in the corresponding ranking list.

## 6 Evaluation Results

The proposed approach is evaluated according to the evaluation model described in the Sect. 5. In order to improve the homogeneity and completeness features, the most appropriate weighting method (in term of F-measure) has been used for the ranking algorithm LambdaMART used in the proposed approach. However, weighting method can be explicitly revealed. Though, we applied the proposed approach for 20 design problems related to the GoF and Douglass pattern collections. However, we give the detail analysis of only one problem given in Sect. 4.4. For this problem, the Composite, Decorator, Adaptor, and strategy are the candidate design patterns; however, the Composite design pattern should be more appropriate choice for a novice designer with respect to expert point of view. The performance of ranking algorithm used in the proposed approach depends on the creation of effective ranking list ranking with respective to relevance to the design problem. In terms of NDCG ranking metric criterion, the ranking of top 4 design patterns (Composite, Decorator, Adaptor and strategy) metric out of 23 design patterns indicate the effectiveness of the ranking of algorithms used in the proposed approach. We observed the average NDCG as 0.85 and 0.78 in case of GoF and Douglass design pattern collection respectively. These results suggest the applicability of the proposed approach.

## 7 Evaluation Results

In our study, we also find some threats. The first threat is related to a number of design pattern collection and design problem(s) which are considered during the evaluation process of our proposed approach. In order to evaluate the significance of results of proposed methodology, we will consider more design pattern collection (such as a security and Duynei's HCI design patterns group) and more examples of design problem(s).

The second threat is related to the incorporation of ranking algorithms. Our promising result based on the ranking function created through LambdaMART, we will consider more list-wise and pair-wise algorithm to improve the effectiveness of the proposed approach.

## 8 Conclusion and Future Work

In this paper, we proposed an approach using text categorization and exploit it through a supervised learning technique ‘Learning to Rank’. We incorporate LambdaMART, a widely used list-wise ranking algorithm in the proposed approach. Subsequently, we also propose an evaluation model in order to determine its effectiveness. We evaluate the proposed approach through GoF and Douglass pattern collections and relevant design problem(s). In terms of NDCG performance metric criterion, we observe the significant performance (NDCG = 0.85 in case of GoF and NDCG-0.78 in case of Douglass pattern collection) of the proposed approach. In the future, we will consider more list-wise, point-wise, and pair-wise ranking algorithm and design pattern collections to improve the effectiveness of the proposed approach.

**Acknowledgments.** This research is supported by the City University of Hong Kong research funds (Project No. 7004683, 7004474 and 7200354).

## References

1. Bass, L., Clements, P., Kazman, R.: *Software Architecture in Practice*, 3rd edn. Addison-Wesley Professional, Upper Saddle River (2012)
2. Wood, W.G.: A practical example of applying attribute-driven design (ADD), Version 2.0, Technical report, Software Engineering Institute (2007)
3. Gamma, E., Helm, R., Johnson, R., Vlissides, J.: *Design Patterns: Elements of Reusable Object-Oriented Software*. Addison-Wesley, Boston (1995)
4. Bouhours, C., Leblance, H., Percebois, C.: Spoiled patterns: how to extend the GoF. *Softw. Qual. J.* **23**, 661–694 (2015)
5. Booch, G.: *Handbook of Software Architecture* (2006). <http://handbookofsoftwarearchitecture.com/>
6. Baraki, H., Kurt, G., Voigtmann, C., Hoffman, A., Kniewel, R., Macek, B-E., Zirfas, J.: Interdisciplinary design patterns for socially aware computing. In: *Proceeding of 37th International Conference on Software Engineering (ICSE)* (2015)
7. Kim, D.K., Khawand, C.E.: An approach to precisely specifying the problem domain of design patterns. *J. Vis. Lang. Comput.* **18**, 560–591 (2007)
8. Hsueh, N.L., Lin, C.-C., Kuo, J.-Y.: Object-oriented design: a goal-driven and pattern-based approach. *J. Softw. Syst. Model.* **8**(1), 1–18 (2007)
9. Kim, D.K., Shen, W.: Evaluating pattern conformance of UML models: a divide and conquer approach and case studies. *Softw. Qual. J.* **16**(3), 329–359 (2008)
10. Hasso, S., Carlson, C.R.: A theoretically-based process for organizing design patterns. In: *Proceedings of 12th Pattern Language of Patterns* (2005)
11. Hotho, A., Nurnberger, A., Paab, G.: A brief survey of text mining. *J. Comput. Linguist. Lang. Technol.* **20**, 19–62 (2005)
12. Khoury, P.E., Mokhtari, A., Coquery, E., Hacid, M.S.: An ontological interface for software developers to select security patterns. In: *Proceedings of 19th International Conference on Database and Expert Systems Application, (DEXA 2008)*, pp. 297–301 (2008)
13. Hasheminejad, S.M.H., Jalili, S.: Design patterns selection: an automatic two-phase method. *J. Syst. Softw.* **85**, 408–424 (2012)

14. Hussain, S., Khan, A.A.K., Ebo, K.B.: A methodology to automate the selection of design patterns. In: Proceeding of 40th Annual Computer Software and Applications Conference (COMPSAC) (2016)
15. Hussain, S., Khan, A.A.K.: Software design patterns classification and selection using text categorization approach. *Appl. Soft Comput.* (2017). doi:[10.1016/j.asoc.2017.04.043](https://doi.org/10.1016/j.asoc.2017.04.043)
16. Uysal, A.K.: An improved global feature selection scheme for text classification. *Expert Syst. Appl.* **43**, 82–92 (2016)
17. Li, H.: A short introduction to ‘Learning to Rank’. *IEICE Trans. Inf. Syst.* **94**(10), 1854–1862 (2011)
18. Wu, Q., Burges, C.J.C., Svore, K.M., Gao, J.: Adapting boosting for information retrieval measures. ‘Learning to Rank’ for Information Retrieval, Microsoft Research (2009)
19. Porter, M.F.: An algorithm for Suffix Stripping. *J. Prog. Electron. Libr. Inf. Syst.* **40**, 211–218 (2006)
20. Huang, A.: Similarity measures for text document clustering. In: Proceedings of NZCSRSC (2008)
21. Douglass, B.P.: *Real-Time Design Patterns: Robust Scalable Architecture for Real-Time Systems*. Addison-Wesley/Longman Publishing Co. Inc., Boston (2002)
22. Silberschatz, A., Galvin, P.B., Gagne, G.: *Operating System Concepts*, 6th edn. Addison-Wesley, Reading (2002)
23. Shalloway, A., Trott, R.: *Design Pattern Explained: A new Perspective on Object Oriented Design*. Addison Wesley, Reading (2001)

# Real-Time Body Gestures Recognition Using Training Set Constrained Reduction

Fabrizio Milazzo<sup>(✉)</sup>, Vito Gentile, Antonio Gentile, and Salvatore Sorce

Ubiquitous Systems and Interfaces Group (USI),  
Università degli Studi di Palermo-Dipartimento dell'Innovazione Industriale e Digitale (DIID),  
Viale delle Scienze, Edificio 6, 90128 Palermo, Italy  
{fabrizio.milazzo, vito.gentile, antonio.gentile,  
salvatore.sorce}@unipa.it  
<http://usi.unipa.it>

**Abstract.** Gesture recognition is an emerging cross-discipline research field, which aims at interpreting human gestures and associating them to a well-defined meaning. It has been used as a mean for supporting human to machine interaction in several applications of robotics, artificial intelligence, and machine learning. In this paper, we propose a system able to recognize human body gestures which implements a constrained training set reduction technique. This allows the system for a real-time execution. The system has been tested on a publicly available dataset of 7,000 gestures, and experimental results have highlighted that at the cost of a little decrease in the maximum achievable recognition accuracy, the required time for recognition can be dramatically reduced.

**Keywords:** Gesture recognition · Real-time systems · Constrained optimization

## 1 Introduction

In the last decade, *Gesture recognition*, a new field of artificial intelligence has grown more and more. It aims to interpret human movements and to associate them to a specific meaning. Here, the term “movement” refers to the motion of either the whole or parts of human body [1].

Gesture recognition was born with the aim of improving human-machine interactions, by making it as simple and natural as possible. Indeed, there are many applications that may take advantage from gesture recognition, e.g.: *health monitoring* [2], *lie detection* [3], *automatic movie subtitling* [4], *online games* [5], *e-tutoring systems* [6], *emotion recognition* [7], *management systems for ambient intelligence* [8, 9] and so on.

Among the others, there are two typical issues that must be addressed in every gesture recognition application: *ensuring real-time processing* and *maximizing recognition accuracy*.

Real-time processing allows recognition of gestures in a negligible time interval; on the other hand, the recognition accuracy represents the probability that the gesture recognition algorithm will properly recognize a gesture.

The main contribution of this work is a novel system for body gesture recognition, which implements a technique based on training set constrained reduction. The key idea

is to reduce as much as possible the size of the training set used for recognition, by taking into account the two aforementioned issues.

The proposed system benefits of the *Dynamic Time Warping* [10] recognition technique, which makes the system independent of gestures length and size.

The rest of the paper is organized as follows: Sect. 2 deepens the discussion and state of the art in gesture recognition and some state of the art solutions; Sect. 3 describes the proposed system for gestures recognition; Sect. 4 highlights the experimental results obtained by using the system with an online available dataset of over 7000 gestures; finally, Sect. 5 describes the conclusions and some possible improvements of our proposal.

## 2 Related Works

In the last twenty years, gesture recognition has been the subject of several researches in the field of pattern recognition and has found many applications in robotics [11] and human-computer interaction [12]. Moreover, the availability of novel technologies has significantly contributed to the growing interest towards the development of gesture recognition algorithms.

While earlier works used RGB cameras as data source [13], the more recent Kinect-like devices (i.e. low-cost devices providing an integrated channel for RGB and depth data [14]) allow for more precise information about the observed gestures.

Indeed, Shotton et al. developed a robust algorithm for human pose estimation from single depth images [15], and thanks to their intuition, nowadays there exist many software libraries able to extract skeletal joints<sup>1</sup> from depth images of humans.

Using the aforementioned joints as basic features, it is possible to extract dynamic and static body gestures. According to Henze et al. [16], gestures are said to be static if they can be described by their position and spatial arrangement only; this class of gestures is also known as postures or poses [17], and they only need a single time frame to be entirely observed. In this work, instead, we will focus on the so-called dynamic gestures, i.e. a sequence of changing postures along a variable time interval.

Many authors have described methods for recognizing gestures by modeling them as temporal sequences of skeletal joints. In this context, two of the most suited and adopted mathematical tools are the Hidden Markov Models (HMMs) and the Dynamic Time Warping (DTW).

For instance, in [18] authors use an algorithm based on a Gaussian Mixture Hidden Markov Model, while in [19] Carmona and Climent have compared the performance of these two tools, showing that DTW is more suited for gesture recognition. Both HMM and DTW need a training stage devoted to learning a mathematical model used in a later stage to recognize new unseen sequences.

Despite the mathematical tool used for recognition, the more complex the learned model is, the more the computation needed for recognizing the sequences will be. To this aim, many algorithms have been recently developed for reducing the complexity of

---

<sup>1</sup> A joint is defined as the point of conjunction between two adjacent bones of the human skeleton.



the learned models. In particular, they belong to the so-called class of *training set reduction* algorithms.

As regards HMM-based solutions, the problem is usually faced up by using dimensionality reduction algorithms as the Principal Component Analysis (PCA) [20]. On the other hand, in DTW-based solutions, the reduction algorithms aims at reducing as much as possible the cardinality of the training set to very few and representative samples named prototypes (see for instance [21, 22]).

With the aim of providing a real-time system for gesture recognition, in this work we propose a system making use of DTW as a mathematical tool for comparing temporal joint sequences of variable length. This choice is in line with findings described in [19], i.e. DTW requires a lower number of training samples to achieve the same performance of HMM. Moreover, we developed a *training set constrained reduction* technique, which at the same time reduces the size of the training set and constrains the accuracy of the recognizer to be over a certain threshold.

### 3 System Description

The purpose of this Section is to describe our proposed system for body gestures recognition. We implemented a *real-time* system, with the aim of keeping as low as possible the computational burden of the recognition task, while maximizing its recognition accuracy.

To this end, we shifted the most of the computation in a learning method aimed at reducing the cardinality of the available training set and, as a consequence, the time complexity of the recognition.

First of all, we assume the availability of a training set named *LG*, made up of pairs in the form of  $\langle \text{Label}, \text{Gesture} \rangle$ .

The “label” component is a text representing the name of the gesture; as an example, a movement of the arm at eye’s height from right to left may be labeled as “Swipe Right To Left”.

As regards the definition of “gesture”, we choose to use the *joint* representation of the human skeleton, so we define a gesture  $G$  of length  $T$  as the sequence of the  $N$  joints coordinates over the time:

$$G = \begin{pmatrix} x_{1,1}y_{1,1}z_{1,1} \cdots x_{1,N}y_{1,N}z_{1,N} \\ x_{2,1}y_{2,2}z_{2,2} \cdots x_{2,N}y_{2,N}z_{2,N} \\ \vdots \\ x_{T,1}y_{T,1}z_{T,1} \cdots x_{T,N}y_{T,N}z_{T,N} \end{pmatrix} \quad (1)$$

In order to maintain the approach as generic as possible, we will make no assumptions about neither the duration nor the volume occupied by the training gestures. The proposed system is thus implemented by two modules:

1. **gesture recognition:** a new incoming gesture is matched to the most similar one in the reduced dataset, and the associated label is provided as output;

2. **training set reduction:** in order to provide real-time performance, here the input  $LG$  dataset is filtered in order to retain only the most representative gestures, named here as “prototypes”, to be used for the recognition task.

### 3.1 Gesture Recognition Module

The role of this module is to accept a new body gesture as a sequence of skeletal joints coordinates and to output a label representing the recognized gesture name.

With the aim of providing real-time performance, we implemented this module as a one-nearest neighbor classifier, which compares the incoming gesture to those in the training set, and returns the label of the nearest one. Mathematically speaking, this is carried out as follows:

$$G^* = \operatorname{argmin}_G \operatorname{Dist}(G^{new}, G), \forall G \in LG \quad (2)$$

where  $G^{new}$  is the gesture to be recognized,  $\operatorname{Dist}(\cdot, \cdot)$  is a distance metric, and  $G^*$  is the nearest gesture in  $LG$ . As a consequence, the recognized label  $L^*$  will be the label component of the  $\langle L^*, G^* \rangle$  pair contained in  $LG$ .

As regards the distance metric, we chose to use the *Dynamic Time Warping* one, which is able to compare gestures of different time length and spatial volume, by using simple insertion and deletion operations.

For reader’s commodity, in the following algorithm we report the steps needed to compute DTW between two gestures  $G^{new}$  and  $G$ :

<i>Algorithm DTW(<math>G^{new}</math>, <math>G</math>)</i>	
<b>Input:</b> $G^{new}$ as a $T_1 \times N \times 3$ matrix	<i>#gesture to be recognized</i>
<b>Input:</b> $G$ as a $T_2 \times N \times 3$ matrix	<i>#gesture in the train set</i>
<b>Output:</b> $x$ as a scalar	<i>#distance between gestures</i>
<ol style="list-style-type: none"> <li>1. <b>Declare</b> <math>DTW</math> as a <math>(T_1 + 1) \times (T_2 + 1)</math> matrix</li> <li>2. <b>for</b> <math>i=1</math> <b>to</b> <math>T_1</math> <b>do</b></li> <li style="padding-left: 20px;">2.1. <math>DTW[0, i] = \text{infinity}</math></li> <li>3. <b>for</b> <math>i=1</math> <b>to</b> <math>T_2</math> <b>do</b></li> <li style="padding-left: 20px;">3.1. <math>DTW[i, 0] = \text{infinity}</math></li> <li>4. <math>DTW[0, 0] = 0</math></li> <li>5. <b>for</b> <math>i=1</math> <b>to</b> <math>T_1</math> <b>do</b></li> <li style="padding-left: 20px;">5.1. <b>for</b> <math>j=1</math> <b>to</b> <math>T_2</math> <b>do</b></li> <li style="padding-left: 40px;">5.1.1. <math>d = L2norm(G^{new}[i], G[j])</math> <span style="float: right;"><i>#distance between frames</i></span></li> <li style="padding-left: 40px;">5.1.2. <math>DTW[i, j] = d + \min\{DTW[i-1, j], DTW[i, j-1], DTW[i-1, j-1]\}</math></li> <li>6. <b>Return</b> <math>x = DTW[T_1, T_2]</math></li> </ol>	

Clearly, the time required by the nearest neighbor classifier is linear with respect to the number of gestures composing the  $LG$  set. In order to allow for real-time recognition, it is important to keep the cardinality of such set as low as possible. This issue is thus be solved by the training set reduction module.

### 3.2 Training Set Reduction Module

The main purpose of this module is to reduce the size of the training set used by the recognizer. For this reason, it must be run *before* new gestures are recognized. In particular, it reduces the cardinality of the  $LG$  training set, as it has a direct influence onto the time complexity of the recognition module.

The idea is to extract only the relevant pairs  $\langle Label, Gesture \rangle$ , which can be seen as a sort of “prototypes” for the training set, and then use such prototypes instead of the whole training set to perform recognition.

The module induces a partition of the original training set  $LG$  by splitting it into two subsets, namely  $P$  (which contains the prototype gestures) and  $NP$  (containing non-prototype gestures), so that  $P \cup NP = LG$  and  $P \cap NP = \emptyset$ .

In order to evaluate how good an induced partition is, we can use the procedure described in Sect. 3.1. In particular, we can recognize the gestures contained in  $NP$  using  $P$  as the training set (instead of the whole  $LG$ ).

Moreover, we define the evaluation function  $M(P, NP) \rightarrow [0..1]$  as the accuracy of the recognition for the induced partition of  $LG$ .

Since the purpose of this module is to lower as much as possible the number of prototypes in  $P$  while keeping as high as possible the value of  $M(P, NP)$ , we apply a gradient descent to the following constrained optimization problem:

$$\begin{aligned} \max \quad & M(P, NP) \\ \min \quad & |P| \\ \theta \leq & M(P, NP) \end{aligned} \quad (3)$$

where  $\theta$  is a lower bound on the accuracy of the recognition in the training stage.

The initial condition is  $P = LG$   $NP = \Phi$ ,  $M(P, NP) = 1$ . Then, the module starts a loop composed of a variable number of rounds, iterated until the constraints are satisfied at equality. During each round, all the samples in  $P$  are removed (one at a time), put in  $NP$ , and labeled with the gradient of  $M$ , computed as follows:

$$\nabla M = M(P^-, NP^+) - M(P, NP) \quad (4)$$

where  $P^-$  and  $NP^+$  indicate the sets obtained by moving one sample gesture from  $P$  into  $NP$ . At the end of each round, gestures in  $P$  are sorted according to their gradients, and the one with the maximum value is definitively put in the  $NP$  set. The loop is iterated until  $M(P, NP)$  remains above the  $\theta$  threshold. In the end, the prototypes in the resulting dataset  $P$ , derived from  $LG$ , will be used for the recognition task. Figure 1 clarifies, with a visual example, the training set reduction flow.

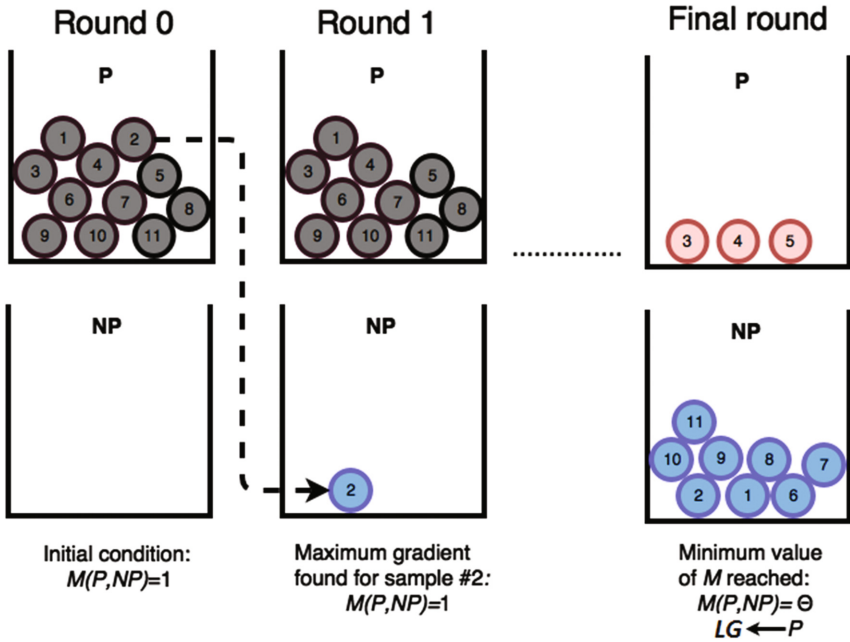


Fig. 1. Example flow of the training set reduction

### 4 Experimental Assessment

The recognition algorithm have been tested in a real deployment, by using the “Chalearn multimodal gesture recognition dataset” [23].

The dataset is made up of over 7000 samples containing each one: a RGB-D video, the gesture joints sequence and a textual label representing the name of the gesture.

The RGB-D videos were acquired by a Microsoft Kinect device, at the rate of 30 FPS, the skeleton data are described by 20 joints per frame, while the textual labels were manually added and represent 20 Italian cultural/anthropological signs, performed by 27 different users. Figure 2 depicts one sample data taken from the dataset.



Fig. 2. RGB, depth, skeletal and textual data of one sample from the dataset.

First of all, we built the  $LG$  dataset by extracting only the  $\langle Label, Gesture \rangle$  pairs from the samples contained in the Chalearn dataset.

We then implemented the modules described in Sects. 3.1 and 3.2 using the Python programming language, and deployed in a Raspberry Pi 3 device (4-core CPU at 1.2 GHz, running a 32-bit Raspbian distribution).

The raw dataset was sub-sampled by randomly choosing from 1000 to 7000 samples (with steps of 1000). Then, the resulting datasets have been divided into train and test by using the leave-1-out technique [24].

The baseline for our comparison is the recognition applied without using training set reduction. The other versions make use of the training set reduction module for three different values of the training accuracy thresholds  $\theta \in \{0.7, 0.8, 0.9\}$ .

Figure 3 depicts the results obtained for: (i) the latency required for recognizing one gesture, (ii) the accuracy of the recognition, and (iii) the number of prototypes retained from the original *LG* dataset.

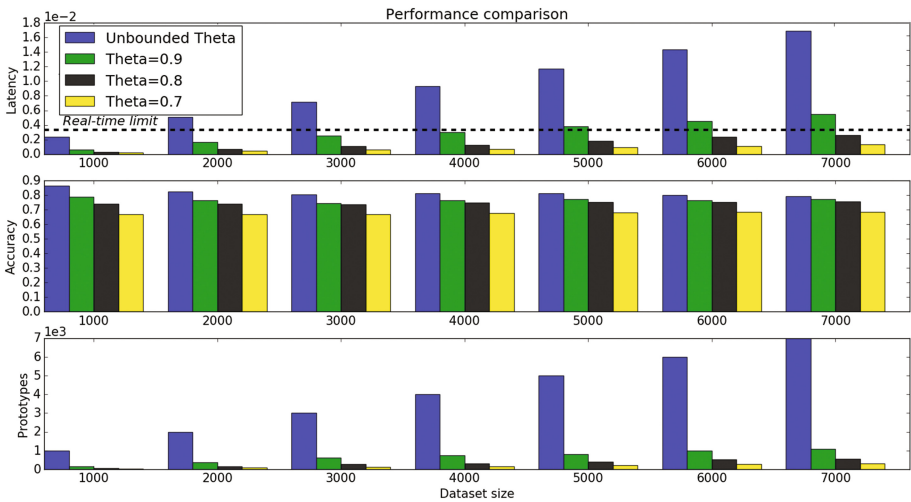


Fig. 3. Performance of the recognition module for different thresholds

The first row reports the latency required for recognizing one new incoming gesture. We set the maximum limit for real-time computation to 3.33 ms (i.e. the maximum available time for recognizing a gesture in a continuous stream of data at 30 FPS).

Unsurprisingly, the recognition module performs very fast for all the cases where training set reduction was applied, while the baseline is very far from real-time performance. We note also that when the training set size goes over 5000 samples, the case for  $\theta = 0.9$  is not real-time compliant.

The second row reports the accuracy of the recognition. The baseline case achieves very good performance with an average recognition accuracy of 0.81, and this is due to the use of the all available samples in the dataset. Anyway, in all the remaining cases, accuracy is only a little bit lower than baseline, ranging between 0.65 and 0.8.

The third row reports the number of retained prototypes, given a certain training accuracy threshold. Interestingly, the number of prototypes after training set reduction is a very small percentage of the whole dataset. It is also worth noting that such number

increases very slowly with respect to the dimensions of the dataset, and this positively affects the timing performance of the recognition module.

Such results highlight that running training set reduction is fundamental because at the cost of a little decrease in the maximum achievable accuracy, then the recognition module becomes 20×, 10× and 5× times faster than the baseline case for accuracy thresholds of 0.7, 0.8 and 0.9 respectively. Moreover, setting a threshold  $\theta = 0.8$  allows the system to achieve the best trade-off between recognition time (always below the real-time limit) and recognition accuracy (slightly less than the baseline case).

## 5 Conclusions

In this paper, we presented a novel approach to recognize body gestures in real-time by applying a training set constrained reduction technique.

Starting from a dataset of  $\langle \text{Label}, \text{Gesture} \rangle$  pairs, the training set reduction module selects the most representative gestures (prototypes) that will be used by the recognition module, implemented as a nearest-neighbor classifier based on Dynamic Time Warping.

We evaluated the performance of the recognition module by running it on a Raspberry Pi 3, using training sets of size ranging from 1000 to 7000 gestures. Moreover, the results highlighted the importance of the training set reduction module, which allows for real-time execution at the cost of a little decrease in the maximum achievable accuracy.

In a future work, we are planning to check performance (time complexity and accuracy) for more sophisticated classifiers, as well as testing the recognizer in-the-wild (i.e. including it in an actual deployment, and testing its performance against end users).

## References

1. Mitra, S., Acharya, T.: Gesture recognition: a survey. *IEEE Trans. Syst. Man Cybern. Part C (Appl. Rev.)* **37**(3), 311–324 (2007)
2. Starner, T., Auxier, J., Ashbrook, D., Gandy, M.: The gesture pendant: a self-illuminating, wearable, infrared computer vision system for home automation control and medical monitoring. In: *The Fourth International Symposium on Wearable Computers* (2000)
3. Davatzikos, C., Ruparel, K., Fan, Y., Shen, D., Acharyya, M., Loughhead, J., Gur, R., Langleben, D.D.: Classifying spatial patterns of brain activity with machine learning methods: application to lie detection. *Neuroimage* **28**(3), 663–668 (2005)
4. Park, S.-B., Yoo, E., Kim, H., Jo, G.-S.: Automatic emotion annotation of movie dialogue using WordNet (2011)
5. Kang, H., Lee, C.W., Jung, K.: Recognition-based gesture spotting in video games. *Pattern Recogn. Lett.* **25**(15), 1701–1714 (2004)
6. Picard, R.W., Picard, R.: *Affective computing*, vol. 252. MIT press, Cambridge (1997)
7. Gentile, V., Milazzo, F., Sorce, S., Gentile, A., Augello, A., Pilato, G.: Body gestures and spoken sentences: a novel approach for revealing user's emotions. In: *11th International Conference on Semantic Computing (ICSC 2017)* (2017)
8. De Paola, A., Lo Re, G., Milazzo, F., Ortolani, M.: Adaptable data models for scalable ambient intelligence scenarios. In: *International Conference on Information Networking (ICOIN)* (2011)

9. Daidone, E., Milazzo, F.: Short-term sensory data prediction in ambient intelligence scenarios. In: *Advances onto the Internet of Things*, pp. 89–103. Springer (2014)
10. Berndt, D.J., Clifford, J.: Using dynamic time warping to find patterns in time series. In: *KDD workshop*, vol. 10, pp. 359–370 (1994)
11. Malima, A.K., Özgür, E., Çetin, M.: A fast algorithm for vision-based hand gesture recognition for robot control. In: *IEEE 14th Signal Processing and Communications Applications*, Antalya, Turkey (2006)
12. Gentile, V., Malizia, A., Sorce, S., Gentile, A.: Designing touchless gestural interactions for public displays in-the-wild. In: Kurosu, M. (ed.) *Human-Computer Interaction: Interaction Technologies*, pp. 24–34. Springer International Publishing, (2015)
13. Wu, Y., Huang, T.S.: Vision-based gesture recognition: a review. In: *Gesture-Based Communication in Human-Computer Interaction*, vol. 1739, pp. 103–115 (2001)
14. Gentile, V., Sorce, S., Gentile, A.: Continuous hand openness detection using a Kinect-like device. In: *Eighth International Conference on Complex, Intelligent and Software Intensive Systems (CISIS)*, Birmingham, UK (2014)
15. Shotton, J., Sharp, T., Kipman, A., Fitzgibbon, A., Finocchio, M., Blake, A., Cook, M., Moore, R.: Real-time human pose recognition in parts from single depth images. In: *Proceedings of the 2011 IEEE Conference on Computer Vision and Pattern Recognition – CVPR 2011* (2011)
16. Henze, N., Löcken, A., Boll, S., Hesselmann, T., Pielot, M.: Free-hand gestures for music playback: deriving gestures with a user-centred process. In: *9th International Conference on Mobile and Ubiquitous Multimedia* (2010)
17. Sorce, S., Gentile, V., Gentile, A.: Real-time hand pose recognition based on a neural network using microsoft Kinect. In: *Eighth International Conference on Broadband and Wireless Computing, Communication and Applications (BWCCA)* (2013)
18. Song, Y., Gu, Y., Wang, P., Liu, Y., Li, A.: A Kinect based gesture recognition algorithm using GMM and HMM. In: *6th International Conference on Biomedical Engineering and Informatics* (2013)
19. Carmona, J.M., Climent, J.: A performance evaluation of HMM and DTW for gesture recognition. In: *17th Iberoamerican Congress (CIARP 2012)*, Buenos Aires, Argentina (2012)
20. Shum, H.P., Ho, E.S., Jiang, Y., Takagi, S.: Real-time posture reconstruction for microsoft Kinect. *IEEE Trans. Cybern.* **43**(5), 1357–1369 (2013)
21. Kasemtaweechok, C., Suwannik, W.: Training set reduction using Geometric Median. In: *15th International Symposium on Communications and Information Technologies (ISCIT)* (2015)
22. Sánchez, J.: High training set size reduction by space partitioning and prototype abstraction. *Pattern Recogn.* **37**(7), 1561–1564 (2004)
23. Escalera, S., González, J., Barò, X., Reyes, M., Lopes, O., Guyon, I., Athitsos, V., Escalante, H.: Multi-modal gesture recognition challenge 2013: Dataset and results. In: *Proceedings of the 15th ACM on International conference on multimodal interaction* (2013)
24. Kohavi, R.: A study of cross-validation and bootstrap for accuracy estimation and model selection. *Ijcai* **14**(2), 1137–1145 (1995)

# Towards Better Population Sizing for Differential Evolution Through Active Population Analysis with Complex Network

Adam Viktorin<sup>(✉)</sup>, Roman Senkerik, Michal Pluhacek,  
and Tomas Kadavy

Faculty of Applied Informatics, Tomas Bata University in Zlin,  
T.G. Masaryka 5555, 760 01 Zlin, Czech Republic  
{aviktorin, senkerik, pluhacek, kadavy}@fai.utb.cz

**Abstract.** This research paper presents an analysis of the population activity in Differential Evolution algorithm (DE) during the optimization process. A state-of-art DE variant – Success-History based Adaptive DE (SHADE) is used and the population activity is analyzed through Complex Network (CN) created from mutation, crossover and selection steps. The analysis is done on the CEC2015 benchmark set and possible future research directions for the population sizing are suggested.

## 1 Introduction

The Differential Evolution (DE) was created in 1995 by Storn and Price [1] and since then it has been one of the best performing tools for numerical optimization. The research community around DE has been active and proposed a plethora of changes to the original algorithm, which were aimed at improving the ability to find the global optima, scalability, and robustness. During the last few years, the Success-History based Adaptive DE (SHADE) algorithm [2] has been one of the most researched DE variants and, it or its improved versions [3–7] have performed very well in CEC single objective optimization competitions [8–10].

SHADE algorithm relies on the automatic adaptation of control parameters (scaling factor  $F$  and crossover rate  $CR$ ) and also on the “current-to- $p$ best/1” mutation strategy with an optional archive of inferior solutions  $A$ , which is inherited from the JADE algorithm [11]. An important common feature of improved SHADE algorithms [3–6] is the linear population size decrease presented in [3], which removes the worst individuals (in terms of objective function value) from the population linearly during the optimization run. In order to evaluate this approach, this paper presents a way to translate the population activity into the Complex Network (CN) as in [12], which is later analyzed. Three analysis metrics are proposed in this paper – active population percentage, generation intersection percentage and average Objective Function Value (OFV) percentage. These metrics are recorded during the optimization of the CEC2015 benchmark set functions [10] and the results are provided and commented. The motivation behind this analysis is to provide interesting future research directions for population sizing in DE based algorithms.

The structure of this paper is as follows: Next two sections describe DE and SHADE algorithms, the section that follows depicts the creation of the complex



network, Sect. 5 provides the experimental setting, Sect. 6 presents the results and their discussion and the whole paper is concluded in Sect. 7.

## 2 Differential Evolution

The DE algorithm is initialized with a random population of individuals  $\mathbf{P}$ , that represent solutions of the optimization problem. The population size  $NP$  is set by the user along with other control parameters – scaling factor  $F$  and crossover rate  $CR$ . In continuous optimization, each individual is composed of a vector  $\mathbf{x}$  of length  $D$ , which is a dimensionality (number of optimized attributes) of the problem, where each vector component represents a value of the corresponding attribute, and the individual also contains the objective function value  $f(\mathbf{x})$ . For each individual in a population, three mutually different individuals are selected for mutation of vectors and resulting mutated vector  $\mathbf{v}$  is combined with the original vector  $\mathbf{x}$  in crossover step. The objective function value  $f(\mathbf{u})$  of the resulting trial vector  $\mathbf{u}$  is evaluated and compared to that of the original individual. When the quality (objective function value) of the trial individual is better, it is placed into the next generation, otherwise, the original individual is placed there. This step is called selection. The process is repeated until the stopping criterion is met (e.g. the maximum number of objective function evaluations, the maximum number of generations, the low bound for diversity between objective function values in population).

### 2.1 Initialization

As aforementioned, the initial population  $\mathbf{P}$ , of size  $NP$ , of individuals is randomly generated. For this purpose, the individual vector  $\mathbf{x}_i$  components are generated by Random Number Generator (RNG) with uniform distribution from the range which is specified for the problem by *lower* and *upper* bounds (1).

$$\mathbf{x}_{j,i} = U[\text{lower}_j, \text{upper}_j] \text{ for } j = 1, \dots, D, \quad (1)$$

where  $i$  is the index of a current individual,  $j$  is the index of current attribute and  $D$  is the dimensionality of the problem.

In the initialization phase, the scaling factor value  $F$  and the crossover rate value  $CR$  has to be assigned as well. The typical range for  $F$  value is  $[0, 2]$  and for  $CR$ , it is  $[0, 1]$ .

### 2.2 Mutation

In the mutation step, three mutually different individuals  $\mathbf{x}_{r1}$ ,  $\mathbf{x}_{r2}$ ,  $\mathbf{x}_{r3}$  are randomly selected from a population and combined in mutation according to the mutation strategy. The original mutation strategy of canonical DE is “rand/1” and is depicted in (2).

$$\mathbf{v}_i = \mathbf{x}_{r1} + F(\mathbf{x}_{r2} - \mathbf{x}_{r3}), \quad (2)$$

where  $r1 \neq r2 \neq r3 \neq i$ ,  $F$  is the scaling factor value and  $\mathbf{v}_i$  is the resulting mutated vector.

### 2.3 Crossover

In the crossover step, mutated vector  $\mathbf{v}_i$  is combined with the original vector  $\mathbf{x}_i$  and they produce trial vector  $\mathbf{u}_i$ . The binomial crossover (3) is used in canonical DE.

$$u_{j,i} = \begin{cases} v_{j,i} & \text{if } U[0, 1] \leq CR \text{ or } j = j_{rand}, \\ x_{j,i} & \text{otherwise} \end{cases}, \quad (3)$$

where  $CR$  is the used crossover rate value and  $j_{rand}$  is an index of an attribute that has to be from the mutated vector  $\mathbf{v}_i$  (ensures generation of a vector with at least one new component).

### 2.4 Selection

The selection step ensures, that the optimization progress will lead to better solutions because it allows only individuals of better or at least equal objective function value to proceed into the next generation  $G + 1$  (4).

$$\mathbf{x}_{i,G+1} = \begin{cases} \mathbf{u}_{i,G} & \text{if } f(\mathbf{u}_{i,G}) \leq f(\mathbf{x}_{i,G}), \\ \mathbf{x}_{i,G} & \text{otherwise} \end{cases}, \quad (4)$$

where  $G$  is the index of the current generation.

The whole DE algorithm is depicted in pseudo-code below.

**Algorithm pseudo-code 1: DE**

Set  $NP$ ,  $CR$ ,  $F$  and stopping criterion;

$G = 0$ ,  $\mathbf{x}_{best} = \{\}$ ;

Randomly initialize (1) population  $\mathbf{P} = (\mathbf{x}_{1,G}, \dots, \mathbf{x}_{NP,G})$ ;

$\mathbf{P}_{new} = \{\}$ ,  $\mathbf{x}_{best} = \text{best from population } \mathbf{P}$ ;

**while** stopping criterion not met

**for**  $i = 1$  to  $NP$  **do**

$\mathbf{x}_{i,G} = \mathbf{P}[i]$ ;

$\mathbf{v}_{i,G}$  by mutation (2);

$\mathbf{u}_{i,G}$  by crossover (3);

**if**  $f(\mathbf{u}_{i,G}) < f(\mathbf{x}_{i,G})$  **then**

$\mathbf{x}_{i,G+1} = \mathbf{u}_{i,G}$ ;

**else**

$\mathbf{x}_{i,G+1} = \mathbf{x}_{i,G}$ ;

**end**

$\mathbf{x}_{i,G+1} \rightarrow \mathbf{P}_{new}$ ;

**end**

$\mathbf{P} = \mathbf{P}_{new}$ ,  $\mathbf{P}_{new} = \{\}$ ,  $\mathbf{x}_{best} = \text{best from population } \mathbf{P}$ ;

**end**

**return**  $\mathbf{x}_{best}$  as the best found solution

### 3 Success-History Based Adaptive Differential Evolution

In SHADE algorithm, the only control parameter that can be set by the user is the population size  $NP$ . Other two ( $F$ ,  $CR$ ) are adapted to the given optimization task, and a new parameter  $H$  is introduced, which determines the size of  $F$  and  $CR$  value memories. The initialization step of the SHADE is, therefore, similar to DE. Mutation, however, is completely different because of the used strategy “current-to- $p$ best/1” and the fact, that it uses different scaling factor value  $F_i$  for each individual. Crossover is still binomial, but similarly to the mutation and scaling factor values, crossover rate value  $CR_i$  is also different for each individual. The selection step is the same and therefore following sections describe only different aspects of initialization, mutation and crossover steps.

#### 3.1 Initialization

As aforementioned, initial population  $\mathbf{P}$  is randomly generated as in DE, but additional memories for  $F$  and  $CR$  values are initialized as well. Both memories have the same size  $H$  and are equally initialized. The memory for  $CR$  values is titled  $\mathbf{M}_{CR}$  and the memory for  $F$  is titled  $\mathbf{M}_F$ . Their initialization is depicted in (5).

$$M_{CR,i} = M_{F,i} = 0.5 \text{ for } i = 1, \dots, H. \quad (5)$$

Also, the external archive of inferior solutions  $\mathbf{A}$  is initialized. Since there are no solutions so far, it is initialized empty  $\mathbf{A} = \emptyset$  and its maximum size is set to  $NP$ .

#### 3.2 Mutation

Mutation strategy “current-to- $p$ best/1” was introduced in [11] and unlike “rand/1”, it combines four mutually different vectors, therefore  $pbest \neq r1 \neq r2 \neq i$  (6).

$$\mathbf{v}_i = \mathbf{x}_i + F_i(\mathbf{x}_{pbest} - \mathbf{x}_i) + F_i(\mathbf{x}_{r1} - \mathbf{x}_{r2}), \quad (6)$$

where  $\mathbf{x}_{pbest}$  is randomly selected from the best  $NP \times p$  best individuals in the current population. The  $p$  value is randomly generated for each mutation by RNG with uniform distribution from the range  $[p_{min}, 0.2]$  [2], where  $p_{min} = 2/NP$ . Vector  $\mathbf{x}_{r1}$  is randomly selected from the current population and vector  $\mathbf{x}_{r2}$  is randomly selected from the union of current population  $\mathbf{P}$  and archive  $\mathbf{A}$ . The scaling factor value  $F_i$  is given by (7).

$$F_i = C[M_{F,r}, 0.1], \quad (7)$$

where  $M_{F,r}$  is a randomly selected value (by index  $r$ ) from  $\mathbf{M}_F$  memory and  $C$  stands for Cauchy distribution. Therefore, the  $F_i$  value is generated from the Cauchy distribution with location parameter value  $M_{F,r}$  and scale parameter value 0.1. If the generated value  $F_i > 1$ , it is truncated to 1 and if it is  $F_i \leq 0$ , it is generated again by (7).

### 3.3 Crossover

Crossover is the same as in (3), but the  $CR$  value is changed to  $CR_i$ , which is generated separately for each individual (8). The value is generated from the Gaussian distribution with mean parameter value of  $M_{CR,r}$ , which is randomly selected (by the same index  $r$  as in mutation) from  $\mathbf{M}_{CR}$  memory and standard deviation value of 0.1.

$$CR_i = N[M_{CR,r}, 0.1]. \quad (8)$$

### 3.4 Historical Memory Updates

Historical memories  $\mathbf{M}_F$  and  $\mathbf{M}_{CR}$  are initialized according to (5), but their components change during the evolution. These memories serve to hold successful values of  $F$  and  $CR$  used in mutation and crossover steps. Successful in terms of producing trial individual better than the original individual. During one generation, these successful values are stored in corresponding arrays  $\mathbf{S}_F$  and  $\mathbf{S}_{CR}$ . After each generation, one cell of  $\mathbf{M}_F$  and  $\mathbf{M}_{CR}$  memories is updated. This cell is given by the index  $k$ , which is initialized to 1 and increases by 1 after each generation. When  $k$  overflows the size limit of memories  $H$ , it is reset to 1. The new value of  $k$ -th cell for  $\mathbf{M}_F$  is calculated by (9) and for  $\mathbf{M}_{CR}$  by (10).

$$M_{F,k} = \begin{cases} \text{mean}_{WL}(\mathbf{S}_F) & \text{if } \mathbf{S}_F \neq \emptyset \\ M_{F,k} & \text{otherwise} \end{cases}, \quad (9)$$

$$M_{CR,k} = \begin{cases} \text{mean}_{WA}(\mathbf{S}_{CR}) & \text{if } \mathbf{S}_{CR} \neq \emptyset \\ M_{CR,k} & \text{otherwise} \end{cases}, \quad (10)$$

where  $\text{mean}_{WL}()$  and  $\text{mean}_{WA}()$  are weighted Lehmer (11) and weighted arithmetic (12) means correspondingly.

$$\text{mean}_{WL}(\mathbf{S}_F) = \frac{\sum_{k=1}^{|\mathbf{S}_F|} w_k \cdot S_{F,k}^2}{\sum_{k=1}^{|\mathbf{S}_F|} w_k \cdot S_{F,k}}, \quad (11)$$

$$\text{mean}_{WA}(\mathbf{S}_{CR}) = \sum_{k=1}^{|\mathbf{S}_{CR}|} w_k \cdot S_{CR,k}, \quad (12)$$

where the weight vector  $\mathbf{w}$  is given by (13) and is based on the improvement in objective function value between trial and original individuals.

$$w_k = \frac{\text{abs}(f(\mathbf{u}_{k,G}) - f(\mathbf{x}_{k,G}))}{\sum_{m=1}^{|\mathbf{S}_{CR}|} \text{abs}(f(\mathbf{u}_{m,G}) - f(\mathbf{x}_{m,G}))}. \quad (13)$$

And since both arrays  $\mathbf{S}_F$  and  $\mathbf{S}_{CR}$  have the same size, it is arbitrary which size will be used for the upper boundary for  $m$  in (13). Complete SHADE algorithm is depicted in pseudo-code below.

**Algorithm pseudo-code 2: SHADE**

```

Set  $NP$ ,  $H$  and stopping criterion;
 $G = 0$ ,  $\mathbf{x}_{best} = \{\}$ ,  $k = 1$ ,  $p_{min} = 2/NP$ ,  $\mathbf{A} = \emptyset$ ;
Randomly initialize (1) population  $\mathbf{P} = (\mathbf{x}_{1,G}, \dots, \mathbf{x}_{NP,G})$ ;
Set  $\mathbf{M}_F$  and  $\mathbf{M}_{CR}$  according to (5);
 $\mathbf{P}_{new} = \{\}$ ,  $\mathbf{x}_{best} = \text{best from population } \mathbf{P}$ ;
while stopping criterion not met
   $\mathbf{S}_F = \emptyset$ ,  $\mathbf{S}_{CR} = \emptyset$ ;
  for  $i = 1$  to  $NP$  do
     $\mathbf{x}_{i,G} = \mathbf{P}[i]$ ;
     $r = U[1, H]$ ,  $p_i = U[p_{min}, 0.2]$ ;
    Set  $F_i$  by (7) and  $CR_i$  by (8);
     $\mathbf{v}_{i,G}$  by mutation (6);
     $\mathbf{u}_{i,G}$  by crossover (3);
    if  $f(\mathbf{u}_{i,G}) < f(\mathbf{x}_{i,G})$  then
       $\mathbf{x}_{i,G+1} = \mathbf{u}_{i,G}$ ;
       $\mathbf{x}_{i,G} \rightarrow \mathbf{A}$ ;
       $F_i \rightarrow \mathbf{S}_F$ ,  $CR_i \rightarrow \mathbf{S}_{CR}$ ;
    else
       $\mathbf{x}_{i,G+1} = \mathbf{x}_{i,G}$ ;
    end
    if  $|\mathbf{A}| > NP$  then randomly delete an ind. from  $\mathbf{A}$ ;
     $\mathbf{x}_{i,G+1} \rightarrow \mathbf{P}_{new}$ ;
  end
  if  $\mathbf{S}_F \neq \emptyset$  and  $\mathbf{S}_{CR} \neq \emptyset$  then
    Update  $\mathbf{M}_{F,k}$  (9) and  $\mathbf{M}_{CR,k}$  (10),  $k++$ ;
    if  $k > H$  then  $k = 1$ , end;
  end
   $\mathbf{P} = \mathbf{P}_{new}$ ,  $\mathbf{P}_{new} = \{\}$ ,  $\mathbf{x}_{best} = \text{best from population } \mathbf{P}$ ;
end
return  $\mathbf{x}_{best}$  as the best found solution

```

## 4 Network Creation

A new CN is created for each generation in the SHADE algorithm run, therefore the information about the population activity is temporal and held only for one generation. CN in this case is undirected and unweighted and consists of  $NP$  nodes, where  $NP$  is the population size (each individual is represented by one node). Edges between nodes are created according to the mutation, crossover and selection steps. If the trial individual  $\mathbf{u}_i$ , which was produced in mutation and crossover succeeds in selection (has better objective function value than the original individual  $\mathbf{x}_i$ ), edges between nodes corresponding to the individuals that helped to produce it ( $\mathbf{x}_{pbest}$ ,  $\mathbf{x}_{r1}$  and  $\mathbf{x}_{r2}$ ) and the

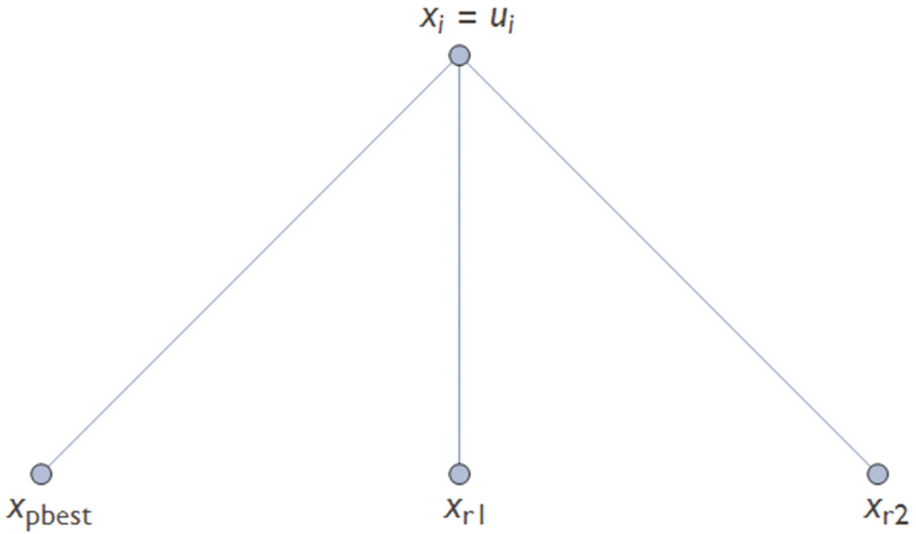


**Fig. 1.** The creation of the network edges after successful mutation.

node corresponding to the original individual  $x_i$  are created. This is depicted in Fig. 1. It is important to note that the nodes are connected to the individual ID, therefore the original individual  $x_i$  and the trial individual  $u_i$  share the same node. The same network creation was used in [12].

## 5 Experimental Setting

For the purpose of the experiment, three new metrics are introduced – active population percentage, generation intersection percentage, and average OFV percentage.

The active population percentage corresponds to the percentage of individuals that are active in one generation. The active individual is the one, that has at least one edge connected to it in the CN (its centrality degree is at least 1).

The generation intersection percentage corresponds to the overlap of the two successive active generations. If all active individuals in the generation are active in the next generation as well, the generation intersection percentage is 100%. This metric in combination with the active population percentage might provide the information about population size needed for the optimization of given problem.

The average OFV percentage corresponds to the average percentage of all active individuals in the generation according to their objective function value. The best individual in the population (not necessarily an active one) has OFV percentage of 100%, the worst one has 0%. This metric should show the advantage/disadvantage of the greedy approach to population decreasing.

These three metrics were recorded for the SHADE algorithm runs on the CEC2015 benchmark set in  $10D$  in accordance with the competition requirements – stopping criterion of  $10,000 \times D$  objective function evaluations and 51 independent runs on

each function. The SHADE algorithm was set as follows: Population size  $NP = 100$  and historical memory size  $H = 10$ .

## 6 Results and Discussion

The behavior of the previously mentioned metrics on the CEC2015 benchmark set functions was divided into three distinct categories.

The first category can be described as the typical behavior of metrics for fast converging functions and include test function 1, 2 and 15. Functions 1 and 2 are unimodal and can be easily solved by the SHADE algorithm. The test function 15 is a composite one, but most of the algorithms converge fast into the local optima of this function and stay there. Which is also SHADE's case. The average population percentage and generation intersection percentage are high and constant (around 80%) during the convergence and then drop to 0% when the convergence phase is over. The same goes for the average OFV percentage. An example of such behavior can be seen in Fig. 2, where the recorded values of all three metrics from 51 runs of test function 2 are averaged and plotted against the generation. The resulting metric history suggests that the linear decrease in population size would not make a difference, but a smaller population of 80 individuals might be sufficient for the problem.

The second category consists of two hybrid functions 10 and 11 and of one composite function 14. Where the interesting fact is that functions 10 and 14 are created from the same set of elemental functions (Schwefel's, Rastrigin's and High Conditioned Elliptic Function). The behavior of the metrics on these functions can be

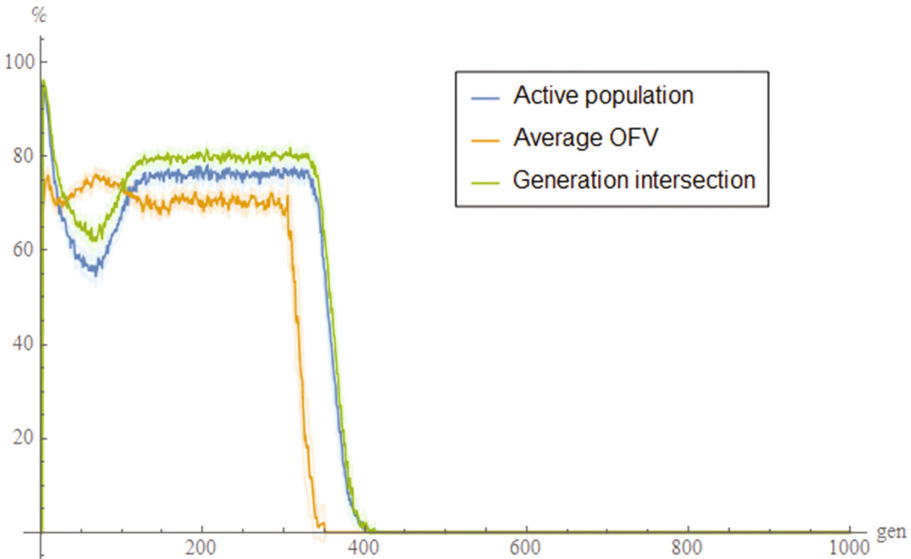


**Fig. 2.** The average history of three metrics on  $f_2$  from the CEC2015 benchmark set with 95% confidence interval in lighter colors.

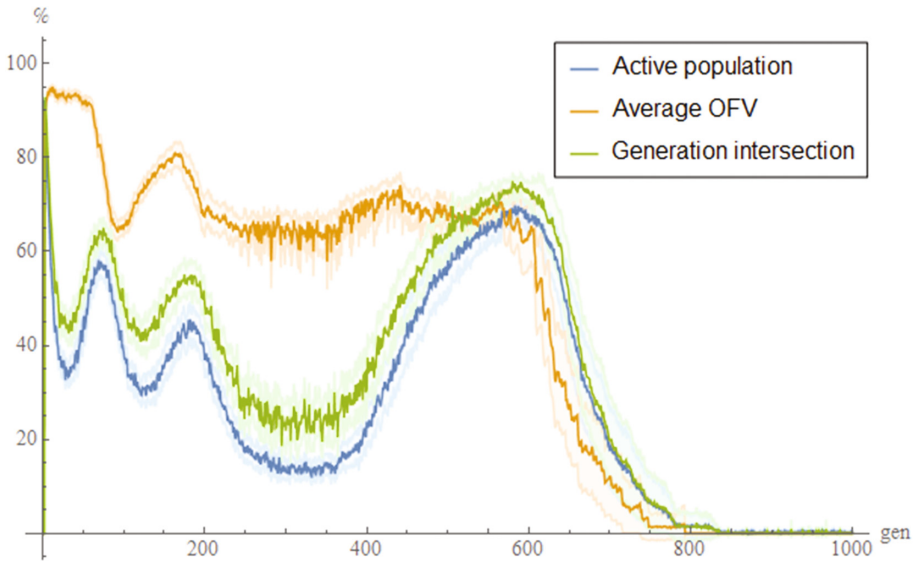


**Fig. 3.** The average history of three metrics on *f10* from the CEC2015 benchmark set with 95% confidence interval in lighter colors.

described as fluctuating. The active population and generation intersection metrics change rapidly over the generations and suggest, that an adaptive approach to the population sizing, in this case, might be more beneficial than a simple greedy linear decrease. An example of this behavior can be seen in Fig. 3, which depicts the average recorded values from 51 independent runs on function 10 from the benchmark set.

The third category contains the remaining test functions 3 to 9 (simple multimodal) and 12 (hybrid) and 13 (composition). The behavior of active population and generation intersection metrics is comparable for these functions. During the first two hundred generations, it decreases from  $\sim 100\%$  to  $\sim 20\%$  and, in most cases (except functions 6 and 8), stays like that for the remaining generations, while the average OFV is mostly quite high and constant (functions 3, 4, 5, 6, 7, 8 and 13) or slowly decreases (functions 9 and 12). The high average OFV percentage supports the advantage of the greedy linear decrease (better individuals stay active in the population) but low value of active population percentage suggests that the linear decrease might be using bigger population than is needed after the first two hundred generations. Also contrarily, the low value of generation intersection percentage shows, that the number of active individuals inter-generationally is higher than the number of active individuals in one generation (different individuals are active in successive generations), therefore an archive of individuals from previous generations might be beneficial along with fewer individuals actively mutated and evaluated in the real population. An example of this behavior can be seen in Fig. 4, which displays average metric history for 51 independent runs of the optimization of function 7.



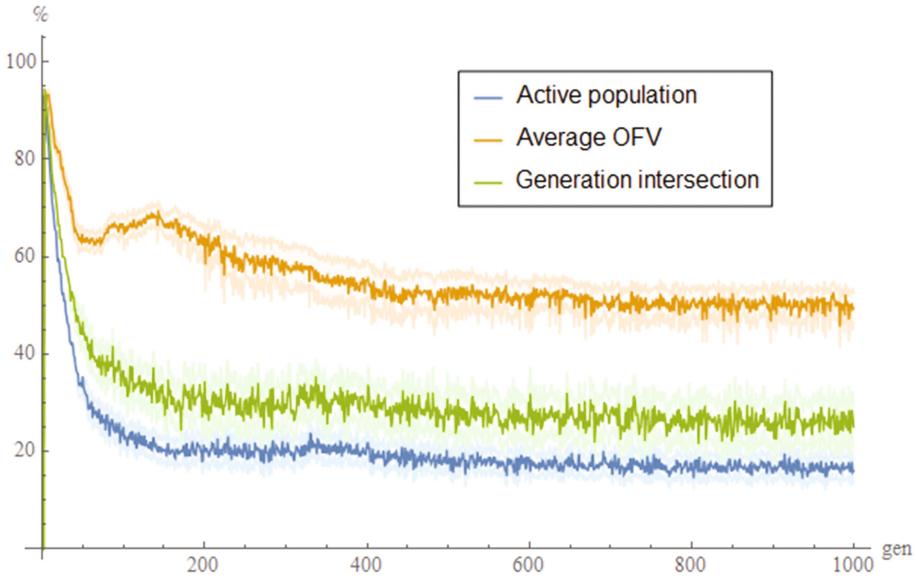


**Fig. 4.** The average history of three metrics on  $f7$  from the CEC2015 benchmark set with 95% confidence interval in lighter colors.

The future research direction might be in using weighted and directed CN and analyzing its interesting properties, such as local dependency [13], which would allow for more precise detection of active individuals.

Due to the page limitation of this submission, the graphs for each test function are not presented here, but were uploaded to the cloud along with the convergence graphs and can be downloaded from there: <https://owncloud.cesnet.cz/index.php/s/5n6Bg5sbY16ufBh>.

## 7 Conclusion

This paper presented an analysis of the SHADE population activity during the optimization of CEC2015 benchmark test functions. In order to do that, the CN was created for each generation of the algorithm and its features were analyzed. This analysis provided interesting future research directions for the population sizing in DE based algorithms and uncovered some weaknesses in the currently most popular linear decrease of the population size.

Findings from this paper will be used in the future research, which will be aimed at adaptive population size mechanism for SHADE algorithm based on the CN features.

**Acknowledgements.** This work was supported by Grant Agency of the Czech Republic – GACR P103/15/06700S, further by the Ministry of Education, Youth and Sports of the Czech Republic within the National Sustainability Programme Project no. LO1303 (MSMT-7778/2014). Also by the European Regional Development Fund under the Project CEBIA-Tech no. CZ.1.05/2.1.00/03.0089 and by Internal Grant Agency of Tomas Bata University under the Projects no. IGA/CebiaTech/2017/004.

## References

1. Storn, R., Price, K.: Differential Evolution - A Simple and Efficient Adaptive Scheme for Global Optimization Over Continuous Spaces, vol. 3. ICSI, Berkeley (1995)
2. Tanabe, R., Fukunaga, A.: Success-history based parameter adaptation for differential evolution. In: 2013 IEEE Congress on Evolutionary Computation (CEC), pp. 71–78. IEEE, June 2013
3. Tanabe, R., Fukunaga, A.S.: Improving the search performance of SHADE using linear population size reduction. In: 2014 IEEE Congress on Evolutionary Computation (CEC), pp. 1658–1665. IEEE, June 2014
4. Brest, J., Maučec, M.S., Bošković, B.: iL-SHADE: Improved L-SHADE algorithm for single objective real-parameter optimization. In: 2016 IEEE Congress on Evolutionary Computation (CEC), pp. 1188–1195. IEEE, July 2016
5. Poláková, R., Tvrđík, J., Bujok, P.: L-SHADE with competing strategies applied to CEC2015 learning-based test suite. In: 2016 IEEE Congress on Evolutionary Computation (CEC), pp. 4790–4796. IEEE, July 2016
6. Awad, N.H., Ali, M.Z., Suganthan, P.N., Reynolds, R.G.: An ensemble sinusoidal parameter adaptation incorporated with L-SHADE for solving CEC2014 benchmark problems. In: 2016 IEEE Congress on Evolutionary Computation (CEC), pp. 2958–2965. IEEE, July 2016
7. Viktorin, A., Pluhacek, M., Senkerik, R.: Success-history based adaptive differential evolution algorithm with multi-chaotic framework for parent selection performance on CEC2014 benchmark set. In: 2016 IEEE Congress on Evolutionary Computation (CEC), pp. 4797–4803. IEEE, July 2016
8. Liang, J.J., Qu, B.Y., Suganthan, P.N., Hernández-Díaz, A.G.: Problem definitions and evaluation criteria for the CEC 2013 special session on real-parameter optimization. Technical report 201212, Computational Intelligence Laboratory, Zhengzhou University, Zhengzhou, China and Nanyang Technological University, Singapore (2013)
9. Liang, J.J., Qu, B.Y., Suganthan, P.N.: Problem definitions and evaluation criteria for the CEC 2014 special session and competition on single objective real-parameter numerical optimization. Zhengzhou China and technical report, Computational Intelligence Laboratory, Zhengzhou University, Nanyang Technological University, Singapore (2013)
10. Liang, J.J., Qu, B.Y., Suganthan, P.N., Chen, Q.: Problem definitions and evaluation criteria for the CEC 2015 competition on learning-based real-parameter single objective optimization. Technical report 201411A, Computational Intelligence Laboratory, Zhengzhou University. Zhengzhou China and technical report, Nanyang Technological University, Singapore (2014)
11. Zhang, J., Sanderson, A.C.: JADE: adaptive differential evolution with optional external archive. *IEEE Trans. Evol. Comput.* **13**(5), 945–958 (2009)
12. Viktorin, A., Pluhacek, M., Senkerik, R.: Network based linear population size reduction in SHADE. In: 2016 International Conference on Intelligent Networking and Collaborative Systems (INCoS), pp. 86–93. IEEE, September 2016
13. Kudělka, M., Zehnalová, Š., Horák, Z., Krömer, P., Snášel, V.: Local dependency in networks. *Int. J. Appl. Math. Comput. Sci.* **25**(2), 281–293 (2015)

# WORDY: A Semi-automatic Methodology Aimed at the Creation of Neologisms Based on a Semantic Network and Blending Devices

Daniele Schicchi<sup>1</sup> and Giovanni Pilato<sup>2</sup>(✉)

<sup>1</sup> Scuola della Scienze di Base e Applicate, University of Palermo,  
Via Archirafi, 28, 90123 Palermo, Italy  
[daniele.schicchi@community.unipa.it](mailto:daniele.schicchi@community.unipa.it)

<sup>2</sup> ICAR - CNR, Italian National Research Council,  
Via U. la Malfa 153, 90146 Palermo, Italy  
[giovanni.pilato@cnr.it](mailto:giovanni.pilato@cnr.it)

**Abstract.** In this paper, we propose a semi-automatic tool, named WORDY, that implements a methodology aimed at speeding-up the process of creation of neologisms. The approach exploits a semantic network, which is explored through the spreading activation methodology and exploits three blending linguistic techniques together with a proper ranking function in order to support companies in the creation of neologisms capable of evoking semantic meaningful associations to customers.

**Keywords:** Creativity · Neologisms · Semantic networks · Blending

## 1 Introduction

The choice of a creative name is a fundamental ingredient to well represent the product or the service that a company wants to promote. A good decision of the name increases the possibility of a successful business because it provides the first image of the product and it defines its identity, being able to communicate the features of the product by evoking semantic associations. The creation of such a name is a challenging and time consuming activity; furthermore, it requires a good knowledge of the product, together with creativity and high linguistic skills. Because of these difficulties, the development of a software that is able to create catchy and meaningful name is hard, and the current automatic generators are based on straightforward combination of random words without the use of semantic meaning.

The field of computational creativity is perhaps the last frontier of Artificial Intelligence and it covers different aspects of cognitive computing [1, 5], and it can help in tackling such a task. The problem of the automatic creation of neologisms has been faced by many authors [12, 16], in particular two recent systems, named Nehova [15] and BrainGene [14] are worth to be mentioned. They have the capability of creating new words on the basis of creativity concepts. Their idea is to convey multiple concepts in a single plausible word, known as *portmanteau*.

Nehova uses two source words provided by the user and in three steps it is able to create catchy neologisms. It makes use of WordNet [9] and TheTopTens [17] to create two sets named “concept set”, then prefixes and suffixes are extracted from the words of concept sets and, with regard to syllables, they are blended by simply concatenating them. The BrainGene’s structure is similar to the Nehova structure with some important differences. BrainGene receives as input some information from the user such as a short description or a list of words that set the topic and then uses them to find a set of priming words. Two matrices that contain statistical information on n-grams are computed combined, while a filtering process selects the “novel” word.

In this paper we present a methodology and an implementation of an intelligent system based on a semantic network and a set of linguistic devices aimed at making it possible to create meaningful and catchy neologisms. More in detail, the presented system, which “gave itself” the name of “WORDY”, uses both semantic networks to represent cognitive process and the “blending” [13] linguistic device that allow, respectively, to retrieve words that are related each other and to create the final artifacts. The use of the bio-inspired spreading activation methodology [4] allows to find unusual logical routes between words in the semantic network. The results proposed by the tool described in this paper are the outcome of a thorough research of terms that can well represent the product object of an advertising campaign combined with the application of a proper linguistic device, making it possible to create catchy words. The system requires some input data from the user, such as the main object, the object’s properties that the user wants to emphasize and some parameters allowing to obtain a wide range of candidates. A scoring procedure allows to rank the novel words and to propose a selection of them to the users.

The remaining part of the paper is structured as follows: in Sect. 2 we illustrate the proposed methodology by describing in detail how the system selects the words to combine, how the blending device is implemented and the ranking procedure of the candidate neologisms; in Sect. 3 we describe the tests and we give the first impressions about the behaviour of the tool; in Sect. 5 we give the final notes and future works.

## 2 WORDY System Description

The basic idea of WORDY is to blend words in a creative manner in order to create catchy, meaningful neologisms. In order to reach this goal, three main problems have to be tackled: how to choose the words to be blended, how to realize an effective blending and how to rank the created words. The three phases are depicted in Fig. 1.

### 2.1 Selection of Words

We think that the choice of appropriate words is a fundamental task to the creation of meaningful, catchy and novel names. For this task we use semantic

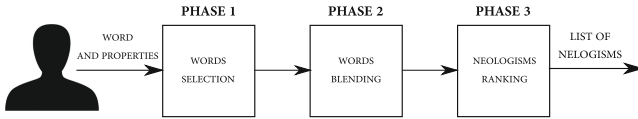


**Fig. 1.** WORDY tool structure and data flow.

networks that allows the system to efficiently chose the words to blend. A semantic network is a graph that represents semantic relations between concepts and makes it possible to emulate cognitive processes [3]. In this case, each node of our network is a word that is connected with other words through edges, which represent semantic relations. We have used an existing semantic network [6] with 9000 manually annotated relations between 4000 mundane concepts; then we have added further relations taken from ConceptNet 5 [10] and deleted the multiwords nodes. ConceptNet is a semantic network containing common sense, cultural and scientific knowledge. Each node of ConceptNet is a word or a short phrase that is connected with some other node through common relations such as: *is part of*, *is locate to*, *is a*, and so on.

At the end of the process, our semantic network contains a single word for each node and about 15000 relations among them. Details about the semantic network are shown in Table 1. We use the bio-inspired spreading activation technique [4] to get a list of words that are connected in the same way that a person, consciously or unconsciously, would do. A person represents the knowledge through a network and tends to associate concepts on the basis of common logical route. Following the common routes does not allow the association of concepts in a creative way and for this reason we need a method that finds new meaningful routes. The spreading activation [7] is a method that makes it possible to emulate the cognitive process for the association of concepts allowing to emphasize unusual logical routes and find words that are related in an unusual way.

**Table 1.** Details about the WORDY’s semantic network. Relation - Number of Edges for relation.

Relation	N. of edges	Relation	N. of edges	Relation	N. of edges
is a	1703	is opposite of	150	used for	5090
is part of	843	desires	680	capable of	1749
is same as	168	is related to	1901	created by	410
is property of	2369	is effect of	160		

According to the technique proposed in Ozabal and Strapparava [12] we allow the user to choose a word that is representative for his business and possibly some other words representing properties that he wants to emphasize. For example, if the user is a chocolate vendor he could insert *cacao* as the main word and *healthy, tasty, sweet* as properties that he wants to emphasize.

The system proposes to the user other properties that are related with the main object not only through *is-property-of* relation but using the spreading activation. From the main word the nodes that are reached by the spreading activation are selected and among these the system chooses words that are *properties*. To check whether a word is a property, the system checks if the candidate word is connected with other words through *is-property-of* relation and it is in the first side of relation. Finally, the words are proposed to the user by ordering them according to their “betweenness centrality” and the user can select some of them. We recall that betweenness centrality of a vertex  $\mathbf{V}$  is a measure of centrality in a graph based on shortest paths between two nodes and represents the number of shortest paths that pass through  $\mathbf{V}$ . Qualitatively, it represents how much a node interacts with others.

The system, for every single property  $\mathbf{P}$ , looks for words that are connected with  $\mathbf{P}$  through *is-property-of* relation and from these it applies the spreading activation. Therefore, the tool collects both words that have exactly the property  $\mathbf{P}$  and words that are strictly related with  $\mathbf{P}$ . The first five words that are retrieved are ordered by centrality and they are proposed to the user who can choose whether to keep all of them or delete some of them.

This way, the system finds out words that are strongly related both with the main concept and with properties specified. The use of these words allows to recall in the listener the meaning of properties by using priming effect and triggering creativity. The priming is an effect proper of the human beings and consists in the automatic association of concepts close to the concept that has been proposed to the listener. For example, if the concept was *lion* the person would think not only to the *animal* but also to concepts close the *lion* concept such as: *strength*, *savannah*, *ferocity* and so on.

Using the priming effect, the system has collected words which represent the properties that have been specified by the user and that are related with the main concept. They can therefore be blended.

In our system the user can choose in addition to the words to be blended the depth of spreading activation. A deeper spreading activation might find words that are related in some interesting way or words that are not, conversely a shallow spreading activation would find word that are related in a trivial way.

Not all the words retrieved are blended together but only some of them. In Ekaterine Keke Bakaradz work [2] she examines the morphology of the words that form the blending words and finds out that some pattern like **noun + noun** are more common than others like **adjective + adverb**. For this reason the system allows the user to choose a parameter  $\mathbf{k}$  that corresponds to first  $\mathbf{k}$  common patterns. The default value of  $\mathbf{k}$  is 3 that corresponds to **noun + noun**, **verb + verb**, **adjective + adjective** patterns. A complete list of patterns is shown in Table 2.

Finally, the words are blended according with patterns using a linguistic device.

**Table 2.** Common patterns.

Position	Pattern
1	<b>noun + noun</b>
2	<b>verb + verb</b>
3	<b>adjective + adjective</b>
4	<b>verb + noun</b>
5	<b>noun + verb</b>
6	<b>adjective + adverb</b>
7	<b>adjective + noun</b>

## 2.2 Blending Words

In Ozbal et al. paper [13] linguistic devices, that are the bases of 1000 brands names, have been explored. For our purpose we have focused our attention on **blending**. This linguistic device consists of forming a word from two or more distinct words through blending their sounds and their meanings.

There exist many type of blending based on how the words are combined. We have exploited three type of combinations.

**Blending 1.** This type of blending combines two words to create neologism that is the concatenation of the prefixes of both words. For example, words **biography** and **picture** can be concatenated using prefixes for the creation of the **biopic** neologism.

Our implementation of this type of blending takes into account the choice of prefixes that represent the word better than others.

The choice of the prefix has been done using the recognition point concept [8]. Recognition point of a word **W** is a point that identifies a part **T** of **W** for which a majority of speakers (e.g. 80%) can recognize **W** from **T**. For example, the recognition point of **mexico** word could be **mex**.

We have decided to use dictionary method to find recognition point through SUBTLEX [11] corpus. It is a corpus that contains 600.000 subtitles of films in the English language. Subtitles are formed by a variety of words that represent different social contexts.

In details, for every prefix **X** of the word **W** we evaluate a list formed by all words that starts with **X**. The list is ordered in descending way based on words frequencies. Finally, we identify position of **W** among the listed words and if it is less than  $\eta$  the prefix is selected.  $\eta$  is a natural number that can be set and it avoids to choose prefix unrepresentative. An example is shown in Fig. 2. If the user chooses a low value of  $\eta$  (e.g.  $\eta \leq 10$ ), the obtained prefix recalls to the listener the word in question because it is more common than others in the list. However setting set  $\eta$  to 1 generates long prefixes that are not very useful for the task of the system of the software because they generate long neologism that usually are not interesting. For this reason we have set  $\eta$  to 10. This value has

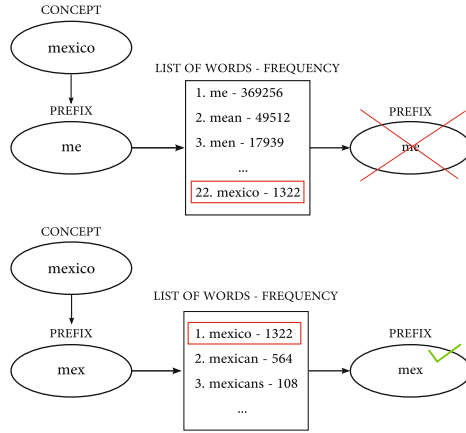


**Fig. 2.** Top: the prefix “me” is not representative because the word “mexico” is at the 22<sup>o</sup> position ( $\geq \eta$ ); Bottom: the prefix “mex” is representative because the word “mexico” is at the 1<sup>o</sup> position ( $\leq \eta$ ).  $\eta = 10$

been obtained by empirical tests and it allows obtaining prefixes which are both short and representative.

WORDY proposes both neologisms and existent words created, because the latter could be creative in an domain context and therefore useful to the representation of the product. Finally, the system concatenates all chosen prefixes of both words.

**Blending 2.** This type of blending combines two words to create neologism that is the concatenation of the prefixes of a first word and suffix of a second word. For example, the words **lion** and **tiger** can be concatenated by using prefixes and suffixes for the creation of **liger** neologism.

For this type of blending we find best prefixes for the first word in the same way of Blending 1. To find best suffixes of second word we readapt the technique for prefixes of Blending 1 to suffixes. In details, for every suffix **S** of the word **W** we evaluate a list formed by all words that ends with **S**. The list is ordered in descending way based on words frequencies. Finally, we identify position of **W** among the listed words and if it is less than  $\eta$  the suffix is selected.

The recognition point can be used also for suffixes. The chosen suffix using recognition point is representative of the word and it allow to the listener to recall the original word from **S**. The concatenation is done in the same way of Blending 1.

**Blending 3.** This type of blending uses the overlapping of the two words to be blended. Blending 3 creates neologism that are formed by the first part of the first word and the last part of the second word. A common neologism obtained



from blending 3 has got a structure like: **first part of first word + overlap between words + last part of second word**; The + sign stands for the concatenation operation. For example, words **drama** and **comedy** can be concatenated using the overlap of the two words for the creation of **dramedy** (*dra+m+edy*) neologism.

To find the maximum overlap between words we have used the well known Longest Common Substring (LCS) algorithm based on dynamic programming. We examine the output matrix of LCS and a relevant maximum value cannot be in the first row or in the last column of the matrix because the neologism must contain at least a letter of both words in addition to the overlap. If the maximum value is not valid the system tries to search another maximum and if there are more than one relevant maximum value the system considers all of them, getting more blended words as results.

Let  $i$  and  $j$  respectively be row index and column index of the matrix, an alternative maximum cannot be contained in the succession  $(i, j)(i + 1, j + 1) \dots (i + 2, j + 2)(i + k, j + k)$  which ends in the last column because in this case when the system concatenates the last part of the second word it would get the same result as in the case of choosing the maximum value in the last column. For example, the words **meaning** and **willing** have got a substring of length 3 that cannot be accepted as maximum value because it is in the last column. An alternative maximum cannot be 2 that is in the succession that ends in the last column. If we choose 2 as maximum we will obtain the source word **willing**. The good maximums are 1 that are not in the succession as shown in Fig. 3.

An index to evaluate the quality of the neologism can be the length of the overlap between the two words. A long overlap recall both source words and for the listener will be more easy recall the words and their meaning. The importance of the overlap raises questions like “*How the overlap affects the quality of the neologism?*” or “*Is the overlap a good index to measure the quality of the neologism?*” that are waiting to find answers.

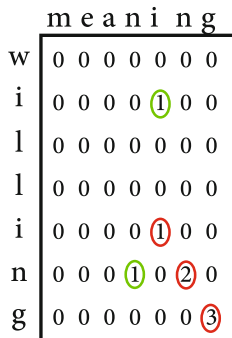


**Fig. 3.** Matrix obtained from LCS algorithm. Good maximum value are circled in green. Bad maximum value are circled in red.

### 2.3 Ranking Neologisms

Among all the words that have been created we need a methodology to distinguish if a word could be catchy or not. Checking if a word is catchy is not a trivial problem and in the state of art, to the best of our knowledge, does not exist an univocal and infallible algorithm that identifies if a word is catchy or creative. For this reason, we have chosen to rank the words in three manners created ad hoc.

In the first way, that can be used only for Blending 3, the system proposes to the user a list of words ordered by the length of overlap. Although it is not clear how much the overlap is a good choice as index we think that a long overlap well represents both source words.

The second way, that can be used for all blending types, is based on the well known Levenshtein distance. The idea is that if a neologism is “near” to a very common English word this will be more familiar for the listener but not trivial because it carries a new meaning. For our test we have gathered from SUBTLEX the 25% of the most common words. The system calculates the distance between the neologisms and the chosen words ordering them by Levenshtein distance in ascending way.

The third way can be used for Blending 1 and Blending 2 and considers the conjunction strings of the candidate prefixes for the concatenation. In details, let  $X_1$  and  $X_2$  be prefixes (or prefix and suffix) that have to be concatenated, we evaluate the concatenation of last  $n$  letters of  $X_1$  and first  $n$  letters of  $X_2$  and we check its frequency among English words. The idea is that if the frequency is high the listener is accustomed to listen that combination of characters which reflects the idea of catchiness and allow to create a good coupling between the parts. This way, the system is able to obtain an order among all candidate neologisms based on the frequencies of the conjunction strings allowing to consider only the catchy words. The tests have been done setting  $n$  to 2 and 4.

## 3 Experimental Results

In this section we want to express the first impressions about the behaviour of the software. We are aware that the tests are not comprehensive but they give the impression that the system can be useful to the creation of creative name.

Evaluation of the system is not a trivial problem because does not exist an algorithm to check if a neologism is creative or meaningful. To face this problem is necessary the collaboration of linguists that can evaluate the quality of created neologisms. Nevertheless, we have done tests obtaining interesting results. Each test has been done using a depth of spreading activation equal to 2.

The first test aims at understanding how the tool could be useful to the creation of a product’s name so we have decided to use the software for the creation of its own name. Indeed, the software’s name “WORDY” has been proposed by the software itself.

We wanted a catchy name that emphasized some property of the software such as the creativity that exhibit the software for the creation of words and

the similarity between the software and an artist that works on words. We have chosen **word** as the main concept and **creative** and **artistic** as properties that we wanted to emphasize. The software has retrieved some other properties such as **articulate**, **fluent** and **clear** that are related to the main concept and it allows us to decide if add some of them. From these we have chosen to add **fluent** property. Then we have chosen **art**, **artist**, **creativity**, **syllable**, **computer** as terms that are related to these properties usable to obtain final results.

The software has proposed very catchy artefacts such us: **wordart** (word + artist), **artword** (artist + word), **syllart** (syllable + artist), **artivity** (artist + creativity), **creatist** (creativity + artist), **arty** (artist + creativity), **wordy** (word + creativity) and **creater** (creativity + computer) that represent well the features of the software.

Both **arty** and **wordy** are not neologisms but in this context they represent a different meaning that is useful to the representation of the software. Finally, we selected **WORDY** because it is a very catchy name and it well represents the mission of the software, creates words with creativity. The parameters that have been used to the creation of WORDY's name are shown in Table 3.

**Table 3.** Parameters used to the creation of WORDY's name

Parameter	Value
Main concept	word
Properties	creativity, artistic, fluent
Chosen words	artist, creativity, syllable, computer
Spreading activation depth	2
Recognition point ( $\eta$ )	10
Number of pattern (k)	3
Freq. conjunction string (n)	4

Obviously, not all the words created by WORDY are catchy and some results such as: **woreativity** (word + creativity), **syllableartist** (syllable + artist), **creativertistic** (creative + artistic) are far from being catchy.

To choose the tool's name, we have examined the results one by one since the number of results was limited but we are aware that examine a long list of names could have been time consuming. For this reason, we have done some test about our ranking methodology.

A first impression about the use of the overlap as quality index is that a long overlap represents well both source words. From empirical tests, it seems that results that come from a long overlap are catchier. For example, **womance** (woman + romance) and **pungenta** (pungent + magenta) have overlap of length 4 and it's clear that they are catchy. Conversely, neologism that have overlap of length 1 such as **oniomato** (onion + tomato), **feminined** (feminine + red), **chocolateet** (chocolate + sweet) seems less catchy.

The ranking based on the Levenshtein distance seems to be useful mainly for catchiness and less for meaningful property. Indeed, a neologism with a low distance from a common English word usually has a nice sound but, since the similarity with a common word, the neologism remembers that word that could have a different meaning. For example, **swear** (sweet + heart) has a 1 distance from **swear**, the neologism result is catchy but it remembers a **swear** word that represents a totally different meaning. A solution could be calculating the Levenshtein distance from a strict corpus of words that regard the domain of application. Nevertheless, it seems that words which have a big distance from common words show details that identify a low catchiness, the big distance suggests some oddities in the neologism. For example, **pungenthusiastic** (pungent + enthusiastic) has a distance 9 from fantastic and it is very far from a catchy word.

The use of the frequencies of conjunction string (see Sect. 2.3) to identify a catchier neologism seems to be effective and it deserves more thorough testing. The first tests show that the neologisms with high conjunction point frequency have got a better sound. The low frequencies of conjunction point reflect the presence of a substring of the neologism which is hardly pronounceable and not very catchy. For instance, **hearchoc** (heart + chocolate) has a conjunction substring **arch** with high frequency and it can be seen that the prefix **hear** and the prefix **choc** are nice coupled. Conversely, **animawweet** (animal + sweet) has got a conjunction substring **mawe** with frequency of 1 and its sound is unattractive.

To understand how the created blending function works, these have been applied to a dataset of existent portmanteau words. The dataset was created ad hoc and it contains 100 words that belong to different categories such as animal, transport, marketing. For each word of the dataset are associated a couple of words that generate it through a blending device. For instance, *liger* will be associated with *lion* and *tiger*.

The three Blending procedures have been applied to each entry of the dataset and then we have checked if among the results there was the portmanteau word contained in the dataset. The results have showed that on the 100 words 69 have been created correctly. Nevertheless the few entries of the dataset, this first test is very encouraging and it makes us confident for the next tests.

## 4 Discussion

The tests show that not only the software allows the user to obtain creative names but it helps users in triggering inspiration by evaluating the software outcomes. Indeed, for example, if during the creation process of WORDY's name the system had proposed only **arty** name, a creative person would have easily created **wordy** by substituting **art** with **word**. This scenario recalls and somehow emulates what happens during the creation process within a creativity group in which the exchange of ideas and the obtained results allow creating new artefacts. For this reason the WORDY's creative properties make it a tool that can be used like a member of a team to collaborate towards the creation of creative names.

The main problem is to find a strategy to understand what are the key features of creative names in order to implement an algorithm that could propose to the user only the most catchy names. The ranking methodologies seem to be useful but they need to be refined and thoroughly tested. Conversely, the Blending implementation seems to work well succeeding to reproduce the 69% of the words contained in the dataset.

Although it could seem at first sight that WORDY is similar to past systems like Nehova or BrainGene, we emphasize some important differences that make it innovative. The main characteristic is that at the base of WORDY there is a semantic network that allows the system to have knowledge about the world and to emulate the cognitive processes of the human beings. The creativity can be interpreted as the capability of looking at the world from a different perspective that, in this context, means to create neologism by associating words in unusual way, triggering also creativity in the listener. The step of selection words in the Nehova system is based on the simple research of synonyms. Conversely, BrainGene tries to emulate the priming effect to find the best candidates words to be blended but showing the weaknesses related to his lack of knowledge of the world. The use of a semantic network allows a continuous improvement of the system, indeed, to obtain other interesting results just changing the network navigation method or by increasing the network's content. WORDY uses different types of blending to create catchy neologism that are not used by other approaches and we try to describe a structure of these linguistic devices taking into account different concepts such as the "recognition point".

The paper tries to face the problem to find the best couple of prefixes (suffixes) and directly tie with the blending device, it describes further interesting measures to test the catchiness and creativity of the results to obtain a score of neologisms. For example, unlike in BrainGene work, we think that the Levenshtein distance can help to identify the catchiness factor in the created neologisms. The methodology shows both strengths and weaknesses. The latter come from the strong indeterminacy of the problems addressed, nevertheless, our initial tests show that the software is useful for accomplish its task. The WORDY structure allows to increase its feature, for instances, through the implementation of other linguistic devices, reinforce its ranking methodologies or improving the semantic network.

## 5 Conclusions

The methodology implemented by WORDY has shown to be effective for creating neologisms that are meaningful, catchy and which represent the main object in a creative way, even the name of the tool "Wordy" has been generated by the methodology.

Although there are other systems that create neologism, today, there is not a standard methodology capable to carefully explain the creativity process. WORDY improves the approach followed by these systems emulating the priming effect through the semantic network and the spreading activation method,

somehow emulating the cognitive processes for the association of concepts. This way, the world knowledge contained in the semantic network together with the spreading activation allow the system to select words following uncommonly route that can be translate to look at reality from a different point of view.

We think that the presented approach which exploits a semantic network could be helpful in better emulating the cognitive process in human beings leading possibly to better results.

In future work we will focus our attention to more tests and improvement of WORDY, exploring new methods to navigate the semantic network. Furthermore, we will test the implementation of new blending devices that can help to create original catchy names and which could be integrated in the tool itself.

## References

1. Augello, A., Infantino, I., Pilato, G., Rizzo, R., Vella, F.: Introducing a creative process on a cognitive architecture. In: *Biologically Inspired Cognitive Architectures*, vol. 6, pp. 131–139, October 2013
2. Bakaradze, E.K.: Principle of the least effort: telescopic word formation. *Int. J. Arts Sci.* **3**(16), 86–105 (2010)
3. Collins, A.M., Quillian, M.R.: Retrieval time from semantic memory. *J. Verbal Learn. Verbal Behav.* **8**(2), 240–247 (1969)
4. Collins, A., Loftus, E.: A spreading-activation theory of semantic processing. *Psychol. Rev.* **82**(6), 407–428 (1975)
5. Colton, S., Wiggins, G.A.: Computational creativity: the final frontier? In: *Proceedings of the 20th European Conference on Artificial Intelligence (ECAI 2012)*, Montpellier, France, pp. 21–26, 27–31 August 2012
6. De Smedt, T., Daelemans, W.: Pattern for Python. *J. Mach. Learn. Res.* **13**, 2063–2067 (2012)
7. Duch, W., Pilichowski, M.: Experiments with computational creativity. *Neural Inf. Proces. Lett. Rev.* **11**(4–6), 123–133 (2007)
8. Gries, S.Th.: Cognitive determinants of subtractive word-formation processes: a corpus-based perspective. *Cogn. Linguist.* **17**(4), 535–558 (2006)
9. Fellbaum, C. (ed.): *WordNet: An Electronic Lexical Database*. MIT Press, Cambridge (1998)
10. Liu, H., Singh, P.: Conceptnet, a practical commonsense reasoning tool-kit. *BT Technol. J.* **22**(4), 211–226 (2004)
11. Mandera, P., Keuleers, E., Wodniecka, Z., Brysbaert, M.: Subtlex-pl: subtitle-based word frequency estimates for Polish. *Behav. Res. Methods* **47**, 471–483 (2015)
12. Ozbal, G., Strapparava, C.: A computational approach to the automation of creative naming. In: *Proceedings of the 50th Annual Meeting of the Association for Computational Linguistics (ACL 2012)*, Jeju Island, Korea, pp. 703–711 (2012)
13. Ozbal, G., Strapparava, C., Guerini, M.: Brand Pitt: a corpus to explore the art of naming. In: *Proceedings of the Eighth International Conference on Language Resources and Evaluation (LREC 2012)*, Istanbul, Turkey, May 2012
14. Pilichowski, M., Duch, W.: BrainGene: computational creativity algorithm that invents novel interesting names. In: *IEEE Symposium on Computational Intelligence for Human-like Intelligence (CIHLI)*, Singapore (2013)

15. Smith, M.R., Hintze, R.S., Ventura, D.: Nehovah: a neologism creator nomen ipsum. In: Proceedings of the International Conference on Computational Creativity, ICCO 2014, pp. 173–181 (2014)
16. Veale, T., Butnariu, C.: Harvesting and understanding on-line neologisms. In: Onysko, A., Michel, S. (eds.) *Cognitive Perspectives on Word Formation*, pp. 393–416. Mouton De Gruyter (2010)
17. [www.thetoptens.com](http://www.thetoptens.com)

# Conveying Audience Emotions Through Humanoid Robot Gestures to an Orchestra During a Live Musical Exhibition

Marcello Giardina<sup>1</sup>(✉), Salvatore Tramonte<sup>1</sup>, Vito Gentile<sup>2</sup>,  
Samuele Vinanzi<sup>1,3</sup>, Antonio Chella<sup>1</sup>, Salvatore Sorce<sup>2</sup>, and Rosario Sorbello<sup>1</sup>

<sup>1</sup> Robotics Lab, Università degli Studi di Palermo - Dipartimento dell'Innovazione Industriale e Digitale (DIID), Viale delle Scienze, Building 6, 90128 Palermo, Italy

{marcelloemanuele.giardina,salvatore.tramonte,vito.gentile,  
antonio.chella,salvatore.sorce,rosario.sorbello}@unipa.it

<sup>2</sup> Ubiquitous Systems and Interfaces Group (USI), Università degli Studi di Palermo - Dipartimento dell'Innovazione Industriale e Digitale (DIID), Viale delle Scienze, Building 6, 90128 Palermo, Italy

<sup>3</sup> Centre for Robotics and Neural Systems, Plymouth University, PL4 8AA, Plymouth, UK

samuele.vinanzi@plymouth.ac.uk

<http://usi.unipa.it>

**Abstract.** In the last twenty years, robotics have been applied in many heterogeneous contexts. Among them, the use of humanoid robots during musical concerts have been proposed and investigated by many authors. In this paper, we propose a contribution in the area of robotics application in music, consisting of a system for conveying audience emotions during a live musical exhibition, by means of a humanoid robot. In particular, we provide all spectators with a mobile app, by means of which they can select a specific color while listening to a piece of music (act). Each color is mapped to an emotion, and the audience preferences are then processed in order to select the next act to be played. This decision, based on the overall emotion felt by the audience, is then communicated by the robot through body gestures to the orchestra. Our first results show that spectators enjoy such kind of interactive musical performance, and are encouraging for further investigations.

**Keywords:** HRI · Musical robotics · Humanoid robotics

## 1 Introduction

In the last decade, we have witnessed a growing interest towards the use of intelligent humanoid robots during common human activities, because of their very “human” aspect and consequent human-like motion capabilities. This gives them the ability to convey emotions during the interactions with humans, and this is the main reason that boosted up the development of humanoid robots



and their consequent availability for common-life applications. There are a lot of robots that are specifically designed to convey emotions, and their shape is often fine-tuned even on the specific emotional field they are intended for.

For example, Emotional Humanoids robot are used to sustain natural empathic conversations with elderly people [20]; or to express emotion and personality [6]; or to aid people with cognitive disorders [1]; or also to support people with serious disabilities such as “ALS” patients [21]. Furthermore, gestures may be suitably used both by humans for the live control of humanoid robots [9], and by humanoid robots to communicate in a “human” way [10].

In the field of the musical performance, we propose that Human-humanoid interaction (*HHI*) allows for designing natural-like settings in which human users and a robotic agent coordinate behaviours and emotions [2] and communicate on the basis of shared phenomenal features in a common environment [19]. Our goal is to build a bond between the two entities giving to a robot the capability to exhibit affective-expressive movements as an emotional mediator of the feelings of the human audience during the musical performance of an orchestra. In this paper, we present a system for conveying audience emotions during a live musical show, using a humanoid robot (namely, a NAO by Aldebaran Robotics) as an orchestra leader. In particular, we provide all spectators with a mobile app, by means of which they can select a specific color (which corresponds to an emotion) during a live performance. Then, audience feelings are used by the robot to address the musicians to play a piece of music with a specific emotional meaning according with the musical composition. The robot directs the orchestra using preset body gestures.

The rest of the paper is arranged as follows. Section 2 presents a brief review of the state of the art in terms of emotion representation and the use of robotics in music; Sect. 3 includes a detailed overview of the whole system; Sect. 4 shows the first results of an evaluation study conducted during an actual deployment of our proposal; finally, Sect. 5 concludes the paper, with some ideas for future works.

## 2 Related Works

Before describing our system in details, in this section we focus on two crucial aspects addressed in this paper: emotion representation and robotics applications in musical context. The first subsection is aimed at describing which frameworks have been studied and implemented in literature in order to quantitatively model emotions. The second one includes some solutions based on the use of robots in musical contexts.

### 2.1 Emotion Representation

Emotions can be described as the human response to adapt himself to the constant environmental stimuli deriving from one’s circumstances, mood, or relationships with others. Emotions are the results of complex psychological and

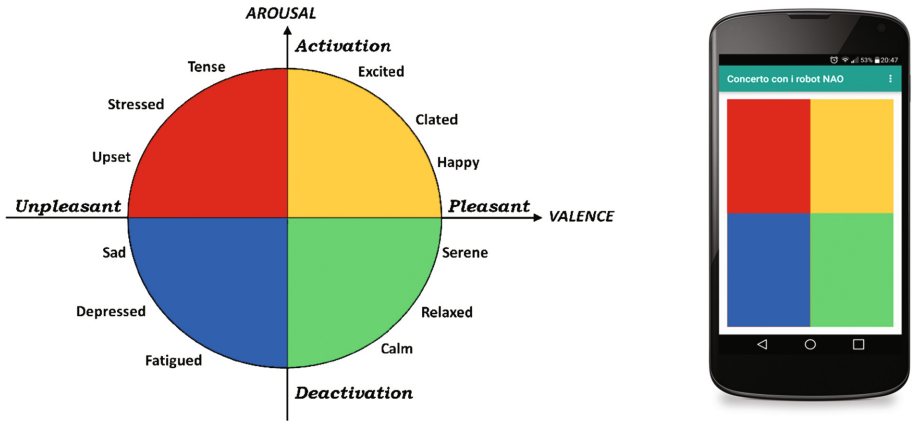


**Fig. 1.** The circumflex model for emotion representation, along with color labeling and its use in the mobile application.

physiological systems activated by the perception of significant environmental events. Many researches have been conducted in order to investigate how to represent emotions and how it is possible recognize them, as shown in [11] or [15]. Among the many approaches illustrated in psychology, the one based on “emotional categories” is one of the most often used [7] in literature, having focus to modelling emotions in according to different and discrete emotion classes and labels. One of the most used approaches has been developed and described by Paul Ekman in [8]. In his work, Ekman claimed that all the emotions can be mapped into a six-dimensional space defined by six basic emotions, namely *anger*, *disgust*, *fear*, *joy*, *sadness* and *surprise*. Using this model it is possible representing a human emotion felt as a balance of the six basic emotions. This advantage, however, may also represent the main drawback of such approach, since non-expert users may consider it overcomplicated to model their feelings. A two-dimensional, alternative to the Ekman’s model, has been described by Russell et al. in [17], and the further extended by Posner et al. in [16]. In these works, authors defined a “circumflex model of affect”, aimed to accurately describe every possible emotion. In particular, authors suggest a two-dimensional structure in which an emotional event may vary quantitatively along two independent dimensional variables. One dimension (*valence*) describes the degree of pleasantness or unpleasantness, whilst the other dimension (*arousal*) indicates the intensity in terms of physiological activation. The combination of these two dimensions generates the subjective emotional feeling. By means of this model, every emotion can be defined as the combination of two different levels of arousal and valence. The emotional categories may be ordered along the aforementioned circumflex, as shown in Fig. 1.

In this work, we opted for the circumflex model to describe the audience emotional responses, as well as the emotional content of the pieces of music of the composition. This allows us for discretizing the whole spectrum of emotions

in four “areas”, one for each quadrant of the circumflex. Each of these areas was associated with a different color: from the first to the fourth quadrant, happiness (yellow), anger (red), sadness (blue) and serenity (green). These colors have been chosen for being associated with the correspondent emotions [3,22].

### 2.2 Robotics in Music

There are several relevant works in the field of Robotics in musical applications. Among them, Hoffman et al. have defined the sense and outcomes of sharing an experience with a robot and this concept has been proposed as *Robotic Experience Companionship* (REC) [12]. Lim et al. proposed a unifying framework to generate emotions across voice, gesture, and music, by representing emotional states as a 4-parameter tuple of speed, intensity, regularity, and extent [13]. McCallum et al. stated that improvised musical interaction are able to provide an improvement of social presence and engagement during long term Human Robot Interaction (HRI) [14]. Burger et al. developed a simple robot with the goal to display its emotions by performing expressive movements during musical performances [5]. Brown et al. derived a framework for implementing happy and sad gestures on a humanoid robotic platform to measure user’s predominant perceived emotions to enhances the social interaction [4]. This short list show the broad interest of the scientific community towards the use of (humanoid) robots to convey emotions both from and to people in a musical context.

## 3 System Description

In this Section, we describe the main building blocks of our system architecture, depicted in Fig. 2.

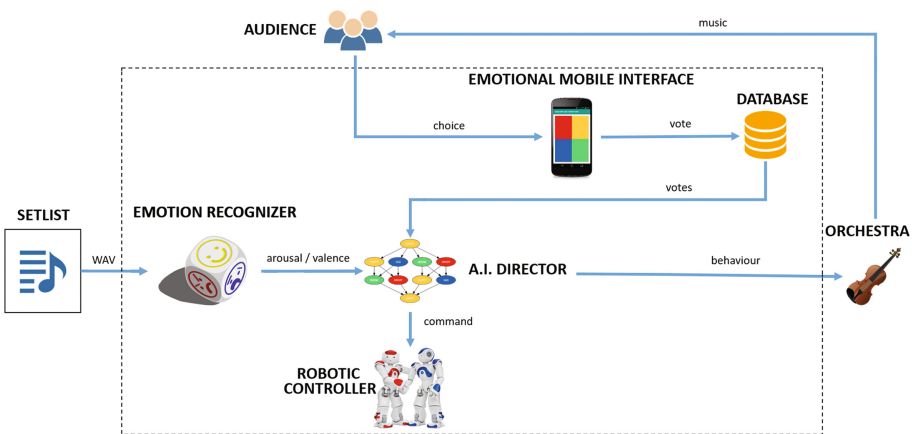


Fig. 2. System architecture.

There are three main actors that produce inputs or receive outputs: the *orchestra*, the *audience* and the *setlist*. The first one is made up of an electronic ensemble (i.e. a group of electronic acoustic speakers controlled by a computer) and an instrumental ensemble that produces music with acoustic instruments. The orchestra's role is to receive the system output in terms of gestures from the robot, and to play according to them.

The second actor of this system is the *audience*, i.e. spectators of the concert who are equipped with a mobile application (namely *NaoMusic*). As explained further in the following Sections, spectators are able to select their preferred colors according to the emotions felt during the musical performance.

The last actor is the *setlist*, i.e. a collection of audio files that together compose the musical structure of the concert. In particular, these musical tracks will be played by the electronic ensemble, acting as the base for the acoustic performance by the instrumental ensemble.

The system architecture is made up of five modules:

- *Emotion Recognizer*: a machine learning module to extract the emotional content from a song;
- *Emotional Mobile Interface*: a mobile app (i.e. the aforementioned *NaoMusic*) that allows users to submit their preferred color, according to the emotions experienced during the concert;
- *Database*: a web-located database that stores all the users' choices;
- *AI Director*: central component that realizes the decision-making process, guiding the evolution of the musical performance;
- *Robotic Controller*: translates the instructions of the *AI Director* module into behaviours for the robot.

Before describing the modules in more details, in the following subsection we present a high-level use case, in order to better clarify how the system works.

### 3.1 Use Case

The concert is preceded by a preparation phase aimed at generating the music to be played by the orchestra. In particular, some musicians compose a few short pieces, which is then processed by a software in order to produce a series of new, original tracks. All the new computer-generated songs, along with the initial ones, are included in the setlist used for the concert.

All these tracks are thus sent to the Emotion Recognizer module, which extracts (as explained later) their emotional content in terms of arousal and valence, from here on called *song\_arousal* and *song\_valence*. The output of this functional block is thus a collection of  $\langle \textit{song\_arousal}, \textit{song\_valence} \rangle$  pairs, one per track in the setlist. This concludes the preparation phase, and the system is now ready for being used in an actual concert.

During the concert, the orchestra starts by playing the introductory music, while the audience is able to express its emotions using the Emotional Mobile Interface (i.e. *NaoMusic*). All the data sent by this application are continuously

stored in a remote Database. When the musical act is close to its conclusion, the AI Director queries the Database to fetch the entries gathered during the current act. Those data are then processed in order to estimate the overall emotional state of the spectators, in terms of a  $\langle \text{song\_arousal}, \text{song\_valence} \rangle$  pair. By using this information, along with the emotional content of the tracks in the setlist, the system selects the song whose emotional content best fits the course of the performance, communicating its choice to the Robotic Controller. This module translates the choice into a behaviour for the robot, which will inform the orchestra about the next song to be played.

In the following we describe each module in more details.

### 3.2 Emotion Recognizer

This module (depicted in Fig. 3) implements a method for allowing identification and extraction of  $\langle \text{arousal}, \text{valence} \rangle$  pairs from a musical track. The emotion recognition capabilities have been implemented through Support Vector Machines (SVMs), trained with the dataset described in [18]. It includes approximately 1000 CC-licensed songs that have been listened and subsequently annotated with their values of arousal and valence through crowdsourcing. The training process uses 34 musical features extracted from each audio track of the aforementioned dataset, which constitute the training set inputs (see [18] for more details). Obviously, the corresponding *arousal* and *valence* annotations are used as outputs. More specifically, two models are created: one for arousal recognition, and the other for valence recognition.

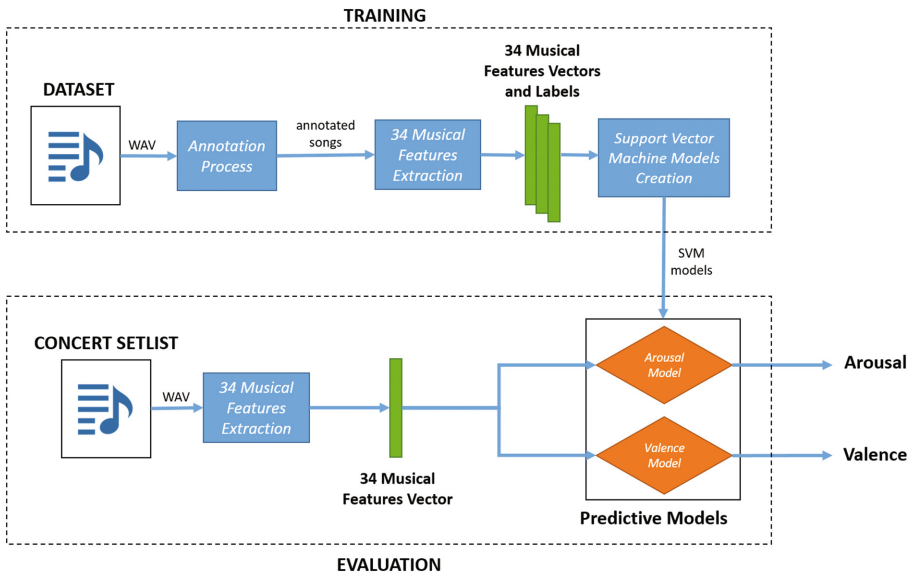


Fig. 3. Emotion recognizer module architecture.

After the training stage, the setlist is processed to extract the aforementioned musical features from each track. These features are then inputted into the two SVMs to obtain the estimated  $\langle arousal, valence \rangle$  pairs.

### 3.3 Emotional Mobile Interface

This module plays a fundamental role in the proposed system, as it represents the interaction point between the audience and the entire system. It consists in a simple and user-friendly mobile application, whose interface is shown in Fig. 1.

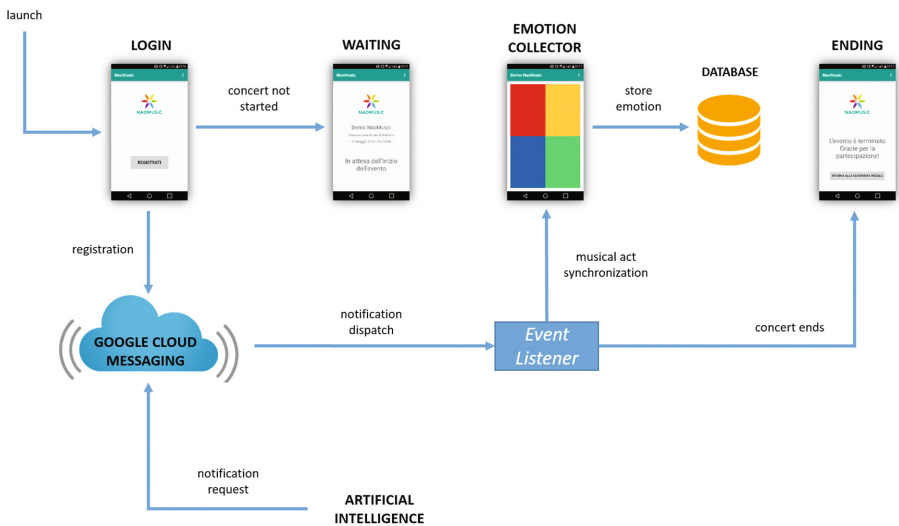


Fig. 4. Emotional mobile interface architecture.

Figure 4 describes the mobile application architecture. The main goal is to create an interface that allows spectators from the audience for expressing their emotional state while listening to the concert. All the votes recorded by all users at the end of each musical act will be used in order to compute the emotion that more faithfully represents the global emotional state of the audience, and that will be used by the AI Director module to decide which song should be played next.

On startup, the mobile devices can receive push notifications by the AI Director module through the Google Cloud Messaging (GCM) infrastructure. Once logged in, the application will move its user into a welcome screen that will persist until a notification will report the beginning of the concert. At this point, the user will be led in the voting screen, where s/he will be able to send the emotion to a remote webserver. This interface will synchronize with the musical act progression, thanks to the notification system, to be able to store the votes

correctly. This screen resembles Russel’s Circumplex Model of Emotions, having four colored tiles that resemble the four emotional categories described in Sect. 2.

It is worth noting that nor before neither during the concert users have been advised on the meaning of the colors: they were only asked to interact with the app as they wish, in order to avoid biases and to stimulate a more instinctive and less reasoned response.

### 3.4 Database

The Database module consists in a simple HTTP server, able to receive GET and POST requests aimed at storing votes to a local MySQL database management system. More precisely, all the votes are firstly sent from the mobile application to a server via GCM, and then stored to the database using REST API. The data are then used from the AI Director module (described in the next subsection), or for further offline analysis.

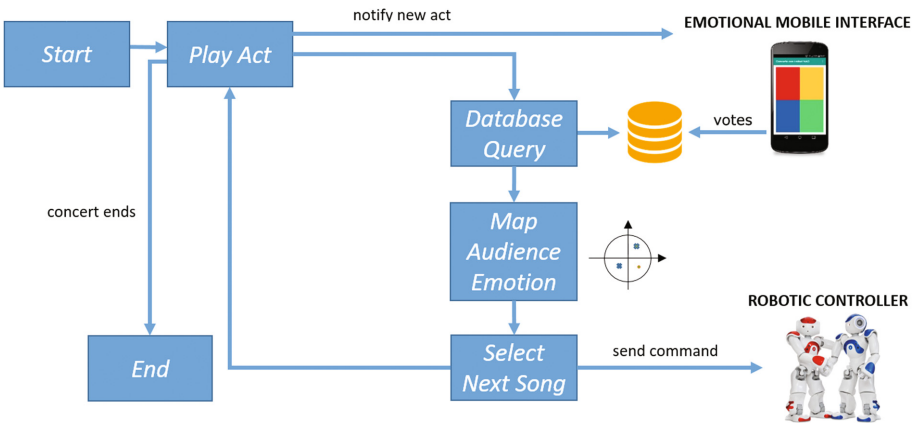


Fig. 5. AI director architecture.

### 3.5 AI Director

This module is the core component, as it contains the artificial intelligence that deals with the real-time management of the concert, taking decisions on the next song to be played (Fig. 5). This module accepts as input the  $\langle \text{song\_arousal}, \text{song\_valence} \rangle$  pair produced by the Emotion Recognizer module.

In order to understand how this module works, it is important to explain the concert structure. It consists in a tree data structure, whose depth represents the number of musical acts, and whose nodes are all the possible songs that can be played in every act (see Fig. 9). The goal of this module is to find an optimal path from the first to the last node, in order to produce the most engaging effect for the spectators based on their emotional response.

At the beginning of the show, the robot will perform an introductory welcome animation and subsequently it will turn towards the musicians in order to communicate via a body gesture the beginning of the first musical act.

For every such acts, the AI Director sends a synchronization notification to the Emotional Mobile interface, then it remains in a waiting state, giving time to the electronic and orchestral ensembles to perform their executions. Shortly before the end of the act, the system will wake up and query the Database to retrieve the spectators' votes collected during the act. This information is used to calculate the audience's predominant emotion. Combining this information with the emotional content of the candidate songs eligible to be performed on the next act, a heuristic search algorithm can be used in order to choose the song that most likely would induce an emotional shift in the audience, while avoiding stalls on the same emotions and abrupt changes. For instance, considering the  $\langle \text{song\_arousal}, \text{song\_valence} \rangle$  pair as a point on the circumflex shown in Fig. 1, its mirrored point (with respect to the main diagonal) represents the opposite emotion, which can be selected for obtaining the highest emotional variability.

### 3.6 Robotic Controller

Once the AI Director chooses the next song (as explained before), the Robotic Controller module will convey this information to the robot, and through it to the performers. This chain of operations is executed in loop for every musical act, until the end of the show.

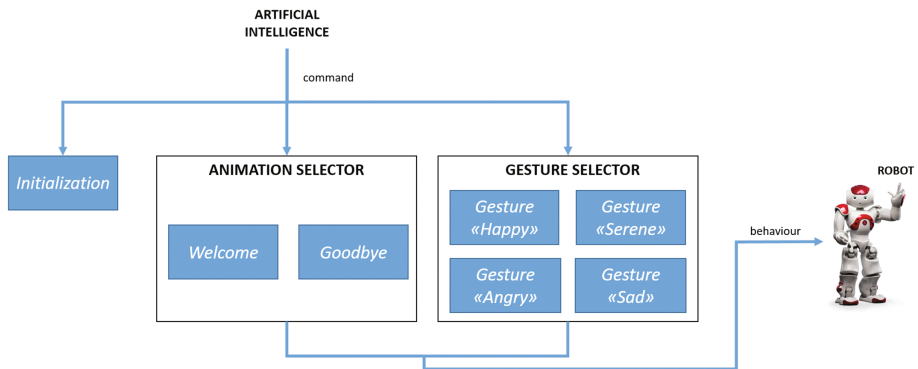


Fig. 6. Robotic controller architecture.

The purpose of this module, whose architecture is shown in Fig. 6, is to model the robotic behaviors that will enable a NAO robot to interact through body gestures with people involved in the show, both spectators and performers.

The robot plays two main roles: it serves both as an announcer, gesticulating and speaking to the audience, and as a musical director, performing movements to instruct the musicians on the next song they should play. The gestures used



for communicating emotions are shown in Fig. 7, and have been designed to be non-ambiguous. These four movements are the robotic embodiments of the outputs from the AI Director module, and each of them is interpreted as one of the four songs that can be played in the next musical act. Each song belongs to an emotional category, which in turn is associated to a color. Thus, the robot will modify the color of his LEDs accordingly, to give a continuous reference to the music players even after the gesture movement is over.

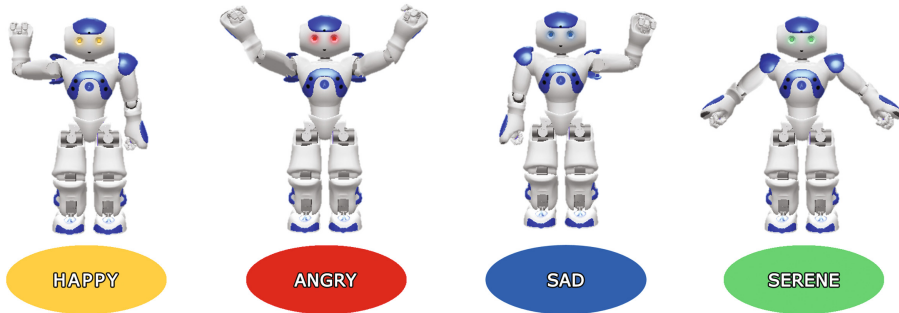


**Fig. 7.** The four robot directional gestures.

## 4 Evaluation

After some preliminary tests, aimed at fixing bugs and tuning some parameters, we tested our system during an actual concert, opened to an audience made by 118 spectators (63 males and 55 females). As explained before, each spectator was given with a mobile application, by means of which they were able to select a color during the concert. At the end of the concert, we have also asked them to fill a questionnaire consisting of 9 questions to be answered with 3-points Likert scales:

1. How frequently do you listen to symphonic music?
2. Do you consider yourself an expert in informatics?
3. Which was the predominant emotion you felt during the concert?
4. Did the robot correctly fulfil the task?
5. Do you believe that the presence of a person instead of the robot might change the effectiveness of the concert?
6. Before the concert, did you expect an emotional involvement from the performance?
7. Did the robot meet your expectations?
8. Did the presence of the robot affect your emotional state?
9. Did you enjoy the concert?

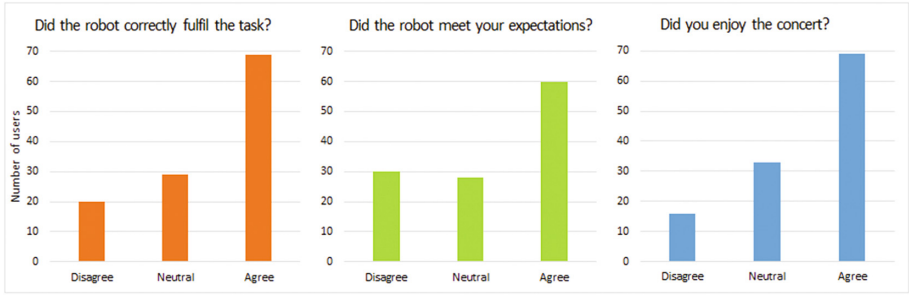


Fig. 8. Users’ answers to questions 4, 7 and 9.

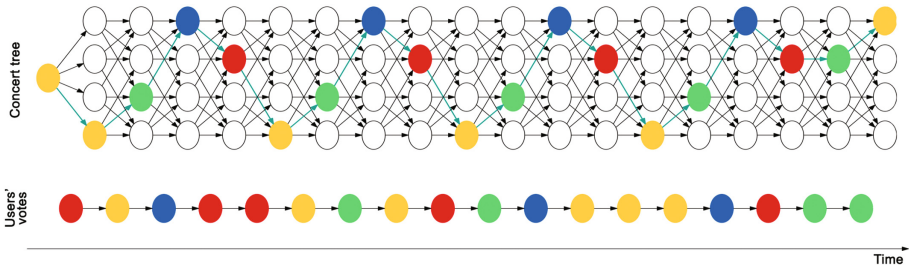


Fig. 9. Comparison between concert tree and users’ votes.

Most of the questions produced answers with mean and median values next to the neutral one. However, it is worth noting that questions 4, 7 and 9 revealed interesting aspects of users’ opinions. As shown in Fig. 8, the majority of users enjoyed the concert, and no relations were noted between neither the level of expertise in informatics nor the users’ habits in attending to such kind of concerts. Moreover, most of the users felt like the robot correctly fulfil the task, and that its behavior meets users’ expectations.

During the concert, the predominant emotion recorded was Serenity (i.e. most of the users chose green). Furthermore, the analysis of users’ responses in terms of the chosen colors (see Fig. 9) shows that they do not always select the emotions corresponding to the songs played by the orchestra. Indeed, according to the output of the emotion recognizer module, the songs played by the orchestra should elicit a specific emotion. The observed differences in users’ choices may be due to external factors, including the presence of the robot. While this consideration needs to be further investigated, this preliminary result is encouraging for future works.

## 5 Conclusion and Future Works

In this paper we presented a system for conveying audience emotions to orchestra musicians through a humanoid robot, and we described its architecture along

with a brief overview of the algorithms we used. We have also discussed the first results collected after the deployment of our system in a real scenario, in particular by evaluating users' opinions during and after a live musical exhibition.

The results are encouraging for further studies. In particular, we noted that most of the users enjoyed the concert, and noted that the robot may have influenced their opinions. While this observation seems encouraging, further investigations are required to strengthen this hypothesis. To this end, we are planning to deploy our system in another live musical exhibition, and to compare it with other solutions, in order to understand the differences between humanoid robots and other kind of hardware in terms of their ability to convey emotions.

**Acknowledgements.** The authors wish to thank the musical ensemble members, the students Corsello, Caravello and the professors Betta, Correnti, D'Aquila and Rapisarda from the Conservatorio di Musica "Vincenzo Bellini" di Palermo for their fundamental contribution for the realization of the musical performance and for their invaluable open-mindedness.

## References

1. Anzalone, S.M., Tilmont, E., Boucenna, S., Xavier, J., Jouen, A.L., Bodeau, N., Maharatna, K., Chetouani, M., Cohen, D., Group, M.S., et al.: How children with autism spectrum disorder behave and explore the 4-dimensional (spatial 3d+ time) environment during a joint attention induction task with a robot. *Res. Autism Spectr. Dis.* **8**(7), 814–826 (2014)
2. Anzalone, S., Cinquegrani, F., Sorbello, R., Chella, A.: An emotional humanoid partner. In: *Proceedings of the 1st International Symposium on Linguistic and Cognitive Approaches to Dialog Agents - A Symposium at the AISB 2010 Convention*, pp. 1–6 (2010)
3. Augello, A., Infantino, I., Pilato, G., Rizzo, R., Vella, F.: Binding representational spaces of colors and emotions for creativity. *Biol. Inspired Cogn. Architectures* **5**, 64–71 (2013)
4. Brown, L., Howard, A.M.: Gestural behavioral implementation on a humanoid robotic platform for effective social interaction. In: *The 23rd IEEE International Symposium on Robot and Human Interactive Communication*, pp. 471–476 (2014)
5. Burger, B., Bresin, R.: Communication of musical expression by means of mobile robot gestures. *J. Multimodal User Interfaces* **3**(1), 109–118 (2010)
6. Chella, A., Sorbello, R., Pilato, G., Vassallo, G., Balistreri, G., Giardina, M.: An architecture with a mobile phone interface for the interaction of a human with a humanoid robot expressing emotions and personality. In: *Congress of the Italian Association for Artificial Intelligence*, pp. 117–126. Springer (2011)
7. Cowie, R., Cornelius, R.R.: Describing the emotional states that are expressed in speech. *Speech Commun.* **40**(1–2), 5–32 (2003)
8. Ekman, P.: *Basic Emotions*, pp. 45–60. Wiley, New York (2005)
9. Gentile, V., Sorce, S., Gentile, A.: Continuous hand openness detection using a kinect-like device. In: *2014 Eighth International Conference on Complex, Intelligent and Software Intensive Systems*, pp. 553–557 (2014)

10. Gentile, V., Sorce, S., Malizia, A., Gentile, A.: Gesture recognition using low-cost devices: Techniques, applications, perspectives (Riconoscimento di gesti mediante dispositivi a basso costo: Tecniche, applicazioni, prospettive). *Mondo Digitale* **15**(63), 161–169 (2016)
11. Gentile, V., Milazzo, F., Sorce, S., Gentile, A., Pilato, G., Augello, A.: Body gestures and spoken sentences: a novel approach for revealing user's emotions. In: *Proceedings of 11th International Conference on Semantic Computing (IEEE ICSC 2017)* (2017)
12. Hoffman, G., Bauman, S., Vanunu, K.: Robotic experience companionship in music listening and video watching. *Pers. Ubiquit. Comput.* **20**(1), 51–63 (2016)
13. Lim, A., Ogata, T., Okuno, H.G.: Towards expressive musical robots: a cross-modal framework for emotional gesture, voice and music. *EURASIP J. Audio Speech Music Process.* **2012**(1), 3 (2012)
14. McCallum, L., McOwan, P.W.: Face the music and glance: how nonverbal behaviour aids human robot relationships based in music. In: *Proceedings of the Tenth Annual ACM/IEEE International Conference on Human-Robot Interaction*, pp. 237–244, HRI 2015, NY, USA. ACM, New York (2015)
15. Meudt, S., Schmidt-Wack, M., Honold, F., Schüssel, F., Weber, M., Schwenker, F., Palm, G.: Going further in affective computing: how emotion recognition can improve adaptive user interaction, pp. 73–103. Springer, Cham (2016)
16. Posner, J., Russel, J.A., Peterson, B.S.: The circumplex model of affect: an integrative approach to affective neuroscience, cognitive development, and psychopathology. *Dev. Psychopathol.* **17**(3), 715–734 (2005)
17. Russell, J.A.: A circumplex model of affect. *J. Pers. Soc. Psychol.* **39**(6), 1161–1178 (1980)
18. Soleymani, M., Caro, M.N., Schmidt, E.M., Sha, C.Y., Yang, Y.H.: 1000 songs for emotional analysis of music. In: *Proceedings of the 2nd ACM International Workshop on Crowdsourcing for Multimedia*, pp. 1–6, CrowdMM 2013, NY, USA. ACM, New York (2013)
19. Sorbello, R., Chella, A., Calí, C., Giardina, M., Nishio, S., Ishiguro, H.: Telenoid android robot as an embodied perceptual social regulation medium engaging natural human-humanoid interaction. *Robot. Auton. Syst.* **62**(9), 1329–1341 (2014). *Intelligent Autonomous Systems*
20. Sorbello, R., Chella, A., Giardina, M., Nishio, S., Ishiguro, H.: An architecture for telenoid robot as empathic conversational android companion for elderly people. In: *Intelligent Autonomous Systems*, vol. 13, pp. 939–953. Springer (2016)
21. Spataro, R., Chella, A., Allison, B., Giardina, M., Sorbello, R., Tramonte, S., Guger, C., La Bella, V.: Reaching and grasping a glass of water by locked-in ALS patients through a BCI-controlled humanoid robot. *Front. Hum. Neurosci.* **11**, 68 (2017)
22. Tkalcíč, M., De Carolis, B., de Gemmis, M., Odić, A., Košir, A.: Introduction to Emotions and Personality in Personalized Systems, pp. 3–11. Springer, Cham (2016)

# A Kernel Support Vector Machine Based Technique for Crohn's Disease Classification in Human Patients

Albert Comelli<sup>1,2</sup>, Maria Chiara Terranova<sup>2</sup>, Laura Scopelliti<sup>2</sup>, Sergio Salerno<sup>2</sup>, Federico Midiri<sup>2</sup>, Giuseppe Lo Re<sup>2</sup>, Giovanni Petrucci<sup>1</sup>, and Salvatore Vitabile<sup>2</sup>(✉)

<sup>1</sup> Dipartimento dell'Innovazione Industriale e Digitale (DIID),  
Università di Palermo, Viale delle Scienze, Ed. 8, 90128 Palermo, PA, Italy  
albert.comelli@unipa.it

<sup>2</sup> Dipartimento di Biopatologia e Biotecnologie Mediche,  
Università di Palermo, Via del Vespro, 129, 90127 Palermo, PA, Italy  
salvatore.vitabile@unipa.it

**Abstract.** In this paper a new technique for classification of patients affected by Crohn's disease (CD) is proposed. The proposed technique is based on a Kernel Support Vector Machine (KSVM) and it adopts a Stratified K-Fold Cross-Validation strategy to enhance the KSVM classifier reliability. Traditional manual classification methods require radiological expertise and they usually are very time-consuming. Accordingly to three expert radiologists, a dataset composed of 300 patients has been selected for KSVM training and validation. Each patient was codified by 22 extracted qualitative features and classified as Positive or Negative as the related histological specimen result showed the CD. The effectiveness of the proposed technique has been proved using a real human patient dataset collected at the University of Palermo Policlinico Hospital (UPPH dataset) and composed of 300 patients. The KSVM classification results have been compared against the histological specimen results, which are the adopted Ground-Truth for CD diagnosis. The achieved results (Sensitivity: 94,80%; Specificity: 100,00%; Negative Predictive Value: 95,06%; Precision: 100,00%; Accuracy: 97,40%; Error: 2,60%) show that the proposed technique results are comparable or even better than manual reference methods reported in literature.

**Keywords:** Kernel support vector machine · K-Fold cross-validation · Crohn's disease classification

## 1 Introduction

Crohn's Disease (CD) is a life-long idiopathic, often debilitating, chronic inflammatory disease of the gut, which can potentially involve the entire gastrointestinal tract [1]. It arises from an interaction between genetic and environmental factors, and it is characterized by granulomatous autoimmune reaction of

the bowel walls, from the mucosal layer to the serosa one, and frequent extra-luminal and extra-intestinal features. The incidence peak is in adolescents and young adults, between 15 and 25 years old [1,2]. CD comprehends a variety of complex phenotypes in terms of disease location and behavior, characterized by different events within time, healing and relapses. This phenotypical heterogeneity depends on many factors: the age of appearance, time elapsed from symptoms to diagnosis, site, extent and behavior of disease, and other anamnestic features [3]. Because of these heterogeneities the last European Consensus by European Crohn's and Colitis Organization (ECCO) agreed on the lack of a single gold standard for diagnosis of CD: "A single gold standard for the diagnosis of CD is not available. The diagnosis is confirmed by clinical evaluation and a combination of endoscopic, histological, radiological, and/or biochemical investigations" [4]. The recent new therapies, both biological ones and immuno-modulators, are very effective in downgrading disease activity and in symptoms control, but their real effect on disease course is mostly unknown. Moreover different therapy strategies must be tailored on disease evolution during treatment, thus allowing to prolong remission, to improve life quality, to prevent or manage hospitalization and surgery, and finally to prevent disability [3]. Imaging plays a pivotal role on disease evaluation during life-time, allowing a non-invasive patients follow up. That's the reason why non ionizing imaging technics must be preferred [3,5]. Enterography magnetic resonance imaging (E-MRI) was recently yielded as useful diagnostic tool that can afford radiation free diagnosis where other imaging examinations have failed, or when involved areas are not easily reachable by endoscopy [2,3,6]. It is considered the gold standard for CD diagnosis and is not able to provide a comprehensive assessment of extra-luminal features and extra-intestinal manifestations of disease [3]. In the last decades, MRI represented a valid technique for evaluation of disease extension and activity, for patient follow-up or for a pre-operative assessment in patients with histologically proven CD [3]. Its role as first step examination in diagnosis for suspected but not confirmed CD was explored only recently, showing high accuracy (sensitivity 93%, specificity 90%) [7]. Up to date, many studies have been published, concerning the use of imaging evaluation in CD diagnosis and grading, although nowadays there is not yet an adequate consensus about its actual reliability in clinical practice [4,8,9]. Because of the widely heterogeneous clinical features of CD, the role of radiologists may be challenging [3,6,10,11]. Nevertheless, worldwide literature has reported typical E-MRI features, which are frequently associated with CD, and whose evaluation may help in diagnosis by imaging [3,10,11]. The possibility of early CD diagnosis has great clinical implications, considering the impact on public health that such a chronic and disabling disease can imply, due to the high economic costs necessary for patients management, and which may be potentially reduced by imaging early diagnosis, and pattern definition [3]. This is particularly important considering that time elapsed from symptoms to diagnosis, site, extent and behavior of disease deeply influence patient prognosis, outcome, therapy, and complications.

Automatic diagnosis of CD is a very challenging task and can have a great clinical implication in CD affected patients. In last years, a lot of approaches to classify MRI images into healthy or unhealthy classes have been proposed. Supervised classification techniques include support vector machine (SVM) [12] and k-nearest neighbors (k-NN) [13, 14]. Unsupervised classification techniques [15, 16] include self-organization feature map (SOFM) [12] and fuzzy c-means [14, 17]. Generally, all these methods achieve good classification results.

Among supervised classification methods, SVMs are common classification methods based on machine learning [18–20]. Compared against other methods such as artificial neural networks, decision trees, and Bayesian networks, SVMs have significant advantages in high accuracy, elegant mathematical tractability, and direct geometric interpretation. Moreover, they do not need a large number of training samples to avoid over-fitting [21].

To the best of our knowledge, there are not SVM based applications for CD in literature. In [22], it has been applied a SVM method for data classification. The SVM modeling is a promising classification approach for predicting medication adherence in Heart Failure (HF) patients. This predictive model helps to stratify the patients so that evidence-based decisions can be made and patients can be managed appropriately. In [23], a novel hybrid system to classify a given MR brain image as either normal or abnormal is proposed. The method employed digital wavelet transform to extract features and principal component analysis (PCA) to reduce the feature space. Afterwards, a KSVM with Radial basis function (RBF) kernel, using particle swarm optimization (PSO) to optimize the parameters  $C$  and  $\sigma$  is adopted. Five-fold cross-validation was utilized to avoid over-fitting. Wavelet transform is an effective tool for feature extraction from MR brain images, because it allows images analysis at various levels of resolution due to its multi-resolution analytic property. This technique requires large storage and it is computationally expensive [24]. PCA is appealing since it effectively reduces data dimensionality and computational cost [25]. In this paper a supervised Crohn's disease patient's classification technique based on Kernel Support Vector Machine (KSVM) algorithm using a Stratified K-Fold Cross Validation strategy is presented. The proposed technique aims to apply a KSVM technique on E-MRI qualitative extracted features to simplify classification task complexity and preserve technique accuracy and quality when compared against manual methods [7].

The article is organized as follows: in Sect. 2 the E-MRI dataset used for development, test, and evaluation of the proposed technique is described; In Sect. 3, the proposed technique is presented; Sect. 4 depicts the archived results and reports some discussions; The final considerations are treated in Sect. 5.

## 2 Materials

The proposed classification technique is based on machine learning algorithms used to classify the proprietary University of Palermo Policlinico Hospital (UPPH) dataset.

## 2.1 University of Palermo Policlinico Hospital Dataset

The dataset consists of 300 MR Enterography examinations of 300 patients coming from University of Palermo Policlinico Hospital, Department of Radiology, (156 females, 144 males, mean age 37,8 years). MR imaging studies were performed with a 1.5-T magnet and surface coils phased array (Signa, GE Medical system, Milwaukee, WI, USA and Achieva, Philips Medical System, Eindhoven, The Netherlands), with the use of paramagnetic contrast media (DOTAREM; Guerbet; USA), after the administration of a spasmolytic agent, unless contraindicated.

In our protocol has been used the following sequences: HASTE thick-slab, Steady State Free Precession, Single Shot Fast Spin Echo, 3D Spoiled Gradient Echo - on axial and coronal planes - and DWI. Patients underwent specific protocol for MR Enterography, that requires 6 hours fasting before the exam, low fiber diet for the preceding 5 days, and the intake from the day before the exam of 2000 ml of water and polyethylene glycol (PEG). Thus allowing to reduce the fecal matter and to provide a better and easier distention of the bowel loops. Upon the arrival to the department, patient is invited to ingest other 1500 ml of water and PEG 40 min before the exam.

The dataset is composed of 300 E-MRI examinations related to 300 patients: 150 are histologically CD proved, and 150 are healthy individuals [3, 10, 11]. Each patient has been codified with a vector of 22 qualitative features. The expert radiologist extracted features are depicted in Table 1.

## 3 Method

The purpose of this study is to develop an automatic tool for CD affected patients classification based on a kernel support vector machine (KSVM) technique.

The description of algorithms and mathematical formalisms used are briefly described.

### 3.1 Features Extraction

Parameters extraction has been elaborated on the basis of the typical E-MRI features of CD affected patients [3, 6, 10, 11], as shown in Fig. 1 and Table 1.

### 3.2 Kernel SVM

The support vector machines (SVM) can be thought as an alternative technique for polynomial classifiers learning, as opposed to classical training methods for neural networks. SVMs can represent complex non-linear functions. The characteristic parameters of the network are obtained by the solution of a quadratic convex programming problem with equality constraints or box type (in which the value of the parameter must be maintained within a range), providing a single global minimum [26]. One of the most popular and reliable SVMs are the kernel SVMs. Kernel SVMs have the following advantages [28]:



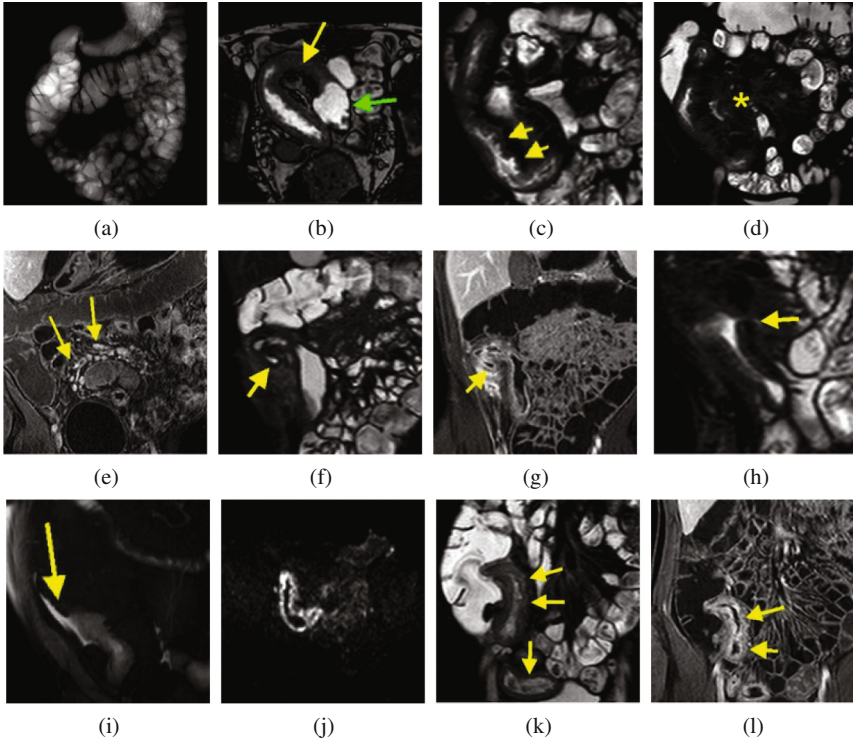


**Fig. 1.** E-MRI CD Features: (a) HASTE Thick slab: Bowel cleansing and distension; (b) Balanced - TrueFISP: Terminal Ileum thickening; length; lumen caliber: substenosis; (c) T2 Single-shot FSE fat-sat: Mucosal layer: pseudo-polyps; (d) T2 Single-shot FSE fat-sat: Fat Wrapping; (e) Post contrast T1 3D spoiled GE: Lymph-nodes; (f) T2 Single-shot FSE fat-sat: Sinus; (g) Post contrast T1 3D spoiled GE: Sinus; (h) T2 Single-shot FSE fat-sat: Fistula; (i) T2 Single-shot FSE fat-sat: Free fluid; (j) DWI: Water diffusion restriction. Hyper-intensity; (k) T2 Single-shot FSE fat-sat: T2 imaging: Hyper-intensity due to severe edema and Terminal Ileum Thickening; (l) Post contrast T1 imaging 3D spoiled GE: Layered pattern contrast enhancement

- Work very well in practice and have been remarkably successful in such diverse fields as natural language categorization, bioinformatics and computer vision;
- Have few tunable parameters;
- Training often involves convex quadratic optimization.

Four common kernels [27] have been used in this work and they are listed in Table 2. For each kernel, there should be at least one adjusting parameter to make the kernel flexible and tailor itself to practical data. Table 2 depicts also the used parameters in each case.

Our task is a two class classification task, labelled as Positive or Negative.

**Table 1.** MR Enterorgraphy extracted features

Sequence types	Features	Parameters
T2 SPAIR/post contrast T1 e-Thrive/BFFE	Termina Ileum thickening	0: None or less than 3 mm thickening 1. Thickening greater than 3 mm
	Length	The length, in cm, of the affected gastrointestinal tract/tracts
	Single lesion/Skip lesions	1: single tract involved: 2: multiple tracts involved
	Fat wrapping	0: Normal mesenteric adipose tissue 1: mesenteric hyperplasia
	Sinus	0: No 1: Yes
	Fistulas	0: No 1: Yes
	Surgery	0: No 1: Yes
	Mucosal layer	0: no mucosal involvement 1: Edema and post-contrast enhancement 2: Inflammatory changes and pseudo-polyps
	Free fluid	0: No 1: Yes
	Pattern	0: no disease features 1: active inflammatory subtype 2: fibrostenotic subtype 3: fistulizing subtype
	Activity	0: no activity 1: mild activity 2: moderate activity 3: severe activity
	Complications	0: No 1: Yes
	Intestinal obstruction	0: No 1: Yes
Post-contrast T1 e-Thrive	Lymph nodes	0: No 1: Yes
	Breathing/ Peristalsis artifacts	0: No 1: Yes
	Post contrast T1 imaging	0: no wall enhancement 1: layered enhancement 2: transmural enhancement
T2 SPAIR	Pseudo-polyps	0: No 1: Yes
	Lumen	0: No changes in lumen caliber 1: Stenosis/Sub-stenosis
	T2W imaging	0: no mural edema 1: mild mural edema 2: severe hyper intensity due to noticeable edema
HASTE thick slab	Bowel cleaning protocol	0: no sufficient preparation 1: adequate bowel loops cleaning and distention
	Bowel distention protocol	0: no sufficient bowel distention: only stomach or duodeno-jejuneal loop 1: PEG has reached the ileocecal junction
DWI	Water diffusion restriction (DWI)	0: free and physiological diffusion, no hyper intensity on DWI 1: mild hyper-intensity 2: Severe hyper intensity

**Table 2.** Four common kernels used in the Support Vector Machine

SVM Kernel	Formula	Parameter
Linear	$K(x, y) = x^T y, x, y \in \mathbb{R}^d$	Linear kernel, meaning dot product
Polynomial	$K(x, y) = (x^T y + r)^n, x, y \in \mathbb{R}^d, r > 0$	Polynomial kernel (order $n = 3$ )
Quadratic	$K(x, y) = (x^T y + r)^2, x, y \in \mathbb{R}^d, r > 0$	Quadratic kernel
Radial basis function (RBF)	$e^{-\frac{\ x-y\ ^2}{2\sigma^2}}, x, y \in \mathbb{R}^d, \sigma > 0$	Gaussian Radial Basis Function kernel (scaling factor $1/2\sigma^2 = 1$ )

### 3.3 The Proposed Technique

The goal of the proposed system is the supervised Crohn’s disease affected patient classification using a KSVM algorithm. Accordingly to the expert radiologists, each E-MRI sequence is codified by a vector composed of 22 qualitative features as depicted in Table 2. KSVM classification performs a two class classification task: accordingly to the related histological specimen result each pattern

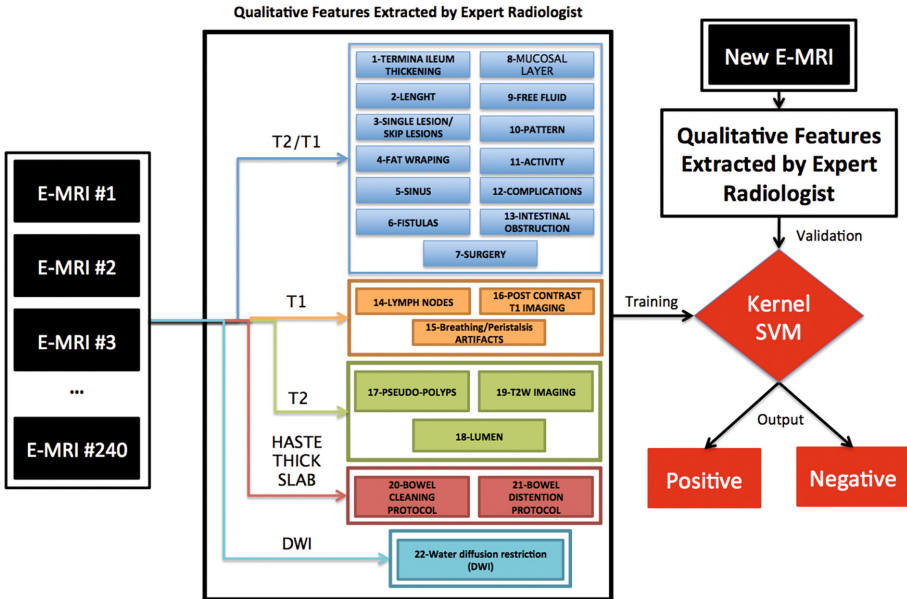


**Fig. 2.** The proposed training and validation workflow: each E-MRI sequence is codified by a vector composed of 22 qualitative features. Accordingly to the related histological specimen result, KSVM training vectors have been labelled. Afterwards, a new E-MRI vector is classified by KSVM.

is classified as Positive or Negative. As pointed out before, our dataset is composed of 300 vectors of 22 qualitative features. The whole dataset is divided into two bins: 80% (240 vectors) of the sampled values are used for the training session, and the remaining 20% (60 vectors) values are used for the validation session:

- 240 vectors composed of 22 qualitative features for KSVM training;
- 60 vectors composed of 22 qualitative features for KSVM validation.

A cross-validation strategy has been also integrated into the proposed technique to enhance classifier reliability and generalization capabilities, and limit over-fitting issues. The proposed training and validation workflow is depicted in Fig. 2.

## 4 Results and Discussions

The proposed technique has been used on the datasets described in the Materials section. To the best of our knowledge, there are not KSVM applications on medical data related to CD. For that reason, it was not possible to propose a direct comparison. To test the effectiveness of the proposed technique, a comparison using four SVMs different kernels (Linear, Polynomial, Quadratic, RBF, as depicted in Table 2) has been performed. When using the linear kernel, the KSVM degrades to original linear SVM.

It is important to underline that the Ground-Truth for CD diagnosis is the histological specimen result. The biopsy is performed under endoscopic examination. Two biopsies from five sites around the colon, including the rectum, are obtained, and then analyzed by expert pathologists of University Hospital Policlinico, for diagnosis confirmation according to European Crohn's and Colitis Organisation's guidelines [4]. As depicted in Tables 3 and 4 the results showed that the proposed technique archives excellent results in both training and validation. Performance measures are then calculated regarding correct/incorrect Patient classification.

Sensitivity, Specificity, Negative Predictive Value, Precision, Accuracy, and Error scores are defined and used as follows:

- Sensitivity: It is defined as the percentage of effective positives that are correctly identified as such:

$$\text{Sensitivity} : \frac{TP}{TP + FN} \quad (1)$$

- Specificity: It is defined as the percentage of effective negatives that are not classified as such:

$$\text{Specificity} : \frac{TN}{TN + FP} \quad (2)$$

- Negative Predictive Value: It is defined as the probability that subjects with a negative test are truly not diseased:

$$NegativePredictiveValue : \frac{TN}{TN + FN} \tag{3}$$

- Precision: It is defined as, related to reproducibility and repeatability, the degree to which repeated classifications under unchanged conditions show the same results:

$$Precision : \frac{TP}{TP + FP} \tag{4}$$

- Accuracy: It is defined as the degree of closeness of classifications of a disease to that disease’s true histological examination:

$$Accuracy : \frac{TP + TN}{TP + FP + FN + TN} \tag{5}$$

- Error: It is defined as the opposite of Accuracy:

$$Error : \frac{FP + FN}{TP + FP + FN + TN} \tag{6}$$

The classification result has been evaluated using three stratified K-Fold validation, with same SVM Linear Kernel. The results are depicted in Table 3.

For 5-Fold cross validation strategy, the whole classification accuracy was 97,00%; for 10-Fold cross validation, was 96,40%; and for 15-Fold cross validation, was 96,40%. The above strategy limited differences are due to the size of the training and validation sets.

**Table 3.** Classification comparison of 3 stratified K-Fold validation strategies using the same SVM Linear Kernel

Classification	Linear SVM Kernel		
	Fold cross validation		
	5	10	15
True Positive	47,00%	46,20%	46,33%
True Negative	50,00%	50,00%	50,00%
False Positive	0,00%	0,00%	0,00%
False Negative	3,00%	3,80%	3,67%
Sensitivity Eq. (1)	94,00%	92,40%	92,67%
Specificity Eq. (2)	100,00%	100,00%	100,00%
Negative Predictive Value Eq. (3)	94,34%	92,94%	93,17%
Precision Eq. (4)	100,00%	100,00%	100,00%
Accuracy Eq. (5)	97,00%	96,20%	96,20%
Error Eq. (6)	3,00%	3,80%	3,80%

Successively the classification result have been compared using four different SVM Kernels, with same 5-Fold cross validation. The results are depicted in Table 4.

Using the Linear kernel, the whole classification accuracy was 97,00%; Using the Polynomial kernel, was 96,40%; Using the the Quadratic kernel, was 96,40%; Using the RBF kernel, was 97,40%. In this particular application domain, RBF kernel answers the best performance also using different K-Fold strategies.

**Table 4.** Classification comparison of 4 different SVM Kernels

Classification	5-Fold cross validation			
	SVMs Kernel			
	Linear	Polynomial	Quadratic	Radial basis function
True Positive	47,00%	46,40%	46,40%	47,40%
True Negative	50,00%	50,00%	50,00%	50,00%
False Positive	0,00%	0,00%	0,00%	0,00%
False Negative	3,00%	3,60%	3,60%	2,60%
Sensitivity Eq. (1)	94,00%	92,80%	92,80%	94,80%
Specificity Eq. (2)	100,00%	100,00%	100,00%	100,00%
Negative Predictive Value Eq. (3)	94,34%	93,28%	93,28%	95,06%
Precision Eq. (4)	100,00%	100,00%	100,00%	100,00%
Accuracy Eq. (5)	97,00%	96,40%	96,40%	97,40%
Error Eq. (6)	3,00%	3,60%	3,60%	2,60%

## 5 Conclusions

In this contribution a KSVM based technique for CD affected human patients classification has been presented. The classification results on the proprietary UPPH dataset composed of 300 patients, each of one codified by 22 qualitative features, have been calculated and compared against the histological specimen results. Histological specimen results are the clinical Ground-Truth for CD diagnosis and have been used for demonstrating the validity of proposed technique.

Sensitivity, Specificity, Negative Predictive Value, Precision, Accuracy, and Error scores obtained using the proposed technique highlight the improvement in accuracy and quality compared to the manual results presented in [7].

The proposed technique has a significant advantage in integrating the cross-validation strategy. This gives its contribution to the classifier generalization capability without showing either over-fitting or sensibility to the selected test dataset. After KSVM training, classifier usability does not require any parameter setting and deep knowledge about the used learning machine technique. So, its degree of acceptance in medical practices can be very high.

## References

1. Maglinte, D.D., Gourtsoyiannis, N., Rex, D., Howard, T.J., Kelvin, F.M.: Classification of small bowel Crohn's subtypes based on multimodality imaging. *Radiol. Clin. North Am.* **41**(2), 285–303 (2003)
2. Bhatnagar, G., Stempel, C., Halligan, S., Taylor, S.A.: Utility of MR enterography and ultrasound for the investigation of small bowel CD. *J. Magn. Reson. Imaging* **45**, 1573–1588 (2016)
3. Lo Re, G., Midiri, M.: *Crohn's Disease: Radiological Features and Clinical-Surgical Correlations*. Springer, Heidelberg (2016)
4. Gomollón, F., Dignass, A., Annese, V., Tilg, H., Van Assche, G., Lindsay, J.O., Peyrin-Biroulet, L., Cullen, G.J., Daperno, M., Kucharzik, T., et al.: 3rd European evidence-based consensus on the diagnosis and management of Crohn's disease 2016: part 1: diagnosis and medical management. *J. Crohns Colitis* **11**, 3–25 (2016). jjw168
5. Peloquin, J.M., Pardi, D.S., Sandborn, W.J., Fletcher, J.G., McCollough, C.H., Schueler, B.A., Kofler, J.A., Enders, F.T., Achenbach, S.J., Loftus, E.V.: Diagnostic ionizing radiation exposure in a population-based cohort of patients with inflammatory bowel disease. *Am. J. Gastroenterol.* **103**(8), 2015–2022 (2008)
6. Sinha, R., Verma, R., Verma, S., Rajesh, A.: Mr enterography of Crohn disease: part 1, rationale, technique, and pitfalls. *Am. J. Roentgenol.* **197**(1), 76–79 (2011)
7. Panes, J., Bouzas, R., Chaparro, M., García-Sánchez, V., Gisbert, J., Martínez de Guereñu, B., Mendoza, J.L., Paredes, J.M., Quiroga, S., Ripollés, T., et al.: Systematic review: the use of ultrasonography, computed tomography and magnetic resonance imaging for the diagnosis, assessment of activity and abdominal complications of Crohn's disease. *Aliment. Pharmacol. Ther.* **34**(2), 125–145 (2011)
8. Steward, M.J., Punwani, S., Proctor, I., Adjei-Gyamfi, Y., Chatterjee, F., Bloom, S., Novelli, M., Halligan, S., Rodriguez-Justo, M., Taylor, S.A.: Non-perforating small bowel CD assessed by MRI enterography: derivation and histopathological validation of an MR-based activity index. *Eur. J. Radiol.* **81**(9), 2080–2088 (2012)
9. Lo Re, G., Cappello, M., Tudisca, C., Galia, M., Randazzo, C., Craxì, A., Camma, C., Giovagnoni, A., Midiri, M.: CT enterography as a powerful tool for the evaluation of inflammatory activity in Crohn's disease: relationship of CT findings with CDAI and acute-phase reactants. *Radiol. Med. (Torino)* **119**(9), 658–666 (2014)
10. Tolan, D.J., Greenhalgh, R., Zealley, I.A., Halligan, S., Taylor, S.A.: Mr enterographic manifestations of small bowel Crohn disease 1. *Radiographics* **30**(2), 367–384 (2010)
11. Sinha, R., Verma, R., Verma, S., Rajesh, A.: Mr enterography of Crohn disease: part 2, imaging and pathologic findings. *Am. J. Roentgenol.* **197**(1), 80–85 (2011)
12. Chaplot, S., Patnaik, L., Jagannathan, N.: Classification of magnetic resonance brain images using wavelets as input to support vector machine and neural network. *Biomed. Signal Process. Control* **1**(1), 86–92 (2006)
13. Cocosco, C.A., Zijdenbos, A.P., Evans, A.C.: A fully automatic and robust brain MRI tissue classification method. *Med. Image Anal.* **7**(4), 513–527 (2003)
14. Agnello, L., Comelli, A., Ardizzone, E., Vitabile, S.: Unsupervised tissue classification of brain MR images for voxel-based morphometry analysis. *Int. J. Imaging Syst. Technol.* **26**(2), 136–150 (2016)
15. Zhang, Y., Wu, L.: Weights optimization of neural network via improved BCO approach. *Prog. Electromagnet. Res.* **83**, 185–198 (2008)

16. Comelli, A., Agnello, L., Vitabile, S.: An ontology-based retrieval system for mammographic reports. In: 2015 IEEE Symposium on Computers and Communication (ISCC), pp. 1001–1006. IEEE (2015)
17. Yeh, J.Y., Fu, J.: A hierarchical genetic algorithm for segmentation of multi-spectral human-brain MRI. *Expert Syst. Appl.* **34**(2), 1285–1295 (2008)
18. Patil, N., Shelokar, P., Jayaraman, V., Kulkarni, B.: Regression models using pattern search assisted least square support vector machines. *Chem. Eng. Res. Des.* **83**(8), 1030–1037 (2005)
19. Wang, F.F., Zhang, Y.R.: The support vector machine for dielectric target detection through a wall. *Prog. Electromagnet. Res. Lett.* **23**, 119–128 (2011)
20. Xu, Y., Guo, Y., Xia, L., Wu, Y.: An support vector regression based nonlinear modeling method for SiC MESFET. *Prog. Electromagnet. Res. Lett.* **2**, 103–114 (2008)
21. Li, D., Yang, W., Wang, S.: Classification of foreign fibers in cotton lint using machine vision and multi-class support vector machine. *Comput. Electron. Agric.* **74**(2), 274–279 (2010)
22. Son, Y.J., Kim, H.G., Kim, E.H., Choi, S., Lee, S.K.: Application of support vector machine for prediction of medication adherence in heart failure patients. *Healthc. Inform. Res.* **16**(4), 253–259 (2010)
23. Zhang, Y., Wang, S., Ji, G., Dong, Z.: An MR brain images classifier system via particle swarm optimization and Kernel support vector machine. *Sci. World J.* **2013**, 9 (2013)
24. Tagluk, M.E., Akin, M., Sezgin, N.: Classification of sleep apnea by using wavelet transform and artificial neural networks. *Expert Syst. Appl.* **37**(2), 1600–1607 (2010)
25. Agnello, L., Comelli, A., Vitabile, S.: Feature dimensionality reduction for mammographic report classification. Springer (2016)
26. Martiskainen, P., Järvinen, M., Skön, J.P., Tiirikainen, J., Kolehmainen, M., Mononen, J.: Cow behaviour pattern recognition using a three-dimensional accelerometer and support vector machines. *Appl. Anim. Behav. Sci.* **119**(1), 32–38 (2009)
27. Deris, A.M., Zain, A.M., Sallehuddin, R.: Overview of support vector machine in modeling machining performances. *Procedia Eng.* **24**, 308–312 (2011)
28. Bermejo, S., Monegal, B., Cabestany, J.: Fish age categorization from otolith images using multi-class support vector machines. *Fish. Res.* **84**(2), 247–253 (2007)



# On the Design of a System to Predict Student's Success

David Bañeres<sup>(✉)</sup> and Montse Serra

IT, Multimedia and Telecommunications Department,  
Open University of Catalonia, Barcelona, Spain  
{dbaneres, mserravi}@uoc.edu

**Abstract.** Predictive models to evaluate student's performance have been widely used in the past. These models have been basically used as a statistical tool to predict whether students will pass a course based on previous background variables such as prior-learning or academic records. These models have a large potential to give support to teachers and learners during the learning process in real time. This paper focuses on the design foundations of a predictive core system. This core system is the essential component to build in the future a predictive support framework. Additionally, experimental results are shown to validate the quality of the designed system.

## 1 Introduction

Learning analytics (LA) appeared to give support to teachers to be aware of the learning process on their courses. The knowledge gathered by these systems helps to generate reports and visualizations on student's performance and actions. Their contribution on acquiring knowledge about how the course is progressing and giving evidences of activities or resources that can be improved is unquestionable.

LA has a limitation. Extensive reports can be generated, dynamic charts can be provided but all this information has to be interpreted, analyzed and, in case of showing some issues on the learning progress, it is the instructor that should find a way to solve the issue and there is no clue related on what will happen in the future.

Here, predictive models arise. They can be defined as the evolution of the LA systems. Based on all the information gathered by the LA systems, the predictive models can see beyond today and forecast future events. Note that, it is a prediction highly dependable on previous observations and, therefore, these models are error-prone. Notorious improvements have been done in prediction models related to the educational context. Since instructors are always concerned about the evolution of their students, extensively research has been performed over the past decades to try to predict student's success. In addition, these models also helped to identify the most influent indicators. Prior-learning, demographic information, student's actions, acquired competences among others are some examples of indicators used to create predictive models.

Predictive models have been extensively used as a statistical tool to understand the student's behavior. However, predictive models similar to LA can be used to give support to teachers on real time or give additional feedback to learners on their learning progress. Here, we refer as "real time" to be able to accurately predict some outcome

related to the course (e.g. acquire a competence or pass the course) with the minimal information related to the students.

The author in [1] specifies a personalized predictive system for an introductory course in digital systems and different predictive models were simulated in order to analyze the quality of them. This personalized system can be extended to support any course and creating highly configurable models according to the personalized characteristics of it. This paper focuses on the design of a system to give support to teachers and learners based on predictive models. The aim of the system is to predict in real time the chances to pass a course based on a different set of indicators. Previous to obtain the complete system, a core predictive module is needed to manage the personalized predictive models. The design of this core module is described in this paper.

The paper is organized as follows. First, related work to prediction models and systems is analyzed in Sect. 2. Section 3 describes the prediction system prototype. The prediction core module is shown in Sects. 4 and 5 summarizes the experimentation results on the designed module. Finally, conclusions and future work can be found in Sect. 6.

## 2 Previous Work

Research in learning analytics and its closely related field of educational data mining, has demonstrated much potential for understanding and optimizing the learning process [2]. To date, much of this research has focused on developing predictive models of academic success and retention [3]. Specifically, the prediction of students at risk of failing a course (i.e., a binary variable with two categories, fail and pass) and the prediction of students' grades (i.e., dependent numeric or classification variable that represents the final mark) have been two commonly reported tasks in the learning analytics and educational data mining literature [4]. These two types of success predictions have been based on the following sources of data such as: data stored in institutional student information systems (e.g., high school grades, socio-economic status, parents' education, and language skills) [5, 6]; trace data recorded by LMS and other online learning environments [7, 8]; and combinations of previous data sources [9, 10].

In addition, many authors, especially those from educational data mining backgrounds, have also reported highly accurate predictions using different classification algorithms such as C4.5, EM, Naïve Bayes, and SVM (Support Vector Machines). The development of these sophisticated machine-learning data mining techniques, as well as big data storage and processing capabilities, has allowed to go beyond traditional reporting about the past and move into an era where we can predict. For instance, students are often direct consumers of learning analytics, particularly through dashboards that support the development of self-regulated learning and insight into one's own learning. Predictive learning analytics helps students at the course level, solutions are also emerging to assist students at the program level by predicting which students may not complete their degree on time or which course would be the best for a specific student to take next.

At this point, research in predictive analytics focused on the capacity for early identification of students at-risk of academic failure allows a proactive approach to implement learning interventions and strategies that target teaching quality and student retention [11]. Despite a big progress in this type of research, a significant challenge remains and many examples of it are patent of the awaken interest.

In [12], “Degree Compass” determines which courses are needed for the student to graduate and ranks them according to how they fit with the sequence of courses in the student’s degree program and their centrality to the university curriculum as a whole. That ranking is then overlaid with a collaborative filtering model that predicts the courses in which the student is most likely to achieve the best grades.

Dashboards such as “Brightspace LeaP by D2L” [13] works with course learning objectives, content, and questions and provides a text representation for each component. It then uses semantic algorithms to find relationships among these components to make intelligent recommendations for what should be presented to a learner to meet a particular learning objective, what questions should be used to determine if a learner has met the objective, and what content items the learner should read if a particular question is answered incorrectly.

Other applications let instructors see where students stack up against each other in a course using specific metrics (i.e., course access, content access, and social learning) overlaid with what those numbers typically mean for academic performance. For example, the “Brightspace Student Success System” [14] developed by D2L uses regression models that predict student grades starting from the first weeks. Instructors can monitor the status of individual students regarding their predicted success.

### 3 Prediction System Prototype

Based on the particular case described in [1], this section describes the design of a more general prediction system. The system architecture is very simple as it is illustrated in Fig. 1. The core system is composed of a machine-learning engine. Different data sources are accepted as incoming data in order to train the models. Additionally, the generated models can be used to provide multiple services based on the knowledge acquired from the classification of the learners.

Each course can define multiple predictive models but it is recommended that a model is associated with a unique course or context. This condition will help to enhance the quality of each model since it will be created and trained based on the characteristics and needs of each particular course. The models will be feed with different indicators based on the available ones and can be created with different methodologies. Here, we propose to use machine-learning algorithms since the algorithms are well-known and no further research is needed in tuning the base machine learning algorithm. Several predictions can be done. Here, we start with the simplest one: *student passes the course or student fails the course*. The problem is a binomial classification problem and the type of the machine-learning algorithm selected is a supervised learning method because data from past students can be used to train the model. We can increase the complexity of the problem or seek other predictions such as predict the score of the student or

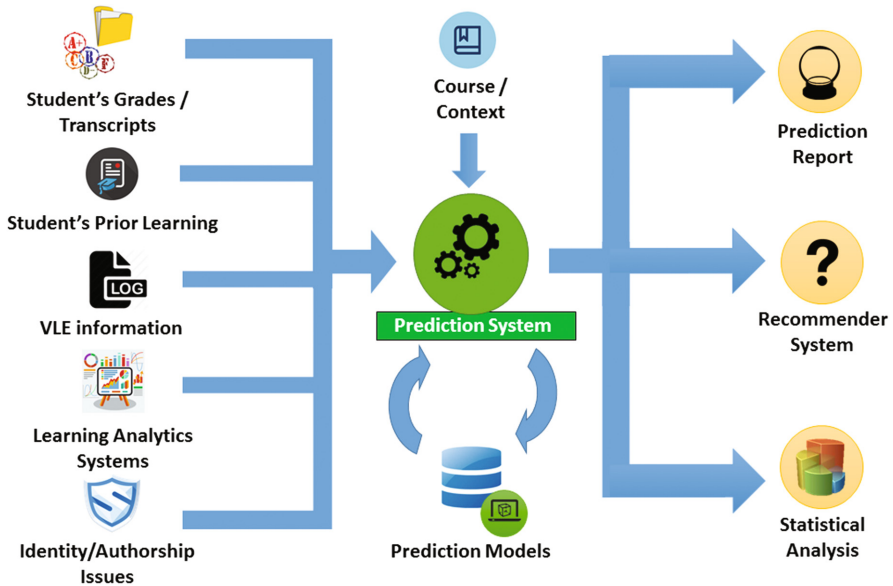


Fig. 1. Design of the prediction system

chances to drop out the course. However, this problem will be different and the algorithms used as well.

The main challenge together with the selection of the best algorithm is the selection of indicators to feed the model. In machine learning, the indicators are denoted as *features*. The model is characterized by the set of features that help to build and specify the model. Few features will generate a poor model with a high failure rate. Many features may generate an over fitted model or some features may be complementary or redundant. A trade-off between simplicity and quality should be found. Note that, the objective is to avoid static models. Thus, they will be dynamically improved by data obtained on each edition of the course. More data will generate in few editions fine-tuned models particularly applicable for each course.

Here, we have identified a set of potential data sources. Note that, this is an incomplete list that can be enlarged in the future:

- Student's grades or transcripts: This data source provides the performance of students in terms of grades. Transcripts are also accepted. A grade for each assessment activity (i.e. continuous, projects, and exams) can be retrieved. Quantitative (numerical) and qualitative (i.e. letter from A to F) grades are both acceptable depending on the type to grading used in the institution.
- Student's prior learning: In the previous section, we have observed that prior learning indicators have a significant impact on predictions mostly in science programs. However, basic knowledge such as mathematics can be broadly used in many specializations. Here, previous knowledge regarding course passed or acquired skills can be used to improve the quality of the models.

- VLE information: During the instructional process, the students interact with the VLE (virtual learning environment) and some actions can be logged. For instance, accessing to learning materials or interaction in the discussion forum. In on face-to-face learning, some learner actions can also be logged manually such as, the participation level during the class, whether she submits some non-assessment activities or she attends all laboratory/practice sessions. Online learning with a VLE is preferable since actions can be registered automatically.
- Learning analytics system: Some courses have tutoring systems or activities using some third-party platforms. These systems tend to store all attempts, accomplishments, and actions performed by the learner and provide an LA interface to report the results. We consider that all additional information related to the progression of the learner can be highly valuable to predict the student's success.
- Identity/authorship issues: This final category refers to all issues detected on the learner based on successful or failed identity or authorship checking. We consider that this information can also be used to create better models. Note that, these indicators have a high impact on models. For instance, a plagiarism detection can be penalized by the academic regulation with a fail score. Thus, this indicator in case of plagiarism detection will have an accuracy of 100% on the model.

Different potential outputs have been identified focused both for learners and for teachers:

- Prediction report: This service can be for learners and instructors. The objective is to predict whether the learner will pass the course based on her current information. Note that, several predictions can also be enabled within the course, i.e. to pass a specific assessment activity or chances to drop out.
- Recommender system: This service can also be used for learners and teachers. For the point of view of the learner, a recommender system should be able to specify which activity (or set of activities) should be done to “probably” pass the course. Also, this recommender system can be integrated into intelligent tutoring systems to create adaptive learning paths. Many common exercises solved by previous learners that have passed the course can be suggested. For the point of view of the instructor, the system could be used to advise the learner during the course and know at any time the progression of the student. A personalized feedback is highly appreciated by learners. Note that, the recommendation information can be easily extracted from rule-based or tree-based machine learning algorithms where the list of rules or the binary decision tree to reach a prediction can be extracted from the model.
- Statistical analysis: This service will be only used by instructors and academic coordinators. Statistical analysis on predictions and correlation among similar courses can be very useful to improve the course design and to share good practices.

In the next section, we will describe the design of the prediction core system.

## 4 Core System Implementation Details

Aforementioned, the objective of this section is to describe the different operations provided by the core system. The main operations are summarized next:

- To create a model (manual): First, the model (or models) for each course must be created. This operation aims to create a model based on the available indicators and select the features to be predicted.
- To gather evidences (automatic): The system must systematically gather evidences for the indicators selected for each model. Different approaches can be used to obtain the data information
- To update the model data information (automatic): At the beginning of each course session (semester), the model data information has to be built or updated based on internal and external sources. This operation creates or improves the data model to be used in the prediction phase.
- To generate a prediction (automatic): Finally, the model data information is used to generate the prediction.

In the next subsections, each operation will be described in detail. We ordered each operation based on the relationship among them.

### 4.1 Operation to Gather Evidences

One of the critical operations of the system is the one responsible for gathering all the evidences. The main challenge of this operation is the interoperability with other services since there is no standard format to describe each evidence. VLE log system uses one data model, student's transcripts or prior learning description are stored in another data warehouse. The same problem arises in the others data source. There are standard ontology models such as IEEE PAPI [15] and IMS LIP [16] but most of the current VLE does not support the export operation in those standard formats.

Another challenge is how this data is retrieved. Some services allow to install modules to send data periodically to other services. Others have some API that can be instantiated to gather information. Our service must be adapted to support all these characteristics.

We propose a data processing flow with two entry points: a server REST API and a client REST API. The server REST API allows to gather periodically information sent by other services. This API is used for services capable of implementing an interface or installing daemon-like processes to send events. The client API is used for the rest of the data sources. Some services are immutable but some interface is offered to query some information. In this case, it is our system that periodically triggers this operation to obtain the data based on a predefined period (i.e. at the beginning of the semester, every week, ...).

The data is formatted to a common data model before the processing step currently defined as the tuple:

⟨provider, student, course, semester, indicator, date, value⟩

Next, the data is validated, clean-up and fixed. Note that, some fields may not be provided (i.e. date may not be relevant when retrieving student's grades) or some errors may appear on the data. The REST APIs performs these operations to obtain valid tuples.

Finally, there is an evidence processor responsible for gathering these tuples and store in the data warehouse. Note that, there is two types of events: (1) events that do not need further processing such as grades or prior-learning information; and (2) events that require further processing. Data such as log events, learning analytics information or security events should be aggregated to be useful for the prediction model. For instance, if the events related to write messages to discussion forums are taken into account, the VLE log system will send this event every time the *student sends a message*. Then, the event processor will be responsible for aggregating this information and for creating an indicator which counts the number of messages.

## 4.2 Operation to Update the Model Data Information

This operation aims to create the data model information. The previous operation stores the indicators as defined by the previous tuple, that is, one row per indicator or event. However, the prediction of data model information uses another format to perform the prediction. The format is the next one:

$$\langle \text{student}, \text{value\_ind\_1}, \text{value\_ind\_2}, \dots, \text{value\_ind\_n} \rangle$$

As we can observe, this format aggregates all information related to one student in one row. This model data information can be updated each time the predictor generator is run. However, this decision can affect the performance of the system negatively.

We decided to create the operation that runs at the beginning of the semester using the information of the indicators of the previous semesters. This operation is straightforward when at least we have the information of a previous semester since an ETL (Extract-Transform-Load) process is executed to transform the data format. However, on new models, some data may not be available (i.e. events send by the VLE systems) mostly related to services that send data to the server REST API. This may produce the first semester with a lower quality model that will be fixed and improved in the next semesters. Another option is to create a first model without taking into account the unavailable indicators. Meanwhile, this data can be retrieved by the system and it will be used for the second semester to train a new model with the full list of indicators.

## 4.3 Operation to Create a Model

This operation is the responsible to support the creation of new models for courses. At this stage of the research, we have decided that this operation is completely manual. It is possible to create semi-automate or fully automate new models based on previous high-quality models created or simulated by the system. However, this is out the scope of this paper.

The data processing flow is composed of an indicator list generator and a manual checker. First, the list of available indicator must be known. There are three options to capture this information:

1. Indicators stored in the data warehouse: This is the simplest one. On a running system where previous semesters of events have been collected, the list of the available indicator can be easily known. Here, a query to the internal indicators is performed
2. Indicators gathered from the client REST API: Similar to the previous operation, on the first semester, the system does not have any indicator information. This option performs a query on the available evidences that can be gathered using the client REST API. Note that, no information is stored in the system. This query only reports the list of available evidences.
3. Indicators gathered from the server REST API: Similar to the client REST API, the list of evidences that can be collected using the server API has to be obtained. Here, we listen within a period (enough to get a full list of evidences) the services that periodically send data to the system.

These three options create a list of available evidences and, finally, using a manual checker, the model is created. The instructor will interact with the manual checker using a simple web form where she selects the list of indicators that will be collected and she will create aggregated indicators for evidences that need further processing. After this selection, there is the option to activate the evidence for the model. This double option stands for the problem related to indicators that are not available for the first semester of the model. The collect selection activates the collecting operation by the evidence processor, while the activate selection enables the indicator for the prediction model. Using these options, we will be able to have models with better quality in the second semester.

Finally, a prediction indicator and trigger event to perform the prediction must be also defined. Here, we assume the indicator the student has passed the course. However, the system is capable to select other indicators, for instance, whether the student will drop out in a certain activity. Note that, we assume a single prediction model. Other variants could be added in the future, such as, multivariate prediction models. Based on the trigger event, we have identified three options: (1) a predefined date, (2) an evidence received in the APIs, such as, the grade for an activity, and (3) manual trigger.

#### 4.4 Operation to Generate a Prediction

The last operation performs the prediction using all the information configured and collected with the previous operations. There is a prediction generator, which is a background process. This process has access to all models of the system and listens for the event that may trigger a model. When a trigger event is received efficiently seeks the prediction models that must be activated.

Then, the prediction is performed for each model (we have the data model information) and for each learner (we have the list of available evidences). At the end of the process, the prediction is stored in the data warehouse, ready to be queried by any service described in Sect. 3.



## 5 Experimental Results

In this section, an experiment has been performed using the core prediction module in one course in the Open University of Catalonia. The objective is to provide real prediction results and to evaluate the accuracy of two prediction models.

First, we describe the configuration of the system. Next, the results are shown with an evaluation of the quality of the models.

### 5.1 Configuration of the System

A prototype of the core module has been implemented with the four operations described in the previous section. Currently, there is no graphical interface in the prediction system and the creation of the system is performed based on an XML file and the output is exported to a CSV file.

The Open University of Catalonia is a fully online university where all the learning process is performed through a custom VLE. Each course has an online classroom where all the learning resources and assessment activities are placed and the learners can interact using a discussion forum. The assessment activities are submitted within the classroom using the CAR (Continuous Assessment Registry) and the grade and personalized feedback is provided using the same tool.

The VLE provides several services in REST APIs to access to a limited information related to the teaching process. Students, activities, grades for activities can be retrieved. Currently, the log information related to student's actions such as interaction in the discussion forum or with the learning resources is not available and only the technical team of the university (i.e. developers, VLE administrators) has access to it.

Based on this limitation, the experiment has been performed only using the information that can be accessed using our client REST API. The interaction with other services has been set as future work. Assessment activities and the activity grades REST API within CAR are queried and the trigger action has been set on the date when the grades are published to learners.

Several models have been created for each course. Precisely, one model for each submitted assessment activity (i.e. one model with only activity 1, one model with activity 1 and 2 and so on) where the prediction indicator is to pass the course (binary variable, pass or fail). Additionally, two variants of each model have been created denoted as pessimistic and optimistic model. The pessimistic model only considers the grade of the activities that the learner has submitted. This model on the first activities of the course has few evidences and the model tends to have a low accuracy. Additionally, the model tends to report that the learner needs a good grade to pass the course. This model is realistic and it can be valuable for the teacher. However, this model is not recommended for learner since it may contribute to discourage to continue when initial low grades are obtained. For this reason, we proposed an optimistic model where a grade of 5 out of 10 is assigned for activities not yet submitted. This model is ideal for learners since it motivates to continue even if bad grades are obtained on first activities. Thus, all these models have been created in the system and they have been assigned to the course.

Finally, the predictor generator has been created based on the experiment performed in [1]. The machine-learning algorithm J48 has been used using the WEKA [17] system. This algorithm has been used since it provided the best performance in cross validation for grades related to the assessment activities. WEKA is a collection of machine learning algorithms for data mining tasks and there is also an API to use the algorithms from JAVA code. The predictor generator outputs a CSV file with the results of the prediction for each model.

## 5.2 Analysis of the Experimental Results in Computer Structure

Computer Structure extends the concepts that have been seen in the previous course of Computer Fundamentals. The aim of this subject is to extend the vision of the basic structure of a computer and to describe the low-level language (assembler). The computer programming is performed in C language doing calls to assembler functions. The student will learn to develop functions in assembler and to add calls to these functions in higher-level languages using their own structures in C language. The learning process requires an investment in time of 10 h for week. The average total investment for a student is 150 h. Note that, this calculation is statistical.

The assessment is divided into 2 continuous assessment activities (CAA) and one compulsory final project (FP). The continuous assessment activities are proposed to check the progressive development of the contents of the course. The compulsory final project is used for the synthesis of all the concepts acquired during the course. The final project is divided into two parts (70% FP1, 30% FP2). The first one FP1 is compulsory to pass. However, there is an optional second submission in case of failing the first one. The second part FP2 is optional to reach the maximum score. There is also a final exam (FE) to evaluate these acquired concepts. The final mark (FM) of the course as we can observe on Eq. 1 is obtained by combining the results of the continuous assessment activities (CAA), the compulsory final project (FP) and a final exam (FE). The project and the exam are mandatory while the CAAs are optional, but they can improve the final mark.

$$FM = \text{MAX}(32, 5\%FE + 32, 5\%FP + 35\%CAAs, 50\%FP + 50\%FE) \quad (1)$$

Computer Structure has a strong relation with the previous course of Computer Fundamentals of the Bachelor of Computer Engineering. This course expands the knowledge of the hardware components that a programmer needs to know to successfully perform his tasks increasing the complexity of the contents. Thus, the high dropout rate that reaches values nearly 45% of enrolled students (over 250 students) in each semester is patent such as in the previous subject, Computer Fundamentals.

Table 1 summarizes the results. No cross validation has been done since it was performed in [1]. We show the accuracy and RMSE (root mean square deviation) for each model taking as training data the information from 2015 Fall and 2016 Spring semester and taking as test set the 2016 Fall semester. For each model, the accuracy and RMSE are calculated globally (General) for the model and distinctively when the model predicts pass or fail. We are interested in observing the model for each prediction.

**Table 1.** Accuracy of the models in Computer Structure

Asses. Act.	Predict.	Pessimistic				Optimistic			
		Total Pred.	Corr. Pred.	Acc.	RMSE	Total Pred.	Corr. Pred.	Acc.	RMSE
CAA1	Pass	99	74	0,74	0,50	239	116	0,48	0,71
	Fail	140	98	0,70	0,54	0	0	0	0
	General	239	172	0,72	0,52	239	116	0,48	0,71
FP1	Pass	88	76	0,86	0,37	239	116	0,48	0,71
	Fail	151	111	0,73	0,51	0	0	0	0
	General	239	187	0,78	0,46	239	116	0,48	0,71
CAA2	Pass	123	103	0,84	0,40	237	114	0,48	0,72
	Fail	116	103	0,89	0,33	2	2	0	1,00
	General	239	206	0,86	0,37	239	116	0,48	0,71
FP1 (2 <sup>nd</sup> chance)	Pass	118	110	0,93	0,26	122	113	0,93	0,27
	Fail	121	115	0,95	0,22	117	114	0,97	0,16
	General	239	225	0,94	0,24	239	227	0,95	0,22
FP2	Pass	120	112	0,93	0,25	120	112	0,93	0,25
	Fail	119	115	0,97	0,18	119	115	0,97	0,18
	General	239	227	0,95	0,22	239	227	0,95	0,22

For the pessimistic model, the accuracy increases on each activity. More data helps to predict better whether a student will pass/fail the course. The accuracy improves from 72% to 95%. Note that, better accuracy also decreases the RMSE of the models. It is interesting to note that the FP1 (second chance) is only for students who failed FP1 and FP2 is optionally for all students. Even in courses with activities not mandatory for all learners (i.e. some students will not have a grade for the activity), the model prediction is highly accurate. Note that, having the optional activity at the end of the course also influences positively on the accuracy. If the pass/fail predictions are analyzed, the accuracy is comparable for both possible values. On starting activities, pass prediction is better. However, the fail prediction is better when more data is available from CAA2.

If the optimistic model is analyzed, we can observe that is inaccurate. For CAA1, FP1 and CAA2, the model is inaccurate. On the FP1 (second chance) is the activity when the model starts to produce accurate predictions. Note that, assuming a grade of 5 out of 10 points for not yet submitted activities produces an error-prone model. It can be a good model for learners to improve the morale when activities are failed. However, it can produce overconfident learners or it can decrease the trust with the model by always predicting a pass prediction even when activities are failed.

## 6 Conclusions and Future Work

In this paper, we have presented the core module of the prediction system that aims to give support to the learning process. This system has a large potential in learning since teachers and learners can have information related to future events based on the current progress. The basic operations of the module have been presented and experimental results based on the real execution of the module has been shown.

There is still a long path to complete the full system. The system needs to experiment to find better accurate models and more indicators are required. VLE integration is critical to obtain this data. Additionally, a graphical interface is needed to show the prediction results. When all this will be ready, the teacher will be able to provide early-personalized feedback to learners that may potentially fail or drop out the course. Trying to reverse the fail predictions by means of this prediction system can be a handicap for instructors.

**Acknowledgments.** This work was funded by SOM Research group and the Spanish Government through the project: TIN2013-45303-P “ICT-FLAG: Enhancing ICT education through Formative assessment, Learning Analytics and Gamification”.

## References

1. Baneres, D.: Towards a particular prediction system to evaluate student's success. In: Proceedings of the 11th International Conference on P2P, Parallel, Grid, Cloud and Internet Computing, pp. 935–945 (2016)
2. Baker, R., Siemens, G.: Educational data mining and learning analytics. In: Sawyer, R.K. (ed.) Cambridge Handbook of the Learning Sciences. Cambridge University Press, Cambridge (2014)
3. Campbell, J., De Blois, P.B., Oblinger, D.G.: Academic analytics. A new tool for a new era. *Educause Rev.* **42**(4), 42–57 (2007)
4. Dawson, S., Gašević, D., Siemens, G., Joksimovic, S.: Current state and future trends: a citation network analysis of the learning analytics field. In: Proceedings of the Fourth International Conference on Learning Analytics and Knowledge, pp. 231–240. ACM, New York (2014)
5. Araque, F., Roldán, C., Salguero, A.: Factors influencing university drop out rates. *Comput. Educ.* **53**(3), 563–574 (2009)
6. Kovacic, Z.J.: Predicting student success by mining enrolment data. *Res. High. Educ. J.* **15**, 1–20 (2012)
7. Agudo-Peregrina, Á.F., Iglesias-Pradas, S., Conde-González, M.Á., Hernández-García, Á.: Can we predict success from log data in VLEs? Classification of interactions for learning analytics and their relation with performance in VLE-supported F2F and online learning. *Comput. Hum. Behav.* **31**, 542–550 (2014)
8. Romero, C., López, M. -I., Luna, J. -M., Ventura, S.: Predicting students' final performance from participation in on-line discussion forums. *Comput. Educ.* **68**, 458–472 (2013). <http://dx.doi.org/10.1016/j.compedu.2013.06.009>
9. Barber, R., Sharkey, M.: Course correction: using analytics to predict course success. In: Proceedings of the 2nd International Conference on Learning Analytics and Knowledge, pp. 259–262. ACM, New York (2012)
10. Jayaprakash, S.M., Moody, E.W., Lauría, E.J.M., Regan, J.R., Baron, J.D.: Early alert of academically at-risk students: an open source analytics initiative. *J. Learn. Anal.* **1**(1), 6–47 (2014)
11. Siemens, G., Long, P.D.: Penetrating the fog: analytics in learning and education. *Educause Rev.* **46**(5), 31–40 (2011)
12. D2L Degree Compass. <https://www.d2l.com>. Accessed 3 July 2017

13. Steven, L., Stephanie D.: Student explorer: a tool for supporting academic advising at scale. In: Proceedings of the First ACM Conference on Learning @ Scale Conference, pp. 175–176 (2014)
14. Brightspace Student Success System. <https://www.d2l.com/products/student-success-system/>. Accessed 3 July 2017
15. Draft Standard for Learning Technology - Public and Private Information (PAPI) for Learners (PAPI Learner) - Core Features, IEEE P1484.2.1/D8 (2001). [http://metadata-standards.org/Document-library/Meeting-reports/SC32WG2/2002-05-Seoul/WG2-SEL-042\\_SC36N0175\\_papi\\_learner\\_core\\_features.pdf](http://metadata-standards.org/Document-library/Meeting-reports/SC32WG2/2002-05-Seoul/WG2-SEL-042_SC36N0175_papi_learner_core_features.pdf). Accessed 3 July 2017
16. IMS Learner Information Packaging Information Model Specification, version 1.0 (2001). <http://www.imsglobal.org/profiles/lipinfo01.html>. Accessed 3 July 2017
17. Hall, M., Frank, E., Holmes, G., Pfahringer, B., Reutemann, P., Witten, I.H.: The WEKA data mining software: an update. SIGKDD Explor. Newslett. **11**(1), 10–18 (2009)

# DoppioGioco. Playing with the Audience in an Interactive Storytelling Platform

Rossana Damiano<sup>1(✉)</sup>, Vincenzo Lombardo<sup>1</sup>, and Antonio Pizzo<sup>2</sup>

<sup>1</sup> Dip. di Informatica and CIRMA, Università di Torino, Turin, Italy  
rossana@di.unito.it, vincenzo.lombardo@unito.it

<sup>2</sup> Dip. di Studi Umanistici and CIRMA, Università di Torino, Turin, Italy  
antonio.pizzo@unito.it

**Abstract.** In this paper, we address the gap between the editing and delivery of stories in interactive digital storytelling. Our system, “DoppioGioco” (DoublePlay), provides a software platform for training authors to deal with the response of the audience since the story editing phase. Offline, the author attaches emotional information to each story chunk; on stage, the author and the audience construct together the storytelling experience, in a software-enabled live game where the system responds at each turn to the emotional response of the audience.

## 1 Introduction

In the last two decades, storytelling practices and contexts have undergone huge changes, as pointed out by media theorists and practitioners [1, 12, 17, 23]: moving from its traditional realms of textual, linear delivery, to the digitally mediated, interactive communication that characterize today’s media, traditional storytelling has migrated to new forms of narration and new narratives types. Following the advent of “transmedia storytelling” [12] brought about by new media, social and mobile media have opened the way to “multi-party, co-constructed narration” [17], with new narrative forms where story and reality mix at the junction of gaming and social experience [1].

As advocated by M.L. Ryan [23] at the onset of this revolution, these changes may have not affected the nature of stories into depth, but have innovated the way stories are presented and the way the audience is engaged. In today’s media, the relationship with the audience has become less obvious, blurring the expectations about the audience’s response granted by traditional forms of storytelling. Given this background, it is necessary for today’s authors to refine their ability to handle the relation with the audience, taking into account the audience response since story editing. In this paper, we describe a software platform that establishes a tight relation between editing and interactive delivery of the story. The platform has been developed with the goal in mind to *train* the creators of narrative contents to write their stories while actively taking into account the response of the audience, and the emotional response in particular.

Traditionally considered an indirect achievement of the gifted storyteller [16], the evocation of an emotional response is less straightforward in digital platforms

than in traditional media [9]. Our system, called DoppioGioco (“DoublePlay”), deconstructs the emotional response of the audience, factorizing it at the chunk level in the story editing phase. Offline, the author attaches emotional information to each story chunk. On stage, the system plays a live game with a simulated audience, reacting at each turn to the audience’s response.

The paper is structured as follows: after explaining the motivations for our work (Sect. 2), we describe the functioning of the system in Sect. 3 and its architecture (Sect. 4). In Sect. 5, we illustrate a real case study in using of the system for training story editors, describing the re-design issues and guidelines emerged from this case study. Discussion and conclusion end the paper.

## 2 Background and Motivations

The inspiration for DoppioGioco draws from two main sources. On the one side, the line of research in studying and designing the experience of the audience [2, 20], situated at the junction of HCI and media studies (see the survey provided by [7]). In particular, [26] reconsiders the notion of “subversive player”, developed in game studies to describe the user’s attempts at breaking the boundaries of the interactivity allowed for by games, with the goal of making this behavior become an intrinsic propellant of the game. On the other side, a relevant source of inspiration is given by the attempts at bringing the paradigm of improvisational theater into interactive storytelling [3, 18, 25]. Typically considered a training tool for dramatic writing, the paradigm of improvisational theater increases the sense of dramatic presence and the engagement of the users, as demonstrated by [25]. The dynamics of improvisational theater has been described by [6] in the perspective of interactive storytelling, using the Decision Cycle from Newell’s Unified Theory of Cognition (*receive* new inputs, *elaborate* new knowledge, *propose* actions to take, *select* one of those actions, *execute* the action) as a conceptual framework for analyzing the way each performer takes advantage of the scene advancing moves of the others.

With respect to the approaches described above, our goal is not only to improve the effectiveness of the storytelling system, but to test an innovation in the paradigm of interactive storytelling for training purposes. Combining the tradition of the improvisational theater [2] with the insights from player studies, the “Decision Cycle” in our system achieves an improvisational dimension through the emotional response of the audience. The narrative component is mostly handled offline, at the story design time. The relationship with the audience is handled by the real time component, which is mainly concerned with emotions, those attached to the story contents and those expressed by the audience. Emotions have received much attention in interactive storytelling, both as a component of artificial characters, and as a feature of the story plot. In artificial character applications, emotions have become part of the processes that generate the character’s behavior [5, 10]. As a property of the story, emotions have been accounted for by a few storytelling systems [11, 21, 27], since the seminal work of Mateas and Stern [15], *Faade*, where the emotional engagement of

the user is controlled by a drama manager that keeps it aligned with the notion of dramatic climax.

Our approach is targeted at digital storytelling applications in new and social media, where story is not seen only as an appealing sequence of incidents, but a looser concatenation of events delivered in an interactive way. This is often the case in situated storytelling (e.g. in storytelling applications for cultural heritage and tourism), where the intrinsic coherence of the story gives way to the emotional engagement of the user. This design goal is achieved by moving the focus from the story level design of the audience response to a local, adjustable level of engagement in story delivery. DoppioGioco puts equal emphasis on editing and delivery, transforming the interactive delivery of story in a tight interplay of the audience's emotional responses and counter-responses by the system.

### 3 DoppioGioco

Consider the following scenario. W.S. jr. is a young author who wants to master the art of interactive storytelling. He intends to captivate the engagement of the audience, and wants to do so through the use of emotions. After conceiving the story line, he has created a number of story chunks that represent the alternative turning points of the plot and has associated each of them with the emotions he figures out in response by the audience. He runs a simulation of the story in front of the imaginary audience: he plays a story chunk, then observes the reaction of the audience: looking at the imaginary audience, he stares at their faces, trying to spot unexpected responses. Sometimes, he decides to please the audience, making the story advance in a way that reverberates the feelings expressed by the audience. Sometimes, he decides to strike the audience with something opposed to the audience's emotional reaction. Rehearsal after rehearsal, W.S. jr. navigates the story with different audiences and different attitudes, until he has attained a deep knowledge of the potential of his own creation. He can now edit the story again, and play it from scratch to find the desired balance of story direction and emotional twists and turns.

The software platform provided by DoppioGioco aims at realizing the scenario described above. Basically, the offline system consists of a navigable story chart annotated with emotions, and rules for managing the attitude towards the emotional reaction of the audience. Each story chunk, or *unit*, corresponds to a media asset that is played when the unit is selected. Online, the system plays the part of the storyteller, whose attitude affects the navigation through the story chart. At each step, the audience reacts to the last played story unit, then the initiative goes to the user: she/he decides whether to empathize with the audience or to antagonize it. The system selects the next unit among the suitable ones, depending on the interplay of the audience's emotional reaction and the selected attitude.

The system has two main functions: the Story Manager is the tool for editing the story units offline and organizing them in a plot; the Stage Manager is the online platform for managing the story advancement in response to the audience's reactions.

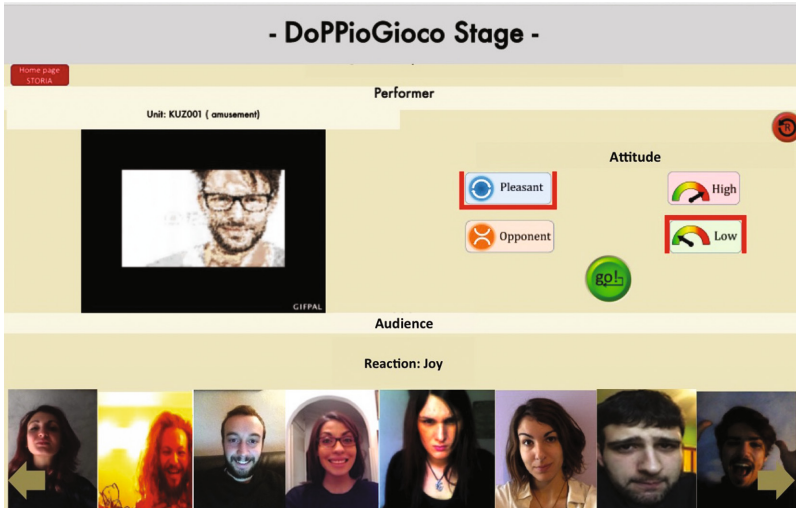




Fig. 1. DoppioGioco. The interface of the Story Manager.

The Story Manager allows the author to create and organize the units offline. Each unit consists of an audiovisual clip and a set of metadata elements describing it, such as title and textual description. For each unit, the author has to provide the information needed to the story engine to create a consistent story at runtime: the precedence relations with the other units, needed to generate a causally motivated story, and the emotions attached to the unit, needed to account for the response of the audience. So, each unit must be tagged with a set of emotions to ensure that the story engine can drive the story advancement based on the combination of the emotional response of the audience and the attitude chosen by the user. Figure 1 shows the interface for the editing of the units. The interface is divided into four areas: the top left area allows managing the unit metadata; the top right area allows uploading and viewing the media asset that realizes the unit (typically, an audiovisual clip); the bottom left area contains the emotion tags: for example, the unit displayed in the figure is tagged with the emotions of “anxiety” and “panic fear”; finally, the bottom right area allows specifying the units that precede and follow the unit. The story chart editing tool (not shown in the figure) allows the author to manipulate the position of the units in the story chart.

When the system is run in the online mode (“on stage”), the Stage Manager enters into play. By selecting an initial unit, the story begins to be told, unit by unit. After each unit, the audience reacts by displaying a set of emotions: like a real audience, the individuals who compose the public may react differently from each other, so the system computes the most frequent emotion. At this point, the author can decide to *please* or *oppose* the audience. After setting the reaction type (“against” or “pro”), the system will pick up the next unit among the continuations allowed by the story chart. If several continuation are compatible with the current story unit and the response of the audience,



**Fig. 2.** DoppioGioco. The interface of the Stage Manager.

the system selects one of them randomly. Figure 2 shows the interface for managing the stage. The interface is horizontally divided into two areas which represent, respectively, the storyteller (top area) and the audience (bottom area). The top area contains, on the left, the last played unit; the right area is occupied by the console for managing the attitude of the reaction to the audience: the four buttons it contains refer to the global parameters of the emotional control of the continuation, namely intensity (low or high) and polarity (negative or positive, i.e. “pro” or “against”). The lower part of the interface contains a button for getting the emotional reaction of the audience (“Get reaction”, not visible in the figure): when pressed, this button reveals the reaction of the audience and the button becomes invisible until the next unit is selected. For attaining a more realistic impression, the facial expressions of the single members of the audience are displayed (in the figure, the emotion of “joy” has been computed by the system for the audience). The “Go” button posited below the console (in green, see Fig. 2) triggers the selection of the next unit: the new unit is loaded, the console is reset and the faces of the audience are replaced by the button “Get reaction”. The system contains also a tool for managing the audience (adding and removing members, attaching a facial expression to the each member’s emotions, etc.). Notice that the reactions of audience are currently simulated by a random mechanism (see Sect. 4.3).

## 4 Bringing the Audience into Play

Following a standard practice in interactive storytelling, in DoppioGioco the story is represented through a plot graph (the story chart), with rules for transitioning from a node to the next one in order to generate a complete story.

#### 4.1 Narrative Model

Formally, the story is structured as a directed graph, where the nodes represent the story units. Edges represent the transition from a unit to the next unit. Nodes with no input edge are start nodes; nodes with no exiting edges are end nodes. Starting from a set of initial nodes, a story is a path traveling from a start node to an end node.

In the online mode, when the next unit is chosen, the clip associated to it is played. Units can be marked as initial or end units (not both). Each unit is labeled with a set of emotion tags, as shown in the previous section: they represent the emotions that the author expects the audience to feel when the unit clip is played. At each step, the story engine computes a set of admissible emotions for the next unit given the reaction type selected by the user. By doing so, emotions reduce the space of the possible stories to the stories that are consistent with the emotion model embedded in the system.

Figure 3 shows the visualization of the story automatically generated by an apposite functionality of the Story Manager: each box represents a unit, the edges represent the possible transitions from a unit to another (as described in Sect. 5, this functionality was added during the re-design following the testing of the system). The design of the graph is inspired by the following principles, aimed at facilitating its interpretation by the user:

- The graph is directed horizontally, distributing left to right the units that implement the shortest path from beginning to end. In particular, on the

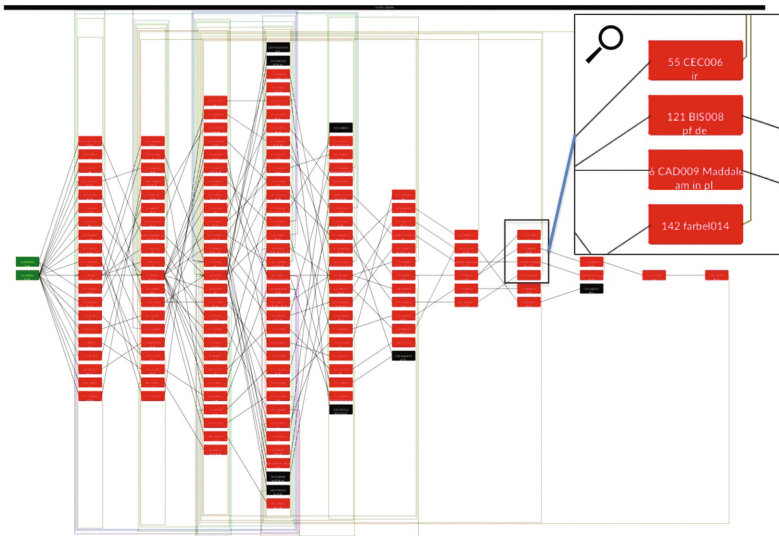


**Fig. 3.** The visualization of the plot. The box in the top left corner shows the details of some units: each unit has an id and a name; for brevity, emotions are replaced by tags: e.g., *ir* for “irritation”.

horizontal axis, units are displayed when they are first reached in moving from the initial units.

- On the vertical dimension, from the middle to the extremes, the nodes maximize the entering edges.
- Paths that are longer than the shortest paths (without repetitions) are represented with the contribution of edges that go back to a unit already introduced.

## 4.2 Annotating Emotions

As mentioned in Sect. 2, different computational models of emotions have been proposed in the last two decades, for purposes that range from the annotation of emotions in media to the generation of emotions in synthetic characters. The former systems typically rely on dimensional models, such as Russell's circumplex model of affect [22] or Plutchik's wheel of emotions [19], which lend themselves to the general description of the affective content of media, while the latter systems tend to draw inspiration from cognitive models of emotions [24], which are easily integrated in goal directed characters.

DoppioGioco relies on the model described in [4]: originally designed to support the creation of a corpus of clips displaying the performance of emotions by human actors (GEMEP), this model is based on an extensive survey of the existing theories and models of emotions, including cognitive and dimensional models. GEMEP, GENEVA Multimodal Emotion Portrayals, is a collection of audio and video recordings featuring actors portraying affective states, with different verbal contents and different modes of expression. Thanks to its syncretic and methodologically robust design, geared on performance, this model is especially suitable to annotate the affective content of media. In GEMEP, emotions are grouped based on two axes: the *polarity* (positive/negative) and the *intensity* (high/low arousal). The combination of these two axes provides four emotions families, each including 3 emotion types: amusement, anxiety, cold anger (irritation), despair, hot anger (rage), fear (panic), interest, joy (elation), pleasure (sensory), pride, relief, and sadness. Within each family, the emotion categories are mainly characterized by different arousal levels (such as fear and despair).

- **Positive, high intensity:** amusement, pride, joy;
- **Positive, low intensity:** relief, interest, pleasure;
- **Negative, high intensity:** hot anger, panic fear, despair;
- **Negative, low intensity:** irritation, anxiety, sadness;

In DoppioGioco, the story units and the reaction of the audience are both annotated with the 12 emotion categories of the GEMEP model. Designed for describing emotions in performance, the GEMEP model accounts for the cognitive emotions, such as fear or anger, that drama studies and narratology consider suitable for the narrative content; more importantly, since the GEMEP model relies on a polarity-based account on emotions, it is suitable to deal with the polarity of the reaction to the audience's response implied by DoppioGioco: the

decision to play against (or pro) the audience can be directly mapped onto the negative/positive dimension of emotions in this model, with “against” corresponding to the “opposite polarity” and “pro” to “same polarity”. The following *Reaction rules*, applied in a cascading way, determine the continuation of the story:

- **R1:** *If the selected choice is **pleasant**, then select the emotion families with the same polarity; else (the storyteller decides to be **opponent**), select the families with opposite polarity.*
- **R2:** Tune the intensity level of the reaction to the selected intensity (low or high), given the polarity established by R1.

In order to emphasize the elements of arbitrariness that characterize a live, interactive performance, a random element was introduced in the selection of the emotions within the selected family: given the available units, the system randomly selects the next unit among the available ones, so that the user does not have complete control on the selection.

For example, consider Fig. 2: the current clip corresponds to the unit KUZ001, tagged as “amusement” and the user has chosen to keep a pleasant attitude toward the audience (the active button, “pleasant”, is outlined in red) and to respond with a low intensity emotion. Following the reaction rules described above, if the audience responds with “joy” (as shown in the figure), the system will choose, among the available units, those that belong to the “Positive, Low intensity” family, namely one of the available units tagged with Relief, Interest and Pleasure.

### 4.3 System Architecture

The architecture of the system encompasses four main modules (see Fig. 4): the Story Manager, the Stage Manager, the Emotion Manager and the Audience Manager. The knowledge about the story and the media assets, created and uploaded offline through the interface displayed in Fig. 1, are embedded, respectively, into the Story Manager and into the Stage Manager (where they are stored in the Media Repository). The system loop orchestrates the interaction of the four modules in the following way:

1. The Audience Manager generates the reaction of the audience. The Audience Manager contains the description of the audience members and manages generates their emotional reaction when requested by the Stage Manager. In the current implementation, this module randomly extracts an emotion for each audience member and computes the most frequent emotion to generate the audience reaction.
2. The Emotion Manager computes emotions compatible with the selected attitude. The Emotion Manager takes as input the audience reaction and the selected attitude, and applies the Reaction Rules to compute the emotions, which become the input to the Story Manager.

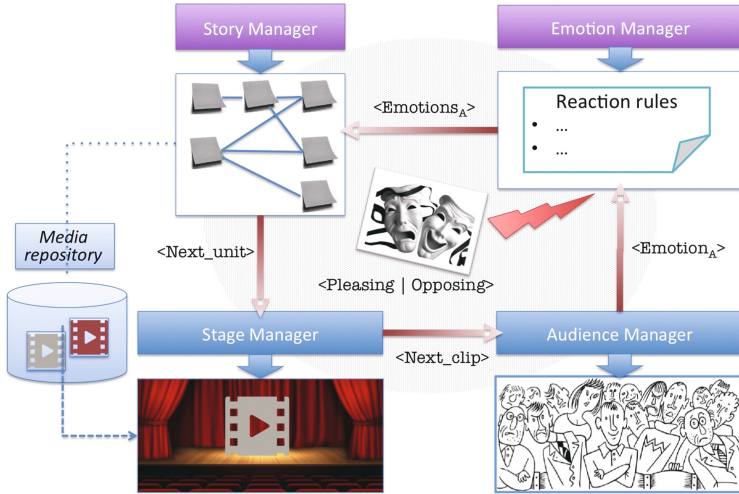


**Fig. 4.** The architecture of DoppioGioco. Red lines represent the control flow of the system.

3. The Story Manager selects the next unit. The Story Manager, the properly called the story engine, consults the story graph to select the possible continuations, filtering out the units that are not emotionally consistent with the attitude chosen for the response to the audience.
4. The Stage Manager takes as input the unit selected by the Story Manager and sends it to the player, activating the reaction console in the interface.

Each module of the system is implemented as a web service, so as to allow the portability of the system across different devices and media. The services are written in PHP and rely on a mySql database. The current interfaces have been developed as web pages and rely on the Ajax technology to support a fluid interaction with the user.

## 5 The System at Work

During the academic years 2015-16 and 2016-17, DoppioGioco provided the online platform for a writing lab targeted at graduate students in Arts and Media at the University of Turin. The goal of the lab was to teach the students to design and produce an interactive story by accounting for the emotions in the relation with the audience. We think that this lab provided a valid test-bed for assessing the potential of the platform for training goals.

The staff consisted of a writing coordinator, a media producer, and a developer. The writing coordinator was in charge of coordinating the conception of the story, the design of the characters and the editing of the story in textual form. The producer coordinated the production of the audiovisual clips that realize

the story units. A developer was included in the staff to debug and redesign the software system timely during the conduction of the laboratory. The first edition included 18 students; the second one, 17 students. A contest was held among the participants to decide the story plot, then the class collaboratively designed the story graph. Finally, the students were divided into small groups and were assigned the editing, annotation and production of the story units. The final product was delivered online.

In the first edition of the lab, the story, entitled “Clark”, was a thriller set in a hospital. In this story, the main character of the story is a hospital worker, Clark, who comes across some apparently paranormal events. With the help of a quite and poised young girl, Magdalene, Clark investigates the origin of the events in a climax of horror. But the tale is nothing but a dream made by Clark before his first day in the new job: the alarm clock rings, and he wakes up. In the second edition of the lab, we tested a looser type of narration, with a romance set in an American smalltown in the Sixties. In this story, entitled “Hot bread”, the characters go through changes in their personal lives as a result of their professional and relational crossroads. The story is more inspired to serial formats (such as TV fictions) than to the classical U-shaped stories that characterizes traditional storytelling.

The experience with DoppioGioco was crucial to develop a writing methodology that takes full advantage of the potential of the platform, and to identify the most suitable narrative type for working with the platform. In general, the students appreciated the approach underlying the system and correctly grasped the relation between the annotation of the units with the emotion tags and the generation of the story in the interplay with the audience. However, during the first year the management of the story graph emerged as main difficulty in using the system, so the plot visualization tool for the analysis of the story was added to the system (see Fig. 3). This led, in the second year of the lab, to a more careful design of the story graph. Thanks to the visualization of the story graph, the participants were able to limit the branching factor of the story by pruning some edges. Moreover, during the story editing, a minimality strategy emerged in the transition from the first to the second edition of the lab: in the second edition, for each family of emotions, only a representative was kept in the annotation, so as to limit the number of continuations by avoiding, at the same time, the proliferation of units and of emotion tags. As a result of the changes in the design and genre of the story, the number of units dropped from 156 in the first edition to 105 in the second edition. Moreover, due to the more thorough design of the story, in the second edition the duration of the story was a function of the intensity of the emotions: more intense audience responses (remember from Sect. 4.2 that intensity was one of the two dimensions of emotions) led to shorter stories, i.e., stories composed of lower number of units.

## 6 Discussion and Conclusion

The tension between the creation of well crafted, consistent story line and the emotional response of the audience was both a challenge and an opportunity

for the trainees. In particular, the factorization of the emotions in story editing, and the dualism between the roles of story editor and producer, were suitable to promote a change of paradigm in their design and editing practices.

The writing labs conducted with the system provided some useful insights for the redesign of the system. Putting forth emotions in the design of the story actually went against the standard practices previously learned by the students, mostly based on causal connections: as a result, designing the story in terms of emotions tended to put at risk the logical consistency of the incidents, requiring a careful control on the story graph. To alleviate this problem, a tool for checking their consistency, similarly to [14] may be added to the system.

The solution adopted in the current version of the system to generate the emotions of the audience was effective for training the students to cope with audience responses, but their randomization was sometimes frustrating. In order to reduce the gap between the author's expectations and the reactions of the audience, the set of emotions may be reduced to a more basic set. Moreover, the management of the audience may be dealt with by a dedicated audience modeling module, as proposed by [8], employing a linked data approach like the one exemplified by [13] to create a more realistic audience simulation from real data.

As future work, we plan to extend the use of the system to other storytelling forms, such as teaching and presentation, and in mixed forms, such as edutainment and infotainment.

## References

1. Alexander, B.: *The New Digital Storytelling: Creating Narratives with New Media: Creating Narratives with New Media*. ABC-CLIO, Santa Barbara (2011)
2. Alrutz, M., Listengarten, J., Wood, M.V.D.: *Playing with Theory in Theatre Practice*. Palgrave Macmillan, Basingstoke (2011)
3. Aylett, R., Louchart, S.: I contain multitudes: creativity and emergent narrative. In: *Proceedings of the 9th ACM Conference on Creativity & Cognition*, pp. 337–340. ACM (2013)
4. Bänziger, T., Scherer, K.R.: Introducing the geneva multimodal emotion portrayal (gemep) corpus. In: Scherer, K.R., Bänziger, T., Roesch, E.B. (eds.) *Blueprint for Affective Computing*, pp. 271–294. Oxford university Press, Oxford (2010)
5. Bates, J., Loyall, A.B., Reilly, W.S.: An architecture for action, emotion, and social behavior. In: Castelfranchi, C., Werner, E. (eds.) *MAAMAW 1992*. LNCS, vol. 830, pp. 55–68. Springer, Heidelberg (1994). doi:[10.1007/3-540-58266-5\\_4](https://doi.org/10.1007/3-540-58266-5_4)
6. Baumer, A., Magerko, B.: Narrative Development in Improvisational Theatre. In: Iurgel, I.A., Zagalo, N., Petta, P. (eds.) *ICIDS 2009*. LNCS, vol. 5915, pp. 140–151. Springer, Heidelberg (2009). doi:[10.1007/978-3-642-10643-9\\_19](https://doi.org/10.1007/978-3-642-10643-9_19)
7. Brooker, W.: *The Audience Studies Reader*. Psychology Press, Hove (2003)
8. Chollet, M., Wörtwein, T., Morency, L.P., Shapiro, A., Scherer, S.: Exploring feedback strategies to improve public speaking: an interactive virtual audience framework. In: *Proceedings of the 2015 ACM International Joint Conference on Pervasive and Ubiquitous Computing*, pp. 1143–1154. ACM (2015)
9. Giovagnoli, M.: *Transmedia Storytelling: Imagery Shapes and Techniques*. Etc Press, Halifax (2011)



10. Gratch, J., Marsella, S.: Tears and fears: modeling emotions and emotional behaviors in synthetic agents. In: Proceedings of the Fifth International Conference On Autonomous Agents, pp. 278–285. ACM (2001)
11. Hernandez, S.P., Bulitko, V., Hilaire, E.S.: Emotion-based interactive storytelling with artificial intelligence. In: *AIIDE* (2014)
12. Jenkins, H.: *Convergence Culture: Where Old and New Media Collide*. NYU press, New York (2006)
13. Kaneko, K., Okada, Y.: Facial expression system using japanese emotional linked data built from knowledge on the web. *Int. J. Space Based Situated Comput.* **4**(3–4), 165–174 (2014)
14. Lombardo, V., Damiano, R.: Semantic annotation of narrative media objects. *Multimedia Tools Appl.* **59**(2), 407–439 (2012)
15. Mateas, M., Stern, A.: *Façade: an experiment in building a fully-realized interactive drama*. In: Game Developers Conference, vol. 2 (2003)
16. Oatley, K.: A taxonomy of the emotions of literary response and a theory of identification in fictional narrative. *Poetics* **23**(1), 53–74 (1995)
17. Page, R.E.: *Stories and Social Media: Identities and Interaction*. Routledge, Abingdon (2013)
18. Perlin, K., Goldberg, A.: *Improv: a system for scripting interactive actors in virtual worlds*. In: Proceedings of the 23rd Conference on Computer Graphics and Interactive Techniques, pp. 205–216. ACM (1996)
19. Plutchik, R.: *Emotion: A Psychoevolutionary Synthesis*. Harpercollins College Division, New York (1980)
20. Reeves, S., Benford, S., O'Malley, C., Fraser, M.: Designing the spectator experience. In: Proceedings of the SIGCHI Conference On Human Factors in Computing Systems, pp. 741–750. ACM (2005)
21. Roberts, D.L., Narayanan, H., Isbell, C.L.: Learning to influence emotional responses for interactive storytelling. In: *AAAI Spring Symposium: Intelligent Narrative Technologies II*, pp. 95–102 (2009)
22. Russell, J.A.: Core affect and the psychological construction of emotion. *Psychol. Rev.* **110**(1), 145 (2003)
23. Ryan, M.: *Avatars of Story*. University of Minnesota Press, Minneapolis (2006)
24. Scherer, K.R.: Appraisal theory. In: Dalglish, T., Power, M. (eds.) *Handbook of Cognition and Emotion*, pp. 637–663. Wiley, Chichester (1999)
25. Swartjes, I., Theune, M.: An experiment in improvised interactive drama. In: Nijholt, A., Reidsma, D., Hondorp, H. (eds.) *Intelligent Technologies for Interactive Entertainment*, pp. 234–239. Springer, Heidelberg (2009)
26. Tanenbaum, J.: How i learned to stop worrying and love the gamer: reframing subversive play in story-based games. In: *Proceedings of DiGRA* (2013)
27. Zagalo, N., Göbel, S., Torres, A., Malkewitz, R., Branco, V.: INSCAPE: emotion expression and experience in an authoring environment. In: Göbel, S., Malkewitz, R., Iurgel, I. (eds.) *TIDSE 2006. LNCS*, vol. 4326, pp. 219–230. Springer, Heidelberg (2006). doi:[10.1007/11944577\\_23](https://doi.org/10.1007/11944577_23)

# BioGrakn: A Knowledge Graph-Based Semantic Database for Biomedical Sciences

Antonio Messina<sup>1</sup>(✉), Haikal Pribadi<sup>2</sup>, Jo Stichbury<sup>2</sup>, Michelangelo Bucci<sup>2</sup>,  
Szymon Klarman<sup>2</sup>, and Alfonso Urso<sup>1</sup>

<sup>1</sup> ICAR-CNR, via Ugo La Malfa 153, 90146 Palermo, Italy  
{antonio.messina,alfonso.urso}@icar.cnr.it

<sup>2</sup> Grakn Labs Ltd, Unit 22, 8 Hornsey Street, London, UK  
{haikal,jo,michelangelo,szymon}@grakn.ai

**Abstract.** The proliferation of biological research data generated and shared openly online is of huge benefit to the scientific community, but there are often significant challenges to overcome before it can be integrated from different sources and re-used to gain new knowledge. This paper introduces BioGrakn, which is a graph-based deductive database, combining the power of knowledge graphs and machine reasoning. BioGrakn illustrates how data can be aggregated and integrated, modelled in all its complexity and contextual specificity, and extended as needed. Built upon GRAKN.AI, it provides an integrated, intelligent database for researchers handling complex data.

**Keywords:** Knowledge representation and reasoning · Semantic web · Semantic data integration · Biomedical · Databases · Knowledge graphs

## 1 Introduction

Nowadays, the amount of biological data available online has proliferated, but this has been accompanied by enormous challenges arising from the need to integrate and connect related information from different sources [1].

Common problems include locating resources, differing data formats, ambiguity and duplication, relationships between data and the sheer volume and granularity of the information. As yet, there is no standard memorization and query format for this kind of data, so each resource usually requires a different approach to be properly handled.

Several classes of bio-molecular data, such as transcriptional regulatory networks and protein-protein interaction networks, interact as complex networks. They can usually be modeled as graphs, where nodes (and their attributes) model biological entities and edges contain relationships between these entities. Since query languages play a key role in the success of databases, in order to allow for efficient queries, these graphs can be stored either in relational or graph databases [2], where the latter by their nature seem to be a *natural* choice.

Examples of the adoption of graph databases in bioinformatics are given by ncRNA-DB [3], Bio4J [4], and BioGraphDB [5].

ncRNA-DB is a NoSQL database based on OrientDB [6] that combines many biological resources to deal with several classes of ncRNA such as miRNA, long-noncoding RNA (lncRNA), circular RNA (circRNA) and their interactions with genes and diseases.

Bio4j is based on a Java library and is an integrated cloud-based data platform, built upon a graph structure on top of Neo4J [7]. For now, it includes data about proteins, GO and enzymes.

Lastly, BioGraphDB integrates several types of data sources to perform bioinformatics analysis using a comprehensive system built on top of OrientDB. It includes data about genes, proteins, microRNAs, molecular pathways, functional annotations, and associations between microRNAs and cancer diseases.

No matter the chosen underlying architecture (relational or NoSQL graphs), every solution should also address the major issue of *semantic integrity*, that is, interpreting the real meaning of data derived from multiple sources or manipulated by various tools [8].

In the biological sciences, Semantic Web database technologies have seen significant adoption over the past decade, with some of the most fundamental and broadly known resources are being the EBI RDF platform [9], BioPortal [10], and Pathway Commons [11]. The uptake of these types of system has been summarized by Pasquier [12], who goes on to analyze the improvements needed before the Semantic Web is taken up by the majority of life science researchers.

Similarly, Livingston et al. describe the problems that persist in data integration, providing a case study of a knowledge base built on 18 large biomedical data sources [13]. KaBOB (the Knowledge Base of Biomedicine) is an integrated knowledge base of biomedical data and allows the underlying data to be queried in terms of biomedical concepts (e.g., genes and gene products, interactions and processes). KaBOB illustrates the concepts of shared identity and shared meaning across heterogeneous biomedical data sources.

Here, we introduce BioGrakn, based on GRAKN.AI [14], which is a deductive database in the form of a knowledge graph, allowing complex data modelling, verification, scaling, querying and analysis.

The database behind GRAKN.AI uses an ontology to facilitate the modelling of extremely complex datasets, functioning as a data schema constraint to guarantee information consistency. GRAKN.AI stores data in a way that allows machines to understand the meaning of information in the complete context of their relationships. Consequently, the semantic layer of Grakn allows computers to process complex information more intelligently, with less human intervention.

## 2 GRAKN.AI

GRAKN.AI is composed of two parts: Grakn (the storage), and Graql (a declarative query language).

## 2.1 Grakn

Grakn is built using several graph computing and distributed computing platforms, such as Apache TinkerPop and Apache Spark. Grakn is designed to be sharded and replicated over a network of distributed machines. The underlying data structure of Grakn is that of a labelled, directed hypergraph (Fig. 1).

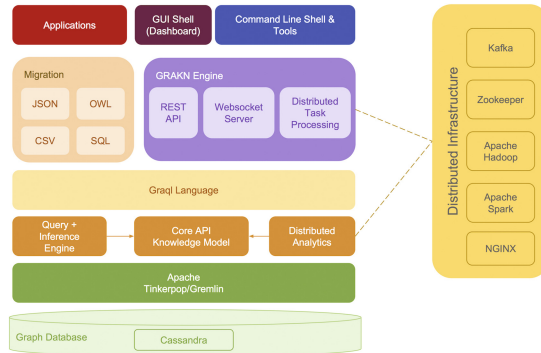


**Fig. 1.** The GRAKN.AI architecture

Grakn exposes a high-level knowledge model, allowing developers to represent their application domain as an ontology, specifying it in terms of entities, resources, relations, and roles. Grakn's ontology modelling constructs include, but are not limited to, data type hierarchy, relation type hierarchy, bi-directional relationships, multi-type relationships, N-ary relationships, relationships in relationships, and so on. Therefore, Grakn can model the real world and all the hierarchies and hyper-relationships contained within it.

## 2.2 Graql

Graql is a declarative, knowledge-oriented graph query language that uses machine reasoning to retrieve explicitly stored and implicitly derived knowledge from Grakn.

When using legacy systems, database queries have to define explicitly the data patterns they are looking for. Graql, on the other hand, will translate a query pattern into all its logical equivalents and evaluate them against the database. This includes, but is not limited to, the inference of types, relationships, context, and pattern combination. In this way, Graql can derive implicit information with concise and intuitive statements, reducing the complexity of expressing intelligent questions.

In Graql, there are different types of queries available: for matching patterns in the graph, inserting or deleting types and instances, and for computing useful information about the graph, such as statistics or shortest path between nodes.<sup>1</sup>

Two inference mechanisms are supported: *type inference*, based on the semantics defined in the ontology, and *rule-based inference*, that involves rules defined by expressions of the form *lhs G1 rhs G2*, where *G1* and *G2* are a pair of Graql patterns. Whenever the left-hand-side (*lhs*) pattern *G1* is found in the data, the right-hand-side (*rhs*) pattern *G2* can be assumed to exist and optionally materialized (inserted).

### 3 Data Sources

The data sources selected for database population are almost the same as those used by BioGraphDB. This way, we can build an integrated database containing resources related to genes, proteins, miRNAs, and metabolic pathways.

Getting into the details, we have considered the following:

- (1) *NCBI Entrez Gene* [15]: provides a lot of genes data, such as interactions with other genes, genomic context, annotated pathways, and so on.
- (2) *Gene Ontology (GO)* [16]: provides annotations for gene products in biological processes, cellular components and molecular functions.
- (3) *UniProt Knowledgebase (UniprotKB)* [17]: the largest public collection of annotated functional information on proteins.
- (4) *Reactome* [18]: contains validated metabolic pathways, each annotated as a set of biological events, dealing with genes and proteins.
- (5) *miRBase* [19]: provides all the known miRNAs sequences and annotations, associated with names, keywords, genomic locations, and references.
- (6) *mirCancer* [20]: contains associations between miRNAs and human cancers.
- (7) *miRNASNP* [21]: aims to provide a resource of the miRNA-related mutations (SNPs) for human and other species.
- (8) *mirTarBase* [22]: list of experimentally validated miRNA-target interactions.
- (9) *miRanda* [23]: list of putative miRNA-target interactions.
- (10) *HGNC* [24]: the HUGO Gene Nomenclature Committee database contains, for each gene symbol, a list of synonyms and a list of corresponding entries in the most popular genes databases.

Many of the above are supplied in *tab-separated values* (TSV) format, a simple text format for storing data in a tabular structure where each record in the table is one line of the text file, and each field value of a record is separated from the next by a tab character. By contrast, miRBase, GO, and UniprotKB are distributed as EMBL text file format [25] and XML format, respectively.

---

<sup>1</sup> Further information about syntax and keywords used by Graql can be found in <https://grakn.ai/pages/documentation/grawl/grawl-overview.html>.

## 4 BioGrakn

### 4.1 The Ontology

The ontology is a formal specification (in Graql) of all the relevant concepts and their meaningful associations in our domain. It must be clearly defined before loading data into the graph. This allows objects and relationships to be categorized into distinct types, enabling *automatic reasoning* over the represented knowledge, such as *inference* (extraction of implicit information from explicit data) and *validation* (discovery of inconsistencies in the data).

Grakn ontologies use four types of concepts for modeling domain knowledge. The categorization of concept types is enforced by declaring every concept type as a subtype of exactly one of the four corresponding built-in concept types: *entity*, *relation*, *role*, and *resource*.

Given the data sources considered in this work, our biological information has been associated to concepts, such as the ad-hoc defined subtypes shown in Table 1.

**Table 1.** Associations between Graql concepts, subtypes and biological information

Concept	Defined subtype	Biological information	Source
Entity	gene	genes	NCBI Entrez Genes
	go	functional annotations	Gene Ontology
	protein	proteins	UniProtKB
	pathway	pathways	Reactome
	mirna	miRNA precursors	miRBase
	mirnaMature	miRNA matures	miRBase
	mirnaSNP	miRNA SNPs	miRNASNP
	cancer	cancers	mirCancer
	proteinAccession	proteins accessions	UniProtKB
	geneName	genes symbols	HGNC
	interaction	miRNA-target interactions	mirTarBase, miRanda
Relation	annotation	links to annotated entities	Gene Ontology
	containing	links to entities contained in pathways	reactome
	precursorOf	precursors-matures relations	miRBase
	regulation	regulations of miRNAs in cancers	mirCancer
	snpMutation	miRNA-mutations relations	miRNASNP
	entity Reference	relations for entities synonyms	UniProtKB, HGNC
	encoding	genes-proteins coding	HGNC
	interactionMiRNA	miRNAs-interactions relations	mirTarBase, miRanda
	interaction—Gene	genes-interactions relations	mirTarBase, miRanda

## 4.2 Data Import

Two ways are supported for migrate data into a Grakn graph, the native migration capabilities and the *Loader Client API*. Both require the preliminary definition of an ontology for the data in Graql.

The former currently supports migration of CSV, JSON, OWL and SQL data. First, in order to map the data to the ontology, some Graql templates must be created. Then, it is possible to invoke the Grakn migration facilities through the shell or the migration API.

Even though most of the considered data sources are supplied in TSV format, a variant of CSV, their complexity and the extreme abundance of data and external references haven't allowed us to create related templates easily and quickly. Also, EMBL and XML source data files are not supported.

For this reason, we have developed an ad-hoc set of Extract-Transform-Load (ETL) tools. They have been written in Java and use the Loader Client API, in order to load large quantities of data into BioGrakn using multithreaded batch loading.

Data consistency and proper relations between entities are guaranteed by precise order of execution of the ETLs. This way, when a data source also refers to others, the presence in the database of all the depending resources is assured.

## 5 Results

In this section, we briefly introduce some illustrative queries and results representing typical bioinformatics problems, starting from the simplest.

### 5.1 Search for Genes Linked to a Particular Gene Ontology Annotation

Let's consider the Gene Ontology annotation "*platelet activating factor biosynthetic process*", that has *GO:0006663* as identifier. In order to find annotated genes, the *annotation* relation, with the functional annotation member equal to our starting identifier, points out all the related annotated entities, from which we extract the genes, printing their symbols and names. The following Graql query returns the desired results, shown in Fig. 2 in graph form:

```
match $go has goId "GO:0006663";
      (functionalAnnotation: $go; annotatedEntity: $gene) isa annotation;
      $gene isa gene;
```

### 5.2 Search for Pathways Linked to a Particular Gene

At a first sight, this seems like the previous problem. However, genes cannot be directly linked to pathways, because Reactome just provides pathway-to-proteins associations. Therefore, we have to go through two relations: *encoding*, that links genes to proteins, and *containing*, that links pathways to proteins. Thus, the Graql query is formed as follows (Fig. 3):

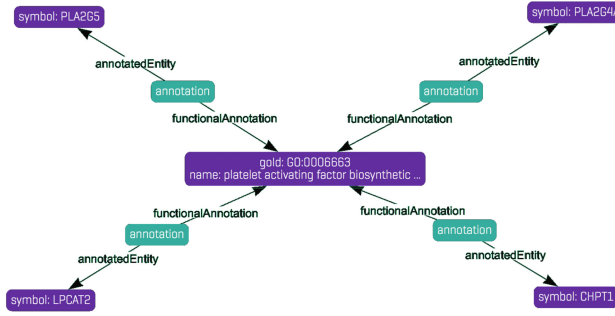


Fig. 2. Graphic results of a search for genes linked to GO annotation *GO:0006663*.

```

match $gene has symbol "LYPLA1";
(encoder: $gene, encoded: $protein) isa encoding;
(precursor: $path, contained: $protein) isa containing;
$path isa pathway;
    
```

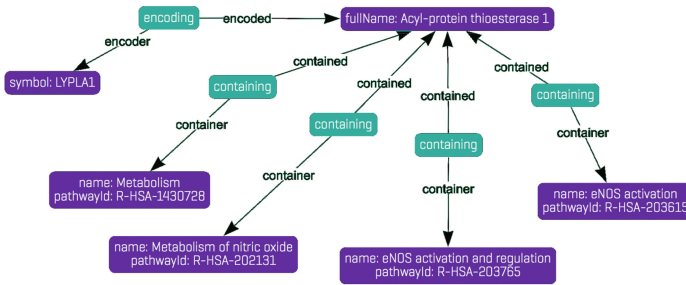


Fig. 3. Graphic results of a search for pathways linked to gene *LYPLA1*.

### 5.3 Differentially Expressed miRNAs Having SNPs in Cancer

Starting from a specific cancer, such as, for example, the *colorectal cancer*, we want to find all the up-regulated differentially expressed (DE) miRNAs that also have validated mutations. Because we are just interested in SNPs existence instead of their details, we can exclude them in the output, by selecting only entities of interest. Results for the following query are shown in Fig. 4:

```

match $cancer isa cancer has name "colorectal cancer";
(upRegulator: $mirna, upRegulated: $cancer) isa upRegulation;
(precursor: $mirna, mature: $mature) isa precursorOf;
(mutated: $mature, snp: $snp) isa snpMutation;
select $cancer, $mirna, $mature;
    
```



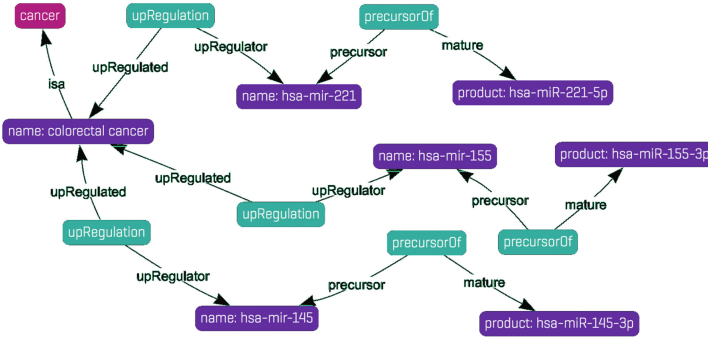


Fig. 4. Looking for DE miRNAs having SNPs for “colorectal cancer”.

### 5.4 Reasoning on Our Biological Data

It is interesting to note how queries can be rearranged when using inference rules, especially the ones corresponding to typical query templates used in the domain of biological sciences.

For instance, considering the example in Subsect. 5.2, we have the following statements, that can be seen as a *set of premises*:

```

    if genes codify proteins
    if proteins belong to pathways
  
```

Thus, it is possible to infer the following *fact*:

```

    then genes can be linked to pathways
  
```

Therefore, we can write an inference rule that infers genes-pathways links:

```

$genesInPathways isa inference-rule
  lhs {
    $gene isa gene; $protein isa protein;
    (encoder: $gene, encoded: $protein) isa encoding;
    (container: $pathway, contained: $protein) isa containing;
  }
  rhs {
    (container: $pathway, contained: $gene) isa containing;
  }
  
```

This rule allows us to rewrite the query reported in Subsect. 5.2 this way:

```

match $gene has symbol "LYPLA1";
  (container: $pathway, contained: $gene) isa containing;
  
```

As expected, the graphic results now show direct links from gene to pathways (Fig. 5).

Similarly, we can heavily rewrite the query in Subsect. 5.4 thanks to an inference rule like this:

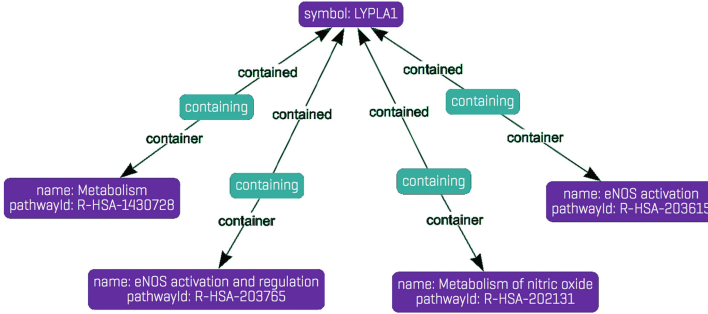


Fig. 5. Graphic results of reasoning on gene-pathways links.

```

$matureWithSNPsByCancer isa inference-rule
lhs {
  $cancer isa cancer; $mirna isa mirna; $mature isa mirnaMature;
  (upRegulator: $mirna, upRegulated: $cancer) isa upRegulation;
  (precursor: $mirna, mature: $mature) isa precursorOf;
  (mutated: $mature, snp: $snp) isa snpMutation;
}
rhs {
  (byCancer: $cancer, mirnaWithSNP: $mature) isa matureWithSNPsByCancer;
}

```

The rewritten query and its results are shown below (Fig. 6).

```

match $cancer isa cancer has name "colorectal cancer";
(byCancer: $cancer, mirnaWithSNP: $mature) isa matureWithSNPsByCancer;

```

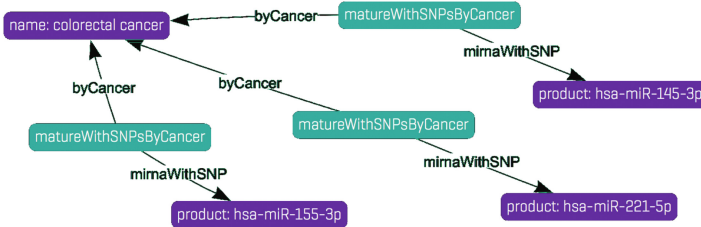


Fig. 6. Graphic results of reasoning on cancers and miRNAs with SNPs.

## 6 Conclusions and Future Works

In this paper, we propose BioGrakn, a graph-based semantic database that takes advantage of the power of knowledge graphs and machine reasoning, to solve problems in the domain of biomedical science. The database has been designed to overcome problems related to the lack of a structural organization and interoperability of publicly available biological resources, ensuring the semantic integrity of data by design.

BioGrakn has been built on top of GRAKN.AI, a distributed knowledge graph database which allows complex data modeling, verification, scaling, querying and analysis. A key step is the definition of an ontology, which facilitates the modeling of complex datasets and guarantees information consistency.

Inference rules allow the extraction of implicit information from explicit data, to achieve logical reasoning over the represented knowledge.

In the short term, further developments are expected, such as the integration of other publicly available biological resources, the use of the native GRAKN.AI migration tools for data migration procedures, and the deployment of an user-friendly web interface.

## References

1. Cheung, K.H., Smith, A.K., Yip, K.Y., Baker, C.J., Gerstein, M.B.: Semantic web approach to database integration in the life sciences. In: *Semantic Web*. Springer, US (2007)
2. Have, C.T., Jensen, L.J.: Are graph databases ready for bioinformatics? *Bioinformatics* **29**(24), 3107–3108 (2013)
3. Bonnici, V., Russo, F., Bombieri, N., Pulvirenti, A., Giugno, R.: Comprehensive reconstruction and visualization of non-coding regulatory networks in human. *Front. Bioeng. Biotechnol.* **2**, 69 (2014). doi:10.3389/fbioe.2014.00069
4. Pareja-Tobes, P., Tobes, R., Manrique, M., Pareja, E., Pareja-Tobes, E.: Bio4j: a high-performance cloud-enabled graph-based data platform. *Era7 bioinformatics*, Technical Report (2015)
5. Fiannaca, A., La Rosa, M., La Paglia, L., Messina, A., Urso, A.: BioGraphDB: a new GraphDB collecting heterogeneous data for bioinformatics analysis. In: *BIOTECHNO 2016: The Eighth International Conference on Bioinformatics, Bio-computational Systems and Biotechnologies*, Lisbon, Portugal, pp. 28–34 (2016)
6. Orient Technologies Ltd: OrientDB Community Edition. <http://orientdb.com>
7. Neo Technology Inc: Neo4J <https://neo4j.com>
8. Pettifer, S., Thorne, D., McDermott, P., Marsh, J., Villéger, A., Kell, D.B., Attwood, T.K.: Visualising biological data: a semantic approach to tool and database integration. *BMC Bioinform.* **10**(6), S19 (2009)
9. Jupp, S., Malone, J., Bolleman, J., Brandizi, M., Davies, M., Garcia, L., Gaulton, A., Gehant, S., Laibe, C., Redaschi, N., Wimalaratne, S.M., Martin, M., Le Novère, N., Parkinson, H., Birney, E., Jenkinson, A.M.: The EBI RDF platform: linked open data for the life sciences. *Bioinformatics* **30**, 1338–1339 (2014). (Oxford, England)
10. Whetzel, P.L., Noy, N.F., Shah, N.H., Alexander, P.R., Nyulas, C., Tudorache, T., Musen, M.A.: BioPortal: enhanced functionality via new web services from the national center for biomedical ontology to access and use ontologies in software applications. *Nucleic Acids Res.* **39**(Web Server issue), W541–W545 (2011)
11. Cerami, E.G., Gross, B.E., Demir, E., Rodchenkov, I., Babur, O., Anwar, N., Schultz, N., Bader, G.D., Sander, C.: Pathway commons, a web resource for biological pathway data. *Nucleic Acids Res.* **39**(Database issue), D685–D690 (2011)
12. Pasquier, C.: Biological data integration using semantic web technologies. *Biochimie* **90**(4), 584–594 (2008)
13. Livingston, K.M., Bada, M., Baumgartner, W.A., Hunter, L.E.: KaBOB: ontology-based semantic integration of biomedical databases. *BMC Bioinform.* **16**(1), 126 (2015)

14. Grakn Labs Ltd: GRAKN.AI. <https://grakn.ai>
15. Schuler, G.D., Epstein, J.A., Ohkawa, H., Kans, J.A.: Entrez: molecular biology database and retrieval system. *Methods Enzymol.* **266**, 141–162 (1996)
16. The gene ontology consortium: gene ontology consortium: going forward. *Nucleic Acids Res.* **43**(D1), 1049–1056 (2015)
17. The UniProt: a hub for protein information. *Nucleic Acids Res.* **43**(D1), 204–212 (2015)
18. Croft, D., Mundo, A.F., Haw, R., Milacic, M., Weiser, J., Wu, G., Caudy, M., Garapati, P., Gillespie, M., Kamdar, M.R., Jassal, B., Jupe, S., Matthews, L., May, B., Palatnik, S., Rothfels, K., Shamovsky, V., Song, H., Williams, M., Birney, E., Hermjakob, H., Stein, L., D'Eustachio, P.: The reactome pathway knowledgebase. *Nucleic Acids Res.* **42**(D1), 472–477 (2014)
19. Kozomara, A., Griffiths-Jones, S.: miRBase: integrating microRNA annotation and deep-sequencing data. *Nucleic Acids Res.* **39**, 152–157 (2011). Database issue
20. Xie, B., Ding, Q., Han, H., Wu, D.: miRCancer: a microRNA-cancer association database constructed by text mining on literature. *Bioinformatics* **29**(5), 638–644 (2013)
21. Gong, J., Tong, Y., Zhang, H.M., Wang, K., Hu, T., Shan, G., Sun, J., Guo, A.Y.: Genome-wide identification of SNPs in microRNA genes and the SNP effects on microRNA target binding and biogenesis. *Hum. Mutat.* **33**(1), 254–263 (2012)
22. Hsu, S.-D., Tseng, Y.-T., Shrestha, S., Lin, Y.-L., Khaleel, A., Chou, C.-H., Chu, C.-F., Huang, H.-Y., Lin, C.-M., Ho, S.-Y., Jian, T.-Y., Lin, F.-M., Chang, T.-H., Weng, S.-L., Liao, K.-W., Liao, I.-E., Liu, C.-C., Huang, H.-D.: miRTarBase update 2014: an information resource for experimentally validated miRNA-target interactions. *Nucleic Acids Res.* **42**(D1), 78–85 (2014)
23. John, B., Enright, A.J., Aravin, A., Tuschl, T., Sander, C., Marks, D.S.: Human microRNA targets. *PLoS Biol.* **2**(11), e363 (2004)
24. Gray, K.A., Yates, B., Seal, R.L., Wright, M.W., Bruford, E.A.: Genenames.org: the HGNC resources in 2015. *Nucleic Acids Res.* **43**(D1), 1079–1085 (2015)
25. Baker, W., Van den Broek, A., Camon, E., Hingamp, P., Sterk, P., Stoesser, G., Tuli, M.A.: The EMBL nucleotide sequence database. *Nucleic Acids Res.* **28**(1), 19–23 (2000)

# Security Infrastructure for Service Oriented Architectures at the Tactical Edge

Vasileios Gkioulos<sup>1(✉)</sup> and Stephen D. Wolthusen<sup>1,2</sup>

<sup>1</sup> Norwegian Information Security Laboratory,  
Norwegian University of Science and Technology, Trondheim, Norway  
{vasileios.gkioulos, stephen.wolthusen}@ntnu.no

<sup>2</sup> School of Mathematics and Information Security, Royal Holloway,  
University of London, Egham, UK

**Abstract.** The requirement for enabling network centric warfare through the accommodation of network-enabled capabilities, promoted the use of service oriented architectures (SOA) within military networks. The initial response of the academic and industrial communities was to utilize standard enterprise SOA. The developed solutions were well adjusted to the strategic domain, where node and network constraints were minimal. Yet, experience gained from the battlefields of the last decade, has proven that the tactical domain imposes a set of unique constraints, that render such solutions inefficient for the tactical edge.

The project TACTICS, supported by the European Defense Agency, focuses on the study and development of a SOA dedicated to tactical networks. In this paper we present the designed security service architecture, as developed in accordance to the requirements identified in our earlier studies. Each service is presented as an architectural element within the TACTICS TSI (Tactical Service Infrastructure), aiming to highlight the distinct functionalities of the security infrastructure towards the efficient enforcement of security controls at the tactical edge.

**Keywords:** Ad-Hoc · Security · Service oriented architectures · Tactical networks · Tactical service infrastructures

## 1 Introduction

The introduction of SOA across the strategic domain of military networks has been promoted by the increasing requirement for the integration of Network Enabled Capabilities (NEC), within the developed C2 (Command and Control) and C4I (Command, Control, Communications, Computers and Intelligence) systems. Extending this paradigm to the tactical domain, is expected to allow the widespread incorporation of Network Centric Warfare (NCW), by improving situational awareness and increasing network flexibility, adaptability and responsiveness at the tactical edge.

However, standard enterprise SOA have been proven across the AoO (Areas of Operations) of recent conflicts to be unsuitable for tactical networks, due to

their rapidly evolving nature and constrained resources. The project TACTICS [1] is oriented towards the theoretical and experimental analysis of contemporary tactical networks, in respect to the feasibility and required adaptations for the deployment of SOA. Consequently, and in accordance to these studies, a Tactical Service Infrastructure (TSI) has been defined and experimentally demonstrated. The TSI architecture [2] was developed according to the NATO Architecture Framework 3.1, including twenty discrete architectural perspectives.

Focusing on the security aspects of such an architecture, our study was initiated by analysing system specific constraints and requirements, arising due to terminal and network characteristics across the three mission stages (Preparation, Execution, Debrief). This allowed the identification of fine-grained security requirements and protection goals, maintaining the necessary distinction between the communication [3] and service domains [4].

Accordingly, these requirements have been translated into corresponding functional characteristics, for a security policy framework and service infrastructure, that would be suitable for the investigated environment. Furthermore, an extended state of the art review, revealed the weaknesses of existing mechanisms but also suitable adaptations that would satisfy the identified requirements under the imposed constraints [5]. These initial studies, allowed us to analyse, define and develop a suitable security policy framework [6], along with the corresponding distribution [7], reconciliation [8] and QoS (Quality of Service) interoperability [9] mechanisms.

In this article we present the core security service infrastructure, as developed within the TACTICS TSI in accordance to the aforementioned studies. These components are suitably adjusted towards satisfying the identified requirements, by facilitating the operation of the developed security policy framework and supporting mechanisms. The remainder of this paper is structured as follows: Sect. 2 presents the functionalities and interactions of each developed service, as an architectural element towards the extraction of valid policy decisions. Subsequently, Sect. 3 includes a discussion over the operational complexity of the security service infrastructure, in accordance to early results from the ongoing field and laboratory experiments/demonstrations.

## 2 TACTICS Security Architecture

The developed security architecture, consists of two distinct groups of services, namely core and functional. The functional services are responsible for the enforcement of the requisite protection goals, by instantiating the distinct mechanisms (e.g. encryption algorithms, access control, intrusion detection), while the core security services are responsible for the governance of these mechanisms, in accordance to predefined security policies. In this section we present these components (Fig. 1), aiming to highlight the processes involved in the extraction of suitable policy decisions (Figs. 2 and 3). It must be noted that the security policy framework developed within TACTICS for the accommodation of the requirements imposed by contemporary tactical SOA, has been presented earlier in detail [6] and is outside the scope of this article.

The main functionalities of each service as presented in Figs. 1, 2 and 3 can be summarised as:

- **Security Handling service**
  1. Initiate the internal policy decision extraction process.
  2. Store and identify the applicability of precomputed policy decisions.
- **Policy Management service**
  1. Control the policy decision extraction process.
  2. Prioritize pending policy decision requests.
- **Policy Decision Point service**
  1. Securely store the prioritized rule stacks that have been defined for each available policy decision request.
- **Metadata Handling service**
  1. Accommodate the defined ontological knowledge base (Including both the Terminological-box and Assertional-box) and the selected inference engines.
  2. Extraction of policy decisions.
- **Contextual Monitoring service**
  1. Monitoring and collection of dynamic attributes.
  2. Generation of statistical and aggregated data.
  3. Triggering of event driven policy decisions to the Security Handling service.
  4. Update of Metadata Handling service A-box to current values.
- **Policy Enforcement Point service**
  1. Translation and enforcement of extracted policy decisions.

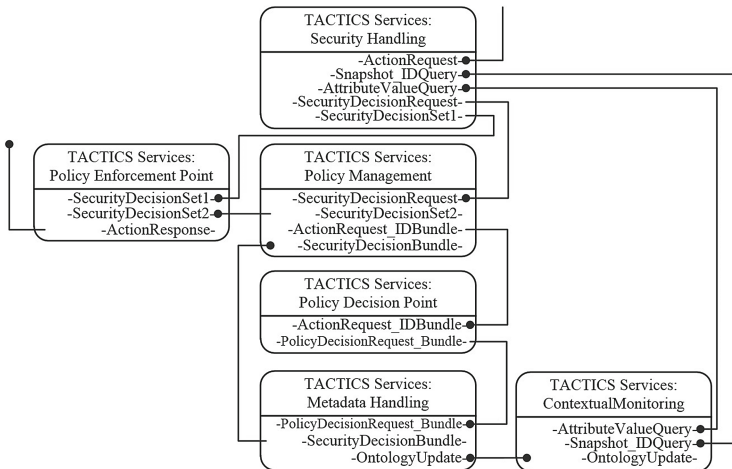


**Fig. 1.** Interfaces of the developed core security services.

### 2.1 Security Handling Service

**Description:** The Security Handling (SH) service operates as the internal to the security architecture action (policy decision) requester. The service can be invoked either externally (By a predefined set of core and functional services, for which the required interfaces have been established for the invocation of corresponding policy decisions) or internally (By the Contextually Monitoring (CM) service, for event driven policy decisions). The service accommodates precomputed policy decisions for the reduction of the computational overhead imposed by the security architecture. These are established at the mission preparation stage, according to a statistical analysis of previous invocation logs and the use of computational intelligence methodologies. Thus, precomputed policy decisions can be established for a constraint range of the required semantics, and after local evaluation, be directly applied without the invocation of the complete security service stack (Fig. 2). When such precomputed policy decisions are not available or applicable, the SHs must compose and forward a security decision request to the subsequent security services, providing all the required information for the adaptation, prioritization and successful extraction of valid policy decisions.

**Invocation:** Invocation Originator  $\implies$  Invocation Form

1. Set of core and functional services (RequestorID)  $\implies$  ActionRequest.
2. Contextual Monitoring (CM) service  $\implies$  Pre-established ActionRequest according to attribute threshold alert.

**Functionalities:** Internal= $*$ , Input= $\implies$ , Output= $\leftarrow$

- 1  $\rightarrow$  Receive ActionRequest
- 2  $*$  Generate ActionRequest.ID



Fig. 2. Sequence diagram for valid precomputed policy decisions.



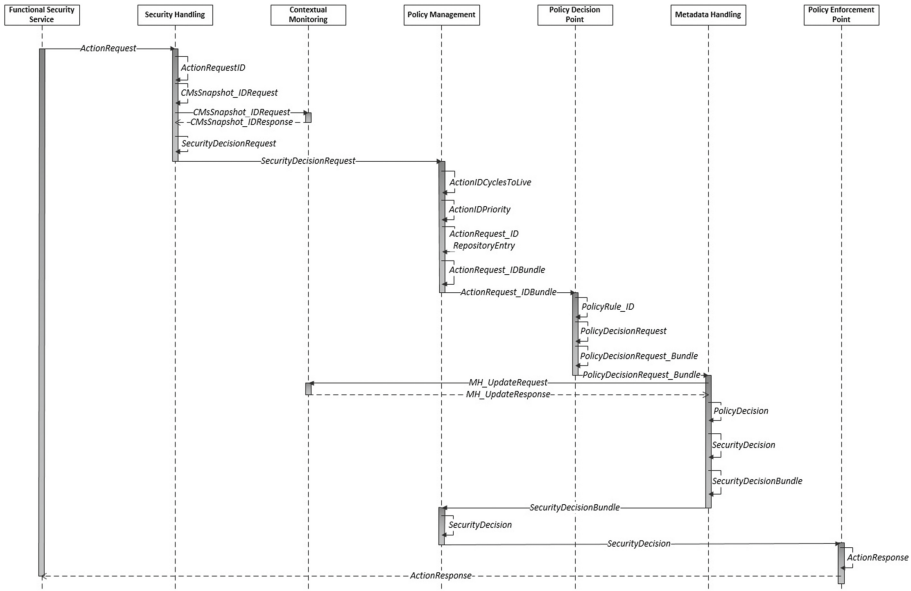


**Fig. 3.** Sequence diagram for the on-line extraction of policy decision.

3-\* Identify existence of precomputed PolicyDecision. According to ActionRequest\_ID

a-\* IF(TRUE)

i-\* Identify required attributes

ii-\* Generate AttributeValuesRequest

iii- Send AttributeValuesRequest to CMs for timely values

iv- Receive AttributeValuesResponse from CMs

v-\* Evaluate attributes of precomputed PolicyDecision

1-\* IF(TRUE)

a-\* Generate SecurityDecision

b- Send SecurityDecision to PEPs for enforcement

2-\* IF(Not TRUE)

a-\* Generate CMsSnapshot\_IDRequest

b- Send CMsSnapshot\_IDRequest to CMs

c- Receive CMsSnapshot\_IDResponse from CMs

d-\* Generate SecurityDecisionRequest

e- Send SecurityDecisionRequest to PMs

b-\* IF(Not TRUE)

i-\* Generate CMsSnapshot\_IDRequest

ii- Send CMsSnapshot\_IDRequest to CMs

iii- Receive CMsSnapshot\_IDResponse from CMs

iv-\* Generate SecurityDecisionRequest

v- Send SecurityDecisionRequest to PMs

## 2.2 Policy Management Service

**Description:** The Policy Management (PM) service operates as the controller of the security services that are involved in the policy decision extraction process. The PMs can be explicitly invoked by the Security Handling (SH) service, or execute functionality according to the input received from the Metadata Handling (MH) service. The invocation from the SHs includes all the required information for the management of a viable policy decision extraction within a security decision request. In addition to the action request related elements, an aggregated metric of the available local node resources (for the prioritization of policy decision requests) and a refresh alert based on predefined constraints (for the update of the MHs to the current state of dynamic semantics) are also included. Upon receipt of a security decision request, the corresponding cycles to live and priority are identified according to the received available resources metric. Consequently, a corresponding entry is generated and included within a repository with all the pending security decision requests. The repository entries are prioritized and a bundle is created, including those requests that can currently be served. The cycles to live of those requests is reduced and the bundle is forwarded to the Policy Decision Point (PDP) service. It must be noted that the cycles to live metric is critical, since it affects the maximum complexity of the policy rule that will be used for the resolution of the security decision request.

**Invocation:** Invocation Originator  $\implies$  Invocation Form

1. Security Handling (SH) service  $\implies$  SecurityDecisionRequest.
2. Metadata Handling (MH) service  $\implies$  SecurityDecisionBundle.

**Functionalities:** Internal= $*$ , Input= $\rightarrow$ , Output= $\leftarrow$

- For invocation type 1:
  - 1 $\rightarrow$  Receive SecurityDecisionRequest from SHs
  - 2 $*$  Extract RefreshAlert from SecurityDecisionRequest
  - 3 $*$  Extract ResourceAvailability from SecurityDecisionRequest
  - 4 $*$  Identify ActionIDCyclesToLive (For the received ActionID)
  - 5 $*$  Identify ActionIDPriority (For the received ActionID)
  - 6 $*$  Generate ActionRequest\_IDRepositoryEntry
  - 7 $*$  Update ActionRequest\_IDRepository (Enter new entry)
  - 8 $*$  Prioritize ActionRequest\_IDRepository (According to 3, 4, 5)
  - 9 $*$  Generate ActionRequest\_IDBundle
  - 10 $*$  Update (Reduce by one) ActionIDCyclesToLive in ActionRequest\_IDRepository  
(For those included in the ActionRequest\_IDBundle)
  - 11 $\leftarrow$  Send ActionRequest\_IDBundle to PDPs
  - 12 $*$  Update ActionRequest\_IDRepository (Remove entries with ActionIDCyclesToLive equal to zero)
- For invocation type 2:
  - 1 $\rightarrow$  Receive SecurityDecisionRequest from MHs
  - 2 $*$  Extract PolicyDecision /s

3-\* *Extract ActionRequest\_ID /s*  
   a-\* *IF(PolicyDecision TRUE)*  
     i-\* *Generate SecurityDecision /s*  
     ii- $\leftarrow$  *Send SecurityDecision/s to PEPs for enforcement*  
     iii-\* *Delete ActionRequest\_IDRepositoryEntry /s*  
   b-\* *IF(PolicyDecision NotTRUE) OR IF(ActionRequest\_IDRepository NotEMPTY)*  
     i-\* *Prioritize ActionRequest\_IDRepository*  
     ii-\* *Generate ActionRequest\_IDBundle*  
     iii-\* *Update (Reduce by one) ActionIDCyclesToLive in ActionRequest\_IDRepository (For those included in the ActionRequest\_IDBundle)*  
     iv- $\leftarrow$  *Send ActionRequest\_IDBundle to PDPs*  
     v-\* *Update ActionRequest\_IDRepository (Remove entries with ActionIDCyclesToLive equal to zero)*

### 2.3 Policy Decision Point Service

**Description:** The Policy Decision Point (PDP) service operates as a repository of the predefined policy rules. Each ActionID is mapped at the mission preparation stage to a set of ActorIDs, SubjectIDs and RequestorIDs in accordance to a corresponding set of semantics (Referring to Services, Information, Networks, Radios, Nodes and Subjects). These mappings constitute the predefined policy rules. Thus, a set of prioritized policy rules of increasing granularity are defined for any given range of the allowed ActionRequest\_IDs. Furthermore, an escape rule of least priority is defined for each ActionRequest\_ID range, in order to allow the enforcement of security policy decisions under heavily constrained local-node and radio resources. The received ActionIDCyclesToLive indicator defines which of the prioritized rules should be utilized for the given policy reasoning cycle. Accordingly, upon receipt of an ActionRequest\_IDBundle, the individual ActionRequest\_IDs are separated and bound to the corresponding policy rules (PolicyRule\_ID). This is achieved by the individual evaluation of their ActionIDCyclesToLive and rule identification across their predefined rule-sets. The generated PolicyDecisionRequest\_Bundle contains these ActionRequest\_ID/PolicyRule\_ID pairs and the received RefreshAlert indicator.

**Invocation:** Invocation Originator  $\implies$  Invocation Form

1. Policy Management (PM) service  $\implies$  SecurityDecisionRequest.

**Functionalities:** Internal=\*, Input= $\rightarrow$ , Output= $\leftarrow$

1- $\rightarrow$  *Receive ActionRequest\_IDBundle from PMs*  
 2-\* *Extract RefreshAlert from ActionRequest\_IDBundle*  
 3-\* *Extract individual ActionRequest\_ID / ActionIDCyclesToLive pairs*  
 4-\* *Identify PolicyRule\_ID according to ActionIDCyclesToLive*  
 5-\* *Generate PolicyDecisionRequest /s*  
 6-\* *Generate PolicyDecisionRequest\_Bundle*  
 7- $\leftarrow$  *Send PolicyDecisionRequest\_Bundle to MHs*

## 2.4 Metadata Handling Service

**Description:** A variety of semantic web frameworks can be used for the implementation of the Metadata Handling (MH) service, such as CubicWeb, RDF4J(Sesame), Mulgara, Open Semantic Framework and Jena. The MHs receives a bundle of policy decision requests and updates the local ontology, if required so by the received RefreshAlert. The value of the RefreshAlert originates from the Contextual Monitoring (CM) service (From CmsSnapshot\_IDResponse), which bound to an ActionRequest initiation, is used to update the local ontology through the MH\_UpdateRequest/Response process. After this update, the exact functionality order depends on the selected semantic web framework. Yet, the required functionalities are: Structure ontological construct > Invoke reasoner > Query local ontology (According to the received PolicyRule\_ID) for policy decision. The result of this process is then matched with the corresponding ActionRequest\_ID and transferred back to the Policy Management (PM) service.

**Invocation:** Invocation Originator  $\implies$  Invocation Form

1. Policy Decision Point (PDP) service  $\implies$  PolicyDecisionRequest\_Bundle.

**Functionalities:** Internal= $*$ , Input= $\implies$ , Output= $\leftarrow$

1 $\leftarrow$  Receive PolicyDecisionRequest\_Bundle from PDPs

2 $*$  Extract RefreshAlert

a $*$  IF RefreshAlert TRUE

i $\leftarrow$  i. Send MH\_UpdateRequest to Contextual Monitoring service

ii $\leftarrow$  Receive MH\_UpdateResponse from CMs

iii $*$  Update local ontology

3 $*$  Extract PolicyDecisionRequest/ s from PolicyDecisionRequest\_Bundle

4 $*$  Create reasoner

5 $*$  Insert ontological terminology and assertions

a $*$  For(all PolicyDecisionRequest/ s)

i $*$  Extract PolicyRule\_ID from PolicyDecisionRequest

ii $*$  Query local ontology according to PolicyRule\_ID

iii $*$  Extract PolicyDecision

iv $*$  Generate SecurityDecision

6 $*$  Generate SecurityDecisionBundle

7 $\leftarrow$  Send SecurityDecisionBundle to Policy Management (PM) service

## 2.5 Contextual Monitoring Service

**Description:** The Contextual Monitoring (CM) service is not strictly bound to the security architecture, since it serves multiple other actors and services including the quality of service (QoS) architecture. The functionalities of CMs relate to the maintenance of local awareness over the context under which the tactical nodes operate, including local and remote dynamic information, related to services, information, networks, radios, nodes and subjects. These information

are collected locally through other services and by exploiting cross layer functionalities. Furthermore, entries in the CMs can be updated globally utilizing policy administration processes. It must be noted that CMs can also generate aggregated and statistical data for use within policy rules of limited priority. This allows the definition of simplified policy rules of limited computational complexity, for use under constrained network or local resources. For the two invocation cases initiated by the Security Handling (SH) service, the CMs only returns timely values of the corresponding attributes. Yet, for the invocation initiated by the Metadata Handling (MH) service, the exact implementation of this process is system specific and can vary significantly in terms of the syntax, context or both, regarding the information transferred through the MH\_UpdateResponse. In this sense, the generated MH\_UpdateResponse may refer to a complete and updated policy copy or only the timely values of the dynamic data and object properties (In which case their incorporation occurs at the MHs, during inserting the ontological terminology and assertions – Line 5 of MHs: functionalities).

**Invocation:** Invocation Originator  $\implies$  Invocation Form

1. Security Handling (SH) service  $\implies$  AttributeValuesRequest.
2. Security Handling (SH) service  $\implies$  CMsSnapshot\_IDRequest.
3. Metadata Handling (MH) service  $\implies$  MH\_UpdateRequest.

**Functionalities:** Internal= $*$ , Input= $\rightarrow$ , Output= $\leftarrow$

- For invocation type 1:
  - 1- $\rightarrow$  *Receive AttributeValuesRequest from SHs*
  - 2- $*$  *Extract requested attributes*
  - 3- $*$  *Extract attribute values*
  - 4- $*$  *Generate AttributeValuesResponse*
  - 5- $\leftarrow$  *Send AttributeValuesResponse to SHs*
- For invocation type 2:
  - 1- $\rightarrow$  *Receive CMsSnapshot\_IDRequest from SHs*
  - 2- $*$  *Extract timely value of ‘ResourceAvailability’ semantic*
  - 3- $*$  *Extract timely value of ‘RefreshAlert’ semantic*
  - 4- $*$  *Generate CMsSnapshot\_IDResponse*
  - 5- $\leftarrow$  *Send CMsSnapshot\_IDResponse to SHs*
- For invocation type 3:
  - 1- $\rightarrow$  *Receive MH\_UpdateRequest from MHs*
  - 2- $*$  *Generate MH\_UpdateResponse*
  - 3- $\leftarrow$  *Send MH\_UpdateResponse to MHs*

## 2.6 Policy Enforcement Point Service

**Description:** The Policy Enforcement Point (PEP) service operates as the output of the core security policy architecture towards the rest of the security or TSI services deployed in the processing pipeline. The role of the PEPs is to identify the service that provides the functionalities required for the enforcement of the policy decision, translate it to a suitable format for enforcement, and communicate it to the initial RequestorID.

**Invocation:** Invocation Originator  $\implies$  Invocation Form

1. Security Handling (SH) service  $\implies$  SecurityDecision.
2. Policy Management (PM) service  $\implies$  SecurityDecision.

**Functionalities:** Internal= $*$ , Input= $\rightarrow$ , Output= $\leftarrow$

1- $\rightarrow$  Receive SecurityDecision from SHs or PMs

2- $*$  Extract RequestorID from ActionRequestID

3- $*$  Generate ActionResponse

4- $\leftarrow$  Send ActionResponse to RequestorID

## 2.7 Functional Security Services

Additionally to the aforementioned core security architecture components, a variety of functional services can be incorporated in a modular manner through the TSI processing pipeline. These services refer to the enforcement of all the predefined protection goals (e.g. cryptography, management of digital certificates, access control, authentication, credential management, integrity protection, information labelling and filtering, security token management, provenance assurance).

In addition to some non security related services (e.g. packet queue, service registry, message session management), these functional security services are expected to invoke the extraction of policy decisions. Therefore, these services are assigned a RequestorID, and incorporate the appropriate interfaces towards the Security Handling service and from the Policy Enforcement Point service (Denoted earlier as the singular ActionRequest and ActionResponse interfaces). These services can be defined following standardized processes. Yet, the developed architecture allows the incorporation of national and tailored solutions, satisfying the requirement for modularity towards the security enforcement mechanisms.

## 3 Test Case Based Validation

As presented earlier, the designed TSI is targeted to the tactical domain. Thus the test cases used for the validation of the designed architecture were developed in accordance to common tactical operations, the experience gained from recent battlefields and the analysis of future requirements. The used tactical operations (e.g. Convoy, Reconnaissance Surveillance and Target Acquisition (RSTA), intervention patrol, medical Evacuation (MEDEVAC), cordon and search, area denial) have been separated to specific use cases (e.g. Blue force tracking, Common Operational Picture (COP) distribution, injection of high mobility nodes, improvised explosive device (IED) detection and report, interoperability with police forces) and detailed episodes (Addressed request/reply, multihop service invocation, service discovery, transitive service delivery, node isolation).

The communication between the defined core security services is achieved using SOAP (Simple Object Access Protocol) messages, allowing the remote

procedure call across the services. It is apparent that the service functionalities as presented earlier, correspond mainly to simple message modifications or substitutions. In this case a dedicated process receives a SOAP message (request) that contains all the required parameters, and transforms it into an invocation of the corresponding method. The resulting SOAP message (response) contains the required parameters for the continuation of the policy decision extraction process. Following this model, as presented in Fig. 3, an `ActionRequest` (according to its components) is mapped to a `SecurityDecisionRequest` by the Security Handling service. Consequently, the `SecurityDecisionRequest` (according to its components) is mapped to an `ActionRequest_IDRepositoryEntry` by the Policy Management service, while the process continues until the extraction of a valid `ActionResponse` towards the corresponding functional security service.

According to the results of our experiments, it is important to note that the complexity and dynamic adaptability of the developed mechanism is situated at the structure of the ontological knowledge base, the governing policy rules, the fine grained definition of action requests and the detailed incorporation of the available semantics, as described earlier [3,5–8]. Contrary to that, the functionalities of the presented core security services are kept at a low complexity level aiming for clear separation of duties within the policy decision extraction process. Thus, the identification of the appropriate `SecurityDecisionRequest` by the Security Handling service is a low complexity matching/querying process, despite of the fine-grained definition of security actions as a conjunction of the security domains (e.g. protection, detection, diligence, response) and network capabilities (e.g. NCV-NATO Capability View).

The executed validation experiments highlighted the functionalities of the Metadata Handling service, and more precisely the reasoning phase (See: Metadata Handling Service/Functionalities/5.a.i to iv), as the process with most significant impact in terms of computational complexity within the policy decision extraction process. Aiming to counteract this obstacle and maintain the support of the required network functionalities, under a constrained operational status or across low capacity nodes, a variety of countermeasures have been deployed within the security policy mechanism, which are visible in the functionalities of the presented services.

- The Security Handling service can incorporate precomputed policy decisions, when this has been deemed necessary at the mission preparation stage.
- The Policy Management service utilises resource availability metrics at the prioritization of the `ActionRequest_IDRepositoryEntries`.
- The Policy Decision Point service connects each `ActionRequest_ID` to a `PolicyRule_ID` in accordance to resource availability metrics. Thus, for each reasoning cycle the complexity of the utilised policy rule depends on the locally available computational capacity. Additionally, as presented earlier, a default policy escape rule must be defined (Across the prioritized dedicated rule stack) for each possible `ActionRequest_ID` for use under highly congested scenarios.

- The Metadata Handling service can incorporate supplementary reasoners (OWL, OWL Mini, OWL Micro) and instances of the local ontological knowledge base, for use under highly congested scenarios.
- Finally, a dedicated policy distribution mechanism has been developed [7], for the purpose of allowing the core security service architecture presented in this article, to be operable across the various platforms deployed within a tactical network.

## 4 Conclusions

Our research within the security aspects of TACTICS is tripartite. The first completed aspect was to analyse the requirements, validate, and recommend suitable controls and mechanisms for their attainment (e.g. Recommendation of suitable solutions for the enforcement of the identified protection goals through the functional services). Consequently, the development of a suitable security policy framework, able to support and govern the functionality of the aforementioned mechanisms was required, and has been developed as presented earlier. The last major contribution towards a tactical SOA, has been presented in this article and relates to the design of a core security service architecture, able to instantiate the functionalities of the other two elements. The developed architecture provides configuration flexibility in a modular manner, while satisfying the defined requirements dynamically under varying network conditions. Additional SOA benefits include the information flow and performance improvement, maintaining the capacity to integrate existing or tailored assets, with reduced development and management cost. In our future work we intent to utilize our existing experimental results with the experience gained from the recent demonstration of the overall TACTICS TSI, towards the fine-grained adaptation of the developed mechanisms to the realistic conditions of contemporary areas of operations.

**Acknowledgments.** The results described in this work were obtained as part of the European Defence Agency project TACTICS (Tactical Service Oriented Architecture). The TACTICS project is jointly undertaken by Patria (FI), Thales Communications & Security (FR), Fraunhofer-Institut für Kommunikation, Informationsverarbeitung und Ergonomie FKIE (DE), Thales Deutschland (DE), Leonardo (IT), Thales Italia (IT), Norwegian University of Science and Technology (NO), ITTI (PL), Military Communication Institute (PL), and their partners, supported by the respective national Ministries of Defence under EDA Contract No. B 0980.

## References

1. Aloisio, A., Autili, M., D'Angelo, A., Viidanoja, A., Leguay, J., Ginzler, T., Lampe, T., Spagnolo, L., Wolthusen, S.D., Flizikowski, A., Sliwa, J.: TACTICS: tactical service oriented architecture, CoRR, vol. abs/1504.07578 (2015)
2. Lampe, T.A., Prasse, C., Diefenbach, A., Ginzler, T., Sliwa, J., McLaughlin, S.: TACTICS TSI architecture. In: International Conference on Military Communications and Information Systems (ICMCIS) (2016)



3. Gkioulos, V., Wolthusen, S.D.: Securing tactical service oriented architectures. In: 2nd International Conference on Security of Smart cities, Industrial Control System and Communications (SSIC) (2016)
4. Gkioulos, V., Wolthusen, S.D.: A risk analysis approach over network centric warfare and tactical service oriented architectures. Submitted for Review at: 7th International Conference on Mathematical Methods, Models and Architectures for Computer Networks Security (2017)
5. Gkioulos, V., Wolthusen, S.D.: Enabling dynamic security policy evaluation for service-oriented architectures in tactical networks. In: Norwegian Information Security Conference (NISK 2015) (2015)
6. Gkioulos, V., Wolthusen, S.D.: A security policy infrastructure for tactical service oriented architectures. In: 2nd Workshop on the Security of Industrial Control Systems and of Cyber-Physical Systems (CyberICPS 2016), in conjunction with ESORICS 2016 (2016)
7. Gkioulos, V., Wolthusen, S.D.: Constraint analysis for security policy partitioning over tactical service oriented architectures. In: Advances in Networking Systems Architectures, Security, and Applications. Advances in Intelligent Systems and Computing. Springer, Heidelberg (2016)
8. Gkioulos, V., Wolthusen, S.D.: Reconciliation of ontologically defined security policies for tactical service oriented architectures. In: International Conference on Future Network Systems and Security, FNSS (2016)
9. Gkioulos, V., Flizikowski, A., Stachowicz, A., Nogalski, D., Gleba, K., Sliwa, J.: Interoperability of security and quality of service policies over tactical SOA. In: IEEE Symposium on Computational Intelligence for Security and Defense Applications (IEEE CISDA 2016) - IEEE Symposium Series on Computational Intelligence (IEEE SSCI 2016) (2016)

# An Application Using a BLE Beacon Model Combined with Fully Autonomous Wheelchair Control

Shugo Miyamoto<sup>1</sup>, Takamasa Koshizen<sup>1(✉)</sup>, Takanari Matsumoto<sup>2</sup>, Hiroaki Kawase<sup>2</sup>, Makoto Higuchi<sup>2</sup>, Yasuo Torimoto<sup>2</sup>, Koji Uno<sup>1</sup>, and Fumiaki Sato<sup>3</sup>

<sup>1</sup> Honda R&D Co. Ltd., Tochigi, Japan  
{Shugo\_Miyamoto, Takamasa\_Koshizen, Koji\_Uno}@n.t.rd.honda.co.jp

<sup>2</sup> Imasen Electric Industrial Co. Ltd., Inuyama, Japan  
{takanari\_matsumoto, hiroaki\_kawase, makoto\_higuchi, yasuo\_torimoto}@imasen.co.jp

<sup>3</sup> Toho University, Tokyo, Japan  
fsato@is.sci.toho-u.ac.jp

**Abstract.** This paper describes a novel technology for controlling a fully autonomous wheelchair, using a Bluetooth Low Energy (BLE) beacon. Our framework, in particular, enables the beacon substrate (Received Signal Strength Indicator) to allow machine learning for fully autonomous wheelchair control, namely for the beacon model. Location awareness is computed for the smooth locomotion control of a motorized wheelchair. As a result, low current consumption is achieved to allow lasting battery life. In this paper, we provide several results relevant to this, and future remarks.

## 1 Introduction

In recent years, interest in autonomous cars has grown dramatically worldwide due to the promotion of a computer vision dedicated to artificial intelligence (AI). In particular, a team of NVIDIA engineering has provided a platform (*e.g.*, powerful GUIs) that uses *deep learning* [1] to teach an autonomous (*i.e.*, self-driving) car to drive [2]. Basically, an autonomous car is a vehicle that is capable of sensing its environment and navigating without human input. It can detect its surroundings using external sensors such as radar, lidar, GPS, and cameras, etc.

Historically, the first autonomous cars were appeared from Carnegie Mellon University in 1984 and Mercedes-Benz in 1987. Prototype autonomous cars have also been developed by not only major car companies, but also by digital disruptors such as Google, Apple, and so on (*e.g.*, [3]).

Figure 1 describes a roadmap of autonomous cars [4], including the different levels and qualities with respect to the autonomous car. In particular, these are divided into *four* levels of driving automation ranging from ‘no’ automation (**Level 1**) to ‘full’ automation (**Level 4**). A key distinction is between **Level 2**, where the human driver performs part of

the dynamic driving task, and **Level 3**, where an automated driving system performs the entire dynamic driving task. Note that dynamic driving tasks include the operational (steering, braking, accelerating, monitoring the vehicle and roadway) and tactile (responding to events, determining where to change lanes, turn, etc.) parts of the driving tasks. If strategic (determining destinations and waypoints) parts of the driving task are taken into consideration, a model predictive control (MPC) is undertaken for “fully” autonomous cars (Level 4). That is, MPC allows a computational model to predict the future dynamics of autonomous cars [5]. These predictions are based on an objective function, where MPC is used to generate data for training purposes. Mamadou et al. [6] have, for instance, shown for achieving high fuel efficiency due to the string stability of *adaptive cruise control* (CACC) concerning MPC.

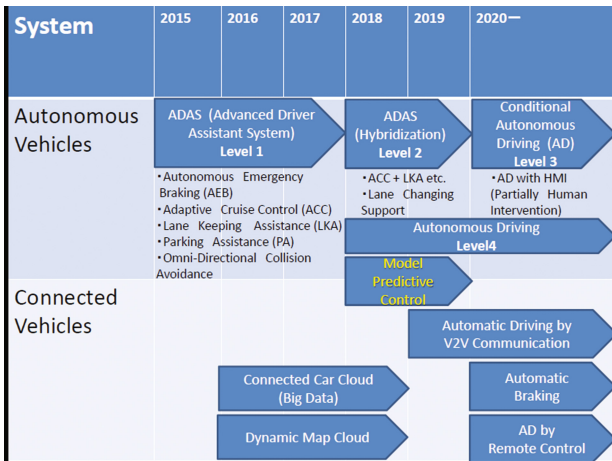


Fig. 1. Roadmap of autonomous vehicles, including connected vehicles.

This paper aims to deploy an MPC-based approach to an autonomous wheelchair. In this respect, we enable a motorized (alternatively called an *electric-powered*) wheelchair to attain full autonomy using an MPC. The spread of motorized wheelchairs will assist elderly people in an aging society in the coming years. By providing an autonomous wheelchair, we are convinced that the elderly will be guaranteed *safer* and *easier* visits outside the home or other road trips.

As with the related studies on semi-autonomous wheelchair locomotion control, WHILL Inc. et al. [7] has built a *remote control* using a smartphone. This technology utilizes the smartphone as a joystick, in order to allow it to localize at any location in an indoor environment. Although many robotics projects have been devoted to developing fully autonomous wheelchairs, in most of their products, object recognition such as radar sensors and camera vision systems are basically used to find the *free space* [8, 9]. This partially originates from SLAM (Simultaneous localization and mapping), which is one of the reprehensive autonomous car technologies [4]. It is a computation for constructing or uploading a map of an unknown environment for self-driving.

SLAM is, however, considered to increase the computation complexity and economical cost when an unknown environment is recognized using a group of external sensors. In order to come to terms with the complexity problem, the proposed architecture for an autonomous wheelchair must be simplified, and BLE beacons are used in consolidation with fully autonomous wheelchair control. In practice, each beacon is attached to a wall or door in an indoor environment to help triangulate the position of the autonomous wheelchair. Most importantly, the beacon produces RSSI (*Received Signal Strength Indicators*) that measure the approximate distance between the smartphone and the beacon. Due to external factors influencing radio waves, such as absorption, interference or diffraction, the RSSI tends to fluctuate. Therefore, we propose to use the machine learning method to help cope with these difficulties.

In machine learning theory, the capability of training models are limited when the quality and/or quantity of training data is insufficient. This *poor* performance of machine learning leads to either under-fitting or over-fitting for training data generation with the RSSI. In order to resolve this problem, a smartphone cloud platform is used to select and to update a training model, the so-called *beacon model*. In practice, the smartphone plays a crucial role in collecting the RSSI in real-time, and then sends it to a cloud server to generate the beacon model automatically. That is, a cloud server can be used to quantify and to analyze the smoothness of the autonomous wheelchair locomotion. In the end, the smooth locomotion of the wheelchair is quantitatively confirmed by a smartphone-cloud platform as shown in Fig. 2.

In this paper, a proposed autonomous wheelchair is introduced. At first, we elucidate our autonomous wheelchair. The beacon model is then explained, concentrating on its computation and performance with the locomotion control system of the wheelchair in particular. The results of current consumption will additionally be concerned with the smooth locomotion of autonomous wheelchair control. Finally, our conclusions and perspectives on the proposed control scheme are provided.

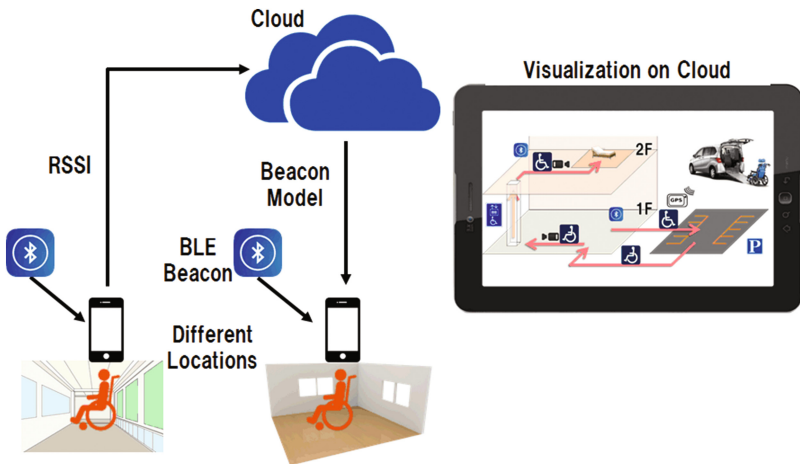


Fig. 2. The smartphone-cloud platform for autonomous wheelchair.

## 2 Background

Several studies have so far shown applications for autonomous wheelchairs, *e.g.* [8, 9]. Especially, Quan et al. have built an autonomous wheelchair with an omni-directional camera and four laser range sensors [8]. In practice, omni-directional camera is used to observe distance and the surrounding environment with a fully overlapping field of visual perception. Moreover, laser range sensors are also used to measure the distance of obstacles, so that an autonomous wheelchair can avoid them. It has a cooperative operation in which a wheelchair is capable of moving in attendance with a person. There is, however, no semantic speech dialogue system, in which a camera is used to capture the human pose and interact with a person. Natural language descriptions have meanwhile been incorporated into an autonomous wheelchair, using a microphone and augmented metric map, *e.g.*, [9]. Nevertheless, the semantic speech dialogue seems to still be immature due to the incapability of language acquisition and robust speech perception. A proposed autonomous wheelchair is engaged for MPC, where beacons learn to generate their models. Importantly, their learned beacons bring into play the location awareness of wheelchair control. It then leads to low energy consumption, by *penalizing* beacon models.

## 3 Proposed Autonomous Wheelchair Control

Autonomous wheelchair control is here proposed with a probabilistic mode, which is computed by a machine learning technique with training data from BLE beacons. The computation of the beacon model is explained here. To begin with, a description of the BLE beacon is provided in Fig. 3.

### 3.1 Description of the Beacon Model

Figure 3 shows a BLE beacon, which is a wireless device producing RSSI, received by a smartphone and used to determine the position of the autonomous wheelchair. It enables our smartphone-cloud platform (Fig. 2) to provide “context-aware” and proximity-based applications using the high quality led by the beacon (Fig. 3).

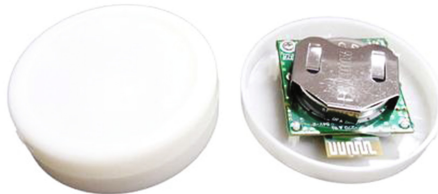


**Fig. 3.** Appearance of BLE beacon. (Diameter: 5 cm, Weight: 28 g)

### 3.1.1 Beacon Attributes

Important issue of a beacon that we are particularly concerned with is “interference”. One of the reasons for using a beacon is to estimate the position of the autonomous wheelchair given an indoor map. In practice, the RSSI is provided by its *radio field intensity*. Generally, interference is caused by multiple beacons in corners of the indoor environment. This is because the beacons proximities are fairly high (e.g., 1 to 2 m), and the RSSI then fluctuates. As a result, the position estimate using beacons could be inaccurate and incorrect. Figure 4 illustrates the outlook of a radio field intensity that can be different from the two specific locations in the ‘straight’ and ‘corner’ regions. Note that a beacon threshold is used to specify a *large* plateau with the RSSI. On the other hand, a beacon model is capable of coping with a small plateau with the RSSI because it is trained the relationship between the sensory pattern and the location. In the corner region, interference often occurs. The RSSI of the corrected beacon is then involved in an “artifact”. That is, we conclude that the beacon model can be more effective that the straight region than for the corner region, in terms of the interference of RSSIs. Next, we shall provide details on the machine learning method to create the beacon model, while dealing with its uncertainty.

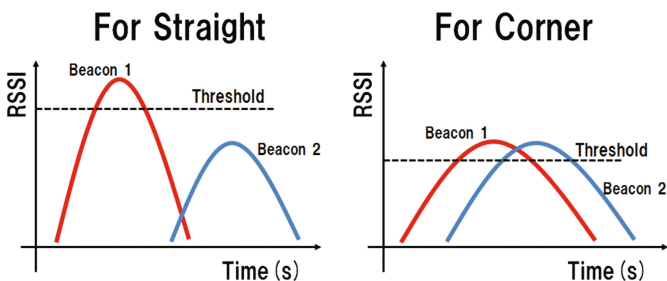


Fig. 4. The difference between the two in accordance with interference. (Straight and corner region are particularly concerned)

### 3.1.2 Beacon Model Using Machine Learning

In order to generate beacon models represented by probability distribution, we used the Expectation Maximization (EM) [10]. In theory, it is an iterative method to discover the maximum likelihood or maximum a posteriori (MAP) estimate of parameters in statistical models, where the probabilistic density can be suitable to deal with uncertainty. Figure 5 shows the algorithmic flow char of the EM algorithm. It has two main steps. The **E** step calculates the value of the parameters, whereas the **M** step calculates the maximum likelihoods. In particular, the EM approximates the Gaussian mixture distribution given Eq. (1), parameterized by the mean  $\mu$  and standard deviation  $\sigma$  when constituting the Gaussian mixture distribution as follows:

$$P(X|L) = \sum_{j=1}^K \frac{\alpha_{jL}}{(2\pi)^{1/2} \sqrt{|\sigma_{jL}|}} \exp\left(-\frac{1}{2}(X - \mu_{jL})^T \sum_{jL}^{-1} (X - \mu_{jL})\right) \quad (1)$$

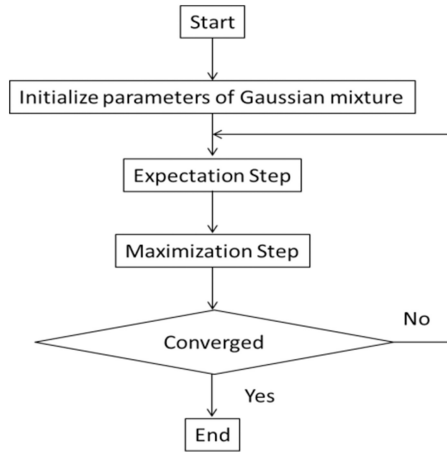


Fig. 5. The algorithm flow of Expectation Maximization.

Where  $X$  denotes the beacon sensor (1-dim). Given 10 beacons, Fig. 6 indeed illustrates the RSSI manifestation, where the autonomous wheelchair is localized at the corner region as shown in Fig. 7. In addition, the label ( $L$ ) is defined by three states as follows:

- Before the wheelchair is to pass through a corner ( $L = 1$ )
- A wheelchair passing through a corner ( $L = 0$ )
- After the wheelchair passes through a corner ( $L = -1$ )

Where  $L$  is a label playing a role in extracting semantic location (*i.e.*, either corner or non-corner) for the wheelchair control as described in Fig. 7.

Three labels are presumed based on the result of the EM (Fig. 5). Note that EM is used for a supervised learning scheme rather than an unsupervised learning one.

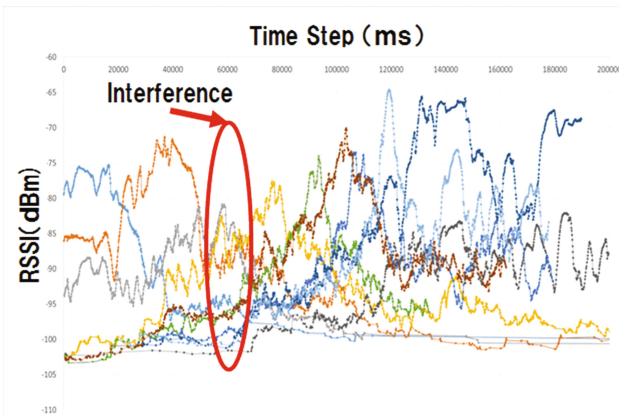


Fig. 6. The RSSI for 10 Beacons.

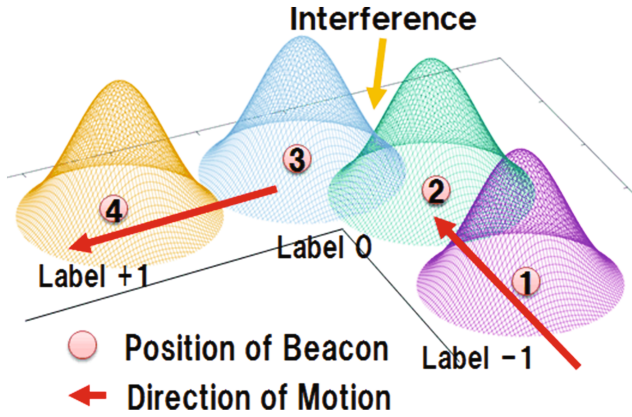


Fig. 7. The semantic location provided by three labels (-1, 0, +1).

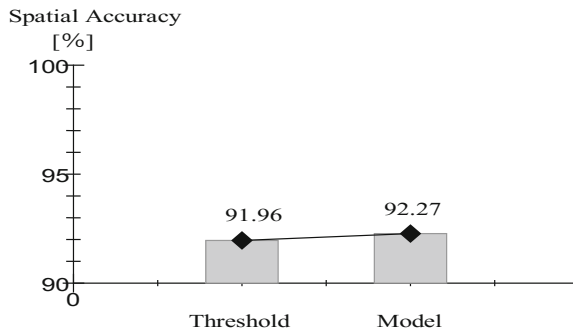


Fig. 8. Comparison: beacon threshold vs. beacon model (N = 60). Note: This result is assumed in the corner region in particular.

Furthermore, Fig. 8 shows the comparison between the beacon threshold and the beacon model for the accuracy rate of labeling the location of the autonomous wheelchair. The result has shown that the beacon model was slightly more accurate than the other by 0.31%. N(= 60) denotes the number of trial numbers. Note that the accuracy may depend significantly on the variation of training examples for beacon model.

### 3.2 Architecture of Autonomous Wheelchair Control

Figure 9 shows the motorized wheelchair for the *front* and the *back* part. As with the front part of the wheelchair, there are two cameras to detect obstacles, whereas for the back part, there is a battery to charge electric energy. If it is considered to reduce the travelling energy of a wheelchair, the number of external sensors should be minimized. Therefore, we propose a behavioral planning framework for fully autonomous vehicles,



using a smartphone and two cameras, as described in Fig. 9. Note that the smartphone collects data from the beacons, and sends it to a cloud server for the wheelchair locomotion in an indoor environment. That is, we obtain position information using a beacon (Fig. 3), with monitoring from a cloud server (Fig. 2).

**3.2.1 The Motorized Wheelchair**

Figure 10 describes the block diagram of the wheelchair control part, which deals with the beacon model, odometry (from wheel encoders) and stereovision using two cameras. Note that there are two modules for the straight and corner regions. The beacon model performs in executing the optimal timing of the behavioral planner (e.g., economic slowdown) to attain smooth locomotion by the wheelchair (Fig. 9).

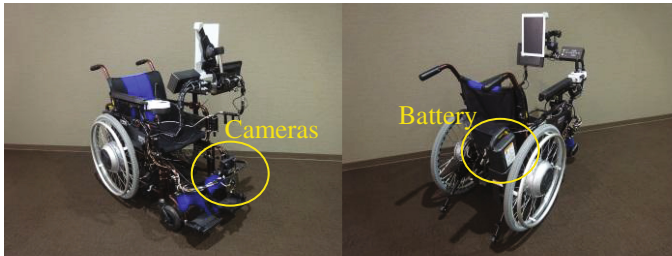


Fig. 9. Outlook of a motorized wheelchair (<http://www.imasengiken.co.jp/en/emc/index.html>)

**3.2.2 The Behavioral Planning of Autonomous Wheelchair Control**

In addition, obstacle detection is implemented by the stereovision system [11], where 3D information is extracted from digital images (see Fig. 11), using two cameras (Fig. 9). Importantly, the obstacle detection is undertaken by the output of the beacon model with our behavioral planning of autonomous wheelchair control (Fig. 10).

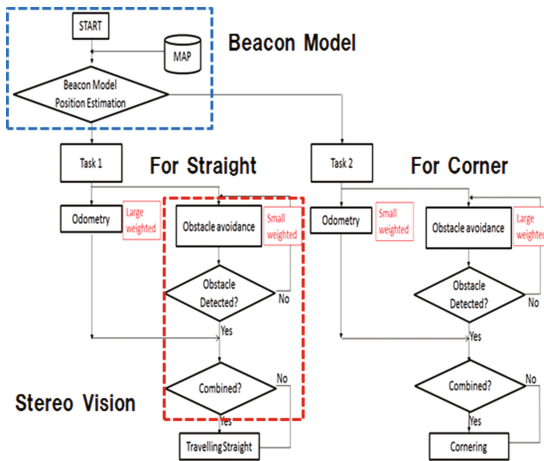
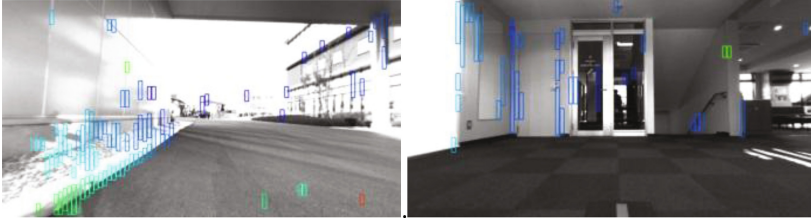
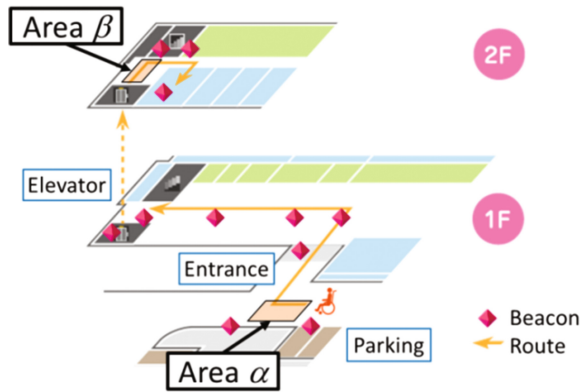


Fig. 10. The behavioral planning of autonomous wheelchair control



**Fig. 11.** Examples of obstacle avoidance using stereovision (Left: corner area  $\beta$  and Right: corner area  $\alpha$  in Fig. 12)



**Fig. 12.** The locomotion map for autonomous wheelchair control

Figure 11 illustrates the two pictures that resulted from our stereovision system with autonomous wheelchair control. With regards to the environment, there are two floors, where the wheelchair proceeds in accordance with the *orange* arrow as described in Fig. 12. An important aspect of the wheelchair locomotion is the two corner areas, namely  $\alpha$  and  $\beta$ , where beacons are severely affected by interference. If this is the case, the response from the motor commands of the wheelchair has a delay in control. As a result, the wheelchair is likely to lose control and *vice versa*.

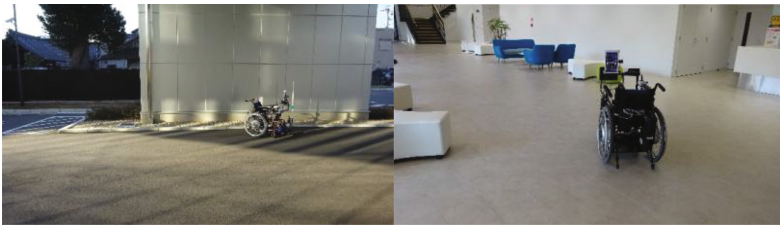


**Fig. 13.** Examples of obstacle avoidance using stereovision (Left: Outdoor case; Right: Indoor case)

### 3.3 Beacon Model as MPC

The beacon model is here described as an MPC in order to attain long battery life. The idea of using a beacon model is to create a quick response to the wheelchair locomotion control. It is reminiscent of electric vehicle concepts. That is, MPC plays a crucial role in achieving fuel economy due to smooth driving without processing the accelerator or the brake pedals aggressively and maintaining a steady velocity as long as possible *e.g.*, [12].

In our framework, smooth driving (or locomotion) allows a model to take into account the timing of possible driving behaviors (especially deceleration) in terms of low energy consumption. In both cases, Fig. 14 shows the delay reduction rate that the beacon model is significantly *shorter* than the beacon threshold by 17.3% for the response time of wheelchair locomotion.

In summary, we conclude that the beacon model can achieve better performance (as shown in Figs. 8 and 13) than the beacon threshold at the corner regions, because it can cope with the uncertainty caused by interference.

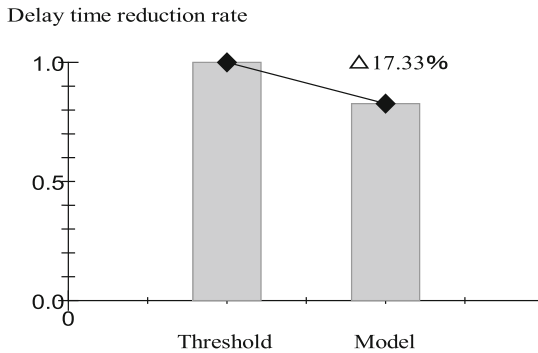


Fig. 14. Comparison: beacon threshold vs. beacon model (N = 30)

#### 3.3.1 Smooth Locomotion by Penalized Beacon Model

The smooth locomotion of wheelchair control using a beacon model has been investigated quantitatively by changing the penalizing factor ( $F_c$ ), as seen in Fig. 15. That is, the beacon model is *penalized* with  $F_c$ . It is apparent that there is a boundary between  $F_c = 20$  and 30. If  $F_c < 30$ , then the wheelchair can move smoothly in particular within areas  $\alpha$  and  $\beta$  in Fig. 12. If  $F_c > 20$ , the effect is then reversed. The reason is as follows. The greater the  $F_c$  value, the greater the radius ( $R$ ) is. Note that when  $R$  is a small value, the wheelchair then moves smoothly for the corner regions (area  $\alpha$  and  $\beta$ ). In summary, when  $R$  has a relatively large, the smooth locomotion of the wheelchair is capable of preventing *tight turns* in the corner regions.

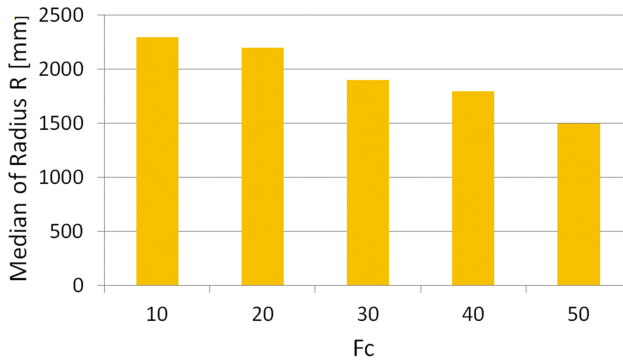


Fig. 15. The relationship between R and Fc

#### 4 Low Current Consumption (LCC) with Beacon Model

Since the wheelchair has an electric battery to move around the specified environment (Fig. 12), low current consumption (LCC) must be taken into account. Our technology, the beacon model, has the feasibility of implementing MPC with an autonomous wheelchair. As has already been shown, MPC improves the degree of smooth driving. Therefore, it is likely to achieve LCC. The framework has been implemented in the proposed autonomous wheelchair control. We shall show here that the beacon model can be effective in terms of LCC, allowing the wheelchair to be able to be localized smoothly, in particular with area  $\alpha$  and  $\beta$  in Fig. 12. Figure 16 describes the *electricity cost* (A/m) in correspondence with Fc, which was changed by 10 to 40. Apparently, we can see a relationship between electricity cost and smooth locomotion in regards to fully autonomous wheelchair. That is, the smaller the value of Fc, the lower the electricity cost is.

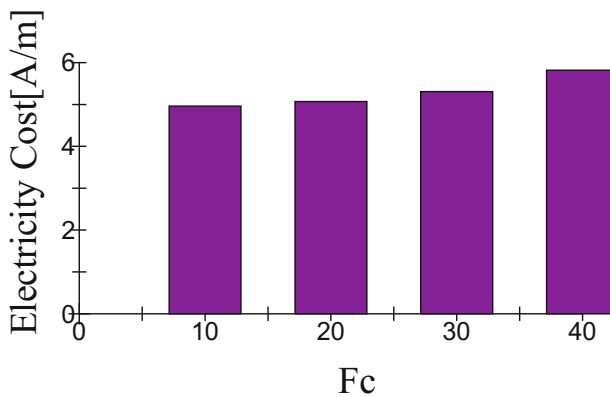


Fig. 16. Electricity cost with Fc (changing 10 to 40)

## 5 Conclusion

In this paper, we propose a novel locomotion control framework for fully autonomous wheelchair. The RSSI-based beacon model is used to estimate the position of the wheelchair. More importantly, it allows a motorized wheelchair to localize autonomously in an indoor location by adding the scheme of a stereovision component for obstacle avoidance.

As a result, the locomotion control of fully autonomous wheelchairs can be smooth. Our preliminary results have shown that low current consumption is attained, and we expect smooth locomotion will lead to the battery life of the autonomous wheelchair lasting as long as possible.

Using the beacon model, the autonomous wheelchair may further be considered functional as follows:

- Robust estimate using beacon model with machine learning technique
- To attain movement stability for proposed autonomous wheelchair control
- Routing guide to location markers using beacons

Accordingly, the functional of a cloud server will be enhanced to collect beacon data and to yield a real-time beacon model, in which a smartphone performs the perceptual and behavioral planner of proposed autonomous wheelchair control.

By deploying the smartphone-based cloud platform with beacons, the structure of the autonomous wheelchair attains simplification and a lighter weight using the beacon model. Therefore, we envision that the *permeation* of autonomous wheelchairs can be increased.

**Acknowledgments.** The authors would like to thank Mr. Syoji Isobe (Honda Automobile R&D Center, Tochigi) for useful and insightful suggestions.

## References

1. Krizhevsky, A., Sutskever, I., Hinton, G.: ImageNet classification with deep convolution neural networks. In: Proceedings of the Advances in Neural Information Processing Systems, vol. 25 (2012)
2. <http://www.nvidia.com/object/autonomous-cars.html>
3. Mehl, R.: The Automotive Industry as a Digital Business. NTT Innovation Institute Inc., CA (2016)
4. Automated Driving Roadmap: ERTRAC task force (connectivity and automated driving) (2015)
5. Gillespie, T.: Fundamental of vehicle dynamics. SAE International (1992)
6. Mamadou, M., Sorkati, A.: Optimization for energy efficient cooperative adaptive cruise control, Master thesis in Chalmers University of Technology, (2016)
7. <http://whill.us/about-company/>
8. Quan, W., Niwa, H., Ishikawa, N., Kobayashi, Y., Kuno, Y.: Assisted care robot based on sociological interaction analysis. Comput. Hum. Behav. (Elsevier) 27(5), 1527–1534 (2011)

9. Hemanchandra, S., Walter, M.: Learning semantic maps through dialogue for a voice-commandable wheelchair. In: Proceedings of the IEEE/RSJ International Conference on Intelligent Robots and Systems (IROS) Workshop on Rehabilitation and Assistive Robotics, Chicago (2014)
10. Dempster, A., Laird, N., Rubin, D.: Maximum Likelihood from incomplete data via EM algorithm. *J. R. Stat. Soc. Ser. B (Methodological)* **39**(1), 1–38 (1977)
11. Kamal, K., Imura, J., Hayakawa, T., Ohata, A., Aihara, K.: Smart driving of a vehicle using model predictive control for improving traffic flow. *IEEE Trans. Intell. Transp. Syst.* **15**(2), 878–888 (2014)

# UnipaBCI a Novel General Software Framework for Brain Computer Interface

Salvatore Tramonte<sup>1</sup>(✉), Rosario Sorbello<sup>1</sup>, Marcello Giardina<sup>1</sup>,  
and Antonio Chella<sup>1,2</sup>

<sup>1</sup> Robotics Lab, Università degli Studi di Palermo - Dipartimento dell’Innovazione Industriale e Digitale (DIID), Viale delle Scienze, Building 6, 90128 Palermo, Italy  
`salvatore.tramonte@unipa.it`

<sup>2</sup> ICAR-CNR, via Ugo La Malfa 153, 90146 Palermo, Italy

**Abstract.** The increasing interest in Brain Computer Interface (BCI) requires new fast, reliable and scalable frameworks that can be used by researchers to develop BCI based high performance applications in efficient and fast ways. In this paper is presented “UnipaBCI”, a general software framework for BCI applications based on electroencephalography (EEG) that can fulfill these new needs. A visual evoked potentials (VEP) application has also been developed using the proposed framework in order to test the modular architecture and the overall performance. Different types of users (*beginners* and *experts* in BCI) have been involved during the “UnipaBCI” experimental test and they have exhibited good and comparable results.

**Keywords:** Brain-Computer Interface (BCI) · Humanoid robot · Assistive technology · Augmentative communication · Rehabilitation · BCI framework

## 1 Introduction

A Brain Computer Interface (BCI) system, is a hardware and software platform that allows humans to interact without using muscles, through the signals generated from brain activity. BCI creates a new channel of communication to transmit the person’s intentions to external devices such as robot, speech synthesizers, assistive devices and prostheses. In consideration of this situation BCI is particularly helpful for people with severe motor disabilities to help them to partially restore their independence [1].

UnipaBCI is a brand new general purpose BCI platform that allows the translation of human thought in external control commands.

## 2 State of the Art

The Brain Computer interface, also known as Brain Machine Interface, (BMI) is a direct channel of communication between the human brain and hardware or

software devices [2]. A first classification of BCIs could be done on the acquisition technique used: invasive [3] and non-invasive [4]. Invasive techniques require neuro-surgery operations to implant electrodes over the neural cortex, while non-invasive techniques use electrodes placed over the head with a cap accordingly to an international montage system [5]. Between the non-invasive techniques it is possible to find many different approaches, one of the most used is based on the *Electroencefalography* (EEG) [6]. It measures the electrical activity of the brain with electrodes disposed over the head. With good temporal resolution and low costs, compared to other techniques, is one of the most used acquisition technique. From EEG it is possible to derive The *Evoked Related Potentials* (ERP) defined as the variation in the voltage of the EEG signals consequently to a sensory stimulation [7]. One of the most used ERPs is the Visual Evoked Potentials (VEP) [8] and in particular the P300 which is elicited by a cognitive process with a latency of 300 ms as a positive deflection in brain activity. Nowadays interaction is largely indirect and mediated by new technologies and devices [9] and many BCI platform have been developed in the last years to enable human interaction. The *BCI2000* [10] is a general purpose software for BCI research. It uses a wide variety of data acquisition, stimulus presentation and brain application. It's development begun 2000 and it's widely used around the world. *OpenVibe* [11] is an open-source software platform to design, test, and use brain-computer interfaces in real and virtual environments. *BCIlab* [12] is an open-source Matlab based toolbox for advanced BCI research. It provides a graphical interface and a scripting language to use many well established methods. The development of different BCI architecture enabled researchers to develop different BCI based applications. Tanaka et al. [13] controlled an electric wheelchair using EEG. In Chen et al. [14] a robot as meal assistance is developed and in Tumanov et al. Chella et al. [15] used a BCI controlled robot to navigate in a museum.

### 3 The UnipaBCI Framework

The general architectural schema of the UnipaBCI system, as shown in Fig. 1 is composed by five main modules: *Acquisition*, *Signal processing*, *User Application*, *Device Controller* and *Control Application*. The architecture has been designed accordingly to the key points stated in [16]. The modular architecture of the UnipaBCI framework makes it easily scalable and flexible to new needs allowing the develop of new features or the removal of the older ones, maintaining the general structure unchanged.

The system provides two operative modalities: *Training* to calibrate the system over the user and *Recognition* to use the system, after it is calibrated, to spell letters and symbols. Next paragraphs will provide an insight on the main parts of the architecture.

#### 3.1 The Acquisition Module

The system is compatible with g.usbAmp, produced by g.tech, a high-performance and high-accuracy biosignal amplifier with 16 simultaneously



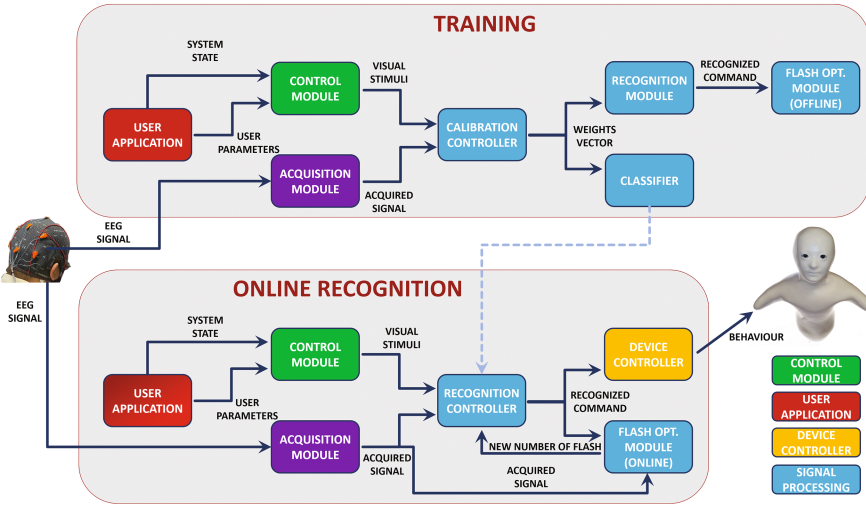


**Fig. 1.** The architectural schema of UnipaBCI framework (Each color of the blocks is related to a specific functionality).

sampled biosignal channels with 24 bits, connected with USB socket to the PC (for details please consult the Guger technology website (<http://www.gtec.at>)). The maximum number of channels, as well as the sample rates and the applicable filters are fully dependent from the hardware. The framework theoretically works with more than one g.usbAmp at the same time but only single device tests have been done for the current implementation. The Acquisition Module is used to connect to the G.usbAmp and to manage the recording of the electrical potentials, defined as raw signals, extracted in real-time from the brain of the user. We selected an acquisition rate of 250 Hz and implemented a Notch filter of 50 Hz. Row signals are band-passed between 1 and 50 Hz with a 6 – th Order Butterworth filter.

### 3.2 The Signal Processing Module

The signal Processing Module is used to extract the relevant features from the raw signal. This module is composed by a pre-processing module, used to remove artifacts from the signal, a training module, dedicated to the calculation of weights of the classifier and a recognition module used to discriminate user’s brain activity. In Fig. 2 is described the architectural schema of the Signal Processing Module.

The signals, acquired and digitalized by the Acquisition module are down-sampled to reduce data dimensionality. To avoid aliasing effects, a preliminary study to find the best reduction factor has been carried out and, based on findings in [17, 18], a reduction factor  $n = 4$  has been set up. In this way, signals originally acquired at 256 Hz are stored with a sample frequency of 64 Hz. We applied a

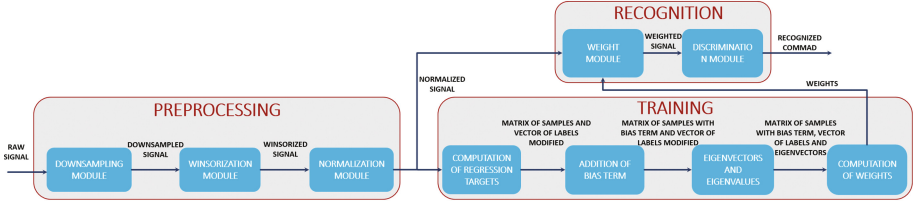


**Fig. 2.** The architectural schema of Signal Processing Module.

to the signal a Winsor window to cut off the outliers values reducing their bias effect. The *Winsorization* module defines a threshold that considers values as outliers, based on median and inter-quartile range and it takes into account only 1% of these values. The signal is then normalized using a z-score method [19]. The algorithm works by subtracting from each feature the mean  $\mu$  and dividing it for the standard deviation  $\sigma$ .

The Training Module implements a Bayesian Linear Classifier [20] that outputs a weights vector to classify the normalized samples obtained from the Preprocessing Module. The brain signals acquired are synchronized with the Visual Stimuli related to two class labels: *target* and *non-target*. The brain signals and the class labels are used by the classifier to discriminate the membership for each stimulus. Brain signals are inserted in a structure called BSP (Brain Save Potentials), with dimension  $[F * N]$  where  $F$  represents the features extracted and  $N$  is the number of normalized samples extracted for each epoch. The epoch size has been set to 600 ms. The *Regression Targets Computation* calculates the regressions targets from the normalized samples using the Bayesian Linear Discriminant Analysis (BLDA) [21]. BLDA is based on the assumption that regression targets are set as  $\frac{N}{N_i}$  where  $N$  is the total training samples and  $N_i$  is the total number of samples for the  $i$ -th class. The *Bias Terms addition* consists in the introduction of a bias term, as a systemic error due to data modelling. The *eigenvectors and eigenvalues calculation* calculates the eigenvectors and the eigenvalues for  $X' = X \cdot X^T$

The weights are calculated using the following equation:

$$p(D|\beta, w) = \left(\frac{\beta}{2\pi}\right)^{\frac{N}{2}} \exp\left(-\frac{\beta}{2} \|X^T w - t\|^2\right) \quad (1)$$

where  $\mathbf{t}$  represent the *regression targets*,  $\mathbf{X}$  are the features in the training matrix,  $\mathbf{D}$  is the pair  $(\mathbf{X}, \mathbf{t})$ ,  $\beta$  is the inverse of the additive noise and  $\mathbf{N}$  is the total number of samples. To calculate the posterior distribution  $w$  it is necessary to calculate the conditional expectation for  $w$  given  $\alpha$ . This distribution is expressed as a multivariate Gaussian distribution with zero mean, expressed as:

$$p(w|\alpha) = \prod_{i=1}^D \left(\frac{\alpha_i}{2\pi}\right)^{\frac{1}{2}} \exp\left(-\frac{1}{2} w^T I'(\alpha) w\right) \quad (2)$$

where  $\mathbf{I}'(\alpha)$  is a diagonal matrix with dimension  $D \times D$ ;  $\alpha_i$  is the inverse of the variance of the distribution of each weight  $w_i$  and it's used to estimate the importance of  $w_i$  in the regression model [22]. From this equations, the algorithm iterates the process and calculates the  $\alpha$  and  $\beta$  values until they are lower than an error  $\epsilon$ . The *Recognition* module is used to recognize the command selected by the user with the BCI device after  $w$  is calculated. The recognition module determines a new vector of signal samples as:

$$m_k = \sum w * x. \quad (3)$$

where  $w$  is the weight vector and  $x$  is the original brain signal. For each  $k$ -th symbol of the interface the  $x$  acquired during the presentation of the  $k$ -th stimulus are summed with the corresponding  $m_k$ :

$$v_k = m_k + x_k \quad (4)$$

The  $k$ -th symbol, corresponding to the maximum  $v_k$  is selected as output of the Signal Processing module.

### 3.3 The User Application Module

The User Application module, shown in Fig. 3, is formed by the Operator console and the User Interface. The operator console is used by the experimenter to set system parameters, choose operational modality (*training*, *recognition*), monitor the experiment and set the network address of external devices. The User Interface provides the stimuli interface and it is formed by a symbolic or alphabetical matrix whose dimension and icons are dynamically selected by the user. Icons could be enlightened in row-column or single square modality. Each item is highlighted with an icon showing the Einstein face, to increase ERPs response [23].

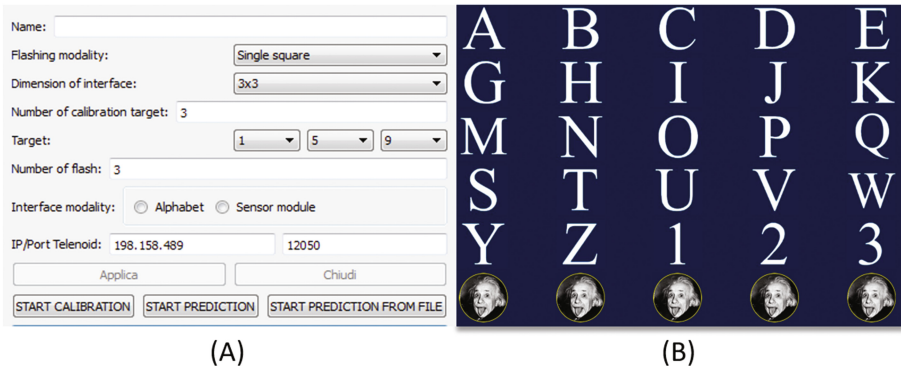


Fig. 3. The operator console (A) and the user interface (B).

### 3.4 The Control Application

The *Control application* module, shown in Fig. 4 is formed by the *States Manager* as the main controller and by three sub-controllers the *Acquisition Controller*, the *Interface Controller* and the *Device Controller*. The *States Manager* is the core of the whole platform. It is the main thread, managing all system states. After the platform has been started, it could be in *Training State* or *Recognition State*. For each of the states it manages the execution and synchronization of the sub-controller. In *Training State* it will activate the *Acquisition Controller* and the *Interface Controller*. In *Recognition State* it will activate the *Acquisition Controller*, the *Interface Controller* and the *Device Controller*. The *Acquisition Controller* is used to manage the EEG signal recording and storing. The *Interface Controller* manages the execution of the user interface and the stimuli synchronization. The *Device Controller* controls the external device, used as final output of the system.

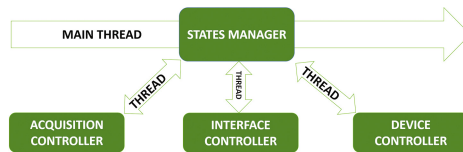


Fig. 4. The control application module.

### 3.5 The Flash Optimization Module

Accordingly to personal differences (e.g. *BCI skills*, *level of concentration*, *stress*) it is not possible to have a prior definition of the right number of stimuli needed to discriminate the P300 potentials. For this reason, in order to find the correct number of stimuli (flashes) to be presented to the user during the trials, two modules have been implemented: one for the training session and the other one for the recognition session.

The *Offline Flash Optimization module* is used to identify the best number of stimuli to be presented to the user based on the percentage of symbols correctly classified in the training set. This module merges the vector of weights  $w$  with the target id representing the expected symbol of the interface user must mentally select. The optimization module calculates the minimum number of flashes needed for the best precision of the system, intended as the probability of correctly classify the id of the target.

The *Online Flash Optimization* is used during the Recognition phase, when there are no prior informations on the target id that user is going to select. For the target id selected the Online Flash Optimization evaluates the minimum number of stimuli for correct selection and set the next iteration stimuli to that value.

### 3.6 The Device Controller Module

The Device Controller module is used to send commands to an external device connected to the system. The Telenoid R1 robot has been connected to the system as an embodied communicator. To detach the platform from the device connected it has been implemented a network interface based on TCP/IP for connection. In this way the robot doesn't need to be in the same physical place as user. Each command selected, it is sent to an *Accumulation Buffer*, until a termination character is selected. The obtained string is translated in an audio file using *Text-To-Speech* API. The Device module also initializes the Network Connection and sends the vocal file to the robot to be reproduced. At the end of the reproduction, Telenoid sends a termination ack to the device module which informs the device controller of the correct termination of the behaviour and enables the system to perform further operations.

## 4 Online Evaluation and Validation

20 subjects took part to the experiment. 10 had previous BCI experience and are defined *Experts*, the remaining never used BCI before and are referred as *Beginners*. We evaluated the precision of the system with both groups and how the Optimization Module increased the bit-rate of the system. To evaluate the system acceptance a questionnaire was filled from users. Finally we evaluated the real-time capabilities of UnipaBCI.

The experiment has been conducted in a controlled light room under the supervision of an experimenter. The experimenter controlled all the phases of the experiment and instructed the participants. Participants were instructed to avoid movements, blinking, swallowing and speaking. To limit the artifacts, it was asked them to focus on the GUI and to mentally count each time the expected item was highlighted. Participants wear a g.Cap with electrodes in Cz, Pz, C3, C4, accordingly the 10–20 montage system [24]. We empirically elided this montage because it provided best results, even with a small number of electrodes. Participants sit at a distance of 40 cm from the interface monitor, a Telenoid robot was connected to the system to provide feedback to the participants on the ongoing of the experiment. In Fig. 5 is reported a schematic description of the experimental environment setup. The experiment has been conducted on 20 healthy subjects with a median age of 23 years, 15 male and 5 female, with an average scholarization of 14 years. 10 of them have been defined as *Expert* since they had a prior knowledge in using BCI (*more than 10 hours in controlling BCI*) while the others five had no prior knowledge of BCI systems. All the participants were informed of the purposes of the study and gave their written informed consent.

### 4.1 The Precision of the System

An experimental session with expert and non expert BCI users has been conducted. In this experiment it has been investigated the precision of the UnipaBCI

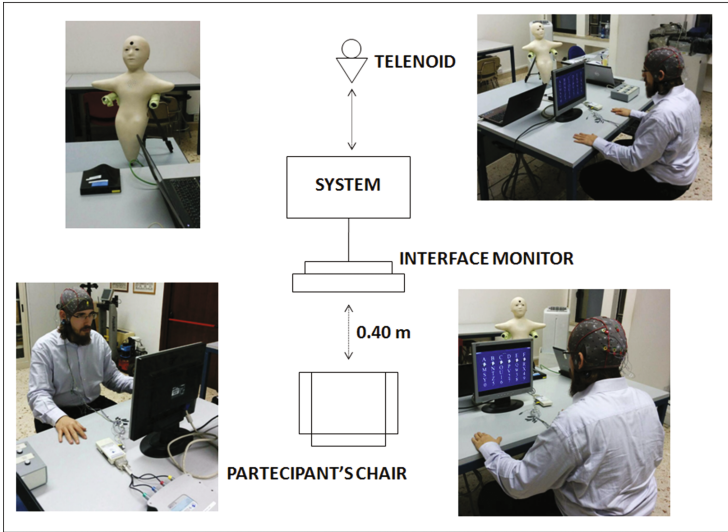


**Fig. 5.** The experimental environment setup.

framework accordingly to personal skills and using different operative modality: *single square* and *row-column* with a  $5 \times 5$  alphabetic interface. In single square mode each target was highlighted separately while in row-column mode for each target, all the row or all the column containing it were highlighted.

The first step consisted in the calibration to train the system over users. For this step a  $5 \times 5$  matrix formed by the first 20 letters of the English alphabet was used. The calibration session was formed by two trials, and each trial was formed by a sequence of three items. A total of 10 enlightenment for each item have been shown to each subject. At the end of the calibration session, the system calculated the attended percentage of success to be used during the recognition session to achieve a prediction of 100% of success for classification. All subjects successful completed the calibration phase with success. This result suggests the BLDA algorithm was able to correctly classify the provided features.

In the recognition modality, subjects were asked to recognize a total of 20 items randomly chosen by the experimenter from a  $5 \times 5$  alphabetic interface. 10 item were presented in *row-column modality* and 10 in *single square mode*. We randomized the stimuli presentation modality between users. Each item was highlighted from 1 to 10 times for 125 ms accordingly the results provided by the Optimization Module. Between two subsequently stimuli, a random time interval between 175 ms and 225 ms was set to avoid users' habituation. Table 1 reports results obtained in row-column (*RC*) alphabetic modality. Experts achieved an hit rate of  $90.00\% \pm 9.43\%$  while beginners successfully completed the task with a precision of  $85.00\% \pm 10.80\%$ . Accordingly to the row-column paradigm used, for a  $5 \times 5$  interface, the total number of possible target is 10. The average number of flash, set by the Optimization module was  $5 \pm 1$  stimuli for Expert and  $9 \pm 1$

stimuli for Beginners (all values are averaged to the closest integer by the Optimization module). In Table 2 are reported results for the single square modality. Experts achieved an average precision of  $85.00\% \pm 13.54\%$  and  $80.00\% \pm 9.43\%$  for non expert users. The average number of flash, set by the Optimization module was  $5 \pm 1$  stimuli for Experts and  $7 \pm 1$  stimuli for Beginners.

**Table 1.** Results for expert and beginners in terms of precision and average number of flash with a  $5 \times 5$  interface and row-column modality

Row - Column mode		S1	S2	S3	S4	S5	S6	S7	S8	S9	S10
Precision	Experts	80.00%	80.00%	100.00%	90.00%	80.00%	100.00%	100.00%	80.00%	100.00%	90.00%
	Beginners	90.00%	80.00%	70.00%	90.00%	100.00%	80.00%	100.00%	70.00%	80.00%	90.00%
Avg flash	Experts	5	6	6	5	5	4	4	5	3	7
	Beginners	9	8	7	9	10	8	10	7	8	9

A statistical analysis of results provided in Tables 1 and 2 are reported in Sect. 5.

**Table 2.** Results for expert and beginners in terms of precision and average number of flash with a  $5 \times 5$  interface and Single Square modality

Single Square mode		S1	S2	S3	S4	S5	S6	S7	S8	S9	S10
Precision	Experts	100.00%	90.00%	90.00%	80.00%	100.00%	80.00%	80.00%	70.00%	60.00%	100.00%
	Beginners	80.00%	80.00%	70.00%	80.00%	70.00%	80.00%	80.00%	70.00%	90.00%	100.00%
Avg flash	Experts	6	4	5	7	5	4	4	5	6	7
	Beginners	4	6	7	8	9	8	6	8	7	7

### 4.2 The Speedup Factor

The **speedup factor**  $F_s$  represents the differences in speed with and without the optimization module active and improves the bitrates of UnipaBCI. It could be described as:

$$F_s = \frac{S * T_{Opt} * St * I}{S * T_{NoOpt} * St * I}$$

where  $S$  is the number of subjects,  $T_{Opt}$  is the total number of target with Optimization Module active,  $T_{NoOpt}$  is the total number of target with Optimization Module inactive  $St$  is the stimuli duration,  $I$  is the inter-stimuli duration. Each stimulus lasted 125 ms, the inter-stimulus was set between 175 and 225 ms and a total of 10 users accomplished a total of 200 trials for each modality (Row - Column and Single Square). Without the Optimization module active, the number of flash was set to 10, while in Tables 1 and 2 are reported the average number of flash used during the experiment In consideration of this, the speedup factor with the optimization module active was 1.49 in Row-Column mode and 1.62 in Single Square mode.

### 4.3 Questionnaire Analysis

At the end of the experiment, we have asked participants to fill a questionnaire consisting of 6 questions to be answered with 3-points Likert scales. All 20 participants filled the questionnaire. The purpose of the questionnaire was to examine the level of user acceptance of UnipaBCI and to have the confirmation that the proposed system meets all the necessary requirement for a BCI framework. From results shown in Fig. 6, it is clearly possible to deduce that users find unipaBCI easy to use (Q1,Q2); the experiment was well prepared (Q4, Q5); even if using the system could be considered quite demanding in terms of focus (Q3), 12/20 subjects were overall satisfied while only two subjects were not satisfied.

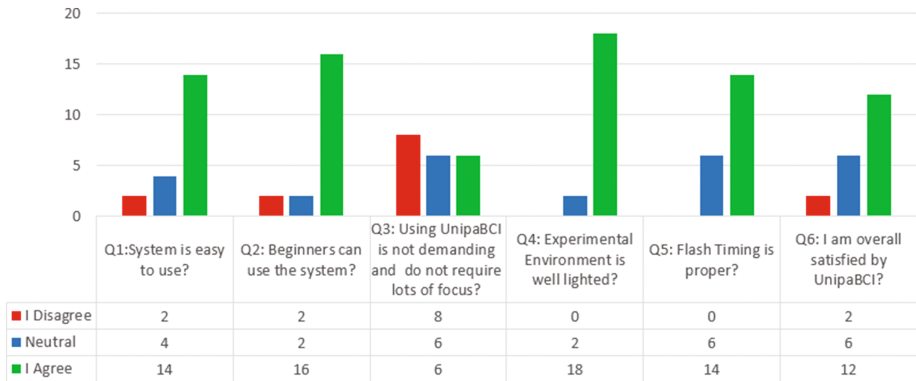


**Fig. 6.** Results of the questionnaire filled from participants after the experiments.

### 4.4 Real Time Capabilities of the UnipaBCI

The framework has been developed using Microsoft Visual Studio 2012 to provide a complete IDE for the code writing. The operating system used to implement UnipaBCI is Windows 10 since it provides more support to the API of the g.usbAmp hardware device used to test the framework. C++ was selected as language, because it introduces a low performance overhead at run-time. GUI and other visual components are implemented in OpenGL. To test the real time capabilities for the UnipaBCI framework we followed the approach stated in [25]. Test was run on a Intel Core i5-4200M with 8 Gb at 2.5 Ghz, with 8 GB ram and integrated graphic card. The processor load was always  $< 30\%$ . Our test has been run at 256 Hz so the acquisition module received a new sample every 39.06 ms. The ADC latency, expressed as the time to acquire a signal for each of 16 channel, was below 3.17 ms. This result proves that the system is able to process every sample and store it before a new one is acquire. The processing latency, expressed as time to get a prediction from the BLDA algorithm was  $4.022 \pm 0.59$  s. The output latency expressed as the time to send the command to the robot was  $< 22$  ms. These results suggest that the most demanding operation is represented



by the BLDA algorithm while others operations are done without any significant jitter so UnipaBCI framework could be effectively used for real-time operations since prediction is done at the end of each trial.

## 5 Discussion

Accordingly to our findings the precision of the system is not statistically affected ( $t(40) = 1.7471$   $p = 0.0887$ ) by flashing modality (Row Columns vs Single Square) so it is possible to conclude the system could be used indifferently in both modalities even if users obtained best results in Row Column modality. Both expert and beginner users achieved good results using UnipaBCI and expertness doesn't seem to statistically affect the performance both in row-square modality ( $t(20) = 1.1028$   $p = 0.2846$ ) and in single square modality ( $t(20) = 0.9583$   $p = 0.3506$ ). It is clearly possible to conclude that the system is performing accurately and that it works even with non expert subjects. Accordingly to the questionnaire, all users, even beginners, found the system easy to use. They noticed quite difficult to follow the flash speeds but they were overall satisfied by UnipaBCI.

Accordingly to the performance test, the system could be used in real-time and present good signal acquisition rate and fast connection to the external agent. The most demanding operation is represented by the features classification.

## 6 Conclusion

In conclusion the UnipaBCI has demonstrated to be a powerful and reliable system able to work efficiently with visual evoked potentials showing a low error rate with Expert and Non Expert subjects. Moreover only a low number of electrodes have been used. The flash optimization module proved that the system was able to adapt over the user expertness by finding the optimal number of stimuli to provide for each trial to avoid stress in the user.

The system is able to work in real-time and suitable to be the ground to develop new BCI functionalities in a fast and reliable way. The UnipaBCI framework will be enriched with new modules to support for other hardware devices; new BCI paradigms like auditory VEP, motor imagery and SSVEP; to develop of new user application to control external devices such as humanoid robots and systems to help impaired users in their everyday life.

**Acknowledgment.** Authors wish to thank Christopher Guger supporting us with his BCI hardware, the master thesis students Rosario Misuraca, Walter Tranchina and Giuseppe Trubia for their support in the framework development.

## References

1. Spataro, R., Chella, A., Allison, B., Giardina, M., Sorbello, R., Tramonte, S., Guger, C., La Bella, V.: Reaching and grasping a glass of water by locked-in ALS patients through a BCI-controlled humanoid robot. *Front. Hum. Neurosci.* **11**, 68 (2017)
2. Amiri, S., Fazel-Rezai, R., Asadpour, V.: A review of hybrid brain-computer interface systems. *Adv. Hum. Comput. Interact.* **2013**, 1 (2013)
3. Lal, T.N., Hinterberger, T., Widman, G., Schröder, M., Hill, J., Rosenstiel, W., Elger, C.E., Birbaumer, N., Schölkopf, B.: Methods towards invasive human brain computer interfaces. In: *Advances in Neural Information Processing Systems*, pp. 737–744 (2004)
4. del R. Millán, J., Ferrez, P.W., Galán, F., Lew, E., Chavarriaga, R.: Non-invasive brain-machine interaction. *Int. J. Pattern Recogn. Artif. Intell.* **22**(05), 959–972 (2008)
5. Tekgul, H., Bourgeois, B.F.D., Gauvreau, K., Bergin, A.M.: Electroencephalography in neonatal seizures: comparison of a reduced and a full 10/20 montage. *Pediatric Neurol.* **32**(3), 155–161 (2005)
6. Guger, C., Edlinger, G., Harkam, W., Niedermayer, I., Pfurtscheller, G.: How many people are able to operate an eeg-based brain-computer interface (BCI)? *IEEE Trans. Neural Syst. Rehabil. Eng.* **11**(2), 145–147 (2003)
7. Walsh, P., Kane, N., Butler, S.: The clinical role of evoked potentials. *J. Neurol. Neurosurg. Psychiatry* **76**(suppl 2), 16–22 (2005)
8. Vallabhaneni, A., Wang, T., He, B.: Brain-computer interface. In: *Neural Engineering*, pp. 85–121. Springer (2005)
9. Gentile, A., Sorce, S., Santangelo, A., Vitabile, S.: Human-to-human interfaces: emerging trends and challenges. *Int. J. Space-Based Situated Comput.* **1**, 3–17 (2011)
10. Schalk, G., McFarland, D.J., Hinterberger, T., Birbaumer, N., Wolpaw, J.R.: BCI 2000: a general-purpose brain-computer interface (BCI) system. *IEEE Trans. Biomed. Eng.* **51**(6), 1034–1043 (2004)
11. Renard, Y., Lotte, F., Gibert, G., Congedo, M., Maby, E., Delannoy, V., Bertrand, O., Lécuyer, A.: Openvibe: an open-source software platform to design, test, and use brain-computer interfaces in real and virtual environments. *Presence Teleoper. Virtual Environ.* **19**(1), 35–53 (2010)
12. Kothe, C.A., Makeig, S.: Estimation of task workload from EEG data: new and current tools and perspectives. In: *2011 Annual International Conference of the IEEE Engineering in Medicine and Biology Society, EMBC*, pp. 6547–6551. IEEE (2011)
13. Tanaka, K., Matsunaga, K., Wang, H.O.: Electroencephalogram-based control of an electric wheelchair. *IEEE Trans. Robot.* **21**(4), 762–766 (2005)
14. Chen, S.-C., Hsu, C.-H., Kuo, H.-C., Zaeni, I.A.E.: The BCI control applied to the interactive autonomous robot with the function of meal assistance. In: *Proceedings of the 3rd International Conference on Intelligent Technologies and Engineering Systems (ICITES 2014)*, pp. 475–483. Springer (2016)
15. Chella, A., Pagello, E., Menegatti, E., Sorbello, R., Anzalone, S.M., Cinquegrani, F., Tonin, L., Piccione, F., Priftis, K., Blanda, C., Buttita, E., Tranchina, E.: A BCI teleoperated museum robotic guide, pp. 783–788 (2009)
16. Mason, S.G., Birch, G.E.: A general framework for brain-computer interface design. *IEEE Trans. Neural Syst. Rehabil. Eng.* **11**(1), 70–85 (2003)

17. Hinterberger, T., Mellinger, J., Birbaumer, N.: The thought translation device: structure of a multimodal brain-computer communication system. In: First International IEEE EMBS Conference on Neural Engineering, Conference Proceedings, pp. 603–606. IEEE (2003)
18. Hinterberger, T., Nijboer, F., Kübler, A., Matuz, T., Furdea, A., Mochty, U., Jordan, M., Lal, T.N., Hill, J., Mellinger, J., et al.: Brain-computer interfaces for communication in paralysis: a clinical experimental approach. *Towards Brain-Computer Interfacing*, pp. 43–64 (2007)
19. Hastings Jr., C., Mosteller, F., Tukey, J.W., Winsor, C.P.: Low moments for small samples: a comparative study of order statistics. *Ann. Math. Stat.* 413–426 (1947)
20. Chen, T., Martin, E.: Bayesian linear regression and variable selection for spectroscopic calibration. *Analytica Chimica Acta* **631**(1), 13–21 (2009)
21. Bishop, C.M.: *Pattern Recognition and Machine Learning*. Springer (2006)
22. MacKay, D.J.C.: Bayesian interpolation. *Neural Comput.* **4**(3), 415–447 (1992)
23. Kaufmann, T., Schulz, S.M., Grünzinger, C., Kübler, A.: Flashing characters with famous faces improves ERP-based brain-computer interface performance. *J. Neural Eng.* **8**(5), 056016 (2011)
24. Teplan, M., et al.: Fundamentals of EEG measurement. *Meas. Sci. Rev.* **2**(2), 1–11 (2002)
25. Wilson, J.A., Mellinger, J., Schalk, G., Williams, J.: A procedure for measuring latencies in brain-computer interfaces. *IEEE Trans. Biomed. Eng.* **57**(7), 1785–1797 (2010)

# XML-VM: An XML-Based Grid Computing Middleware

Alfredo Cuzzocrea<sup>1</sup>(✉), Enzo Mumolo<sup>2</sup>, Marco Tassarotto<sup>2</sup>, Giorgio Mario Grasso<sup>3</sup>,  
and Danilo Amendola<sup>4</sup>

<sup>1</sup> DIA Department, University of Trieste and ICAR-CNR, Trieste, Italy  
alfredo.cuzzocrea@dia.units.it

<sup>2</sup> DIA Department, University of Trieste, Trieste, Italy  
mumolo@units.it, marco.tassarotto@regione.fvg.it

<sup>3</sup> CSECS Department, University of Messina, Messina, Italy  
gmgrasso@unime.it

<sup>4</sup> IRCCS Bonino-Pulejo, Messina, Italy  
danilo.amendola@gmail.com

**Abstract.** This paper describes a novel distributing computing middleware named XML-VM. Its architecture is inspired by the ‘Grid Computing’ paradigm. The proposed system improves many characteristics of previous Grid systems, in particular the description of the distributed computation, the distribution of the code and the execution times. XML is a markup language commonly used to interchange arbitrary data over the Internet. The idea behind this work is to use XML to describe algorithms; XML documents are distributed by means of XML-RPC, interpreted and executed using virtual machines. XML-VM is an assembly-like language, coded in XML. Parsing of XML-VM programs is performed with a fast SAX parser for JAVA. XML-VM interpreter is coded in JAVA. Several algorithms are written in XML-VM and executed in a distributed environment. Representative experimental results are reported.

## 1 Introduction

In the last decade, there has been an increasing interest in the development of systems for distributed computing aiming at sharing computing resources available on a large scale. These systems exploit the unused CPU cycles of a potentially enormous number of computers available in internet, conveying to a final user a large computing power at a very low cost. At a smaller scale, they exploit the unused CPU cycles of the computers available in the current intranet. These implementations originated the computing paradigm known as “GRID Computing” [1–4]. For instance, classical environments for which these framework are *medical information systems* (e.g., [22, 23]).

Grid computing aims at creating the illusion of a simple yet powerful virtual computer. Actually, the computing power is provided by a large collection of connected systems. There are many important applications requiring a large amount of processing power, for example systems for weather prediction using computational models, systems for the solution of theoretical physics and astronomy problems, simulations of complex systems, financial markets prediction systems and many other. The computing

environments for GRID computing are usually very heterogeneous from a hardware and software point of views; thus, the first problem to be faced is the necessity of developing virtual machines to make the computation infrastructure independent from the various platforms. Of course, the most important characteristics of a virtual machine are the easiness of use, performance, security and scalability. Java is one of the most popular virtual machine. The Java virtual machine has been designed for running in various computing environments, from dedicated systems to general-purpose machines. However, generally Java requires a remarkable amount of computing and memory resources for compilation and execution.

One of the problems of the known Grid systems is that they are typically built around a monolithic architecture: the remote computing node selected to execute a certain application must also execute locally the verification functions, the security management, compilation and optimisation. Consequently, these monolithic architectures generally are limited in terms of security and scalability, opening to a large field of research [5]. Other known problems come from the lack of grid enabled software, making it difficult to easily obtain software solutions.

This paper proposes a contribution in this field of research, developing a middleware that hides to the programmer the complexity of the available distributed architecture. The issues that we have treated designing the middleware are system performance, addressed by means of efficient distribution and interpretation tools, and the security, addressed using of SSH protocols. The architecture we propose in this paper is based on the XML meta-language, which is a programming language normally used for describing data structures. The key point of this work is that rather than using XML to describe data we use XML to describe algorithms. Distribution of XML-VM code is performed using XML-RPC high performance protocol. Parsing and interpretation of XML-VM documents is performed in JAVA.

Using XML as a framework to describe both data and algorithms we provide a common base that different platforms can manage in different ways. One way may be to use transformation sheets, and another way is to write an interpret using an appropriate programming language.

This paper is structured as follows. Section 2 deals with the state of the art, describing in particular a representative Grid system highlighting its positive aspects and defects. In Sect. 3, we describe the architecture of the system. In Sect. 4, we summarize the XML-VM language, while in Sect. 5 we describe some information on parsing and interpretation of a XML-VM program. In Sect. 6, some experimental result are shown. In Sect. 7, some final remarks are reported.

## 2 Related Work

This project is inspired by the large scale distributed computing systems for research purposes developed over the years. The Great Internet Mersenne Prime Search (GIMPS) project [6] started in 1996. The goal of GIMPS is to find Mersenne primes, namely prime number of the form  $M_n = 2^n - 1$  for some integer  $n$ , using computers connected via internet. The SETI@Home project [7] started in 1997 to identify non-random radio

patterns generated by some form of intelligent life, excluding at the same time random signal patterns generated by natural phenomena like stars and supernovas. The Einstein@Home project [8] was officially launched in 2005 for searching signals from rotating neutron stars using gravitational-wave detectors. In each of these projects, huge amount of data is processed using a parallel computing approach: data is broken in small packets, and each packet is sent to the computers distributed across the Internet which offer their free CPU times for the processing. This is done using a special software downloaded from a web site. Usually this software acts as a traditional screen saver, however it contains the implementation of the data processing algorithms and the procedures for receiving data and transmitting results to the main server. The algorithms implemented on the GRID are always the same, while the data to be processed is varying; such a SIMD model is only suitable to particular computations. Namely, if we do not have a completely separable problem, or if the routines being executed on the data are varying, or if a single node needs additional remote tasks, the reported GRID computational model becomes absolutely inadequate.

Other approaches for building a distributed programming system are based on Java virtual machines [9]. Some approaches give the programmer an unique environment in which the threads are distributed on the different nodes by the operating system. This solution is quite complex to develop, since many problems arise concerning both implementation and performance. Projects following this approach include the IBM cluster VM for Java, the Kaffe virtual machine and the JDSM [10].

Other approaches are based on the development of communication mechanisms such as, for example, message passing. A typical approach of this kind is RMI (Remote Method Invocation). Other approaches are based on extensions of Java with parallel programming linguistic constructs. An example of this latter approach is JavaParty, developed at the University of Karlsruhe [11].

Other approaches are based on CORBA [12]. Miro [13] is an object oriented layered client/server robot middleware system based on ACE [14] and the associated real-time CORBA ORB, TAO.

The middleware described in this paper is of SIMD type. One of its feature is that it is able to distribute the computing load transparently to the programmer.

### 3 System Architecture

The architecture of the distributed system described in this paper, namely XML-VM, is depicted in Fig.1. XML-VM is structured according to a peer-to-peer principles. A central node provides a simple terminal for the collection of the result and the measurements of the performances of the system. The central node does not know nearly anything about what is happening in the remote nodes, where the computation effectively takes place. Each node decides if and when to call other remote nodes and the method to execute. On the central node a particular daemon is running, called 'name resolve daemon', which knows the IP of the available remote nodes. A generic node 'A', when it needs to fork a procedure on a remote node, calls the central node for the individuation and resolution of the address of an available remote node. At this point, node 'A' contacts

directly the remote node for the execution of an algorithm; this procedure is executed each time a remote call is needed. Clearly, node 'A' must join the conclusion of the remote call by waiting for the return of results. In our system, the distribution of the XML code on the distributed nodes is performed using the Fork statement.

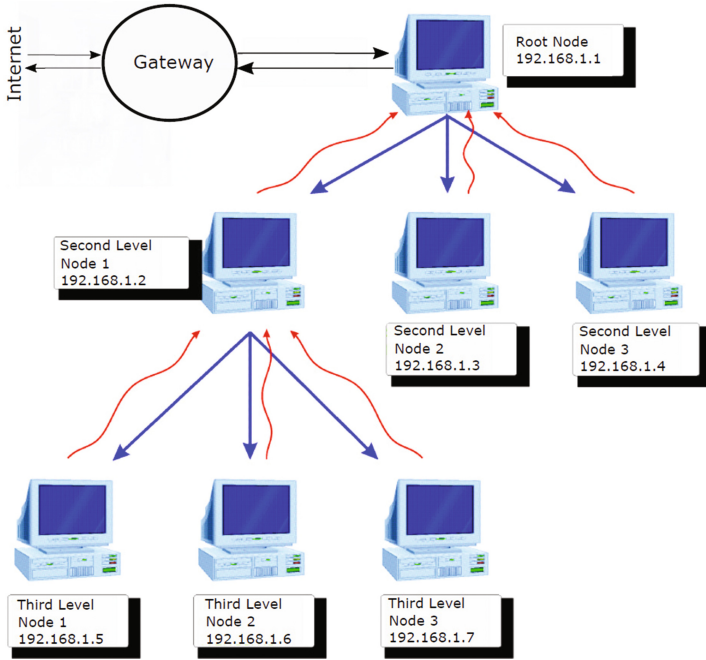


**Fig. 1.** XML-VM System Architecture. The gateway computer is the Root Node. Every other computer is a computational node and it is configured as root or leaf in a logical tree structure. Each node has a reference to its higher-level node and a to a local IP table.

```
<FORK id clone results>  
    ...data and algorithms to be executed in the remote node,  
    expressed in XML-VM...  
</FORK>
```

Fork implements the following actions: first, an available node is sought in the local table, then the code and data are sent to the remote node with XML-RPC.

Synchronization is performed using the Join statement. The Join tag has the following syntax: <JOIN id/> and implements the following operation: waits for the termination of the remote node and returns the results to the calling environment using the XML-RPC response.

## 4 The Fork/Join Linguistic Framework

The Fork/Join linguistic framework has been introduced by M. Conway [15] and J. Dennis [16] in the '60. Starting from the initial definition, many programming languages used the Fork/Join concept in several ways. The Fork/Join operations has been largely studied from a queueing point of view [17–19]. The Fork/Join linguistic framework is available in Java [20]. Fork generates a concurrent thread of execution, while the Join waits for its termination; in this way it is possible to build concurrency.

In Fig. 2 a system of concurrent processes is shown using an interpretation of the Fork operation based on a data type defined by the language, *process*, which is used as an operand of Join to specify the process to synchronize with. A similar approach for the implementation of Fork/Join is used in this work.

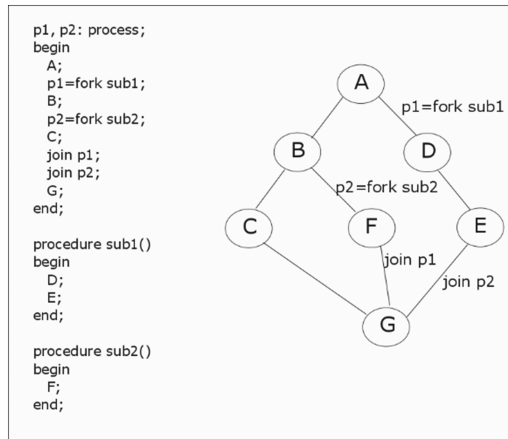
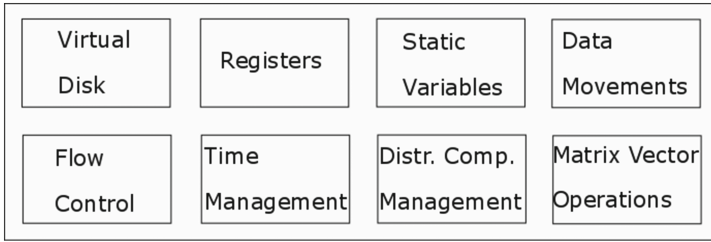


Fig. 2. Example of a Fork/Join concurrent processes with a predefined data type

## 5 The Language XML-VM

In this Section, we summarize the main characteristics of the XML-VM language. First of all, it is worth noting that two sets of memory are generated, declared in Java as Array of Object, which simulate registry and a virtual disk available to the virtual machine. The registry is constituted by 32 cells numbered from 0 to 31, while the virtual disk is constituted by 10000 blocks of data, numbered from 0 to 9999. All the data related operations take place on the virtual disk; this means that, for example, if we want to make a simple sum of two numbers, the numbers must be stored in two data cells of the virtual disk. There are no variables, and every operation must be performed specifying the involved cells of memory; from this point of view, XML-VM is an assembler-like language (Fig. 3).





**Fig. 3.** The architecture of XML-VM

All the mathematical and logical instructions of the language take only place on registers. The storage of data on the virtual disk is performed exclusively through the STORE instruction. Instead, the LOAD instruction is the only instruction that allows to copy the content of the cells of the virtual disk into the registers. Ten different data types are implemented in the language; nine of them follow the Java data types: int, long, short, byte, float, double, Boolean, char and string while the tenth data type, defined in XML-VM as “index”, represents a pointer to another data cell in the virtual disk or in a register. The index data type can be used by the load, store and procedure call operations; moreover, this type is fundamental for programming loops. The syntax of the language exploits the use of tags attributes as integrating parts of the instructions, while nesting of tags is rare. This decision was taken in order to facilitate the XML-VM code writing.

### 5.1 Parsing and Interpretation

The parser performs a complete analysis of the XML-VM document, expanding all the tags, attributes and values. One of the most complete and used XML parser is the Apache Xerces XML Parser. Xerces supports SAX 1.0 and 2.0; SAX stands for Simple Api for XML. Once we completed the first version of XML-VM virtual machine, embedding the XML-RPC protocol for communication between remote nodes, we noticed a decrease of performance due to the slowness of the XML parser. In order to overcome this overhead we decided to use the Piccolo XML Parser for Java [21], which is a light and fast SAX 1, SAX 2 and JAXP parser. Piccolo is very fast and it has been integrated in our system. The high performance reached is mainly due to the fact that the parser does not process the Data Type Definition (DTD). The interpreter of XML-VM language is written in Java for portability reasons; the interpreter executes the actions associated to the XML tags as they are analyzed by the parser.

Let us consider the architecture depicted in Fig. 1. The following points are required:

- 1 – it is necessary to install on each machine the XML-VM virtual machine; the virtual machine is started and works as a service, waiting for remote requests.
- 2 – on the central node, we install the same XML-VM virtual machine and the name resolve daemon used by remote nodes.
- 3 – the sources of the algorithms to be executed are published through a web server reachable by all the nodes.
- 4 – now we are ready to launch the distributed execution of the program.

The pseudocode of the interpret is reported as follows.

```

public Object startExe (Object[]arg,xmlvm Machine)throws
Exception {
    Initialize XML-VM stack, registry end virtual disk;
    Search the Tag Labels;
    Save the (name, position) couples in the
    LabelIis tarray;
    Verify that all the document is included in
    <XMLVM>...</XMLVM> Tags;
    Find the Tags <START/> or <STRUCT/>;
    Set 'i'=<START/>Tag position;
    try {
        for(i<tag.getChildrenCount();
        if (i-th Tag in ADD LOAD MOV STORE SUB MUL
        DIV
                                COMP LOCALCALL CALL FORK JOIN
                                CONV ELEV OPER e RANDOM)
        then
            execute the Tag service routine;
        else{
            if START and LABEL do nothing;
            if STRUCT restore information;
            if JEQ, JNEQ, JGR, JNGR execute the
            associated routines;
            if RETURN execute the Return(tag)
            routine;
            if SHOW list registry content;
            if QUIT exit;
        }
    }
    } catch(Exception e)
    Measure the time interval from initialization to
    last detected Tag;
    Send the time measure to the name resolution
    routine using XML-RPC;
    End routine;
}

```

In the following we report the pseudocode of the implementation of the Fork instructions.

```

public void Fork(xmlvm tag) throws Exception {
    Extract TO, IP, FILE, NAME and CLONE attributes;
    If (IP.charAt(0) == 'N'){
        Make an RPC call to the Name Resolution
        Module to get the IP corresponding to the
        identifier stored in IP;
        IP = true IP returned by the name resolution
        module;
        args = registry and virtual disk address
        indicated by CLONE;
        virtual disk = ``*RESERVED*``;
        ForkThread remoteCall = new ForkThread();
        RemoteCall.start();
    }
}

```

We now report the pseudocode of the implementation of the Join instruction.

```

public void Join(xmlvm tag) throws Exception {
    Extract TO and TOPOINTED attributes;
    if(TO.compareTo('') != 0)
        Verify that the TO cells are still not
        *RESERVED*;
        Otherwise, start a cycle to continuously
        monitor the cells;
    Else{
        Verify that TOPOINTED cells are still not
        *RESERVED*;
        Otherwise, start a cycle to continuously
        monitor the cells
    }
}

```

## 6 Experimental Results

We report some experimental results about typical performance of the Grid computing system presented in this paper. In general, the efficiency of a distributed application is related to various factors: the network speed, the homogeneity of the machines which participate to the Grid, the degree of parallelism of the algorithm.

Our experimental study is performed on fifteen computers available in the laboratory intranet. Each computer, based on an Intel Core I5 running at 3.40 GHz, is a XMLVM node. Three simple applications are written in XML-VM and executed on this network. The first application is the sum of two billions of integer numbers. The whole series of numbers is split in small sections whose summation is distributed among the nodes. The second application is the computation of the  $\pi$  number by solving this integral:

$$\int_0^1 \frac{4}{1+x^2} dx = \pi$$

where the [0–1] interval is divided in two billion sections distributed among the network. The third application a quicksort sorting algorithm executed on a sequence of two billion integers. The quicksort algorithm is implemented in the XML-VM distributed computing framework.

These simple problems allow us to study the behavior of XML-VM executing a large number of operations. Clearly, the computing time is dependent on the number of machines used in parallel for the elaboration of the algorithms.

The applications are executed on fifteen nodes and the execution time of each node is summed and divided by fifteen. To analyze the overhead of XML parsing, the parsing time of each node is averaged over the nodes too. The results are reported in Table 1.

**Table 1.** Medium Parsing and Execution Times and Parsing Overhead.

Application	Average parsing time	Average execution time	Percentage
Sum	384 ms	5814.32 ms	0.066%
Integral	531 ms	10662.81 ms	0.05%
QuickSort	518 ms	7727.3 ms	0.067%

The first application is executed on a number of nodes from one to fifteen. What it is expected is that the execution time  $T(n)$  follows an hyperbolic behavior, since the  $T(n)$  function should be of the type  $1/n$ , where  $n$  is the number of machines involved in the

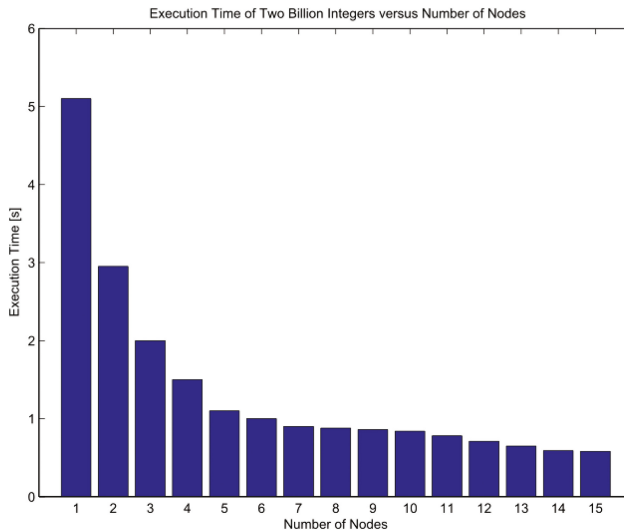


**Fig. 4.** Execution time in seconds of the sum of the two billion integer versus the number of distributed nodes.

distributed computation. The measured values are shown in Fig. 4. The absolute time versus the number of machines follows a hyperbolic curve as expected.

In Fig. 5 we report the speedup of the execution time required by the sum operation performed on the distributed system compared with the execution time of the same operation on a single i5 computer.

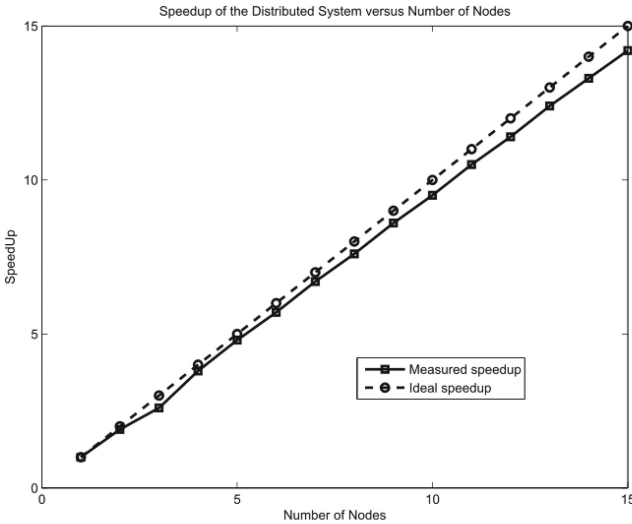


**Fig. 5.** Speedup of the execution time obtained with the XML-VM distributed system compared to the execution time on a single node.

The speedup approximately follows the theoretical behavior.

## 7 Conclusions and Final Remarks

In this paper we dealt with the problem to design and develop an efficient architecture for realizing a computing system based on the Grid approach. We describe a Grid system based on XML. Many distributed applications are described. This work is based on the idea to use XML for describing algorithms. By means of XML it is possible to realize an efficient Grid system; the distribution of the algorithms, which is done by means of HTTP protocols, is very fast, the code execution is quickly performed by a fast XML parsing and by means of an interpreter we wrote in JAVA. The scalability of the system is realized efficiently with a name resolve daemon. Due to these reasons, the system performance compare very favorably with other solutions based on the distribution of Java code.

We develop a language, called XML-VM, for describing algorithms, as well an XML-VM interpreter to execute these algorithms. Each distributed machine runs locally the parser and the interpreter, whose execution is very efficient. The distribution of the methods is efficiently performed with XML-RPC and HTTPS protocols. Experimental

results show that the practical behavior of the system is in agreement with the theoretical expectations.

Many problems are still open. The distribution of the workload, that is how to choose the distributed nodes, has not been considered. Another open aspect is the fault tolerance of the system. Similarly, we did not consider the problems related to the programming of complex algorithms; this problem could be mitigated by the development of a high-level language to XML-VM translator. Also, privacy (e.g., [24]) and performance (e.g., [25]) are still open problems.

In conclusion, in view of the increasing importance of the Grid computing and of the possible future developments of this research, such as adaptive metaphors (e.g., [26]), we believe that this paper can give a remarkable contribute in several theoretical and applicative fields.

## References

1. Strong, P.: Enterprise grid computing. *Distrib. Comput.* **3**(6), 18 (2005)
2. Gullapalli, S.: Atlas: an intelligent, performant framework for web-based grid computing. In: *ACM SIGSOFT FS*, pp. 1154–1156, 13–18 November (2016)
3. Sharma, S., Chhabra, A., Sharma, S.: Comparative analysis of scheduling algorithms for grid computing. In: *International Conference on Advances in Computing, Communications and Informatics*, Kochi, India, 10–13 August (2015)
4. Abidi, L., Cerin, C., Jemni, M.: Desktop grid computing at the age of the web. In: Park, J.J. (Jong Hyuk), Arabnia, H.R., Kim, C., Shi, W., Gil, J.-M. (eds.) *GPC 2013*. LNCS, vol. 7861, pp. 253–261. Springer, Heidelberg (2013). doi:[10.1007/978-3-642-38027-3\\_27](https://doi.org/10.1007/978-3-642-38027-3_27)
5. Geetha, R., Ramyachitra, D.: Security issues in grid computing. In: *International Conference on Research Trends in Computer Technologies (ICRTCT – 2013)*, pp. 33–37 (2013)
6. Quan-quan, G.A.O.: Research development of great internet mersenne primes search project. *Math. Pract. Theory* **10**, 028 (2010). CNKI J.
7. Anderson, P., Cobb, J., Korpela, E., Lebofsky, M., Werthimer, D.: SETI@home: an experiment in public-resource computing. *Commun. ACM* **45**(11), 56–61 (2002)
8. Aasi, J., et al.: Einstein@Home all-sky search for periodic gravitational waves in LIGO S5 data. *Phys. Rev. D* **87**, 042001[1–29] (2013)
9. Baker, M.A., Grove, M., Shafi, A.: Parallel and distributed computing with java. In: *Symposium on Parallel and Distributed Computing* (2006)
10. Sodha, Y., Nakada, H., Natsuoka, S.: Implementation of a portable software DSM in Java. In: *Proceedings of the 2001 Joint ACM-ISCOPE Conference on Java Grande* (2001)
11. Philippsen, M., Zenger, M.: JavaParty - transparent remote objects in java. *Concurr. Pract. Exp.* **9**(11), 1225–1242 (1997)
12. Yang, Z., Duddy, K.: CORBA: a platform for distributed object computing. *Oper. Syst. Rev.* **30**(2), 4–31 (1996)
13. Kraetzschmar, G., Utz, H., Sablatnög, S., Enderle, S., Palm, G.: Miro — middleware for cooperative robotics. In: Birk, A., Coradeschi, S., Tadokoro, S. (eds.) *RoboCup 2001*. LNCS, vol. 2377, pp. 411–416. Springer, Heidelberg (2002). doi:[10.1007/3-540-45603-1\\_52](https://doi.org/10.1007/3-540-45603-1_52)
14. Schmidt, D.C.: ACE: an object-oriented framework for developing distributed applications. In: *Proceedings of the 6th USENIX C++ Technical Conference*, (Cambridge, Massachusetts). USENIX Association, April 1994

15. Conway, M.: Multiprocessing system design. In: Proceedings of the AFIPS Fall Computer Conference (1963)
16. Dennis, J.G., Van Horn, E.C.: Programming semantics for multiprogramming computations. *Commun. ACM* **9**(3), 143–155 (1966)
17. Chen, R.J.: A hybrid solution of fork/join synchronization in parallel queues. *IEEE Trans. Parallel Distrib. Syst.* **12**(8), 829–845 (2001)
18. Nelson, R., Tantawi, A.N.: Approximate analysis of fork/join synchronization in parallel queues. *IEEE Trans. Comput.* **37**(6), 739–743 (1988)
19. Liu, Y.C., Peros, H.G.: A decomposition procedure for the analysis of a closed fork/join queuing system. *IEEE Trans. Comput.* **40**(3), 365–370 (1991)
20. Lea, D.: A java fork/join framework. In: ACM Java Grande 2000 Conference, 3–5 June 2000 (2000)
21. Sosnoski, D.M.: XML documents on the run. *JavaWorld*, APR 26 (2002)
22. Montagnat, J., Jouvenot, D., Pera, C., Frohner, Á., Kunszt, P.Z., Koblitz, B., Santos, N., Loomis, C.: Bridging clinical information systems and grid middleware: a medical data manager. In: *HealthGrid 2006*, pp. 14–24 (2006)
23. Ramos-Pollán, R., Guevara-López, M.A., Oliveira, E.C.: A software framework for building biomedical machine learning classifiers through grid computing resources. *J. Med. Syst.* **36**(4), 2245–2257 (2012)
24. Cuzzocrea, A.: Privacy and security of big data: current challenges and future research perspectives. In: *Proceedings of ACM PSBD 2014* (2014)
25. Cuzzocrea, A., Matrangolo, U.: Analytical synopses for approximate query answering in OLAP environments. In: Galindo, F., Takizawa, M., Traunmüller, R. (eds.) *DEXA 2004. LNCS*, vol. 3180, pp. 359–370. Springer, Heidelberg (2004). doi:[10.1007/978-3-540-30075-5\\_35](https://doi.org/10.1007/978-3-540-30075-5_35)
26. Cannataro, M., Cuzzocrea, A., Pugliese, A.: A probabilistic approach to model adaptive hypermedia systems. In: *Proceedings of WebDyn 2001* (2001)

# Intelligent Sensor Data Fusion for Supporting Advanced Smart Health Processes

Alfredo Cuzzocrea<sup>1</sup>(✉), Fernando Ferri<sup>2</sup>, and Patrizia Grifoni<sup>2</sup>

<sup>1</sup> DIA Department, University of Trieste and ICAR-CNR, Trieste, Italy  
alfredo.cuzzocrea@dia.units.it

<sup>2</sup> IRPPS-CNR, Rome, Italy  
{fernando.ferri, patrizia.grifoni}@irpps.cnr.it

**Abstract.** Smart cities applications are now very relevant in both the academic and industrial settings. Smart health processes are among the most significant cases of smart cities applications, where the goal is to determine effective and efficient decision-making processes in the context of healthcare management. One way to achieve this goal is just introducing novel sensor data fusion algorithms and techniques, as to take advantages from the mature area of sensor data management and processing. This article proposes a system based on sensors data to identify the most appropriate solution to be activated when a health problem arises. In particular, the proposed system allows identifying anomalies, their assessment and their management.

## 1 Introduction

*Smart cities applications* are now very relevant in both the academic and industrial settings. In this class of applications, intelligent methods, techniques and algorithms are combined to effectively and efficiently manage data produced by sensors and derive decision making processes (e.g., [15–18]).

Among several approaches, one relevant is represented by *data fusion methods*, where the idea is to combine sensor data coming from heterogeneous data sources in order to improve the overall knowledge discovery task.

*Smart health processes* are among the most significant cases of smart cities applications, where the goal is to determine effective and efficient decision making processes in the context of healthcare management. One way to achieve this goal is just introducing novel sensor data fusion algorithms and techniques, as to take advantages from the mature area of sensor data management and processing. On the other hand, performance (e.g., [12]) and privacy (e.g., [13]) concerns are also relevant in these settings.

Due to the lifestyle and environmental changes, as well as healthcare improvements and increased life expectancy, the management of chronic diseases is more and more becoming one of the most important focus of new health policies being currently the leading cause of adult death and disability worldwide [1]. Currently health care services tend to be fragmented, curative, hospital-based and disease-oriented rather than person-centered. On the contrary, chronic diseases and multi-morbidity require a more integrated and people-centered approaches to service delivery [8] and, by the use of ICT solutions, a better coordinate care across providers and service settings can be applied [2, 6]:



- at *micro* level, to support the empowerment of citizens (better-informed patients and careers have the potential to improve the quality of clinical care by facilitating the provision of feedback to individual health professionals on the outcomes of care they deliver);
- at *meso* level, to integrate multi-professional teams and institutions;
- at *macro* level, to allow better planning of services based on epidemiological investigations and outcomes.

New organizational models of healthcare are needed; in this perspective patients becomes partners in the process, contributing to almost every decision or action level and integration between hospital and home care are needed [7].

Various methodologies were provided in the literature for managing health care processes and clinical trials [4, 5, 10].

In order to support the possibility for chronic patients to safely live in not hospitalized environments (either at home or in residential structures) it becomes crucial to manage critical events. Several elements have to be considered in order to identify and activate the most appropriate solutions. A clear identification of the specific health need associated with a level of severity, the mapping of the healthcare processes with associated resources that could provide an answer to the health need, criteria of preferences to refine selection once the minimum set of health criteria are satisfied (e.g. distance between the subject and the health service, previous experiences between the specific subject and the specific health operators, preferences expressed by the patient).

To overcome the aforementioned critical issues, a system has been developed for the automatic identification of the most appropriate solution to be activated when a health problem arises. The system acts at the previously mentioned *meso* and *micro* levels to orchestrate the available resources/actors in order to meet the patient needs.

The present work describes the system and reports its testing in a simulated environment. This paper extends the paper [11].

## 2 Proposed Methodology

### 2.1 Case Study

A simulated case study was used to design and test the system (no real interventions were executed). The specific health context is described:

- *Patient*: subjects living at home and suffering from chronic cardiovascular issues;
- *Analyzed parameters to define the health status*: body temperature, arterial bloody pressure (min and max), hearth rate;
- *Health issue*: 3 different health issues are identified, with an associated level of life-risk, based on the available parameters: fewer (low risk), infarction (medium risk), stroke (high risk);
- *Social/Health resources to be activated*: specialized physician, general practitioner, nurse, social operator;
- *Health organizations*: City Hospitals (Florence, Italy);
- *Healthcare processes*: three generic healthcare processes are defined to be activated based on the specific health issue.

The specific problem to solve with the implemented system was:

*Which are the best protocol to activate and the most appropriate resource to involve when a specific health issue arise?*

The case study organized to test whether the system is able to correctly address the above reported problem consists of:

- a simulated list of patients with their geographical coordinates (real addresses in Florence, Italy);
- a simulated list of health organizations with their geographical coordinates (real addresses in Florence);
- a simulated list of social/health professionals with their specialization and geographical coordinates (real addresses in Florence);
- a simulated list of previous interventions where the combination of patients-operator was reported and a level of satisfaction expressed by the patient was stored;
- a simulated list of health events characterized by a combination of the aforementioned 4 parameters.

The system was fed with the simulated lists and piloted with the simulated events. The system responses was then manually analyzed for validation to check whether:

- the health issues were correctly identified from the comprehensive analysis of raw clinical data;
- the specific healthcare protocol was correctly activated once the health events were classified;
- the most appropriate resource was identified based on minimum level of expertise required by the health event, current availability of professionals, level of urgency in requiring an intervention, previous experiences between the specific patient and the social/health resource, patient satisfaction, geographical location.

## **2.2 Activating Healthcare Resources Based on Multiple Sensor Data and Processes Modelling**

The process for activating healthcare resources is modelled by using the *Business Process Model and Notation* (BPMN) [3], and it consists of different steps:

1. identification of the anomalies;
2. assessment of the anomalies;
3. management of the anomalies.

### **2.2.1 Identification of Anomalies**

The healthcare resources are asynchronously activated by abnormal values detected by sensors. The asynchronous activation determines a check for detecting potential anomalies.

For identifying the anomaly, we made use of the theory of *Dempster-Shafer*, as this method does not require a priori knowledge of the event and allows to assign a degree

of uncertainty regarding a given situation. Although the theory of Dempster-Shafer is computationally complex, because it is closely linked to the number of elements of the frame of discernment  $\Theta$ , in this case the frame of discernment is formed by only 2 elements:

$$\Theta = \{[Normal], [Abnormal]\} \tag{1}$$

Consequently, we can go to define the power set, formed by all the possible combinations of the elements of the frame of discernment, such as:

$$2^\Theta = \{[], [Normal], [Abnormal], [Normal, Abnormal]\} \tag{2}$$

The model is based on the mass function for each sensor described by:

$$m_{S_i}(Normal) = (1 + e^{(v_i - t_i)})^{-1} m_{S_i}(Abnormal) = 1 - m_{S_i}(Normal) \tag{3}$$

where  $v_i$  indicates the measured value to be analyzed and  $t_i$  gives the threshold value relative to the sensor  $i$ .

The value  $m_{S_i}(Normal)$  is obtained by logistic regression with sigmoid function so that the results are comprised between 0 and 1. Logistic regression is a special case of generalized linear model. It is a regression model applied in cases where the dependent variable is dichotomous, that is attributable to the values 0 and 1 (as are all the variables that take only two values: true or false, male or female, healthy or sick, etc.). The regression formalizes and solves the problem of a functional relationship between variables measured on the basis of sample data extracted from a hypothetical infinite population.

More formally, the regression is a method of estimating the conditional expectation of a dependent variable, or endogenous  $y$ , given the values of other variables or exogenous,  $x_1, \dots, x_k$ , namely:

$$E[y|x_1, \dots, x_k] \tag{4}$$

They have at their disposal a number  $n$  of sensors each one concerning a specific characteristic, such as temperature, minimum pressure, maximum pressure, heartbeats, etc. After assigning the masses to each feature, or to each sensor  $S_i$ :

$$\begin{matrix} m_{S_1}(Normal), \dots, m_{S_n}(Normal) \\ m_{S_1}(Abnormal), \dots, m_{S_n}(Abnormal) \end{matrix} \tag{5}$$

Through the combination rule of Dempster, we obtain:

$$m_{12}(A) = \frac{\sum_{B \cap C} m_1(B)m_2(C)}{1 - \sum_{B \cap C} m_1(B)m_2(C)} \tag{6}$$

It is carried out the fusion of the  $m_{S_i}(Normal)$  so that to obtain a single mass and general to determine the situation “Normal”, or  $m(Normal)$ . It runs the same procedure

for the  $m_{S_i}(Abnormal)$  in order to obtain the single mass and to determine the general situation “*Abnormal*”, i.e.  $m(Abnormal)$ .

The results obtained are then compared. They determine an emergency situation if:

$$m(Abnormal) >> m(Normal) \quad (7)$$

then, the measurement recorded data outliers, and intervention is required.

If:

$$m(Normal) > m(Abnormal) \quad (8)$$

then, measurements showed values in the media and no action is required.

### 2.2.2 Assessment of Anomalies

After identifying the occurrence of a fault it is necessary to decide the most appropriate procedure. However, the choice of the appropriate method depends on the assessment of the risk level of the situation. Based on the risk assessment it can be turned on an appropriate method. Given  $x$  as value of risk assessment for the present situation, then if:

- $x > \text{maximum threshold of risk}$ , then the *procedure A* will be performed;
- if  $\text{minimum threshold of risk} < x < \text{maximum threshold of risk}$ , will run *procedure B*;
- $x < \text{minimum threshold of risk}$ , in this case the *procedure C* will be performed.

The *procedure A* is activated in situations of high alarm, or when the level of risk is greater than the maximum threshold level of risk. This procedure is also applied when an abnormal situation is identified and the ontology diseases module has not been able to provide information about the type of pathology in progress. In this case it is very risky to the rescue intervention to domicile and it is preferable the immediate hospitalization of the patient through the management of an emergency. Patient information will then be analyzed and a request for emergency assistance will be sent to the public hospital in the same cluster of the patient or hospital neighboring if the necessary resources are not available.

The *procedure B* is applied in situations of average - high risk or when the level of risk is between a threshold value of minimal risk and a threshold value of maximum risk. In that case the intervention of rescue can be performed in the patient home by the competent professionals. The objective of this procedure is to identify the most suitable professionals, among all the available, to carry out the rescue by using the detected information from the devices.

We have implemented the algorithm using the structure of Greedy algorithms, that, at each iteration, choose the best solution at that time, or it is identified excellent local. This choice was dictated by the fact that there may be cases where the health professional “preferred” may be unavailable at the time of the call. The algorithm for the *procedure B* involves the following steps:

**Step 1.** The step allows the identification of potential health care professionals. For identification the following information are considered: patient, kind of potential problem and a level of risk. The step identifies a list of health care professionals that meet the following characteristics:

- the types of professionals is among the medical specialists or general practitioner eventually supported by nurses or social professionals;
- the professionals of the list must belong to the same cluster as the patient.

**Step 2a.** If the list is not empty, for each operator on the list it is calculated the value of preference; otherwise:

**Step 2b.** It goes back to Step 1 by changing the selection criteria of health workers to be included in the list as follows:

- the types of health care professionals is among the general practitioners or doctors specialized in managing the type of anomalies;
- the health professionals must belong to the cluster closest to the cluster analyzed in the first iteration.

**Step 3.** It was chosen for the intervention the health professional that has the highest value of preference.

The *procedure C* is applied in low risk situations or in routine activities such as changing a drip. The low level of risk can be managed by the nursing staff, social support professionals or relatives of the patient with the support and under the control of the staff. The algorithm for the *procedure C* involves the following steps:

**Step 1.** The step allows the identification of potential health care professionals. For identification the following information are considered: patient, kind of potential problem and a level of risk. The step identifies a list of health care professionals that meet the following characteristics:

- the types of professionals is among the nurses or social professionals;
- the professionals of the list must belong to the same cluster as the patient.

**Step 2a.** If the list is not empty, for each operator on the list it is calculated the value of preference; otherwise:

**Step 2b.** It goes back to Step 1 by changing the selection criteria of health workers to be included in the list as follows:

- the types of health care professionals is among the nurses or social professionals specialized in managing the type of anomalies;
- the health professionals must belong to the cluster closest to the cluster analyzed in the first iteration.

**Step 3.** It was chosen for the intervention the health professional that has the highest value of preference.

### 2.2.3 Management of Anomalies

The management of the anomalies is based on information on patients, kind of anomaly, available healthcare personnel, history of interventions to favor already consolidated matches between patients and the health operators and to consider the patient satisfaction on previous interventions.

To facilitate the choice of the health care professionals to be sent for the aid has been introduced the value of preference. The preference value is based on four parameters, described below, that are normalized and combined. The four parameters are:

**Frequency:** percentage of interventions of health professional  $X$  on the patient  $Y$ . The number of interventions made by the health professional  $X$  on patient  $Y$  is computed using the table of the “history of the interventions”. This value is compared with the total number of operations carried out by  $X$ . The percentage of the interventions made by  $X$  to  $Y$  will be then obtained, that is (combination rule of Dempster):

$$\%(interventions\ of\ X) = \frac{\text{Number of intervention of } X \text{ on } Y}{\text{Number of total intervention of } X} \quad (9)$$

The Frequency parameter feature is quite important as the project is mainly targeted to elderly people and for these users is preferable to have operators already known. This creates a more serene and trustful collaboration between professional and patient. It was therefore decided to give a 40% weight to this feature and accordingly the value of the coefficient is 0.4.

**Score:** preferences of the patient  $Y$  for the health professional  $X$ . The table of “history of the interventions” is used to analyze all the feedback left by the patient  $Y$  related to the health professional  $X$ . Each patient can give a value ranging from 1 to 5 to the health professional. The total score is obtained by an arithmetic average of the scores given by the patient  $Y$  to the health professional  $X$ , the value obtained will be rounded to the nearest integer. This parameter is useful, however it is not the most efficient and significant in the choice of the health professional, then we assigned a weight of 10 and accordingly the value of the coefficient is 0.1.

**Distance:** distance between patient  $Y$  and health professional  $X$ . The distance between the healthcare personnel and patients has influence on costs and the quality of services and must be evaluated in assigning and planning resources [9]. The distance is calculated by the geodesic distance, between the healthcare professional and the patient. A health professional is “available” when he is in his workplace, while it is “not available” as soon he leaves the workplace to go to make a rescue or when off duty. Scores are obtained based on the distance between the two seats going to prefer, and then assigning a higher score, the association between operator and patient with minimum distance. This feature appears to be the most important because the proximity is a key point in the speed of the operation, it will thus be considered with a weight of 30%. Accordingly, it will be multiplied by a coefficient of 0.3.

**Relevance:** type of the HCP, the following categories are considered: *Medical specialists; General practitioners; Nurses; Social professionals.*

The preference, depending on the severity of the situation, will be paid to the choice of a medical specialist or a general practitioner than that of a social professional. This feature presents importance of 20%, and then will be multiplied by a coefficient of 0.2.

The preference value is provided by the combination of the values of the characteristics, weighted according to their importance, and the availability of a health professional. The availability value of a health professional, as already mentioned, can be “available”, and then has a value equal to 1, or “not available” and has a value equal to 0. Obviously, in the case of non-availability of a health professional, his preference

value will be cancelled and then he will be “excluded” from the list of possible candidates to perform the surgery. The preference value is then defined as:

$$Preference\_value_Y = D \cdot \sum_i (Coeff_i \times Score_i) \quad (10)$$

where we denote by:

- $D$ , the availability of the health professional  $Y$ , that can be 0 or 1;
- $Coeff_i$ , the coefficient of the characteristic  $i$ ;
- $Score_i$ , the score obtained by the health professional  $Y$  with respect to the feature  $i$

### 3 Experimental Results

To implement all the algorithms we used the Java programming language of the web platform. Process modelling was performed using the BPMN standard, the models were incorporated into Java code using software Camunda, which offers a graphic panel to enable the realization of the process model. The association between the Java classes and the corresponding elements of the BPMN model is via XML. The proposed approach allows activating healthcare resources based on multiple sensor data and processes modelling in different operative contexts. In this paper, we present a simulation based on the Florence area, with a simulated list of health structures, social/health professionals, patients and sensors capturing data for cardiologic patients.

In Florence there are five public hospitals, therefore our value  $k$ , which is the number of clusters, will be just equal to 5. As centroids of the five clusters were chosen coordinates (represented in the form of latitude and longitude) obtained by the addresses of the hospitals themselves. Figure 1 shows the arrangement of the centroid on the map of the city and assigned patients.

First, we assumed the presence of 4 different sensors, whose measurement include:

- $S_1$  that detects the basal temperature, wherein abnormal values are the temperatures higher than 37;
- $S_2$  that detects the minimum pressure, where abnormal values are greater than 85;
- $S_3$  that detects the maximum pressure, where abnormal values are greater than 140;
- $S_4$  that detects heartbeats, where abnormal values are greater than 86.

If the sensors have detected the following values:

$S1$	$S2$	$S3$	$S4$
39	85	180	85

Analyzing the values of the patient, the algorithm detects the presence of an abnormal situation. It was also created a knowledge base (based on ontologies) for simulating the identification of the type of event identified. The combination of the values of the four sensors provided us information on the following possible conditions: fever, heart attack, stroke. An emergency can be activated after checking by

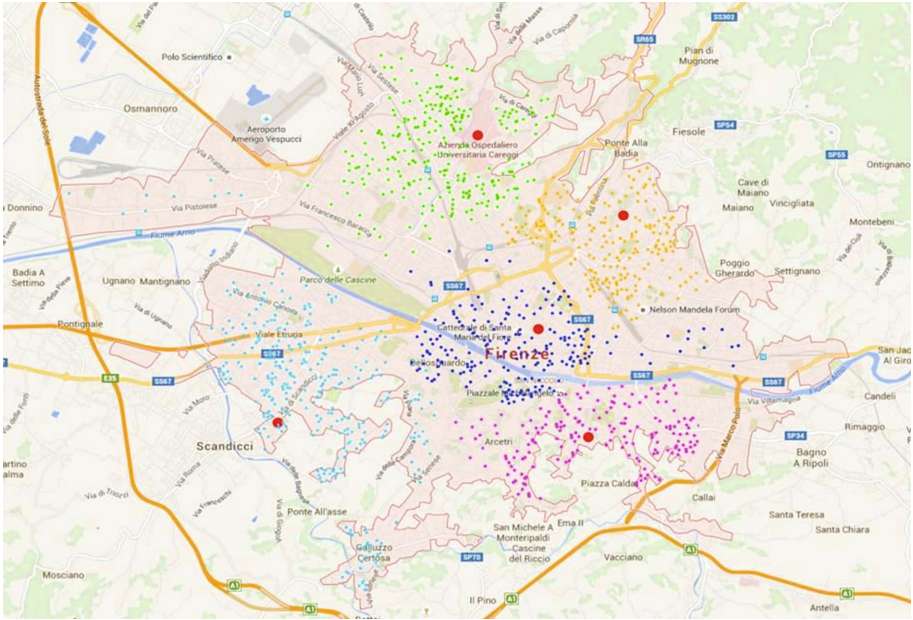


Fig. 1. Centroids on the map of the city and assigned patients

phone the presence of other symptoms like abrupt loss of vision, speech, or the ability to understand speech. As an alternative may be asked to the patient to apply a sensor to verify the presence of a stroke.

The overall module has been tested simulating different data from sensors for activating different procedures and social/healthcare resources.

## 4 Conclusions and Future Work

The increased life expectancy has led the majority of the population over the age of 65, defined elderly, to play an important role in today's society. The increasingly frenetic rhythms of everyday life have done that the elderly are alone more and more. Minimize response time, thanks to the system, allows avoiding situations extremely dangerous for patients, allowing in extreme case, to save their life. Currently the "weights" to be attributed to each feature, used to calculate the level of attractiveness (in terms of preference value) of a health professional, are considered statically and pre-defined. In a future evolution it could be considered to provide patients with the opportunity to register their preferences degree for each feature. The location of the healthcare professionals is currently regarded as fixed and defined on the basis of the registered office.

As a future work the algorithm can be upgraded to allow for identifying the GPS position of the healthcare professionals, even according to adaptive methods (e.g., [14]). Based on this information it can be calculated the position of the operator that is



closer to the patient; this will make more efficient the algorithm for the choice of the operator minimizing intervention times.

## References

1. Alwan, A., Armstrong, T., Bettcher, D., et al.: Global Status Report on Noncommunicable Diseases. World Health Organization, Geneva (2010)
2. Anderson, G.: Chronic Care: Making the Case for Ongoing Care. Robert Wood Johnson Foundation (2010). <http://www.rwjf.org/content/dam/farm/>
3. BPMN Specification - Business Process Model and Notation
4. Fazi, P., Grifoni, P., Luzi, D., Ricci, F.L., Vignetti, M.: Is workflow technology suitable to represent and manage clinical trials? *Stud. Health Technol. Inform.* **77**, 302–306 (2000)
5. Grifoni, P., Luzi, D., Merialdo, P., Ricci, F.L.: ATREUS: a model for the conceptual representation of a workflow. In: *Proceedings of DEXA Workshop 1997*. IEEE Press (1997)
6. Grone, O., Garcia-Barbero, M.: Integrated care: a position paper of the WHO European office for integrated health care services. *Int. J. Integr. Care* **1**, e21 (2001)
7. Sabato, E., Leo, C.G., Sabina, S.: Continuity of health care in patients with chronic respiratory insufficiency: a macro-model of care integration between hospital and home. *Multidisciplinary Respir. Med.* **4**(2), 112–120 (2009)
8. WHO: Global Strategy on People-centred and Integrated Health Services. <http://www.who.int/servicedeliverysafety/areas/people-centred-care/en/>
9. Rafanelli, M., Ferri, F., Maceratini, R., Sindoni, G.: An object oriented decision support system for the planning of health resource allocation. *Comput. Methods Programs Biomed.* **48**(1–2), 163–168 (1995)
10. Ferri, F., Pisanelli, D.M., Ricci, F.L.: An object-oriented model for a multimedia patient folder management system. *ACM SIGBIO Newsl.* **16**, 2–18 (1996)
11. Ferri, F., Grifoni, P., Leo, C.G., Mincarone, P., Sabina, S.: Health and assistance processes modelling and management at home and in residential structures by fusing sensor data. In: *Proceedings of LTC 2015* (2015)
12. Cuzzocrea, A.: Privacy and security of big data: current challenges and future research perspectives. In: *Proceedings of ACM PSBD 2014* (2014)
13. Cuzzocrea, A., Matrangolo, U.: Analytical synopses for approximate query answering in OLAP environments. In: *Proceedings of DEXA 2004* (2004)
14. Cannataro, M., Cuzzocrea, A., Pugliese, A.: A probabilistic approach to model adaptive hypermedia systems. In: *Proceedings of WebDyn 2001* (2001)
15. Cuzzocrea, A., Fortino, G., Rana, O.F.: Managing data and processes in cloud-enabled large-scale sensor networks: state-of-the-art and future research directions. In: *Proceedings of CCGRID 2013* (2013)
16. Zhang, P., Deng, Q., Liu, X., Yang, R., Zhang, H.: Emergency-oriented spatiotemporal trajectory pattern recognition by intelligent sensor devices. *IEEE Access* **5**, 3687–3697 (2017)
17. Lai, C.-F., Hwang, R.-H., Lai, Y.-H.: An intelligent body posture analysis model using multi-sensors for long-term physical rehabilitation. *J. Med. Syst.* **41**(4), 1–15 (2017)
18. Hu, J.-X., Chen, C.-L., Fan, C.-L., Wang, K.-H.: An intelligent and secure health monitoring scheme using IoT sensor based on cloud computing. *J. Sens.* **2017**, 1–11 (2017)

# Hardware Design of a Smart Meter Communication Interface for Smart Grids

William Richard Kintzel<sup>1</sup>(✉), Mauro Marcelo Mattos<sup>2</sup>, and Altamir Rosani Borges<sup>2</sup>

<sup>1</sup> WEG Drives & Controls – Automation, Jaraguá do Sul, SC, Brazil  
wiriki@gmail.com

<sup>2</sup> FURB – University of Blumenau, Blumenau, SC, Brazil  
{mattos,arb}@furb.br

**Abstract.** Internet of Things (IoT) is a reality and nowadays a great effort is being devoted to connecting in a ubiquitous network different types of appliances. In this context, the Smart Grid (SG) is currently a widely discussed subject throughout the world, and this technology is promoting a paradigm shift for the electric sector. The deployment of the Advanced Metering Infrastructure (AMI), which supports remote interaction between the electric utility and the consumer through smart meters, is the first step for a future smart grid. This work presents an electrical meter communication solution applied to AMI in the last mile. The paper describes the hardware development process of a remote communication interface for electricity meters, which involves radio frequency and power line communication technologies. The work is based on a real demand, which will be used in an AMI pilot project of an electric power company in Brazil. The paper presents the design requirements, hardware architecture, testing requirements and results related to the remote communication interface in question.

## 1 Introduction

One of the major global initiatives in the electricity sector today is related to the development of a smarter grid model, which promises a great transformation towards the modernization of this sector and in the form of relationship between the various actors involved, mainly in companies and consumers of electricity. In this context, points that the smart grid is related to the integration of the 20th century traditional electrical power grid with the most recent 21st telecommunication and information technologies enabling efficient resource utilization to optimize energy consumption, install and manage distributed energy sources, as well as to exchange the generated power [1].

The process of deploying and operating a smart metering network presents many challenges. The main one is the selection of communication technology that provides the most reliable and cost-effective performance for the largest number of smart meters. In this context, the study for systematization of the process of hardware development of a remote communication interface for electricity meters in smart grid model, is characterized as a current topic of extreme relevance both in the theoretical and practical point of view. The results of the experiments in the field, through the smart metering pilot

project, will certainly bring contributions to assist in the future decisions of implantation of the solution in large scale.

The electrical power system (EPS) encompasses a broad infrastructure involving a set of facilities and equipment for the generation, transmission and distribution of electricity to residential, commercial and industrial consumers. The traditional power grid is characterized by a hierarchical system, where generation is centralized in large power plants that are at the top of the chain supplying many consumers located at the base of the chain. The electricity flow is unidirectional and consumers do not interact in the operation [2].

Although the current system has been able to provide the necessary power source, continuous demand growth, increased use of renewable energy resources, use of sustainable systems, availability of electricity at competitive prices, the security of supply and infrastructure aging became the motivators for the development of the Smart Grid (SG) [3]. This is currently the main world innovation initiative in the electricity sector. The move to a smarter grid promises to change every business model in this industry and its relationship to all stakeholders, involving and affecting power utilities, regulatory agencies, energy service providers, policy makers, technology and automation providers and all consumers of electricity [4].

The SG refers to the next generation of the electrical power grid that aims at a cleaner and more efficient (economic) power system, reliable and able to supply the demand, through the integration of advanced information, communication and electronic technologies. SG will introduce a distributed and centered system in consumer that becomes a more active agent for the system. The modern communication infrastructure will play a key role in the management, control and optimization of different devices and systems in SG. In addition, information and communication technologies will provide to power grid the capability to support bidirectional flow of electricity and information, isolate and re-establish power outages more quickly, facilitate the integration of renewable energy sources in power grid and empower consumers to optimize their electricity consumption [5].

This project is based on a real demand, with results homologated by the Brazilian Agency of Telecommunications (Anatel), and made available to a next stage that is the production of thousands pieces that will be used in a pilot project of advanced metering infrastructure in a Brazilian municipality planned to start in 2017.

## 2 Smart Grid Conceptual Model

The National Institute of Standards and Technology (NIST) [6], has developed a conceptual model, which is also adopted by other standards organizations such as IEC, as a basis for describing the architecture of smart grids. This conceptual model divides the SG into seven domains: generation, transmission, distribution, consumers, markets, service providers and operations. Each domain contains one or more actors, which are typically devices, computer systems, or software programs capable of making decisions and exchanging information necessary to run applications (automated processes). The domains

interact through secure communication interfaces and electrical connections, each of which can be bi-directional flow (Fig. 1).

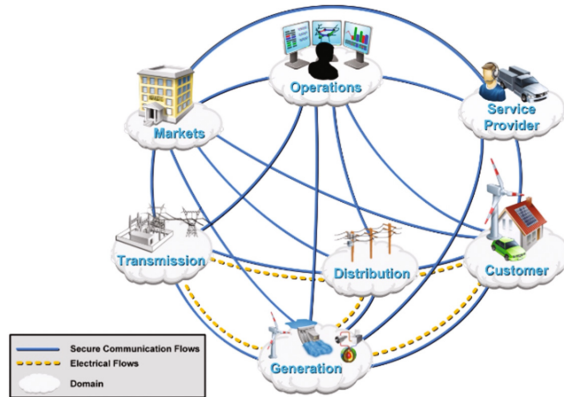


**Fig. 1.** Smart grid conceptual model [6].

The characteristics that distinguish a SG according to the National Laboratory of Energy Technology of the United States (NETL) [7] are: (a) Active participation by consumers, i.e. the ability to involve consumers in the processes of planning and operating the power grid, providing information in a timely manner, with control options; (b) Accommodate all generation and storage options: ability to integrate a wide variety of generation (including distributed generation) and storage systems, using simplified and standardized interconnection processes to support a “plug-and-play” connection level; (c) Enable new products, services and markets: enables the creation of new electricity markets, involving services and technologies that allow consumers and stakeholders to provide their energy resources to the electricity market. Consumers will have the opportunity to choose between competing services. Products related to energy efficiency will also be offered as market options; (d) Provide power quality: the ability to continuously provide electricity quality to consumer expectations and needs; (e) Optimize asset utilization and operate efficiently: the ability to apply the latest control and monitoring technologies to optimize the use of assets, by reducing operating and maintenance expenses; (f) Self-healing: ability to quickly detect, analyze, take corrective actions, and recover from faults or failures; and (g) Operate resiliently against external attack: ability to make the system less vulnerable and more protected against physical attacks (including natural disasters) and virtual attacks (cyber attacks).

## 2.1 Advanced Metering Infrastructure

The advanced metering infrastructure (AMI) corresponds to one of the main functionalities of smart grid and is considered as the basis for its implementation and operation. AMI involves a set of hardware (equipment and/or devices) and software (application) technologies, which are employed in measuring, collecting and analyzing electricity

consumption data and system operations through remote and bi-directional communication between smart meters, installed on the consumer premises, and the control/operations system of the electric power distribution utility. Because of the bi-directional communication feature, AMI provides the utility with unprecedented system management capability, significantly improving consumer services, enabling them to receive near real-time information about the cost of electric power and to make optimal decisions about their use. In summary, it is possible to understand AMI as the product of measurement and communication infrastructures for data acquisition purposes, as well as sending information and commands remotely.

The AMI system can be divided into three subsystems [9]: (a) Data Collection: mainly composed of smart meter located in the dependencies of the consumers and that are connected in network. These smart meters can be aggregated into data concentrator units that act as routers or indeed as data concentrators, collecting data from smart meters and sending them to the utility's central system through the communication network; (b) Communication Network: comprises the bi-directional data transmission network between the metering network (consumer) and the utility; and (c) Data Reception and Management: it represents the center of data management and control of the measurement system, within the scope of the utility.

The formation of an AMI solution integrates several components, among them, the technologically fundamental elements that serve as parameterization for the entire conceptualization of the AMI model include [8, 10]: (a) Smart meters: are advanced metering devices capable of collecting information about the use of electricity, water or gas, and have a communication interface for transmitting data to the utility, as well as receiving information / commands from it; (b) Communication Infrastructure: refers to the different types of architecture and communication networks that are available to perform the AMI, encompassing the various means and communication technologies between smart meters and utility, such as: power line communication, radio frequency, public networks (i.e., fixed telephony, cellular), among others; (c) Head-End System (HES): involves set of equipment that collects a large amount of data from all smart meters and manages the various types of communications and meters in the network; and (d) Meter Data Management System (MDMS): is a database management system that encompasses the acquisition, processing and storage of data generated by the smart meter and made available through HES, and that act an analytical tool for interacting with other information systems in order to provide useful information for the utilities actions. Includes network equipment, servers and database.

According to Guide for Smart Grid Interoperability of Energy Technology and Information Technology Operation with the Electric Power System (EPS), End-Use Applications, and Loads [11], the end-to-end communication model for smart grid involves: (a) Networks at customer premises which may vary according to their size and the number of devices they serve, and can be classified into: Home Area Network (HAN), Building Area Network (BAN) and Industrial Area Network (IAN); (b) Neighborhood Area Network (NAN) which are networks used to collect information generated by networks at customer premises and in general this network is related to the AMI installed to collect consumer measurement data for the utility. NAN networks constitute the last mile of smart grid, intermediate between the customer premises and the

distribution grid; (c) Field Area Network (FAN): are used in distribution grid to monitor and control various field devices (isolators, feeders and transformers). As FANs cover the entire distribution grid, they can also serve for communication of utilities, providing communication and monitoring services for technical personnel responsible for the operation and maintenance of the power grid; and (d) Wide Area Network (WAN): which are networks that cover long distances, capable of interconnecting between the facilities/dependencies in the generation and transmission domains, and provide communication links to SG's backbone. They are connected to the WAN segment: the substation network, used for protection, monitoring and automation services; and also the local network of power utility. The WAN allows, through the backhaul network, the communication from the control and operation center of the utility to NAN/FAN in the distribution domain.

### 2.2 Communication Architecture for Smart Metering

The communication architecture for smart metering through the AMI is shown in Fig. 2. In this SG subsystem, each smart meter installed on consumer premises, in general, connects with another to form a possible network topology in mesh characterizing the NAN or the last mile network.

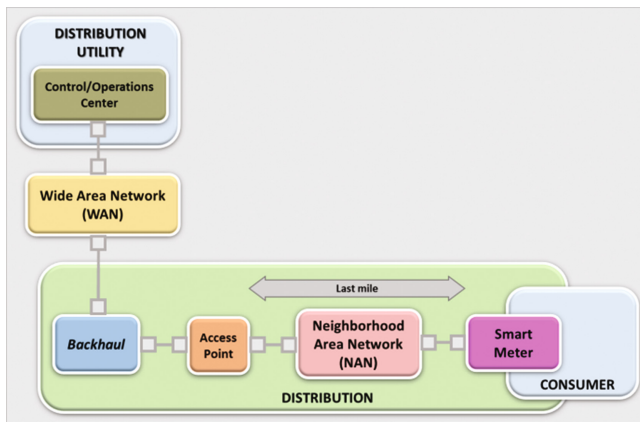


Fig. 2. Network architecture for AMI. Based on [11].

The NAN and backhaul networks have delimited coverage to a specific area, but of great capillarity, and are implemented to allow the integration of the dependencies of the consumers to the dependencies of the electric power distribution utility through WAN. More specifically, NAN implements the network capillarity required to service each individual consumer, while the backhaul segment connects communication technologies between NAN and WAN. Also between backhaul and NAN, there may be the Access Point (AP) which is a device that collects and aggregates data (data concentrator) from smart meters through the NAN. The system is completed with the WAN, which is characterized by covering an extensive geographic area and using higher bandwidth

transmission technologies, capable of interconnecting the meter network in distribution domain to the center of control/operations of the electric power distribution utility.

### 2.3 Communication Technologies for Last Mile

Last mile networks play an important role in the infrastructure of smart grids. They are designed to support a growing variety of applications, among them, the management and measurement of the use of electricity with a network of connectivity between smart meters. The design of such network depends not only on the application layer requirements, but also on the nature of its physical layer (PHY) and media access control (MAC). The adoption of standards based on internet protocol (IP) facilitates the integration of NANs within the end-to-end network architecture [12]. There are several communication technologies and standards that can be deployed at the NAN. In the context studied and presented in this work, are the technologies of wireless communication by radiofrequency below one gigahertz (RF Sub-GHz) and wired by narrow band power line communication (NB-PLC), based on the open standards IEEE 802.15.4g for RF and IEEE 1901.2 for PLC, which are fully aligned with the architecture in IP layers and well suited to the last mile of the AMI network. The communication networks for smart metering purposes should also present such qualities as reliability, robustness and self-recovery, and for this the mesh topology becomes an attractive option for this type of application [5].

## 3 Project Testing Scenario

The AMI system in question is an initiative project of a national electric power distribution utility, as a pilot project for proof of concept of a smart metering solution. The aim is to establish functionalities such as telemetry, remote disconnection and reconnection, fault location in low voltage grid, energy balance. This AMI pilot project is part of a structuring smart grid project, aimed at developing, deploying and demonstrating of smart metering functionality. Its main characteristic is to use the concept of living laboratory in an environment with high density of consumption and urban complexity. With this project, the utility intends to apply the model to the other areas of its concession.

The scenario chosen for the field test corresponds to a metropolis that represents an area of about 60 thousand km<sup>2</sup>. The region is covered by a primary network of about 300 km, and has annual consumption exceeded of 1,200 GWh. The pilot project will include more than fifty thousand customers of different profiles: residences, businesses and industries, benefiting a population of about 250 thousand inhabitants.

The architecture of the AMI Distribution Pilot Project is composed of single phase and poly phase smart meters installed at the consumers premises. The last mile communication network will be characterized by the formation of a mesh network, using a routing scheme that defines a structure based on the tree topology, and that has in Cisco® router the root of the network. The meter's remote communication interface will allow the operation of one physical medium each time, and the logic will be to use the PLC

mode when the RF is not available. The RF mode will operate in 902 to 907.5 MHz and 915 to 928 MHz frequency ranges, and the PLC in the 35 to 89 kHz frequency range.

## 4 Project Development

The project involved two steps: the hardware and the firmware. The hardware development process consisted of capturing the electronic schematic of the RF and PLC communication interface for smart metering from an electronic reference design provided and supported by Cisco®, through a development partnership (Cisco Developer Network program) with company WEG<sup>1</sup> that is developing the project. The electronic circuit was the detailed (component positioning and routing of the electrical connections) on a printed circuit board. Prototypes were assembled and tested, then forwarded to Cisco® validation and certification, as well as certification and approval at Anatel. In the end, it was obtained the hardware of a remote communication interface for electricity meter approved according to test requirements, and considering the manufacturing process of the company. The firmware design of the remote communication interface in question is not part of the scope of this work.

### 4.1 Project Requirements

According to the technical specification elaborated by the national electrical power distribution utility involved in this project, in the chapter that is about the remote communication interface, the electricity meter to be provided must integrate an RF and PLC communication interface, these technologies being compatible with those of the Cisco® CGR 1240 router. Thus, the hardware design of the remote communication interface shall have the following characteristics: (a) follow the Cisco® electronic reference design to maintain the functionality and interoperability of the AMI communication system; (b) PLC shall use IEEE 1901.2 standard technology, in the CENELEC A frequency band with frequency restriction according to Anatel regulation, and OFDM modulation; (c) RF communication shall use technology in the IEEE 802.15.4g standard, in the ISM 915 MHz frequency band with frequency restriction according to Anatel regulation, and MR-FSK modulation; (d) provide processing capability compatible with Cisco® firmware, containing the stacks and protocols of communication for both the PLC and RF interface.

In addition, there are also design requirements in question: (a) contemplate a single hardware containing the two communication technologies; (b) provide an interface connection with the electricity meter; (c) receive supply voltages from the electricity meter, including energy storage circuit to perform last gasp functionality; (d) meet Anatel certification tests; and (e) have compatible size to fit the electricity meter used for testing.

---

<sup>1</sup> <http://www.weg.net/institutional/BR/en/>.



## 4.2 Hardware Architecture

The main feature of the hardware developed is to provide communication through the RF and PLC technologies, and thus to allow a more available and efficient communication, since the limitations and the specific potentials of each technology can act in a complementary way. The hardware architecture consists of five functional blocks: (a) Processing Unit; (b) RF interface; (c) PLC interface; (d) Supply voltage; and (e) Connection with the Meter.

The microcontroller (MCU Host), part of processing unit, is the main element of the electronic architecture of the communication interface because it is responsible for controlling the RF and PLC interfaces, and interaction with the meter's processing unit. It features a 32-bit ARM Cortex M3 core with operating frequency up to 120 MHz, 1 MB Flash and 128 kB SRAM. The processing unit also contains additional 64 Mb Flash memory to extend the system's data storage capacity, and additional 8 Mb SRAM memory to allow the firmware to run; The RF interface, supported by the IEEE 802.15.4g standard, is implemented using a radio frequency transceiver in conjunction with an RF amplifier. The RF transceiver has the following key features of RF performance: (a) Receiver sensitivity:  $-110$  dBm at 50 kbps; (b) Programmable output power up to  $+16$  dBm; (c) Supported modulation formats: 2FSK, 4FSK, 4GFSK, MSK, OOK; and (d) Supports up to 1.25 Mbps data rate in transmission and receive. The RF amplifier features transmit output power up to  $+30$  dBm. Antenna features 1 dBi peak gain with linear polarization; The PLC interface, which supports the IEEE 1902.1 standard, is implemented using a microcontroller whose purpose is to perform the PLC modem functionality, together with an analog unit (AFE PLC) for conditioning communication signals in power grid. The microcontroller (MCU PLC) has 32 bits with operating frequency up to 90 MHz, 256 kB MB Flash and 100 kB SRAM. The AFE PLC has the following characteristics: (a) protection against over temperature and over current conditions; (b) power amplifier output capacity up to 1.5 A; (c) supports CENELEC frequency band A, B, C, D; (d) supports FSK, SFSK and OFDM modulations; (e) receive sensitivity:  $20 \mu\text{VRMS}$  (typical); (f) programmable transmit and receive filters; and (g) programmable transmit and receive gain control. The PLC interface also contains the isolated part of the zero crossing and line coupling circuits; The supply voltage functional block, receives the supply voltages  $+15$  V and  $+6$  V generated in the electricity meter. The block contains two linear DC voltage regulators, which convert the  $+6$  V supply voltage to the  $+3.3$  V and  $+4$  V voltages. It also contains two electronic switches to enable the  $+3.3$  V and  $+15$  V at the PLC interface. The  $+3.3$  V and  $+4$  V voltage are used to power the RF interface, and the processing unit is powered with  $+3.3$  V. The electronic switches are commanded to open in the execution of the last gasp functionality, with the purpose of reducing consumption in the energy backup; Finally, the connection with the meter, it features a connector  $20 \times 2$  pins that provides supply voltage and signal exchange of the RF and PLC communication interface.

### 4.3 Test Requirements

There are three sets of tests to be performed and defined as requirements for approval of the hardware prototype of the RF and PLC communication interface for the electricity meter: (a) Developer verification tests: these are the verification tests of the prototype of the electronic board in question, executed during the product development stage, within the company; (b) Cisco® interoperability verification tests: these are external lab tests run by the Cisco® development team that result in a certificate of compatibility with Cisco® communication technology; and (c) Anatel certification tests: these tests are run in an external laboratory, which results are managed by Anatel Designated Certification Organization, which analyzes them according to the acceptance criteria, and elaborates a final document containing all the necessary information for certification of the communication device and homologation with Anatel.

## 5 Test Results

This chapter presents the electronic board of the RF and PLC communication interface developed for the WEG electricity smart meter, and the results of tests performed to approve the hardware prototype in question in this work.

During the hardware development process of the RF and PLC communication interface, four versions of electronic board prototypes were developed. The first one was designed to perform initial testing and hardware recognition, to support the beginning of firmware development, and it has already been designed to meet the internal limitations of the communication module where the electronic board is housed. The second one was designed with care in relation to the issues of EMI in the electronic board, and with concern for EMC which is a requirement of testing for certification of the product in Anatel. The third one was tried to improve the thermal dissipation of the components of higher heating in the PCBs, and to minimize the influence of the heating of these components on the other circuits. And the fourth prototype (Fig. 3) was developed to further accommodate some requests for the manufacturing process of the printed circuit board supplier and the electronic board assembly process in the company. This last version of electronic board was then considered ready to start the Anatel certification testing.

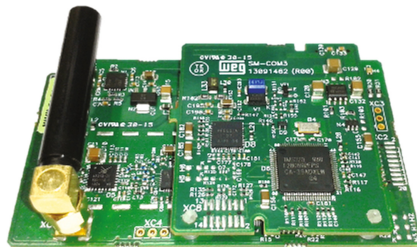


**Fig. 3.** The final version of electronic board.

The functionalities of the electronic board of the RF and PLC interface were verified in the execution of the hardware test plan elaborated for such purpose, which included: (a) Verification of the supply voltage of the electronic board; (b) Programming of MCU Host and MCU PLC processing units; (c) Testing of electronic circuits, which used a hardware diagnostic tool (firmware on MCU Host) provided by Cisco®. The RF and PLC transmission signals (Figs. 4 and 5) were verified using a transmission test tool (firmware on MCU Host) provided by Cisco® too, which allow to configure the range of the operating frequency and the transmit output power; (d) Verification of the temperature in points on the electronic board, considering extreme operating conditions; and (e) Consumption evaluation of the electronic board operating in RF or PLC mode, at maximum power transmission.

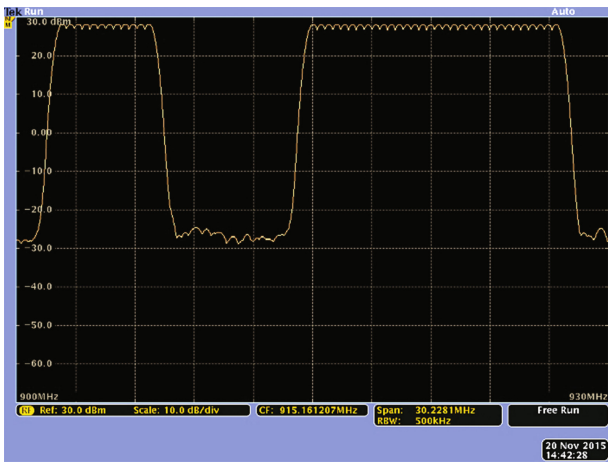


Fig. 4. RF transmission signal.

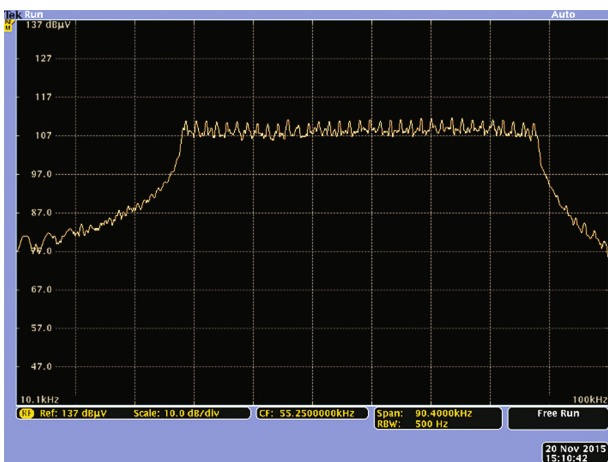


Fig. 5. PLC transmission signal.

The Cisco® certification process begins after preliminary testing of the RF and PLC communication interface. The preliminary tests are executed by company, and in short, correspond to a hardware diagnostic test (executed on Development Verification Test) and the connectivity test of the remote communication interface, operating as a RF and/ or PLC node in a mesh network formed with a router Cisco® CGR 1240. The Fig. 6 shows the result for the connectivity test, with the network structure composed of a Cisco® CGR 1240 router and ten smart meters (among single phase and poly phase) was installed in an internal environment, each one containing the RF and PLC communication interface. All of them were connected to the same circuit of the power grid for sharing a PLC communication channel. The remote communication interfaces were programmed with the firmware containing the stack and protocols of communications provided by Cisco®. A set of qualified meters in the preliminary tests were forwarded to Cisco® for certification the interoperability with Cisco® communication system. The certification includes functional and system tests related to the RF and PLC communication interface installed on electricity meter by company. All tests foreseen as a priority in the test plan developed by Cisco® were executed and approved. The report shows that the RF and PLC communication interface for the electricity meter by company presented the expected behavior for the Cisco® communication solution, forming a multi-hop network with both RF and PLC links for the same network. Finally, the report announces that the hardware of the RF and PLC communication interface of this work has obtained the approval of compatibility with the Cisco® communication solution; and recommends the implementation of electricity meters with RF and PLC communication interface for the AMI Distribution Pilot Project.

```

CGR1000#show wpan 4/1 rpl stree
----- WPAN RPL SLOT TREE [4] -----

[2015:DEAD:BEEF:CAFE:207:8108:D3:911B]
  \-- (PLC) -- 2015:DEAD:BEEF:CAFE:21E5:605F:B01E:BD1E
  \-- (PLC) -- 2015:DEAD:BEEF:CAFE:5460:5902:22A6:A300
    \-- (RF ) -- 2015:DEAD:BEEF:CAFE:A43A:C9D7:84A:7A45
  \-- (RF ) -- 2015:DEAD:BEEF:CAFE:81C9:5848:F987:310F
  \-- (RF ) -- 2015:DEAD:BEEF:CAFE:9D9F:4FFD:7E7F:9FB7
  \-- (PLC) -- 2015:DEAD:BEEF:CAFE:C122:B6D:B8B7:9A7D
  \-- (RF ) -- 2015:DEAD:BEEF:CAFE:CC5C:6702:93DC:2094
    \-- (RF ) -- 2015:DEAD:BEEF:CAFE:4598:58D6:DF7A:9F2C
  \-- (PLC) -- 2015:DEAD:BEEF:CAFE:F12F:2BC7:AEAF:3936
    \-- (RF ) -- 2015:DEAD:BEEF:CAFE:8ED:B0D1:D2E9:B978

RPL SLOT TREE: Num.DataEntries 10, Num.GraphNodes 11 (external 0) (RF 6) (PLC 4)
    
```

**Fig. 6.** Network diagram formed with RF and PLC nodes.

The Anatel certification process was also completed with the issuance of certificates of conformity by Anatel designated certification organization, one for the single-phase model of smart meter and another for the family of poly phase models. Therefore, the smart meters by company were certified as telecommunication equipment type Transceiver with Restricted Radiation Transceiver with Spread Spectrum in Category II, which also has Narrowband PLC Transceiver.

## 6 Conclusions

The present work approaches the smart grid model with emphasis on the functionality of the advanced metering infrastructure. Specifically, is presented a communication solution for electricity meter related to the last mile segment of the communication network of a smart metering system.

The paper presented the development stages that resulted in the construction of a RF and PLC communication hardware in electricity meters to be applied in a project pilot of smart metering. The design methodology of the hardware in question involved the compatibility with technical requirements established by the electrical power distribution utility and compliance with the restrictions of the electricity meter manufacturer. The physical prototype was tested and certified compatible with Cisco® communication technology, chosen by the utility as communication solution. The design was also adequate and prepared for product-level manufacturing, and obtained approval at Anatel, which authorizes its installation in the field and its commercialization in the national territory.

Although it is part of a large-scale pilot project, this work will serve as a reference for new projects in the area, because besides presenting and justifying the steps of construction the hardware solution for remote data communication of an electricity meter, also were reported the concerns, the difficulties and/or needs observed during its development to meet both functional and certification aspects, as well as manufacturing as a product.

## References

1. Al-Ali, A.R., Aburukba, R.: Role of internet of things in the smart grid technology. *J. Comput. Commun.* **3**, 229–233 (2015)
2. Farhangi, H.: The path of the smart grid. *IEEE Power Energy Mag.* **8**(1), 18–28 (2010)
3. International Electrotechnical Commission: IEC Smart Grid Standardization Roadmap, June 2010. <http://www.iec.ch/smartgrid/roadmap/>
4. U.S. Department of Energy: The Smart Grid: An Introduction (2008). <http://energy.gov/>
5. Hossain, E., Han, Z., Poor, H.V.: *Smart Grid Communications and Networking*. Cambridge University Press, New York (2012)
6. National Institute of Standards and Technology: NIST Framework and Roadmap for Smart Grid Interoperability Standards, Release 3.0. NIST, Gaithersburg (2014). <http://www.nist.gov/smartgrid/>
7. National Energy Technology Laboratory: A Vision for the Smart Grid, June 2009. <https://www.smartgrid.gov/>
8. National Energy Technology Laboratory: Advanced Metering Infrastructure, February 2008. <https://www.netl.doe.gov/>
9. European Technology Platform for Smart Grids: Strategic Deployment Document for Europe's Electricity Networks of the Future, September 2008. <http://www.smartgrids.eu/>
10. Mohassel, R.R., Fung, A.S., Mohammadi, F., Raahemifar, K.: A survey on advanced metering infrastructure and its application in smart grids. In: *27th Canadian Conference on Electrical and Computer Engineering (CCECE)*, pp. 1–8. IEEE, May 2014

11. International Electrical and Electronics Engineers: IEEE 2030: Guide for Smart Grid Interoperability of Energy Technology and Information Technology Operation with the Electric Power System (EPS), End-Use Applications, and Loads, New York (2011)
12. Cisco Systems Incorporation: A Standardized and Flexible IPv6 Architecture for Field Area Networks: Smart-Grid Last-Mile Infrastructure. White Paper, January 2014. <http://www.cisco.com/>

# Performance Analysis of WRF Simulations in a Public Cloud and HPC Environment

Klodiana Goga<sup>1</sup>(✉), Antonio Parodi<sup>2</sup>, Pietro Ruiu<sup>1</sup>, and Olivier Terzo<sup>1</sup>

<sup>1</sup> Istituto Superiore Mario Boella (ISMB), Torino, Italy  
{goga,ruiu,terzo}@ismb.it

<sup>2</sup> CIMA Research Foundation, Savona, Italy  
antonio.parodi@cimafoundation.org

**Abstract.** The Weather Research and Forecasting (WRF) Model is a numerical weather prediction system designed for both atmospheric research and operational forecasting needs. WRF requires a large amount of CPU power which increases drastically if WRF is used to model a big geographical area with a high resolution. To satisfy the computational demand WRF requires large number of computing resources through infrastructures such as clusters in grid or cloud. In this paper the performance analysis of different WRF simulations to the Amazon Web Services (AWS) cloud computing environment (single node and cluster) compared to that of a HCP cluster is presented.

## 1 Introduction

The Weather Research and Forecasting (WRF) Model [1] is a numerical weather prediction system designed for both atmospheric research and operational forecasting needs. It is made up by two dynamical cores, a data assimilation system, and a software architecture facilitating parallel computation and system extensibility. An alternative approach to the traditional HPC infrastructures is to use public cloud computing services [2]. All major IT players (Amazon, Google, Microsoft, IBM) have their own cloud offering, making available to users powerful computing resources. These resources can be sized based on users needed and can be configured at almost all levels of the IT stack (infrastructure, platform, application) in a selfservice manner, enabling great flexibility and easy access [3]. As well as the majority of cloud providers adopt a pay-per-use model, the public cloud usage brings also economic benefits because there are no initial investments and the user knows at any time how much is spending. Many research work has been done to evaluate the performance of HPC applications in cloud environments including climate modelling (Evangelinos and Hill 2008) [4], e-science [5], chemo-hydrodynamics [6], bioinformatics [7]. Cloud performance studies also considered also WRF model performance Duran-Limon, H.A., Flores-Contreras, J., Parlavantzas, N., et al. Earth Sci Inform (2016) [8] presented a lightweight virtualization approach for efficiently running the WRF model in cloud environment. Many research work has been done to evaluate the performance of HPC

applications in cloud environments. These results all indicate that cloud execution for communication-intensive applications are affected by a performance overhead.

In this paper is presented a performance comparison of the same WRF simulation of 6 h carried out on the Amazon Web Services (AWS) and on the LRZ Cluster. The motivation to accomplish such an experiment is to specifically assess the suitability of cloud computing technologies to effectively process CPU intensive parallel simulations like WRF and more generally, to analyze the Cloud Computing potential in the WRF framework. In the public cloud environment the tests have been carried out in two different configurations. The first one uses single virtual machines while the second one uses clusters. Such an approach has been driven by the motivation of evaluating the performance of WRF in a distributed environment compared to that of a single node with the same number of cores.

## 2 Testing Environment

### 2.1 Cluster HPC Deployment

SuperMUC is the name of the high-end supercomputer at the Leibniz-Rechenzentrum (Leibniz Supercomputing Centre) in Garching near Munich (the MUC suffix is borrowed from the Munich airport code). With more than 241,000 cores and a combined peak performance of the two installation phases of more than 6.8 Petaflop/s (=1015 Floating Point Operations per second), it is one of the fastest supercomputers in the world (Fig. 1).

The LRZ Linux Cluster [9] consists of several segments with different types of interconnect and different sizes of shared memory. All systems have a (virtual) 64 bit address space.

- Intel Xeon based 4-way nodes for serial processing
- MPP Cluster with 16-way AMD-based nodes and QDR Infiniband interconnect (system will be retired)
- CoolMUC2 Cluster with 28-way Haswell-based nodes and FDR14 Infiniband interconnect
- Intel Broadwell based 6 TByte shared memory server HP DL580.

LRZ Linux cluster has different capabilities such as shared and distributed memory, large software portfolio, flexible usage due to various available memory sizes, parallelization by message passing (MPI), shared memory parallelization with OpenMP or pthreads, mixed (hybrid) programming with MPI and OpenMP. On all HPC systems at LRZ, the SLURM scheduler is used to execute parallel jobs.

### 2.2 Cloud Deployment

The simulations has been carried out on the Elastic Compute Cloud (EC2) of Amazon Web Services (AWS). Amazon Web Services is a cloud services platform,



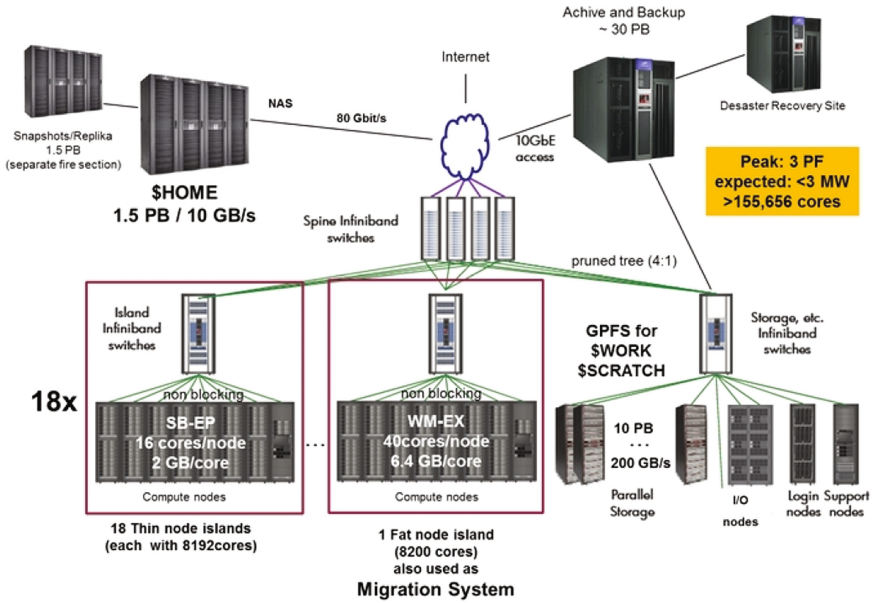


Fig. 1. SuperMUC architecture

offering compute power, database storage, content delivery and other functionality to the users.

For the test purposes have been used different types of services. Firstly has been created an AMI (Amazon Machine Image) [10] HVM (Hardware Virtual Machine) with Ubuntu 16.06 in which have been installed WRF 3.8.1. An AMI provides the information required to launch an instance (virtual server) in the cloud.

Amazon Machine Images (AMI) use one of two types of virtualization: paravirtual (PV) or hardware virtual machine (HVM). HVM AMIs are presented with a fully virtualized set of hardware and boot by executing the master boot record of the root block device of the image. This virtualization type provides the ability to run an operating system directly on top of a virtual machine without any modification, as if it were run on the bare-metal hardware. HVM guests can take advantage of hardware extensions that provide fast access to the underlying hardware on the host system(eg. CPU virtualization). In order to take advantage of enhanced networking features of AWS the usage of HVM AMIs is required. Enhanced networking uses single root I/O virtualization (SR-IOV<sup>1</sup>) to provide high-performance networking capabilities on supported instance types. Enhanced networking provides higher bandwidth, higher packet

<sup>1</sup> SR-IOV is a method of device virtualization that provides higher I/O performance and lower CPU utilization when compared to traditional virtualized network interfaces.

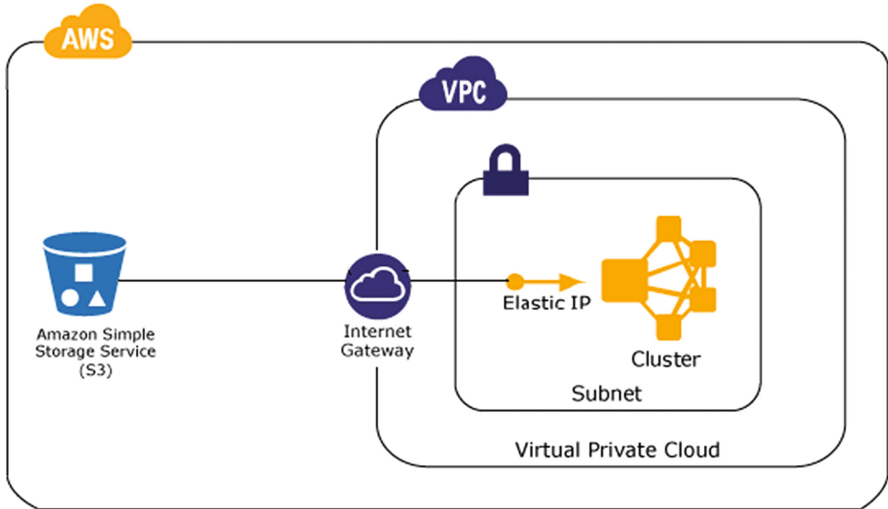


Fig. 2. cfnCluster architecture

per second (PPS) performance, and consistently lower inter-instance latencies. For our test especially in the cluster configuration this feature is very important.

In the cluster test, have been used CfnCluster [11] (Cloud Formation Cluster) which is a framework based on Amazon Cloud Formation [12] that deploys and maintains high performance computing clusters on Amazon Web Services (AWS). CloudFormation enables users to use a template file to create and delete a collection of resources together as a single unit called a stack. CfnCluster template as described in Fig. 2 allows the developers to create a stack which contains VPC [13], S3 [14] and EC2 resources. The template is stored in S3 (Simple Storage Service) it can be called using the AWS APIs in order to launch a stack. The instances (virtual machines) of the cluster are launched inside a VPC (Virtual Private Cloud) which is a logically isolated section of AWS in which resources can be launched in a completely defined virtual network. The users have full control of the virtual networking environment (IP address range selection, subnet creation, route tables configuration, network gateways and multiple layers of security (security groups and network access control lists).

CfnCluster supports different types of job schedulers to be used with the cluster (eg. SGE, openlava, torque, or slurm). For these tests has been used SGE (Sun Grid Engine). In these tests the cluster is made up by e master node and different worker nodes, all within the same VPC, subnet and placement group<sup>2</sup>. As described more in detail in Sect. 3 the instances used in these tests are M4, C3, and X1 type.

<sup>2</sup> A placement group is a logical grouping of instances within a single Availability Zone. Placement groups are recommended for applications that benefit from low network latency, high network throughput, or both.

- M4 instances are the latest generation of General Purpose Instances. This family provides a balance of compute, memory, and network resources, and it is a good choice for many applications.
- C3 instances are Compute-optimized instances, featuring the high performing processors.
- X1 instances are optimized for large-scale, enterprise-class, in-memory applications.

Amazon EC2 has multiple storage option, the instances used in this tests are based on EBS. EBS [15] is a durable, block-level storage volume that can be attached to a single, running Amazon EC2 instance. For all the instances in these tests have been used General Purpose (SSD) root devices which is an SSD-backed, general purpose EBS volume type suitable for a broad range of workloads, including small to medium sized databases, development and test environments, and boot volumes.

An Amazon EBS-optimized instance uses an optimized configuration stack and provides additional, dedicated capacity for Amazon EBS I/O. This optimization provides the best performance for the EBS volumes by minimizing contention between Amazon EBS I/O and other traffic from the instance. EBS-optimized instances deliver dedicated bandwidth to Amazon EBS, with options between 500 Mbps and 12,000 Mbps, depending on the instance type used. General Purpose SSD (gp2) volumes are designed to deliver within 10% of their baseline and burst performance 99% of the time in a given year.

### 3 Experimental Tests

The WRF experiment adopted to compare the scaling and computational performances on the LRZ cluster and on a public cloud environment is described hereafter. Two two-way nested domains at cloud-permitting (domain d01, 6 km) and cloud-resolving (domain d02, 2 km) grid spacing have been adopted: d01 corresponds to  $321 \times 319 \times 42$  grid points, while d02 corresponds to  $697 \times 739 \times 42$  grid points. This domains setup has been adopted because it is comparable to a typical numerical weather prediction configuration at fine grid spacing in operational mode (Fig. 3).

The WRF physics setup corresponds to the one typically adopted for the modeling of severe thunderstorms events over complex topography areas (Fiori et al. 2014) [16]. More specifically, the double-moment Thompson microphysics (Thompson et al. 2004) [17], and the YSU planetary boundary layer parameterization (Hong et al. 2006) [18].

#### 3.1 Cluster HPC Tests

LRZ's target for the architecture [19] is a combination of a large number of thin and medium sized compute nodes with and 64 GByte (Phase 2) of memory, and a smaller number of fat compute nodes with 256 GByte memory. The network

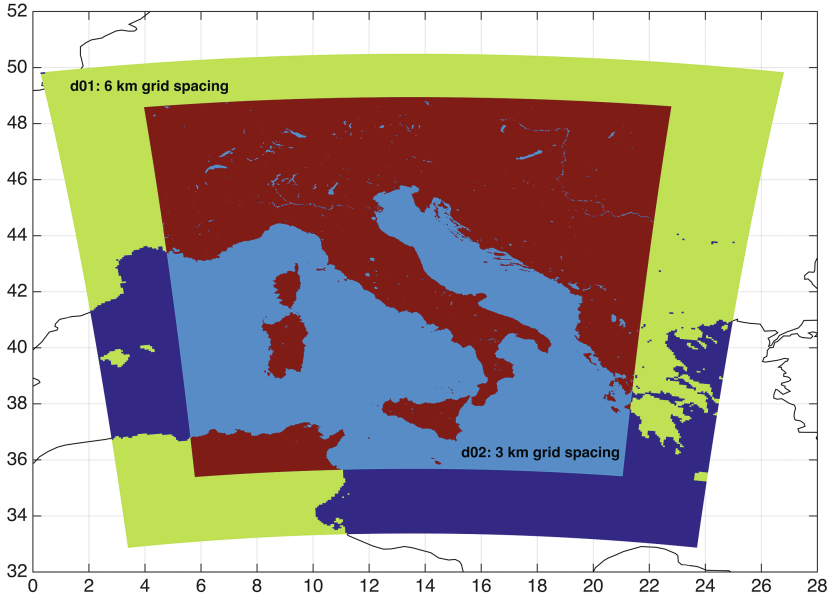


**Fig. 3.** WRF domains experimental tests

interconnect between the nodes allows excellent scaling of parallel applications up to the level of more than 10,000 tasks. SuperMUC consists of 18 Thin Node Islands based on Intel Sandy Bridge-EP processor technology, 6 Thin Node Islands based on Intel Haswell-EP processor technology and one Fat Node Island based on Intel Westmere-EX processor technology. Each Island contains more than 8,192 cores. All compute nodes within an individual Island are connected via a fully non-blocking Infiniband network (Phase 1: FDR10 for the Thin nodes of Phase 1, FDR14 for the Haswell nodes of Phase 2 and QDR for the Fat Nodes). Above the Island level, the pruned interconnect enables a bi-directional bi-section bandwidth ratio of 4:1 (intra-Island/interIsland).

The tests executed on the LRZ Linux Cluster concern the execution of an 1 h simulation prediction using a varying number of cores, namely 64, 80, 96, 128, 256, and 512. The hardware characteristics of the LRZ Linux Cluster [9] are shown in the Table 1

### 3.1.1 Two Compute Nodes Cluster

In this test configuration the CfnCluster framework is used. In this configuration we have a master node and two worker nodes.

The test are executed by the worker nodes so in the first column of the Table 2 is represented the total number of cores of the two worker nodes, and is not taken into account the number of cores of the master node. The total number of cores in this configuration is the same used for the single node configuration in order to have comparable results. In this configuration we have in addition

**Table 1.** LRZ Linux cluster environment

System	Processor type	#Processors per node	#Cores per node	RAM per node	Storage bandwidth GB/s
CooLMUC[1] (MPP[1])	AMD Opteron 6128HE (Magny-Cours) 8-core, 2.0GHz	2	16	16	2
CooLMUC2 (MPP2)	Intel Xeon E5-2690v3 (Haswell) 14-core, 2.6GHz	2	28	64	2

**Table 2.** Two compute nodes cluster testing environment

Total nr. of cores	Single VM nr. of cores	Name	Processor type	Single VM RAM (GiB)	Dedicated EBS bandwidth (Mbps)	Storage (GB)
2 <sup>a</sup>	2	m4.large	Intel(R) Xeon(R) CPU E5-2676 v3 @ 2.40GHz	8	450	EBS only
8	4	m4.xlarge	Intel(R) Xeon(R) CPU E5-2686 v4 @ 2.30GHz	16	750	EBS only
16	8	m4.2xlarge	Intel(R) Xeon(R) CPU E5-2676 v3 @ 2.40GHz	32	1000	EBS only
32	16	m4.4xlarge	Intel(R) Xeon(R) CPU E5-2686 v4 @ 2.30GHz	64	2000	EBS only
64	32	c3.8xlarge	Intel(R) Xeon(R) CPU E5-2680 v2 @ 2.80GHz	60	-	SSD 2 × 320
80	40	m4.16xlarge	Intel(R) Xeon(R) CPU E5-2686 v4 @ 2.30GHz	256	10000	EBS only
96	48	m4.16xlarge	Intel(R) Xeon(R) CPU E5-2686 v4 @ 2.30GHz	256	10000	EBS only
128	64	m4.16xlarge	Intel(R) Xeon(R) CPU E5-2686 v4 @ 2.30GHz	256	10000	EBS only
256	128	x1.32xlarge	Intel(R) Xeon(R) CPU E7-8880 v3 @ 2.30GHz	1.952	10.000	SSD 2 × 1920

<sup>a</sup>Master Node

the 256 core simulation which was made possible by using two worker nodes of 128 core each. All the instances in these tests have a General Purpose (SSD) root devices which is an SSD-backed, general purpose EBS volume type. The M4 and X1 instances have dedicated bandwidth to Amazon EBS, which varies from 750 Mbps and 10,000 Mbps, depending on the instance type used. The C3 instances have not a dedicated EBS bandwidth.

### 3.1.2 Four Compute Nodes Cluster

Also in this test configuration is used the CfnCluster framework. In this configuration we have a master node and four worker nodes.

**Table 3.** Four compute nodes cluster testing environment

Total nr. of cores	Single VM nr. of cores	Name	Processor type	Single VM RAM (GiB)	Dedicated EBS bandwidth (Mbps)	Storage (GB)
2 <sup>a</sup>	2	m4.large	Intel(R) Xeon(R) CPU E5-2676 v3 @ 2.40GHz	8	450	EBS only
64	16	m4.4xlarge	Intel(R) Xeon(R) CPU E5-2686 v4 @ 2.30GHz	64	2000	EBS only
80	20	c3.8xlarge	Intel(R) Xeon(R) CPU E5-2680 v2 @ 2.80GHz	60	-	SSD 2 × 320
96	24	c3.8xlarge	Intel(R) Xeon(R) CPU E5-2680 v2 @ 2.80GHz	60	-	SSD 2 × 320
128	32	c3.8xlarge	Intel(R) Xeon(R) CPU E5-2680 v2 @ 2.80GHz	60	-	SSD 2 × 320
256	64	m4.16xlarge	Intel(R) Xeon(R) CPU E5-2686 v4 @ 2.30GHz	256	10000	EBS only
512	128	x1.32xlarge	Intel(R) Xeon(R) CPU E7-8880 v3 @ 2.30GHz	1.952	10.000	SSD 2 × 1920

<sup>a</sup>Master Node

The test are executed by the worker nodes so in the first column of the Table 2 is represented the total number of cores of the two worker nodes, and is not taken into account the number of cores of the master node. The total number of cores in this configuration is 64, 80, 96, 128, 256, 512 vCores. In this configuration we have in addition the 512 core simulation which was made possible by using four worker nodes of 128 core each.

All the instances in these tests have a General Purpose (SSD) root devices which is an SSD-backed, general purpose EBS volume type. The M4 and X1

instances have dedicated bandwidth to Amazon EBS, which varies from 2000 Mbps and 10,000 Mbps, depending on the instance type used. The C3 instances have not a dedicated EBS bandwidth.

**3.1.3 Results**

In this section, an experimental analysis aimed at evaluating the simulation performances in terms of processing times when the number of EC2 instances increases (in particular with 1, 2, 4 worker nodes) and how this differs from the processing time of the LRZ cluster. In the Table 4 is reported the total simulation time necessary to perform 6 h of WRF simulations, for the different configurations in the AWS cloud.

**Table 4.** AWS total simulation time

Total nr. of cores	Single node total simulation time (6 h) [seconds]	Two compute nodes cluster total simulation time (6 h) [seconds]	Four compute nodes cluster total simulation time (6 h) [seconds]
8	58200	51120	-
16	33600	30300	-
32	19860	16860	-
64	14400	11400	10260
80	11340	9600	10200
96	10500	10800	10020
128	7260	7140	6060
256	-	4620	6240
512	-	-	3780

In the Fig. 4 we can see a graph of the total simulation time in AWS for every configuration. The lowest simulation time is achieved by using the cluster simulation of four nodes with 512 core. By this graph can be deduced that by increasing the number of cores and the number of nodes we can achieve lower simulation time of WRF.

As well as there during the tests, in order to have a certain amount of cores have been used different types of instances with different characteristics in terms of CPU type, RAM memory etc. the authors considered to evaluate how the total simulation time was affected by the RAM/CPU ratio. The graph in the Fig. 5 represents the relation between the RAM/CPU ratio and the simulation time in all the different configurations in AWS. The bar graphs represent the total RAM and total number of cores ratio while the line graphs represent the total simulation time. In this graph can be notices that the simulation time is not

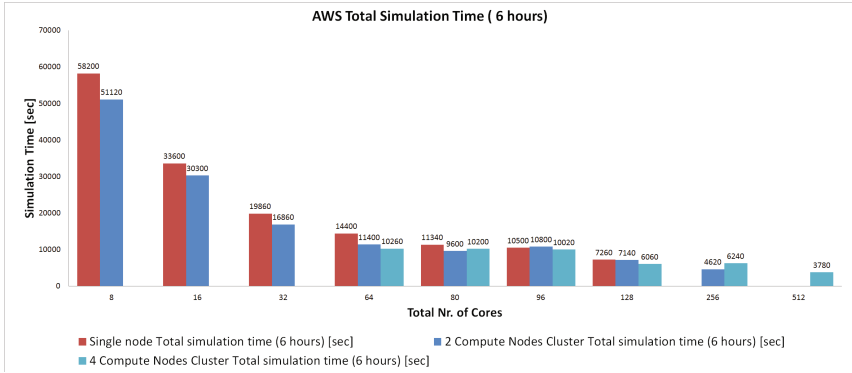


Fig. 4. AWS total simulation time

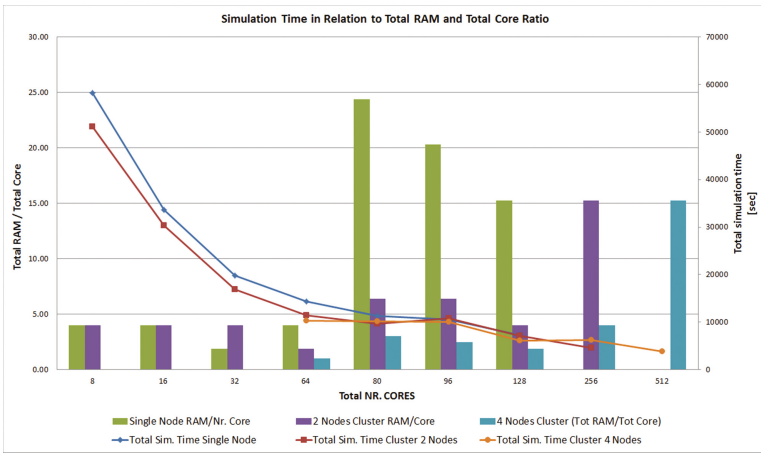


Fig. 5. Simulation time in relation to total RAM and total core ratio

affected much by the RAM/CPU ratio but the lower simulation time is more related to the increasing number of cores and the parallelization.

In the Fig. 6 is represented a comparison of an hour of WRF simulation carried out by the LRZ cluster, in a single node AWS instance, in AWS two nodes cluster and in AWS four nodes cluster for a number of cores that vary from 64 to 512. It includes also a theoretical performance presentation.

For all the configurations by increasing the number of cores is possible to reduce the simulation time. We have the best performance in the AWS four nodes cluster until it reaches 128 cores after in 256 and 512 simulation the performance slows down and does not follow the previous trend. This can be addressed to the fact that the simulation using 96, 128 have been used the Compute-optimized instances c3.8xlarge (see Table 3). In all cases the AWS cloud simulation from 64 core to 128 core represent a better performance comparing to the theoretical



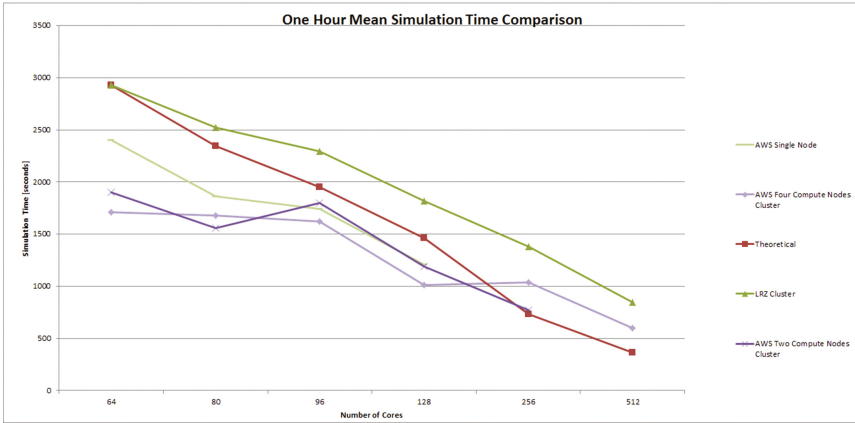


**Fig. 6.** One hour mean simulation time comparison

performance. And in all cases the AWS cloud simulation performs better than the LRZ cluster.

In the Table 5 is even more evident the fact that the total simulation time therefore the performance, are influenced more by the CPU than by the RAM, in fact the lower simulation time is achieved when using multiple instances (four worker nodes cluster) with CPU of 2.8 GHz frequency.

**Table 5.** AWS simulation time, total RAM and CPU frequency

CPU	Single node			Cluster 2 nodes			Cluster 4 nodes		
	RAM	CPU frequency [GHz]	Total sim. time [sec]	Tot. RAM	CPU frequency [GHz]	Total sim. time [sec]	Tot. RAM	CPU frequency [GHz]	Total Sim. Time [sec]
64	256	2,3	14400	120	2,8	11400	64	2,3	10260
80	1952	2,3	11340	512	2,3	9600	240	2,8	10200
96	1952	2,3	10500	512	2,3	10800	240	2,8	10020
128	1952	2,3	7260	512	2,3	7140	240	2,8	6060

## 4 Conclusions and Future Work

In this paper, has been presented 6 h WRF simulation in the AWS public cloud environment and in the LRZ cluster. The aim was to investigate the parallel performances which are achieved within the cloud environment. The experimental tests carried out on the LRZ cluster highlighted different performances compared to the AWS test. This work represents a first step towards the development of Cloud Computing platforms for WRF simulations managing huge data flows

that have to be processed in short times or on a continuous basis to meet not only scientific but also operative scenarios.

Future test can be performed by using containers [20] instead of virtual machines in a cloud infrastructure in order to improve flexibility, performance and the resource usage of the cloud resources.

## References

1. The weather research & forecasting model. <http://www.wrf-model.org/index.php>. Accessed 06 Mar 2017
2. Thackston, R., Fortenberry, R.C.: The performance of low-cost commercial cloud computing as an alternative in computational chemistry. *J. Comput. Chem.* **36**(12), 926–933 (2015)
3. Zhang, Q., Cheng, L., Boutaba, R.: Cloud computing: state-of-the-art and research challenges. *J. Internet Serv. Appl.* **1**(1), 7–18 (2010)
4. Evangelinos, C., Hill, C.N.: Cloud computing for parallel scientific HPC applications: feasibility of running coupled atmosphere-ocean climate models on Amazon’s EC2. In: *The 1st Workshop on Cloud Computing and its Applications (CCA)* (2008)
5. Zinno, I., Elefante, S., Mossucca, L., De Luca, C., Manunta, M., Terzo, O., Lanari, R., Casu, F.: A first assessment of the p-sbas dinsar algorithm performances within a cloud computing environment. *IEEE J. Sel. Top. Appl. Earth Obs. Remote Sens.* **8**(10), 4675–4686 (2015)
6. Pilosu, L., Ruiu, P., Goga, K., Budroni, M.A.: Automated cloud computing approach for the simulation of chemo-hydrodynamic problems. In: *2016 10th International Conference on Complex, Intelligent, and Software Intensive Systems (CISIS)*, pp. 438–443. IEEE (2016)
7. Mossucca, L., Terzo, O., Goga, K., Acquaviva, A., Abate, F., Provenzano, R.: NGS workflow optimization using a hybrid cloud infrastructure. *Int. J. Adv. Netw. Serv.* **5**(3 & 4), 2012 (2012)
8. Flores-Contreras, J., Parlavantzas, N., Duran-Limon, H.A.: Efficient execution of the WRF model, other HPC applications in the cloud. *Earth Sci. Inform.* **9**(Issue 3), 365–382 (2016). doi:10.1007/s12145-016-0253-7
9. Overview of the cluster configuration. <https://www.lrz.de/services/compute/linux-cluster/overview/>. Accessed 30 Jan 2017
10. Amazon machine image (AMI). <http://docs.aws.amazon.com/AWSEC2/latest/UserGuide/AMIs.html>. Accessed 06 Mar 2017
11. Amazon cfnccluster. <https://aws.amazon.com/hpc/cfncluster/>. Accessed 06 Mar 2017
12. Aws cloudformation. <https://aws.amazon.com/cloudformation/>. Accessed 06 Mar 2017
13. Aws virtual private cloud (VPC). <https://aws.amazon.com/vpc/>. Accessed 06 Mar 2017
14. Amazon simple storage service (s3). <https://aws.amazon.com/s3/>. Accessed 06 Mar 2017
15. Amazon elastic block store. <https://aws.amazon.com/ebs/>. Accessed 06 Mar 2017
16. Fiori, E., Comellas, A., Molini, L., Rebori, N., Siccardi, F., Gochis, D.J., Tanelli, S., Parodi, A.: Analysis and hindcast simulations of an extreme rainfall event in the mediterranean area: the genoa 2011 case. *Atmos. Res.* **138**, 13–29 (2014)

17. Rasmussen, R.M., Thompson, G., Manning, K.: Explicit forecasts of winter precipitation using an improved bulk microphysics scheme. Part I: Description and sensitivity analysis. *Mon. Weather Rev.* **132**(2), 519–542 (2004)
18. Hong, S.-Y., Noh, Y., Dudhia, J.: A new vertical diffusion package with an explicit treatment of entrainment processes. *Mon. Weather Rev.* **134**(9), 2318–2341 (2006)
19. Supermuc petascale system. <https://www.lrz.de/services/compute/supermuc/systemdescription/Flyer.pdf>. Accessed 15 Mar 2017
20. Docker. <https://www.docker.com/what-docker#/overview>. Accessed 06 Mar 2017

# HyperLoom Possibilities for Executing Scientific Workflows on the Cloud

Vojtech Cima<sup>1</sup>(✉), Stanislav Böhm<sup>1</sup>, Jan Martinovič<sup>1</sup>, Jiří Dvorský<sup>1</sup>,  
Thomas J. Ashby<sup>2</sup>, and Vladimír Chupakhin<sup>3</sup>

<sup>1</sup> IT4Innovations, VŠB Technical University of Ostrava, Ostrava, Czech Republic  
{vojtech.cima,stanislav.bohm,jan.martinovic,jiri.dvorsky}@vsb.cz

<sup>2</sup> IMEC, Brussels, Belgium  
ashby@imec.be

<sup>3</sup> Janssen Pharmaceutica NV, Brussels, Belgium  
vchupakh@its.jnj.com

**Abstract.** We have developed HyperLoom - a platform for defining and executing scientific workflows in large-scale HPC systems. The computational tasks in such workflows often have non-trivial dependency patterns, unknown execution time and unknown sizes of generated outputs. HyperLoom enables to efficiently execute the workflows respecting task requirements and cluster resources agnostically to the shape or size of the workflow. Although HPC infrastructures provide an unbeatable performance, they may be unavailable or too expensive especially for small to medium workloads. Moreover, for some workloads, due to HPCs not very flexible resource allocation policy, the system energy efficiency may not be optimal at some stages of the execution. In contrast, current public cloud providers such as Amazon, Google or Exoscale allow users a comfortable and elastic way of deploying, scaling and disposing a virtualized cluster of almost any size. In this paper, we describe HyperLoom virtualization and evaluate its performance in a virtualized environment using workflows of various shapes and sizes. Finally, we discuss the Hyperloom potential for its expansion to cloud environments.

**Keywords:** Cloud · Virtualization · Distributed environments · Scientific workflows · HPC

## 1 Introduction

The rapid growth of resource demanding workloads such as machine learning applications which take advantage of large-scale infrastructures is being reflected in service offerings of major public cloud providers. For example, Amazon's AWS [1] offers instance types with up to 16 CPUs (64 vCPUs) and hundreds GB of RAM, similarly Exoscale [4] offers instance types with up to 16 CPUs and 128 GB RAM. The performance of the compute instances with such specifications is directly comparable with compute nodes in HPC systems. But unlike the HPC systems, these can be deployed on demand in just a few seconds in

seemingly any imaginable scale. As the gap between HPC systems and other virtualized distributed environments such as clouds decreases, more HPC solutions are being ported to the cloud.

Although the trend in Cloud Computing is to shift workloads to lighter virtualization solutions such as containers, the virtualization overhead is still present. Nonetheless, for many use cases is the overhead either acceptable, insignificant or compensated by other factors.

In this paper, we describe a virtualization of HyperLoom - originally an HPC solution for defining and executing scientific workflows and compare the performance of the virtualized HyperLoom to the performance of the bare metal deployment.

The paper is organized as follows. Section 2 describes important properties of scientific workflows. Section 3 introduces HyperLoom - an HPC solution for defining and executing such workflows. In Sect. 4, we overview standard virtualization solutions and discuss their suitability for virtualization of HyperLoom's components. We evaluate HyperLoom performance in Sect. 5. Finally, we conclude in Sect. 6.

## 2 Scientific Workflows

Many scientific workloads are composed of several consecutive computational phases. These are then often chained into more complex flows, such as, for example, model cross-validation combined with hyper-parameter search, which results in pipelines in a shape of large directed acyclic computational graphs - *plans*, whose nodes represent computational units - *tasks*. Figure 1 shows an example of such a graph.

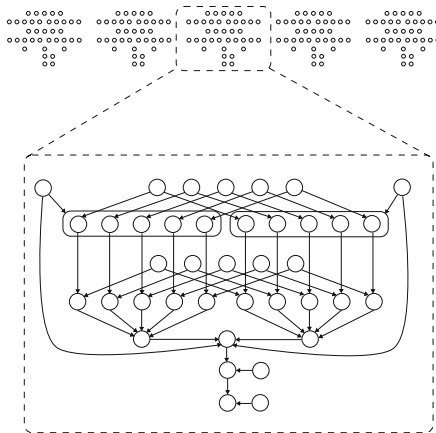


**Fig. 1.** Example of a scientific pipeline visualized as a directed acyclic graph.

## 2.1 Workflow Properties

We have identified a set of properties which, we believe, apply to the most of the scientific workflows. Different scientific workloads are defined by plans of various shapes and sizes. Plans may contain millions of tasks of the various types with non-trivial inter-task dependencies. Generally, a plan can take the shape of any directed acyclic graph. Furthermore, the execution time of individual tasks is typically not known before the execution finishes and may vary from milliseconds (short-running tasks) to days (long-running tasks). Similarly, the size of the outputs produced by the tasks may not be known in advance. Distributed environments, namely HPC clusters, may contain thousands of computational nodes. Moreover, different computational nodes may provide various resource types with different capacities. All of the listed properties have a significant impact on the workflow execution. Ideally, we look for a solution that minimizes the execution time agnostically to those properties.

## 3 HyperLoom

HyperLoom is a platform for defining and executing scientific workflows in distributed environments designed for HPC systems. The ultimate goal of HyperLoom is to minimize the overall plan execution time respecting tasks' and environment's resource constraints.

Other tools for scheduling tasks in distributed environments exist such as Spark [16], HTCondor [11] or Hadoop [14]. If we only consider solutions that allow defining inter-task dependencies, we name SciLuigi [12], DAGman [8], Pegasus [9] and Dask/Distributed [13]. The first three are designed for more coarse-grain tasks. Moreover, in these tools, the inter-task data transfer is done through a shared file system which introduces another performance bottleneck for some use cases, namely in the scenarios with a large number of tasks where a large number of files to be created imposes a significant load on the distributed file system. Also, in all of the cases, the tools do not provide an easy way of chaining third party applications and provide so an arbitrary functionality.

To mitigate the limitations of the competing solutions while respecting the properties listed in Sect. 2.1, HyperLoom contains the following design features. The core of HyperLoom is implemented in C++. Plans can be easily defined and executed using the client application implemented in Python. Since the execution time of individual tasks is not known in advance, Hyperloom implements an optimized dynamic scheduler that schedules the tasks reactively with a low overhead. Moreover, the scheduler respects task dependencies and prioritizes placements that induce the smallest possible inter-node data transfer. The data produced by tasks are by default kept directly in memory and can be accessed by any other task from any other node directly with no additional overhead imposed on the server or the underlying file system. HyperLoom allows chaining and execution of third-party applications in the same manner as any other native task type. It is also possible to define custom task types.

### 3.1 Architecture

Figure 2 illustrates the main components of HyperLoom. HyperLoom consists of a *server* process that manages *worker* processes that run on computational nodes and a *client* component providing an user interface to HyperLoom.

**Client** allows users to programmatically chain computational tasks into a plan and submit the plan to server. It also provides a functionality to gather results of the submitted tasks after computation finishes. **Server** receives and decomposes a plan and reactively schedules tasks to run on available computational resources provided by workers. **Workers** execute and run tasks as scheduled by server and inform the server about the state of task execution. This modular architecture allows connecting an arbitrary number of workers which is the keystone for HyperLoom scalability.

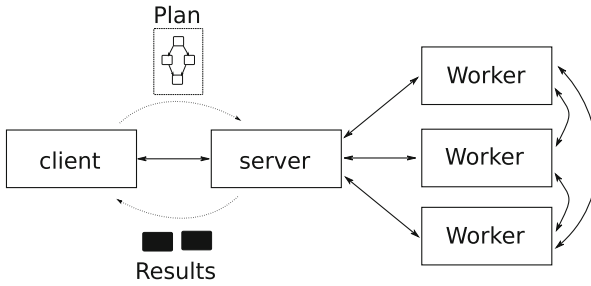


Fig. 2. HyperLoom architecture.

## 4 Virtualization

In this section, we introduce the main motivation for the virtualization of the HyperLoom infrastructure, overview well-known virtualization solutions and discuss the potential of their usage in the HyperLoom context.

### 4.1 Motivation for HyperLoom Virtualization

HyperLoom has been designed as a high-performance solution in the context of HPC systems. Nonetheless, we realize some of the disadvantages of such systems such as inflexible resource management, limited offerings and high administration overhead comparing to the cloud solutions. We foresee that the HyperLoom virtualization is a key step for its expansion to the cloud world that will allow on-demand and flexible deployment of HyperLoom at infrastructures other than HPC which may be easier to access for some of the potential users.

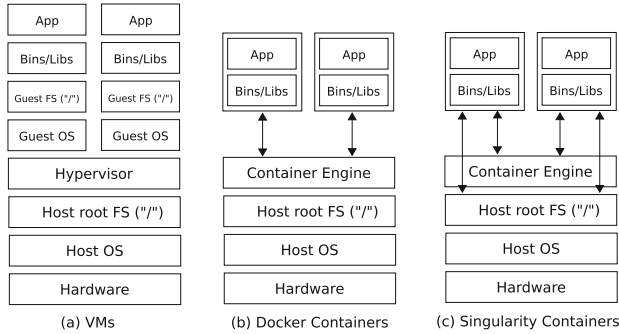


**Fig. 3.** Virtualization solution: (a) Virtual machines, (b) Docker containers, (c) Singularity containers.

## 4.2 Virtualization Solutions

One of the best-known virtualization solutions used nowadays is the concept of virtual machines (VMs) powered by various hypervisors. While the VMs dominated the market not so many years ago, many workloads are being shifted to lighter virtualization platforms such as containers. The adoption of container platforms such as Docker [2] is reportedly increasing. Containers, in contrast to heavier VMs, allow almost an instant execution of a containerized application or a service while still providing a certain level of isolation from the host machine. This shift allows developers to build and ship more flexible and scalable applications available as-a-service. Although Docker has been proven numerous times to work well in cloud environments and provide a centralized catalog - Docker Hub [3] containing many ready-to-run Docker images, the Docker daemon process requires a privileged user (root) to run which makes it unlikely to be widely adopted by HPC centers. Singularity [5], in contrast to Docker, is a containerization solution that does not require the daemon process being owned by root which makes it a containerization solution of choice for many HPC systems. Moreover, Singularity is compatible with existing Docker images including those in Docker Hub. Figure 3 illustrates the main architectural differences between (a) a standard virtual machine, (b) a Docker container and (c) a Singularity container.

## 4.3 HyperLoom Virtualization

We have virtualized the key components of HyperLoom - *server* and *worker* using Ubuntu 16.04 as the base Docker image for creating a container with HyperLoom binaries and the underlying library stack. Although we have only containerized HyperLoom using Docker image, we don't foresee any potential issues creating a HyperLoom virtual machine which would provide the same functionality with higher virtualization overhead. We have decided to use containers mainly due to the lighter virtualization layer sacrificing the full process isolation in favor of higher performance and also due to their increasing popularity in the community.



## 5 Performance Evaluation

In this section, we discuss HyperLoom performance. Concretely, we compare plan execution time with and without virtualization scaling the environments up to 64 compute nodes on which we execute various synthetic and a real test case scenarios.

### 5.1 Testbed Description

We have carried out all the experiments on a testbed with up to 64 identical physical computational nodes, each with two 12-core Intel Xeon E5-2680v3 processors (2.5 GHz) [6] and 128 GB of physical memory. All the nodes are interconnected by an InfiniBand [15] network (56 Gbps). All nodes run Red Hat Enterprise Linux [10] 6.5 OS. As a virtualization layer, we use Singularity Launcher with HyperLoom components containerized using a Docker container based on Ubuntu 16.04 image. The virtualized deployment is depicted in Fig. 4.

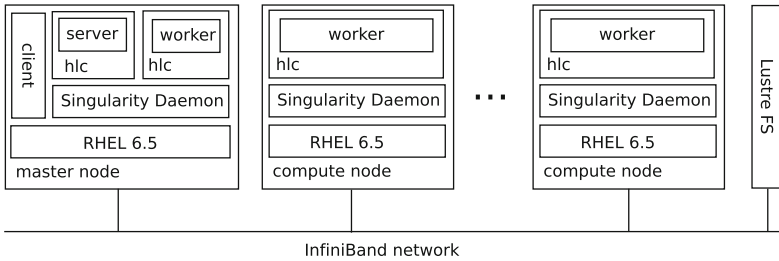


Fig. 4. Virtualized HyperLoom infrastructure.

### 5.2 Methodology and Metrics

We measure the total execution time (execution duration) from the time when a plan is submitted to the server to the time when the computation finishes. To illustrate the virtualization overhead, we also compute and plot the relative execution time by normalizing the plan execution time in virtualized environment by the execution time of the native execution. The test scenarios are described more in detail in Sect. 5.3 below. All experiments were replicated three times and the total execution time averaged to moderate potential unforeseen system deviation which might affect the performance.

### 5.3 Test Scenarios

We have designed several test case scenarios devoted to evaluate different corner cases as well as to evaluate HyperLoom performance and scalability for workflows used in practice. As an example of real-world scenario, we demonstrate a

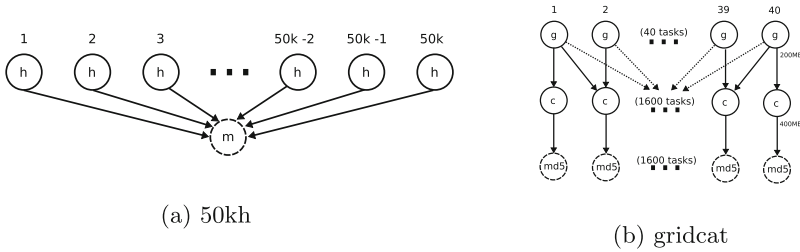


**Fig. 5.** Visualization of the (a) *50kh* and (b) *gridcat* test case scenarios.

performance of a scientific workflow derived from a pipeline used for novel drug discovery. Below, we briefly describe our test cases more in detail.

*50kh* - a synthetic test case designed to benchmark scheduling overhead. As depicted in Fig. 5a, the assembled plan contains 50k independent and identical short running tasks - *h*-nodes (running *hostname* command) followed by a task that merges outputs from all of them - *m*-node.

*gridcat* - a synthetic test case designed to simulate more complex workflows. The assembled plan contains tasks of various sizes chained together, so it induces a significant inter-worker data transfer when scheduled inappropriately. Concretely, as visualized in Fig. 5b, we create 40 tasks which each generate a 200 MB output, followed by tasks representing a concatenation of every possible pair from the first layer resulting in 1600 tasks (each 400 MB of output), the last layer of tasks then computes the *md5* hash of the concatenated data.

*mlchemo* - a real-world test case derived from an existing scientific workflow which performs a nested cross-validation ( $5 \times 5$ ) with hyperparameter search to find an optimal parametrization of machine-learning based models used for compound activity prediction. The plan contains a mix of long-running tasks such as modeling and validation done by LibSVM [7] - a widely used support vector machine implementation, short running tasks for supporting tasks such as averaging values and others. The shape of this plan is very similar to the plan depicted in Fig. 1.

## 5.4 Experiments

Table 1 contains total execution time values [s] for each of the test case scenarios using both, the virtualized (sing.) and the native (native) HyperLoom deployment. The total execution time for both of the synthetic test cases (*50kh*, *gridcat*) varies from seconds to minutes depending on the cluster size. We remind that these test cases were designed to artificially stress HyperLoom components with the increasing cluster size and thus we do not observe the inverse proportionality between the cluster size and the total execution time values. The scalability of Loom is more evident in the *mlchemo* test case, where the total execution time steadily decreases with the increasing cluster size.

**Table 1.** Comparison of the plan execution time [s] using native and virtualized HyperLoom deployment (*50kh*, *gridcat*, *mlchemo*).

# nodes	<i>50kh</i>		<i>gridcat</i>		<i>mlchemo</i>	
	Native	Sing.	Native	Sing.	Native	Sing.
1	48.84	44.37	112.08	115.03	28,796.97	31257.13
2	23.41	20.97	76.00	83.53	14123.65	15,279.46
4	12.19	10.56	49.05	48.80	7,025.58	7,599.67
8	7.48	6.38	35.37	35.75	3,547.31	3,851.36
16	10.09	9.89	34.85	42.49	1,815.60	1,989.85
24	13.59	14.53	31.94	48.78	1,255.27	1,370.00
32	18.11	16.80	38.96	37.01	956.81	1,053.71
64	34.28	33.99	50.68	43.59	559.27	595.12

Figure 6 visualizes the virtualization overhead by plotting the relative execution time for the respective test case scenarios.

None of the synthetic test cases - *50kh* (Fig. 6a) nor *gridcat* have confidently confirmed the expected performance degradation caused by the virtualization layer. On the contrary, for the *gridcat* test case, the virtualized deployment of HyperLoom performed slightly better than the native deployment in 7 out of 8 cases (1, 2, 4, 8, 16, 32, 64 workers) with  $\sigma = 0.069$ . The *gridcat* test case (Fig. 6b) introduces significantly higher variance ( $\sigma = 0.193$ ) in the relative execution time of the virtualized deployment with varying cluster size. In this test case, the virtualized infrastructure performed slightly better in 3 out of 8 cases (4, 32, 64 workers).

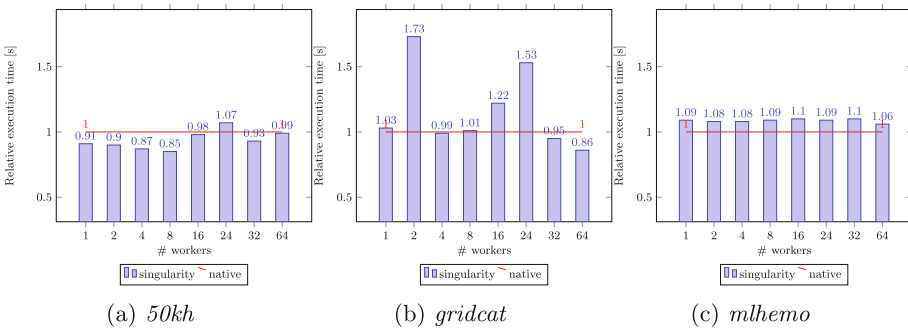


**Fig. 6.** Relative execution time of the (a) *50kh*, (b) *gridcat* and (c) *mlchemo* test cases executed on virtualized infrastructure (singularity) normalized to the execution time of the test cases executed on native HyperLoom infrastructure (native baseline) using up to 64 nodes (24 CPUs each).

A representative of real-world HyperLoom usage - the *mlchemo* test case (Fig. 6c) uniformly confirmed the expected performance degradation caused by the added virtualization layer. The virtualized deployment of HyperLoom is in this case in average 9% slower than the native alternative. Notably, in this case, we observe a very low variation ( $\sigma = 0.01$ ) in the relative execution time values with varying cluster size.

Considering the non-trivial size and complexity of the *mlchemo* test case, whose execution time varied from more than 8 h (1 worker) to less than 20 min (64 workers), we argue that these results may be generalized to other large-scale real-world workloads more objectively than the results obtained using the synthetic test cases.

## 6 Conclusion

We have successfully virtualized HyperLoom components using Docker images with Singularity Launcher and compared the performance of such a virtualized infrastructure to native HyperLoom deployment in an HPC environment.

Despite the fact that HyperLoom was initially designed for HPC systems, we have shown its potential of being used in a cloud or other virtualized environments which brings HyperLoom closer to a much broader audience. Although cloud providers offer a flexible lease of machines which performance is comparable to those in HPC systems, the network solutions used in HPC systems offer incomparably higher inter-node throughput and latency.

We have shown that the degradation of HyperLoom performance caused by the virtualization layer is in average  $\sim 9\%$  for the test case designed to simulate real-world scenarios. Nevertheless, some of the synthetic test cases in virtualized environment slightly outperformed the performance of the bare metal HyperLoom deployment. This suggests that advantages of virtualization such as the availability of the newest versions of application dependencies may outweigh the overhead of virtualization layer itself.

Although we have virtualized HyperLoom so it can find its audience outside the HPC community, we believe that virtualization is also beneficial for HPC systems as it has the potential to enable more applications on such systems without the need for the applications themselves being directly compatible with the underlying operating systems.

Although we have only discussed fix-sized HyperLoom deployments, in elastic cloud environments, we foresee a potential for HyperLoom to become significantly much more energy efficient by scaling the deployment up/down (potentially in/out) based on current workers utilization which is one of the subjects for future work.

**Acknowledgements.** This project has received funding from the European Union's Horizon 2020 Research and Innovation programme under Grant Agreement No. 671555. This work was supported by The Ministry of Education, Youth and Sports from the National Programme of Sustainability (NPU II) project IT4Innovations excellence in science - LQ1602 and by the IT4Innovations infrastructure which is supported from the Large Infrastructures for Research, Experimental Development and Innovations project IT4Innovations National Supercomputing Center LM2015070.

## References

1. Amazon AWS. <https://aws.amazon.com/>
2. Docker. <https://www.docker.com/>
3. Docker Hub. <https://hub.docker.com/>
4. Exoscale. <https://www.exoscale.ch/>
5. Singularity. <http://singularity.lbl.gov/>
6. Specsheat - Processor Intel Xeon E5 2680. <http://ark.intel.com/products/81908/Intel-Xeon-Processor-E5-2680-v3-30M-Cache-2.50-GHz>
7. Chang, C.-C., Lin, C.-J.: Libsvm: a library for support vector machines. *ACM Trans. Intell. Syst. Technol. (TIST)* **2**(3), 27 (2011)
8. Chen, W., Deelman, E.: Workflow overhead analysis and optimizations. In: *Proceedings of the 6th Workshop on Workflows in Support of Large-Scale Science, WORKS 2011*, New York, NY, USA, pp. 11–20. ACM (2011)
9. Deelman, E., Singh, G., Mei-Hui, S., Blythe, J., Gil, Y., Kesselman, C., Mehta, G., Vahi, K., BruceBerriman, G., Good, J., Laity, A., Jacob, J.C., Katz, D.S.: Pegasus: a framework for mapping complex scientific workflows onto distributed systems. *Sci. Program.* **13**(3), 219–237 (2005)
10. Red Hat: Red hat enterprise linux (2017). <https://www.redhat.com/en/technologies/linux-platforms/enterprise-linux>. Accessed 31 Mar 2017
11. HTCondor: Htcondor (2017). <https://research.cs.wisc.edu/htcondor/index.html>. Accessed 31 Mar 2017
12. Lampa, S., Alvarsson, J., Spjuth, O.: Towards agile large-scale predictive modelling in drug discovery with flow-based programming design principles. *J. Cheminformatics* **8**(1), 67 (2016)
13. Rocklin, M.: Dask: parallel computation with blocked algorithms and task scheduling. In: *Proceedings of the 14th Python in Science Conference*, pp. 130–136. Citeseer (2015)
14. White, T.: *Hadoop: The Definitive Guide*, 1st edn. O'Reilly Media Inc., Sebastopol (2009)
15. Wikipedia: Infiniband – wikipedia, the free encyclopedia (2017). <https://en.wikipedia.org/w/index.php?title=InfiniBand&oldid=772443735>. Accessed 31 Mar 2017
16. Zaharia, M., Xin, R.S., Wendell, P., Das, T., Armbrust, M., Dave, A., Meng, X., Rosen, J., Venkataraman, S., Franklin, M.J., et al.: Apache spark: a unified engine for big data processing. *Commun. ACM* **59**(11), 56–65 (2016)

# A Scalable and Low-Power FPGA-Aware Network-on-Chip Architecture

Somnath Mazumdar<sup>1</sup>(✉), Alberto Scionti<sup>2</sup>, Antoni Portero<sup>3</sup>, Jan Martinović<sup>3</sup>,  
and Olivier Terzo<sup>2</sup>

<sup>1</sup> Università di Siena, Siena, Italy  
mazumdar@dii.unisi.it

<sup>2</sup> Istituto Superiore Mario Boella (ISMB), Torino, Italy  
{scionti,terzo}@ismb.it

<sup>3</sup> IT4Innovations, VSB-University of Ostrava, Poruba, Czech Republic  
{antonio.portero,jan.martinovic}@vsb.cz

**Abstract.** The growing demand for high-performance capabilities in data centers (DCs) leads to adopt heterogeneous solutions. The advantage of specialised hardware is a better support for different types of workloads, and a reduction of the power consumption. Among the others, FPGAs offer the unique capability to provide hardware specialisation and low power consumption. In this context, large arrays of simple and reconfigurable processing elements (PEs), known as coarse-grain reconfigurable arrays (CGRAs), represent a flexible solution for supporting heterogeneous workloads through a specialised instruction set that provides high performance in specific application domains (e.g., image recognition, patterns classification). However, efficient and scalable interconnections are required to sustain throughput and performance of CGRAs. To this end, networks-on-chip (NoCs) have been recognised as a viable solution for better data packet communication. In this paper, we propose an FPGA-aware NoC design targeting CGRAs with 128+ PEs. The proposed design leverages on a two-level topology to scale well with the increasing number of PEs, while the introduction of a software-defined reconfiguration capability offers the opportunity to tailor the set of resources assigned to a specific application. Partitions of physical resources (i.e., *virtual domains*) are built over the physical topology to meet the required performance, as well as to ease sharing physical chip resources among applications. Experimental evaluation shows the efficiency of our solution regarding used FPGA resources and power consumption.

## 1 Introduction

The growing demand for performance and energy saving is the major driver of the silicon industry. Nowadays, it is possible to integrate several billions of transistors on the same die to implement more powerful on-chip functions. The growing

---

S. Mazumdar and A. Scionti—Both the authors contributed equally.

demand for performance is also transforming the DCs' infrastructure, aiming at exhibiting higher levels of energy efficiency. Thus, heterogeneous solutions, including field programmable gate arrays (FPGAs), are incorporated into the DCs' racks (e.g., the Bing Search engine). FPGAs are of particular interest, since they help to implement large and effective *coarse-grain reconfigurable arrays* (CGRAs), providing an extremely high level of parallelism.

Supporting such high parallelism requires an effective interconnection subsystem which can efficiently move data among different PEs. Bus-based interconnections are quickly dominated by the physical limits in driving signals, since the capacitive load increases with the number of connected devices. Rings show a similar drawback, once connecting a large number of cores (i.e., tens to hundreds of PEs). Packet-switched networks (i.e., NoCs) are scalable and offer deterministic performance, while supporting chip exposing a substantial number of nodes. NoCs represent one of the most efficient candidates for implementing on FPGA devices an effective interconnection for high-performance and low power CGRAs. NoCs can be characterised by considering the topology and the microarchitecture of routers forming the interconnection. The topology defines how nodes in the network are connected each other, while the adopted routing algorithm determines the microarchitecture of the routers. The router microarchitecture in turn influences the number of cycles needed to forward a data packet towards its destination. Among the others, the 2D-mesh topology is the most adopted. It efficiently connects all the nodes and helps to keep the router microarchitecture simple. On the other hand, router architects aim at reducing the number of cycles required by a data packet to reach the output port by exploiting variants of the basic crossbar-based design. However, one of the main drawbacks of such designs is the large area and power cost that a large network (hundreds of PEs) presents. In fact, the majority of the router area and power budget is consumed by the input buffers and the crossbar switch. In [1] authors have shown that connecting 256 cores using conventional 2D-mesh NoC can consume up to 45% of the total energy.

This paper proposes a hybrid NoC architecture for alleviating the area and power cost of conventional 2D-mesh networks. In this work, a group of four PEs are connected by a simpler but efficient ring, while each group directly connects to a crossbar-based 2D-mesh router. Using this design, the majority of the data traffic is kept inside the rings (traffic localisation), as well as the area cost is reduced. For instance, connecting 256 PEs only requires a  $4 \times 4$  array instead of 256 routers as in a purely flattened configuration. Synthesis results on FPGA confirmed our expectations: the number of resources consumed by our solution and the overall power consumption is not significant, leaving more space for implementing advanced PE functions. In addition, performance and throughput can be further improved by exploiting the proposed adaptation mechanism, without negatively affecting the efficiency (e.g., multiple instances of the application can run in parallel).

## 2 Background

In past years, the attention of the research community for efficient NoC architectures has grown, focusing on different aspects of the design. Some proposed works are on: low latency router microarchitectures [2], power efficient routers [3], improved topologies [4, 5]. Hierarchical topologies [6–8] have also been proposed as a solution to the scaling problem of NoCs. HiRD [6] is a hierarchical ring-based NoC design for improved energy efficiency, where buffers within individual rings are not used. It provides buffer support between different levels of the ring hierarchy. Flits are deflected in the rings upon the saturation of buffers. CSquare [9] proposes a way of clustering routers. Routers are grouped resembling a tree-like organisation. The authors showed that this topological design improves throughput, providing better scalability. Transportation network inspired NoC (tNoC) [10] is another proposed hierarchical ring topology, employing a hybrid packet-flit approach, credit-based flow control mechanism for better scalability, as well as priority-based arbitration for achieving better performance. Some works also focused on hybridization of routers to provide better performance and scalability. In [7], a two-tier hierarchical topology consisting of local networks managed through a bus, and a global network controlled by a low-radix mesh router have been proposed. Authors showed that the proposed topology could reduce the latency, power consumption and energy-delay product only for localised communication-based applications. Concentrated mesh (CMesh) [11] is also a modified mesh architecture with replicated sub-networks, where express channels are used to incorporate the second network without increasing the die area and wire length. This approach aims at reducing the hop count and load imbalance. Channel lengths are kept short to reduce energy dissipation, while express channels are used to improve energy efficiency. Recently, adaptation mechanisms have been integrated into the router microarchitectures, with the aim of both improving performance and lowering power consumption by activating only the resources that effectively are required by the application. Panthre [12] integrates reconfiguration features in the microarchitecture of a traditional 2D-mesh router. On the other hand, in [13] authors integrate reconfiguration capabilities into a ring-based design, allowing application software to control the configuration phase directly. In this paper, we propose a scalable NoC architecture aimed at providing high performance (i.e., improved throughput and reduced latency) in a small power envelope, along with a low area cost. To achieve this, our architecture combines a hierarchical topology design and an adaptation mechanism.

## 3 System Architecture

Our proposed NoC architecture supports high-speed and low-cost communications in CGRAs composed of a large set of PEs (i.e., specifically, 128 or more). The instruction set architecture (ISA) of PEs can be customized for achieving better performance while keeping low power consumption. Each PE is coupled



with a lightweight switch representing the primary communication interface. The proposed design leverages on a two-level organization of the interconnection. It allows for a better exploitation of the principle of locality of computations, and also reduces the network traffic between distant PEs. In a large CGRA configuration data moving data and synchronizing PEs' activity quickly becomes a bottleneck. Data-driven program execution models (PXM) and effective thread scheduling policies must be integrated to avoid performance loss, and to preserve energy efficiency advantages [14–16]. In our design, 4 PEs are grouped together to form a local cluster called *ringlet* (i.e., the first level of the topology). PEs inside a ringlet are connected through a bi-directional ring, while one of the PEs also supports the communication with the mesh router (i.e., the *ring master*). Up to 4 ringlets are directly attached to a single mesh router, forming a *physical domain* (i.e., the second level of our topology). Physical domains are connected each other through a high-speed 2D-mesh network, which serves less frequent data exchange among PEs placed far away. By combining these two physical topologies, our scalable design results in a higher throughput capacity, lower communication latency, and better energy efficiency, with regards to conventional flattened 2D-mesh designs (i.e., local rings consume less power respect to 2D-mesh routers, although they serve more frequent packet exchanges). The proposed hybrid topology exploits the fact that most of the communication in a parallel application affects a group of resources (i.e., PEs and routers) that are close to each other [7]. Since, the larger portion of the interconnection is represented by rings, the area cost can also be reduced by our approach. For instance, Fig. 1 shows an instantiation of the proposed CGRA architecture: a  $4 \times 4$  fabric providing up to 256 PEs organized into 16 physical domains.

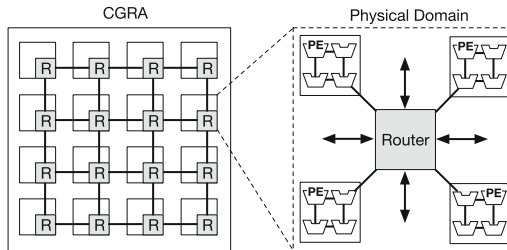


**Fig. 1.** An example of instantiation of the proposed CGRA architecture: up to 256 PEs are grouped into a  $4 \times 4$  fabric of physical domains.

### 3.1 Mesh Router Microarchitecture

The 2D-mesh router is based on the traditional architectural design: a set of input channels are connected to the front-side of a crossbar switch, which enables the packet transfer to a corresponding set of output channels. Input and output channels are formed by FIFO buffers which allow to temporary store packets in-flight every time the output channels/links are busy. Generally, the size of the FIFO

buffers can differ between input and output channels (typically output channels are smaller). In a conventional 2D-mesh topology only five channels are required to enable chip communication (i.e., east, west, north, south and local PE link). However, since the router also connects up to 4 ringlets, the number of channels is extended to eight: a group of 4 channels are used to steer network traffic inside the physical domain (i.e., moving traffic among local ringlets), while other 4 channels extend the communication among physical domains (i.e., separated routers). Figure 2 shows the detailed microarchitecture of our proposed 2D-mesh router. Network traffic can be differentiated in a NoC by introducing multiple buffers for each input channel (i.e., *virtual channels* – VCs). Although VC offers higher flexibility for managing network traffic but introducing more VCs can add complexity to the router. Nonetheless, VCs are essential to ensure dead-lock free communications with standard routing protocols (e.g., X-Y dimension order routing – XY-DoR). To support VCs, the routing logic needs to drive a two-stage selection policy: (i) each input channel is arbitrated to select one of the VC, (ii) input channels are arbitrated to transfer packets to the output channels. The first step is accomplished by the VC allocator (VA) module, while the second step is performed by the switch allocator (SA) module.

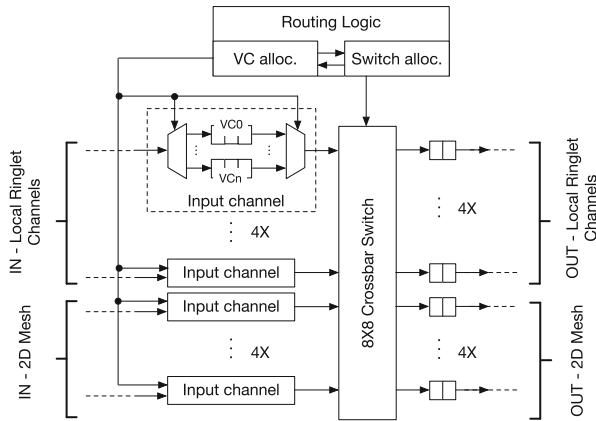


**Fig. 2.** Internal microarchitecture of the 2D-mesh router connecting up to 4 ringlets. A router with all the ringlets connected to, it forms a physical domain.

Interestingly, single-flit packets represent the large segment of the network traffic for real applications [17]. With the aim of keeping the microarchitecture complexity low, we considered a *single flit* data packet. In our design, the data packet length is 42-bits, where 32-bits are used to transport data payload, and the remaining 10-bits are devoted to carrying header information. The size of the packet has been chosen to take into account that increasing the packet size, leads to a quadratic increment of the internal crossbar switch area cost. For that reason, we maintained the packet size as small as possible [18]. Also, it is worth to

note that many applications require short machine words (e.g., artificial neural networks), thus well fitting with our selected packet length. Every time a new flit is received, the corresponding header enables the routing logic to compute the correct destination port. At the same time, the VA and SA modules are enabled to select which flit has to reach the destination port. To maximize the network throughput, more aggressive speculation techniques can be applied, so that VA and SA operations can be performed in parallel. The entire flit transfer can be restricted to a single cycle due to the following design choices: *(i)* the adoption of the store-and-forward mode, *(ii)* small size packets (i.e., single-flit packets with a short length), and *(iii)* the application of speculative allocation techniques.

### 3.2 Ring Switch Microarchitecture

Ring switches are the basic blocks to implement the proposed hierarchical NoC design. Specifically, each *ring switch* (RS) is responsible for forwarding traffic over the ring, as well as extracting traffic from the ring and further injecting it into the 2D-mesh (or forwarding it to the local PE). Figure 3 shows the microarchitecture of an RS. Two multiplexers/demultiplexers (MUXs/DEMUXs) are used to manage the traffic travelling on the ring in both the directions. Each MUX/DEMUX is coupled with a small buffer to temporary store packets that must be extracted from the ring. Compared to ordinary crossbar-based routers, an RS uses smaller input buffers. In fact, MUX/DEMUX modules support prioritization of the traffic: flits traversing the MUX/DEMUX in the same direction have higher priority over data packets that need to be injected. Thus, only few buffer entries are required to avoid flits (packets) to be dropped. Traffic prioritization also allows the rings to support higher operational frequencies, compared to ordinary crossbar-based routers. The interface towards the local PE is implemented through a third MUX and a local buffer. Similar to the buffers used to manage traffic moving in the ring, also buffers at the PE interface can be kept small: extraction of the flits from the ring has a higher priority on traffic injection since this help to reduce the pressure on the internal buffers. Specifically, a round robin (RR) policy is used to drive the selection of the input to transfer to the output port using the MUX. Finally, traffic prioritization helps to keep a simple control logic for governing the switch operations. Figure 3 shows in red, the portion of the microarchitecture devoted to interface the RS with the 2D-mesh router. This interface is composed of a MUX to inject the traffic in the router, and an input channel for storing flits that have to be injected in the ring or that have to be presented to the local PE. The MUX contains the arbitration logic that allows selecting flits to forward in the input channel of the router. It is worth to observe that the RS is interfaced with a dedicated input channel, thus preventing contention with other traffic sources. Similarly to the PE interface, traffic injection in the router has higher priority, since this reduces pressure on the local ring buffers. Conversely, the traffic that is extracted from the router is temporarily stored in a dedicated input channel, resembling the input structures available in the mesh router. Such inputs present the same number of VCs to

manage different classes of traffic correctly and to avoid deadlocks. An RR policy is applied to such VCs to avoid buffer exhaustion and traffic starvation. The adoption of such microarchitecture allows reducing the area cost of the proposed solution, as well as to lowering the overall power consumption. If implemented on an ASIC device, the interface with the router can be avoided in those RS that are not connected to it (i.e., only a single RS in a ringlet is interfaced with the router – the master RS). Similarly, when synthesised on an FPGA, it can be both disabled (reducing the overall power consumption) and avoided (in that case, the two different ring structures of the RS must be provided to the synthesis tool).

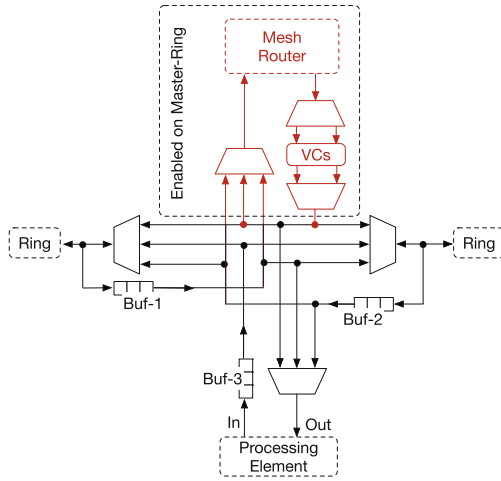


**Fig. 3.** Internal microarchitecture of the RS. The link with the router is enabled only on a single switch (master) within the ringlet.

### 4 Reconfigurability

To meet the required level of performance, many applications may demand the capability of the underlying hardware to dynamically adapt to the behavioral changes over time. Our solution leverages on a simple, but effective interface with the application software for dynamically configuring the network topology. The proposed solution allows the software to directly control the mesh routers for the purpose of creating custom virtual topologies. In such way, the physical resources of the CGRA are partitioned, allowing the creation of multiple *virtual domains*. Virtual domains also allow reserving resources for multiple applications (or multiple instances of the same application) running on the same chip, thus avoiding interferences among them. Figure 4 shows an example of the creation of such virtual domains. Two mesh routers share two ringlets each, better adapting to the application behavior: red arrows in the figure shows how traffic flowing

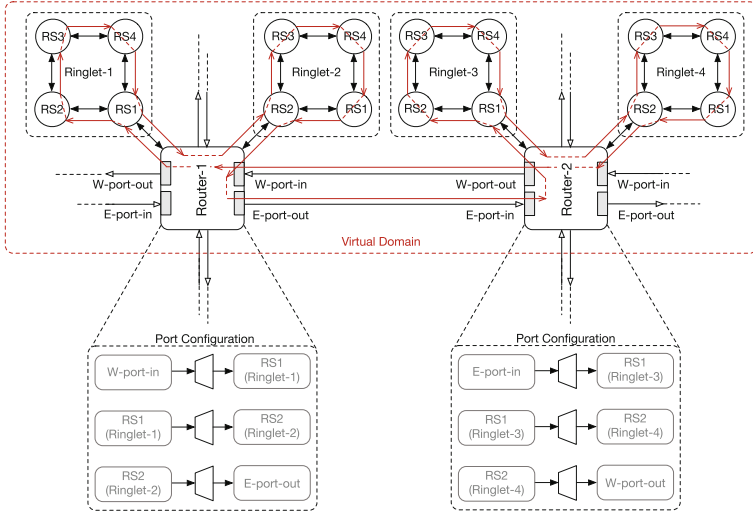


**Fig. 4.** Virtual domain configuration: 4 ringlets are virtually connected to form a single cluster of resources.

in one direction moves through the global virtual ring. Only the routers need to be configured to correctly steer the traffic between the global mesh and the local ringlets. Through our software interface, crossbar switches are configured in such way traffic is maintained inside the virtual ring (i.e., the red path in Fig. 4). For instance, the west input port of Router-1 is configured to directly forward traffic into the input buffer of the  $RS_1$  switch (Ringlet-1). Similarly, traffic exiting  $RS_1$  switch is steered in the  $RS_2$  switch belonging to Ringlet-2. Finally, traffic that flows away  $RS_2$  on Ringlet-2 is injected in the east output port of Router-1. Similar to Router-1, also the other router is configured to inject/eject traffic from the local ringlets, providing a behavior like a global ring structure. In addition, the configuration of routers can be further extended to support a bidirectional flow of the flits within the virtual ring.

Routers are configured through a software interface, which consists of a minimalistic set of instructions executed by PEs:

- *ENABLE\_CFG*: enables the selected router to use a specific configuration for the input/output ports. Whenever a specific configuration is enabled, the output signals of the arbitration and routing logic are overrun by the user configuration.
- *DISABLE\_CFG*: disables the user defined configuration. In such way, the whole physical resources of the chip are exposed to the application.
- *LOAD\_CFG*: specifies the router configuration, by transferring the information contained in a PE's general purpose register. In the case of short length registers (e.g., targeting neural network applications), more than one register is needed to keep the entire router configuration.

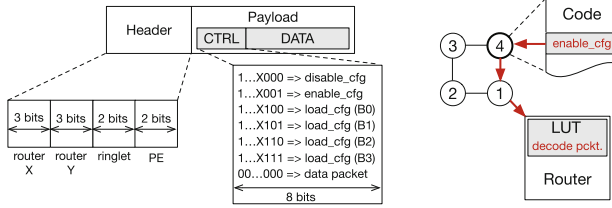


**Fig. 5.** Single-flit packet organization (left) and the corresponding 2D-mesh router configuration enabled by special instructions (right).

The payload of our data packet is partitioned into *control* (CTRL) and *data* fields (see Fig. 5). The most significant bit (MSB) of the control field (8-bits long) allows the router logic to check if a configuration action is required or not. Configuration flits carry all the configuration information. Every time the MSB is asserted, the remaining 7-bits provide the indication of the specific command. To reduce the complexity of the logic, only the three least significant bits (LSBs) are used, leaving space for future extensions. The router configuration requires that for each input port, the set of output ports that traffic can flow through is defined. Such set is specified using a single byte, where each bit controls part of the crossbar switch MUXs associated with the specific input port. Thus the whole router configuration requires 8 bytes. The entire router configuration is completed sending four subsequent flits, each bringing the configuration of two ports (for the sake of simplicity, input and output ports are numbered progressively). Figure 5 (right) shows an example of router configuration: once the PE<sub>4</sub> on the ringlet executes the ENABLE\_CFG instruction, a corresponding packet is sent to the router, where a look-up table (LUT) is used to decode it, and to enable the configuration (previously loaded). Figure 6 depicts the hardware extension that we integrated into the routers to allow the dynamic configuration. To keep simple the design, a 64-bits internal register holds the configuration of the input ports (i.e., lower 32-bits contains the configuration of the four local ringlets attached to the router, while the upper 32-bits refer to the configuration

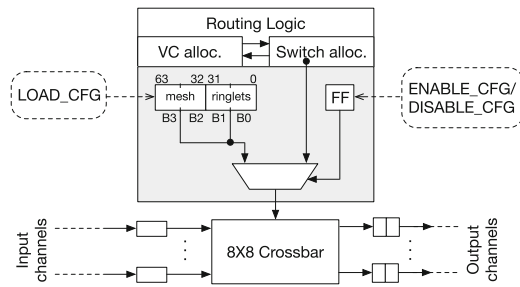


**Fig. 6.** The extended 2D-mesh router microarchitecture supporting dynamic reconfiguration capabilities.

of the mesh ports of the router). `LOAD_CFG` packets directly load configuration bytes in the correct position within such register. On the other hand, `ENABLE_CFG` and `DISABLE_CFG` flits affect the selection of a MUX, which in turn allows applying the configuration provided by the routing arbitration logic or bypassing it.

## 5 Evaluation

We evaluated the effectiveness of the proposed NoC architecture regarding scalability, area cost and power consumption. All the experiments were performed on a Xilinx Kintex-7 ultra-scale device. The Xilinx Vivado 2016.4 design suite was used to simulate, synthesize, and perform the place-and-route operation. The entire synthesis and placement process were performed considering the instantiation of both the modified mesh router and a variable number of ringlets (ranging from 1 to 32). To correctly manage traffic, input ports in the router have two VCs. To reduce the latency for reaching the output port while keeping low the complexity of the control logic, routers implement a store-and-forward (SAF) packet switching strategy, where the SA arbitration employs an RR strategy. Routing logic implements the X-Y DoR algorithm to provide deterministic routing. The router operates with a four-stage pipeline, that can be optimized by integrating speculative logic to reduce the number of cycles required to forward flits.

We evaluated the throughput and average packet latency for a configuration with multiple physical domains (up to 128 PEs) by simulating the injection of uniform random traffic in the network (injection rate equals to 1.0 packet/cycle). Experimental results show the capability of the proposed design to scale very well: average latency increases from 90 cycles (16 PEs) to 155 cycles (128+ PEs grouped into  $4 \times 4$  physical domains), while the throughput increases from 12 packets/cycle (16 PEs) to 172 packets/cycle (128+ PEs).

### 5.1 Area Cost and Power Consumption

We evaluated the area cost for implementing our design by measuring the number of FPGA resources consumed by the synthesis and place-and-route processes when instantiating groups of ringlets and the mesh router.

We have reported the following resources as the percentage of the whole set of available ones on the selected FPGA device (mid-size): the number of look-up tables (LUTs), registers (FFs), and Block RAMs (BRAMs – each 36 Kbits in size). From the reported values our claim of the effectiveness of the proposed design is confirmed. It is interesting to note that the implementation of the 16 RSs (i.e., 4 ringlets composing a physical domain) requires less than 1% of the whole FPGA resources (except for the BRAMs). However, scaling the number of ringlets, some of the BRAMs can be shared (further resource saving). Nevertheless, scaling up to 128 PEs on a mid-size FPGA device consumes less than 41% of the resources (i.e., BRAMS, LUTs and FFs in total), thus leaving

**Table 1.** FPGA resources utilization: percentage of the total number of LUTs, FFs and BRAMs. Within brackets we reported values before the place-and-route process (i.e., synthesis results only for the ringlets' configurations).

Module	PEs	LUTs		FFs		BRAMs	
Router	–	0.77%	–	0.34%	–	1.52%	–
Ringlet	$1 \times 4$	0.05%	(0.29%)	0.08%	(0.11%)	1.06%	(2.41%)
Ringlet	$2 \times 4$	0.12%	(0.51%)	0.17%	(0.18%)	3.15%	(4.63%)
Ringlet	$4 \times 4$	0.29%	(0.92%)	0.34%	(0.35%)	6.30%	(9.26%)
Ringlet	$8 \times 4$	0.58%	(1.92%)	0.68%	(0.68%)	12.22%	(18.52%)
Ringlet	$16 \times 4$	0.74%	(3.90%)	1.01%	(1.34%)	18.15%	(37.04%)
Ringlet	$32 \times 4$	1.34%	(7.87%)	2.00%	(2.67%)	37.77%	(74.07%)

enough space for the PEs' logic. Figure 7 shows the results of the placement of a  $4 \times 4$  array of RSs on the FPGA device. The complete synthesis results are reported in the Table 1 for different configurations of the ringlets (ranging from 4 PEs arranged as a single ringlet to 128 PEs arranged as 32 ringlets with 4 PEs each). Finally, it is worth noting that the proposed design does not consume a single DSP resource (the number of clock buffers consumed is constant irrespective of the configuration and it is below 1%), thus leaving space for the PE's logic to explore the free DSPs.

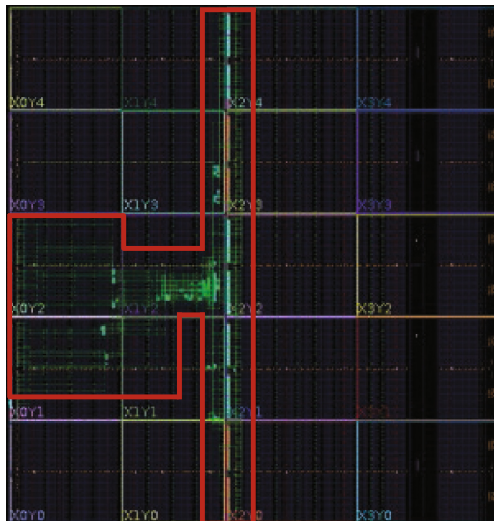


**Fig. 7.** Result of the place-and-route process for a  $4 \times 4$  array of RSs (i.e., 4 ringlets). Red box highlights the area of FPGA device where resources are used.



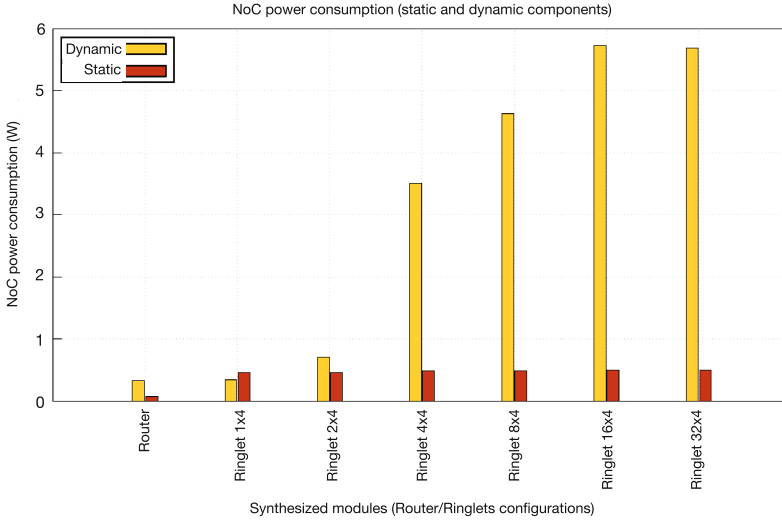


**Fig. 8.** Static and dynamic components of the NoC power consumption.

From the results is evident that for small size NoC implementations (i.e., up to 8 PEs) the static component dominates the power consumption of the system (this is mainly due to the leakage effects, which results in a static power consumption of the entire device). Figure 8 provides the split of static and dynamic components of the power consumption for different NoC configurations. Conversely, increasing the size of the NoC (i.e., more than 16 PEs), dynamic component dominates the total power consumption. For our design, we found a static power consumption equals to 806.0 mW (324.0 mW ascribed to the router and 482.0 mW to 4 ringlets). On the other hand, the dynamic power consumption for the mesh router is only 75.0 mW, while the ringlets consume up to 3.502 W. Considering that (dynamic) power consumption does not increase linearly with the number of active PEs. Thus, we expect our solution capable of scaling towards 128+ PEs without a substantial increase in the power consumption (e.g., ringlets configured as a  $32 \times 4$  array consume 5.683 W as a dynamic component). All these results demonstrate the effectiveness of the proposed design as the main interconnect for large CGRAs.

## 6 Conclusion

The continuous improvements in manufacturing technologies make the adoption of accelerators in Cloud domain easy. In this paper, we present the architecture of a scalable NoC-based interconnect, which relies on a hybrid topology to provide scalability and power/area efficiency at the same time. Such interconnection

could be the core block for building highly parallel accelerators. FPGAs offer the opportunity to create large arrays of customised PEs (i.e., customized CGRAs) targeting new frameworks (e.g., deep learning frameworks). Experimental results confirm our proposed design supports low packet latency, low power consumption and also resource efficiency (FPGA friendly). Scalability is demonstrated with a configuration containing more than 128 nodes, as well as power consumption and area cost of our solution is very low on a mid-range FPGA device, making the proposed architecture well suited for highly parallel CGRAs.

**Acknowledgement.** This work is partially supported by the European Union H2020 program through the OPERA project (grant no. 688386), and by the Ministry of Education, Youth and Sports of the National Programme for Sustainability II (NPUII) under the project “IT4Innovations excellence in science – LQ1602”.

## References

1. Curtis Harting, R., et al.: Energy and performance benefits of active messages. Concurrent VLSI Architectures Group, Stanford University. Technical report, 131 (2012)
2. Amit, K., et al.: Express virtual channels: towards the ideal interconnection fabric. ACM SIGARCH Comput. Architect. News **35**(2), 150–161 (2007)
3. Hangsheng, W., et al.: Power-driven design of router microarchitectures in on-chip networks. In: IEEE/ACM, Micro (2003)
4. Kim, J., et al.: Technology-driven, highly-scalable dragonfly topology. ACM SIGARCH Comput. Architect. News **36**, 77–88 (2008)
5. Kim, J., et al.: Flattened butterfly topology for on-chip networks. In: IEEE/ACM, Micro, pp. 172–182 (2007)
6. Ausavarungnirun, R., et al.: A case for hierarchical rings with deflection routing: an energy-efficient on-chip communication substrate. Parallel Comput. **54**, 29–45 (2016)
7. Reetuparna, D., et al.: Design and evaluation of a hierarchical on-chip interconnect for next-generation CMPS. In: IEEE HPCA (2009)
8. Bourduas, S., et al.: A hybrid ring/mesh interconnect for network-on-chip using hierarchical rings for global routing. In: NOCS, pp. 195–204. IEEE (2007)
9. Zheng, N., et al.: Csquare: a new kilo-core-oriented topology. Microprocess. Microsyst. **39**(4), 313–320 (2015)
10. Kim, H., et al.: Transportation-network-inspired network-on-chip. In: IEEE HPCA (2014)
11. Balfour, J., et al.: Design tradeoffs for tiled CMP on-chip networks. In: Proceedings of the 20th Annual International Conference on Supercomputing, pp. 187–198. ACM (2006)
12. Parikh, R., et al.: Power-aware NOCS through routing and topology reconfiguration. In: Proceedings of the 51st Annual Design Automation Conference (2014)
13. Scionti, A., Mazumdar, S., Portero, A.: Software defined network-on-chip for scalable CMPS. In: IEEE HPCS, pp. 112–115 (2016)
14. Zhu, S.: Hardware implementation based on FPGA of semaphore management in  $\mu\text{C}/\text{OS-II}$  real-time operating system. IJGUC **6**(3–4), 192–199 (2015)
15. Lynar, T.M., et al.: Resource allocation to conserve energy in distributed computing. IJGUC **2**(1), 1–10 (2011)

16. Kipp, A., et al.: Applying green metrics to optimise the energy-consumption footprint of it service centres. *Int. J. Space-Based Situated Comput.* **2**(3), 158–174 (2012)
17. Sheng, M., et al.: Whole packet forwarding: efficient design of fully adaptive routing algorithms for networks-on-chip. In: *IEEE HPCA* (2012)
18. Junghee, L., et al.: Do we need wide flits in networks-on-chip? In: *IEEE ISVLSI* (2013)

# Design of a Control System Card for Frequency Inverter in FPGA

Horacio Matsuura<sup>1(✉)</sup>, Mauro Marcelo Mattos<sup>2(✉)</sup>, and Luiz Henrique Meyer<sup>2(✉)</sup>

<sup>1</sup> WEG Drives & Controls - Automação Ltda., Jaraguá do Sul, SC, Brazil  
matsuura.horacio@gmail.com

<sup>2</sup> FURB – University of Blumenau, Blumenau, SC, Brazil  
{mattos,meyer}@furb.br

**Abstract.** Nowadays much energy has been allocated to what is being called the Internet of Things (IOT) but little attention has been devoted to the infrastructure aspects to support this designed model, particularly for industries wishing to embark on the IOT era. This work describes the design and implementation of scalar control software for induction motors based in FPGA technology, with emphasis on control features based on PWM and Space Vector Modulation techniques as a proof of concept project. From the perspective of the scientific methodology, the present work is classified as an applied research (regarding the nature of the study), quantitative (regarding the approach to the problem) and explanatory (regarding the objectives). As for the technical procedures to carry out the work, the case study was used from the context of the company that produces frequency inverters where the project is being executed. To achieve the main objective was instantiated a “soft processor” in FPGA and specified and implemented scalar control algorithms (and helper functions) that allowed validating the hardware implementation. In addition, were performed a set of tests on pilot hardware and an evaluation of results is presented.

## 1 Introduction

Since the introduction of thyristor or semiconductor-controlled rectifier (SCR) in the mid-1950s, technology has evolved and directly impacted traditional methods of power conversion and control. This impact translates into the reduction of size and cost in the components used in the construction of power electronic converters, which has been experiencing a reduction in size and cost. This process has also impacted on the performance and cost-effectiveness aspects of modern AC (alternating current) drive systems. As a result, there was a rapid expansion in the use of AC drives in industrial applications, and this growth was accelerated with the realization of the great capacity to improve the performance of these applications. The introduction of the microprocessors enabled a universal hardware design with flexible software control, facilitating integrated and complete factory automation [3].

In addition, the processing power of the microprocessors allows for numerous possibilities of sophistication in the drive control systems, whether with traditional induction

motors and synchronous motors, or not so traditional brushless DC motors and variable reluctance machines [2].

These advances allowed many variable speed drive applications that required precise and stable speed, torque, or position controls with long-term stability, good transient performance, and high efficiency to migrate from DC motors to AC motors.

DC motors meet some of these requirements, but their mechanical commutator is often undesirable due to the need for regular maintenance. This feature introduces a level of difficulty when the application does not allow interruptions or when the motor is in an inaccessible position.

AC motors such as the squirrel cage induction motor and synchronous reluctance motors and permanent magnet synchronous motors do not have mechanical brushes and have a robust construction, which allows reliable operation at high speeds, without the need for maintenance.

The simpler rotor construction also results in lower cost motors and a higher power/weight ratio. Unfortunately, induction motors and synchronous motors are inflexible in speed when operated on standard frequency constant power supply, as is the case of electric utilities that offer 60 Hz (or 50 Hz) fixed frequency power supplies.

The synchronous motors operate synchronously at a speed that is determined by the frequency of the power supply and by the number of poles to which the stator is wound. Induction motors run slightly below the synchronous speed [12, 13]. For intermittent low speed operation, the induction motor stator voltage control is satisfactory. However, efficient speed control over a wide operating range for synchronous motors or induction motors is only possible when an adjustable frequency power supply is available. These characteristics have meant that in the last decades there has been a rapid expansion in the use of frequency inverters, mainly in the industry. This factor led to the emergence of a virtuous circle, where the demand for the use of frequency inverters in increasingly demanding processes leads to the increasing need for evolution also in all the components that constitute the drive.

At the same time as the evolution of electronic devices dealing with power electronics itself (semiconductors), the evolution of devices such as microprocessors, microcontrollers and digital signal processing (DSP) also allowed for significant advances in control strategies (requiring considerable processing capacity), ranging, for instance, from scalar control to vector control to modulation techniques that optimize control for a desired characteristic.

With the advent of the Internet of Things (IoT) [4–7] we are experiencing the emergence of a new technology ecosystem involving an increase in new technologies, skills and infrastructure support, including new hardware platforms, new networks, new operating systems, new cloud services which require adaptation in energy infrastructure technologies, for example.

The motivation for the realization of this project occurred in the context of a traditional world-class company that develops frequency inverters for the market.

The project was developed as proof of concept that served to evaluate the adequacy of new technologies to support the demands of: (a) Internet of Things (IoT); (b) flexibility of insertion/removal of plug-ins modules, embedded PLC functions and hot swap; (c) integrated functional safety; (d) modularity between the control and power stages

and (e) efficiency. As additional software requirements were included: (a) functional safety related to IEC 61508; (b) industrial communication networks that allow the parameterization and control of the inverters, new protocols (SymbiNet and BACnet); (c) built-in Programmable Logic Controller (PLC) functions that allow the user to implement drives that are much more complex than those allowed by the I/O by Ladder programming; and (d) additional features for the Human Machine Interface (HMI) as well as the possibility of displaying graphics of the inverter signals (currents, voltages, temperatures and etc.) as a function of time, USB port for monitoring/Parameter change, online help, IP66 protection, Cyrillic text input and CJK characters (Chinese, Japanese, Korean).

At the same time, this project must meet the following performance requirements: (a) allow to change the topology of the power hardware with the least possible effort (being able to configure converters of 6, 12 and 18 pulses); and (b) allow a regular increase in the switching frequency of the inverter switches from the current 10 kHz to 15 kHz or more (which would imply maximum duty cycles of 67  $\mu$ s).

This paper is organized as follows: the first section presents an introduction with the research theme, the second presents the main concepts, the third section describes the hardware/software design, the fourth section describes the test model used and the fifth section presents the conclusions and Future work.

## 2 Main Concepts

### 2.1 FPGA

According to [1] the Field Programmable Gate Array (FPGA) are truly revolutionary devices that mix the benefits of hardware and software. They implement circuits as realized in a hardware project, providing tremendous benefits particularly in performance over purely software-based projects, and can be reprogrammed cheaply and easily. Unlike Application Specific Integrated Circuits (ASIC) where the device is custom-tailored for a particular project, FPGAs can be programmed and reprogrammed to meet the requirements or functionalities of the desired application [1, 14].

Although FPGAs of the One-Time Programmable Type (OTP) are in the market, the dominant type is based on Static Random Access Memory (SRAM) that can be reprogrammed as the project evolves. In this way, FPGAs allow designers to change their designs until the end of their development cycle (and eventually, even after the final product has been manufactured and deployed in the field). For example, Xilinx FPGAs allow field updates to be performed remotely, eliminating the associated costs for re-designing or manually updating electronic systems [8].

Since customizing an FPGA basically involves storing values in memory locations, the creation of FPGA-based circuits involves the process of creating a string of bits to be loaded into the device. Although there are tools for doing this from software languages, schemas, and other formats, FPGA designers usually start with a document written in a hardware description language or Hardware Description Language (HDL), such as Verilog or Very High Speed Integrated Circuits Hardware Description Language (VHDL). This abstract design is optimized to fit into the available logical structure of

the FPGA by means of a series of steps that involve the following steps [1]: (a) logical synthesis that converts logical constructions of high level and code of behavior in logical doors; (b) mapping to separate the ports in clusters that more closely match the logical resources of the FPGA being used; (c) assignment of logical groupings to specific logical blocks; (d) determination of interconnection routes that carry user signals; (e) generation of the binary file containing the necessary resources of the project; and (f) load the binary file on the device.

## 2.2 Microblaze Software Processor

The main component of the FPGA project involves the instantiation of a MicroBlaze Soft Processor Core [9] where the software will be developed for motor control and associated functions. This is a 32-bit RISC processor with an instruction set optimized for embedded applications, widely used in diverse applications such as medical, automotive, consumer goods, communications infrastructure beyond industrial.

It is quite versatile and highly configurable, with more than 70 configuration options such as instruction/data caching, Floating Point Unit (FPU), Memory Management Unit (MMU) and more. Its flexibility allows you to select the memory characteristics, peripherals and interfaces that best fit the user's design in a single component. It can be optimized for performance (5 state pipeline) or for area (3 state pipeline). Supports Processor Local Bus (PLB) or Advanced eXtensible Interface (AXI) interfaces.

## 2.3 Frequency Inverters

Frequency inverters or simply inverters, are commonly referred to in the literature as a series of other designations such as variable speed drive or variable frequency drive. They are devices that converts the fixed voltage and frequency of the electrical supply network, supplied by the utility, into variable voltage and frequency. This feature is especially useful for applications with electric motors, where speed variation is commonly required in a wide range of applications. Therefore, frequency inverters are, as a rule, used to drive electric motors.

One of the great advantages of using frequency inverters is that, depending on the characteristics of the load, it is possible to achieve a high degree of efficiency of the application by the speed variation, which will certainly imply an increase in energy efficiency in a time in which the costs of the energy and production difficulties increase every day. Inverters usually also act as protection devices for the system driven against the most varied electrical power supply disturbances, such as voltage variations, overloads and imbalance between phases.

The classic basic structure of the power stage of a frequency inverter consists of three main blocks: a rectifier stage at the input, an intermediate stage consisting of a bank of capacitors and filter circuits and the output stage which is the inverter stage itself formed by transistors of type Insulated Gate Bipolar Transistor (IGBT) acting as keys. The transformation of the fixed frequency power supply to a variable frequency power supply is done in two steps: (a) the AC power supply is rectified generating a DC source and (b) the DC voltage is then modulated at an AC voltage at the desired frequency. It is by

means of the synchronized opening and closing control of the inverter stage switches that the effect of controlling the output voltage and frequency and consequently varying the speed of a motor coupled to the output of the frequency inverter is achieved [11]. This control technique is known as Pulse Width Modulation (PWM) [10] and is also used in other fields of Engineering such as Communication Systems. In modern frequency inverters, the PWM control is implemented digitally through embedded microprocessor systems.

## 2.4 Main Functionalities

The main functions to be implemented in software are Acceleration/Deceleration Ramps, Scalar Control for Induction Motors (Volts/Hz) and Space Vector Modulation. With this set of functions, it is possible to validate with good precision the necessary hardware and software control requirements for a final commercial product. It is also possible to test and validate much of the power hardware.

## 3 Hardware Card Design

The hardware design of the card was based almost exclusively on FPGA design. The XC6SLX45 chip is part of Xilinx's Spartan-6 family, whose features are cost-optimized, delivering industry-leading connectivity features such as high pin logic rates, reduced tunnels and a diverse number of I/O supported. Manufactured with 45 nm technology, the devices are ideal for a variety of applications in many areas, inclusive in industrial automation. Ease of integration into the user's system, increase processing speed, reduce costs, reduce consumption and increase development productivity are some of the advantages pointed out by the manufacturer Xilinx.

Some characteristics that corroborate the adoption of this technology are: (a) more than 40 I/O standards available; (b) up to 8 low-power transceivers at 3.2 GB 800 Mb/s DDR3 with integrated memory controller; (c) MicroBlaze Soft Processor IP eliminates the need for an external processor; (d) option of core supply voltages in 1.2 V or 1.0 V; (e) zero consumption in Power-down mode; and (f) ISE Design Suite for Windows and Linux for the development of the logical part of FPGA in VHDL language.

In the scope of this project were implemented in VHDL the projects described below: (a) instantiation of the IP of the MicroBlaze Soft Processor, where will be developed the algorithms of control of the motor; (b) implementation of multiple PWM channels (9 pairs can trigger up to 18 keys) with dead time insertion, dead time compensation, pulse feedback and minimum pulse width. This configuration allows, in addition to the standard topology of a three-phase converter using six switches, to drive different topologies such as a matrix converter or a back-to-back structure; (c) multiple fault inputs that disable the PWM pulses; (d) two trigger outputs (at the switching frequency) for simultaneous and simultaneous reading of signals on the two channels of the A/D converters (fundamental for reading the output currents); (e) an output for actuation of the IGBT of the braking resistor for regenerated energy dissipation for the DC bus via the braking resistor; (f) an output for interruption generation when faults are detected in



the operation of the inverter; (g) a clock input; (h) a reset input; (i) nine PWM feedback inputs for dead time compensation; (j) an input for earth fault signaling; (k) an input for overcurrent fault signaling; (l) an input for signaling other generic faults; (m) interface channel with SDRAM memory; (n) interface channel with user interface card; (o) implementation of a fast UART channel with automatic read/write buffer; (p) calculation of CRC; and (q) interface channel with safety card.

The tool used for software development in MicroBlaze Soft Processor is the Software Development Kit (SDK) provided by Xilinx. The SDK includes an Eclipse-based development interface and GCC compiler. The operating system used is FreeRTOS. The floating-point unit of the processor in question was used.

Within the scope of this project, the following algorithms were developed: (a) acceleration/deceleration ramps; (b) scalar control for induction motors; and (c) PWM (space vector modulation) modulation. The implementation of these algorithms made it possible, once the speed reference was provided, to drive an induction motor connected to the inverter output, as shown in Fig. 1.



**Fig. 1.** Software components.

Although it did not meet all the control software requirements specified, this implementation was enough for validation of control and power hardware, and thermal, electromagnetic and mechanical compatibility projects. For the design of the acceleration/deceleration ramp (Fig. 2a) the following functionalities were implemented: (a) two sets of ramps with independently adjusted acceleration and deceleration times; (b) selection between ramp 1 or ramp 2 via parameter, via digital input, via network command or via SoftPLC command; (c) selection between linear ramp or “S” ramp (future implementation); (d) user adjustable ramp1 acceleration time from 0.0 s to 999.9 s, factory preset at 20.0 s; (e) user adjustable ramp1 deceleration time from 0.0 s to 999.9 s, factory preset at 20.0 s; (f) ramp-up time 2 adjustable by the user from 0.0 s to 999.9 s, factory preset at 20.0 s; (g) user adjustable ramp2 deceleration time from 0.0 s to 999.9 s, factory preset at 20.0 s; (h) user-adjustable max. Permissible speed from 0 to 65000 rpm, factory preset at 1800 rpm; (i) acceleration time was defined as the time for the engine to accelerate from 0 rpm (stopped) to the maximum speed defined by the user (in rpm); and (j) deceleration time was defined as the time for the motor to decelerate from the maximum speed defined by the user (in rpm) to 0 rpm (stopped).

The design of the Scalar Control Module (V/Hz or V/f) is because the Volts/Hz ratio in an induction motor remains approximately constant up to the synchronous motor speed, typically 60 Hz or 50 Hz. So, the flux and, consequently, the torque remain approximately constant in this region. Above the synchronous speed the Volts/Hz ratio is no longer constant and the flux and torque decrease. For this reason, this operating region is called the field weakening region. Based on these characteristics the V/Hz control implements a curve according to Fig. 2b.

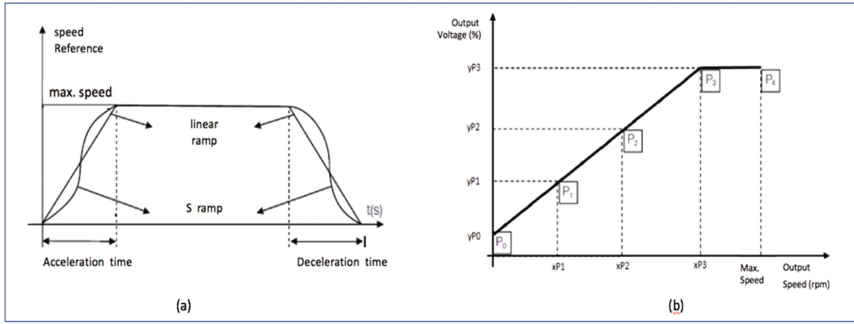


**Fig. 2.** (a) Acceleration/deceleration ramps and linear/curve “S”. (b) Curve V/Hz (rpm).

These points shown in Fig. 2b define the curve as three straight line segments defined by their respective line equations, as described below:

$$U_{0-1} = s_{0-1} \times (ref - xP0) + yP0, \quad \text{para } xP0 \leq ref \leq xP1 \quad (1)$$

$$U_{1-2} = s_{1-2} \times (ref - xP1) + yP1, \quad \text{para } xP1 \leq ref \leq xP2 \quad (2)$$

$$U_{2-3} = s_{2-3} \times (ref - xP2) + yP2, \quad \text{para } xP2 \leq ref \leq xP3 \quad (3)$$

where  $ref$  = speed reference for control provided by ramp output and where:

$$s_{0-1} = \frac{yP1 - yP0}{xP1 - xP0} \quad (4)$$

$$s_{1-2} = \frac{yP2 - yP1}{xP2 - xP1} \quad (5)$$

$$s_{2-3} = \frac{yP3 - yP2}{xP3 - xP2} \quad (6)$$

The project of the SVM (Space Vector Modulation) module contains the following implemented requirements: (a) user-adjustable switching frequency from 1.5 kHz to 16.0 kHz, factory preset at 4.0 kHz; (b) implementation of the floating point algorithm; (c) must be compatible for future use with other control types such as VVW control, senseless vector control and vector control with encoder for induction motors and permanent magnet motors; (d) implementation with the possibility of entering the region of over modulation; (e) without dead time implementation, this function will be implemented in FPGA logic; (f) without implementation of minimum pulse time, this function will be implemented in FPGA logic; (g) without implementation of pulse feedback, this function will be implemented in FPGA logic; and (h) implementation of the Space Vector Modulation (SVM) algorithm [10].

### 4 Project Validation

To test the implemented model, some cases of use of commands sent by a system operator were simulated. The testRampComm variable is already initialized with the GenEnable = ON command. The test starts by making Enable = ON, causing the reference to start to accelerate until it receives the Hold = ON command when it stops accelerating and remains at the same value. After a while the Hold = OFF command will re-initialize until it receives a GenEnable = OFF command that disables the drive.

After some time, the Enable = ON command enables the reference to accelerate again until it receives an Enable = OFF, when it starts to decelerate. Before it stops, it again receives the command Enable = ON and accelerates to the reference value set by the user. Remains for a while when you receive a command rotationDirection = CCW (counter clockwise) to reverse the direction of rotation. It then decelerates to zero and reactivates in the reverse direction until it reaches the user-defined reference value again. The results are presented at Fig. 3.

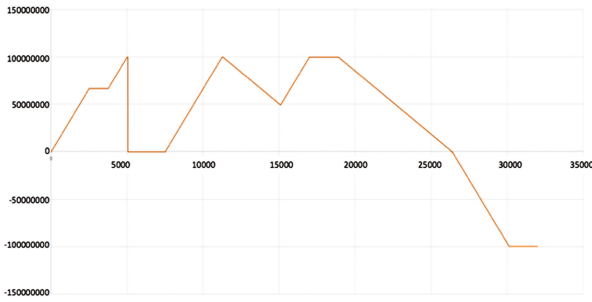


Fig. 3. Ramp module unit test.

In the test of the space vector modulation module, each iteration simulates a step in the switching frequency given a reference of 1800 rpm. Figure 4a shows the typical waveform of the percentages of time for each of the three phases in percent (axis y) as a function of the angle  $\theta$  (x-axis).

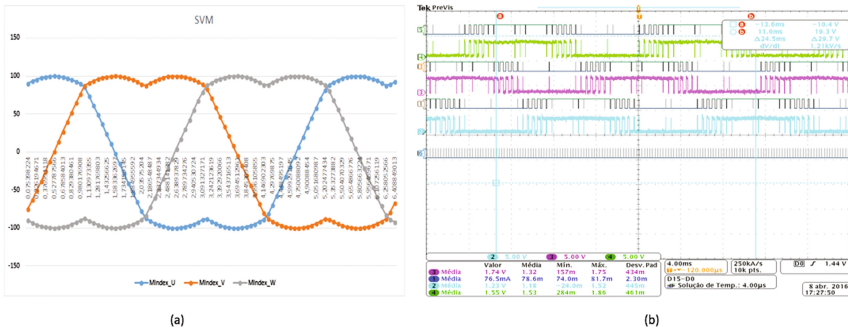


Fig. 4. (a) Unit test for SVM module. (b) IGBT trigger signals.

For software development, a reduced prototype was built for benchtop use, making it easier to integrate with the software development tools available on the bench without the need to go to the laboratory.

Another advantage of this prototype is to also meet the safety standards regarding the use of high voltage equipment in the workplace. The control hardware cards are the same as the actual product, so the software used is also the same. For the power hardware, a special card with a nominal 30 V AC input voltage was developed to drive a special 30 V 60 Hz/0.25 Hz motor.

To validate a scenario between the pulses generated by the FPGA and the actual activation of the keys we present the Fig. 4b where you can see in channels 2, 3 and 4 the actual actuation of the keys in the gates of the IGBT. In the digital bus, in lanes 1, 3 and 5 the commands for the same keys in the output of the FPGA. The signal of the switching frequency, defined by the AD trigger signal, is also observed in path 6.

Another test tried to verify the operation of the drive in 15 Hz. Figure 5b shows the current signal measured at one of the output phases with the motor being driven at 15 Hz (450 rpm).

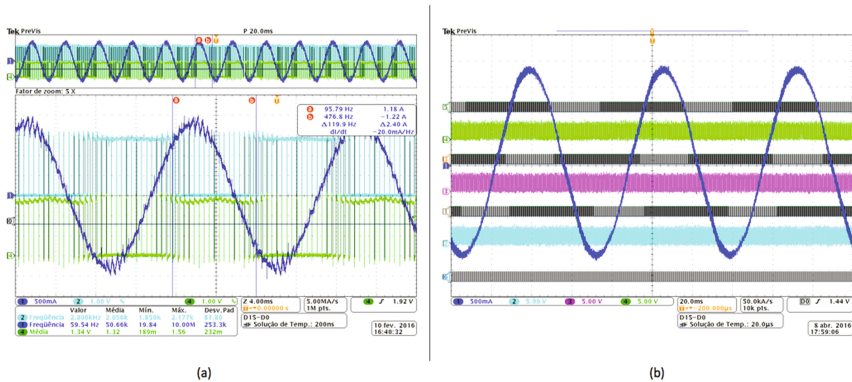


Fig. 5. (a) Sample test in a 15 Hz drive (b) Sample drive at 1800 rpm without over modulation.

It can be seen in Fig. 5a that the current distortion is very small with an over modulation of approximately 5%. More tests should be done with real prototypes to base this issue as this current prototype still has very low power.

## 5 Conclusions and Further Work

The present work deals with the design and implementation of scalar control software for induction motors based on FPGA technology, with emphasis on control features based on PWM and Space Vector Modulation. Specifically, a solution for implementing the scalar control code (and accessory functions) for induction motor drive and the implementation of external logic to the processor in the FPGA required for the control is presented.

The work includes the instantiation of the soft processor in the chosen FPGA and specified and implemented the scalar control code (and accessory functions) to drive the induction motor. Also, the implementation of the external logic to the soft processor required to support the control functions was performed. In addition, validation tests and an evaluation of the results obtained were carried out.

The tests carried out showed that, from a software development point of view, the use of a soft processor instantiated in an FPGA has little or no influence over development in conventional microcontrollers. It is a transparent process for the developer.

This project served as proof of concept for new projects in power control within the company, as well as presenting and justifying the steps of building the hardware and software solution of the FPGA and reported the concerns, difficulties and/or needs observed during the project to achieve the proposed objectives, particularly regarding the functional aspect of the final product.

It may be considered that from the point of view of control hardware design, flexibility for change or new implementations opens a new range of possibilities in a context where the demands for agile and flexible product development open new business prospects. Although the tests of the present project are in the initial phase, these indicate high reliability of the component, being subjected to thermal tests and electromagnetic compatibility. Comparing this solution with the previous one (using conventional microcontrollers) there is the disadvantage that the current design has a higher cost. It is expected to compensate cost with the flexibility and agility achieved to leverage new business. It should be noted that in the product used as reference, where the maximum duty cycle is 100  $\mu$ s, it is already clearly observed that in the worst working condition, i.e. operation in sensorless vector control mode and communication networks active the response of the HMI is significantly affected, both in response to keyboard inputs and in updating output data to the display.

Finally, the domain of the technologies used in this project and the knowledge acquired in the development of this study allowed the mapping of complementary modules such as the development of: (a) accessory functions module for scalar control improvement such as slip compensation, drop voltage in stator resistance compensation, energy savings function; (b) vector control module for induction motor; (c) vector control module for permanent magnet motor; (d) vector control module for reluctance motors; (e) regenerative converter module; (f) active filter module; (g) matrix converter module; and (h) back-to-back converter module.

## References

1. Hauck, S., Dehon, A.: Reconfigurable Computing: the Theory and Practice of FPGA-Based Computation. (Kaufmann, M. (ed.)) (2008)
2. Murphy, J.M., Turnbull, F.G.: Power Electronic Control of AC Motors. Oxford Pergamon Press, Elmsford (1988)
3. On Semiconductor: Thyristor Theory and Design Considerations Handbook: HBD855/D Rev. 1, Phoenix (2006). [http://www.onsemi.com/pub\\_link/Collateral/HBD855-D.PDF](http://www.onsemi.com/pub_link/Collateral/HBD855-D.PDF). Accessed 12 May 2015

4. Rayes, A., Samer, S.: Internet of things: from hype to reality. In: Jamalipour, A., Ruggieri, M., Nikookar, H. (eds.) *The road to Digitization*. River Publisher Series in Communications, Denmark, vol. 49, 338p (2016)
5. Sethi, P., Sarangi, S.T.: Internet of things: architectures, protocols, and applications. *J. Electr. Comput. Eng.* **2017** (2017). Article ID 9324035, 25 pages. <https://doi.org/10.1155/2017/9324035>
6. Vermesan, O., Fress, P.: *Internet of things – from research and innovation to market deployment*. River Publishers Series in Communication (2014). ISBN: 87-93102-94-1
7. Vermesan, O., Friess, P., Guillemin, P., et al.: *Internet of things strategic research roadmap*. In: *Internet of Things: Global Technological and Societal Trends*, vol. 1, pp. 9–52 (2011)
8. Xilinx: DS162 - Spartan-6 FPGA Data Sheet: DC and Switching Characteristics (ver3.1.1, 3276 KB) (2016). [https://www.xilinx.com/support/documentation/data\\_sheets/ds162.pdf](https://www.xilinx.com/support/documentation/data_sheets/ds162.pdf). Accessed 5 Mar 2016
9. Xilinx: *MicroBlaze Processor Reference Guide*, v5.3 (2011). [http://www.xilinx.com/support/documentation/sw\\_manuals/mb\\_ref\\_guide.pdf](http://www.xilinx.com/support/documentation/sw_manuals/mb_ref_guide.pdf). Accessed 3 Apr 2015
10. Holmes, D.G., Lipo, T.A.: *Pulse Width Modulation for Power Converters: Principles and Practice*. Wiley, Hoboken (2003)
11. Mohan, N.: *Power Electronics: A First Course*. Wiley, Hoboken (2012)
12. Kosow, I.L.: *Máquinas Elétricas e Transformadores*, 5 edn. Globo, Porto Alegre (1985). (F.L. Soares., Trans.)
13. Krause, P.C., Wasynczuk, O., Sudhoff, S.D.: *Analysis of Electric Machinery and Drive Systems*, 2a edn. Wiley, New York (2002)
14. Zhu, S.: Hardware implementation based on FPGA of semaphore management in  $\mu\text{C}/\text{OS-II}$  real-time operating system. *Int. J. Grid Util. Comput.* **6**(3/4), 192–199 (2015)

# Ising-Model Optimizer with Parallel-Trial Bit-Sieve Engine

Satoshi Matsubara<sup>1(✉)</sup>, Hirotaka Tamura<sup>1</sup>, Motomu Takatsu<sup>1</sup>, Danny Yoo<sup>2</sup>, Behraz Vatankhahghadim<sup>2</sup>, Hironobu Yamasaki<sup>1</sup>, Toshiyuki Miyazawa<sup>1</sup>, Sanroku Tsukamoto<sup>1</sup>, Yasuhiro Watanabe<sup>1</sup>, Kazuya Takemoto<sup>1</sup>, and Ali Sheikholeslami<sup>2</sup>

<sup>1</sup> Fujitsu Laboratories Ltd., Kawasaki, Japan  
s-matsubara@jp.fujitsu.com

<sup>2</sup> University of Toronto, Toronto, Canada

**Abstract.** We propose a hardware architecture for solving combinatorial optimization problems and implemented it on an FPGA. The hardware minimizes the energy of Ising model with 1,024 state variables fully connectable through 16-bit weights, which ease restrictions on mapping problems onto the Ising model. The system uses a hardware bit-sieve engine that performs a Markov-chain Monte-Carlo search with a parallel-evaluation of the energy increment prior to the bit selection, achieving a speedup while guaranteeing convergence. The engine is implemented on an Arria 10 GX FPGA and solves 32-city traveling salesman problems  $10^4$  times faster than simulated annealing running on a 3.5-GHz Intel Xeon E5-1620v3 processor.

## 1 Introduction

In order to overcome the performance limitations of current computer systems while the Moore's-law trend that has been leading the growth of the performance is going to stop within a few years, dedicated accelerators [1–3] for specific applications are becoming popular. Since the architecture of the accelerator is tailored to a particular application, a slightest change in the application often requires a redesigning of the hardware to maintain its performance. Thus, exploring a method which covers a wide range of applications is very important.

Optimization using Ising model [4–7] covers a wide variety of applications ranging from NP-hard combinatorial optimization to machine learning. Thus, it has a potential to provide higher performance due to specialization, yet keeping versatility to be used for various purposes. Slow convergence of optimizing scheme based on Ising model, however, hindered the practical use of the method so far. Hoping for an exponential speedup over Ising model optimization, quantum annealing has been proposed in [8, 9] based on the principle of superconducting. Since the operating principle of the quantum annealing is different from the conventional computing, integrating it with existing computer system is one of the major challenges. In addition, the quantum devices used

to build the quantum annealers still need innovation to expand the scale. For example, due to the lack of connectivity among the bits, the applicability is very limited.

Thus, in this paper we propose a massively parallel architecture to optimize the energy of Ising model by Markov chain Monte Carlo (MCMC) search with a significant speedup over the conventional methods. The architecture processes 1,024 parallel bits which are fully connectable through 16-bit weights. We implement the architecture on an Altera Arria 10 GX FPGA [10], and as a case study we evaluated a 32-city travelling salesman problem (TSP). Experimental results reveal that our proposed architecture achieves ~12,000× speedup over a software process running on a 3.5 GHz Intel Xeon E5-1620v3 processor.

## 2 Operating Principle

The proposed hardware consists of a Server and multiple engines, each of which performs a MCMC stochastic search to minimize the Ising energy as defined in (1):

$$E(X) = - \sum_{\{i,j\}} W_{ij}x_i x_j - \sum_i b_i x_i, (i = 1, 2, \dots, N) \tag{1}$$

where  $x_i \in \{0, 1\}$  is the state variable or bit,  $X = (x_1, x_2, \dots, x_N)$  is the vector representation of the state variables,  $N$  is the number of bits,  $W_{ij}$  is the connection weight between bit  $i$  and bit  $j$ , and  $b_i$  is the bias term. The values of the weights and bias terms are supplied from the Server to the engine before starting the stochastic search (Fig. 1). Multiple engines can be used either to extend the number of the bits or enhance the speed of stochastic convergence [11].

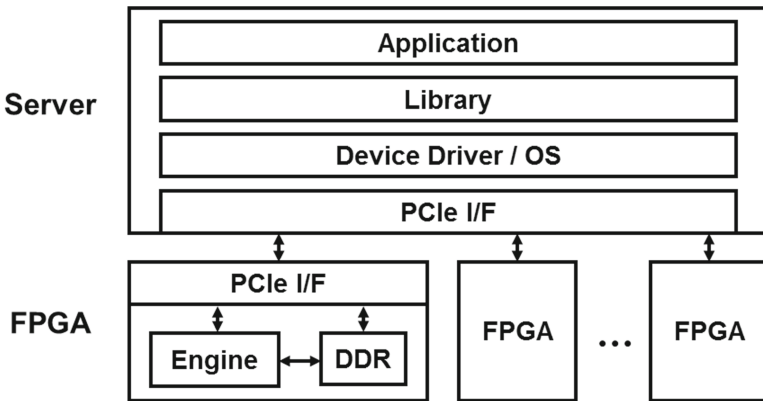


Fig. 1. Ising-model optimizing system

The search in the engine is done by stochastically picking a move based on the increment in the energy when the state moves to a neighboring state  $X^{(i)}$ . The neighboring state is generated from the current state  $X = (x_1, x_2, \dots, x_N)$  by flipping the value of  $x_i$



to  $1 - x_i$ . The corresponding energy increment  $\Delta E_i$  is calculated from the local field  $h_i$  of the bit  $i$  as

$$\Delta E_i(X) = -(1 - 2x_i)h_i(X) \quad \text{where} \quad h_i(X) = \sum_j W_{ij}x_j + b_i \quad (2)$$

Unlike implementations with an artificial bit that outputs logical “1” with the probability of a sigmoid function on the local field, the hardware explicitly evaluates the energy increment using (2) and applies an acceptance criterion such as the Metropolis or Gibbs criteria. This enables a modification of the acceptance criterion so as to achieve faster convergence to an optimum solution. The hardware differs from classical MCMC methods, where a bit  $i$  is first selected and subsequently the energy increment  $\Delta E_i$  is evaluated, in that the energy increment evaluation is executed in parallel for all  $i$  prior to selecting the bit to be examined (Fig. 2).

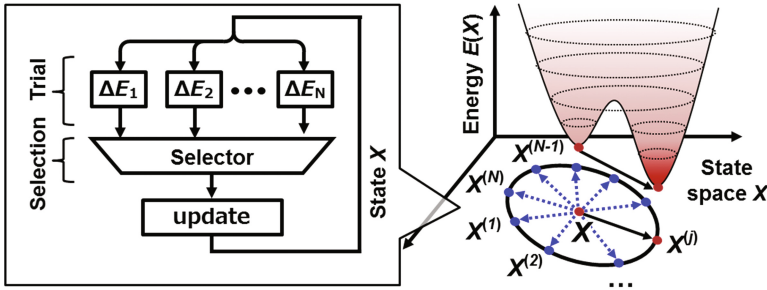


Fig. 2. Optimizing Ising model with parallel trial

### 3 Engine Implementation

Since only one state variable changes its value during the update phase, the values of the local fields are calculated using DeGloria’s algorithm [12]: when the variable  $x_j$  is flipped to  $1 - x_j$ , each local field is updated by adding its increment  $\delta h_i$  to the current value stored in a register.

$$\delta h_i^{(j)} = W_{ij}(1 - 2x_j) \quad (3)$$

Thus, the total number of the multiplier-accumulators becomes 1/1023 that of a straightforward implementation in which the local field is directly calculated from (2).

In this design, the number of bits in the engine is 1024, and any two bits, bit  $i$  and bit  $j$ , can be connected through the weight  $W_{ij}$ , independent of other bit-pair connections. The weight values are expressed in 16-bit fixed-point signed binary code, the local fields  $h_i$  in 27-bit signed binary, and the bias terms  $b_i$  in 26-bit signed binary. The bias term is implicitly given by setting the initial values of  $h_i$  and  $x_i$  so that the latter part of (2) holds.

The trial criterion used in the trial phase is chosen as either Gibbs or Metropolis [13] ones:

$$A(\Delta E_i) = \begin{cases} \min[1, \exp(-\beta \cdot \Delta E_i)] & \text{Metropolis} \\ 1/[1 + \exp(\beta \cdot \Delta E_i)] & \text{Gibbs} \end{cases} \quad (4)$$

where  $A(\Delta E_i)$  is the acceptance probability of  $x_i$  flipping to  $1 - x_i$ , and  $\beta(= 1/T)$  is the inverse temperature. In the parallel trial scheme, an acceptance decision block (ADB) in each bit compares the value of  $\Delta E_i$  with a numerical noise to produce a binary flag that becomes “1” with the probability given by (4). The numerical noise is generated from a random number  $r_i$  uniformly distributed between 0 and 1 by a table that produces  $A^{-1}(r_i)$  (Fig. 3). The resulting flag bit indicates whether the corresponding state variable is a candidate to change its value when selected.

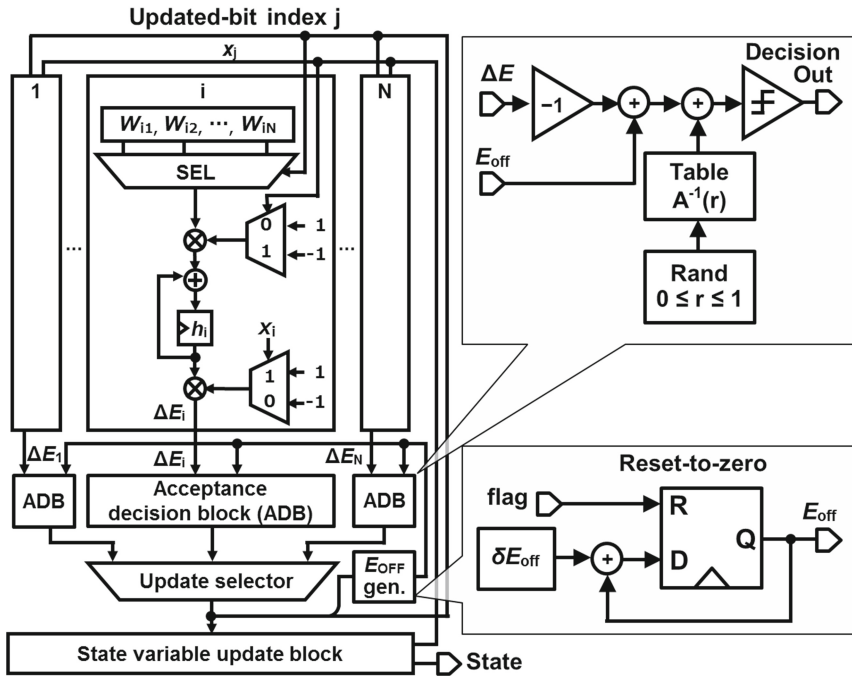
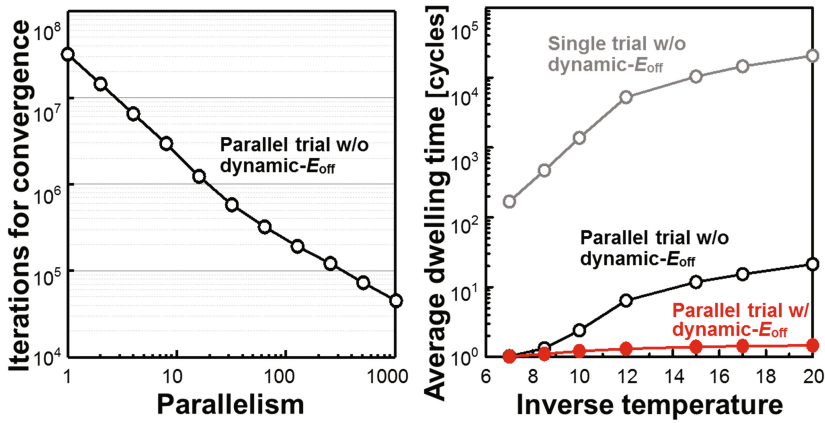


Fig. 3. Bit-sieve engine architecture

The update selector selects a single state variable from the state variables having the flag value of “1”. Ten stages of two-to-one selectors perform the selection and the flag and index generation.

Simulations showed that the number of trial/update cycles to reach the global minimum for a 32-city TSP is inversely proportional to the number of neighbors that are examined in parallel [Fig. 4(a)]. Unlike a parallel updating scheme where several state variables are updated in parallel, this scheme guarantees convergence without requiring knowledge of the problem structure.



**Fig. 4.** Effects of acceleration techniques, (a) speedup by parallel trial, and (b) reduction of average dwelling time at a state

When the state is at a local minimum of the Ising energy function, the probability to move to a new state is much smaller than one. This makes the system stay at the same local-minimum state for many cycles, making the convergence slower.

To reduce the number of cycles staying at a local minimum, we implemented a scheme to subtract a positive offset  $E_{off}$  from the energy increment (Fig. 3), which is approximately equivalent to multiplying a common constant factor  $\exp(\beta \cdot E_{off}) > 1$  to the state-flip acceptance probabilities. This technique shortens the time spent in a local minimum [Fig. 4(b)] as in the rejection-free Metropolis scheme [14–16], in which the probability of moving to another state is made one. To achieve this, an offset generator generates the offset dynamically by adding a constant increment to the offset value when there is no move to a new state. When there is a state-variable flip, the offset value is reset to zero.

## 4 Benchmark Results

The proposed optimizer was implemented on an Altera Arria 10 GX FPGA with a 1 GB DDR4 SDRAM development board clocked at 100 MHz. It took five clock cycles per trial phase, resulting in the search at 20.4 G(=  $1,024 \times 100\text{MHz}/5$ ) trials/s. As a benchmark, the time-to-solution metrics with 99% confidence for 32-city TSPs were evaluated. When none of the parallel trial and dynamic energy offsetting was used, the hardware was about two times faster than those of an in-house simulated annealing performing at 13.7 M trials/s, running on a 3.5-GHz Intel Xeon E5-1620v3 processor. When the 1,024-parallel trial was applied, an additional speedup factor of about 1,000 times was obtained. When the dynamic-energy offset scheme was used in addition to the parallel trial, another 6 $\times$  speedup was added, resulting in a 12,000 $\times$  speedup over the processor (Fig. 5).

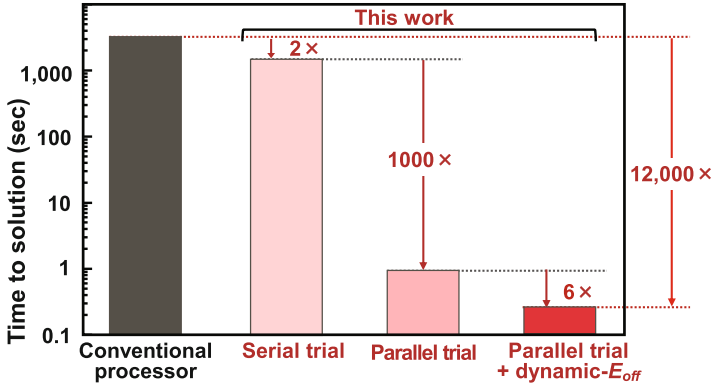


**Fig. 5.** Measured results for 32-city TSPs, (a) tour-length error versus number of iteration, and (b) speed comparison in terms of time-to-solution metrics

## 5 Conclusion

This work demonstrates an architecture of hardware for combinatorial optimization problems. The operation of the hardware is based on minimizing the energy of Ising model using Markov-Chain Monte Carlo search. In the proposed architecture, the speed of the convergence is enhanced by using a 1,024-parallel-trial Monte Carlo search. Compared to the CMOS dedicated hardware for optimizing general Ising energy reported so far, this work has the highest weight resolution with full connectivity with the highest trial-per-second metric (Table 1).

**Table 1.** Performance comparison

	Ref. [6]	Ref. [7]	This work
Number of bits	1,438	20 K	1 K
Weight range	64 k (16-bit)	3 (+1/0/-1)	64 k (16-bit)
Clock frequency	20 MHz	100 MHz	100 MHz
Search rate (trial/s)	490 K	Not described	20.4 G
Technology	Xilinx3090 FPGAs, 0.8 $\mu$ m	ASIC 60-nm CMOS	Arria 10 GX FPGA, 20 nm

## References

1. Merolla, P.A., et al.: A million spiking-neuron integrated circuit with a scalable communication network and interface. *Science* **345**(6197), 668–673 (2014)
2. Akopyan, F., et al.: TrueNorth: design and tool flow of a 65 mW 1 million neuron programmable neuromorphic chip. *IEEE Trans Comput. Aided Des. Integr. Circ. Syst.* **34**, 1537–1557 (2015)
3. Jouppi, N.P., et al.: In-datacenter performance analysis of a tensor processing unit. In: *Proceedings of 44<sup>th</sup> International Symposium on Computer Architecture*, June 2017

4. Hopfield, J.J.: Neural networks and physical systems with emergent collective computational abilities. *Proc. Natl. Acad. Sci.* **79**, 2254–2558 (1982)
5. Aarts, Emile H.L., Korst, Jan H.M.: Boltzmann machines and their applications. In: Bakker, J.W., Nijman, A.J., Treleaven, P.C. (eds.) *PARLE 1987*. LNCS, vol. 258, pp. 34–50. Springer, Heidelberg (1987). doi:[10.1007/3-540-17943-7\\_119](https://doi.org/10.1007/3-540-17943-7_119)
6. Skubiszewski, M.: An exact hardware implementation of the boltzmann machine. In: *Proceedings of the Fourth IEEE Symposium on Parallel and Distributed Processing*, pp. 107–110 (1992)
7. Yamaoka, M., et al.: 20 k-spin Ising Chip for Combinational Optimization Problem with CMOS Annealing. *ISSCC 2015 digest of technical papers*, pp. 1–3, February 2015
8. Johnson, M.W., et al.: Quantum annealing with manufactured spins. *Nature* **473**, 194–198 (2011)
9. Bunyk, P., et al.: Architectural considerations in the design of a superconducting quantum annealing processor. *IEEE Trans. Appl. Supercond.* **24**(4), 1–10 (2014)
10. ALTERA: Arria 10 FPGA development kit user guide, May 2016
11. Hukushima, K., Nemoto, K.: Exchange monte carlo method and application to spin glass simulations. *J. Phys. Soc. Jpn.* **65**, 1604 (1996)
12. DeGloria, A., et al.: Application specific parallel architectures. In: *Proceedings of First International Conference on Massively Parallel Computing Systems (MPCS)*, pp. 497–512 (1994)
13. Metropolis, N., et al.: Equation of state calculations by fast computing machines. *J. Chem. Phys.* **21**, 1087 (1953)
14. Bortz, et al.: A new algorithm for monte carlo simulation of ising spin systems. *J. Comput. Phys.* **17**, 10–18 (1985)
15. Schulze, T.P.: Efficient kinetic Monte Carlo simulation. *J. Comput. Phys.* **227**, 2455–2462 (2008)
16. Zhu, H., et al.: Boltzmann Machine with Non-rejective Move. *IEICE Trans. Fundam.* **E85-A**, 1229–1235 (2002)

# An FPGA Based Heterogeneous Redundant Control System Using Controller Virtualization

Masaharu Tanaka<sup>1(✉)</sup>, Haruhi Eto<sup>1</sup>, Nobumasa Matsui<sup>2</sup>, and Fujio Kurokawa<sup>1</sup>

<sup>1</sup> Nagasaki University, 1-14 Bunkyo-machi, Nagasaki 852-8521, Japan  
{mhtanaka, haruhi-eto, fkurokaw}@nagasaki-u.ac.jp

<sup>2</sup> Nagasaki Institute of Applied Science, 536 Aba-machi, Nagasaki 851-0193, Japan  
MATSUI\_Nobumasa@NIAS.ac.jp

**Abstract.** This paper describes heterogeneous redundancy of FPGA based control system using cloud. Since conventional cloud servers have problems in responsiveness, we propose the concept and architecture of controller virtualization using FPGAs. However, we should consider the negative effect on the controllability by the communication delay when control is performed using the cloud. We evaluated the stability of control using cloud by means of a simulation for a representative process control model.

## 1 Introduction

Recently, the value creation of data by IoT(Internet of Things) and Industry 4.0 which is said to be the 4th Industrial Revolution is attracting big attention. Improving productivity is the most important task for the industry, and it is necessary to improve the availability ratio of production facilities in order to improve productivity. Therefore, to improve the reliability of industrial controllers by means of IoT is absolutely essential for realizing the value creation.

In general, redundancy of the controller is adopted as a method for increasing the reliability. For example, when the controller board is duplexed, if a fault occurs on controlling side, switching the control to the other side, thereby enabling the control to be continued without stopping the system. Multiple controllers are nothing special in modern automated production facilities for sensing, motor control, etc. Therefore, when simply configuring a duplex configuration of hardware, there are problems such as increase in cost, increase in power consumption of equipment and increase in installation space.

In this paper, we propose a heterogeneous redundancy system of controllers using cloud, assuming that production system will be connected to the cloud via Internet. When the controller stops due to a fault, the cloud replaces the control process so that the system can be continuously operated. The proposed method is low cost, small size and energy saving compared with the redundancy of the controller hardware, and improvement of the more reliability can be expected than a single configuration without duplexing. However, when operating the controller on the cloud, the conventional virtual server has a problem in responsiveness. When control processing is performed in the cloud,

there is concern about the negative influence on controllability due to communication delay as well.

Therefore, we propose FPGA-based controller virtualization against the first problem. Improvement in responsiveness can be expected by utilizing dedicated circuit and simultaneous parallel processing, which is a feature of FPGA. For the second problem, we evaluated the negative influence of controllability due to communication delay by simulation, and confirmed that the influence is within practically acceptable range.

The structure of this paper is as follows. The Sect. 2 describes the problems of the conventional system. In the Sect. 3, we propose heterogeneous redundancy of controller using controller virtualization. Section 4 describes the experiment by simulation and its results. In Sect. 5 discusses future issues, before a summary section.

## 2 Problem of Conventional Method

### 2.1 Redundant Control System

A duplex configuration as a redundant system is a mechanism in which the standby system is arranged and operated as a backup in preparation for the occurrence of some failure in a part of the system from the normal time so as to maintain the function of the entire system even after a failure. Typical configuration of the duplex system is shown in Fig. 1. It is a mechanism that can always operate, and can instantly switch to the standby side when a failure occurs in the running side. A redundant system applies to controllers of facilities that greatly affects socio economic activities if its function falls or becomes unavailable, such as social infrastructure systems.

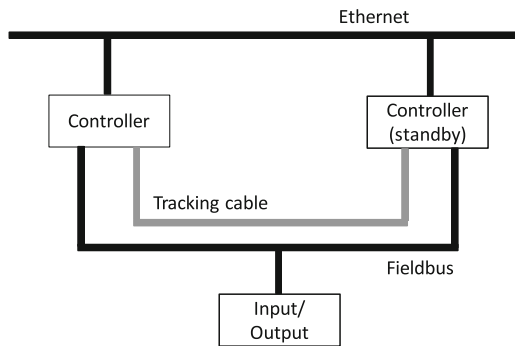


Fig. 1. Structure of redundant control system.

In the conventional duplex system, since the redundancy is realized by installing two identical hardware, there were the following problems.

- Cost increase due to duplication of hardware
- Increase Power consumption
- Need more space for installation

In this paper, in order to alleviate the above problems in the duplex system, we consider application of a system assuming to place the standby controller in the cloud server.

## 2.2 Problem of Conventional Cloud Control System

A cloud control system has been proposed in which devices such as sensors and actuators in a control system are connected to the cloud via the Internet, and control operations are executed from the cloud server [1]. It is said that by using a cloud server located at a geographically distant from the controlled object, the control system can be easily restored at the time of a disaster. In addition, it is said that it is possible to flexibly increase or decrease the performance of the control operation with respect to the scale of the control system and the number of customers.

In general, the control system is required to have real time processing ability that performing process is completed within a predetermined time. In the cloud server, since various processes coexist in the background, variation in response time becomes large. Therefore, a method of balancing the load among the servers has been proposed [1].

However, in the conventional load balancing algorithm, response delay of one cycle can occur due to the mechanism. Therefore, when the conventional method is used for the standby side of redundant system, it can be said that it is difficult to apply it to an application that emphasizes responsiveness. In the conventional method, there has been no discussion on the evaluation of communication delay and the influence on the controllability.

As proposed in the next section, controllers using FPGAs with feature of low latency can be considered to be powerful solutions for virtualization.

## 3 Heterogeneous Redundant Control System Using Controller Virtualization

### 3.1 Basic Concept of Controller Virtualization

In virtualization of controller, focusing on responsiveness, which is a problem of conventional cloud systems, the followings are basic ideas to solve the problem. First, FPGA-based controllers are used for cloud servers to improve responsiveness of control function. For example, it is to make FPGA in which multiple controllers installed performs like server virtualization.

Secondly, in order to improve the responsiveness of the communication process, it is to realize a novel communication protocol for the FPGA circuit. TCP/IP is generally used on the Internet, and the process of TCP/IP is the main cause of the impaired responsiveness, and a new communication protocol specialized for applications that emphasize responsiveness has been required.

There are three patterns of example in conventional virtualization generally as follows.



- Type1: Segment and use computer resources: Operate as if multiple servers are running on one server.
- Type2: Synthesize computer resources and use: a representative example is storage virtualization that multiple disks are handled as one large virtual disk.
- Type3: Running on heterogeneous computer: A representative example is a Java virtual machine, making Java language program executable on deferent models of computers.

The controller virtualization proposed in this paper can be said to be a concept of hybridizing Type 1 and Type 2.

A specific configuration example of controller virtualization is shown in Fig. 2. The FPGA based controller shown in Fig. 2 is a control equipment installed at the site, and it is composed of a controller using an FPGA based on the basic idea. I/O is a module that performs input and output with sensors, motors and actuators, and is connected to the controller via a field bus or the like.

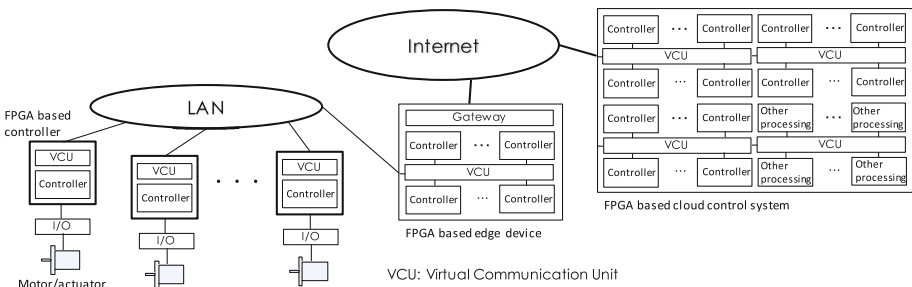


**Fig. 2.** Structure of controller virtualization.

Virtualized controllers are installed in cloud servers and edge devices. Edge devices are installed in the LAN such as in factory premises, especially when high responsiveness is required. Here shown an example in which the edge server is provided with the function of Gateway. VCU is an abbreviation for Virtual Communication Unit. This unit performs its own Virtual Communication Protocol (VCP) to realize controller virtualization. The VCU is implemented as a common circuit on each of FPGA base controller, FPGA base edge device and FPGA base cloud control system.

For example, after the start of operation, if a larger resource than the initially designed is temporarily required due to some circumstances, additional resources can be added as controllers on FPGA-based edge devices and FPGA-based cloud control systems. Since it is not required to modify the control equipment on the site, the solution can be realized in a short time at low cost. In addition, by analyzing the data collected from the sensors, applications such as failure prediction of equipment and machine learning are conceivable. We are currently designing and producing prototypes for VCU, VCP and FPGA base controllers.

### 3.2 Heterogeneous Redundant Control System

Figure 3 shows the configuration of heterogeneous redundancy of control system using controller virtualization. In the proposed method, the control side of the duplex system is placed at the site and the standby side is arranged in the cloud control system. When the on-site controller controls, controller communicates with the I/O module directly via the field bus. The internal state of the control side of the control system is transmitted to the standby side on the cloud control system via the gateway and the Internet every predetermined cycle time. This is called tracking communication.

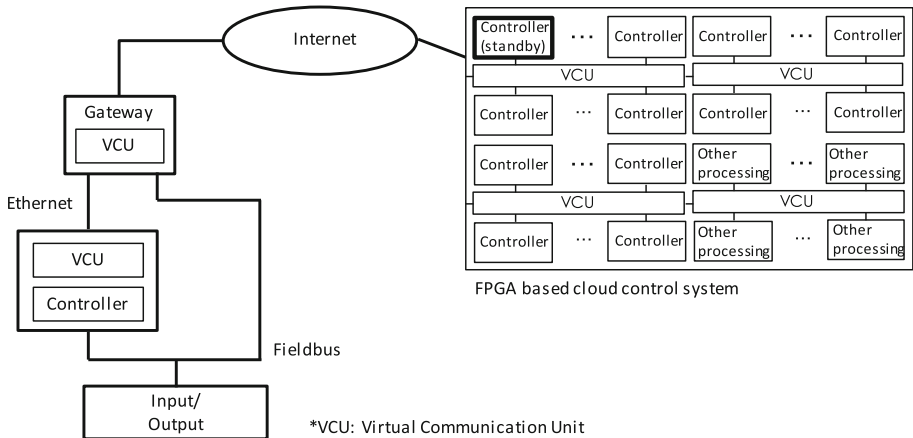


**Fig. 3.** Structure of heterogeneous redundant control system.

When a fault occurs on the control side, control is passed to the standby side. When the standby side performs control, the controller on the cloud control system communicates control signals with the I/O module via the Internet, the gateway and the field bus. Therefore, there is a communication delay caused by passing through the Internet and Gateway, so it is an important issue to study the influence on the controllability due to the dead time and limited control cycle. In Sect. 4, evaluation by simulation of this issue is described.

### 3.3 Architecture of VCU and FPGA Based Controller

Here we describe the architecture of the virtual communication unit and the FPGA base controller.

The requirements of VCU are described below.

- It is possible to select any physical layer
- Implementation by software including FPGA is required.
- To ensure a flexible frame configuration.
- To make it possible to define the structure of the frame header according to the application

- Time synchronization is available.

Features are shown below.

- It is possible to construct a system that does not have to be conscious of inside and outside of the device, and because it has great scalability, it is easy to expand the system.
- Since it does not depend on the physical layer of communication, the major system modification is possible easily such as change of communication system.
- Since it is possible to define a frame header configuration suitable for the application, for example, it is possible to construct a protocol specialized for responsiveness.

Figure 4 shows the architecture of VCU. As shown in Fig. 4, the VCU consists of three layers. The roles of each layer are as follows.

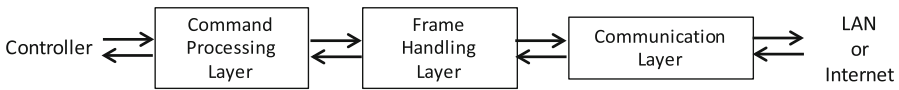


Fig. 4. Architecture of VCU.

Command Processing Layer: Send/receive commands, specify the physical address of the destination

Frame Handling Layer: Generation and decoding of virtual communication frame

Communication Layer: Execution of Layer 2 communication processing, generation and decoding of MAC frame

Figure 5 shows the architecture of the FPGA based controller. The proposed architecture assumes the implementation of PLC (Programmable Logic Controller) which is

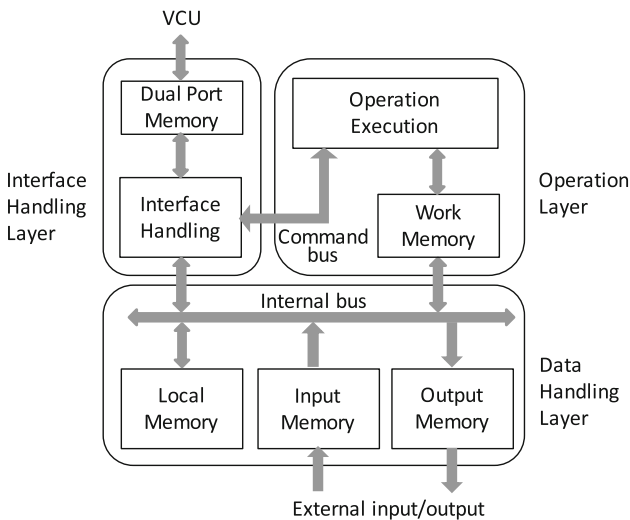


Fig. 5. Architecture of FPGA based controller.

a widely used general purpose controller. This architecture consists of three layers. The functions of each layer are as follows.

Interface Handling Layer:	Execution of command transmission and receiving with other controllers, execution of interface with VCU
Operation Layer:	Execution of commands, execution of arithmetic operation
Data Handling Layer:	Execution of general data processing (memory processing, input/output processing)

Features are shown below.

- As the architecture, the external interface and the internal data path configuration are defined, and the processing (command) in “Interface Handling” and “Operation Execution” are defined according to the application.
- The same architecture can also be implemented on FPGA based edge device and FPGA based cloud control system.
- The arithmetic operation function in “Operation Execution” can be composed of an ALU-based processor or dedicated circuit.
- For “Operation Execution”, it is possible to implement functions other than PLC, for example, signal processing, statistical processing, artificial intelligence algorithm and the like. However, those with a large circuit scale are desirably placed in edges and clouds.

Conventional research on the use of FPGAs in PLC has proposed a method for converting PLC languages such as ladder to hardware description language (HDL) [2] and proposal of processor architecture of CPU dedicated to PLC [3–5].

The architecture proposed in this paper can be recognized to be a processor architecture of a new concept that has a conventional processor architecture in the “Operation Layer”, an internal memory in the “Data Handling Layer” and an interface with VCU in the “Interface Handling Layer”. This internal memory and the interface with VCU are necessary elements to realize controller virtualization on the cloud.

## 4 Simulation and Results

### 4.1 Simulation Method

In order to evaluate the effect on controllability caused by transmission delay of signals due to communication and execution cycle of control to be considered when controlling from the controller on the cloud, simulation was carried out with a computer using MATLAB. Here, as a representative control model, third-order lag model as temperature control and first order lag model as pressure control were used. In the simulation model, the control period is simulated by the discrete time width of the control calculation. The time delay due to communication is defined as a dead time between the output of the PID control and the process model input, and between the process model output and the feedback input of the PID control. Figure 6 shows the block diagram of the pressure

control simulation model, and Fig. 7 shows the block diagram of the temperature control simulation model.

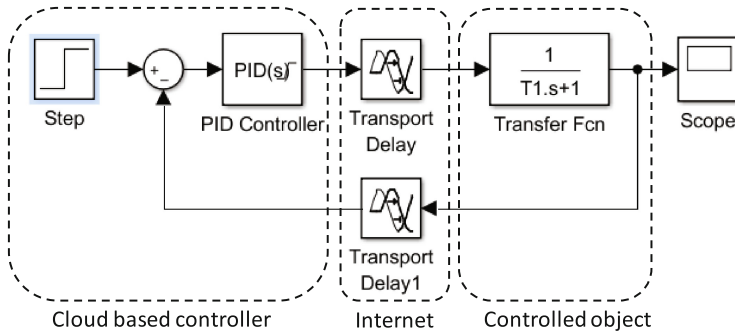


Fig. 6. Simulation model of pressure control.

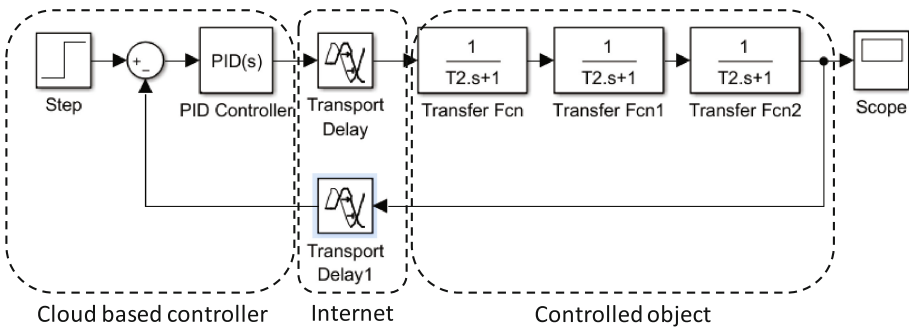


Fig. 7. Simulation model of temperature control.

In the simulation, the time constant of the model was set to 1 s. Transmission delay time was set to 1 ms, 2 ms, 5 ms, 10 ms, 50 ms, 100 ms or 200 ms. The control period was set to 1 ms, 10 ms, 50 ms, 100 ms or 200 ms for each delay time. A simulation was executed at every combination of transmission delay time and control cycle, and the result were shown in a step response waveform and a Bode diagram, and the gain margin and phase margin at that time were obtained. Since the time constant of the model is 1 s, the discrete time width is set to 200 ms or less in consideration of sampling theorem.

As the delay time changes, the dynamic characteristics of the process changes. The optimal parameters (proportional control P, integral control I, differential control D, filter coefficient N) of PID control also change. Therefore, when changing delay time, the optimum parameters were obtained by MATLAB/Simulink’s PID auto tuner.

## 4.2 Simulation Results

Figures 8 and 9 show the gain margin and the phase margin against the communication delay time and the discrete time width (dt) of the pressure control respectively.

Figures 10 and 11 show the gain margin and the phase margin against the communication delay time and the discrete time width ( $dt$ ) of the temperature control respectively.

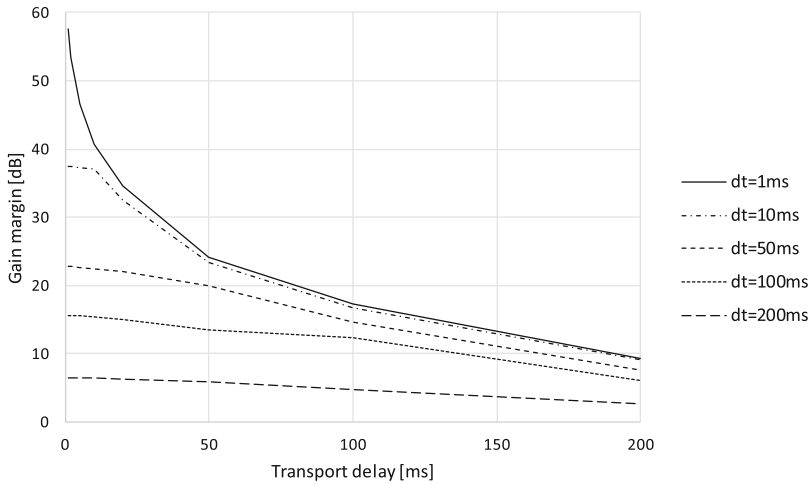


**Fig. 8.** Gain margin of pressure control.

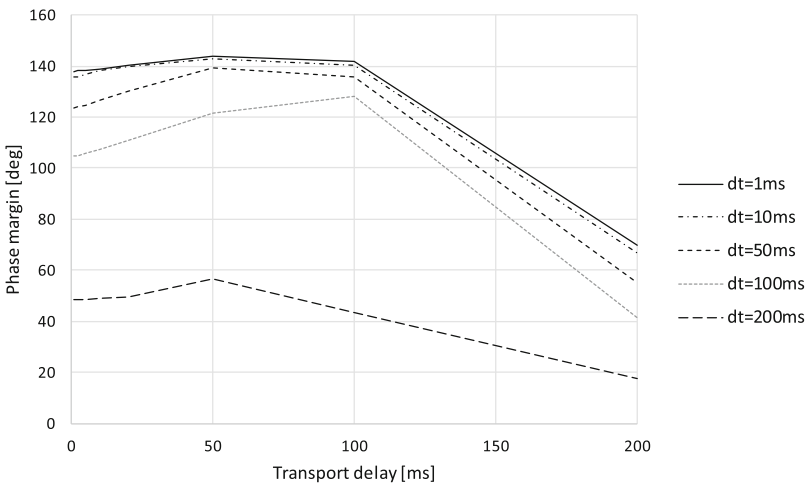


**Fig. 9.** Phase margin of pressure control.

Generally, if the gain margin is 20 dB or more and the phase margin is  $60^\circ$  or more, it is empirically known that the control is in the stable range. Therefore, from the simulation results, it was found that, in both pressure control and temperature control, if the control period is 50 ms or less and the communication delay is 50 ms or less, the stable control range is satisfied.

From the simulation results, it can be observed that the gain margin and the phase margin gradually decrease as the communication delay increases at a constant control

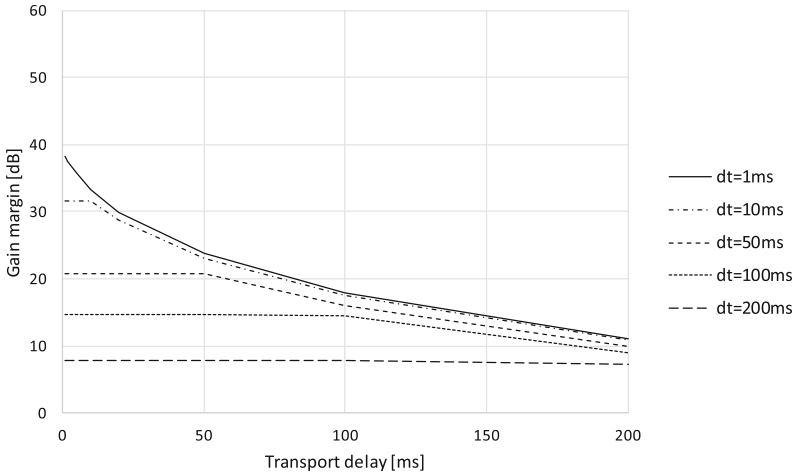


Fig. 10. Gain margin of temperature control.

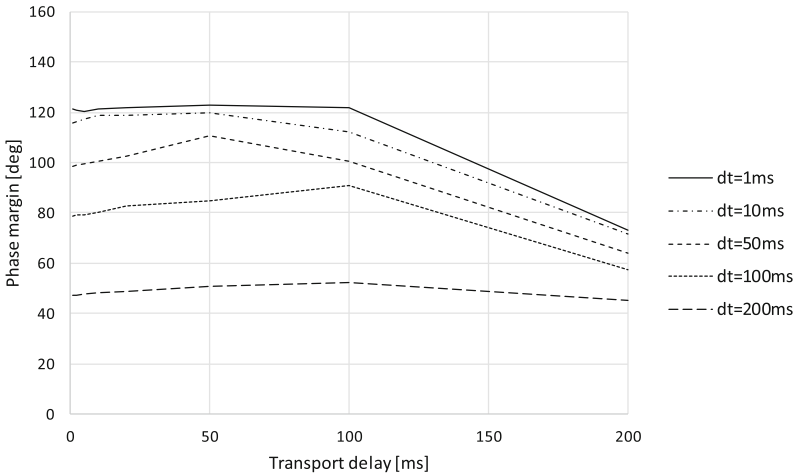


Fig. 11. Phase margin of temperature control.

period. In particular, the reduction of the gain margin is conspicuous. This is considered to be due to the performance of the PID auto tuner.

## 5 Discussion and Future Work

From the simulation results, it was found that if the control period is 50 ms or less and the communication delay is 50 ms or less, it is possible to control stably. It is generally said that it takes about 50 ms to communicate with the cloud system which is 1000 km

away through Internet, but a communication common carrier says that it is able to communicate in 5 ms with a dedicated communication line.

As the communication delay increases, the gain margin decreases, and when the delay is 100 ms or more, the stability is affected. Observing the parameter adjustment result of the PID auto tuner, the derivative element became zero at the delay of 20 ms or less. On the other hand, it is found that it is trying to make the derivative element effective from the delay of 50 ms or more. While PID control can only compensate limitedly against the effect of communication delay, it can be expected to improve the controllability from the cloud by means of adaptive control using the estimated communication delay model [6, 7].

In this simulation, the communication delay was fixed. In an actual communication environment, since variations in communication delay are assumed, it is necessary to evaluate in addition to the application of the above-described communication delay estimation model, and which is a future task.

For the VCU and the FPGA base controller, design and production of prototype are currently in progress. For future work, it is necessary to design the architecture, design and the prototype, manufacture and evaluate about the FPGA based edge device and the FPGA based cloud control system as well.

Furthermore, demonstration experiment with heterogeneous redundancy which is constructed using prototype will be carried out in actual Internet environment.

## 6 Conclusion

We proposed a heterogeneous redundancy system of controllers using the cloud, assuming that they will normally be connected to the cloud via the Internet. When operating the controller on the cloud, the conventional virtual server has a problem in responsiveness. Hence, we proposed FPGA-based controller virtualization and designed its architecture. Improvement in responsiveness can be expected by making use of dedicated circuit and concurrent processing which are the characteristic of FPGA.

On the other hand, when control processing is performed in the cloud, the influence on controllability due to communication delay is concerned. Therefore, the effect of controllability due to communication delay was evaluated by simulation, and we clarified the range in which control can stably perform without practical problem even with communication delay.

The future tasks are improvement of controllability by applying adaptive control with communication delay estimation model, design and production of prototype, demonstration experiment in actual Internet environment.

## References

1. Ohnishi, N., Takanaka, T., Nakatani, H.: Load balancing of processing servers for cloud control system. *Electron. Commun. Japan* **99**(10), 71–80 (2016)



2. Ichikawa, S., Akinaka, M., Hata, H., Ikeda, R., Yamamoto, H.: An FPGA implementation of hard-wired sequence control system based on PLC software. *IEEJ Trans. Electr. Electron. Eng.* **6**, 367–375 (2011)
3. Koo, K., Rho, G.S., Kwon, W.H., Park, J., Chang, N.: Architectural design of an RISC processor for programmable logic controllers. *J. Syst. Archit.* **44**(5), 311–325 (1998). Publisher: Elsevier, Netherlands
4. Chmiel, M., Mocha, J., Hryniewicz, E., Milik, A.: Central Processing Units for PLC implementation in Virtex-4 FPGA. In: *Proceedings of the 18th IFAC World Congress, Milano, Italy, 28 August–2 September 2001*
5. Chmiel, M., Kulisz, J., Czerwinski, R., Krzyzyk, A., Rosol, M., Smolarek, P.: An IEC 61131-3-based PLC implemented by means of an FPGA. *Microprocess. Microsyst.* **44**, 28–37 (2016)
6. Astrom, K.J., Wittenmark, B.: *Adaptive Control*. 2<sup>nd</sup> edn. Dover Publications, Mineola (2008)
7. Matsui, N., Kurokawa, F.: An improved model-based controller for power turbine generators on grid system of shipboard. *IEEE Trans. Indus. Appl.* **48**(4), 1237–1242 (2012)

# Power Performance Analysis of FPGA-Based Particle Filtering for Realtime Object Tracking

Akane Tahara, Yoshiki Hayashida, Theint Theint Thu,  
Yuichiro Shibata<sup>(✉)</sup>, and Kiyoshi Oguri

Nagasaki University, 1-14 Bunkyo-machi, Nagasaki 852-8521, Japan  
{tahara,yoshiki,theinttt}@pca.cis.nagasaki-u.ac.jp,  
{shibata,oguri}@cis.nagasaki-u.ac.jp

**Abstract.** Real-time image processing with a compact FPGA-based architecture plays a key role in dynamic state-space models. This paper presents an energy efficient FPGA acceleration architecture of a particle filter, which is based on stream processing structure with a parallel resampling algorithm. Particle filters solve the state estimation problems with three steps: prediction, likelihood calculation and resampling. By accomplishing the resampling in a valid pixel area of an input image frame, while executing prediction in a synchronization region, our approach achieves real-time object tracking. This paper mainly highlights implementation alternatives using different clock frequencies and resource usages of FPGA. The result shows the comparisons of power consumption for the compact architecture with an accelerated clock frequency (135 MHz) compared to the larger circuit size with clock frequency (27 MHz). Interestingly, the larger architecture with a slower clock frequency shows lower power consumption.

## 1 Introduction

The recent technological developments of object tracking enhance the security camera, automatic driving, and so on. Particle filters [1] have become popular among nonparametric filters in marker-less tracking applications. Study of real-time stream processing on FPGAs is also popular to fulfill the demands for fast and robust object tracking with low energy consumption. Image-based features for particle filters using color histogram were introduced by [10]. Particle filtering approximates the density directly as a finite number of samples whereas the extended Kalman filter cannot approximate without a Gaussian. The color-based particle filter enables an embedded implementation in [6]. However, the parallel implementation does not offer in their tracking system. The resampling operation is the bottleneck in real-time particle filter implementation [2, 3]. To solve this problem, the particles are resampled using Independent Metropolis-Hastings (IMH) resampling method and the root mean square error is used to measure the accuracy [8]. Although they could apply the parallel particle filter implementation successfully with the high speed and accurate estimation performance on FPGA, they did not fully parallelize the particles due to lack of hardware resources.

In this paper, we discuss efficient FPGA acceleration architectures for particle filters based on a stream-based structure [5, 9] with the FPGA optimized resampling (FO-resampling) [11]. In addition to our previous work [12], we compare several implementation articles focusing on a tradeoff between power efficiency and resource requirements.

The rest of the paper is organized as follows. Section 2 outlines the algorithm of particle filters. The implementation of the system is described in detail in Sect. 3. Section 4 shows the evaluation results and discussion. Finally, we draw some conclusions and describe the scope of the future work in Sect. 5.

## 2 Particle Filter Algorithm

### 2.1 Particle Filter

Particle filtering is a recursive filter that provides the estimation of nonlinear and non-Gaussian processes. It consists of three steps: prediction, likelihood calculation and resampling as shown in Fig. 1. In the prediction step, states of each particle in the next time step are estimated based on target motion models [4]. Prediction utilizes the previous observations to predict the state of a system in future time instants. In general, some noises are added to states to adjust the irregular movement. In a simple example with a uniform linear motion model in which each particle has a position and velocity as a state, the prediction can be performed as

$$x_t = x_{t-1} + v_{x_{t-1}} + n_x, \tag{1}$$

$$y_t = y_{t-1} + v_{y_{t-1}} + n_y, \tag{2}$$

$$v_{x_t} = v_{x_{t-1}} + n_{vx}, \tag{3}$$

$$v_{y_t} = v_{y_{t-1}} + n_{vy}, \tag{4}$$

where  $x_t$  and  $y_t$  are the coordinates of particle at time  $t$ , while  $v_{x_t}$  and  $v_{y_t}$  are velocities.  $n_x$  and  $n_y$  stand for the positioning noises and  $n_{vx}$  and  $n_{vy}$  are the velocity noises, which are randomly generated. In the likelihood calculation step, for each particle, it is evaluated how much the state of the particle is in

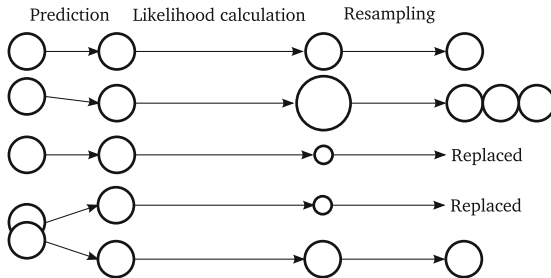


Fig. 1. Overview of a particle filter

agreement with the actual measurement. The weight calculation for the sampled particle ( $w_t$ ) is given by

$$w_t = p(z_t|x_t), \quad (5)$$

where  $z_t$  denotes the current sensor measurement. Finally, resampling induces the loss of diversity to decrease the variance of particles. The particles with small weights are eliminated and the particles with big weights are replicated in the resampling step.

## 2.2 FPGA Optimized Resampling (FO-resampling)

During resampling, information of all the particles are needed, making parallel implementation on an FPGA difficult. As a solution to this problem, FO-resampling method [11], which can update weights of particles without the interrelationships between former and current particles, has been proposed. The pseudocode for FO-resampling algorithm is described in Fig. 2. Here,  $M$  is the total number of particles, while  $B$  denotes the number of virtual particles for each real particle.  $\hat{x}_{i,n}$  represents a virtual particle and is randomly generated around a real particle  $x_i$ .  $r$  is randomly generated from a uniform distribution over  $[-1, 1]$ . The standard deviation ( $\sigma_{x_i}$ ) measures the spread of  $\hat{x}_{i,n}$  around  $x_i$ . To the highest possible weight, the value of  $\sigma_{x_i}$  varies inversely with the initial weight. The weight of virtual particle  $\hat{w}_{i,n}$  is obtained from the likelihood calculation of virtual particle with the observation ( $z_t$ ) at the location of object ( $\hat{x}_{i,n}$ ). Then,  $\hat{w}_{i,n}$  is compared with  $w_i$ . If  $\hat{w}_{i,n}$  is greater than  $w_i$ ,  $x_i$  and  $w_i$  will be replaced by  $\hat{x}_{i,n}$  and  $\hat{w}_{i,n}$ , respectively whereas  $x_i$  and  $w_i$  will keep the values for other conditions. After  $B$  iterations, all  $x_i$  values are used for posterior estimation. Since all particles are not related to each other, parallel resampling enables an efficient chip area on FPGAs.

```

1: for  $i = 1$  to  $M$  do
2:   for  $n = 1$  to  $B$  do
3:      $\hat{x}_{i,n} = x_i + \sigma_{x_i} \times r$ 
4:      $\hat{w}_{i,n} = p(z_t|\hat{x}_{i,n})$ 
5:     if  $\hat{w}_{i,n} > w_i$  then
6:        $x_i = \hat{x}_{i,n}$ 
7:        $w_i = \hat{w}_{i,n}$ 
8:     end if
9:   end for
10: end for

```

**Fig. 2.** Pseudocode of parallel resampling process using virtual particles

### 3 Implementation

#### 3.1 Overview of the System

We aspire a highly efficient object tracking system by mapping FO-resampling process. As an example, we designed and implemented a color-based object tracking system, which tracks a red object. Figure 3 shows an overview of a process flow of the system. Pixel data inputs from camera interface are streamed to the system for 1 pixel per 1 clock cycle. Streamed pixel data is then given to weight calculation step, and the weight of pixel data are calculated in a pipelined manner. Compared with the weight of real and virtual particles in weight comparison step, the maximum weight of particles are replaced as real particles. The entire system is managed by a 4-state controller, which are initialization of real particles, prediction of real particles, placement of virtual particles, and weight comparison of real particles and virtual particles (resampling). As shown in Fig. 4, the weight comparison is processed in valid pixel region in a pipeline, while the prediction and the setting of virtual particles are processed in the synchronization region of the frame. All real particle weights and coordinates processed in the weight comparison step are streamed to the weighted center calculation step, and the weighted center of real particles are calculated as the position of the target object. Finally, the calculated center is outputted with video images in the weighted center drawing step.

Figure 5 presents structure of Baseline design, which is a straightforward implementation of our approach. Firstly, RGB color values are converted into a hue to calculate the weight of the particle with coordinate signals  $(h_w, v_w)$ . Then, likelihoods are compared with  $M$  real particles each of which includes  $B$  virtual particles. After selecting the maximum weight of each particle, the maximum positions and velocities are selected when it comes to the maximum weight of  $M$  particles. After parallel resampling, the positions and velocities of real particles are the same as the number of  $M$ . Finally, the weighted center of gravity of positions of all the real particles is calculated. In this implementation, the entire

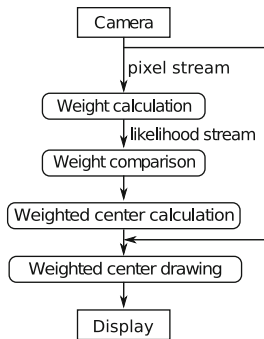


**Fig. 3.** Overview of the process flow

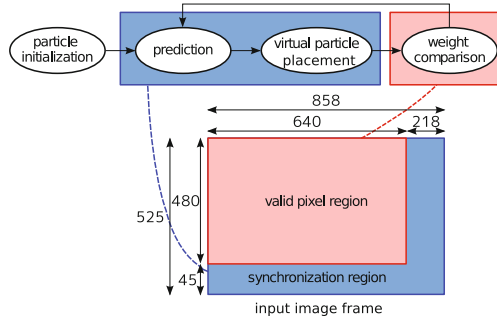


Fig. 4. State transition diagram of weight comparison step

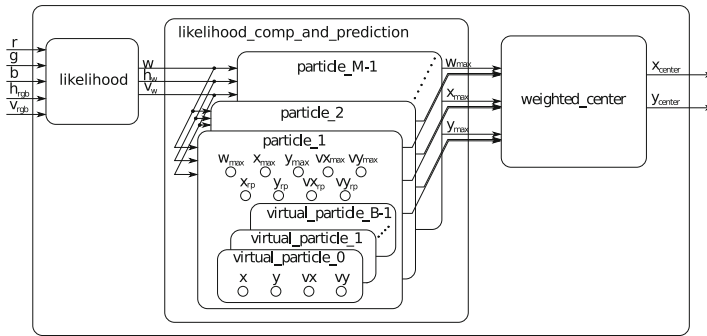


Fig. 5. Overview of a particle filter module for the Baseline design

system clock is synchronized with a camera pixel clock, which is 27 MHz for  $640 \times 480$ -pixel images with 60 fps.

In addition, we implemented three design alternatives: RSync, 5x\_LUT and 5x\_BRAM. In the Baseline design, logic for updating velocities of each particle in the resampling module becomes bottleneck, since all the resampling operations are performed every clock cycle in the valid pixel region. In contrast, RSync design updates velocities in the synchronization region, while still performing weight comparisons in the valid pixel region. This modification allows us to use sequential logic for velocity update, which can reduce required hardware size. As Fig. 6 shows, BRAM with a 29-bit width and a depth of 50 is used to store velocities of the particles in the synchronization region.

Another concern of the Baseline design is that the entire circuit is synchronized with camera pixel clock of 27 Hz, which is quite slower than typical FPGA designs. By increasing the clock frequency, multiple operations for particles can be executed with a single arithmetic module in a time-sharing manner, which can also result in reduction of required hardware resources. Following to this idea, the other two designs, 5x\_LUT and 5x\_BRAM, utilizes a 5 times higher clock

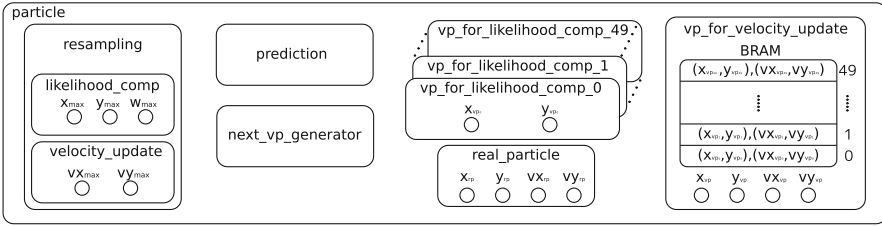


Fig. 6. Overview of a particle module for RSync

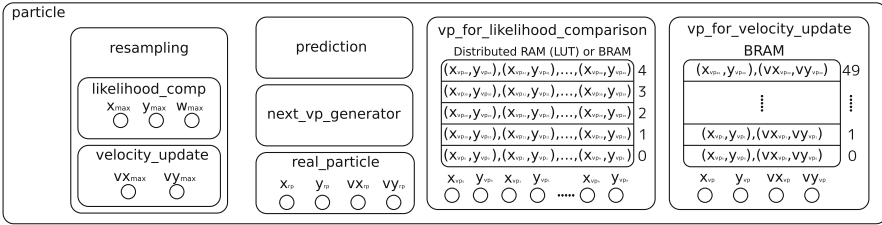


Fig. 7. Overview of a particle module for 5x.LUT and 5x.BRAM

Table 1. Implemented design alternatives

Design	Description
Baseline	Baseline design in which the entire system is synchronized with the pixel clock frequency of 27 MHz
RSync	Update of velocities of particles for resampling is sequentially executed in the synchronization region
5x.LUT	Resource sharing using a 5 times clock frequency (135 MHz). LUTs (distributed RAMs) are used to store virtual particles
5x.BRAM	Resource sharing using a 5 times clock frequency (135 MHz). BRAMs are used to store virtual particles

frequency (135 MHz). To enable resource sharing in these designs, the states of particles are stored in on-chip memory as Fig. 7 shows. While 5x.LUT implements this memory using LUTs as distributed RAM, 5x.BRAM utilized BRAM. The aforementioned evaluated design alternatives are summarized in Table 1.

### 3.2 Prediction

The prediction step estimates the state transition of each particle from the prior state at time  $(t - 1)$  to the posterior state at time  $(t)$ . In this implementation, we utilized the simple prediction model described in Eqs. (1)–(4). We defined the random noises for each particle using the two random number generators

within the ranges of  $n_x = \pm 30$ ,  $n_y = \pm 30$ ,  $n_{vx} = \pm 10$  and  $n_{vy} = \pm 10$ . Finally, the coordinates and velocities of next particles are given by the prior state of related particle with noises.

### 3.3 Virtual Particle Arrangement

As described in Fig. 2, virtual particles are arranged to coordinate the real particles. The value of  $\sigma_{x_i}$  is calculated taking into account efficiency of FPGA implementation as

$$\sigma_{x_i} = \left\lfloor \frac{1023 - w_i}{16} \right\rfloor. \tag{6}$$

The  $x$  and  $y$  coordinates of each virtual particle are defined using the tolerances of  $\pm \sigma_{x_i}$  to avoid too big or too small dispersion of virtual particles around one real particle. The division process with the divisor of 16 can be replaced with simple shift wiring on FPGAs.

### 3.4 Weight Calculation

For color detection in image processing, the color space conversion from RGB to HSI (hue, saturation and intensity) has been widely used. Hue value can be calculated as follows:

$$H = \begin{cases} 42 + \left\lfloor \frac{42(G - B)}{\delta} \right\rfloor & \text{if } R = \max(R, G, B), \delta > \frac{\max(R, G, B)}{2}, \\ 126 + \left\lfloor \frac{42(B - R)}{\delta} \right\rfloor & \text{if } G = \max(R, G, B), \delta > \frac{\max(R, G, B)}{2}, \\ 210 + \left\lfloor \frac{42(R - G)}{\delta} \right\rfloor & \text{if } B = \max(R, G, B), \delta > \frac{\max(R, G, B)}{2}, \\ -1 & \text{otherwise,} \end{cases} \tag{7}$$

$$\delta = \max(R, G, B) - \min(R, G, B), \tag{8}$$

where  $R$ ,  $G$ , and  $B$  are 8-bit color intensities for red, green and blue, while  $H$  is a hue value ranging from  $-1$  to  $252$ . The difference value of hue ( $H_d$ ) is calculated as

$$H_d = \min(|H - H_t|, 253 - |H - H_t|), \tag{9}$$

where the hue of the tracked object ( $H_t$ ) is set to 40 in this implementation, for tracking red objects. Finally, for the object localization, the weight of the particle ( $w$ ) is given by

$$w = \begin{cases} \left\lfloor \alpha \exp\left(-\frac{H_d^2}{2s^2}\right) \right\rfloor & \text{if } H \neq -1, R \geq 64, \\ 0 & \text{otherwise,} \end{cases} \tag{10}$$



where  $\alpha$  denotes a parameter related to the scale of weights, and  $s$  represents a parameter indicating the spread of the distribution of the weight (dispersion). In this implementation, we applied  $\alpha = 1023$  and  $s = 20$  for Eq. (10).

### 3.5 Weight Comparison

Maximum likelihood calculation employs the choice of  $x_{max}$ ,  $y_{max}$  and  $w_{max}$  from the same coordinates as shown in Fig. 8. For hardware structure, one real particle is rounded by predefined virtual particles. For example, if we select the number of real particles ( $M = 100$ ) and the number of virtual particles ( $B = 50$ ), one process includes one real particle and fifty virtual particles, and this process works one hundred times in parallel. Accordingly, the likelihoods of stream processing are compared to the respective coordinates of one real particle and 0 to 49 virtual particles. When the coordinates of likelihood stream and that of real or virtual particle are same initially, the coordinates and weight become  $x_{max}$ ,  $y_{max}$  and  $w_{max}$ . Then, the same process performs as the previous one and the weight of current coordinates are compared with the previous maximum weight. After comparing the weights of one real particle and fifty virtual particles, we select the maximum weight value with the related coordinates and velocities of  $x$  and  $y$ .

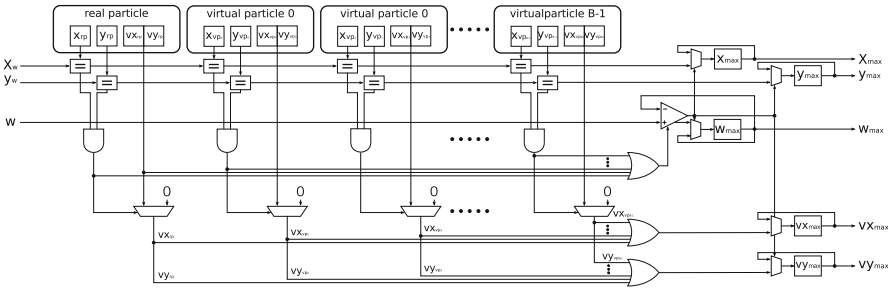
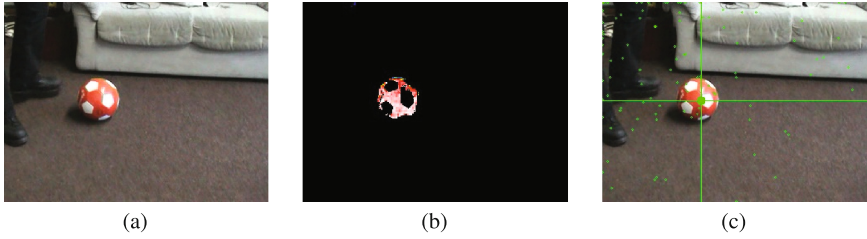


Fig. 8. Weight comparison module

### 3.6 Center of Gravity Calculation

To the tracking of a moving model, center of gravity calculation purposes for the demonstration and estimation of the object position across the frame. The center of gravity calculation of a frame is given by

$$g(x, y) = \left( \frac{\sum_{i=1}^M x_i w_i}{\sum_{i=1}^M w_i}, \frac{\sum_{i=1}^M y_i w_i}{\sum_{i=1}^M w_i} \right), \tag{11}$$



**Fig. 9.** Tracking example. (a) captured image from a benchmark video [7]. (b) corresponding image of weight representation. (c) object detection result.

where  $x_i$ ,  $y_i$ , and  $w_i$  represent the  $x$  and  $y$  coordinates, and weight of  $i$ -th real particle, respectively. After the calculation, the center of gravity known as the intersection point of two lines in lime-green color is drawn on the object for tracing the trajectories of object. Figure 9 shows an execution example of the implemented object tracking system (Table 3).

## 4 Evaluation and Discussion

We implemented the proposed system on a Kintex-7 XC7K325T FPGA using Xilinx Vivado 2016.3. Based on our primary evaluation on tracking accuracy [12], the number of real particles ( $M$ ) and the number of virtual particles ( $B$ ) were set to 100 and 50, respectively. Table 2 shows the FPGA implementation results and the performance. Among the four design alternatives, the 5x\_LUT design was successfully implemented on a smaller FPGA chip (XC7K160T), demonstrating that resource sharing with a high clock frequency leads to the compact architecture and the cost down. Although 5x\_BRAM achieved the highest resource reduction rates in terms of LUTs and FFs, it consumed about 80% of the BRAM

**Table 2.** FPGA mapping results for each design

Design and FPGA	Baseline XC7K325T	RSync XC7K325T	5x_LUT XC7K325T	5x_LUT XC7K160T	5x_BRAM XC7K325T
LUT	160,940 (78.97%)	102,750 (50.42%)	81,895 (40.18%)	81,868 (80.74%)	69,203 (33.96%)
FF	177,229 (43.48%)	156,119 (38.30%)	106,646 (26.16%)	106,646 (52.59%)	68,646 (16.84%)
BRAM	0 (0.00%)	51 (11.46%)	51 (11.46%)	51 (15.69%)	351 (78.88%)
DSP48E	408 (48.57%)	203 (24.17%)	203 (24.17%)	203 (33.83%)	203 (24.17%)
Max freq. (MHz)	28.00	33.70	139.38	141.18	141.25
Throughput (fps)	62.16	74.81	61.88	62.68	62.72

**Table 3.** Latencies for each process (clock cycles)

Process	Baseline	RSync	5x_LUT	5x_BRAM
Likelihood calculation	3	3	7	
Resampling	411,622	411,672	2,058,162	
Prediction & weighted center calculation	136	136	137	
Total latency	411,761	411,811	2,058,306	
Available clock cycles in one frame	450,450	450,450	2,252,250	

offered by XC7K325T. That is why this design cannot fit in the smaller chip. In terms of throughputs, more than 60 fps was shown for every design, demonstrating the realtime performance for input video images.

Table 3 summarizes the latencies of object tracking process for one frame. The table also shows breakdowns of the total latencies into three sub-processes: calculation of likelihood, resampling, and prediction including calculation of the weighted center of particles. The prediction and the calculation of the weighted center are executed in parallel. As shown in the table, the resampling clearly dominates the total latency, since this process is performed in parallel with pixel input in a pipelined manner. Nevertheless, in-frame performance are achieved for all the design alternatives, since the total latencies were 411,761 clock cycles for Baseline, 411,811 for RSync, and 2,058,306 for 5x\_LUT and 5x\_BRAM, which are less than the available clock cycles for one frame. Note that 5 times clock cycles are available for 5x\_LUT and 5x\_BRAM, since the clock frequency is increased by 5 times than Baseline and RSync. The latency of resampling for RSync was slightly increased compared to Baseline, since the process of updating velocities of particles was change to be sequentially executed in the synchronization region. Al though this is a cost of hardware size reduction, it is acceptable since there is still an enough margin of clock cycles for one frame.

To discuss the tradeoff between the time-sharing of hardware resources and power consumption, we estimated power consumption with Xilinx Vivado tool, and the results are shown in Table 4. By comparing 5x\_LUT on XC7K325T and the same design on XC7K160T, approximately 6% of total on-chip power reduction was shown. However, the power consumption for 5x\_LUT on XC7K160T was 2.7 to 3.0 times higher than the designs synchronized with the camera clock.

**Table 4.** Power consumption comparison

Power [W]	Baseline XC7K325T	RSync XC7K325T	5x_LUT XC7K325T	5x_LUT XC7K160T	5x_BRAM XC7K325T
Dynamic	0.842	0.772	2.289	2.186	3.530
Static	0.165	0.169	0.179	0.127	0.209
Total on-chip	1.008	0.941	2.469	2.314	3.740

That is, the increase in power consumption caused by the increase in the clock frequency cannot be compensated by downsizing the chip. In summary, large designs with a slow clock frequency were more efficient than smaller designs with a fast clock frequency in terms of power consumption.

Finally, for performance comparison, we implemented the same algorithm in software and executed on an embedded system equipped with a 900-MHz ARM Cortex-A7U CPU and 1-GB memory managed by Raspbian Jessie Linux OS. The software was described in C++ with the OpenCV library, and input images were given from a file. The measured throughput for the software implementation was 19.5 fps. As a result, it was shown that our FPGA implementation achieved 3.1 to 3.8 higher throughputs.

## 5 Conclusion

This paper discussed particle filter architectures for stream image processing on FPGA. The implementation experiment on a KC7K325T FPGA revealed that the proposed architecture achieved realtime performance of 60 fps for VGA images without using any external memory devices. In addition, by introducing a higher clock frequency than the pixel clock and by improving a balance of resource utilization, we demonstrated our design can be fitted in a smaller XC7K160T FPGA. However, it was also shown that the power consumption for a smaller design with a 5 times clock frequency was increased by 2.7 to 3.0 times, compared to a design implemented on a larger chip synchronizing with a slow camera pixel clock. Our challenging future work includes the evaluation of particle filters with a large number of particles for non-rigid objects and to find the best tradeoff point between chip size and clock frequency.

## References

1. Arulampalam, M.S., Maskell, S., Gordon, N., Clapp, T.: A tutorial on particle filters for online nonlinear/non-Gaussian Bayesian tracking. *IEEE Trans. Sig. Process.* **50**(2), 174–188 (2002)
2. Athalye, A., Bolic, M., Hong, S., Djuric, P.M.: Architectures and memory schemes for sampling and resampling in particle filters. *Proc. IEEE Digital Sig. Process. Workshop* **1**, 92–96 (2004)
3. Athalye, A., Bolic, M., Hong, S., Djuric, P.M.: Generic hardware architectures for sampling and resampling in particle filters. *EURASIP J. Appl. Sig. Process.* **17**, 2888–2902 (2005)
4. Bräunl, T.: *Embedded Robotics: Mobile Robot Design and Applications with Embedded Systems*. Springer, Heidelberg (2008)
5. Dohi, K., Yorita, Y., Shibata, Y., Oguri, K.: Pattern compression of FAST corner detection for efficient hardware implementation. In: *Proceedings of the International Conference on Field Programmable Logic and Applications*, pp. 478–481 (2011)
6. Fleck, S., Strasser, W.: Adaptive probabilistic tracking embedded in a smart camera. In: *IEEE Computer Society Conference on Computer Vision and Pattern Recognition*, pp. 134–134 (2005)

7. Klein, D.A.: BoBoT - Bonn benchmark on tracking. <http://www.iai.uni-bonn.de/~kleind/tracking/>
8. Miao, L., Zhang, J.J., Chakrabarti, C., Papandreou-Suppappola, A.: A new parallel implementation for particle filters and its application to adaptive waveform design. In: Proceedings of the IEEE Workshop on Signal Processing Systems, pp. 19–24 (2010)
9. Negi, K., Dohi, K., Shibata, Y., Oguri, K.: Deep pipelined one-chip FPGA implementation of a real-time image-based human detection algorithm. In: Proceedings of the International Conference on Field-Programmable Technology, pp. 1–8 (2011)
10. Nummiaro, K., Koller-Meier, E., Gool, L.V.: An adaptive color-based particle filter. *Image Vis. Comput.* **21**, 99–110 (2003)
11. Schwiigelshohn, F., Ossovski, E., Hübner, M.: A fully parallel particle filter architecture for FPGAs. In: Proceedings of the International Symposium on Applied Reconfigurable Computing, pp. 91–102 (2015)
12. Tahara, A., Hayashida, Y., Thu, T.T., Shibata, Y., Oguri, K.: FPGA-based real-time object tracking using a particle filter with stream architecture. In: Proceedings of the International Symposium on Computing and Networking, pp. 422–428 (2016)

# HLS-Based FPGA Acceleration of Building-Cube Stencil Computation

Rie Soejima, Yuichiro Shibata<sup>(✉)</sup>, and Kiyoshi Oguri

Nagasaki University, 1-14 Bunkyo-machi, Nagasaki 852-8521, Japan  
soejima@pca.cis.nagasaki-u.ac.jp, {shibata,oguri}@cis.nagasaki-u.ac.jp

**Abstract.** This paper presents design and implementation of a framework for high-level synthesis (HLS), which allows easy description and acceleration of stencil computation with building-cube method (BCM) on FPGAs. The BCM is one of adaptive mesh refinement methods, which can reduce computational costs by using various granularity of cubes depending on computational precision required by target models. By placing some restrictions on size ratios between adjacent cubes, the BCM offers affinity to parallel processing. However, non-continuous memory access imposed by the irregular cubes does not straightforwardly match with stream processing on FPGA accelerators. To fill this gap, we design and implement a BCM framework as a class library on a high-level synthesis environment. The framework automatically generates mechanisms required for the BCM, such as reordering modules of data streams and data interpolation hardware between different cubes. The proposed framework is evaluated in terms of computing performance, memory performance and required hardware resources on a Maxeler Technologies FPGA accelerator. The results reveal that a performance overhead of data exchange between different sizes of cubes is reasonably small.

## 1 Introduction

Stencil computation is a well-known design pattern, in which a same pattern of operations is iteratively applied for each element of a mesh of data. In scientific stencil applications, higher computational accuracy can be achieved by increasing the resolution of the data mesh. However, this also requires large amount of computational costs and memory usage. To cope with this problem, an adaptive mesh refinement method called building cube method (BCM) has been proposed [4, 5]. In the BCM, the simulation space is divided into an orthogonal grid with various sizes of elements called cubes. In most scientific simulations, in terms of computational accuracy, required mesh resolution is not uniform in the entire simulation space. Thus, by using coarse-grained cubes for the regions where high resolution is not required, the BCM can reduce the computational costs. At the same time, to increase affinity to parallel processing, the BCM imposes restrictions on a size ratio between adjacent cubes.

The stencil computation can be effectively implemented on FPGA accelerators as a form of stream processing with deep pipelined custom hardware

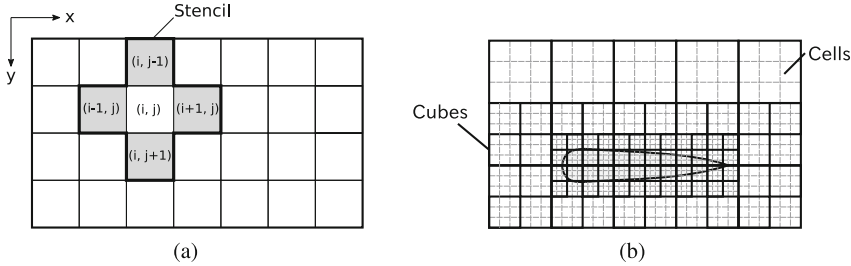


**Fig. 1.** Example of BCM mesh. (a) stencil. (b) cubes and cells.

modules [2, 6–8, 10, 11]. Although productivity of application development was a main drawback of FPGA accelerators, recent advances in high level synthesis (HLS) technologies are mending the problem. HLS frameworks for stencil computation for FPGA accelerators have been also implemented [12]. However, there are hardly any attempts to develop an HLS framework for the BCM, since an irregular mesh topology introduced by the BCM makes it difficult to straightforwardly utilize stream processing [9]. In this paper, we implement a framework for stencil computation with the BCM as a class library on MaxCompiler, which is a Java-based HLS system developed by Maxeler Technologies for their FPGA accelerators. We also evaluate the efficiency and overhead of the mechanism by implementing an example application with the proposed framework.

## 2 Building Cube Method (BCM)

In stencil computation, an operation with a same data reference pattern (a stencil) is iteratively applied for all the data elements. Figure 1(a) shows an example of a 2-D stencil, where a next step value of the element at  $(i, j)$  is calculated using the current values of  $(i, j - 1)$ ,  $(i - 1, j)$ ,  $(i + 1, j)$ , and  $(i, j + 1)$ . In multidimensional stencil computation for a large amount of computational space, spatial locality of memory access is reduced, since locations of the data elements referenced by the stencil are scattered on the memory space. Therefore, a blocking method, in which the computational space is divided into small regions is widely used [1]. In addition, to achieve a good balance between spatial locality and efficient DMA transfer, a multi-level blocking method, where each block is divided into further small regions, is often utilized [12]. The computation for each block is not self-contained, since some data elements in adjacent blocks must be read out by the stencil. Such data elements are called halos.

BCM is one of adaptive mesh refinement methods, in which the simulation space is divided into various sizes of cubes, and the computation is performed for each cube. Each cube is further divided into an equal-sized mesh called cells, which are the elements of computing. By unifying the size ratio between adjacent different-sized cubes, BCM introduces some sort of mutual similarity in computing. In addition, the meshing is performed so that every cube has

the same number of cells. This uniformed structure makes the BCM suitable for parallel processing in spite of the variety of cube sizes. However, on the boundary between different sizes of cubes, different resolution of halos needs to be accessed. Therefore, some mechanisms are required to interpolate the values of halos. The size of each cube is given depending on a target model of the simulation. To reduce the computational cost, coarse-grained cubes are utilized for regions where a high degree of arithmetic precision is not required. Figure 1(b) illustrates an example of BCM meshing, where the solid lines show cube boundaries while the dashed lines show cell boundaries.

### 3 MaxCompiler

MaxCompiler is an HLS tool developed by Maxeler Technologies as a development environment for high performance computing on their FPGA accelerators called Data Flow Engines (DFEs). The MaxCompiler offers a stream-oriented programming model, where users describe desired applications in a Java based dedicated language called MaxJ. Based on user descriptions, the compiler generates arithmetic pipelines, PCIe interface, DRAM interface, APIs on a host machine and so on. In this paper, we used a DFE MAX3424A equipped with a Xilinx Virtex-6 SX475T FPGA and 6 banks of 4-GB DDRIII memory modules.

Major hardware modules implemented on the FPGA by MaxCompiler are kernels and managers. A kernel is user-designed custom computational hardware, which typically consists of many pipelined arithmetic units. A manager provides interface among the accelerator, the host PC, and external memory. It is also used for setting hardware parameters such as the clock frequency and degree of parallelism for the arithmetic pipelines. The programming model hides architectural details from users such as latencies of arithmetic units and pipeline stalls. The compiler automatically generates a stall control mechanism for the pipelines. The dataflow on the FPGA is implemented as a simplex stream. The compiler also automatically generates FIFOs on input and output ports to absorb speed differences of streams.

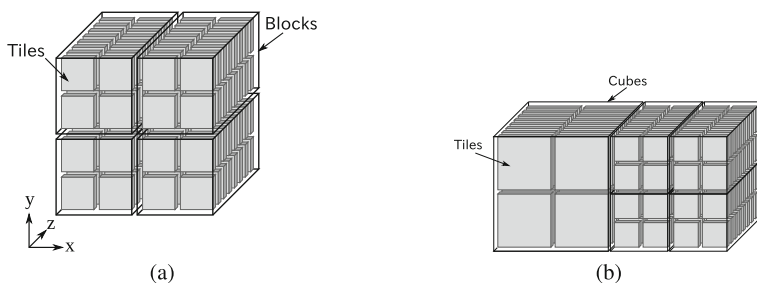


**Fig. 2.** Blocking methods. (a) two-level blocking. (b) BCM blocking.



### 4 Design and Implementation of BCM Framework

We implemented an HLS framework for stencil computing based on BCM as a class library on the Maxeler’s environment. In this BCM framework, the idea of a two-level blocking method [12] is adopted. The simulation space is divided into 3-D regions called blocks and each block is further divided into 2-D small regions called tiles. While the calculation is performed block by block, DRAM access is performed tile by tile. As Fig. 2(a) shows, the block decomposition is performed only for the  $x$  and  $y$  directions, since blocking in the  $z$  direction does not increase spatial locality. The optimal block size depends on the stencil form used in applications, while the optimal tile size depends on the burst size of DRAM access. With this framework, users can designate tile size ( $T_W, T_H$ ), block size ( $B_W, B_H$ ), the clock frequency of kernels  $F_s$ , the memory access frequency  $F_{mem}$ , a degree of parallelism of pipelines, and so on, at synthesis time. We extended the two-level blocking framework to support BCM as shown in Fig. 2(b). Cubes in BCM correspond to blocks in the two-level blocking, while cells in each cube are managed by a unit of tiles. In order to avoid confusion, we call cubes blocks, henceforth.

Figure 3 shows the dataflow of the BCM, and Table 1 shows the classes implemented in the framework. Using these classes, users can describe stencil computation, optimize memory access, and designate architectural parameters. The framework also provides a memory profiler to help users evaluate and optimize the memory access performance. The data stored in DRAM is read out tile by tile and reordered for each block in the Transposition class. Then, user-described arithmetic kernels performs calculation in a block-by-block manner. The calculation results are reordered again in units of tiles and are written back to the DRAM. DRAM access of each data stream is controlled by the AddressCommandGenerator class.

Since different block sizes are mixed in the BCM, a mechanism to obtain block size information is needed. Therefore, we provide an additional data stream to convey the information. In the BCM framework, the DRAM data is read out

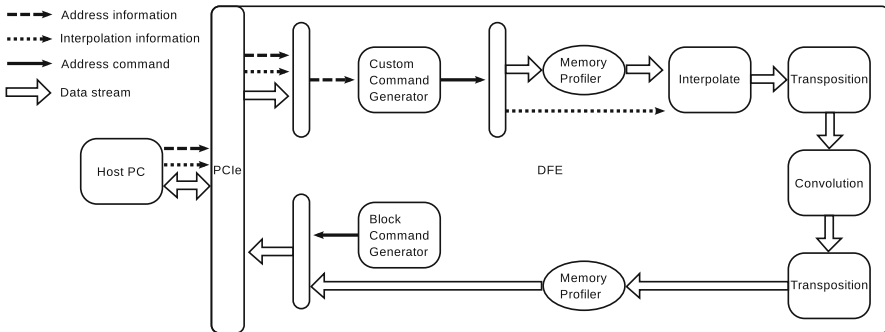


Fig. 3. Dataflow of the implemented BCM framework

**Table 1.** Classes implemented in BCM framework

Class names	Functionality
ConvolutionKernel	Modules for stencil computation
Transposition	Interconversion tiles and blocks
MemoryProfiler	Measurement of memory performance
SimpleManager	Management of kernels and streams
AddressCommandGenerator	Generation of DRAM access commands for streams
CustomCommandGenerator	Generation of DRAM access commands for input streams
BlockCommandGenerator	Generation of DRAM access commands for output streams
Interpolate	Halo data processing and interpolation

tile by tile and is sent to the Interpolate class, where a special data process such as interpolation of halos is performed to adjust boundaries between different size blocks. DRAM access operations for input streams and output streams are controlled by the CustomCommandGenerator class and the BlockCommandGenerator class, respectively. For comparison, we also implemented a baseline framework without BCM support, which is called FD framework, henceforth.

#### 4.1 Interpolation of Halos

The Interpolate class receives input streams of the stencil computation and an additional stream for information on interpolation of halos, and performs data processing of halos for each tile. Here, two different types of data processing are required: fine blocks to coarse blocks (FtoC) and coarse blocks to fine blocks (CtoF).

These data reference methods are illustrated in Fig. 4. In FtoC, an external data value is interpolated by taking an average of two halo elements as shown in Fig. 4(a). In CtoF, on the other hand, the same halo element is accessed twice as shown in Fig. 4(b). The location of halos to be accessed also varies depending on positional relationship between tiles. The BCM framework determines necessity of FtoC or CtoF based on the positional relationship of halos for each tile at compile time. This information is stored in the DRAM and input into the



**Fig. 4.** Halo processing between different size of blocks. (a) fine to coarse. (b) coarse to fine.

Interpolate class as a stream at run time. One Interpolate class object is instantiated for each input stream.

## 4.2 Generation of DRAM Access Commands

In the BCM, irregularity of DRAM access is introduced for input streams due to halos in different sizes of blocks. On the other hand, DRAM access made by output streams of arithmetic kernels is regular, since the output streams do not have any halos. Therefore, the BCM framework provides different classes for input and output streams to control DRAM access.

DRAM access for input streams is managed by CustomCommandGenerator class, which receives address information as an input stream at execution time. Based on this address information, this class generates address commands required for DRAM access and outputs them as an output stream. The address information is prepared on the host application at compile time, by analyzing how the simulation space is divided into blocks. When fetching multiple tiles that are continuous on the DRAM, a series of access is combined into one address command.

DRAM access made by output streams is controlled by BlockCommandGenerator class. This class receives block size and parameters designated by users and calculates DRAM addresses to be accessed. Then, address commands are generated and outputted. The address commands outputted by these two classes are passed to the DRAM controller so that required memory access is performed for the corresponding streams.

## 5 Application for Evaluation

As an application example of 3-D stencil computation, heat conduction simulations with an explicit method were implemented using the FD framework and the BCM framework. Figure 5 shows part of the arithmetic kernel of the 3-D heat conduction simulation described with the BCM framework. In this simulation, two input streams for thermal values  $T$  and diffusion coefficients  $\alpha$  and one output stream for thermal values  $T$  are utilized for the computation. Moreover, to obtain size information for each element, an additional stream for Scale is provided. In Lines 2 to 19, I/O parameters are configured and initialized. Here, the streams for  $\alpha$  and Scale are firstly received as an array of structure (AOS) in a single stream. Then, they are decomposed for each. The stencil is configured for the  $x$  and  $y$  directions in Lines 22 to 30 and for the  $z$  direction in Lines 32 to 39. In Lines 42 and 43, the heat diffusion equation is described. Scale values affect only for the  $x$  and  $y$  directions, since all the elements has the same size in the  $z$  direction in this implementation.

In the implementation with the FD framework, on the other hand, only two input streams for the thermal values  $T$  and the diffusion coefficients  $\alpha$  are utilized, and the Scale stream is not provided. In addition, only one stencil description is needed to cover all the three directions.

```

1  /*Define input stream*/
2  DFEVector<DFEVar> inT
3  = addInputStream("inT",v_type, 1, 1, 1, 1, 1, 1);
4  DFEVector<DFEVar> AlphaScale
5  = addInputStream("AlphaScale", v_type_NoOffset);
6
7  DFEVector<DFEVar> Alpha
8  = AlphaScale.slice(32, 32).cast(v_type);
9  DFEVector<DFEVar> Scale
10 = AlphaScale.slice(0, 32).cast(v_type);
11
12 /*Define output stream*/
13 DFEVector<DFEVar> outT = constant.vect(v_type, 0);
14
15 /*Scalar input scaler*/
16 DFEVar DeltaT = addInputScalar("DeltaT", type);
17 DFEVar DeltaXX_1 = addInputScalar("DeltaXX", type);
18 DFEVar DeltaYY_1 = addInputScalar("DeltaYY", type);
19 DFEVar DeltaZZ_1 = addInputScalar("DeltaZZ", type);
20
21 /*Make stencil for xy dimation*/
22 DFEVar coeffX_xy[]
23 = {DeltaXX_1,
24    constant.var(type, -2) * (DeltaXX_1 + DeltaYY_1),
25    DeltaXX_1};
26 DFEVar coeffY_xy[] = {DeltaYY_1, DeltaYY_1};
27 DFEVar coeffZ_xy[] = {};
28 Stencil S_xy
29 = new XStencil(-1, 1, -1, 1, 0, 0,
30               coeffX_xy, coeffY_xy, coeffZ_xy);
31
32 /*Make stencil for z dimation*/
33 DFEVar coeffX_z[]
34 = {constant.var(type, -2) * (DeltaZZ_1)};
35 DFEVar coeffY_z[] = {};
36 DFEVar coeffZ_z[] = {DeltaZZ_1, DeltaZZ_1};
37 Stencil S_z
38 = new XStencil( 0, 0, 0, 0, -1, 1,
39               coeffX_z, coeffY_z, coeffZ_z);
40
41 /*Computations*/
42 outT = inT + DeltaT * Alpha *
43       (Scale * convolve(inT, S_xy) + convolve(inT, S_z));
44
45 /* Output */
46 addOutputStream("outT", outT);

```

Fig. 5. Part of heat conduction simulation described with BCM framework

## 6 Evaluation and Discussions

To reveal how the simulation performance and hardware size are affected by supporting the BCM, we evaluated the heat conduction simulation in terms of required FPGA resources, execution performance and memory performance. The host PC utilized for the evaluation was equipped with a 2.8-GHz Intel Core i7-2600S, 16-GB DDRIII memory, and a MAX3424A DFE and managed by CentOS6.4. The design was compiled and mapped on the FPGA using MaxCompiler Version 2013.3 and Xilinx ISE 13.3. The design parameters of the evaluated heat conduction simulators were  $(B_W, B_H) = (32, 24)$ ,  $(T_W, T_H) = (16, 12)$ ,  $F_s = 150$  MHz, and  $F_m = 300$  MHz. For arithmetic kernels, single-precision floating point arithmetic units were utilized. For performance evaluations, the three simulation models shown in Fig. 6 were evaluated. The FD model, which was executed by the FD framework for comparison, divides the simulation space into same-sized 5 blocks as shown in Fig. 6(a). For BCM execution, the other two

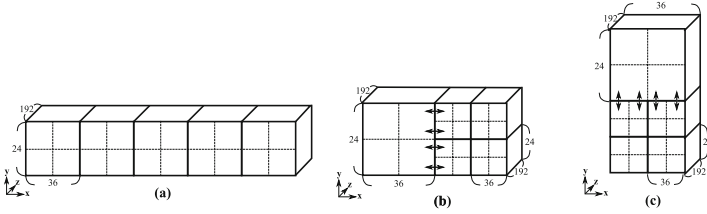


**Fig. 6.** Evaluated blocking. (a) FD model. (b) Divide-X model. (c) Divide-Y model.

models called Divide-X model (Fig. 6(b)) and Divide-Y model (Fig. 6(c)) were implemented, where 1 large block and 4 small blocks were utilized. The difference between Divide-X and Divide-Y is the direction of block arrangement. These three models have the same amount of data with the block size of (32, 24, 192).

### 6.1 Overhead in FPGA Resources

By comparing FPGA resource utilization for the heat conduction simulations implemented by the FD framework and BCM framework, we evaluated an overhead in hardware size for supporting the BCM. The evaluated implementations were the FD model by the FD framework and Divide-X by the BCM framework. Note that the resource amounts required for Divide-X and Divide-Y are the same, since hardware generated by the BCM framework does not depend on simulation models.

**Table 2.** Comparison of resource utilization

Resources	FD framework	BCM framework	Increase ratio (%)
LUTs	45,516 (15.3%)	59,349 (19.9%)	30.3
FFs	68,636 (11.5%)	91,958 (15.5%)	33.8
BRAMs	223 (20.9%)	344 (32.3%)	54.2
DSPs	41 (2.03%)	49 (2.43%)	19.5

Table 2 summarizes resource utilization for each implementation and the increase ratio in resources compared to the FD framework. Figure 7 shows the breakdown of utilized resources for each stream in the generated hardware except the arithmetic kernel. As these evaluation results show, utilization of each FPGA resource was increased by supporting the BCM. DSP blocks, which were mainly utilized for the arithmetic kernel, increased by 19.5% due to the additional multiplications introduced by the stream of Scale. The increases in LUTs and FFs were 82.4% and 18.2%, respectively. This was mainly due to the additional process of average calculation of halos in the Interpolate class.

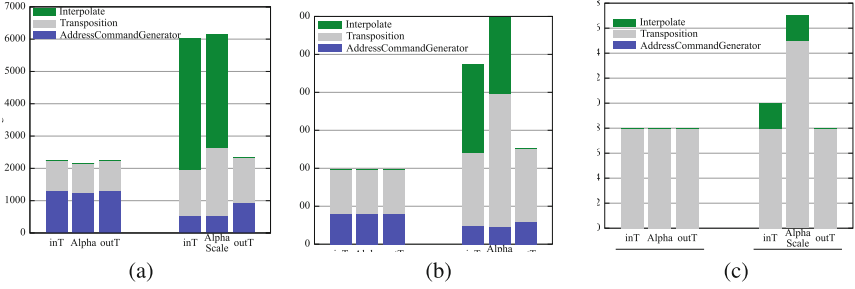


**Fig. 7.** Breakdowns of resource utilization for each stream. (a) LUTs. (b) FFs. (c) BRAM.

By supporting the BCM, the latency of the overall application pipeline was also increased, and additional pipeline registers were introduced for controlling stalls. That is why even in the Transposition class, whose functionality is the same as the BCM framework, LUTs and FFs for the inT and outT streams were increased by up to 51.1% and 65.6%, respectively. Furthermore, the BCM framework needs the additional stream of Scale to obtain information on block size. In this implementation, the streams of  $\alpha$  and Scale were combined into the AlphaScale stream in an AOS manner, and thus the number of input streams was not increased. However, the data width of the AlphaScale stream was doubled, compared to the Alpha stream in the original FD framework. As a result, LUTs, FFs and BRAM used for the AlphaScale stream were increased by 130%, 196% and 87.5%, respectively.

On the other hand, the resource utilization for the DRAM access control class was decreased. Especially in the CustomCommandGenerator class, which manages input streams, LUTs and FFs were decreased by up to 59.3% and 39.6%, respectively, compared to the AddressCommandGenerator class in the FD framework. While the AddressCommandGenerator class calculates the memory addresses to be accessed by various parameters, the CustomCommandGenerator class uses address information given by the host application. Therefore, the resource utilization for address calculation was reduced. As a tradeoff, however, DRAM utilization was increased since address information needs to be stored in DRAM in advance.

**Table 3.** Impacts of BCM on performance

Models	Exec. time (sec)	Throughput (GB/sec)	Drop ratio (%)
FD	$2.02 \times 10^{-2}$	$1.36 \times 10^{-1}$	-
Divide-X	$2.08 \times 10^{-2}$	$1.32 \times 10^{-1}$	2.68
Divide-Y	$2.07 \times 10^{-2}$	$1.32 \times 10^{-1}$	2.46

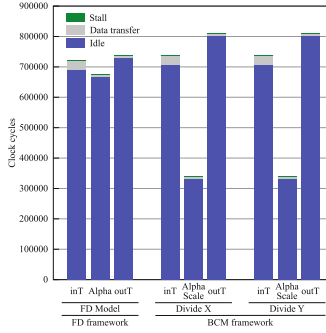


Fig. 8. Memory profiling results of heat conduction simulations

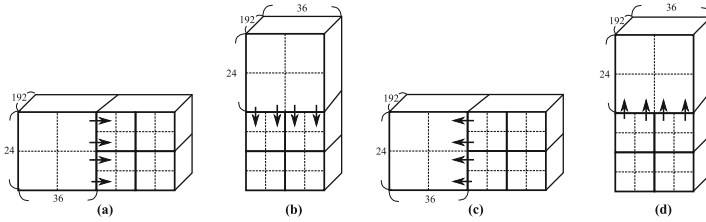
## 6.2 Performance Overhead

Table 3 shows the execution time, throughput, and throughput degradation ratio compared to the FD model for the three simulation models depicted in Fig. 6. The performance degradation imposed by the BCM was up to 2.68% in terms of the throughput. Figure 8 plots the results of memory profiling. The memory profiler counts the number of events in a state machine of the memory controller. The counted events are (1) Data transfer, where valid data was transferred, (2) Stall, where requested data was not ready and not transferred, and (3) Idle, where the memory controller was in an idle state. As the profiling results show, the Idle counts of the inT and outT streams for both Divide-X and Divide-Y were increased 2.46% and 10.0%, respectively. This is mainly due to the increase in the latency imposed by the BCM. On the other hand, the Idle counts of the AlphaScale stream were significantly reduced compared to the Alpha stream in the FD model. This suggests the additional stream for block size and interpolate information of the BCM did not become a bottleneck of the memory access as far as this application is concerned.

Comparing Divide-X with Divide-Y, Divide-Y was slightly better in terms of both execution performance and memory performance. In addition, the data size of the address information stored in DRAM was  $9.73 \times 10^{-5}$  GB for Divide-X, while it was  $9.44 \times 10^{-5}$  GB for Divide-Y. This reduction was made by combining multiple access commands for the halo elements continuously arranged in the DRAM. That is, block decomposition in the  $y$  direction has an advantage in the BCM framework.

## 6.3 Characteristic of Halo Data Processing

To reveal performance characteristics for each halo data processing, 4 evaluation models illustrated in Fig. 9, where reference to halos was restricted to one direction, were implemented and evaluated. While the models in Fig. 9(a) and (b) performed CtoF processing, the models in (c) and (d) performed FtoC processing. For all the models, the same block size of (32, 24, 192) was utilized.



**Fig. 9.** Halo data processing evaluation models. (a) CtoF Divide-X. (b) CtoF Divide-Y. (c) FtoC Divide-X. (d) FtoC Divide-Y.

Table 4 summarizes the execution time and execution throughput for each model, and Fig. 10 plots the memory profiling results. As the results in Table 4 show, the performance of the FtoC processing was worse than that of the CtoF processing regardless of blocking directions. Also in terms of memory performance, the idle counts of FtoC for the AlphaScale and outT streams were increased by 12.7% and 10.0%, respectively, compared to CtoF processing. These performance differences between FtoC and CtoF reflect the fact that FtoC needs average interpolation of halos while CtoF just reads out the same halos multiple times.

**Table 4.** Evaluation results for each halo data processing

Models		Exec. time (sec)	Throughput (GB/sec)
CtoF	Divide X	$2.02 \times 10^{-2}$	$1.36 \times 10^{-1}$
	Divide Y	$2.02 \times 10^{-2}$	$1.36 \times 10^{-1}$
FtoC	Divide X	$2.08 \times 10^{-2}$	$1.32 \times 10^{-1}$
	Divide Y	$2.08 \times 10^{-2}$	$1.32 \times 10^{-1}$

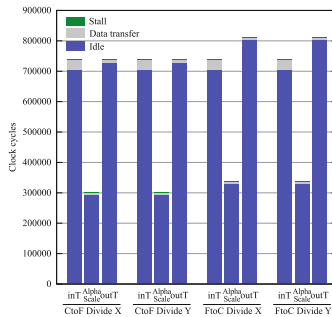


**Fig. 10.** Memory profiling results for halo data processing



## 7 Conclusion

In this paper, we implemented a framework for stencil computation with the BCM as a class library on the MaxCompiler environment. As a result of empirical evaluation of a 3-D heat conduction simulation implemented by the proposed BCM framework, it was revealed that the BCM increased BRAM usage by up to 54.2% and degraded the performance by up to 2.68%. However, these overheads are considered to be reasonably small, since the BCM can significantly reduce the computational cost by using coarse grained cells. Our future work includes to implement more sophisticated halo processing [3], and to make more practical evaluation with large-scale applications.

## References

1. Datta, K., Murphy, M., Volkov, V., Williams, S., Carter, J., Oliker, L., Patterson, D., Shalf, J., Yelick, K.: Stencil computation optimization and auto-tuning on state-of-the-art multicore architectures. In: Proceedings of ACM/IEEE Conference on Supercomputing (SC), pp. 4:1–4:12 (2008)
2. Giefers, H., Plessl, C., Förstner, J.: Accelerating finite difference time domain simulations with reconfigurable dataflow computers. *ACM SIGARCH Comput. Archit. News* **41**(5), 65–70 (2013)
3. Hiroe, Y., Takehiko, S.: Non-hydrostatic atmospheric cut cell model on a block-structured mesh. *Atmos. Sci. Lett.* **13**(1), 29–35 (2012)
4. Ishida, T., Takahashi, S., Nakasashi, K.: Efficient and robust Cartesian mesh generation for building-cube method. *J. Comput. Sci. Technol.* **2**(4), 435–446 (2008)
5. Kim, L.S., Nakahashi, K., Jeong, H.K., Ha, M.Y.: High-density mesh flow computations by building-cube method. *J. Mech. Sci. Technol.* **21**(8), 1306–1319 (2007)
6. Mencer, O.: ASC: a stream compiler for computing with FPGAs. *IEEE Trans. Comput. Aided Des. Integr. Circ. Syst.* **25**(9), 1603–1617 (2006)
7. Okina, K., Soejima, R., Fukumoto, K., Shibata, Y., Oguri, K.: Power performance profiling of 3-d stencil computation on an FPGA accelerator for efficient pipeline optimization. *SIGARCH Comput. Archit. News* **43**(4), 9–14 (2016)
8. Sano, K.: FPGA-based systolic computational-memory array for scalable stencil computations. In: High-Performance Computing Using FPGAs, pp. 279–303. Springer (2013)
9. Sano, K., Chiba, R., Ueno, T., Suzuki, H., Ito, R., Yamamoto, S.: FPGA-based custom computing architecture for large-scale fluid simulation with building cube method. *ACM SIGARCH Comput. Archit. News* **42**(4), 45–50 (2014)
10. Sato, Y., Inoguchi, Y., Luk, W., Nakamura, T.: Evaluating reconfigurable dataflow computing using the Himeno benchmark. In: Proceedings of International Conference on Reconfigurable Computing and FPGAs (ReConFig), pp. 1–7 (2012)
11. Schneider, S., Hirzel, M., Burga, G., Wu, K.K.: Safe data parallelism for general streaming. *IEEE Trans. Comput.* **64**(2), 504–517 (2015)
12. Soejima, R., Okina, K., Dohi, K., Shibata, Y., Oguri, K.: A memory profiling framework for stencil computation on an FPGA accelerator with high level synthesis. *ACM SIGARCH Comput. Archit. News* **42**(4), 69–74 (2014)

# Enriching Remote Control Applications with Fog Computing

Claudio Fiandrino<sup>1</sup>, Paolo Giaccone<sup>2</sup>, Ahsan Mahmood<sup>2(✉)</sup>, and Luca Maioli<sup>2</sup>

<sup>1</sup> Imdea Networks Institute, Madrid, Spain  
`claudio.fiandrino@imdea.org`

<sup>2</sup> Dip. di Elettronica e Telecomunicazioni, Politecnico di Torino, Turin, Italy  
{Paolo.Giaccone,Ahsan.Mahmood,Luca.Maioli}@polito.it

**Abstract.** Fog computing has emerged in the recent years as a paradigm tailored to serve geo-distributed applications requiring low latency. Remote Control (RC) applications allow a mobile device to control another device from remote. To enrich Quality of Experience (QoE) of RC applications, in this paper we investigate the use of fog computing as a viable platform to offload computation of tasks that would be expensive if performed locally on a mobile device. The proposed approach, supported with next 5G communication systems, will enable a Tactile Internet experience. In this paper we study and compare offload policies to accommodate tasks in the fog platform and analyze the requirements to minimize outages.

**Keywords:** Fog computing · Mobile edge computing · Cellular networks

## 1 Introduction

Mobile cloud applications are nowadays essential in our day lives. Among the others, they are used for business and entertainment purposes. However, mobile devices such as smartphones, laptops and wearables are resource constrained, i.e., they have limited energy and computing capabilities at disposal. Mobile cloud and fog computing paradigms overcome such issue through offloading [4, 11, 19]. Offloading is a technique applied to traffic [8] or computation [14]. Computation offloading augments the capabilities of mobile devices by moving the processing of tasks to the cloud. This allows the mobile devices to (i) prolong the battery lifetime as processing heavy tasks locally is energy-costly, (ii) to run sophisticated tasks that the local limited processing capabilities would not permit [12].

Remote Control (RC) applications allow a mobile device, typically a smartphone, to control remotely another device such as a drone or a robot [15]. Typically the control requires line of sight, however with future 5G networks the requirement will not be necessary anymore. RC applications allow the controller to perform actions by means of the controlled device, e.g., taking a picture from a

---

Claudio developed this work as a PhD student at the University of Luxembourg.

drone. Being resource constrained, batteries and computing capabilities of both controller and controlled devices are limited, thus enriching the applications with functionalities that are non strictly necessary is difficult. For example, performing object detection over a picture taken by the drone can be prohibitive for both the drone and the smartphone. Similarly, performing on-demand statistical analysis may improve robot and automation systems, but it can only be feasible with the help of the cloud [10]. Through offloading, the task becomes then feasible. However it is important that communication overhead is compatible with the small latency required by real-time RC applications. For example, RC applications like drone control require latency to be in the order of ms [3].

The expected requirements for future fifth-generation (5G) wireless systems foresee an improvement in latency from 15 ms of current 4G networks to 1 ms [2]. Levering the ultra-responsive connectivity of 5G systems, RC applications will become an important part of the Tactile Internet vision [18]. Tactile Internet aims at shifting the current content-delivery paradigm of the Internet into a skill-delivery. The ultimate goal is to create a medium capable of transporting touch and other senses. To illustrate with an example, real-time robot applications may suffer service inefficiency (e.g., environment recognition), which can be compensated with human expertise (e.g., through video streaming on RC applications).

In this paper we advocate the use of fog computing to enrich the Quality of Experience (QoE) of RC applications in view of enabling a ultra-responsive Tactile Internet experience. In more details, we investigate the process of allocating computing resources required to perform the tasks<sup>1</sup> such as object recognition that augment the QoE. This process is network-aware, i.e., to maintain a tight synchronization between the controller and the controlled device, communication resources need to be carefully selected. In this work we rely on existing technologies, and not on 5G systems, to verify feasibility constraints. We categorize the tasks according to their suitability to be offloaded in the fog platform or not. Specifically, we identify tasks that must be offloaded in the fog platform because of time constraints, tasks that can be executed either in the fog or in the remote cloud, and tasks that cannot be offloaded in the fog platform because of privacy concerns or because they require external and proprietary software to be executed.

## 2 A Primer on Fog Computing

The concept of fog computing was initially proposed by Cisco to render the network edge capable of cloud computing [5], hence it is also known as *edge computing*. Fog computing is specifically designed to cater for geographically distributed applications which have stringent low latency requirements and context awareness [17]. Consequently it is foreseen that fog computing will play a major role in the development of Internet of Things (IoT) [6]. To this end, various research efforts are being conducted on fog computing platforms supporting

---

<sup>1</sup> In the reminder of the paper, we use the terms tasks and jobs interchangeably.

IoT applications to assess their efficacy and resource management [1, 16]. The IoT front-end consists of mobile devices which have different computing, networking and storage capabilities. Local processing units called *cloudlets* can be utilized for temporary storage and processing [7]; these include desktop PCs or notebooks. The cloud, which centralizes the processing and backup, can receive the aggregated data from the cloudlets. In vehicular networks, [13] proposes a fog computing approach to place content caches at the network edges; the approach is shown to perform remarkably well as compared to the centralized caching approach, in particular for location-specific applications.

### 3 Resource Allocation in the Fog Platform

The aim of this section is to present the problem of resource allocation for task offloading in the fog platform. First, the general architecture and the main interacting entities are described. Afterwards, the classification of the jobs that must be offloaded on the remote platforms is introduced. Lastly, the offload policies for assigning the jobs either to the edge platform or to the external cloud are presented.

#### *Network Architecture*

In RC applications, the end-user devices, being resource constrained, are unable to enhance the QoE perceived by the users. One viable solution is to offload the computationally intensive tasks to external resources. Therefore, we envision a network topology where computational platforms are placed both in the cloud and the edge.

The general network architecture, as shown in Fig. 1, is divided into three levels. At the first (user) level, we have a generic user equipment, typically a tablet or a smartphone, acting as controller, and a remote controlled device, typically a drone or a robot. We assume both the devices are connected to the second (access) level of the network through three possible access networks: (i) a generic WiFi network, e.g. through an access point connected to the ADSL access network of an ISP; (ii) an LTE cellular network; (iii) a telecommunication operator's public WiFi network. The last kind of network has been recently introduced by the operators in addition to their existing cellular infrastructure [4]. We assume that edge servers, which users can access to offload some of their jobs, are only available inside the LTE and the operator's WiFi networks.

Finally, the third level in the considered network architecture consists of the global Internet where external cloud servers are available for the execution of users' tasks as well.

#### *Job Definition*

In the following, we concentrate just on the jobs that must be offloaded, assuming that other tasks are running locally in the user devices. Each job is associated with a maximum allowed delay for its processing, denoted as *job deadline*. We assume that the users offload the jobs to the edge servers present in the LTE network or in the public WiFi network, or to the external cloud present in Internet.

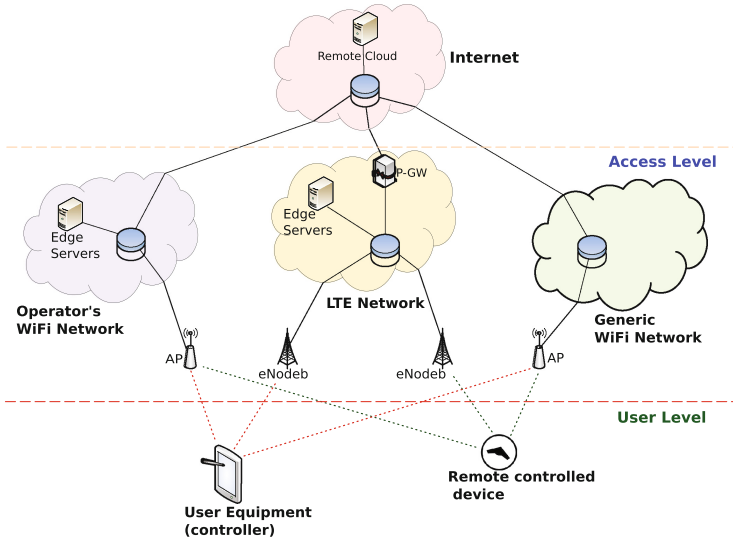


**Fig. 1.** Network architecture and topology enabling fog-computing capabilities in LTE and operator’s WiFi networks.

The range of jobs requested to be processed remotely depends on the scenario as well as on the required processing capabilities. Example of such remote jobs are the following: processing of raw data acquired by a robot, elaboration of digital media (pictures or videos) taken by a drone, object recognition, tasks that require external softwares and services of third-party companies. Moreover, there can also be latency constraints associated with some jobs, limiting them to be processed only at the edge instead of the cloud.

Taking into account the wide range of applications and the latency constraints, we define three classes of jobs as explained in Table 1. Class C jobs are typically the ones requiring third-party software or services, hence such jobs can only be executed in the cloud. Class E jobs can be executed only in the edge platform due to strict latency constraints. Finally, class H jobs are the ones with no latency constraints, so they can be run either in the cloud or in the edge platform.

**Table 1.** Job classification

JOBS CLASS	DESCRIPTION
C (Cloud)	Job can be executed only in the cloud
E (Edge)	Job can be executed only in the edge servers
H (Hybrid)	Job can run either in the cloud or in the edge servers

When a new job arrives, there may not be enough resources available to run the job and thus the offload allocation fails. This is denoted as *blocking event*.

### ***Offload Allocation Policies***

The allocation policy is responsible to choose where to run a particular job that must be offloaded, based on two possible options: either on the edge servers, or on the cloud. Based on our previous job classification, we consider only class H jobs, for which the allocation decision is not immediate. In our work we formulate the following four policies in order to handle class H jobs:

- *First Fit* (FF): Class H jobs are assigned to the edge servers as long as the resources are available, otherwise they are assigned to the external cloud. The idea is to exploit the resources in the edge servers as much as possible in order to minimize delays. As a consequence, the edge servers may become saturated, due to the limited resources, and cause blocking of class E jobs.
- *All Away* (AA): Class H jobs are allocated to the external cloud. The aim is to keep the resources, in the edge servers, available for class E jobs.
- *Load Based* (LB): Class H jobs are allocated to the external cloud only if the load on the edge servers is over 50 percent, otherwise they are executed in the edge servers.
- *Balanced Split* (BS): If the resources are available at the edge, class H jobs are allocated to the edge servers with 0.5 probability, otherwise they are allocated to the external cloud.

## **4 Performance Evaluation**

We developed an ad-hoc event-driven simulator in C language in order to compare the different offload allocation policies for a generic job arrival process.

The simulator was developed to capture the unique features of the proposed system model explained in Sect. 3. Based on the network architecture shown in Fig. 1, we deduced a simplified network topology, in which we associated a constant communication delay between any pair of entities involved in the communication process.

The workflow of the simulator is shown in Fig. 2. The first step is the random generation of a job that belongs to one of the classes defined in Table 1. In the simulations, we assume that all classes of jobs arrive with an equal probability, following a Poisson process. We also assume that the cloud has always enough resources to accommodate any number of jobs.

If the generated job belongs to class C, it is sent to the external cloud for execution. After the processing of the job, the results are delivered to the user. If the computation results reach the user within the job deadline, the job is *completed*, otherwise it is considered *failed*. If the generated job belongs to class E, the simulator checks the available resources in the edge servers. If not enough resources are available, the job is *blocked*. Otherwise, the job is sent to the edge servers and the results are sent back to the user, and checked if they satisfy the deadline. Lastly, in the specific case of class H job, the offload policy, chosen

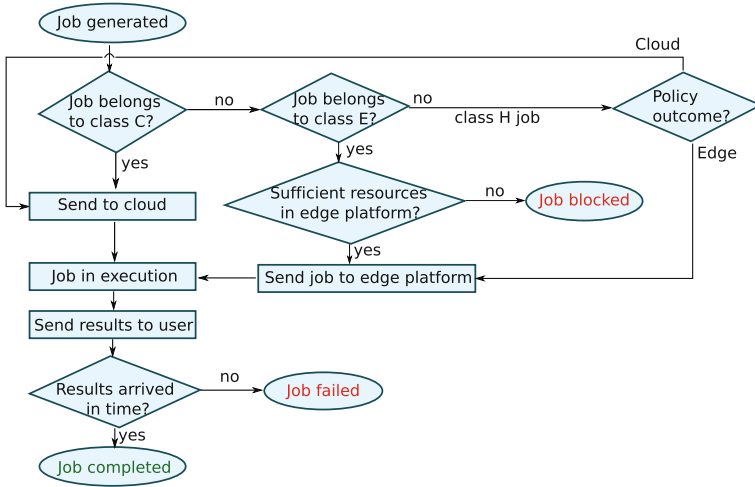


**Fig. 2.** Workflow of the simulator

among the four ones described in Sect. 3, determines whether the job should be executed in the edge platform or the cloud.

Table 2 describes all the set of the parameters used for our evaluation. The parameters are divided into three groups: network, edge platform and job related parameters. As shown in Fig. 1, the user devices are connected with the operator’s WiFi, LTE and the generic WiFi networks present in the access level. Each of the three networks presents a different access scenario characterized by different parameters. Therefore, we define the network parameters, such as delay, uplink rate and downlink rate, separately for each access network.

As mentioned, the jobs can be allocated either to the edge platform or the cloud. Differently from the cloud, equipped with unlimited computational resources, the edge platform is composed of a limited number of servers available in the LTE network and in the operator’s WiFi network. For each edge server, we define the number of virtual CPUs (VCPUs) and their processing capabilities.

Finally, we have the job related parameters which depend on the kind of task required to be processed. We assume a generic image processing job, where a user sends a raw image to the edge platform or the cloud and requests to send the processed image to the other user. The selected parameters in Table 2 reflect such choice.

Given an allocation policy, 5000 simulation runs are executed. In each run, the job arrival rate is increased, ranging from 1 to 5000 jobs per second. In addition, for each of the simulation parameters that takes a range of values in Table 2, we generate a uniformly distributed value in the considered range.

**Table 2.** Simulation Parameters

Parameter	Description	Value
NETWORK PARAMETERS		
LTE delay	LTE access and core network delay	5–9 ms
OP-WiFi delay	Operator’s WiFi access and network delay	10–20 ms
G-WiFi delay	Generic WiFi access and network delay	8–20 ms
Internet delay	Delay in a one way trip over the Internet	15 ms <sup>a</sup>
Tx G-WiFi	Uplink rate of the generic WiFi network	7.2 Mbps
Rx G-WiFi	Downlink rate of the generic WiFi network	20 Mbps
Tx LTE	Uplink rate of LTE network	3.3–5 Mbps <sup>b</sup>
Rx LTE	Downlink rate of LTE network	20–50 Mbps <sup>b</sup>
Tx OP-WiFi	Uplink rate of the operator’s WiFi network	3.2–4.4 Mbps
Rx OP-WiFi	Downlink rate of the operator’s WiFi network	8.8–9 Mbps
EDGE PLATFORM PARAMETERS		
Max servers	Number of edge servers	20
Max VCPUs	Number of VCPUs available on each edge server	10
VCPU speed	Processing speed of a single VCPU	1400 MIPS <sup>c</sup>
JOB PARAMETERS		
Job load	Processing requirements of a job	700 MI (million instructions)
Input size	Amount of data uploaded while requesting a job	3 MB
Output Size	Amount of data downloaded while receiving results	1.1 MB
Deadline	Maximum amount of time at disposal to process and deliver the job successfully	7 sec

<sup>a</sup>Verizon IP latency statistics. Available at: <http://www.verizonenterprise.com/about/network/latency/>

<sup>b</sup>Verizon offered speed on LTE. Available at: <http://www.verizonwireless.com/mobile-living/network-and-plans/4g-lte-speeds-compared-to-home-network/>

<sup>c</sup>Amazon m3.medium vcpu benchmark. Available at: <https://s3.amazonaws.com/cloudharmony/geekbench3.3.1.6/aws:ec2/m3.medium/ebs/sa-east-1/2014-11-12/2636/369105-9/geekbench.html>

## 4.1 Numerical Results

We start by comparing the four offload policies in order to find out the best policy among them. Then, we perform the server utilization analysis to evaluate the minimum number of servers required in the edge platform for a given job arrival rate.



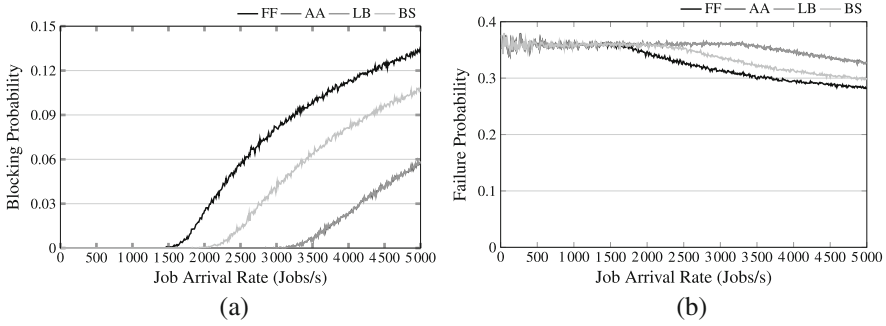


**Fig. 3.** Global blocking probability (a) and Global failure probability (b)

### Offload Allocation Policy Comparison

The allocation policies are compared in terms of their global blocking probability and global failure probability as shown in Figs. 3a and b respectively. The global blocking probability represents the fraction of *blocked jobs*, while the global failure probability represents the fraction of *failed jobs*, in the overall system. As a reminder, the First Fit (FF) policy allocates the class H jobs to the edge platform with a higher priority. This causes the edge servers to saturate sooner (in comparison to the other policies) and thus increasing the number of blocked jobs. However, since more jobs get executed at the edge, the number of failed jobs reduces. On the other hand, the All Away (AA) policy allocates all of the class H jobs to the cloud. As a consequence, the number of blocked jobs are reduced, but at the expense of the increase in the number of failed jobs. Therefore, AA and FF are the best policies in terms of global blocking probability and global failure probability respectively. The LB policy, which assigns jobs to the edge servers based on a given load, behaves similarly to AA for high load. Indeed, when the job arrival rate is high, the load of the class E jobs on the edge servers is high as well. Thus, almost all of the class H jobs are allocated to the cloud. The behavior of the BS policy remains in between FF and AA.

In order to find the overall best policy, we have computed the summation of global blocking and failure probabilities (i.e. 1 minus the probability that the job is completed) and based on this we have observed that AA policy is the best among all the other offload policies. Thus, for the following investigations we will consider only AA policy.

Figure 4 shows the blocking and the failure probabilities in LTE and WiFi networks. It is evident that the failure probability of WiFi networks is higher than that of LTE network, due to the fact that the overall delay of WiFi network is greater than the delay of LTE network. As a result, the processed jobs traversing WiFi networks are more likely to arrive after the deadline. In addition, the downlink rate of LTE is also higher as compared to that of the WiFi networks. Moreover, for low job arrival rate, the blocking probability is zero in both LTE and the WiFi networks. This is because there are sufficient resources available

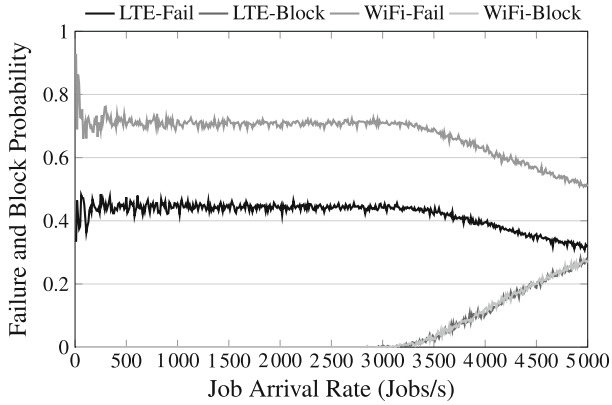


**Fig. 4.** Failure and blocking probabilities for LTE and WiFi networks for the All Away (AA) offloading policy

in the edge servers to accommodate class E jobs, while both class C and class H jobs are allocated to the cloud. Once the resources are exhausted, at a job arrival rate of about 3200 jobs/s, class E jobs begin to get blocked and the blocking probability starts to increase. This phenomenon decreases the failure probability as the blocked jobs do not consume additional network and computing resources, thus allowing more jobs that are executed in the cloud to arrive at the user device within the deadline.

### *Server Utilization Analysis*

This second part of results focuses on the server utilization in the edge platform. Our design aim is to quantify the number of servers required to sustain a given job arrival rate while maintaining the blocking probability under 1%. Here, we are only interested in the blocking probability as it depends on the capacity of the edge platform. The failure probability, on the other hand, depends mainly on the network performance. Our previous results have shown that AA policy outperforms the other policies in terms of blocking probability. However, to evaluate the worst case scenario, useful for a safe design of the edge platform, we consider the FF policy which gives the highest blocking probability, according to Fig. 3a.

We assume that the pseudo-sinusoidal traffic pattern during 24 h of a working day, as measured in [9], is followed by the job arrival rate, as shown in Fig. 5. In the figure, the job arrival rate is normalized to its peak value.

We evaluate the required number of edge servers in two different scenarios: a small community with few users and a peak arrival rate set at 1100 jobs/s; and a large community, similar to a city, with a large number of users and a peak arrival rate set at 100,000 jobs/s. Figure 6a shows the number of servers needed to satisfy the job requests at the blocking probability of 1% throughout the day for the small community scenario. In this case, the number of servers required

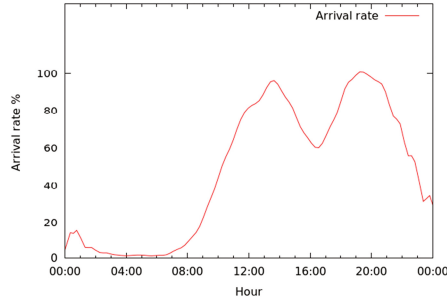


**Fig. 5.** Normalized arrival rate during 24 h of a working day

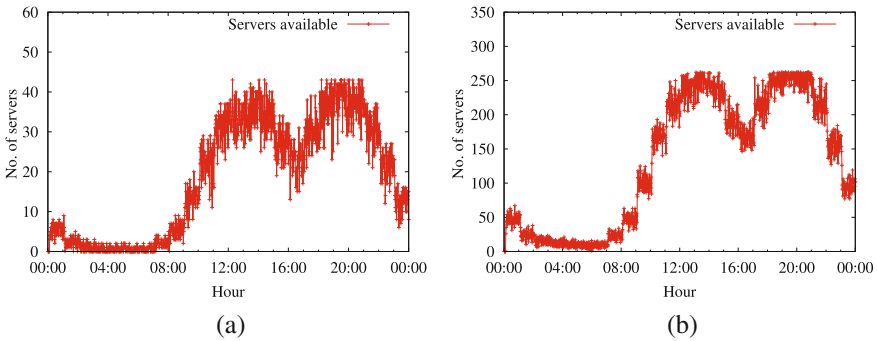


**Fig. 6.** Small community evaluation, blocking probability=1%, FF policy (a) and Large community evaluation, blocking probability=1%, FF policy (b)

at the peak hour is 43. Similarly, Fig. 6b shows the number of servers for the large community scenario. Here, the number of servers required at the peak hour is 262. It is worth to note the step behavior of the number of required servers, due to the policy that tends to consolidate the usage of the edge servers. Only when all the edge servers are saturated, then a new set of servers is activated to accommodate the new requests.

## 5 Conclusion

Enriching remote control applications with advanced capabilities can be highly expensive, in terms of required computational power and energy, for a resource constrained user device. Fog computing is a promising alternative to offload computationally expensive jobs away from the user device to the edge. In this paper, we present a network architecture where a communication infrastructure, based on LTE and WiFi networks, is equipped with fog and cloud computing platforms. We categorize the jobs to be offloaded specifically in the edge (E), cloud (C) or in both (H) according to their suitability. Moreover, we define a set of 4 offload policies to manage class H jobs. The All Away (AA) policy

outperforms the other policies in terms of the global blocking probability as it offloads all of the class H jobs to the cloud, thus decreasing the load on the edge servers. In terms of the global failure probability, the First Fit (FF) policy performs better than the other policies as it offloads the class H jobs at a higher priority to the edge servers, thus reducing the latency and meeting the deadline. Furthermore, we quantify the number of edge servers required to sustain a given job arrival rate while maintaining the blocking probability under 1%, in two scenarios, consisting of small and large communities.

## References

1. Aazam, M., Huh, E.N.: Fog computing micro datacenter based dynamic resource estimation and pricing model for IoT. In: IEEE International Conference on Advanced Information Networking and Applications (AINA), pp. 687–694 (2015)
2. Andrews, J.G., Buzzi, S., Choi, W., Hanly, S.V., Lozano, A., Soong, A.C.K., Zhang, J.C.: What will 5G be? IEEE J. Sel. Areas Commun. **32**(6), 1065–1082 (2014)
3. Asadpour, M., den Bergh, B.V., Giustiniano, D., Hummel, K.A., Pollin, S., Plattner, B.: Micro aerial vehicle networks: an experimental analysis of challenges and opportunities. IEEE Commun. Mag. **52**(7), 141–149 (2014)
4. Balasubramanian, A., Mahajan, R., Venkataramani, A.: Augmenting mobile 3G using WiFi. In: 8th International Conference on Mobile Systems, Applications, and Services, MobiSys, pp. 209–222. ACM (2010)
5. Bonomi, F., Milito, R., Natarajan, P., Zhu, J.: Fog computing: a platform for Internet of Things and analytics. In: Big Data and Internet of Things: A Roadmap for Smart Environments, pp. 169–186. Springer (2014)
6. Bonomi, F., Milito, R., Zhu, J., Addepalli, S.: Fog computing and its role in the Internet of Things. In: 1st Workshop on Mobile Cloud Computing, MCC, pp. 13–16. ACM (2012)
7. Chen, M., Hao, Y., Li, Y., Lai, C.F., Wu, D.: On the computation offloading at ad hoc cloudlet: architecture and service modes. IEEE Commun. Mag. **53**(6), 18–24 (2015)
8. Fiandrino, C., Kliazovich, D., Bouvry, P., Zomaya, A.Y.: Network-assisted offloading for mobile cloud applications. In: IEEE International Conference on Communications (ICC), pp. 5833–5838 (2015)
9. Hohwald, H., Frías-Martínez, E., Oliver, N.: User modeling for telecommunication applications: experiences and practical implications. In: International Conference on User Modeling, Adaptation and Personalization, pp. 327–338. Springer (2010)
10. Kehoe, B., Patil, S., Abbeel, P., Goldberg, K.: A survey of research on cloud robotics and automation. IEEE Trans. Autom. Sci. Eng. **12**(2), 398–409 (2015)
11. Kumar, K., Lu, Y.H.: Cloud computing for mobile users: can offloading computation save energy? Computer **43**(4), 51–56 (2010)
12. Mach, P., Becvar, Z.: Mobile edge computing: a survey on architecture and computation offloading. IEEE Commun. Surv. Tutorials (2017)
13. Malandrino, F., Chiasserini, C., Kirkpatrick, S.: The price of fog: a data-driven study on caching architectures in vehicular networks. In: 1st International Workshop on Internet of Vehicles and Vehicles of Internet, IoV-VoI, pp. 37–42 (2016)
14. Ragona, C., Granelli, F., Fiandrino, C., Kliazovich, D., Bouvry, P.: Energy-efficient computation offloading for wearable devices and smartphones in mobile cloud computing. In: IEEE Global Communications Conference (GLOBECOM), pp. 1–6 (2015)

15. Rouanet, P., Oudeyer, P.Y., Danieau, F., Filliat, D.: The impact of human-robot interfaces on the learning of visual objects. *IEEE Trans. Rob.* **29**(2), 525–541 (2013)
16. Sarkar, S., Chatterjee, S., Misra, S.: Assessment of the suitability of fog computing in the context of Internet of Things. *IEEE Trans. Cloud Comput.* (2015)
17. Sciarrone, A., Fiandrino, C., Bisio, I., Lavagetto, F., Kliazovich, D., Bouvry, P.: Smart probabilistic fingerprinting for indoor localization over fog computing platforms. In: 5th IEEE International Conference on Cloud Networking (CloudNet), pp. 39–44 (2016)
18. Simsek, M., Aijaz, A., Dohler, M., Sachs, J., Fettweis, G.: 5G-enabled tactile internet, pp. 460–473 (2016)
19. Wang, S., Zhang, X., Zhang, Y., Wang, L., Yang, J., Wang, W.: A survey on mobile edge networks: convergence of computing, caching and communications. *IEEE Access* **5**, 6757–6779 (2017)

**The 11th International Workshop  
on Engineering Complex Distributed  
Systems (ECDS-2017)**

# Dynamic MAC Protocol Designed for UAV Collision Avoidance System

Xiao Ou Song<sup>(✉)</sup>

Engineering University of CAPF, Xi'an, Shanxi, China  
e\_miracle@163.com

**Abstract.** During the formation flight of Unmanned Aerial Vehicles (UAVs), avoiding collision with intruders and other UAVs is very important. A key technique of collision avoidance is the real-time delivery of risk related warning messages among UAVs. In UR-MAC, a frame is composed of contention slots and transmission slots. When there is no warning message, each UAV accesses the channel like a TDMA protocol. Otherwise, the warning messages can contend to occupy any already assigned transmission slot. The UAV with higher emergency level has shorter waiting time to claim to occupy the coming transmission slot. Then the other UAVs choose the proper maneuvers to avoid the forthcoming collisions. The simulation results show that the UR-MAC efficiently reduces the delivery latency of warning messages and the collision probability in a UAV formation.

## 1 Introduction

Flying ad hoc network (FANET) [1] has received considerable attention around the world. FANET can provide various safety-related services. As a typical representation, cooperative collision avoidance systems have been studied in the past years [2], which helps to reduce the probability of aircrafts collisions and the corresponding damage significantly. To facilitate safety applications in UAV formation, the collision avoidance techniques have significantly evolved recently. The collision avoidance in UAV formation involves two parts: The first one is gathering the information of the surrounding UAVs and other mobile obstacles; the second one is making the optimal maneuver to avoid the collision and notifying the other UAVs. We assume that every UAV is equipped with Electro-Optic sensors [3] to sense the intruders, and the UAVs can exchange speed and position information through warning messages. UAVs flying in formation use the warning messages transmitted through UR-MAC protocol to maintain a safe distance between each other.

Many priority based MAC protocols has been proposed to transmit the delay sensitive data in time. Z-MAC [4] combines the advantage of CSMA's low latency under low throughput and TDMA's high channel utilization under high throughput. A series of priority based MAC mechanisms are proposed to enable traffic with higher priority to hijack the transmission bandwidth of the traffic with lower priority. Alert [5] is a priority based FDMA protocol to collect the event-triggered urgent messages from a

group of sensor nodes with minimum latency. Priority MAC [6] classifies the traffic into four different priorities. The lowest two type of traffic use TDMA method to access the channel, and the highest two type of traffic not only use the TDMA method but also the CSMA method to access the channel. However, we did not find any paper involved in how to classify the messages into different priority for UAV formation collision avoidance system. In the domain of collision avoidance system, the vehicular MAC protocols [7, 8] have already been evolved significantly compared to UAV MAC protocols. Fortunately, the MAC protocols in collision avoidance systems of vehicles and UAVs share something in common. R-MAC [9] is a protocol tailored for vehicular cooperative collision avoidance applications. R-MAC uses TDMA segment to transmit beacons and CSMA segment to transmit warning messages. C-RACCA [10] is a cluster based risk-aware cooperative collision avoidance system for vehicles. C-RACCA includes an IEEE 802.11 based MAC protocol in which the medium-access delay of each vehicle is set as a function of its emergency level. The C-RACCA MAC ascertains that the vehicles with high probability of meeting an emergency situation should enjoy short contention windows. A number of other MAC protocols designed for delay sensitive application can be found in [11], where mission-critical applications are defined as applications demanding data delivery bounds in the time and reliability domains. But none of the MAC protocols is specially designed for UAV formation collision avoidance.

This paper proposes a priority based MAC protocol designed both for delay sensitive traffic and delay tolerate traffic in UAV collision avoidance system. The delay of the unpredictable and emergency traffic generated from the collision avoidance system would lead to a mass in the UAV formation. Moreover, the delay may result in collisions under some severe conditions. To overcome these shortcomings, we study efficient delivery of different messages in automatic collision avoidance system of UAV formation. Delay sensitive traffic is the warning messages triggered by UAVs which experience a hazard or collisions. And the delay sensitive traffic should be propagated to surrounding UAVs as soon as possible to inform them of the forthcoming collision. So the delay sensitive traffic has a higher priority compared with delay-tolerate traffic, and should be sent earlier than the delay-tolerate traffic. UAVs involved in collision avoidance may make maneuvers simultaneously to avoid collision, which leads to an undesired chain reaction in the formation, especially in close formation flight. So the UAV with more emergency should make a maneuver first and send its warning message first. To the best of our knowledge, UR-MAC is the first priority based MAC protocol compatible with UAV formation collision avoidance system. This paper is organized as follows. In Sect. 2, we briefly review the model of network, mobility and collision avoidance. In Sect. 3, we offer the details UR-MAC, including the frame structure, emergency calculation, and the contention schemes. In Sect. 4, the results of our study are presented, dealing with the comparison of warning messages delivery latency and probability of collisions. In Sect. 5 we conclude by noting that UR-MAC is an efficient protocol to deliver the warning messages in time and reduce the collisions probability.



## 2 The System Model

### 2.1 Network and Mobility Model

We assume that there are  $N$  UAVs in a single formation. In the formation, every UAV is in the communication range of the other ones. So there is no hidden terminal. Each UAV is equipped with satellite navigation system, so the coordination and the velocity information are obtained by each UAV. The UR-MAC protocol is applied to the scenario that one or more intruders rush into the UAV formation.

We assume that every UAV maintains its flight height if no intruder is detected. The UAVs won't change their moving state unless the collision avoidance maneuvers are taken. If  $n_k$  finds that it is going to collide with  $n_i$ , it has two choices to avoid the collision. One solution is  $n_k$  making a roll maneuver and another one is  $n_k$  making a pitching maneuver. In fact, some kinds of fixed-wing UAVs can make more complex maneuvers to avoid the collision, which combines roll maneuver, pitching maneuver, and acceleration or deceleration. But the complex maneuvers are liable to incur accidents under adverse airstream condition. Moreover, some kinds of UAVs are not designed with highly dynamic maneuvers characters. So we only consider the case of roll maneuver or pitching maneuver to avoid a collision.

### 2.2 Collision Avoidance Model

## 3 System Overview

### 3.1 The Dynamic Slots Allocation Scheme

Applying the IEEE 802.11 MAC protocol [12], a node first listens to the channel if it wants to transmit. If the channel is idle (no active transmitters), the node is permitted to transmit. Otherwise, the node will defer its transmission and uses a binary exponential backoff scheme to randomize the start time of transmissions. However, this backoff scheme significantly increases the data delivery latency. Consequently, when transmitting the delay sensitive critical warning messages, the effectiveness of the original 802.11 MAC protocol decreases substantially. The high latency in the transmission of a warning message will lead to scenarios that some UAVs will not have enough time to avoid the forthcoming collision.

The medium access control protocols of the UAV formation need to make sure that the access delay remains as short as possible in emergent scenario. Specifically tailored for UAV formation environments, we propose an effective collision avoidance scheme. There are two kinds of traffic with different priority. One type of traffic is delay-tolerate ordinary data, called M1. Another type of traffic is delay sensitive collision warning messages, called M2. M1 is the traffic class of lower priority, which aims at providing delay-tolerate service. M2 is the traffic class of higher priority, which aims at providing timely warning messages for collision avoidance maneuvers. Due to its unpredictability, it should not be scheduled using the TDMA protocol. A UAV prioritizes the packets in

its output buffer: the packet with the higher priority in the buffer shall be transmitted firstly, whereas the other packets in the buffer have to wait for next slot assigned to the UAV. UR-MAC enables high-priority traffic to defer the lower priority traffic.

M1 uses the TDMA protocol to access the wireless medium. M2 uses a hybrid protocol involving CSMA and TDMA techniques to access the wireless medium. M1 traffic is allowed to transmit only at its assigned transmission slot. Before M1 traffic transmission, the channel should be listened. If the channel keeps idle during the contention slot, M1 is allowed to transmit. Otherwise, it has to wait to the next assigned transmission slot. A busy-channel case is caused by higher priority traffic M2.

When a UAV has M2 data to transmit, it will contend to occupy the forthcoming transmission slot, even if the slot belongs to another UAV. In the formation there are many UAVs, each UAV will make its maneuvers to avoid the forthcoming collision and send warning messages. The warning messages include position and speed vector. So there are more than one UAV to generate M2 traffic. In order to reduce the media access collisions, a dynamic contention window based CSMA scheme is proposed.

### 3.2 The Dynamic Slots Allocation Scheme

In the contention stage, UR-MAC sets the medium-access delay of an individual UAV's M2 data as a function of its emergency level. This strategy attempts to guarantee that the most likely colliding UAV has the shortest delivery latency. This feature can prevent the chain collisions and reduce the associated damage. So the emergency level should be calculated firstly by researching the maneuver patterns of collision avoidance.

The coordination of  $n_k$  is  $(x_k, y_k, z_k) = (0, 0, 0)$ , the coordination of  $n_i$  is  $(x_i, y_i, z_i)$ , the velocity of  $n_k$  is  $(v_{kx}, v_{ky}, v_{kz}) = (0, v, 0)$  and the velocity of  $n_i$  is  $(v_{ix}, v_{iy}, v_{iz})$ . In the collision instance of Fig. 1, we seem the intruder  $n_i$  as static, and  $n_k$  as moving with relative speed  $(v_{ix}-v_{kx}, v_{ix}-v_{kx}, v_{ix}-v_{kx})$ . This scheme simplifies the calculation.

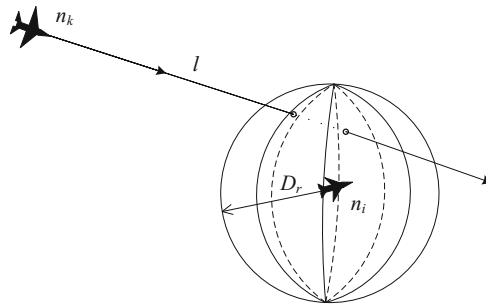


**Fig. 1.** A collision instance between two UAVs is illustrated. We assume that each UAV has collision sphere zone with radius  $D_r$ , as depicted in this figure. When the distance between two UAVs is less than  $D_r$ , Near Mid-Air Collision occurs.

**Emergency calculation.** The time from the beginning to the end of roll maneuver is very short compared to that of pitching maneuver. The rate of climb and the rate of

descending in pitching maneuver are limited by the dynamic performance of the UAVs. So the pitching maneuver is a slow process.

If a UAV make a roll maneuver, its emergency is proportional to the maneuver time. That is because the longer the maneuver time is, the harder a UAV can avoid a collision.

The formation rule set the maximum  $a$  is  $\pi/2$ . So the normalization of the emergency level for roll maneuver is as shown in (1).

$$E_r = \frac{2a}{\pi} \quad (1)$$

If a UAV makes a pitching maneuver, its emergency is proportional to absolute value of its  $v_{kz}$ . The higher  $|v_{kz}|$  is, the harder a UAV can avoid a collision. So the normalization of the emergency level for pitching maneuver is as shown in (2).

$$E_p = \frac{|v_{kz}|}{v_p} \quad (2)$$

$v_p$  is the maximum descending speed. The final emergency level of a UAV is express as:

$$E = \min(E_x, E_p) \quad (3)$$

UAV in the formation treats other UAVs as intruders to avoid collisions. If an intruder rushes into the UAV formation and  $n_k$  is the first UAV that makes a maneuver to avoid the forthcoming collision with the intruder, the maneuver of  $n_k$  will bring a chain of reactions to other UAVs in the formation to avoid the potential collisions caused by  $n_k$  and the intruder. The consequent maneuvers of other UAVs would cause more maneuvers until all of the UAVs are safe.

If  $n_k$  makes a pitching maneuver, the other UAVs treat  $n_k$  as an ordinary intruder. If  $n_k$  makes a roll maneuver, the reaction of the other UAVs should follow the following steps.

When  $n_k$  makes a roll maneuver, its flying path is part of a circle before the bank angle of  $n_k$  returning to zero at position  $s$ . Actually, the circle radius is much longer than the curved path. So we use the beeline between the position that  $n_k$  starts a roll maneuver and position  $s$  as  $n_k$ 's moving path. This approximation can simplify the collision avoidance calculation with little accuracy loss. Then  $n_k$  can be treated as an ordinary intruder by other UAVs.

If there is only one intruder, the maneuver time can be calculated following the steps illustrated in Fig. 2. If there is more than one intruder, a UAV has different schemes to avoid the collisions with different intruders. A UAV is only able to choose a single maneuver at the same time. When there is more one intruder, a UAV calculates the emergency of all the four schemes: left turn roll maneuver, right turn roll maneuver, climb pitching maneuver and descent pitching maneuver. Calculated as (1) and (2), the corresponding emergency of the above schemes is  $E_{r_l}$ ,  $E_{r_r}$ ,  $E_{p_c}$  and  $E_{p_d}$ , respectively. For each maneuver scheme, the maximum emergency of all the intruders is reserved in the end. For a maneuver scheme, only the maneuver corresponding to the maximum emergency can avoid all the collisions. At last, the minimum emergency  $E_f$  to avoid all

the collisions is the minimum reserved emergency of all the four maneuver schemes. The maneuver corresponding to emergency  $E_f$  is the optimal maneuver to avoid all the collisions.

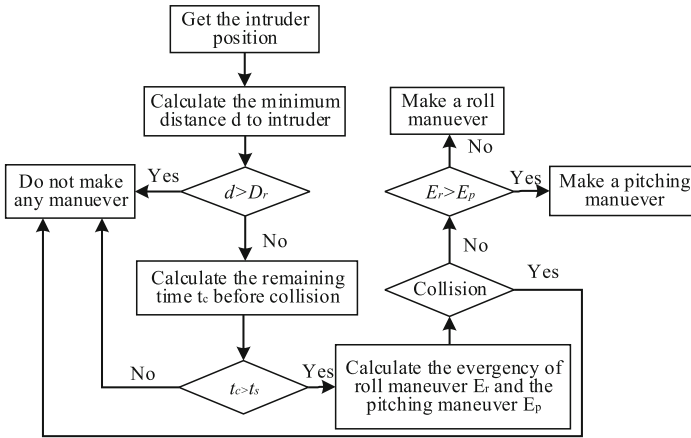


**Fig. 2.** The steps required for collision avoidance is illustrated. A UAV can detect an intruder by its own airborne sensors or being informed by other UAVs through wireless communication. When a UAV  $n_k$  in the formation finds an intruder, it calculates the minimum distance  $d$  to the intruder if both of them don't change their current moving status. If  $d > D_r$ , the intruder is far enough that no collision will happen. Otherwise,  $n_k$  will collide with the intruder if no maneuver is taken. Then  $n_k$  calculates the remaining time  $t_c$  before collision. If  $t_c$  is longer than a predefined threshold  $t_s$ , it means that the moving status of the UAV will change before the collision. In this case,  $n_k$  need not make any maneuver. If  $t_c < t_s$ ,  $n_k$  should make a roll maneuver or a pitching maneuver to avoid the forthcoming collision. By the algorithm proposed in Sect. 3.2 of this paper, the emergency level of roll maneuver and pitching maneuver are calculated respectively. If the emergency level of roll maneuver is larger than pitching maneuver,  $n_k$  chooses to make a pitching maneuver. Otherwise,  $n_k$  chooses to make a roll maneuver.

**The contention window calculation.** Suppose the length of contention slot is  $l_c$  and the length of transmission slot is  $l_t$ . In our proposed UR-MAC protocol, when transmitting the warning messages (M2 traffic), the contention window of a given UAV  $n_k$  is computed based on the following equation:

$$CW = [t + l_c - \beta E_f - \Delta, t + l_c - \beta E_f + \Delta] \tag{4}$$

where  $t$  is the start time of a contention slot in Fig. 3,  $\beta$  is a constant factor,  $\Delta$  is a constant value,  $CW = [t, t + l_c]$

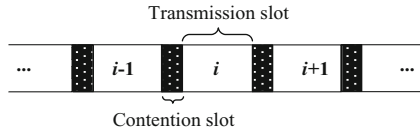


**Fig. 3.** The dynamic slots allocation scheme is illustrated. In the UAV formation, each UAV is assigned a time slot to transmit data. A contention slot is inserted before every transmission slot in this figure. All the contention slots and transmission slots compose a time frame. The length of transmission slot is 10 ms, and the contention slot is 1 ms.

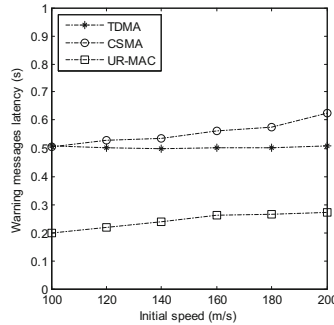


**Fig. 4.** The average warning message delivery latency for different initial speed of UAVs is depicted. It can be deduced from this figure that the average warning message delivery latency increases when the initial speed of UAVs in the formation increases using the CSMA and UR-MAC protocols.

When a UAV avoids a forthcoming collision by making a maneuver, it should immediately broadcast its detailed maneuver messages to other UAVs. The emergency of these messages are calculated according to Sect. 3.2 of this paper. If the emergency of these messages is  $E_f$ , the UAV should send a RTS message at a random time in CW according to (4). The first UAV that sends the RTS message will occupy the corresponding transmission slot. If another UAV’s warning message’ emergency level is less than the first UAV, it will not make any maneuver, then, it recalculates its emergency level and contends in the next transmission slot.

### 4 Simulation Results

In order to verify the effectiveness of our proposed MAC protocol, numerical simulations are performed. In the simulation, a group of UAVs move towards a same target from their initial airspace. The diameter of the initial airspace that the UAVs are deployed is 1000 m. The UAVs are deployed in the initial airspace randomly, and the distance between any two UAVs is further than 100 m. When simulating the scenarios that an intruder is rushing into a UAV formation from different directions 1000 times.

In the simulation, the horizontal speed of all the UAVs is constant, and the vertical speed of the UAVs varies from 0 to  $V_p$ . The initial center and the target position have

the same altitude. When the simulation starts, the moving vector of each UAV is the same as the vector between center of the initial airspace and the target position, which means that each UAV flies horizontally at first. Since the maximum detection range of the sensors is about 3 km for an intruder with size dimension 5 m [13], an intruder will not be detected until its distance to a UAV is less than 3 km.

As comparison terms, we use CSMA and TDMA protocols. The CSMA protocol is based on IEEE MAC protocol that uses the exponential back-off algorithm to calculate contention windows of the UAVs. The length of a slot in TDMA protocol is equal to the sum of the contention slot length and the transmission slot length in the UR-MAC.

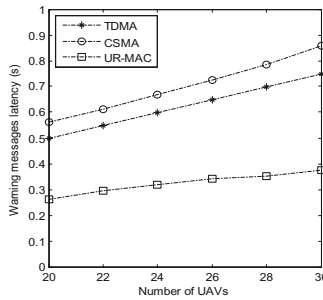


**Fig. 5.** The average warning message delivery latency for different number of UAVs is depicted. It can be deduced from this figure that the average warning message delivery latencies of TDMA, CSMA and UR-MAC protocols increases when the number of UAVs in the formation increases. The number of collisions for various initial speeds in the case of CSMA, TDMA and the proposed UR-MAC protocols are plotted in Fig. 6.

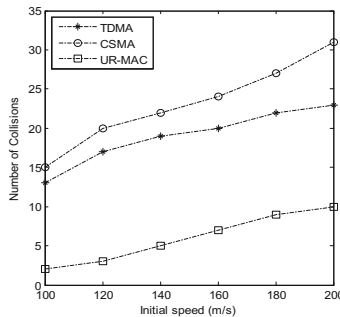


**Fig. 6.** The number of collisions for various initial speeds in the case of CSMA, TDMA and the proposed UR-MAC protocols is showed. It can be deduced that the number of collisions increases as the initial speed increases when the above three protocols are adopted. That is because when the initial flying speed increases, the reacting time for the UAVs to avoid collisions decreases. When the CSMA protocol is used, the collision number is biggest. That is because the warning messages delivery latency is longest among the three protocols in Fig. 4. The longer the warning messages delivery latency is, the more likely a UAV can't make the optimal maneuver in time to avoid the forthcoming collisions. The results demonstrate that the proposed UR-MAC scheme helps reduce the collisions significantly compared to the traditional TDMA and CSMA protocols.

The priority based scheme enables a UAV to prioritize packets in its output buffer: the M2 traffic packets have higher priority in the buffer and should be transmitted firstly, whereas M1 traffic packets in the buffer would have to wait for future slots assigned to this UAV.

Corresponding to Fig. 5, the longer the warning messages delivery latency is, the more collisions will come. The results demonstrate that the proposed UR-MAC scheme helps reduce the collisions significantly compared to the traditional TDMA and CSMA protocols when the number of UAVs increases (Fig. 7).

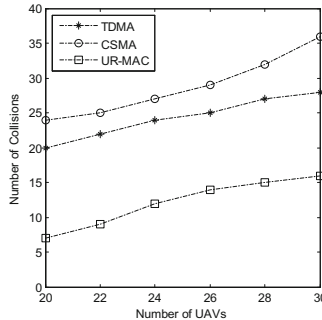


**Fig. 7.** The number of collisions for different number of UAVs is depicted. It can be deduced that the number of collisions increases as the number of UAVs in the formation increases when using TDMA, CSMA and UR-MAC protocols. That is because when the number of UAVs increases, the interval distances among the UAVs decreases, which reduces the space for collision avoidance maneuver.

## 5 Conclusions and Future Work

This paper proposes a specially designed dynamic MAC protocol, UR-MAC, to facilitate the collision avoidance system. The priority based scheme of UR-MAC confirms the timely delivery of the warning messages. The contention window of each UAV is calculated according to the emergency level. UR-MAC protocol let the most likely colliding UAV make a maneuver firstly, which efficiently reduces the collision probability when an intruder is rushing into the formation. The simulation results show that UR-MAC protocol reduces the warning messages latency and the collision number. So UR-MAC is an efficient MAC protocol to enhance the performance of UAV collision avoidance system. In the future work, we want to calculate the contention window based on more complex collision avoidance maneuvers.

## References

1. İlker, B., Ozgur, K.S., Şamil, T.: Flying Ad-Hoc networks (FANETs): A survey. *J. Ad Hoc Networks* **11**(3), 1254–1270 (2013)
2. Sarena, B., Takeo, F.: Learning-based p-persistent CSMA for secondary users of cognitive radio networks. *J. Space-Based Situated Comput.* **3**(2), 102–112 (2013)

3. Tetsuya, S., Junko, N.: DCR-MAC: a data channel recommending MAC for multi-channel WLANs toward the higher throughput performance. *J. Grid Util. Comput.* **5**(3), 168–177 (2015)
4. Injong, R., Ajit, W., Mahesh, A., et al.: Z-MAC: a hybrid MAC for wireless sensor networks. *J. IEEE/ACM Trans. Networking* **16**(3), 511–524 (2008)
5. Tetsuya, S., Junko, N.: DCR-MAC: a data channel recommending MAC for multi-channel WLANs toward the higher throughput performance. *J. Space-Based Situated Comput.* **5**(3), 168–177 (2015)
6. Wei, S., Tingting, Z., Filip, B., Mikael, G.: Priority MAC: a priority-enhanced MAC protocol for critical traffic in industrial wireless sensor and actuator networks. *J. IEEE Trans. Ind. Inform.* **10**(1), 824–835 (2014)
7. Biswas, S., Tatchikou, R., Dion, F.: Vehicle-to-vehicle wireless communication protocols for enhancing highway traffic safety. *J. IEEE Commun. Mag.* **44**(1), 74–82 (2006)
8. Palazzi, C.E., Rocchetti, M., Ferretti, S.: An intervehicular communication architecture for safety and entertainment. *J. IEEE Trans. Intell. Transp. Syst.* **11**(1), 90–99 (2010)
9. Weijie, G., Liusheng, H., Long, C., et al.: R-MAC: risk-aware dynamic MAC protocol for vehicular cooperative collision avoidance system. *J. Distrib. Sens. Networks* **9**(5), 1–14 (2013)
10. Tarik, T., Abderrahim, B., Khaled, B.: Toward an effective risk-conscious and collaborative vehicular collision avoidance system. *J. IEEE Trans. Veh. Technol.* **59**(3), 1474–1486 (2010)
11. Petcharat, S., Utz, R., Andrew, S.: A survey of MAC protocols for mission-critical applications in wireless sensor networks. *J. IEEE Commun. Surv. Tutorials* **14**(2), 240–264 (2012)
12. IEEE. IEEE Standard for Wireless LAN Medium Access Control (MAC) and Physical Layer (PHY) Specifications (1999)
13. Giancarmine, F.: Multisensor based fully autonomous non-cooperative collision avoidance system for UAVs. Unpublished master's thesis, Italy (2009)



# A Method for Estimating the Camera Parameters Based on Vanishing Points

Wan Fang, Li HaiNing, Jin HuaZhong<sup>(✉)</sup>, Lei GuangBo,  
and Ruan Ou

Hubei University of Technology, Wuhan, China  
devwaf@qq.com, galaxy0522@163.com

**Abstract.** This paper presented MMVD vanishing points detection algorithm which was inspired by multi-model estimation. It was operated in image pixel space, not parameter space. We first gave some vanishing points estimation model assumption based on the lines' position and angle of each other. Then, the model assumption was used to construct the correlation matrix for line segments clustering and vanishing points estimation. Clustering algorithm produced vanishing points and they were refined by the EM algorithm to improve the accuracy. Experiments showed that the detection speed was good and the detection result can ensure good accuracy.

**Keywords:** Multi-model · EM · Clustering · Vanishing point

## 1 Introduction

In graphical perspective, a vanishing point was a point in the picture plane that was the intersection of the projections (or drawings) of a set of parallel lines in space on to the picture plane. When the set of parallels was perpendicular to the picture plane, the construction was known as one-point perspective and their vanishing point corresponds to the oculus or eye point from which the image should be viewed for correct perspective geometry.

Based on the vanishing point, we could calibrate the camera. But there were two key problems. One was the detection of vanishing point. The precision of vanishing point directly determined the accuracy of camera calibration. If the point accuracy was not high, it could lead to camera calibration error. On the other hand, computation efficiency was crucial. Only the fast vanishing point detection method could be used for real-time large-scale 3d reconstruction, but most of the existing vanishing point detection algorithms were unable to meet the requirements. Bazin [1] said, in the past 30 years, although a lot of research was carried out, but no one was completely satisfactory, the difficulty was that this was a pathological problem. For example, the iterative detection algorithm of vanishing point often produced local minima, the orthogonality calculation of vanishing point was complex, and the data may contain a large number of outliers and so on. Even so, because the camera self-calibration could provide an automatic way to obtain the initial position and orientation of the camera which was valuable for image-based 3d reconstruction, the rapid detection of vanishing point had been highly valued by researchers.

## 2 Related Research

Caprile was first to use vanishing point to calculate the main point and rotation matrix [2], many researchers carried out related work, but they all assumed that part of camera parameters were known. Haralick [3] did not directly use vanishing point, using a rectangular projection in the image. Wilczkowiak [4] used the relationship between parallel lines to estimate projection matrix, whose essence was using of vanishing point calibration. Chen [5] used a uniform grid on the assumption that the focal length was known, which was the equivalent of artificial designated two vanishing point direction. These methods have the requirements of constraint conditions, which are specified in a single image by hand.

Recent year, Orghidan [6], Lopes [7] and Dong [8] used structured light features to calibrate the camera, indirectly used vanishing points. Wang [9] used a hexahedral as the calibration target to generate vanishing line. These vanishing lines contained effective geometric constraint information for the calculation of camera direction and focal length, but this calibration condition was too strict. Grammatikopoulos [10] used multiple images, each of which was calibrated by the internal reference of the camera. Using the direct geometric reasoning method, the absolute quadric curve was used in essence. Because only two vanishing points existed on multiple images, his algorithm could be addressed to the polygon like objects. Similarly, in the method of Stevenson [11], the calibration equation was simplified by motion control of multiple cameras.

These calibration methods basically needed constraint conditions such as camera moving track, or some manually specified marks in the image. In fact, the geometrical characteristic of structured 3d scene in images itself could provide similar constraints for camera calibration.

## 3 MMVD Algorithm

LSD [12] proposed a method of line segment detection which could provide linear time complexity, and the error rate was very low. We took it to help detect line segments.

In this paper, according to the features of 3D scene structure, we put forward a MMVD vanishing point detection algorithm for multi-model estimation. Multi-model estimation method was inspired by Toldo [13]. The workflow of the algorithm was as described:

- (1) Construction of line subset and vanishing point model hypothesis
- (2) Compute a Correlation matrix
- (3) Line segments clustering and vanishing point estimation
- (4) EM optimization

The following sections will focus on the process of each step to describe the algorithm in detail. Here it was some definitions used in the algorithm:

$L$  denoted an array of line segments detected by line segments,  $L_s$  denoted a line subset of  $L$ , and was a collection of line segments used for vanishing point estimation.  $e_n$  signified the detected  $n$  segment,  $e_n^s$  denoted the starting point coordinate of line

segment  $n$ ,  $e_n^e$  denoted the end coordinates of the line segments  $n$ , and  $e_n^m$  denoted the midpoint coordinates of line segment  $n$ .

### 3.1 Construction of Line Subset and Vanishing Point Model Hypothesis

Model hypothesis was only the initial value which would be modified in repeated calculation. Original line segments set we named it  $L$ , which usually contained a lot of external data or error data, so line subset was to be constructed to remove these data points. Vanishing point model hypothesis was also built from this subset.

SampleSetConstruct algorithm was described as followed:

---

```

Input: L parameters: M (vanishing point count)
Output: Ls, lineSeg[] and VP[] (M) initial vanishing point
estimation
1  foreach line l in LineSegAll[] do
2      for(i=0;i++;i<M )
3          if lineSeg[i].size<size then
4              addLineSeg(lineSeg[i]); //find the nearest line
5          else
6              ModelHypothesis(lineSeg[i]) //generate VP
7              endif
8      endfor
9  endfor

```

Size of  $L_s$ (line segments) was  $N$ . Assuming that there were  $M$  vanishing points estimations, then the algorithm traversed in  $L$  space. Each two line segments formed a minimum sampling set  $lineSeg[i]$ , and estimated a vanishing point. Model Hypothesis calculated intersection of line pair, as the model hypothesis of vanishing point. We could think that the hypothesis was not accurate, but it had a theoretical basis to be an initial value, which was the spatial relationship of line segment and vanishing point. Sample Set Construct could find pair for each line segment, unless it was obviously an outlier. Figure 1 described the process of constructing the model hypothesis and vanishing point line subset.

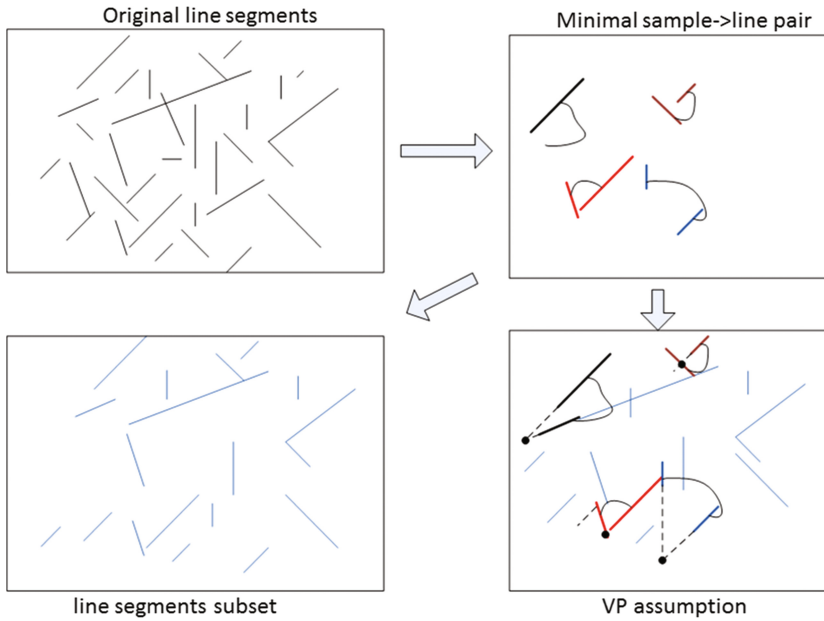


**Fig. 1.** From the original line segments, we can easily classify them into one-one pair form, so, each pair had two lines and became the start of clustering. From now on, line subset and model hypothesis of vanishing point was constructed iteratively.

### 3.2 Correlation Matrix

Correlation matrix determined the correlation of  $L_s$  and  $M$  vanishing points, which constructed a consistency metric relation. Set center line of  $v_m$  and  $e_n$  as  $l_n$ , we should compute the angle between the reference line  $l_n$  and line segment  $e_n$ . If  $\theta$  was greater than a certain threshold, we asserted that there was no correlation between line and vanishing point (Fig. 2).

$$\theta(e_n, l_n) = \arccos \frac{e_n \cdot l_n}{|e_n||l_n|} \tag{1}$$

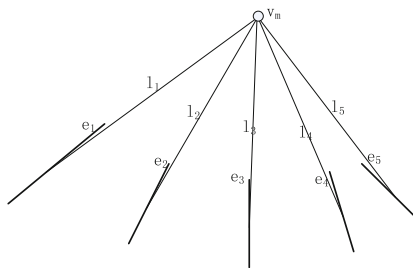


**Fig. 2.** We used reference line to estimate relationship between  $v_m$  and  $e_n$

In the correlation matrix  $R_{N \times M}$ , each row were  $N$  segments of the subset  $L_s$ , column represented  $M$  models of vanishing point. Each element of matrix was valued as the correlation degree:

$$R_{N \times M} = R(v_m, e_n) \quad (2)$$

When the correlation matrix built, hypothesis of position of vanishing point obtained support on numerical value and relationship between vanishing point and line segment formed a good initial state of clustering iteration. Next was the clustering and estimation.

### 3.3 Line Segments Clustering and Vanishing Point Estimation

When the initial state of clustering was ready, in this step, the main work was to cluster the line in `RelateMatrix`, and generate vanishing point estimation for each cluster. Obviously, this was an iteration process. Vanishing point hypothesis in previous section could be modified. Clustering method decided which line belong to which class and also decided the result of vanishing point. In the clustering process, we used Jaccard [14] distance to classify the data. At the end of the iteration, the distance between all line segments is less than the specified threshold  $D$ .

Then it was to estimate vanishing point of each cluster. Line segment clustering of each step resulted in the estimation value of a multi-model. Each model corresponded to a vanishing point direction. Calculation formula according to the distance of the vanishing point was as followed:

$$v_j = \operatorname{argmin} \sum_{i,j=(1..m)} d(e_i, vp_j) \quad (3)$$

The formula meant that for the cluster, the point could be the vanishing point because it had the minimum average distance to lines in this cluster. This formula was good at computation and weak at accuracy, which avoided least square solution.

In the process of clustering, each class was taken into calculation several times until class distance was greater than a threshold  $D$ . The number of iterations depended on the distribution of line segments in the image and the setting of the distance threshold.

### 3.4 EM Optimization

In this step, we tried to overcome our weakness in vanishing point estimation accuracy. The clustering process described above most likely to split multiple classes which corresponded to same vanishing point. EM method [15] was to refine the clustering results for the purpose of optimization. Now, we wanted to obtain vanishing point estimation of high reliability with EM optimization. In this section, we designed an EM algorithm, while the  $n$  lines and  $m$  vanishing points were known. It was transformed into a problem of using maximum likelihood function to estimate direction of lines.

$$\max \prod_{i=1}^M p(v_m) = \sum_{i=1}^M \log p(v_m) \quad (4)$$

assumed:

$$p(v_m|e_n) = \frac{1}{w_{mn}\sqrt{2\pi}\sigma_i} \exp\left(\frac{-\theta_{mn}^2}{2\sigma_i^2}\right) \quad (5)$$

Among them,  $\theta_{mn} = \sin^{-1}(v_m \cdot e_n)$ , was angle of line direction and the direction of the vanishing point.  $w_{mn}$  was the weight, which could be obtained by calculating the largest eigenvalue of the symmetric matrix, where  $C_m$  was the covariance matrix of the edge.

In M step,  $\sigma_i^2$ ,  $p(e_n)$  and  $e_n$  was estimated to make a maximum likelihood function.

$$p(e_n) \approx \frac{1}{N} \sum_{m=1}^M p(e_n|v_m) \quad (6)$$

$$\sigma_i^2 \approx \frac{\sum_{m=1}^M \theta_{mn}^2 p(e_n|v_m)}{Np(e_n)} \quad (7)$$

Because  $\theta_{mn} = \sin^{-1}(v_m \cdot e_n) \approx v_m \cdot e_n$ , then  $e_n$  can be used with the right direction of the linear least squares estimation formula:

$$\min_{e_n} \left\| (W_n^{m \times m} A_n^{m \times 3} e_n) \right\|^2 \quad (8)$$

$W$  was a diagonal matrix containing weight  $p(e_n|v_m)$ ,  $A$  was vanishing point matrix. Through the SVD decomposition, we could to find the vector that was related to the direction of line  $e_n$ .

## 4 Experiment

### 4.1 Efficiency of Vanishing Point Estimation

We took York Urban database [16] as our experiment data, including indoor and outdoor images. Camera model was Panasonic DMC-LC80, image size at 640 \* 480.

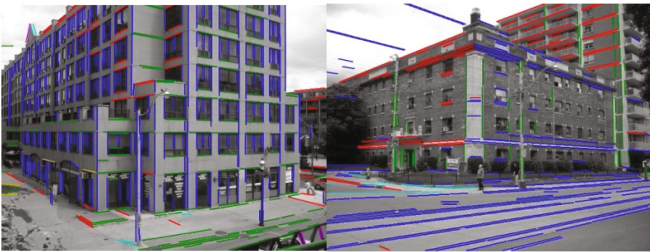


**Fig. 3.** Lines extracted in orthogonal directions of outdoor scenes



**Fig. 4.** Lines extracted in orthogonal directions of indoor scenes

The following figure was the result of line detection and the three vertical edges were obtained by line segment clustering (Figs. 3 and 4).

We compared our method with Denis' [16]. Table 1 showed the performance results of vanishing point estimation. In the step of line segment extracting, several algorithms were quite like in performance. But in the step of vanishing point estimation, MMVD algorithm and MMVD + EM had obvious advantages.

**Table 1.** VP estimation performance comparison

Algorithm	Lines number	Line extracting time(s)	VP estimation time (s)	Total Time(s)
Denis	1532	67	1445	1512
MMVD	1021	45	513	558
MMVD + EM	1021	45	535	581

It could be seen that for images of different sizes, even using EM optimization, the convergence speed was very fast, it only took a few iterations to end. For images with size of  $1024 * 1024$  or larger, Denis algorithm failed.

The images in Figs. 5 and 6 were rendered from the scene of a real-time digital city with a resolution of  $2048 \times 1024$ . For the large image, the MMVD algorithm could perform within 20 s, which could meet the needs of practical application.

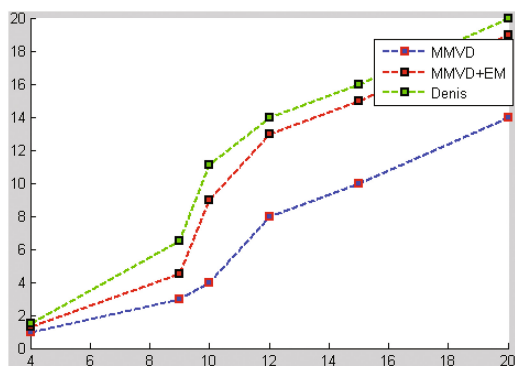


**Fig. 5.** Performance comparison of several algorithms on different size images

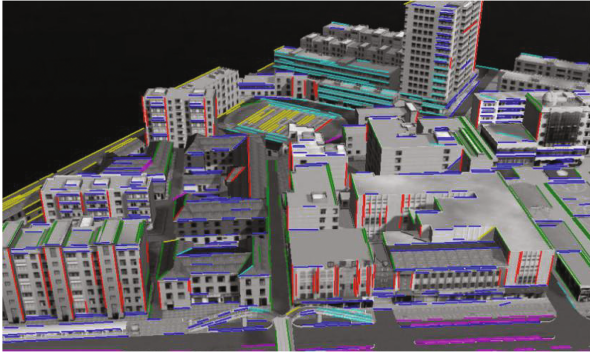


**Fig. 6.** Line extraction results of scene rendering in digital city project

## 4.2 Accuracy of Vanishing Point Estimation

For the vanishing points detected by MMVD algorithm, we used the algorithm proposed by Caprile [2] to calculate the focal length. And, we compared to the focal length provided by York Urban database to verify the accuracy of our estimation algorithm (Table 2).

**Table 2.** Comparison of principal distance and real principal

Image Num	P1020826	P1020830	P1020833	P1020177	P1020847
MMVD Focal	672.5933	672.5621	671.55	672.3515	672.2451
Original Focal	672.6122	672.6122	672.6122	672.6122	672.6122

The experiment used indoor and outdoor images. We used algorithm proposed by Caprile to calculate the focal length. From the experimental results, it could be seen that the error of camera focal length and the actual focal length calculated is small, proving high accuracy of the estimate algorithm.

## 5 Summary

An important feature of three-dimensional structural scene was the presence of three orthogonal directions, each orthogonal direction in the finite or infinity image plane formed vanishing point. The orthogonal vanishing points can be used for the self-calibration of the camera, and was more convenient than other manual calibration methods. In this paper, a vanishing point detection method of multi-model consensus estimation was proposed. This method used the detected line, using line segment clustering to achieve the estimation of multiple vanishing point, and then optimized the results through the EM algorithm. Experiments proved that, the algorithm could quickly and accurately estimate the vanishing point and compute camera parameters.



**Acknowledgement.** The work was supported by the Educational Commission of Hubei Province of China (No. D20151401) and the Green Industry Technology Leading Project of Hubei University of Technology (No. ZZTS2017006).

## References

1. Bazin, J.C., Seo, Y., Démonceaux, C., Vasseur, P., Ikeuchi, K., Kweon, I., Pollefeys, M.: Globally optimal line clustering and vanishing point estimation in Manhattan world. In: CVPR, pp. 638–645 (2012)
2. Caprile, B., Torre, V.: Using vanishing points for camera calibration. In: IJCV, pp. 127–40 (1990)
3. Haralick, R.M., Shapiro, L.G.: Computer and Robot Vision, vol. 2. Addison-Wesley, Boston (1993)
4. Wilczkowiak, M., Boyer, E., Sturm, P.: Camera calibration and 3D reconstruction from single images using parallelepipeds. In: Proceedings of Eighth IEEE International Conference on Computer Vision, ICCV 2001, vol. 1, pp. 142–148. IEEE (2001)
5. Chen, W., Jiang, B.C.: 3-D camera calibration using vanishing point concept. *Comput. Vis. Patten Recogn.* **24**, 57–67 (1991)
6. Orghidan, R., Salvi, J., Gordan, M., et al.: Structured light self-calibration with vanishing points. *Mach. Vis. Appl.* **25**(2), 489–500 (2014)
7. Lopes, F., Silva, H., Almeida, J.M., et al.: Structured light system calibration for perception in underwater tanks. In: Iberian Conference on Pattern Recognition and Image Analysis, pp. 111–120 (2015)
8. Dong, S., He, B., Lin, C., et al.: Calibration method for a structured light measurement system with two different focal length cameras. *Measurement* **73**, 462–472 (2015)
9. Wang, L.L., Tsai, W.H.: Camera calibration by vanishing lines for 3-D computer vision. *IEEE Trans. Pattern Anal. Mach. Intell.* **13**, 370–376 (1991)
10. Grammatikopoulos, L., Karras, G., Petsa, E.: Camera calibration combining images with two vanishing points. *Int. Arch. Photogrammetry Remote Sens. Spat. Inf. Sci.* **35**(5), 99–104 (2004)
11. Stevenson, D., Fleck, M.: Robot aerobics: four easy steps to a more flexible calibration. In: ICCV 1995, p. 34–39 (1995)
12. Von Gioi, R.G., Jakubowicz, J., Morel, J.M., et al.: LSD: a fast line segment detector with a false detection control. *IEEE Trans. Pattern Anal. Mach. Intell.* **32**(4), 722–732 (2010)
13. Toldo, R., Fusiello, A.: Robust multiple structures estimation with J-Linkage. In: Forsyth, D., Torr, P., Zisserman, A. (eds.) ECCV 2008. LNCS, vol. 5302, pp. 537–547. Springer, Heidelberg (2008). doi:[10.1007/978-3-540-88682-2\\_41](https://doi.org/10.1007/978-3-540-88682-2_41)
14. Jaccard, J. (ed.): *Interaction Effects in Logistic Regression*, vol. 135. Sage Publications, Thousand Oaks (2001)
15. Dempster, A.P., Laird, N.M., Rubin, D.B.: Maximum likelihood from incomplete data via the EM algorithm. *J. Roy. Stat. Soc. Ser. B (Methodological)*, pp. 1–38 (1977)
16. Denis, P., Elder, J., Estrada, F.: Efficient edge-based methods for estimating manhattan frames in urban imagery. In: European Conference on Computer Vision, part II, pp. 197–210 (2008)

# Research and Construction of the Full-Service IP High-Speed Intelligent Bearer Network for the Digital Oil Field

Xian Zhang<sup>(✉)</sup>, YuMin Feng, and XiaoHui Song

HuaBei Oil Communication Company,  
No.008, HuiZhan Street, Renqiu, Hebei, China  
{tx\_zhangx, tx\_fym, tx\_songxh}@petrochina.com.cn

**Abstract.** The construction of the basic bearer network is the “road network project” of digital oil field information field, which is the “highway” to connect the information application platforms, data centers and terminal users. Start with digital oil field, this thesis analyzes the construction of the basic networks, as well as the syncretic technology development status, the prospective development tendency and the popularization and application prospects. This thesis also confirms the method of development, clarifies the approach of evolution, and shows different periods of evolution and phased technical points.

According to research construction, a full-service hosted network based on IP has been constructed, which realizes service intelligence control. The era of digital oil field cloud data center has been opened, the loading problem of the multiple business data from production and operation has been solved, the terminals under the cloud construction mode and the data centers has been satisfied.

## 1 Introduction

Development of the IP-based telecommunications service propels the IP network to bear the traditional telecommunications service. Customers and services both propose new requirements for the bearer network, such as a routed metropolitan area network (MAN), differentiated access modes, diversified services, and layered networks. Due to the lack of the current network devices and structures, the traditional MAN cannot meet the multi-service development requirements. To provide increasing user bandwidth, elaborate service quality, and overall service development, it is imperative to reconstruct the current network and build a new full-service IP high-speed Intelligent bearer network.

The full-service IP high-speed Intelligent bearer network integrates traditional services and emerging services to expand services from simple communications to various information systems, making it more integrated and comprehensive while also improving the informationization level of the digital oil field. Additionally, it promotes the integration of the three networks at the technical, service, terminal, transmission network, and operation monitoring layers, which can perfect the information security system, adjust the service structure, disperse operation risks, optimize resource configurations, and quickly enhance international competitiveness.

The construction of the full-service IP high-speed Intelligent bearer network for the digital oil field is a basic and meaningful project. The bearer network is the road

network in the information field, as well as the highway that connects information application platforms, data centers, and terminal users. Without scientific and rigorous planning in advance, breaking points and dead zones may appear on the network, thus forming isolated information islands. Without an intelligent and efficient management mode, broad roads will still be congested and turn into large parking lots, while information application platforms may be hard to sustain like uprooted trees. Without scientific and thorough application maintenance policies, advanced infrastructures may have a short lifespan and the maintenance and operation costs may increase. Deeper research on the bearer network can provide scientific support for the development of information and communications constructions, as well as promote the complete, sequential, and smooth implementation of information and communications services. Research achievements can directly provide information services for both individual and enterprise users of the digital oil field. By planning and deploying highways for network application platforms and data centers while also formulating corresponding traffic rules and road operation maintenance regulations, the informationization construction of the digital oil field can be promoted.

## 2 Main Body

### 2.1 Research Object

With the sharp increase of the data scale for the digital oil field and rapid change of service structures, the original basic bearer network cannot meet the requirements of the current service structures and needs to be technically upgraded and improved in the following four aspects:

- (1) Full-service integration: The full-service integration bearing is not only an inevitable trend of network development in the future, but also a critical point for cost reduction and efficiency increases in enterprise network operations. To implement the full-service integration bearing, two challenges must be solved: the integration of service information content and the integration of the service bearer transmission network.
- (2) IP-based service: A unified IP bearer network is adopted to simplify and optimize the network structure, provide network flexibility, and make full use of the transmission bandwidth, thus saving network investments and O&M costs for carriers.
- (3) High-speed network bandwidth: It is predicted that the traffic flows on the backbone network in China will rise at the rate of more than 50% over the next 5 to 10 years. As the broadband service develops, there will be a tendency of “coarse granule” in the IP service sector. The bandwidth requirements for the optical transmission network (OTN) are increasing day by day and the OTN has a trend of both long distance and large-volume transmissions.
- (4) Intelligent network: As more and more service data gradually accesses the IP bearer network, different services have different requirements on the network. Multiple types of service data functioning on the same bearer network will certainly bring different risks.

## 2.2 Ideas and Content

**Technical Ideas.** In the construction of full-service IP high-speed Intelligent bearer networks for the digital oil field, TCP/IP protocol must be adopted during the upgrading and improvement processes of all service networks. This means that the voice service network is changed from the program controlled switching network to the software switching network; the data network is optimized and upgraded to the IP multi-service bearer platform; and the front-end system of the cable network in the original ASI mode is gradually constructed based on the IP. It finds the point for network integration during the upgrade and improvement, as well as uses applications with key technologies for network integration based on the interconnection between the service networks. Services penetrate and intersect with each other in order to blur terminal boundaries and enable the same terminal to provide multiple types of services. Furthermore, it constructs the virtual data network based on the broadband MAN MPLS VPN and powerful multi-service bearing capabilities for automatic oil and gas production, intelligent mining services, informationalized enterprise management, and digital security protection in order to promote the construction of the digital oil field.

**Content.** Our research focuses on the following aspects:

### (1) Integration of the access network

As required by FTTx and aiming to realize FTTH, the all-around resource optimization and upgrades are performed on the access network in order to construct a communications network with wired and wireless connections everywhere, providing information highways for voice, data, and video applications. A bidirectional access network is built using the passive optical network (PON) for the broadcast transmissions of TV signals and the bidirectional interaction in the mode of a single fiber with three waves. Furthermore, it provides access channels for broadband network access and other digital data services.

### (2) Integration of the backbone transmission network

This project uses the Wavelength Division Multiplexing technology to expand the original star transmission networks that use optical fibers supplemented by microwaves into OTN self-healing optical ring networks. In this way, the quality and quantity of the backbone transmission networks are both improved.

### (3) Construction of the IP full-service bearer platform

An IP full-service bearer platform is constructed by deploying the MPLS VPN protocol, upgrading the backbone network from 1 Gigabit to 10 Gigabits, establishing the full-service QoS security system, constructing the integrated network management system and network security systems, and also supporting the IPv6 protocol in order to integrate multiple services. The platform mainly includes the following parts:

Part 1: Entire architecture of the full-service bearer network

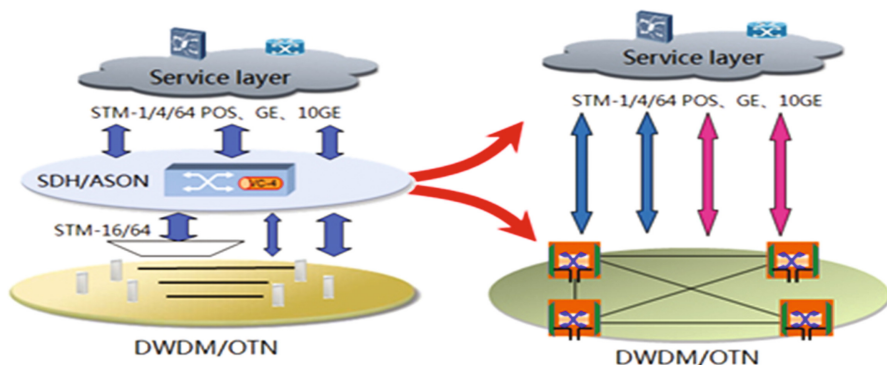


**Fig. 1.** Evolution of the architecture of the full-service bearer network

As shown in Fig. 1, the architecture of the transmission network is evolving from the IP over SDH to the IP over WDM. This is because single-service communications networks cannot meet service development requirements any more and full-service bearer networks are required. Furthermore, as the network rate and granule grow, the application environment has more demanding requirements for network robustness. All of these factors make the construction of the full-service high-speed bearer network more significant.

Part 2: The full-service integration and bearer technology of the core network

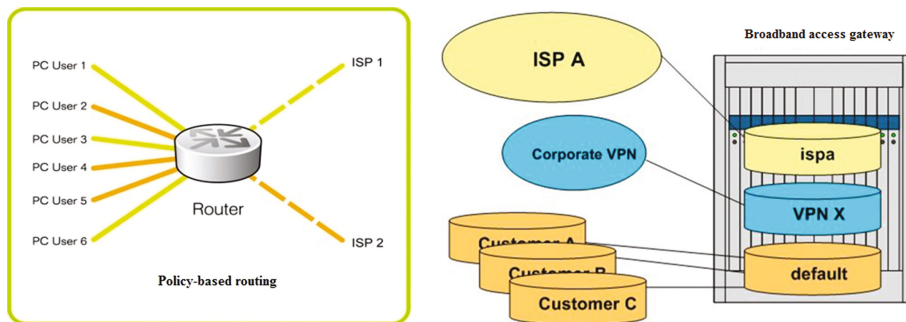


**Fig. 2.** Technologies related to full-service integration and bearing

Further researches on policy-based routing and virtual routing technologies on the core network create conditions for placing multiple services on the same bearer network (Fig. 2).

Part 3: Full-service Intelligent access technology on the access network

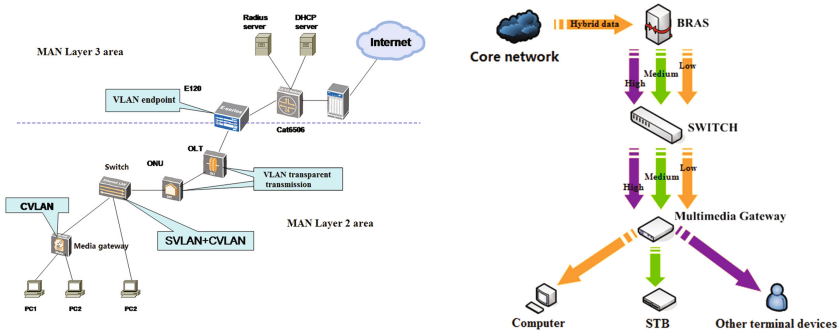


Fig. 3. Full-service Intelligent access technology

As shown in Fig. 3, a unified access network is constructed and the access mode of a single fiber with three waves is innovatively used. A reverse Q in Q encapsulation and decapsulation is implemented through the joint work of the Layer 2 and Layer 3 switches and multimedia gateway on the IP access network in order to ensure stable and transparent transmissions of the different types of services. At the same time, the QoS technology is studied. QoS policies are planned to be deployed on the entire network to ensure the normal functioning of services.

Part 4: Technologies of the backbone bearer network and wireless access network

By engaging in deep research regarding the transmission technology of the backbone bearer network, an evolution route is planned for the high-speed Intelligent bearer network whereas the actual environment is being upgraded and expanded. Furthermore, to have a deeper understanding of the TD-LTE, McWiLL, and WIFI technologies, a network access demonstration area is set up in the production and living places of the digital oil field in order to provide examples for large-scale promotion.

Part 5: Implementation of full-service bearer network services

A FTTH + FTTB network is deployed using Passive Optical Network (PON) so that voice, Internet, and TV services can be integrated onto the same access network, building an end-to-end communications process at the service access layer and transmission layer.

2.3 Research Result

This project forms an IP-based full-service bearer network, constructs the N\*10GE mode between the data center and area center of the digital oil field, opens up an era of large data volume in the cloud data center of the digital oil field, solves the bearing of multi-service data such as voice, videos, and images collected during production, as well as meets the future large-bandwidth requirements between application platforms,

terminals and data centers in the cloud architecture mode. We have made five significant innovations during the project implementation:

- (1) Integrating and applying such technologies as Q in Q, virtual routing, and policy-based routing in order to construct a 3D access model with one network and multiple planes

We adopt virtual routes and policy-based routing technologies at the aggregation layer of the IP bearer network as well as innovatively apply the Q in Q technology at the access layer (multimedia gateway side) for logical isolation of our users and services so that different services of different users are allocated with different VLANs, accounts, and IP addresses on terminals. This provides internal routing control and security guarantees for multiple services on the same IP bearer network. The deployment and innovation of this policy construct a 3D access model with one network and multiple planes in order to effectively support the evolution of private enterprise networks from the integration of three networks to the FTTH.

- (2) Making high-density IP encapsulation on ASI signals for lossless transmissions of cable TVs at ultra-remote distances

At the live distribution network layer, a video scheduling and distribution network is constructed by partitioning independent channels on the OTN with a separated data communications network. In addition, high-density IP encapsulation is performed on the scrambled ASI signals at the front end of the digital TV so that the program transmission flows are scheduled and distributed on the network as multicast packets. This allows users from different production units to flexibly select TV programs, improving the forwarding efficiency of the platform and system running reliability. More importantly, digital TV programs are logically separated from other Internet data and VOD unicast video distribution services from the bottom-layer transmission channel to the data communications network meeting the high QoS requirements on digital TV programs while also ensuring high security, high reliability, and low delays of video distribution services. The innovative application of this technology overcomes the disadvantages of the analog optical transmission modes at an ultra-remote distance, such as serious CSO/CTB deterioration, non-linear distortion, and multiplexing reception interference. In this case, cable TV can be transmitted without losing service during ultra-remote distance transmissions, which meets the requirements of cable TV signal coverage for remote wells, queues, and stations.

- (3) Innovating on the service granule layered forwarding mode and network management monitoring mode, improving network usage, stability, reliability, and reducing operation costs

In the IP over the WDM architecture of the OTN, the transmission modes of services on the optical layer and IP layer are optimized based on service granule levels in accordance with the features of the optical fiber links and packet switching. This means that the traffic flows of larger granules are forwarded through the optical layer instead of the grouping layer, whereas traffic flows of either medium or small granules are aggregated on the grouping layer before being transmitted through the optical layer. Furthermore, by optimizing the optical channel routing and wavelength assignment (RWA),

communications resources can be fully utilized and the network structure is flattened, both protecting the current network device investments and saving network construction and operation costs.

Regarding aspects of monitoring, management, and protection, the SC + FIU + OSC mode, with which the monitoring function was originally independently performed by the SDH layer, but is now performed by the SDH and WDM layers, is established. This solves the problem that network elements may be detached from management when indicators of optical fibers deteriorate or optical fibers are broken, enhancing the robustness of the network management function.

- (4) Integrating advantageous resources of private networks to set up the TS + PON network integration mode of a single fiber with three waves

Depending on communications and TV network resources, a network integration mode of a single fiber with three waves is created on the transmission network, on which waves at the length of 1310 nm and 1490 nm respectively transmit EPON uplink and downlink signals, while waves at the length of 1550 nm transmit TS code streams. The highly-isolated C-Band Er-Yb co-doped double-clad fiber magnifying technology is adopted and the CATV module that integrates the WDM function is developed to ensure physical isolation of both radio signals and IP signals on the family multimedia gateway ONU. This mode gives full use to the advantages of cable TV networks, such as broad channel resources, strong anti-interference capability, and high-definition signals with capacities that can be smoothly expanded. Since the CATV does not occupy data network resources, the bandwidth pressure on the core network is greatly reduced and high-definition TV signals and high-quality sound effects are ensured.

- (5) Carefully design data encapsulation and service switchovers, as well as a protection mechanism to ensure full-service end-to-end OAM and service quality protection while also improving the core processing capability of the bearer network

An overall and elaborate design has been made utilizing a data encapsulation multiplexing format, the service bandwidth development trend, multiplexing at the optical and electrical layer, and a service switchover with a protection mechanism by collaborated planning of IP and OTN in accordance with the multi-service integration and bearing features on the private networks of the digital oil field. A service quality and management network structure model of the full-service bearer private network have been established to provide end-to-end OAM and service quality protection for various services, improving the processing capabilities of the core platform, meeting rapid bandwidth development requirements, and implementing Intelligent management and control of all services throughout the network.

### 3 Conclusions

The full-service IP high-speed Intelligent bearer network for the digital oil field is not the equivalent to the traditional integrated network defined either in or outside of China; it does not mean the physical combination of the telecommunications network, Internet, and radio and TV networks, rather, it refers to the integration of higher-level



service applications, presented as a technical consistency. This implies that it should have interconnection for seamless coverage at the network layer, mutual penetration and intersection at the service layer, and a unified IP protocol at the application layer. After technical reconstruction, infrastructures of the three networks can provide comprehensive multimedia communications services such as voice, data, and images. It aims to share network resources to its maximum capacity, avoid low-level duplicated construction, as well as form a widely applicable, easily maintained, and low-cost basic platform for high-speed bandwidth multimedia full-service information.

After studying related technologies both in and outside of China, we have found that there has been no full-service IP high-speed Intelligent bearer network in the domestic oil field enterprises or other enterprises with large-scale private networks. There is no available reference either for construction concepts or implementation schemes. We have found that most enterprises still use the traditional networking mode, in which different networks are set up for different services but have limited service integration and bearing capabilities. This reflects that different service departments inside an enterprise do not share basic bearer network resources with each other, let alone have the ability to integrate high-level service applications. Thus, the construction of the full-service IP high-speed Intelligent bearer network for the digital oil field will certainly make a difference for oil field enterprises and provide construction ideas and reference schemes for other oil fields or domestic enterprises with large-scale private networks.

A multi-service basic operation platform is able to shield differences on different networks and protocols from the bottom layer and provide reconstitutable open capabilities in order to quickly generate applications. These functions solve both service problems and bearer isolations. In this way, the platform can offer powerful service capabilities for both 4G and 5G networks in the future, as well as ensure a complete service development environment. The service layers and technical layers are made to be continuously improved and perfected; the network bearing capability is greatly enhanced; and the network operation reliability is significantly enlarged. Furthermore, the network transmission capacity is multiplied, providing large space and strict quality guarantees for both large-scale and multi-service transmissions. This platform can bear several digital and data services including voice, videos, and images. Additionally, it can provide higher bandwidth, more service access, higher group bearing efficiency, faster and more flexible service deployment, more refined resource scheduling, differentiated service level agreement (SLA), and a lower total cost of ownership (TCO). There are also comprehensive information services provided for full-service operations and unified customer service experience provision capabilities.

A network is a strategic resource of an enterprise. An efficient and advanced network supports high-quality services. We will continue to make technical innovations regarding network quality, service support, and operation management for the full-service IP high-speed Intelligent bearer network to stabilize the foundation of network services, optimize the basic network, aim for the IP-based network development trend, as well as increase our investments in full-service IP high-speed Intelligent bearer networks. We will provide the industry-leading full-service IP high-speed Intelligent bearer network in order to offer a suggestive basis for the digitalization and informationalization of CNPC, which will be profoundly influential on the informationalization construction of other domestic enterprises with large-scale private networks.

# Verification Using Multi-agent Simulation for Evacuation Guidance with Robots

Ryuta Sugie<sup>(✉)</sup>, Takahiro Uchiya, and Ichi Takumi

Nagoya Institute of Technology, Gokiso-chou, Showa-ku, Nagoya 466-8555, Japan  
sugie@uchiya.nitech.ac.jp, {t-uchiya,takumi}@nitech.ac.jp

**Abstract.** In recent years, Japan has been adversely affected to a severe degree by the effects of a strong earthquake disaster. In such dire times, appropriate disaster prevention behaviors are important to reduce damage. Evacuation behavior to outside areas is one disaster mitigation behavior. Evacuation drills are regularly performed at large facilities such as schools so that appropriate evacuation measures can be taken. However, in times of disaster, guide staff members might be absent at night. It might be difficult for staff members to guide evacuees because of secondary disasters such as smoke caused by fire. To provide assistance reliably, a disaster prevention system can be constructed with robots, instead of people, to perform dynamic guidance in accordance with evacuation route situations. The final goal is to develop a robotic disaster prevention system. As described herein, we can verify the effectiveness of evacuation guidance with robots using multi-agent simulations.

## 1 Introduction

Evacuation from inside areas is one disaster prevention behavior after the earthquake. During evacuation drills, guide staff members can give instructions at the designated area. However, the guide staff member might be absent at night despite the disaster.

Moreover, it is difficult to prepare for disasters with measures to meet all circumstances and conditions. For example, we cannot pass through fire to get to an exit. In addition, guide staff cannot guide evacuees through smoke caused by a fire. For these reasons, it is necessary for robots to perform dynamic guidance according to a situation. Therefore, we propose a disaster prevention system in which robots undertake dynamic evacuation guidance instead of a human.

It is necessary to conduct experiments by changing various factors such as guidance methods, place of instillation, and robot performance to introduce the robot into the disaster prevention system. If we experiment on actual machines, then the cost will increase in terms of both time and money. As described herein, we aim to verify the effectiveness of evacuation guidance with robots in a virtual environment using multi-agent simulation.

Existing studies using multi-agent simulations include the following. Okaya [1] conducted investigations of dynamic evacuation guidance involving evacuees

and guide staff. Tanaka [2] used a small unmanned aerial vehicle for evacuation guidance as one means of information transmission.

As described herein, we use multi-agent simulator `artisoc` [3]. `artisoc` was developed by Kozo Keikaku Engineering Inc. to construct and simulate multi-agent systems. Fundamentally, the descriptive language used for `artisoc`'s execution rules conforms to Microsoft Corporation's VisualBasic [4]. Additionally, types and functions are prepared for agents.

This paper's organization is the following. We explain our proposed method in Sect. 2. The evaluation experience of our multi-agent simulation is presented in Sect. 3. Finally, conclusions are explained in Sect. 4.

## 2 Proposed Method

As described in this paper, we assume indoor dynamic evacuation guidance by Unmanned Ground Vehicles<sup>1</sup>. There are guidance methods of roughly two types using UGVs. The first is indirect evacuation guidance by which the direction of the exit is transmitted by UGV visually, such as with arrows or in an auditory way, as with voice guidance. It is helpful for evacuees who understand the route to the exit to change the route to avoid the risk posed by a secondary disaster. The second is direct evacuation guidance by which UGV leads evacuees to the exit. It is helpful for evacuees who do not understand the exit used for evacuation.

We propose two scenarios dealing with indirect evacuation guidance and direct evacuation guidance respectively by UGV agent. Thereby, we verify dynamic evacuation guidance using UGV.

### 2.1 Scenario 1 – Discovery of Fire and Call for Evacuation

Fire occurs the most frequently as a secondary disaster after an earthquake. It might be possible to pass through the route around the room where a fire occurs. However, risks exist such as smoke, so this route should be avoided. In the first scenario, fire agents and smoke agents are created in case of a fire. When a patrol UGV agent detects smoke agents generated from fire agents, it performs indirect evacuation guidance. A patrol UGV agent calls to surrounding evacuees agents to avoid the route filled by smoke. Figure 1 presents the protocol of scenario 1.

### 2.2 Scenario 2 – Evacuation Guidance Considering Visitors

Direct evacuation guidance by UGV is effective mainly for those who are delayed in their evacuation. For example, at a university, it is thought that students and faculty members are familiar with buildings and that they understand the exit. However, it is difficult for visitors to understand the exit of the building when they have come to the building for the first time. Therefore, they evacuate slowly. We create student agents and visitor agents to reproduce this situation.

---

<sup>1</sup> UGV.

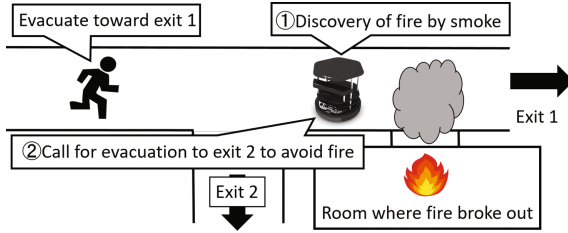


Fig. 1. Scenario 1 – discovery of fire and call for evacuation.

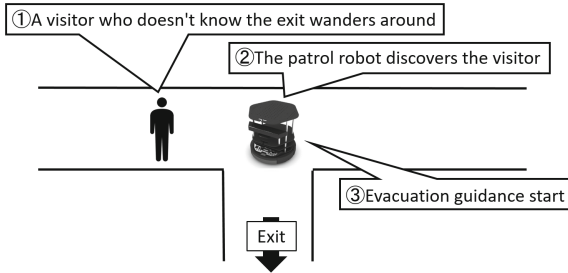


Fig. 2. Scenario 2 – evacuation guidance considering visitors.

Student agents evacuate after the earthquake. However, visitor agents do not understand the exit and wander around. In scenario 2, when a patrol UGV agent finds visitor agents, evacuation guidance starts. Figure 2 presents the protocol of scenario 2.

### 2.3 Modeling Evacuation Behavior

#### Status setting

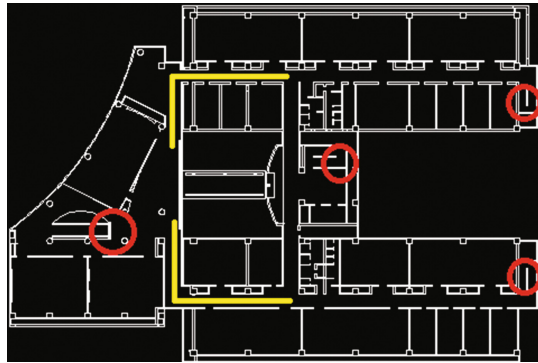
This simulation assumes evacuation behavior at Nagoya Institute of Technology Building 2 – Second floor. The four circles in Fig. 3 shows the exit. Table 1 shows the defined behavior of each agent. The evacuees are 100 student agents. As evacuation behaviors, everyone must ensure their own safety immediately after the earthquake [5]. There is an announcement to start evacuation after 90 s. The timing of evacuation is set randomly for each evacuee over 90 s. The termination condition of the simulation is eight minutes elapsed time or the complete evacuation of all agents. Up to two UGV agents are arranged. They patrol on the yellow line in Fig. 3.

#### Map settings

We created the cell space of  $80 \times 120$  based on Fig. 3. The size of one cell is 0.6 m square. This was set as a useful size that can cover the human body, as referred from a report of the relevant literature [7].

**Table 1.** Agent action list.

Agent	Action
UGV	After disaster occurrence: patrol the designated area Detect smoke: Call to surrounding evacuees by voice Find a visitor: Performance of evacuation guidance
Student	Evacuate to the nearest exit
Visitor	When there are other evacuees nearby: Follow up If not: Wandering around
Fire	Occur from a random room after a certain time
Smoke	Be filled at constant speed The Student agent die in smoke agents for 30 s

**Fig. 3.** Map of Nagoya Institute of Technology building 2 – second floor.

### Elapsed time of 1 step

Generally, it is said that the human walking speed is 4 km/h ( $\approx 1.1$  m/s). Because it is a calculation that can walk about 1.2 m (=2 cells) in 1 s, the elapsed time of 1 step is set to 0.5 s.

## 3 Evaluation Experiment

We conducted experiments of two types in scenario 1 and one type of experiment in scenario 2.

### 3.1 Scenario 1

#### 3.1.1 Experiment 1

In Experiment 1, we experiment with guidance methods. No matter where a fire occurs, smoke easily reaches the center of the experiment site. For that reason, it is dangerous to use the center staircase for evacuation guidance. Therefore,

we present a contrasting case using the central staircase with a case not using it in simulation.

### Experimental Method and Result

The student agent position, the UGV agent position, the fire location, and the fire occurrence time are fixed. These maintain the reproducibility. Table 2 shows each average value from ten trials conducted on the following five experimental patterns.

1. No UGV agent
2. One UGV agent and Use central staircase
3. Two UGV agents and Use central staircase
4. One UGV agent and Do not use central staircase
5. Two UGV agents and Do not use central staircase

In addition, Fig. 4 presents the simulation execution window when the central staircase is used. Figure 5 shows the simulation execution window when it is not used. Both use two UGV agents.

**Table 2.** Scenario 1 – Result of Experiment 1.

Central staircase	-	Use		Do not use	
Number of UGV	0	1	2	1	2
Number of steps	642.5	631.6	573.1	644.9	604.2
Number of induced people	-	4.7	12.9	4.3	14.7
Number of induced evacuation-success people	-	0.2	7.6	3	11.9
Number of evacuation-failed people	9.1	8	6	6	3.1
Moving distance of evacuee	108.6	120.9	118.7	116	118.8
Number of steps touching smoke	678.7	669	405.7	538.4	250.5
Fire occurrence time	362				
Fire detection time	-	485.8	421.7	486.4	420.8

### Consideration

First, when using the central staircase, we compare the numbers of UGV agents.

When one UGV agent was launched, the number of evacuation-failed people and the number of steps touching smoke decreased. The moving distance of evacuees increased. An increase in the evacuee moving distance is probably attributable to the evacuation route change.

A great difference existing between one UGV agent pattern and two UGV agents pattern is that the fire detection time became faster and the number of induced people increased greatly. As a result, the number of evacuation-failed people and the number of steps touching smoke were reduced.

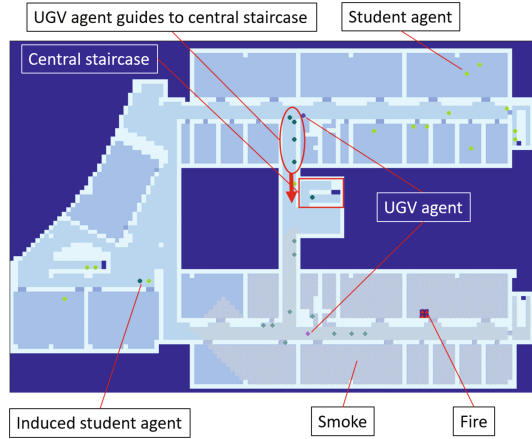


**Fig. 4.** Scenario 1 – when the central staircase is used.

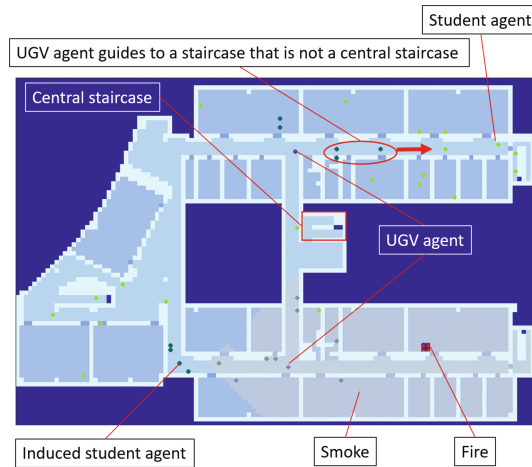


**Fig. 5.** Scenario 1 – when the central staircase is not used.

From the results presented above, it is probably effective to use UGV agents for evacuation guidance. In addition, the best results were obtained when using two UGV agents.

Next, we contrast a case using the central staircase with a case not using it. We consider the case of two UGV agents. When the central staircase was used, the induced evacuation-success people were 60% of the number of induced people. However, when the central staircase was not used, that increased to 80%. Furthermore, the number of evacuation-failed people was halved. The number of steps touching smoke was reduced by 40%. Results show that a guidance method not using the central staircase is probably effective.

### 3.1.2 Experiment 2

In Experiment 2, we examined the change of the number of evacuation-failed people by fire detection time. We simulated how the number of evacuees fails by delaying fire detection.

#### Experimental method and Result

The fire detection time was taken as 240 steps after the start of the simulation. The evacuee position and the fire location are random every time. Experiments were conducted with two UGV agents. This experiment uses the evacuation guidance method not using the central staircase conducted in Experiment 1. The scatter plot (Fig. 6) shows the fire detection time and the number of evacuation-failed people of simulation results in 100 iterations.

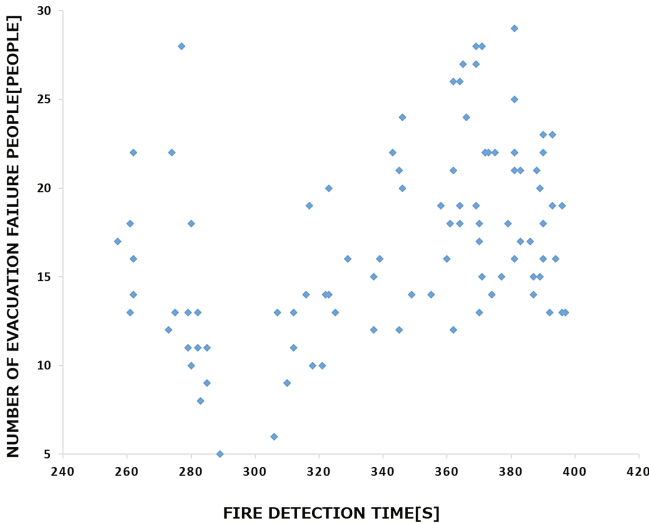


Fig. 6. Result of experiment 2.

#### Consideration

Fire detection time varies between 260 steps and 400 steps depending on where the fire occurred. The number of evacuation-failed people was concentrated between 10 and 20 people. Although variations exist overall, the faster the fire detection is, the fewer the evacuation-failed people tend to be. Additionally, later fire detection is associated with larger numbers of evacuation-failed people. One finds that early fire detection time leads to evacuation-failed people of fewer than 10; late fire detection leads to 25 or more evacuation-failed people.

The results presented above imply that more rapid fire detection is an important factor for reducing the number of evacuation-failed people.



### 3.2 Scenario 2

#### Experimental Method and Result

The evacuee and visitor positions are fixed. These maintain reproducibility. The simulation was performed with three patterns of UGV agent from zero to two. Table 3 presents the average value obtained from iterating this trial 10 times. Figure 7 portrays the simulation execution window.

**Table 3.** Scenario 2 – Result of experiment.

Number of UGV	0	1	2
Number of steps	603	559.5	531.5
Moving distance of evacuee	114.2	118.1	114.4
Number of induced people	-	1.5	0.9

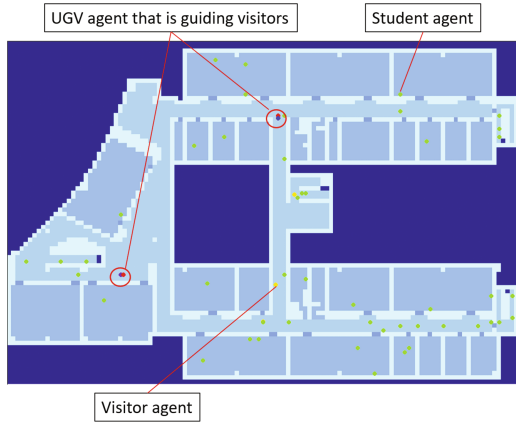


**Fig. 7.** Scenario 2 – simulation execution window.

#### Consideration

Comparing cases with no UGV agent pattern and one UGV agent pattern reveals that the number of steps was reduced by about 40 steps. Moreover, comparison of a one-UGV agent pattern and a two-UGV agent pattern shows that the number of steps in the latter was reduced by approximately 30 steps. The considerations presented above indicate the possibility of shortening the evacuation time by guiding the wandering visitor agents.

However, the number of induced people has decreased by 0.6 people when the UGV agent pattern is increased from one to two. We guess that visitor agents were able to follow student agents successfully in a two UGV agent pattern. The difference between one UGV agent pattern and two UGV agents pattern

is whether they can find a visitor agent who has not evacuated. Thereby, we inferred that the number of steps could be reduced.

The effectiveness of UGV agents can be confirmed. However, the problem of this experiment is that the share of visitor agents is much smaller than that of the student agents. It is easy for visitor agents to follow student agents. Consequently, it is necessary to consider parameters that can reproduce situations that are difficult to follow-up.

## 4 Conclusion

The purpose of this research is construction of a system for prompt evacuation guidance without human intervention. The system uses a robot that performs dynamic evacuation guidance autonomously in the event of a disaster. To construct a system, we verified the use of robots by multi-agent simulation in this paper.

For the proposed method, we classified the evacuation guidance methods to be conducted by the robot into two types: indirect evacuation guidance and direct evacuation guidance. Additionally, we proposed a scenario reproducing each evacuation guidance method.

In Scenario 1, we conducted two experiments. Experiment 1 verified the effectiveness and evacuation guidance method of UGV. Results demonstrated the effectiveness of UGV and showed that the evacuation guidance method not using the central staircase is effective. Experiment 2 investigated the relation between the fire detection time and the number of evacuation-failed people. Results show that the number of evacuation-failed people increased as the fire detection time increased.

In scenario 2, we showed that using UGV to guide visitors is effective. Additionally, we explained the problems of the experiment.

Finally, we shall introduce future works.

- UGV action range and UGV operating method  
In this paper, UGV action range and UGV operating method were fixed. We believe that the efficiency of evacuation guidance will increase by changing these factors.
- Considering route including obstacle  
Rubble may be generated by the earthquake. Evacuees may be deprived of sight on the route full of smoke. We need to consider obstacles which hinder evacuation. Evacuation guidance that does not use exit of route where obstacle occurred is necessary.

## References

1. Okaya, M., Takahashi, T.: Evacuation simulation for dynamic evacuation management. IEICE Tech. Rep. AI **112**(477), 7–11 (2013)
2. Tanaka, K., Furuichi, M.: Effectiveness of guiding evacuees by UAVs using multi-agent simulation. Forum Inf. Technol. **14**(4), 473–474 (2015)
3. Kozo Keikaku Engineering Inc.: artisoc. <http://mas.kke.co.jp/>
4. Visual Basic 6. <http://www.vb6.us/>
5. Tokyo Metropolitan Disaster Prevention Homepage - Behavior Manual on Earthquake Occurrence. <http://www.bousai.metro.tokyo.jp/bousai/1000026/1000276.html>
6. Ministry of Land, Infrastructure and Transport and Tourism - Fourth Underground City Safe Evacuation Measures Examination Committee. [http://www.mlit.go.jp/toshi/toshi\\_gairo\\_tk\\_000052.html](http://www.mlit.go.jp/toshi/toshi_gairo_tk_000052.html)
7. Oshino, M.: Evacuation behavior simulation using multi agent model. Chuo University (2005)

# Development Support Mechanism for Deep Learning Agent on DASH Agent Framework

Kento Watanabe<sup>1</sup>(✉), Takahiro Uchiya<sup>1</sup>, Ichi Takumi<sup>1</sup>, and Tetsuo Kinoshita<sup>2</sup>

<sup>1</sup> Nagoya Institute of Technology, Gokiso-chou, Showa-ku, Nagoya 466-8555, Japan  
watanabe@uchiya.nitech.ac.jp, {t-uchiya,takumi}@nitech.ac.jp

<sup>2</sup> Tohoku University, Katahira 2-1-1, Aoba-ku, Sendai 980-8577, Japan  
kino@riec.tohoku.ac.jp

**Abstract.** Agent-Oriented Computing is an effective method introduced in recent years to meet diverse needs. For such computing, we use the DASH agent framework, which can develop an agent with learning capability. However, it is difficult to develop a versatile agent for applications such as image recognition and speech recognition using the current development environment. Deep learning can be used to resolve this difficulty. Using deep learning is difficult for ordinary developers because it requires detailed knowledge. Therefore, we propose development support of a “deep learning agent” to simplify development by ordinary developers.

## 1 Introduction

Various requests have arisen along with the rapid spread of the internet in recent years. Such requests demand a flexible system that can respond easily to various needs. Agent-oriented computing can support such flexible systems and meet user requirements.

An agent is software that works instead of the user to achieve some goal. It operates autonomously while communicating with other software or people. Agents with learning ability are called a “Learning Agents”. Learning agents learn intelligent actions based on past experience.

An agent framework exists to develop and operate agent systems. It can develop agent systems easily. Developers can develop learning agents with traditional agent frameworks. Nevertheless, few agent frameworks support development of learning agents. Developers must program all actions for an agent. Therefore, they must learn specialized knowledge related to machine learning. Consequently, ordinary developers have difficulty developing learning agents.

The “Development Tool of Q-Nash Learning Agent for Intelligent System” [2] was developed in earlier studies to support learning agent development. This study achieved support of learning agent development to the DASH agent framework by adding development support functions for learning agents. Using the framework presented in this paper, ordinary developers can develop learning agents without programming complicated actions. However, it is difficult to develop an advanced learning agent to perform more difficult learning such as

image recognition and speech recognition. Therefore, there is a limit to the difficulties that current agent-oriented computing can resolve.

As described in this paper, we propose the addition of new learning functions by deep learning to a DASH framework. Deep learning, a machine learning algorithm for neural networks, is widely used for applications such as image recognition and speech recognition.

Moreover, we propose support of “learning agent with deep learning” development for ordinary developers who have no detailed knowledge of deep learning. Consequently, the framework reduces the developer’s burden and the development time of the learning agent.

## 2 DASH Agent Framework

For this research, we use DASH Framework and the agent in DASH. Therefore, we explain these in this section.

### 2.1 Outline

Distributed Agent System based on Hybrid architecture (DASH) [1] is a framework for developing and using an agent system. DASH comprises a repository to accumulate and manage agents and workplaces where agents are generated and operated. This is called a Repository-based multiagent framework. By managing agents in a repository, a user first requests a service to a workplace. Second, a workplace notifies the task to a repository. Then, a repository generates an agent system in the workplace and agents in the agent system will run and provide services to a user (Fig. 1).

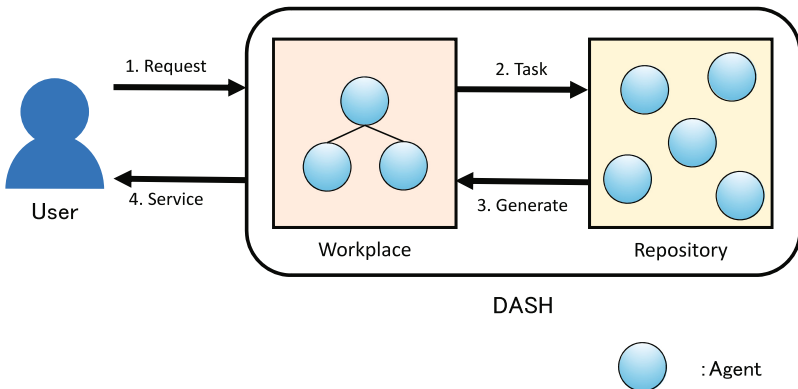


Fig. 1. DASH agent framework.

### 2.2 Agent in DASH

An agent in DASH is a rule-based model agent and described by texts. An agent has a Domain Knowledge-base, which is a mechanism to decide an action (Fig. 2).

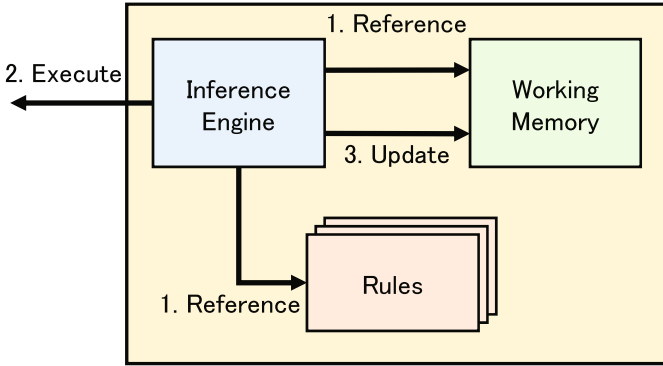


Fig. 2. Domain knowledge-base of DASH agent.

Domain Knowledge-base comprises the Inference Engine, the Working Memory, and Rules. Explanations of these respective components are presented below.

#### Inference Engine

The inference engine refers to states in the working memory and controls the operation-knowledge. It searches for a rule by rules. Then an agent operates.

#### Working Memory

The working memory stores information an agent receives.

#### Rules

The rules store the operation-knowledge as an if-then rule.

An agent in DASH behavior is explained below.

1. The inference engine refers to the working memory and the rules when the agent receives a message.
2. The inference engine controls the operation-knowledge searches for a rule which matches the state that is reformed to the working memory. Then, the rule is executed.
3. If states of the working memory are updated by executing the selected rule, then the inference engine refers to the working memory and updates it.
4. The agent repeats 1. – 3. to operate.

## 3 Proposed Method

There is difficulty by which the range of tasks which agents can process is limited in the current DASH framework. As described in this paper, we solve the problem by adding development support functions of deep learning to the DASH framework.

### 3.1 Introduction of Deep Learning

Deep learning is a subfield of machine learning algorithms using multilayer neural networks. It is applicable to manifoldness such as image recognition and speech recognition, and to show the precision of high recognition. Therefore, deep learning is excellent as the method of machine learning. As described in this paper, we use convolutional neural networks for agent learning functions.

A convolutional neural network consists of a Convolutional Layer, Pooling Layer, and a Fully Connected Layer (Fig. 3).

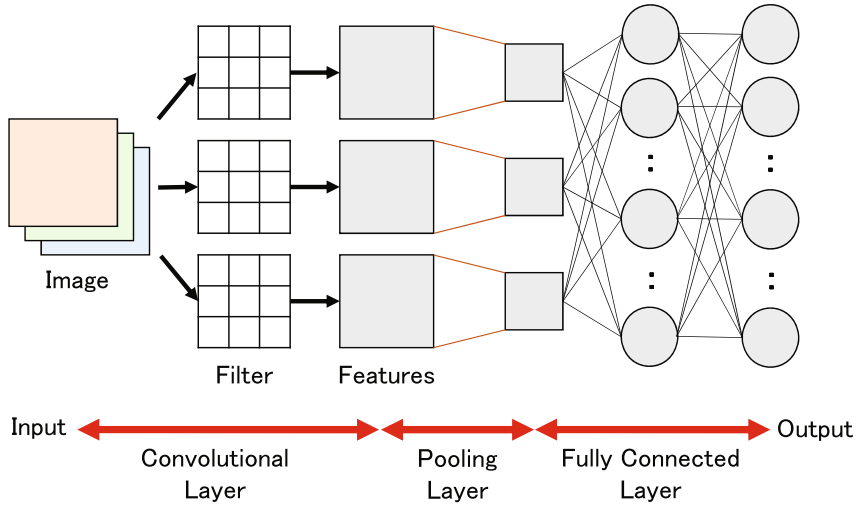


Fig. 3. Convolutional neural network.

An explanation of these is presented below.

#### Convolutional Layer

The convolutional layer has learnable filters. Each filter is spatially small. This layer outputs feature maps by convolving neighbor input nodes with every filter. A feature map expresses topical features such as the edge of an input image.

#### Pooling Layer

The pooling layer compresses an input image by propagating only the largest value in neighbor input nodes.

#### Fully Connected Layer

The fully connected layer is used to classify types of images after the convolutional layer or pooling layer. Every connection learns by the Backpropagation Algorithm.

Deep learning is a great method, but using deep learning is difficult for ordinary developers because it requires technical knowledge such as the intricate deep learning algorithm. Moreover, many deep learning parameters must be set.

### 3.2 Development Support Functions

Our proposed functions are presented in Fig. 4. In this way, the proposed method consists of a Deep Learning Function for an agent to learn by deep learning and a Development Support Mechanism to support parameter setting and confirmation of the learning situation from the DASH framework.

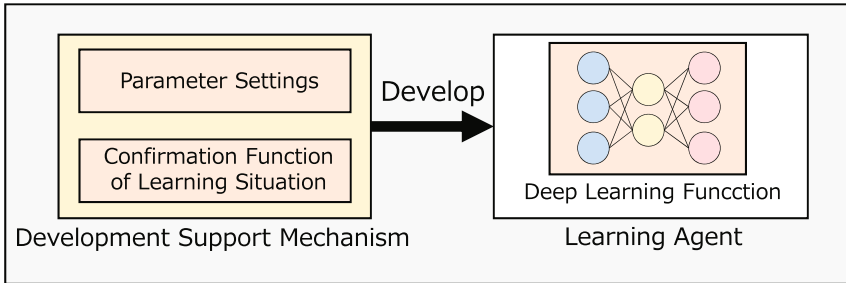


Fig. 4. Development support functions.

This study was designed to support an agent developer on the occasion of development of an agent equipped with a deep learning function. A developer with no detailed knowledge related to deep learning cannot use the algorithm of deep learning to develop a learning agent [3]. As described herein, we support development and operation of deep learning agent with proposed functions from DASH framework and load the deep learning function into an agent. Therefore, we reduce an agent developer's burden and enable an agent to learn by deep learning.

The functions we added are explained below.

#### 3.2.1 Deep Learning Function

The deep learning function is presented in Fig. 5. This acts mutually with the whole inference module. An agent calls the deep learning function from the inference engine in the inference module. The execution result of deep learning function is stored in the working memory in the inference module.

The deep learning function is divided into the Learning Function and the Identifying Function.

##### Learning Function

The learning function is a function to learn the neural network in the proposed function. A learning agent with parameters set in the agent framework reads a training dataset described by the private format to learn. The training dataset describes input images and classes which they come into. An agent saves the result of learning to an external file as a trained model after learning. The trained model enables a learning agent to use the identifying function by reading the training model file.



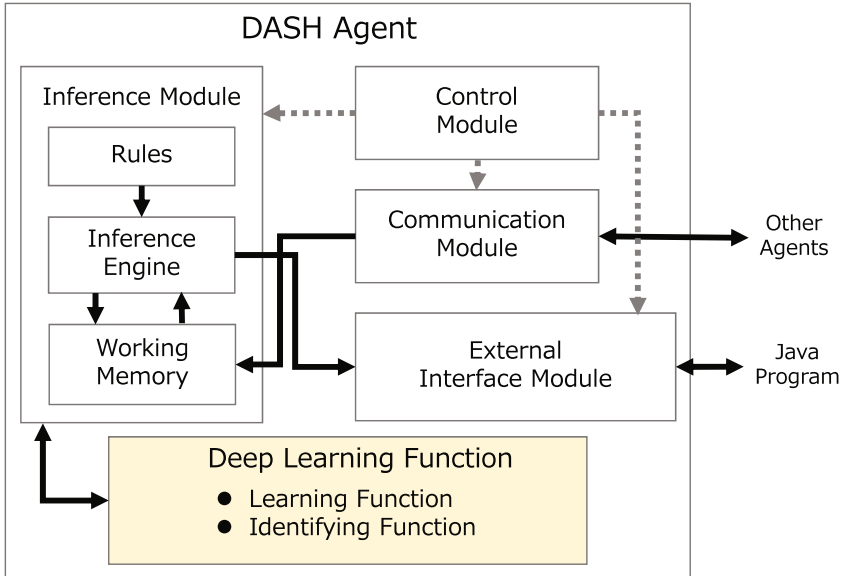


Fig. 5. DASH Agent with deep learning function.

### Identifying Function

The identifying function is a function for classifying the input image by giving the input to a learning agent. First, the development support mechanism reads the training model generated by the learning function. Then, the development support mechanism generates the learning agent with the trained model. Subsequently, the agent reads the input image converted into the private format. Finally, the agent identifies the input and operates based on the identified result.

### 3.2.2 Parameter Setting Function

One problem is that the parameters which must be set by the developer are complex and multifarious. To solve the problem, we introduce the parameter setting function to set various parameters easily on the GUI. When a learning agent with deep learning function starts, the parameter setting function is executed automatically. Settings such as necessary parameters and a trained model are set by the function.

### 3.2.3 Learning Situation Confirmation Function

The confirmation function of learning situation is a function to check on a learning agent's situation during training (Fig. 6). For example, progress of training, execution time, estimated remaining time, and accuracy of training as the information indicated by the function.

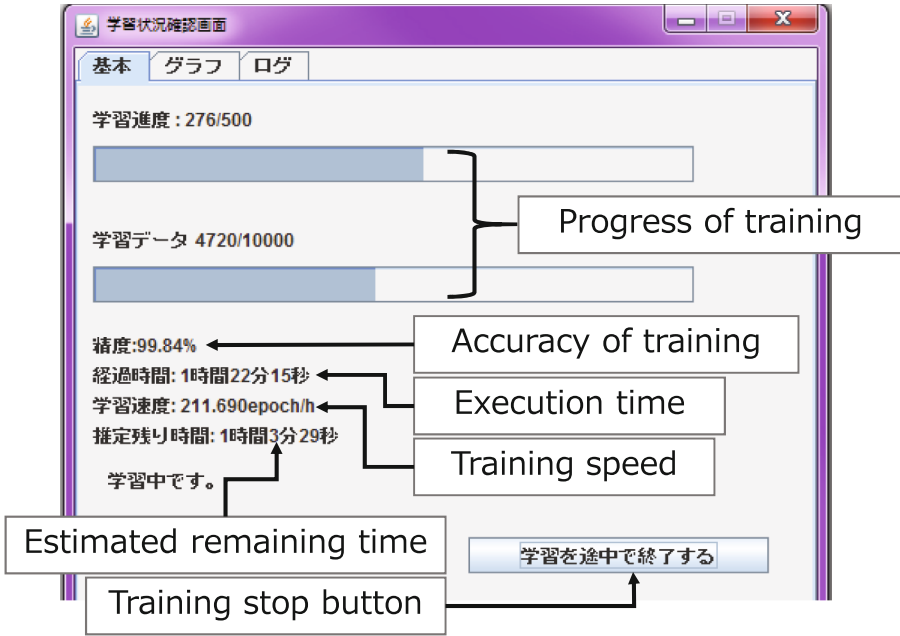


Fig. 6. Confirmation function of the learning situation.

The accuracy is the percentage showing how right training data can be identified by the trained model. A developer can visually confirm the transition of accuracy with automatic drawing of the graph function.

## 4 Experiment

We conducted evaluation experiments for the proposed functions.

### 4.1 Experiment A

We investigated the number of steps required in learning agent development to validate the developer's burden reduction.

#### 4.1.1 Outline

First, we defined respective operations of the following A, B, and C as steps followed during learning agent development.

- A: Describe the code of an agent (every 1 line, 1 step)
- B: Press a button or a check box on the GUI
- C: Input a text on the GUI

Then, we investigated the number of steps until a training agent learns or an identifying agent identifies some input data. We measured the number of the steps after activation of the DASH framework. The goal of a training agent was to execute a training action. The goal of an identifying agent was to execute an identifying action.

#### 4.1.2 Result

Results presented in Table 1 confirmed that development of a learning agent is possible using only a few steps.

**Table 1.** Results of experiment A

Process	A	B	C	Total steps
Develop training agent	14	3	0	17
Set training agent parameters	0	6	12	18
Total of training agent	14	9	12	35
Develop identifying agent	14	3	0	17
Set parameters of identifying agents	0	3	0	3
Total of identifying agents	14	6	0	20

## 4.2 Experiment B

We performed a questionnaire to validate the developer's burden reduction and ascertain whether the proposed functions are convenient.

### 4.2.1 Outline

Four students of our university developed a learning agent. We asked them about the usability of the proposed functions.

### 4.2.2 Result

Each question item and answer is presented in Table 2. Results showed that the proposed mechanism received high evaluations for all questions. Therefore, we infer from the results that the proposed functions are effective in terms of development support of a learning agent.

**Table 2.** Results of experiment B

Question	Average	Standard deviation
Did you develop a learning agent easily?	4.25	0.50
Did you set the parameters of a learning agent easily?	4.00	0.82
Did you operate the parameter settings function rightly?	3.75	1.26
Did you feel that the confirmation function of learning situation is useful?	4.25	0.50

## 5 Conclusion

The goal of this research was to realize various movements of an agent and to support the development of a learning agent for general developers.

We achieved development support of a learning agent with deep learning on a DASH agent framework. The proposed functions can reduce the development burden. We also confirmed the convenience of the proposed functions using evaluation experiments. Results show that the proposed mechanism enables ordinary developers to develop a learning agent with deep learning.

Future research is expected to introduce reinforcement learning with deep learning such as Deep Q-Network [4] to realize autonomous learning of an agent and to widen the range of agent applications.

## References

1. Uchiya, T., Hara, H., Sugarawa, K., Kinoshita, T.: Repository based multiagent framework for developing agent systems. IGI Global 60–79 (2011). Chap. 4
2. Hibino, M., Uchiya, T., Takumi, I., Kinoshita, T.: Development tool of Q-nash learning agent for intelligent system. In: The 18th International Conference on Network-Based Information Systems, pp. 581–585 (2015)
3. Kurotaki, H., Matsuo, Y.: Knowledges and usages of deep learning. In: The 28th Annual Conference of the Japanese Society for Artificial Intelligence (2014)
4. Volodymyr, M., Koray, K., David, S., Andrei, A.R., Joel, V., Marc, G.B., Alex, G., Martin, R., Andreas, K.F., Georg, O., Stig, P., Charles, B., Amir, S., Ioannis, A., Helen, K., Dharshan, K., Daan, W., Shane, L., Demis, H.: Human-level control through deep reinforcement learning. *Nature* **518**(7540), 529–533 (2015)

**The 10th International Workshop  
on Engineering Parallel  
and Multi-Core Systems  
(ePaMus-2017)**

# A Bayes Classifier-Based OVFD Algorithm for Massive Stream Data Mining on Big Data Platform

Liangde Li<sup>1</sup>, Peng Li<sup>2,3</sup>(✉), He Xu<sup>2,3</sup>, and Fangzhou Chen<sup>2</sup>

<sup>1</sup> School of Electronic Science and Engineering,  
Nanjing University of Posts and Telecommunications, Nanjing 210023, China

<sup>2</sup> School of Computer Science,  
Nanjing University of Posts and Telecommunications, Nanjing 210003, China  
lipeng@njupt.edu.cn

<sup>3</sup> Jiangsu High Technology Research Key Laboratory for WSN,  
Nanjing 210003, Jiangsu Province, China

**Abstract.** Recently, online incremental data mining has become an immensely growing area of research for stream data mining. VFDT algorithm, as an excellent incremental decision tree classification algorithm, is widely used in online data mining. To optimize VFDT algorithm, a dynamic tie-breaking threshold strategy and a pre-pruning mechanism strategy are utilized to achieve the reduction of the scale of decision tree. Furthermore, Bayes classifier is applied to leaf nodes of Hoeffding decision tree, which promotes the improvement of classification accuracy. In this paper, this improved algorithm is called OVFD (Optimized VFDT) algorithm. To improve the performance of OVFD for massive streaming data processing, an implementation scheme of OVFD Algorithm on MapReduce Platform is proposed in our paper. Considering the need for real-time computing, the implementation scheme on Storm Platform is designed. Three comparison experiments are designed to compare the scale, the classification accuracy and the execution time of decision tree of three algorithm generate. The simulation results reveal that compared with C4.5 and VFDT algorithm, OVFD algorithm can effectively reduce the scale of the decision tree, achieves the improvement of classification accuracy as well.

## 1 Introduction

Streaming data mining refers to the search for valuable information from fast, large, and continuous data streams [1]. Streaming data is ordered, continuous and constantly changing, unlike the traditional static data, which is stored in the hard disk or memory [2].

Classification technology plays an increasingly important role in data mining [3–5]. Decision tree is a popular classification algorithm. ID3 algorithm, C4.5 algorithm and CART algorithm are the traditional decision tree algorithm with high performance [6, 7]. Many researches show that ID3 algorithm tends to the ignorant of the best attributes [8]. C4.5 algorithm conducts the information gain ratio as criterion, which achieves improvement for the generalization ability of decision tree [9], but this algorithm tends to get local optimal result [10, 11]. Domingos proposed VFDT algorithm in 2000 [12],

which is a popular method of incremental mining, widely used in streaming data classification. VFDT algorithm [13] utilizes Hoeffding inequality to determine the minimum number of samples required for a leaf node to convert to an internal node. It can be proved that VFDT algorithm shares infinite approximate accuracy with decision tree constructed with all input data streams [13, 14].

In order to achieve the processing of massive data streams, cloud computing technology must be adopted [15–17]. MapReduce is a programming model introduced by Google [18], which has developed into a big data processing programming model [19, 20]. Many big data processing applications, such as Hadoop, Storm, adopt computing framework based on MapReduce [21].

Sharmishta Desai implemented VFDT in Hadoop cluster [22], but their distributed computing solution for VFDT algorithm do not achieve effective parallelization. Besides, Hadoop saves intermediate results on disk, which leads to requirement for lots of I/O operations [23], so Hadoop cannot achieve real-time streaming data processing for VFDT algorithm. Storm is Apache's open source project [24], similar to Hadoop MapReduce computing framework. Storm is an open source distributed real-time computing system, which is a perfect distributed real-time computing system [25].

The structure of paper is as follows: Sect. 2 extends VFDT algorithm to Optimized algorithm, two strategies to reduce the scale of Hoeffding decision tree and the strategy of using Bayes classifiers on leaf nodes are also discussed. Section 3 puts forward the distributed computing method in the MapReduce platform. Section 4 discussed the detail implementation scheme of OVFD algorithm on Storm Platform. Section 4 designs experiments to compare the performance of three algorithm on Storm, the conclusion of experimental results are also discussed in this section. Finally, the conclusions are described in Sect. 5.

## 2 Optimized VFDT Algorithm

### 2.1 Moderated VFDT Algorithm

The VFDT algorithm can adopt information gain, information gain ratio and Gini index as criterion of selecting the optimal attribute, and Hoeffding inequality is used as the condition to determine the node splitting. For  $n$  independent observations of a random variable  $r$ , whose range is  $R$ . Hoeffding bounds [26] illustrates that the true mean of  $r$  is at least  $\bar{r} - \varepsilon$ , with the possibility of  $1 - \delta$ , where  $\bar{r}$  is the observed mean of samples.  $\varepsilon$  is defined by

$$\varepsilon = \sqrt{\frac{R^2 \ln(1/\delta)}{2n}} \quad (1)$$

When the evaluation function of several attributes is very close, it is difficult for VFDT to identify the best attribute, the active splitting coefficient  $\tau$ , is introduced to take the initiative to select the decision attribute and realize the splitting of the leaf node.

The Moderated VFDT algorithm extends the VFDT algorithm from two aspects as follows [27]:

**Dynamic tie-breaking threshold:** For traditional VFDT algorithm, tie-breaking threshold  $\tau$  is a user-defined fixed value. The dynamic tie-breaking strategy means that  $\tau$  is calculated as the mean of Hoeffding bound.  $\tau$  is updated with a new node splitting, which is given by

$$\tau_k = \frac{\sum_{i=1}^k HB_{\text{bound}_k}}{k} \xrightarrow{\text{a new splitting}} \tau_{k+1} = \frac{\sum_{i=1}^k HB_{\text{bound}_k} + \varepsilon_{k+1}}{k+1} \quad (2)$$

**Pre-pruning mechanism:** To reduce the depth of decision tree, a light-weight pre-pruning mechanism is utilized to constrain the splitting. For incremental decision tree, pre-pruning mechanism is more suitable than post-pruning mechanism because training samples continue to arrive. If the splitting of leaf nodes cannot lead to the improvement of classification accuracy, the splitting of these leaf nodes will be prohibited.

## 2.2 Improving Moderated VFDT Algorithm Based on Bayes Classification

Bayes classifier is the classifier with the lowest classification error rate in the existing classifier. Its theoretical basis is a basic statistical classification model. To improve the classification accuracy of decision tree, we blend Hoeffding decision tree and Bayes classifier. Suppose attribute vector  $X = (x_1; x_2; \dots; x_d)$ , where  $d$  is the number of attributes. The possibility of  $X$  is classified as class  $Y = y_j$  is defined by

$$P(Y = y_j|X) = \frac{P(Y = y_j) \prod_{i=1}^d P(x_i|Y = y_j)}{P(X)} \quad (3)$$

To apply Bayes classifier to Hoeffding decision tree, the number of samples with class  $y_j$  in training samples is recorded, denoted as  $N_j$ , the number of the number of samples with class  $y_j$  and attribute  $x_i$  in training samples is record, denoted as  $M_j$ . According to law of large numbers, for leaf nodes, Bayes classifier is used to predict its class, which significantly improve classification accuracy. When a test sample arrives, the conditional probability is obtained, the class to which the sample belongs is easy to get

$$h_{nb}(X) = \underset{y \in Y}{\operatorname{argmax}} P(Y = y_j) \prod_{i=1}^d P(x_i|Y = y_j) = \operatorname{argmax}_{y \in Y} \frac{N_j}{N_0} \prod_{i=1}^d \frac{M_j}{N_j} \quad (4)$$

Where  $N_0$  is total numbers of training sample.

## 3 Distributed Computing Scheme for OVFD Algorithm

### 3.1 Parallelization Scheme of OVFD Algorithm

**Horizontal Parallelism scheme.** Whenever the data streams comes to the cluster, the samples is divided into several data blocks, assigned to different slave nodes, and the execution flow chart is shown as follows (Fig. 1):



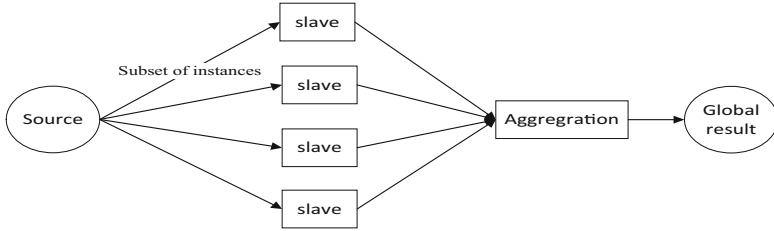


Fig. 1. Distributed computing based on horizontal parallelism

**Vertical Parallelism scheme.** When data source sends data streams to the cluster, the master node accepts the data. The data streams is divided into several data blocks according to the attributes, each data block contains the statistics of all samples of one or more attributes. The execution flow chart is shown as follows (Fig. 2):

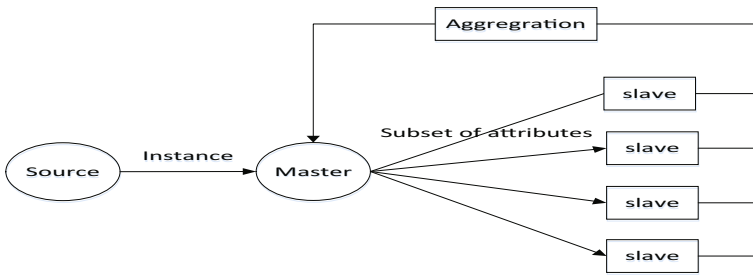


Fig. 2. Distributed computing based on vertical parallelism

### 3.2 Implementation Scheme of OVFD T Algorithm in MapReduce Environment

**Split Phase.** The training samples traverse from the root until it reaches the leaf node. The Split function divides the samples into several data blocks according to their attributes. Each data block contains all samples of one or more attributes. Each sample is written into memory with specific format  $\langle leafID|attributeID|class \rangle$ . The pseudo-code implementation of this stage is shown in Table 1.

Table 1. Pseudo-code implementation of Split phase

---

**Algorithm 2:** Split()

---

1. for each example  $s$  from  $S$  do
2. sort  $s$  into a leaf  $l$  based on its attribute vector
3. Update the number of examples seen at leaf  $l$ :  $n_l \leftarrow n_l + 1$
4. if  $n_l \bmod n_{min} = 0$  and examples at leaf not all of same category then
5. Push  $l$  into the list of splitting leaf
6. for each example seen at  $l$
7. Transform its format into:  $\langle leafID|attributeID|class \rangle$

---

**Map phase.** Firstly, the slaves read the data blocks generated in the Split phase. Secondly, each slave node calculates the evaluation function of corresponding attributes. Thirdly, the attribute  $X_a^{local}$  with the local highest evaluation function and the other one  $X_b^{local}$  with the local second highest evaluation function will be selected. Finally, let  $Key_1 = \langle leafID | X_a^{local} | X_b^{local} \rangle$ ,  $Value_1 = \langle G(X_a^{local}) | X_b^{local} \rangle$ . The result is returned with key-value pairs format. The pseudo-code implementation of this phase is shown in Table 2.

**Table 2.** Pseudo-code implementation of Map phase

---

**Algorithm 3: Map(block)**

---

1. Update corresponding statistics Table
  2. Get leafID l from block
  3. **for** each attribute  $X_i$  seen at l
  4.     Compute  $G(X_i)$
  5.     Find the attribute  $X_a^{local}$  with the highest G
  6.     Find the attribute  $X_b^{local}$  with the second highest G
  7.     Let  $Key_1 = \langle leafID | X_a^{local} | X_b^{local} \rangle$
  8.     Let  $Value_1 = \langle G(X_a^{local}) | X_b^{local} \rangle$
- 

**Combine Phase.** The key values generated by the Map phase are integrated to obtain the attributes with the highest evaluation function and the second highest evaluation function on each leaf node. Finally, the results are returned in the form of key pairs.

**Reduce Phase.** The cluster assigns the calculation task to the different slave nodes according to the different key and the corresponding value. Reduce function is run on the slave node, which aims at the calculation of Hoeffding bound to get the decision attribute. Finally, the state of Hoeffding decision tree and  $\tau$  is updated. The pseudo-code implementation of this stage is shown in Table 3.

**Table 3.** Pseudo-code implementation of Reduce phase

---

**Algorithm 5: Reduce ( )**

---

**Input:**  $\langle Key_2 | Value_2 \rangle$  pairs from Combine phase

---

1. Calculate Hoeffding bound  $\epsilon = \sqrt{\frac{R^2 \ln(1/\delta)}{2n_l}}$
  2. **if**  $X_a \neq X_\emptyset$  and  $(G(X_a) - G(X_b) > \epsilon)$  or  $\epsilon < \tau$
  3.     Convert leaf l to an internal node
  4.     **if** the generalization ability of decision tree is get improved
  5.     Split leaf l with  $X_a$
  6.     Update  $\tau = \frac{\tau_{k+1} + \sum_{i=1}^k \tau_i}{k+1}$
-

## 4 The Implementation Scheme of OVFD T on Storm Cluster

### 4.1 Implemental Hoeffding Decision Tree Construction Module

As Fig. 3 shows, after getting training samples from Kafka Spout, Split bolt runs the Split function, which aims at updating the statistics after the sample arrives. Map bolts are responsible for finding the attribute with the local highest evaluation function, the other one with the second local highest evaluation function. Combine bolts focus on the aggregation of the calculation result of Map bolt, so as to the globally best attribute and the second best attribute. Reduce bolts concentrate on the calculation of Hoeffding boundary and the selection of decision attribute, carrying out pre-pruning mechanism to restrain the depth exploration of Hoeffding decision tree and implementing the serialization store of Hoeffding tree to Redis.

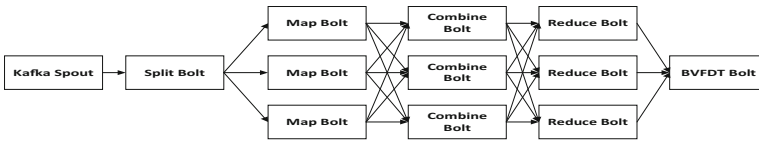


Fig. 3. The structure of decision tree construction module

### 4.2 Classification Module

Classification module contains the Datapro bolt, the Bayes classification bolt and the Prediction bolt. Datapro bolts use random packets to pull data from Kafka Spout, so that the number of samples processed by each task is approximately the same. Bayes classification Bolts also take random packets from Datapro bolts, run Bayes classifier programming to obtain the class samples belong to. Finally, the Global grouping is used to distribute the classified samples to the Prediction Bolt, achieving the results of serialization stored in Redis.

## 5 Experiment on Storm

### 5.1 Experimental Methodology

**Clusters Configuration.** We arranged our cluster environment in three physical hosts, including Zookeeper 3.4.9 version, Storm 1.0.3 version, Kafka 2.8.1 version, Redis using 3.2.8 version.

**Data Source.** The training samples and test samples source is a random sampling and combination of the KDDCUP1999 Data. The algorithm reads the outline file KDDCUP.names before reading the data stream. The KDDCUP1999 contains 41 attributes and 23 data categories.

## 5.2 Comparison of Performance of Three Algorithms

To verify the efficiency and accuracy of VFDT and OVFD algorithms, three algorithms of C4.5, VFDT and OVFD are evaluated by three aspects: tree scale, execution time and classification accuracy.

**Tree scale comparison.** The decision tree of the three algorithms is generated by the training samples with the sample capacity of 1000, 15000, 25000, 35000, and 45000, and the number of nodes of the decision tree is counted. Figure 4 shows the histogram that the number of decision tree nodes increases as the capacity of training samples increases.

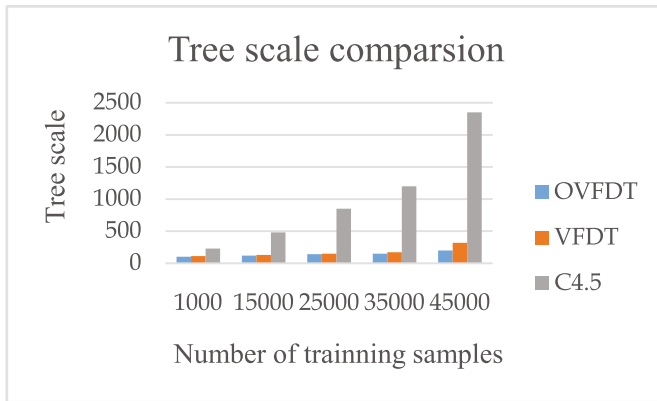


**Fig. 4.** Comparison of tree scale of three algorithms

By analyzing the histogram above, we can conclude that:

- (1) When the capacity of training samples is small, there exists tiny difference between the number of decision tree nodes generated by the three algorithms, but OVFDT algorithm and VFDT algorithm tend to generate less nodes compared with C4.5 algorithm.
- (2) With the increase of the number of training samples, the relationship between the speed at which the decision tree nodes are generated by three algorithm is:  $OVFDT < VFDT \ll C4.5$ .

The conclusions above prove that dynamic tie-breaking strategy and pre-pruning strategy achieve the reduction of tree scale, which leads to lesser memory consumption and makes OVFDT algorithm more suitable for data streaming mining due its lightness.

**Execution time comparison.** The decision tree of the three algorithms is generated by the training samples with the sample capacity of 1000, 15000, 25000, 35000, and 45000, and the number of nodes of the decision tree is counted. Figure 5 shows the histogram that the number of decision tree nodes increases the training samples increases.

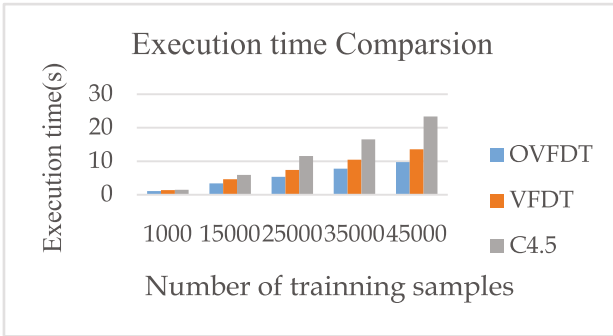


Fig. 5. Comparison of execution time of three algorithms

By analyzing the histogram above, we can conclude that:

- (1) When the training data is small, the execution time of the three algorithms is not very different, but the execution time of the OVFDT algorithm tends to be smaller than the other two algorithms
- (2) As the number of training samples increases, the relationship between the rate of change in the execution time of the three algorithms is  $OVFDT < VFDT \ll C4.5$ .

The conclusion above proves that dynamic tie-breaking strategy and pre-pruning strategy achieve the reduction of execution time of building decision tree, which leads to lesser learning time consumption.

**Accuracy comparison.** For the decision tree generated by the previous experiment, the test set with the sample capacity of 10,0000 is tested. Figure 6 shows the accuracy diagram.

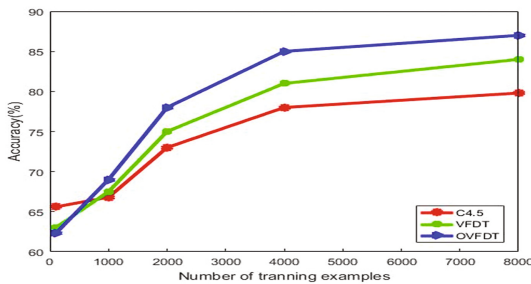


Fig. 6. The accuracy diagram

By analyzing the curves in the graph, we can conclude that:

- (1) When the capacity of training samples is small,OVFDT algorithm is less accurate than VFDT and C4.5, which may be due to the capacity of training samples is too small, so that the calculation of Bayes conditional probability is not accurate enough;

- (2) With the increase in the capacity of the training samples, the accuracy of the three algorithms is: OVFD  $>$  VFDT  $>$  C4.5, which shows that the accuracy of OVFD algorithm is higher than VFDT and C4.5 algorithm.

The conclusions above prove that the strategy that using Bayes classifier on leaf nodes promotes the improvement of classification accuracy.

## 6 Conclusion

This paper proposes an optimized VFDT(OVFD) algorithm, which effectively improve the improvement of VFDT algorithm form two aspects. Dynamic tie-breaking threshold and pre-pruning mechanism are adopted to reduce the scale of Hoeffding decision tree, Bayes classifier is utilized in leaf nodes to improve the classification accuracy. Furthermore, vertical parallelism scheme is adopted to achieve the distributed computing of OVFD, and the detail implementation schemes of Split phase, Map phase, Combine phase, Reduce phase in MapReduce Platform are designed. Considering the need for real-time computing, Storm is chosen to implement OVFD algorithm. To verify the scale and accuracy of our newly proposed algorithm, three comparison experiments are designed to compare the scale, the classification accuracy and the execution time of decision tree generated by three algorithm. Experimental results present that OVFD algorithm effectively improve the performance of Hoeffding decision tree.

**Acknowledgments.** The subject is sponsored by the National Natural Science Foundation of P. R. China (No. 61373017, No. 61572260, No. 61572261, No. 61672296, No. 61602261), the Natural Science Foundation of Jiangsu Province (No. BK20140886, No. BK20140888, No. BK20160089), Scientific & Technological Support Project of Jiangsu Province (No. BE2015702, No. BE2016777, BE2016185), China Postdoctoral Science Foundation (No. 2014M551636, No. 2014M561696), Jiangsu Planned Projects for Postdoctoral Research Funds (No. 1302090B, No. 1401005B), Jiangsu High Technology Research Key Laboratory for Wireless Sensor Networks Foundation (No. WSNLBZY201508).

## References

1. Wu, X., Zhu, X., Wu, G.Q., et al.: Data mining with big data. *IEEE Trans. Knowl. Data Eng.* **26**, 97–107 (2014)
2. Tan, P.N.: *Introduction to Data Mining*. Pearson Education India, Upper Saddle River (2006)
3. Wu, K., Kang, J., Chi, K.: Research on fault diagnosis method using improved multi-class classification algorithm and relevance vector machine. *Int. J. Inform. Technol. Web Eng. (IJITWE)* **10**, 1–16 (2015)
4. Pradhan, R., Sharma, D.K.: TemporalClassifier: Classification of implicit query on temporal profiles. *Int. J. Inform. Technol. Web Eng. (IJITWE)* **10**, 44–66 (2015)
5. Wu, Z., Lin, T., Tang, N.: Explore the use of handwriting information and machine learning techniques in evaluating mental workload. *Int. J. Technol. Hum. Interac. (IJTHI)* **12**, 18–32 (2016)
6. Dietterich, T.G.: Ensemble methods in machine learning. In: Kittler, J., Roli, F. (eds.) *MCS 2000*. LNCS, vol. 1857, pp. 1–15. Springer, Heidelberg (2000). doi:[10.1007/3-540-45014-9\\_1](https://doi.org/10.1007/3-540-45014-9_1)

7. Domingos, P., Hulten, G.: Mining high-speed data streams. In: Proceedings of the Sixth ACM SIGKDD International Conference on Knowledge Discovery and Data Mining, pp. 71–80. ACM (2000)
8. De Mántaras, R.L.: A distance-based attribute selection measure for decision tree induction. *Mach. Learn.* **6**, 81–92 (1991)
9. Friedman, J.H., Kohavi, R., Yun, Y.: Lazy decision trees, pp. 717–724 (1996)
10. Shah, S., Chauhan, N.C., Bhandari, S.D.: Incremental mining of association rules: a survey. *Int. J. Comput. Sci. Inform. Technol.* **3**, 4071–4074 (2012)
11. Mitra, S., Pal, S.K., Mitra, P.: Data mining in soft computing framework: a survey. *IEEE Trans. Neural Networks* **13**, 3–14 (2002)
12. Hulten, G., Spencer, L., Domingos, P.: Mining time-changing data streams. In: Proceedings of the Seventh ACM SIGKDD International Conference on Knowledge Discovery and Data Mining, pp. 97–106. ACM (2001)
13. Last, M.: Online classification of nonstationary data streams. *Intell. Data Anal.* **6**, 129–147 (2002)
14. Song, X., He, H., Niu, S., et al.: A data streams analysis strategy based on hoeffding tree with concept drift on Hadoop system. In: 2016 International Conference on Advanced Cloud and Big Data (CBD), pp. 45–48. IEEE (2016)
15. Su, Z., Sun, C., Li, H., et al.: A method for efficient parallel computation of Tate pairing. *Int. J. Grid Util. Comput.* **3**, 43–52 (2012)
16. Petrlc, R., Sekula, S., Sorge, C.: A privacy-friendly architecture for future cloud computing. *Int. J. Grid Util. Comput.* **26**(4), 265–277 (2013)
17. Yuriyama, M., Kushida, T.: Integrated cloud computing environment with IT resources and sensor devices. *Int. J. Space-Based Situated Comput.* **1**, 163–173 (2011)
18. Dean, J., Ghemawat, S.: MapReduce: simplified data processing on large clusters. *Commun. ACM* **51**, 107–113 (2008)
19. Mori, T., Nakashima, M., Ito, T.: SpACCE: a sophisticated ad hoc cloud computing environment built by server migration to facilitate distributed collaboration. *Int. J. Space-Based Situated Comput.* **2**, 230–239 (2012)
20. Mezghani, K., Ayadi, F.: *Int. J. Technol. Hum. Interact. (IJTHI)* **12**, 1–20 (2016)
21. Urbani J, Margara A, Jacobs C, et al. AJIRA: a lightweight distributed middleware for MapReduce and stream processing. In: 2014 IEEE 34th International Conference on Distributed Computing Systems (ICDCS), pp. 545–554. IEEE (2014)
22. Desai, S., Roy, S., Patel, B., et al.: Very Fast Decision Tree (VFDT) algorithm on Hadoop. In: 2016 International Conference on Computing Communication Control and automation (ICCUBEA), pp. 1–7. IEEE (2016)
23. Joshi, SB.: Apache hadoop performance-tuning methodologies and best practices. In: Proceedings of the 3rd ACM/SPEC International Conference on Performance Engineering, pp. 241–242. ACM (2012)
24. Toshniwal, A., Taneja, S., Shukla, A., et al.: Storm@ twitter. In: Proceedings of the 2014 ACM SIGMOD International Conference on Management of Data, pp. 147–156. ACM (2014)
25. Xin, R.S., Gonzalez, J.E., Franklin, M.J., et al.: Graphx: a resilient distributed graph system on Storm. In: First International Workshop on Graph Data Management Experiences and Systems. ACM (2013)
26. Hoeffding, W.: Probability inequalities for sums of bounded random variables. *J. Am. Stat. Assoc.* **58**, 13–30 (1963)
27. Li, F., Liu, Q.: An improved algorithm of decision trees for streaming data based on VFDT. In: IEEE International Symposium on Information Science and Engineering, ISISE 2008, vol. 1, pp. 597–600 (2008)

# Congestion Aware Routing for On-Chip Communication in NoC Systems

Gul N. Khan<sup>(✉)</sup> and Stephen Chui

Electrical and Computer Engineering, Ryerson University,  
350 Victoria Street, Toronto, ON M5B 2K3, Canada  
gnkhan@ee.ryerson.ca

**Abstract.** Adaptive on-chip communication is critical to the design of multi-core system-on-chip. Wormhole routers provide an effective mechanism to exchange data among the multiple cores in the NoC. Efficient packet allocation can improve the performance of adaptive wormhole routing by prioritizing uncongested packets to reach their destinations first. This paper presents a routing methodology that collects traffic/congestion information, and employs it to prioritize long distance traveling packets during high congestion. Each NoC router collects traffic/congestion information from its nearby routers and makes routing decisions to select some packets for travelling first that can reach their destination cores faster. We utilize header flits to carry congestion information rather than adding dedicated communication links among the routers. It saves extra communication links between routers, and simpler SoC layout is achieved due to fewer inter-connection wires. Our NoC router design improves the NoC throughput. The experimental results indicate performance improvement for long distance traffic.

**Keywords:** Multi/many core SoCs · Network-on-chip systems · NoC router micro-architecture · On-chip communication · Virtual channel and switch allocation

## 1 Introduction

Multi-core SoCs (System-on-a-Chip) have evolved with new on-chip applications. Processing, memory and other IP cores require higher on-chip communication bandwidth, which traditional bus-based SoCs cannot provide. Network-on-chip (NoC) has higher bandwidth and allows easier growth of multi-core systems. However, NoCs cannot handle large scale data transfers and efforts are being made to reduce congestion to increase the overall throughput of the NoC systems. Congestion in the NoC can be improved by reducing the latency. Generally, NoCs employ virtual channel (VC) based wormhole routing. The use of dynamic buffering allows each individual VC to increase its buffer size to accommodate the remaining flits of a packet to reduce blocking [1]. However, dynamic buffering based VCs have their own problems such as complexity, intervention among VCs, etc.

Early adaptive routers made their packet routing decisions based on the traffic information of their neighbors [2]. An initial adaptive NoC router switches to adaptive routing for a traffic congestion threshold. There are many advantages of adaptive



routing as compared to deterministic (e.g. XY) routing. However, in contrast to pure deterministic routing such as DOR (Dimension Order Routing), adaptive routing can result in deadlocks. The Odd-Even turn model has been proposed as one of the solutions for deadlock and live lock free adaptive routing [2]. The adaptive routing proposed by Kim et al. employs direction mapped VCs to prevent deadlocks [3]. In direction mapped VC allocation, each VC is mapped to an output direction that automatically eliminates any cyclic routing patterns. Escape VC was proposed by Duato as an alternate to prevent deadlock [4]. A specific Escape VC is designated for utilization to achieve deadlock free routing. Utilizing a sideband network for the transmission of congestion data has been proposed by different researchers [5–7]. Gratz et al. proposed Regional Congestion Awareness (RCA) methodology, that considers the congestion beyond the direct neighbors to improve throughput [5]. It is also argued that destination based adaptive routing algorithms (DAR and DBAR) perform better than regional adaptive routing techniques [6, 7]. The architectures proposed use a sideband network. Adaptive routing could be further improved by utilizing a Global Congestion Awareness (GCA) mechanism [8]. We present a congestion aware NoC router that provides higher performance during congestion while operating at near saturation traffic situations.

## 2 Overview and Motivation

A typical wormhole NoC router is shown in Fig. 1. The micro-architecture of a traditional router consists of input and output ports, an arbiter, and a crossbar switch. In this paper, the input-ports contain the VC buffers, and the output-ports are simple data buses. After buffering a flit, the input-port issues a request signal to the arbiter. The arbiter accommodates VC and Switch allocators and performs arbitration among the potential VC flits that make request to access the crossbar and other shared resources [9]. The crossbar switch can be configured to connect any input buffer of the router to any output port, where one input-port is connected to only one output-port.

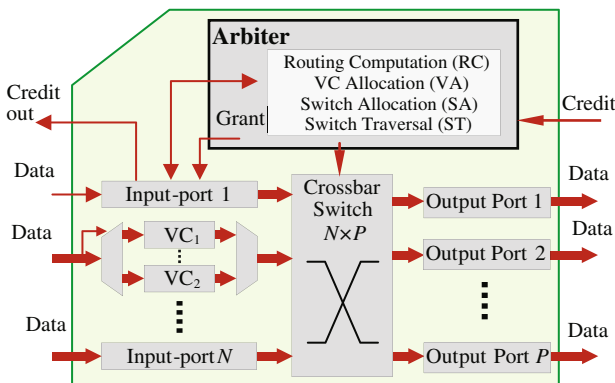


**Fig. 1.** Typical wormhole NoC router

Destination-based congestion-aware adaptive routing improves latency in the NoC for high traffic situations. Most of the regional congestion aware based NoC routing research is focused on improving the latency and throughput by refining the routing mechanism. The baseline NoC routers use round-robin (RR) scheme for both VC and switch allocation due to its simplicity. There are numerous benefits of using the round-robin VC and switch allocation; however, this scheme is not efficient in different traffic scenarios. Organization of packets in a specific order will certainly allocate a packet to a congested VC and the packet may not be able to travel in the NoC efficiently. For limited number of VCs, allocating an alternate packet that has no congestion on its path will improve the overall NoC latency and throughput.

One of the ways to present performance of on-chip communication network is latency, which is the time taken by a packet to reach its destination. There are mainly two categories of latency that can be measured for various traffic patterns. Average latency is commonly used to evaluate the performance of the NoC. However, for average latency, some packets experiencing high latency may be hidden. Maximum latency represents the worst-case scenario, where a packet would experience the highest latency. Usually packets that travel between the routers/cores located at the opposite ends of a 2D-mesh NoC suffer the worst latencies.

### 3 Congestion Aware NoC Routing

In congested NoCs, a packet can spend most of its time waiting for a VC assignment which is a buffer slot in the downstream router. The waiting time for a packet traveling long distance from the current router to its destination will not increase significantly if that packet is held in-between until the alleviation of congestion. The benefit of allocating available VCs to another packet with lower delays to its destination will allow that packet to traverse the NoC quickly. Some applications have traffic patterns, which usually varies with periods of packet burst. In an unsaturated NoC, active packets facing delays (due to congestion) in reaching their destinations will wait until the alleviation of congestion before continuing their journey in the NoC.

Regional adaptive routing algorithms such as RCA, DAR, DBAR and GCA utilize congestion information during the routing decision making process [5–8]. In addition to utilizing the congestion data for adaptive routing, we propose to use the information for VC allocation to improve performance. In place of RR-based VC allocation, we present a congestion-aware VC allocator to prioritize uncongested VCs to allocate them first. It is particularly useful when only a limited number of VCs are available. In addition to prioritizing the allocation by the VC allocator, a similar process is applied to the switch allocator. Considering that certain packets would take longer to reach their destinations, prioritization can be applied to packets that would be stuck in the NoC due to congestion. These packets are usually the ones that travel longer distance across the NoC as they have more chances to wait as allocation may fail for them. It increases the average latency as these packets are likely to spend significant amount of time while waiting in a congested region of the NoC.

The allocation methodology in NoC router is customized to improve the performance for all the packets. The methodology is improved by lowering the priority of

long distance packets under congested conditions that results in better NoC latency. There are two approaches to alter round-robin arbitration i.e. either by changing how VCs are allocated or how flits are allocated by the switch allocator.

### 3.1 VC/Switch Allocation

VC allocation is a critical process where the arriving packets are assigned a VC identification (VCID) in the downstream router. Fairness and deadlock avoidance are considered during this process. We propose to amend the RR-based allocation to ensure that no packets are starved while improving the latency and throughput of the NoC. With the destination-based adaptive routing, congestion is determined for the current source to the destination router. Using the congestion information, a modified round-robin methodology will deny any VC allocation requests if a packet path to the destination is greater than a threshold (number of hops). For an  $N \times N$  mesh NoC, we use a threshold of  $N * 3/2$  in this paper. If congestion persists for that packet, it is also important to avoid starvation. A counter register is used to track the number of cycles that the packet is held on waiting. When the counter reaches to a maximum allowed wait time, the packet is treated as uncongested and would be allocated in a round-robin way. Figure 2a illustrates our proposed VC allocation mechanism. Switch allocation is a process where flits are selected for crossbar traversal at every clock cycle. Under normal circumstances, RR-based process accepts request of only one VC at a time and then prioritizes it for the next VC request. To improve average latency for prioritized long distance packets, the scheme is modified to permit these packets to allow two flits to be allocated in consecutive cycles before allowing the round-robin counter to increment for the next VC. The amended switch allocation process is given in Fig. 2b.

Packets have a prioritization flag to indicate that the packet can be prioritized. It is important to limit the number of packets being prioritized to avoid non-prioritized packets from starving. Normally for a 2D-mesh NoC, only packets traveling longer distances (i.e. packets traveling from one corner to another) are prioritized. Our congestion-aware adaptive routing (CAAR) can be extended for QoS applications where certain packets are given priority to ensure lower latency. Our VC allocation procedure of Fig. 2a, determines if the CAAR mechanism will prioritize any VC allocation requests or not. When an unassigned packet requests for an output VCID and it is prioritized, CAAR would ignore (based on congestion data) the non-prioritized requests and perform allocation between prioritized requests.

### 3.2 Congestion Aware Adaptive Router Micro-Architecture

In addition to the NoC router components shown in Fig. 1, CAAR router has a header extractor, congestion awareness component, (input) port pre-selection and header replacement components at the output-ports as shown in Fig. 3. Moreover, CAAR router also employs congestion awareness prioritization for VC (CVA) and switch arbitration (CSA). CVA mechanism given in Fig. 2a only prioritizes VC allocation while CSA only prioritizes the switch allocation following the CSA mechanism

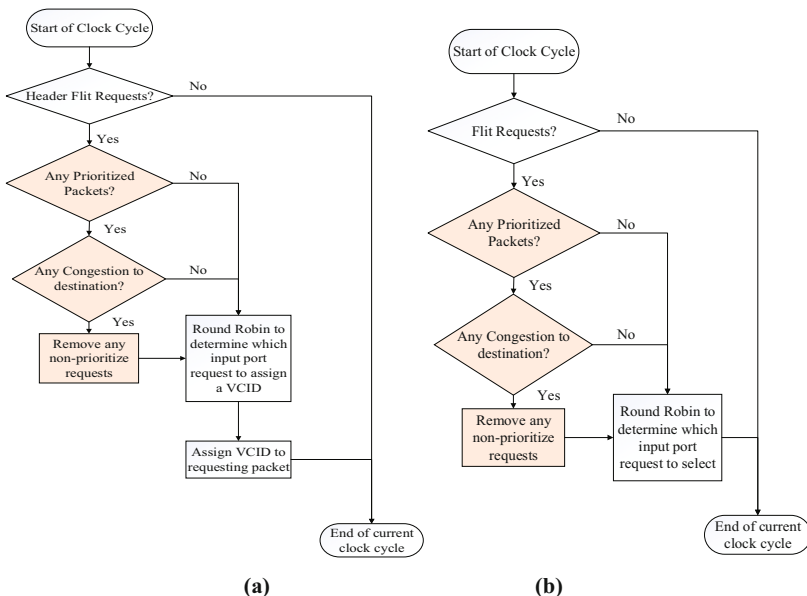


**Fig. 2.** (a) CVA: Congestion-aware VC allocation (b) CSA: Congestion-aware switch allocation

illustrated in Fig. 2b. The proposed CAAR router micro-architecture is a pipelined adaptive NoC router based on the baseline adaptive router [3]. The router consists of five stages: Buffer Write (BW), Route Computation (RC), VC allocation (VA), Switch Allocation (SA) and Crossbar Traversal (XT). Moreover, one cycle is required for channel Link Traversal (LT). Look-ahead routing is leveraged to allow the router output directions that can be pre-selected to remove the BW stage from the pipeline. A flit that arrives at the router will traverse the allocators immediately in parallel to buffering if the flit fails to win an output port. Speculative switch allocation is utilized to allow both VA and SA stages to proceed in parallel.

In our proposed CAAR router, the number of available VCs is used as a congestion evaluation metric. Ma and others have employed single-bit information to represent the congestion state of specific router known as DBAR [7]. Based on the same idea, each router propagates congestion information to its neighboring (specifically upstream) routers. We embed the congestion information in the header flits instead of a sideband network used in DAR [6] and DBAR [7]. Our methodology is an extended version of RCA mechanism [5]. The recently proposed NoCs have 128-bit size flits with many unused bits in the header flit. The congestion information would require a minimum of 1-bit per router or 8-16 bits in total for an  $8 \times 8$  mesh topology NoC. We utilize a destination based congestion table to track traffic conditions, which is similar to DAR and DBAR techniques. The congestion table is updated as new congestion information becomes available. The routing computation would utilize this table to make decisions for adaptive routing. Figure 4 shows the organization of header flit to accommodate congestion information. A congestion data unit would monitor the link for traffic congestion information and update the information at a specific interval if desired.

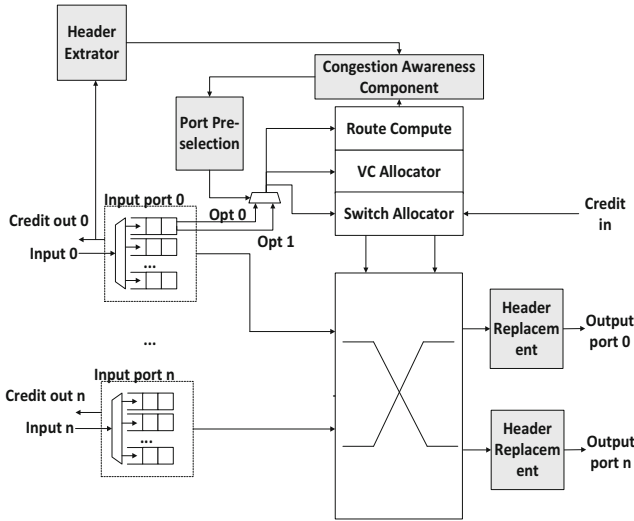


Fig. 3. CAAR router micro-architecture.

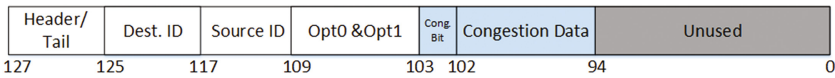
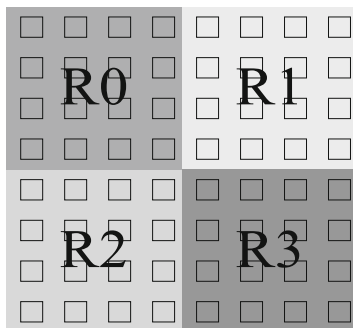


Fig. 4. Packet organization.

### 4 Experimental Results

A transaction level SystemC simulator is used to model the micro-architecture of our CAAR router presented in this paper. The pipelined NoC router employs three cycles: one for VC and switch allocation, 2<sup>nd</sup> for crossbar traversal and the third cycle for link traversal. CAAR performance is evaluated by employing synthetic traffic. Flits are injected into the NoC at a constant rate. For uniform traffic, each source node (core/router) sends a packet to a different destination. In a 2D mesh of N×N size NoC, Transpose traffic is generated by sending packets from all the source nodes (i, j) to destination nodes (j, i). Where a node (i, j) represents the core/router placed at row i and column j of a 2D mesh. In the case of Shuffle traffic, packets are sent from (i, j) to (2\*i, 2\*j) if 2\*i < N or else to (2\*(i-N-1), 2\*j). Regional uniform traffic is most likely to send packets within a region but sometimes send packets to elsewhere in the NoC. This type of traffic has a higher likelihood as NoC organizations would likely to have more cores, which communicate with the closest one. Figure 5 shows the partitioning of an 8 × 8 mesh NoC into four regions (R0, R1, R2 and R3) where each region is a 4 × 4 mesh. This type of organization can also be expanded to 16 × 16 mesh NoCs.



**Fig. 5.** Uniform traffic regions.

The NoC is setup in the form of  $4 \times 4$  and higher 2D-mesh topologies. The router employs 8 VCs with 5 flit-slots per VC. The simulation is warmed up with 10,000 cycles before the performance measurement is started. Then the packets are monitored for another 100,000 cycles to obtain an average-latency based performance. The delay threshold for determining the existence of congestion is carefully selected. Since RCA type methodology is used to obtain congestion, the congestion values are aligned with the congestion data. It is important to determine if any congestion is significant to use the priority-based arbitration scheme in CAAR or a certain amount of congestion is necessary to be present before CAAR's priority based arbitration is enabled. To determine how the threshold value affects the arbitration, different values are evaluated at different injection rates.

We have chosen the utilized VCs as the congestion measuring metric. For example, with eight VCs available, four or more occupied VCs are considered as a congested region in the NoC. It means that half of the VCs are free in the region where the packet will be transmitted. In our experiments, 80% of the traffic is sent within the region and the remaining 20% packets are sent to elsewhere in the NoC. We also need another threshold to determine long distance packets for prioritization in both CVA and CSA mechanisms. For an  $N \times N$  mesh NoC, we have employed a threshold of  $N * 3/2$  (i.e.  $> 12$  for  $4 \times 4$  size mesh NoC) hops. Our methodology is intended to be used for large NoC systems (e.g.  $8 \times 8$  or higher size mesh NoCs) as more packets of larger NoCs travel long distances. We have also evaluated our CAAR methodology for a smaller size  $4 \times 4$  2D-mesh NoC to determine its applicability for smaller NoC systems.

We have implemented the baseline adaptive routing (local) [3] for comparison with RCA [5], and a modified DBAR [7] architecture without sideband links for congestion data transmission. CAAR methodology is compared with the past techniques for Uniform and Transpose traffic patterns and the results are presented in Figs. 6a and b. We measured average latency and it is evident from the results that CAAR have similar or better performance as compared to past techniques. We also present the average latency for  $8 \times 8$  mesh NoCs in Fig. 7.

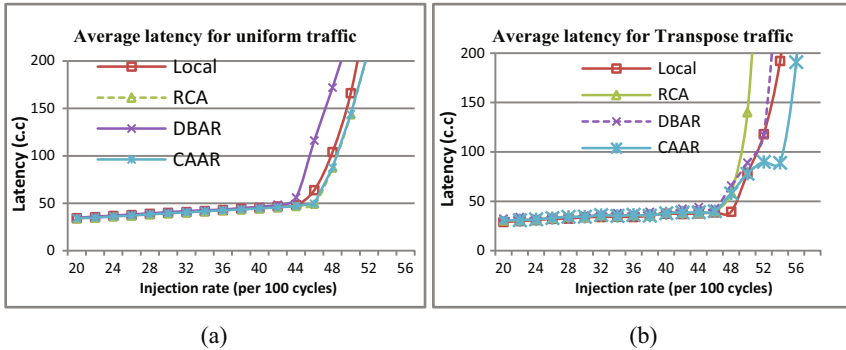


Fig. 6. 4 × 4 mesh NoC average latency for 8 VCs.

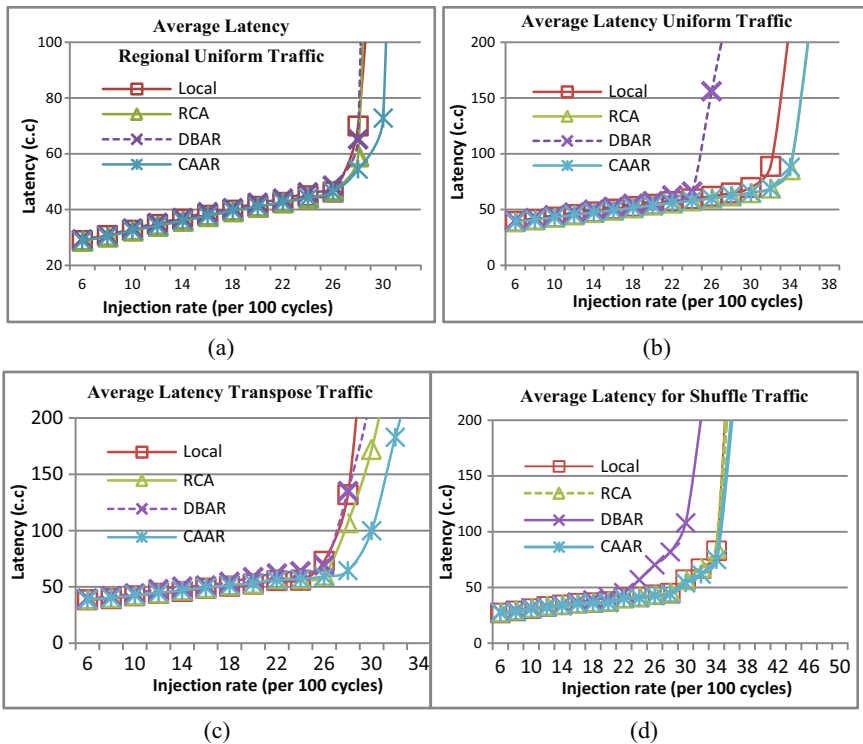


Fig. 7. 8 × 8 mesh NoC performance (Average Latency) for different traffic patterns.

Our CAAR mechanism has shown an improvement of 10-11% in the average latency for uniform and regional uniform traffic (see Figs. 7a and b). As compared to past techniques, our methodology has better average latency when majority of the packets are sent to the neighboring routers with a few packets being sent to longer distances in the NoC. In the case of Shuffle traffic, CAAR performs at par or slightly

better than the RCA mechanism as shown in Fig. 7d. Shuffle traffic rarely have long distance traveling packets. CAAR does perform better for Transpose traffic with 7% improvement over the RCA as indicate by the results of Fig. 7c. Transpose traffic has some packets traveling across the NoC, which allowed those packets to be prioritized under congested conditions.

CAAR based NoC performance has also been investigated for larger  $16 \times 16$  NoC. For Uniform traffic, CAAR outperforms all the past methods (RCA, DBAR, local) in terms of lower average-latency and saturation at higher injection rates as shown in Fig. 8a. For regional uniform traffic, CAAR shows a 4% improvement over RCA and local traffic as per results shown in Fig. 8b. We define the long-distance packets are those, which travel for twelve or more hops. The long-distance packet travelling distance is about a quarter of the distance in a  $16 \times 16$  2D-mesh NoC. In this way, there are more packets that are considered long distance for prioritizing in the CAAR resulting in lower improvement as compared to  $8 \times 8$  mesh NoC. We have also compared CAAR performance with the GCA methodology that uses header flits to carry congestion information at the global level in the NoC. The average latency results of GCA methodology is drawn as dotted line and our CAAR methodology outperforms GCA for high traffic situations when the injection rates are beyond 17 and 20 for uniform and shuffle traffics respectively.

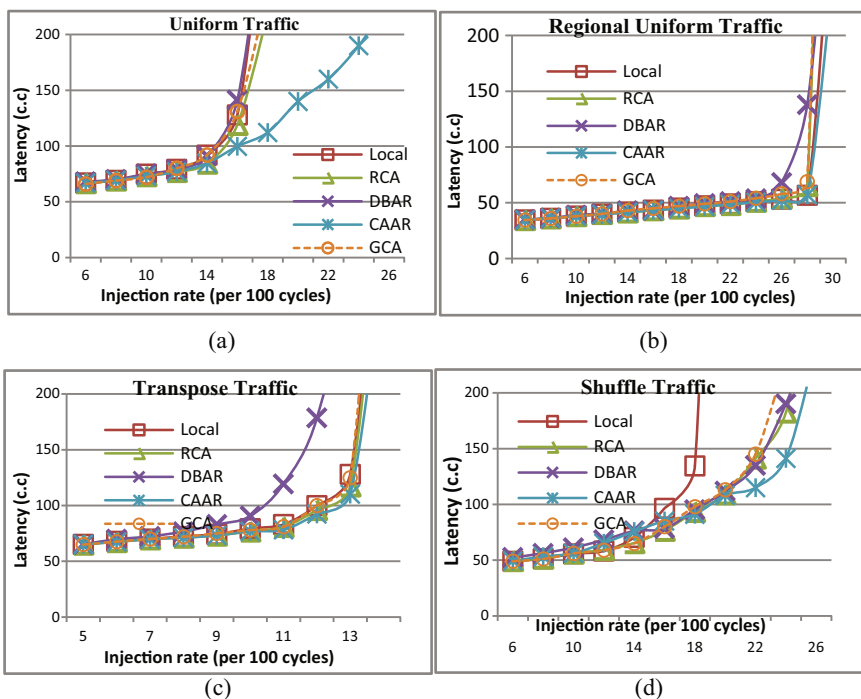


Fig. 8.  $16 \times 16$  mesh 8VC NoC performance (average latency) for different traffic



## 5 Conclusions

This paper presents a novel approach to improve NoC latency and throughput by packet prioritization. The objective is to reduce NoC latency and improve NoC throughput by using congestion information. Our adaptive routing employs regional congestion to improve packet routing in high traffic NoCs. We have expanded the regional congestion awareness data to other parts of the router, primarily to the arbiters to improve packet selection for both VC and switch allocators. A new methodology of Congestion Aware Adaptive Routing (CAAR) is designed to prioritize the allocation of packets that suffer higher latency while travelling long distances between source and destination cores. CAAR also removes the sideband network to transfer congestion data. CAAR methodology shows significant performance improvement.

**Acknowledgments.** The authors acknowledge the financial support of NSERC discovery and FEAS, Ryerson University DRF grants. Authors also acknowledge CMC microsystems, Canada for providing high performance computer systems and CAD tools.

## References

1. Nicopoulos, C., Park, D., Kim, J., Vijaykrishnam, N., Yousif, M.S., Das, C.R.: ViChaR: a dynamic virtual channel regulator for Network-on-Chip router. In: Proceedings of the International Symposium on Microarchitecture, pp. 333–344 (2006)
2. Hu, J., Marculescu, R.: DyAD-Smart routing for Network-on-Chip. In: Proceedings of the Design Automation Conference, San Diego, CA, pp. 260–263, July 2004
3. Kim, J., Park, D., Vijaykrishnam, N., Das, C.R.: A low latency router supporting adaptivity for on-chip interconnects. In: Proceedings of the Design Automation Conference, pp. 559–564, June 2005
4. Duato, J.: A new theory of deadlock-free adaptive routing in wormhole networks. *IEEE Trans. Parallel Distributive Syst.* **4**(12), 1320–1331 (1993)
5. Gratz, P., Grot, B., Keckler, S.W.: Regional congestion awareness for load balance in Network-on-Chip. In: Proceedings of the IEEE International Symposium on High Performance Computer Architecture, Salt Lake City, pp. 203–214, April 2008
6. Lin, B., Ramanujam, R.S.: Destination-based adaptive routing on 2D mesh networks. In: Proceedings of the International Conference on Architectures Networking and Communication Systems, pp. 1–12, October 2010
7. Ma, S., Enright-Jerger, N., Wang, Z.: DBAR: An efficient routing algorithm to support multiple concurrent applications in Network-on-Chip. In: Proceedings of the International Symposium Computers and their Applications, pp. 413–424, June 2011
8. Ramakrishna, M., Gratz, P., Sprintson, A.: GCA: Global congestion awareness for load balance in Network-on-Chip. In: Proceedings of the IEEE International Symposium NoC, Tempe, pp. 1–8, April 2013
9. Becker D., Dally, W.: Allocator implementations for Network-on-Chip routers. In: Proceedings of the International Conference on High Performance Computing Networking, Storage & Analysis, Portland, OR, pp. 1–12, November 2009

# Data Locality Aware Algorithm for Task Execution on Distributed, Cloud Based Environments

Mihai Bica and Dorian Gorgan<sup>(✉)</sup>

Technical University of Cluj-Napoca, Cluj-Napoca, Romania  
{mihai.bica,dorian.gorgan}@cs.utcluj.ro

**Abstract.** A solution that proactively analyzes the shape of the operator graph of a task based cloud application is studied in this paper. Based on the analysis of the execution graph and operator metadata, the nodes of the execution graph are properly clustered so that highly connected operators are scheduled on the same or nearby computing resources. Two graph partitioning algorithms are studied, implemented and compared. The graph partitioning efficiency is visually analyzed and compared by using existing graph visualization software.

**Keywords:** Graph partitioning · Distributed systems · Application execution

## 1 Introduction

Running complex applications on cloud [6] based distributed environments requires a profound understanding of the application that needs to be run and a deep understanding of the environment [8] on which the application will run. Task based applications are described as a series of tasks defined by a dependency graph.

One of the most challenging problems is to plan data movement and to move the code closer to data rather than to move the data closer to the code. To obtain a reduced data movement plan. The execution service must execute the next sequential operators very close to the location on which the previous sequential operators were launched.

If the tasks are simple to parallelize, then the job of the scheduler is to simply distribute tasks that follow a Poisson distribution [1] on the available computing resources.

The purpose of the algorithm presented in this paper is to keep data fragmentation to a minimum and to increase as much as possible the data locality [6] so that the required data will be very close to the location of the operators which need the respective data.

To obtain such a behavior, the cloud execution service must understand the shape and the structure of the whole application that will be launched. This way,

the system can reserve some virtual machines for some tasks because previous dependent tasks were executed on the respective machine.

This strategy reduces data fragmentation and increases the chances of having data pieces already cached in the RAM or HDD of the virtual machine. To understand the shape and the structure of the application, the execution service needs to read and statically analyze the dependencies of the operators.

## 2 Related Work

Various scientific domains like geographic analysis of satellite images are using distributed datasets with processing applications that are described and structured as scientific workflows. In [3] is described a particle swarm based optimization algorithm for scheduling workflow based applications.

In the paper [4] is described a Breadth First Search (BFS) algorithm that scans the execution graph and takes each branch from the graph and computes an estimation. Based on the calculated estimation, a deadline for each task is estimated. After the deadlines were estimated for each branch or task group, the nodes from a group are distributed based on a Markov Decision Process [5] model.

Several algorithms were tested in [7] by using a randomly Directed Acyclic graph (DAG). The problem of energy efficiency is studied in [9]. The most power hungry component in a computer is the CPU, but other components like disks, memory and network devices use significant energy so that an idle computer can use 60% of peak power usage. In [9] is stated that it is necessary to reduce the number of hops in network packers. Application data locality and application properties can also be used to design good distributed schedulers that use data placement strategies to reduce the energy consumption.

An approach for task scheduling is presented in [10] based on priority and quota. Graph multi partitioning is studied in [12] using techniques like spectral graph bipartitioning for calculating the global bipartitioning solution.

YARN [11] is a resource negotiator. It analyses an application and allocates the required infrastructure resources, then runs and monitor the application. Simple migration to different cloud providers is studied in [13] in which is mentioned that most of the applications should be migrated to Docker containers because will simplify large application deployment.

We observed that a scheduling solution which takes into account the data locality and the shape of the application is needed. In this paper we present an algorithm that considers execution locality as being important, having the benefit of reducing internal data movement inside a cloud datacenter.

## 3 Workflow Description and Task Model

Cloud task based applications can be defined by describing the workflow of the application like a graph. In such a graph description, the nodes of the graph represent functions of the application or operators of the application. The dependent

nodes are connected by a directed edge, the weight of the edge represents the size of the data that needs to be sent to the next operator. A simplified view of such of graph is represented in Fig. 1.

The data source nodes contain estimation metadata which tells how much data input is required for the first set of operators that are being executed. The operator nodes, denoted with OP, contain metadata like a formula which helps to estimate how much output data is generated based on the input data size.

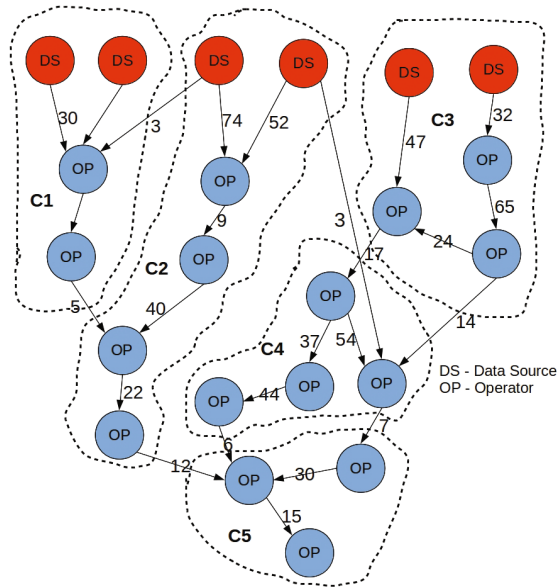


**Fig. 1.** Clustering the application workflow graph.

It is observed in the Fig. 1, that the dataflow estimations are calculated and represented on the directed edges of the graph. All the nodes from inside of a cluster are highly coupled, while the clusters are as loosely coupled as possible.

The execution service will ensure that the nodes from within a cluster will be scheduled on the same virtual machine. This will increase data locality [6] so that all the necessary files to execute a cluster of operators are stored on the same machine.

The problem of cutting the graph into clusters of size at most  $S$ , while making sure that the total cut size is minimal, falls under the category of NP-hard problems. Approximation solutions for these NP-hard problems are found using heuristics and approximation algorithms.

## 4 Cost Model

Before discussing the algorithm, it is necessary to further detail the attributes of operators and the attributes of edges. The operators have some recommended

$$\begin{aligned}
 CostOP_{CPU} &= \frac{fAlgEstimCPU_{Cycles}(DataSize)}{SystemAvailable_{CPU}} \\
 CostOP_{Memory} &= fAlgEstimMemory(DataSize) \\
 CostOP_{OutputStorage} &= fAlgEstimOutput(DataSize)
 \end{aligned}$$

**Fig. 2.** Calculating the cost estimation for operators.

computing resource requirements. Such resources for an operator are the CPU usage, RAM usage and temporary disk storage requirement. Such requirements can be defined like in the Fig. 2.

Variable  $CostOP_{CPU}$  represents an estimation of how many CPU cycles the operator needs to consume based on the amount of input data and the properties of the algorithm. Variable  $CostOP_{Memory}$  represents the required system memory to run the operator for a certain size of input data and the variable  $CostOP_{OutputStorage}$  represents the required space to store temporary data. We have to attribute to the cost of the graph edges, the value of the  $CostOP_{OutputStorage}$  variable.

The estimation functions  $fAlgEstim*$  are specified by the operator metadata, being embedded inside the operator package.

A cluster has three types of costs: CPU cost, Memory cost and Storage cost. Each kind of cost is the sum of the costs of the operators contained in the respective cluster.

## 5 Breadth First Search Clustering Algorithm

The approach of this algorithm is to start with a random node, grow a cluster from that node by adding the most connected neighbor node to the existing cluster. The cluster can grow until it will reach the maximum limits.

Because the weights of the edges of the graph represent the amount of data transmitted by one operator to the next operator, grouping the graph nodes by the edge weights will ensure that one operator cluster is loosely connected to another operator cluster.

Grouping the operators into clusters is described in the Algorithms 1, 2.

The Algorithms 1, 2 has an array of *clusters*, which stores the final result. The main function that is called first is named *bfs\_clusterize\_graph* which has the role of selecting unmarked nodes to start the clustering from them. If no unmarked nodes are available, it means that the algorithm finished the execution. As input, the function *bfs\_clusterize\_graph* gets an initialized graph. This graph can be based on any kind of representation, in this paper we implemented the graph as a list of edges and a list of object vertexes.

The *grow\_bfs\_cluster(vertex, index)* keeps adding to the current cluster the most connected unmarked available vertex. Once the cluster has reached a maximum size it cannot grow any more. At this point, vertexes are not added any more to the current cluster. The execution returns back to

**Algorithm 1.** BFSClustering

---

```

Algorithm BFS_clustering:
clusters = []
procedure bfs_clusterize_graph(Graph g):
  cluster_index = 0
  for vertex in g.vertices:
    if vertex not marked:
      grow_bfs_cluster(vertex,
                      cluster_index)
      cluster_index++
procedure grow_bfs_cluster(vertex, index):
  cluster = clusters[index]
  cluster.add_vertex(vertex)
  while continue:
    max_node = get_max_connected_node(
                                      cluster)
    cluster.add(max_node)
    mark(max_node)
    continue = not cluster_is_large(cluster)

```

---

*bfs\_clusterize\_graph()* where it will search for unmarked nodes from which to start a possible cluster. One problem of this algorithm is that at the end of the process the formed clusters contain a small number of nodes. Or simply, at the end of the process the probability to grow small clusters is higher than the probability to grow the larger clusters.

The maximum cost of a cluster is determined by the configurations of the virtual machines, which are usually fixed and they depend on the type of the service offered by the cloud provider.

## 6 Stoer Wagner Based Clustering

Another heuristic for finding a good enough solution is to take a minimum cut algorithm and to run it multiple times. The minimum cut algorithm splits a weighted graph into two sets which are less connected. The procedure can be repeated until we remain with graph partitions of the desired size.

The algorithm described in this section is an adaptation for the min-cut Stoer-Wagner algorithm [2] to our problem, that is to cluster the graph in loosely coupled graphs of max dimension. Our adaptation runs this minimum cut algorithm multiple times to obtain several clusters.

In Fig. 3 is the pseudocode of the Stoer-Wagner algorithm based approach. The first function that is called is *sw\_graph\_clustering(Graphg)* and it starts by adding the current graph to the clusters array.

The *clusters* array will hold the final results, will contain the node clusters which were partitioned from the main graph. After the whole graph was added to the solution array, a test is made.

**Algorithm 2.** BFS Clustering - Part 2

---

```

procedure cluster_is_large(Cluster c):
  if CostClusterCPU(c) > MAX_CPU:
    return True
  if CostClustMemo(c) > MAX_MEM:
    return True
  if CostClustStor(c) > MAX_STOR:
    return True
  return False
procedure get_max_connected_node(cluster):
  max_edge_weight = 0
  max_node = None
  for node in cluster.vertices:
    for neigh in node.getneighbours():
      if edge.weight > max_edge_weight:
        max_node = edge.weight
        max_edge_weight = edge.weight
  return max_node

```

---

This test determines if the current cluster is too big or if it is too small. If the cluster is too big, it will be splitted into two clusters, by the min-cut algorithm represented by the function *split\_graph\_by\_min\_cut(Clusterc)* from the paper [2].

If the current cluster was split, the current graph is removed from the solution, because it is too large and the two new possible smaller graphs are added to the solution. This do while loop continues to iterate through the items from the solution array. If a split is made, the loop restarts, if splits are not made during N iterations, where N is the number clusters, then it means that we computed small clusters.

The function *cluster\_is\_large(Cluster c)* checks if a cluster requires more capacity than it is available on a VM. Min. cut function *split\_graph\_by\_min\_cut* is described in the paper [2].

## 7 Testing the BFS Clustering

For testing of the clustering algorithms we generated random input data and started a visual analysis of clustering process. We also analyze the algorithms from an implementation point of view, and we estimate the performance of the algorithms and discuss implementation difficulties.

For visual observation of the resulted clusters, graphviz graph plotting software was used. This library supports reading a text file in dot format and generates a PNG image for visualization of the graph described in the input file.

---

**Algorithm 3.** Stoer Wagner Based Clustering

---

```

Algorithm stoer_wagner_clustering:
clusters = []
procedure sw_graph_clustering(Graph g):
  clusters.add(g)
  do:
    repeat = False
    for cluster c in clusters:
      if cluster_is_large(c):
        clust1, clust2 =
          split_graph_by_min_cut(c)
        clusters.remove(c)
        clusters.add(clust1, clust2)
        repeat = True
  while repeat

```

---

Testing data from Fig. 3 was generated using a random graph generation algorithm. The test graph is not directed because direction of the edges does not influence the locality.

The Fig. 3 is obtained by running the clustering based on breadth first search algorithm on the input graph which is not colored. Each cluster is represented with a different color. The largest clusters are the cyan, red1, blue and red2 clusters. They are the largest because each time the search algorithm starts it picks a random node to start growing a cluster.

As the execution time passes, lonely nodes are missed for getting grouped inside clusters because of reaching maximum cluster dimensions. These lonely nodes are not very coupled to clusters and can be eventually grouped together into several clusters or they can be added to existing clusters increasing cluster costs where cost is not filled to the maximum capacity.

The algorithm can scan fast large sized graphs. For example, the result from the Fig. 4 was computed in under 100 ms. The Fig. 4 has 100 nodes connected with random edge weights between 0 and 100 and the maximum cluster capacity is 300.

We can observe the effects of randomly picking start nodes. This has the effect to produce firstly large clusters, because the first clusters have room to grow, because the graph contains plenty of unused nodes. As the number of used nodes increases the size of the clusters will gradually decrease.



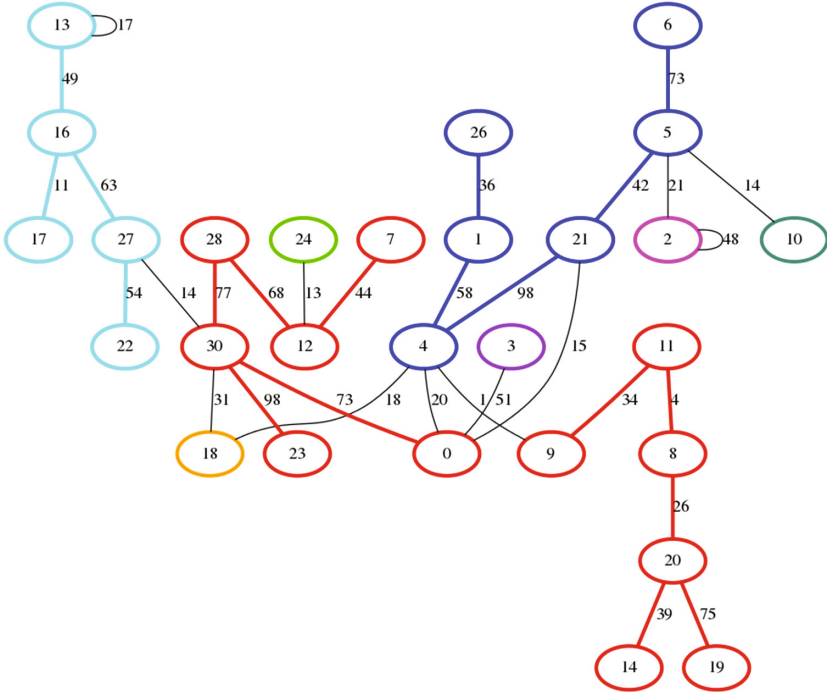


Fig. 3. Each cluster is colored. This is a dot representation of the execution graph.

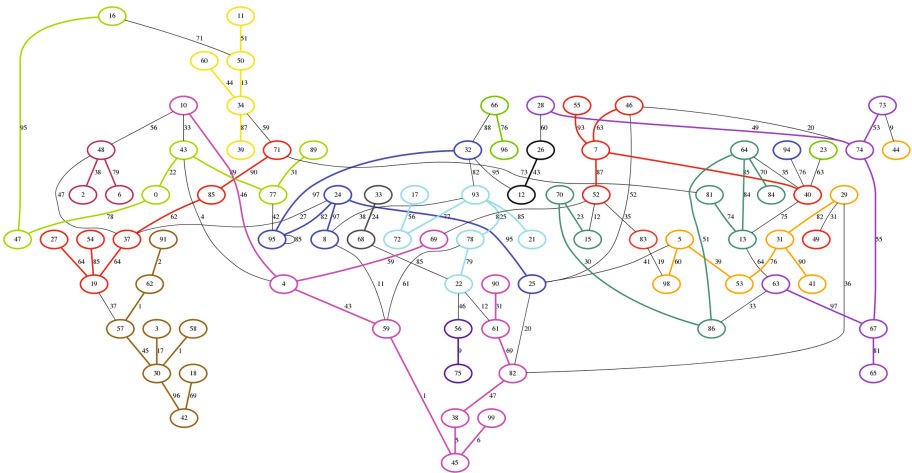


Fig. 4. Each cluster is colored. This is a dot representation of the clusters, this random example has 100 nodes.

## 8 Testing the SW Clustering Method

This algorithm was implemented on a graph data structure which is represented as a list of edges.

The algorithm starts with a random node and adds it to set  $A$ . After this step, the most connected nodes to  $A$  are added in order. This creates list of ordered nodes. The last node is connected by the graph through a set of edges. These edges can be part of the minimum cut solution, like described by [2]. After the possible cut is stored, the last two nodes are merged and this repeats until the graph is only a single large node.

A disadvantage of this algorithm is that it is requiring to merge nodes. Merging nodes will complicate the data structure of the nodes. Each node, needs now to store an extra set of children nodes.

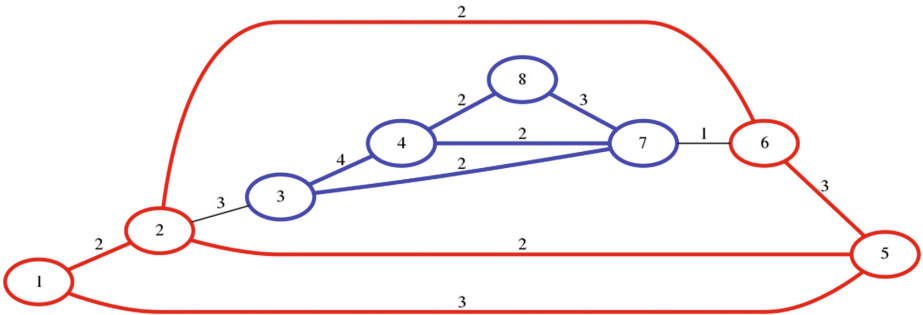


**Fig. 5.** Resulted graph clusters (red and blue) after running the Stoer Wagner [2] algorithm on test input data.

For testing data, we used the same graph from work [2], the one represented in Fig. 5, but not colored. Because the solution based on min cut Stoer Wagner algorithm is more complex than the first algorithm the execution time is worse than the execution time for the first algorithm. For clustering a 10 nodes graph, the execution time was about 100 ms, the same as the execution time in which the first BFS based algorithm is clustering 100 nodes.

## 9 Conclusions

Two algorithms for clustering were tested experimentally and the quality of the clusters was analyzed visually with the graphviz visualization library. Each algorithm behaves differently and has its own advantages and disadvantages. The first algorithm presented in the paper is efficient and the quality of clusterization is good for both large and small clusters. This algorithm is well suited for the implementation of a scheduling module for the distributed task based applications.

A main disadvantage is that both algorithms generate small lost clusters. Another disadvantage of the second algorithm is the complexity and slowness in a real world scenario. Merging nodes, deleting edges, mapping nodes on super nodes, and splitting large clusters into smaller clusters recursively, are very costly operations and increase dramatically the complexity of the code.

Overall we conclude that the first algorithm is not perfect, but better than the second one and good enough to be used for cluster based scheduling. It runs fast enough on large input data and offers good clustering for large and even for small data sets. It can be easily customized, because it has a reduced complexity, and can be easily parallelized as well. As a future improvement, this algorithm needs to have an associated module that computes the estimated execution time, so that distribution of tasks is also based on the required deadline.

## References

1. Li, L.: An optimistic differentiated service job scheduling system for cloud computing service users and providers. In: 2009 Third International Conference on Multimedia and Ubiquitous Engineering, MUE 2009, pp. 295–299. IEEE (2009)
2. Stoer, M., Wagner, F.: A simple min-cut algorithm. *J. ACM (JACM)* **44**(4), 585–591 (1997)
3. Pandey, S., et al.: A particle swarm optimization-based heuristic for scheduling workflow applications in cloud computing environments. In: 2010 24th IEEE international conference on Advanced information networking and applications (AINA). IEEE (2010)
4. Yu, J., Buyya, R., Tham, C.K.: Cost-based scheduling of scientific workflow applications on utility grids. In: 2005 First International Conference on e-Science and Grid Computing. IEEE (2005)
5. Sulistio, A., Buyya, R.: A grid simulation infrastructure supporting advance reservation. In: 16th International Conference on Parallel and Distributed Computing and Systems (PDCS 2004) (2004)
6. Foster, I., et al.: Cloud computing and grid computing 360-degree compared. In: 2008 Grid Computing Environments Workshop, GCE 2008. IEEE (2008)
7. Li, J., et al.: Online optimization for scheduling preemptable tasks on IaaS cloud systems. *J. Parallel Distrib. Comput.* **72**(5), 666–677 (2012)
8. Buyya, R., Ranjan, R., Calheiros, R.N.: Modeling and simulation of scalable Cloud computing environments and the CloudSim toolkit: challenges and opportunities. In: 2009 International Conference on High Performance Computing and Simulation, HPCS 2009. IEEE (2009)
9. Berl, A., et al.: Energy-efficient cloud computing. *Comput. J.* **53**(7), 1045–1051 (2010)
10. Verma, A., et al.: Large-scale cluster management at Google with Borg. In: Proceedings of the Tenth European Conference on Computer Systems. ACM (2015)
11. Vavilapalli, V.K., et al.: Apache hadoop yarn: yet another resource negotiator. In: Proceedings of the 4th Annual Symposium on Cloud Computing. ACM (2013)
12. Dhillon, I.S.: Co-clustering documents and words using bipartite spectral graph partitioning. In: Proceedings of the Seventh ACM SIGKDD International Conference on Knowledge Discovery and Data Mining. ACM (2001)
13. Linthicum, D.S.: Moving to autonomous and self-migrating containers for cloud applications. *IEEE Cloud Comput.* **3**(6), 6–9 (2016)

# Asynchronous Page-Rank Computation in Spark

Chao Li<sup>(✉)</sup>, JianXia Chen, Zhi Yang, and WuYan Chen

School of Computer, Hubei University of Technology, Wuhan 430068, China  
lich.mail@163.com

**Abstract.** High efficiency page-rank computation is motivated by issues that bulk synchronous parallel computing model has high-cost synchronous barriers, and asynchronous communication can avoid long-waiting time. By operations of updating inside RDDs, iteration can step into the next round without the barrier of synchronization among all partitions. Experiment results indicate that our method can improve the execution speed significantly compared to Graphx.

**Keywords:** Asynchronous computation · Page-rank · Spark

## 1 Introduction

Large-scale graph-structured computation usually involves a massive amount of data and potentially requires numerous iterations to complete. To perform iterative processing in a timely manner is a challenging issue [1]. To address this challenge, several graph-parallel abstractions including Pregel [2] and GraphLab [3] were developed to solve computational problems. These frameworks exploit vertex-centric [4] programming model, which simply let the vertices perform the update in lock steps.

Though BSP model has clear logical workflow and can be easily implemented, existing graph-based iterative processing algorithms might degrade performance in the perspectives of slow convergence, high communication overhead. Moreover, traditional frameworks have to store intermediate iterative result during the whole process. Obviously, accessing data through I/O would lead higher cost than in memory. To address above inefficiency in processing page-rank computation, an efficient method for asynchronous accumulation computation in Spark has been proposed in this paper.

The rest of the paper is organized as follows. Section 2 presents the asynchronous graph-based computation in Spark, followed by introducing implementation details in Sect. 3. The experimental results are shown in Sect. 4, and we conclude the paper in Sect. 5.

## 2 Related Work

In this section, we first introduce fundamental ideal about RDD [5] (Resilient Distributed Datasets), the core conception that Graphx leverages to store the attributes of vertexes and edges. Then, sufficient conditions that asynchronous iteration should be

satisfied are present. By RDD, RDD-based asynchronous communication for graph-based iterative computation is proposed.

## 2.1 Graphx and RDD

Graphx is a typical BSP model, which has the same computing strategy as other synchronous computing frameworks, but the difference from the others is that Graphx leverage RDD to store vertex and edge attribute. Although Graphx perform in-memory computations in a fault-tolerant manner by policies of cache and persistence, which can generate an RDD of messages and keep vertex states in memory, updating state of vertex attribute can be performed until all the attribute blocks sent from all the other edge partitions arrive.

## 2.2 Asynchronous Iteration

To bypass the synchronous barrier, asynchronous iteration was proposed [6, 7]. In graph-based iterative processing, each vertex  $i$  graph maintains a state which is updated iteratively based on the states of its in-neighbours and expressed as follows.

$$s_i^k = g(s_1^{k-1}, s_2^{k-1}, \dots, s_{n_i}^{k-1}). \quad (1)$$

where  $s_i^k$  is the state of vertex  $i$  after the  $k^{th}$  iteration, and  $n_i$  is the number of vertex  $i$ 's in-neighbors. In practice, many graph-based iterative computation can also be rewritten as

$$s_i^k = f_1(s_1^{k-1}) \oplus f_2(s_2^{k-1}) \oplus \dots \oplus f_{n_i}(s_{n_i}^{k-1}) \oplus c_i. \quad (2)$$

Where  $f_j(s_j)$  is a function denoting the effect of an in-neighbour  $j$ 's state on the state of vertex  $i$ ,  $\oplus$  is an abstract operator which is often a simple operation, such as addition. Moreover, if function  $f_j(s_j)$  has the distributive property and  $\oplus$  is both associative and commutative, letting  $s_j^k = s_j^{k-1} \oplus \Delta s_j^k$ , an iterative computation can be obtained with a simple manipulation on the previous equation:

$$\begin{aligned} s_i^k &= s_i^{k-1} \oplus \Delta s_i^k \\ \Delta s_i^k &= \sum_{j=1}^{n_i} \oplus f_j(\Delta s_j^{k-1}). \end{aligned} \quad (3)$$

Since the  $\oplus$  operation is both associative and commutative, the iterative order of state updating becomes irrelevant and the accumulation of the changes for the state update of a vertex can be done at any time in any order [8, 9]. Therefore, asynchronous processing allows the state changes to be more quickly broadcast to other vertices to improve convergence.

### 2.3 RDD-Based Asynchronous Communication

For many problems, the state updating can be done asynchronously [10], and page-rank computation can satisfy the above conditions. However, if a fine-grained scheme is adopted to push state changes from one partition to another, the cascade effect will dramatically increase the overhead of communication.

Moreover, asynchronous iteration might perform useless computations. An activated vertex pulls all its in-neighbors' values, but not all of them have been updated. In that case, asynchronous iteration performs a useless computation. Recognizing these problems, we take advantage of both RDDs and asynchronous iteration that enable more efficient transmission. In the following section, we present the implementation in detail.

## 3 Implementation

### 3.1 Asynchronous RDD-Based Iterative Computation

To process the iterative result as quickly as possible, we propose that remote procedure call protocol (RPC), which has already been employed in Graphx is feasible for the reliable transmission between vertex RDD and edge RDD.

Firstly, we construct `RpcEndpoints` of Vertex RDDs and Edge RDDs. In that way, vertex can perform the sensible update at any time in the vertex RDD based on the most recent states of its in-neighbors sent from edge partitions, and edge partition can aggregate messages along edges as soon as receiving the state updating of source vertexes sent from vertex partitions.

Besides, the attributes of vertexes and edges have been stored in vertex RDDs and edge RDDs respectively, and from the perspective of asynchronous communication, the relationship between vertex RDDs and edge RDDs has been set up in RPC environment. To asynchronously process the state updating of vertex attribute, state updating should be carefully designed in Vertex RDD to guarantee the validity of computing result.

### 3.2 State Updating in Vertex RDD

To process messages sent from edge RDDs and improve the efficiency of asynchronous computation, we separate the function of receiving, processing and sending by setting up receive thread, update thread and send thread inside the `RpcEndpoints` of vertex RDDs.

Besides, the `RpcEndPoint` of vertex RDD are operated with receive thread and update thread respectively. Once partial function in `RpcEndPoint` of vertex RDD is invoked, receive thread put blocks into vertex attribute block buffer. Then, update thread executes blocks periodically from the buffer. It first checks whether the current processed vertex exists in the vertex attribute state table. If there exists, update thread combines the mapped value and update the corresponding vertex attribute in state table.

## 4 Evaluation

This section evaluates the method for page-rank computation with a series of experiments. The experiments are performed on a cluster of local machines, which consists of 2 commodity machines. Each machine has Intel Xeon E5-2620 with 5-core at 2.5 GHz CPU, 8 GB of RAM, running a Linux operation system with kernel version 2.6.32.

### 4.1 Preparation

We use Google Webgraph [11] for PageRank computation. In Webgraph, nodes represent web pages and directed edges represent hyperlinks between them. The basic statistic about the dataset is that the number of nodes is 875,713, the number of edges is 5,105,039 and the number of triangles is 13,391,903.

Moreover, PageRank [12], a typical graph algorithm proposed for ranking web pages in web applications, which also satisfies the condition of asynchronous computation, is employed as benchmark. The formula of PageRank algorithm is defined as follows.

$$R_j^k = d * \sum_{\{i|(i \rightarrow \varphi) \in E\}} \frac{R_i^{k-1}}{|N(i)|} + (1 - d). \quad (4)$$

where  $d$  is a damping factor, we set  $d$  is 0.85. At the beginning of iteration, the initial message is 0 for all the vertexes, which means that therefore delta value is 0.15 at first iteration for all vertexes is the weight set on the edges based on the out degree. Then we analyze and transform the page rank algorithm, and define the following functions in Scala to run the iterative algorithm.

We first split the dataset into partitions and setup `RpcEndPoint` for each RDD partition. Depending on the strategy of hash partition, 6 parts of edge RDDs and 6 parts of vertex RDD have been built.

After that, we execute a Pregel-like iterative vertex-parallel abstraction according to the asynchronous method. The user-defined vertex-program ‘vprog’ is executed in parallel on each vertex in each RDD, receiving any inbound messages and computing a new value for the vertex. The ‘sendMsg’ function is then invoked on all out-edges and is used to compute an optional message to the destination vertex. The ‘mergeMsg’ function is a commutative associative function used to combine messages destined to the same vertex. Graph-based iteration runs in this method until deltas of all vertex are not changed, we terminate the iteration.

### 4.2 Experiment Results

We compare synchronous and asynchronous method of iterative computation on running time and communication overhead in the context of PageRank computation. Figure 1 shows the PageRank running time on Google Webgraph on our local cluster. Note that, the data loading time is also included in the total running time.

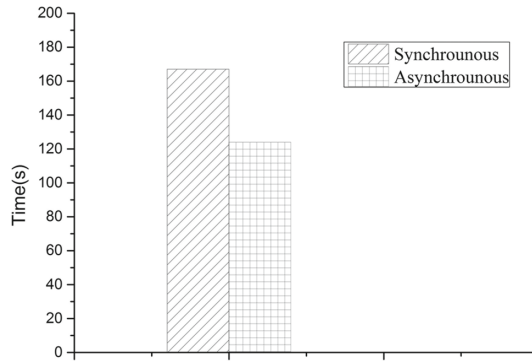


**Fig. 1.** Running time of PageRank for Google Webgraph on local cluster

Figure 1 demonstrate that we need 21 iterations and more than 160 s to converge in Pregel, while the asynchronous method performs the update without waiting for the synchronous barriers, and ignores the useless updates, by which the running time is significantly reduced to less than 120 s.

On the other hand, we compare the communication efficiency and measure the relative communication overhead in Fig. 2.

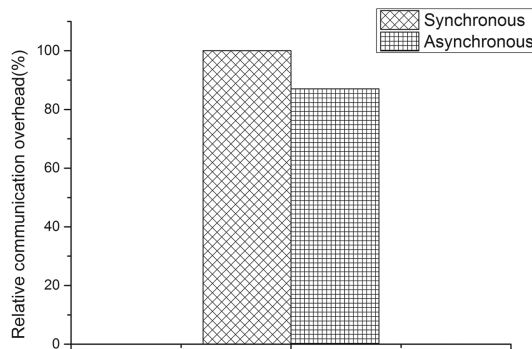


**Fig. 2.** Relative communication overhead of asynchronous method to Graphx

Figure 2 demonstrates that the relative communication overhead of asynchronous method to synchronous counterpart in Graphx is less than around 20%.

By synchronous computation, all the vertices in the RDD have to perform the update once and only once before stepping into the next round [13], while in asynchronous context, the update sequence can follow any order without any restriction in different RDDs. Although the asynchronous method accumulates the received delta for the same vertex, and not immediately send the updating state of vertexes until the accumulated delta is above the threshold in the RDD, the frequency of sending blocks to other RpcEndpoints of RDDs in asynchronous method is still little higher than



synchronous, while the capacity of sending blocks in asynchronous method is less than synchronous counterpart [14, 15], which leads to insignificantly improvement in the perspective of communication overhead.

## 5 Conclusions

In this paper, we implement our method for asynchronous page-rank computation in Spark. Through the RDD-based asynchronous communication, we deploy the method on local cluster to evaluate its performance. The experiment results demonstrate that the relative execution speed is improved against the synchronous counterpart in Graphx.

**Acknowledgments.** This work is supported by the Scientific Research Project of Education Department of HuBei Province under Grant no. Q20141410.

## References

1. Dean, J., Ghemawat, S.: MapReduce: simplified data processing on large clusters. *Commun. ACM* **51**(1), 107–113 (2004)
2. Malewicz, G., Austern, M.H., Bik, A.J.C., Dehnert, J.C., Horn, I., Leiser, N., Czajkowski, G.: Pregel: a system for large-scale graph processing. In: *Proceedings of the 2010 ACM SIGMOD International Conference on Management of Data*, pp. 135–146. ACM Press (2010)
3. Low, Y., Gonzalez, J., Kyrola, A., Bickson, D., Guestrin, C., Hellerstein, J.M.: Distributed GraphLab: a framework for machine learning and data mining in the cloud. *Proc. VLDB Endow.* **5**(8), 716–727 (2012)
4. Tian, Y.Y., Balmin, A., Corsten, S.A., Tatikonda, S., Mcpherson, J.: From “think like a vertex” to “think like a graph”. *Proc. VLDB Endow.* **7**(3), 193–204 (2013)
5. Zaharia, M., Chowdhury, M., Das, T., Dave, A., Ma, J., McCauley, M., Franklin, M.J., Shenker, S., Stoica, I.: Resilient distributed datasets: a fault-tolerant abstraction for in-memory cluster computing, *Usenix Conference on Networked Systems Design & Implementation*, p. 2 (2012)
6. Baudet, G.M.: Asynchronous iterative methods for multiprocessors. *J. ACM* **25**(2), 226–244 (1978)
7. Zhang, Y., Gao, Q., Gao, L., Wang, C.R.: Accelerate large-scale iterative computation through asynchronous accumulative updates. In: *Proceedings of the 3rd Workshop on Scientific Cloud Computing Date*, pp 13–22. ACM Press (2012)
8. Wang, G., Xie, W., Demers, A., Gehrke, J.: Asynchronous large-scale graph processing made easy. In: *Proceedings of Biennial CIDR*, pp. 1–12 (2013)
9. Zhang, Y., Gao, Q., Gao, L., Wang, C.: Maiter: a message-passing distributed framework for accumulative iterative computation. *Technical report* (2012)
10. Yu, W., Lin, X., Zhang, W.: Towards efficient SimRank computation on large networks. In: *Proceedings of the 2013 IEEE 29th International Conference on Data Engineering (ICDE)*, pp. 601–612. IEEE (2013)
11. Stanford Dataset Collection. <http://snap.stanford.edu/data/>

12. McSherry, F.: A uniform approach to accelerated pagerank computation. In: Proceedings of the International Conference WWW, pp. 575–582 (2005)
13. Bertsekas, D.P.: Distributed asynchronous computation of fixed points. *Math. Program.* **27** (1), 107–120 (1983)
14. Yuan, F., Chang, K., Chen-Chuan, W., Lauw, H.: RoundTripRank: graph-based proximity with importance and specificity. In: Proceedings of the ICED, pp. 613–624 (2013)
15. Zhang, Y., Gao, Q., Gao, L., Wang, C.R.: Prlter: a distributed framework for prioritized iterative computations. In: Proceedings of the 2nd ACM Symposium on Cloud Computing, p. 1. ACM Press (2011)

**The 10th International Workshop  
on Intelligent Informatics and Natural  
Inspired Computing  
(IINIC- 2017)**

# Energy-Aware Routing in A4SDN

G. Cammarata<sup>1,2</sup>, A. Di Stefano<sup>1</sup>, G. Morana<sup>2</sup>(✉), and D. Zito<sup>2</sup>

<sup>1</sup> DIEEI, University of Catania, Catania, Italy

<sup>2</sup> C3DNA, Cupertino, CA, USA  
giovanni@c3dna.com

**Abstract.** The concept of Green Computing and, more specifically, energy-aware solutions have gained attention in the last years in many fields of ICT: network management is one of those. Today, power consumption is considered a fundamental parameter, as well as latency, bandwidth or error rate, to take into account when a new routing strategy is designed.

In this paper the authors introduce an energy-aware extension of the A4SDN, an algorithm for traffic engineering on SDN based on the Alienated Ant Algorithm, a heuristic solution inspired by a non-natural behaviour of ants colonies.

In order to evaluate its performance, the proposed energy-aware approach is compared with the standard A4SDN and with two deterministic solution based on Dijkstra's Algorithm.

## 1 Introduction

The design of energy efficient systems is, today, a major challenge in ICT.

The increasing demand in term of computation, storage and bandwidth for ICT services have been directly translated in an increasing demand of power energy. In an article titled "Power, Pollution and the Internet" [23], the New York Times pointed out that energy consumption of Data Centres is close to 30 billion watts worldwide, equivalent to the output of 30 nuclear power plants.

A large portion of the energy consumption in ICT is due to the network services.

In the last years, many solutions have been proposed to improve the energy efficiency of networks: power consumption has became, as well as latency, bandwidth and error rate, a fundamental parameter to take into account when a new routing strategy is designed. The flexibility in network management provided by the advent of Software-Defined Networking (SDN) [28] has further simplified and boosted these type of solutions.

In this paper the authors introduce an energy-aware extension of the A4SDN [9–11], an algorithm for traffic engineering on SDN based on the Alienated Ant Algorithm (AAA), a heuristic solution inspired by a non-natural behaviour of ants colonies. As any other AAA solutions, eA4SDN takes its decisions minimising the value of pheromone on the available paths, here emulated by the energy needed to managed routing operations. In order to evaluate its performance,

the proposed energy-aware approach is compared with the standard A4SDN and with two deterministic solution based on Dijkstra’s Algorithm. The rest of the paper is organised as follows: Sect. 2 discusses some Related Work; Sect. 3 gives an overview about SDN, OpenFlow and the considered energy model; Sect. 4 outlines the AAA-based algorithms; Sect. 4.4 describes the results of the performance evaluation; finally, the conclusions are briefly given in Sect. 5.

## 2 Related Work

In a recent work, Assefa and Ozkasap [4] provide a classification about all the current solutions for reducing energy consumption in SDNs.

Two are the main approaches commonly used: (I) put in “sleep mode” the hosts/resources not used (or not frequently used) and (II) balancing the geographical distribution of the hosts/resources in order to minimise the hops per request.

Two examples of the first approach are [19,20]: in these works the network automatically adapt itself to workload changes by turning on and off physical servers, reducing costs the number and the type of the underlying resources.

A very similar approach is adopted also in [3] and in [30] (for Content Delivery Networks): in this last, in particular, the authors propose a solution in order to minimise the needed start/stop operations for the “sleeping” resources.

Examples of the second approach, instead, are [1, 5, 16, 22]: all of them focus their solution on a smart placement of the resources in order to minimise the electricity cost for packets delivery.

To the best of the authors knowledge this is the first work that investigates the opportunity to use a bio-inspired approach to reduce the energy consumption on SDN environments.

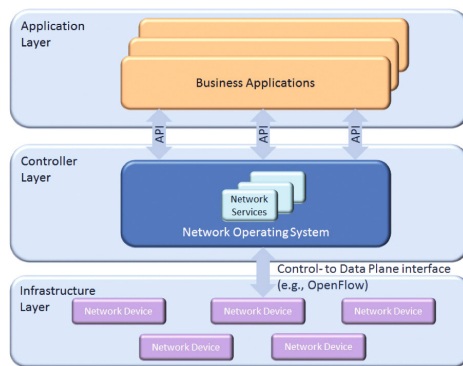


Fig. 1. SDN architecture (image from [28])

## 3 Background

### 3.1 SDN and Openflow

According to the Open Networking Foundation (ONF) [28], software-defined networking (SDN) is a networking architecture in which the traffic control and forwarding (data plane) functions are decoupled. The network intelligence is logically centralised in software-based SDN Controllers, which have a global view of the network and provide a programmable interface that allows to abstract the underlying network infrastructure. As a result, the network appears to the applications (and to policy engines, too) as a single, logical switch. Figure 1 depicts a logical view of the SDN architecture.

The SDN architecture can operate with different types of switches and at different protocol layers: it is extremely dynamic, manageable, cost-effective, and adaptable and provide to administrators unprecedented programmability, automation, and control. The key component of a Software Defined Network is its Controller (e.g., OpenDayLight [25], FloodLight [8], Pox/Nox [26], Onos [24]), which represents the conjunction point between the applications that manage the network (via the Northbound API) and the underlying network appliances (via the Southbound API).

The Northbound APIs enables external applications to program the network behaviour, providing basic network functions such as path computation, loop avoidance, smart routing, security and so on. There are several function offered on top of SDN but there not exist a single set of Northbound APIs: they represent the most nebulous component in a SDN environment.

The Southbound APIs represent the communication channel between SDN controllers and switches and routers of the network.

Today, although several solutions (both open and proprietary) exist, the most-used and well-know Southbound API implementation is represented by OpenFlow [29]. OpenFlow was the first standard communications interface defined between the control and forwarding layers of an SDN architecture. OpenFlow allows direct access to and manipulation of the forwarding plane of network devices, both physical and virtual (hypervisor-based). Differently from a classical one, in a OpenFlow-enabled switch or router the fast packet forwarding (data path) and the high level routing decisions (control path) are decoupled: the data path portion still resides on the switch, while high-level routing decisions are moved to the SDN controller.

### 3.2 Energy Model

The energy model considered in this paper was introduced by Kaup et al. in [7], where it is described in details.

In that paper the authors provide a model for the power consumption of SDN-enabled networking devices, with a specific focus on two devices, i.e. an OpenFlow-based hardware switch and a server running Open vSwitch.

The model, which takes care of all the operations related with the routing process (not limited only to packet forwarding but including the ones for switches configuration and management), is able to approssimate the consumed energy with an error of less than 8% for the software switch and less than 1% for the hardware switch.

According to that model, the power consumption of a switch, here defined as  $P_{switch}$ , is:

$$P_{switch} = P_{base} + P_{config} + P_{control} + P_{OF} \tag{1}$$

where:

- $P_{base}$  is static power needed to keep active the device;
- $P_{config}$  is the power used by the assigned configuration, i.e. related with the number active ports or with the configured line speed;
- $P_{control}$  is the power needed to control the network traffic, i.e. the packets involved in the network management;
- $P_{OF}$  is the power consumed by the traffic processed by OpenFlow.

Going into details, the  $P_{config}$  is:

$$P_{config} = \sum_i^{N_{activePorts}} s_i \cdot P_{port} \tag{2}$$

where:

- $N_{activePorts}$  is the number of active ports;
- $s_i$  is a value proportional to the configured speed of the port;
- $P_{port}$  is the power consumption of the  $i$  port at the full speed.

The  $P_{control}$  is:

$$P_{control} = r_{packetIn} \cdot E_{packetIn} + r_{FlowMod} \cdot E_{FlowMod} \tag{3}$$

where:

- $r_{packetIn}$  is the rate of outgoing *packetIn* messages;
- $E_{packetIn}$  is the energy needed to manage a *packetIn* message;
- $r_{FlowMod}$  is the rate of incoming *FlowMod* messages;
- $E_{FlowMod}$  is the energy needed to manage a *FlowMod* message.

Finally,  $P_{OF}$  is:

$$P_{OF} = \sum_i^{N_{flows}} r_{packets}(i) [ \sum_j^{N_{matches}} \mu_{match}(i \cdot j) \cdot e_{match}(j) ] + \sum_k^{N_{actions}} \mu_{action}(i \cdot k) \cdot e_{action}(k) \tag{4}$$

where:

- $N_{flows}$  is the number of active flows;
- $r_{packets}(i)$  is the packet rate for the  $i$ th flow;
- $e_{match}(j)$  is the energy consumed for each match ( $\mu_{match}(i \cdot j) \neq 0$  only if the match happens);
- $e_{action}(j)$  is the energy consumed for each action undertaken if the match happens ( $\mu_{action}(i \cdot j) \neq 0$  only if the action is performed).

As explained in [7], this last component can be removed due to its small impact on the overall power consumption.

The power model adopted in this paper, as a consequence, is:

$$P_{switchHW} = P_{base} + P_{config} + P_{control} \quad (5)$$

## 4 eA4SDN

eA4SDN is an evolution of the Adaptive Alienated Ant Algorithm for Software-Defined Networking (A4SDN), a distributed, adaptive, load-balancing bio-inspired algorithm for traffic engineering on Software-Defined Networks.

The Alienated Ant Algorithm (AAA, [2, 17]), i.e. the heuristic solution at the heart of the A4SDN, is a special case of Ant Colony Optimisation (ACO, [18]) solutions that takes advantages from a *non natural* behaviour of the ants, forcing them to spread themselves over all the available paths rather than converge to a single one.

### 4.1 Ant Colony Optimisation Solutions

Starting from the late 90's, many algorithms [6, 15, 27] have been developed, in different scenarios, in order to emulate the self-organisation ability of ants: this led to the definition of a well-structured class of stochastic, population-based meta-heuristics algorithms, known as Ant Colony Optimization (ACO).

ACO-based solutions have been mainly used to solve combinatorial and multi-constraint optimisation problems: each problems is firstly modelled to fit into the *shortest path* problem on a weighted graph and then a set of software agents, the *artificial ants*, build solutions by moving on the graph imitating their counterpart in the natural environments trying to maximise a given metric expressed in terms of pheromone quantity.

All ACO algorithms follow a simple three-steps pattern: *selection*, *reinforcement* and finally *evaporation*. The *selection* step consists in the selection of a set of candidates among the available paths which connect the nest to food source, basing on a probabilistic function. This function evaluates the pheromone on each node and assigns it a probability to be selected proportional to the quantity of associated pheromone.

Once identified a path, each ant marks it, reinforcing the current pheromone trail. By means of this step of *reinforcement*, each ant increments pheromone



only on one path, increasing the probability to choose again the same path in the next iteration. This simple mechanism guarantees the convergence of all ants on the paths that optimise the distance between the nest and the food.

Finally, the *evaporation* mechanism consists in the progressive decrement of the pheromone over all the paths proportionally to the elapsed time. Forcing the reduction of the pheromone quantity guarantees, after a given amount of time, that the less covered paths will be removed by the set of feasible solutions. Conversely, the paths (usually a single one) where the pheromone is stronger are highlighted.

## 4.2 From AAA to eA4SDN

ACO based algorithms are particularly suitable and easy-to-apply for all those scenarios where the conditions over the paths (e.g. the cost, the weight) are fixed or, at most, they change slowly. This is mainly due to the path selection mechanism that, forcing the convergence to a unique path, it needs to know all results in advance before to choose the best one.

AAA is an ACO-based algorithm based on a different interpretation of pheromone trails that simplifies the management of those scenarios where the conditions over the paths change in an unpredictable way, as for flows management in time-variant networks.

AAA takes into account the behaviour of an ideal alienated ant that prefers the paths where it can find the least number of other ants. In order to achieve this it smells pheromone trails but, instead of following the path where the pheromone trail is stronger (as the other normal ants), it takes the path with the lighter one. Therefore, releasing on a path an additional quantity of pheromone means to reduce the probability that it could be selected from other alienated ants.

In A4SDN, the quantity of pheromone has been considered proportional to the number of packets crossing each network device, making possible to build a routing solution able to:

- Rapidly explore all the graph/network and perform a dynamic load balancing among all its edges;
- Provide a reasonable response time related to the routing among the edges;
- Adapt its selected paths making on changing of load and network conditions (load balancing).

eA4SDN, instead, is designed to balance the energy consumption on each switch, not the packets: the pheromone, here, is represented by the energy consumed in the routing activities and, as a consequence, the paths selection is done minimising the Eq. 5.

## 4.3 Algorithms, Testbed and Settings

In order to evaluate the effectiveness of the proposed solution, we compared the energy-aware version of the A4SDN (eA4SDN) with the standard A4SDN

solution and with two other different solutions based on Dijkstra's shortest path algorithm, named respectively DA (i.e., Dijkstra's algorithm) and EDA (i.e., Extended Dijkstra's algorithm, EDA).

Both these solutions, introduced in [9] and already compared in a different environment with the A4SDN in [11], build their own routing tables taking into account the shortest path among each couple of switches available in the network: both DA and EDA calculated the shortest path using as a weight the bandwidth of the link connected each couple of nodes but whereas DA calculated the shortest path statically only when the network is created, the EDA solution does it cyclically, considering also the actual load on links as the A4SDN does.

All the mentioned algorithms have been implemented using OpenDaylight as SDN controller. In particular, the A4SDN Orchestrator has been implemented atop OpenDaylight, interfacing them through jFlowLight 0.9.1 [14].

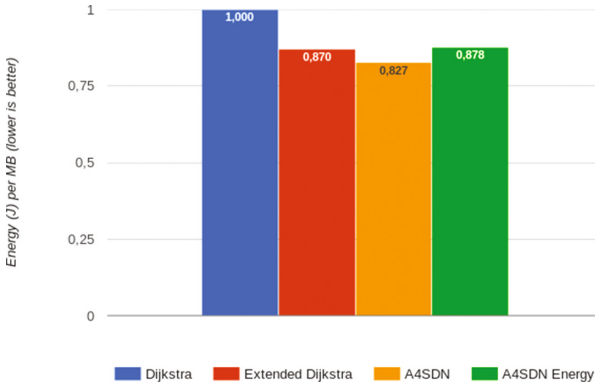
The evaluation has been done on top of the Internet2's Advanced Layer 3 Service topology [12] simulated with Mininet [21]. The Internet 2 is an optical-fibre network composed by 1 SDN Controller and 10 OpenFlow switches: it connects over 60,000 U.S. educational, research, government and institutions, from primary and secondary schools to community colleges and universities, public libraries and museums to health care organisations. A detailed list of the parameters value considered in the test environment are given in Table 1.

The load used for evaluating the behaviour of each algorithm has been generated using Iperf [13] and configured to keep network overload.

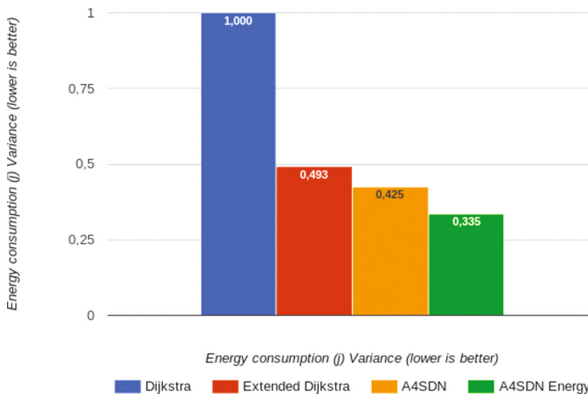
All the algorithms have been compared taking into account 4 different aspects: Throughput, Delay, Packet loss and Energy consumption. Throughput has been measured using the Iperf *bandwidth measurement* tool. Delay and Packet loss have been measured by using the *ping* tool. Energy consumption has been measured using the model in Sect. 3.2.

#### 4.4 Performance Evaluations

The Fig. 2 shows the average cost (in terms of energy, Joule) for delivering 1 MB of data. The best result is obtained by the A4SDN solution that uses about 5.5% less energy than eA4SDN and EDA (the difference between them is less than 1%) and about 21% than DA. This result is easy to explain: A4SDN is designed to balance, and as a consequence to minimise, the amount of packets crossing (IN/OUT) any switch, i.e. the  $P_{control}$ , which represents the biggest components in Eq. 5 when, as it happens in the considered testing scenario, the network is active and loaded. eA4SDN, instead, is designed to balance the energy consumption on each switch, i.e. the entire Eq. 5. The Fig. 3 shows the variance of energy consumption across all the switches of the considered network: as it is easy to note, eA4SDN is able to arrange the routing in order to keep the level of energy consumption well balanced all over the network. In a homogenous environment (as the one taken into account) characterised by a  $P_{base}$  (i.e. static consumption) equals in each switch, the difference in energy consumption is only due to the dynamic aspects of the routing: the higher the consumption, the higher the rules and packets managed, the more important the role played by



**Fig. 2.** Internet 2 Energy consumption Average per MB

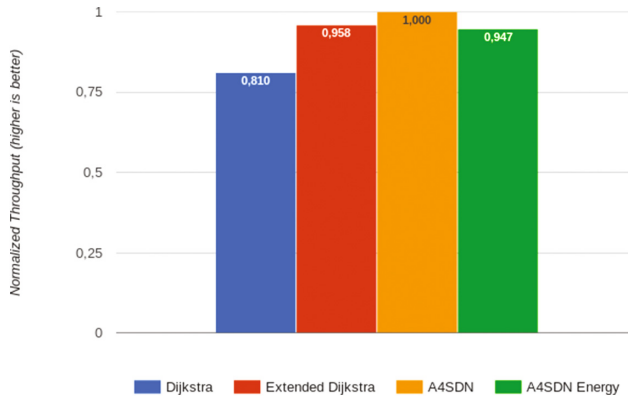
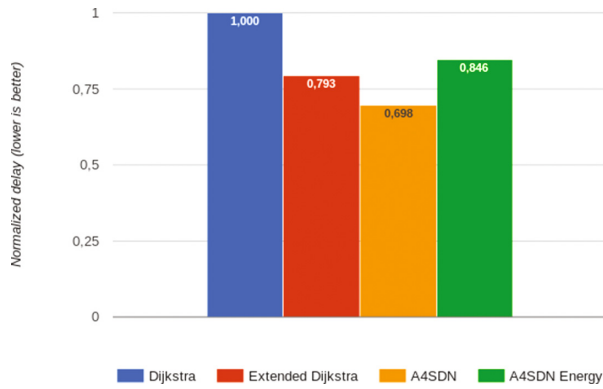
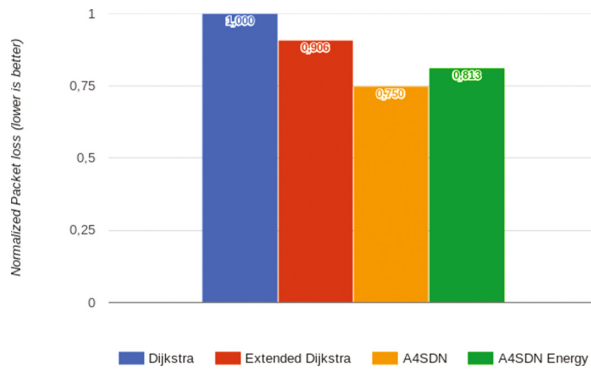


**Fig. 3.** Internet 2: Overall Energy Consumption Variance

each switch in the routing schema. As a consequence, a high value of variance is directly related with both a lower number of switch involved in the routing activities and an asymmetric distribution of the workload: this explains the high value of EDA (47.2% bigger than eA4SDN) and DA (about 300% bigger than eA4SDN) that, being based on Dijkstra’s algorithm, tend to use a well defined path (or paths) for their routing solutions.

From the energy consumption prospective, however, the lower the number of involved switches, the higher the wastefulness of “passive” energy, i.e. the energy needed to keep active those portions of network under-utilised or not used at all. Under this view, the eA4SDN has the best performance in terms of energy consumption.

The A4SDN, instead, is the best solution for all the other considered aspects. As expected, the dynamic and adaptive load balancing capability of A4SDN makes it the best solution in term of throughput. In particular, as shown in Fig. 4,

**Fig. 4.** Internet 2 Throughput**Fig. 5.** Internet 2 Delay**Fig. 6.** Internet 2 Packet Loss

**Table 1.** Internet 2 testbed

Link bandwidth	10 Mbps
Link propagation delay	10 ms
Number of servers	2
Number of switches	10
Number of edges	15
SDN controller	OpenDayLight 0.2.3 Helium-SR3
SDN enabled network	Mininet 2.2.1
OpenFlow version	1.3.0
jFlowLight version	0.9.1
Iperf version	3.0.7
Ping	-
Testing time	300 s

the throughput measured for A4SDN is 23.4% better the one measured for DA, 4.36% better than EDA and 5.59% better than its Energy-aware version. eA4SDN and EDA have the same performance (EDA is about 1% better).

The Fig. 5 summarises the results about performance of each algorithm in terms of average delay per transmitted packet. Also in this case, A4SDN performs better than the other solutions. Its ability to prevent congestion, together its load balancing capability, makes A4SDN able to delivery packets, in average, 43.2% faster than DA, 13.6% than EDA and 21.2% than eA4SDN. The poor performance of DA is easily explained by the fact that it uses static paths and then it is not able to react to traffic congestions: when a path tagged as “shortest” becomes congested, the DA is not able to modify it, continuing to forward packets on it and then to feed the congestions. On the contrary, EDA is able to react to congestion searching for a new shortest path: this allows it to perform 26% better than its static version. The ability to avoid congestions strongly influences also the probability of loosing packets during the routing activities. As shown in Fig. 6, both AAA-based solutions (A4SDN and eA4SDN) perform better that the solutions based on Dijkstra’s algorithm. Although the standard version of the A4SDN has again the best performance (8.4% better than eA4SDN, 20.8% better than EDA and 33.3% than DA) also the eA4SDN performs much better than EDA (11.2%) and DA(23%), underlying the important of avoiding congestions, which represent the only cause of packet loss in this scenario.

## 5 Conclusion

In this paper the authors have introduced eA4SDN, an energy-aware algorithm for traffic engineering on SDN based on the A4SDN, a heuristic, bio-inspired solution already introduced in [11].

As any other ACO-oriented solutions, eA4SDN takes its decisions basing on the value of pheromone, here emulated by the energy needed to managed routing operations. In particular, eA4SDN designs its routing paths minimising, step by step, the energy used by each switch (see Eq. 5).

In order to evaluate its performance, the proposed energy-aware approach has been compared with the standard A4SDN and with two deterministic solution based on Dijkstra's Algorithm: the results have demonstrated that eA4SDN is able to minimise the amount of "passive" energy, i.e. the energy needed to keep active portions of network under-utilised or not used at all.

## References

1. Buyya, R., Beloglazov, A., Abawajy, J.: Energy-aware resource allocation heuristics for efficient management of data centers for cloud computing. *Future Gener. Comput. Syst.* **28**(5), 755–768 (2012)
2. Morana, G., Di Stefano, A.: A bio-inspired distributed algorithm to improve scheduling performance of multi-broker grids. *Nat. Comput.* **11**(4), 687–700 (2012)
3. Marinescu, D.C., Paya, A.: Energy-aware load balancing policies for the cloud ecosystem. In: 2014 IEEE International Parallel & Distributed Processing Symposium Workshops (IPDPSW), pp. 823–832. IEEE (2014)
4. Ozkasap, O., Assefa, B.G.: State-of-the-art energy efficiency approaches in software defined networking. In: ICN 2015, p. 268 (2015)
5. Papuzzo, G., Mastroianni, C., Meo, M.: Probabilistic consolidation of virtual machines in self-organizing cloud data centers. *IEEE Trans. Cloud Comput.* **1**(2), 215–228 (2013)
6. Lee, C.N., Chou, T.Y., Chiang, C.W., Lee, Y.C.: Ant colony optimisation for task matching and scheduling. In: IEE Proceedings of Computers and Digital Techniques, vol. 153, pp. 373–380. IET (2006)
7. Hausheer, D., Kaup, F., Melnikowitsch, S.: Measuring and modeling the power consumption of openflow switches. In: 2014 10th International Conference on Network and Service Management (CNSM), pp. 181–186. IEEE (2014)
8. Floodlight website (2017). <http://www.projectfloodlight.org/floodlight/>. Accessed 3 Apr 2017
9. Morana, G., Zito, D., Cammarata, G., Di Stefano, A.: A4sdn - adaptive alienated ant algorithm for software-defined networking, pp. 344–350. IEEE (2015)
10. Morana, G., Zito, D., Cammarata, G., Di Stefano, A.: Assdn: a framework for adaptive strategies for software-defined networking. In: 2016 IEEE 25th International Conference on Enabling Technologies: Infrastructure for Collaborative Enterprises (WETICE), pp. 101–106. IEEE (2016)
11. Morana, G., Zito, D., Cammarata, G., Di Stefano, A.: Evaluating the performance of a4sdn on various network topologies. In: 2016 IEEE International Parallel and Distributed Processing Symposium Workshops, pp. 801–808. IEEE (2016)
12. Internet 2 layer 3. <http://www.internet2.edu/products-services/advanced-networking/layer-3-services/>. Accessed 3 Apr 2017
13. Iperf website (2015). <https://github.com/esnet/iperf>. Accessed 3 Apr 2017
14. jflowlight website. <https://github.com/giovannicammarata/jflowlight>. Accessed 3 Apr 2017
15. Sun, W.H., Sim, K.M.: Ant colony optimization for routing and load-balancing: survey and new directions. *IEEE Trans. Syst. Man Cybern.* **33**(5), 560–572 (2003)

16. Xie, L., Liu, W., Rao, L., Liu, X.: Minimizing electricity cost: optimization of distributed internet data centers in a multi-electricity-market environment. In: 2010 Proceedings IEEE INFOCOM, pp. 1–9. IEEE (2010)
17. Morana, G., Bandieramonte, M., Di Stefano, A.: Grid jobs scheduling: the alienated ant algorithm solution. *Multiagent Grid Syst.* **6**(3), 225–243 (2010)
18. Blum, C., Dorigo, M.: Ant colony optimization theory: a survey. *J. Theoret. Comput. Sci.* **344**(2), 243–278 (2005)
19. Humphrey, M., Mao, M.: Auto-scaling to minimize cost and meet application deadlines in cloud workflows. In: 2011 International Conference for High Performance Computing, Networking, Storage and Analysis (SC), pp. 1–12. IEEE (2011)
20. Humphrey, M., Mao, M., Li, J.: Cloud auto-scaling with deadline and budget constraints. In: 2010 11th IEEE/ACM International Conference on Grid Computing (GRID), pp. 41–48. IEEE (2010)
21. Mininet website. <http://mininet.org/>. Accessed 3 Apr 2017
22. Quang-Hung, N., Thoai, N.: Energy-efficient vm scheduling in iaas clouds. In: Dang, T.K., Wagner, R., Küng, J., Thoai, N., Takizawa, M., Neuhold, E. (eds.) FDSE 2015. LNCS, vol. 9446, pp. 198–210. Springer, Cham (2015). doi:[10.1007/978-3-319-26135-5\\_15](https://doi.org/10.1007/978-3-319-26135-5_15)
23. The new york times (2015). <http://www.nytimes.com/2012/09/23/technology/data-centers-waste-vast-amounts-of-energy-belying-industry-image.html>. Accessed 3 Apr 2017
24. Onos website (2015). <http://onosproject.org/>. Accessed 3 Apr 2017
25. Opendaylight website (2015). <http://www.opendaylight.org/>. Accessed 3 Apr 2017
26. Pox/nox website (2015). <http://www.noxrepo.org/>. Accessed 3 Apr 2017
27. Bruten, J., Schoonderwoerd, R., Holland, O.: Ant-like agents for load balancing in telecommunications networks. In: Proceedings of the First International Conference on Autonomous Agents, pp. 209–216. ACM (1997)
28. Sdn website. <https://www.opennetworking.org/sdn-resources/sdn-definition>. Accessed 3 Apr 2017
29. OpenFlow Switch Specification. Version 1.4.0, 14 october 2013
30. Ramesh, K., Shenoy, P., Mathew, V., Sitaraman, B.: Energy-aware load balancing in content delivery networks. In: 2012 Proceedings IEEE INFOCOM, pp. 954–962. IEEE (2012)

# Energy Optimization Algorithm Based on Data Density Correlation in Wireless Sensor Network

Jiang Wanyuan<sup>1</sup>, Li Peng<sup>1,2(✉)</sup>, Xu He<sup>1,2</sup>, and Nie Huqing<sup>1</sup>

<sup>1</sup> School of Computer Science & Technology,  
Nanjing University of Posts and Telecommunications, Nanjing 210003, China  
lipeng@njupt.edu.cn

<sup>2</sup> Jiangsu High Technology Research Key Laboratory  
for Wireless Sensor Networks, Nanjing 210003, Jiangsu, China

**Abstract.** It's importance to send the typical data from sampled data to the sink node in wireless sensor network. Compared with actual data, the representative data are always imprecise. Moreover, the energy consumption is huge. In order to minimize the energy consumption and improve the data accuracy, this paper presents the data fusion model PCCDNCD (correlation degree base on the Pearson correlation coefficient, the distance factor and the number of neighbor nodes, PCCDNCD). The correlation degree formula which can characterize the node from three aspects and classify nodes into three types precisely, is based on the Pearson correlation coefficient, the distance of nodes and the number of neighboring nodes. Nodes are classified into typical, ordinary and isolated nodes. In addition, the typical and isolated nodes are responsible for transferring data, while ordinary nodes are not required. The results show that the typical data achieved by the PCCDNCD method have higher degree of accuracy than the data from PCC (the Pearson correlation coefficient, PCC) and DDCD (the data density correlation degree, DDCD) methods. Meanwhile PCCDNCD algorithm has a low energy consumption.

**Keywords:** Wireless sensor networks · Data density · Data fusion · Energy optimization

## 1 Introduction

WSN (wireless sensor network, WSN) has obtained wide attention, which is regarded as the most important basis supporting technology of internet of things [1]. Sensor nodes deploy randomly, and it is difficult to replace the battery or additional energy. In order to describe the physical characteristics of the perception area accurately and reliably, a lot of nodes are required to cover the sensing area. However, this will cause the overlapping of sensor nodes' monitoring region, leading to the redundancy of neighboring sensor nodes' data. Therefore, ensuring the quality of the network, minimizing the energy consumption of each node, and eventually improving network life cycle has become one of the key technologies of WSN.



WSN energy consumption relates to distance between nodes and the amount of data [2, 3]. Currently, one of the method to reduce the energy consumption is the data fusion method. Compared with uploading the data to each node directly, data fusion method can greatly reduce data redundancy and the amount of data transmitted over the network, reducing energy consumption and prolonging the network lifetime [4, 5].

According to the fusion strategies, we can divide the data fusion methods into three kinds: in-network inquiry, data compression and representation [6]. The kind of in-network inquiry takes a long time to receive a reply from WSN. The second kind is high complexity. So we focuses on the third type.

## 2 Related Works

Representative data fusion algorithm is on the basis of correlation of nodes [7]. Document [8] proposed the Pearson's correlation coefficient to describe the correlation. But the correlation value has related to the number of the data  $n$ . it is inappropriate to determine the linear relationship between two variables via the correlation coefficient.

Literature [9, 10] proposed a correlation formula based on the statistics feature of data. It builds a cluster get a tolerant error approximate results, avoiding unexpected data, while existing large errors. And when applied it to the WSN, it seems to have some problems such as consume more energy in the clustering process, and the complexity in calculation process of correlation.

Document [11] presented the data density correlation formula DDCD that exploited the difference between the node data. It reflected not only the aggregation degree of nodes within a certain domain data, but also the position of a node relative to a certain area. Compared with the correlation on the basis of distance, the DDCD was better in accuracy. However, the data difference between nodes is not convenient to measure. Case the distance between two nodes are far apart, while data with little difference, the data transmission between nodes wastes much energy.

Based on the analysis, this paper presents a data density correlation formula based on the Pearson's correlation coefficient of sample data, distance between nodes and the number of the neighbor nodes. The main idea of the method is dividing the nodes into three types: isolated nodes, ordinary nodes and representative nodes. Isolated nodes upload the information separately, representative nodes represent the ordinary nodes to upload sampled data, greatly reducing the amount of data transmitted.

## 3 Define of the Data Density Correlation Degree

### 3.1 Formula of Data Density Correlation Degree

Data density correlation degree formula proposed is to divide the nodes into three types. The three main aspects of the formula is PCC based on the sample data, the distance between nodes and the neighbor nodes within a range of the node. The formula 1 is shown as follows.

$$\text{sim}(n) = \begin{cases} 0 & N < \text{minpts}, p_l < 0.8 \\ a_1 \sum p_i / N + a_2(1 - d/r) + a_3(1 - 1/\exp(N - \text{minpts})) & N \geq \text{minpts}, p_l \geq 0.8 \end{cases} \quad (1)$$

Where n is the current node, sim(n) represents the data density correlation degree of the current node, pi is the PCC between nodes, N indicates the number of neighbor nodes within a scope of the node where PCC is greater than 0.8. Seen as Table 1, PCC between 0.8 to 1.0 are highly relevant. In order to ensure a strong correlation between the experimental data, so we select 0.8 as the threshold value. Minpts represents the minimum threshold number of neighbor nodes, where we consider it as 2. d is the average distance between node n to its neighbor nodes set N, r is the distance threshold between nodes, a1, a2 and a3 are the weighted coefficients, with a1 + a2 + a3 = 1.

### 3.2 Pearson Correlation Coefficient

The first part of formula 1 represents the average value of PCC [12] between node n and its N neighbor nodes' data objects. pi is the correlation between nodes from the sampling data level. It is calculated as formula 2.

$$PCC(X, Y) = \frac{\sum_i (x_i - \bar{x}_i)(y_i - \bar{y}_i)}{\sqrt{\sum_i (x_i - \bar{x}_i)^2} \sqrt{\sum_i (y_i - \bar{y}_i)^2}} \quad (2)$$

Where X and Y represent the sample data come from two nodes respectively, xi and yi represent the sampled data in the i time, x̄i and ȳi are the average value of the sampled data. Table 1 is adopted to determine the strength of the correlation of two variables. Here we consider the PCC threshold value of two nodes' sample data is 0.8.

### 3.3 Physical Location of the Nodes

In the second part of formula 1, d represents an average distance between two nodes of the physical location, and distance function is calculated by Euclidean distance function. Suppose there are two nodes A and B in the network that the coordinates of point A is (x0, y0) and point B is (x1, y1) so the euclidean distance is computed by formula 3.

**Table 1.** Relationship between Pearson correlation coefficient and correlation coefficient

PCC	Correlation
0	Completely related
0-0.2	Very weak related
0.2-0.4	Weak related
0.4-0.6	Medium related
0.6-0.8	Strong related
0.8-1.0	Very strong related
1	Completely related

$$d = \sqrt{(x_0 - x_1)^2 + (y_0 - y_1)^2} \quad (3)$$

The part measures the relationship between two nodes from distance level,  $r$  is the distance threshold value. Obviously, the distance closer, the sampled data similar, the correlation degree of nodes greater. As can be seen from the formula 3, with the increasing of physical distance  $d$  between two nodes, the node correlation  $\text{sim}(n)$  decreases, with the decreasing of  $d$ , and  $\text{sim}(n)$  becomes larger.

### 3.4 Number of Neighbor Nodes

In the third part of the formula 1,  $N$  is the number of neighbor nodes meet the criteria. The more the number of neighbors, the stronger the representation of data density correlation [13]. It can be seen that as  $N$  increasing, the third part is also increased. Conversely if the value  $N$  decreases, it shows the fewer the neighbor nodes and the smaller the data density node.

It can be seen in the formula 1 that the first part is directly related to the sample data, the importance is greater than the other two. The second part describes the physical location of the nodes, which has the necessary connection with the sampling results. Due to the number of nodes in the dense regions with little difference, thus the third part has the smallest importance. So the individual weight values are set as follows:  $a_1 = 1/2$ ,  $a_2 = 1/3$ ,  $a_3 = 1/6$ .

We can see that the collaboration between the various information can ensure the accuracy of the data density correlation. And the data density correlation formula  $\text{sim}(n)$  this article defined is range at  $[0-1]$ , PCC threshold is about 0.8 to ensure that  $\text{sim}(n)$  not impact by the irrelevant data, and the value  $\text{minpts}$  ensures that node  $n$  has the minimum number of neighbor nodes.

If the data density correlation degree of sensor node is  $\text{Sim}(n)$  defined by (1), then we can obtain the properties of  $\text{Sim}(n)$  as:

- (1)  $\text{Sim}(n)$  increases with the increase of  $p_i$ ;
- (2)  $\text{Sim}(n)$  increases with the decreases of  $d$ ;
- (3)  $\text{Sim}(n)$  increases with the increase of the number of neighbor nodes;

Thus in formula 1,  $\text{sim}(n)$  can reflect the correlation between the node  $n$  and its neighbor nodes.

## 4 Data Fusion Algorithm Based on Data Density Correlation

### 4.1 Classification of Nodes

The paper adopts the data density correlation formula 1 to characterize the nodes, and the nodes can be divided into three types: the representative nodes, the ordinary nodes and the isolated nodes, shown as follows.

- (1) Representative Node: A node named  $n$ , with  $N$  nodes where the Pearson coefficient between node  $n$ ' sample data and nodes  $N$ ' ( $N \geq \text{minpts}$ ) sample data is greater than 0.8. The representative nodes represent the  $N$  nodes within a certain range to transmit the collected data to the sink node, reducing the amount of data transmitted and reducing energy consumption.
- (2) Isolated Node: A node named  $b$ , if the PCC with all other nodes' sampled data is less than 0.8,  $b$  node is regarded as the isolated node, so that data must be uploaded individually to the sink node.
- (3) Ordinary Node: Between node  $n$  and node  $b$  is one of the  $N$  neighbor nodes of  $n$  node, which is responsible for helping representative nodes to transmit data to sink node.

Isolated nodes upload data to the sink node separately, so as to ensure the integrity of the information. Representative nodes substitute the ordinary nodes with a high degree of similarity to transmit the collected data to the sink node, to ensure the comprehensiveness and avoiding the redundancy of information.

The process of data density correlation fusion algorithm is to use the defined of data density correlation as an index, select the appropriate representative nodes of the local area and transmit collected data to the sink node, reducing the amount of data transmitted and saving energy consumption.

## 4.2 Implement Process of PCCDNCD Algorithm

Fusion algorithm is interpreted as follows.

Assuming the number of nodes in WSN is  $n$ . At the beginning, all the sensor nodes have to send a message containing the geographic location to the base station. Since the position of base station is fixed so we can build a two-dimensional coordinate system, in which the position of base station is at  $(0,0)$  point, so that we can obtain the location information of other nodes which make up the initial entire network.

- (1) Firstly, each node calculates the PCC on the basis of sample data.
- (2) If PCC are less than 0.8, we consider the node as isolated node.
- (3) If the remaining nodes meet the definition of representative nodes, according to the formula 1, it calculates the data density correlation of the node, followed by calculating the value  $\text{sim}(n)$  of all nodes meet the definition of representative nodes.
- (4) It selects the largest value  $\text{sim}(n)$  and records its neighbor nodes into the set  $\text{inclusterNode}()$ , the nodes not within the neighbor range are in the set  $\text{outclusterNode}()$ .
- (5) Repeat the above steps 1–4 where nodes in the set  $\text{clusterNode}()$ , until all nodes' division is complete.

After executing the above algorithm, nodes are divided into representative nodes, isolated nodes or ordinary nodes. The representative nodes hold the largest  $\text{sim}(n)$ , and the set  $\text{inclusterNode}()$  save the ordinary nodes. The data density correlation degree of this ordinary nodes and representative nodes. The ordinary nodes and the node data

density correlation if relative large, the representative nodes upload the data to the sink node on behalf of the ordinary nodes. Isolated nodes are the nodes which inclusterNode() set is empty.

## 5 Simulation and Analysis

### 5.1 Simulation Environment and Parameter Settings

MATLAB is adopted as simulation platform, we assume that the WSN consists of 100 sensor nodes and nodes are randomly distributed in the 100 m \* 100 m area, detecting temperature of the area, and the remote base station locate in coordinates (50, 175). Supposing that base station is deployed outside of the region which has the supplementary energy source; nodes are the same and static randomly deployed in a region; the initial energy of nodes is the same; and the spread channel of the transmitting and receiving is symmetrical.

The communication model in the document [14, 15] be adopted. Suppose the distance between two nodes is  $d$ , the wireless coverage radius is  $r$ , so that the energy consumption of transfer 1 bit is calculated by formula 4; Node consume energy when receive 1 bit data is calculated by formula 5 (Fig. 1 and Table 2).

$$E_{TX}(ld) = \begin{cases} lE_{elec} + le_{fs}d^2, & d < d_0 \\ lE_{elec} + le_{mp}d^4, & d > d_0 \end{cases} \tag{4}$$

$$E_{RX}(l) = lE_{elec} \tag{5}$$

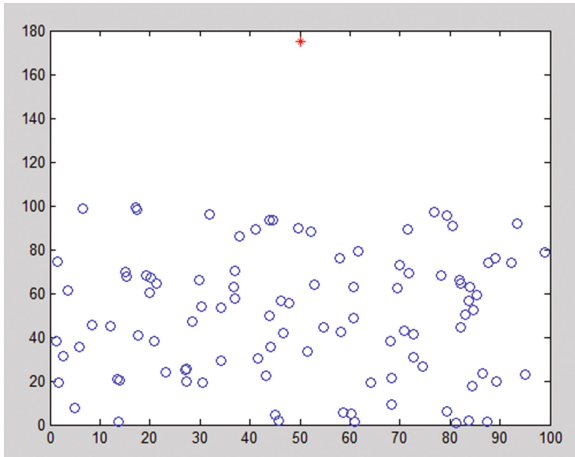


Fig. 1. Initial node scene

**Table 2.** Simulation parameters table

Parameter name	Values
Network area	(100 m * 100 m)
Base station coordinate	(50 m, 175 m)
Number of nodes	100
Initial energy	2 J
Transmission and reception circuit consumes	50 nJ/bit
Amplifiers factor (space)	10 pJ/bit·m <sup>-2</sup>
Amplifiers factor 2 (multipath propagation)	0.0013 pJ/bit·m <sup>-4</sup>
Data fusion energy	5 nJ/bit-signal - 1
Packet size	4000 bit

## 5.2 Fusion Performance Index and Comparison

### 5.2.1 Fusion Algorithm Performance Index

We use the data error between typical nodes and ordinary nodes to measure the data fusion effect. Considering  $n$  sensor nodes  $p_1, p_2 \dots p_n$ , with data  $d_1, d_2 \dots d_n$  respectively. And  $p_n$  is the representative data. Then the error is shown in formula 6, the molecular is the relative error between  $p_0$  and  $p_i$ . Therefore, the global average relative error could be used to measure the performance of the algorithm. The fusion effect between global representative nodes and ordinary nodes is shown in formula 7, where  $k$  represents the number of regional division in a WSN,  $\bar{E}$  is the average relative error with in the area  $i$ .

$$\bar{\varepsilon} = \frac{\sum_{i=1}^{n-1} (p_n - p_i)/p_n}{n - 1} \quad (6)$$

$$\bar{E} = \frac{\sum_{i=1}^k \bar{\varepsilon}_i}{k} \quad (7)$$

### 5.2.2 Fusion Effect

PCC data fusion algorithm proposed by the document [8] based on the PCC. Data fusion needs to upload a large number of sample data, while the calculation process is simple.

The DDCD data fusion algorithm in the literature [11] adopts the number of neighbor nodes, and the deviation between sampled data of the nodes. It not only reflects the aggregation degree of data within a certain domain, but also the position of a node relative to a certain area.

Figure 2 shows the fusion result of each data fusion algorithm in the sampling time, characterized global relative error and time functions. The smaller global relative error, the better fusion result in the representative nodes. The PCCDNC proposed by this paper exhibits the smallest global relative error compared with the other two algorithms, which indicates PCCDNC has better fusion effect than DDCD and PCC.

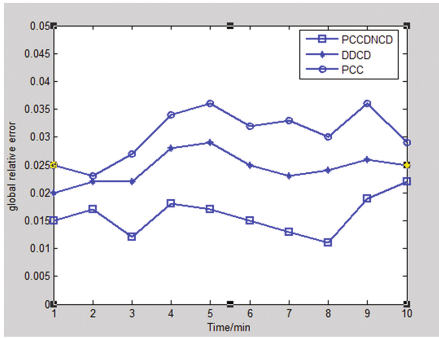


Fig. 2. Comparison of each algorithm global relative error

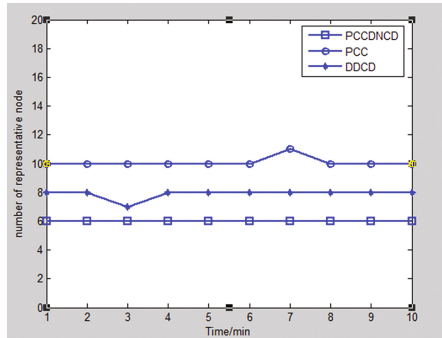


Fig. 3. Number of representative nodes in each algorithm

Figure 3 compares the number of representative nodes in each algorithm. As can be seen from the Fig. 3, the number of representative nodes selected in PCCDNCD algorithm is slightly less than DDCD algorithm, and much less than PCC algorithm. A small number of representative nodes in the network illustrates smaller amount of data to be transferred, which can also reduce the energy consumption of WSN.

Figure 4 shows the number of isolated nodes in each algorithm. The number of isolation nodes selected in PCCDNCD is less than DDCD, and much less than PCC algorithm. A small number of isolated nodes in the network illustrates smaller amount of data to be transferred, leading to reduce the energy consumption of WSN.

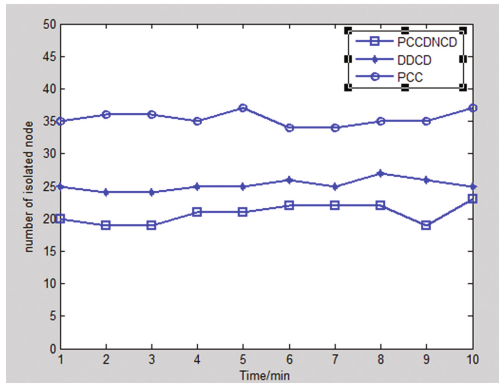


Fig. 4. Number of isolated nodes in each algorithm

### 5.3 Energy Consumption Analysis of Fusion Algorithm

PCC fusion algorithm with respect to the proposed PCCDNCD data fusion algorithm can save much energy in the data upload process. The energy consumption between DDCD algorithm and the PCCDNCD algorithm proposed in this paper makes almost

**Table 3.** Proportion of each type of node

Name of algorithm	Percentage of representative nodes	Percentage of isolated nodes	Percentage of representative and isolated nodes
PCC	10%	35%	45%
DDCD	8%	25%	33%
PCCDNCD	6%	20%	26%

no difference, but in the transmission phase of representative nodes, the energy consumption of PCCNCD algorithm is lower than the DDCD algorithm (Table 3).

It can be seen that in the number of isolated nodes and representative nodes, PCCDNCD algorithm has advantages over PCC algorithm and DDCD algorithm, which can save energy in the data transmission phase.

When the WSN becomes stable, isolated and representatives nodes upload data, thus PCC algorithm requires the largest amount of data transferred, PCCDNCD algorithm is superior to PCC and DDCD algorithm.

## 6 Conclusion

In this paper, the data density correlation degree and the PCCDNCD is proposed, based on the energy consumption model in WSN. For the defects of other correlation formula, the data density correlation degree formula proposed is association with the PCC of sample data, the distance of nodes and the number of neighboring nodes. At the same time, we apply the correlation formula to the WSN for data fusion, classifying the nodes in the network and electing suitable and representative nodes to transit information.

Simulation results show that data density correlation fusion algorithm can effectively reduce the amount of data transmitted over the network, reducing energy consumption and providing more accurate description, comparing with the method PCC and DDCD. In conclusion, the PCCDNCD fusion method is more energy conservation and obtains the performance of better data representation than the other two methods. Therefore, PCCDNCD fusion method is more useful for the WSN network, where the sampled data change slowly over the time.

**Acknowledgments.** The subject is sponsored by the National Natural Science Foundation of P.R. China (No. 61373017, No. 61572260, No. 61572261, No. 61672296, No. 61602261), the Natural Science Foundation of Jiangsu Province (No. BK20140886, No. BK20140888, No. BK20160089), Scientific & Technological Support Project of Jiangsu Province (No. BE2015702, No. BE2016777, BE2016185), China Postdoctoral Science Foundation (No. 2014M551636, No. 2014M561696), Jiangsu Planned Projects for Postdoctoral Research Funds (No. 1302090B, No. 1401005B), Jiangsu High Technology Research Key Laboratory for Wireless Sensor Networks Foundation (No. WSNLBZY201508).



## References

1. Zhang, J., Yang, T., Zhao, C.: Energy-efficient and self-adaptive routing algorithm based on event-driven in wireless sensor network. *Int. J. Grid Utility Comput.* **7**, 41–49 (2016)
2. Xia, J., Yun, R., Yu, K., Yin, F., Wang, H., Bu, Z.: A coordinated mechanism for multimode user equipment accessing wireless sensor network. *Int. J. Grid Utility Comput.* **5**, 1–10 (2014)
3. Rahman, M.N., Matin, M.A.: Efficient algorithm for prolonging network lifetime of wireless sensor networks. *Tsinghua Sci. Technol.* **6**, 561–568 (2011)
4. Boyinbode, O., Le, H., Takizawa, M.: A survey on clustering algorithms for wireless sensor networks. *Int. J. Space Based Situated Comput.* **1**, 130–136 (2011)
5. Meng, N., Wang, J., Kodama, E., Takata, T.: Reducing data leakage possibility resulted from eavesdropping in wireless sensor network. *Int. J. Space Based Situated Comput.* **3**, 55–65 (2013)
6. Xin, G., Feiqi, D.: Routing protocol and data fusion technology research in wireless sensor network. South China University of Technology (2013)
7. Hao, L., Jijun, Z.: Data fusion research based on the correlation of data fusion in wireless sensor networks. Hebei University of Engineering (2013)
8. Guyeux, C., Makhoul, A., Bahi, J.M.: A security framework for wireless sensor networks: theory and practice. *Int. J. Inf. Technol. Web Eng.* **10**, 47–74 (2015)
9. Yuan, J., Chen, H.: The optimized clustering technique based on spatial-correlation in wireless sensor networks. In: *Proceedings of IEEE Youth Conference on 2009 Information, Computing and Telecommunication*, pp. 411–414. IEEE, Beijing (2009)
10. Bouaziz, R., Krichen, F., Coulette, B.: C-SCRIP: collaborative security pattern integration process. *Int. J. Inf. Technol. Web Eng.* **10**, 31–46 (2015)
11. Yuan, F., Zhan, Y., Wang, Y.: Data density correlation degree clustering method for data aggregation in WSN. *IEEE Sens. J.* **4**, 1089–1098 (2014)
12. Solis, E.D.B., Neto, A.M., Huallpa, B.N.: Pearson's correlation coefficient for discarding redundant information: velodyne lidar data analysis. In: *2015 12th Latin American Robotics Symposium and 2015 3rd Brazilian Symposium on Robotics (LARS-SBR)*, pp. 116–119 (2015)
13. Liu, Q., Xiong, Y.: The research of recommendation algorithm based on collaborative filtering. University of Science and Technology of China (2013)
14. Yang, K., Liu, S., Li, X., Wang, X.A.: D-S evidence theory based trust detection scheme in wireless sensor networks. *Int. J. Technol. Hum. Interact.* **12**, 48–59 (2016)
15. Li, X., He, Y., Niu, B., Yang, K., Li, H.: An exact and efficient privacy-preserving spatiotemporal matching in mobile social networks. *Int. J. Technol. Hum. Interact.* **12**, 36–47 (2016)

# Design and Implementation of Urban Vehicle Positioning System Based on RFID, GPS and LBS

Cong Qian<sup>1,2</sup>, He Xu<sup>1,2</sup>✉, Peng Li<sup>1,2</sup>, and Yizhuo Wang<sup>3</sup>

<sup>1</sup> School of Computer Science, Nanjing University of Posts and Telecommunications, Nanjing, China

1227388900@qq.com, {xuhe, lipeng}@njupt.edu.cn

<sup>2</sup> Jiangsu High Technology Research Key Laboratory for Wireless Sensor Networks, Nanjing, China

<sup>3</sup> Bell Honors School, Nanjing University of Posts and Telecommunications, Nanjing, China  
838726806@qq.com

**Abstract.** In order to monitor the mobile vehicles efficiently and judge the congestion status under complex condition of road and traffic, Radio frequency identification (RFID) technology is used to realize the dynamic identification and information exchange of the vehicles together with using the advantage of technologies of Global Positioning System (GPS) and Location Based Service (LBS) to get the precise position of vehicle. LBS technology is used to realize the function of showing the congestion status under complex condition of road and traffic, and the status of the vehicle can be shown to users by electronic map on website. The model of vehicle monitoring is designed and the system is implemented and tested on the basis of combination of RFID, GPS and LBS, which can be of great significance to the information construction of traffic detection.

## 1 Introduction

With the rapid development of the country's economic construction, the city scale and population extends increasingly, together with the contradiction of people, vehicle and road. The problems of the management of the road traffic caused by the urbanization and motorization become increasingly serious [1]. The traffic is almost paralyzed around the holidays, when the issue of traffic is very obvious. Usually, government gives priority to the development of urban public transport as to improve urban residential environment, construct a harmony society and promote the sustainable development of cities. Strengthening the safety supervision of public transport and vehicle routing could reduce congestion and security risks as well as to promote the development of intelligent transportation systems.

As we all knows, the routes of urban public transport are fixed, so they are monitored not to select the best route but use Global Positioning System (GPS) to track their real-time position to be arranged conveniently to facilitate passengers and improve the utilization rate of the vehicle. This goals require the application of Radio frequency identification technology (RFID) systems. In order to provide greater convenience for passengers and vehicle schedule in monitoring, we can set up RFID monitoring points

at key positions such as stations, platforms, tunnel, bridge, etc. to realize the dynamic identification of vehicles and toll collection making up for the weak signal of GPS in these key points which lead to the inaccurate positioning [2]. The Singapore bus (SBS) assemble the on-board computer and the GPS locator on each bus, and each platform is equipped with a passenger display board. The central control computers of the intelligent transportation system tracks and monitors every bus at all time, which can monitor the arrival time and even the attendance of every bus. Passengers can view the operation of the bus on the passenger display board on the platform to reduce the waiting time and plan their own itinerary better and also can help managers to adjust their departure frequency better at the same time [3].

RFID is a kind of communication technology, which can identify the specific target and read the relevant data through the wireless signal identifying the mechanical or no-eye contact between the system and the specific target [4]. RFID component contains at least three parts: tag, reader and antenna. The complete RFID systems is also equipped with computer communication network. RFID technology is favored and used widely by virtue of the advantages of its easy read, rapid identification, large capacity, long life time, strong penetration, high security, high positioning accuracy, etc., while other technologies like bar code cannot match. The development of RFID technology in the transportation area is very fast since the 80s of the last century, which has been widely used in vehicle management, logistics management, arrival time prediction of transportation vehicle, smart cards, vehicle positioning, etc. In the intelligent transportation system, the technology of RFID automatic identification can accurately draw the vehicle information. The GPS receiver gets the real-time vehicle location information through uninterrupted 24 h and then displays and analysis the location information on the electric map through the powerful LBS technology [5]. In this paper, the RFID storage and positioning function are combined with the GPS technology, and the road traffic conditions are displayed by using LBS technology to control and manage the city's vehicle traffic conditions.

## 2 RFID System Architecture

In this paper, the RFID tag is used to identifications of the specific vehicle in the urban intelligent transportation system. A complete RFID system consists of reader, tag, antenna and communication network [6], which structure is shown in Fig. 1. Compared with the conventional traffic data detection, RFID-based systems is more efficient and cost saving. It accelerates the information of traffic detection and has the following advantages:

### 1. Fast read-write and long identification distance

As long as an object pasted with a RFID tag appears in the effective recognition range of reader, it can be detected immediately and dynamic identification. In the intelligent transportation system, the readers are arranged in the key intersection and tunnel location, where the tags exchange information with readers in a non-contact style. The

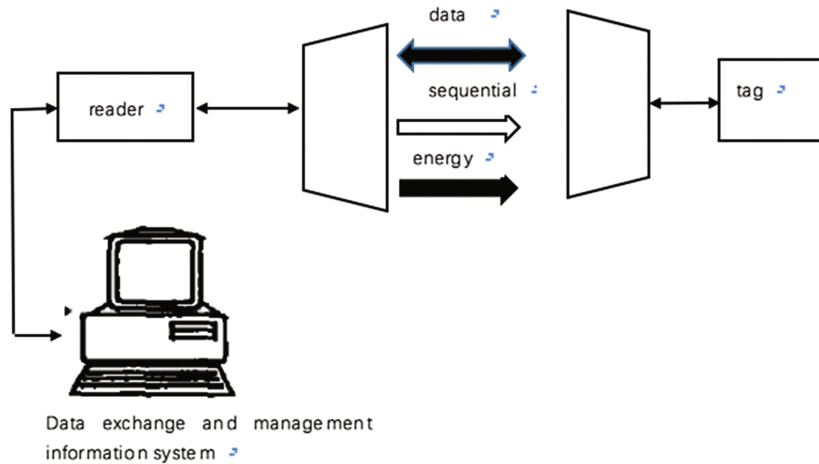


**Fig. 1.** RFID systems

recognition distance can reach dozens or even hundreds of meters, which makes the identification more reliable and no time delay.

## 2. High reliability

RFID tag communicates with a reader in a non-contact style, while a car in a high speed can also correctly be identified. The anti-collision algorithm can be used to achieve multi-target recognition, which can avoid the errors in reading and writing or missed information caused by bad communication environment. The tag has a high pollution resistance, which can be read and written normally even in dusty and dirty environment.

## 3. High safety

In RFID systems, the RFID tag can be pasted on the car. Because the tag has a large storage capacity, it can store a lot of information about the vehicle, such as the information of driver, the car information and rated passenger capacity, etc. The information of tags can be encrypted to prevent privacy leaks, such as use of PUF encryption algorithm.

The working principle of RFID based vehicle system is: (1) the reader sends the encrypted information through the antenna to the RFID tag pasted in the vehicle; (2) when the tag enter into the range of reader work area, the tag gets energy and sends the encoded information to the reader through the built-in RF antenna; (3) the RF antenna of reader receives the carrier signal which is transmitted by the tag, and the effective information processed by the reader will be sent to the computer to complete identification. Thus, the automatic management can be realized. RFID systems is shown in Fig. 1.

The feasibility of RFID based vehicle system has the following advantages:

Standard: Since the international RFID standard has some regulations, if it is used locally (a city or a province and even a country) is feasible. It's necessary to consider the issue of the application standards.

Low cost: In intelligent vehicle system, active tag is used. Although the cost is much more expensive than the passive tag, it reads farther and has high security and large storage. The proportion of RFID cost is very small compared with the cost of vehicle.

Mature technology: Active tags has a very mature technology in security, confidentiality and privacy protection.

In the intelligent vehicle system, the RFID tags can be pasted in the car class or the dashboard, which can be used in the car while driving without parking. The data processing speed of the traffic management system can reach 3000 kbps after testing in some provinces while the vehicle speed can reach 300 km/h. The reader can be directly installed on the platform or the intersection and tunnel with large traffic flow. The data can be transmitted to the control center through the network to realize the function of toll collection, speeding monitoring, positioning and so on.

In this system, the main function of RFID is used to dynamically identify the specific information of the vehicle for actual position control and monitoring system, and GPS also plays a major role. The intelligent equipment in the era has a rapid development, everyone can easily enjoy the convenience brought by GPS with good applicability. We can easily monitor the position of the vehicle by using the LBS technology like Baidu Map. But it has restriction that GPS is suitable for outdoor areas. GPS will be no signal in the airtight place like tunnel. The RFID systems can be used to locate the tag accurately in indoor environment. The RFID system is set up in the airtight place with large traffic flow which can make up for the lack of GPS. RFID can realize the uninterrupted vehicle tracking and positioning [7]. The RFID systems are used in the urban traffic networks or highways and other highly monitored places. In many large data processing like position and vehicle, the cloud computing technology can also play a role. Therefore, the collaborative work based on GPS, LBS and RFID technologies can solve the operation of automatic identification, dynamic monitoring and accurate management of vehicles.

### 3 Review of Localization Algorithm

As mentioned above, the GPS signal is weak in tunnel and other indoor environment. These places can set up with RFID system. In this paper, we make use of RFID positioning technology to make up for the disadvantage of GPS in these places, which improves the positioning accuracy of the positioning system.

There are many kinds of methods of RFID positioning such as AOA (based on angle), TDOA, RSSI (based on signal intensity), and PDOA (based on phase) etc. [8]. Each algorithm has its own characteristics and advantages and disadvantages. We choose two algorithms which are more suitable for our system.

#### 1. AOA localization algorithm (based on angle)

The idea of AOA positioning algorithm is measuring the arrival direction of the RFID signal from reader through antenna array and then calculate and measure the angle between the reader and the tag. The directivity of the single antenna is limited, so at least two antenna arrays is necessary to complete the AOA positioning. The position information of tag can be obtained based on the angle and known reference tags. The

intersection of signal of RFID tag detected is the location of tag which is also the positioning of the tag.

The AOA positioning algorithm schematic is shown in Fig. 2.

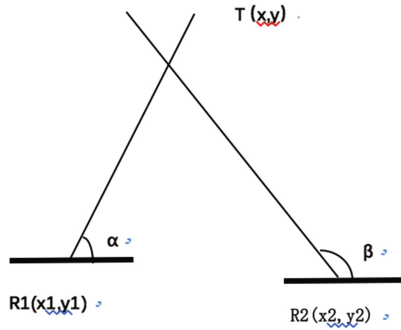


Fig. 2. Diagram of AOA localization algorithm

The following equations can be obtained from Fig. 2:

$$\begin{cases} \tan\alpha = \frac{y - y_1}{x - x_1}; \\ \tan(\pi - \beta) = \tan\beta = \frac{y - y_2}{x_1 - x} \end{cases} \quad (3.1)$$

Then the location is obtained to be tested of tag T:

$$\begin{cases} x = \frac{y_2 - y_1 + x_1 \tan\alpha - x_2 \tan\beta}{\tan\alpha - \tan\beta}; \\ y = \frac{\tan\alpha y_2 - \tan\beta y_1 + \tan\beta \tan\alpha (x_1 - x_2)}{\tan\alpha - \tan\beta} \end{cases} \quad (3.2)$$

All in all, the idea of AOA sitioning requires high sensitivity and resolution of antenna, and additional expensive array with strong direction equipped is necessary, so its positioning accuracy is high, and these costs are fully acceptable relative to the costs and objects of positioning system.

## 2. PDOA localization algorithm (based on phase)

The idea of PDOA is combined with the discrete spectrum correction technology to extract the phase between the frequency of emission signal and received signal, calculating the change of the phase and getting the distance between the tag and the reader through relevant calculation. Dual frequency or multi frequency can be used to avoid the influence of phase period ambiguity. That is, the phase difference measured by the difference frequency signals is transmitted by the reader through the same distance to get the distance to calculate the location of the tag to be positioned. According to the principle of passive RFID backscattering, the reader transmits the carrier signal whose

frequency is  $f$ , then the passive RFID tag returns a portion of the carrier signal to the reader when the signal is received, thus the reader demodulates the carrier signal of the tag returns and then get the change of signal phase  $\theta$  between the reader and the tag. Assuming that the distance between the tag and the reader is  $d$ , the time difference between the carrier signal transmitted from the reader and received from the tag is  $\Delta t$ , radio waves travels at the speed of light in the air at  $c = 3 * 10^8$  m/s, so we can get:

$$d = \frac{1}{2}c\Delta t \tag{3.3}$$

Assuming the phase changes between carrier signal transmitted from the reader and received from the tag is  $\theta$ , then:

$$\theta = 2\pi f\Delta t \tag{3.4}$$

We can draw the following formula:

$$d = \frac{\theta}{4\pi f}c \tag{3.5}$$

The  $\theta$  can be expressed as the sum of  $n$  (positive integer) cycles and a lack of whole cycle:  $\Delta\theta$  (in the range of  $[0-2\text{PI}]$ ), and  $c = f\lambda$ , so:

$$d = \frac{n\lambda}{2} + \frac{\lambda\Delta\theta}{4\pi} \tag{3.6}$$

According to the actual situation, the variable  $n$  cannot be solved obviously, the positioning range is generally a few meters to tens of meters, the range of electromagnetic waves is wide, the ultra-high frequency RFID band is generally 900 MHz. If the variable  $\Delta\theta$  is used to solve the value of  $d$ , the phase will appear the error of  $2n\pi$  fuzzy condition because the RFID can only output phase between  $[0-2\pi]$ . In order to eliminate the error, the problem of phase ambiguity can be solved by using the dual frequency [9]. That is, the distance between the reader and the tag is constant, assuming the carrier signal from the reader are  $f_1$  and  $f_2$  respectively, the corresponding phase variation from the tag to reader are  $\theta_1$  and  $\theta_2$ . If the two phase fuzzy circles are equal, only two phase subtraction can solve the problem of phase ambiguity. According to the following formula:

$$\theta_i = \frac{4\pi d f_i}{c} \quad (i = 1, 2) \tag{3.7}$$

Then we can get:

$$d = \frac{c\Delta\theta}{4\pi\Delta f} \tag{3.8}$$

Where  $\Delta\theta = \theta_1 - \theta_2$ ,  $\Delta f = f_1 - f_2$ .

Thus, the distance is obtained. Then the position of the tag is measured by using the three-trilateral measurement method. The PDOA requires little signal strength, just demodulates the signal carrier returned by the tag which is tested to measure the phase changing and to measure the distance. The measurement precision is high, and the cost is not high, so the PDOA positioning algorithm has been widely used.

In this paper, because the RFID based vehicle system is set up in the complex environment like the bridge, tunnel with large vehicle flow, we can bury the antenna in the ground to avoid the influence of environmental disturbance on the work of RFID systems.

### 4 Design of Vehicle Positioning System

Urban intelligent vehicle positioning system is a service system based on modern electronic information technology. Its prominent feature is the collection, processing, distribution, exchange, analysis and utilization of data as the main aim to provide traceable and a variety of services for traffic participants. In this paper, we design a city intelligent vehicle positioning system based on RFID, GPS and LBS technology, which can realize the function of monitoring, querying and releasing the dispatched information and quick response.

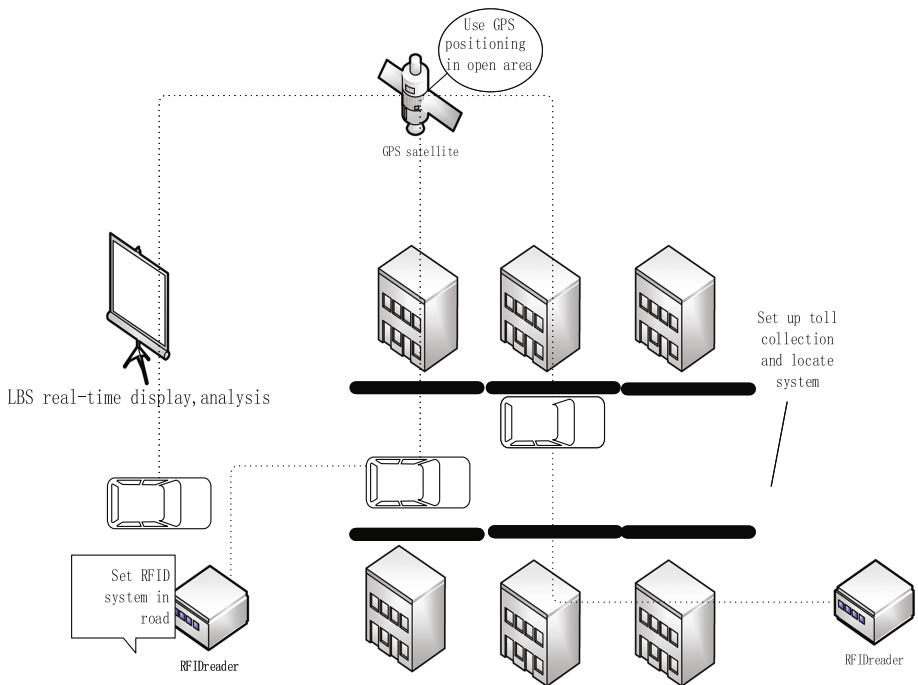


Fig. 3. The model of intelligent transportation system based on GPS, LBS and RFID



The system is divided into five subsystems: vehicle trajectory query, traffic information monitoring, speeding detection, toll collection system, vehicle scheduling. As shown in Fig. 3, the main function of toll collection system is vehicle tagging in the high-speed road and tunnel with large traffic flow, dynamic identification of the tag information equipped with the vehicle, deducting the cost of the corresponding vehicle through the tag to identify the status information of the vehicle. The road information monitoring and speed detection module is to monitor vehicle using LBS, GPS services and associate RFID tags for each vehicle to realize the monitoring and detection of vehicle, detecting the vehicle speed and warning of over-speeding, determining the vehicle arrival time and location. By using RFID reader to scan the tag in the vehicle and complement with GPS data, it completes the precise positioning of the vehicles. We can schedule the vehicles flexibly according to road traffic when the congestion condition is occurred. Vehicle trajectory query subsystem uses the LBS services to track the trajectory of the vehicle to achieve the traceability function. The following Fig. 3 shows the system model.

Intelligent transportation system is a complex and comprehensive system, and we cannot consider it just only a car or a road. The combination of vehicles and roads and the use of modern computer technology can be efficient and real-time monitoring for traffic conditions. We present the combination of GPS, LBS and RFID which is a complex system that can be able to query any vehicle in system about its location, trajectory and condition.

The main process is as the following: RFID tags is pasted with vehicle information in a vehicle to be monitored, installing a GPS receiver with network function. Then the vehicle receives the GPS signal and transmits the location and speed to the monitoring center and data storage center, RFID systems is set to communicate with vehicles in a non-contact style and locate the vehicles. The monitoring center takes advantage of the LBS technology to receive the data and display it on the electric map so as to learn the city's road conditions and vehicle information which can be further analyzed and operated. The LBS technology current has a rapid development. For instance, the Baidu Map and Gaode Map services have a variety of very strong application Programming Interfaces [10], which can be called directly to complete the required functions. In addition, it is necessary to define a powerful data flow interface which enables the system to display the real-time location of the vehicle and the traffic condition that the system do not collapse with a lot of real-time data to receive.

## 5 Implementation and Test

The hardware configuration of RFID reader is the Impinj R420 readers equipped with two antennas as shown in Fig. 4, and the two antennas installed relatively. The reader connects to the center computer through the Ethernet connection cable to communication. In our realized system, the mobile part of this system takes advantage of the android smart phone with network function, calling the Baidu Map SDK to develop and implementation. It can record the trajectory and location of the vehicle and upload the location and other data of the vehicle through socket network programming. The development

of the browser interface makes use of the Javascript programming language to call the Baidu Map API and uses the Oracle database for data storage, the electric display is shown in Fig. 5. The implementation system can locate the specific vehicle pasted with the tag is show as Figs. 5, 6 and 7.

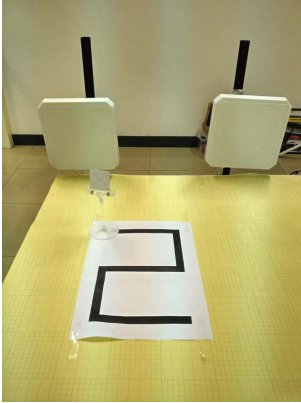


Fig. 4. Hardware system

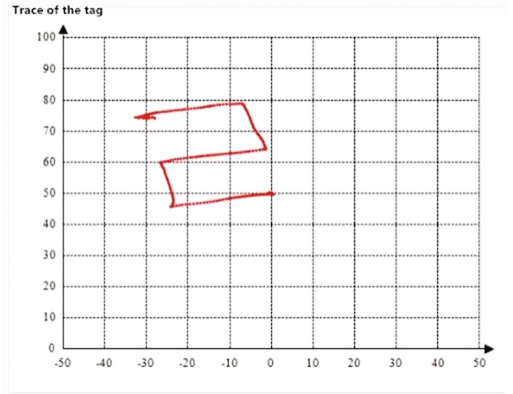


Fig. 5. Display of the trajectory

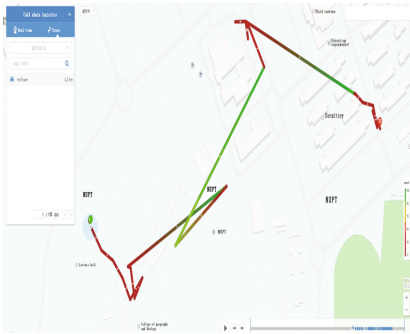


Fig. 6. LBS electric map display

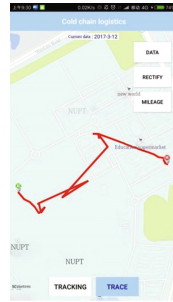


Fig. 7. Vehicle track display

The system is divided into five subsystems: Vehicle Trajectory query, traffic information monitoring, speeding detection, toll collection system, vehicle scheduling. We develop the mobile and the Web by calling the Baidu Map LBS services to monitor the location of the vehicles and upload the data to the monitoring center through the network for further operation. Experimental results show that the city intelligent transportation system based on RFID, LBS, GPS introduced in this paper can locate and track the vehicles on real-time and accurately, and it can query the state of the vehicles, which makes the traffic monitoring more transparent, information-based and cost-effective.

## 6 Conclusions

In the process of urban traffic regulation, taking advantage of the RFID technology to identify and interact with vehicle information dynamically to realize the accurate positioning and ensure the consistency of the information and the GPS information, it can track the real-time location of the vehicles, query the data of road condition and vehicle status and save the costs of city traffic management. With the support of the powerful LBS technology, we realize the monitoring and information management of traffic state. It can reduce the time of interaction between the various links to speed up the efficiency of the vehicle scheduling and emergency detection, and make the information of all aspects of the traffic management to be more transparent and accurate.

**Acknowledgments.** This work is financially supported by the National Natural Science Foundation of P.R. China (No. 61373017, No. 61572260, No. 61572261, No. 61672296, No. 61602261), the Natural Science Foundation of Jiangsu Province (No. BK20140886, No. BK20140888), Scientific & Technological Support Project of Jiangsu Province (No. BE2015702, BE2016185, No. BE2016777), Natural Science Key Fund for Colleges and Universities in Jiangsu Province (No. 12KJA520002), China Postdoctoral Science Foundation (No. 2014M551636, No. 2014M561696), Jiangsu Planned Projects for Postdoctoral Research Funds (No. 1302090B, No. 1401005B), Jiangsu Postgraduate Scientific Research and Innovation Projects (SJLX16\_0326), Project of Jiangsu High Technology Research Key Laboratory for Wireless Sensor Networks (WSNLBZY201509), NUPTSF (Grant No. NY214060, No. NY214061) and the STITP projects of Bell Honors School of NUPT (No. ZD201606 and No. YB201615).

## References

1. Toral, S.L., Gregor, D., Vargas, M., et al.: Distributed urban traffic applications based on CORBA event services. *Int. J. Space Based Situated Comput.* **1**(1), 86–97 (2011)
2. Liu, T., Yang, L., Lin, Q., et al.: Anchor-free backscatter positioning for RFID tags with high accuracy. In: *Proceedings of INFOCOM*, pp. 379–387 (2014)
3. Dobkin, D.M.: *The RF in RFID: UHF RFID in Practice*. Newnes, Waltham (2012)
4. Sakurai, S.: Prediction of sales volume based on the RFID data collected from apparel shops. *Int. J. Space Based Situated Comput.* **1**(2–3), 174–182 (2011)
5. Nam, S., Park, M., Kim, K., et al.: A study on the regulations and market of Location Based Service (LBS). *J. Internet Comput. Serv.* **15**(4), 141–152 (2014)
6. Wang, J., Katabi, D.: Dude, where's my card? RFID positioning that works with multipath and non-line of sight. *ACM SIGCOMM Comput. Commun. Rev.* **43**(4), 51–62 (2013)
7. Beyerle, G., Zus, F.: Open-loop GPS signal tracking at low elevation angles from a ground-based observation site. *Atmos. Meas. Tech.* **10**(1), 15–34 (2017)
8. Gomez-Gil, J., Alonso-Garcia, S., Gómez-Gil, F.J., et al.: A simple method to improve autonomous GPS positioning for tractors. *Sensors* **11**(6), 5630–5644 (2011)
9. Wang, E., Zhao, W., Cai, M.: Research on improving accuracy of GPS positioning based on particle filter. In: *8th IEEE Conference on Industrial Electronics and Applications (ICIEA)*, pp. 1167–1171 (2013)
10. Yang, L., Yang, G., Zhang, Q., et al.: Management and analysis platform of radio coverage data based on Baidu map. In: *Fifth International Conference on Instrumentation and Measurement, Computer, Communication and Control (IMCCC)*, pp. 369–372 (2015)

# Radio Spectrum Management for Cognitive Radio Based on Fuzzy Neural Methodology

Hang Yang<sup>1</sup>(✉), Yuan Liang<sup>2</sup>, Jingcheng Miao<sup>3</sup>, and Dongmei Zhao<sup>1</sup>

<sup>1</sup> Naval Aeronautical Engineering Institute Qingdao Branch,  
Qingdao, Shandong, China

13576150@qq.com

<sup>2</sup> Air Force Engineering University, Xi'an, Shanxi, China  
e\_miracle@163.com

<sup>3</sup> Engineering University of CAPF, Xi'an, Shanxi, China  
zhongdcz@qq.com

**Abstract.** According to the limited available spectrum and the inefficiency in the spectrum usage, a fuzzy neural network based system for Cognitive Radio is proposed to implement the spectrum sense. Parameters like signal strength, node velocity and distance are transmitted as inputs through the fuzzy logic dispose and reinforcement learning, and the decision is taken whether to take up the unused spectrum. The system is less complex and consumes little time, and the results are consistent with the theory. The system can be simulated for dynamic spectrum management, and be implemented in real environment.

## 1 Introduction

With the rapid development of science and technology, people have more knowledge about nature and more exploitation of the natural resources, the definition of which is not limited to regional resource but expands to time resource, space resource, frequency resource, power resource and so on. The spectrum, a non-renewable natural resource used widely because of fast advancements in wireless communication technology, is being faced with physical scarcity. And the current spectrum allocation scheme will definitely cause spectrum congestion. In addition to spectrum allocation, the legacy command-and-control regulation will make physical scarcity and underutilization of spectrum more serious. According to a report published by the Federal Communications Commission (FCC), the use efficiency of distributed ratio spectrum only has 10%–80%. The performance of military equipment like radar and radio stations which has large quantity, high distribution density, strong power and complex electromagnetic environment, is continuously constrained by limited spectrum resource. The efficiency of spectrum access is significant to the reliability and robustness of military network, especially mobile communication system, for which the efficient usage of spectrum is directly related to the quality of battlefield communication and even the change of battlefield situations.

The most advanced dynamic spectrum management is in fact to optimize spectrum access, which is ultimately applied to the settlement of Cognitive Radio (CR) problems. It is obvious that the realization of future dynamic spectrum management relies on the

development of CR. When it comes to the concrete implementation of CR, many domestic and international scientific research institutions and scholars have made in-depth and practical explorations, building the model in new framework to realize real-time dynamic spectrum access. The papers proposed building spectrum management system based on fuzzy logic in consideration of parameters like distance, signal strength, node velocity and availability of unknown spectrum, to implement dynamic spectrum sense and spectrum strategy. The system can use effectively the fuzzy characteristic of detected objects to simulate human reasoning ability based on the concept of fuzzy logic to some extent, strengthening the adaptability and practicability of spectrum sense. But the fuzzy logic must be built on knowledge database including expert advice. And if the controller is executed, the reasoning regulation, based on fuzzy logic, will be determined and lose the brain-empowered characteristic. The primary purpose of this paper is to combine fuzzy logic with neural network technology, making full use of their complementarity characteristic, to build Fuzzy Neural Network (FNN). FNN system has the ability of fuzzy management and adaptive learning, providing a better approach of spectrum sense for CR.

## 2 The Capability Structure of CR

Reconfigurability and awareness are two significant capabilities of Cognitive Radio. With knowledge of the capabilities needed by the system, radio configurator poses a comprehensive analysis on function unit library and select proper resources to reconfigure the radio system to make it better, which is done by SDR. And the system can achieve corresponding awareness information and implement adaptive management through being aware of its surrounding environment. This paper proposes that applying FNN structure in adaptive algorithms module is able to implement the awareness capability of CR (Fig. 1).

The rule set and membership function of fuzzy system is generally determined by experience, for which the system designed in this way lacks the capabilities of self-adaption and learning. To implement intelligent control of fuzzy system, we can use the learning methodology of neural network to automatically design and modulate the

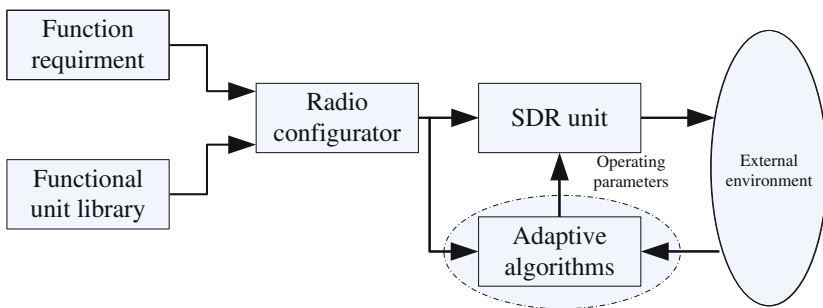


**Fig. 1.** Cognitive Radio, a radio system, is based on software defined radio and adaptive to environment, and the system functional diagram is pictured.

rule set and membership function of fuzzy system by making analysis and process of the input and output data. The fuzzy neural network combines fuzzy system and neural network in full consideration of their complementation and includes logical reasoning, linguistic computing and nonlinear dynamics, which reflects its multiple capabilities (e.g. learning, association, recognition, self-adaption and fuzzy information processing).

### 3 Fuzzy Neural Network

#### 3.1 The Structure of Fuzzy Neural Network

Layer 1: Input layer. There are 3 inputs, and there are 3 nodes.

$$f_i^1 = u_i^1, \phi_i^1 = f_i^1 \quad i = 1, 2, 3 \quad (1)$$

Layer 2: Membership function layer. Nodes on Layer 2 correspond to fuzzification of input variables. An input of FNN has independently 3 fuzzy sets, and then Layer 2 has 9 nodes. Membership function is implemented by a Gaussian function.

$$f_i^2 = -\frac{(u_i^2 - m_i^2)^2}{(\sigma_i^2)^2}, \phi_i^2 = e^{f_i^2} \quad i = 1, \dots, 9 \quad (2)$$

Layer 3: “AND” layer. FNN has 3 inputs, and each input has 3 fuzzy sets. There are 27 fuzzy reasoning rules according the fuzzy logic rules. Layer 3 supplies the logical AND operation, for which synthetic function on Layer 3 selects the minimum operation as follows.

$$f_i^3 = \min(\phi_j^2), \phi_i^3 = f_i^3 \quad i = 1, 2, \dots, 27 \quad (3)$$

The  $j$  in the formula (3) denotes the  $j$ th node on Layer 2.

Layer 4: “OR” layer. The logical OR operation is denoted by summation notation. Considering each input has 3 fuzzy sets, the synthetic function and activation function are as follows.

$$f_i^4 = \sum \phi_j^3, \phi_i^4 = \min(1, f_i^4) \quad i = 1, 2, 3 \quad (4)$$

Layer 5: Output layer. Layer 5 provides service for de-fuzzy according to the principle of maximum membership degree, for which we select the one with the maximum membership degree in the fuzzy sets of reasoning conclusion to make the output more exact.

$$f^5 = \sum \omega_i u_i^5, a^5 = \frac{f^5}{\sum u_i^5} \quad (5)$$

The  $i$  in the formula (5) denotes the  $i$ th node on Layer 4. And the  $\omega_i$  is the weights on Layer 5.

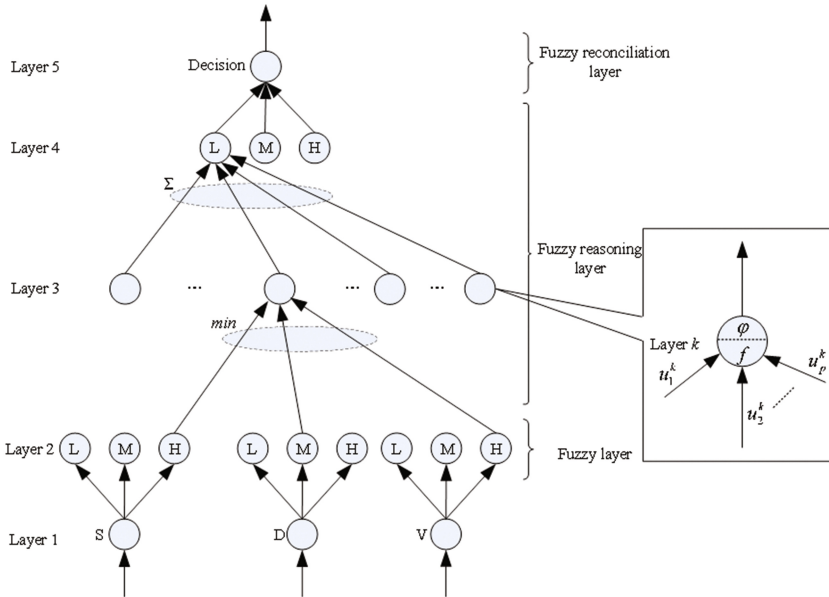


**Fig. 2.** The network system is a 3-input 1-output system. And the right of Fig. 2 is the structure of single neuron node. The  $i$ th input signal is denoted by  $u_i^k$  at Layer  $k$ . The synthetic function and activation function of neural networks are defined separately by  $f$  and  $\phi$ . The model structure is composed of 5 layers. According to the structure diagram on the left of Fig. 2, the synthetic function and activation function of all layers are dissected as follows.

Neuron status on each layer of FNN is gradually transferred to next layer, because of which we can decide whether relevant frequency band is occupied and make corresponding strategies through transmission and processing of some parameters (e.g. node velocity, distance and signal intensity of surrounding environment) (Fig. 2).

### 3.2 The Strengthened Learning of FNN

Adjustable parameters in FNN include the mean and variance of membership function on Layer 2 and the de-fuzzy weights on Layer 5. In order to strengthen learning, it is feasible to implement adaptive modulation of multilayer network by using BP (Back-Propagation Network), a learning algorithm of neural networks, in FNN. BP is used to work out the error between neurons and find out the self-adaption law of adjustable parameters. The definition of reinforcement function is given by

$$e(t) = (p_0 - p(t)) \tag{6}$$

The  $p_0$  in formula (6) denotes default error rate and  $p(t)$  is practical error rate at time  $t$ . And the error function denoted by

$$E(t) = \frac{1}{2} e(t)^2 = \frac{1}{2} ((p_0 - p(t)))^2 \quad (7)$$

The general learning rule of adjustable parameters described by

$$l(t+1) = l(t) + \gamma \left( -\frac{\partial E(t)}{\partial l(t)} \right) \quad (8)$$

The  $l$  in formula (8) denotes adjustable parameters and  $\gamma$  is relevant learning efficiency.

The value of  $\omega_i$ , an adjustable parameter of Layer 5, is defined by

$$\frac{\partial p(t)}{\partial \omega_i(t)} = \frac{\partial p(t)}{\partial \varphi^5(t)} \frac{\partial \varphi^5(t)}{\partial \omega_i(t)} = \frac{\partial p(t)}{\partial \varphi^5(t)} \frac{\partial \varphi^5(t)}{\partial f^5(t)} \frac{\partial f^5(t)}{\partial \omega_i(t)} \quad (9)$$

The definition of reinforcement signal transferred between Layer 2 and Layer 5 is given by

$$\delta_i^2 = \frac{\partial E(t)}{\partial \varphi_i^2} = \sum_n \frac{\partial E(t)}{\partial u_n^4} \sum_k \frac{\partial u_n^4}{\partial u_k^3} \frac{\partial u_k^3}{\partial \varphi_i^2} \quad (10)$$

$$\frac{\partial E(t)}{\partial u_n^4} = r(t) \cdot \frac{m_n^5 \sigma_n^5 \left( \sum_{j \in T_n} \sigma_j^5 \varphi_j^5 \right) - \left( \sum_{j \in T_n} m_j^5 \sigma_j^5 \varphi_j^5 \right) \sigma_n^5}{\left( \sum_{j \in T_n} \sigma_j^5 \varphi_j^5 \right)^2} \quad (11)$$

$$\frac{\partial u_n^4}{\partial u_k^3} = \begin{cases} 1, & \text{if the } k\text{th node on layer 3} \\ & \text{is connected to} \\ & \text{the } n\text{th node on layer 4} \\ 0, & \text{otherwise} \end{cases} \quad (12)$$

$$\frac{\partial u_k^3}{\partial f_i^2} = \begin{cases} 1, & \text{if the } k\text{th input and} \\ & \text{the first node on layer} \\ & \text{2 meet the minimum norm} \\ 0, & \text{otherwise} \end{cases} \quad (13)$$

In conclusion, the learning algorithm of adjustable parameters is as follows

$$\omega_i^5(t+1) = \omega_i^5(t) + \gamma_1 \cdot \frac{\partial p(t)}{\partial \varphi^5(t)} \frac{\partial \varphi^5(t)}{\partial f^5(t)} \frac{\partial f^5(t)}{\partial \omega_i(t)} \quad (14)$$

$$m_i^2(t+1) = m_i^2(t) + \gamma_2 \cdot \delta_i^2 \cdot e_i^2 \cdot \frac{2(u_i^2 - m_i^2)}{(\sigma_i^2)^2} \quad (15)$$



$$\sigma_i^2(t+1) = \sigma_i^2(t) + \gamma_3 \cdot \delta_i^2 \cdot e^{f_i} \cdot \frac{2(u_i^2 - m_i^2)^2}{(\sigma_i^2)^3} \tag{16}$$

The  $\gamma$  in formulas above represent the learning efficiency of relevant algorithm.

The 3 algorithms of adjustable parameters above can implement the strengthened learning of FNN and then FNN will have both the processing ability of fuzzy algorithms and self-adaption ability of neural network.

## 4 The Analysis and Results of Simulations

### 4.1 Input/Output Relationship

The structure of 3-input 1-output system is discussed in chapter 3. The signal energy of PU is denoted by S, and D represents the distance between PU and SU, and V denotes the node velocity of SU relative to PU, and Decision, the value of which is 0–1, denote the possibility of changes in frequency band. The system takes S, D and V as the input variables and Decision as the output variable. According to the fuzzy reasoning rules [5], giving V and D fixed values, we get it through programmatic implementation in MATLAB 7.0 and find out the relationship between output and two other inputs, which is showed in Figs. 3 and 4.

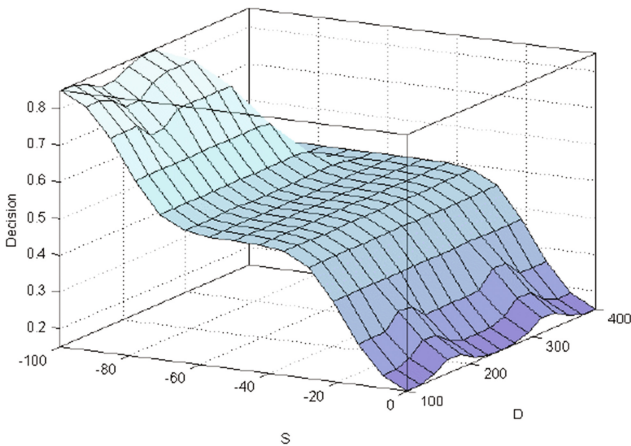
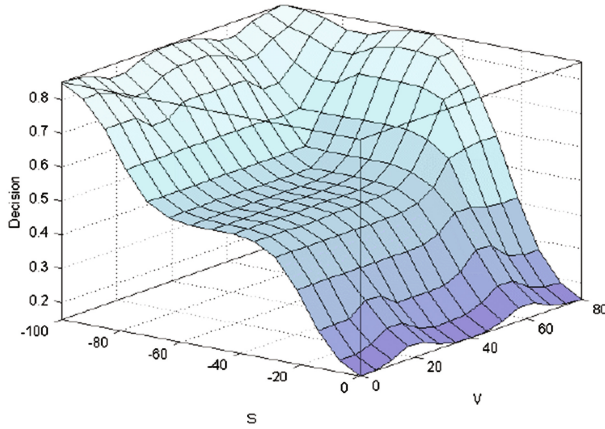


Fig. 3. With V equal to 40 km/h, the lower values of both S and D are, the higher value of D is.



**Fig. 4.** The spectrum access decision between S and V ( $D = 500$  m). With  $D$  equal to 500 m, Decision becomes high if S is low enough and V is high enough.

### 4.2 The Curve of Strengthened Learning

According to the derivation process of strengthened learning, with  $p_0$  equal to 5%, we figure out the corresponding reinforcement function by MATLAB programming and draw a curve of strengthened learning, which is pictured in Fig. 5.

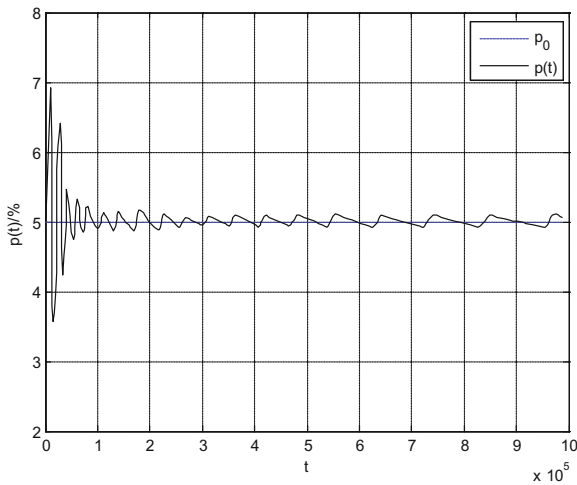


**Fig. 5.** With the default error rate equal to 5%, the practical error rate fluctuates near the default error rate after a finite amount of time, which represents that the result of strengthened learning is satisfying. In addition, the changes of curve become more and more even, which illustrates that the modulation velocity is fast when initial step length is relatively big, but it becomes slower and even stable when step length becomes gradually small.

## 5 Conclusion

In short, it is more and more obvious that the physical scarcity of spectrum and the inefficiency in the spectrum usage is limiting the development of communication technology. Cognitive Radio has become a main trend of solving such spectrum problems because of its high flexibility and wide-ranging practicality. In this paper, we build the FNN system to provide a new methodology of spectrum sense for CR. FNN selects some parameters (e.g. energy, distance, velocity) in environment as system inputs and decision chosen by frequency band as system output, and is endowed with the ability of both fuzzy processing and self-learning. The simulations reveal that the FNN system is able to efficiently help CR detect the changes of environment and make reasonable strategies by comprehensive analysis, which embodies the efficient spectrum sense and spectrum strategy. The structure of simulations is simple, feasible and time-saving, and the calculation of algorithm can be implemented in corresponding hardware circuit, which means that it is friendly to concrete application and practical system.

## References

1. Akyildiz, I.F.: Spectrum management in cognitive radio networks. In: *Networking and Communications* (2008)
2. Zheng, H., Shi, J., Cao, I.: Group-mobility-aware spectrum management for future digital battlefields. In: *Military Communications Conference*, pp. 23–25 (2006)
3. Ren, G.: Potential game for dynamic spectrum management in cognitive radio networks. *J. Inf. Comput. Sci.* **10**(6), 1805–1817 (2013)
4. Suchański, M., Gajewski, P.: Dynamic spectrum management in legacy military communication systems. In: *Communications and Information Systems Conference*, pp. 1–5 (2012)
5. Bhattacharya, P.P., Khandelwal, R., Gera, R., et al.: Smart radio spectrum management for cognitive radio. *Int. J. Distrib. Parallel Syst.* **2**(4), 12–24 (2011)
6. Ejaz, W., Hasan, N., Aslam, S., et al.: Fuzzy logic based spectrum sensing for cognitive radio networks. In: *2011 Fifth International Conference on Next Generation Mobile Applications and Services*, pp. 185–189 (2011)
7. Xin, X.: *Principle and Technology of Software Defined Radio*, pp. 211–212. The Press of Xidian University, Xi'an (2008)

# Optimized Energy Efficient Routing Using Dynamic Clustering in Wireless Sensor Networks

M.Z. Siddiqi<sup>1</sup>, N. Ilyas<sup>2</sup>, A. Aziz<sup>2</sup>, H. Kiran<sup>1</sup>, S. Arif<sup>1</sup>, J. Tahir<sup>1</sup>, U. Qasim<sup>3</sup>,  
Z.A. Khan<sup>4</sup>, and N. Javaid<sup>1</sup>(✉)

<sup>1</sup> COMSATS Institute of Information and Technology, Islamabad 44000, Pakistan  
[nadeemjavaidqau@gmail.com](mailto:nadeemjavaidqau@gmail.com)

<sup>2</sup> Department of Computer Sciences, Lahore Leads University, Lahore 54000,  
Pakistan

<sup>3</sup> Cameron Library, University of Alberta, Edmonton, AB T6G 2J8, Canada

<sup>4</sup> Computer Information Science, Higher Colleges of Technology, Fujairah 4114,  
United Arab Emirates  
<http://www.njavaid.com>

**Abstract.** Energy efficient routing, minimum network lifetime, adaptation to continuous variation in topology of nodes and high energy consumption for data transmission are the major limitations in Wireless Sensor Networks (WSNs). Different routing techniques of WSNs have been presented to tackle the above mentioned challenges. These techniques are Direct Transmission Mechanism (DTM), Chain Based Routing (CBR) and Hierarchical Clustering (HC) for network lifetime maximization. Nevertheless, the available solutions are suitable for limited range network but not for scalable networks. Moreover, these techniques do not address the variable clustering approach in terms of energy efficiency and the hot spot problem. In this work, an efficient algorithm is proposed to enhance lifetime and stability period of the entire systems by meeting the all available constraints.

**Keywords:** Wireless sensor networks · Network lifetime · Scalable networks

## 1 Introduction

Wireless Sensor Networks (WSNs) comprised of large number of tiny nodes that have limited resources such as limited energy and low memory. The sensors have sensing and routing capabilities and are deployed in targeted region to monitor attributes like health-care, weather monitoring, tarhet field imaging, disaster management, precision agriculture, temperature and humidity [1]. Usually, these tiny nodes collect information from the environment and sends it to the Base Station (BS) for further signal processing. Due to its significant importance, WSN has gained enough attention among researchers to get maximum advantage of this field. In WSN, network lifetime maximization and efficient data gathering are big challenges for research community. Consequently, different solutions have

been proposed to solve given problems. Clustering is considered one of those classic approaches for energy efficient routing in WSN. In this scheme, Clusters Head (CH) is selected by BS, from alive nodes, on the basis of certain probability. Other nodes associate with CH on the basis of minimum distance criteria [2]. The Low Energy Adaptive Clustering Hierarchy (LEACH) [3] achieves uniform distribution of energy using clustering approach. There is a limitation in LEACH that the nodes that lies near the BS send data to CH at larger distance instead of direct sending to BS (Fig. 1).

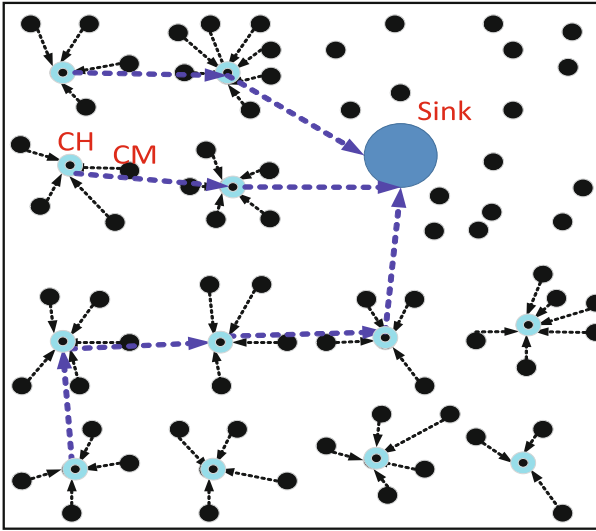


Fig. 1. Cluster Formation in WSN

Furthermore, [4] proposed a Multi-hop LEACH. In this protocol, the authors used two types of communication, intra cluster and inter cluster communication. In multi-hop inter cluster communication, the sensors transmit their data to CH that further transmit the information to the BS through hierarchal chain of CHs. They shown in their result that, multi hop LEACH was more energy efficient than conventional LEACH. However, hot spot problem is still exist with unbalanced cluster size problem. The [5] gave the idea of mobile nodes. They divided whole network into sub regions with fixed BS in such a way that over all communication distance could be squeezed. Authors in [6] developed a strategy in which each node communicate with the closest neighbor to establish a chain. The node with more residual energy was selected as Leader Node (LN). This node was responsible to collect information from nearby devices in order to forward data to static BS. Thus, the energy consumption cost was reduced. However, there is a disadvantage of this protocol as well. The data follows maximum number of paths to reach the destination (BS) which requires large amount of energy. On the other hand, [7] worked on improving the energy consumption.

In this protocol, BS had information about the residual energy of each node. The node with more remaining power in comparison to others was chosen as CH. The shortcomings to this protocol was that, communication distance was skipped in their work. Also, BS does not finalize its decision regarding the node selection, if a node does not exist in the range of communication.

The researchers in [8] presented a novel protocol which is a combination of clustering scheme of LEACH, chain formation protocol of PEGASIS, and also cluster organization of LEACH-C. This protocol is very complex for implementation point of view. In contrast, [9] determined hybrid technique of LEACH and PEGASIS to enhance the network lifetime.

Chain-Chain Based Routing Protocol (CCBRP) was developed by [10]. In this scheme, network area was divided into number of chains. Nodes, in each chain, transmit their sensed data to selected LN (called primary level). Rest of the nodes associated with this primary level behaves as secondary levels. Compression was performed at leader nodes to relaying the information to BS. H. Fahim et al., presented Energy Hole Repairing Depth Based Routing (EHRDBR) and Interference-bandwidth aware Depth Based Routing (IDBR) protocols to minimized the energy consumption in order to maximize the network lifetime, throughput and maintained end to end delay upto certain level [11]. For the throughput problem [12] proposed an Optimized Region Based Efficient Data (AORED) routing protocol which is employed on Connecting Dominating Set (CDS) of wireless nodes. CDS was used to create virtual backbone of communicating nodes in the network. As a result, overall transmission rate was enhanced.

In [13] author proposed a scheme named Distributed Energy-Efficient Clustering (DEEC) used in heterogeneous wireless sensor networks. In this scheme the cluster-heads are elected by a probability based on the ratio between residual energy of each node and the energy of the network. The energy expenditure of nodes is controlled by the adaptive approach. DEEC uses average energy of the network as reference energy.

Enhanced Distributed Energy Efficient Clustering (E-DEEC) Scheme was investigated to enhance the network, lifetime and stability, and maximized the energy level of the network [14]. They maintained the heterogeneity in the system with the introduction of particular super nodes that have energy more than normal. On the other hand, [15] author proposed a technique named Enhanced Developed Distributed Energy Efficient Clustering (EDDEEC) for Heterogeneous Wireless Sensor Networks. This scheme exploited adaptive energy protocol that dynamically changes the probability of nodes to allocate equal amount of energy among the tiny sensors. They not only measured stability period, network lifetime but also the number of packets transmitted to the BS. Nonetheless, the energy still consume earlier as the load increases. In the same way, [16] worked to maximize the throughput and lifetime of the network using the linear programming. They presented Adaptive Clustering Habit (ACH)<sup>2</sup> scheme to fulfill the all available constraints. On the other hand, [17] proposed stable election protocol for the lifetime problem. Since so much work has already been done to optimize the energy consumption but network lifetime enhancement is still

challenging for the researchers. Therefore, in this research paper, we present an energy efficient routing scheme for lifetime maximization.

## 2 Motivation

Main research challenges in above protocols are hot spot problems, low data delivery ratio, decreased network lifetime and high energy consumption. Therefore, major inefficiencies in the traditional WSNs routing schemes are as follows: Due to dynamic conditions, there are certain limitations that include; no failure detection, and limited storage capacity etc. In Multi-hop scheme, the nodes closer to sink die more quickly due to heavy load of relaying the data of distant nodes, and hence deplete energy more quickly, which is named as hot spot problem. In case of rotating the neighbors of sink, the energy consumption for data relaying is balanced up to some extent, however, nodes would require extra energy from the already limited energy source. The above mentioned routing protocol enhance the network lifetime and stability period up to some extent, however none of them focus on the dynamic clustering mechanism to balance the energy consumption. In our research work, we aim to design an energy efficient routing scheme using dynamic clustering for network lifetime maximization with low energy consumption. We mainly focus on the variable size clusters in network area. The clusters near the sink are smaller in size in order to overcome the energy hole problem. The variable size clustering enhances the stability period, network lifetime with reduced energy consumption.

### 2.1 Problem Statement

The concern of network lifetime maximization is considered major problem in WSNs. Thus, mitigation of transmit power consumption will be helpful in increasing network's lifetime. Therefore, our aim is to escalating the network's lifetime by fulfilling the available constraints. Mathematically the problem can be formulated as,

$$\max \sum_{i=1}^N (T) \quad (1)$$

s.t.

$$C1: \sum_{i=1}^{(N-ch)} \Phi(Kr_i + d_i \leq d_{total}) \forall i \in n, \quad (2)$$

$$C2: \sum_{i=1}^{(N-ch)} \alpha(Kr_i + Kt_i) \leq E_{total} \forall i \in n, \quad (3)$$

$$C3: d_{ik} = d_{ij} + u \forall i, j, k \in n, \quad (4)$$

$$C4: d_{ij} \leq C_{ij} \forall i, j \in n, \quad (5)$$

$$C5: d_{ij} \geq 0, \alpha \geq 0 \quad (6)$$

The first constraint i.e. C1 describes that “k” number of bits received by each CH, and  $d_i$  is the amount of data sensed by each CH should be less than the total amount of flow in the network. C2 shows the upper limit of the energy. The energy required to transmit or received “k” number of bits must be upper bounded by total energy of the network. Condition three indicates that data flow from one CH to another is exceeded by amount of u. where, u is the amount of data sensed by CH. C4 depicts that data flow between two CHs must be upper bounded by total capacity of that particular link.

### 3 EERDC: The Proposed Protocol

The proposed protocol EERDC is present in detail. In our proposed protocol, a static sink is deployed at the middle of network field. The sensor nodes are deployed in the network field. The dimension of network field is fixed, however the cluster within the network field is variable depending upon the criteria. We take following assumptions in EERDC.

- Static Sink (SS) has unlimited energy resources, processing, memory and computational capability.
- Formation of variable sized cluster depending upon some criteria.
- Random deployment of nodes in the network field.

In EERDC, the Static Sink (SS) is deployed at the centre and sensor nodes are randomly deployed. Virtually we have divided the whole network into different regions with different size of cluster. In other way we can say that the network area has three types of cluster size in order to minimize the energy consumption during transmission. The nodes sense the data from surroundings and then transmit to closest Cluster Head (CH). The CH transmits the aggregated data from Cluster Member (CM) to next minimum distance CH. Finally, the data is forwarded to SS located at the centre of network field. The optimal association of CM with CH minimizes the energy consumption which leads to maximization of stability and network lifetime. CH has less burden to transmit data packet which leads to make maximum nodes alive for longer period of time and hence transmit for longer duration. Therefore, the overall data gathering of network enhances.

#### 3.1 Detailed Description of EERDC

This section explain the detailed working of our proposed protocol. EERDC operates in two phases:

- Initialization Section
- Data transmission phase.



### 3.2 Initialization Section

During initialization part, the sensor nodes are deployed randomly in the network area having  $100 \times 100$  m. After deployment, the SS is deployed at the mid of the network. The nodes generate random numbers in each round, and these numbers are then compared with the threshold value calculated by the following formula. The CHs are selected based on random probability and these CHs are rotated to balance the energy consumption. Moreover, the fusion and data aggregation responsibilities are performed by CHs.

$$Th(i) = \frac{p}{1 - p(\text{mod}(r, \frac{1}{p}))} \quad (7)$$

where,  $p$  represents the probability of electing the CHs in the network and  $r$  is number of rounds. In each round, a node  $i$  generates a number. This available number is compared with the threshold value which is calculated by an Eq. 7. If the value of threshold is greater than the random number, that node is selected as CH for current round. The same process is repeated to elect CHs for the next coming rounds.

#### 3.2.1 Dynamic Clustering

In case of SS approach, the nodes which lies in the vicinity of SS die out more quickly due to two reason:

- Relaying the data of far end clusters.
- CHs aggregate the data from own CM (Same size of clusters near the SS leads to over burden the nodes in the vicinity of sink).

In order to overcome the above mentioned problems. We, therefore, devised a criteria of dynamic clustering which includes:

- Virtual division of network field.
- Variable sized clusters formation.

In our protocol the network area is virtually divided into three regions with different size of clusters.

- Cluster Region1 (CR1).
- Cluster Region2 (CR2).
- Cluster Region3 (CR3).

In dynamic clustering approach the CM association with CH is restricted in order to balances the energy consumption. Once the CH is selected in the vicinity of SS, the CMs are restricted to certain threshold value in order to minimize the burden on CHs near the sink. In CR1, the size of cluster is larger as compared to CR2 and CR3. The maximum number of CM associates themselves with CHs in the CR1. However, in CR2 the association of CMs with CHs is restricted in order to balances the energy consumption. In CR3, the CMs associations with

CHs is further restricted to minimum threshold value in order to release the burden of innermost nodes (nodes in the vicinity of SS). The above mentioned virtual formation of region with variable clustering decreases the burden of data packet on the innermost nodes which leads to enhance their network lifetime. As a result when network lifetime increases the more number of nodes will be alive for longer duration and hence the nodes sense for longer duration and transmit to closest CHs. The enhance network lifetime increases the stability period and overall network throughput.

### 3.3 Data Transmission Phase

After the formation of virtual regions (CR1, CR2, CR3) and dynamic clustering with respect to each region, the nodes in the network field sense the data from surroundings. The CMs sense data and then transmit to nearest CHs. The CHs are responsible for data aggregation and fusion. The CHs in the CR1 transmitted the aggregated data to CHs of CR2. The CHs of CR2 onwards transmit the incoming data to CHs of CR3. At the end, the CHs in the CR3 directly transmit the bundle of aggregated data to SS exist at the centre of network field. This process will repeat in each round until the whole network die out. The SS then transmits the data to any remote destination for any further processing and evaluation.

## 4 Simulation Results

We evaluate our proposed protocol EERDC with SEP and LEACH in terms of network throughput, network lifetime and stability period. The nodes are randomly deployed within an area of  $100\text{ m} \times 100\text{ m}$ . The BS has unlimited computational energy resources. The initial energy given to each sensor node is  $0.5\text{ J}$ . The data packet size is fixed throughout the network lifetime which is  $4000\text{ bits}$ . The sensor nodes which exist at the corner of network field transmit their data to nearest CHs. These CHs forward the received data to next optimal CHs until the data reached to BS. The Medium Access Control (MAC) and physical layer issues are ignored in our case like interference, multi-path fading and co-channel interference etc. The parameters used in our proposed work is given in Table 1. Following metrics are used for the evaluation of EERDC:

- **Dead Nodes:** The amount of energy consumed by nodes during sensing, transmission and reception of data packets is directly relates to rate of dead node.
- **Stability Period:** The duration between start of network till the death of first node is called stability period. The unit of stability period is time (sec).
- **Network Lifetime:** The total amount of time between start of network till the depletion of whole network is called network lifetime. It is measured in time (sec).
- **Network Throughput:** The number of data packets successfully received at the base station is called network throughput. The scientific unit of network throughput is bit/s.

**Table 1.** Parameters used in simulation

Parameters	Values
Network size	100 m × 100 m
Number of nodes	100
Initial energy of normal nodes	0.5 J
Packet size	4000 bits
Transmitter/Receiver electronics	50 nJ/bit
Data aggregation energy	50 nJ/bit/signal
Transmitter amplifier(if $d < d_0$ )	10 pJ/bit/m <sup>2</sup>
Transmitter amplifier(if $d > d_0$ )	0.0013 pJ/bit/m <sup>4</sup>
Speed of light	$3 \times 10^8$ ms/s
Number of BS	1

- Packet Dropped: The number of packet dropped during transmission.
- CH Count: The number of CHs elected in every round is called CH count.

### 4.1 Number of Dead Nodes

Figure 2 depicted the rate of dead nodes in three respective protocols EERDC, SEP, LEACH and  $(ACH)^2$ . LEACH has low stability period due to random election of CHs. The SEP has more stability period as compared to LEACH due to CHs election on the basis of remaining energy. In addition,  $(ACH)^2$  has

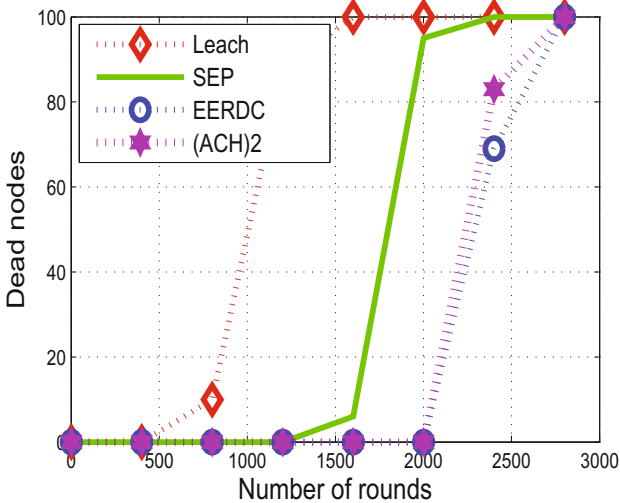


**Fig. 2.** Number of dead nodes

enhanced stability period as compared to LEACH and SEP. However, in EERDC the dynamic clustering approach further reduces the energy consumption which leads to increases the stability period as shown in Fig. 2.

### 4.2 Network Throughput

Figure 3 shows the network throughput of EERDC, SEP, LEACH and  $(ACH)^2$ . The LEACH has low network throughput as compared to EERDC. This is due to the unbalance energy consumption in LEACH which leads to reduced network throughput. The EERDC has more network throughput as compared to LEACH and SEP due to balance energy consumption. The more nodes are alive for longer duration and transmit data packets to nearest CHs. Moreover, the advantage of dynamic clustering approach efficiently balances the energy consumption. This will increases the network throughput of EERDC as shown in Fig. 3. The network throughput of EERDC and  $(ACH)^2$  is linear due to balance energy consumption.

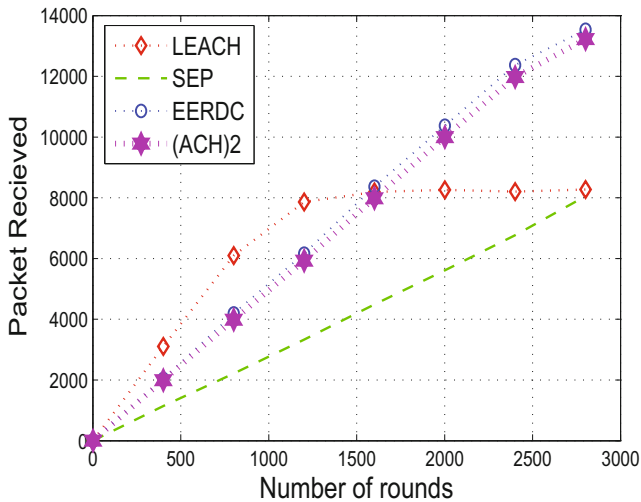


Fig. 3. Network throughput

## 5 Conclusions

In this paper, we have proposed an Energy Efficient routing scheme by using Dynamic clustering in Wireless Sensor Network. We virtually divided the network into three regions. The different size of clusters are formed in three different regions in order to balance the energy consumption of whole network. The dynamic clustering approach overcome the hot spot problem which leads to increase the stability period and network lifetime. Moreover, due to balance energy consumption the maximum amount of nodes alive fore longer duration which result in enhanced network throughput.

## References

1. Gilbert, E.P.K., Kaliaperumal, B., Rajsingh, E.B.: Research issues in wireless sensor network applications: a survey. *Int. J. Inf. Electron. Eng.* **2**(5), 702 (2012)
2. Heinzelman, W.R., Chandrakasan, A., Balakrishnan, H.: Energy-efficient communication protocol for wireless microsensor networks. In: *IEEE International conference on System Sciences*, pp. 10–14 (2000)
3. Handy, M.J., Haase, M., Timmermann, D.: Low energy adaptive clustering hierarchy with deterministic cluster-head selection. In: *International Workshop on Mobile and Wireless Communications Network*, pp. 368–372 (2002)
4. Israr, N., Awan, I.: Coverage based intercluster communication for load balancing in wireless sensor networks. In: *IEEE International Conference on Advanced Information Networking and Applications AINAW*, pp. 923–928 (2007)
5. Nguyen, L.T., Defago, X., Beuran, R., Shinoda, Y.: An energy efficient routing scheme for mobile wireless sensor networks. In: *IEEE International Symposium on Wireless Communication Systems ISWCS*, pp. 568–572 (2008)
6. Lindsey, S., Raghavendra, C.S.: Pegasus: power-efficient gathering in sensor information systems. In: *IEEE Aerospace conference*, pp. 3–1125 (2002)
7. Muruganathan, S.D., Ma, D.C., Bhasin, R., Fapojuwo, A.O.: A centralized energy-efficient routing protocol for wireless sensor networks. *IEEE Commun. Mag.* **43**(3), 8–13 (2005)
8. Zhang, Z., Yan, L., Pan, W., Luo, B., Liu, J., Li, X.: Routing protocol based on cluster-head-chaining incorporating leach and pegasus. *Chin. J. Sens. Actuators* **8**, 27–31 (2010)
9. Tang, F., You, I., Guo, S., Guo, M., Ma, Y.: A chain-cluster based routing algorithm for wireless sensor networks. *J. Intell. Manufact.* **23**(4), 1305–1313 (2012)
10. Ali, S.A., Refaay, S.K.: Chain-chain based routing protocol. *Int. J. Comput. Sci. Issues IJCSI* **8**(3), 83–87 (2011)
11. Fahim, H., et al.: Interference and bandwidth aware depth based routing protocols in underwater WSNs. In: *9th IEEE International Conference on Innovative Mobile and Internet Services in Ubiquitous Computing, Blumenau*, pp. 78–85 (2015)
12. Faheem, H., Ilyas, N., ul Muneer, S., Tanvir, S.: Connected dominating set based optimized routing protocol for wireless sensor networks. *Int. J. Adv. Comput. Sci. Appl. (IJACSA)* **7**(Issue 11), 322–331 (2016)
13. Qing, L., Zhu, Q., Wang, M.: Design of a distributed energy-efficient clustering algorithm for heterogeneous wireless sensor networks. *Comput. Commun.* **29**(12), 2230–2237 (2006)
14. Saini, P., Sharma, A.K.: Energy efficient scheme for clustering protocol prolonging the lifetime of heterogeneous wireless sensor networks. *Int. J. Comput. Appl.* **6**(2), 30–36 (2010)
15. Javaid, N., Qureshi, T., Khan, A., Iqbal, A., Akhtar, E., Ishfaq, M.: Eddeec-enhanced developed distributed energy-efficient clustering for heterogeneous wireless sensor networks. *Procedia Comput. Sci.* **19**, 914–919 (2013)
16. Ahmad, A., Javaid, N., Khan, Z.A., Qasim, U., Alghamdi, T.A.: (ACH)<sup>2</sup>: routing scheme to maximize lifetime and throughput of wireless sensor networks. *IEEE Sens. J.* **14**(10), 3516–3532 (2010)
17. Smaragdakis, G., Matta, I., Bestavros, A.: Sep: a stable election protocol for clustered heterogeneous wireless sensor networks. In: *Second International Workshop on Sensor and Actor Network Protocols and Applications (SANPA)*, pp. 1–11 (2004)

# Quantitative Deliberation Model and the Method of Consensus Building

Xuan Li, Caiquan Xiong<sup>(✉)</sup>, Jiabao Guo, and Gang Liu

School of Computer Science,  
Hubei University of Technology, Wuhan 430068, China  
x\_cquan@163.com

**Abstract.** Deliberation is an effective method to solve complex problems. Unlike the persuasion and negotiation, deliberation is necessary to consider uncertainty information representation and processing. This paper proposes a quantitative deliberation model (QuDM) based on IBIS. Firstly, the IBIS model is simplified, without considering the specialization and generalization of the issue in the model, and the argument is divided into two parts: the premise and the conclusion. Premise and conclusion are all called statement. Then the uncertainty of argument's premise and the intensity of argument are expressed by certainty-factors. In order to determine the certainty-factors of positions, a consensus building method is proposed, and the credibility values of all statements are calculated by a recursive algorithm. Finally, an example is used to verify the validity and rationality of the proposed method.

## 1 Introduction

Deliberation is an important means for groups to solve complex problems [1]. Deliberation model is a formalized or graphical description of the process of deliberation. It is the theoretical basis of computer-aided group decision support system [2] and debate-based multi-agent interaction system [3]. A good deliberation model can not only describe the daily deliberation dialogue, but also support the dialogue process guidance and consensus building. In deliberation dialogue process, the modality words such as “certain”, “very likely”, “may”, “impossible” are often used, so there are some uncertain information in deliberation. Each subject in the deliberation dialogue has no individual goal, but has its own belief, therefore contradictions and conflicts exist in the deliberation process, and thus persuasion dialogue will be activated in deliberation dialogue [4], and the issue will be solved via argumentation reasoning [5]. Hence, the deliberation dialogue model needs to describe the process of group thinking which is from divergence to convergence, and to introduce uncertainty reasoning and argumentation method. The content of the model includes: (i) the structural decomposition of utterance information, (ii) the description of dialogue deduction process, and the algorithm of consensus building.

At present, most of argumentation models only describe the information of a certain stage or a certain part of the deliberation dialogue process, and do not provide a comprehensive depiction of the process. For example, the Toutmin model [6] focuses on the description of the argument structure, whereas does not describe the attack and

support relationship between arguments. Issue-Based Information System (IBIS) [7] describes the decision making process of proposing the position to a issue and giving the argument to the position, but the model neither represent the multi-level argumentation structure to the position, nor propose the method to determine the final acceptable position. Dung's Abstract Argumentation Framework (AAF) [3, 8] describes the attack relationship between arguments and puts forward the corresponding extended semantics, but it doesn't consider the support relationship between arguments, nor the attack strength. Currently, deliberation dialogue models are built mostly on the basis of the above models, either via integration or via extension. There are some researches on multi-agent deliberation dialogues at present [9, 10], but these researches mostly focus on dialogue protocol, and do not propose corresponding approaches for argument quantification and evaluation.

In view of the above problems, this paper proposes a quantitative deliberation model (QuDM) based on IBIS (Issue Based Information System). In the model, argumentation and uncertainty reasoning are introduced to calculate the certainty-factors of positions. The process of argumentation on a position is described as a dialogue tree, and the whole deliberation is described as a dialogue forest with the position being its root node. A consensus building method is proposed to calculate the final certainty-factors of positions.

## 2 IBIS: Issue-Based Information System

Issue-Based Information System (IBIS) [11] invented by Werner Kunz and Horst Rittel in 1970 is an argumentation-based method to tackling wicked, complex and ill-defined problems. The arguments of the problems usually involve multiple stakeholders (e.g., designers, customers, implementers).

IBIS consists of four main nodes:

Issues: These are issues that need to be addressed.

Positions: These are responses to questions. Typically, the set of ideas that respond to an issue represents the spectrum of perspectives on the issue.

Arguments: These can be arguments supporting (pros) or arguments against (cons) a position. The complete set of arguments that respond to an idea represents the multiplicity of viewpoints on it. Arguments are laid out and linked to either the positions or other arguments.

Further issues: These may emerge during the process and be linked to either the positions or the arguments. In engineering design, positions and arguments may correspond to viewpoints of different experts or stakeholders so that each move may also be regarded as a step in a dialectical process.

There are nine kinds of links in IBIS. A position responds-to an issue, and this is the only place the responds-to link can be used. Arguments must be linked to their positions with either supports or objects-to links. Issues may be generalized or specialized, and may also be-questioned or be-suggested by other issues, positions, and arguments. As an escape mechanism, other nodes may connect to any other node type with other links (Fig. 1).

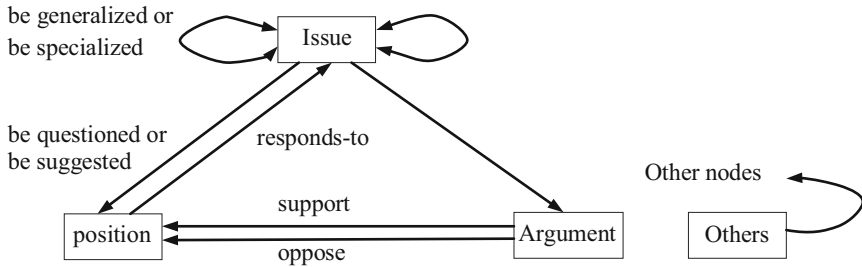


Fig. 1. The model of IBIS

### 3 Quantitative Deliberation Model

The deliberation is conducted via dialogue [4]. Utterance is the basic unit of dialogue, the utterance from the structure can be decomposed into two parts of the conclusion and the premise. The premise and conclusions are collectively referred to as statements. In the consultation process, the expert usually uses an initial score to indicate the degree of support for the conclusion or the support/opposition to another statement.

We will define an argument evaluation algorithm in Sect. 4 to obtain the final credibility values of deliberation. Based on these requirements, a quantitative deliberation dialog framework is proposed by simplifying and quantifying the IBIS model.

**Definition 1 (Statement).** The statement is a positive description of things, which is the basic unit of an utterance. for two statements  $h_1, h_2$ , if they are logically equal, then denoted as  $h_1 \equiv h_2$ ; if they are logically opposite, then denoted as  $h_1 \equiv \neg h_2$ . the set of all statements is denoted as  $L$ .

**Definition 2 (Issue).** The issue is the object of the deliberation dialogue, the entire deliberation dialogue is directed to an issue denoted as  $t$ . The issue is generally represented as statements, hence  $t \in L$ .

**Definition 3 (Position).** The position is the alternative solution to the issue. The set of all the positions is denoted as  $P$ . The position is also represented as the statement, hence  $P \subseteq L$ .

**Definition 4 (Argument).** An utterance with definite claim and corresponding foundation is called argument. The argument can be represented as a 2-tuple  $A = \langle H, h \rangle$ , where  $H = \{h_1, \dots, h_n\}$  is called as the premise set of the argument,  $h_i \in L (1 \leq i \leq n)$  as the premise of the argument,  $h_i \in L$  as the conclusion of the argument. The set of all arguments is denoted as  $A$ .

An argument have zero or multiple premises, there exist “and” relationship among premises, and at most one conclusion.

**Definition 5 (Dialogue).** For two arguments  $A_1 = \langle H_1, h_1 \rangle, A_2 = \langle H_2, h_2 \rangle$ , if  $h_1 \in H_2$ , then  $A_1$  is called the dialogue to  $A_2$ , denoted as  $\langle A_1, A_2 \rangle$ . Dialogue is actually a response of one argument to another.



A position is a special argument with only one premise to an issue, called root argument or position argument. Root argument can be represented as  $A_p = \langle \{p\}, t \rangle$  denotes a position, and  $t$  is the issue of deliberation dialogue.

In the actual deliberation dialogue, the argument contains some uncertainty. We use fuzzy argument to represent the uncertainty.

**Definition 6 (Fuzzy argument).** Fuzzy argument is a 4-tuple  $A = \langle H, d(), h, cf() \rangle$ , which  $H = \{h_1, \dots, h_k\}, h_i \in L (1 \leq i \leq k)$  is called the premise of the argument,  $h \in L$  is called the conclusion of the argument.  $d() : A \rightarrow [-1, 1]$  is the argument strength mapping function, which represents the strength of the support from argument premise  $H$  to the conclusion  $h$ . For an argument  $A$ , if  $d(A) > 0$ , it means the argument premise support the conclusion; if  $d(A) < 0$ , it means the premise oppose the conclusion; if  $d(A) = 0$ , it means the argument does not take effect in the deliberation dialogue.  $cf() : L \rightarrow [0, 1]$  is the certainty-factor function of an argument premise,  $cf(h_i)$  represent the certainty-factor of the argument premise  $h_i$ .

This definition is the quantification of the IBIS model, with which the consensus value of the position can be calculated, and the acceptability of the position can be determined according to the consensus value.

**Definition 7 (Deliberation Framework).** The deliberation framework is a 4-tuple:  $DDT = (L, t, A, D)$ , where  $L$  is a set of statements,  $t$  is the issue of the deliberation dialogue,  $A$  is an argument set,  $D \subseteq A \times A$  is a dialogue set.

Deliberation framework can be represented in a dialogue graph (shown in Fig. 2). In the graph, the rounded rectangle represents the statement, and the circle represents the argument. A connection line pointing from an argument to a statement represents the argumentation relationship between an argument and a statement, where the statement is the premise of the argument.

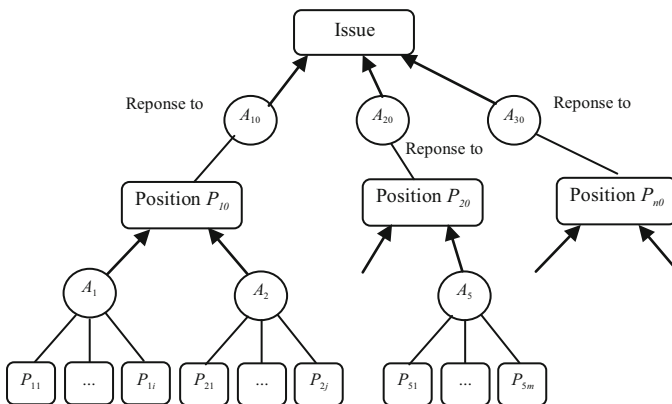


Fig. 2. The deliberation dialogue graph

The key to the extension of IBIS model is to increase the multiple argumentation of the position, namely, the structure of the argument, thus forming a dialogue tree rooted in the first argument.

**Definition 8 (Dialogue Tree).** Dialogue tree is a finite set of  $n(n \geq 1)$  arguments where the root argument is taken as the root node. In any dialogue tree, there is one and only one argument  $A_0$  which is called the root. When  $n > 1$ , the arguments other than the root argument can be divided into  $m(m > 0)$  disjoint finite sets of  $T_1, \dots, T_m$ , where  $T_i (1 \leq i \leq m)$  itself is a dialogue tree, called the subtree of  $A_0$ , and  $\langle A_1, A_0 \rangle \in \mathcal{D}$ , where  $A_i$  is the root argument of  $T_i$ .

The root node of the dialogue tree is the position argument which contains only one premise, that is, a position proposed by an expert.

**Definition 9 (Dialogue Forest).** The set of  $n(n \geq 0)$  disjoint dialogue trees is called dialogue forest.

Dialogue forest is an abstract description of the whole deliberation dialogue process. Dialogue forest is composed of a number of dialogue trees, and each tree describes the argumentation inference process to a position. There are as many positions in the dialogue process as there are dialogue trees in the dialogue forest. If the certainty-factor of the premise of the position argument (i.e. the position) of each dialogue tree can be calculated and the positions are sorted by their certainty-factors, then the result of the whole deliberation dialogue can be determined.

## 4 Calculation of Consensus Values in QuDM

In the actual deliberation process, the experts give the argument not only to set the premise and conclusion, but also set the premise of the credibility of each statement  $\{cf(h_1), cf(h_2), \dots, cf(h_n)\}$  and argument credibility  $d$ . The argument conclusion credibility depends on the premise of credibility and argument credibility. With the deliberation going on, the controversy prerequisites will be subject to changes in the response of other argument, so that the credibility of the argument conclusions changes. Argument evaluation algorithm is to calculate the deliberation dialogue framework as a prerequisite for the argument and the credibility of the statement.

### 4.1 Credibility of Argument's Conclusion

(1) Calculate the credibility of the first Argument's conclusion

Argument  $A = \{H, d, h, cf()\}$  is first argument, argument strength of  $A$  is  $d$ .  $H = \{h_1, \dots, h_n\}, h_i \in \mathcal{L}(1 \leq i \leq n)$ . Argument statements  $h_1, \dots, h_n$ , the initial credibility of the value were  $cf(h_1), cf(h_2), \dots, cf(h_n)$ . That  $h$  is not a premise for any argument, then the conclusion of the credibility of  $h$  is:

$$cf(h) = cf(H) \times d \tag{1}$$

where  $cf(H) = \min\{cf(h_i) \mid (0 \leq i \leq n)\}$ .

(2) Calculate the credibility of the non-controversial conclusion

If the argument  $A = \{H, d, h, cf()\}$  is not the first argument, that  $h$  is a premise for the argument  $B$ , that is  $h \in pre(B)$ , Since the premise of  $h$  as argument  $B$  has been set the credibility  $cf^0(h)$ , then the purpose of argument  $A$  is to modify the credibility of  $h$ , so the credibility of  $h$  should be  $cf^0(h)$  with the  $cf(H) \times d$  synthesis.

Argument  $A = \{H, d, h, cf()\}$ ,  $h$  is a premise of the argument  $B$ , its initial credibility is  $cf^0(h)$ , then  $h$  is the response of  $A$ , its credibility is

$$cf(h) = \begin{cases} cf^0(h) + (1 - cf^0(h)) \times cf(H) \times d, & \text{while } 0 \leq d \leq 1 \\ cf^0(h), & \text{while } d = 0 \\ cf^0(h)(1 + cf(H) \times d), & \text{while } -1 \leq d \leq 0 \end{cases} \tag{2}$$

The value of the  $cf(h)$  is in  $[0, 1]$ , which satisfies the statement credibility. The proof of the formula can be found in [12].

### 4.2 Credibility Synthesis Algorithm

If an argument received a number of controversial responses, a credibility synthesis is required.

Consider the two cases of argument. There is a argument  $A^1 = \{H^1, d^1, h, cf^1()\}$  and  $A^2 = \{H^2, d^2, h, cf^2()\}$ ,  $h \in pre(B)$ , the argument  $A^1, A^2$  at the same time on the premise of argument  $B$  to respond to  $h$ . Set the initial credibility for  $h$ . The reliability of the synthesis can take the following steps:

Step1: According to formula 1, calculating the credibility of  $cf^1(h), cf^2(h)$  argument  $A^1, A^2$  conclusion  $h$ .

Step2: Using the formula 3 [13] synthesize the  $cf^1(h), cf^2(h)$ . Formula 3 is as follows, where is  $cf_{1,2}(h)$  the comprehensive credibility value for the conclusion  $h$  of the sub-arguments.

$$cf_{1,2}(h) = \begin{cases} cf_1(h) + cf_2(h) - cf_1(h)cf_2(h), & \text{while } cf_1(h) \geq 0 \ \& \ cf_2(h) \geq 0 \\ cf_1(h) + cf_2(h) + cf_1(h)cf_2(h), & \text{while } cf_1(h) \geq 0 \ \& \ cf_2(h) \geq 0 \\ \frac{cf_1(h) + cf_2(h)}{1 - \min\{|cf_1(h)|, |cf_2(h)|\}}, & \text{while } cf_1(h) \times cf_2(h) \leq 0 \end{cases} \tag{3}$$

Step3: According to formula 2, combining the initial credibility of the premise  $h$  of  $A$ , the credibility value of the premise  $h$  after the impact of  $B, C$  is calculated.

Using formula 3 and formula 2 to compute an argument synthesis value in the context of a number of arguments responses to the case of credibility.

The argument evaluation algorithm is described as follows:

```

Argument_Create()
While(deliberation is not over);
{
  Produce a new argument  $P$ ;
  IF( $P$  is frist argument);
    Use formula (1)to calculate the credibility values of the argument node  $P$ ;
  ELSE
    Certainty-factor_revision( $P$ );
  ENDIF
}ENDWHILE
Certainty-factor_revision( $P$ );
{
  Use formula (1)to calculate the credibility values of the argument node  $P$ ;
  Search the argument  $p$  that response argument  $Q$  and premise  $h$ ;
  Use formula (2) to re-synthesize the son argument  $Q$ ;
  Use formula (3)to calculate  $cf(h)$ ;
  Use formula (1)to calculate the credibility values of the argument node  $Q$ ;
  IF( $Q$  is not frist argument)
    Certainty-factor_revision( $Q$ );
  ENDIF
}

```

## 5 Example Analysis

Assuming that a group conducts a deliberation dialogue on an issue. During the course of the dialogue, three positions  $A_0$ ,  $B_0$ ,  $C_0$  are proposed, and then the three positions will be argued, and three deliberation dialogue trees are formed. The corresponding deliberation tree is shown in Fig. 3, and the corresponding initial values are shown in Table 1.

In the Table 2, when generating a new argument and calling the certainty of the transfer algorithm, only the certainty of the statement from the newly generated node will be updated. And the certainty of the conclusion  $h$  will be updated at each time node. The change process is  $0.45 \rightarrow 0.3202 \rightarrow 0.4212$ .

At this time node, the conclusion  $P$  is unacceptable, and it can be seen that the method is used to calculate the certainty of the stated statement and to determine the final acceptable set of statements based on the stated certainty threshold.

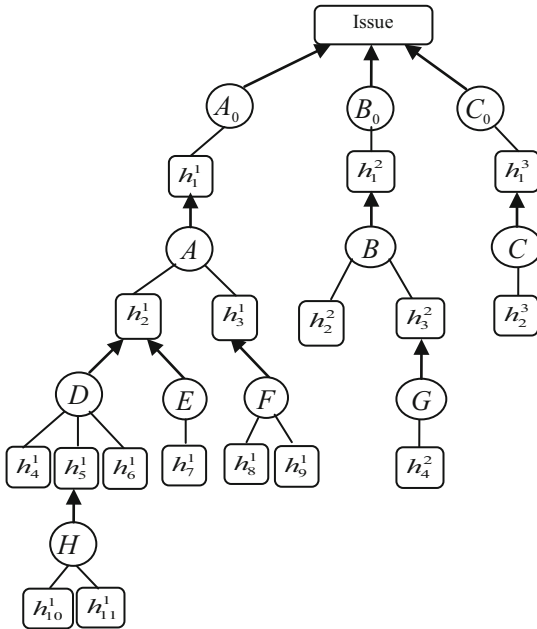


Fig. 3. An example of argumentation

Table 1. Initial value of the dialog graph

Argument	Precondition set	Argument conclusion	Argument Credibility	Argument prerequisites initial credibility
A	$\{h_2^1, h_3^1\}$	$h_1^1$	0.9	$cf(h_2^1)^0 = 0.5, cf(h_3^1)^0 = 0.9$
B	$\{h_2^2, h_3^2\}$	$h_1^2$	0.7	$cf(h_2^2)^0 = 0.8, cf(h_3^2)^0 = 0.3$
C	$\{h_2^3\}$	$h_1^3$	0.5	$cf(P_2^3)^0 = 0.8$
D	$\{h_4^1, h_5^1, h_6^1\}$	$h_2^1$	-0.9	$cf(h_4^1)^0 = 0.8, cf(h_5^1)^0 = 0.9, cf(h_6^1)^0 = 0.7$
E	$\{h_7^1\}$	$h_2^1$	0.8	$cf(h_7^1)^0 = 0.6$
F	$\{h_8^1, h_9^1\}$	$h_3^1$	-0.8	$cf(h_8^1)^0 = 0.7, cf(h_9^1)^0 = 0.6$
G	$\{h_4^2\}$	$h_3^2$	-0.8	$cf(h_4^2)^0 = 0.5$
H	$\{h_{10}^1, h_{11}^1\}$	$h_5^1$	-0.7	$cf(h_{10}^1)^0 = 0.6, cf(h_{11}^1)^0 = 0.8$

Table 2. Certainty-Factor of statements in timeline

Time line	$h_1^1$	$h_1^2$	$h_1^3$	$h_2^1$	$h_3^1$	$h_5^1$	$h_3^2$
1	-	-	-	0.5	0.9	0.9	0.3
2	0.45	0.21	0.4	0.3558	0.468	0.522	0.18
3	0.3202	0.126	0.4	0.5096	0.468	0.522	0.18
4	0.4212	0.126	0.4	0.5096	0.468	0.522	0.18

## 6 Conclusion

Deliberation model should fully describe the deliberation process, including the structural decomposition of the argument node, the relationship representation between the argument nodes and the corresponding argument evaluation algorithm. Unlike the persuasion and deliberation dialogues, deliberation dialogue is necessary to introduce uncertainty information representation and processing. In the course of deliberation dialogue, there is also individual belief inconsistency, which needs to embed the persuasion dialogue elements to deal with, that is, need to introduce the argumentation reasoning. The proposed model can meet the above requirements. First, the argument node is decomposed into defeasible rules which consist of a number of premises and a conclusion, reflecting the internal structure of the argument node. Second, IBIS model is reduced and extended so that it can not only represent the actual deliberation dialogue, but also facilitate the evaluation of arguments. Reduction is to restrict the generalization and specialization of the issue so as to only solve a single problem. Extension is to increase the multi-layer argument structure, and to model the entire deliberation dialogue process as a dialogue forest, in which the root node of each dialogue tree corresponds to a position. Third, the quantitative representation of the argument premise and the argument strength are added. And the consensus evaluation method is proposed. The final consensus value of the position is obtained by recursive operation, and the algorithm is reasonable and efficient. The proposed method has been used in computer-aided argument support system, and achieved good results. In order to apply to multi-agent interactive system, further work should be done, including utterance information symbolization, agent belief representation and belief library construction, argument generation and dialogue protocol design.

**Acknowledgments.** This research is supported by National Natural Science Foundation of China under grant number 61075059, 61300127.

## References

1. Modgil, S., Toni, F., Bex, F., Bratko, I., Chesñevar, C., Dvořák, W., Falappa, M., Fan, X., Gaggl, S., García, A., González, M., Gordon, T., Leite, J., Možina, M., Reed, C., Simari, G., Szeider, S., Torroni, P., Woltran, S.: The added value of argumentation. In: Ossowski, S. (ed.) *Agreement Technologies*, vol. 8, pp. 357–403. Springer, Dordrecht (2013)
2. Scheuer, O., Loll, F., Pinkwart, N., McLaren, B.: Computer-supported argumentation: a review of the state of the art. *Comput. Support. Learn.* **5**, 43–102 (2010)
3. Heras, S., Jordán, J., Botti, V., Julián, V.: Case-based strategies for argumentation dialogues in agent societies. *Inf. Sci.* **223**, 1–30 (2013)
4. Walton, D.N., Krabbe, E.C.W.: *Commitment in Dialogue: Basic Concepts of Interpersonal Reasoning*. State University of New York Press, Albany, NY, USA (1995)
5. Amgoud, L., Maudet, N., Parsons, S.: Modelling dialogues using argumentation. In: 4th International Conference on MultiAgent Systems (ICMAS 2000), pp. 7–12. IEEE Press (2000)
6. Toulmin, S.E.: *The Uses of Argument*. Cambridge University Press, Cambridge (1958)

7. Kunz, W., Rittel, H.W.J.: *Issues as Elements of Information Systems*. University of California, Berkeley (1970)
8. Dung, P.M.: On the acceptability of arguments and its fundamental role in nonmonotonic reasoning, logic programming and n-person games. *Artif. Intell.* **77**, 321–357 (1995)
9. Eric, M.K., John-Jules, C.M., Prakken, H., Vreeswijk, G.: A formal argumentation framework for deliberation dialogues. In: *Proceedings of the 7th International Workshop on Argumentation in Multi-Agent Systems*, pp. 73–90 (2010)
10. McBurney, P., Hitchcock, D., Parsons, S.: The eightfold way of deliberation dialogue. *Int. J. Intell. Syst.* **22**, 95–132 (2007)
11. Conklin, J., Bergman, M.: gIBIS: a hypertext tool for exploratory policy discussion. *ACM Trans. Office Inform. Syst.* **6**, 303–331 (1988)
12. Xiong, C.Q., Ouyang, Y., Mei, Q.: Argumentation model based on certainty-factor and algorithms of argument evaluation. *J. Softw.* **25**, 1225–1238 (2014)
13. Shortliffe, E.H., Buchanan, B.G.: A model of inexact reasoning in medicine. *Math. Bio.* **23**, 351–379 (1975)

**The 8th International Workshop  
on Frontiers on Complex, Intelligent  
and Software Intensive Systems  
(FCISIS-2017)**



# Distinguishing Property for Full Round KECCAK- $f$ Permutation

Maolin Li<sup>1</sup> and Lu Cheng<sup>2</sup>(✉)

<sup>1</sup> Nan Kai University Binhai College, Tianjin 301900, China  
maolinwork@163.com

<sup>2</sup> Engineering University of Armed Police Force, Xi'an 710086, China  
18302972151@163.com

**Abstract.** Hash function is one of the most important cryptographic primitives. It plays a vital role in security communication to protect data's integrity and authenticity. KECCAK is a hash function selected by NIST as the winner of the SHA-3 competition. The inner primitive of KECCAK is a permutation named by KECCAK- $f$ . In this paper, we present improved bounds for the degree of the inverse of iterated KECCAK- $f$ . By using this bound, we improve the zero-sum distinguisher of full 24 rounds KECCAK- $f$  permutation by lowering the size of the zero-sum partition from  $2^{1579}$  to  $2^{1573}$ .

## 1 Introduction

Distributed Computing and Network Communication has been developed rapidly. However, it brings with serious security concerns like verifying the integrity and authenticity of the transmitted data. Hash function is one of the most important cryptographic primitives. It plays a vital role in security communication to protect data's integrity and authenticity. To achieve this, technique called "Hashing" is employed which relies on a family of Hash Functions.

KECCAK is the Hash Function selected as the winner of NIST Hash Function Competition. SHA-3 is not meant to replace SHA-2 since there is no significant attacks on SHA-2 have been demonstrated. But it is designed in response to the need to find an alternative and dissimilar construct for Cryptographic Hash that is more fortified to attacks.

The security of hash function is very important for data's integrity and authenticity. The algebraic degrees of hash functions have been studied for analyzing their security. A secure hash function is expected a high algebraic degree. A relative low degree of the inner permutation can be used to construct higher-order differential distinguishers, or zero-sum structures, which has been investigated in [1–3].

The hash function KECCAK, has a permutation based internal function and employs the sponge construction [4]. The internal function is named by KECCAK- $f$ , which is composed of several iterations of very similar round transformations. In previous works, the algebraic degree of iterated KECCAK- $f$  has been investigated. Based on the bound of degree, a zero-sum distinguisher for the 16-rounds KECCAK- $f$  permutation was first given in [1]. Later, zero-sum distinguishers for more rounds KECCAK- $f$  permutation

were obtained [2, 5–7], which came from the lower bound of degree in iterated  $\text{KECCAK-}f$ . The known lowest size of zero-sum partition of full 24 rounds  $\text{KECCAK-}f$  is  $2^{1579}$  [7]. This result comes from an improvement of the bound for the degree of iterated permutations for a special category of SP-networks in case of the inverse of  $\text{KECCAK-}f$  [6].

In this paper, we study the property of  $\text{KECCAK}$  and observe that the bound on degree of iterated inverse of  $\text{KECCAK-}f$  in [6] can be re-proved, and that help us lower the size of zero-sum partition of full rounds  $\text{KECCAK-}f$ .

The remainder of the paper is organized as follows. The preliminaries of  $\text{KECCAK-}f$  permutation and zero-sum partition properties are given in Sect. 2. The new bound on the degree of iterated inverse of  $\text{KECCAK-}f$  permutation is proposed in Sect. 3. Section 4 discusses the distinguishing property for full round  $\text{KECCAK-}f$  and at last, Sect. 5 summarizes this paper.

## 2 Preliminaries

In this section, we first describe the Sponge Construction and  $\text{KECCAK-}f$  permutation and then present the property of *Zero sum Partitions*.

### 2.1 Sponge Function

$\text{KECCAK}$  adopts the structure of Sponge Construction [8]. Based on a fixed-length permutation (or transformation) and on a padding rule, this mode of operation builds a function mapping variable-length input to variable-length output. It takes an element of  $F_2^*$  as input, i.e., a binary string of any length, and returns a binary string with any requested length, i.e., an element of  $F_2^n$  with  $n$  a user-supplied value. It operates on a finite state by iteratively applying the inner permutation to it, interleaved with the entry of input or the retrieval of output.

The sponge construction operates on a state of  $b = (r + c)$  bits. The value  $r$  is called bit-rate and  $c$  is called capacity. The sum  $b = (r + c)$  determines the width of  $\text{KECCAK-}f$  permutation which is used in the Sponge Construction (Fig. 1).

Firstly, the input string is padded with a reversible padding rule and cut into blocks of  $r$  bits. Then the  $b$  bits of the state are initialized to zero and the sponge construction proceeds in two phases:

- (1) In the absorbing phase, the  $r$ -bit input blocks are XORed into the first  $r$  bits of the state, interleaved with applications of the function  $f$ . When all input blocks are processed, the sponge construction switches to the squeezing phase.
- (2) In the squeezing phase, the first  $r$  bits of the state are returned as output blocks, interleaved with applications of the function  $f$ . The number of output blocks is chosen at will by the user.

The sponge construction uses  $r + c$  bits of state, of which  $r$  are updated with message bits between each application of  $\text{KECCAK-}f$  during the absorbing phase and



**Table 1.** Boolean components of  $\chi$ .

Output	Corresponding Boolean function
$\chi_0$	$x_0 + x_2 + x_1x_2$
$\chi_1$	$x_1 + x_3 + x_2x_3$
$\chi_2$	$x_2 + x_4 + x_3x_4$
$\chi_3$	$x_0 + x_3 + x_0x_4$
$\chi_4$	$x_1 + x_4 + x_0x_1$

**Table 2.** Boolean components of  $\chi^{-1}$ .

Output	Corresponding boolean function
$\chi_0^{-1}$	$x_0 + x_2 + x_4 + x_1x_2 + x_1x_4 + x_3x_4 + x_1x_3x_4$
$\chi_1^{-1}$	$x_0 + x_1 + x_3 + x_0x_2 + x_0x_4 + x_2x_3 + x_0x_2x_4$
$\chi_2^{-1}$	$x_1 + x_2 + x_4 + x_0x_1 + x_1x_3 + x_3x_4 + x_0x_1x_3$
$\chi_3^{-1}$	$x_0 + x_2 + x_3 + x_0x_4 + x_1x_2 + x_2x_4 + x_1x_2x_4$
$\chi_4^{-1}$	$x_1 + x_3 + x_4 + x_0x_1 + x_0x_3 + x_2x_3 + x_0x_2x_3$

**Definition 1.** Let  $F$  be a function from  $F_2^n$  into  $F_2^m$ . A zero-sum for  $F$  of size  $K$  is a subset  $\{x_1, \dots, x_K\} \subset F_2^n$  of elements which sum to zero and for which the corresponding images by  $F$  also sum to zero, i.e.

$$\sum_{i=1}^K x_i = \sum_{i=1}^K F(x_i) = 0.$$

In the above definition, the sum is defined by the addition in  $F_2^n$  (and in  $F_2^m$ ), i.e., the bitwise exclusive-or. Since it is expected that a randomly chosen function does not have many zero-sums, the existence of several such sets of inputs can be seen as a distinguish property of  $F$ .

A stronger distinguishing property named zero - sum partition targets permutation on  $F_2^n$  was also proposed.

**Definition 2.** Let  $P$  be a permutation from  $F_2^n$  into  $F_2^m$ . A zero-sum partition for  $P$  of size  $K = 2^k$  is a collection of  $2^{n-k}$  disjoint zero-sums  $X_i = \{x_{i,1}, \dots, x_{i,2^k}\} \subset F_2^n$ , i.e.

$$\cup_{i=1}^{2^{n-k}} X_i = F_2^n \text{ and } \sum_{j=1}^{2^k} x_{i,j} = \sum_{j=1}^{2^k} P(x_{i,j}) = 0, \forall 1 \leq i \leq 2^{n-k}.$$

The existence of zero-sum structures has been investigated in [1, 3, 9] and so on.

### 3 A New Bound on the Degree of KECCAK- $f$ Permutation

For an iterated function, the existence of zero-sums is usually due either to the particular structure of the round transformation or to a low degree. The algebraic degree of  $F$  provides some particular zero-sums, which correspond to all affine subspaces of  $F_2^n$  with dimension  $(\deg(F) + 1)$ . Proposition 1 gives the relation between the degree and the zero-sums.

**Proposition 1 [10].** Let  $F$  be a function from  $F_2^n$  into  $F_2^m$ . For every subspace  $V$  of dimension  $(\deg F + 1)$  we have

$$D_V F(x) = 0, \text{ for every } x \text{ in } F_2^n.$$

In the following, we will present a new bound of the degree of KECCAK- $f$  permutation.

**Observation.** For the boolean components of  $\chi^{-1}$ , let  $\delta_k$  be the maximal degree of the product of any  $k$  coordinates of  $\chi^{-1}$ , we have,

$$\delta_1 = 3, \delta_2 = 3, \delta_3 = 4, \delta_4 = 4.$$

In Crypto 2010, Boura et al. presented an improved upper bound for iterated permutation with a nonlinear layer composed of parallel applications of a number of balanced S boxes. In this paper, by using the similar proof idea, and combining some techniques of linear combination, we get the following bound for KECCAK family.

**Theorem 1.** Let  $F : F_2^n \rightarrow F_2^n$  denotes the nonlinear layer of KECCAK- $f$ , and  $F$  corresponding to the concatenation of  $m$  smaller balanced S boxes. Then, for any function  $G$  from  $F_2^n$  to  $F_2^l$ , we have

$$\deg(G \circ F) \leq \frac{\deg(G)}{2} + \frac{5}{2}m.$$

Proof. Denote by  $\pi$  the product of  $d$  output of coordinates of  $F$ , some of the coordinates involved in  $\pi$  may belong to the same S box. Then, for any  $i, 1 \leq i \leq 5$ , we denote by  $\pi_i$  the integer corresponding to the numbers of S boxes for which exactly  $i$  coordinates are involved in  $\pi$ . Thus,

$$\deg(\pi) \leq \max_{(x_1, \dots, x_5)} \sum_{i=1}^5 \delta_i x_i,$$

where the maximum is taken over all vectors  $(x_1, \dots, x_5)$  satisfying

$$\sum_{i=1}^5 ix_i = d \text{ and } \sum_{i=1}^5 x_i = m.$$

we have

$$\begin{aligned}
 \text{deg}(\pi) - d &\leq \sum_{i=1}^4 \delta_i x_i - \sum_{i=1}^4 i x_i \\
 &= 3x_1 + 3x_2 + 4x_3 + 4x_4 - (x_1 + 2x_2 + 3x_3 + 4x_4) \\
 &= 2x_1 + x_2 + x_3 \\
 &\leq 2m - (x_2 + x_3 + 2x_4 + 2x_5) \\
 &= 2m - \frac{1}{2}(2x_2 + 3x_3 + 4x_4 + 4x_5) \\
 &\leq 2m - \frac{1}{2}(x_2 + 2x_3 + 3x_4 + 4x_5) \\
 &\leq 2m - \frac{1}{2}(d - m).
 \end{aligned}$$

From the above inequality, we can easily deduce that

$$\text{deg}(\pi) \leq \frac{d}{2} + \frac{5}{2}m,$$

which ends our proof.

In KECCAK family,  $m$  is the number of S boxes in nonlinear layer, and  $m = 320$  for SHA-3 candidate. We denote the degree of  $r$  iterations of the inverse of KECCAK- $f$  by  $R^{-r}$ . By combining bound in Theorem 1 with the trivial bound, we get the bound on  $\text{deg}(R^{-r})$ . This upper bound as well as the bounds given in [6, 7] are listed in Table 3.

**Table 3.** Upper bounds on  $\text{deg } R^{-r}$

Round	Bound in [6]	Bound in [7]	Our bound
1	3	3	3
2	9	9	9
3	27	27	27
4	81	81	81
5	243	243	243
6	729	729	729
7	1309	1309	1164
8	1503	1454	1382
9	1567	1532	1491
10	1589	1566	1545
11	1596	1583	1572
12	1598	1591	1586
13	1599	1595	1593
14		1597	1596
15		1598	1598
16		1599	1599

## 4 Improved Distinguishing Properties for Full Round KECCAK- $f$

With the bounds of this paper and [6], we can use the technique presented in [2] to find zero-sum partitions for the full KECCAK- $f$  permutation. The technique in details we refer [2]. Note that the inverse of the first 11 rounds of KECCAK- $f$  has degree at most 1572, and the last 12 rounds with degree at most 1536 [6]. We consider the intermediate states after the linear layer  $L = \pi \circ \rho \circ \theta$  in the 12-th round, and choose any subspace  $V$  in  $F_2^{1600}$  corresponding to a collections of 1573 bits, implying  $\dim V = 1573$ . Then, the sets

$$X_a = \{(G_{11} \circ L^{-1})(a+z), z \in V\}, a \in F_2^{1600},$$

from a zero-sum partition of size  $2^{1573}$  for the full round KECCAK- $f$  since  $\dim V$  at most 1 more than both 1572 and 1536, where  $G_{11}$  denotes the inverse of the first 11 rounds.

## 5 Conclusion

Hash function is one of the most important cryptographic primitives. As the winner of NIST Hash Function Competition, KECCAK adopts the Sponge Construction, in which KECCAK- $f$  permutations is the core function. KECCAK- $f$  with the fixed-length output and variable length output can be used for hashing, MAC Computation etc. In addition it can also be used for symmetric key encryption and random number generation. This makes KECCAK one of most suitable candidate for multi-core processor architecture. In this paper, we improved the bound for the degree of the iterated inverse of KECCAK- $f$  permutation. This bounds leads to a zero-sum partition of full 24 rounds KECCAK- $f$  with size of  $2^{1573}$ , and the size is the lowest one among the known results. However, even if it points out that KECCAK- $f$  does not have an ideal behavior, this property does not seem to affect the security of KECCAK.

**Acknowledgments.** The authors would like to thank the anonymous referees for their valuable remarks and their helpful comments.

## References

1. Aumasson, J.P., Meier, W.: Zero-sum distinguishers for reduced KECCAK- $f$  and for the core functions of Luffa and Hamsi. In: Presented at the Rump Session of Cryptographic Hardware and Embedded Systems (CHES 2009) (2009)
2. Boura, C., Canteaut, A.: Zero-sum distinguishers for iterated permutation and application to KECCAK- $f$  and Hamsi-256. In: Selected Areas in Cryptography (SAC 2010). LNCS, vol. 6544, pp. 1–17. Springer, Heidelberg (2010)
3. Watanabe, D., Hatano, Y., Yamada, T., Kaneko, T.: Higher order differential attacks on step-reduced variants of luffa v1. In: Fast Software Encryption (FSE 2010). LNCS, vol. 6147, pp. 270–285. Springer, Heidelberg (2010)

4. Bertoni, G., Daemen, J., Peeters, M., Assche, G.V.: The KECCAK sponge function family. Main document. Submission to NIST (Round 2) (2009)
5. Boura, C., Canteaut, A.: A zero-sum property for the KECCAK-f permutation with 18 rounds. In: IEEE International Symposium on Information Theory 2010, 1–9 2010, Austin, Texas: United States (2010)
6. Boura, C., Canteaut, A., Canniere, C.D.: Higher-order differential properties of KECCAK and luffa. In: FSE 2011. LNCS, vol. 6733, pp. 252–269. Springer, Heidelberg (2011)
7. Duan, M., Lai, X.J.: Improved zero-sum distinguisher for full round KECCAK-f permutation. *Sci. Bullet.* **75**(6), 694–697 (2012)
8. Bertoni, G., Daemen, J., Peeters, M., Assche, G. V.: Keccak implementation overview: [keccak.noekeon.org/Keccak-implementation-3.2](http://keccak.noekeon.org/Keccak-implementation-3.2)
9. Knudsen, L.R., Rijmen, V.: Known-key distinguishers for some block ciphers. In: ASIACRYPT 2007. LNCS, vol. 4833, pp. 315–324. Springer, Heidelberg (2007)
10. Knudsen, L.R.: Truncated and higher order differentials. In: Fast Software Encryption (FSE 1994). LNCS, vol. 1008, pp. 196–211. Springer, Heidelberg (1995)



# Optimal Control of Carrier-Based Aircraft Steam Launching Valve

Chengtao Cai<sup>1</sup>(✉), Yujia Cui<sup>1</sup>, and Yanhua Liang<sup>2</sup>

<sup>1</sup> College of Automation, Harbin Engineering University, Harbin 150001, China  
caichengtao@hrbeu.edu.cn

<sup>2</sup> College of Electrical and Control Engineering,  
Heilongjiang University of Science and Technology, Harbin 150022, China

**Abstract.** In order to study the launching valve that can make the carrier-based aircraft take off smoothly, the steam catapult system is analyzed. The model of the steam storage cylinder, the cylinder, the launching valve and the carrier-based aircraft are under construction. In the case of a given opening degree of the launching valve, the simulation system is established. The performance parameters vary with time can be got. A series of launching valve opening degree curves are drawn to study the control of the launching valve. By simulation, the corresponding acceleration curves can be obtained and the peak-to-average ratios are calculated. At last, by analyzing, it is demonstrated that the launching valve has a beneficial influence on the carrier-based aircraft taking off performance.

**Keywords:** Launching valve · Steam catapult system · Carrier-based aircraft · Catapult take off

## 1 Introduction

At present, the carrier-based aircraft mainly uses the steam catapult to take off from the aircraft carrier [1]. The control process of the steam catapult system is performed by the hydraulic servo control system. The control object of the system is a launching valve provided between the steam storage cylinder and the cylinder [2]. The carrier-based aircraft is controlled by the steam, which is sent by the launching valve. In this way, the carrier-based aircraft takes off the aircraft carrier accurately at the end of the power stroke. In the above control process, as the law of how to open the launching valve directly affects the performance of the system, the most critical step is to control the opening degree of the launching valve to control the amount of steam [3].

Over a long period of time, there are few published literature on the steam catapult technology, and the main study is the carrier-based aircraft catapult takes off process, which rarely involves the working mechanism and the control law of the launching valve.

This paper aims to study the control technology of the launching valve. Firstly, the research on the steam catapult taking off system is carried out. On the basis of the establishment of the steam storage cylinder, the cylinder, the launching valve and the carrier-based aircraft taking off models, the simulation of the steam catapult system is obtained. The launching valve opening degree curves are designed. Through the

simulation system, the acceleration curves can be got. After multiple calculations, the control law of the launching valve can be summarized.

## 2 Steam Catapult System

The steam catapult system consists of the steam storage cylinder, the cylinder and the launching valve [4]. A large amount of steam stored in the steam storage cylinder is supplied to the cylinder through the launching valve. This steam can promote the cylinder piston movement, and then produce ejection force. The structure of the steam catapult is shown in Fig. 1.

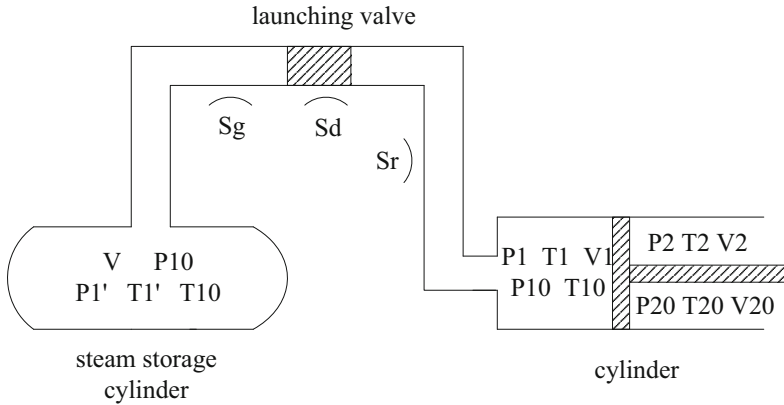


Fig. 1. Structure of the steam catapult

### 2.1 Steam Storage Cylinder

The steam storage cylinder is a kind of energy storage equipment, in a very short period of time, it can provide large steam for the equipment. Hot water and steam are stored in the steam storage cylinder [5].

As shown in Fig. 1, the volume of the steam storage cylinder is  $V$ , its initial temperature and pressure are  $T_{10}$  and  $P_{10}$ . When the time is  $t$ , the temperature inside the cylinder is  $T'_1$  and the pressure is  $P'_1$ .  $S_d$  is the area, which is composed of the pipe area and the simplified area of steam treatment components. The cylinder inlet area is  $S_r$ . The initial temperature and pressure of the cylinder are  $P_{10}$  and  $T_{10}$ . When the time is  $t$ , the temperature, pressure and volume of the cylinder rodless cavity are  $P_1$ ,  $T_1$  and  $V_1$ .

The degassing process is adiabatic, and the relationship between the state quantities satisfies Eqs. (1)–(5) [6]. In the following equations,  $\omega_{e1}$  is the scale factor.  $b_1$  is the critical pressure ratio, in this paper, its value is 0.46.  $S$  is the throttle area.  $V$  is the volume of the steam storage cylinder.  $\kappa$  is the specific heat ratio, its value is 1.135. The flow rate of the steam storage cylinder is  $Q_{m1}$ .

$$\omega_{e1} = \begin{cases} \sqrt{1 - \left(\frac{\sigma_1 - b_1}{1 - b_1}\right)^2} & b_1 < \sigma_1 = \frac{P_1}{P_{10}} \leq 1 \\ 1 & \sigma_1 = \frac{P_1}{P_{10}} \leq b_1 \end{cases} \quad (1)$$

$$S = \frac{1.46\sqrt{1 - b_1}}{\sqrt{\frac{1}{S_g^2} + \frac{1}{S_d^2} + \frac{1}{S_r^2}}} \quad (2)$$

$$T_1' = T_{10} \left(\frac{P_{10}}{P_1'}\right)^{\frac{1-\kappa}{\kappa}} \quad (3)$$

$$Q_{m1} = \frac{SP_1' \sqrt{1 - b_1}}{\sqrt{RT_1'}} \omega_{e1} \quad (4)$$

$$\frac{dP_1'}{dt} = -\frac{\kappa RT_1' Q_{m1}}{V} \quad (5)$$

## 2.2 Cylinder

The cylinder work process model is presented in Fig. 1. The steam pressure of the cylinder is  $P_1'$  and the temperature is  $T_1'$ . The area of the cylinder rodless cavity is  $A_1$ . Its initial temperature and pressure are  $T_{10}$  and  $P_{10}$ . The area of the cylinder rod cavity is  $A_2$ . Its initial temperature and pressure are  $T_{10}$  and  $P_{20}$ . When the time is  $t$ , the temperature, pressure and volume of the cylinder rodless cavity are  $T_1$ ,  $P_1$  and  $V_1$ , the temperature, pressure and volume of the cylinder rod cavity are  $T_2$ ,  $P_2$  and  $V_2$ . The total displacement of piston motion is  $S$ . The actual displacement of the piston is  $X$ .

Depending on the dynamic characteristics of the typical double acting pneumatic transmission system, the working process of the cylinder can be obtained. Its internal reaction is similar to the steam storage cylinder. The equations are similar to above.

## 2.3 Launching Valve

The launching valve is an essential component of the steam catapult system. The ejection force can be regulated by adjusting the opening degree of the launching valve. The structure of the launching valve is shown in Fig. 2.

The working principle of the launching valve is illustrated below. The oil is injected into the valve body from the hydraulic port so that the liquid enters the opening chamber of the launching valve. The measuring rod is subjected to the downward thrust, which causes the lifting head between the steam storage cylinder and the cylinder to descend. Thus, the launching valve opens. The steam in the steam storage cylinder starts to work in the cylinder. The opening degree of the launching valve varies with the change of the oil flowing into the opening chamber. At the same time, oil from the closing chamber flows out through the two outlet ports.

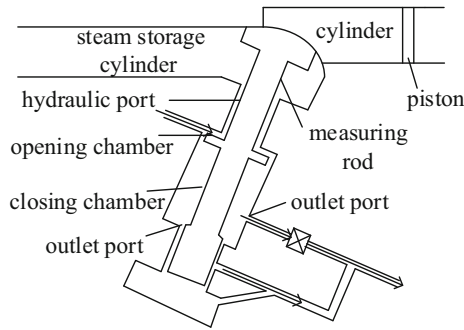


Fig. 2. Structure of the launching valve

The displacement of the measuring rod is determined by the velocity of the oil flowing into the opening chamber and flowing out of the sealed chamber. This is the launching valve opening degree. Depending on the above process, we can get separate ejection force for different types carrier-based aircraft to take off.

### 3 Carrier-Based Aircraft Catapult Taking Off Simulation

#### 3.1 Modeling of Carrier-Based Aircraft Catapult Taking Off

The force analysis of carrier-based aircraft catapult takes off as shown in Fig. 3 [7].

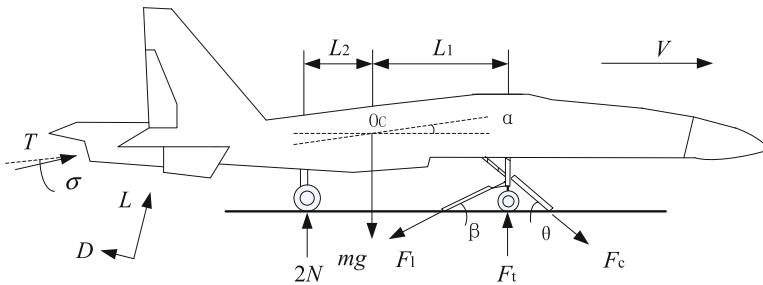


Fig. 3. Carrier-based aircraft catapult taking off process

The catapult taking off process is divided into six stages [8]. Since the six stages of the kinematic model principle are the same, the ejection slip stage is taken as an example.

In the following Eqs. (6)–(10),  $F$  is the ejection force applied to the horizontal direction of the carrier-based aircraft.  $S_1$  represents the ejection distance of the aircraft.  $V_{w/d}$  is the deck wind speed.  $V$  is the speed of the carrier-based aircraft.  $V_A$  is the speed of the air.  $C_L$  is the lift coefficient.  $C_D$  is the resistance coefficient.  $S$  is the equivalent wing area of the aircraft.  $L_m$  is a distance of the nose landing gear shaft to the lift action point.

$$V_A = V + V_{w/d} \tag{6}$$

$$D = \frac{1}{2} C_D \rho S V_A^2 \tag{7}$$

$$L = \frac{1}{2} C_L \rho S V_A^2 \tag{8}$$

$$Y_n = \frac{L_m}{L_1 + L_2} L \tag{9}$$

$$F_c \sin \theta + T \cos(\alpha + \sigma) - Y_n \sin \alpha - D \cos \alpha = ma \tag{10}$$

### 3.2 Simulation and Result Analysis

MATLAB software is utilized to simulate the model. This article refers to the C13 type steam catapult [7]. The relevant parameters are shown in Table 1.

**Table 1.** Relevant parameters.

Parameter	Parameter value	Parameter unit
Initial pressure of steam storage cylinder	5220000	Pa
Initial temperature of steam storage cylinder	570	K
Volume of steam storage cylinder	70	m <sup>3</sup>
Initial pressure of cylinder	100000	Pa
Initial temperature of cylinder	570	K
Piston quality	1000	Kg
Quality of carrier-based aircraft	27500	Kg

According to the above parameters, the carrier-based aircraft characteristics are shown in Fig. 4.

## 4 Optimal Control of Launching Valve

As can be observed in the model above, the faster the launching valve is opened, the shorter the diversion lever disconnects. The launching valve opening degree determines the amount of steam flowing through the launching valve and the amount of steam consumed at the end of the ejection.

The control law of the launching valve can not only affect the ejection characteristics in the acceleration process but also can control the total energy of the catapult output.

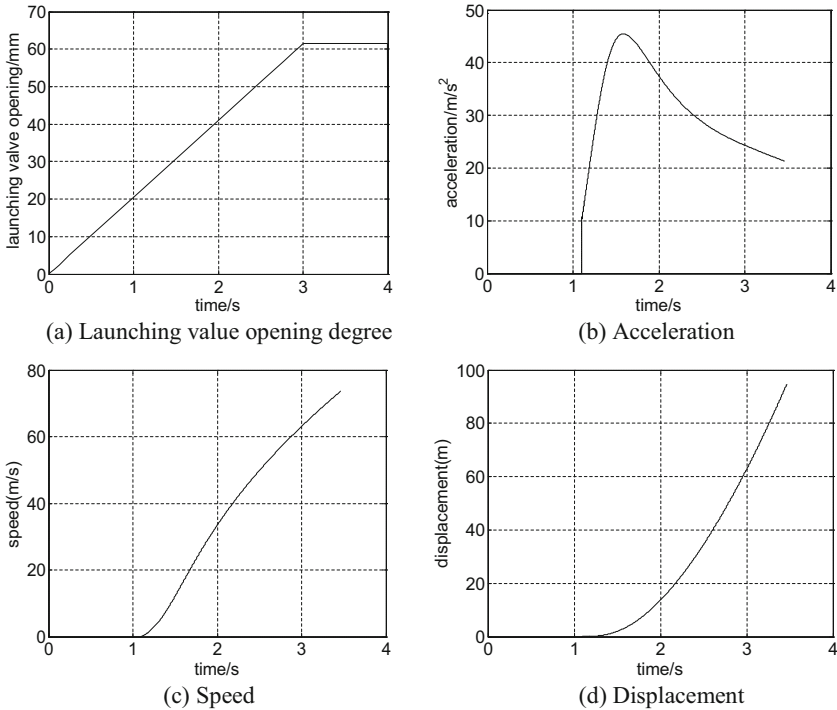


Fig. 4. Carrier-based aircraft steam catapult characteristics

### 4.1 Selection of Steam Launching Valve Opening Degree Curves

In order to maintain the sum of the launching valve opening degree is the same, the following method is utilized to draw the curves.

There is an integral called Riemann points. It is defined as the image of the function on the Cartesian coordinate system is divided into numerous rectangles by a straight line parallel to the y-axis. Then the rectangles on this interval are accumulated. What is obtained is the area of the image of the function on the interval. The core idea of the Riemann integral is an attempt to calculate the integral value by infinite approximation. Like this, the launching valve opening degree curves are infinitely approximated, divided, and then summed.

Each moment of the launching valve opening degree is added until the launching valve is closed. In fact, it also equates to compute the integral along the launching valve opening degree curves. The flow area of the launching valve is proportional to the launching valve opening degree. The curves can be drawn under the conditions that they last the same amount of time and possess the same image area.

## 4.2 Construction of Launching Valve Control System

A number of the launching valve opening degree curves are designed which are opened at the same time. Then, the simulation of each valve opening degree is carried out. The corresponding acceleration curve is obtained. By calculation, the law of how to open the launching valve is summed up, which can make the carrier-based aircraft take off smoothly. The opening degree curves of the launching valve are shown in Fig. 5. In this paper, four representative curves are given.

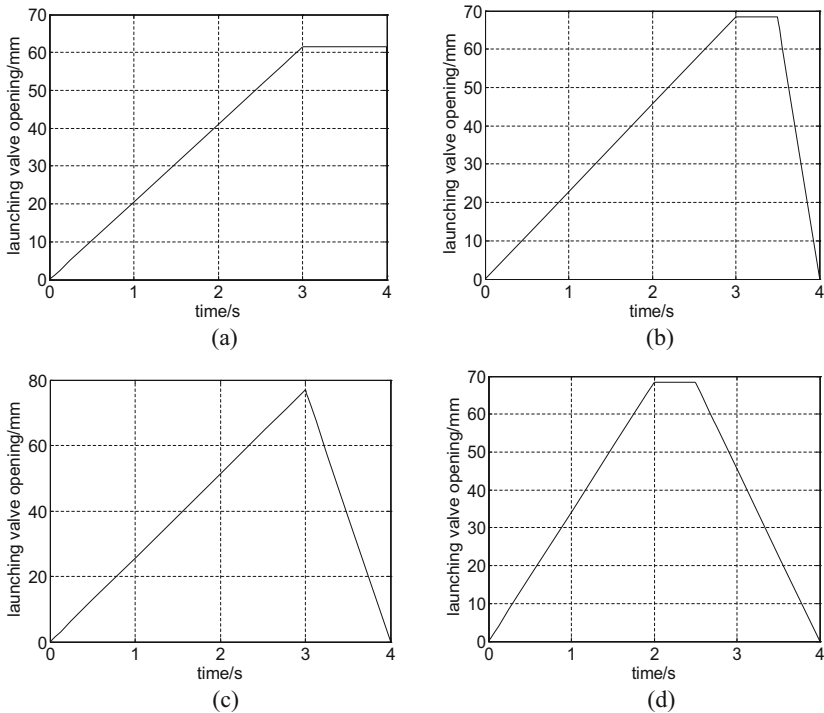


**Fig. 5.** Launching valve opening degree

In the case of a certain ejection distance of the aircraft, the launching valve opening degree curves are brought into the simulation system. The acceleration curves of the carrier-based aircraft can be achieved. They are shown in Fig. 6.

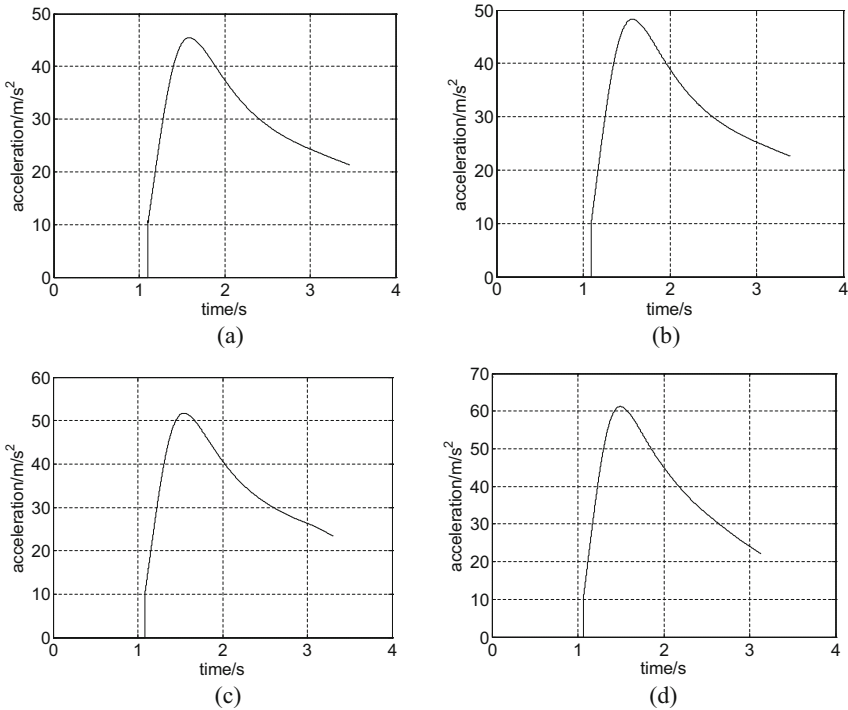


**Fig. 6.** Acceleration

### 4.3 Analysis of Steam Launching Valve Control System Results

The stability of the curve can be obtained by the peak-to-average ratio [9]. When the ratio gets closer to 1, the peak is closer to the mean. Namely, the acceleration changes smoother. By calculating the peak-to-average ratio of each acceleration curve, the results are gotten in Table 2.

**Table 2.** Peak-to-average ratio.

Acceleration curve number	Peak	Average	Peak-to-average ratio
a	45.4298	31.1034	1.4606
b	48.2766	32.9458	1.4653
c	51.7262	35.1181	1.4729
d	61.2138	39.7893	1.5384

From Table 2, we can see that from (a) to (d), the peak-to-average ratio is increasing. The reason can be summarized from the launching valve opening degree curves. In (a), the launching valve opening degree continues to grow in 3s. After that, the maximum of the launching valve opening degree is maintained until the ejection process ends. In (b), the launching valve opening degree also continues to increase until



3s. When the launching valve opening degree reaches its maximum, it maintains for 0.5s. Then, the launching valve is turned off in 1s. In (c), the launching valve is opened in 3s. Afterward, the launching valve opening degree is reduced until the ejection ends. In (d), the launching valve opening degree continues to increase in 2s. And then, the maximum is kept for 0.5s. At last, the launching valve is closed until the end.

It can be seen from (a) to (b), when the time of the two launching valves reach the maximum is the same, the value of the peak-to-average ratio decreases, with the growing of time that the maximum of the launching valve opening degree remains longer. This law is also applicable to (b) and (c). And what's more, in (b) and (d), when the time of the two launching valves keep the maximum is the same, the longer of the launching valve opening degree rises, the smaller the peak-to-average ratio will be.

It can be summed up that the longer the launching valve reaches the maximum and maintains the maximum, the smaller the peak-to-average ratio will be, the more stable the acceleration changes, the more smoothly the carrier-based aircraft takes off.

## 5 Conclusions

The carrier-based catapult aircraft taking off model is established. By simulation, it shows that the model of the carrier-based aircraft system given in this article can be applied to study the effect of the launching valve. Then, the launching valve opening degree curves are designed. The acceleration of the carrier-based aircraft can be obtained under the different launching valve opening degree. According to the multiple calculation and analyses, the laws of how to open the launching valve can be got. The longer the launching value reaches the maximum and the longer the launching value maintains the maximum, the smaller the peak-to-average ratio will be, the more stable the acceleration changes, the more smoothly the carrier-based aircraft takes off.

The law of the launching valve opening conforms to the actual processes. The model lays a foundation for the carrier-based aircraft taking off simulation and the study of the aircraft taking off safety.

**Acknowledgement.** This work was supported in part by the National Natural Science Foundation of China (No. 61673129,51674109) and the Harbin Application Research Funds (2016RQXJ096).

## References

1. Becherini, G., Fraia, S.D., Tellini, B.: Analysis of the dynamic behavior of a linear induction type catapult. *IEEE Trans. Plasma Sci.* **39**, 59–64 (2011)
2. Liu, C.G., Liu, L.Y., Zi, L.H., et al.: Assessment and regression analysis on instant catapult steam explosion pretreatment of corn stover. *Bioresour. Technol.* **166**, 368–372 (2014)
3. Jin, J., Yan, Z., Hu, J.: Modeling and simulation of dynamic performance of horizontal steam-launch system. *J. Cent. South Univ.* **20**, 3604–3611 (2013)
4. Cheng, G., Ni, H., Sun, F.: Modeling and simulation research on naval steam-power aircraft launch system. *J. Wuhan univ. Technol. (Transp. Sci. Eng.)* **34**, 301–305 (2010)

5. Stevanovic, V.D., Maslovaric, B., Prica, S.: Dynamics of steam accumulation. *Appl. Therm. Eng.* **37**, 73–79 (2012)
6. Liu, J.: Study on the ejection process of the UAV catapult supplied by gas cylinder. Zhengzhou University (2013)
7. Zhang, L., Feng, Y., Xue, X.: Dynamics simulation of carrier based aircraft steam catapult. *Aeronaut. Comput. Tech.* **42**, 29–33 (2012)
8. Li, X.: Simulation of key technology of launch and land for carrier-based aircraft. Harbin Engineering University (2012)
9. Yan, Z., Jin, J., Zhu, Y.: Research on control strategy of a horizontal steam-launch system. *Ship Sci. Technol.* **35**, 126–129 (2013)

# Design and Implementation of Food Safety Traceability System Based on RFID Technology

Jie Ding<sup>1,2</sup>, He Xu<sup>1,2(✉)</sup>, Peng Li<sup>1,2</sup>, and Runyu Xie<sup>3</sup>

<sup>1</sup> School of Computer Science,  
Nanjing University of Posts and Telecommunications, Nanjing, China  
1248395233@qq.com

<sup>2</sup> Jiangsu High Technology Research Key Laboratory  
for Wireless Sensor Networks, Nanjing, China  
{xuhe, lipeng}@njupt.edu.cn

<sup>3</sup> Bell Honors School,  
Nanjing University of Posts and Telecommunications, Nanjing, China  
578107039@qq.com

**Abstract.** Food safety is a crucial event concerned with people's healthy. In recent years, the situation of food safety accidents occurs frequently. The main reasons leading to this situation is lack of food security mechanism, and the information is not timely updated on all aspects of food from production to consumption, which could not be found when the food safety problems occur. For this case, this paper is based on RFID technology, combined with existing food production, warehousing and logistics, and proposes a comprehensive food safety traceability system. The system is designed and implemented, which can improve the productivity of food enterprises in the production section, reduce the error rate of storage and logistic links, and enhance food security, which also improves information sharing and enhances the competitiveness of food enterprises.

## 1 Introduction

Food safety has changed into a major concern of the community [1]. The whole process of food traceability is an important means to guarantee the quality and security of the production enterprises, implement the main responsibility for quality and security, improve the production quality management and build a safe society consumption environment, which is a powerful weapon against criminals. At present, Chinese traceability system is under a stage of development, because of the high technique requirement, it is difficult to implement and needs large investment. Due to enterprises lacks of credibility and other reasons, most of the food enterprises cannot hold the implementation of food safety process traceability system, especially for the small and medium enterprises.

Radio frequency identification (RFID), unlike other automatic identification technology, which does not require identification of contact, can work in severe conditions such as dense fog, heavy snow, under-mine, etc. [2–4]. At the same time, RFID technology can also discriminate various tags, greatly improves the efficiency of

identification. Owing to these superiorities of RFID technology, it is also known as one of the most promising applications in the 21st Century.

The food industry is the livelihood of our industry [5, 6]. The healthy development of food is related to the people's health problems, so the national development of food industry is showing enough attention, which has promulgated many laws to regulate domestic food production and circulation. Because the degree of information of food industry is not high and the way of collecting information is slow, much information cannot be achieved in all aspects of food production, warehousing, logistics, sales and timely sharing, which results in China's food industry supply chain efficiency is low [7, 8]. And because the link information cannot achieve efficient acquisition, real-time sharing and transparent management cannot deal with. In the management process aiming at counterfeit and inferior food safety problems cannot be proceeded in a timely manner, when the responsibility is not easy to implement. The food industry production, circulation and sales problems mainly include the following respects.

- (1) In the edible production, producers have no real-time understanding of downstream manufacturers, inventories and sales, which is unable to adjust production according to sales and results in underproduction or overproduction. This is not conducive to sustainable development of enterprises.
- (2) The illegal manufacturers use various ways to avoid to be checked for national food authority, indiscriminate production of counterfeit and inferior food. However, the national food inspection authority does not have effective methods in the investigation, which led to a lot of circulation of fake and shoddy foods on the market, and seriously affects physical and mental health of human.
- (3) Because storage and logistics use manual operation, which increases the intensity of staffs, but also aggrandizes the rate of false goods, according to the related survey that the rate of warehousing and logistics link error has reached more than 30%. Rework time has spent a great deal of error correction, which gives negative impact of corporate reputation.
- (4) Because of the blind spots of food circulation management, some organizations sale this wanton offsite series of goods, gain a great deal of illegal income, seriously harm to the rightful business benefits, undermine the workings of market rules, and stunt the sound trend of the food industry. There are two reasons in the food industry. First of all, it lacks an efficient means of information collection followed by the manufacturing, warehousing and logistics. Marketing aspects lack an effective sharing information in real time. If RFID technology is used in the food industry and the particular software is designed for food industry management, the issues discussed above can be solved in some aspects.

In this paper, RFID traceability system is proposed by using RFID technology and Internet. The system has the following advantages: the data is automatically collection and recognition using characteristics of RFID which can help enterprise to fast obtain object information; and the Internet technology, coding technology and e-commerce technology are combined with and used to achieve on target in any time at any locations in fast recognition, which is effective for target to be tracked and dates back. This can change existed business process achieved information to be fast shared, speed up logistics running, perfect enterprise existing warehouse process, achieve out

automatically storage, read and statistics, and improve the management efficiency and the quality and traceability of products.

## 2 RFID Anti-counterfeiting Technology

RFID electronic tag is divided into five categories according to its function [9]. It is used only with information storage function, which do not have the ability to deal with the password in Class1 type tags. Products using EPC (Electronic Product Code) code for the unique identification of the product [10, 11], in line with the current standards for the development of the Internet of things. The standard EPC encoding structure contains: EPC-64, EPC-96 and EPC-256. Considering the current development of mainstream encoding system, the cost and liquor shipments, EPC-96 encoding is chosen in this paper, where the encoding length is divided into four parts: 96bit, 8bit, 28bit and 24bit, which contains manufacturer identification code, product classification code and serial number. For the uniform manufacturer, the manufacturer identification code is the same. For the uniform type of product, the product classification code is the same. And the serial number of each commodity is distinguished. In this paper, the Hash function is used to extract the digital digest of the EPC code, and the encryption is used to prevent the forgery and tamper of the EPC code. Hash function in the current application is a wide range of MD5. For example, it is used in the private key RSA encryption algorithm.

At the production period, manufacturers extract the EPC encoded MD5 digest, and use private key to encrypt, digital signatures are stored in the database. Signature is stored in the RFID tags in the user area. During the authentication phase, there are two steps. The verification phase is shown in Fig. 1. The first step is to match the database: TID is encoded into EPC encoding and validated in the database, if EPC encoding and TID coding is incorrect, then the tag is not valid. The second step is to verify the signature, where the signature verification is shown in Fig. 2. TID is encoded as MD5 process to read, the expected digest is obtained and to be abstracted after RSA encryption algorithm is used to form the number of signatures; signature and read the summary of the user area to compare, if they are equal, the tag is valid, then product specific information will be submitted to a database and returns a result, otherwise it is invalid.

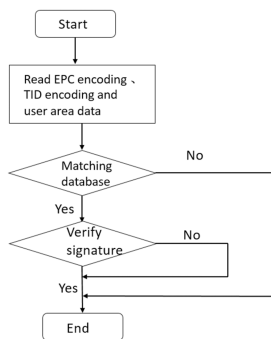


Fig. 1. Anti-counterfeiting process

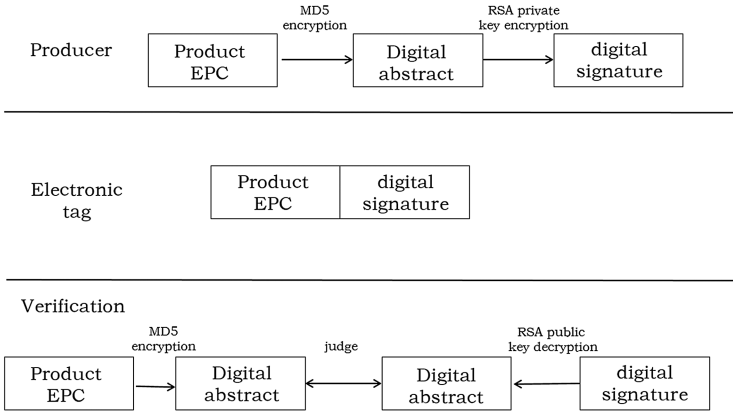


Fig. 2. The signature verification process

According to the requirements of system security and cost control, passive UHF Class 1 type RFID electronic tags are used in this paper. According to the tag design, there are two kinds of destruction method which is software and hardware. The destruction of the software is to send the kill command to the tag through the authorized reader, which makes the tag permanently damaged. It needs the tag to have self-destruct function, which makes the manufacturing cost is higher. When it is the sale to consumers like wine, it no longer has a query anti-counterfeiting function, which may be inappropriate for drinking and often not necessary to immediate donation to other wine. While the hardware system uses the tag storage module and antenna where the tag is divided into two parts, and the tag is pasted between the bottle and the cap. When the cap is opened, the storage module and the antenna is physical separation, and the permanent damage of the tag will cause the tag cannot be used again.

For information transfer stage, manufacturers and dealers use their own private key to encrypt data and send to the security center. Under the prerequisite of guaranteeing the security of private key, fraud cannot be fabricated and tampered with the information which can ensure the security of communication phases. Because the tag EPC is encoded as MD5 and the RSA encryption is used, an attacker cannot forge a digital signature, which puts an end to the possibility of counterfeiting and tampering the EPC code. Even if we could estimate the EPC encoding of factory goods, its signature cannot be forged about the tag.

In conclusion, this system uses RFID technology to control food security, which is able to meet the security needs, has large amount of information to be stored and strong environmental adaptation, verification efficiency, and supports the product traceability function. From the above analysis, we can see that criminals can hardly try to disguise the legitimate manufacturers to attack security center or forgery or tampering tag. However, RSA encryption crack problem is inevitable, and the difficulty of RSA problem is due to the current level of technology which cannot break in the effective time. Although the RFID security has many superiorities, it also confronts with some troubles: (1) The early cost of the security system construction is higher.

(2) The security process requires the reader to support, and ordinary users cannot read tag information. Along with the expansion of mobile phone functions, the mobile phone which can scan electronic tag has emerged. As the mobile phones are used more and more popular, it will solve this problem.

### 3 Design of RFID Based Food Safety System

The system is composed of user management module, information acquisition module, supervision module, user recommendation module and product traceability. The structure is shown in Fig. 3.

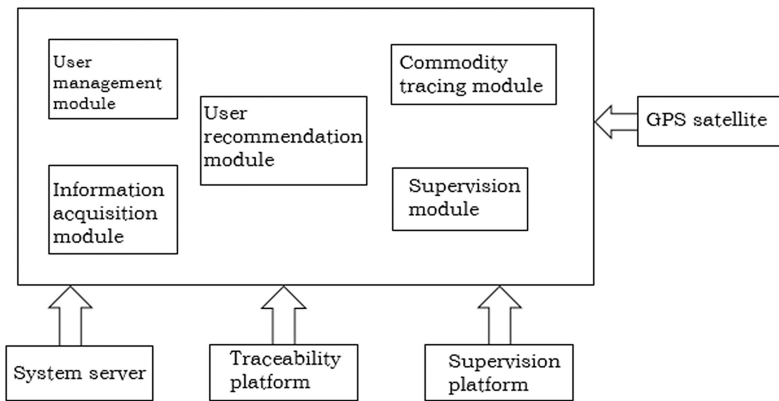


Fig. 3. System module overview

The user management module: it is used by administrator for producers, processors, logistics companies and other enterprises. It needs to fill in the registration information and login, which is easy to grasp the dynamic information of products.

The information acquisition module is used for the enterprise to collect the information into the system database. For example, manufacturers, their name, address, contact information and other information of goods are selected into the database.

The supervision module is used to monitor the product from the production link to the sales of the abnormal situation, and then report to the relevant enterprises and send warning messages.

The user recommendation module is used for the consumer to express opinion to the system. Manufacturers use it to improve their products and support better service to consumers.

The product traceability module is to offer “reverse back” function for consumers. When users purchase goods, through inputting the tracing number in mobile phone dish (manual input, or shooting, identity number, bar code), it can use the data service center for production, where the information may include the source of food manufacture date, back information of transportation node. The flow chart of this module is shown in Fig. 4.

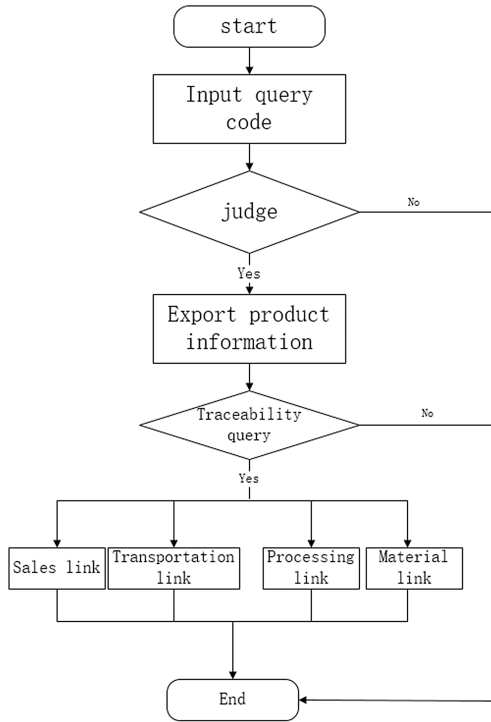


Fig. 4. Traceability module process

The logic database of system uses E-R diagram to show. The E-R diagram is the abbreviation of entity relation graph (Entity Relationship Diagram), which provides the method of representing entity type, attribute and relation. It is an effective method to describe the conceptual structure model of the real world. In the following E-R diagram, a rectangle represents an entity, and a diamond indicates a corresponding relation. Where the 1 sides of the diamond are represented by a pair of 1 pairs of relations, and the relation between the 1 and the n is represented by 1 pairs of relations, and the m and the n represent many-to-many relationships. Here are a few important E-R diagrams.

Figure 5 shows the logical relationship among the entities in the production process, such as administrator, production information, the box tag information, the operator and so on.

Figure 6 shows the logical relationship among the entities in the storage link, such as the goods, administrator, inventory, documents, information and so on.

Figure 7 shows the logical relationship among the entities in the sales link, such as drivers, administrator, logistics information and so on.

The food industry contains a large number of types of food, and the realized system gives the dairy industry as an example to design. In this system, the amount of data is complex, the design data table entity table includes the administrator, producers, processors and statistics information.

Here are the system most important tables.



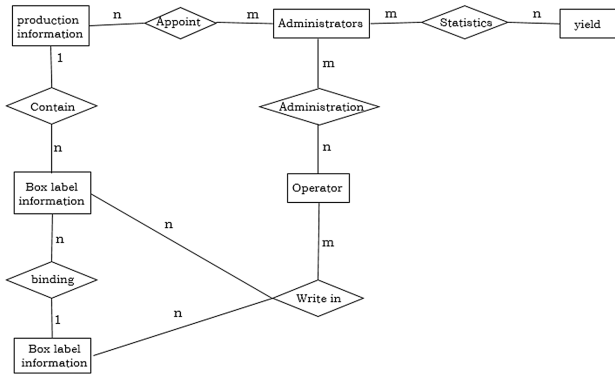


Fig. 5. E-R diagram of production link

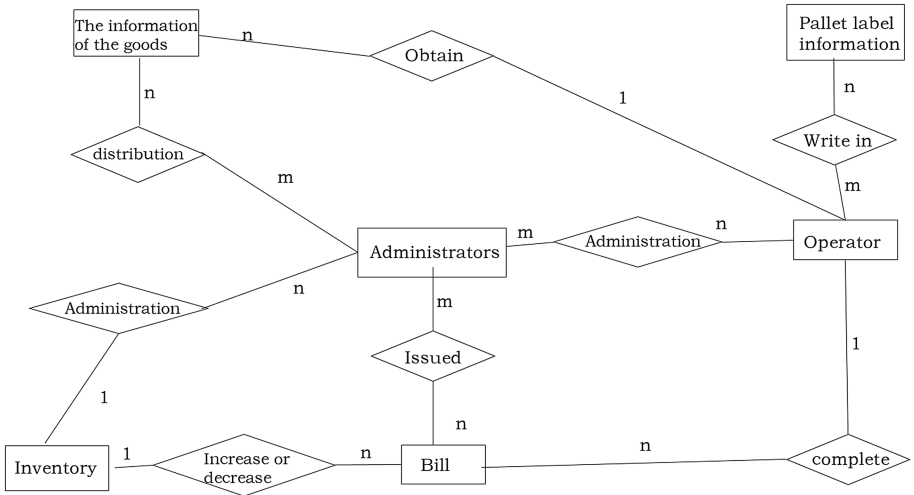


Fig. 6. E-R diagram of storage link

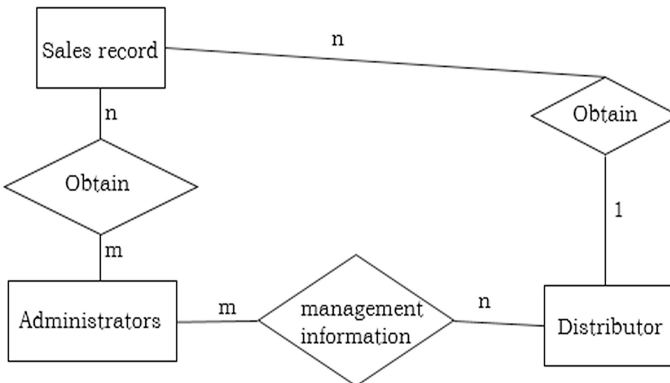


Fig. 7. E-R diagram of sale link

The Table 1 mainly stores a box of milk binding information, including the basic information of milk and the status of sales information.

**Table 1.** The milk information table

Field name	Field type	Field description
Xbox_num	Int(11)	Milk box number
Mbox_num	Int(11)	Milk mbox number
Xiaoshou	Varchar2(60)	Sales status
Milk_name	Varghar2(60)	Milk name
Milk_date	Date	Date of manufacture
FactoryName	Varchar2(60)	Processing factory
FactoryClass	Varchar2(60)	Milk category
Milk_yuan	Varchar2(60)	Milk ingredients
Line	Varchar2(60)	Production line
Product_pihao	Int(11)	Batch number
Team	Varchar2(60)	Production team
Inspector	Varchar2(60)	Inspector

The Table 2 mainly stores the data about the logistics link.

**Table 2.** The logistics information table

Field name	Field type	Field description
Mbox_num	Varchar2(60)	Milk mbox number
Van_num	Varchar2(60)	Truck number
Start_di	Varchar2(60)	Originating place
End_di	Varchar2(60)	Destination
Sell_company	Varchar2(60)	Name of manufacturer
Transport_zhuang	Varchar2(60)	Transport status
Driver_name	Varchar2(60)	Driver name
Driver_iphone	Varchar2(60)	Driver telnumber

The Table 3 mainly stores the main repository of environmental information.

**Table 3.** The warehouse table

Field name	Field type	Field description
Mbox_num	Varchar2(60)	Milk mbox number
Cangku_num	Varchar2(60)	Warehouse number
Temperature	Varchar2(60)	Warehouse humidity
Humidity	Varchar2(60)	Warehouse temperature

## 4 Implementation

The system uses B/S architecture, and Oracle 12C is used as the background database. Tomcat 9.0 is used as the server software. JDK8.0, myeclipse10.0 and struts 2.3.16 are the corresponding software development environment.

The RFID reader of Fig. 8 can scan the RFID Tag information. In the server, it completes the security functions of RFID-based food management system.

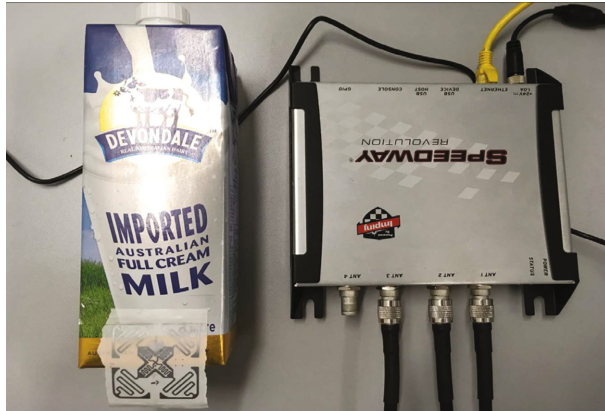


Fig. 8. Milk and RFID tag

This interface of Fig. 9 is the information query module. Users can enter the product code in this interface to query the information about the product.



Fig. 9. Query interface

## 5 Conclusion

In this paper, RFID technology is used in the food industry, and we design a system for food security. Combined with existing food production, warehousing, logistics, we propose a comprehensive application system of food safety traceability system. The security tracking system is designed and implemented, which can improve productivity of food enterprises in the production section, reduce the error rate of storage and logistics links, and enhance food security, which also improves information sharing and enhances the competitiveness of food enterprises.

**Acknowledgments.** This work is financially supported by the National Natural Science Foundation of P. R. China (No. 61373017, No. 61572260, No. 61572261, No. 61672296, No. 61602261), the Natural Science Foundation of Jiangsu Province (No. BK20140886, No. BK20140888), Scientific & Technological Support Project of Jiangsu Province (No. BE2015702, BE2016185, No. BE2016777), Natural Science Key Fund for Colleges and Universities in Jiangsu Province (No. 12KJA520002), China Postdoctoral Science Foundation (No. 2014M551636, No. 2014M561696), Jiangsu Planned Projects for Postdoctoral Research Funds (No. 1302090B, No. 1401005B), Jiangsu Postgraduate Scientific Research and Innovation Projects (SJLX16\_0326), Project of Jiangsu High Technology Research Key Laboratory for Wireless Sensor Networks (WSNLBZY201509), NUPTSF (Grant No. NY214060, No. NY214061) and the STITP projects of Bell Honors School of NUPT (No. ZD201606 and No. YB201615).

## References

1. Cordell, D., White, S.: Tracking phosphorus security: indicators of phosphorus vulnerability in the global food system. *Food Secur.* **7**(2), 337–350 (2015)
2. Sula, A., Spaho, E., Matsuo, K., et al.: A new system for supporting children with autism spectrum disorder based on IoT and P2P technology. *Int. J. Space Based Situated Comput.* **4**(1), 55–64 (2014)
3. Pereira, R., Pereira, E.G.: Future internet: trends and challenges. *Int. J. Space Based Situated Comput.* **5**(3), 159–167 (2015)
4. Sakurai, S.: Prediction of sales volume based on the RFID data collected from apparel shops. *Int. J. Space Based Situated Comput.* **1**(2–3), 174–182 (2011)
5. Malla, Y.B.: Impact of community forestry policy on rural livelihoods and food security in Nepal. *Unasyilva* **51**(202), 37–45 (2016)
6. Larochez-Dupraz, C., Huchet-Bourdon, M.: Agricultural support and vulnerability of food security to trade in developing countries. *Food Secur.* **8**(6), 1191–1206 (2016)
7. Ramanujam, N., Chow, S.: Towards a human dignity based approach to food security: lessons from China and India. *Front. Law China* **11**(2), 243–265 (2016)
8. Smyth, S.J., Phillips, P.W.B., Kerr, W.A.: EU failing FAO challenge to improve global food security. *Trends Biotechnol.* **34**(7), 521–523 (2016)
9. Ahson, S.A., Ilyas, M.: *RFID Handbook: Applications, Technology, Security, and Privacy*. CRC Press, Boca Raton (2008)
10. Tseng, C.W., Yu-Chang, C., Huang, C.H.: A design of GS1 EPCglobal application level events extension for IoT applications. *IEICE Trans. Inf. Syst.* **99**(1), 30–39 (2016)
11. Tolcha, Y., Kim, D.: Distributed event-based resource-oriented EPCglobal middleware using GPC. In: 2016 IEEE International Conference on RFID Technology and Applications (RFID-TA), pp. 29–34. IEEE (2016)

# PaEffExtr: A Method to Extract Effect Statements Automatically from Patents

Na Deng<sup>1</sup>(✉), Xu Chen<sup>2</sup>, Ou Ruan<sup>1</sup>, Chunzhi Wang<sup>1</sup>, Zhiwei Ye<sup>1</sup>,  
and Jingbai Tian<sup>1</sup>

<sup>1</sup> School of Computer, Hubei University of Technology, Wuhan, China  
iamdengna@163.com

<sup>2</sup> School of Information and Safety Engineering,  
Zhongnan University of Economics and Law, Wuhan, China  
chenxu@zuel.edu.cn

**Abstract.** Patents contain a lot of technical, economic and legal information, and they are the main references of enterprises' technological innovation. As a tool of patent analysis and mining, technology/effect matrix provides important support for technological innovation and avoidance. In the process of building technology/effect matrix, most of current technical efficiency annotation is by manually work, which requires heavy labor. Considering the distribution and morphological characteristics of patent abstract texts, this paper proposes a multi-features fused scoring algorithm named PaEffExtr, which automatically extracts effect statements from patent abstract texts. The experimental results show that the algorithm has good recall and accuracy.

## 1 Introduction

With the development of society, people are more and more aware of the tremendous changes in our life brought about by innovation. As one of the most important ways to protect innovation, patent has been paid more and more attention. More and more patents are accumulated in the worldwide since the amount of patents applications increases year by year. Because patents contain rich technology, economy and law information, patent analysis and mining has become an important research topic in the field of data mining. Nowadays, with the rapid development of market economy, enterprises have to seize the highland of technology for sustainable development. Technology/effect matrix is a tool of patent analysis and mining. It can help enterprises to find technology vacant areas and minefields, and provides important support for technological innovation and avoidance. In the process of building technology/effect matrix, the annotation of technology/effect is a rather important step. At present, technology/effect is mostly by manual annotation, requiring a lot of heavy manual labor. In addition, manual annotation is subjective, for the same patent, different annotators may have different ways, which may bring hidden trouble for patent mining. This paper aims to solve these problems.

## 2 Related Work

In recent years, there are many research on patent analysis and mining at home and abroad. [1] investigated multiple research questions related to patent documents, including patent retrieval, patent classification, and patent visualization. [2] used OPTICS algorithm and k-nearest neighbor to implement clustering analysis of patent information. [3, 4] tried to focus on vacant technology forecasting, by using K-medoids or Bayesian. [5] gave a survey on different text clustering techniques for patent analysis. [6] used self-organizing map (SOM) approach to cluster patents into different quality groups and used support vector machine (SVM) to build up the patent quality classification model. [7] studied the patent document classification problem by deep learning. [8] focused on keyword strategies for applying text-mining to patent data and addressed four factors about key words.

In the domain of patent technology effect matrix, there are also some but not many research [9–15]. Japanese scholars [9, 10] were the earliest to study on technology effect matrix of Japanese and English language patents. [11] applied semantic role labeling to create technology-effect matrix. [12] proposed a method for matrix structure construction based on feature degree and lexical model. [13] gave one kind method based on conditional random field model (CRFs) to recognize effect phrases.

In the authors' previous work about patent analysis and mining [14–17], we mainly focused on the removal of stop words in patents, intelligent recommendation of the traditional Chinese medicine patents and effect annotation. In the research about annotation, we found that the same patent inventor has his/her preferred style of writing; thus, using co-training method, effect statements' extraction is divided into chain extraction and keywords extraction, which iteratively annotate effect statements in patent abstract. However, the limitation of this method is that it is easy to produce misjudgment. That is, some statements that are closely related to each other but actually not effect statements will be deemed as effect statements falsely. In this paper, making use the distribution and morphological characteristics of patent effect statements, and trying to make the extraction algorithm more general, but not limited to a patent inventor, we propose a multi-features fused scoring algorithm for automatic extraction of effect statements.

The rest of paper is organized as follows: Sect. 3 analyzed and summarized the characteristics of Chinese patent abstract, including distribution and morphological characteristics of effect statements. Section 4 described the automatic annotation algorithm PaEffExtr in detail. Section 5 analyzed and explained the experimental results. Section 6 concluded the paper and prospected the future work.

## 3 Characteristics of Patent Abstracts

Generally, a patent text consists of title, abstract, claim and specification. Patent abstract is a summary of the whole content of the patent text. It is short, but contains the composition structure of the invention, technologies used, design principles, functions, scope of application and other important information. Therefore, patent abstract is the data source of many patent mining experiments. In patent abstract, there is usually a description of the function and application scope of the invention, which is called as

patent effect. The purpose of this paper is to automatically extract effect statements from Chinese patent abstracts.

In order to facilitate the following explanation, two definitions are given as follows:

**Definition 1: patent effect statements**

A collection of statements describing the function and application scope of the invention in the text of patent abstract, denoted as ES. From the perspective of linguistics, the elements in this collection are not necessarily close to each other in the abstract text.

**Definition 2: patent effect clause**

The element in patent effect statements, denoted as ec. From the perspective of linguistics, patent effect clause may be a single sentence, and also may be a clause in a long sentence.

So we can say that  $ES = \{ec\}$ .

After observing a large number of patent abstracts, we found that effect statements had two obvious characteristics.

- (1) Distribution characteristic: in patent abstracts, the positions of effect clauses follow certain rules. In many cases effect clauses appear at the end of the abstract, in a few cases appear in the head of the abstract, in rare cases in the middle of the abstract. Sometimes, all of the effect clauses in a patent abstract are distributed in multiple places, but in many cases, all the effect clauses appear in a continuous way.
- (2) Morphological characteristic: because effect statements describe the function and the scope of application of the invention, there are often specific clue words in effect clauses. These clue words may be used to guide the emergence of an effect clause, and may also indicate which aspects have changed, what changes have been made and so on.

According to different situations, we divide the clue words into the following categories.

- (1) leading word: a word used to guide the emergence of effect clause. For example: “have”, “can”, “apply to”, “used to”, “make”, etc.
- (2) facet word: a word used to indicate which aspects have changed brought by a patent invention. For example: “cost”, “performance”, “quality”, “efficiency”, etc.
- (3) changing word: a word reveals what changes have been made by a patent invention. For example: “improve”, “simple”, “lower”, “avoid” and so on.
- (4) degree word: a word used to indicate the extent to which a patent invention have changed. For example: “significant”, “obvious”, etc.

## 4 Multi-features Fused Scoring Algorithm

According to the introduction above, we find that effect clauses in patent abstract have its obvious distribution and morphological characteristics. Those clauses at specific locations and containing clue words are more likely to be effect clauses than other clauses. Therefore, we design a multi-features fused scoring algorithm, based on the

location information and whether containing clue words, to give score to each clause, and choose those with high scores as effect clauses.

#### 4.1 Calculation of Distribution Score

There is no mandatory requirement for the writing of abstract text of patents, so patent applicants usually write according to their own habits and preferences. Through the observation we found that in many cases, functions and application scope of patents are located in the tail of the abstracts, in few cases are in the head, in rare cases are in the middle, even sometimes there is not any effect statement in some abstract. In addition, the use of punctuation marks is also very arbitrary. Some applicants are accustomed to use periods to separate the patent structure, technology, design principle, function and application range, some tend to use a semicolon, and some only use commas directly. In this paper, we will use the comma, semicolon, periods etc. as delimiter, to separate abstract into clauses. We calculate distribution score using the following method.

With regard to a patent abstract text  $T$ , we use  $C$  to represent the set of all its clauses. For the  $i$ th clause  $c_i$ , its distribution score is calculated as:

$$D_i = \begin{cases} \gamma_1 & \text{when } 0 < i < \frac{N}{3} \\ \gamma_2 & \text{when } \frac{N}{3} \leq i < \frac{2N}{3} \\ \gamma_3 & \text{when } \frac{2N}{3} \leq i \leq N \end{cases} \quad (\gamma_1 + \gamma_2 + \gamma_3 = 1) \quad (1)$$

In Formula 1,  $|C| = N$ ,  $D_i$  represents the distribution score of  $c_i$ . The abstract text is divided into 3 parts, each of which is given a single weight.

#### 4.2 Calculation of Morphological Score

Because the clauses containing clue words are more likely to be effect clauses than others, so we check whether the clause contains clue words and how many clue words to calculate morphological score.

The collection of clue words is the key to calculate morphological score. Through the observation, we found that clue words appear frequently in effect statements, so we use statistical methods to find them. By manually annotating effect clauses of a certain number of patents, looking for high-frequency words, artificial screening, and several rounds repeated, we constitute a clue words set called ClueWords.

With regard to a patent abstract text  $T$  and  $i$ th clause, the morphological score is calculated as follows.

$$M_i = \lambda k_i \quad (2)$$

In (2),  $k_i$  represents the number of clue words contained in  $c_i$ .



### 4.3 Algorithm PaEffExtr

In summary, for the  $i$ th clause in a patent abstract text T, the score is calculated as follows:

$$Score_i = \alpha D_i + \beta M_i \quad (\alpha + \beta = 1) \quad (3)$$

Here,  $\alpha$  and  $\beta$  are the weights of  $D_i$  and  $M_i$  respectively.

The following is the algorithm of extracting effect statements from patent abstract.

Algorithm PaEffExtr:

Input: Patent abstract text, denoted as T, the set of all ClueWords, denoted as {ClueWords}, parameters  $\gamma_1, \gamma_2, \gamma_3, \lambda, \alpha, \beta$  and threshold  $th$

Output: The set of all annotated effect clauses, denoted as ES

Begin

    Separate T into clauses by punctuations;

    For each clause  $c_i$ :

        Calculate position score  $D_i$  of  $c_i$  using (1);

        Segment  $c_i$  into words by NLPPIR, denoted as {words};

$k_i=0$ ;

        For each word w in {words}:

            If w in {ClueWords}:

$k_i++$ ;

        End for

        Calculate morphological score  $D_i$  of  $c_i$  using (2);

$Score_i = \alpha D_i + \beta M_i$

        If  $Score_i > th$ :  $ES = ES \cup \{c_i\}$ ;

    End for

End

In this algorithm, firstly, the abstract text is separated into clauses with the period, comma, semicolon, colon, question mark, brackets and spaces. According to each clause's position, distribution score is calculated; secondly, segment words for each clause using NLPPIR [18], count the number of clue words and calculate morphological score; thirdly, fuse distribution score and morphological scores together, and calculate the total score; finally, put all the clauses with the total score higher than the threshold into the set of effect clauses.

It is not difficult to see that the constitution of clue words set is the key point of the algorithm, since the accuracy of the set directly affects the accuracy of the algorithm. In order to ensure the integrity and usefulness of clue word set, we use the idea of iteration to collect clues words. First of all, annotate some patents manually, find out the high-frequency words, after artificial screening, keep high-quality ones as the initial set

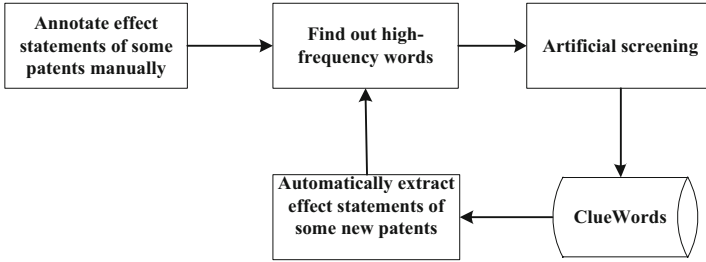


Fig. 1. The constitution process of clue words set

of clue words; then use the automatic extraction algorithm above to extract effect clauses of more patents, find out high-frequency words again, artificial selection, add new clue words into the initial clue words set; repeat iteratively until the clue word set arrive to a stable state. As shown in Fig. 1.

#### 4.4 Evaluation of Algorithm

In this paper, we compare automatically annotated effect statements with those manually annotated, using two indicators: precision and recall to evaluate the effectiveness of the algorithm.

Assuming that for the *i*th patent abstract, the set of effect clauses by manual annotation is  $P_i$ , and the set of effect clauses by automatic annotation is  $Q_i$ , then, the precision and recall of our algorithm on this patent abstract are computed as the following.

$$\text{Precision}_i = \begin{cases} \frac{|P_i \cap Q_i|}{|Q_i|} & \text{when } |P_i| > 0 \text{ and } |Q_i| > 0 \\ 1 & \text{when } |P_i| = 0 \text{ and } |Q_i| = 0 \\ 0 & \text{when } |P_i| > 0 \text{ and } |Q_i| = 0 \\ 0 & \text{when } |P_i| = 0 \text{ and } |Q_i| > 0 \end{cases} \quad (4)$$

$$\text{Recall}_i = \begin{cases} \frac{|P_i \cap Q_i|}{|P_i|} & \text{when } |P_i| > 0 \text{ and } |Q_i| > 0 \\ 1 & \text{when } |P_i| = 0 \\ 0 & \text{when } |P_i| > 0 \text{ and } |Q_i| = 0 \end{cases} \quad (5)$$

Generally speaking, for N patent abstracts, the precision and recall of our algorithm are computed as the following.

$$\text{Precision} = \frac{1}{N} \sum_{i=1}^N \text{Precision}_i \quad (6)$$

$$\text{Recall} = \frac{1}{N} \sum_{i=1}^N \text{Recall}_i \quad (7)$$

## 5 Experiments

We use Java language to implement the algorithm, with 50,000 patent abstracts from Chinese universities and research institutions as the data source. In this section, the experimental results are given.

### 5.1 Clue Words

Table 1 exhibits part of clue words after several rounds of algorithm operation and manual screening.

**Table 1.** Some clue words

function	can	have	use	effect	obvious	fit for
beneficial	get	achieve	time	precision	advantage	widely
increase	low	simplify	capacity	stable	quality	side effect
outstanding	thus	shorten	range	influence	prospect	optimization
feasible	solve	treat	price	advantage	favorable	improve
important	act	solid	easy	cheap	thorough	sensibility
application	speed	high	avoid	reliability	promote	significant

### 5.2 Comparative Experiments

By setting different parameters and thresholds, the precision and recall of the algorithm are compared. Table 2 shows the evaluation results of 24 groups of experiments with different parameters. We can find some rules from these results.

- Rule 1: We can see that when  $\gamma_1, \gamma_2, \gamma_3$  values as 0.3, 0.2 and 0.5 respectively, the algorithm will get better precision and recall, since effect clauses prefer to be located in the tail the head of the abstract text.
- Rule 2: The differences brought by the weights of  $\alpha$  and  $\beta$  are not obvious.
- Rule 3: When the threshold is improved, the precision increases, but the recall reduces.
- Rule 4: When  $\lambda$  changes from 0.2 to 0.1, the precision increases, but the recall reduces.
- Rule 5: Group 9, 23 and 24 have the best precision, and Group 15 has the best recall.

### 5.3 Runtime

Figure 2 shows when the parameters and threshold are set to fixed values ( $\gamma_1 = 0.2, \gamma_2 = 0.1, \gamma_3 = 0.7, \lambda = 0.2, \alpha = 0.3, \beta = 0.7, th = 0.35$ ), the runtimes of our algorithm on different number of patent texts. It can be seen that the time complexity of our algorithm is approximately linear.

**Table 2.** Evaluation results of 24 groups of experiments with different parameters

Group no.	$\gamma_1$	$\gamma_2$	$\gamma_3$	$\lambda$	$\alpha$	$\beta$	Threshold	Precision	Recall
1	0.333	0.333	0.333	0.2	0.5	0.5	0.3	0.612	0.659
2	0.2	0.1	0.7	0.2	0.5	0.5	0.3	0.470	0.764
3	0.3	0.2	0.5	0.2	0.5	0.5	0.3	0.565	0.765
4	0.333	0.333	0.333	0.2	0.3	0.7	0.3	0.614	0.659
5	0.2	0.1	0.7	0.2	0.3	0.7	0.3	0.565	0.765
6	0.3	0.2	0.5	0.2	0.3	0.7	0.3	0.612	0.659
7	0.333	0.333	0.333	0.2	0.5	0.5	0.4	0.678	0.494
8	0.2	0.1	0.7	0.2	0.5	0.5	0.4	0.654	0.741
9	0.3	0.2	0.5	0.2	0.5	0.5	0.4	0.736	0.675
10	0.333	0.333	0.333	0.2	0.5	0.5	0.35	0.614	0.659
11	0.2	0.1	0.7	0.2	0.5	0.5	0.35	0.488	0.764
12	0.3	0.2	0.5	0.2	0.5	0.5	0.35	0.618	0.760
13	0.333	0.333	0.333	0.1	0.5	0.5	0.2	0.437	0.773
14	0.2	0.1	0.7	0.1	0.5	0.5	0.2	0.470	0.764
15	0.3	0.2	0.5	0.1	0.5	0.5	0.2	0.401	0.778
16	0.333	0.333	0.333	0.1	0.5	0.5	0.3	0.678	0.494
17	0.2	0.1	0.7	0.1	0.5	0.5	0.3	0.495	0.731
18	0.3	0.2	0.5	0.1	0.5	0.5	0.3	0.654	0.741
19	0.333	0.333	0.333	0.2	0.4	0.6	0.3	0.612	0.659
20	0.2	0.1	0.7	0.2	0.4	0.6	0.3	0.618	0.760
21	0.3	0.2	0.5	0.2	0.4	0.6	0.3	0.565	0.765
22	0.333	0.333	0.333	0.2	0.4	0.6	0.4	0.678	0.494
23	0.2	0.1	0.7	0.2	0.4	0.6	0.4	0.736	0.675
24	0.3	0.2	0.5	0.2	0.4	0.6	0.4	0.736	0.675

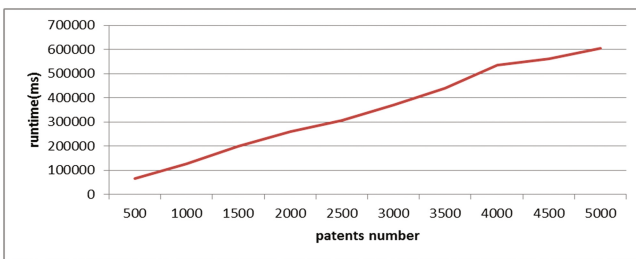


**Fig. 2.** The runtime of the algorithm

## 6 Conclusion and Future Work

In order to reduce the burden of patent annotators, this paper presents an automatic extraction algorithm of effect statements in Chinese patent abstracts. This algorithm uses distribution and morphological characteristics of effect statements, construct a clue

words thesaurus, and use scoring method to extract effect statements automatically. The algorithm is simple and direct, and has satisfying experimental results. It can also be extended to the automatic annotation of other patents information, such as technical words, coordinative phrases, and so on.

**Acknowledgments.** This paper was supported by Research Foundation for Advanced Talents of Hubei University of Technology (No. BSQD12131), the Fundamental Research Funds for the Young Teachers' Innovation project of Zhongnan University of Economics and Law (No. 2014147), the Educational Commission of Hubei Province of China (No. D20151401) and the Green Industry Technology Leading Project of Hubei University of Technology (No. ZZTS2017006).

## References

1. Zhang, L., Li, L., Li, T.: Patent mining. *ACM SIGKDD Explor. Newsletter* **16**(2), 1–19 (2015)
2. Fan, Y., Hongguang, F.U., Wen, Y.: Patent information clustering technique based on latent Dirichlet allocation model. *J. Comput. Appl.* (2013)
3. Jun, S., Sang, S.P., Dong, S.J.: Technology forecasting using matrix map and patent clustering. *Ind. Manag. Data Syst.* **112**(5), 786–807 (2012)
4. Choi, S., Jun, S.: Vacant technology forecasting using new Bayesian patent clustering. *Technol. Anal. Strateg. Manag.* **26**(3), 241–251 (2014)
5. Sharma, A.: A Survey On Different Text Clustering Techniques For Patent Analysis. *Esrta Publications* (2012)
6. Wu, J.L., Chang, P.C., Tsao, C.C., et al.: A patent quality analysis and classification system using self-organizing maps with support vector machine. *Appl. Soft Comput.* **41**, 305–316 (2016)
7. Xia, B., Baoan, L.I., Lv, X.: Research on patent document classification based on deep learning. In: *International Conference on Artificial Intelligence and Industrial Engineering* (2016)
8. Noh, H., Jo, Y., Lee, S.: Keyword selection and processing strategy for applying text mining to patent analysis. *Expert Syst. Appl.* **42**(9), 4348–4360 (2015)
9. Nonaka, H., Kobayahi, A., Sakaji, H., et al.: Extraction of the effect and the technology terms from a patent document. In: *International Conference on Computers and Industrial Engineering*, pp. 1–6. *IEEE* (2010)
10. Nonaka, H., Kobayashi, A., Sakaji, H., et al.: Extraction of effect and technology terms from a patent document (theory and methodology). *J. Jpn. Ind. Manag. Assoc.* **63**, 105–111 (2012)
11. He, Y., Li, Y., Meng, L.: A new method of creating patent technology-effect matrix based on semantic role labeling. In: *International Conference on Identification, Information, and Knowledge in the Internet of Things*, pp. 58–61. *IEEE* (2015)
12. Chen, Y.: Research of patent technology-effect matrix construction based on feature degree and lexical model. *New Technology of Library & Information Service* (2012)
13. Hou, T., Lv, X.Q., Xu, L.P.: Chinese patent efficacy phrase recognition. *Appl. Mech. Mater.* **743**, 510–514 (2015)

14. Chen, X., Deng, N.: A semi-supervised machine learning method for Chinese patent effect annotation. In: International Conference on Cyber-Enabled Distributed Computing and Knowledge Discovery, pp. 243–250. IEEE Computer Society (2015)
15. Chen, X., Peng, Z., Zeng, C.: A co-training based method for Chinese patent semantic annotation. In: ACM International Conference on Information and Knowledge Management, pp. 2379–2382. ACM (2012)
16. Deng, N., Chen, X.: Automatically generation and evaluation of stop words list for Chinese patents. *Telkommnika* **13**(4), 1414 (2015)
17. Deng, N., Chen, X., Li, D.: Intelligent recommendation of Chinese traditional medicine patents supporting new medicine's R&D. *J. Comput. Theor. Nanosci.* **13**, 5907–5913 (2016)
18. <http://ictclas.nlpir.org/newsDetail?DocId=387>

# An Efficient Data Aggregation Scheme in Privacy-Preserving Smart Grid Communications with a High Practicability

Bofeng Pan<sup>1</sup>, Peng Zeng<sup>1(✉)</sup>, and Kim-Kwang Raymond Choo<sup>2</sup>

<sup>1</sup> Shanghai Key Laboratory of Trustworthy Computing,  
East China Normal University, Shanghai, China  
panbofeng@hotmail.com, pzeng@sei.ecnu.edu.cn

<sup>2</sup> Department of Information Systems and Cyber Security, University of Texas at  
San Antonio, San Antonio, TX, USA  
raymond.choo@fulbrightmail.org

**Abstract.** Smart grids allow real-time monitoring and management of electricity usage, etc. to meet the varying demands of end users. In this paper, we propose an efficient data aggregation scheme in privacy-preserving smart grid communications. Specifically, users in our scheme can be divided into several groups of any size according to different criteria (e.g. geographic regions and desired features), and the control center (e.g. government, utility provider) can obtain real-time electricity usage information of each group in a privacy-preserving manner. This allows control center to conduct fine-grained analysis and make informed decisions.

**Keywords:** Smart grid · Privacy-preserving · Data aggregation · Data analysis

## 1 Introduction

Smart grids provide an intelligent way of managing, distributing, monitoring, and billing electricity usage, as well as providing utility providers predictive maintenance, self-healing and analytical (e.g. data can be analyzed to predict future usage) capabilities. A smart grid generally consists of smart meters (SMs) installed at user's premises, a gateway (GW), and a control center (CC) – see Fig. 1. Each user in a residential area has a SM installed, which unlike traditional meters has the ability of handling simple operations. For example, SM periodically collects electricity usage data and reports the data to a local GW. The GW pre-processes these received data and forwards the processed data to the CC for further analysis and processing. The CC, acting as the brain of the smart grid, can monitor grid status, balance electricity load, optimize energy consumption, etc., in real-time based on the received data [1].

In a smart grid, there may also exist a trusted authority (TA). For example, for schemes presented in [2–6], TA is tasked with initializing the system and

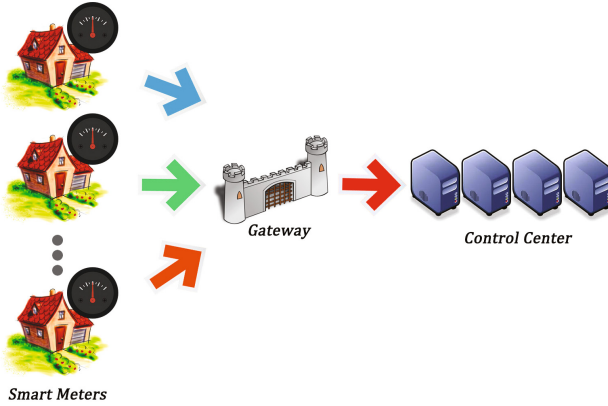


Fig. 1. Common smart grid structure

distributing the keys for the entities involved in a smart grid. However, having an additional entity (i.e. TA) may increase the complexity and overheads of the infrastructure; thus, when designing the scheme in this paper, we do not require a TA.

Similar to other consumer technologies, smart grids can be targeted by attackers for criminal exploitation (e.g. exploiting vulnerabilities in smart grids, particularly in resource-constrained nodes, to exfiltrate or modify data, as well as compromising the privacy of users) [7–12]. For example, unlike traditional power grids where metering data are only read monthly or half monthly, more detailed and granular electricity usage data are collected at much shorter time intervals in smart grids. Such data in the wrong hands would compromise the privacy of users (e.g. usage patterns, types of household devices and appliances, and daytime habits) [10]. Thus, it is important to provide a secure manner for the CC to obtain computation results of smart meter readings without revealing other non-essential information about individual users. When designing security solutions, we also need to consider the computational limitations in smart meters (e.g. limited battery life). Wherever possible, we should transfer the heavy computational tasks from resource-constrained smart meters to entities with higher computational capability (e.g. CC). We also need to take deployment requirements into the design. For example, a smart grid can consist of a large number of smart meters which may be divided into several groups according to different criteria. For example, the smart meters can be divided into groups based on their user properties (e.g. household groups, school groups, and shop groups), geographic regions (e.g. cities such as Beijing and Shanghai, and states such as Texas and California), etc. CC also needs to obtain different statistical information of these individual groups for fine-grained analysis.

Existing privacy-preserving solutions for ensuring the privacy of users (e.g. user electricity usage data) are mainly based on homomorphic encryption cryptosystems. Generally, these approaches require a semi-trusted third party to



obtain some statistic functions (e.g. summation, average, variance, and skewness) of all electricity usage data, but without learning anything about the data of individual user. Thus, ensuring the privacy of users. Schemes such as those reported in [13–16] offer complex solutions to achieve privacy-preserving in smart grid. In these schemes, smart meters need to encrypt the usage data and transfer the encrypted data to each other multiple times; thus, incurring costs during calculations and data transfers. Schemes such as those reported in [17–21]) offer a relatively simple and efficient privacy-preserving solution, but these schemes are based on a stable structure with little flexibility.

As discussed earlier, a smart grid generally consists of a large number of entities playing different roles. For example, company users have more electricity usage requirements compared to householder users. Therefore, a smart grid should provide the feature of differentiating between different user groups; thus, the importance of fine-grained analysis. Erkin [22] proposed a privacy-preserving data aggregation scheme in which users are divided into different groups and CC can obtain the power usage summation of each group. In the scheme, if a meter of some group  $G_i$  generates a ciphertext  $g^m r^n h^{n-\alpha}$ , then to cancel out the blinded item (power of  $h$ ) there must have another meter of the same group  $G_i$  which computes ciphertext of the form  $g^{m'} r'^n h^{n+\alpha}$ , where  $n$  is an RSA module,  $h \in \mathbb{Z}_n$  is a hash value,  $g, g', r, r' \in \mathbb{Z}_n^*$  and  $m, m', \alpha \in \mathbb{Z}_n$  are random numbers. A key limitation of this scheme is the requirement for the groups to have even number of users.

In this paper, we propose a new efficient privacy-preserving aggregation scheme for smart grid communications. Our scheme does not require the presence of a trusted third party, and allows users to be divided into different groups of any size. In addition, CC can obtain electricity usage data summations of each group in a privacy-preserving manner, which enables the CC to conduct fine-grained analysis to inform decision making.

We will present the preliminaries next.

## 2 Preliminaries

In this section, we briefly introduce our system model, the Chinese Remainder Theorem (CRT) and Paillier public-key encryption (PKE) scheme.

### 2.1 System Model

The system model considered in this paper consists of a control center (CC), a gateway (GW), and some users divided into  $k$  groups  $G_i, 1 \leq i \leq k$ , based on some preferred properties - see Fig. 2. The smart meters report the electricity usage data to GW in a fixed time interval (e.g. every 15 min). Then, GW aggregates all received reports from the meters and forwards the aggregated results to CC. Finally, CC analyzes and processes the electricity usage data summations of each group (e.g. real-time power pricing decisions, detecting power leakage, allocating

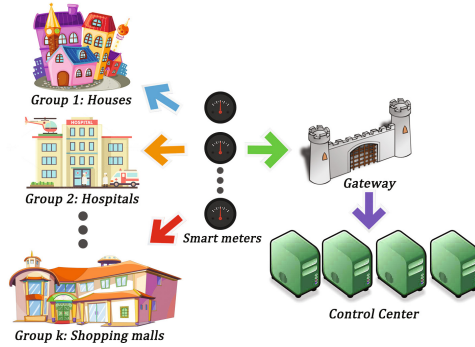


Fig. 2. Our system model

appropriate resources to deal with peak demands, such as providing more electricity for air-conditioners during hot weather). However, both GW and CC should not learn any information of electricity usage data of individual user.

### 2.2 Chinese Remainder Theorem

Let  $m_1, m_2, \dots, m_k$  be  $k$  pairwise co-prime integers and  $M := m_1 m_2 \dots m_k$ . Assume that  $b_1, b_2, \dots, b_k$  are  $k$  random integers satisfying  $0 \leq b_i < m_i, 1 \leq i \leq k$ . CRT states that there is a unique solution in  $\mathbb{Z}_M$  to the congruence equation

$$\begin{cases} x = b_1 \text{ mod } m_1 \\ x = b_2 \text{ mod } m_2 \\ \vdots \\ x = b_k \text{ mod } m_k \end{cases}$$

and the solution can be computed as

$$x = b_1 y_1 M_1 + b_2 y_2 M_2 + \dots + b_k y_k M_k \text{ mod } M,$$

where  $M_i := M/m_i$  and  $y_i := M_i^{-1} \text{ mod } m_i, 1 \leq i \leq k$ .

In this paper, we use CRT to compress multiple summations of electricity usage data of different user groups into a single element in  $\mathbb{Z}_M$ . The single summation for each user group can be recovered by simple modulating the corresponding  $m_i$ .

### 2.3 Paillier PKE Scheme [23]

Let  $n = pq$  be a product of two large primes  $p$  and  $q$ ,  $\phi(n) = (p - 1)(q - 1)$  the Euler’s function and  $\lambda = \lambda(n) = \text{lcm}(p - 1, q - 1)$  the Carmichael’s function of  $n$ .

$\mathcal{B}_\alpha \subset \mathbb{Z}_{n^2}^*$  denotes the set of all elements of order  $n\alpha$  and by  $\mathcal{B}$  their disjoint union for  $\alpha = 1, \dots, \lambda$ . Further, we define a function  $L$  over the set

$$\mathcal{S}_n = \{u < n^2 \mid u = 1 \pmod n\}$$

by

$$L(u) = \frac{u-1}{n}, \quad \forall u \in \mathcal{S}_n.$$

Then, the public key is  $pk = (n, g)$ , where  $g$  is randomly chosen from  $\mathcal{B}$ , and the private key is  $sk = \lambda$ .

**Encryption:** For any plaintext  $m \in \mathbb{Z}_n^*$ , select a random  $r < \mathbb{Z}_n^*$ , and the ciphertext can be calculated as

$$c = E_{pk}(m, r) = g^m \cdot r^n \pmod{n^2}.$$

**Decryption:** For ciphertext  $c \in \mathbb{Z}_{n^2}^*$ , the plaintext can be recovered as  $m = \frac{L(c^\lambda \pmod{n^2})}{L(g^\lambda \pmod{n^2})} \pmod n$ .

The additive homomorphic property of the Paillier PKE scheme is as follows: for any  $m_1, m_2 \in \mathbb{Z}_n$  and  $r_1, r_2 \in \mathbb{Z}_n^*$ , we have

$$\begin{aligned} & E_{pk}(m_1, r_1) \cdot E_{pk}(m_2, r_2) \pmod{n^2} \\ &= (g^{m_1} \cdot r_1^n) \cdot (g^{m_2} \cdot r_2^n) \pmod{n^2} \\ &= g^{m_1+m_2} \cdot (r_1 r_2)^n \pmod{n^2} \\ &= E_{pk}(m_1 + m_2, r_1 r_2) \end{aligned}$$

We will use this homomorphic property to design our scheme described in Sect. 3.

### 3 Proposed Scheme

Our scheme consists of four components, as described below.

#### 3.1 Setup

CC initializes the system, by first choosing two large primes  $p, q$  and setting  $n = pq$ . Then, CC chooses a random element  $g \in \mathcal{B}$  and generates a pair of public-private key  $(pk_{CC} = (g, n), sk_{CC} = \lambda = \text{lcm}(p-1, q-1))$  as in the Paillier PKE scheme.

Assume that we divide all users into  $k$  different groups  $G_i$  and each group has  $n_i$  users  $u_{i,j}$ ,  $1 \leq i \leq k$ ,  $1 \leq j \leq n_i$ . CC generates  $k$  pairwise co-prime integers  $m_1, m_2, \dots, m_k$  and sends them to GW.

Upon receiving  $k$  integers  $m_i$ ,  $1 \leq i \leq k$ , GW executes the following steps.

- (1) GW computes  $M := m_1 m_2 \cdots m_k$  and  $M_i := M/m_i$  for each  $i = 1, 2, \dots, k$ .

- (2) For each user group  $G_i$ ,  $1 \leq i \leq k$ , GW randomly chooses  $n_i$  integers  $r_{i,1}, r_{i,2}, \dots, r_{i,n_i}$  and computes  $r_{i,0}$ , s.t.

$$r_{i,1} + r_{i,2} + \dots + r_{i,n_i} + r_{i,0} = n. \tag{1}$$

- (3) GW broadcasts  $M_i$  and  $M$  among user group  $G_i$  and sends  $r_{i,j}$  to user  $u_{i,j}$  via a secure channel for each  $i = 1, 2, \dots, k$ ,  $j = 1, 2, \dots, n_i$ .
- (4) GW saves secretly  $r_{i,0}$ ,  $i = 1, 2, \dots, k$ , to its local database.

Finally, we assume that there is a secure hash function  $H : \{0, 1\}^* \rightarrow \mathbb{Z}_n^*$ , which is publicly known to each entity in the system.

### 3.2 Reporting

The reporting time interval is divided to  $\ell$  fixed time points  $T = \{t_1, t_2, \dots, t_\ell\}$  and the electricity usage data of user  $u_{i,j}$  at time point  $t_\gamma$  is  $s_{i,j,\gamma}$ ,  $1 \leq i \leq k$ ,  $1 \leq j \leq n_i$ ,  $1 \leq \gamma \leq \ell$ . To report  $s_{i,j,\gamma}$  to CC in a privacy-preserving manner, each user  $u_{i,j}$  executes the following computations.

- (1) Compute  $m_i = M/M_i$  and  $y_i := M_i^{-1} \bmod m_i$ .
- (2) Compute  $h_\gamma := H(t_\gamma)$  and  $s'_{i,j,\gamma} := s_{i,j,\gamma} \cdot y_i \cdot M_i \bmod M$ .
- (3) Randomly choose  $r_{i,j,\gamma} \in \mathbb{Z}_n^*$  and compute  $c_{i,j,\gamma} := g^{s'_{i,j,\gamma}} \cdot r_{i,j,\gamma}^n \cdot h_\gamma^{r_{i,j,\gamma}} \bmod n^2$ .
- (4) Send  $c_{i,j,\gamma}$  to GW.

### 3.3 Aggregation

Upon receiving the ciphertext data  $c_{i,j,\gamma}$  of all users at time point  $t_\gamma$ ,  $1 \leq i \leq k$ ,  $1 \leq j \leq n_i$ ,  $1 \leq \gamma \leq \ell$ , GW can aggregate them by executing the following:

- (1) GW computes  $h_\gamma = H(t_\gamma)$ .
- (2) With the private data  $r_{i,0}$ ,  $1 \leq i \leq k$ , GW computes  $R_\gamma := h_\gamma^{\sum_{i=1}^k r_{i,0}}$ .
- (3) GW computes the aggregated result  $C$  as

$$\begin{aligned} C &:= \left( \prod_{i=1}^k \prod_{j=1}^{n_i} c_{i,j,\gamma} \right) \cdot R_\gamma \bmod n^2 \\ &= \left( \prod_{i=1}^k \prod_{j=1}^{n_i} g^{s'_{i,j,\gamma}} r_{i,j,\gamma}^n h_\gamma^{r_{i,j,\gamma}} \right) \left( h_\gamma^{\sum_{i=1}^k r_{i,0}} \right) \bmod n^2 \\ &= \prod_{i=1}^k \left( g^{\sum_{j=1}^{n_i} s'_{i,j,\gamma}} \left( \prod_{j=1}^{n_i} r_{i,j,\gamma} \right)^n h_\gamma^{\sum_{j=1}^{n_i} r_{i,j,\gamma}} \right) \cdot \left( h_\gamma^{\sum_{i=1}^k r_{i,0}} \right) \bmod n^2 \end{aligned}$$

$$\begin{aligned}
 &= \left( g^{\sum_{i=1}^k \sum_{j=1}^{n_i} s'_{i,j,\gamma}} \right) \left( \prod_{i=1}^k \prod_{j=1}^{n_i} r_{i,j,\gamma} \right)^n \left( h_\gamma^{\sum_{i=1}^k \sum_{j=1}^{n_i} r_{i,j}} \right) \cdot \left( h_\gamma^{\sum_{i=1}^k r_{i,0}} \right) \bmod n^2 \\
 &= \left( g^{\sum_{i=1}^k \sum_{j=1}^{n_i} s'_{i,j,\gamma}} \right) \left( \prod_{i=1}^k \prod_{j=1}^{n_i} r_{i,j,\gamma} \right)^n \cdot \left( h_\gamma^{\sum_{i=1}^k \left( r_{i,0} + \sum_{j=1}^{n_i} r_{i,j} \right)} \right) \bmod n^2 \\
 &= \left( g^{\sum_{i=1}^k \sum_{j=1}^{n_i} s'_{i,j,\gamma}} \right) \left( h_\gamma^k \prod_{i=1}^k \prod_{j=1}^{n_i} r_{i,j,\gamma} \right)^n \bmod n^2.
 \end{aligned}$$

The last equation holds because, for any  $i = 1, 2, \dots, k$ , we have  $\sum_{j=0}^{n_i} r_{i,j} = n$  by Eq. (1).

- (4) GW sends  $C$  to the CC for further processing and analysis.

### 3.4 Obtain Group Readings

When CC obtains ciphertext  $C$  from GW at time point  $t_\gamma$ , CC can compute the summations  $S_i$  of electricity usage data for each group  $G_i$ ,  $i = 1, 2, \dots, k$ . Specially, CC performs the following calculations with his/her private-key  $\lambda$  and parameters  $m_1, m_2, \dots, m_k$ .

- (1) With the decryption key  $\lambda$ , CC obtains

$$S := \sum_{i=1}^k \sum_{j=1}^{n_i} s'_{i,j,\gamma}$$

by computing  $\frac{L(C^\lambda \bmod n^2)}{L(g^\lambda \bmod n^2)} \bmod n$ . According to the constructions of  $s'_{i,j,k}$ ,  $1 \leq i \leq k$ ,  $1 \leq j \leq n_i$ , we have

$$S := \sum_{i=1}^k \sum_{j=1}^{n_i} s'_{i,j,\gamma} = \sum_{i=1}^k \left( \sum_{j=1}^{n_i} s_{i,j,\gamma} \right) \cdot y_i \cdot M_i \bmod M,$$

where  $y_i = M_i^{-1} \bmod m_i$ ,  $i = 1, 2, \dots, k$ .

- (2) For each user group  $G_i$ ,  $1 \leq i \leq k$ , CC computes the summation of the electricity usage data of the users in  $G_i$  as  $S_i := S \bmod m_i = \sum_{j=1}^{n_i} s_{i,j,\gamma}$ . It is clear that the latter equation holds due to CRT.

## 4 Security Analysis

In this section, we consider a powerful adversary  $\mathcal{A}$  against the system proposed in Sect. 3. We assume that adversary  $\mathcal{A}$  can eavesdrop on the communication channel and wishes to obtain the information of individual user data.

First, we assume that  $\mathcal{A}$  eavesdrops on reports transmitted from users in the group  $G_i$  to the GW at the time point  $t_\gamma$  and thus gets some reports in the form:

$$c_{i,j,\gamma} = g^{s'_{i,j,\gamma}} \cdot r_{i,j,\gamma}^n \cdot h_\gamma^{r_{i,j,\gamma}} \text{ mod } n^2.$$

But  $\mathcal{A}$  can't decrypt  $c_{i,j,\gamma}$  to get the  $s'_{i,j,\gamma}$  because  $\mathcal{A}$  is unable to cancel out the blinding factor  $h_\gamma^{r_{i,j,\gamma}}$ . Further, even  $\mathcal{A}$  gets the private key  $r_{i,j}$  of the user  $u_{i,j}$  in exceptional cases, it is still unable to get  $s'_{i,j,\gamma}$  without the decryption key  $\lambda$  of Paillier PKE scheme owned by the CC.

On the other hand, we assume that the adversary  $\mathcal{A}$  eavesdrops the communication between GW and CC and obtains the aggregated result

$$C = \left( g^{\sum_{i=1}^k \sum_{j=1}^{n_i} s'_{i,j,\gamma}} \right) \left( h_\gamma^k \prod_{i=1}^k \prod_{j=1}^{n_i} r_{i,j,\gamma} \right)^n \text{ mod } n^2.$$

Without the decryption key  $sk_{CC} = \lambda$ ,  $\mathcal{A}$  is unable to recover the summation  $\sum_{i=1}^k \sum_{j=1}^{n_i} s'_{i,j,\gamma}$  of electricity usage data of all users. This is due to the security of the underpinning Paillier PKE scheme (we refer interested readers to [23] for a detailed security analysis of the Paillier scheme).

Next, we consider the case that  $\mathcal{A}$  eavesdrops on communications from users to GW and from GW to CC. As per above analysis,  $\mathcal{A}$  is unable to obtain individual user data  $s'_{i,j,\gamma}$  from  $c_{i,j,\gamma}$  or user data summation  $\sum_{i=1}^k \sum_{j=1}^{n_i} s'_{i,j,\gamma}$  from ciphertext  $C$ , as long as the decryption key  $sk_{CC} = \lambda$  is not exposed. On the other hand, it is clear that  $\mathcal{A}$  is unable to obtain the key  $sk_{CC} = \lambda$  because it is generated and maintained securely by CC (and CC has a vested interest to ensure the security of these keys, due to reputation and legal implications). Thus, the privacy of users is assured.

Finally, we consider the privacy-preserving issue under the case that either GW or CC is honest-but-curious. Recall that the ciphertext transmitted from individual user  $u_{i,j}$  to GW at time point  $\gamma$  is of the form  $c_{i,j,\gamma} = g^{s'_{i,j,\gamma}} \cdot r_{i,j,\gamma}^n \cdot h_\gamma^{r_{i,j,\gamma}}$ , which has two randomly disturbed items  $r_{i,j,\gamma}^n$  and  $h_\gamma^{r_{i,j,\gamma}}$ . It is clear that CC is not able to obtain the value  $s'_{i,j,\gamma}$  without the secret  $r_{i,j}$  to cancel out the disturbance  $h_\gamma^{r_{i,j}}$ . Similar argument for GW which does not have the secret  $\lambda$ . In other words, neither GW nor CC are able to retrieve  $s'_{i,j,\gamma}$  and, thus, obtain the sensitive data  $s_{i,j,\gamma}$  of individual user  $u_{i,j}$ . This holds unless both GW and CC collude.

## 5 Communication Overheads

In this section, we evaluate the communication overheads of our scheme against those of the privacy-preserving scheme of Erkin and Tsudik [19], in terms of individual user communication and the overall communication overheads. Assume that the parameters  $p$  and  $q$  in the Paillier scheme have the same size  $\kappa = 512$  bits,  $X := 1024$  bits is the size of the modular  $n$ , and  $\ell$  the number of users

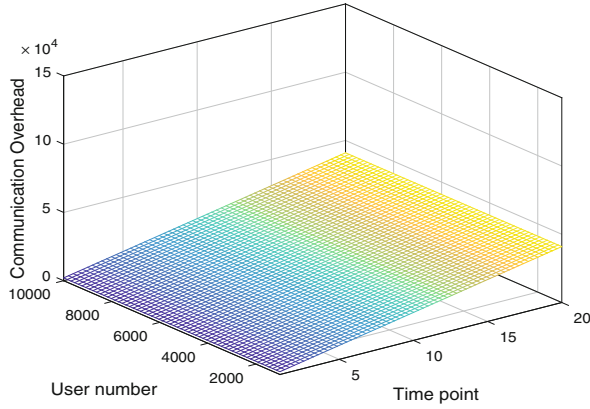


**Fig. 3.** Individual communication overheads of our scheme

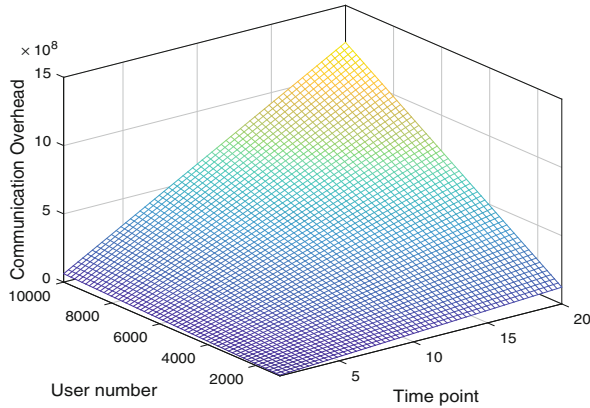


**Fig. 4.** Individual communication overheads of Erkin-Tsudik scheme [19]

in the smart grid. The transmission between the individual user  $u_{i,j}$  and GW at time point  $\gamma$  is ciphertext  $c_{i,j,\gamma}$ ; thus, the communication overhead of individual user is  $2X$  bits. In Erkin-Tsudik scheme, each user needs to exchange random numbers and broadcasts his/her reports to all other users at each time point, which results in  $6(\ell - 1)X$  bits communication overheads for the individual user. Figures 3 and 4 illustrate the communication overheads of our scheme and Erkin-Tsudik scheme, respectively.

In Erkin-Tsudik scheme, each user (rather than GW) broadcasts individual report to all other users; thus, overall communication overheads are  $6\ell(\ell - 1)X$  bits. On the other hand, overall communications in our scheme include  $\ell$  individual communications (from each  $\ell$  user to GW) and one-time communication (from GW to CC). This results in an overall communication overheads of size

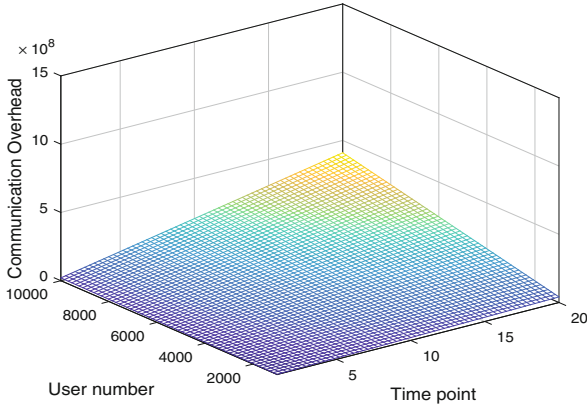


**Fig. 5.** Overall communication overheads of our scheme

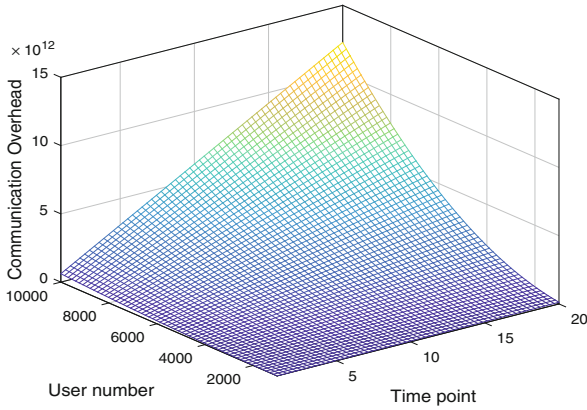


**Fig. 6.** Overall communication overheads of Erkin-Tsudik scheme [19]

$(2\ell+2)X$ . Figures 5 and 6 respectively show the overall communication overheads of our scheme and Erkin-Tsudik scheme.

## 6 Conclusion

Designing efficient data aggregation schemes for privacy-preserving smart grid communications is likely to remain a topic of interest in the foreseeable future, partly due to the constant evolution of smart grid technologies and user and provider requirements.

In this paper, we proposed a privacy-preserving data aggregation scheme for smart grids. The proposed scheme is flexible since it allows users to be divided into different groups of any size. Using the Paillier public-key encryption scheme



and the Chinese Remainder Theorem, the control center is able to obtain electricity usage data summations of each user group without compromising the privacy of any individual user. We demonstrated the security of the proposed scheme. We also evaluated the performance with those of the scheme of Erkin and Tsudik [19], which demonstrated that our scheme has lower communication overheads and is more practicable.

**Acknowledgement.** The work was supported in part by the NSFC-Zhejiang Joint Fund for the Integration of Industrialization and Informatization under Grant No. U1509219, the Shanghai Natural Science Foundation under Grant No. 17ZR1408400, the National Natural Science Foundation of China under Grant No. 61632012, and the Shanghai Sailing Program under Grant No. 17YF1404300.

## References

1. Meng, W., Ma, R., Chen, H.H.: Smart grid neighborhood area networks: a survey. *IEEE Netw.* **28**(1), 24–32 (2014)
2. Bao, H., Lu, R.: A new differentially private data aggregation with fault tolerance for smart grid communications. *IEEE Internet Things J.* **2**(3), 248–258 (2015)
3. Bao, H., Lu, R.: A lightweight data aggregation scheme achieving privacy preservation and data integrity with differential privacy and fault tolerance. *Peer-to-Peer Networking Appl.* **10**, 1–16 (2015)
4. Chen, L., Lu, R., Cao, Z.: PDAFT: a privacy-preserving data aggregation scheme with fault tolerance for smart grid communications. *Peer-to-Peer Networking Appl.* **8**(6), 1122–1132 (2015)
5. Lu, R., Alharbi, K., Lin, X.: A novel privacy-preserving set aggregation scheme for smart grid communications. In: *IEEE Global Communications Conference (GLOBECOM)*, pp. 1–6. IEEE (2015)
6. Ni, J., Zhang, K., Lin, X., et al.: EDAT: efficient data aggregation without TTP for privacy-assured smart metering. In: *2016 IEEE International Conference on Communications (ICC)*, pp. 1–6. IEEE (2016)
7. Chen, L., Lu, R., Cao, Z., et al.: MuDA: multifunctional data aggregation in privacy-preserving smart grid communications. *Peer-to-Peer Networking Appl.* **8**(5), 777–792 (2015)
8. Jiang, R., Lu, R., Choo, K.-K.R.: Achieving high performance and privacy-preserving query over encrypted multidimensional big metering data. *Future Gener. Comput. Syst.* (in Press). [10.1016/j.future.2016.05.005](https://doi.org/10.1016/j.future.2016.05.005)
9. Li, B., Lu, R., Wang, W., Choo, K.-K.R.: Distributed host-based collaborative detection for false data injection attacks in smart grid cyber-physical system. *J. Parallel Distrib. Comput.* (in Press). [10.1016/j.jpdc.2016.12.012](https://doi.org/10.1016/j.jpdc.2016.12.012)
10. Lu, R.: *Privacy-enhancing aggregation techniques for smart grid communications*. Springer (2016)
11. Yang, J., Cheng, R., Liu, W., et al.: Cryptanalysis and improvement of smart prepayment meter protocol in standard Q/GDW 365. *Int. J. Grid Util. Comput.* **4**(1), 40–46 (2013)
12. Rathnayaka, A.J.D., Potdar, V.M., Dillon, T.S., et al.: Formation of virtual community groups to manage prosumers in smart grids. *Int. J. Grid Util. Comput.* **6**(1), 47–56 (2014)

13. Wen, M., Lu, R., Lei, J.: ECQ: an efficient conjunctive query scheme over encrypted multidimensional data in smart grid. In: IEEE Global Communications Conference (GLOBECOM), pp. 796–801. IEEE (2013)
14. Hajny, J., Dzurenda, P., Malina, L.: Privacy-enhanced data collection scheme for smart-metering. In: International Conference on Information Security and Cryptology, pp. 413–429. Springer (2015)
15. Rial, A., Danezis, G.: Privacy-preserving smart metering. In: Proceedings of the 10th Annual ACM Workshop on Privacy in the Electronic Society, pp. 49–60. ACM (2011)
16. Borges, F., Volk, F., Mühlhäuser, M.: Efficient, verifiable, secure, and privacy-friendly computations for the smart grid. In: Innovative Smart Grid Technologies Conference (ISGT), pp. 1–5. IEEE Power & Energy Society, IEEE (2015)
17. Li, F., Luo, B., Liu, P.: Secure information aggregation for smart grids using homomorphic encryption. In: 2010 First IEEE International Conference on Smart Grid Communications (SmartGridComm), pp. 327–332. IEEE (2010)
18. Jung, T., Li, X.Y., Wan, M.: Collusion-tolerable privacy-preserving sum and product calculation without secure channel. *IEEE Trans. Dependable Secure Comput.* **12**(1), 45–57 (2015)
19. Erkin, Z., Tsudik, G.: Private computation of spatial and temporal power consumption with smart meters. In: International Conference on Applied Cryptography and Network Security, pp. 561–577. Springer, Heidelberg (2012)
20. Kursawe, K., Danezis, G., Kohlweiss, M.: Privacy-friendly aggregation for the smart-grid. In: International Symposium on Privacy Enhancing Technologies Symposium, pp. 175–191. Springer, Heidelberg (2011)
21. Sui, Z., Niedermeier, M., de Meer, H.: A robust and efficient secure aggregation scheme in smart grids. In: International Conference on Critical Information Infrastructures Security, pp. 171–182. Springer (2015)
22. Erkin, Z.: Private data aggregation with groups for smart grids in a dynamic setting using CRT. In: IEEE International Workshop on Information Forensics and Security (WIFS), pp. 1–6. IEEE (2015)
23. Paillier, P.: Public-key cryptosystems based on composite degree residuosity classes. In: International Conference on the Theory and Applications of Cryptographic Techniques, pp. 223–238. Springer, Heidelberg (1999)

# A Hot Area Mobility Model for Ad Hoc Networks Based on Mining Real Traces of Human

Lingyun Jiang<sup>1,2(✉)</sup>, Fan He<sup>1</sup>, Zhiqiang Zou<sup>1,2</sup>, Zhengyuan Wang<sup>1</sup>,  
and Lijuan Sun<sup>1,2</sup>

<sup>1</sup> School of Computer Science, Nanjing University of Posts  
and Telecommunications, Nanjing, China

{jianglingyun, zouzq, sunlj}@njupt.edu.cn

<sup>2</sup> Jiangsu High Technology Research Key Laboratory  
for Wireless Sensor Networks, Nanjing, China  
137569450@qq.com, 397248731@qq.com

**Abstract.** Mobility Model decides how the users move has a great impact on the topology of the Ad hoc networks. In order to reveal human mobile preferences in the real world, by mining two location-based social network data sets, we discover three regular patterns: (1) the complementary cumulative distribution of the number of hot areas of users and the degree of hot areas follows heavy-tail flight distribution; (2) the number of hot areas of the user has stability across time slots; (3) the user's hot area and user's social relationship has a weak correlation. A new model called HAMM (Hot Area Movement Model) is put forward based on the above three regular patterns. To validate HAMM, we implement it by extending ONE platform. The experimental results show that HAMM is superior to the baseline SLAW and TLW that relies on more parameters with higher complexity.

## 1 Introduction

Since movement pattern of the mobile node (MN) is found to have significant impact on the topology of the Ad hoc networks. [1], it is required that mobility models emulate movements of MNs in a realistic way. Currently there are two types of mobility models used in the simulation of networks: traces and synthetic models [2], traces provide accurate information because they involve a large number of participants and an appropriately long observation period. However, new network environments of the Ad hoc networks are not easily modeled if traces have not yet been created. So synthetic mobility models are widely used which attempt to realistically represent the behaviors of MNs without the use of traces.

Mobility Models are divided into two types: entity mobility models and group mobility models. There are several widely used entity mobility models for Ad hoc networks such as Random Walk Mobility Model(RW) [3], Random Waypoint Mobility Model(RWP) [4], Random Direction Mobility Model(RD) [5], Gauss-Markov Mobility

Model(GM) [6] which can't describe the characteristics of human movement [7]. There are several group mobility models such as Reference Point Group Mobility Model (RPG) [8], Nomadic Community Mobility Model(NC) [9], Working Day Mobility model(WDM) [10] which try to describe the characteristics of human group activities but can't guarantee that inter-contact times between MNs follows the heavy tailed distribution. Levy walk Mobility Model (TLW) [11] and Self-Similar Least Action Walk Mobility Model, SLAW) [12] try to reflect the property of human mobile, but are very complex and difficult to understand and seldom used in performance simulation of Ad hoc networks.

In this paper, we address the issue of providing a simple-used and easy-understanding mobility model which can reflect human mobile preference, and put forward a mobility model called HAMM based on mining two human mobile data sets in the real world. The remainder of this paper is organized as follows. In Sect. 2, we mine human mobility pattern in data sets of location-based social networks and illustrate three discovered regular patterns. Thereafter, in Sect. 3 we propose the mobility model HAMM and present the experimental results. Finally, in Sect. 4 we draw the conclusion and discuss some possible future directions.

## 2 Mining Human Mobility in Location-Based Social Networks

In order to reveal human mobile preferences in the real world, by mining two location-based social network data sets, we discover three regular patterns before building mobility model. Compared to traditional cellphone data from GPS trackers or telecommunication companies, LBSN (location-based social networks) data not only has social-spatial properties, large-scale, but also has sparse properties and semantic indication properties [13]. In this paper, we choose two data sets from Stanford University which are shown in Table 1. Check-in point distribution maps of Gowalla [14] and Brightkite [15] are shown in Fig. 1.

**Table 1.** Facts about studied traces.

Trace source	Brightkite	Gowalla
Time/duration of trace	2008/4–2010/10	2009/2–2010/10
The number of users	58228	196591
The number of check-in	4491143	6442890

As can be seen from Fig. 1, the check-in point looks particularly dense in some areas but sparse in other areas, which accords with the aggregation of human mobile: there are always more people in the center of the city. In this section, we introduce our analysis by defining the two metrics related to the hot area, we try to find the distribution law of two metrics which are used to formulate the human mobility, then consider the stability of the representation of a given user, and correlation detection between user hot spots and social relationships.

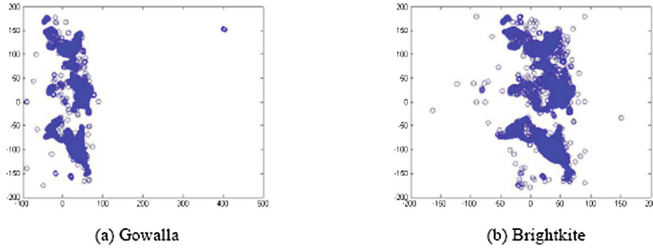


Fig. 1. Check-in point distribution maps of Gowalla and Brightkite.

### 2.1 The Distribution Law of the Human Mobility

In order to analyze the human mobility phenomenon, we formalize the user’s check-in points as a set of points  $p = \{p_1, p_2, \dots, p_i, \dots, p_w\}$ , and  $p_i$  is a check-in point which is defined using a triple of latitude, longitude and timestamp. We divide the whole research region into  $n * n$  grids  $G = \{g(1, 1), \dots, g(x, y), g(n, n)\}$ , thus all check-in points can be mapped into a grid  $g(x, y)$ . Let  $f_i(t, g(x, y))$  denote the number of check-in points of user  $i$  in  $g(x, y)$  during the time  $t \in [t_1, t_2]$ , if  $f_i(t, g(x, y)) > 0$ , then  $g(x, y)$  is regarded as a hot area of user  $i$  during the time  $t \in [t_1, t_2]$ . Two metrics related to the hot area are defined:  $h(i, t)$  denotes the number of hot areas of user  $i$  during the time  $t$  which can be calculated by Eq. (1) and  $ha(g(x, y), t)$  denotes the number of users in  $g(x, y)$  during the time  $t$  which can be calculated by Eq. (2).

$$h(i, t) = \sum_{x=1}^n \sum_{y=1}^n \eta_i(t, g(x, y)) \quad \eta_i(t, g(x, y)) = \begin{cases} 0 & f_i(t, g(x, y)) = 0 \\ 1 & f_i(t, g(x, y)) > 0 \end{cases} \quad (1)$$

$$ha(g(x, y), t) = \sum_{i=1}^m \eta_i(t, g(x, y)) \quad \eta_i(t, g(x, y)) = \begin{cases} 0 & f_i(t, g(x, y)) = 0 \\ 1 & f_i(t, g(x, y)) > 0 \end{cases} \quad (2)$$

We count  $h(i, t)$  with different  $n$  (we pre-process the two data sets and delete those users whose check-in number is less than 200). Statistical results demonstrate that more than 95% percent of users’  $h(i, t)$  is less than 1.25% of the total number of hot spots with different  $n$  granularity in Gowalla (when  $n$  is set to 20, the value of  $h(i, t)$  is less than 5, when  $n$  is set to 40, the value of  $h(i, t)$  is less than 20, when  $n$  is set to 60, the value of  $h(i, t)$  is less than 45), and that more than 94.8 percent of users’  $h(i, t)$  is less than 1.25% of the total number of hot spots with different  $n$  granularity in Brightkite. The complementary cumulative distribution maps of  $h(i, t)$  in Gowalla and Brightkite are shown in Figs. 2 and 3 respectively, which can be well approximated by heavy-tail flight distributions(formulated by Eq. (3)), and which is identical with the daily life experience: most people’s activities are concentrated in a limited number of areas, only a small number of people’s activities areas vary greatly.

$$p(X > x) = (x/x_{\min})^{-k} \quad (3)$$

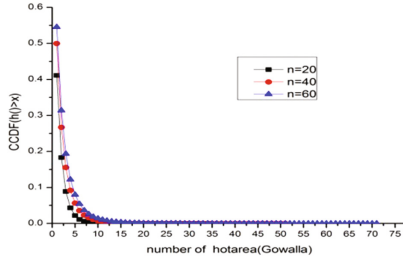


Fig. 2. The complementary cumulative distribution map of  $h(i, t)$  in Gowalla.

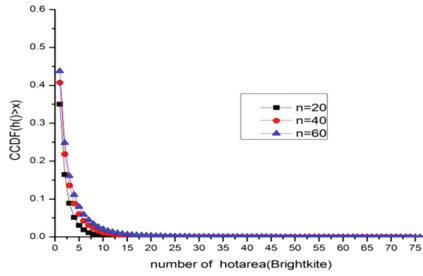


Fig. 3. The complementary cumulative distribution map of  $h(i, t)$  in Brightkite.

We do the similar work to count  $ha(g(x, y), t)$ , and the complementary cumulative distribution maps of  $ha(g(x, y), t)$  in Gowalla and Brightkite are shown in Figs. 4 and 5 respectively, which can also well approximated by heavy-tail flight distributions, and which is also identical with the daily life experience.

### 2.2 The Stability of the Human Mobile

The stability of a user’s mobility pattern representation across time is a decisive factor for whether the representation can be leveraged to predict the user’s future behavior. In order to quantify how stable the representation of a user’s mobility pattern, we use the

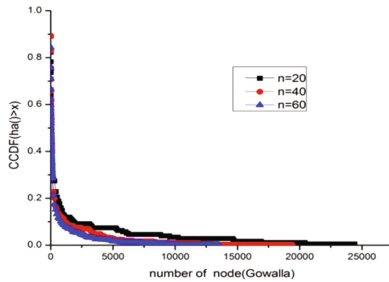


Fig. 4. The complementary cumulative distribution map of  $ha(g(x, y), t)$  in Gowalla.

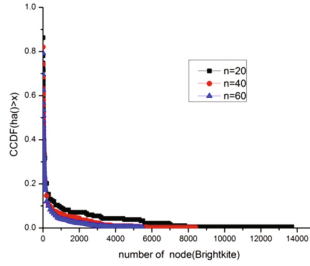


Fig. 5. The complementary cumulative distribution map of  $ha(g(x,y),t)$  in Brightkite.

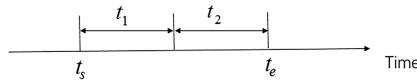


Fig. 6. The illustration of  $t_1$  and  $t_2$ .

similarity metric defined in Eq. (4), where the elapsed time from the first check-in time ( $t_e$ ) to the last one( $t_s$ ) is divided equally into  $t_1$  and  $t_2$ , as illustrated in Fig. 6. The smaller the value of  $r_i(t_1, t_2)$  is, the cross slot stability of the user  $i$  is stronger.

$$r_i(t_1, t_2) = \frac{|h(i, t_1) - h(i, t_2)|}{|h(i, t_1) + h(i, t_2)|} \tag{4}$$

We select those users whose check-in times are greater than 1000 (there are 443 users in Gowalla and 1035 users in Brightkite), and calculate the value of  $r_i(t_1, t_2)$  which are illustrated by Figs. 7 and 8 respectively ( $n = 500$ ).

As can be seen from Fig. 7, there are more than 95% users'  $r_i(t_1, t_2)$  are less than 0.05, and all users'  $r_i(t_1, t_2)$  are not more than 0.08. The statistical results seem not so optimistic in Brightkite seen from Fig. 8, in which there are only more than 78% users'  $r_i(t_1, t_2)$  is less than 0.3, and there are 3 users'  $r_i(t_1, t_2)$  is bigger than 0.8. We analyze the 3 users thoroughly: ID 634 user checked in the website at the beginning of time 2009-09-19 to time 2009-02-24 frequently (2081 times), and seldom checked in the time 2009-02-24 to the end of time 2010-07-30 (only 19 times) which results in a large value of  $r_i(t_1, t_2)$ , ID 1891 user has the same reason where there are 1923 check-in times from 2008-11-30 to 2009-11-9 and only 177 times from 2009-11-9 to 2010-10-17, ID 1891 user has the different reason where there are only 2 hot areas from 2008-08-14 to 2009-03-15 and 35 hot areas from 2009-03-15 to 2009-10-16. The results of the above analysis show that the distribution hot area of the majority of users is stable across time, which means that the representation of hot area can be used as a metric of user's mobility pattern.

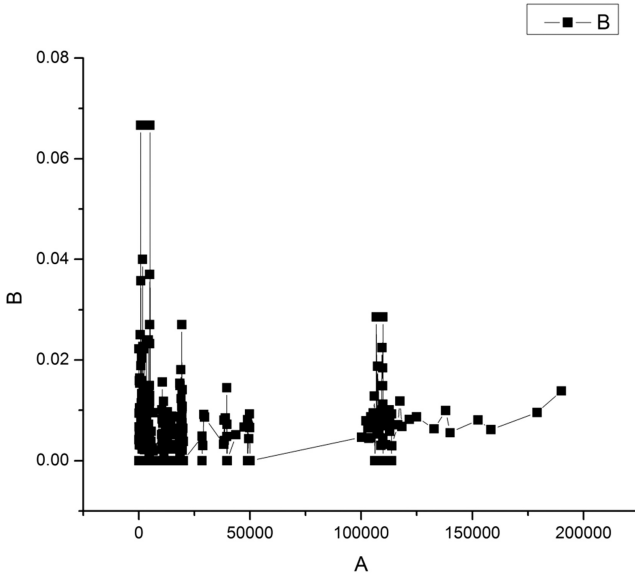


Fig. 7.  $r_i(t_1, t_2)$  in Gowalla.

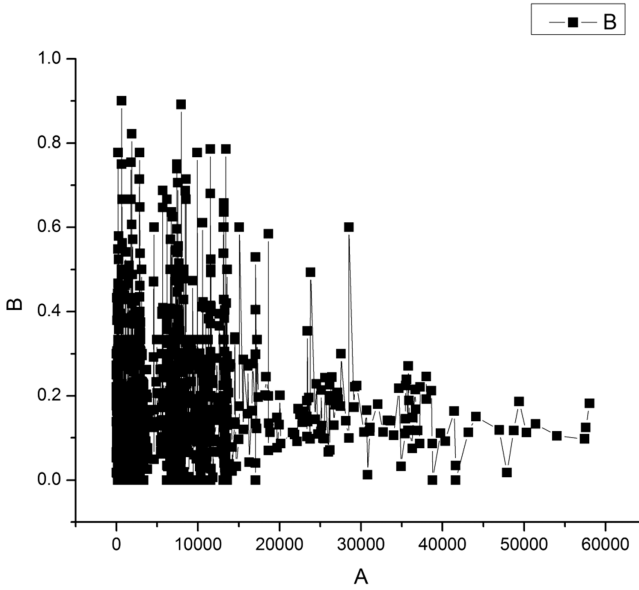


Fig. 8.  $r_i(t_1, t_2)$  in Brightkite.



### 2.3 The Correlation Detection Between User Hot Spots and Social Relationships

In order to verify whether the user's social relations have significant effect to user's mobility, we select 334 users whose number of friends are more than 250 in the Gowalla\_edges subset of the Gowalla, and the ID of those users are put into the set A. Then we sort the users according to the total number of hot areas in Gowalla\_totalCheckins subset and select top 334 users, and the ID of those users are put into the set B. We find the intersection of A and B is only 9. We do the similar work with Brightkite, we select 402 users whose number of friends are more than 100 and put the ID of those users into the set C. Then we select top 402 users in Brightkite\_edges, and put the ID of those users into the set D. We find the intersection of C and D is only 31.

These experiments show that there is no(weak) consistent relationship between the number of friends on the social network and the scope of activities in the real world. Therefore, the social relationship can be ignored to ensure the simple and easy representation of user mobility in considering the construction of the mobile model of the real world.

## 3 Hot Area Mobility Model Design and Evaluation

In the following section we develop a model of human mobility named Hot Area Mobility Model(HAMM) based on the mined patterns mentioned above, and implement it by extending ONE platform [16].

The basic framework of HAMM is simple-used and its construction way can be illustrated by Fig. 9. For the users of HAMM, they only need to set the simulation world-size, number of MNs and number of hot areas and their coordinates, then select the way to move between hot areas ('1' means moving from one hot area to another by RW [3], '2' means moving by the shortest path), HAMM can assign to the number of hot areas for each MN according to the Pareto distribution and then assign several hot areas to each MN according to the Pareto distribution where the MN can only travel within its own hot areas. Each MN move independently and its initial position is its home hot area which has the biggest  $ha(g(x, y), t)$ .

We implement HAMM in the ONE platform [16] ( $x_{\min}$  is set to 1 and  $k$  is set to 1.75 in Eq. (3)). For the users of HAMM, they can customize their mobile model only need to change the related parameters in 'default\_settings.txt'. There are four testing trajectories illustrated by Fig. 10. (there are 30 MNs and 15 hot areas in (a), and 20 MNs and 15 hot areas in (b), 30 MNs and 10 hot areas in (c), 20 MNs and 10 hot areas in (d)), and the trajectories of RWP, TLW and SLAW were described in [4, 11, 12]. As can be seen from Fig. 10, the trajectory of HAMM is similar to SLAW although there are only four parameters set by users which can reflect the property of human mobile.

In order to further analyze the characteristics of HAMM, we count the inter-contact time(ICT) of 15 hot areas, the Complementary Cumulative Distribution of the inter-contact times of two MNs are illustrated by Fig. 11, in which the blue dotted lines mean average time interval between all MNs and the time distribution accords with a truncated power-law distribution [17, 18].

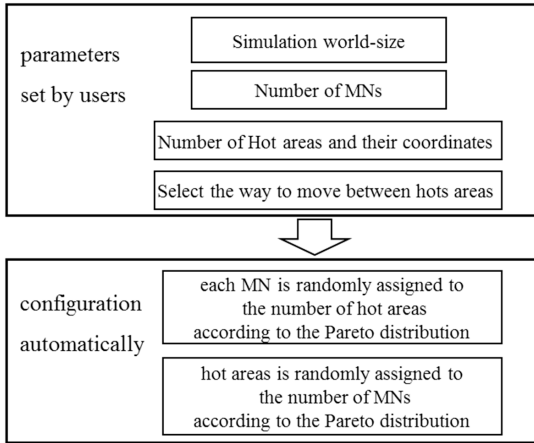


Fig. 9. Framework of HAMM.

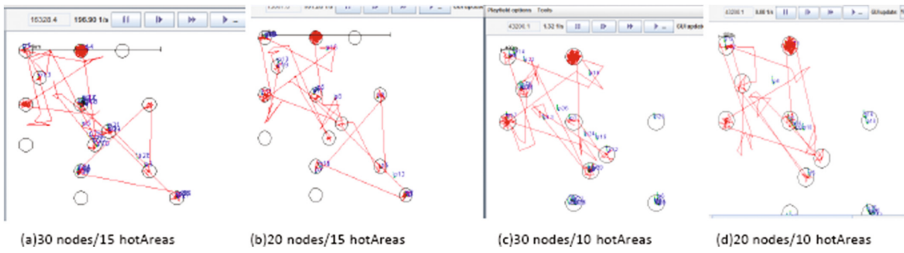


Fig. 10. Four testing trajectories of HAMM

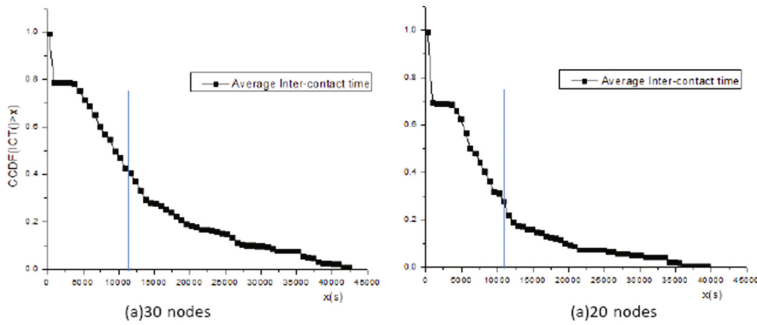


Fig. 11. The Complementary Cumulative Distribution of the inter-contact times HAMM.

## 4 Conclusion

In this paper, we address the fundamental research issue: how to design a simple-used and easy-understanding mobility model which can reflect human mobile preference. We investigate patterns of human mobility on two large location-based social network check-in data sets and find three common patterns of human mobility which are used to design a simple and generic mobility model HAMM. The simulation results show that HAMM is capable of reflecting human mobile preference that the complementary cumulative distribution of the inter-contact times of two MNs follows the truncated power-law distribution, which can be extended and applied to the human-centric mobile network (such as mobile crowd sensing network, social network and so on). In the future work, we will explore the quality aware incentive mechanisms in more complex scenarios. For example, how to prevent co-cheating using the history of mobility traces and the completed tasks list of participants.

**Acknowledgments.** The subject was sponsored by the National Natural Science Foundation of P. R. China (No. 61572261, 61472193, 61373138, 61572260, 61373017, and 41571389), the Scientific and Technological Support Project (Society) of Jiangsu Province (No. BE2014718), Postdoctoral Foundation (No. 2016T90485), the Sixth Talent Peaks Project of Jiangsu Province (No. DZXX-017), Project of Jiangsu Province (BE2015702), Open Project of Jiangsu High Technology Research Key Laboratory for Wireless Sensor Networks (WSNLBZY201518, WSNLBZY201519), Jiangsu Postgraduate Scientific Research and Innovation Projects (CXLX12\_0482).

## References

1. Jiang, L.Y., Feng, Y., Sun, L.J.: Impact analysis of movement model on opportunistic network routing protocols. *J. Nanjing Univ. Posts Telecommun. (Nat. Sci. Ed.)* **35**(5), 32–40 (2015)
2. Camp, T., Boleng, J., Davies, V.: A survey of mobility models for ad hoc network research. *Wirel. Commun. Mob. Comput.* **2**(5), 483–502 (2002)
3. Einstein, A.: *Investigations on the theory of the Brownian Movement*, pp. 2–18. Dover Publications, New York (1926)
4. Johnson, D.B., Maltz, D.A.: Dynamic source routing in ad hoc wireless networks. *Mob. Comput.* **353**, 153–181 (1996)
5. Royer, E.M., Melliarsmith, P.M., Moser, L.E.: An analysis of the optimum node density for ad hoc mobile networks. In: *IEEE International Conference on Communications*, pp. 857–861. IEEE (2001)
6. Liang, B., Haas, Z.J.: Predictive distance-based mobility management for PCS networks. In: *Eighteenth Joint Conference of the IEEE Computer and Communications Societies, INFOCOM 1999, Proceedings*, vol. 3, pp. 1377–1384. IEEE (1999)
7. Yoon, J., Liu, M., Noble, B.: Random waypoint considered harmful. In: *Joint Conference of the IEEE Computer and Communications Societies*, vol. 2, pp. 1312–1321 (2003)
8. Hong, X., Gerla, M., Pei, G., Chiang, C.C.: A group mobility model for ad hoc wireless networks. In: *ACM International Workshop on Modeling*, pp. 53–60 (1970)

9. Nchez, M., Manzoni, P.: ANEJOS: a java based simulator for ad hoc networks. *Future Gener. Comput. Syst.* **17**(5), 573–583 (2001)
10. Ekman, F., Keränen, A., Karvo, J., Ott, J.: Working day movement model. In: *ACM Sigmobile Workshop on Mobility Models, Mobilitymodels, DBLP 2008*, pp. 33–40 Hong Kong, China, May 2008
11. Rhee, I., Shin, M., Hong, S., Lee, K.: On the levy-walk nature of human mobility. *IEEE/ACM Trans. Netw.* **19**(3), 630–643 (2011)
12. Munjal, A., Navidi, W.C., Camp, T.: Steady-state of the slaw mobility model. *J. Commun.* **9**(4), 322–331 (2014)
13. Gao, H., Liu, H.: Mining human mobility in location-based social networks. *Synth. Lect. Data Mining Knowl. Discov.* **7**(2), 1–115 (2015)
14. Gowalla. <http://snap.stanford.edu/data/loc-gowalla.html>
15. Brightkite. <http://snap.stanford.edu/data/loc-brightkite.html>
16. Keränen, A., Ott, J., Kärkkäinen, T.: The ONE simulator for DTN protocol evaluation. In: *International Conference on Simulation TOOLS and Techniques* (p. 55). ICST (Institute for Computer Sciences, Social-Informatics and Telecommunications Engineering) (2009)
17. Karagiannis, T., Boudec, J.Y.L., Vojnović, M.: Power law and exponential decay of inter contact times between mobile devices. In: *ACM International Conference on Mobile Computing and Networking*, vol. 9, pp. 183–194. ACM (2007)
18. Masahiro, H., Elis, K., Makoto, I., Leonard, B.: Evaluation of MANET protocols for different indoor environments: results from a real MANET testbed. *Int. J. Space-Based Situated Comput.* **2**(2), 71–82 (2012)

**The 8th International Workshop  
on Virtual Environment  
and Network-Oriented Applications  
(VENOA 2017)**

# A Parameter Optimization Tool and Its Application to Throughput Estimation Model for Wireless LAN

Nobuo Funabiki<sup>1</sup>(✉), Chihiro Taniguchi<sup>1</sup>, Kyaw Soe Lwin<sup>1</sup>,  
Khin Khin Zaw<sup>1</sup>, and Wen-Chung Kao<sup>2</sup>

<sup>1</sup> Department of Electrical Engineering,  
National Taiwan Normal University, Taipei, Taiwan  
[funabiki@okayama-u.ac.jp](mailto:funabiki@okayama-u.ac.jp)

<sup>2</sup> Department of Electrical Engineering,  
National Taiwan Normal University, Taipei, Taiwan  
[jungkao@ntnu.edu.tw](mailto:jungkao@ntnu.edu.tw)

**Abstract.** Most of algorithms or logics to solve mathematical problems adopt multiple parameters such as coefficients and thresholds whose values should be carefully selected to enhance the performance. Conventionally, their developers or users tune them by trial and error, where they repeat to apply algorithms or logics with proper parameter values to available input data sets and modify them based on the results. As a result, this tuning process may consume a great deal of energy and not always provide the optimal ones. In this paper, we present a versatile *parameter optimization tool* to explore optimal values of parameters for various algorithms/logics. We show the effectiveness through applications for the *throughput estimation model* for wireless local-area networks, with the extension of the model.

## 1 Introduction

Most of algorithms or logics to solve mathematical problems have multiple parameters such as coefficients and thresholds whose values may critically affect their performance and thus should be carefully selected. Conventionally, it will take a considerable of trials and errors for developers or users to tune the values. They will select the proper values for the parameters and apply the algorithm/logic using them to available input data sets. Then, by evaluating the results, they modify the values of specific parameters and repeat the process. As a result, the tuning process of parameters may consume a great deal of energy, and may not always provide the optimal ones, because the results principally depend on adopting input data sets.

In this paper, we present a *parameter optimization tool* that can be extensively used for a variety of algorithms or logics to explore their optimal parameter values. For now, the target algorithm or logic whose parameters are optimized

---

This work is partially supported by JSPS KAKENHI (16K00127).

by the proposed tool is called the *logic*, and the program to implement a logic is the *logic program*. The proposed tool is separated from the logic program so that the developers of logic programs can implement them independently, if they follow the few conditions to use this tool, which will be discussed later.

This tool adopts a local search method to detect optimal parameter values. This method jointly uses the *tabu table* and the *hill-climbing function* to avoid a local minimum convergence [1,2]. More specifically, this algorithm repeats three phases: (1) to prepare three sets of parameters whose values are slightly changed between them by following the given specification, (2) to apply the logic program with them using input data sets, and (3) to select the best parameter value set among them which returns the best score or evaluation result that is output from the logic program.

In this paper, we apply the proposed tool to optimize the parameters of the *throughput estimation model* for the wireless communication link in a wireless local-area network (WLAN) [3-5]. The accurate throughput estimation model plays an important role in designing efficient WLAN systems [6-8]. Our model first calculates the receiving signal strength at the receiver using the *Log distance path loss model* [9]. Then, it calculates the throughput using the *sigmoid function* originally. Each model/function has several parameters to be tuned, which are optimized by the tool. By comparing the throughput estimation errors between the manual tuning and the tool, the effectiveness of the tool is verified.

In [10], *Dakota* was presented as a software tool with similar functions. It has been developed by the Sundia National Research Laboratory in USA as open source software. The comparisons with our tool will be involved in future works.

The rest of this paper is organized as follows: Sects. 2 and 3 present the proposed parameter optimization tool and its adopted algorithm respectively. Section 4 shows the application to the throughput estimation model for WLANs. Finally, Sect. 5 remarks the conclusion of this paper with future works.

## 2 Parameter Optimization Tool

In this section, we present the proposed parameter optimization tool. The parameter optimization tool is independent from the logic program for generalization, running the program as its child process. The effectiveness of the parameter values to run the logic program is evaluated by the output score from the program given in the output file. This tool searches the parameter values that maximize or minimize the output score. Currently, it is implemented by *Java* as a desktop application. In future works, it will be implemented as a Web application.

A user of the tool is required to prepare the following five files.

### 1. Parameter Specification File

The parameter specification file describes the condition how to change the value of each parameter during the search process. “parameter.csv” must be used as the file name. Each line in this file reflects the specification for one parameter, and must describe in the order of “parameter name”, “initial value”, “lower limit”, “upper limit”, and “change step”. The *change step* indicates one step

change size of the parameter value when the tool changes it to generate a new value. For example, when the *parameter name* is  $x$ , the *initial value* is 50, the *lower limit* is 0, the *upper limit* is 100, and the *change step* is 5,  $x$  is initially assigned 50 and then, it can be changed to 0, 5, . . . , 100 during the optimization process.

## 2. Logic Program File

The logic program file is a binary code file to run the logic, which can be executed through the command line. Any name is possible for this file. This file must satisfy the following two conditions:

- (1) When the program is executed, it receives the path for the parameter file in the argument and applies the parameter values in the file to the algorithm/logic.
- (2) When the program is completed, it outputs the score as the evaluation value in the text file “result.txt”.

With (1), the logic program can read the parameter values that are generated by the tool. With (2), the tool can read the score that is calculated in the logic program. For example, the parameter file for the previous example with three parameters is described as follows when their initial ones are used:

## 3. Sample Input Data File

The sample input data file contains the input data set to the logic program such that the result of the logic program is evaluated and used to optimize the parameter values in the tool. To improve the accuracy of the obtained parameter values, multimodal sample input data sets should be collected and adopted in the tool.

## 4. Score Output File

The score output file contains the score from the logic program to evaluate the current parameter values. The score can be given by the difference between measured and estimated throughputs in the throughput estimation model, the cost function for an optimization problem, and the S/N ratio for a signal processing filter.

## 5. Script File for Execution

The script file describes the sequence of the commands to execute the logic program. The file name must be “run.sh”. It describes the paths to the input files for the logic program. By modifying this script file, the user can change the name and the arguments for the logic program, and may run multiple logic programs sequentially to obtain one score. In the following example, line 10 executes the Java logic program with three paths to the input files. When the logic program is executed with multiple sample input data files continuously, the array to describe these files should be prepared and the loop procedure be adopted.



Example of “run.sh”.

```

01: #!/bin/bash
02: DIR=$(cd $(dirname $0); pwd)
03: PARAMETER_FILE=$1
04: cd "$DIR"
05: #folder for sample input data files
06: INPUT_DIR="./file/3f_ap1/"
07: #measurement data file
08: MEASUREMENT_FILE="./file/evaluate/
    indoor_3f_ap1.csv"
09: #execute the logic program
10: java -jar ThroughputEstimation.jar
    ${INPUT_DIR} ${MEASUREMENT_FILE}
    $PARAMETER_FILE
11: #move ‘result.txt’ to folder of parameter file
12: mv result.txt ‘dirname $PARAMETER_FILE’

```

The processing flow of the proposed tool is shown as follows:

- (1) The parameter optimization tool ( $T$ ) generates the initial parameter file by copying the initial values in the parameter specification file.
- (2)  $T$  executes the script file using the current parameter file.
  - (a) The logic program ( $L$ ) reads one sample input data file.
  - (b)  $L$  computes the algorithm/logic.
  - (c)  $L$  writes the score in the score output file.
- (3)  $T$  reads the score from the score output file.
- (4) When the termination condition is satisfied,  $T$  goes to (5), otherwise goes to (6).
- (5)  $T$  changes the parameter file based on the algorithm in the next section, and goes to (2).
- (6)  $T$  selects the parameter values with the best score and outputs it.

### 3 Parameter Optimization Algorithm

In this section, we describe the parameter optimization algorithm in the tool [1,2]. The following symbols are used in the algorithm:

- $P$ : the set of the  $n$  parameters for the algorithm/logic in the logic program whose values should be optimized.
- $p_i$ : the  $i$ th parameter in  $P$  ( $1 \leq i \leq n$ ).
- $\Delta p_i$ : the change step for  $p_i$ .
- $t_i$ : the tabu period for  $p_i$  in the tabu table.
- $S(P)$ : the score of the algorithm/logic using  $P$ .
- $P_{best}$ : the best set of the parameters.
- $S(P_{best})$ : the score of the algorithm/logic where  $P_{best}$  is used.
- $L$ : the log or cache of generated parameter values and their scores.

The algorithm procedure that minimizes the score is described as follows:

- (1) Clear the generated parameter log  $L$ .
- (2) Set the initial value in the parameter file for any  $p_i$  in  $P$ , and set 0 for any tabu period  $t_i$ , and set a large value for  $S(P_{best})$ .
- (3) Generate the neighborhood parameter value sets for  $P$  by:
  - (a) Randomly select one parameter  $p_i$  for  $t_i = 0$ .
  - (b) Calculate parameter values of  $p_i^-$  and  $p_i^+$  by:

$$\begin{aligned} p_i^- &= p_i - \Delta p_i, \text{ if } p_i > \text{lower limit,} \\ p_i^+ &= p_i + \Delta p_i, \text{ if } p_i < \text{upper limit.} \end{aligned} \quad (1)$$

- (c) Generate the neighborhood parameter value sets  $P^-$  and  $P^+$  by replacing  $p_i$  by  $p_i^-$  or  $p_i^+$ :

$$\begin{aligned} P^- &= \{p_1, p_2, \dots, p_i^-, \dots, p_n\} \\ P^+ &= \{p_1, p_2, \dots, p_i^+, \dots, p_n\} \end{aligned}$$

- (4) When  $P$  ( $P^-, P^+$ ) exists in  $L$ , obtain  $S(P)$  ( $S(P^-), S(P^+)$ ) from  $L$ . Otherwise, execute the logic program using  $P$  ( $P^-, P^+$ ) to obtain  $S(P)$  ( $S(P^-), S(P^+)$ ), and write  $P$  and  $S(P)$  ( $P^-$  and  $S(P^-), P^+$  and  $S(P^+)$ ) into  $L$ .
- (5) Compare  $S(P)$ ,  $S(P^-)$ , and  $S(P^+)$ , and select the parameter value set that has the largest one among them.
- (6) Update the tabu period by:
  - (a) Decrement  $t_i$  by  $-1$  if  $t_i > 0$ .
  - (b) Set the given constant tabu period  $TB$  for  $t_i$  if  $S(P)$  is largest at (5) and  $p_i$  is selected at (3)(a).
- (7) When  $S(P)$  is continuously largest at (5) for the given constant times, go to (8). Otherwise, go to (3).
- (8) When the hill-climbing procedure in (9) is applied for the given constant times  $HT$ , terminate the algorithm and output  $P_{best}$ . Otherwise, go to (9).
- (9) Apply the hill-climbing procedure:
  - (a) If  $S(P) < S(P_{best})$ , update  $P_{best}$  and  $S(P_{best})$  by  $P$  and  $S(P)$ .
  - (a) Reset  $P$  by  $P_{best}$ .
  - (c) Randomly select  $p_i$  in  $P$ , and randomly change the value of  $p_i$  within its range.
  - (d) Go to (3).

## 4 Application to Throughput Estimation Model for WLAN

In this section, we reveal the application results of the proposed tool to the throughput estimation model for WLAN in [3,4] with the model extension to improve the accuracy.

## 4.1 Overview of Throughput Estimation Model

This model estimates the throughput or transmission speed of a wireless communication link between a source node and a destination node in WLAN. First, this model estimates the receiving signal strength at the destination node using the *Log distance path loss model* by considering the distance and the obstacles between the end nodes. Next, it estimates the throughput using the *sigmoid function* from the receiving signal strength. Each function has several parameters that can affect the estimation accuracy. In [4], three network fields composed of multiple small rooms are considered, and throughputs between APs and hosts in different locations were measured using *Iperf* [11] and estimated by the model, where the parameter values for the model were tuned manually. For now, we discuss the results regarding that the source node is an AP and the destination node is a host.

The results in [4] show that prominent differences exist in specific links between estimated throughputs and measured ones. As the reason, they estimated that the model only considers the *direct signal* along the *line of sight (LOS)* at the host. It does not consider the *multipath effect* due to the *indirect signal* reflected at the walls, even if the indirect signal is stronger than the direct signal. The direct signal becomes exceedingly weak when it passes several walls or obstacles along the path. If the indirect signal passes only a few walls, the receiving signal strength of the host of this indirect signal can be much larger and the estimated throughput can be increased.

Therefore, to consider such indirect signals, we propose the extension of the throughput estimation model. For simplicity, we assume that for each host in the field, there exists a *reflecting point* on the wall in the same room such that the signal strength of the AP is the largest, and the indirect signal reaches the host through this reflecting point after the signal is attenuated there.

## 4.2 Input and Output Files

The input files to the logic program for the throughput estimation model are as follows:

- Network field file: it describes the set of the two coordinates of the end points on each wall and the wall type.
- Device coordinate file: it describes the set of the coordinates for one AP and plural hosts.
- Reflecting point file: it describes the set of the coordinates of the reflecting points for the hosts.
- Parameter file: it describes the parameter values of the model.
- Sample input data file: it describes the measured signal strengths and throughput at the hosts.

The summation of the absolute value of the difference between each measured and estimated throughput is output as the score for the current parameter values in the score output file.

### 4.3 Throughput Estimation Procedure

The computation procedure of the throughput estimation model including the extension is as follows:

- (1) Calculate the Euclid distance  $d$  ( $m$ ) for each link (AP/host pair) by:

$$d = \sqrt{(AP_x - H_x)^2 + (AP_y - H_y)^2} \quad (2)$$

where  $AP_x$  and  $AP_y$  represent the  $x$  and  $y$  coordinates for the AP, and  $H_x$  and  $H_y$  represent the  $x$  and  $y$  coordinates for the host.

- (2) Find the walls intersecting with the link. Here, the link and the wall are regarded as line segments where their intersection is judged by considering the intersection between the two line segments.
- (3) Estimate the receiving signal strength at the host using the Log distance path loss mode and consider the indirect signal:
- (a) Calculate the receiving signal strength  $P_{dir}$  at the host through the direct signal:

$$P_{dir} = P_1 - 10\alpha \log_{10} d - \sum_k n_k W_k \quad (3)$$

where  $P_{dir}$  represents the receiving signal strength ( $dBm$ ) at the host with the distance  $d$  ( $m$ ) from the AP,  $P_1$  does the signal strength ( $dBm$ ) at the host with  $1m$  distance from the source node,  $\alpha$  does the attenuation factor that should be optimized,  $n_k$  does the number of walls with type  $k$ , and  $W_k$  does the signal attenuation factor ( $dBm$ ) of the type  $k$  wall.

- (b) Calculate the receiving signal strength through the indirect signal:
- (1) Calculate the receiving signal strength  $P_{ref}$  ( $dBm$ ) at the reflecting point for each host using (4).
- (2) Calculate the receiving signal strength  $P_{ind}$  ( $dBm$ ) at the host by the indirect signal, where the receiving signal strength at (1) is used as the transmitting signal strength from the reflecting point using (5).

$$P_{ref} = P_1 - 10\alpha \log_{10} r - \sum_k n_k W_k \quad (4)$$

$$P_{ind} = P_r - 10\alpha \log_{10} t - W_{ref} \quad (5)$$

where  $r$  ( $m$ ) represents the distance between the AP and the reflecting point,  $t$  ( $m$ ) does the distance between the reflecting point and the host, and  $W_{ref}$  ( $dBm$ ) does the attenuation factor at the reflecting point.

- (c) Select the larger one between  $P_{dir}$  and  $P_{ind}$  for the receiving signal strength  $P_h$  ( $dBm$ ) at the host.
- (4) Calculate the estimated throughput  $S_h$  ( $Mbps$ ) using the sigmoid function in (6).

$$S_h = \frac{a}{1 + \exp(\frac{P_h - b}{c})} \quad (6)$$

where  $a$ ,  $b$ , and  $c$  are constant coefficients.

#### 4.4 Application of Tool

By applying the proposed tool, the values of the parameters for the throughput estimation model, namely,  $P_1$ ,  $\alpha$ ,  $W_k$ , and  $W_{ref}$  in (3), (5), and (4), and  $a$ ,  $b$ , and  $c$  in (6) are optimized.  $W_k$  is prepared for each wall type. In this paper, the corridor wall ( $k = 1$ ), the partition wall ( $k = 2$ ), the intervening wall ( $k = 3$ ), the glass wall ( $k = 4$ ), and the elevator wall ( $k = 5$ ) are considered. For the parameters in the parameter optimization algorithm,  $TB = 16$  and  $HT = 10$  are adopted. For the sample input data files, the measurement results in [4] are used in the application of the tool.

The three network fields in [4] are considered. Here, in field#1, one additional AP is allocated between the hosts 307-3 and Ref-3 and one AP is at the center in D307, in addition to the AP in [4]. In field#2, two additional APs are also allocated at the similar positions as in field#1. The reflecting point for each host is manually selected. Because field#1 and field#2 are located in the same building on different floors, all the sample input data sets measured with six

**Table 1.** Throughput estimation errors.

AP	method	model	ave.	max.	min.	var.
field#1 AP1	manual	conv.	9.42	18.7	0.62	38.7
	tool	conv.	5.15	20.74	0.01	46.2
	tool	extend.	5.81	22.6	0	56.0
field#1 AP2	manual	conv.	11.4	26.0	0.58	65.9
	tool	conv.	9.81	20.9	0.97	48.5
	tool	extend.	9.20	19.3	0	51.6
field#1 AP3	manual	conv.	17.3	34.4	0.44	89.0
	tool	conv.	16.5	47.3	5.22	146.9
	tool	extend.	16.2	46.6	3.24	146.5
field#2 AP1	manual	conv.	19.1	34.6	5.07	90.8
	tool	conv.	13.2	31.5	1.19	62.6
	tool	extend.	12.6	31.4	0.51	64.0
field#2 AP2	manual	conv.	18.7	31.8	4.96	64.6
	tool	conv.	12.6	21.2	3.08	24.6
	tool	extend.	12.3	21.0	2.10	33.8
field#2 AP3	manual	conv.	15.4	33.9	0.46	80.3
	tool	conv.	17.5	41.0	0.65	149.7
	tool	extend.	18.1	42.0	0.81	148.4
field#3 AP1	manual	conv.	13.2	38.2	0.83	116.7
	tool	conv.	6.75	1.45	0	28.5
	tool	extend.	5.05	15.82	0	25.8

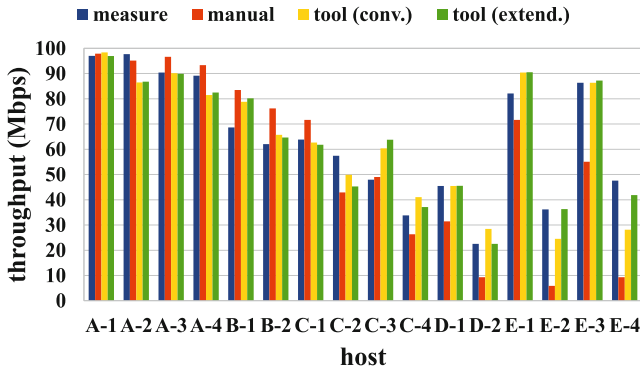


Fig. 1. Throughputs for AP1 in field#3.

APs and 28 hosts in the two fields are used together to select the optimal values of the parameters.

Then, we compute the throughput estimation model using the optimized parameter values. Table 1 summarizes the average, maximum, and minimum scores or estimation errors and the variances for each AP in the three fields. For reference, Fig. 1 shows the measured and estimated throughputs for the hosts with AP1 in field#3. Table 1 indicates that the accuracy of the throughput estimations of the model is generally improved by the tool, although it is degraded for certain hosts. The analysis of the reason and the provision will be explored in future works. The accuracy for the two hosts, E-2 and E-4, with AP1 in field#3, is greatly improved by the extended model. These results have verified the contribution of the proposed tool and model extension in this paper.

## 5 Conclusion

This paper presented a versatile parameter optimization tool to find optimal values of parameters for various algorithms or logics to solve mathematical problems. The effectiveness of the tool was confirmed through applications to the throughput estimation model for wireless local-area networks, where the extension of the model was also presented to enhance the accuracy. In future works, the tool will be applied to different algorithms/logics for verifications, and the user interface will be improved including the implementation of the Web application.

## References

1. Sekioka, T., Funabiki, N., Higashino, T.: A proposal of an improved function synthesis algorithm using genetic programming. *IEICE Trans. D1* **J83–D–I(4)**, 407–417 (2000)
2. Sekioka, T., Yokogawa, Y., Funabiki, N., Higashino, T., Yamada, T., Mori, E.: A proposal of a lip contour approximation method using the function synthesis. *IEICE Trans. D2* **J84–D–II(3)**, 459–470 (2001)
3. Mamun, M.S.A., Islam, M.E., Funabiki, N., Kuribayashi, M., Lai, I.-W.: An active access-point configuration algorithm for elastic wireless local-area network system using heterogeneous devices. *Int. J. Network. Comput.* **6(2)**, 395–419 (2016)
4. Lwin, K.S., Funabiki, N., Zaw, K.K., Mamun, M.S.A., Kuribayashi, M.: A minimax approach for access-point setup optimization using throughput measurements in IEEE802.11n wireless networks. In: *Proceedings of the CANDAR 2016* (2016)
5. Funabiki, N., Lwin, K.S., Kuribayashi, M., Lai, I.W.: Throughput measurements for access-point installation optimization in IEEE802.11n wireless networks. In: *Proceedings of the IEEE ICCE-TW*, pp. 218–219 (2016)
6. Gibney, A.M., Klepal, M., Pesch, D.: A wireless local area network modeling tool for scalable indoor access point placement optimization. In: *Proceedings of the SpringSim*, pp. 163–170 (2010)
7. Farkas, K., Huszák, Á., Gódor, G.: Optimization of Wi-Fi access point placement for indoor localization. *Network. Commun.* **1(1)**, 28–33 (2013)
8. Safna, R.F., Manoshantha, E.J.N., Suraweera, S.A.T.S., Dissanayake, M.B.: Optimization of wireless pathloss model JTC for access point placement in wireless local area network. In: *Proceedings of the RSEA 2015*, pp. 235–238 (2015)
9. Faria, D.B.: Modeling signal attenuation in IEEE 802.11 wireless LANs. Technical Report, TR-Kpp. 06-0118, Stanford University (2005)
10. Dakota. <https://dakota.sandia.gov/>
11. ACD.net, Iperf Speed Testing. [http://support.acd.net/wiki/index.php?title=Iperf\\_Speed\\_Testing](http://support.acd.net/wiki/index.php?title=Iperf_Speed_Testing)

# Virtual IP Network Practice System with Software Agent

Nobukazu Iguchi<sup>(✉)</sup>

School of Science and Engineering, Kindai University, Osaka, Japan  
iguchi@info.kindai.ac.jp

**Abstract.** It is important for beginning network engineering students to frequently practice setting up fundamental IP networks according to predetermined procedures. We have been developing NetPowerLab, a hands-on IP network practice system that uses virtual machines to provide an IP network learning environment. In this paper, we report the new development of IP network practice system with software agents. Software agents operate as a teacher or a cooperative student. The new system has three mode. The tutorial mode is used by beginner students with software agent operating as teacher. The practice mode is used by intermediate students with software agent operating as intermediate cooperative student. The troubleshooting mode is used by advanced students with software agent operating as advanced cooperative student. We describe outline of the system and software agent for IP network practice in this paper.

## 1 Introduction

Hands-on practical learning for network engineers has been held at many educational institutions [1]. It is important for beginning network engineering students to frequently practice setting up fundamental IP networks according to predetermined procedures.

However, in practical learning with real networking devices, each student requires two or more devices. For example, some experiments, such as routing information protocol (RIP) work, require multiple routers. Thus, it is not easy for students to prepare freely available and adequate practice network environments. Therefore, we have developed a learning system for practicing IP networking skills on a single PC [2, 3]. We have named this system NetPowerLab.

NetPowerLab is a learning system designed for undergraduate networking courses. The primary goal of this system is to facilitate learning the setup and configuration of routers and hosts, using standard commands. NetPowerLab can be used to develop skills outside the classroom environment, which can augment the overall learning experience.

Cooperative learning is held in network practice class. More than one students build single IP network together cooperatively in cooperative learning. Through Cooperative learning, students execute mainly three items; (1) explaining of own operations, (2) discussing with other students and (3) finding misoperations of another student [4, 5]. In this way, cooperative learning has several benefits for students. Therefore, we developed cooperative learning environment for NetPowerLab with software agents. Using software agents, students can practice cooperative learning of network practice by oneself at any time.



In this paper, we report the new development of IP network practice system with software agents. Software agents operate as a teacher or a cooperative student. The new system has three mode; (1) tutorial mode, (2) practice mode and (3) troubleshooting mode. The tutorial mode is used by beginner students with software agent operating as teacher. The practice mode is used by intermediate students with software agent operating as intermediate cooperative student. The troubleshooting mode is used by advanced students with software agent operating as advanced cooperative student.

We describe outline of the system and software agents for network practice in this paper.

## 2 NetPowerLab Overview

We describe the system architecture of NetPowerLab that is fundamental system of this research. The NetPowerLab is a hands-on IP network practice system that uses virtual machines. The NetPowerLab functions are illustrated in Fig. 1 [6]. As previously mentioned, the purpose of our system is to provide a training environment for the construction of virtual IP-based networks on a single PC.

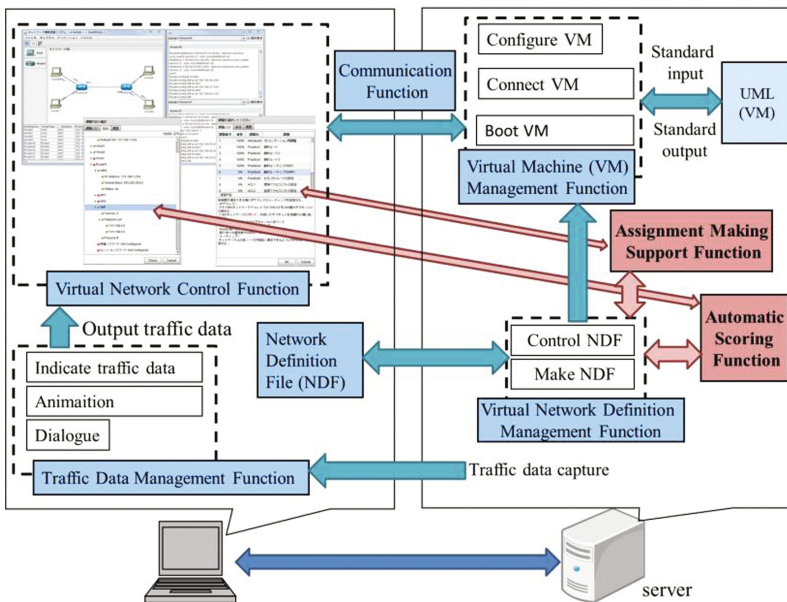


Fig. 1. System architecture of NetPowerLab.

We developed NetPowerLab using virtual Linux environment software. NetPowerLab was developed using a client-server model. The previous version of NetPowerLab consisted of the following components: virtual network control, virtual machine

management, traffic data management, virtual network definition management, communication function and automatic scoring function. In this study, we have developed and implemented the software agents for network practice.

We implemented NetPowerLab using UML [7], which is a virtual Linux environment. UML was selected because it is freely available and allows remodelling of source programs. In addition, UML has fully functional networking. Furthermore, multiple instances of UML can be employed simultaneously on a single general performance PC because it consumes little computing resources.

In NetPowerLab, we use virtual machines that remodel UML as virtual networking devices, including routers, hosts and hubs. We have developed functions to operate virtual machines by Java. All virtual machines operate on the server side, and students use a web-browser-based graphical user interface (GUI) to operate the virtual machines.

As related works of this study, various learning systems and networking tools for networking education have been developed and examined [8–10]. Some virtual router projects have also been undertaken [11, 12]. The aim of these projects is construction of software-based routers and visualization of internal router behaviors. A teaching system designed for undergraduate and graduate networking courses has been developed by Casado et al. [13, 14]. This system is implemented using a virtual router, and each student can build a router in user space. This system is used to teach implementation of internet routers. In addition, a learning system for LAN administrators using user-mode Linux (UML) has been developed by Tateiwa et al. [15]. This system is similar to our system; however, our practical goals are different. Training with Tateiwa's system focuses on the application layer, such as server software and firewalls. Our system is focused on the physical layer, such as the setup and configuration of routers.

### 3 Software Agent for Network Practice

Generally, software agent is defined as follows; (1) agents do not work at own discretion, (2) agents do not need user's instruction, (3) agents wait for designated events, (4) when conditions are complete, agents start to work. In this paper, we have developed software agents for network practice according to these items. We implemented software agents for network practice by Java. Figure 2 shows system overview with software agent.

Software agents for network practice that we have developed in this paper work as follows. Software agents wait for student's operation and software agents use student's operation as trigger. When students input some network commands, software agents start to run. Software agents define next work by the operation of student and software agents for network practice will work according to predefined file.

Software agents run according to SOF (Software agent Operating File). SOF is predefined by teacher. SOF includes three information; device name, input command, interval time. The device name means network devices that are handled by software agent. The input command means setup commands that are used by software agent. And software agent executes input commands at each interval time. Figure 3 shows a sample of SOF.

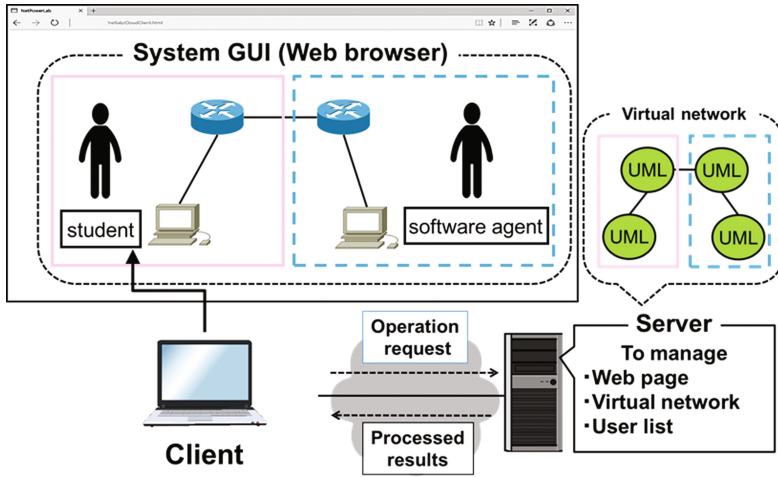


Fig. 2. System overview with software agent.

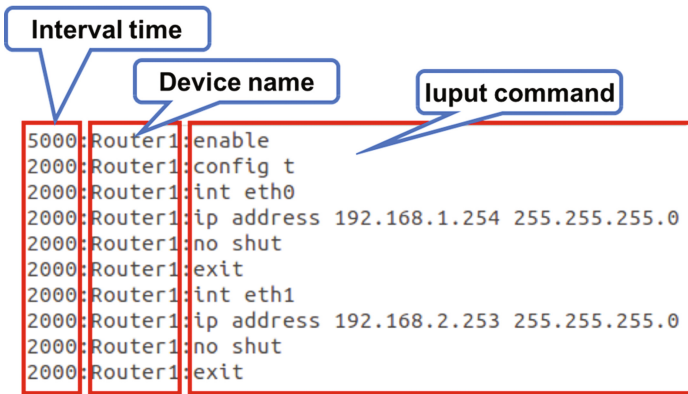


Fig. 3. A sample of SOF.

The new system has three mode; tutorial mode, practice mode and troubleshooting mode. The tutorial mode is used by beginner students with software agent operating as teacher. The practice mode is used by intermediate students with software agent operating as intermediate cooperative student. The troubleshooting mode is used by advanced students with software agent operating as advanced cooperative student.

Beginner students learn how to setup IP networks and how to use commands on the system with software agent operating as teacher at tutorial mode. Teacher agent always indicates a correct answer.

Intermediate students build IP networks according to predetermined procedures with software agent operating as intermediate cooperative student at practice mode. Intermediate student and software agent build one IP network in collectively work. Software agent always configure network devices correctly in this mode.

Advanced students lean network troubleshooting with software agent operating as advanced cooperative student at troubleshooting mode. Software agent configures network devices incorrect in a purposeful way at this mode. Student points out incorrect items of configuration of software agent side devices. Then student reconfigures incorrect items of software agent side devices.

As previously mentioned, SOF is predefined by teacher. To define SOF, teachers have to configure network devices that are going to be assigned for software agent. At this time, we have to determine and make two types of SOF. One is used for tutorial mode and practice mode, the other is used for troubleshooting mode.

### 4 Using the System

Students practice to build networks according to predetermined procedures on GUI as shown in Fig. 4. The GUI works on Web browser as client. Predetermined procedures of practice assignment are directed by teacher. As previously mentioned, the system has three mode. Students use this GUI on all mode. When students select practice assignment, virtual network devices boot up automatically. And network topology is shown on network topology pane. Students input commands through console pane. Inputted commands are shown on operation history pane.

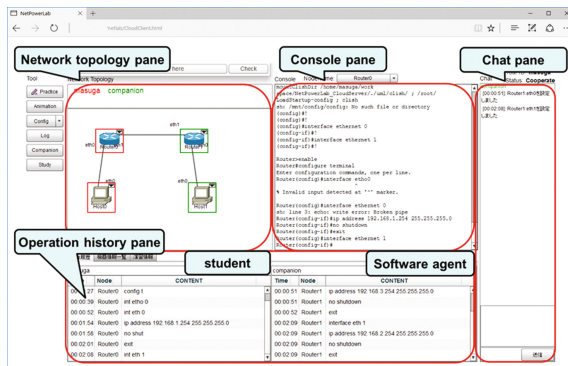


Fig. 4. GUI of cooperative practice with software agent.

Beginner students use the tutorial mode. In the tutorial mode, software agent operates as teacher. Beginner students learn how to setup IP networks and how to use commands. Teacher agent always indicates a correct answer. In this mode, we use key commands. Key commands are included in SOF. Key commands determine actions of software agent in coursework assignment. When student enters one of the key command, the software agent execute related commands. Students are able to see setup commands that are operated by software agent. Figure 5 shows an example of tutorial mode. For example, when student enters a command to start configuration of network interface, software agent as teacher enters a series of commands for network interface configuration immediately.

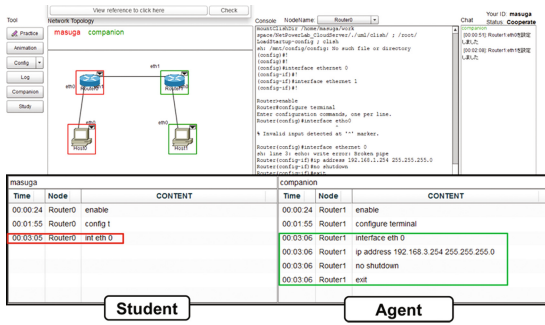


Fig. 5. An example of tutorial mode.

When students complete their practice assignment, students verify whether their operation are correct or not correct. To check operations, students use the automatic scoring function. The automatic scoring function compares the correct configuration file with the student’s configuration file to score the work. Figure 6 shows an example of scoring results provided by the automatic scoring function. This function displays the following items.

- score (percentage of correct items)
- correct items (green check mark)
- incorrect items (red check mark)
- detailed information about incorrect items.

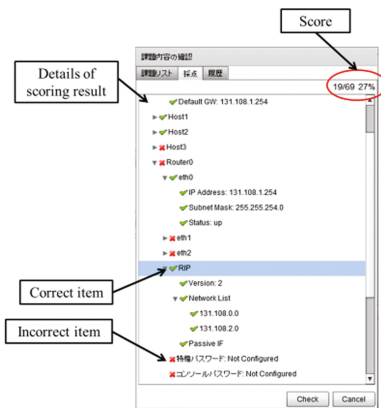


Fig. 6. An example of scoring results.

Using the automatic scoring function, students can perform self-guided training and testing. In addition, many students can practice collaboratively in a classroom environment, and teachers do not have to check and score student solutions manually.

The practice mode is used by intermediate students with software agent operating as intermediate cooperative student. Intermediate students build IP networks according

to predetermined procedures with software agent operating as cooperative student at practice mode. Intermediate student and software agent build one IP network in collectively work. Software agents always configure network devices correctly in this mode.

In this mode, students are not able to see setup commands that are inputted by software agent. And students are not able to refer software agent's operation. As shown in Fig. 7, the operation history pane of software agent is invisible. Therefore, students can not know whether software agent complete practice assignments or not.

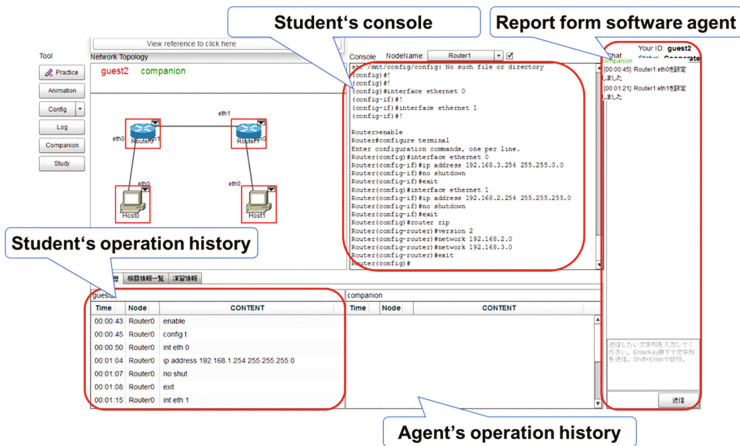


Fig. 7. GUI for practice mode.

In the practice mode, students use chat pane in place of agent's operation history pane. And students use an operating situation report function. This function displays a report of operating situations of software agent. Reports are shown in the chat pane of GUI. Figure 8 shows an example of operating situation report. As show in Fig. 8, this report displays no commands. And this report displays minimum information of operation. When students complete their practice assignment and students recognize software agent done, students check whether their operation are correct or not correct using by the automatic scoring function.



Fig. 8. An example of operating situation report.

The troubleshooting mode is used by advanced students with software agent operating as advanced cooperative student. Advanced students learn network troubleshooting with software agent operating as cooperative student at troubleshooting mode. Software agent configures network devices incorrect in a purposeful way at this mode. Student points out incorrect items of configuration of software agent side devices. To point out incorrect items, students verify operation history pane of software agent side as shown in Fig. 9. Figure 10 shows an example of incorrect item. Here, student found subnet mask of software agent side router was not right.

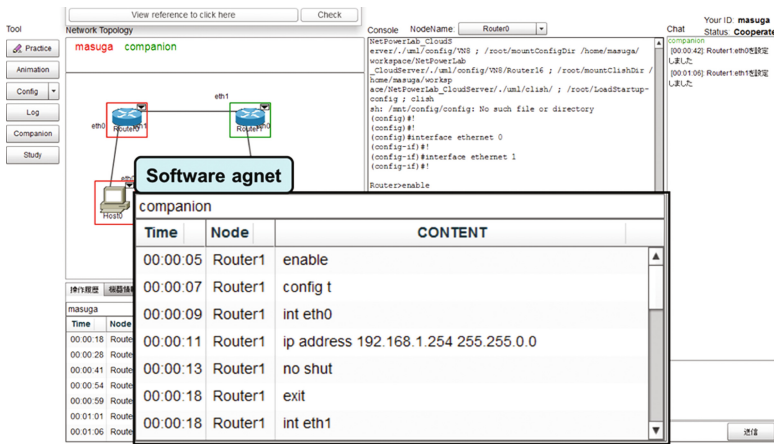


Fig. 9. An example troubleshooting mode 1.

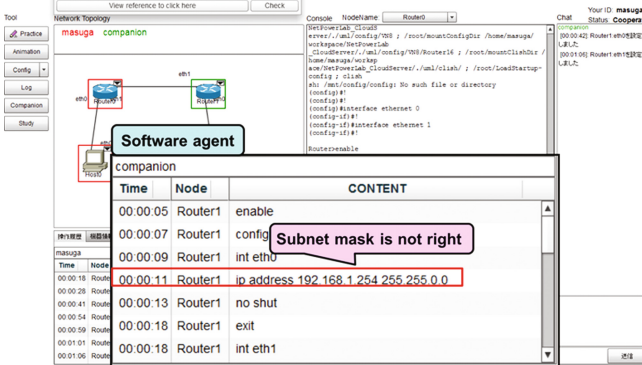


Fig. 10. An example of troubleshooting mode 2.

Then student reconfigures incorrect items of software agent side devices. To reconfigure incorrect items, students are able to get permission of operation of software agent's console as shown in Fig. 11. When students complete their practice assignment, students check whether his/her operation are correct or not correct using by the automatic scoring function.

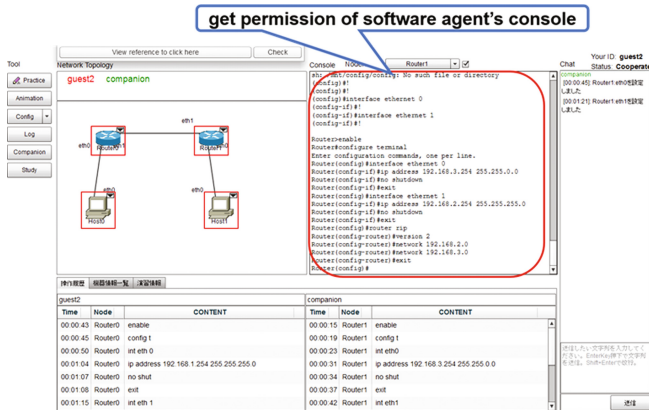


Fig. 11. An example of troubleshooting mode 3.

## 5 Conclusions

We have developed the hands-on practice system to learn IP network skills on PC. Using this system, students are able to practice network skills freely and virtually on PC.

In this paper, we described the new development of the IP network practice system with software agents. Software agents operate as teacher or cooperative student. The new system has three mode. The tutorial mode is used by beginner students with software agent operating as teacher. The practice mode is used by intermediate students with software agent operating as intermediate cooperative student. The troubleshooting mode is used by advanced students with software agent operating as advanced cooperative student. By providing this system, students are able to do self-service training and testing all in one place.

At this time, we have to determine and make two types of SOF (Software agent Operating File). We are going to develop a function that automatically make two types of SOF from single configuration file as future work. Additionally, we are going to develop a function that automatically makes several kinds of practice assignments for troubleshooting.

In next semester, we are planning to introduce this system to our CNA class partly. And, we are going to determine if this system is efficient for learning of IP network building skill.

**Acknowledgments.** This work was supported by JSPS KAKENHI Grant Number JP15K01046.

## References

1. Cisco Systems: Cisco Networking Academy. <http://www.cisco.com/web/learning/netacad/>. Accessed Mar 2017



2. Iguchi, N.: Development of a system to support computer network construction practice using virtual router. *IPJS J.* **52**(3), 1412–1423 (2011)
3. Iguchi, N., Kitazawa, Y.: Development of hands-on IP network construction practice system used in campus cloud computing. In: *Proceedings of 2012 Sixth International Conference on Complex, Intelligent, and Software Intensive System*, pp. 711–716 (2012)
4. Gordon, A., Hall, L.: A Collaborative learning environment for data modeling. In: *Proceedings of the Eleventh International Florida Artificial Intelligence Research Symposium Conference* pp. 156–162 (1998)
5. Kasai, T., Okamoto, O.: Collaboration among agents in a virtual collaborative learning environment. *IPJS J.* **40**(11), 3934–3945 (1999)
6. Iguchi, I.: Development of a self-study and testing function for NetPowerLab, an IP networking practice system. *Int. J. Space-Based Situat. Comput.* **4**(3/4) (2014)
7. Dike, J.: *User Mode Linux*. Prentice Hall, USA (2006)
8. Bruce, K., Ilona, B.: A virtual learning environment for real-world networking. In: *Proceedings of Informing Science+IT Education Conference 2003* pp. 671–683 (2003)
9. Steve, L., Willis, M., Wei, Z.: Virtual networking lab (VNL): its concepts and implementation. In: *Proceedings of the 2001 American Society for Engineering Education Annual Conference & Exposition* (2001)
10. Galan, F., Fernandez, D., Ruiz, J., Walid, O., Miguel, T.: Use of virtualization tools in computer network laboratories. In: *Proceedings of the 5th International Conference on Information Technology Based Higher Education and Training* pp. 209–214 (2004)
11. Kohler, E., Morris, R., Chen, B., Jannotti, J., Kaashoek, M.F.: The click modular router. *ACM Trans. Comput. Syst.* **18**(3), 263–297 (2000)
12. VRouter: VRouter Project. <http://nrg.cs.ucl.ac.uk/vrouter/>. Accessed Mar 2017
13. Casado, M., Vijayaraghvan, V., Appenzeller, G., McKeown, N.: The stanford virtual router. *ACM SIGCOMM Comput. Commun. Rev.* **32**(3), 26 (2002)
14. Casado, M., McKeown, N.: The virtual network system. In: *ACM SIGCSE 2005* pp. 76–80 (2005)
15. Tateiwa, Y., Yasuda, T., Yokoi, S.: Development of a system to visualize computer network behavior for learning to associate LAN construction skills with TCP/IP theory, based on virtual environment software. *IPJS J.* **48**(4), 1684–1694 (2007)

# Creating Learning Materials by Learners Themselves Using Partial Bookmarking for Web Curation

Takehiro Nagatomo, Takahiro Tachibana, Keizo Sato, and Makoto Nakashima<sup>(✉)</sup>

Oita University, 700 Dannoharu, Oita-shi, 870-1192, Japan  
{v16e3013,v1353041,k-sato,nakasima}@oita-u.ac.jp

**Abstract.** Creating a learning material by a learner oneself is an effective way of nurturing their ability to become independent-minded learners. Although web curation is a familiar way for the learner to interact with up-to-date knowledge regarding several subjects, recent popular applications for web curation, e.g., SNSs, are deficient in their ability to support free-form curation of the web contents for authoring the learning material. We have developed a new authoring environment by employing an enhanced web browser which enables a new kind of bookmarking, named partial bookmarking, which supports learners in collecting any portion of a web page and allows the learner to organize these portions simultaneously in any layout or format. We have conducted a case study of 15 university students using a developed environment for creating learning materials and then derived considerable design patterns of web curation by means of a visual grounded theory analysis.

## 1 Introduction

Learning materials are important tools which can guide students towards active learning, through taking control of their own learning experiences and nurturing their ability to become independent-minded learners. These materials are usually designed for students to enable them study individually with less assistance or input from people around them. These consist of perhaps hints about the subject itself, e.g., information resources, a brief explanation of solutions, practice quizzes, etc., and are prepared by lecturers. The core elements of active learning are student activities and engagement in the learning process. Instead of merely using lecturer-made learning materials, if the students themselves collect appropriate information or tips and organize them into different kinds of materials to complete homework assignments and/or study in advance in their chosen subject, it is of great assistance in stimulating the students to comprehend the learning content individually. Web curation [5], i.e., collecting and organizing the informative tips on the web for later browsing or sharing them with other people, are everyday activities, especially for the youth of today. It can be said that web curation must be one of the most convenient ways to create learning materials for learners.

Popular SNSs on the web, e.g., Pinterest [7] and Tumblr [9], are typical applications of web curation. These services allow a large number of people to curate the contents of web pages, and then arrange the curated contents according to parameters such as

recency and popularity or predefined templates. This easy arrangement provides the advantage of being able to collect the most interesting contents, but provides little support for articulating relationships among the curated contents [5]. For the learner, arranging and combining many portions of the web pages in consideration of their relationships' are significant activities that aid concentration and maintaining focus on the task in hand. The web curation application IdeaMâché [3] allows users to freely curate and arrange the elements of HTML, e.g., image, movie, or document division element. However, there is one constraint: it is impossible to fragment these elements in curation.

In this paper, we introduce a new environment enabling web curation for the learner to create learning materials themselves. In the environment, the enhanced web browser [6] allows the learner to collect any portion of a web page referring to the learning subject and to author a hypertext as a learning material by arranging these portions. The enhanced web browser has a mechanism, named partial bookmarking, which makes transclusion available for authoring the hypertext regardless of document structure involving modularize documents written in languages for hypertext such as XML or HTML on the web. Thus the learner can collect any portion of a web document element they like, even if it is a part of an image or a combination of some parts of multiple elements. We also analyse the design patterns of learning materials through the case study, and clarify the effectiveness of partial bookmarking for creating the learning materials on the enhanced web browser.

We conducted a case study in which 15 university students participated and were asked to create the learning materials for a class in their curriculum with the enhanced web browser. Through a visual grounded theory analysis [4] of the created learning materials to investigate concrete visual actions and interactions with the enhanced web browser, we derived 4 major patterns in creating learning materials and defined districted categories within each major pattern. Although three of the four major patterns were identical to the ones derived in the pregnant research about web curation in visual thinking [5], one major pattern was found in our environment. This major pattern named *scrapbook*, clarified the importance of free-form transclusion in creating learning materials: about 50% of the contents of learning materials consisted of the fragments of web document elements. This shows that many participants wanted to curate the contents on the web pages without feeling shackled by document structure, since web document elements do not always correspond to the information unit required to be curated by learners. For this reason, partial bookmarking with the enhanced web browser was shown to be an effective method in the process of web curation.

## 2 Related Work

Several services or systems have been available to curate the web contents. In this section, we describe the problems with these systems. SNSs, e.g., Pinterest [7], Tumblr [9] are popular web curation services. The curated contents by users are organized in linear or in board shaped style according to the ranking algorithms based on recency or popularity [5]. Thus, to create the learning materials, these services are deficient in their ability to arrange the curated web contents according to the relationships between them.

IdeaMâché [3] has been developed to solve the above problem. This web curation application allows the user to freely rearrange the curated contents of web pages like a photograph album. The units to be curated by this application, however, are pre-designed linkable objects, such as HTML objects. Evernote Web Clipper [2], an add-on for a web browser, enables the browser to record the part/whole of the web page in free-form. However, this application focuses on recording the content and sharing it with other users, and as a result, this is not designed for simultaneously collecting multiple parts of the web pages to express their relationships.

### 3 Creating Learning Materials by Partial Bookmarking

Figure 1 shows the process flow when creating the learning materials for a subject using partial bookmarking for web curation in our environment. The learner uses the enhanced web browser which consists of two areas: browsing area and authoring area. The former includes a web browser with multiple tabs, where the learner searches a web page including informative contents about the subject, and then selects a single portion of the web page or trims the unnecessary part, which the user wants to record its content from as a reference of the subject. The portion is able to be arranged to author the learning material on the latter area. As shown in the figure, creating the learning material is preceded by partial bookmarking some portions and arranging them as elements of a learning material, just as it is when considering these relationships.

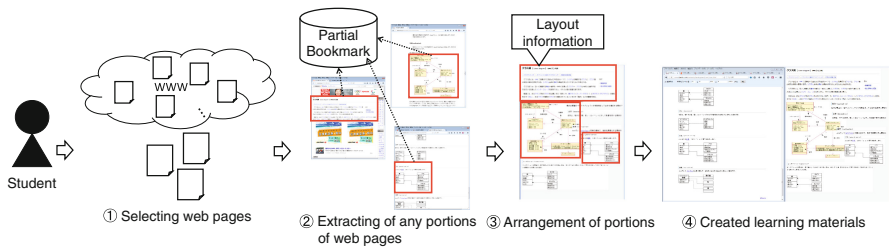


**Fig. 1.** Outline of creating learning materials with web curation

To realize this process, the enhanced web browser fulfils the following requirements:

- (i) Enable collecting the information for identifying any portion on a web page.
- (ii) Enable displaying only the portion as it is displayed on the web browser.
- (iii) Enable arranging the displayed portions in any layout or format as the learner likes to author a learning material.
- (iv) Enable sharing the authored learning material with other learners without infringement of copyright.

In the following, the mechanism of partial bookmarking which is to fulfil the first and fourth requirement, is described. Following that, we describe the procedure of enhancing a web browser to utilize partial bookmarking for creating learning materials as a hypertext, which meets the second and the third requirements.

### 3.1 Partial Bookmarking

The mechanism of partial bookmarking [6] records the necessary information, i.e., partial bookmark, needed for identifying any portion of a web page to reload it on the web browser. Whereas the mechanism of usual bookmarking only records the URL of a web page to be bookmarked to access again later, partial bookmarking records two types of information: location and action information. The former includes the coordinates of the region of the portion on the web browser beside the URL of the web page, including the portion which the user is interested in and wants to access again later. The latter includes the sequence of events that occurred on the web browser, e.g., button/scroll down, or key down which are performed when the user found the portion.

The left half of Fig. 2 shows an example of a partial bookmark written in XML, which identifies the portion of a dashed line in the right half of the figure. As shown in Fig. 2, the partial bookmark can identify any portion of a web page displayed on the web browser without the need to rely on any document structure, i.e., web document element; that is, **its contents are not to be duplicated even if the portion is a part of an image or a movie clip.**

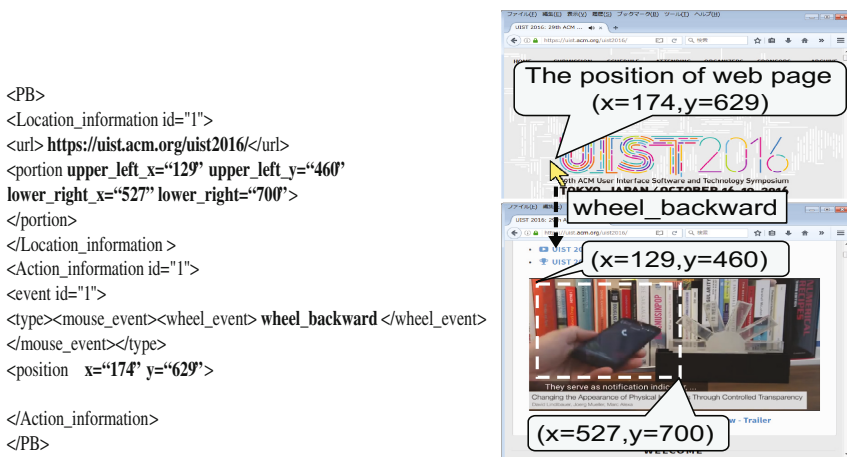


Fig. 2. A partial bookmark

### 3.2 The Enhanced Web Browser

Figure 3 shows the architecture of the enhanced web browser [6] in which two areas for browsing the web pages and authoring the learning materials have been included. The authoring area has an individual window, named p-window, which mirrors only the portion identified by the partial bookmark on the tab's window. They are designed as movable so as to enable the learner arrange them freely to create learning materials. Although the browsing area is seemingly a traditional web browser with multiple tabs, it allows the learner to select any portion of a web page and record the partial bookmark for that portion. To record the partial bookmark and display the content of the p-window according to the

information in the partial bookmark, PB handler employs the technique [1, 8] of intervening image/event-information between the learner and the web browser. This handler reproduces the events recorded in the partial bookmark, sends them to the web browser, and mirrors the image of the portion reloaded on the web browser to the p-window. Note that the reference web pages for p-windows are always loaded on the tab's windows. Thus the portion to be bookmarked is shown as it is displayed on the tab's window, and the dynamic changes on the web page are always updated on the p-window.

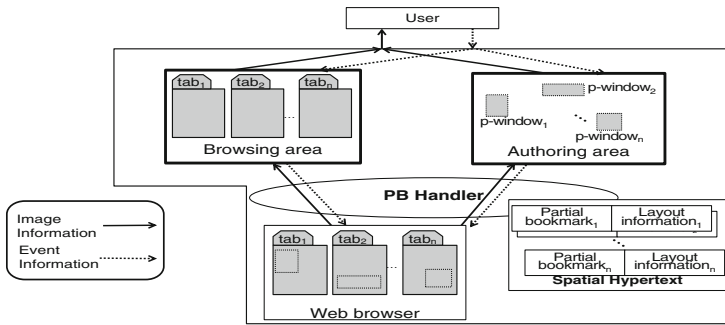


Fig. 3. The architecture of the enhanced web browser

## 4 Case Study

We were deeply interested in the user experience of the enhanced web browser in creating learning materials when the learners had no restriction in collecting and arranging the web contents. To analyse the experience we conducted a case study of university students. We took a visual grounded theory approach using the data aggregated in the case study and clarified the design patterns in terms of how web contents were arranged as learning materials.

### 4.1 Task

The university students (4 females and 11 males) of a computer science course participated in our case study and created 15 learning materials through web curation by using the enhanced web browser. Each participant created the learning material for one class, which they had already taken, by way of homework to help oneself comprehend the content of the class. Note that each of them were asked to select one class from among the five classes shown below, so as to balance the number of learning materials created for each class.

- Computer Network (Lecture)
- Knowledge Processing (Lecture)
- Database Seminar (Laboratory)
- Software Development Laboratory II (Laboratory)
- Computer System Experiments (Experiment)

After having created the learning material, each participant was interviewed about their intention when creating it.

## 4.2 Data Analysis

We performed a visual grounded theory analysis to clarify the design patterns of the learning materials, i.e., context of creation of the learning materials, based on the data pool which consisted of the 15 learning materials created along with the interview results. The process flow is as follows:

- (1) Interpret each created learning material in terms of its visual forms and write down its characteristic in a sentence.
- (2) Fragment the written sentences for each material and the interview result from the author of the material into the smallest meaningful phrases.
- (3) Assign the interpretive codes to these phrases to carefully review data.

**Table 1.** Design patterns of learning materials

Design pattern	Sub pattern	Definition	# of occurrences
<i>Scrapbook</i>		The arrangement of any portion of web page	
	<i>Fixed/single</i>	The portion consists of a single web element	11
	<i>Fixed/multiple</i>	The portion consists of multiple web elements	10
	<i>Partial/single</i>	The portion is a portion of single web element	7
	<i>Partial/multiple</i>	The portion consists of the portions of multiple web elements	9
<i>Group*</i>		The arrangement of elements to delineate distinct subsets	
	<i>Conjunction</i>	The use of partial overlap to strongly connect multiple elements	9
	<i>Spatial*</i>	The use of positioning to create white space, which clearly separates one or more sets of elements	11
<i>Path*</i>		The elements are arranged into one or more legible sequences	
	<i>Linear*</i>	A single, ordered sequence	12
	<i>Non-linear*</i>	Branching, with subsequences that fork and junction, and/or with multiple connected elements	5
<i>Morphology*</i>		The arrangement of elements corresponds to a recognizable form	
	<i>Concrete*</i>	The corresponding form is a text or a reference	12
	<i>Abstract*</i>	The corresponding form is a class schedule	3

The patterns marked \* are identical to the ones derived in [5].

- (4) Organize the codes into categories in terms of the arrangement pattern of web contents and then summarize the codes of each.
- (5) Define the core categories through combining similar categories, and finding relationships between them.

In our study, we assigned 173 codes and organized 18 categories. We used these categories to derive the design patterns in creating learning materials through web curation. As a result, we derived 4 core categories as design patterns shown in Table 1. For example, the two categories, summarized as “*various web elements selection*” and “*various portions selection*” were joined together to become the category named “*scrapbook.*” We also identified the distinct categories as sub patterns within each design pattern. Although the 3 design patterns and 5 sub patterns having asterisks were the same ones which were found in the previous study [5] of web curation for visual thinking, we found 2 unique design patterns in creating learning materials under the situation in which the learner can curate any part of a web page.

## 5 Design Patterns in Creating Learning Materials

We describe the characteristic of the unique design patterns found in our case study in creating learning materials. We also discuss the effectiveness of the enhanced web browser in terms of the user experience through creation of learning materials.

### 5.1 Design Patterns

**Scrapbook.** The design pattern *scrapbook* assembles any portion of a web element selected by the learner regardless of the document structure. A typical example was shown in Fig. 4. There are four distinct sub patterns, i.e., four different ways of assembling a portion of a web page.

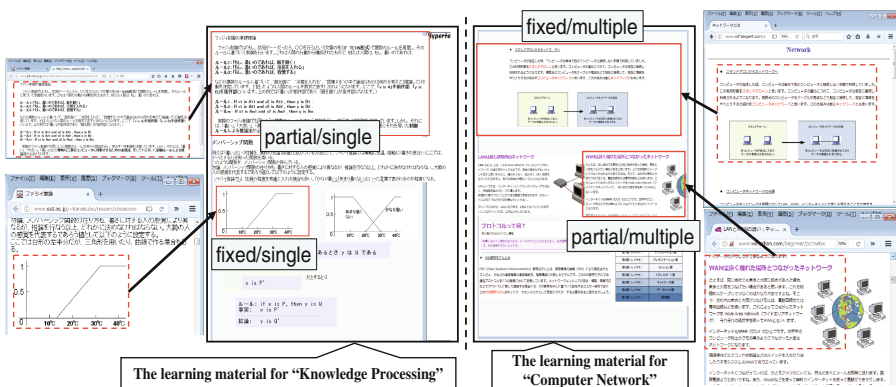


Fig. 4. Example of *scrapbook*.



The sub pattern *fixed/single* uses a single web element of the web page just as when creating learning materials. This pattern is always exhibited in web curation using IdeaMâché or Evernote which presupposes the document structure on the Web. In the learning material for “Knowledge Processing” in Fig. 4, this pattern was exhibited in partial bookmarking the image element of the whole graph. The sub pattern *fixed/multiple* arranges the multiple web elements of a web page as they are. In this learning material, the two image elements of diagrams along with their descriptions were simultaneously bookmarked.

The sub patterns *partial/single* and *partial/multiple* emerged through partial bookmarking of a portion of a single web element or portions of multiple web elements, respectively. The top of the learning material in the left half of Fig. 4 exhibits *partial/single* in which a part of paragraph on a web page was curated. In the learning material for “Computer Network,” *partial/multiple* arranges the portions of multiple elements, where half of the image and a part of its description were combined as an element of the learning material.

**Group/Conjunction.** The sub pattern *conjunction* forms a tight material which is packed with multiple elements without white space. Figure 5 shows an example of the learning material for the class “Software Development Laboratory II.” The author packed the portions of four web pages about UML in a tight format as if writing a textbook. Although this sub pattern is partially comparable to the sub pattern of overlapping the elements in the previous study [5], our study results showed that *conjunction* partially overlaps the elements or pushes them up next to each other in order to group them in as legible a way as possible. It can be said that this pattern shows the learners’ obsessive-compulsive desire to exhaustively collect the information about the subject when creating learning materials.

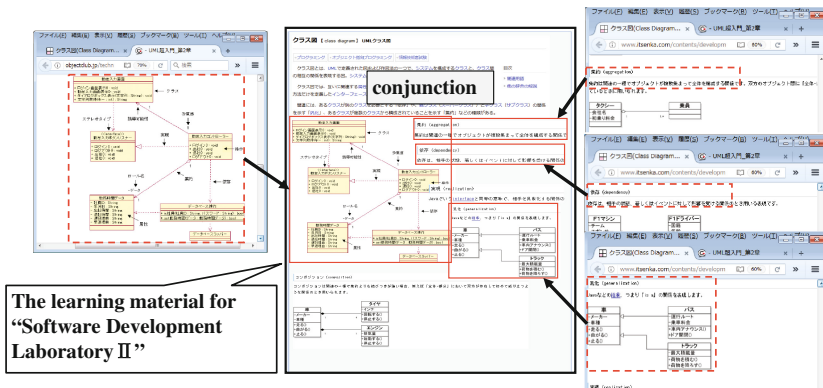


Fig. 5. Example of group

### 5.2 Design Intentions

The design patterns mentioned above are the results of analysis based on the behavior of the participants as learners in creating learning materials. From another perspective, we could categorize the learning materials in terms of the design intention of the learners. We found three typical intentions to make three types of materials; *glossary*, *links page*, and *textbook (reference)*. Figure 6 shows the typical learning material which was made according to each of these intentions. From the interview results, we deduced that these intentions changed depending on which learning style was considered effective by the learners for self-learning.

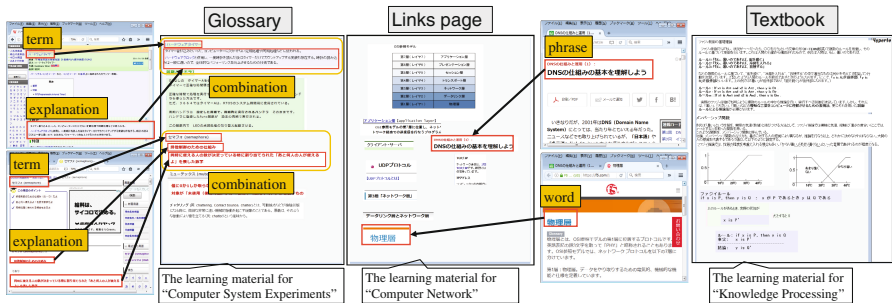


Fig. 6. The types of learning materials.

**Glossary:** The authors of this material type intended to curate as much useful information as possible so as to aid understanding of the terms introduced in the class rather than learning detailed solutions of various problems. Thus, the material consists of explanations about given terms, where the design pattern *path* was the regular one used for combining the term to its explanation.

**Links page:** This type of learning material consists of some anchors to the web pages. Each author of this material type performed partial bookmarking of the portion for the word or phrase in a web page including its explanation. These portions are arranged in the pattern *spatial* of the major design pattern *group*. The author intended to use such a word or phrase as anchor text on the learning material to refer to the web page including informative knowledge.

Almost all authors of this type of learning material tended to collect the information for exploring a certain problem related to the subject and wanted to study the class practically. Thereby, these materials included not only just abstract content but concrete content also, e.g., graphs, figures, and/or computer programs, and combined them. There were numerous variations of design patterns and as a result we could not see a regular design pattern for this type of learning material.

As seen from the above, the design intentions of the learners when creating learning materials by themselves are widely variable. In other words, the partial bookmarking on the enhanced web browser accommodates free form web curation or transclusion which meets the learners' requirements when creating learning materials. The unique design

pattern *scrap* derived in our study emerged in all the learning materials. Figure 7 shows the emerging ratio of each sub pattern of *scrapbook*. The total ratio of sub patterns *fixed/single* and *fixed/partial* which the traditional applications of web curation only allow to create, was about 54%; on the flip side, the sub patterns *partial/single* and *partial/multiple* which only the enhanced web browser can afford to create, accounted about 46% of all the curation. It can be said that web curation for creating learning materials should allow learners use any portion of a web page regardless of document structure. So, from the viewpoint of a curation technique, partial bookmarking on the enhanced web browser provides an indispensable function for the learners to create learning materials, and therefore stimulate and enhance their active learning ability and technique.

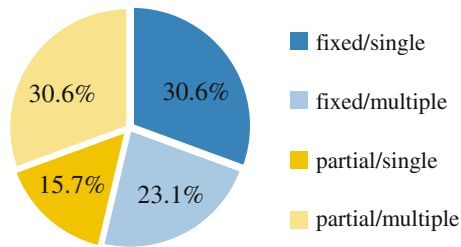


Fig. 7. The emerging ratios of sub patterns of *scrap*

## 6 Conclusions

We investigated how learners interact with the enhanced web browser in which partial bookmarking is available for free-form web curation or transclusion. The visual grounded theory analysis through the data set obtained from the case study clarified the characteristics of design of learning materials. The derived design patterns in creating learning materials revealed the advantage of the notion of partial bookmarking and the valuableness of free-form web curation for the learners in active learning.

Free-form web curation including partial bookmarking is still in its infancy [5]. We also know the set of design patterns derived from such a small amount of participants and learning materials is not complete. A long-term case study in which we provide the enhanced web browser for university students to support their active learning should be conducted so as to substantiate this study.

## References

1. Abe, Y., Matsusako, K., Kirimura, K., Tamura, M., Nakashima, M., Ito, T.: Tolerant sharing of a single-user application among multiple users in collaborative work. In: Companion Proceedings, CSCW2010, pp. 555–556. ACM Press (2010)
2. Evernote Web Clipper. <https://evernote.com/intl/jp/webclipper/?downloaded> Accessed 3 Feb 2017
3. IdeaMâché. <https://ideamache.ecologylab.net/>. Accessed 3 Feb 2017

4. Konecki, K.T.: Visual grounded theory: a methodological outline and examples from empirical work. *Revija za sociologiju* **41**(2), 131–160 (2011)
5. Lupfer, N., Kerne, A., Webb, A.M., Linder, R.: Patterns of free-form curation: visual thinking with web content. In: Proceedings of MM 2016, pp. 12–21 (2016)
6. Nagatomo, T., Tachibana, T., Sato, K., Nakashima, M.: Partial bookmarking: a structure-independent mechanism of transclusion for a portion of any web page. In: Proceedings of UIST 2016 Adjunct, pp. 185–186 (2016)
7. Pinterest. <https://jp.pinterest.com/>. Accessed 3 Feb 2017
8. Sato, K., Adachi, Y., Nakashima, M., Ito, T.: A mechanism of trailing the footprint for the previously visited web pages to ease a meta-knowledge-based search. In: Proceedings of NBS2012, pp. 298–305 (2012)
9. Tumblr. <https://www.tumblr.com/dashboard>. Accessed 3 Feb 2017

# Autonomous Decentralized System for Knowledge Refinement of Contents Published over Networks

Takuma Horiuchi<sup>1</sup> and Shinji Sugawara<sup>2</sup>(✉)

<sup>1</sup> Nagoya Institute of Technology, Gokiso-cho, Showa-ku, Nagoya 466-8555, Japan  
h-takuma@mcl.nitech.ac.jp

<sup>2</sup> Chiba Institute of Technology, 2-17-1 Tsudanuma, Narashino 275-0016, Japan  
shinji.sugawara@it-chiba.ac.jp

**Abstract.** Recently, a large number of useful contents are accumulated in large-scale networks like the Internet. On the other hand, plural sources often provide slightly different content concerning a same knowledge, and this causes incoherence of the knowledge for the network users. This paper proposes an autonomous decentralized knowledge refinement system that provides reliable knowledge to the users. This system consists of plural subsystems, and they autonomously subscribe contents from a lot of content sources over the network, refine and reconstruct the contents, and publish reliable knowledge. The effectiveness of this system is evaluated by computer simulations.

## 1 Introduction

Currently, a large number of useful content items are accumulated in large-scale networks like the Internet. Each of the content items is independently managed in a content source and the items are exchanged among a lot of network users. In such environment, large-scale networks are recognized as if they were a huge database, and we called this *super distributed environment* of information [1, 2].

Although there are a lot of valuable contents in super distributed environment, users are at risk of retrieving an obsolete or wrong contents because some content sources neglect appropriate updates, some publish misconceived contents, and even the other might publish disinformation on purpose. On top of that, there is another problem of resource discovery [3], i.e., a useful content for a user might lie buried in the huge amount of the other contents in the network, and this makes discovery of the content very difficult. Furthermore, if there is an inconsistency among the plural content sources publishing the same topic, users are needed to judge which content is reliable. In this case, it is difficult for the user to select the content to retrieve if he/she does not have enough literacy.

In order to solve these problems, a variety of researches have been done. Especially, there are a lot of studies to find out the reliability of WWW (World Wide Web) content sources over the Internet [4, 5]. The main aim of these researches is getting highly reliable content items by subscribing contents only from highly

reliable content sources. [6] mentions that because content publishing processes seriously influence the quality of the content, the processes themselves that prompt the sources to publish highly reliable contents must be important.

However, these researches mainly aim to get highly reliable contents by estimating the reliability of content sources, or achieving the appropriate publishing processes for making highly reliable contents, and they do not take the approach of retrieving a lot of content items from plural content sources publishing a certain topic, selecting reliable parts from them, and reconstructing the most reliable one. On top of that, it seems to be inappropriate for a user to judge that the content from a single source must be reliable, even if the source is extremely reliable.

Therefore, in order to retrieve reliable contents, we proposed a method that subscribes a content from plural sources publishing the same topic, clears off wrong or obsolete parts by judging from the view points of freshness of the content, reliability of the source, and commonality of the parts forming the content, and reconstruct the content consisting of the most reliable parts in [7–9]. We called this process “*knowledge refinement*.” Furthermore, we introduced a concept of *autonomous decentralized system* [10], and proposed a content refinement method that subscribes contents from plural sources and publishes the refined contents to the users autonomously [9].

## 2 Assumed Environment

The environment in which the proposed system works is assumed as follows.

- A lot of content sources exist in a large-scale network. Each content published in its source can be independently and freely updated and deleted by its owner user. Also, a new content of another topic can be added in every source.
- Each content is made up and published in a source according to the observations of an actual event occurred in an object existed in the real world, and the observations of the object continue at a certain frequency by the owner of the content and the source.
- The owner might update his/her content along with the change of the object itself or its condition.
- Each content published in its source includes errors with a certain probability.
- Each content source has a preference about the topic to publish, and the preference is known.
- A published content can be divided into fragments, each of which has a minimum meaning and has a counterpart fragment in each of the other content items of the same topic.
- Each fragment is so small that its meaning or possessing data is identical to a word, and each of such words belongs to a known finite set.

The concept of knowledge refinement assumed in this paper is illustrated in Fig. 1. This system subscribes contents partially including errors from a lot of sources scattered in the network, refines the contents, reorganizes them as a reliable knowledge, and finally publishes it to the other users.

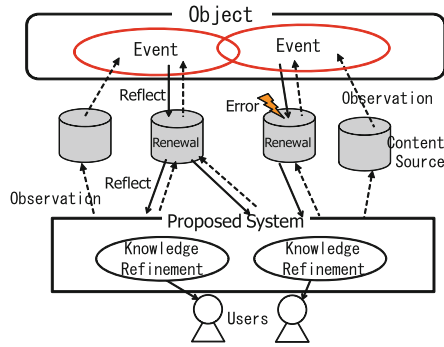


Fig. 1. Concept of knowledge refinement.

### 3 Proposed System

#### 3.1 Proposed System Architecture

The architecture of “Proposed System” shown in Fig. 1 is illustrated in detail in Fig. 2, which is designed as a layered autonomous decentralized system. It has layered data field (DF) [10] for contents exchange. This system mainly consists of databases (DBs) that subscribe contents from the content sources, DFs, and gateways (GWs). DBs are categorized into large classifications at first, then broken down furthermore into small classifications, according to published topics. An item of large classifications corresponds to a lower DF, and an item of small classification corresponds to a DB on the Fig. 2. Hence a lower DF bundles some DBs classified into a same large classification.

Each DB broadcasts its possessing content items with content codes in the directly connected lower DF periodically. This content code is defined uniquely according to the content and its classification. Also at the same time, each DB, i.e., the owner user of the DB, retrieves only the content items with content codes fallen within its interesting category. Some content items with special content codes that are preliminarily registered in GWs can go to another lower DF getting through upper DF, and the content items are broadcasted in that lower DF. Because most of the content items fallen within the similar categories are retrieved by DBs bundled in the same lower DF, this kind of limited contents exchange is effective for the system to reduce wasted traffic, except only a small number of special content items that are categorized into different plural classifications at the same time, which are allowed to be subscribed by DBs bundled in another lower DFs, too.

Each DB observes content sources that publish its interesting topic. If there is another DB that has the same preference of subscribing topic, bundled in the same lower DF, two DBs can share the load of the observations together and the system can reduce the data sending costs.

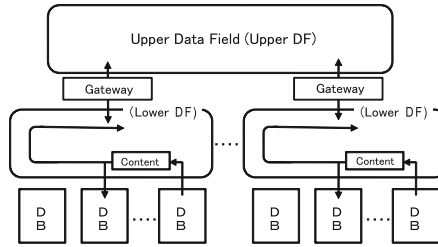


**Fig. 2.** Proposed system architecture.

### 3.2 Algorithm of DB Behavior

Each DB behaves as a main part of the system according to the following algorithm in order to autonomously publish reliable contents to the users. There are mainly six functions explained below.

#### 1. *Observing content sources*

Each DB observes its interesting sources and retrieve updated contents, if any, with content codes fallen within its favorite category. If a DB detects that a topic heretofore published is eliminated from the source, the DB lets the others know about it. Then all the DBs subscribing the missing topic remove their content items corresponding to the topic.

#### 2. *Sharing retrieved contents*

When a DB acquires an update of a subscribing content, the DB sends the updated content item and its metadata (updated time, reliability of the source mentioned later, etc.) to the other DBs through DFs, appending its content code.

#### 3. *Knowledge refinement*

Each DB executes content refinement process for its retrieved content items corresponding to its interesting topic. In the knowledge refinement, each content is divided into fragments and the reliability of each fragment is calculated according to the freshness of the content, the reliability of its publishing source, and the commonness of the fragment with the others retrieved from different sources. The detail of knowledge refinement algorithm is illustrated in [8], and omit the description from this paper because of space limitations.

#### 4. *Publish content items*

Each DB publishes content items refined according to the above method on its favorite topics.

#### 5. *Derive reliability of content sources*

Each DB derives the reliability of all content sources every  $t_p$  (constant) period. The reliability of a source is defined as the average ratio of the number of fragments adopted as a refined knowledge to the number of whole published fragments from the source for past  $t_p$  period. The initial value is set to 0.5.

#### 6. *Abort of source subscribing*

When the reliability of a source falls below a threshold  $\beta$ , abort subscribing



of the source and let the other DBs know this abort through DFs. The DBs noticed about the abort remove the content subscribed from the source.

### 3.3 Content Code Management

In the proposed system, each DB discriminates its favorite content items from the others by content codes. GWs have two lists of content codes in order to exchange content items among DBs using white list filtering, one is for a DB's content retrieval from the outside of its DF (subscribing direction), and the other is for a DB's content provision to the outside of its DF (publishing direction). Content items staying in upper and lower DFs are directed by GWs according to the lists of both directions, i.e., content items the content codes of which are on the list are allowed to slip through the GW, and the others are blocked. In order to manage the content codes, a DB that decides to subscribe a content from the DB in the other DF sends back an acknowledgment message when receiving the content item. Also, when a DB publishes a content item of a new category with a new content code, the content item is sent to all of the upper DFs regardless of the GWs' white list filters by using a special transmission mode, and reaches every DBs. The operations of registrations and deletions of content codes in the GWs' white lists for both directions are described as follows.

#### (a) Subscribing direction

When a content code is registered in subscribing direction, GW passes content items with the code to its lower DF.

##### (i) Registration

Each DB registers some content codes of its preliminarily assigned category to the list of subscribing direction beforehand. Besides, when a DB finds a new kind of content to subscribe from the new contents floating out from the other DFs, the DB adds the corresponding content code on the list of the GW of its DF in subscribing direction, in order to pass the same kind of content items to the DF. The acknowledgment messages from content receiving DBs, mentioned above, are sent to the DB providing the new content item regardless of the GWs filters.

##### (ii) Deletion

In the case that a content item slips through a GW in subscribing direction and reaches a DF from the outside but no DB subscribes the content item in the DF, the GW decides that the corresponding content code on its white list is unnecessary and delete it from the list of subscribing direction.

#### (b) Publishing direction

When a content code is registered in publishing direction, GW passes content items with the code to its upper DF.

##### (i) Registration

Each DB registers some content codes of its preliminarily assigned category to the list of publishing direction beforehand. Besides, when a DB finds a new kind of content from content sources and decides to publish it to the DBs of the other DF, the DB send the content item with its

content code by using a special transmission mode mentioned above. If an acknowledgment returns from a subscriber located outside DF, the DB adds the corresponding content code on the list of the GW of its DF in publishing direction, in order to pass the content through the GW of the DF.

(ii) Deletion

In the case that a content item slips through a GW in publishing direction and goes out to the upper DF but no acknowledgment message returns i.e., no DB subscribes the content item in the outside DF, the GW decides that the corresponding content code on its white list is unnecessary and delete it from the list of publishing direction.

## 4 Evaluation

### 4.1 Evaluation Method

The effectiveness of the system is evaluated by computer simulations from the viewpoints of  $F$ -measure and total cost. Total cost,  $E$ , consists of processing cost,  $E_p$ , as load on computers for browsing content sources and content refinement, and communication cost,  $E_c$ , as network loads for sending content items and messages, and content source browsing.  $F$ -measure,  $F_m$ , is defined as a harmonic mean of precision,  $P_r$ , and recall,  $R_e$ .

In this paper, precision is defined by the number of very satisfied content items from the viewpoint of the system user divided by the total number of content items provided by the system. On the other hand, recall is defined by the number of very satisfied content items provided by the system divided by the number of very satisfied content items to be found by infinite effort.  $F_m$  is shown as follows.

$$F_m = \frac{2 \cdot P_r \cdot R_e}{P_r + R_e} \quad (1)$$

Total cost,  $E$ , is defined as follows.  $W$  is a weight for changing importance of  $E_c$  and  $E_p$ .

$$E = W \cdot E_c + E_p \quad (2)$$

In this paper, we admit effectiveness of the system only if the total cost  $E$  is sufficiently suppressed, and wrong and obsolete fragments of the refined contents are adequately reduced, under the environment presented in Sect. 2.

### 4.2 Systems to Be Compared

- Majority oriented scheme system (MOS)

In the process of knowledge refinement, this system uses only majority vote for content fragments. The most common word is selected as the most probable word in each fragment of the content. The content consisting of the set of the fragments is provided to the user. The rest of the system configuration is just the same with the proposed system.

- Single DF system (SDF)  
This system has a single DF and all of DBs are connected in the same DF. The rest of the system configuration is just the same with the proposed system.
- No collaboration system (NC)  
DBs in this system do not communicate each other and do not exchange their content items. Each of DBs just retrieves contents from the content sources and refines the knowledge by itself independently. The rest of the system configuration is just the same with the proposed system.

### 4.3 Simulation Conditions

Specific parameters for the computer simulations are shown below in Table 1, and some conditions are assumed as follows.

**Table 1.** Parameters.

Parameters	Value
Number of content sources	200
Number of fragments consisting of a content item	1600
Number of all words belonging to $U$	10
Simulation time [unit time]	200
Number of simulation runs	100
Recalculation interval of content sources' reliability: $t_p$ [unit time]	10
Number of DBs	16
Number of lower DFs	4

- A fact, consisting of 1,600 fragments and observed by content sources is given; each fragment of the fact is given a word selected randomly, updated randomly to simulate the temporal variation of the fact; the number of updated fragments is given according to Poisson distribution with the mean arrival rate of 100.
- Each content source monitors some facts, revises their content items according to the temporal alteration of the facts, and re-publishes the updated content item; the probability for each content source to behave like this per unit time is 0.5.
- The initial number of publishing content items in each content source is given by a uniform distribution of [1, 625].
- Discarding randomly selected content and new content publishing according to the newly found fact occur respectively per unit time in each content source; the number of both discarding and new publishing content items are given by Poisson distribution respectively; the mean arrival rate of the distribution is defined by the number of publishing content items of the content source divided by 50.

- Each content source includes some error fragment in its publishing content item both mistakenly and intentionally; the probability of error occurrence is simulated by using Zipf distribution the maximum probability of which is set to 0.9.
- Threshold  $\beta$  to control the proposed system is set to the values between 0.3 to 0.9.

#### 4.4 Simulation Results and Discussions

Simulation results is shown in Figs. 3, 4, 5, 6 and 7. Parameter  $\alpha$  is set to 20.0 in every cases so that  $F$ -measure becomes maximum value.

$F$ -measures of all the methods are compared in Fig. 3. While the parameter  $\beta$  is set smaller, proposed system achieves the highest  $F$ -measure as with SDF, and higher than MOS. In this condition, because there are a lot of content items subscribed from the different DBs, majority vote for freshly published candidates selects reliable words of fragments successfully, thus proposed system gets higher  $F$ -measure than MOS which uses only majority vote.

However,  $F$ -measure of proposed system decreases rapidly along with the increase of  $\beta$ . In this situation, the number of content items DBs can subscribe reduces, and a lot of abortions of subscription occur. Then, recall value decreases and at the same time, precision is also reduced because of the difficulty of precise knowledge refinement. NC's  $F$ -measure is obviously lower than that of the other systems because DBs do not communicate with each other, and therefore each DB has fewer number of content items to be used for knowledge refinement.

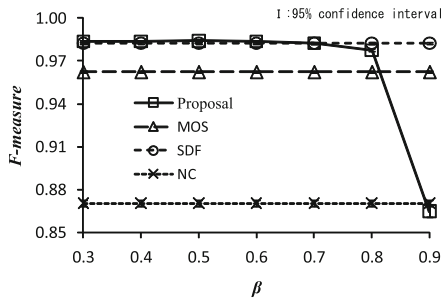


Fig. 3. Relationship between  $\beta$  and  $F$ -measures.

Processing costs are compared in Fig. 4. In the case of using the proposed system, processing cost gradually gets smaller along with the increase of  $\beta$ . This is caused because a lot of content subscriptions are aborted and the content refinement load is reduced when a small number of reliable contents are subscribed. The other systems without abortions of subscription need processing cost at almost the same level regardless of  $\beta$ .

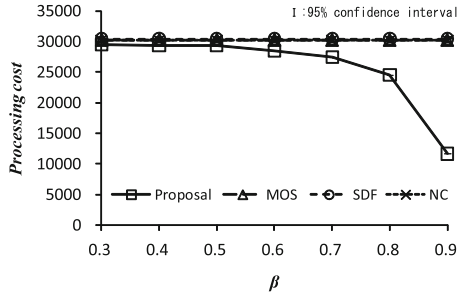


Fig. 4. Relationship between  $\beta$  and processing costs.

Communication costs are illustrated in Fig. 5. Proposed system reduces the cost along with the increase of  $\beta$  for the same reason with the above. In the case of using SDF, communication cost becomes larger than that of the other systems because this system has only a single DF and all of content items are shared by all of DBs, whereas the proposed system is divided into some DFs according to their main topics and DBs seldom have the opportunity to send content items of different kinds, then reduces communication cost. NC costs the lowest for communications, because DBs do not communicate with each other.

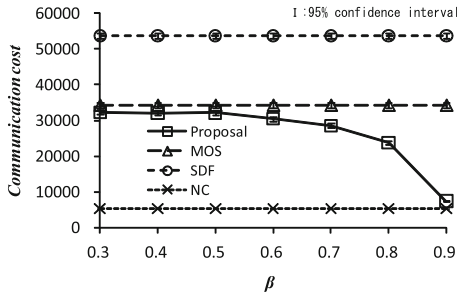


Fig. 5. Relationship between  $\beta$  and communication costs.

From the above, it turns out that the lower  $\beta$  is set to, the higher  $F$ -measure tends to be in the case of using proposed system. Because the aim of this research is to give correct contents to users, if we assume that the providing contents are correct enough when  $F$ -measure is larger than 0.95, the systems providing sufficiently reliable contents should be MOS, SDF, and proposed system with setting  $\beta$  to 0.8 or less.  $F$ -measures and total costs of these systems are compared in Figs. 6 and 7 respectively.

These figures show that proposed system with setting  $\beta$  to 0.8 reduces the total cost better than MOS and SDF in the both cases of  $W$  set to 0.5 (the situation that processing cost is twice as expensive as communication cost) and 2.0 (vice versa), and at the same time, keeps  $F$ -measure sufficiently as high as SDF.

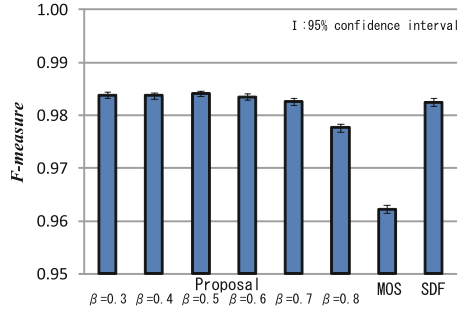


Fig. 6. Comparison of  $F$ -measures.

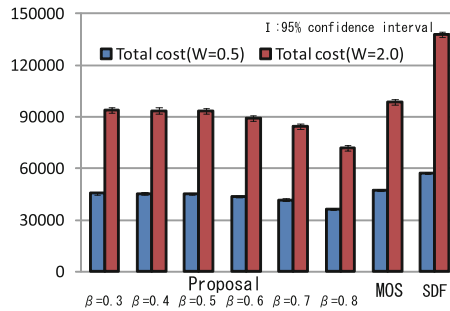


Fig. 7. Comparison of total costs.

In the case of changing the conditions such as giving different maximum error-inclusion probability and different distribution of error-inclusion frequency, proposed system does not lose its superiority. Therefore, in the condition mentioned above, proposed system with appropriate  $\beta$  can be the most effective than the others.

## 5 Conclusions

We proposed an autonomous decentralized system for knowledge refinement which provides users with reliable content items efficiently, by subscribing a content from a lot of sources over the Internet, decomposing it into fragments, extracting the most probable value of each fragment by focusing on its commonality, freshness, and reliability of its source, and reconstructing the refined content item, under the rapidly changing environment. And we showed the effectiveness of the system comparing with others by using computer simulations.

**Acknowledgements.** The authors would like to thank Professor Yutaka Ishibashi at Nagoya Institute of Technology, Nagoya, Japan, for precious advices and discussions.

## References

1. Sugawara, S., Yamaoka, K., Sakai, Y.: A study on image searching method in super distributed database. In: Conference Rec. IEEE Globecom 1997, pp. 737–740 (1997)
2. Sugawara, S., Yamaoka, K., Sakai, Y.: A study on efficient information searches with agents for large-scale networks. In: Conference Rec. IEEE Globecom 1999, pp. 1954–1958 (1999)
3. Bowman, C.M., Danzing, P.B., Manber, U., Schwartz, M.F.: Scalable internet resource discovery: research problems and approaches. *Commun. ACM* **37**(8), 98–107 (1994)
4. Gil, Y., Ratnakar, V.: Trusting information sources one citizen at a time. In: Proceedings of the 1st International Semantic Web Conference (2002)
5. Takehara, M., Nakajima, S., Sumiya, K., Tanaka, K.: A trust value calculation method for web searching based on blogs. *DBSJ Lett.* **3**(1), 101–104 (2004). (in Japanese)
6. Kato, Y., Kurohashi, S., Emoto, H.: Credibility of information content: concepts and evaluation technology. JSAI Technical report, SIG-SWO-A602-01 (2006). (in Japanese)
7. Sugawara, S., Sonehara, N., Watanabe, K.: Information retrieval for theoretical trust communications. In: Proceedings of the First Workshop on Information Credibility on the Web (WICOW), pp. 89–96 (2007)
8. Sugawara, S., Sonehara, N.: An efficient information retrieval from plural independent databases partially unreliable. In: Proceedings of the IASTED European Conference: Internet and Multimedia Systems and Applications, IMSA, pp. 148–153 (2007)
9. Horiuchi, T., Sugawara, S., Ishibashi, Y.: An information refinement with use of autonomous distributed databases. IEICE Technical report, IA2009-82, pp. 1–6 (2010). (in Japanese)
10. Mori, K.: Autonomous Decentralized Systems: Concept, Data Field Architecture and Future Trends. In: IEEE ISADS, vol. 93, pp. 28–34 (1993)

# A Device Status Visualization System Based on Mobile Markerless AR Technology

Toshiyuki Haramaki<sup>(✉)</sup> and Hiroaki Nishino

Division of Computer Science and Intelligent Systems, Faculty of Science and Technology,  
Oita University, Oita, Japan  
{haramaki, hn}@oita-u.ac.jp

**Abstract.** In order to effectively manage computer and network infrastructure, administrators need to appropriately understand the latest state of the whole system. When managing new servers and communication equipment, accurately grasping current situation is particularly important. In this paper, we propose a status visualization system based on AR (Augmented Reality) which supports administrators in actual management work environments. The proposed system graphically visualizes state information of a specific device such as a server or a network switch via a head mounted display (HMD) worn by a system administrator. It also visualizes logical and physical network structures consisting of servers and switches. This system assists the administrators for efficiently executing computer device management tasks. In addition, it helps them to master practical knowledge and skills related to servers and networks.

## 1 Introduction

In organizations such as companies and universities, the required operation of IT infrastructure including computer systems and networks is expanding. In order to maintain its operation, a team of multiple IT engineers is usually composed for the management. In order to efficiently manage and maintain IT infrastructure and services, management team members need to understand the current state of the whole system. Additionally, the IT infrastructure is dynamically deployed and frequently reformed in response to changes in the organization's activities and scale. When supporting new projects and their services in the organization, it is essential for extending the functions and performance of the IT infrastructure. Therefore, the configuration of the IT initial infrastructure currently in operation may be different from the current configuration. Properly managing these change histories and steadily operating the whole system is a very important task in computer system management.

However, there are some cases where the person in charging of the whole system does not accurately grasp the entire situation of the IT infrastructure currently in operation. Furthermore, the actual change contents done in the field may not correctly be reflected in the configuration management information. In universities, if there are some problems with computer and network systems, education and its management activities are affected by serious problems. In addition, any problems for the research computer



systems cause serious problems to the research activities. Daily monitoring and maintenance tasks are essential for ensuring the stable system operation and services in these environments.

CWIS (Campus Wide Information System), which is operated for education and research activities by universities and other higher education institutions, consists of various kinds of servers, computers and network equipment. Because many teachers and students are using the system, so many problems are happening in malfunctioning the system. If a serious failure occurs in the education system, many lectures and exercises cannot be conducted. Inadequacies in the research system may adversely affect the progress of the research activities. Grasping the whole system status and conducting stable operation increases the labor and expense of management tasks.

Therefore, in order to reduce the cost of acquiring the information necessary for managing the IT infrastructure, we are working on the research and development of a system that visualizes management information of IT infrastructure with simple operations. As a research result to date, we designed and implemented several methods for visualizing the system and network organizations and we implemented a network topology visualization system. This system enables the administrator to easily check the latest VLAN configuration information of a specific device. The system graphically presents the VLAN information set in a network device through an HMD worn by a user using AR (Augmented Reality) technology. The system can automatically identify the target network device observed by the user. It can reduce the operation cost for the system administrator to confirm the state of the network device and perform management task.

In this paper, we propose additional functions for visualizing information obtained from physical servers constituting real physical networks and virtual servers operating in a virtual environment. In addition, we will explain the mechanism for visualizing all the devices making up the whole computer system and the mechanism for identifying some failures caused in the system.

## 2 Related Work

In this research, we aim to visualize the status information of all the devices making up the IT infrastructure. We have worked on the research for effectively visualizing the network topology based on AR technology and achieved certain results. When visualizing information with AR, it is very important to identify the target on which the information is presented. We have been studying some ways to identify target devices in our previous studies. In this section, we explain the outline of our previous research that we have been working on and the methods on the visualization using the AR technique we used in the studies.

Figure 1 shows an overview of the VLAN visualizer that we first proposed and implemented to solve the visualization problem [1]. As preparation, it is necessary to paste a special unique marker on the network device to be visualized. Designating the marker specifies the device to visualize among many switches. An operator who uses the visualization system wears an HMD (Head Mounted Display) equipped with a

camera. The orientation of the camera is directed toward the user's line of sight. Therefore, the marker affixed to the front panel of the apparatus can be easily gazed. The VLAN visualizer extracts the IP address of the target device from the database that stores the marker pattern and the individual information of the corresponding device (IP address, the physical layout of the port array on its front panel, etc.). The system queries the device using its detected IP address and acquires its VLAN configuration information defined on each port. Finally, the system graphically displays the acquired VLAN information near the device via the HMD.

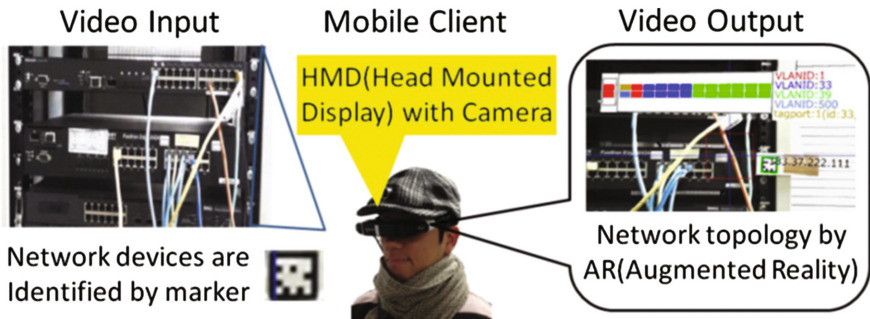


**Fig. 1.** Overview of initial VLAN visualizer.

In marker-based device identification adopted by the VLAN visualizer, it is necessary to paste physical markers specific to each target device beforehand. Information on the device and marker pattern corresponding to the device need to be registered in the database. Large companies and CWIS consist of hundreds or thousands of network devices. Thus, to identify these devices in the manner described above, huge number of markers should be made and defined. This is another problem causing a new burden for administrators. Additionally, because of the organizational evolution, the organization's IT infrastructure should frequently be changed. As a result, keeping the link between the marker and the target device up-to-date will force the administrator to make continuous efforts. Because of these issues, we reviewed the system architecture and improved its device identification method.

Then, we proposed another method using image information is designed and adopted as a new device identification method [2]. The flow of the new device identification method is shown in Fig. 2. Instead of attaching a physical marker to the device for identifying the device, this technique uses the features acquired from the captured image of the target device for identification. This allows the user to identify the actual device without using a physical marker. When using the system, the user needs to capture all devices as preprocessing for identification. Then, we replaced the marker-based object identification supported by the initial VLAN visualizer to the new image-based method.

Unlike the device identification by physical markers, online device image registration function is added and the target device image is taken on site to identify the device using its image features. The problems related to marker management was solved by introducing this vision-based device identification method. However, since the appearance of network



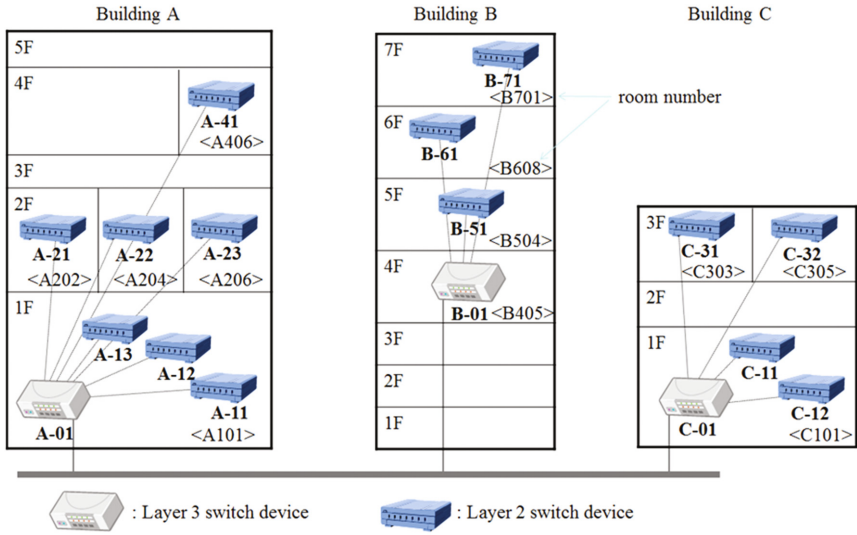


Fig. 3. A network configuration visualized by the previous system.

Figure 4 shows the network configuration to visualize by the enhanced system proposed in this paper. The devices are operated within the organization for actual educational research. Although the previous system can only visualize the network

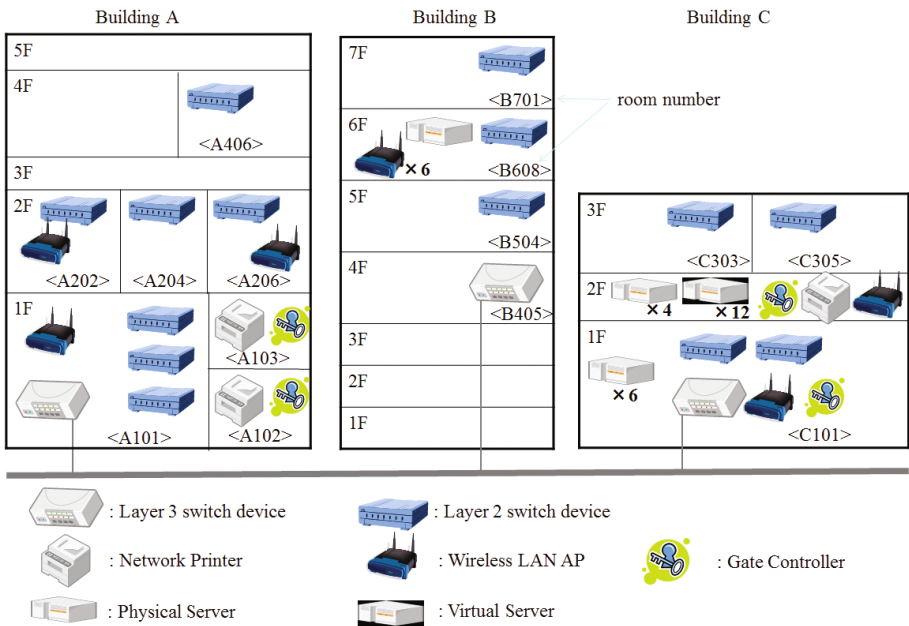


Fig. 4. A network configuration visualized by the new system.

configuration including L2 and L3 switches as shown in Fig. 3, the proposed system can also visualize additional components such as application servers, file servers, network printers, virtual servers, wireless LAN APs (access points), and routers. There are also surveillance cameras and gate controllers managing access to rooms to visualized in the system.

### 3.1 Extend the Target Device for Visualization

Figure 5 shows how to present configuration information when visualizing a server. It is very important to monitor equipment and networks in the IT infrastructure. If the system properly visualizes the currently monitoring device and informs the administrator of the occurrences of any troubles, he/she can rapidly solve the problem. If the administrator can analyze the equipment information monitored in the past, he/she may also predict the occurrence of future accidents and to prevent the failures beforehand.

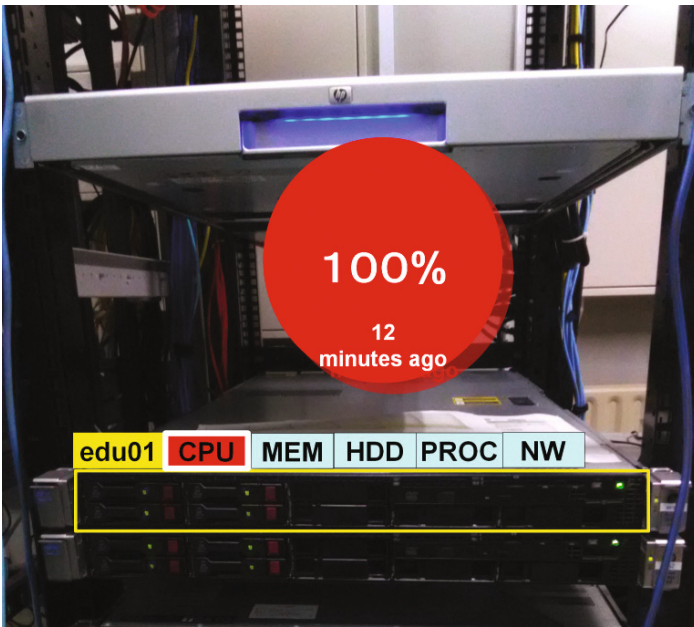


Fig. 5. Server status visualization example by the proposed system.

### 3.2 Introduction of Inexpensive Monitoring Agent Device

In the case of normal maintenance or fault recovery, the required information by management staff should be varies. If a serious malfunction occurs due to device failure, information to pinpoint the cause should be presented. After the reason of the cause is identified, information useful and necessary for solving the problem should be shown. If the reason is physical disconnection occurred in the network, the system may not

possible to monitor the state in the disconnected part. In such a situation, we introduce an inexpensive IoT monitoring device as an alternative monitoring and visualization system.

The monitoring agent using IoT forms a special network with dedicated communication function between monitoring devices using BLE (Bluetooth Low Energy) technology in addition to wired and wireless LAN communications. As a result, even if any failures occur in a part of the wired or the wireless LAN, the communication link between the monitoring agents can be continued. Figure 6 shows the outline of the IoT-based monitoring agent system for monitoring any failures occurred in the system.

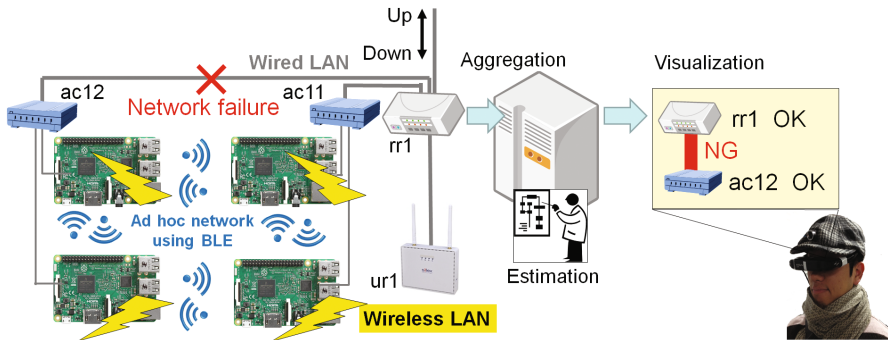


Fig. 6. Network monitoring agent based on IoT.

As shown in the figure, if the physical link between “rr1” and “ac12” loses for some reasons, the previous system cannot get information about the ac12 because the rr1 cannot communicate on the downstream side of the port to the ac12. If the network monitoring agent forming a unique ad hoc communication path is built, the system can confirm the living of the device ac12 and identify the cause of the failure. It is useful in identifying the cause and solving the problem in any failures including physical disconnection. If the user accumulates and analyzes information about these happenings for a long term, he/she can estimate and present such critical events in the future management task.

## 4 Preliminary Experiments

As for implementation of the network monitoring agent proposed in this paper, Zabbix was introduced into the system. Zabbix has a comprehensive information monitoring function that dynamically acquires information from devices such as servers and network devices. By installing the Zabbix agent on a monitoring server, the system can send status information to the Zabbix main unit of the server and check the CPU usage rate and HDD usage status in real time. For servers without Zabbix agent installed, the system can send the servers’ living confirmation for each port via HTTP and SMTP. Operation information of network devices can be acquired from the MIB (Management

Information Base) of the target device using SNMP (Simple Network Management Protocol) for real-time monitoring.

The system monitoring agent is implemented using Raspberry Pi 3. Raspberry Pi 3 is an inexpensive IoT open source hardware and Linux based Raspbian OS runs on each board. The monitoring agent application and the ad hoc network application are running on that OS. The ad hoc network application is implemented based on the iBeacon standard and all information is exchanged using BLE (Bluetooth Low Energy) technology based on the standard.

As a preliminary experiment, we installed an agent for monitoring wireless LAN radio field strength implemented by multiple Raspberry Pi 3 components in the actual network environment, and we conducted an ad hoc communication test using BLE. Since communication on the upper and lower floors of the experimental environment was unstable, it is desirable to install multiple ad hoc networks on the same floor when building an ad hoc network. If multiple wireless LAN APs are installed in the floor, it is possible to communicate via different link if any failures occur in the current wireless link.

## 5 Conclusions

We proposed a system to visualize information of all the devices constituting a network infrastructure. It helps administrators for efficiently managing the whole network. In this paper, we described a method to visualize the entire system including servers in addition to network devices. The proposed system consists of a system monitoring agent, servers, and mobile AR clients. The administrator uses the mobile AR client system implemented using an HMD device and performs the management task. The wireless communication function incorporated in the HMD simultaneously detects Wi-Fi signal strengths receivable at the administrator's current position. Based on the obtained information, the system estimates the physical location of the administrator, such as the building and floor he/she is currently working on.

A camera incorporated in the HMD continuously captures the image of the target device being monitored by the administrator. Additionally, sensor information that varies according to the administrator's movements is captured by the IMU embedded in the HMD. The image and sensor information are combined for automatically identifying the target device in the administrator's vision. The client queries the server for the management information of the identified device and the server returns it as a graphical image. The client renders it via the user's HMD display.

Several preliminary experiments were conducted to verify the effectiveness of the extended visualization function proposed in the paper. We investigated whether the cause of the problem could accurately and quickly be identified. As a result, when a node in the network topology fails, the monitoring agent works effectively to identify the cause of the failure.

In the future, we would like to further verify the usefulness of the proposed visualization function by using in actual management tasks. We also plan to implement a function to help users for predicting the current operating state based on the past

operation history and graphically presenting the result. To make the system more efficient, a mechanism for predicting the occurrence of management risks and accidents with high probability by machine learning based on a large amount of observation data is another challenge.

**Acknowledgments.** This work was supported by JSPS KAKENHI Grant Number 15K00277.

## References

1. Nagatomo, Y., Nishino, H., Kagawa, T.: An AR-based VLAN visualizer. In: Proceedings of the 2014 IEEE International Conference on ICCE-TW, pp. 117–118 (2014)
2. Haramaki, T., Nishino, H.: A network topology visualization system based on mobile AR technology. In: Proceedings of the 29th IEEE International Conference on AINA-2015, pp. 442–447 (2015)
3. Haramaki, T., Nishino, H.: A device identification method for AR-based network topology visualization. In: Proceedings of the 10th International Conference on BWCCA-2015, pp. 255–262 (2015)
4. Haramaki, T., Nishino, H.: A sensor fusion approach for network visualization. In: Proceedings of the 2016 IEEE International Conference on ICCE-TW, pp. 222–223 (2016)



# A Color Scheme Explorer Based on a Practical Color Design Framework

Satoru Miura and Hiroaki Nishino<sup>(✉)</sup>

Division of Computer Science and Intelligent Systems,  
Faculty of Science and Technology, Oita University, Oita, Japan  
sigsig490@gmail.com, hn@oita-u.ac.jp

**Abstract.** Color scheme design is an important process when designing artwork such as illustrations and graphics. Appropriate coloring maximizes the functional and emotional effects of the work. However, there is no unique solution for properly designing the layout of multiple colors. A designer must have enough skills and experiences for accurately presenting his/her targeting impressive quality of the work. This paper proposes a method for automatically creating and presenting a set of candidate color layouts by adjusting a few carefully selected color parameters with color harmony. It enables designers to readily explore various color scheme candidates while considering color harmony of the work. We implemented a color design support system based on the proposed method and conducted experiments for validation.

## 1 Introduction

Color scheme design is an important process when designing artistic products such as corporate logos, event posters, and web pages. Appropriate coloring greatly enhances the impressions and emotional effects of the products. However, there is no standard method or algorithm for exploring the best color scheme fitting to a design concept. Additionally, knowledge about color harmony is required to produce an optimum solution with harmonious color selection. Therefore, the color design is quite a difficult and tedious task even for experienced designers.

Designers commonly use their preferred photo retouching and/or drawing tools to create the products. Although these tools provide extensive functions for drawing and composing graphics, functions for supporting creative design aspects such as proposing a color scheme with harmony are insufficient. Therefore, the designers need to select an appropriate color set from the full color spectrum and explore the optimum scheme by trial and error. Such task requires a lot of time and efforts to find the best one. Because the experienced designers likely to select biased color sets depending on their preferences, resulting color scheme may fall into mannerism.

In this paper, we propose a color scheme design support system using a color coordinate system called Practical Color Co-ordinate System (PCCS). It is used by expert designers as a framework for analyzing and designing color scheme with color harmony. The proposed system automatically generates various candidate images by painting a target image based on a set of simple color appearance parameters specified

by a user. The user can easily explore and find the optimum one matching the user's design concept among the candidate images.

Figure 1 shows a simple example for designing a logo painted by two or three colors. The pieces in Fig. 1(a) use two complementary colors that are exact opposite colors in a color space. This coloring technique enhances the contrast between characters and background included in a logo. The pieces in Fig. 1(b) use three colors that are equidistant on the hue circle as explained in Sect. 3.1. Three colors in this technique are well balanced and can express a sense of stability for coloring a logo. The pieces in Fig. 1(c) unify a whole logo image with a single hue as a dominant color and change the image impression with tone. Hue and tone are explained in Sect. 3.1. The upper four images use blue as a dominant color for expressing cold impressions while the lower four use red for depicting warm impressions. The pieces in Fig. 1(d) unify a whole logo image with a single tone and change the image impression with hue color. The upper and lower four images use "light" and "dark" tones, respectively. Although the images in the same tone are painted in different colors, they give a unified impression.

Designers who know the above-mentioned techniques can select hues and tones by themselves and find an optimum color scheme. They should, however, waste time to do it by trial and error. The proposed system automatically generates various images by randomly selecting a specific hue and tone combination among user specified hues and tones. It significantly reduces the time to find the best one. The user iterates the process of hue/tone selection and candidate image generation until he/she finds the optimum image fitting to his/her design concept. We designed the system operation as simple as possible so that even beginners can easily use it.

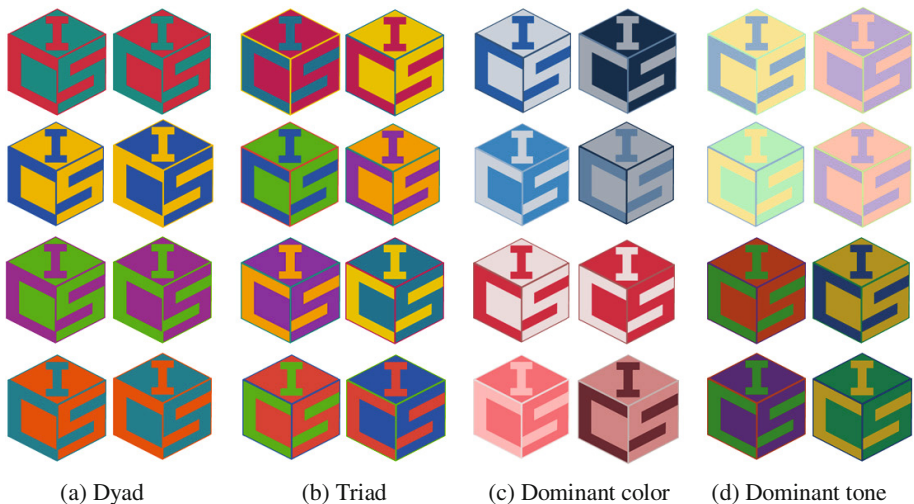


**Fig. 1.** Four coloring techniques applied to the logo design: (a) *Dyad* technique for coloring a logo using two complementary color pair. (b) *Triad* technique for coloring a logo using three colors that are equidistant on the hue circle. (c) *Dominant color* technique for coloring a logo using a single color with different tones. (d) *Dominant tone* technique for coloring a logo using a single tone with different hues.

## 2 Related Work

There are some previous research activities supporting color design process. Among them, Interactive Genetic Algorithm (IGA) is a powerful framework enabling unskilled designers and novices to easily creating their own artwork based on their personal preferences [1–3]. An IGA-based system firstly takes an initial model as an input data and randomly generates multiple objects based on the model for user’s review. Next, the user rates each object and requests the system for generating a set of new objects. Then, the system reproduces new objects by evolving the current objects. It uses a set of GA operations such as cross over and mutation for the evolution. While normal GA uses a predefined fitness function for calculating the fitness value of each object, IGA applies the user’s rates as fitness values when performing the GA operations. The process of the user’s rating and the system’s evolution is iterated until the user finds an optimal solution. In this way, IGA involves user’s preference or sensitivity into the object optimization process.

There are some other trials for applying the PCCS color system to color design process. Fukuda et al. applied PCCS for extracting personal preferred colors and coloring patterns [4]. They collected and analyzed color illustrations made by multiple subjects using an IGA-based design system. They confirmed that quantitatively extracting a representative color and a coloring pattern from a subject’s illustration can be possible by using PCCS. Ogawa et al. tried to analyze the relationship between human feeling and color using PCCS [5]. They categorize a set of image words expressing specific color combinations into clusters and developed a design support system based on the derived clusters.

All these activities target at developing techniques enabling users to easily create their favorite color scheme without using specialized knowledge and skills. Our target is experienced users who can produce their original products. We propose a method enabling experts to dramatically improve a time-consuming process that is to explore and find the best harmonious color scheme among enormous possibilities. Additionally, we show the proposed method is effective for beginners by supporting a set of carefully-selected operations.

## 3 System Implementation

### 3.1 Practical Color Co-ordinate System

PCCS (Practical Color Co-ordinate System) is a color system developed by the Japan Color Research Institute in 1964 [6]. It enables users to practically perform color design for various targets and easily select a combination of harmonious colors. It is used in a wide range of color design processes such as survey, planning, analysis, and education. It allows the users to effectively design harmonious color scheme by simply combining two color parameters “hue” and “tone”.

Hue is a color appearance parameter such as red, green, and blue. Figure 2 shows the PCCS hue circle presenting relationships between color hues. It organizes 24 hues around a circle, centering on psychological four primary colors consisting of red,

yellow, green, and blue. Each hue is labeled with a number from 1 to 24 and a hue symbol such as “pR (purplish-Red)” and “bG (bluish-Green)”. Diagonal color pairs on the circle are complementary colors as shown in Fig. 2, so the users can select a specific pair on the circle for making dyad color schemes as shown in Fig. 1(a). Similarly, if they select three colors that are equidistant on the circle (those connected by a triangle in Fig. 2), they can make triad color schemes as exemplified in Fig. 1(b).

Tone is a color concept integrating lightness and saturation as shown in Fig. 3. It consists of 17 elements including 12 chromatic and 5 achromatic color sets. Each tone element is labeled with an adjective word such as “v (vivid)” and “dk (dark)”, so the users can easily perceive the brightness and colorfulness of each tone. In the PCCS color system, the users can indicate a specific color with its tone symbol and hue number such as “v2 (vivid red)” and “dk18 (dark blue)”. Changing the tone parameter with a fixed hue color produces dominant color schemes as exemplified in Fig. 1(c) and the reverse case produces dominant tone schemes as shown in Fig. 1(d).

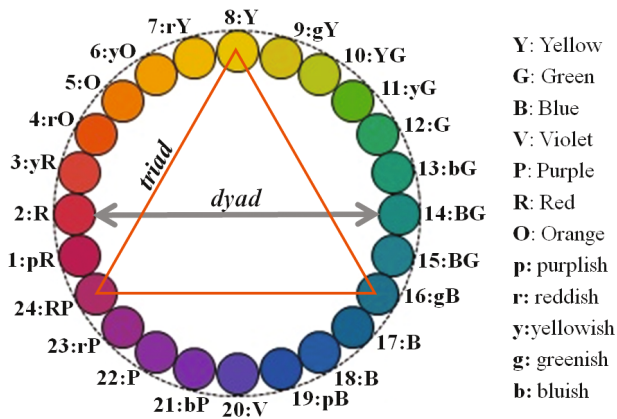


Fig. 2. PCCS hue circle.

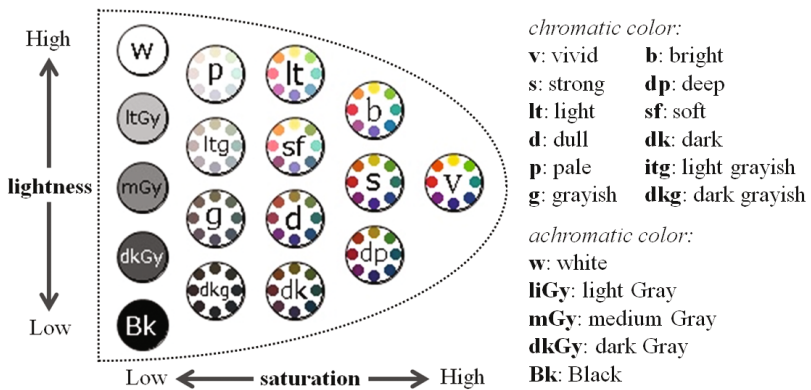


Fig. 3. PCCS tone concept.

### 3.2 Color Scheme Design Flow

Figure 4 shows the processing flow of the proposed system. Firstly, the user needs to prepare a temporary color layout image to clearly indicate regions where different colors are painted. The figure uses a logo design example consisting of three regions painted in different colors: characters, backgrounds, and edges. The system reads the temporary image and analyzes it for extracting the indicated regions. It automatically detects the connected regions and labels them using the component labeling function supported by OpenCV. Then, the system creates three mask images equal to the number of the detected regions.

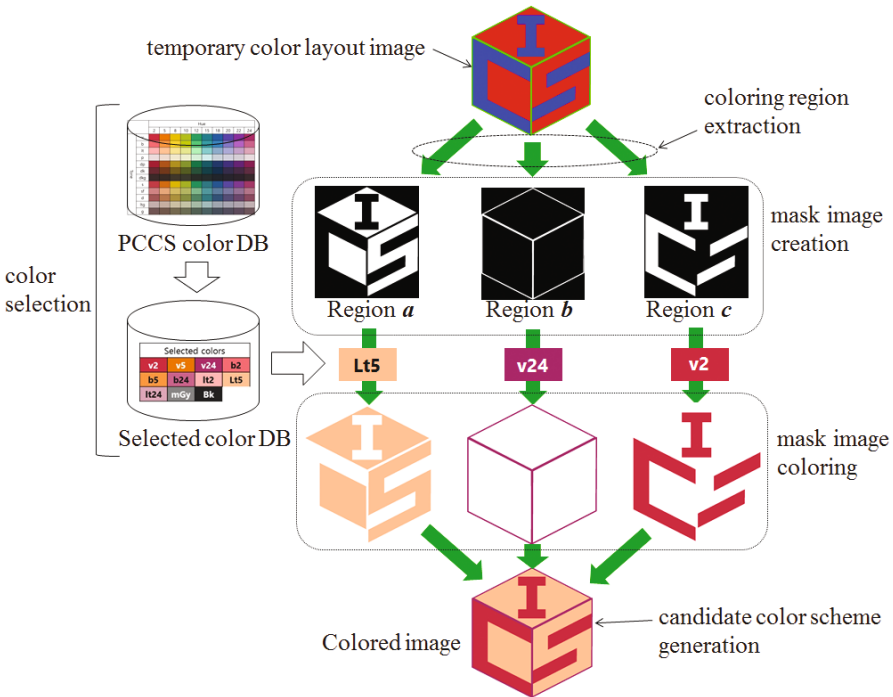


Fig. 4. Color scheme design flow.

Then, the system randomly paints white regions in each mask image to create a color scheme candidate. The painting process wastes time if it needs to select appropriate color combinations among a huge color set. Therefore, the system selects a subset of colors among all colors defined in the PCCS color database before painting the regions.

The color selection is made based on the PCCS color parameters, hues and tones, specified by the user. In the PCCS color database, total 293 color records are defined. This is the sum of 5 achromatic tones and 288 colors which is the product of 24 hues and 12 chromatic tones. If the user specifies four hues and three chromatic tones, the

system selects 12 colors and saves them in a separated database, the selected color database. Then, the system randomly selects a color from the database for painting each mask image. It significantly narrows down the selection range of paint colors while preserving the fitness with the user's design concept.

After that, the system merges all mask images painted by different colors and generates a candidate color scheme. The system iterates the painting process sixteen times and presents all the different sixteen candidate images on a monitor as shown in Fig. 5. The color selection, mask image coloring, and candidate color scheme generation parts in Fig. 4 are repeated until the user finds the best color scheme.

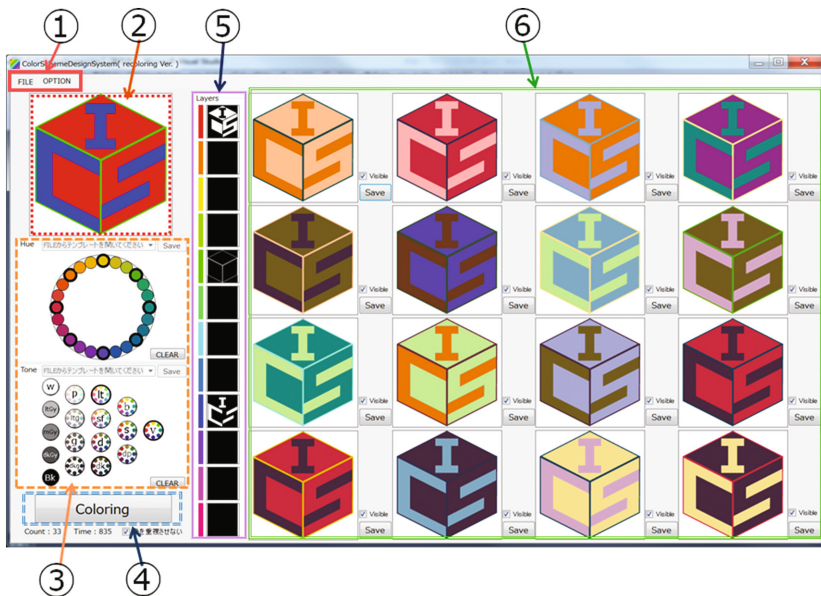


Fig. 5. Snapshot of system GUI.

### 3.3 System GUI

Figure 5 shows the system operation screen. The following numbered items correspond to the numbers shown in the figure.

1. *System menu*: This is a pull-down menu including system operations such as file input and color parameter setting. The FILE tab is used to specify the name of a temporary color layout image file and load it into the system. The OPTION tab is to change the number of hues for showing in the color parameter setting panel.
2. *Temporary color layout image display window*: The temporary color layout image specified in the system menu's FILE tab is displayed in this area.
3. *Color parameter setting panel*: The hue and tone parameters in the PCCS color system are set in this panel. The user can select a specific hue by clicking it in the hue circle and select a tone by clicking a corresponding icon. The selected hues and

tones are highlighted with a thick black contour and they can be released by clicking again. The selected hue and tone combination can be saved and restored through the system menu's OPTION tab. It enables to share a specific hue and tone combination with others and reuse it between different coloring targets.

4. *Coloring execution button*: This button activates the coloring operation using the indicated temporary color layout image and selected color parameters.
5. *Mask image display window*: A set of mask images made by analyzing the temporary color layout image is displayed in this area.
6. *Color scheme display window*: Sixteen preview images of color scheme candidates are displayed in this area. Each preview sub-window has the "Visible" check box for switching image display on/off and the "Save" button for saving the image. Directly clicking a preview image enlarges it for checking details and comparing with other images.

## 4 Preliminary Experiments

We performed experiments for verifying the effectiveness of the system for designing color scheme. We asked a dozen university students for coloring the logo under two different themes such as "pleasant" and "futuristic" logos. We set the former as a practical and easy to imagine theme while the latter is an abstract and hard to imagine one. Some of them have some experiences for using photo-retouch software for creating digital artwork. Figure 6(a) shows example logos made under the "pleasant" theme and Fig. 6(b) shows "futuristic" logo examples.

We observed a tendency for using similar colors and tones in the same theme among different subjects. In the case of the "pleasant" logo, the subjects tend to use warm colors and soft tones while they prefer to use cold colors and dark tones in the "futuristic" logo. Because our target user is experienced designers, we assumed the production time for the experienced subjects was shorter than that of the novices. The experts should be

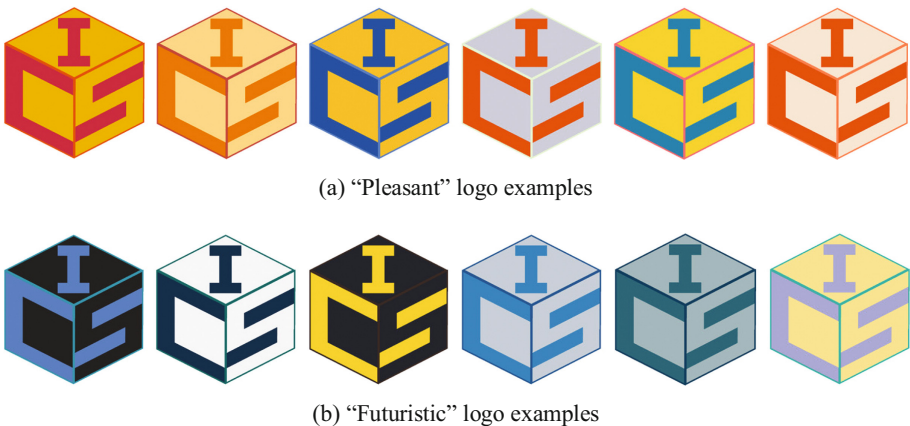


**Fig. 6.** Colored logo examples produced in the experiment.

better for understanding the PCCS-based color design functions and finding the best image expressing the theme among various candidate color schemes. We, however, found the opposite results. The most novices completed a coloring task in about three to four minutes and there were not so much differences between individuals. On the other hand, the experienced subjects tended to spend longer time for coloring a logo. We also observed clearer differences between experienced individuals for their production time. A subject finished in about two minutes by quickly deciding his best design while the other subject took more than 10 min for carefully checking the candidate images one by one. Although we need to conduct quantitative experiments by employing more subjects, we verified the practicality of the system to some extent enabling both experienced users and novices for exploring color design under a specific theme.

We also adopted the system for making a real brochure of our department. Figure 7 shows an example brochure designed to give a unified and staid mood by using blue as a base color and yellow for emphasizing some items. Figure 8 shows other example designed to be more colorful by painting a different color for each item. The example shown in Fig. 9 is similar with the example in Fig. 8, but the background of each item is painted in its item color while the example in Fig. 8 uses the same background color. The designer stated that he was able to create a set of drafts and easily choice several good ones as final products. He added that the system is useful for real design environment because it enables to create multiple color schemes with different moods from a single source image. The deliverables can be targeted at various customers with different ages, occupations, and needs.



Fig. 7. A brochure design painted in a few color for all items.





## 5 Conclusions

The color scheme design usually is a painful and time consuming task because possible color combinations explosively increase depending on the number of painting regions. We proposed a method for designing color scheme with preserving harmony based on the PCCS color system. The proposed method automatically generates multiple color schemes as candidate images based on two color parameters, hue and tone, specified by a user. It simultaneously displays the generated images in a list form, and the user can easily compare them for exploring a good one fitting with the product concept. He/she can iterate the color scheme exploration by changing the parameters and executing new candidate image generation until he/she gets a satisfactory output. We implemented a color design support system based on the proposed method and conducted some experiments for verifying the effectiveness of the system.

In the near future, we would like to conduct more comprehensive experiments with larger number of subjects for quantitatively testing the practicality and applicability of the system in real design issues.

**Acknowledgments.** This work was supported by JSPS KAKENHI Grant Number 15K00277.

## References

1. Hsiao, S.-W., Hsu, C.-F., Tan, K.-W.: A consultation and simulation system for product color planning based on interactive genetic algorithms. *Color Res. Appl.* **38**(5), 375–390 (2013)
2. Inoue, H., Yuan, D., Iwatani, K.: Color combination support systems using interactive evolutionary computation. *J. Jpn. Soc. Fuzzy Theor. Intell. Inf.* **21**(5), 757–767 (2009). (in Japanese)
3. Kagawa, T., Nishino, H., Utsumiya, K.: An interactive surface design method for 3D geometrical shapes. *Int. J. Comput. Syst. Sci. Eng.* **27**(1), 63–72 (2012)
4. Fukada, Y., Mitsukura, Y., Fukumi, M.: The extraction of the personal coloration pattern for color design system. In: *Proceedings of the SCIS & ISIS 2008*, pp. 598–603 (2008)
5. Ogawa, S., Hagiwara, M.: Color combination support system using image words clustering. *Trans. Jpn. Soc. Kansei Eng.* **15**(2), 287–296 (2016). (in Japanese)
6. Wakata, T., Saito, M.: A study of color impression about “tone” in PCCS color system. *J. Color Sci. Assoc. Jpn.* **36**, 224–225 (2012)

# Performance Testing of Mass Distributed Abyss Storage Prototype for SMB

ByungRae Cha<sup>1,2(✉)</sup>, YoonSeok Cha<sup>2</sup>, Sun Park<sup>1</sup>, and JongWon Kim<sup>1</sup>

<sup>1</sup> School of Electrical Engineering and Computer Science, GIST, Gwangju, Korea  
brcha@smartx.kr, {sunpark, jongwon}@gist.ac.kr

<sup>2</sup> GenoTech Inc., Gwangju, Korea  
dxcha@naver.com

**Abstract.** The trends in ICT are concentrated in IoT, Bigdata, and Cloud Computing. These megatrends do not operate independently, and mass storage technology is essential as large computing technology is needed in the background to support them. In order to evaluate the performance of high-capacity storage based on open source Ceph, we carry out the demonstration test of abyss storage with domestic and overseas sites using educational network: KOREN. In addition, storage media and network bonding are tested to evaluate the performance of the storage itself.

## 1 Introduction

Most new technologies improve product performance, and these technologies are called persistent technologies. Persistent technologies can be either disconnected or radical because of their nature, but many of them have a gradual character. Sometimes destructive technologies arise, and innovative technologies bring to market a value proposition that is quite different from what was used in the past. We intend to develop high-capacity, distributed storage and network acceleration technologies based on open source to gain the opportunity of transition and growth from existing storage technologies of existing leading companies to innovative storage technologies for emerging small and medium enterprises. For this, we are using open source Ceph.

Ceph is an open source project launched to implement large software-defined storage using Intel processor-based general purpose hardware. Thus, costs and limitations, and storage services are possible without a monopoly. In this paper, disk media performance test, network bonding, and network traffic test of KOREN network are performed to improve performance of mass storage based on open source Ceph.

## 2 Design and Implementation of Mass Abyss Storage Prototype

Open source Ceph for mass storage is a Linux distributed file system of a petabyte scale and started with a doctoral research project on Sage Weil's storage systems at UCSC (University of California, Santa Cruz).

The architecture and interaction with open-source Ceph system can be expressed as shown in Fig. 1(a), and Fig. 1(b) briefly shows the Ceph self-healing and data triplexation procedures. The benefits of open source Ceph include the next-generation architecture, integrated storage, and openness and scalability, as shown in Fig. 1(c). Thus, Open source Ceph comes with a built-in benchmarking SW tool called the RADOS bench, which can be used to measure the performance of Ceph clusters at the resource pool level [1, 2].

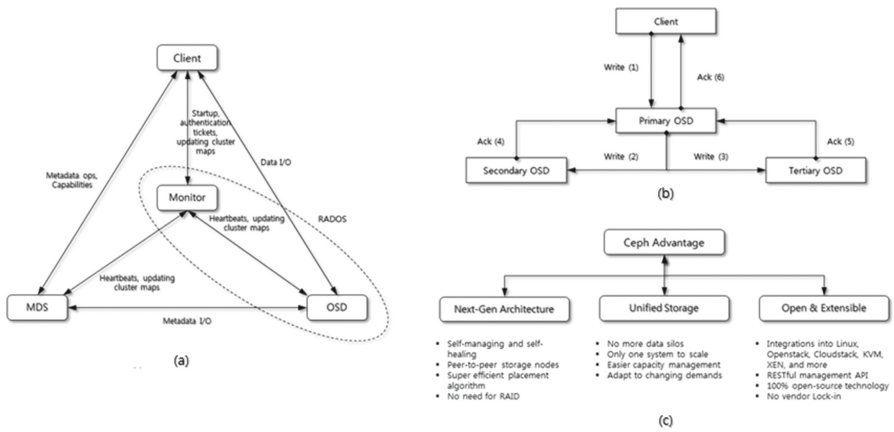


Fig. 1. Architecture & interaction, triplexation, and benefits of open source Ceph.

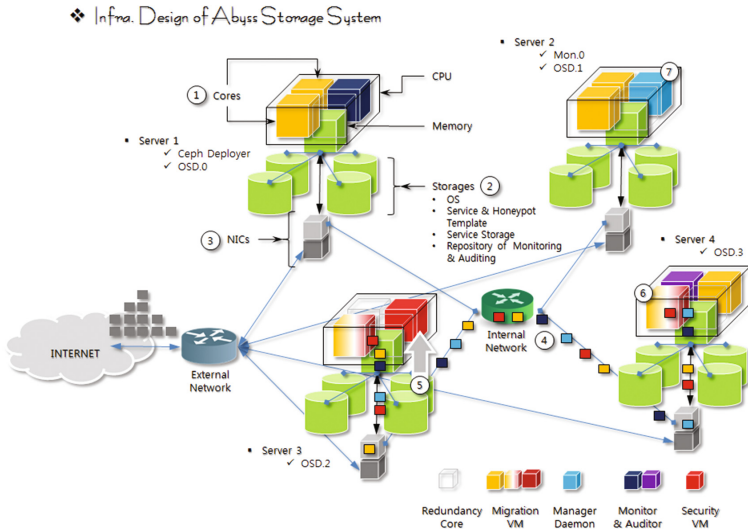


Fig. 2. Concept diagram of mass distributed Abyss Storage.

The logical components of the mass volume Abyss Storage Server for SMB is shown in Fig. 2, and H/W prototype of the Abyss Storage, 3D rendering image and the 3D printing result of the product case are shown in Fig. 3, respectively.

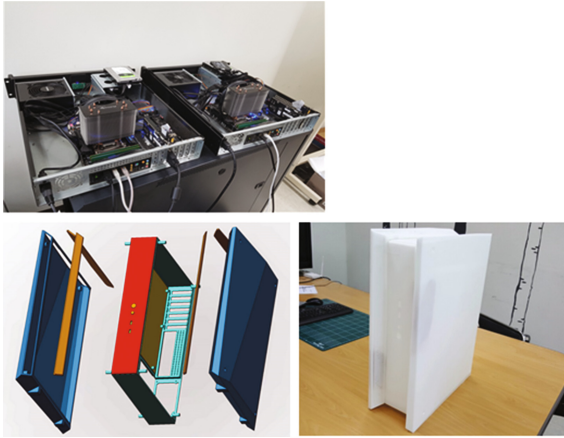


Fig. 3. H/W prototype and 3D printing product of Abyss Storage.

### 3 Performance Testing of Abyss Storage Prototype

In order to improve performance of Abyss Storage, we tested performance of storage media by disk types, bonding for acceleration of internal network of storage, and network traffic test using KOREN network.

#### 3.1 Disk Media Test of Abyss Storage

The disk tests of Abyss Storage servers were performed by disk media types (HDD, SSHD (Solid State Hybrid Drive), and SSD). Using RADOS Bench SW, we performed

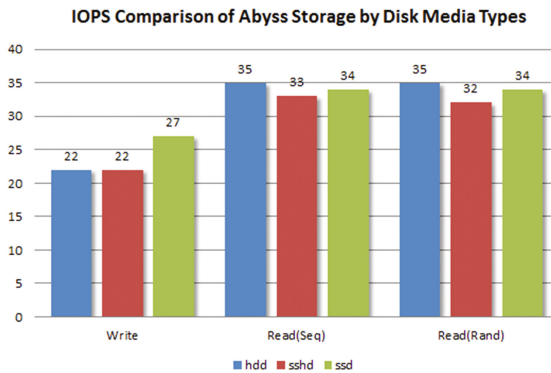
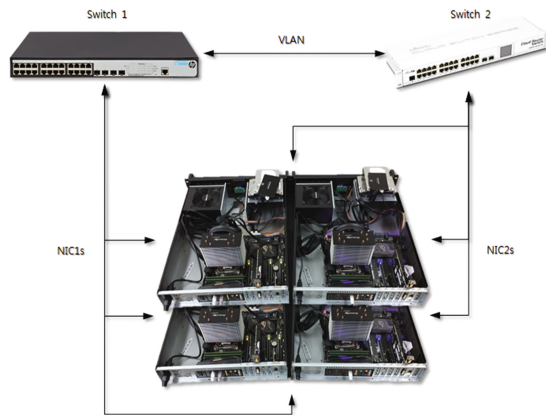


Fig. 4. IOPS comparison of Abyss Storage by disk media types.

the read and write operation of disk media types for 10 s and recorded the average of IOPS (input/output operations per second) using RADOS Bench SW as shown in Fig. 4.

### 3.2 Network Acceleration by Bonding

For network acceleration of Abyss Storage, the internal network of Abyss Storage cluster is bonded with two 1 GB switches into VLAN as shown in Fig. 5. We performed the tests of write, sequence read, and random read operation between general network and bonding network, and Fig. 6 shows the average IOPS comparison of test results. Test results of the system with network bonding for network acceleration were improved by at least 170% more than general network system.



**Fig. 5.** Network bonding of Abyss Storage cluster.

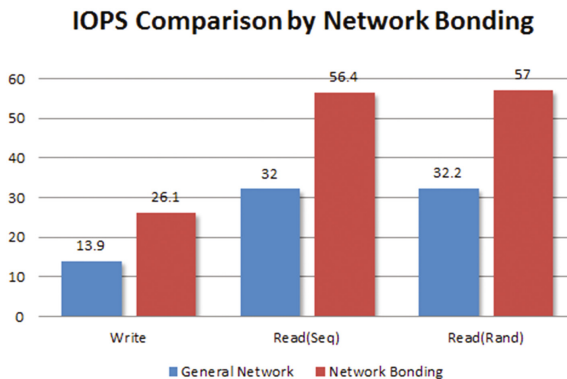


**Fig. 6.** IOPS Comparison between General Network and Bonding Network.

### 3.3 International Network Traffic Test

We performed network traffic test through uploading and downloading of multimedia data between GIST in Korea and Myren in Malaysia. Figure 7 presents the testbed for real network performance test between domestic and oversea.

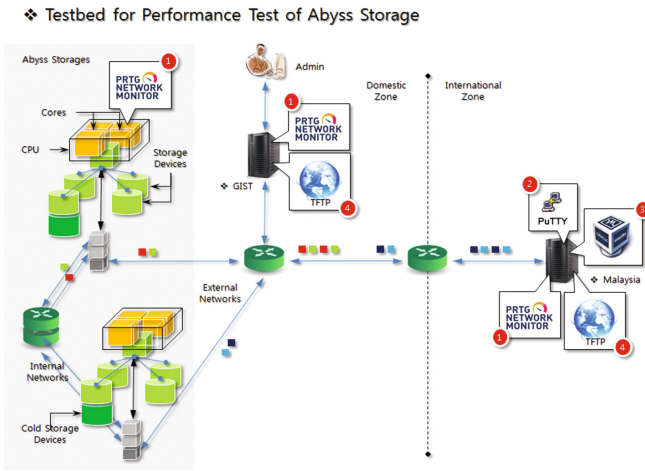
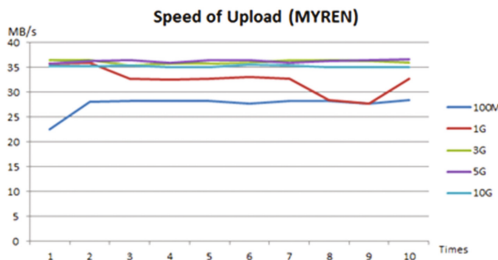
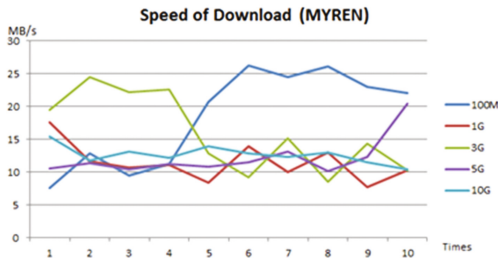


Fig. 7. Testbed of Abyss Storage prototype for network performance test using KOREN.



(a) Test Results of Upload Speed between GIST and MYREN



(b) Test Results of Download Speed between GIST and MYREN

Fig. 8. Test Results of Upload and Download Speed between GIST and MYREN.

Figure 8 shows the upload and download speeds for each file capacity between Myren in Malaysia and the developed Abyss Storage. Specially, comparing the figures shows that the variance among download speeds is much higher than the upload speed. And we measured the external network traffic of Abyss Storage and the internal network traffic inside Abyss Storage cluster using SpeedoMeter [3], a network real-time monitoring tool, as shown in Fig. 9.

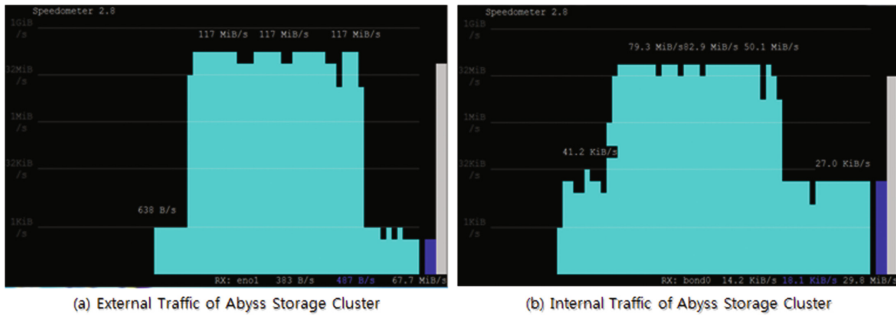


Fig. 9. External and Internal Traffics of Abyss Storage Cluster

## 4 Conclusions

In this paper, the performance tests of the developed mass volume distributed Abyss Storage prototype and real-world tests using KOREN network have been carried out. Based on this, we intend to explore ways to improve performance. Detailed tests to improve performance include performance testing of read and write operations for each disk medium of storage, testing by network bonding, and testing of network traffic between domestic and overseas sites.

**Acknowledgments.** This work was supported by the Technology Development Project for Startup-Growth of SMBA. [No. S2385742, Development of open source-based mass volume distributed storage and network accelerator technology].

## References

1. Singh, K.: Learning Ceph, January 2015
2. Singh, K.: Ceph Cookbook, pp. 270–272, February 2016
3. SpeedoMeter. <https://hub.docker.com/r/opennsm/speedometer/~/dockerfile/>



# 3D Model Generation of Cattle Using Multiple Depth-Maps for ICT Agriculture

Naoto Maki<sup>1</sup>, Shohei Nakamura<sup>1</sup>, Shigeru Takano<sup>2</sup>, and Yoshihiro Okada<sup>1,3</sup>✉

<sup>1</sup> Graduate School of Information Science and Electrical Engineering,  
Kyushu University, Fukuoka, Japan  
maki.naoto@gmail.com, gult4rk0z0000@gmail.com,  
okada@inf.kyushu-u.ac.jp

<sup>2</sup> Center for Co-evolutional Social System, Kyushu University, Fukuoka, Japan  
takano@inf.kyushu-u.ac.jp

<sup>3</sup> Innovation Center for Educational Resources, Kyushu University Library,  
Kyushu University, Fukuoka, Japan

**Abstract.** This paper proposes new system that generates 3D models of cattle from their multiple depth-maps for estimating their BCS (body condition scores). Various works of the agriculture are almost tedious and the use of advanced ICT is possible to improve such works. Currently, the authors have been studying such an ICT agriculture research whose targets are beef cattle. The goal of this study is to capture 3D shape information of cattle accurately for the estimation of their BCS. BCS are important data for checking whether cattle grow appropriately. However, it is very difficult to capture such information even using a commercial 3D scanner because cattle are animals and always moving. Then, the authors propose the use of multiple depth-maps of a cow simultaneously captured by multiple Kinect sensors at a different viewpoint to generate its 3D model. The problems in this case are the calibration of Kinect sensors and the synchronization of their depth-maps capturing. This paper describes how the authors solve these problems, and it shows several results of actually obtained 3D models of cattle using the proposed system.

## 1 Introduction

Recent advances of ICT have made possible to improve various activities of our daily life. As for agriculture fields, there have been many researches about the use of ICT. This paper also treats ICT agriculture especially about beef cattle. In this paper, we propose new system that generates 3D models of cattle from their multiple depth-maps for estimating their BCS (body condition scores). To produce good beef, delicious beef, it is important to know how cattle grow. Not only slim cattle but also fat cattle are not good. Good beef cattle should grow appropriately in good body conditions. Although we need body condition scores (BCS) [1] of cattle for that, it is not easy to measure BCS. Therefore, in this study, we want to make such task easier using ICT than ever. Its goal is to capture 3D shape information of cattle for the estimation of their body condition scores. It is very difficult to capture the body shape information of cattle even using a

commercial 3D scanner because they are animals and always moving. Another reason is that the color of beef cattle is almost black as shown in Fig. 1 and then a 3D scanner like a laser range finder is not available.



**Fig. 1.** Beef cattle.

As the first trial [2], we used multiple RGB cameras to capture silhouette images of a cow and employ the shape-from-silhouette method [3] to generate its 3D model. Actually, we captured multiple RGB camera images of cows and generated their 3D models. Then, we found that the generated 3D models' volumes of cows have positive correlation with their weights. This result says that the estimation of cows' weights is possible from multiple RGB camera images of them. However, in this case, there is still the problem that we have to make silhouette images for each cow manually. We think it may be impossible to generate perfect silhouette images automatically because of various background images and the influence of sun shining.

Then, in this paper, we propose new system of multiple Kinect sensors. The problems in this system are the calibration of Kinect sensors and the synchronization of their depth-maps capturing. This paper describes how we solve these problems, and it shows several results of actually obtained 3D models of cattle using the proposed system.

The remainder of this paper is organized as follows: First of all, next Sect. 2 introduces related work. Section 3 introduces an overview of our proposed system consisting of 6 Kinect sensors, and in Sect. 4, we explain the details of its functionalities and show actually captured 3D models of cattle. Finally, we conclude the paper in Sect. 5.

## 2 Related Work

In this research, we restore 3D shape data from depth-maps acquired by Kinect sensors. As a research to restore the three-dimensional shape of a target object from a two-dimensional image taken with a camera, Shape-from-shading method [4] restores the shape of an object surface from a change in brightness. From the density distribution of the texture of an object surface, Shape-from-texture method [5] reconstructs the shape, and from multiple focus images taken with varying focus, Shape-from-focus method [6]

reconstructs the shape. Li et al. [7] estimates the depth map from the color image and restores the three-dimensional shape. Fremont et al. [8] studied a method of restoring the entire circumference shape of an object by placing an object on a rotating table.

Acquiring the entire circumference shape of an object using a three-dimensional measurement system is basically carried out in three steps of capturing multiple depth data from a different direction, aligning the depth data and integrating them. Contactless scanning method is currently the mainstream in acquiring depth data. There are an active method which measures by irradiating light or sound waves, and a passive method which does not irradiate anything. Triangulation is a commonly used principle. Triangulation is a surveying method that determines the position of a point by measuring the angle from a certain known point to an unknown point to be measured. In three-dimensional scanning, two cameras are used in the passive system, one camera in the active system, and a projector that emits infrared rays. In recent years, inexpensive sensors such as Kinect and RealSense have been produced, and depth data can be easily acquired. As the alignment method, there are ICP [9] and a method [10] using the distance between points and polygons. As an integration method, there is the Marching/Cubes method [11] and others.

The research of this paper is aimed at restoring a more accurate three-dimensional shape. As mentioned in the previous section, our final purpose is to estimate values such as body weights from the reconstructed three-dimensional shapes. Kinect can easily acquire depth data with the high performance sensor and abundant library. In order to restore the complete three-dimensional shape of an object, it is necessary to capture the object not only from one direction but also from plural directions. However, since the target is a living animal, when taking time from one direction with one camera, its shape changes for each image. From the above viewpoint, in this research, we use multiple Kinects and acquire 3D shape data by taking multiple depth-maps of a cow from a different direction at the same time. Also, by using point cloud data and its library, processing of noise removal and integration of depth data can be realized.

### 3 Proposed System of 6 Kinect Sensors

In this section, we introduce our system actually constructed in this research. The purpose of this system is to acquire three-dimensional shape data of cattle. In the research, using three or more Kinect v2 for Windows produced by Microsoft, three-dimensional partial point cloud data from multiple directions of a cow is acquired and the data is integrated to restore the three-dimensional shape of the cow. The placement of the Kinect sensors used in the experiment was actually decided by trial and error. First, we prepared two pole-stands each of which two Kinect sensors are installed to surrounding of a cow. From the captured results, we found that 4 Kinect sensors are not enough because a cow is black so that each Kinect sensor should be close to the cow for correctly capturing its depth-map. As a result, 4 Kinect sensors cannot cover the whole body of the cow. Then, as shown in Fig. 2, we decided to use 6 Kinect sensors in our proposed system. It consists of two pole-stands each of which has three sets of Kinect sensors. Kinect sensors cannot run without connecting to a Windows PC. In this system,

we used a small box PC equipped with Windows 10 OS and connected to each Kinect sensor. The system includes a local network through the router and each PC communicates with the master PC controlling the system in the network, and receives instructions from the master PC to capture. Visual Studio 2015 and Visual C++ were used for making the programs of capturing and processing of point clouds.



**Fig. 2.** Proposed system of 6 Kinect sensors.

As Kinect v2 is the next generation of Kinect for Windows (Kinect v1) produced from Microsoft and can easily obtain information such as depth and skeleton similarly to Kinect v1, attentions from researchers and developers have been drawn all over the world. The depth sensor of Kinect v2 adopts TOF (Time of Flight) which obtains depth information from the time when the transmitted infrared ray is reflected and returned. Kinect was originally developed as a natural sensor for games. It can recognize human joints with this depth sensor and RGB camera, and it makes possible to operate games using the movement of the human body. In this research, we also use 3D depth sensor and RGB camera to acquire three-dimensional shape data of cattle.

As a library to handle Kinect, Microsoft provides Kinect for Windows SDK. The SDK makes it easy to use Kinect's basic functions such as acquiring color images and obtaining depth images. In this research, we used Kinect for Windows SDK 2.0. Kinect's RGB camera and depth sensor capture at 30 fps and data is recorded in the cache. In this system, when there is an instruction from the master PC, the most recent image at that time is saved as PNG format image and PCD(Point Cloud Data) on the PC respectively. PCD is a data format representing point cloud data and is a format supported by PCL(Point Cloud Library) [12] described in next Section. The method of acquiring point cloud data with Kinect is shown below.

The depth sensor of Kinect v2 returns the depth image of  $512 \times 424$  pixels as an output. The value of a pixel describes the distance from the sensor to the surface of the object in mm. From the position and value of each pixel, the coordinate value in the three-dimensional Cartesian coordinate system centered on the depth sensor can be calculated. By calculating the coordinates of each pixel on the three-dimensional space from the depth image in this way and outputting it as a point, three-dimensional point cloud data can be obtained.

## 4 3D Model Generation by 6 Kinect Sensors System

All of the processes to generate 3D model data of cattle in our proposed system are (A) Taking Kinect sensor calibration images, (B) Taking depth-maps for each cow, and (C) 3D model data generation for each cow by aligning 6 depth-maps and integrating them. In the following subsections, we explain the details of these processes.

### 4.1 (A) Taking Kinect Sensor Calibration Images

For generating 3D model data for each cow from its 6 depth-maps, we need the position and orientation information of each Kinect sensor. To obtain such information, we employ OpenCV [13] function `cv:solvePnP` and we took a calibration image for each Kinect sensor by the same Kinect sensor's RGB-camera as shown in the left part of Fig. 3. The right part of the figure is the contents of its calibration file corresponding to the calibration image. For the calibration, we made a cuboid frame that has 12 vertices shown in the left part of the figure. The  $x$ ,  $y$ ,  $z$  coordinate values of 12 vertices of the cuboid frame become those shown in the lower part of the calibration file. The upper part indicates  $x$ ,  $y$  coordinate values (position) for each of the 12 vertices in the calibration image. Unfortunately, we had to make the calibration files manually.

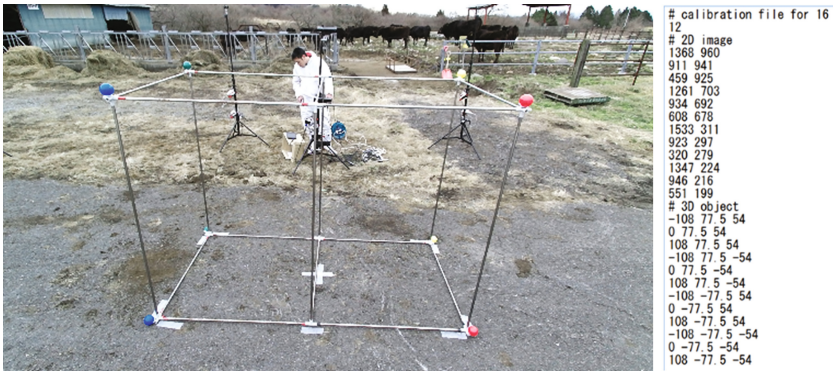


Fig. 3. Calibration image of Kinect sensor (left) and the contents of its calibration file (right).

### 4.2 (B) Taking Depth-Maps for Each Cow

After taking Kinect sensor calibration images for all cameras, we took 6 depth-maps for each cow by 6 Kinect sensors. Figure 4 shows Point Cloud Data(PCD) obtained from one depth-map of a cow. A cow is animal and always moving. So somebody has to control the cow to not move. Therefore, in every PCD, one person wore a white cloth is included.

To obtain accurately 6 Point Cloud Data for each cow from 6 Kinect sensors' depth-maps, the system must capture the 6 depth-maps at the same time. For that, we employ UDP/Multicast communication between each small box PC and the master PC, and



**Fig. 4.** PCD obtained from the depth-map of a cow.

checked how long the total communication delay is among the 6 Kinect sensors. Figure 5 shows 6 RGB-camera images of the 6 Kinect sensors each of which includes the digital timer on a note PC that counts a time by a step of 0.01 s. We tried 20 times checking the total communication delay and found that the average total delay is 86 ms. This value seems acceptable for our purpose because it is possible for us to control a cow not to move in 0.1 s.



**Fig. 5.** Measurement of communication delay.

### 4.3 (C) 3D Model Data Generation for Each Cow

After the processes of (A) to (B), we can obtain Point Cloud Data of 6 Kinect sensors for each cow. However, we have to apply some filters to PCD for the quality improvement because raw data apt to include noise.

#### **Pass-through filter**

The most straightforward and simple filter among the filters is a pass-through filter. Since the depth sensor of Kinect v2 can acquire depth images in the range of 0.5 to 8.0 meters in depth, the background and others are reflected in the raw data in addition to the object. The pass-through filter designates a range on the three-dimensional coordinate, and

removes all points outside or inside the range. In this research, when the size and position of a target object can be predicted to some extent in advance, it is an effective filter. The left part of Fig. 6 is an image using the pass-through filter for the data of Fig. 4.



**Fig. 6.** PCD obtained after applying Pass-through filter (left), Voxel grid filter (middle), Outlier filter (right) to PCD of Fig. 4.

#### **Voxel grid filter (Down sampling filter)**

Since Kinect acquires point clouds from  $512 \times 424$  pixels, the number of data points to be acquired exceeds 200,000. Because large data need long time to calculate, it is necessary to perform down sampling to the extent that shape is not impaired. A voxel grid filter is one of down-sampling filters provided by PCL. This filter divides the three-dimensional space in which the point cloud data exists into a lattice shape and replaces the points in each cube with one point which is the barycenter thereof. The middle part of Fig. 6 is an image obtained by applying a voxel grid filter to the data of Fig. 4 as the voxel size is  $3 \times 3 \times 3$  cm.

**Outlier filter** Point cloud data includes erroneous data as the noise due to poor infrared rays depending on the color or brightness of the measurement surface, measurement of the edge of the object and so on. Among these noises, obviously erroneous points are called outliers, and if there are outliers it is difficult to calculate feature quantities to be described later. Therefore, it is necessary to remove these outliers. Outlier removal can be performed as follows: First, for all points on the data, the filter calculates the average distance to all neighbor points. Assume that the distribution is a normal distribution and remove all points with a larger mean distance than the values obtained from the mean and variance as outliers. The right part of Fig. 6 is an image obtained by applying an outlier filter to the data of Fig. 4.

#### **4.4 Integration of PCD**

In order to integrate the 3D point cloud data of a cow acquired by each Kinect sensor, it is necessary to correctly comprehend and superimpose their positional relationship. As methods for this, we describe the following two.

##### **Alignment by ICP algorithm**

PCL provides a registration function by an ICP (Iterative Closest Point) algorithm as a method of aligning point clouds in the registration module. The ICP algorithm automatically performs alignment of two point clouds. The flow in which ICP aligns the two point groups P and Q is as follows: First, for all points of one point group P, the nearest

neighbor point is found out from the other point group  $Q$ , and this point is set as a corresponding point. A coordinate transformation that minimizes the distance between corresponding points is obtained and applied to  $P$ , and this process is repeated. At this time, depending on the initial positions of  $P$  and  $Q$ , local solutions may occur. Therefore, before using ICP, it is necessary to adjust coarse initial position. Here, we explain how to use SAC-IA (Sample Consensus Initial Alignment) function in PCL.

SAC-IA is a method of performing initial positioning by RANSAC (Random Sample Consensus) algorithm. RANSAC extracts a plurality of feature points from each of two point groups. Then, these feature points are randomly associated with each other, and coordinate conversion is performed so that the feature points are closest to each other. This process is performed a certain number of times, and the conversion when the feature point error becomes the smallest is adopted. By applying this transformation, rough positioning is carried out. Since SAC-IA uses feature points, it is necessary to obtain feature points before the above. Therefore, the feature points are estimated, and positioning is performed with the flow of execution of SAC-IA and execution of ICP. Here, FPFH (FastPoint Feature Histograms) is used as a feature quantity.

For the two point clouds in Fig. 7, ICP was performed. The left part of Fig. 8 is an image obtained by overlapping point groups with each other in a state of not being aligned. The right part of Fig. 8 shows the execution result of ICP algorithm. It can be said that although there are errors, they are almost overlapped together.

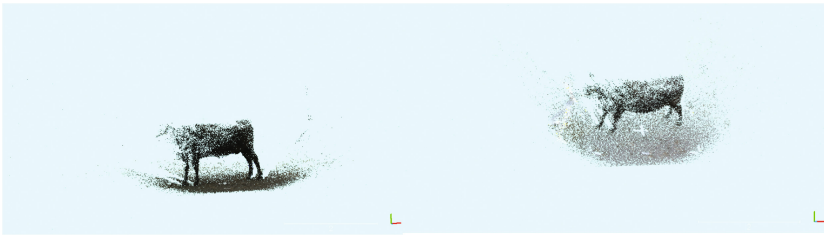


**Fig. 7.** Two PCD obtained from each of two depth-maps of a cow.



**Fig. 8.** PCD merged by two PCD of Fig. 7 without the alignment of ICP algorithm (left) and with the alignment of ICP algorithm (right).

### **Alignment by calibration of Kinect sensors**

Integration of point clouds by ICP is not realized unless there is enough overlap between two point groups. Also, depending on the shape of a target object, it may not be able to



integrate them well. Therefore, we apply a method of aligning point groups by calculating the position and direction of Kinect sensor at the time of acquiring the point group, not using the internal data of the point group.

Figure 9 shows the integrated PCD obtained with the alignment by calibration of Kinect sensors. Furthermore, Fig. 10 shows the refined PCD by applying Pass-through filter and Voxel grid filter to PCD of Fig. 9. In comparison with Fig. 11, we can say that the 3D model of a cow obtained by the proposed system in this paper is more accurate rather than Shape-from-Silhouette method described in [2].

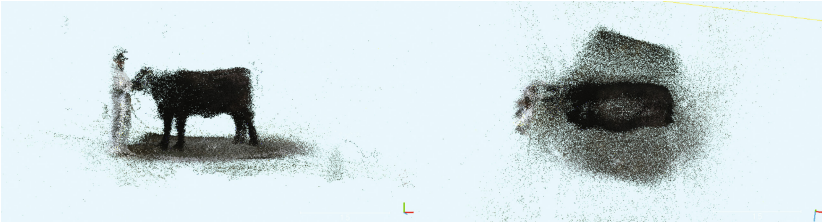


Fig. 9. Integrated PCD obtained with the alignment by calibration of Kinect sensors.

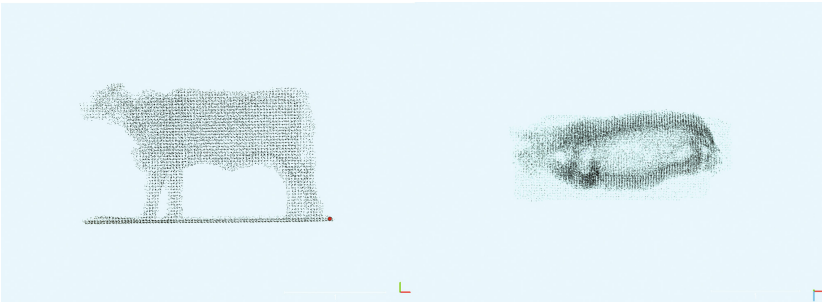


Fig. 10. PCD obtained after applying Pass-through and Voxel grid filters to PCD of Fig. 9.

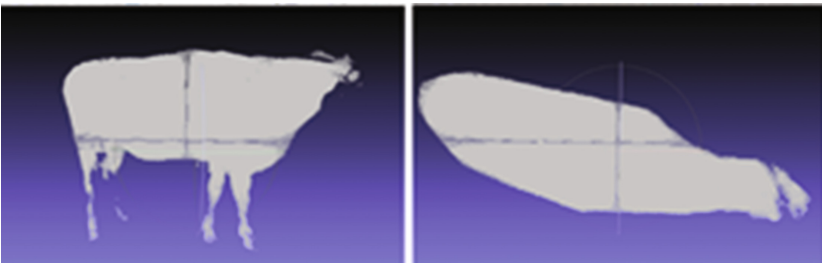


Fig. 11. 3D model of a cow obtained by Shape-from-Silhouette method using 16 RGB-cameras.

## 5 Conclusions

In this paper, we proposed new system to capture cattle using multiple Kinect v2 sensors and to integrate partial point cloud data of each cow by calibrating the Kinect sensors' positions and orientations using their calibration images. Actually, we developed the system and captured 3D model data of a cow.

In the current system, there is still much room for improvement. For example, before starting capturing, we have to power-on each small box PC and execute a capturing program. These operations become troublesome because each small box PC does not have any input/output devices such as a display monitor and a keyboard. In addition, although not mentioned in the paper, since the sun is shining and backlighting cannot obtain depth data well, it is necessary to devise a method such as attaching a roof, but in that case, it is a problem that the apparatus becomes large-scaled. Even in compositing point clouds, the coordinates of the device should be entered manually from each calibration image, but this work needs long time and much cost. Therefore, we should make a program to handle this automatically. This is one of our future work.

## References

1. Dairy, N.Z.: Body Condition Scoring, 27 January 2017. <https://www.dairynz.co.nz/animal/herd-management/body-condition-scoring/>
2. Xiang, Y., et al.: 3D model generation of cattle by shape-from-Silhouette method for ICT agriculture. IEEE CS Press, pp. 617–622 (2016)
3. Olsson, K., Persson, T.: Shape from Silhouette scanner - creating a digital 3D model of a real object by analyzing photos from multiple views. Master's thesis, MSC in Media Technology and Engineering, University of Linköping, Sweden (2001)
4. Ruo, Z., et al.: Shape from shading: a survey. IEEE Trans. Pattern Anal. Mach. Intell. **21**, 690–706 (1999)
5. Blake, A., Buelthoff, H.H., Sheinberg, D.: Shape from texture: ideal observers and human psychophysics. Vis. Res. **33**(12), 1723–1737 (1993)
6. Nayar, S., Nakagawa, Y.: Shape from focus. IEEE Trans. Pattern Anal. Mach. Intell. **16**(8), 824–831 (1994)
7. Li, J., et al.: Bundled depth-map merging for multi-view stereo. In: Computer Vision and Pattern Recognition, pp. 2769–2776 (2010)
8. Fremont, V., Chellali, R.: Turntable-based 3D object reconstruction. IEEE Cybern. Intell. Syst. **2**, 1277–1282 (2004)
9. Besl, P., McKay, N.: A method for registration of 3-D shapes. IEEE Trans. Pattern Anal. Mach. Intell. **14**(2), 239–256 (1992)
10. Yang, C., Medioni, G.: Object modelling by registration of multiple range images. Image Vis. Comput. **10**, 145–155 (1992)
11. Lorensen, W., Cline, H.: Marching cubes: a high resolution 3D surface construction algorithm. ACM SIGGRAPH Comput. Graph. **21**(4), 163–169 (1987)
12. Willow Garage, “PCL”, 3 February 2017. <http://pointclouds.org/>
13. Itseez, “OpenCV”, 3 February 2017. <http://opencv.org/>

# The Ubiquitous Greenhouse for Technology Education in Junior High School

Kazuaki Yoshihara<sup>1</sup>(✉), Kiko Fujimori<sup>2</sup>, and Kenzi Watanabe<sup>1</sup>

<sup>1</sup> Graduate School of Education, Hiroshima University, 1-1-1 Kagamiyama, Higashihiroshima, Hiroshima 739-8524, Japan  
{m153581, wtnbk}@hiroshima-u.ac.jp

<sup>2</sup> School of Education, Hiroshima University, 1-1-1 Kagamiyama, Higashihiroshima, Hiroshima 739-8524, Japan  
b135244@hiroshima-u.ac.jp

**Abstract.** We have developed the Ubiquitous Greenhouse as a project based learning content that students can comprehensively learn contents of technology education in junior high school. We conducted experiments on plant growth using the Ubiquitous Greenhouse. We used Raspberry Pi for control system. Raspberry Pi acquires weather data of remote areas in real time, and reproduced the Ubiquitous Greenhouse by controlling multiple home appliances based on the data. In the plant growth experiments, we compare plants growth between the open air and the Ubiquitous Greenhouse. As the results, there were clear differences in plants growth.

## 1 Introduction

These are four fields of learning contents in technology education in junior high school in Japan. The first is materials and their processing. The second is energy conversion. The third is nurturing living things. The fourth is information processing. The objective of technology education in junior high school in Japan is to enable students to acquire fundamental and basic knowledges and skills related to the four fields through practical and hands-on learning activities such as production (monodukuri), while also fostering the ability and attitude to evaluate and utilize technology properly. It is also important to cultivate problem solving skills against challenges in order that students respond autonomously to the changing society [1]. There is a project based learning as a problem-solving type learning method. In order to be a learning content for project based learning, it is necessary for learning content to include a learning process that students find and solve challenges themselves.

We propose the Ubiquitous Greenhouse as a project based learning content that students can comprehensively learn the four fields of technology education. The Ubiquitous Greenhouse is a greenhouse that can reproduce a weather of a remote place in real time by controlling greenhouse using remote meteorological data.

Some studies have showed measurement of remote places such as Field server and LiveE! Project [2]. Other studies have showed cultivation support system by controlling

weather inside a greenhouse [3]. However little study has been done to reproduce a weather of a remote place in real time by controlling greenhouse. Unlike existing controlled greenhouse, junior high school students can experience production of the Ubiquitous Greenhouse. Through a production of the Ubiquitous Greenhouse, students can learn the learning contents of technology education. The Ubiquitous Greenhouse can be a practical and an experimental learning content for project based learning by using as a teaching material from a development stage.

In this paper, we describe development of the Ubiquitous Greenhouse as a project based learning content and a plant breeding experiments using it.

## 2 The Ubiquitous Greenhouse

### 2.1 Overview

Junior high school students can comprehensively learning the four fields. The data aggregation server acquires the weather data measured by the remote measurement system via the Internet. With this content, junior high school students can learn about information processing. Based on the acquired data, the server controls the Greenhouse in real time. With this content, they can learn about energy conversion. In the Ubiquitous Greenhouse, it is possible to reproduce plant growth in a remote place. With this content, they can learn materials and their processing and nurturing living things.

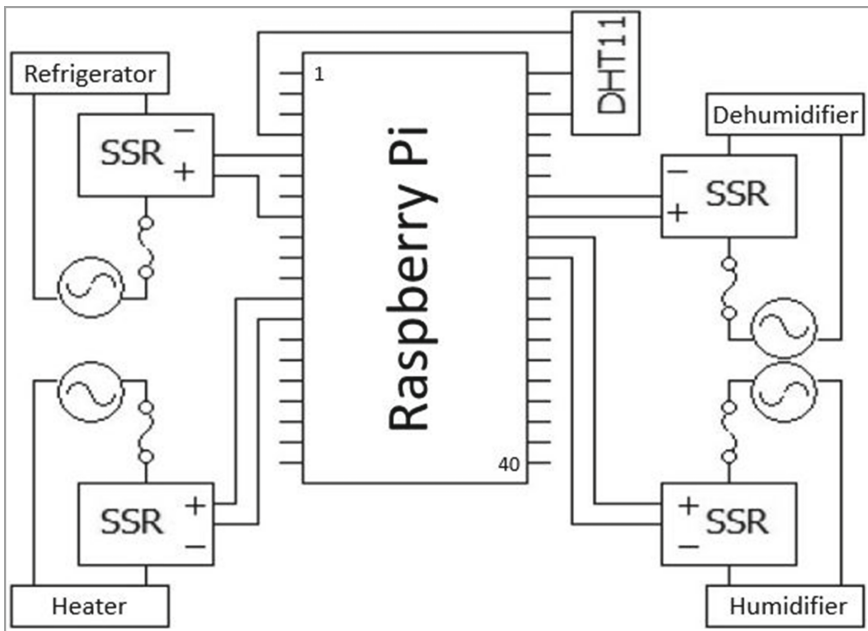


Fig. 1. Circuit diagram of the Ubiquitous Greenhouse

Figure 1 shows the circuit diagram of the Ubiquitous Greenhouse. The Ubiquitous Greenhouse consists of four home appliances, the first is a refrigerator, the second is a heater, the third is a dehumidifier, and the fourth is a humidifier. DHT11 was used to measure weather data in the Ubiquitous Greenhouse. We used Raspberry Pi for control system. Solid-state relay was used to control multiple appliances. Figure 2 shows the Ubiquitous Greenhouse.



**Fig. 2.** The Ubiquitous Greenhouse

## 2.2 Solid-State Relay

A solid-state relay is an electric switching device that switches on and off. The input terminals of the solid-state relays are connected to I/O pins of the Raspberry Pi by soldering. Since it is not desirable that the output terminals of a solid-state relay were connected to a power cord of a home appliance, it is connected to an extension cord by processing it. Fuses were inserted within the extension cords. Radiators were attached the solid-state relays connected to the refrigerator and the heater because they got very hot.

## 2.3 Measurement of Temperature and Humidity in the Ubiquitous Greenhouse

We used DHT11 to measure temperature and a humidity inside the Ubiquitous Greenhouse. DHT11 is a digital temperature and humidity sensor [4]. It used a capacitive humidity sensor and a thermistor to measure the surrounding air, and spits out a digital signal on the data pin. Raspberry Pi acquire the data of temperature and humidity by connecting the three cords of DHT11. We have created an instrument shelter for DHT11 because DHT11 can not measure properly without an instrument shelter.

## 2.4 Acquisition of Temperature and Humidity Data of Remote Places

Raspberry Pi acquire the data of AmeDAS on the Web published by the Japan Meteorological Agency. We used the Beautiful Soup module which is a Python library for Web scraping [5]. Raspberry Pi extracts the latest temperature and humidity data every one hour.

## 2.5 Control Home Appliances

Raspberry Pi compares temperature and humidity data of a remote place with temperature and a humidity data in the Ubiquitous Greenhouse. Raspberry Pi controls home appliances based on the comparison result. For example, if temperature in a remote place is higher than temperature in the Ubiquitous Greenhouse, Raspberry Pi turns on the heater so that temperature in the Ubiquitous Greenhouse is closer to temperature in a remote place.

# 3 The Plant Grow Experiments

We conducted plant grow experiments using the Ubiquitous Greenhouse. We selected a radish and white radish sprouts so as plants to use for experiments because they growth easily and quickly. We selected Naha City as a remote place to reproduce in the Ubiquitous Greenhouse. We cultivated plants in the outside air of Higashihiroshima City to compare with the Ubiquitous Greenhouse.

On December 12, 2016, we prepared two same plastic containers and plants four seeds of radish in each container. We placed one container in the Ubiquitous Greenhouse and the other in the outside air of Higashihiroshiima City. We put water in each container about 50 ml once a day. After 6 days, the radish in the Ubiquitous Greenhouse germinated, but it in outside air of Higashihiroshima City did not change. After 10 days, the radish in the Ubiquitous Greenhouse grew to the length of the stem to 7.2 cm, but it in outside air of Higashihiroshima City did not change. Figure 3 shows comparison the lengths of the radishes stems and the temperature between Higashihiroshima City and the Ubiquitous Greenhouse during the radish grow experiment. According Fig. 3, the temperature in Higashi Hiroshima City is generally considerably lower than the temperature in the Ubiquitous Greenhouse. The temperature in the Ubiquitous Greenhouse is suitable for these plants growth. However, the temperature of Higashihiroshima City is not suitable for the radish growth. Figure 4 shows comparing the temperature and humidity while raising radish between the Ubiquitous Greenhouse and Naha City. Despite some errors, the Ubiquitous Greenhouse reproduced the temperature and humidity of Naha City in general.

On January 10, 2017, we prepared the two same plastic container and put the wet paper towel and sow 20 seeds of white radish sprouts in each container. We placed one container in the Ubiquitous Greenhouse and the other in the outside air of Higashihiroshiima City. We put water in each container about 50 ml each day. After 2 days, the radish in the Ubiquitous Greenhouse germinated, but it in outside air of Higashihiroshima City did not change. After 12 days, the radish in the Ubiquitous Greenhouse grew to the

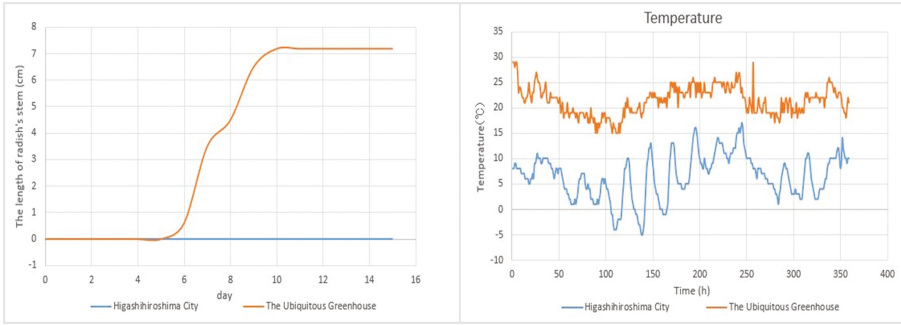


**Fig. 3.** Comparison the lengths of the radishes stem and the temperature between Higashihiroshima City and the Ubiquitous Greenhouse

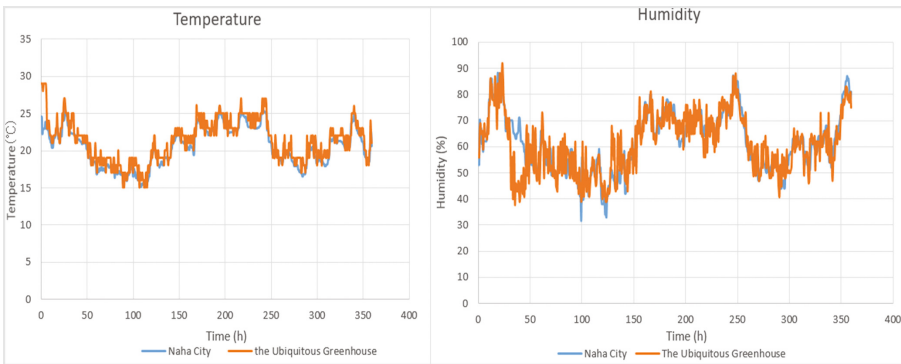


**Fig. 4.** Comparison of temperature and humidity during the radish grow experiment

length of the stem to 11.5 cm, but it in outside air of Higashihiroshima City did not change. Figure 5 shows comparison the lengths of the radishes stems and the temperature between Higashihiroshima City and the Ubiquitous Greenhouse during the white radish sprouts grow experiment. According Fig. 5, the temperature in Higashi Hiroshima City is generally considerably lower than the temperature in the Ubiquitous Greenhouse. The temperature in the Ubiquitous Greenhouse is suitable for white radish sprouts growth. However, the temperature of Higashihiroshima City is not suitable for white radish growth. Figure 6 shows two graphs comparing the temperature and humidity while raising white radish sprouts between the Ubiquitous Greenhouse and Naha City. The Ubiquitous Greenhouse reproduced the temperature and humidity of Naha City in general as well as the radish grow experiment.

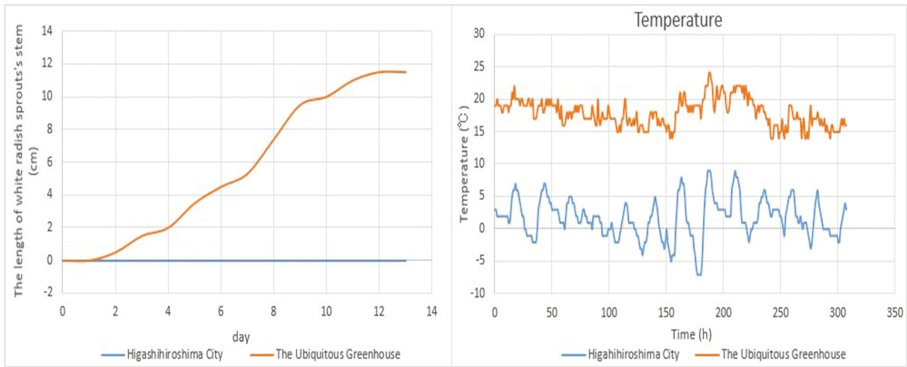


**Fig. 5.** Comparison the lengths of the white radish sprouts stem and the temperature between Higashihiroshima City and the Ubiquitous Greenhouse

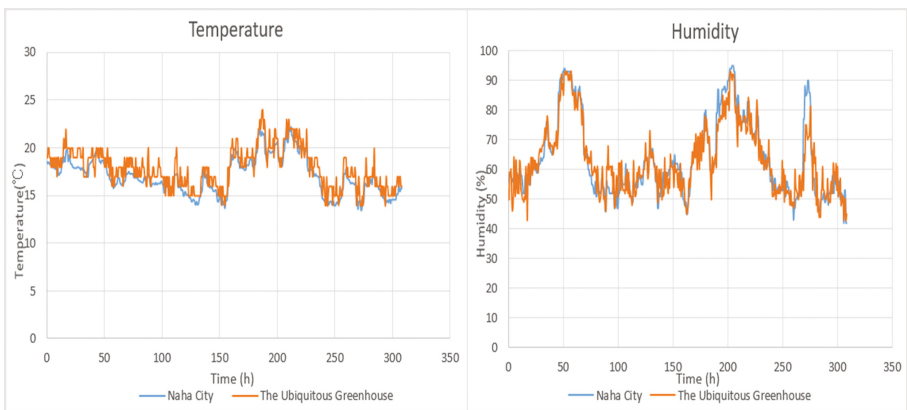


**Fig. 6.** Comparison of temperature and humidity during white radish sprouts experiment

## 4 Conclusion

In this paper, we have described details of the Ubiquitous Greenhouse for technology education in junior high school. After that, we have described plants growth experiments using the Ubiquitous Greenhouse.

Junior high school students can comprehensively learn the learning contents of technology education by using the Ubiquitous Greenhouse from the development stage as a teaching material. In addition, the Ubiquitous Greenhouse can be project-based learning content by challenging unresolved study.

We have been planning to use the Ubiquitous Greenhouse at the junior high school.

**Acknowledgement.** This work was supported by JSPS KAKENHI Grant Number JP15K00481.



## References

1. The MEXT: Junior High School Teaching Guide for the Japanese Course of Study. Technology and Home Economics. Daiichi Gakushusha Tokyo (2008). In Japanese
2. Ezaki, H.: LiveE! Project. [http://www.keieihonbu.com/live\\_e\\_july10\\_2006.pdf](http://www.keieihonbu.com/live_e_july10_2006.pdf). Accessed 13 Mar 2017. In Japanese
3. eLAB experience: FieldServer. <http://www.elab-experience.com/fieldserver>. Accessed 13 Mar 2017. In Japanese
4. DFROBOT, DHT11 Temperature and Humidity Sensor V2 SKU: DFR0067. [https://www.dfrobot.com/wiki/index.php/DHT11\\_Temperature\\_and\\_Humidity\\_Sensor\\_V2\\_SKU:\\_DFR0067](https://www.dfrobot.com/wiki/index.php/DHT11_Temperature_and_Humidity_Sensor_V2_SKU:_DFR0067). Accessed 13 Feb 2017
5. Ryan, M.: Web Scraping with Python. O'Reilly, Tokyo. In Japanese

# Log Data Visualization and Analysis for Supporting Medical Image Diagnosis

Tsuneo Kagawa<sup>1(✉)</sup>, Shuichi Tanoue<sup>2(✉)</sup>, and Hiroaki Nishino<sup>1(✉)</sup>

<sup>1</sup> Oita University, Oita, Japan

{t-kagawa,hn}@oita-u.ac.jp

<sup>2</sup> Kurume University, Kurume, Japan

tanoue\_shuichi@med.kurume-u.ac.jp

**Abstract.** Computer Aided Diagnosis (CAD) has become one of the most important for medical activities. However, radiologists have to cost their time and efforts to investigate these medical images. It is strongly required to reduce their burden without debasing the quality of imaging diagnosis. So we have considered about how to learn from experimental information of veteran radiologists because not only logical knowledge but also experiments are required for accuracy diagnosis. In this paper, we acquire operation log data and analyze difference between experienced and inexperienced discuss about supporting method for medical imaging with these experimental information.

## 1 Introduction

Recently, Computer Aided Diagnosis (CAD) has been advanced with a major research subjects in medical imaging and diagnostic radiology [1]. Computed Tomography (CT) and Magnetic Resonance Imaging (MRI) are most advanced and these are basically collection of tiny horizontal or vertical sliced images. Currently, highly-sophisticated scanning technology has enabled to capture so high resolution images that 3-dimensional graphics can be re-constructed. Radiologists can obtain a very large volume of image sequence from only a patient. Though advanced CAD technique have improved accuracy of diagnosis, it becomes more difficult that radiologists have to investigate the image sequences and detect abnormalities from them because these images include much various information. For example, it is said that the number of images per a case is over 500 and daily totally they must investigate over 10 thousands of images. Radiologists have keep attention for investigating many medical images for a long time but they must perform exact diagnostic imaging. It suffers to the doctors a great eyestrain while they watch them much more carefully.

Many researches on CAD technique have developed methods to detect abnormalities automatically from images and they have successfully provided very powerful functions for imaging diagnosis [2–4], especially with applying machine learning technique, such as deep learning. However, appearance of abnormalities is so various because they are depending on cases of disease, degree of illness, location in the body and so on. Furthermore, medical feature, such as the age,

the gender or constitution of a patient, greatly influenced to view of these images. There is another assistance method to emphasize some features in the images with heuristics to improve the quality of medical imaging. However, the reliability of diagnosis is largely attributable to that of emphasized images. Additionally, they are necessary to have the knowledge of medical image processing for radiologists. They should investigate abnormalities and determine the types of diseases finally by themselves although with powerful assistance of computers, because even small error is sometimes critical in medical imaging diagnosis. Especially, lesions of false-positive of very serious for them. In the process of diagnosis, experience is one of important factor for smooth and accurate diagnosis.

We study about a supporting method for reducing the burden of medical images investigation and for more correct diagnosis. It is necessary to reduce the burden for abnormality detection without debasing the quality of imaging diagnosis. We have studied about computer supported diagnosis with applying medical image processing and multi-modal user interface [6]. In our study, we have developed a user action log acquisition tool to find difference between experienced and inexperienced radiologists. Especially, young and inexperienced students must train their skill to investigate images smoothly. So we have considered about how to learn from experimental information of veteran radiologists because not only logical knowledge but also experiments are required for accuracy diagnosis [5]. In this paper, we acquire operation log data and analyze difference between experienced and inexperienced discuss about supporting method for medical imaging with these experimental information.

## 2 Operation Log Data

### 2.1 Data Acquisition

A medical image viewer has developed to acquire radiologists' operation log data and we applied this tool for real experienced radiologists and medical students. Figure 1 shows a user interface of our viewer. Users can control images forward or

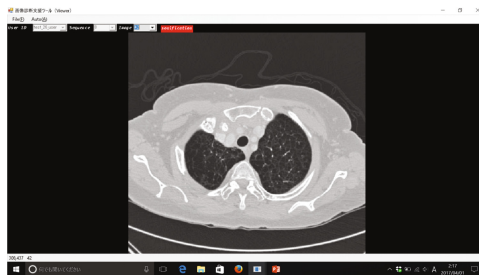


**Fig. 1.** A simple medical image viewer that can record user operation log data. User can control images forward and backward with mouse or keyboards and click the abnormalities in the displayed image with their mouse.

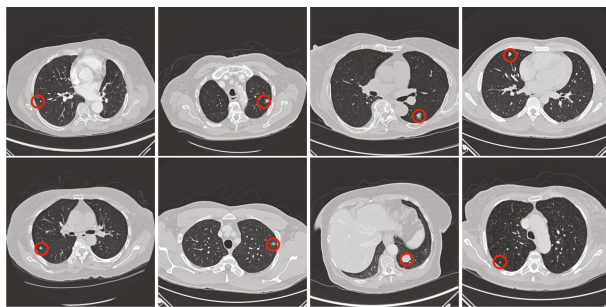


**Fig. 2.** 8 target images with nodule in lung. Radiologists have to find nodule within blood vessel. In this experiment, subjects investigate these 8 image sequence including abnormalities (surrounded with red circles) as tasks.

**Table 1.** The number of images included in each sequence and nodule size.

Sequence #	Number of images	Size of nodule
1	285	Tiny
2	413	Small
3	332	Medium
4	292	Small
5	202	Small
6	338	Small
7	272	Big
8	307	Tiny

backward in the sequence with their mouse wheels or keyboards. In our experiment, 8 types of CT image sequence are prepared as detection experimental tasks and they all are for nodule cases in human lung. Figure 2 shows image examples of nodules and Table 1 shows the number of images included in each sequence. Users as subjects have to detect nodule in many blood vessel. When users detect some abnormalities, they should specify the location of them. Nodule positions and images included them are preregistered in the tool. If they could click the right position in a right image, basically they are represented by a circle with 30 pixels radius in the correct images, they finish investigation for the sequence.

## 2.2 Operation Log Data

While users investigate the images, this experimental image viewer records log data with timer information as below:

- Image ID number in the sequence.
- Viewing time(seconds).
- Specified position (if mouse clicked).

Figure 3 shows an example of operation log data. This logging function is finished by users' mouse clicking to the correct position of an abnormality in image ID 134, as shown in Fig. 1 for an example.

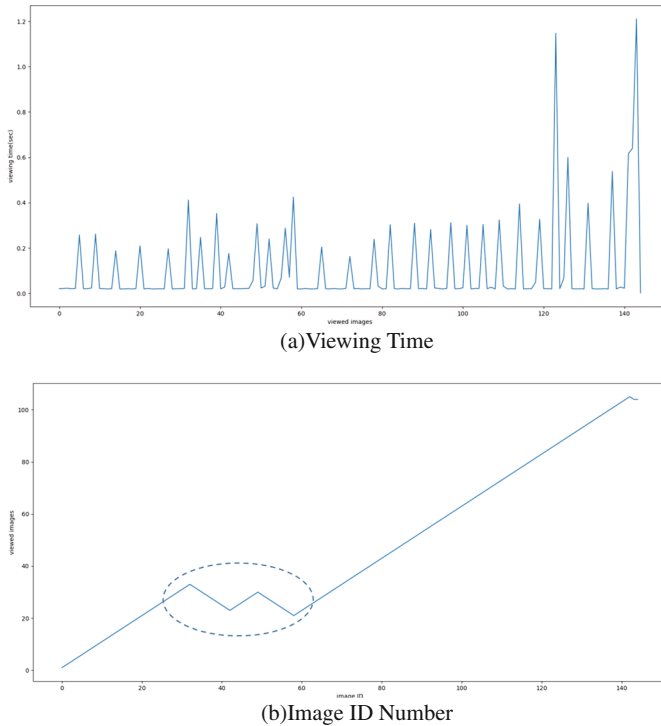
#	Image ID	Viewing time(sec)	Specified position
1	0	0.144	
2	1	0.528	
3	2	0.025	
4	3	0.071	
5	4	0.032	
⋮	⋮	⋮	⋮
151	134	2.048	(119,325)

Fig. 3. An Example of operation log data in medical image diagnosis.

With this interface, currently, 7 real radiologists have investigated 8 image sequences 2 times. So we have obtained 14 types of operation log data for each image sequence, 112 data sets in total. On the other hand, 3 medical students have experimented the same image sequence 1 time, so 3 types of log data, 24 sets, are obtained.

### 2.3 Log Data Visualization

At first, it is important to visualize feature of users' operation, such as rapidness of viewing and number of viewed images. A simple line chart is applied to visualize these log data. Figure 4(a) shows viewing time per a image to detect abnormalities. Vertical axis is viewing time, horizontal axis is counting number of viewed images. This graph means that a user has found nodule in the 151th image, not ID is 151, in total 39.178 s. On the other hand, Fig. 4(b) shows image feeding direction of operation, forwards or backwards. Vertical axis is image ID number, horizontal axis is counting number of viewed image same to Fig. 4(a). Users can watch images in forward or backward order in this user interface. We can count the number of viewed for each image from this graph.



**Fig. 4.** An example of a simple line chart of viewing time for sample 1 in Fig. 2. A radiologist check totally 151 images and total time for investigation is 39.178 s. Chart (a) shows viewing time per single image until abnormality detection, (b) shows changing images forward or backward. In this case, user views images between image ID 20 and ID 30 in 2 or 3 times, as shown in dotted line circle.

### 3 Operation Analysis

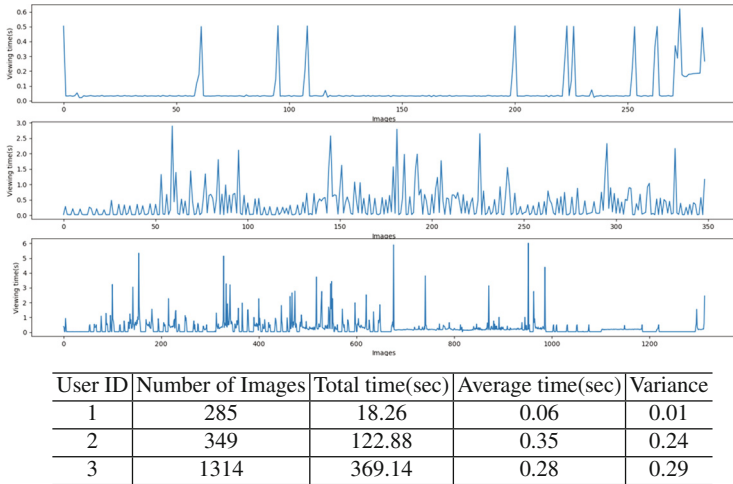
#### 3.1 Comparison Between Experienced and Inexperienced

Figure 5 shows 3 examples of viewing times of experienced radiologists, who have experienced about 3 or 4 years, to detect abnormalities from an image sequence 4 shown in Fig. 2. Figure 6 similarly shows viewing times of inexperienced medical students, who have medical knowledge but little experiment of image diagnosis.

Each figure shows statistical values, number of images, total time, average time and variance. Number of images is the counted number of images while their investigation. Total time is whole investigation time and average time is average time per single image. Variance is from each viewed time. In this case, there is significant difference in average of viewing times per image and variance of viewing times between experienced and inexperienced. They are the same in the whole log data of the other image sequences.



**Fig. 5.** Log data of 3 experienced radiologists’ operations. It can be clearly found their operations are stable, because variance of viewing time is very small. Furthermore, some periodical actions are commonly found while their operations.



**Fig. 6.** Log data of 3 inexperienced medical students’ operations. A medical imaging diagnosis system with sounds. While a physician can view images, certain sounds are provided to him.

There are following tendencies in these log data:

- There are some small periodic peaks in experienced radiologists’ operation.
- Operation of experienced radiologists seem almost uniformity and very smooth.

- There are random peaks in students' operation.
- Medical students have spent more times to investigate each single image than experienced.

Many users have controlled with their mouse wheels to view medical images in the experiment. Experienced radiologists operate mouse wheel regularly. Actually, we have interviewed some subjects after logging experiments, they said that they are not focused in some image but glance whole every single image when detecting abnormalities. Furthermore they unconsciously pay attention for the difference between recent viewing image and previous or subsequent one. It is assumed that they don't weighted to investigate a single image but they focus on 3-dimensional structure estimated from neighboring images, including previous and next image. It is very effective to distinguish nodule from blood vessel because their 3-dimensional structure in lung are long and winding. On the other hand, medical students weighted to watch and seek abnormalities in an image, so their investigation become step by step.

As a result, experienced radiologists utilize 3 dimensional structural feature from difference between images. In contrast, students cannot perform such structural investigations. So they may search abnormalities by features derived from a single image. There can be tendency that student view the same image again and again in this analysis.

### 3.2 Analysis of Image View Operations

In the next step, we reconfigure image-viewing time and counting numbers to investigate the relationship between viewing times and each image. Figure 7 is a histogram that shows the sum of average times and counts of viewing per each image with 7 experienced radiologists, in the case of sequence 4. Vertical axis is viewing time and counts, horizontal axis is image ID. Solid lines represent average

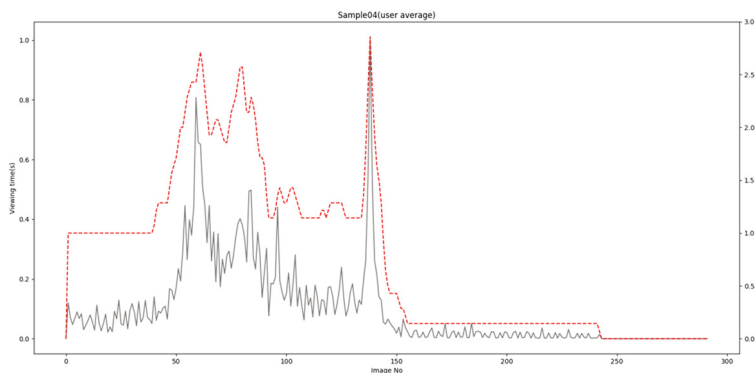


**Fig. 7.** A time-image histogram in sequence 4. Some images besides nodule are viewed by many radiologists for a long time or many times.



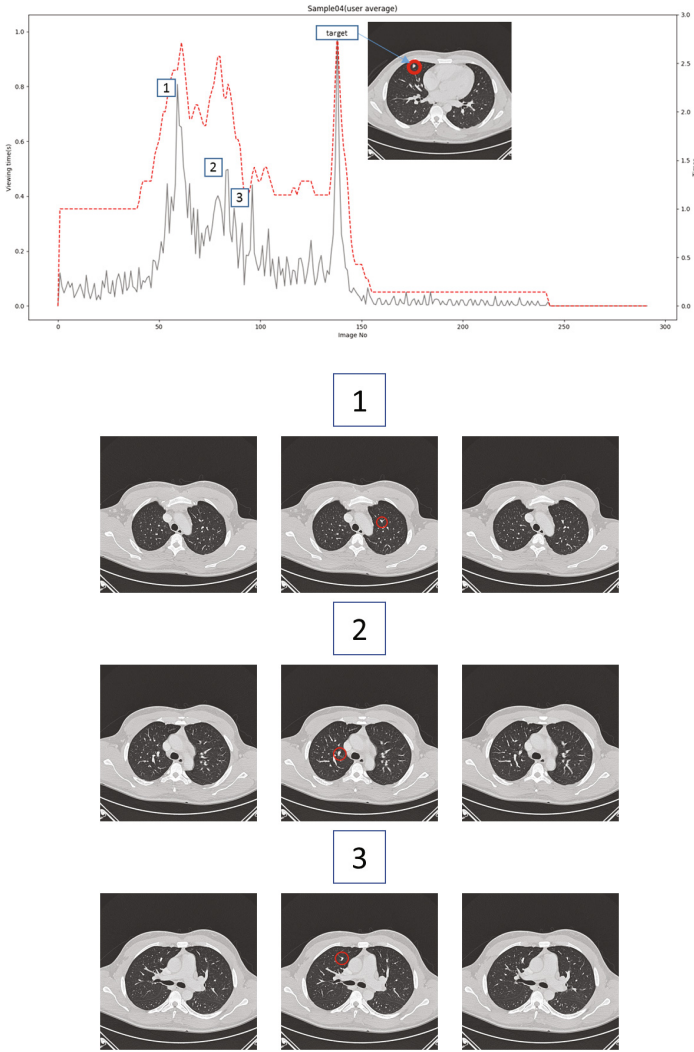


**Fig. 8.** Picked up images for sequence 4 with histogram (Fig. 7). In this case, some radiologists have viewed for a long time, such as 1 to 3 images. Additionally, each images are displayed with previous and next image in the sequence. Experienced radiologists unconsciously find 3-dimensional structure derived from sequential difference among images.

times and dashed one shows average counts. So it is possible to find which image is watched long time and carefully. In this case, target nodule is appeared in image ID from 135 to 142. This histogram represents viewing time assigned for each image is non-uniformed distribution. There are some peaks besides images including target nodule. It may means that there are some tendencies to pay attention for medical image investigation.

## 4 Discussion

Figure 8 shows picked up image that users have viewed for a long time, with their previous and next images in the original sequences. It is remarkable that there are some focused images while investigation. There are some regions in red circle shown in Fig. 8 that they seem like target nodules.

However, according to interview with them, even much experienced radiologists cannot successfully explain how to detect abnormalities rapidly because they seem to find some features unconsciously. As mentioned in Sect. 3.1, experienced radiologists pay attention for 3-dimensional structural information between previous and next images in the sequence. They unconsciously find 3-dimensional structure derived from sequential difference among images.

When students learn medical image diagnosis, at first, they will learn to investigate the images smoothly. Experienced operation log, especially their image handling and focusing information, are very important for inexperienced. It is necessary to support them to enable to find some 3-dimensional information from the sequence of images. To construct effectively educational tool, some quantification should be required to define importance of each image and feed them while medical imaging. Image importance will be estimated to apply these features for a medical imaging support system.

Correspondence between unconscious focused images and geometric feature is also very important information to support medical imaging. However, the current experiment is not large enough for evaluating our supporting method because the type of nodules in the lung seem to be resemble. Evaluating to the similarity between nodules are necessary and more data acquisition is required for more detail analysis. To apply these consequences for supporting medical image diagnosis, features derived from such unconsciously focused images are important because they may include some rules in the much experience of imaging diagnosis.

## 5 Conclusion

In this paper, we visualize radiologists' operation for diagnosis of medical image. The difference between students and radiologists are clarified from this visualized log data. Students try to find the abnormalities from single image, while experienced radiologists smoothly view the images and detect rapidly. It is necessary to utilize more detail information about medical images and to find correspondence difference feature and these features. Machine learning technique is very effective

for that. After that, evaluating to the similarity between nodules are necessary and more data acquisition is required for more detail analysis. To display image importance, multi-modal information supplying such as sound, vibration are effective because visually presentation of information to viewer may inhibit to their concentration.

**Acknowledgment.** This work was supported by JSPS KAKENHI Grant Number 24500148 and 24603018.

## References

1. Doi, K.: Current status and future potential of computer aided diagnosis in medical imaging. *Br. J. Radiol.* **78**(1), S3–S19 (2005)
2. Cheng, J.Z., Ni, D., Chou, Y.H., Qin, J., Tiu, C.M., Chang, Y.C., Huang, C.S., Shen, D., Chen, C.M.: Computer-aided diagnosis with deep learning architecture: applications to breast lesions in US images and pulmonary nodules in CT scans. *Nat. Sci. Rep.* **6**, 24454 (2016)
3. Samala, R.K., Chan, H.P., Hadjiiski, L., Cha, K., Helvie, M.A.: Deep-learning convolution neural network for computer-aided detection of microcalcifications in digital breast tomosynthesis. *Proc. SPIE* **9785**, 97850Y-1 (2016)
4. Kumar, D., Wong, A., Clausi, D.A.: Lung nodule classification using deep features in CT images. In: *Proceedings of the 2015 12th Conference on Computer and Robot Vision, CRV 2015*, pp. 133–138 (2015)
5. Maura, M., Dobashi, Y., Yamamoto, T.: A study on importance estimation of medical images by learning users' Operation History, IEIECE Technical report, ITS2010-33, IE2010-108, pp. 41–45 (2010)
6. Kagawa, T., Tanoue, S., Kiyosue, H., Mori, H., Nishino, H.: A sonification method for medical images to support diagnostic imaging. In: *Proceedings of the 4th International Workshop on Virtual Environment and Network Oriented Applications VENOA-2014 of CISIS-2014*, pp. 771–776 (2014)

# Study on Data Utilization of Regional Industry in Cross-Cutting and Systematic Regional Community Networks

Eiji Aoki<sup>(✉)</sup>, Zenjiro Oba, and Ritsuko Watanabe

Institute for Hyper Network Society, Oita City, Japan  
{blue, z-ohba, watanabe}@hyper.or.jp

**Abstract.** It is possible to collect enormous big data by IoT. Everything is converted into data. In all existing industries, there is the possibility of dramatically improving productivity by devising and utilizing those data. In addition to improving productivity, the creation of new industries is expected in the coming era of AI. Based on such time axis of the real world, what kind of activities should be implemented in the region? Sensor sharing is required for regional IoT network configuration and it is necessary to utilize the collected big data by industry or purpose of regional activity. The problems that are thought are how to make common consciousness of sharing sensor group, how to develop sensor platform, how to distinguish between opened data and concealed data, how to protect security, how to check the ownership of data, and so on. We try to consider the possibility of social experiment concerning data utilization of regional industry.

## 1 Introduction

Since its establishment in 1993, Institute for Hyper Network Society has consistently promoted local informatization. The regional informatization policy in Japan has been implemented by Ministry of Internal Affairs and Communications (former Ministry of Posts and Telecommunications) and some ministries from 1980s, with the name of information media, new media, multimedia, etc. The policy goal is the construction of the information infrastructure. And it involves activating the local community, according to inviting information industries to the region, enriching local medical care and welfare by telemedicine, improving information literacy by introducing information equipment into the educational field, dissolving regional information disparity and increasing tourists by the publicity of regional information. It also overlaps with the history of the Internet where commercial services began in 1994. In this era called the information revolution, were software and networks fully used in Japan? Were white-collar staffs able to improve the productivity of the administrative system? Were they able to contribute to solving social problems and regional issues? It is doubtful in light of the present situation.

Japan became the world's first super-aged society in 2007, and the population declining society that began in 2011. They could bring the increase of marginal settlements and the disappearance of local governments, and these issues to face in the

future are serious. Against those issues, in order for each region to be able to create an autonomous and sustainable society making full use of its respective characteristics, it is necessary to utilize data in the regional society. It covers regional industries in all fields ranging from primary industries to tertiary industries. We propose the establishment of “Cross-cutting and Systematic Regional Community networks” for its practice. Technical innovation with the Internet as a trigger has been rapidly progressing for the past 20 years and the sense of speed will increase in the future. It appears in the discussion of world experts on technical point of singularity that “AI becomes wiser than human being for the first time in human history”. In general, it was understood as arrival in 2045, but in fact, since IoT and AI began to put into practical use from around 2016 in full scale, technology development has been accelerated, and it will arrive in 2029 that Raymond Kurzweil predicts. Moreover, the original meaning of singularity is the moment that “the limits of the human brain with around 100 trillion extremely slow synapsis are transcended by civilization coupled with human beings and machines”. It is also required to capture the flow of these times in the region.

## 2 Background

Institute for Hyper Network Society organized the study group of “Cross-cutting and Systematic Regional Community Networks” in 2016. This study grope has discussed about how to deal with these various problems, variety of diversity of efforts for complicated tasks in rural areas such as low birthrate and aging population, rapid development of ICT (CPS, AI, wearable devices, communication methods), manifestation of light and dark in science and technology, globalization and economic growth in Asia. For example, visualization of efforts for problem extraction, formation of “Cross-cutting and Systematic Regional Community Networks” for solving these problems, construction of regional network type community aiming for mutual complementation and cooperation, collaboration with Asia, and autonomy of ICT companies. Table 1 shows the classification of research theme and keywords: [1, 4].

### 2.1 IoT Promotion Consortium

In October 2015, Ministry of Internal Affairs and Communications, Ministry of Economy, Trade and Industry, related ministries and agencies established “IoT Promotion Consortium”. The object is to establish the system to promote the development and demonstration of technologies related to IoT promotion and the creation of new business models by industry, academia and government participation and collaboration. The consortium has two working groups, the Technology Development WG (Smart IoT Promotion Forum) and the Advanced Model Business Promotion WG (IoT Promotion Laboratory), each secretariat is composed of the National Institute of Information and Communications Technology (NICT) and the General Foundation Japan Information Economic and Social Promotion Association (JIPDEC). The other are IoT security WG and data distribution promotion WG as expert WG.

**Table 1.** The study groups of “Cross-cutting and Systematic Regional Community Networks”

Groups	Theme	Keywords
Regional ICT	Regional security	Cyber defense, Regional joint security center
	Regional construction method of sustainable system	Collaborative system construction with automatic generation tool
Regional education, culture, art	Regional human resource development by industry-academia collaboration	International human resource development, Iterative learning of practice and theory, Educational participation with company experts
	Regional harmonization among art, culture, science with network use	Promotion of human resource development, Collaboration among industry, academia, government and private cooperation, Systematic cooperation of arts facilities libraries, universities, etc.
Regional health, agriculture, tourism	Regional environment, energy learning type tourism	Purpose type tourism, Attractive education for science and engineering, Experiment type learning, Factory tour
	Network type regional creation	Coordination of regional industries, Social activity environment for helping the elders (Platinum Concept Network)
	Regional complete recycling agriculture	Production & quality control of agricultural products, Organic cultivation, Sustainable agriculture, forestry and fisheries production (advancement of agricultural products)

It can predict that measures aimed at the public and private sectors will become full-fledged in each country with the development of new production process and the creation of service industry corresponding to the IoT era, the aim of optimizing the entire supply chain in the future. In reforming the global industrial structure, as evidenced by the movement of Industrial Internet Consortium (IIC) in the United States and Industry 4.0 in Germany. In Japan as well, from the policy such as “Revision of Japan Revitalization Strategy 2015 Investment & Productivity Revolution to the Future” (June 30, 2015), the time to respond to IoT, Big Data and AI era started. In the future, it is a measure to invite domestic and foreign IoT related investment and to activate activities of Japanese related industries to demonstrate their presence in the global economy.

## 2.2 Regional Promotion of IoT Implementation Task Force

Ministry of Internal Affairs and Communications wants to grasp progressing situation and issues to promote regional IoT until 2020. In September 2016, the framework of

“Regional Promotion of IoT Implementation Task Force” was started for the aim of taking necessary countermeasures for that purpose. Task Force consists of two sub-committees, the Human Resources Literacy Subcommittee and the Regional Resources Utilization Subcommittee. IoT, Big Data and AI are strongly expected as an effective tool, which is effective for improving residents’ services through the utilization of local residents, administrative and enterprise data, creating new business and employment in the area, and solving further regional problems. Along with the era of full-scale commercialization of IoT, these will extract regional issues based on the results of demonstration projects so far and promote strong horizontal development. It will propagate over every corners of the whole countries in Japan by grasping the progress situation and obvious problems, and taking necessary countermeasures.

**Activity Contents.** To promote regional IoT until 2020, “Public Roadmap for Promotion of Regional IoT Implementation” and “Primary Recommendations for the Realization of Roadmap” were announced in December 2016. As a background, there are the following issues surrounding the area. (1) Progress in population decline and aging, (2) Acceleration of central concentration in Tokyo, (3) Sluggish regional economy. As shown in Figs. 1 and 2, the areas already working on these are partly, and there are many municipalities that are interested in these, but actual concrete actions are hard to tackle. The issues of regional implementation are budget constraints, uncertainty about concrete usage images and benefits, shortage of human resources, establishment of a promotion system for public-private partnerships.

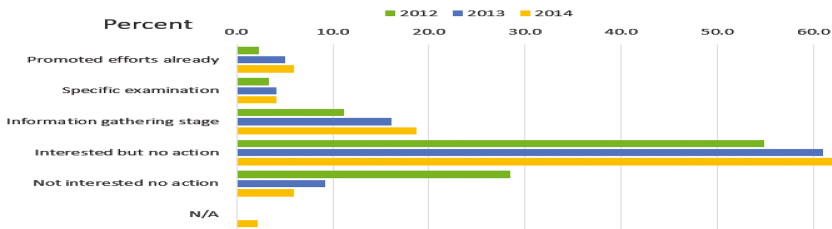


**Fig. 1.** Efforts to create the city utilizing ICT (Source: Ministry of Internal Affairs and Communications 2014)

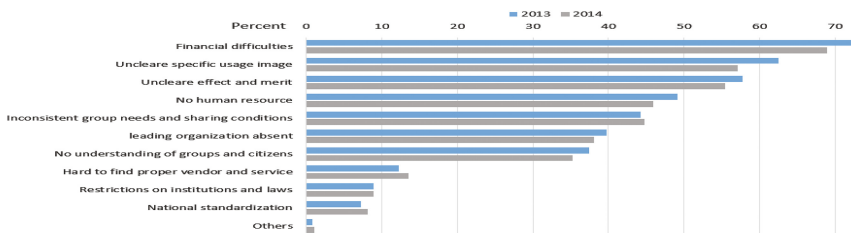


**Fig. 2.** Immediate task to advance ICT city planning (Source: Ministry of Internal Affairs and Communications 2014)

“Primary Recommendations for the Realization of the Roadmap”, for the implementation of regional IoT requires, points out the importance that major players in each field deepen their meaning and understanding of regional IoT and act on their own initiative. First, establish a promotion system on relevant ministries and organizations for each major field of roadmap. Next, urgent action should start in order to establish a comprehensive promotion system of “Vertical Thread” which enhances momentum in each field, “Horizontal Thread” to promote regional cooperation, and “Diagonal Thread” spinning regionally across fields.

### 2.3 IoT Promotion Laboratory

In October 2015, it established as one of its working group (Advanced Model Business Promotion WG) with the inauguration of the IoT Promotion Consortium. There three laboratory principles (growth potential and leadership, spillover (openness), sociality), based on that identify and select individual IoT projects and thoroughly support them from the viewpoint of corporate collaboration, funds and regulations, and improve the environment such as regulatory reform and institution formation for implementation of large scale society.

**Activity Contents.** Specific activities are advanced short-term individual projects toward commercialization and a medium-term demonstration project towards social implementation. Regulatory reform deregulates on the obstruction of business development, and implements new rule on social implementation of projects. There are activity items, (1) IT Lab Connection (theme-based corporate collaboration, project composition event), (2) Solution Matching, (3) Big Data Analysis Contest, (4) Data Innovation Workshop, (5) IoT Lab Selection (support for joint public and private funds and regulations), (6) Lab Demonstration (testbed demonstration). There are also such items as “Cross Platform Framework” and “Regional Economic Activation Framework” that links with the concept of “Cross-cutting and Systematic Regional Community Networks”.

**Regional IoT Promotion Laboratory.** Ministry of Economy, Trade and Industry and IoT Promotion Laboratory select the regional version of IoT promotion laboratory and provide supports. That is for the effort to create IoT projects in rural areas. The first selection of the regional version of IoT promotion laboratory was 29 areas in July 2016. In addition, the second step selected 24 areas newly in March 2017.

## 3 Social Experiment for Regional Implementation

As I mentioned, the progress of aging in Japan is fast, and how does declining population society affect industry? How will it concern with local economy and local government administration in the future? The world focuses Japan as an elderly developed country, and overseas companies that concern with it have started to open some research centers in Japan. The solution to halt the decline of the region activity due to the declining birthrate and aging population of human beings should grasp the



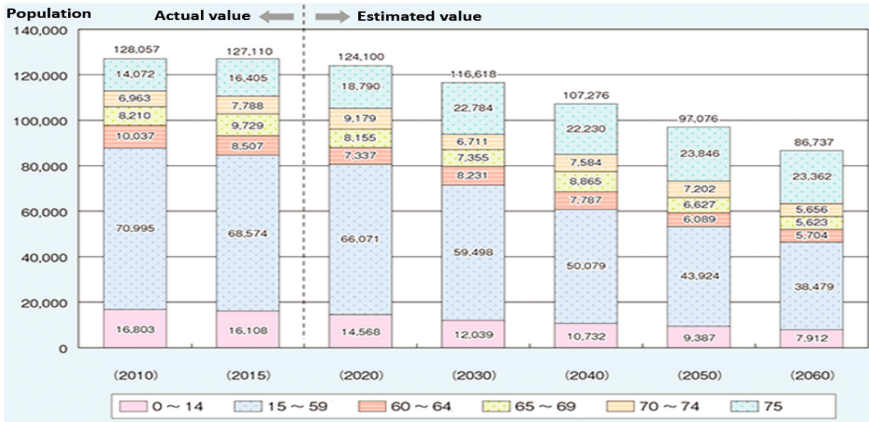


**Fig. 3.** According to the National Institute of Population and Social Security Studies “Japan’s estimated future population (estimated in January 2012)” birth middle (death middle). The forecast is that the total population in 2060 will decrease to approximately 87 million people. Future population estimate by age category (Source: Aged Society White Paper 2016 Cabinet Office)

actual industrial activities in each region and visualize it for the citizens, and in order to accomplish the purpose, it is necessary to cooperate and complement with industry, government, academics and private sector (Fig. 3).

The various policies for the local creation that the current administration stipulates aims at improving the concentration of Tokyo’s one pole, stopping the declining population at rural areas, and raising the vitality of the whole areas in Japan. The accelerating declining population in Japan as a whole is a major burden to Japan’s economic society and is attributable to the population inflow into the Tokyo area, which estimate to continue in the future. On the other hand, as shown in Fig. 4, the ratio of people who wish to migrate from Tokyo area to the district is nearly half.

The government distributes grants to regional comprehensive strategies of local governments as a new type of grant, such as regional creation promotion subsidies and regional creation acceleration subsidies. These are used for pioneering projects

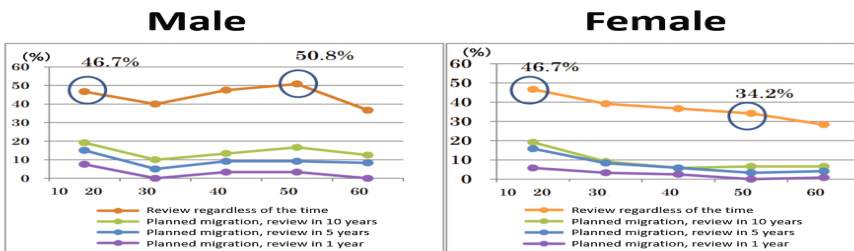


**Fig. 4.** About half of them are considering emigration to rural areas in the future. In terms of age group and gender. (Source: Cabinet Secretariat “Survey on Intention on Future Migration of Tokyo Residents” Outline of Results (August 2014))

requiring local autonomy and public-private interlocking. As a metaphor government supports to shoot three arrows on rural areas, (1) information support arrows, (2) human resources support arrows, (3) financial support arrows, but it is fundamentally hard to solve these problems. As mentioned above, many national support measures such as frameworks and policies that are suitable for IoT era launched. A centralized mechanism that the current political, administrative and economic system, and human resources concentrate on Tokyo, is the weak points of the vertical division administration. It is necessary for us to recognize that the limits of solving the rural problems can be also visible in reality. Therefore, we are conceiving the regional IoT implementation, social experiments to demonstrate by utilizing IoT in the region, the possibility to become an important breakthrough and to demonstrate it.

### 3.1 IoT Utilization in the Nursing Care Industry

Oita prefecture has long been a regional function as a recuperation and recreation area due to hot spring resources, but depopulation due to aging and outflow of other young people in the prefecture is progressing. However, there are cases where the number of inhabitants increases as in Bungo Ono area, and local creation becomes possible by increasing the attractiveness of the area. In this social experiment for regional implementation, the objective is to realize “Mimamori System” as “regional communication support” that realizes “elderly peaceful usual” and “nursing care with no burden and no regrets”. In this section, (1) “robot vision” which does not use visible part for human dignity (privacy) protection, (2) “extraordinary detection/change measurement” derived by human model’s action pattern derivation and “reliable care based on numbers”, (3) Sharing information for principal/living family/doctor/community to achieve early and appropriate response in case of emergency. At the same time, we will tackle “persistence” through training of community-oriented human resources: [2, 3] (Table 2).

**Table 2.** Research and development on community collaborative “safety nursing care” system including human resource development for attractive regional creation where elderly people and their families can live with a smile

Method	Item	Contents
Phase I	Verification of prototype sensor	Regional verification and grasp needs
	Detection/notification system	Commercialization of prototype sensor and integration of existing system
	Behavior pattern collection/analysis	Database construction and dangerous motion detection by behavior analysis
	Regional activation	Marketing and analysis for region
Phase II	Field validation at model area	Model quantification and evaluation
	Expansion of region and attraction of region	Regional categorization and regional attraction of Phase I target model

**R&D Achievement Goal.** In Phase I, we will achieve numerical data on the sensitivity and scope of survey of prototype sensors. First, we set up a prototype sensor in the model area and check the residents' needs in parallel with data collection. Next, we try the commercialization of prototype sensors for practical field verification and deployment. Database construction of ten households that is behavior patterns of everyday life data and falling detection in hazard motion detection. Abnormality detection by behavior analysis when elderly go out. We grasp in order to revitalize the community and the degree of contribution to the improvement of the living conditions of local residents and the revitalization of local communities and economic activities.

In Phase II, we will achieve field verification (model digitization and evaluation) in the model area (2 districts). It will quantify "robustness" and "flexibility" as a model area different from Phase I. Moreover set the goal of "district classification" of regional models accumulated through regional collaboration. Here, we focus on the "movement pattern on the regional scale" in the regional culture.

### 3.2 IoT Utilization in Kunisaki Peninsula Area of Oita Prefecture

Oita prefecture is rich region with nature as it is called "country of wealthy". Among them, Kunisaki Peninsula Area is region of old Japanese culture of Shinto Buddhism consciousness. This area is consisted of Kitsuki City, Kunisaki City, City of Bungotakada, Usa City, Himeshima Village. The agriculture, forestry and fisheries industries in the area is certified as "World Agricultural Heritage" in May 2013, that brings rich agricultural and forest products and has ecosystems through the efficient natural cycle of land and sea (Kunisaki Peninsula). It has recycling type agriculture and has tourism resources. In recent years, tourists from domestic and foreign countries, particularly Asia, are conscious of their own health, and so interested in foods and beverages. These areas are suitable for the production of healthy agricultural products. Elderly people's experience is valuable resources in harvesting natural herbal medicinal herbs, medicinal herb cultivation and food development. Agricultural products in the herbal area have respectively characteristics, so they are unsuitable for mass production and need cooperative complementation in the area. Therefore, actual experiments could create diverse industries by utilizing IoT at the regional network activities, such as herbal research and map creation in cooperation with residents, networking of mountainous areas, preparation of eco-cars and emergency calls necessary for elderly people, food and drinks with medicinal herbs and herbs, and development of souvenirs.

There is Ritsumeikan Asia Pacific University (about 6,000 students) in Beppu City, and faculty and staff from diverse countries (about 90 countries) are engaged in research and learning. Also in relation to medicinal herbs, it is coordinated with Mie University. In social experiments, with the cooperation of these faculty/staff/students/graduates, we plan to market sightseeing, foods and drinks for Asia, and connect to concrete network type production and tourist attraction measures. It will step up to the cross-sectional projects of purpose type tourism in the future, utilizing regional resources such as expansion to network cooperation for healthy vegetable production, factory facilities with state-of-the-art technology for environment and energy system, and facilities incorporating geothermal power generation and hot spring power generation.

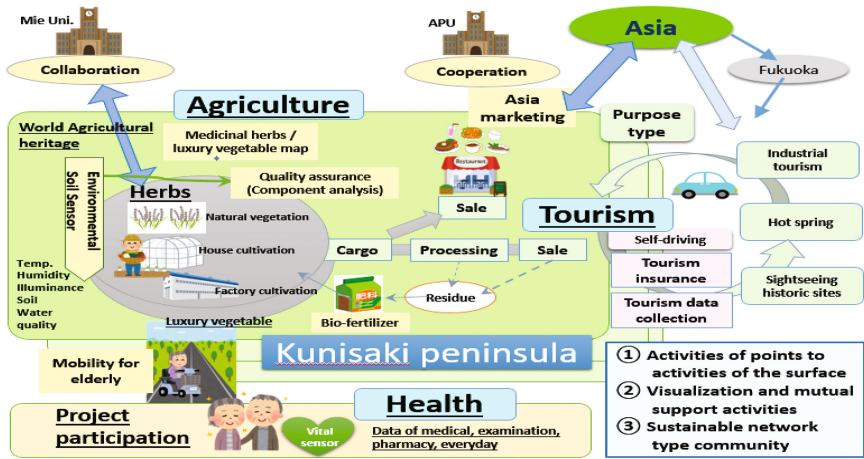


Fig. 5. Experimental concept for regional health, agriculture, tourism promotion plan by utilizing IoT

That is getting worried about human resource development of “manufacturing in Japan”, because young generations haven not an interest in the advancement of science and engineering. Therefore, showing the dynamic facilities that are operating at the manufacturing sites causes them to take an interest in technologies. In addition learning type tourism happens to be arise. Based on the above results, we will promote regional creation of sensor network industry, supporting the development of agriculture and tourism industry based on the improvement of the working environment of the elderly by forming “Cross-cutting and Systematic Regional Community Networks” (Fig. 5) [5].

**R&D Achievement Goal.** Issues to overcome in creating and deploying IoT services are vertical competition by industry and competition in the same industry. The solution is to cooperate in the region, complementing the local administration. Specifically, IoT data utilization and data accumulation from climate sensors/soil sensors, observation cameras, database construction and development of data utilization system are important. Sustainable production and quality control based on those, development and sale of products related to food and drink that involve medicinal herbs, and participation of elderly people experienced in them is indispensable. Showing the work of lively elderly workers gives visitors an impression of healthy areas. Agricultural products and sightseeing are oriented toward domestic and foreign, especially Asia. Consider utilization of IoT data, including local companies, according to openness and concealment for competition and cooperation for regional economic creation and revitalization of the region.

## 4 Future Works

The momentum of IoT has grown nationwide, demonstration experiments are proceeding with unique ideas in various regions. It is doubtful of whether successful cases or failed cases can truly provide regional features. There are not a few projects left to consulting

firms from the center or leaving them to advisers. There is issue that is not networking for effective collaboration where intellectuals live in the region. One of them is the influence of vertical industry group based on vertically divided administration. Another is ideas of residents that the analog world rather than the digital world is important and there are sense of security and vested rights, such as a sudden change does not come.

However, it is clear that ICT's power is necessary for solving social problems and improving productivity. Rather than treat by Buzzword, being able to firmly deal with IoT era could not repeat the past that has stagnated over the Internet for 20 years. The important thing is change from the region. Even in China, the information revolution is progressing rapidly in Shenzhen, not Beijing and Shanghai, which are dominated by the conventional system. Similarly, in the United States, promotion of various social experiments on the West Coast including Silicon Valley is driving the innovation, not on the East Coast of Establishment.

In order to establish "Cross-cutting and Systematic Regional Community Networks", it is important to utilize various resources in the region. In addition to resources related to industry, it is time to utilize effectively public network lines and sensors, information systems, hardware and software, statistical data connected to it. What we need is the planning of systems and methods, the software aspects for that, and measures against the previous precedent, and further human resources development that utilizes IoT, education for industry people and young people. IoT is important in the region rather than in Tokyo, the policy that consider at singularity such as dialogue with sensors, human resource development that can respond to changing ages.

## References

1. Aoki, E., Oba, Z., Watanabe, R.: Study on cross-cutting and systematic regional community networks. In: Proceedings of the 10th International Conference on Complex, Intelligent, and Software Intensive Systems (CISIS 2016), pp. 599–604, 6–8 July 2016
2. Aoki, E., Yoshitake, S., Kubo, M.: Study on sensor networks for elderly people living alone at home. In: Proceedings of 2015 International Conference on Consumer Electronics-Taiwan (ICCE-TW), pp. 132–133, 6–8 June 2015
3. Aoki, E., Yoshitake, S., Kubo, M.: Study on a nursing system using information communication technology. In: Proceedings of the 8th International Conference on Complex, Intelligent, and Software Intensive Systems (CISIS 2014), pp. 631–636, 2–4 July 2014
4. Watanabe, R., Ehara, H., Aoki, E.: Study and practice on information technology in an educational field using a cloud service and SNS. In: Proceedings of the 7th International Conference on Complex, Intelligent, and Software Intensive Systems (CISIS 2013), pp. 760–765, 3–5 July 2013
5. Aoki, E., Kudo, K., Fukuda, A., Nakanishi, T., Tagashira, S., Okayasu, T., Tsuruda, N., Yamasaki, S., Imura, Y.: Study on knowledge management platform about the field of agricultural infomatization. In: Proceedings of the 6th International Conference on Complex, Intelligent, and Software Intensive Systems (CISIS 2012), pp. 705–710, 4–6 June 2012

# Photo Alive!: Elderly Oriented Social Communication Service

Masooma Zehra Syeda<sup>1,2(✉)</sup>, Meeree Park<sup>1,3</sup>, and Yong-Moo Kwon<sup>1,2</sup>

<sup>1</sup> Center for Imaging Media Research, Korea Institute of Science and Technology,  
Hwarangno 14-Gil 5, Seongbuk-Gu, Seoul 02792, Republic of Korea  
masooma\_zehra@hotmail.com, alfl8514@naver.com, ymk@kist.re.kr

<sup>2</sup> University of Science and Technology, 217 Gajeongno, Yuseong-Gu, Daejeon  
34113, Republic of Korea

<sup>3</sup> Seoul National University of Science and Technology,  
232 Gongneungno, Nowon-Gu, Seoul 01811, Republic of Korea

**Abstract.** Technological predilection among different generations for social interaction affected intergenerational communication gap. The rapid intensification of internet and increased technological mediums create digital divide among younger generation and elderly. Regrettably most elderly are unable to use Social media. Elderly people left behind in many areas of digital services platforms and technological skills. In this paper, we proposed a unique system for intergenerational communication based on digital family photos named as “Photo Alive!” to diminished intergenerational interaction problems. The development includes implementation and design of photo-based tagging service and photo-based interaction service with smart aging techniques. We concentrate on captivate of elderly in social media using digital photos with specific goal to enhance social interaction with family members, friends, and younger generation by providing elderly easy user interaction mediums on elderly tangible social service. The preliminary evaluation results indicate that the system is elderly friendly for social communication.

**Keywords:** Intergenerational communication · Elderly · Social interaction · Photo Alive! · Family photos

## 1 Introduction

The comparative measurement of the world population of aged 60 years or over is projecting too high from mere 56% to 1.4 billion from 2015 to 2030, and by 2050 the elderly aged population is estimated to approximately 2.1 billion which is more than double of 2015 [1]. The largest number of older age population accretion pattern is predicted in other countries China, United States, India, Japan, and Germany assembled into 48% of whole globe older population in 2015. According to research of aging and the use of internet, Only a 20% of the population over 54 years old used internet on average 37% once completed attitudinal measures a week while post messages on social sites and usage of social media counted only 20% in EU27 member states which

evidenced intergenerational gap in terms of technological preferences [4]. Elderly constitutes an essential part of our society played role in economic and social growth while lack of interaction and communication mediums, improper dexterity of devices usage leads, towards anxiety, loneliness, and social isolation. Due to make aged people technological strong, many economical consideration suggested that elderly must be considered in the development of future technologies so efforts involved to overcome web access problems in case of keyboard input offered recommendations for typing accuracy [2]. Aged people are very fond of communicating among family members and friends to share their opinions, experiences, suggestions in order to utilize their precious time. In the modern era of digitalized social world, while everyone exploiting social services, elderly need to use modern communication mediums and easy interaction techniques to interact with family and friends conveniently. Elderly prefer social inter-vened established on face-to-face communication, letter, telephone as much as messages, On the other hand, Social networking sites revolutionized digital world caused emergence in different generations. A national survey is conducted among 1,520 adults at March 7-April 4, 2016 found that Facebook remains to be America's most liked social networking platform by a substantial margin (79%) now use Facebook, more than double the share that uses Twitter (24%), Pinterest (31%), Instagram (32%) or LinkedIn (29%) [3].

Elderly needs more attention and interaction in a period of above 60s which owned to loss spouse, family, and friends, In this case, Social interaction should be heightened to maintain elderly mental stability and health issues. Due to the finite knowledge of modern technology, elderly are far away methods of communication promoted by the younger generation. Engagement of elderly and younger generation established an interesting effort in [5]. The author has developed the cloud-based application as a social connector that able to improve synchronous and asynchronous social interaction with relatives. Our Purpose to improve the mood of older adults, encourage them to take part in social media based on photos and smart mediums.

The adoption of technology by older adult's substantially declined and digital divide increased. Researcher in [6], divided roles of family members, seniors and caregivers according to related tasks, although presented social network tailored for emotional comfort to digitally involve all seniors and share their life experiences by YouTube upload widget to allow users to share their videos on YouTube. The Younger generation seems to be more active towards social networks and elderly manifest lack of confidence to adopt the new digital technology, afraid of destroying gadgets considered themselves to digital illiterates. This difference in adaptation digital technology is the origin of lacking behind elderly from modern era technology that cause intergenerational communication gap.

Therefore, we declare our system, "Photo Alive!" that is an elderly oriented photo-based social communication medium for boosting individual's reminiscence. In every era, photos reinvigorate old memories and facilitate story collection of past moments. In our system digital photos has been considered as a source of medium to interaction and communication, rejuvenate memory organization by a healthy conversation among elderly and family members based on photos. "Photo Alive!" Creates series of emotional attachment provides elderly an interactive and unique medium to instigate family

conversations by exploring the photos cultivate social communication with novelty by filling colors of life in photos. Furthermore, “Photo Alive!” developed Photo-based tagging services like Voice messages, family relationships and social information tagging also provided Photo-based interaction techniques to compose elderly friendly live environment by Email and Voice message sending, SNS Voice and Camera taken pictures Posting, Voice/Video Call with elderly supported interfaces with TV, remote control, voice, and touchpad. Moreover, we elaborated smart social service for elderly named “EasyFace” to digitally include all seniors irrespective of their educational level, or technological skills strengthen socially, improve mental condition and contribute pleasant entertainment in their lives by experienced photos with SNS voice posting, comments, messages, emotional connection materials with elderly friendly interfaces so elderly do not need worry about impairments.

Next section reports related work and previous approaches. Section 3 shows the architecture of Photo Alive! And its modules. Section 4 presents the Photo-based several services. Section 5 defines features of Photo Alive! And describes main usage scenarios. Section 6 discusses the preliminary evaluation. Section 7 elaborate conclusion and further work.

## 2 Related Work and Previous Approaches

In this section we explain about existing techniques, for promoting active aging author proposed paper based communication with Social network application [7] provided Tlatosketch, a digital frame and digital pen based on Anoto technology and paper combination authorize elderly to send hand written messages to Facebook [Tlatoque] client produced older adult with access to Facebook. The effort is to articulate design availability of digital pen and paper for expression media of elderly While Photo Alive! elaborated not only easy interfaces like voice, touchpad and Voice but also Social integration with digital photos comfortably to know for elderly who want to communicate, who commented on their photos, at what time they post or share, how many likes with not only sightseeing but also provided speech communication which specify story of “EasyFace” while on the other hand, in our system Voice balloon is generated for voice message tagging among elderly and family members for remove social barriers.

An interesting and joyful effort has been made in [10] to participate elderly and younger generation by means of computer games. The authors have developed a game known as Age Invader where children and elderly play game in the physical environment while parents can participate virtually in real time remotely via the internet. The purpose of Age invader is for a family digital game suitable for different age groups amiable for social family interaction.

Several projects proposed for tangible interaction for social communication. The authors in [8, 9] indicated one family extended case study about authoring process of audio enhanced paper photos for memory collection with livescribed pen for embed audio in a certain area in a paper photo. Therefore their system neglected to focus memory enhancement to identify who embed audio. On contrary, our system emphasize preserving memory to identify who is tagging voice message. Similarly, in EasyFace,



it is easy for elderly to experience who post activities, messages and share digital photos over Social media. While in voice balloon W2W concept is allocated where elderly can understand who tagged voice message to whom.

D. Harley [12] presented case study of 79 years old video blogger “Peter”, about analyzation of his first eight video blogs. Youtube allow official users to display their own videos on the web promotes a certain form of video blogging and permits comments on others videos either in text comments or take use of videos. To promote intergenerational communication Peter posted small episodic videos about his life with help of YouTube services and post comments on new materials. This research concludes YouTube creates Intergenerational connections as an alternative to entertainment media among the younger generation. In our case, Photo Alive! Provided photos support for several other social interaction mediums with multimodal human-computer interaction techniques. By making a video is just attractiveness for a limited time as across elderly may feel fed up while Photo Alive! Generates Intergenerational communication with advanced gadgets and interaction mediums.

### 3 Photo Alive! Architecture

The Photo Alive!, an interactive social captivate for elderly considers all family members and senior population played a role of mediator contain the theme of photos that is unique and ebullient service to connect different age groups aims to increase closeness bridging intergenerational communication. Client-1 elderly are often noticed to be more comfortable with prior gadgets like Television, radio, and telephone. Considered elderly preferences we design an elderly friendly interactive social content platform. In Our developed system we have used PC stick, that turn HDMI television into home entertainment computer with using comfortable interaction modalities TV, remote control, camera, voice, touch pad and hand written an email. While Client-2 Family member and younger generation prefer modern gadgets and Social media without hesitation with simple few clicks they can enter into the social smart world, using several gadgets (game console, computer, smart TV, smartphone, tablet etc.) at the same time. Where they can utilize their time by sharing, suggestion, involving in life events and occasions, as the scenario is shown in Fig. 1. However elderly are unable to use modish equipment frequently, they can use SNS through “Photo Alive!” Our system is web hosted securely with database connectivity of storing data and all information of the application, having three idiosyncratic modules of audible, readable and connectable. Audible module compromises audio tagging with recorder.js and voice balloon feature with Web speech API in particular photo faces, which characterized STT (speech to text), so elderly can record as well visualize the spoken messages. Readable module has contents which are visible with the elderly requirement in large fonts and large buttons incorporated family information relating family member’s name, relationship, and social information. Connectable contemplated voice posting, sending an email and Video communication which is a consequence for connectivity among elderly and younger generation.

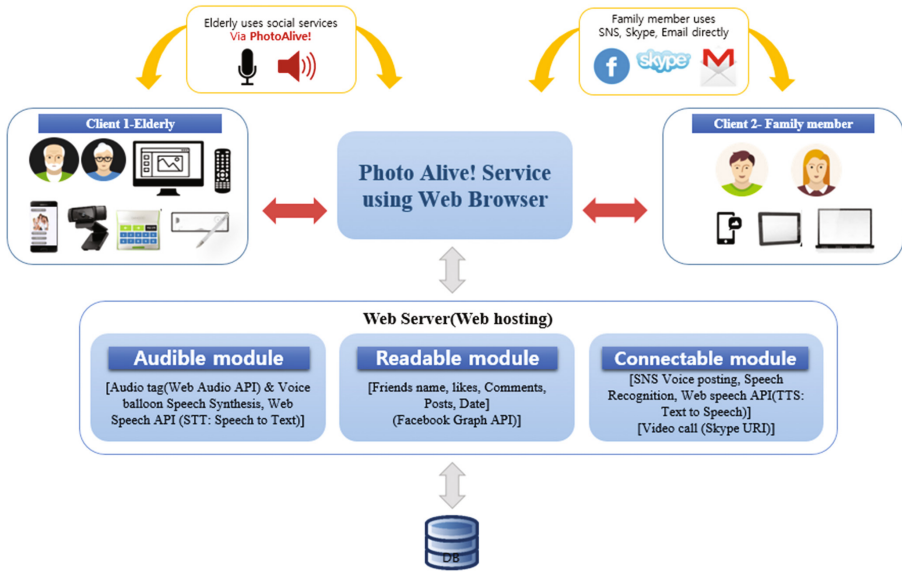


Fig. 1. Photo Alive! Architecture

#### 4 Photo-Based Services for Seniors

Our system can play a key role to reinvigorate senior's lifestyle who feels isolate from this digital world using digital photos. Therefore we declared salient features of our system consisted of Photo view service where elderly experienced photo gallery, by their own wish of forward, backward and also automatic viewing. Ultimately we provided Photo tagging service that consisted of Voice message recording, listening, firstly voice message is recorded over detected face over photos and with the usage of easy communication medium like remote control elderly can experience voice messages. Photo Alive! Have readable module where elderly and younger generation authenticates their names and relationships. To overcome the limitations of technology for presence awareness, elderly must know about social information and interaction techniques of the younger generation so in Photo-based interaction elderly can inquire each family member information. Additionally, we have implemented Photo tagging management functionalities include save and edit function to allow the user to enter information to avoid memory loss.

Mediated or face-to-face interactions within groups, family or institutional contexts it is better to know psychological prosperity of older adults [11], maintain familial and professional relationships are important for emotional health of elderly, In context of this busy era for every age factor human, It is noticed that in retirement age, the elderly are busy in passionate tasks and also they involve in communicating with family members. Photo Alive! Provided them Voice-command supports speech to text, hand written letter and camera support snapshot photos for sending an email. For face to face

communication in the digital domain, video communication is accommodated for relaxing communication.

## 5 Features and Services

### 5.1 Elderly Friendly Interface

Guidelines and techniques for a web application for disable people, as well as elderly, affirmed in [13], they mentioned about the important issue of web accessibility with age-related impairments that has been occurred in older age such as, vision, hearing, cognitive and physical abilities. For the development of web-based elderly oriented tangible service for enhancing social communication, we focused on easy and influencing web service for elderly which is RWD (responsive web design) framework indisputable approach for elderly access from Television preferably Speech recognition and Speech synthesis operate by remote control keys because elderly are more familiar with old gadgets. As like older are feel relax while using them just key information can enjoy them our web tangible service, seniors can also use touch interface of the mobile phone.

### 5.2 Photos and Voice Balloon

Photos are one of the interactive media for elderly, reminds us our past memories and good times. Photos can be used as intercourse material for communication among elderly and younger generation either in paper format or digital photos. In comparison, with the increasing digital media it is necessary to meet with modern needs of the world especially for elderly who are fond of digital gadgets but due to lack of knowledge, they are unable to match their requirements to converge family gatherings and convey their suggestions and messages. We developed Photo Alive! Which referred Photo based voice messaging service called as “Voice balloon”, promoted to rejoin memories and recall amuse moments with family members spend together. Photos are the best source of commemoration, act as a friend, caregiver and family member if they contain the qualities of sharing, talking, listening, and attention especially to overcome loneliness. The older age is very sensitive after retirement, elderly need assistance. On pondering upon disturbance in age factor we declared a distinct feature for recording voice with speech synthesis. In this case elderly and younger generation can communicate each other by embed audio in voice balloon seems beautiful and significant sensible conversation media, contemplate the impairments of elderly. In our application, we combined photos and voice to bring liveliness in revelation between elderly and family members. After uploading photos in the system using the camera for live photos or photo gallery. It will detect the number of faces in given photos. By detection of faces in photos, our system determined Kairos API by scanning over photos looking for a pattern that match a typical face with optional parameter minHeadScale. This intrinsically tells kairos how many faces photo have. This identification reminds elderly how many family members are present in a photo. Simultaneously Voice balloon is generated when faces are detected on photos for leaving or recording a voice message. We used Web Speech API, which converts speech to text. Elderly with impairment face no problem because in the case

of vision problem elderly can experience voice message, similarly in hearing impairment elderly can visualize messages. For this we specified especially communication mediums for interaction is remote control keys which are easy to interact on basis of color, number and shape of faces it is easily diagnosed for elderly who leave the voice message for them and for whom they want to record their voice balloon message which is shown in Fig. 2.

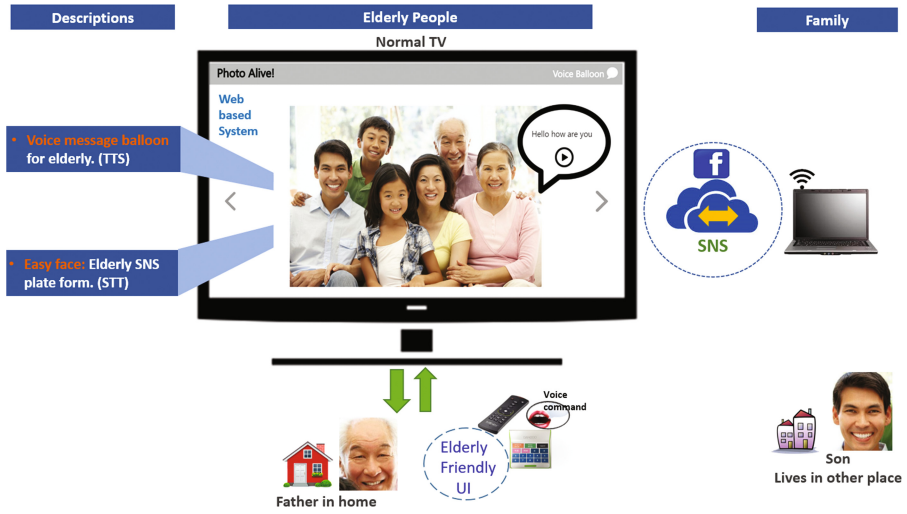


Fig. 2. Photo Alive! Elderly Friendly environment

Voice balloon contained easy conversation for elderly with photos where older people create liveliness in photos with an easy way for them to know with colour and number system elderly can easily easily recognize who tag voice message for them with who to whom scenario. Voice balloon provided interaction as well as amusement for recreation of memories with new diversions of media and elegant user interfaces which encounter elderly’s web accessibility easy and affordable which is considering ongoing topic in most research.

### 5.3 EasyFace

Social media and social network are now an essential part of our lives. Now a days, Rest of the world including stakeholders, younger generation, family members and friends huge percentage of world considered social media is a part of daily life for sharing life events, exchange experiences, emotional feedback, activities, tag presence over social networks to interconnect with loved ones, majority of senior population lack behind to share their expertise and life events due to emerging media digital era. In order to avoid digital divide, older people also need to socialize for enrich physical and mentally, need is arise for senior’s to use easy social interaction mediums. So, we introduced comfortable social communication medium for elderly with society on digital platform. Photo

Alive!, an elderly oriented Social platform compromises media processing unit for receiving the media content from the SNS server and the additional information for the media content and displaying the received additional information on a display. Disparate from text-based SNS such as Twitter and Facebook, it is audio-based SNS where elderly can socially involve with easy interactivity.

Computer-mediated technologies facilitate digital literates (younger generation, friends etc.) to create and share ideas via virtual community networks in a fully supported manner while leaving comments or like post, messages we will be able to tell the person our opinions. Digital illiterate are not aware of electronic communications. The study is conducted [14] to assume encouraging and discouraging factors for 124-internet using elders finished attitudinal measures about benefits of SNS, website accessibility, trust in SNS by TAM (Technology acceptance model) predict the prevalence of SNS, it was proved greater perceived easiness over the internet predict greater intention to use SNS. Hence to make a valuable social approach to elderly over the internet integrated Social service “EasyFace” declared for elderly an easy social platform where elderly can encounter SNS photos, comments, SNS posts, SNS sentiments with who to whom concept. Elderlies are capable of enduring who want to communicate with the extraordinary theme of photo-based, we able to get profile photo of a family member who wishes to meet elderly on a virtual environment and senior population follows EasyFace through the voice guide and some sort of voice format. Ex) Voice guide can tell them what is currently happened on their Photo Alive! SNS service. This feature can be applied to full fill the requirements of elderly. For this purpose, Speech recognition can recognize text over SNS platform using TTS (Text to speech) technology Fig. 3, show interface of EasyFace.

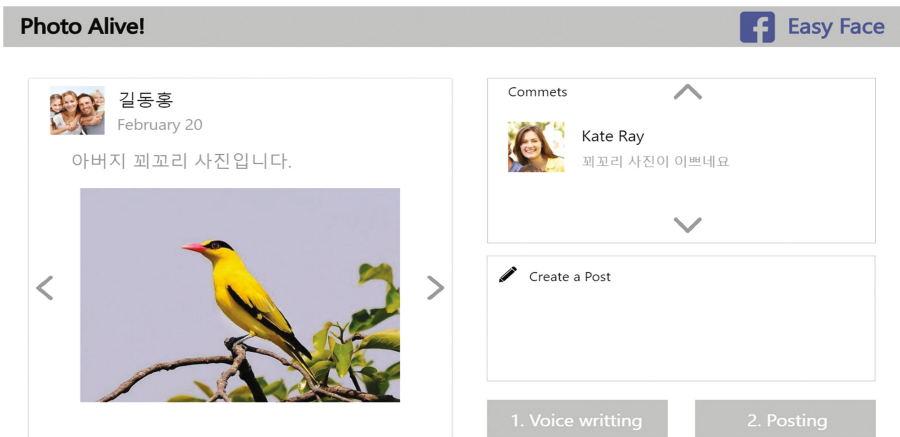


Fig. 3. Photo Alive! EasyFace

Moreover, elderly can able voice posting over SNS which is not currently found on local services. This is specifically designed for elderly people using web speech API, with Speech synthesis or STT (speech to text) aims to develop positive feeling in elderly

and improve quality of life of older adults to reassure elderly that they are not alone, Inventions to connect the digital divide by providing a platform for the elderly to interact with younger generations. A new SNS platform for elderly people using photo where elderly can experience photos, emotion of that photos having likes from SNS, where this photo is taken having location of photo and also comment linkage being interactive and entertaining as a way to communicate with the elderly and the younger generation.

#### 5.4 Photo Alive! App

According to research [16], a prototype framework OldGen is developed on generic mobile devices by dissociating the software user interface, makes the user interface portable it could be moved between different phone hardware consisted messages, phone book and add new contact options for elderly. We proposed smart aging technique with social interaction “Photo Alive! App” for elderly where elderly can fulfill their physically as well as socially communication requirements by capturing live images from camera smartphone and send to Photo Alive! Desktop, another service is provided for sending email on specific contacts and also on other contacts by typing email address as well as elderly can send Camera took photos to Facebook for socially and mentally pleasant communication with family members. The interface is shown in Fig. 4.



Fig. 4. Interface Photo Alive! App

## 6 Preliminary Evaluation

In this section, we discuss the preliminary evaluation of the developed system and interface methods for older aged people. Teixeira in [15] potentially contributed a user study to learn about user behavior (elderly people) towards improving audiovisual and social media by multimodal HCI. Our target group is elderly aged from 60 to 80 years old elderly. For the provision of tangible services for elderly, we tested our service by older women aged 76 in Korea. First, we inquired about modern gadgets Personal computer, keyboard, and mouse. In this case, she realized that to pointing area of mouse and touchpad is not perfectly as younger generation selected. She said, “I want to use these

smart devices but it gave tough time and I forgot how to use these”. We predicted that digital interfaces are hard to manage them, they like this era of digital world and their gadgets but they feel difficulty to proceed. Usability testing methods included TV based service and smartphone service of Photo Alive. We made a scale from 1 to 5, 1 assigned to difficult and 5 assigned to easy, as elderly marked on some parameters. On the basis of her comments, we enhanced communication ability in elderly by initiated more easy interface and mediums by evaluating different task and asked questions about Photo Alive!, by provided them Photo Alive! Environment included Television, remote control, touch pad and Photo Alive! Smart aging app and asked some questions. The response showed below which concluded evaluation question and answers:

**Photo Alive and Social Services:**

Questions:

1. Smart Younger generation services are easy to use in Photo Alive?
2. The interface is evolutionary for elderly?
3. Elderly are satisfied with the services?

Answer: Elderly marked “YES” option.

We evaluate smartphone app of elderly by handle smartphone camera by elderly and utilize their smart gallery by intergenerational communication like send to Photo Alive! send to email and send to Facebook for social interaction. We got a positive response and enhanced our service comprised communication with social network services, recording and playing voice messages of family members as mention in Fig. 5.

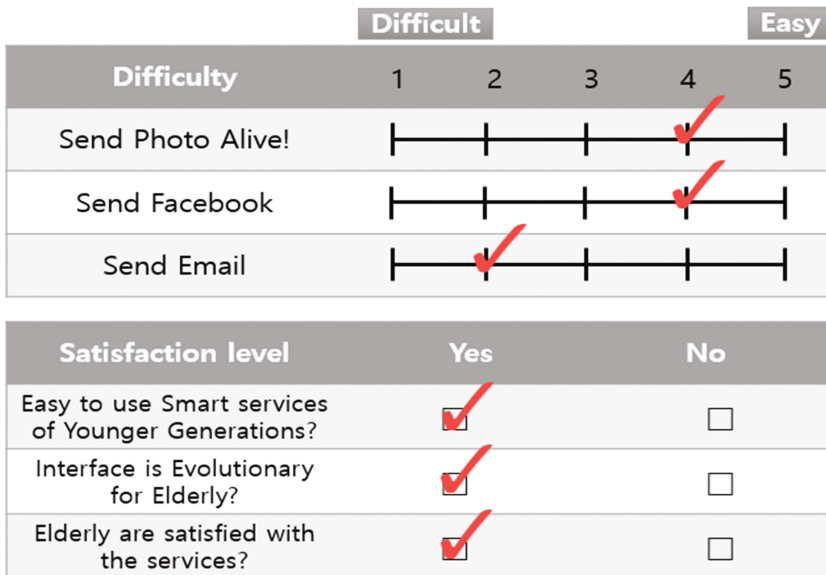


Fig. 5. Photo Alive! smart app evaluation

***Observer Comments:***

The observer pondered how elderly use digital gadgets. Elderly found difficulty to operate mouse, keys function and typing text, while understanding service aspect and intuitiveness elderly have a lack of prior understanding of email and Facebook services as they have no concept of Facebook and email. Other problem factors depending on network and server status, the picture display time delay, although the user is intended to achieve a goal, elder women is satisfied with services.

## 7 Conclusion and Future Work

Elderly are in minority to use smart devices and social network services as relevance they miss opportunities to stay in contact with family members and loved ones. To reinforcement socially connected we presented Photo Alive! For enrich family memory and facilitate to share photos, ideas, activities, and media among intergenerational family communication. We proposed smart interfaces for elderly like remote control, touchpad, voice with home entertainment premises which catalyzed human interaction. Furthermore, we granted several services for elderly to build generation and digital gap resulted photo based view service, photo-based tagging, photo-based social interaction, Voice message balloon and EasyFace: an interactive social communication medium comprises STT and TTS for elderly, provided medium of connection for younger generation while in first preliminary evaluation participant is enthusiastic to experience unique media, an effort to involve elderly socially and mentally aware digital technology. We are planning to enhance User experience to evaluate Photo Alive! in more wider aspects, to know about elderly's web accessibility needs and requirements include physical and cognitive impairments. We want to test elderly friendly oriented plate form to know about their opinion and suggestions bringing an intergenerational communication more powerful tool for future.

**Acknowledgements.** This work is supported by a project entitled with "Development of Tangible Social Media Technology for Smart Aging" of Korea Institute of Science and Technology.

## References

1. United Nations: World Population Ageing 2015. United Nations, New York (2015)
2. Hanson, V.L., I.T.J. Watson Research Center: Web Access for Elderly Citizens, WUAUC 2001 Proceedings EC/NSF Workshop on Universal Accessibility of Ubiquitous Computing, pp. 14–18, May 2001
3. Pew Research Center. <http://www.pewinternet.org/2016/11/11/social-media-update-2016/>. Accessed 04 Apr 2017
4. Milligan, C., Passey, D.: State of art Ageing and the use of the internet, current engagement and future needs, October 2011
5. Munoz, D., Gutierrez, F., Ochoa, S.F., Baloian, N.: Enhancing social interaction between older adults and their families. In: Ambient Assisted Living and Active Aging, IWAAL 2013, pp. 47–54. Springer, December 2013



6. Marcelino, I., Laza, R., Pereira, A.: SSN: senior social network for improving quality of life. *Distribut. Sensor Netw.* SAGE Journals, July 2016
7. Cornejo, R., Weibel, N., Tentori, M., Favela, J.: Promoting active aging with a paper-based SNS application. *IEEE Pervasive Health*, December 2015
8. Piper, A.M., Weibel, N., Hollan, J.: Audio-enhanced paper photos: encouraging social interaction at age 105. In: *Proceedings of the 2013 Conference on Computer Supported Cooperative Work, CSCW 2013*, pp. 215–224, February 2013
9. Piper, A.M., Weibel, N., Hollan, J.: Designing audio-enhanced paper photos for older adult emotion wellbeing in communication therapy. *Int. J. Hum. Comput. Stud.* **72**, 629–639 (2014). ScienceDirect
10. Khoo, E.T., David Cheok, A., Duy Nguyen, T.H., Pan, Z.: Age invaders: social and physical inter-generational mixed reality family entertainment. In: *Virtual Reality 2008*, pp. 3–16 (2008)
11. Hummert, M.L.: Communication with older adults. In: *Encyclopedia of Geropsychology*, pp. 569–575, January 2017
12. Harley, D., Fitzpatrick, G.: YouTube and intergenerational communication: the case of Geriatric 1927. In: *Universal Access in the Information Society*, pp. 5–20. Springer, May 2008
13. W3C: Web accessibility and older people: meeting the needs of ageing web users, March 2017. <https://www.w3.org/WAI/older-users/2017>
14. Braun, M.T.: Obstacles to social networking website use among older adults. *Comput. Hum. Behav.* **2013**, 673–680 (2014)
15. Vítor, T.: Improving elderly access to audiovisual and social media, using a multimodal human-computer interface. Thesis, Department of Information Science and Technology, October 2011
16. Olwal, A., Lachanas, D., Zacharouli, E.: OldGen: Mobile phone personalization for older adults. In: *Proceeding of the SIGCHI Conference on Human Factors in Computer Systems, CHI 2011*, pp. 3393–3396, May 2011

# Realizing Diverse Services Over Hyper-converged Boxes with SmartX Automation Framework

JongWon Kim<sup>(✉)</sup>

School of Electrical Engineering and Computer Science,  
GIST (Gwangju Institute of Science and Technology), Gwangju, Korea  
jongwon@nm.gist.ac.kr

**Abstract.** In this paper, we discuss about a DevOps-oriented automation approach to effectively realize diverse services over distributed hyper-converged boxes, which is aligned with the emerging ICT infrastructure transformation toward converged SDI (Software-Defined Infrastructure). By leveraging diverse open-source software and hardware, SmartX automation software framework attempts to streamline the service realization with the API-based integration of provisioning, visibility, orchestration, intelligence, visualization, and security/federation functions.

## 1 Introduction

To prepare for emerging software-driven digital transformation, ICT (Information and Communications Technology) infrastructure is undergoing long-term shifts toward converged SDI (software-defined infrastructure). As depicted in the bottom of Fig. 1, the undergoing shift for converged SDI leverages the harmonized orchestration of SDN (Software-Defined Networking)/NFV (Network Functions Virtualization), 5G-ready mobile, and Cloud technologies. On top of SDI-based open, composable, and federated resource infrastructure, the dominant Cloud-based capabilities are gradually mixed with AI (artificial intelligence) & BigData analytics. Also Cloud-based capabilities at the core of SDI are tied with the emerging foundations for Industrial Internet of Things (I<sup>2</sup>oT), which involves versatile smart and mobile things<sup>1</sup>. Thus, the resulting open platforms with diverse open APIs are consumed by container-leveraged cloud-native SaaS-style applications to enable the agile and economic realizations of diversified human-defined services, which are intermingled with open data ecosystem.

Also, in order to match the ever-increasing demands for agile service prototyping experiments, various playgrounds (i.e., testbed environments) are constructed and gradually evolved from isolated small-scale islands towards automated large-scale federated ones, especially under the context of FI (Future Internet) testbeds [1]. At the same time the needs for SDI-centric playgrounds have emerged from early 2010, while open-source

---

<sup>1</sup> As an example, to enable diverse types of IoT-Cloud services, end-side IoT and core-side Clouds are effectively tied with the enhanced inter-connection support from edge computing/networking.

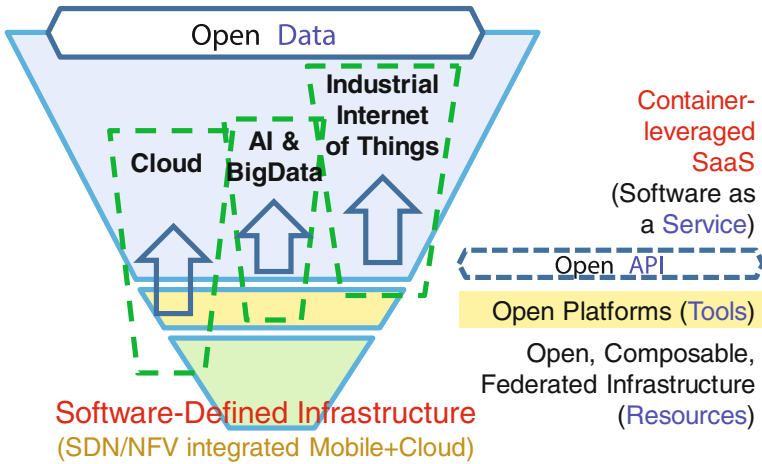


Fig. 1. Enabling data-oriented intelligent services with SDI-based open platforms.

software and hardware communities are growing fast to assist the buildout and operation of open, composable, and federated playgrounds. As depicted in Fig. 2, nowadays, it has become de-facto trends among global playground owners to leverage open-source software and hardware for their converged-SDI-ready playgrounds.

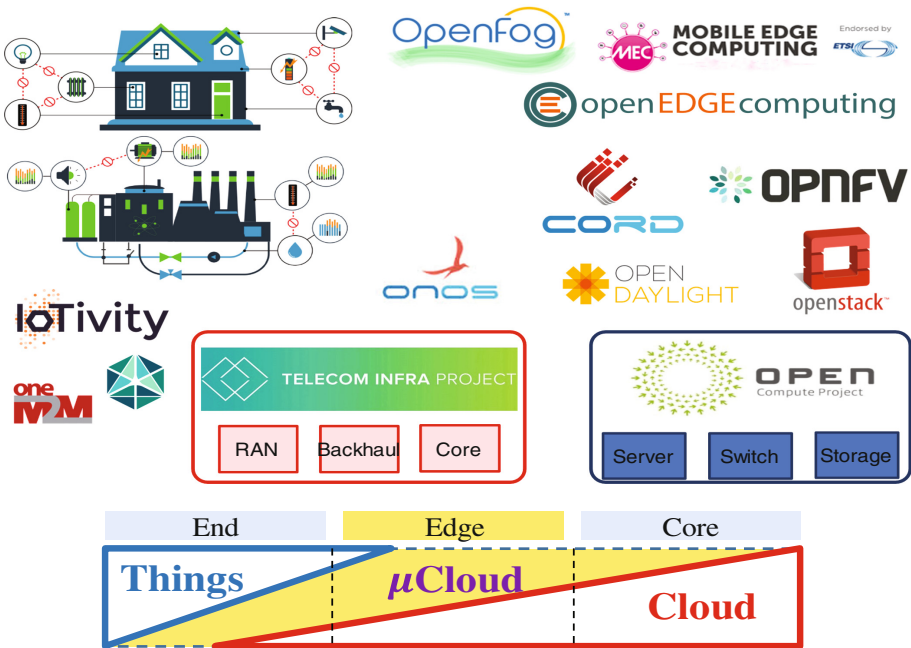
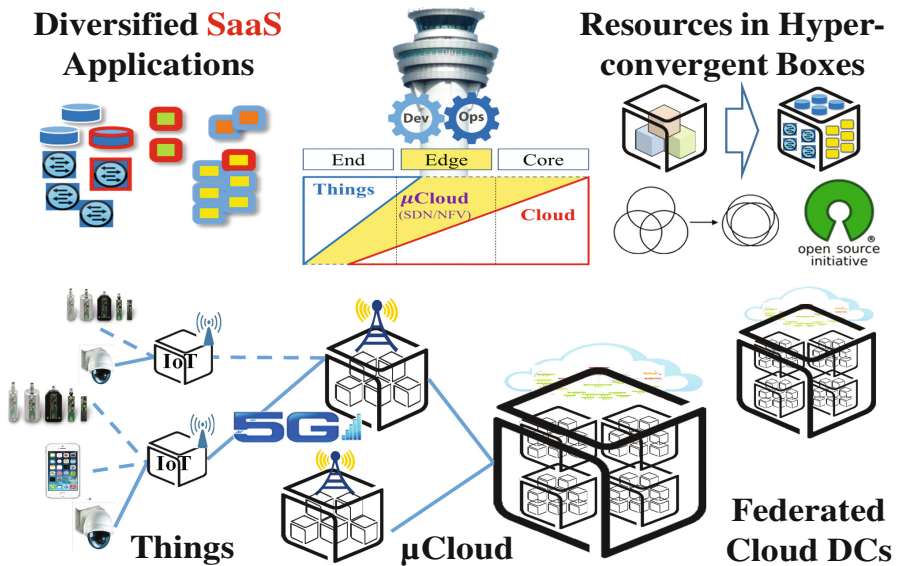


Fig. 2. Converged SDI with open-source software and hardware.

## 2 Diverse SaaS-Leveraged Services with Hyper-converged Boxes

In this context of converged-SDI-ready playgrounds, it is very crucial to flexibly and economically cope with the increasing requirements for diverse service realizations. Thus, as shown in Fig. 3, the adoption of hyper-converged boxes is quite useful to enable converged-SDI-ready playgrounds. As evidenced in our experience of building and operating a shared SDI-centric playground, named as OF@TEIN Playground [2–5], this kind of simplified resource pooling could be efficiently and economically achieved with hyper-converged (i.e., compute/networking/storage integrated) SmartX Boxes<sup>2</sup>.



**Fig. 3.** Diversified SaaS-style services with hyper-converged boxes over SDI-ready playgrounds.

Also, with the automation power of DevOps (Developers and Operators) paradigm, the diversified cloud-native services can be created by flexibly utilizing the dynamically-provisioned resource pools [6, 7]. For example, as depicted in Fig. 3, we can enable the agile service realization by orchestrating IoT-Cloud function-based services with small-and-large distributed hyper-converged SmartX Boxes [4, 5]. Thus, by linking it with three SmartX building-block abstractions such as ‘Box’, ‘Functions’, and ‘Inter-Connect’, as shown in Fig. 4, we can complete the workflow of creating, testing, and launching diversified user-defined services. In doing this, we need to address the challenges such as automated provisioning (e.g., zero-touch installation and configuration), instant and persistent visibility (to-be-expanded for distributed real-time intelligence),

<sup>2</sup> Hyper-converged boxes are illustrated in the upper-right corner of Fig. 3. Also, biggest-size box in Fig. 3 stands for the unified assembly of small-size boxes, as implied by the notion of ‘Data Center as a Computer’ [8].

and lifecycle orchestration (e.g., resource scaling & continuous integration, policy-based management & security/safety). Also, it is required to manipulate the appropriate mix-and-match of p (baremetal) + v (virtual) + c (containerized) functions and their associated inter-connections.

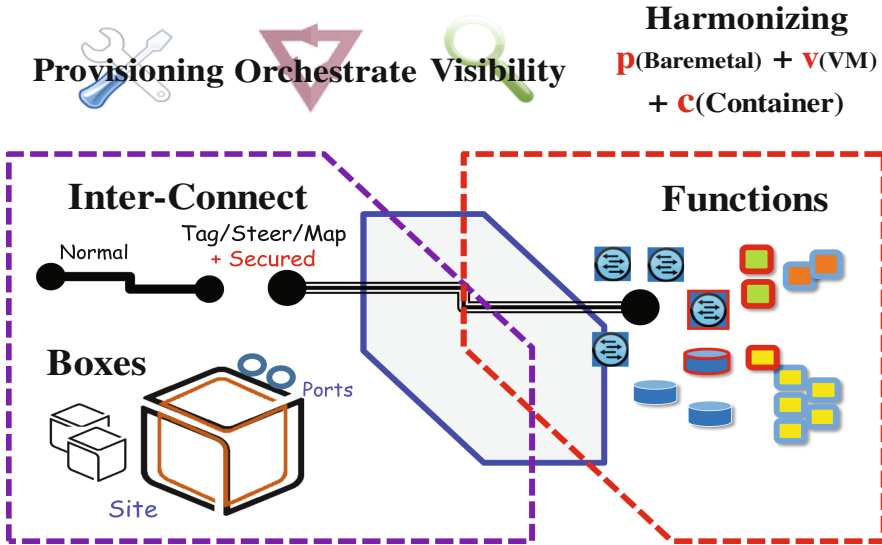


Fig. 4. Box/Inter-Connect/Functions abstraction for agile service realization.

### 3 SmartX Automation Software Framework

Based on the above service realization vision over futuristic SDI-ready ICT infrastructure, we attempt to develop the appropriate software-driven automation framework for upcoming user-defined services, especially, by fully utilizing DevOps-based automation on top of hyper-converged SmartX Boxes. Thus, as depicted in Fig. 5, the design and implementation for SmartX automation software framework is initiated and being continuously refined from 2014. As shown in Fig. 5, the latest version of SmartX automation software framework consists of 4 main building blocks for Provisioning, Visibility, Orchestration, and Intelligence, respectively. Also it is augmented by two vertical building blocks, such as Security & Federation and Visualization. In addition, the specified lifecycle aspects according to the targeted service domains are incorporated by considering the whole ecosystem, as shown in the upper portion of Fig. 5.

Finally, if we summarize the above user-defined service realization over converged-SDI-ready ICT infrastructure, it could be represented as shown in Fig. 6.

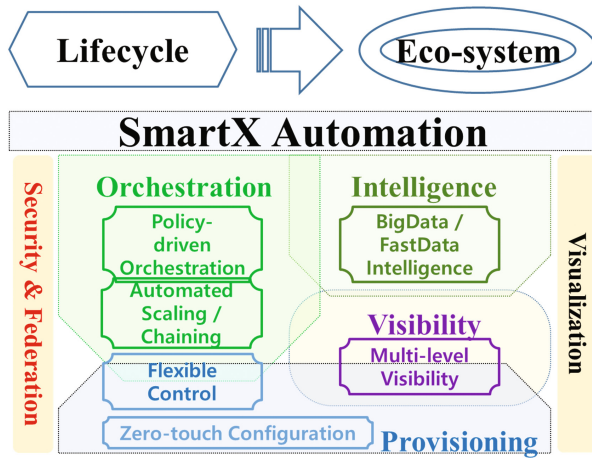


Fig. 5. SmartX automaton software framework.

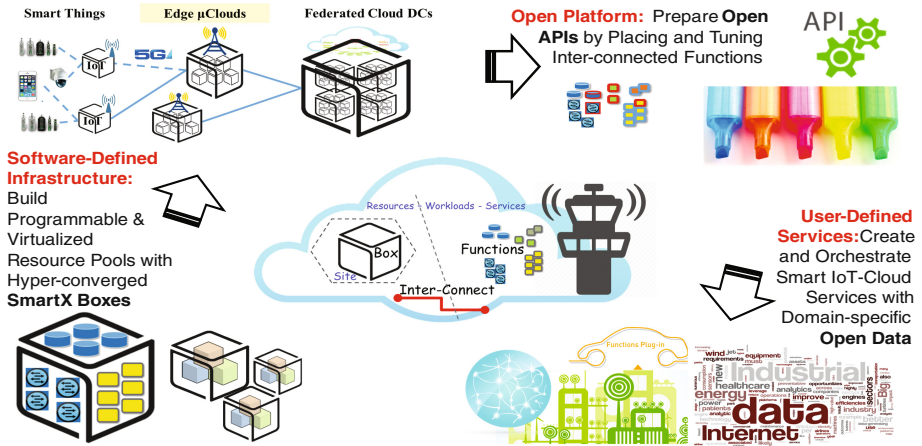


Fig. 6. Realizing diverse services over hyper-converged boxes with SmartX automation framework.

## 4 Conclusion

By leveraging diverse open-source software and hardware, SmartX automation software framework is introduced to streamline the API-based service realization over hyper-converged boxes.

**Acknowledgments.** This work was supported in part by Institute for Information & communications Technology Promotion (IITP) grant funded by the Korea government (MSIP) (No. B0190-15-2012, Global SDN/NFV Open-Source Software Core Module/Function Development) and in part by Institute for Information & communications Technology Promotion

(IITP) grant funded by the Korea government (MSIP) (No. R7117-16-0218, Development of Automated SaaS Compatibility Techniques over Hybrid/Multisite Clouds).

## References

1. Berman, M., Chase, J.S., Landweber, L., Nakao, A., Ott, M., Raychaudhuri, D., Ricci, R., Seskar, I.: GENI: a federated testbed for innovative network experiments. *Comput. Netw.* **61**, 5–23 (2014)
2. Kim, J.: Realizing futuristic service composition with programmable and virtualized pools of unified resources. In: *Proceedings of the International Conference on Future Internet Technologies (CFI 2013)*, Beijing, China, June 2013
3. Risdianto, A.C., Na, T., Kim, J.: Running lifecycle experiments over SDN-enabled OF@TEIN testbed. In: *Proceedings of the IEEE ICCE*, Danang, Vietnam, July 2014
4. Risdianto, A.C., Shin, J., Kim, J.: Building and operating distributed SDN-Cloud testbed with hyper-convergent SmartX Boxes. In: *Proceedings of the 6th EAI International Conference on Cloud Computing (CloudComp 2015)*, Daejeon, Korea, October 2015
5. Risdianto, A.C., Ling, T.C., Tsai, P.-W., Yang, C.-S., Kim, J.: Leveraging open-source software for federated multisite SDN-cloud playground. In: *Proceedings of the Open-Source Software Networking (OSSN) Workshop as part of 2016 IEEE NetSoft Conference and Workshops (NetSoft)*, Seoul, Korea, pp. 423–427, June 2016
6. Balalaie, A., Heydarnoori, A., Jamshidi, P.: Microservices architecture enables DevOps: migration to a cloud-native architecture. *IEEE Softw.* **33**(3), 42–52 (2016)
7. Evans, P.C., Annunziata, M.: *Industrial Internet: Pushing the boundaries of minds and machines*, General Electric White Paper, November 2012
8. Barroso, L.A., Hölzle, U.: *The Datacenter as a Computer: An Introduction to the Design of Warehouse-Scale Machines*. *Synthesis Lectures on Computer Architecture*, vol. 4.1, pp. 1–108 (2009)

**The 7th Semantic Web/Cloud  
Information and Services Discovery  
and Management (SWISM-2017)**



# A Target Driven Approach Supporting Data Diversified Generation in IoT Applications

Flora Amato<sup>1</sup>(✉), Beniamino Di Martino<sup>2</sup>, Fiammetta Marulli<sup>2</sup>,  
Antonino Mazzeo<sup>1</sup>, and Francesco Moscato<sup>3</sup>

<sup>1</sup> DIETI, Università degli Studi di Napoli Federico II,  
via Claudio, 21, 80125 Naples, Italy

{flora.amato,mazzeo}@unina.it

<sup>2</sup> DIII, Università della Campania “Luigi Vanvitelli”,  
via Roma, 29, 81031 Aversa, CE, Italy

{beniamino.dimartino,fiammetta.marulli}@unina.it

<sup>3</sup> DiSciPol, Università della Campania “Luigi Vanvitelli”,  
via Roma, 29, 81031 Aversa, CE, Italy

francesco.moscato@unicampania.it

**Abstract.** Smart IoT technologies have the potential to make a breakthrough in the support of Cultural Heritage (CH), by providing information and communication technology to effectively enhance current models of art recreation and enjoyment. To turn such potential into reality, IoT-based technological solutions for CH should be designed by taking into account two main factors: on the one hand, they must be able to involve and attract different types of users, on the other they must avoid focusing users’ attention solely on the smartness and novelty of the supporting technologies, thus diverting them from living the experience of being in a cultural site. To this aim, endowing IoT applications with anthropic interfaces seems a promising way to explore, and most prominent among such interfaces are those based on capabilities for Natural Language Understanding and Generation. A set of linguistic resources and Natural Language Generation (NLG) techniques are needed in order to reach this goal, which we describe and characterize here through the case study of a workflow that supports the automatic generation of artworks.

## 1 Introduction

Internet of Things (IoT) represents an effective mean to support understanding of Cultural Heritage (CH), by enhancing people’s awareness about its effective value. Smart cultural sites are a meaningful application of IoT into CH, aiming to involve visitors with more amazing and personalized experiences in living culture. “Talking” museums exploit a novel approach in the story telling of an art exhibition. More generally, cultural objects and sites (sculptures, drawings, buildings, etc.) are enabled to tell visitors about their stories, when supported by intelligent infrastructures. In this scenario, a not trivial and not yet deeply investigated issue concerns the selection and organization of knowledge delivered to users. IoT enables objects to communicate each other, but what they should be able to tell and how they could communicate with their human

interlocutors should not be taken for granted. Users, differencing by cultural and social background, by age and sensitivity, have to be approached in different ways, in order to reach an effective engagement with the context they are experimenting. A first effort in this direction could be the proposal of the same contents (artworks biographies) in different appearances. Natural Language provides a most direct way to transfer knowledge at different levels of conceptual density. The opportunity provided by the evolution of the technologies of Natural Language Processing is thus of making more fluid and universal the process of knowledge transfer. Indeed, unfolding domain knowledge is one way to bring to larger audience contents that would be otherwise restricted to specialists. This has been done so far in a manual way through the skills of divulgators and popular science writers. Technology provides now a way to make this transfer both less expensive and more widespread. Extracting knowledge and then generating from it suitably communicable text in natural language are the two related subtasks that need be fulfilled in order to attain the general goal. This paper provides a contribution to making substantial this combination through the exploitation of conceptual knowledge and of a workflow (Moscato 2004; 2014) that can produce strongly customized textual descriptions. A target-driven approach is proposed to automatically generate multiple texts from the same information core. An extended case study is described to demonstrate the effectiveness of the proposed model and approach in the Cultural Heritage application domain, to compare and position this contribution within the current state of the art and to outline future directions. The main contribution of this work is the proposal of a novel processing workflow for automatic generation of natural language textual resources, based on a multidimensional knowledge model. The multidimensionality feature of the proposed model can be explained as its capability of suggesting the exploration and the collection, in a single instantiation, of multiple knowledge dimensions, intervening into a text generation process that would be able to produce differenced and contextualized documents, thus resulting effectively useful for users' enjoyment. In other words, this multidimensional model supports natural language generation processes, by strongly focusing on diversified textual generations, derived from the same information sources, and by the exploitation of paraphrases generation techniques. It allows the adoption of a target-driven approach, taking into account features differencing target audiences (users and applications), thus supporting the processing interactions between schema instantiation and linguistic skills from the Discourse component and the relevant knowledge base from the Content components. The "target" term is used in this context to mean a target language, a target domain, target users and target applications enjoying and exploiting, respectively, textual representations.

## 2 Background and Related Works

Current Internet of Things (IoT) smart technologies set an effective milestone in supporting novel models for enjoying Art and Cultural Heritage (Amato 2013; 2014). The "speaking" artworks and smart museum (Marulli 2016) evidence recent successful applications. This type of applications implements very exciting and advanced solutions, provided with intelligent profiling systems for multimedia contents tailoring (Bordoni 2013; Ardissono 2011), but it turns into a too strongly device-driven

approach. Indeed, the experience of users visiting cultural sites or artworks exhibitions, is strongly mediated by the usage of personal smart devices or provided AVR displays (e.g., the Oculus Rift display). An increasing number of present researches focuses on studying the “appeal” and the appreciation level of such technologies against users’ emotions and involvement, when they are applied to CH domain. Some preliminary results from these studies (Benedusi 2015) highlighted a still not significant increase or improvement in the cultural attitudes and sensitivity of the users, after a “smart” visit experience. Smart cultural approaches should be able to engage users really, without jeopardizing their interest towards the cultural context or the support offered by smart Information Technologies (ITs).

Therefore, main limitations of available smart cultural service infrastructures consist exactly in the way they set the communication paradigm between visitors and cultural objects. Better-profiled interactions, exploiting the means of human-like natural interactions and natural language could help in overtaking these problems (Colace 2005; 2013). In (Vallifuoco 2016) a human-like driven approach, based on Natural Language interactions and holographic projections is exploited to experiment new models for art recreations.

After all, the easiest way for a user to acquire information and to express his/her needs and preferences regarding a desired service or condition, is to use natural language.

In order to offer more engaging experiences, a not trivial issue concerns the selection and organization of an appropriate knowledge to transfer to users. They, differing by cultural and social background, by age and sensitivity, have to be approached in different ways, if the goal is an effective engagement with the context they are experimenting. In (Marulli 2015) an authoring platform for automatic generation of tailored textual artworks descriptions is proposed, basing on users’ profiling information (e.g., art biographies in the shape of little fables for schoolchildren).

A survey on recent Natural Language Generation (NLG) Systems is provided in (Ramos 2016); authors give a general perspective on current systems and open issues related to this research area. A more specific system, designed to support CH domain is Natural OWL, presented in (Galanis 2008; Androutsopoulos 2013). In this last contribution, a NLG engine is implemented to build structured textual artworks descriptions, basing on cultural objects ontologies as lexical vocabulary and documents plan to establish the phrasing structures. Natural OWL is able to generate automatically simpler or more complex textual descriptions in two different languages, English or Greek. System feeds with a lexical ontology (Di Martino 2010), a micro-plan for text structure and users’ profile information. Entities vocabularies are fixed for all type of users and the profiling information are used to modify some text features, as length. So, the general appearance of the textual description keeps quite unchanged but such a system represents an important and really working example of authoring system in the CH domain. Paraphrasing adoption can enhance NLG processes, by proving diversified but equivalent forms for the same concepts.

Paraphrasing generation techniques are deeply investigated in (Androutsopoulos 2010); here, the authors provide a very complete survey on available strategies of automatic paraphrasing and textual entailment generation strategies. Finally, from studying and experimenting solutions currently provided by the recent literature and the related scientific community, very few are natural language generation (NLG) systems

available and effectively able to generate something more appreciable than an ontology verbalization. Such type of systems is strongly dependent on the target generation language and most of them support only English Language or are customized for very specific aims.

Furthermore, no NLG systems dealing with Italian language are currently available, too; but, going beyond the obvious specificity of target language, most of systems aren't able to provide a sufficient level of flexibility and customization to support an effective differenced textual generation. Some types of customizations are allowed (e.g., the selection of facts to be included or not, the order in which facts will be presented, the sentence form (active or passive)) according the selection of a target type of users, but generally the produced textual descriptions, describing the same topic, result very little differenced but in their length (shorter or longer) and in the order in which information are presented. No mechanisms to support a diversified vocabulary and lexicon adoption according to the target user are provided, as well as strong paraphrasing strategies exploitation, in order to clarify and enrich facts explanation with more details, are not employed.

### 3 The Proposed Approach

This section presents a workflow for an automatic generation of diversified textual resources, also underlying the authoring platform FEDRO (Marulli 2015), exploited as an application system to test the proposed approach.

The basic core of this NLG workflow is a multidimensional model for the representation of conceptual knowledge, providing the opportunity to take into account more knowledge aspects in a single instance. The research questions, which the proposed model of knowledge tried to answer, are the following ones:

1. *Which strategies and which dimensions of knowledge are effectively involved to overtake limitations in producing differenced textual descriptions from the same data core?*
2. *What we need to coordinate these multiple interacting dimensions to support a successful natural language generation process?*

Most of efforts were addressed to identify how to make feasible a tangible and sensible improvement in an NLG process.

As in the most common NLG systems, the proposed workflow is made of three main steps, as Fig. 1 shows. Furthermore, a typical content source is represented by domain ontologies, usually fulfilled by domain experts.

The first step of such an NLG process is the *Content Selection*, in which relevant facts that will be included in the final story have to be explicitly selected. The second step is called *Document Planning*, in which selected facts from the ontology are "verbalized" in the form of Natural Language sentences and their appearance order is established. Numbers and gender cases concordances are also established in this step. Finally, the *Surface Realization* step is typically involved with an improvement process of the textual expressing forms for sentences provided by the previous stage, thus dealing with a more fluent and coherent organization of these sentences in a final

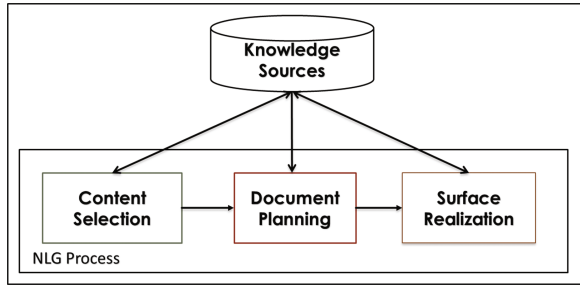


Fig. 1. Typical NLG process

whole composition, presented in a correct and human readable form. Figure 2 shows a domain ontology snippet, representing a typical organization of knowledge supporting NLG processes as facts sources.

Typically, as it happens also in Natural OWL, one of the most relevant contribution among the NLG systems dealing with Cultural Heritage domain, users' profiling for text generation is taken into account in the Content Selection and Document Planning steps.

In particular, by selecting a target user's type, main text customizations consist in selecting which facts have to be included for each kind of users, in which order these facts should appear in the narration and the selection of the referring expressions, as part of the ontology facts verbalization. It is possible to select a set of provided expressing forms, which are semantically equivalent.

A passive or an active form, as an example, can be selected to express to same fact in a different shape. This opportunity is offered by lexical and grammar resources, providing some paraphrasing possibilities, for the same concept. A typical set of paraphrasing expressions we can exploit is the following one:

- (1) *X painted Y.*
- (2) *Y was painted by X.*
- (3) *X is most known for his painting Y.*
- (4) *Y is a painting created by X.*
- (5) *Y is a masterpiece by X.*

This type of customizations mainly influences the length of the final composition, as the total amount of information transmitted to users and introduce a light form of diversification for automatic text generation from the same core knowledge. After populating domain ontology with information about artworks of interest, the NLG process can be started. An example of a textual generations that can be obtained by adopting native Natural OWL lexicon and grammars resources, for English Language, is shown in Table 1.

Column 1 shows a longer version for a textual description, typically generated for a not specific kind of users, a tourist, for example. Column 2, on the other side, shows a shorter description, with a little variation for the presented facts This second version is simpler and probably more suitable for schoolchildren and for not very expert audiences in art matter. Automatically generated textual descriptions appears quite simple

```

▼<rdf:RDF xmlns:rdf="http://www.w3.org/1999/02/22-rdf-syntax-ns#"
  ontologies.com/Ontology1386155618.owl">
  <owl:Ontology rdf:about=""/>
  ▶<owl:Class rdf:ID="Room">...</owl:Class>
  ▶<owl:Class rdf:ID="ConservationStatus">...</owl:Class>
  ▼<owl:Class rdf:ID="Sculptor">
    ▼<rdfs:subClassOf>
      <owl:Class rdf:ID="Artist"/>
    </rdfs:subClassOf>
  </owl:Class>
  ▼<owl:Class rdf:about="#Artist">
    ▼<rdfs:subClassOf>
      <owl:Class rdf:ID="Person"/>
    </rdfs:subClassOf>
  </owl:Class>
  ▶<owl:Class rdf:ID="Restorer">...</owl:Class>
  ▶<owl:Class rdf:ID="RestorationType">...</owl:Class>
  ▼<owl:Class rdf:about="#Person">
    <rdfs:subClassOf rdf:resource="#ENTITY"/>
  </owl:Class>
  ▶<owl:Class rdf:ID="Signature">...</owl:Class>
  ▶<owl:Class rdf:ID="Exhibit">...</owl:Class>
  ▶<owl:Class rdf:ID="CreationDate">...</owl:Class>
  ▶<owl:Class rdf:ID="Length">...</owl:Class>
  ▶<owl:Class rdf:ID="Born_country">...</owl:Class>
  ▶<owl:Class rdf:ID="Statue">...</owl:Class>
  ▶<owl:Class rdf:about="#Dimension">...</owl:Class>
  ▶<owl:Class rdf:ID="Depth">...</owl:Class>
  ▶<owl:Class rdf:ID="Origin">...</owl:Class>
  ▶<owl:Class rdf:ID="City">...</owl:Class>
  ▶<owl:Class rdf:ID="RestorationDate">...</owl:Class>
  ▶<owl:Class rdf:ID="OriginStory">...</owl:Class>
  ▶<owl:Class rdf:about="#Location">...</owl:Class>
  ▼<owl:Class rdf:ID="Death_year">
    ▼<rdfs:subClassOf>
      <owl:Class rdf:about="#Artist_inf"/>
    </rdfs:subClassOf>
  </owl:Class>
  ▼<owl:Class rdf:ID="Ambient">
    <rdfs:subClassOf rdf:resource="#Location"/>
  </owl:Class>
  ▼<owl:Class rdf:ID="Head">
    <rdfs:subClassOf rdf:resource="#Exhibit"/>
  </owl:Class>
  ▶<owl:Class rdf:ID="Death_country">...</owl:Class>
  ▶<owl:Class rdf:ID="Material">...</owl:Class>
  ▶<owl:Class rdf:ID="Technique">...</owl:Class>
  ▶<owl:Class rdf:ID="LocationSignature">...</owl:Class>
  ▶<owl:Class rdf:about="#Restoration">...</owl:Class>
  ▶<owl:Class rdf:ID="Museum">...</owl:Class>
  ▶<owl:Class rdf:ID="Customer">...</owl:Class>
  ▼<owl:Class rdf:ID="Born_year">
    ▼<rdfs:subClassOf>

```

**Fig. 2.** A domain ontology snippet

and fluent, but their general structure is substantially unchanged. By considering textual generations for a different kind of users, we can observe a diversification in length and in the number of facts included, but the presentation form for the whole composition is quite unchanged. In such a way, it is quite easy to obtain a big amount of textual descriptions for multiple artworks but not substantial diversifications are allowed in the output. Linguist resources available in the NLG process mainly influence the quality and the diversification level of the produced textual documents. Therefore, a first step toward an improvement of such kind of process is represented by the integration (Amato 2010) in the NLG process of more linguistic resources in order to enrich the generated descriptions. But more powerful linguistic resources (lexical and grammars) need not only to be added but they need to be annotated, in order to make feasible an effective target driven approach.

**Table 1.** Automatic generated text samples

Text example 1: Long version	Text example 2: Short version
<p>The Pietà is a sculpture in Carrara marble, realized in the Renaissance period by Michelangelo Buonarroti. He was born in Caprese in 1475 and he died in Rome in 1564. This work is housed in St. Peter's Basilica, Vatican City. The statue was commissioned for the French Cardinal Jean de Bilhères, who was a representative in Rome. The sculpture was made for the cardinal's funeral monument, but was moved to its current location, the first chapel on the right as one enters the basilica, in the 18th century. It is the only piece Michelangelo ever signed. This famous work of art depicts the body of Jesus on the lap of his mother Mary after the Crucifixion. Michelangelo's interpretation of the Pietà is unprecedented in Italian sculpture. It is an important work as it balances the Renaissance ideals of classical beauty with naturalism</p>	<p>The Pietà is a sculpture in Carrara marble, realized by Michelangelo Buonarroti. He was born in Caprese in 1475 and he died in Rome in 1564. This work is housed in St. Peter's Basilica, Vatican City. This sculpture is the only piece Michelangelo ever signed. This famous work of art depicts the body of Jesus on the lap of his mother Mary after the Crucifixion Mary, also called the Madonna in Catholic faith, is represented as a very beautiful and young mother. Pietà represents one of the Michelangelo's masterpieces and it is a sculpture famous for its beauty and naturalness</p>

## 4 Conclusion and Future Directions

Knowledge represents the basic core of our Cultural Heritage and Natural Language provides us with prime versatile means of construing experience at multiple levels of organization, storing and exchanging knowledge and information encoded as linguistic meaning. The linguistic verbalization of segmented data is a young field still in its early stages, which has a solid formal base and whose real potential is still waiting to be uncovered. To face with these issues, this work shows the research activity conducted with the aim of exploring and scientifically describing knowledge structure and organization involved in textual resources generation. Thus, a novel and feasible processing workflow, producing strongly customized textual descriptions is proposed. By exploiting paraphrases generation techniques and target users', applications and domains characterizations, a target-driven approach is proposed to generate automatically multiple instances for a textual description, sharing the same information core but differencing in the lexical and expressive form. A case study, in the Cultural Heritage domain, is described to demonstrate the effectiveness and the feasibility of the proposed model and approach, thus providing the means for comparing and positioning this contribution with current state and future directions. The final aim is to automatically generate customized artworks descriptions for different type of users and different type of target applications, feeding smart IoT cultural applications. In this perspective, from current literature, no other contributions are strongly focused on this issue or implement similar approaches for the same aim. A further novelty aspect is the choice to generate

simplified descriptions in the shape of fables, in order to make culture and art environment more charming for children audiences.

As future work, there is the possibility of exploiting different top level text analysis and semantic based strategies and interactive users' experiences and evaluations, to improve the quality of generated textual descriptions. Finally, a related open issue, object of future investigations, is the absence of a standard human or automatic evaluation metrics to establish a text quality baseline. The results of a pilot generation study showed this model is feasible and the results immediately useful.

## References

- Androutsopoulos, I., Malakasiotis, P.: A survey of paraphrasing and textual entailment methods. *J. Artif. Intell. Res.* **38**, 135–187 (2010)
- Androutsopoulos, I., Lampouras, G., Galanis, D.: Generating natural language descriptions from OWL ontologies: the natural OWL system. *J. Artif. Intell. Res.* **48**, 671–715 (2013)
- Ardissono, L., Kufflik, T., Petrelli, D.: Personalization in cultural heritage: the road travelled and the one ahead. *User Model. User-Adap. Inter.* **22**(1), 73–99 (2012). *The Journal of Personalization Research*
- Benedusi, P., Marulli, F., Racioppi, A., Ungaro, L.: What's the matter with cultural heritage tweets? An ontology-based approach for CH sensitivity estimation in social network activities. In: *Proceedings of 2015 IEEE SITIS 2015*. IEEE (2015)
- Bordonì, L., Ardissono, L., Barceló, J.A., Chella, A., de Gemmis, M., Gena, C., Iaquinta, L., Lops, P., Mele, F., Musto, C., Narducci, F., Semeraro, G., Sorgente, A.: The contribution of AI to enhance understanding of Cultural Heritage. *Intelligenza Artificiale* **7**(2), 101–112 (2013)
- Galanis, D., Karakatsiotis, G., Androutsopoulos, I.: How to install Natural OWL (2008). <http://www.ling.helsinki.fi/kit/2008s/clt310gen/docs/NaturalOWL-README.pdf>
- Getty Vocabularies (2016). <http://www.gettyvocabularies.edu>
- Colace, F., De Santo, M., Greco, L.: A probabilistic approach to tweets' sentiment classification. In: *Proceedings of 2013 Humaine Association Conference on Affective Computing and Intelligent Interaction, ACII 2013*, pp. 37–42 (2013). Art. no. 6681404
- Colace, F., Foggia, P., Percannella, G.: A probabilistic framework for TV-news stories detection and classification. In: *2005 IEEE International Conference on Multimedia and Expo, ICME 2005*, pp. 1350–1353 (2005). Art. no. 1521680
- Amato, F., Casola, V., Gaglione, A., Mazzeo, A.: A common data model for sensor network integration. In: *CISIS 2010 - The 4th International Conference on Complex, Intelligent and Software Intensive Systems*, pp. 1081–1086 (2010). Art. no. 5447269
- Marulli, F., Pareschi, R., Baldacci, D.: The internet of speaking things and its applications to Cultural Heritage. In: *Proceedings of IoTBD2016 Conference, SCITEPRESS 2016* (2016)
- Moscato, F.: Model driven engineering and verification of composite cloud services in MetaMORP(h)OSY. In: *Proceedings of 2014 International Conference on Intelligent Networking and Collaborative Systems, IEEE INCoS 2014*, pp. 635–640 (2014). Art. no. 7057162
- Di Martino, B., Moscato, F.: An ontology based methodology for automated algorithms recognition in source code. In: *CISIS 2010 the 4th International Conference on Complex, Intelligent and Software Intensive Systems*, pp. 1111–1116 (2010). Art. no. 5447280



- Moscato, F., Mazzocca, N., Vittorini, V.: Workflow principles applied to multi-solution analysis of dependable distributed systems. In: Proceedings of the Euromicro Conference on Parallel, Distributed and Network-based Proceeding, pp. 134–141 (2004)
- Marulli, F.: IoT to enhance understanding of cultural heritage: fedro authoring platform, artworks telling their fables. In: EAI FABULOUS 2015, pp. 270–276. Springer (2015)
- Ramos-Soto, A., Bugarin, A., Barro, S.: On the role of linguistic descriptions of data in the building of natural language generation systems. *Fuzzy Sets Syst.* **285**, 31–51 (2016). ISSN 0165-0114
- Szpektor, I., Tanev, H., Dagan, I., Coppola, B.: Scaling web-based acquisition of entailment relations. In: Proceedings of the Conference on EMNLP, Barcelona, Spain (2004)
- Amato, F., Barbareschi, M., Casola, V., Mazzeo, A.: An FPGA-based smart classifier for decision support systems. *Stud. Comput. Intell.* **511**, 289–299 (2014)
- Amato, F., Barbareschi, M., Casola, V., Mazzeo, A., Romano, S.: Towards automatic generation of hardware classifiers. In: Lecture Notes in Computer Science (including subseries Lecture Notes in Artificial Intelligence and Lecture Notes in Bioinformatics). LNCS (PART 2), vol. 8286, pp. 125–132 (2013). doi:[10.1007/978-3-319-03889-6\\_14](https://doi.org/10.1007/978-3-319-03889-6_14)
- Aversa, R., Avvenuti, M., Cuomo, A., Di Martino, B., Di Modica, G., Distefano, S., Puliafito, A., Rak, M., Tomarchio, O., Vecchio, A., Venticinque, S., Villano, U.: The cloud@Home project: towards a new enhanced computing paradigm. In: Lecture Notes in Computer Science (including subseries Lecture Notes in Artificial Intelligence and Lecture Notes in Bioinformatics). LNCS, vol. 6586, pp. 555–562 (2011)
- Vallifuoco, L., Marulli, F.: The imitation game to cultural heritage: a human-like interaction driven approach for supporting art recreation. In: Proceedings of 5th EAI International Conference: ArtsIT, Interactivity and Game Creation (ArtsIT2016). Springer (2016)

# Smart Communities of Intelligent Software Agents for Collaborating and Semantically Interoperable Micro-Grids

Rocco Aversa<sup>1</sup>, Beniamino Di Martino<sup>1</sup>, Geir Horn<sup>2</sup>, Svein Hallsteinsen<sup>3</sup>,  
Salvatore Venticinque<sup>1</sup>(✉), and Shanshan Jiang<sup>3</sup>

<sup>1</sup> University of Campania “Luigi Vanvitelli”, via Roma 29, 81031 Aversa, Italy  
`salvatore.venticinque@unicampania.it`

<sup>2</sup> University of Oslo, P.O. Box 1080 Blindern, Oslo, Norway

<sup>3</sup> SINTEF, P.O. Box 4760 Sluppen, Trondheim, Norway

**Abstract.** CoSSMic was an European project that developed a multi-agent solution for smart management of energy from shared photovoltaic panels by photovoltaic panels. Software agents implements collaborating consumer and producer devices negotiating energy over a peer-to-peer (P2P) overlay. The emergent behavior of the multi-agent system was an optimal schedule of energy consumption. This paper summarize main results of the project including techniques, open source technologies and data.

**Keywords:** Multi-agent systems · Smart grid · Smart energy

## 1 Introduction

The world is facing a climate crisis forcing us all to move away from fossil fuel to renewable energies. However, integrating a large fraction of locally produced and difficult to control renewable energy into the public electric energy grid is challenging [7]. There are many ways renewable energy can be generated, and the economical feasibility depends on local conditions. Wind and waves are often abundant in coastal regions, and most of the world’s population lives in areas where insolation is abundant. However, a major obstacle to the profitability of photovoltaic (PV) systems is the misalignment of mid-day peak production and evening and night time energy consumption since this misalignment is normally mitigated by expensive batteries.

The CoSSMic project has investigated how “energy smart neighbourhoods” could contribute to alleviating this problem. An energy smart neighbourhood means a neighbourhood where the buildings coordinate to maximize the self-consumption of the locally produced electrical energy and reduce consumption and feed-in peaks towards the public grid. The project has developed a prototype Cyber-Physical System of coordinated smart micro-grids where human users and intelligent devices collaborate to realize energy smart neighbourhoods, and a

simulation facility where the system can be executed in a simulated environment to study the effects of such collaborative behaviour [11]. The core idea is to increase the consumption of green energy produced by photovoltaic panels by demand side management of electrical loads that can be shifted in time. The objective is to start the loads at times where they can run only on solar energy given the weather forecast predicted energy production. The monitoring and data collecting part of the system has been installed in a number of buildings for more than a year collecting detailed data about energy consumption and production, and this data has been used to simulate the effect of the coordinated scheduling of flexible appliances. The software platform has been implemented using open source technologies, and is available as open source. Different deployment models have been investigated, to exploit the flexibility of Cloud [2], while at the same time taking into account security issues.

## 2 Architecture

The CoSSMic architecture adopts a highly distributed agent based P2P approach where each consuming and producing device in the neighborhood is represented by an agent. Batteries are represented by a coupled pair of agents, one responsible for the charging and one responsible for the discharging. The agents of a neighborhood negotiate to adapt the consumption to the predicted production shifting loads in time within constraints set by the inhabitants. This architecture has several advantages. It allows for easy creation and evolution of energy smart neighborhoods not requiring central organizational or computing support. It reports device failures. It implements a scalable solution by partitioning the optimization problem scaling exponentially in the number of devices. It avoids privacy concern confining private data inside each household. A household is considered as a microgrid and can be a building, a group of buildings or a part of a building. The household has a home gateway, which executes the intelligence based on distributed computing and is also responsible for communication both with devices within the household and with other neighbours. Interconnected gateways represent collaborating microgrids that form neighborhoods. Each microgrid is an autonomous subsystem until it joins a neighborhood. The agents in a neighborhood make up a multi-agent system (MAS) and they communicate with each other directly, *e.g.*, a consumer agent can negotiate with any producer agent in the whole neighborhood. The MAS forms a P2P overlay to support communication and negotiation among agents as well as neighborhood management. The overall architecture for a microgrid is depicted in Fig. 1. The *Graphical user interface* allows users to (re-)plan tasks, configure the system, set policies, preferences and constraints, monitor the energy usage of the household and status of the neighborhood, and see how the household contributes to and the benefits from participating in the neighborhood. The *Prediction* component computes forecasts for the PV production and the prices for electric power exchange with the public grid, based on third party services and knowledge about the house and its PV installations. The *Task manager* serves as the master agent

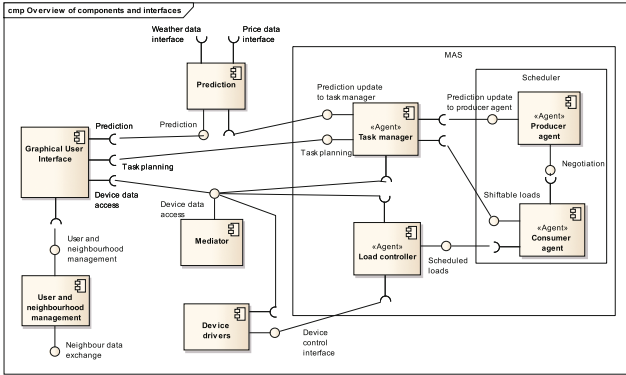


Fig. 1. Overview of components and interfaces

of the multi-agent system negotiating the load scheduling. It creates producer and consumer agents to represent the producer and consumer devices of the household, and manages a list of planned tasks for the household. The *Scheduler* implements distributed load scheduling and is responsible for negotiating load scheduling in the whole neighborhood. It consists of Consumer and Producer agents. The *Consumer agents* negotiate power delivery agreements with the *Producer agents* of the whole neighborhood and scheduling of the loads with the other households, and returns assigned start times for the loads. The *Load controller* executes the loads according to their schedule. The *Mediator* provides device management and data storage services. The *Device drivers* are responsible for the low-level integration and communication with the various devices connected to the system. The *User and neighborhood management* component is in charge of keeping track of the users of the system and their roles and privileges, and the other households that are members of the neighborhood. A more complete description of the architecture is provided in [11].

### 3 Results and Achievements

#### 3.1 Platform

The CoSSMic technological platform has been conceived to run both on general purpose computers and on embedded systems like Raspberry. At lower level a number of device drivers have been developed using different technologies. JAVA and Python programs, but also bash scripts have been implemented to interface the heterogeneous devices installed at the trial sites. Examples of devices are smart meters, smart plugs or inverter of photovoltaic plants. Consuming devices like air conditioners, freezers, fridges, or washing machines installed in the household did not provide open interface and they have always been connected via smart plugs. Drivers implement different communication protocols and connect by heterogeneous interfaces. The CoSSMic mediator is based on

Emoncms<sup>1</sup>, a powerful open-source web-app for processing, logging and visualising energy, temperature and other environmental data, developed in PHP. The original software has been extended by integrating new functionalities to the core modules, and developing new modules. In particular the new modules implement the CoSSMic graphical user interface; the installation and management of smart devices; virtual devices, learning capabilities, and the API for load management and communication with the multi-agent system. These new modules complement the API of Emoncms with the CoSSMic API.

The multi-agent system of the CoSSMic platform has been developed using two different technologies, Python and C++. All agents communicate by the XMPP protocol. A light XMPP server runs in each CoSSMic platform providing the needed communication services and to allowing for the execution of a single instance of the platform. In this condition the schedule includes just the local devices and the energy exchange is optimized between local consumer and the household's PV plant, if it exists. Two instances of the CoSSMic platform communicate via XMPP server-to-server connections. The SPADE2<sup>2</sup> Python library provides to the developers a set of API to develop agents based applications and a light XMPP server itself. One of the python agents is responsible to interface with the mediator. It uses the CoSSMic API and accepts REST-full HTTP requests to receive from the mediator requests, which are forwarded to other agents. Consumer and producer agents are instead different threads of one process. They have been developed in C++ as a Theron<sup>3</sup> application. They implement the one-to-one energy negotiation described in Sect. 3.4 that produces, as emergent behaviour of the whole neighborhood, the optimal schedule of consumptions. The platform has been published open source at<sup>4</sup> as a set of public repositories, each one documented by its own wiki.

### 3.2 Semantic Interoperability

The CoSSMic platform will include a semantic layer that will provide abstract description of the functionalities offered and the data exchanged by IoT enabled devices, appliances and sensors with the CoSSMic software components by means of a semantic model realized through ontologies.

Actually IoT enabled devices, appliances and sensors have interfaces that often are proprietary and not standardised. To allow such devices to be seamlessly integrated within the CoSSMic infrastructure, it is necessary to translate their Application Programming Interfaces (APIs) into a homogeneous and interoperable form. This translation has to be specific to the protocol used by every device (and appliance and sensors), and in principle it needs one translator for each device interfaced. Such translators will typically in the future be provided by the device manufacturers, or third parties can develop and sell them

---

<sup>1</sup> <http://www.emoncms.org>.

<sup>2</sup> <https://github.com/javipalanca/spade>.

<sup>3</sup> <http://www.theron-library.com>.

<sup>4</sup> [http://bitbucket.org/cossmic\\_release](http://bitbucket.org/cossmic_release)

to system integrators developing applications accessing such devices. CoSSMic is bootstrapping this ecosystem by developing such translators for the devices needed for the end-user demonstrations within the project. The main innovation in this activity is the definition of a semantic representation based on the available ontologies for the Smart Energy domain. Despite the multitude of available ontologies, the integration of these for heterogeneous sources of information and various domains is non-trivial. We are surveying available ontologies, and will select, evaluate and combine the most promising of these for the purpose of application integration. Furthermore we are integrating the existing ontologies by complementing them with additional information able to represent the APIs of the involved devices, appliances and sensors, in an agnostic way with respect to the vendor specific protocols and interfaces. Such integrated ontology will be the reference model to enable the definition of agnostic (non-vendor specific) APIs, and (hopefully automated) production of adapters and wrappers allowing a seamless integration and interoperability with the software layer of the CoSSMic platform, and exposing services to external platforms.

### 3.3 Learning Capability

Learning capabilities allows the CoSSMic platform to model and predict the energy profiles of the user's consuming appliances. In particular different device categories have been designed, and for each of them a learning model has been defined. We defined as single-run devices those, those devices which have not a periodic behavior and are not usually interrupted, like washing machines and dish-washers. Continuously-run devices have instead periodic behaviors. In this case the internal controller periodically switches on the device according to other parameters like the temperature in case of freezers and heat-pumps. Finally electric vehicles are considered as energy storages, which can be charged until they are full or the charge reaches a target level at a different power rate that is between a minimum value and a maximum one. The learning process is implemented as an automata that follows the status of the appliances. The automata input is the power consumed by the device. The transaction from a status to another one is triggered comparing the power value and a threshold that identifies the noise. The automata detects the starting and the stopping time and the stop of the device, or can be moved to a waiting status if the run must be delayed. Others parameters, like the necessary time under the threshold to detect the switch off, are used to configure the learning process. For single-run devices the life-cycle of the learning automata updated the consumption profile at the end of any run. Collected energy samples during the last runs are used. The learned profile is represented as a B-spine, that approximates the interleaved samples by a set of polynomial curves which minimize the mean square error, described in [9]. In the case of continuously run device the lack of open interface to monitor temperature and other parameters, and the unfeasible interaction of the internal controller, motivated the design of a different learning technique. In particular the next working cycle is predicted to be equal to the previous one. With this assumption the switch on of the device can be delayed after the next

predicted start time according to the scheduler indication. A maximum delay is allowed and also the daily cumulative delay cannot exceed a fixed threshold. The tuning of these parameters is another issue that has been investigated by experience, analyzing the collected measures. Devices are controlled by switching off and on the same smart-plug that provides energy information. These original learning models and their open source implementation, both as component of the CoSSMic platform and as tools for off-line analysis of collected data are results of the project. Such tools allow for analyzing time-series, for identifying automatically runs and for their supervised clustering to distinguish automatically programs and to filter erroneous detections.

### 3.4 Optimization Model

The core of the system is a distributed multi-agent system [3,4] where software agents collaborate to produce as emergent behaviour the optimal schedule of executions of users' appliances in accordance with constraints defined by the users [1]. One to one negotiations are used as a solution for the distributed optimization of device schedule [6,13]. For this reason it can be defined as a virtual market for energy negotiation and brokering [5]. The CoSSMic approach consists of two steps described in the following sections.

When a load is submitted, a consumer agent is created in the system, and it will select a producer to provide the energy needed by the load. If this producer has sufficient energy according to its prediction to start the load between the load's earliest start time and its latest start time, it will assign a start time to the load. If not, it will refuse the allocation, and the consumer agent will select another producer. It could happen that this new load will make a more optimal consumption of a producer's predicted energy production than its current set of load assignments. In this case the producer could cancel any of the previously assigned loads. Each of these rejected consumer agents will then have to select other producers to serve their needs. The selection process repeats until every load has assigned a start time from a producer. As the consumer agents act autonomously, this is a game where each play corresponds to a consumer selecting a producer, and the epoch of the game is the number of plays needed to have a new solution when the system is perturbed by either a new prediction or the arrival of a new load to the system. A particular set of assignments, *i.e.* bindings of loads to producers, is called a *configuration* of the game. The game will always converge to a configuration provided that the grid accepts to start any load within its allowed start time interval given by the load's earliest start time and its latest start time. This condition must be met even if one uses a grid model that is artificially limited in order to avoid peaks, meaning that peak avoidance cannot be guaranteed if there is no feasible schedule for the loads that have selected the grid as their producer under the maximum grid peak limit. Furthermore, the game is cooperative [10], because all the involved consumers and producers jointly tries to minimise the grid energy consumed by the neighbourhood.

A consumer's selection of a producer is carried out using a *variable structure stochastic automaton* (VSSA) [12]: A consumer has a probability vector  $\mathbf{p} = [p_1, \dots, p_n]^T$  with one probability for each producer, the grid inclusive. This vector represents a probability distribution with  $\sum_i p_i = 1$ . For each play, the consumer agent selects a candidate producer according to this empirical probability distribution, and this Producer Agent either accepts to provide energy to the consumer, or rejects it. Should the system be loaded, and all PV producers refuse the consumer, the grid is the only candidate producer and will be selected with probability one.

Classical scheduling originated in manufacturing disciplines and considers the problem of *assigning* a set of  $n$  jobs onto  $m$  machines. Each job  $j$  is assumed to have a known processing time on machine  $i$ . It should be noted that classical scheduling only implicitly considers the resources provided by the machine, *i.e.* the capacity of the machine is reflected in the time it takes to complete the job on that machine. The situation considered here is different in that the "machine" is a PV system that provides time variant resources, and the scheduling problem is to start the time variant "jobs" that are the assigned loads according to the resource availability on the "machine". The load profiles are *continuous* and once a load has started it will have to run to completion, *i.e.* the problem is a non-preemptive single-machine scheduling problem. In contrast to classical scheduling problems, the PV Producer Agent may start two or more loads with overlapping execution periods if the predicted production profile allow this. In contrast to the combinatorial assignment problem, a *relaxed* form of the problem is considered here where it is possible to acquire additional resources for PV Producer Agent to supply the loads with energy since it can supplement with energy from the grid. This will guarantee that the problem has a solution, and transform the problem to non-linear programme to find the schedule that minimises the cost of the additional resources, *i.e.* the grid energy [8]. Each PV Producer Agent solves independently an optimisation problem to find the schedule for the loads assigned to it given its predicted energy production, and the distributed optimisation allows better scaling in the number of consumer tasks than a centralised optimisation problem.

### 3.5 Trials and Data

The CoSSMic platform has been deployed at two different trials sites, in province of Caserta (Italy) and in City of Konstanz (Germany). In all installations the CoSSMic platform executed on Raspberry P2 or on Raspberry P3, using respectively the Linux distribution Raspbian Wheezy or Jessie. Delays and bureaucratic constraints limited the installation in province of Caserta to one private building, three public schools and a public swimming pool. Also the kind and the number of monitored devices were limited. A smart meter and a smart plug was installed in the private house and two or three smart-meters were installed in each public building to measure consumptions. such devices communicate via zigbee to a wifi gateway that allows for reading data of each meter using a Modbus protocol over TCP. The energy production by photo-voltaic plants



was measured by using the web interface of the inverters, which were equipped with a network interface. The CoSSMic installations in Konstanz were under the responsibility of (ISC) (*International Solar Energy Research Center Konstanz*). Trials are more heterogeneous and include a larger number of devices and buildings. Trials include 4 industries, 2 schools and 6 private houses, In Table 1 a summary of trials information is provided. We collected data for more than one year in Konstanz and for a much more limited period in province of Caserta. The first column shows the trial identifications (IDs), while the second column contains the number of monitored devices. Then we have the starting date and the last date of the observation period. Finally we have the sum of monitored days and hours for each trial. They are not equal to the duration of the observation period multiplied for the number of devices because of downtime, voluntary disconnection of power grid in the school during nights and in weekends, because some devices have been installed later or because other kind of system failures or maintenance.

**Table 1.** Summary of trials results

Trial-id	Devices	From	To	#days	#hours
ce01	2	October 20, 2016	January 11, 2017	1	18
ce02	4	October 17, 2016	January 27, 2017	738	17
ce03	3	October 26, 2016	January 11, 2017	145	13
ce04	2	October 19, 2016	January 11, 2017	96	6
kn01	3	October 13, 2015	February 8, 2017	1012	14
kn03	6	October 29, 2015	February 9, 2017	1707	14
kn04	20	October 13, 2015	February 8, 2017	8802	14
kn05	1	October 3, 2015	October 17, 2016	368	13
kn06	1	October 21, 2016	January 17, 2017	43	6
kn07	6	April 22, 2015	February 8, 2017	3332	11
kn08	5	April 1, 2015	February 8, 2017	2079	8
kn09	8	December 11, 2014	February 8, 2017	3959	13
kn10	9	October 3, 2015	February 8, 2017	4277	14
kn11	4	October 26, 2015	February 8, 2017	1768	12
kn012	7	October 24, 2015	February 8, 2017	2350	10

### 3.6 Simulation and Emulation Tools

The deployment of CoSSMic software on real trials for testing and evaluation purpose introduces a number of drawbacks. On one hand the support of the user to run the devices or to reproduce some relevant conditions for testing or evaluation purpose is needed. However the user is already annoyed during the usual utilization because of faults and limitations that characterize a research

prototype. On the other hand, even if only real trials can be used for collecting data, the existing installations provide limitations in terms of number of devices, heterogeneity of devices, number of households and non-deterministic conditions for reproducing testing condition. However, for testing purposes the platform can be configured to read data collected in the past, and to write them in the system would be running at the current time. The configuration allows for selecting which devices must be emulated and for each device a different starting date-time can be set. This allows both to emulate the execution of a trials in the past, but also to let it run in laboratory with additional real devices, or virtual ones. In fact application which simulate virtual devices have been developed at the beginning of the project to test the platform without real installations. They are also available as an open source package.

A simulation tool was designed to overcome the limited representativeness of our real trials, finding out more about how the collective and individual benefits of the approach depends on the configuration of the neighbourhood, the accuracy of weather forecasts, the price models of the energy providers, and so on. In this way the analysis of the collected data in the trials could be complemented with data coming from a simulator, where we can replay the observed user and device behaviors, varying a number of other factors, such as the configuration of the neighborhood, the number of PVs, the capacity of the storage systems, the frequency of weather forecasts updates, the price models of the public grid, etc. In addition, using the simulation approach, it could be possible to investigate how the CoSSMic distributed system scales with increasing number of households and devices in a neighborhood. Since the main goal of the simulator is to generate more data for the evaluation stage of the project, the key design constraint of the tool has been to obtain a model that exactly reproduces (i.e. reusing the developed software components) the main steps of the real prototype software such as: the creation of the shift able loads; the negotiation and optimization stage using a distributed algorithm; the production of the scheduled loads. The simulator is a discrete event simulator (DES) where the system events appear at different times. Each event has marked with a timestamp and produces a change of state in the system.

## 4 Conclusion

This paper provided an overview about the results achieved by the research activity of the CoSSMic project. We presented an innovative system architecture for energy smart neighbourhoods that has been implemented by an open source prototype. Data has been collected from trial installations in 17 buildings where the monitoring part of the prototype has been installed for up to more than a year gathering detailed data on local energy production and use. The development activities provided open source tools facilitating the execution and observation of the prototype implementation in a simulated environment. Other results include the analysis of regulations, cost models and tariffs for the electric energy sector and their relationship to CoSSMic energy smart neighbourhoods. The proposed

P2P solution demonstrated to be scalable, by partitioning an optimisation problem of exponential complexity, but still providing good improvements in terms of optimality. Future work aims at improving the degree of desired stability for further involving the users without annoying them and the engineering of the platform that would enable the road-map designed for exploitation.

**Acknowledgements.** The project Collaborating Smart Solar-powered Micro-grids (CoSSMic) has received funding from the European Union's Seventh Framework Programme for research, technological development and demonstration under grant agreement no FP7-SMARTCITIES-2013-608806.

## References

1. Amato, A., Aversa, R., Di Martino, B., Scialdone, M., Venticinque, S., Hallsteinsen, S., Horn, G.: Software agents for collaborating smart solar-powered micro-grids, vol. 7, pp. 125–133. Springer, Heidelberg (2014)
2. Amato, A., Aversa, R., Ficco, M., Venticinque, S.: Cosmic smart grid migration in federated clouds, pp. 103–108. IEEE Inc. (2016)
3. Amato, A., Di Martino, B., Scialdone, M., Venticinque, S.: An agent-based approach for smart energy grids, vol. 2, pp. 164–171. SciTePress (2014)
4. Amato, A., di Martino, B., Scialdone, M., Venticinque, S.: Multi-agent negotiation of decentralized energy production in smart micro-grid. *Stud. Comput. Intell.* **570**, 155–160 (2015)
5. Amato, A., Martino, B., Scialdone, M., Venticinque, S.: A virtual market for energy negotiation and brokering, pp. 162–168. IEEE Inc. (2015)
6. Amato, A., Martino, B., Scialdone, M., Venticinque, S.: Distributed architecture for agents-based energy negotiation in solar powered micro-grids. *Concurrency Comput.* **28**(4), 1275–1290 (2016)
7. CIRED Working Group on Smart Grids: Smart grids on the distribution level - hype or vision? Cired's point of view. Technical report, May 2013
8. Horn, G.: Scheduling time variant jobs on a time variant resource. In: Hanzálek, Z., Kendall, G., McCollum, B., Sucha, P. (eds.) *The 7th Multidisciplinary International Conference on Scheduling: Theory and Applications (MISTA 2015)*, Czech Republic, pp. 914–917, August 2015
9. Horn, G., Venticinque, S., Amato, A.: Inferring appliance load profiles from measurements. *LNCS*, vol. 9258, pp. 118–130 (2015)
10. Curiel, I.: *Cooperative Game Theory and Applications - Cooperative Games Arising from Combinatorial Optimization, Theory and Decision Library C: Game Theory, Social Choice, Decision Theory, and Optimization*, vol. 16. Springer, Heidelberg (1997)
11. Jiang, S., Venticinque, S., Horn, G., Hallsteinsen, S., Noebels, M.: A distributed agent-based system for coordinating smart solar-powered microgrids. In: *Proceedings of SAI Computing Conference 2016*, pp. 71–79. IEEE (2016)
12. Narendra, K.S., Thathachar, M.A.L.: *Learning Automata: An Introduction*. Prentice Hall, Upper Saddle River (1989)
13. Tasquier, L., Scialdone, M., Aversa, R., Venticinque, S.: Agent based negotiation of decentralized energy production. *Stud. Comput. Intell.* **570**, 59–67 (2015)

# A Simulation Approach for the Optimization of Solar Powered Smart Migro-Grids

Alba Amato<sup>1(✉)</sup>, Rocco Aversa<sup>2</sup>, Beniamino Di Martino<sup>2</sup>,  
Marco Scialdone<sup>2</sup>, and Salvatore Venticinque<sup>2</sup>

<sup>1</sup> Istituto di Calcolo e Reti ad Alte Prestazioni, CNR,  
via Castellino 111, Napoli, Italy  
`alba.amato@icar.cnr.it`

<sup>2</sup> Department of Industrial and Information Engineering,  
University of Campania “Luigi Vanvitelli”, Via Roma 29, Aversa, Italy  
{`rocco.aversa,beniamino.dimartino,marco.scialdone,`  
`salvatore.venticinque`}@unicampania.it

**Abstract.** A smart micro-grid requires information technology to fast detect and control grid instabilities and to validate that processes will work as designed. But real power grid can not be used for testing and validation, so it is convenient to develop tools to simulate the real system. A relevant challenge in this field is the modeling of the grid, including sensors, control, communication network and computational components using software simulation. But the choice of the simulator depends on the research questions to be answered and possible existing simulation tools to combine with. In this paper we present a simulator we have designed and developed in the context of the CoSSMic project in order to test and control system behavior when anomalies are injected or initial conditions are modified and in order to analyze system performance and quality of service.

**Keywords:** Multi-agent systems · Smart energy · Simulation

## 1 Introduction

A smart grid is an electricity network that uses digital and other advanced technologies to monitor and manage the transport of electricity from all generation sources to meet the varying electricity demands of end-users [1]. The main goal of smart grids is to co-ordinate the needs and capabilities of all generators, grid operators, end-users and electricity market stakeholders in order to operate all parts of the system as efficiently as possible, minimising costs and environmental impacts while maximising system reliability, resilience and stability [1]. To reach the goal, a smart grid requires information technology to fast detect and control grid instabilities and to validate that processes will work as designed. But real power grid can not be used for testing and validation, so it is convenient to develop tools to simulate the real system. A relevant challenge in this field is the modeling of the grid, including sensors, control, communication network and

computational components using software simulation. A simulator should take in account the different resources connected to the power grid that can range from time-series based load models up to detailed models of renewable energies or storages. Most of the current simulators for smart grid scenarios originate in simulation of electric power systems, control circuits or agent based markets [8] and it is hard to decide whether a particular simulator fits the whole smart grid system or only parts of it. As demonstrated in [8], the choice of the simulator depends on the research questions to be answered and possible existing simulation tools to combine with. In this paper we present a simulator we have designed and developed in the context of the CoSSMic project [3] in order to test and control the energy exchange, the system's behaviour when initial conditions are modified or anomalies are injected, the system's performance and the quality of service.

## 2 The CoSSMic Scenario and Limitations

CoSSMic (Collaborating Smart Solarpowered Micro-grids, FP7-SMARTCITIES-2013) is an ICT European project that aims at providing a higher degree of predictability of power delivery [3]. The basic idea is to optimize the schedule of energy loads, according to the availability of production by PV panels, recovering the lack of alignment of production and consumption of each user, in order to maximize self-consumption of the neighbourhood. The behaviour of the smart micro-grids will be governed by reward based business models, ensuring sufficient rewards to the users willing to share resources and collaborate to optimize the overall performance of the neighbourhood power grid. This system requires sharing of information in order to exchange power excess production and storage capacity in accordance with policies defined by the each cluster member and other relevant information, such as input from weather stations, weather forecasts, and habits and plans of inhabitants.

An important mechanism for the project is the design and development of a system of software agents, which are able to negotiate the scheduling of power sources and energy storage [2], over a peer-to-peer overlay [4]. Agents will act autonomously guided by rules and policies set by the users and agree on a coordinated behavior towards the central power grid [5]. An expert systems will suggest the user which device would be better to schedule and when, learning from user plans, energy behaviours of devices and actual energy consumption/production and continuously improving its expertise. The research activities focus on the deployment and validation of the system over the computational grid provided by the project [6]. This will allow household and neighbourhood power optimisation and sales to the network. In addition CoSSMic will provide a higher degree of predictability of power deliveries for the large power companies, and it will satisfy the requirements and achieve the benefits discussed above. CoSSMic research partners are Stiftelsen Sintef, International Solar Energy Research Center Konstanz, Second University of Naples, Norges Teknisk-Naturvitenskapelige Universitet, Sunny Solartechnik, Boukje.com Consulting. City of Konstanz in

Germany and province of Caserta in Italy are project partners that provide trial sites for experimental activities and validation of results. CoSSMic Trials have been set up in Konstanz and Caserta. Real trials limit the investigation of effectiveness of CoSSMic solution because of many reasons. First of all the neighborhood is limited to households participating in the project. Number of households and monitored devices is limited by effort and budget of the project, so evaluation of what happens when the size of the neighborhood increases is not possible. Information collected by trials are limited to the observation of available appliances and PV plants. For example it is not possible to change the number and the dimension of PV panels to evaluate which improvements could be obtained. It is not even possible to evaluate the behavior of the system with different weather conditions or changing user's habits. Moreover the heterogeneity of devices requires additional effort for developing different drivers for each different device. There is no possibility to inject faults to analyze how the system would react. Finally an expert system, which supports the user to plan the usage of his device, or that suggest to increase the dimension of is PV plant, would learn slowly, that is run by run. For these reasons we proposed a methodology based on simulation that provides the possibility to increase the diversity and the amount of data that could be analyzed in order to collect feedback and useful information to test and improve the CoSSMic solution. The main idea is to integrate existing real households and devices, but also to simulate them in order to make a large-scale test of devices to make sure that the solution will be able to adapt to high-volume data and still be able to deliver high-quality reliable services and near real time processing and views on the acquired information. The advantages of simulation over the use of real systems are numerous. First, it is possible to vary the input in order to replicate, modify and generate devices and user's behaviors. Second, the injection of faults is not critical, so avoiding device's damages and other collateral effects. Third, the system becomes more observable and controllable in different situations. In fact it is possible to simulate the change of the weather conditions, or simply investigate the service improvement or its degradation with different the amount of available information collected from the real-field. Moreover the simulation gives the possibility to improve the optimization algorithm and to verify the improvements in the learning. In fact the real system must be able to collect data and to process them in a time slot that is as short as the measured power can be supposed constant. By simulation we can change the dynamic of the system reaction and of power variation to investigate limitations and capabilities of available technologies. The proposed simulator is useful also to improve the learning processes and the optimization algorithm. The idea is to simulate different weather condition and prediction models, speeding up the process even using several parallel executions. Moreover, injecting faults during simulation it is possible to investigate and eventually improve the reliability of the proposed solution. The simulation results can be analyzed off-line to evaluate the effectiveness of the approach and to foresee improvements and reconfiguration of real neighborhoods.

Such information can be used even to train the expert system and to distribute new updates of his knowledge base to all neighbors.

### 3 Simulator Design

Figure 1 shows the architecture of the simulator. In the Central Data Repository the inputs for the simulation together with the simulation results are contained. The inputs are represented by historical data coming from the trials and the configuration of the households composing the neighbourhood. The Setup Module stores the configuration in the Central Data Repository and gives the start signal of the simulation to the dispatcher. The Dispatcher is an agent that reads data about configuration from the Central Data Repository and queries the Virtual Solar Panels to have a prediction of energy production. This information is useful to submit tasks for the households' devices to the Load Scheduler: this one can embed the existing MAS platform and produces the scheduled loads. The Virtual Solar Panels block represents a set of solar panels with different features and power capacity. It can be queried by device manager to have the value of the production or by the dispatcher to have the forecasting. Once the Dispatcher has received the ASTs from the Load Scheduler, it can give the start signal to the Device Manager. The Device Manager reads the consumption profile from virtual devices and the production profile from the virtual solar panels. When it collected the profiles, it stores the relative time series in the Simulation Data Repository. The Simulation Data Repository contains all simulation results and it is accessed by the Viewer, a web application that enables to analyse the time series through graphs. Finally, the simulator has a Trainer block that is an expert system that learns and improves his knowledge to suggest to the user how to use devices to optimize energy utilization. A prototype of the simulator was implemented. All the technologies used for the implementation are open source. The prototype has a web interface that interacts with the Setup Module that is implemented in PHP. The Central Data Repository is realized through a MySQL database. The Simulation Data Repository is implemented by a Time Series Database (TSDB) that is a software system that is optimized for handling time series data. A time series can be seen as an array of numbers indexed by time. In some fields these time series are called profiles, curves, or traces. As TSDB we decide to use InfluxDB<sup>1</sup> an open-source distributed time series database with no external dependencies where everything is managed as a time series. It provides some standard functions like min, max, sum, count, mean, median, percentiles, and more. As viewer we chose Grafana<sup>2</sup>, an open source, feature rich metrics dashboard and graph editor for different Time Series DB such as Graphite, InfluxDB and OpenTSDB. It allows to create fast and flexible client side graphs with a multitude of options. Grafana is organized in dashboards where it is possible to add and manage several type of graphs. It offers the possibility to connect and interact with InfluxDB through a query editor.

<sup>1</sup> <https://influxdb.com/>.

<sup>2</sup> <http://grafana.org/>.

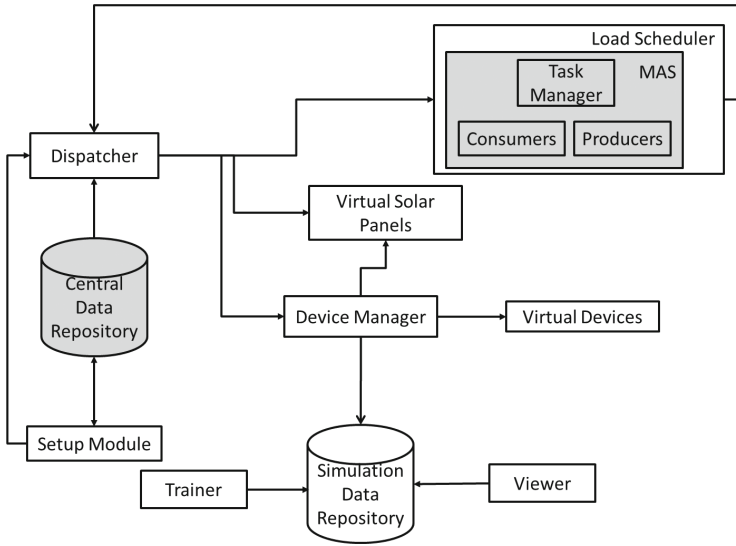


Fig. 1. Simulator architecture

The Virtual Solar Panels block has been implemented as a web application similar to the virtual devices. In the early stages of the work we have taken into account the characteristics of the appliances in order to allow adequate modeling of them. The main issues identified were: time curve of the power required for the operating cycle; frequency of use on a daily basis; duration of the operating cycle. As is well known, each appliance is characterized by a specific profile of the load, which describes the time trend of power generated to and from the network by the device itself. To generate a simulation closer to reality, it would then need to use the correct profiles for each appliance that is going to simulate. The possibility to replicate devices and configure their energetic behaviour is relevant to increase the dimension and the diversity of the simulated neighbourhood. Virtual Devices simulate real-world devices, both producers and consumers of electricity. Device categories include PV panels, household workloads, washing machine, clothes dryers, refrigerators and others. Many templates are currently available for creating different instances of devices belonging to each available category. Different methodologies have been used to simulate virtual devices:

- Many templates of PV panels use historical data collected from some on-line archives that are available in Internet for both Italian and German plants. For example *solarlog.it* website (available at <http://www.solar-log.it/>) provides on-line web access to the information about plants and to their real-time monitoring measures. It is possible to visualize the power measured with a sampling period of 5 min, but also the archived data are available. We downloaded and stored such data for some plants of interests since the January 1<sup>st</sup>2012. Power is measured every 5 min and stored in a database.



- Other PV panel templates of trials are implemented by analytical models which accept as input historical data about irradiation, plant characteristics and information from billing reports. In order to have information about production profiles of our trials already at the beginning of the project we collected monthly reports of owners and were able to get the monthly production from their electricity bills. In particular plant information allowed us to simulate an hourly profile that takes into account the information about PV panel installation plant, the Albedo and the type of photovoltaic that can be chosen among fixed or sun tracking uniaxial, biaxial, uniaxial concentration. We normalized the average daily profile according to the monthly production for that user and total irradiation of each day of the year.
- Consuming appliances have been virtualized using energy profiles provided in related work. For example [7] provided, for some kind of devices, time series measured at different sample rate and for different operation mode.

In order to simulate a real neighbourhood, and to increase the number of virtual devices available in the repository, it is needed to import data collected during trials. A different model has been defined to virtualize PV panels and consuming appliances. For each PV panel trials information include two time series per day: prediction of production and energy measures. In our trials prediction are updated at midnight 6 PM, 12PM, 18PM and the time horizon is 8 h. We allow to eventually change them for simulation purpose. We can also simulate a true prediction replacing it with the energy measures of that day. In the case of consuming appliances we have different measures for each run, both in the case of single run and periodic run devices. Dynamic profiling is needed to model the energy consumption because it may change run by run and according to the current working mode. In fact the energy consumption of an appliance can change dynamically depending on the working condition. For example the washing machine consumption can be affected by the water temperature and will consume less in summer than in winter. In this case for each run we have two time series related to the predicted consumption, which during trials is learned from previous runs, and real consumption measured from the start time to the stop time. For each run we define the following meta-data: start time, sequence, operation mode of the device, day of the year. A compact representation of time series is built reusing the learning and prediction mechanisms developed by the CoSSMic project. The optimization of task scheduling depends on the awareness about energy loads and on precision of prediction of energy produced by solar panels. Load requirements in terms of earliest start time and latest start time are provided by the user and can be manually configured for simulation purpose, randomly generated or inferred by user's habits during trials. The Optimization Module of the simulation tool is the same software component, which implements the load scheduler of the CoSSMic platform. It allows to simulate the effectiveness of CoSSMic scheduler with different neighborhood configurations. The CoSSMic optimization algorithm implemented by a multi-agent application composed of producer agents and consumer agent which exchange energy and schedule loads to maximize the global self-consumption. The description of the

negotiation strategy is out of the scope in this paper, in fact a different optimization algorithm can be replaced and simulated by extending the component interface and implementing the protocol.

## 4 Experimental Results

In order to test the simulator and validate the CoSSMic approach, we set up a testbed and designed a testing scenarios. The objective was to evaluate the increment of self-consumption in a neighborhood using the CoSSMic platform. The experiments were conducted simulating a neighborhood with six houses that represent real trials in Konstanz. Table 1 reports the devices of each house.

**Table 1.** Neighborhood configuration

House 1	Heat Pump Washing Machine Freezer Dishwasher Solar Panel - 10Kw	House 2	Heater Pump Dishwasher Washing Machine Freezer
House 3	Refrigerator Freezer Dishwasher Washing Machine Solar Panel - 5Kw	House 4	Electric Car Heater Pump Refrigerator Freezer Dishwasher Washing Machine Solar Panel - 10Kw
House 5	Refrigerator Dishwasher Washing Machine	House 6	Freezer Dishwasher Washing Machine Heater Pump Solar Panel - 9Kw

Profiles of devices are the actual time series collected in the corresponding trials in Konstanz. It means that there will be not errors due to prediction of consumption. Using the presented configuration we chose a day for each season. Each day has been simulated 10 times to compute average values, which depend on random probabilities used by the scheduler. We computed the global self-consumption for the neighborhood in two cases.

In the first test, the CoSSMic platform optimizes the schedule, i.e. there is both sharing of energy among neighbors and shift of devices start according to the optimized schedule. The same flexibility was defined for the starting of each device. In particular we allowed a default delay of 2 h.

In the second test we did not allow for any delay. The agents will negotiate the exchange of energy, but there will be no shift of device execution and the

schedule equal to the fixed plan. This is just to evaluate the sharing capability without user’s flexibility.

In both the previous cases the self-consumption is computed by Eq. 1, where  $P_i(t_j)$  is the energy provided in the time interval  $[t_{j-1}, t_j]$  by the producer  $i$  and  $C_k(t_j)$  is the energy consumed by the device  $k$ . The self-consumption in the corresponding time slot has been defined as  $sc(t_j)$  and the sum of self-consumption over the day in all neighborhood is  $SC$ . Moreover the day has been divided in 288 time-slots of five minutes,  $n$  is and the number of consuming devices and  $m$  is the number of PV plants in the neighborhood.

$$SC = \sum_{j=1}^{288} sc(t_j) \text{ where} \tag{1}$$

$$sc(t_j) = \begin{cases} \sum_{k=1}^n C_k(t_j) & \text{if } \sum_{i=1}^m P_i(t_j) > \sum k = 1^n C_k(t_j) \\ \sum_{i=1}^m P_i(t_j) & \text{otherwise} \end{cases}$$

In the second tests we also computed the sum of households self-consumption, supposing that without CoSSMic, they consume on site what they can from the PV plant and the remaining production, if any, flows to the Grid.

Table 2 reports all the results in terms of absolute energy self-consumed and self-consumption as percentage of PV energy consumed by the neighborhood.

It must be observed that the difference between the last two columns represents the amount of energy that is not consumed by the households on site, and hopefully is still consumed into the neighborhood by any other households before flow to the rest of the Grid. This amount of energy is the minimum available for negotiation by CoSSMic when the user does not provide flexibility. On the other hand, when flexibility of two hours is provided for each consuming appliance, we observe that the amount of energy, which can be negotiated, and self-consumed in the neighborhood increases, eventually increasing or decreasing the self-consumption on site of each household.

**Table 2.** Neighborhood self-consumption: with CoSSMic, with sharing but without scheduling and without sharing and scheduling

Date	Self-consumption with optimal schedule [Wh]	Self-consumption with 0 flexibility [Wh]	Sum of households self-consumptions [Wh]
21/02/2016	32620, 1271	26389, 8674	12944, 2886
16/04/2016	37311, 5388	28097, 4537	25195, 3501
13/07/2016	27549, 7638	22553, 8168	12853, 5472
15/10/2016	28948, 6913	20746, 7826	13267, 3494

Table 3 shows the increment of self-consumption (in percentage) due to the energy sharing within the neighborhood with and without flexibility. Obviously a reward mechanism must compensate each user, whose own self-consumption could decrease, according to how much energy she shared with the neighborhood and the flexibility of her plan.

**Table 3.** Increment of self-consumption due to the sharing mechanism.

Date	CoSSMic improvement
21/02/2016	8,1%
16/04/2016	12,9%
13/07/2016	8,7%
15/10/2016	8,5%

We are working on other experiments, considering larger intervals of time, to be able to generalize these results.

## 5 Conclusion

The paper presents the design of a simulator, that we have developed in the context of CoSSMic project in order to overcome the limitations of real trials, which have been setup during the project activities. The proposed simulator is useful also to improve the learning process and the optimization algorithm. The expected benefits are improvements of prediction and of learning process, better optimization algorithms, analyzing results obtained by simulating different weather conditions, models, neighborhood configuration, even using several parallel executions. Future works include the exploitation of simulation results to speed-up the training process of an expert system which aims at supporting the user to plan the utilization of her device. Updates of the knowledge base will be distributed to the CoSSMic instances to augment the expertise of local systems.

**Acknowledgements.** This work has been supported by CoSSMic (Collaborating Smart Solar-powered Micro-grids - FP7-SMARTCITIES-2013).

## References

1. Agency, I.E.: Technology roadmap: smart grids. ESE discussion papers, Paris (2011). [www.iea.org/papers/2011/smartgrids\\_roadmap.pdf](http://www.iea.org/papers/2011/smartgrids_roadmap.pdf)
2. Amato, A., Di Martino, B., Scialdone, M., Venticinque, S., Hallsteinsen, S., Jiang, S.: A distributed system for smart energy negotiation. *Lecture Notes in Computer Science (including subseries Lecture Notes in Artificial Intelligence and Lecture Notes in Bioinformatics)*, vol. 8729, pp. 422–434 (2014)
3. Amato, A., Aversa, R., Di Martino, B., Scialdone, M., Venticinque, S., Hallsteinsen, S., Horn, G.: Software agents for collaborating smart solar-powered micro-grids. In: Caporarello, L., Di Martino, B., Martinez, M. (eds.) *Smart Organizations and Smart Artifacts, Lecture Notes in Information Systems and Organisation*, vol. 7, pp. 125–133. Springer (2014)
4. Amato, A., Di Martino, B., Scialdone, M., Venticinque, S.: An agent-based approach for smart energy grids. In: *6th International Conference on Agents and Artificial Intelligence - Agents (ICAART-2014)*, vol. 2, pp. 164–171. SciTePress, Angers, France, March 2014

5. Amato, A., Di Martino, B., Scialdone, M., Venticinque, S.: Multi-agent negotiation of decentralized energy production in smart micro-grid. In: Camacho, D., Braubach, L., Venticinque, S., Badica, C. (eds.) *Intelligent Distributed Computing VIII, Studies in Computational Intelligence*, vol. 570, pp. 155–160. Springer (2015)
6. Amato, A., Martino, B.D., Scialdone, M., Venticinque, S.: Design and evaluation of P2P overlays for energy negotiation in smart micro-grid. *Comput. Stand. Interfaces* **44**, 159–168 (2016)
7. Pipattanasomporn, M., Kuzlu, M., Rahman, S., Teklu, Y.: Load profiles of selected major household appliances and their demand response opportunities. *IEEE Trans. Smart Grid* **5**(2), 742–750 (2014)
8. Pochacker, M., Sobe, A., Elmenreich, W.: Simulating the smart grid. In: *PowerTech (POWERTECH)*, 2013 IEEE Grenoble, pp. 1–6. IEEE (2013)

# A Security Metric Catalogue for Cloud Applications

Valentina Casola<sup>1</sup>, Alessandra De Benedictis<sup>1</sup>(✉), Massimiliano Rak<sup>2</sup>,  
and Umberto Villano<sup>3</sup>

<sup>1</sup> DIETI, University of Naples Federico II, Naples, Italy  
{casolav,alessandra.debenedictis}@unina.it

<sup>2</sup> DII, University of Campania Luigi Vanvitelli, Aversa, Italy  
massimiliano.rak@unicampania.it

<sup>3</sup> DING, University of Sannio, Benevento, Italy  
villano@unisannio.it

**Abstract.** Cloud monitoring and, above all, security monitoring, is of fundamental importance for both providers and consumers. The availability of effective security metrics and related monitoring tools would not only improve the trust of consumers in acquired services and the control of providers over their infrastructures, but it would also enable the adoption of security-oriented Service Level Agreements stating formal guarantees about measurable security parameters.

In this paper, we discuss a Security SLA model including the concepts needed to formalize security metrics and security-oriented Service Level Objectives in compliance with existing standards, and present a novel Security Metric Catalogue collecting several metrics that can be used to monitor the level of security provided by a cloud or multi-cloud application.

## 1 Introduction

Cloud monitoring, which involves dynamically tracking several Quality of Service (QoS) parameters related to exploited virtualized and physical resources, is a very important task for both providers and consumers. Among the possible QoS parameters to monitor, those related to the level of security provided by a cloud service or cloud application are of utmost importance, since they may help detect and mitigate the risks posed by existing threats [12]. Unfortunately, security monitoring is typically less developed than operational performance monitoring, not only in the cloud environment but also in other contexts. For what regards cloud computing, a possible reason for this dearth is related to the cost model and to the elasticity properties of the cloud, for which performance is the key element to measure. More in general, security monitoring is less spread (and less implemented by current providers) than performance monitoring due to the lack of a set of formalized and shared security metrics [6,7].

It is worth noting that the lack of well-known security metrics is the main inhibitor factor that prevents providers from explicitly including security guarantees in their Service Level Agreements (SLAs). In fact, many big cloud service

providers (CSPs) do currently offer SLAs for their services, but these SLAs only include performance-related Service Level Objective (SLOs), mainly referred to availability and response time. Cloud security and security monitoring are hot topics that are being largely addressed by both Academia and standardization bodies in recent years. Several security metrics have been proposed in the context of European projects such as A4Cloud [1], SPECS [3,9] and MUSA [2]. Meanwhile, the International Organization for Standardization is currently working on the ISO/IEC CD 19086-2 standard, focused on the identification of a metric model for SLAs.

In this paper, we discuss a complete Security SLA model that includes the concepts needed to formalize security metrics and SLOs in compliance with the latest standardization results. We present a novel Security Metric Catalogue, initially developed in the context of the closed EU FP7 project SPECS and then refined by the ongoing H2020 MUSA project, which can be used to monitor the level of security provided by a cloud or multi-cloud application. The catalogue collects some of the recent security metrics proposals coming from previous projects and existing standard initiatives and scientific literature, plus additional metrics identified after a detailed analysis of the current cloud application landscape. In addition, the catalogue is supported by a web application developed to make it publicly accessible from the Internet, which is also described in this paper.

The remainder of this paper is structured as follows: in Sect. 2 a discussion on the existing work on security metrics is presented. In Sect. 3, the Security SLA and the metric models are illustrated in details. In Sect. 4, the Security Metric Catalogue is presented and some details are given on how the metrics were collected and categorized. Finally, in Sect. 5 we draw our conclusions.

## 2 Background on Security Metrics

A metric is a standard of measurement that can be used to measure a given characteristic of a system. In particular, metrics provide knowledge about how system characteristics are measured (i.e., about the measurement process and the interpretation of the measurement results) and enable the repeatability, reproducibility, and comparability of measurements and measurement results related to those characteristics. In the cloud environment, several popular Quality of Service (QoS) metrics such as availability, response time, CPU load, packet loss rate etc., are widely used by cloud providers to measure the performance of the offered services and to set related guarantees toward prospective customers in their public SLAs. Unfortunately, as anticipated in Sect. 1, despite the strong interest in security shown by both cloud customers and providers, current CSPs still do not offer security guarantees in their SLAs due to the lack of well-know quantifiable security metrics.

As pointed out in [19] in 2009, while several definitions of security metrics as well as guidelines for their identification do exist, relatively little has been reported on actual metrics to use in practice. This is still true, since several metrics have been proposed related both to organizational and technical aspects

but they are often qualitative and hard to measure, and thus not suited for the definition of SLOs. Nevertheless, some initiatives are worth to be mentioned that identified interesting metrics for security evaluation. In 2008, the NIST proposed in [15] a few program-level and system-level measures including information security programmatic measures, and measures compliant with some of the minimum security requirements set by the Federal Information Processing Standard 200 (FIPS 200), corresponding to a subset of the security control families defined in the NIST Security Control Framework [16]. In 2010, the Center for Internet Security (CIS) put together more than one hundred industry experts to gather a set of metrics aimed to collect and analyze data on security processes performance and outcomes. The result was a set of twenty-eight metric definitions related to Incident Management, Vulnerability Management, Patch Management, Application Security, Configuration Management, Change Management and Financial Metrics [10].

Some recent European projects have also addressed the problem of security evaluation and of security metric definition. A4Cloud [1] had, as one of its objectives, that of developing measurement techniques for the non-functional properties that influence or are influenced by accountability. Towards this aim, the A4Cloud Consortium released in 2013 a list of accountability attributes and of associated measurement techniques [4]. More focused on SLAs and on the introduction of security attributes in cloud SLAs, the SPECS project [3, 9] developed a framework for the set-up and deployment of secure cloud applications through the automated management of the associated Security SLA life-cycle, consisting in the phases of negotiation, enforcement and monitoring. Security evaluation and monitoring and security metrics identification were one of the main topics covered by the project. In fact, the SPECS partners were engaged in the definition of the standard ISO/IEC 19086-2 [13], which aims at proposing a technical model and template for documenting cloud SLA metrics (not only security-related). During these activities, the development of a machine-readable catalogue of metrics (including security metrics) based on the proposed model was launched [18]. The metrics belonging to the SPECS catalogue were directly related to the set of security enforcement mechanisms identified to add security capabilities on top of cloud services in an *as-a-service* fashion, and provided an effective means to monitor how well a given security feature is enforced in a system [17]. The SPECS security metric catalogue was adopted and extended by the ongoing MUSA project [2], which is aimed at releasing a DevOps environment aimed at supporting the security-by-design development and the automated deployment of multi-cloud applications. Additional metrics were considered, based on an analysis of the most relevant features of current cloud and multi-cloud applications and on available monitoring systems [14].

### 3 The Reference Security SLA Model

The UML diagram in Fig. 1 illustrates the Security SLA model proposed in the context of the SPECS project [8], based on the WS-Agreement (WSAG) specification [5] and extended to model specific security-related information including



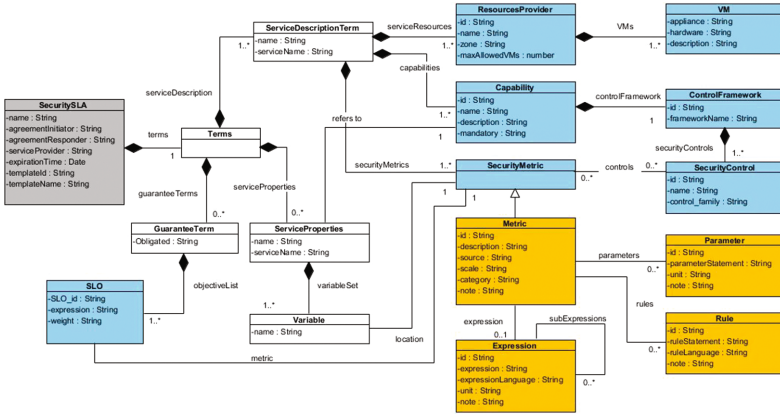


Fig. 1. The SLA model

security metrics. In Fig. 1, the security extensions to WSAG are highlighted in light blue, the original WSAG concepts are reported in white boxes, and the ISO/IEC 19086-2 compliant metric model is highlighted in orange.

As prescribed by the WSAG specification, a Security SLA is provided with basic information such as the agreement name and the expiration date, and by other context information. It includes a *Terms* section that is comprised of the *Service Description Term* and the *Guarantee Term* subsections, which were both extended to explicitly include security-related information. Service Description Terms define the functionalities delivered under the agreement (by means of a domain-specific description). Note that, according to the SPECS vision, in order to enable the automatic enforcement of security, *secure* services are built by adding security features offered as-a-service on top of *bare* infrastructure services (i.e., virtual machines). Therefore, in order to enrich the WSAG specification with security-related information, a security-based domain-specific service term description was proposed, made of the following three sections:

- *Resources Provider*: it describes the available infrastructure resource providers and the appliances they offer (operating system, HW/SW features, etc.);
- *Capabilities*: it reports the security capabilities offered on top of the services covered by the agreement, defined as sets of security controls belonging to a Security Framework (e.g., the NIST Security Control Framework [16] or the Cloud Security Alliance’s Cloud Control Matrix [11]).
- *Security Metrics*: it includes the specification of the security metrics referenced in the service properties section and used to define Security SLOs in the guarantee terms section (see the following). As said, the model is compliant with the current version of the ISO/IEC 19086-2 metrics model, as the security metric concept inherits from the ISO/IEC 19086-2 specification. Note that, in this model, security metrics are associated with security

controls, since they may be used to monitor the fulfillment of a security control or to enforce a given configuration of a control.

The Terms section includes also the *Service properties* section, used to define measurable and exposed properties associated with a service. In the SPECS model, each service property is explicitly associated with a security capability (since it is used to check the enforcement of related security controls), and contains a set of variables, referring to security metrics and representing the actual parameters adopted in SLO expressions. SLOs are specified in the Guarantee Terms section by means of the `CustomServiceLevel` item of the WSAG specification, and are characterized by a SLO id and the related expression. Moreover, in our model, each SLO is assigned a weight by the service customer, which represents the level of importance that its fulfillment has with respect to the overall agreement. An SLO is referred to a specific security metric, as highlighted in the model.

A metric is characterized by a set of information including an id, a description, the organization/individual who created the metric, the scale (nominal, ordinal, interval, or ratio), the category (group of similar metrics to which the metric belongs), and additional notes. Metrics may be defined through *Expressions*, which specify how to calculate their value, and they may be further specified through *Rules*, which indicate possible ways to conduct the measurement of the metric value, and *Parameters*, which represent possible constants used in the Expression of the metric.

## 4 The Security Metric Catalogue

In this section, we introduce the proposed Security Metric Catalogue. As anticipated, the catalogue collects several metrics from multiple sources. In particular, we considered the metrics identified in the A4Cloud and SPECS projects, those introduced by the Center for Internet Security and the NIST 800-55r1 Special Publication, and several additional metrics found in the context of the MUSA project.

The Security Metric Catalogue includes heterogeneous metrics, which significantly differ from one another based on several aspects. Looking at the main goal of defining security metrics, namely measuring how secure a system is, it is possible to identify a first class of metrics, referred to as **technical monitorable metrics**, which actually give information on the *level of security* of the system under observation by taking into account the detection of specific events of interest (detection of attacks or of exposed vulnerabilities). These metrics can be typically monitored with classical monitoring tools and give an information on how well the system was configured or on how much the system is at risk. In many cases, these metrics may be used to specify a customer's security requirements in an SLO (e.g., the customer may require that the *% of incidents reported within required time frame = 100%*). It should be noted, however, that it makes sense to use a metric of this kind in an SLO only if the customer is provided with the means to monitor it (directly or indirectly) and if the desired value (or range of values) set for the metric is somehow under the control of the

**Table 1.** Metric categories

Categories ID	Categories Name	Description
LOC	Level of configuration	This category represents the set-up of a given configuration defined in terms of a <i>level</i> . The level is typically an integer in a given interval ( <b>LevelSet</b> ) that determines in a non ambiguous way the actual configuration put in place in the system
FOP	Frequency of operation	This category represents the frequency used to perform a given operation and is typically expressed in terms of the interval between two subsequent operations
FA	Feature activation	This category represents the activation (ON/OFF) of a given feature. This is typically obtained by turning on a specific already feature of a component/protocol or by activating proper ad-hoc mechanisms
AV	Availability	This category represents the condition that a given system or component is available and properly working. It may be defined in terms of a time percentage or as a simple yes/no value (system up/system down)
NOE	Number of events/elements	This category represents a measure of the number of certain events (or condition occurrences) collected in a given time frame
PERC	Percentage of items	This category represents the percentage of elements (over a defined set) that satisfy a certain condition. It is typically used for organizational and management purposes
COST	Cost	This category represents the cost of occurred incidents or performed actions
MTTC	Mean time to complete operation	This category represents the average time needed to complete a generic operation
MTBE	Interval between two events	This category represents the average time between two events
DL	Data location	This category defines a geographical location

provider. For instance, it makes no sense to set an SLO like *number of attack attempts*  $< 100$  because the provider cannot control the behaviour of attackers but only limit the resulting damage. On the other hand, the **number of attack attempts** metric is very useful to measure the risk that a system is subject to based on the interest of attackers in perpetrating attacks.

**Table 2.** The proposed security metrics

Metric Name	Description	Categories	Controls
Data availability	Percentage of time in which data access is available to data owners	AV	CP-6, CP-9, CP-10, IR-4, SC-5, SC-6, SI-13
Service availability	Percentage of time in which service access is available to users	AV	CP-7, CP-10, IR-4, SC-5, SC-6, SI-13
Total expenses due to compensatory damages	Total expenses incurred due to compensatory damages	COST	IR-4
Average expenses due to compensatory damages	Average expenses due to compensatory damages per upheld complaint/incident	COST	IR-4, IR-5
Cost of Incidents	Total cost to the organization from security incidents occurring during the metric time period	COST	SI-4, IR-4, IR-5
Mean Cost of Incidence	Mean cost to the organization from security incidents identified relative to the number of incidents that occurred during the metric time period	COST	SI-4, IR-4, IR-5
Mean Incident Recovery Cost	Cost of returning business systems to their pre-incident condition	COST	IR-4, IR-8
Mean Cost to Patch	Effort required for patch management activities	COST	SI-2
Datacenter Location	Localization of the data center infrastructure for governance and compliance purposes	DL	CP-6, SC-32, SA-9(5)
Write-Serializability (WS) Activation	Detection of any WS violation to user's stored data in a defined period of time and notification to the user	FA	SC-6
Read-Freshness (RF) Activation	Detection of any RF violation to user's stored data in a defined period of time and notification to the user	FA	CP-2(4), CP-2(6), CP-6(1), CP-9, CP-9(6), CP-10, SI-7, SI-7(1), SI-7(2), SI-7(5)
Forward Secrecy (FS) Activation	Enforcement of the FS capability (encrypted data sent through a TLS session cannot be decrypted even if the data used to generate the cryptographic credentials for that session are compromised)	FA	SC-12, SC-23
HTTP Strict Transport Security Activation	Activation of the feature of the HTTP transport layer that declares the web content available only over a secure HTTP connection	FA	SC-43
HTTP to HTTPS Redirect Activation	Activation of the feature of the HTTP delivery service that forces clients to use only secure HTTP protocol	FA	SC-8
Secure Cookies Enforcement	Activation of the feature of the HTTP protocol that forces the clients to download session cookies, delivered by the HTTP services, only through a secured HTTP communication	FA	SC-29
Certificate Pinning Activation	Activation of the feature of the HTTP protocol allowing the verification of the SSL certificates between the client and the HTTP service where the hash of the public certificate is pinned into the HTTP response	FA	SC-17
Vulnerability Scanning Frequency	Frequency of software vulnerability scanning operations	FOP	CA-7, RA-5
Vulnerability-List Update Frequency	Frequency of the vulnerability list update (from an available repository such as OVAL/NDV)	FOP	CA-7(3), RA-5(1)
SW Update Check Frequency	Frequency of checks for updates and upgrades of vulnerable installed libraries	FOP	CA-7, RA-5

(continued)

**Table 2.** (continued)

Metric Name	Description	Categories	Controls
Audit Record Generation Frequency	Average frequency of audit records review and analysis for inappropriate activity	FOP	AU-1, AU-2, AU-3, AU-6
Level of confidentiality	Level of confidentiality achieved by a system regarding client data independently of the means used to achieve this objective	LOC	SC-8
Key Exposure Level	Level of protection of cryptographic secrets, from a cloud client point of view	LOC	SC-12, SC-13
Account of Privacy and Security Training	Quality of the accounts given with respect to the privacy training and awareness programs in place	LOC	AT-4
Data Isolation Testing Level	Level of testing that has been done by the cloud provider to assess how well data isolation is implemented	LOC	
Type of consent	Type of consent obtained for collecting, using and sharing private data	LOC	IP-1, AU-13
Type of notice	Type of privacy notice provided by the collecting organization, depending on how the privacy notice is offered to the data subjects	LOC	TR-1
Procedures for Data Subject Access Requests	Quality of the procedures in place for guaranteeing data subjects' access to their personal information (levels defined by organization)	LOC	IP-2
Readability (Flesch Reading Ease Test)	Level of readability of a given text, computed from the number of sentences, words and syllables (based on the Flesch Reading Ease Test)	LOC	IP-1
Rank of Responsibility for Privacy	Level within the organization hierarchy at which the person responsible for privacy is located (defined by organization)	LOC	AR-1
Log Unalterability	Level of protection of the log management systems against tampering	LOC	
Identity Assurance	Quality of the authentication mechanisms in place	LOC	AC-1, AC-2, AC-3, SC-23
Type of incident notification	Quality of the notification procedures after a privacy incident or breach	LOC	SI-4
Cryptographic Strength	Strength of a cryptosystem in terms of the expected number of operations required to defeat the underlying cryptographic mechanism. (cf. <a href="https://www.keylength.com/en/3/">https://www.keylength.com/en/3/</a> )	LOC	SC-13
Level of Redundancy	Number of replicas of a software component that are set-up and kept active at the same time during system operation	LOC	CP-2, SC-5, SC-36
Level of Diversity	Number of different SW/HW replicas of a software component that are set-up and kept active at the same time during system operation	LOC	CP-2, SC-5, SC-29

A different class of metrics is the one of **technical enforceable metrics**: they are preferably used for the enforcement of specific security configurations/controls (e.g., the HTTPS\_ON metric identifies whether the automatic redirect from the HTTP to the HTTPS protocol is implemented in web connections) and can be measured by simply checking the current system configuration. Finally, **management metrics** refer to the way an organization sets-up its secu-

rity policies and procedures and handles security incidents (an example of metric of this kind is the **cost of incidents**). These metrics may be used in SLOs since they represent high-level requirements that target organization aspects and can be measured by simply checking how the system is configured. Also, they may be used to configure the target system, when possible, with the parameters defined by the customers.

As previously mentioned, metrics can be grouped by categories that have similar characteristics in terms of the adopted measurement procedure. Our Security Metric Catalogue in particular, considers the metric categories reported in Table 1.

Note that the LOC, FOP, FA, and DL metric categories are very relevant for security configuration, in addition to being easily monitorable. In fact, it is quite common to have SLOs expressed in terms of the desired configuration of some parameter (e.g., the length of the key in a known cryptographic algorithm, the frequency of vulnerability scans to carry out on a server, the activation of a specific version of a protocol, the admissible locations for storing personal data), and often their fulfillment can be verified by checking system logs or by using other available assessment tools (e.g., the Qualsys Platform for the assessment of security and compliance of IT assets). Metrics belonging to the AV, NOE, and MTBE categories include monitorable metrics that give an idea of how well the system was configured with respect to incident detection, mitigation and resolution, (e.g., the number of incidents that belongs to the NOE category gives an idea of how well an Intrusion Detection and Prevention System has been configured), while COST or PERC metrics are mostly referred to management aspects.

Table 2 reports some security metrics belonging to the AV, FA, COST, and LOC categories, along with the associated controls (if any). The complete list of metrics is available online at [18] together with all the related information on associated expression, unit, rule and parameters that could not be included here for space issues.

## 5 Conclusions

In this paper, we presented a Security Metric Catalogue resulting from the analysis of several sources represented by past and ongoing projects dealing with cloud security and by several standardization efforts, both in draft and in final version. The catalogue introduced in the paper is compliant with the latest directives from ISO regarding the structure and format of metrics, and is integrated in the machine-readable format proposed by the recent SPECS project for Security SLAs. We reported thirty-five metrics over more than ninety metrics collected so-far, classified based on a set of categories with similar measurement characteristics.

**Acknowledgment.** This research is partially supported by the grant FP7-ICT-2013-11-610795 (SPECS) and H2020-ICT-07-2014-644429 (MUSA).

## References

1. A4Cloud project web site (2017). <http://www.a4cloud.eu/>
2. MUSA project web site (2017). <http://www.musa-project.eu>
3. SPECS project web site (2017). <http://www.specs-project.eu>
4. A4Cloud Consortium: Deliverable D: 35.1: Metrics for Accountability. (2013). <http://www.a4cloud.eu/sites/default/files/D35.1%20Metrics%20for%20accountability.pdf>
5. Andrieux, A., Czajkowski, K., Dan, A., Keahey, K., Ludwig, H., Nakata, T., Pruyne, J., Rofrano, J., Tuecke, S., Xu, M.: Web services agreement specification (WS-Agreement). In: Global Grid Forum. The Global Grid Forum (GGF) (2004)
6. Casola, V., De Benedictis, A., Rak, M.: On the Adoption of Security SLAs in the Cloud. In: Felici, M., Fernández-Gago, C. (eds.) A4Cloud 2014. LNCS, vol. 8937, pp. 45–62. Springer, Cham (2015). doi:[10.1007/978-3-319-17199-9\\_2](https://doi.org/10.1007/978-3-319-17199-9_2)
7. Casola, V., De Benedictis, A., Rak, M.: Security monitoring in the cloud: an SLA-based approach. In: 2015 10th International Conference on Availability, Reliability and Security (ARES), pp. 749–755 (2015). doi:[10.1109/ARES.2015.74](https://doi.org/10.1109/ARES.2015.74)(2015)
8. Casola, V., De Benedictis, A., Rak, M., Modic, J., Erascu, M.: Automatically enforcing security slas in the cloud. *IEEE Trans. Serv. Comput.* **PP**(99), 1 (2016). doi:[10.1109/TSC.2016.2540630](https://doi.org/10.1109/TSC.2016.2540630)
9. Casola, V., De Benedictis, A., Rak, M., Villano, U.: Preliminary design of a platform-as-a-service to provide security in cloud. In: CLOSER 2014 - Proceedings of the 4th International Conference on Cloud Computing and Services Science, Barcelona, Spain, 3–5 April 2014, pp. 752–757 (2014)
10. Center for Internet Security: The CIS Security Metrics v1.1.0. (2010). [https://benchmarks.cisecurity.org/tools2/metrics/cis\\_security\\_metrics\\_v1.1.0.pdf](https://benchmarks.cisecurity.org/tools2/metrics/cis_security_metrics_v1.1.0.pdf)
11. Cloud Security Alliance: Cloud Control Matrix v3.0. <https://cloudsecurityalliance.org/download/cloud-controls-matrix-v3/>
12. Cloud Security Alliance: The Treacherous Twelve, Cloud Computing Top Threats in 2016 (2016). <https://cloudsecurityalliance.org/download/the-treacherous-twelve-cloud-computing-top-threats-in-2016/>
13. International Organization for Standardization: ISO/IEC CD 19086–2. Information Technology - Cloud computing - Service level agreement (SLA) framework - Part 2: Metric Model (2017). <https://www.iso.org/standard/67546.html>
14. MUSA Consortium: Deliverable D2.1: Initial Sbd methods for multi-cloud applications (2016). <http://www.tut.fi/musa-project/wp-content/uploads/2017/02/MUSA-D2.1-Initial-Sbd-methods-for-multi-cloud-applications.pdf>
15. National Institute of Standards and Technology: NIST Special Publication 800–55 Rev1. Performance measurement guide for information security (2008). <http://nvlpubs.nist.gov/nistpubs/Legacy/SP/nistspecialpublication800-55r1.pdf>
16. National Institute of Standards and Technology: NIST SP-800-53: Recommended Security Controls for Federal Information Systems (2013)
17. SPECS Consortium: Deliverable D4.3.2: Implementation of the enforcement SLA components - Intermediary (2015). <http://www.specs-project.eu/publications/public-deliverables/d4-3-2/>
18. SPECS Consortium: The SPECS Security Metric Catalogue (2017). [http://apps.specs-project.eu/specs-app-security\\_metric\\_catalogue/](http://apps.specs-project.eu/specs-app-security_metric_catalogue/)
19. Jansen, W.: NIST Interagency/Internal Report (NISTIR) - 7564. Directions in Security Metrics Research (2009). <http://nvlpubs.nist.gov/nistpubs/Legacy/IR/nistir7564.pdf>

# Providing Sensor Services by Data Correlation: The #SmartME Approach

Nidhi Kushwaha<sup>1</sup>(✉), Giovanni Merlino<sup>1</sup>, Longo Francesco<sup>1</sup>, Bruneo Dario<sup>1</sup>,  
Antonio Puliafito<sup>1</sup>, and O.P. Vyas<sup>2</sup>

<sup>1</sup> Department of Engineering, University of Messina, Messina, Italy  
kushwaha.nidhi12@gmail.com,

{gmerlino,flongo,dbruneo,apuliafito}@unime.it

<sup>2</sup> Department of Information Technology, IIIT-Naya Raipur, Raipur, India  
opv@iiitnr.edu.in

**Abstract.** In the current era Internet is the most used medium for sharing and retrieving the information for building applications which are commonly developed for enhancing the user experience in terms of comfort, communication. For this, the need of real-time sensor data gains importance. The data collected from the physical objects should be easily available for different applications. Semantic representation of the sensor data directly addresses the problem of storing it in logical, easily accessible and extensible manner. Our paper works towards converting the already collected sensor data of the #SmartME project into semantic format and also proposes real-time storage of semantically enriched sensor data. To build applications using these sensor data the authors consider mainly three kinds of sensors, i.e., Temperature, Humidity, Pressure. Predicting the observed value of any sensor data is the main aim of this work. The analysis leverages other sensors & environmental parameters such as Date, Time, Longitude, Latitude, Altitude etc. Correlation among these parameters and the accuracy of the predicted results showed the suitability of our proposed idea.

**Keywords:** SmartME · IoT · Sensor network · Stack4Things · Semantic web · Data mining · Correlations

## 1 Introduction

A Smart City concept incorporates advanced Information and Communication Technologies for providing the services for the betterment of the citizens. These key services depend not only on the needs of the citizens but also on the region/area where the city is located. As per the recent prediction of Cisco Systems and World Health Organization in 2015, it was noticed that more than 60% of the world's population will live in cities by 2050 [6]. This shifts certainly raise challenges for the basic needs of a person such as water, electricity, fuel supply, building cost-effective infrastructures, proper drainage, waste, air-pollution, parking, traffic, transportation, street lighting management system, healthcare,



education system, safety and security services. For building such type of applications, the domain of the Internet of Things (IoT), Semantic Web, Social Web and Machine Learning have been exploited in recent years. The main components of IoT are sensors, smart phones & other embedded portable, devices and their internet connectivity. Connectivity helps in leveraging the raw data for building smart applications. Semantic and Social Web provide supporting knowledge for making the applications even smarter. Furthermore, Semantic Web technologies have the ability to annotate sensor's raw data & observation by specific domain ontology. This annotations enhance the interpretability of the sensor data. It also allows to build an application without the overhead of heterogeneous sources of data. Semantic annotation of sensor data provides an opportunity to do deep queries. For example, IBM proposed a model [9,10] to diagnose the faulty sensors deployed in a building by expressing the rules through Semantic Web. The correlation logic among different sensors has been explored for diagnosing the faulty sensor. However, Machine Learning acts as a complement for smart applications by analysing the previously collected data and acts making predictions based on it. For example, by doing predictive analysis, Chicago is controlling the rodent population. The application is able to determine which trash dumps are most likely to be full and attract more rats in the near future.

In this paper the authors summarize the recent applications developed in semantic sensor areas. The paper first outlines the conversion of raw data into Semantic Web for the running #SmartME project. Secondly, the authors proposes an idea on how correlation between sensors can be taken into consideration for predicting unspecified/destroyed sensors deployed in a specific location.

## 2 Related Work

Sensors are becoming popular these days to collect huge amount of specific information about real world surroundings. However, these sensors cannot work alone for providing the services smart cities need. To provide the systematic description of sensor networks various attempts were made in the past such as, Sensor Web Enablement (SWE) developed by the Open Geospatial Consortium (OGC) that are widely being adopted by industry, government organizations and academia. SWE provides XML representation for sensor description, thus limited to only syntactical representations [12], rather than semantics. Moreover, semantics of data provide the interpretability of sensor data & observations in terms of machine-readability. This interpretability helps to provide high-level information to the application's user and devises the application more user-friendly as well as easy to use.

Semantic Sensor Web [11] and Semantic Sensor Network (SSN) Ontology [7] have been proposed to define sensor data model for describing the sensor and their services. They also provide uniform descriptions and high-level interfaces for sensors and actuators. The semantic description of sensors mitigates the complexities involved in the heterogeneity of data collection and in the underlying technologies being used for sensors and actuator devices. It has the capability to

provides low-level information about sensor data, as well as high-level reasoning for human understandability. For example, information about the sensor type, observation, respective board (where the sensor is connected), location name and accuracy of measurement are defined as low-level information about sensors. On the other hand, analysing the relation between sensors and recommend the user with personalized weather prediction is called as high-level information. Furthermore, the collection of sensor observations for building applications requires Cloud real-time storage to analyse the sensors data in various combinations for smart applications. Predicting thermal comfort of employees was proposed by Kojima in 2008 [4]. To achieve it, 21 sensor were deployed inside a room. The paper utilizes thermal comfort data from employees in parallel with other physically located sensors. On the other hand, [8] proposed the service infrastructure for semantic sensor data storage and querying. The paper considered the parking spots and empty room examples and described the information related in semantic formats. Also, the authors investigated about the automatic registration of a new sensors by automatically annotating the sensors with appropriate description. Different ontologies were merged such as Dolce Ultralite, the W3C Semantic Sensor Network (SSN-XG), Event model ontology to support cross-domain descriptions. Ploennings et al. in 2014 [10] proposed a diagnosis model for smart building application. This diagnosis model uses semantic information or cause-effect-relationships between sensors. Mainly the approach used two type of sensors i.e. Temperature and Occupancy sensors. The defect of temperature sensors were deduced by the occupancy and cooling sensors. The authors extended the SSN ontology by modifying it specifically for the building infrastructure. The approach was used as a common model for all the buildings create automatically the similar physical model for them. Consoli et al. [2] gathered Catania municipality data from different sources/formats and made them available online as semantic knowledge base. The authors introduced different techniques to convert JSON, XML, SQL Server database and Excel files into RDF format. The goal of this approach is to boost the semantic data based smart city applications for more relevant information retrieval and processing, without the overhead of complexities involved in it.

Recently, authors in [1,5] proposed a project named #SmartME which aims to create a Cloud based infrastructure to model IoT and to control the smart objects remotely. This Smart City infrastructure provides a unique view for all the smart objects located in the different parts of the smart cities. In this infrastructure, the IoT nodes comprise different types of sensors (Temperature, Humidity, Brightness, Noise, Pressure) that are attached to Arduino YUN boards. These boards are able to send the information to the CKAN repository through the Stack4Things cloud infrastructure. The Stack4Things framework was developed by Mobile and Distributed System (MDLSLab) at the University of Messina, Italy. Lightning-rod on the client side and Iotronic at the server side are the main building blocks of the Stack4things technology. Stack4Things Lightning-rod runs on the micro-processor unit of the smart boards (e.g., Arduino YUN). It interacts with the OS tools and services of the

board as well as sensing and actuating resources through I/O pins. On the other hand, Stack4Things Iotronic provides an OpenStack service to the end user for managing the board resources remotely. The users can manage the boards via REST APIs or using the Stack4Things command line client. The logic deployed by Stack4Things pushing the data from Arduino YUN boards to store them in CKAN repository, is written under the guise of Node.js plug-ins at the client side, i.e. in Lightning-rod. The sensors data are currently in standalone (raw) format and also have less interpretability for the application developer. To enhance the experience of sensor data acquisition and to link them logically a semantic layer should be there. Furthermore, siloed information from unrelated sensors would not help to build a smart applications. Thus, there is a need to develop a prediction layer for analysing the appropriate correlated sensor to build a smart application. So, this work focuses on how to provide semantic interoperability to the Stack4Things infrastructure and to investigate the correlation between sensors, for building simple but effective smart applications.

### 3 Semantic Integration

In this paper, we described the work done to incorporate the semantic layer within Stack4Things and also to provide sensor correlations. In our case, to store the information into Virtuoso RDF storage a Node.js plugin file has been modified so that it can send the RDF data at the same time when it is being sent to the CKAN repository for storage. Thus, it enables us to store real-time data in the RDF format.

Furthermore, to store previous data into the storage, the RDF4J 2.2 Java framework has been exploited. Using this framework the CKAN data has been converted directly into Turtle format and later on inserted into the same storage. We stored the converted file on a monthly basis. For example, “2016-04.ttl” file contains all the sensor information of April 2016. All active board’s information has been collected from the CKAN repository. To access these data using the same vocabularies we modified the SSN ontology by re-using three basic ontologies i.e., DateTime.owl, SSN.owl, wgs84pos.rdf, in the Protege tool. We used URI design specifications for choosing the appropriate URIs for “SmartMe.owl” ontology. After storing this information we are able to extract specific information using SPARQL queries. For example, for a particular board, we can retrieve label of the board, geolocation (latitude, longitude, altitude), Manufacturer name, Model of the board, Time and Date of the deployment. Furthermore, for a particular property of a sensor, the SPARQL query can retrieve boardID, observed value, day of the week, date of observation(YYYY-MM-DD), time of observation (hh:mm:ss), unit of the observation type, geo-location, maximum-minimum observation values for a certain time period, and also, group the sensor data by date, week and month. For example, Fig. 2 retrieved the values of temperature sensor (connected to a specific board) gathered over a certain time period grouped by month. The results of this query has been shown in Fig. 3. Moreover, Figs. 4 and 5 provide the list of the specific boards (i.e. manufacturer

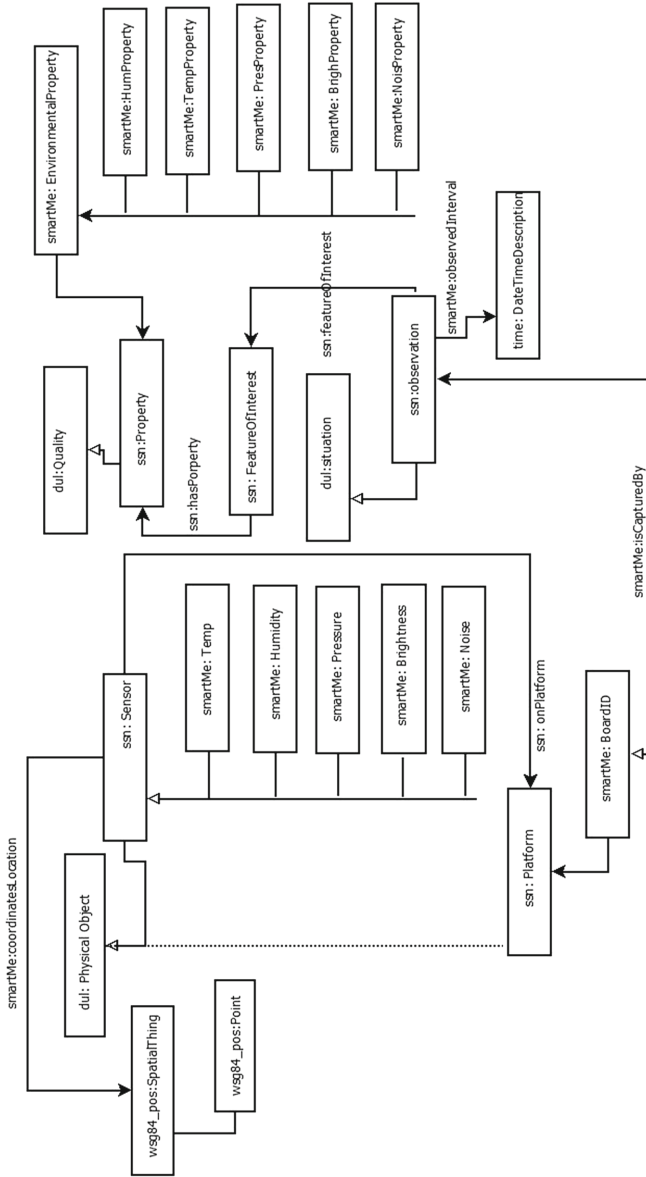


Fig. 1. SmartMe ontology description

= “Arduino” & model = “Yun”) hosting a specific kind (i.e. manufacturer = “Honeywell” & model = “HIH-4030131 Series”) of sensors. As shown in Fig. 1, the ontology has been developed in the Protege tool by integrating DateTime, Geographical ontologies with SSN ontology. The URIs have been selected with the consideration of pattern based ontology design techniques. All the five sensors of #SmartME project are defined as sub-class of the sensor class. The observation property of each sensors is created as a subclass of the Environmental Property of sensor. Sensor observation is related to the time and Date description, for which the vocabulary of DateTime ontology has been exploited. Our SmartME ontology is closely related to the idea described in by Atemezing et al. This modified ontology with the converted data (i.e., inside from CKAN) gets stored in virtuoso RDF storage for querying.

We collected data from 20 Arduino YUN boards, which have been active since May 2016. The data have been converted from Comma Separated Values (CSV) to RDF and stored into the Virtuoso RDF storage. For CSV data generation, Python code is used to automatically fetches data<sup>1</sup> from the CKAN repository and store it into CSV files. These files are then used to generate TTL (Turtle, a RDF serialization) files using RDF4J library. The fields of the CSV file are as follows:

- BoardID
- SensorID
- Observation Type
- Observation Value
- Day of Week
- Date
- Month
- Year
- Hour
- Minute
- Second
- Zone
- Latitude
- Longitude
- Altitude

All the .ttl files and SmartMe ontology have been stored in Virtuoso RDF storage. To insert the real-time data captured by the sensors, we used HTTP POST code<sup>2</sup> inside Node.js plugin file. This Node.js plugin is being used by the Lightning-rod component of the Stack4Things. We stored all the real-time as well previously collected data in “<https://smartMe.linkeddata.org>” graph of Virtuoso RDF Storage. Note that, this graph also contains “smartMe.owl” as well as other required ontologies.

The overall view of the project has been shown in Fig. 6. The figure depicts real-time sensor data being stored in both CKAN and Virtuoso RDF Storage. We converted the already stored CKAN data into RDF format using RDF4J 2.2. It helps us to analyse previously stored data as well. In future we are planning to link data with GeoNames Ontology for further data enhancement. Also, provide an interface with virtuoso global server for user interaction and analysis.

<sup>1</sup> <http://smartme-data.unime.it/organization/smartme>.

<sup>2</sup> <https://virtuoso.openlinksw.com/dataspace/doc/dav/wiki/Main/VirtGraphProtocolCURLEXamples>.

```
PREFIX smartMe: <http://smartMe.linkeddata.org/ontology/>
PREFIX geo: <http://www.w3.org/2003/01/geo/vgs84_pos#>
PREFIX board: <http://smartMe.linkeddata.org/resource/Board/>
PREFIX point: <http://smartMe.linkeddata.org/resource/Point/>
PREFIX prop: <http://smartMe.linkeddata.org/resource/>
PREFIX rdfs: <http://www.w3.org/2000/01/rdf-schema#>
PREFIX time: <http://www.w3.org/2006/time#>
PREFIX ssn: <http://purl.oclc.org/NET/ssnx/ssn#>

select distinct ?BoardName ?latitude ?longitude ?altitude ?dateTime ?day
?Tempvalue
{?board a <http://smartMe.linkeddata.org/ontology/Board>;
  rdfs:label ?BoardName;
  geo:location ?point.
  ?point geo:alt ?altitude.
  ?point geo:lat ?latitude.
  ?point geo:long ?longitude.
  ?observed ssn:observedBy ?board;
  ssn:observedProperty ?property;
  prop:observedInterval ?Time;
  prop:Temp ?Tempvalue.
  ?Time time:hasBeginning ?begins.
  ?begins time:inXSDDate ?dateTime;
  time:inDate ?DataTimeInfo.
  ?DataTimeInfo time:dayOfWeek ?day;
  time:month ?month;
  time:timeZone ?zone.
  FILTER ( ?dateTime <"2017-01-26T23:29:58"^^xsd:dateTime ||
?dateTime>"2016-01-26T23:29:58"^^xsd:dateTime)
} GROUP BY ?month limit 50
```

Fig. 2. Query to fetch Temperature Sensor data over a specific interval

BoardName	latitude	longitude	altitude	dateTime	day	Tempvalue
"Board sme-01-0019"@en	"15.51349528"	"38.16164638"	"142"	2016-04-22T17:29:52	"Tuesday"	16.83293676314554
"Board sme-01-0019"@en	"15.51349528"	"38.16164638"	"142"	2016-11-23T17:33:17	"Wednesday"	17.440052699127705
"Board dip-scienze-co.psi.ped.cul"@en	"15.55599"	"38.19941"	"0"	2016-11-30T17:47:40	"Wednesday"	12.401368164919631
"Board dip-scienze-co.psi.ped.cul"@en	"15.55599"	"38.19941"	"0"	2016-12-01T10:14:59	"Thursday"	14.542305815905252
"Board dip-scienze-co.psi.ped.cul"@en	"15.55599"	"38.19941"	"0"	2016-12-01T10:25:03	"Thursday"	14.542305815905252
"Board dip-scienze-co.psi.ped.cul"@en	"15.55599"	"38.19941"	"0"	2016-12-02T10:39:58	"Friday"	15.63564717789792
"Board dip-scienze-co.psi.ped.cul"@en	"15.55599"	"38.19941"	"0"	2016-12-02T12:00:21	"Friday"	16.919307735293557
"Board dip-scienze-co.psi.ped.cul"@en	"15.55599"	"38.19941"	"0"	2016-12-02T12:20:29	"Friday"	17.789606784575963
"Board dip-scienze-co.psi.ped.cul"@en	"15.55599"	"38.19941"	"0"	2016-12-01T14:46:42	"Thursday"	17.782088493678885
"Board dip-scienze-co.psi.ped.cul"@en	"15.55599"	"38.19941"	"0"	2016-12-02T00:50:20	"Friday"	14.542305815905252
"Board dip-scienze-co.psi.ped.cul"@en	"15.55599"	"38.19941"	"0"	2016-12-03T03:05:48	"Saturday"	14.876948323266106
"Board dip-scienze-co.psi.ped.cul"@en	"15.55599"	"38.19941"	"0"	2016-12-03T03:56:06	"Saturday"	14.209161274117264

Fig. 3. Result of query shown in Fig. 2

```
PREFIX smartMe: <http://smartMe.linkeddata.org/ontology/>
PREFIX rdfs: <http://www.w3.org/2000/01/rdf-schema#>
PREFIX prop: <http://smartMe.linkeddata.org/ontology/>
PREFIX ssn: <http://purl.oclc.org/NET/ssnx/ssn#>

select ?Board {?SensorID prop:model "HHH-4030131 Series"^^xsd:string;
prop:manufacturer "Honeywell"^^xsd:string;
ssn:onPlatform ?BoardID.
?BoardID prop:manufacturer "Arduino";
prop:model "Yun";
rdfs:label ?Board.}
```

Fig. 4. Query to list of specific boards hosting specific kind of sensors

Board
"Board sme-01-0022"@en
"Board rettorato"@en
"Board sme-01-0013"@en
"Board sme-01-0015 - FabLab Messina"@en
"Board facolta-ingegneria"@en
"Board sme-01-0010"@en
"Board sme-01-0021"@en
"Board sme-01-0024"@en
"Board sme-01-0012"@en

Fig. 5. Result of query shown in Fig. 4

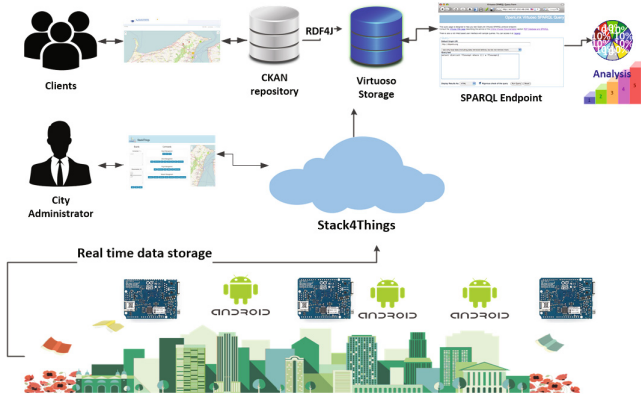


Fig. 6. SmartMe workflow description

## 4 Sensors Correlation Analysis

In this section we describe the correlation analysis among the sensors deployed in the various areas of Messina under the #SmartME project. Our main aim for this analysis is to check, whether the correlation between sensors can assist for predicting the value of unavailable sensor. More specifically, this phenomena can help for building a cost effective Smart city, where huge number of sensors need to be deployed.

The sensors that are important for our analysis are Temperature, Humidity, Pressure. To check the correlation of Temperature sensor with the environmental features captured parallel, we define “Temperature Value” as the predicted attribute (i.e., class label). The attributes for mining are as follows:

- Temperature Value
- Humidity Value
- Pressure Value
- Day of Week
- Date
- Month
- Year
- Hour
- Minute
- Second
- Zone
- Latitude
- Longitude
- Altitude

Random Forest and Linear Regression have been used for checking the accuracy of the model. We have chosen these two algorithms because of their ability to work with numeric class attribute. The algorithms model the data captured by the sensors for predicting the Temperature sensor values. The accuracy/error results with # of Instances has been shown in Table 1. The prediction has been made on the monthly captured different files. It shows the precision of prediction for different subsets of dataset. The correlation column shows the closeness of actual and predicted Temperature sensor’s value. Fourth and fifth columns represent Mean Absolute Error (MAE) and Root Mean Square Error (RMSE) for predicting Temperature Value. Thus, we can say that Random Forest algorithm is independent of number of Instances and worked better then Linear Regression algorithm. The results illustrate that it is feasible to predict a sensor, given the other feature variables i.e. different sensors, specific location (latitude, longitude, altitude, zone), date (Date, Month, Year) and time (Hour, Minute, Second).

We also perform feature selection method to know the important features in the observed data with the “Temperature Value” as a class label. The Correlation-based Feature Selection (CFS) algorithm [3] of feature selection with Greedy Ranker has been used with various subset of datasets. We found for 70% of subsets the algorithm ranked the attributes in following order: Humidity, Latitude, Longitude, Hour, Zone, Altitude, Date, Pressure, Second, Month, Minute, Second, Day of Week. For example, Fig. 7 shows the relationship of Temperature with Humidity & Pressure sensors for a subset of dataset. It shows Humidity is negatively correlated to Temperature while Pressure is constant with varying Temperature. This analysis shows the correlation between different sensors can be exploited for predicting an unavailable(undeployed, failed, broken) sensor.

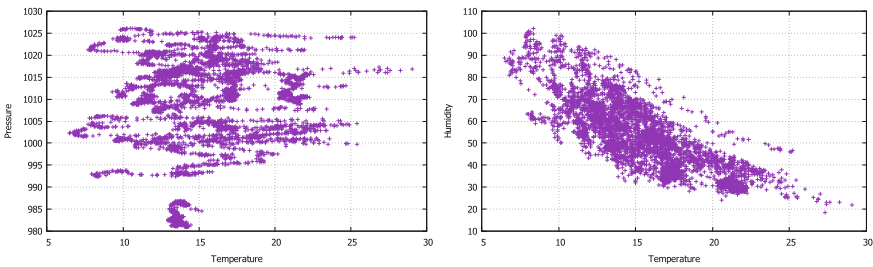


Fig. 7. SmartMe temperature and pressure, humidity correlation



**Table 1.** Analysis on different instances where, # of attributes = 13, Class label = Temperature value

Algorithm	Instances	Correlation	MAE	RMSE
Linear regression	4717	0.8963	1.2638	1.6148
Random forest		0.9943	0.2613	0.3956
Linear regression	4987	0.8835	1.3347	1.7247
Random forest		0.9986	0.185	0.307
Linear regression	7801	0.8354	2.5056	3.1417
Random forest		0.9948	0.4156	0.606
Linear regression	10000	0.8013	1.2437	1.5647
Random forest		0.9786	0.176	0.214
Linear regression	15233	0.9269	0.9901	1.2892
Random forest		0.9969	0.1849	0.2727

This scenario can help in the situation where buying large number of specific sensors would be too costly. Thus, the substitution of a certain subset by other low costly but related sensors would be beneficial in terms of cost effectiveness. It would also help to diagnose the problematic sensor that behaves incorrectly in presence of other sensors.

## 5 Conclusion and Future Work

We proposed a novel approach for converting real-time as well as stored sensor data into RDF format. The #SmartME project infrastructure has been exploited to enable real-time sensor data conversion and storage. The semantic conversion annotates the raw sensor data, provides a unified model for sensors and observations description, and also assists application developer in terms of deep data acquisition as well as quick application building. Also, we observed that correlation between sensors can be leveraged for prediction of data from unavailable sensor. For sensor data prediction we used a data mining tool and analysed the correlation between two sensors and also some environmental parameters. We found that we can rely on the sensor as well as environmental parameters to predict values of specific sensors. In this paper we report some preliminary results of the outgoing work.

## References

1. Bruneo, D., Distefano, S., Longo, F., Merlino, G.: An IOT testbed for the software defined city vision: the # smartme project. In: 2016 IEEE International Conference on Smart Computing (SMARTCOMP), pp. 1–6. IEEE (2016)

2. Consoli, S., Mongiovic, M., Nuzzolese, A.G., Peroni, S., Presutti, V., Reforgiato Recupero, D., Spampinato, D.: A smart city data model based on semantics best practice and principles. In: Proceedings of the 24th International Conference on World Wide Web, pp. 1395–1400. ACM (2015)
3. Han, J.: Data Mining: Concepts and Techniques. Morgan Kaufmann Publishers Inc., San Francisco (2005)
4. Kojima, K.: Prediction of individual thermal sensation using unspecified sensors in sensor networks. In: International Conference on Control, Automation and Systems, ICCAS 2008, pp. 123–126. IEEE (2008)
5. Longo, F., Bruneo, D., Distefano, S., Merlino, G., Puliafito, A.: Stack4things: a sensing-and-actuation-as-a-service framework for IOT and cloud integration. *Ann. Telecommun.* **72**, 1–18 (2016)
6. Maddox, T.: Smart cities: 6 essential technologies (2016). <http://www.techrepublic.com/article/smart-cities-6-essential-technologies/>. Accessed 26 Mar 2017
7. Neuhaus, H., Compton, M.: The semantic sensor network ontology. In: AGILE Workshop on Challenges in Geospatial Data Harmonisation, Hannover, Germany, pp. 1–33 (2009)
8. Pfisterer, D., Romer, K., Bimschas, D., Kleine, O., Mietz, R., Truong, C., Hasemann, H., Kröller, A., Pagel, M., Hauswirth, M., et al.: Spitfire: toward a semantic web of things. *IEEE Commun. Mag.* **49**(11), 40–48 (2011)
9. Ploennigs, J., Schumann, A., Lécué, F.: Adapting semantic sensor networks for smart building diagnosis. In: Mika, P., Tudorache, T., Bernstein, A., Welty, C., Knoblock, C., Vrandečić, D., Groth, P., Noy, N., Janowicz, K., Goble, C. (eds.) ISWC 2014. LNCS, vol. 8797, pp. 308–323. Springer, Cham (2014). doi:[10.1007/978-3-319-11915-1\\_20](https://doi.org/10.1007/978-3-319-11915-1_20)
10. Ploennigs, J., Schumann, A., Lecue, F.: Extending semantic sensor networks for automatically tackling smart building problems. In: Proceedings of the Twenty-first European Conference on Artificial Intelligence, pp. 1211–1212. IOS Press (2014)
11. Sheth, A., Henson, C., Sahoo, S.S.: Semantic sensor web. *IEEE Internet Comput.* **12**(4), 78–83 (2008)
12. Wei, W., Barnaghi, P.: Semantic annotation and reasoning for sensor data. In: European Conference on Smart Sensing and Context, pp. 66–76. Springer (2009)

# A Fuzzy Prolog and Ontology Driven Framework for Medical Diagnosis Using IoT Devices

Beniamino Di Martino<sup>(✉)</sup>, Antonio Esposito, Salvatore Liguori,  
Francesco Ospedale, Salvatore Augusto Maisto, and Stefania Nacchia

Università degli Studi della Campania “Luigi Vanvitelli”,  
via Roma 4, 81031 Aversa, Italy  
beniamino.dimartino@unina.it,  
{salvatore.liguori,francesco.ospedale}@studenti.unina2.it,  
{antonio.esposito,salvatoreaugusto.maisto,  
stefania.nacchia}@unicampania.it

**Abstract.** Advances in medical care and computer technology in recent decades have expanded the parameters of the traditional domain of medical services. This scenario has created new opportunities for building applications to provide enterprise services in an efficient, diverse and highly dynamic environment.

Moreover the IoT revolution is redesigning modern health care with promising technological prospect and has made IT-based healthcare systems expensive, competitive and complex. Their complexity is also enhanced by the use of semantic models which allow the detection and prediction of a patient health anomalies and the therapy management is produced accordingly.

In this paper will be presented a prototypical framework that, starting from the stream analysis and processing coming from wearable devices, tries to detect the possible health anomalies in real time and, through a heuristic and ontology-driven approach capable of reasoning on the patient's conditions, it gives hints about possible diseases that are currently going on.

## 1 Introduction

The healthcare domain is a big and significant area where people, different organizations and various institutions get services as well as provide services at the same time. It is one of the few areas that have a huge amount of domain knowledge. A significant part of this knowledge is composed of the data that is produced by the medical devices and sensors. The ever-growing environment of IoT makes the continuous monitoring and assisting of a patient possible even if they are not at the hospital or in whatever healthcare structure. The devices are capable enough to transmit vital sign data from a patient's home to the hospital staff, allowing them to have a real time monitoring of patient's health. These devices use wirelessly connected *glucometers*, *scales*, *heart rate* and *blood pressure* monitors. The best feature of all these devices is the possibility to wear them, to have them monitoring the person who's wearing them 24/7.

Accordingly to this way of handling healthcare new software architectures, data model, middlewares have expanded significantly and, as a consequence, the number of applications based on the IoT has boomed as well. These applications have some unique characteristics: they are autonomous in their data capture patterns, have event transferring capabilities and provide strong interoperability or network connectivity. Due to these specific features (ubiquity, pervasiveness, miniaturization of components, etc.) researchers and engineers are constantly pushing the boundaries of technology creating applications that have a real and concrete impact on the cure and well-being improvement of the patients.

However just the real-time analysis of the data coming from the sensors and devices sometimes may not be enough for having a complete clinical picture of a patient, therefore many applications, that will be presented in following sections, are integrated with a semantic inference engine that allows a more precise and early detection of possible symptoms and provides a basic understanding of the concepts that serve as building blocks for further processing.

In this paper we focus on the description of the methodology and the subsequent prototypical framework developed with the objective of detecting anomalies in the data coming from wearable e-health sensors and devices and associates these anomalies with possible symptoms, and then making a list of possible diseases using fuzzy logic techniques and ontology-driven approach capable of reasoning on the patient's conditions.

The remainder of the paper is structured as follows: in Sect. 2 we present the various works related not only to the semantic based technologies used in healthcare scenarios. In Sect. 3 an overview of the whole architecture is given, with a focus on the knowledge base used underneath the framework; Sect. 4 deals with the core component and processing phase of the framework, and at last, some considerations and an outlook on future research will be presented in Sect. 5.

## 2 Related Work

The thriving interest towards the Internet of Things has caused a rapid development of related technologies in all sectors of Human activities. The Health-care has been among the faster to adopt IoT technologies. Smart sensors and connected Health devices have been largely applied to provide interesting medical-oriented services, and many studies and researches have been carried out on the topic.

**Wearable Devices** represent an important resource for IoT based health-care services. Such devices are light, non-intrusive, generally cheap and provide a large amount of functions (pulse detection, temperature sampling, movement) which all represent interesting characteristics. The work presented in [3] provides an integrated solution, based on sensors communicating on a wireless network, which supports health-care applications. Software applications for the remote monitoring of patients, based on mobile devices and connected wearables, have been also proposed and applied to real test cases, such as the one proposed in [15].

**Ambient Assisted Living** (AAL) is probably the most noticeable class of Health services based on IoT technologies. With this term, we refer to specialized IoT platforms, supported by artificial intelligence, that are able to address the health care of elders or people with limited capabilities to move. In [16] the authors propose an interesting AAL framework, based on an IoT architecture which covers several aspects of sensors' orchestration, such as automation, security, control, and communication. The architecture includes algorithms that, based on existing medical knowledge, detect health problems in elderly people.

A similar goal is pursued by the platform described in [7] where the authors describe an IoT platform for the detection and monitoring of adverse reactions to drug assumptions. The system, which falls in the **Adverse Drug Reaction** (ADR) class, analyses the patients' general conditions during the drug assumption and try to detect anomalies which can be related to the specific medication. A database of potential allergic reactions and the medical history of the patients (previous allergies, intolerance to specific components, concurrent maladies) are combined with the data coming from sensors to determine adverse reactions before the drug assumption.

One crucial aspect that all Health-care services need to address is represented by the vast amount of maladies and related symptoms which should be considered during the monitoring of a patient's vitals. Indeed, while the detection of symptoms is important, the identification of the proper malady is even more crucial. Ontologies and semantics have been largely apply to describe both symptoms and maladies, and to determine connections among them [2]. A semantic medical monitoring system based on IoT sensors has been proposed in [18], while in [17] the authors describe a ubiquitous data-accessing method to collect, integrate, and interoperate IoT data for emergency medical services, based on a semantic knowledge base.

The approach described in the present paper takes in consideration several of the aspects described here, starting from the use of Wearable Devices to collect data streams regarding patients' health status, and arriving to the application of semantic web technologies to relate symptoms to potential maladies.

### 3 Architecture Overview

The architecture presented in this section highlights the most important components of the framework that has been realised and also how and according to which format the data is exchanged between the various components. The components that are described are hardware appliances and devices as well as software tools, and they communicate and cooperate to make the diagnosis. The architecture is composed of four main components:

- **Smart Wearable Sensors:** this level represents the base of the whole architecture.
- **Knowledge Base:** the knowledge base is a composition of various medical ontologies and is handled by an ad-hoc component.



*muscle electromyography signals, glucose levels etc.* These broad sensing portfolio makes MySignals the most complete eHealth platform in the market.

All the data gathered by MySignals is encrypted and sent to the user's private account at Libelium Cloud through WiFi or Bluetooth. Data can be stored in the Libelium Cloud or being sent to a third party Cloud Server. The data can be visualized in a tablet or smart phone with Android or iPhone Apps. Libelium offers also two different API's for developers to access the information. The Android/iOS API allows to get information directly from MySignals using Bluetooth Low Energy (BLE). The Cloud API allows to access to the user's private account and get the information previously stored to be visualized in a third party platform [1].

Data can be visualized in standalone mode, sent to the Cloud in order to perform permanent storage or visualized and stored in real time by sending the data directly to a Smartphone.

### 3.2 Knowledge Base

In order to process the data generated by wearable sensors, context information models are needed, and context information models are defined by using one of the most effective method among the model representation methods: *Ontologies* [8]. Ontologies can be used to store semantic concepts that represent phenomena and attributes from the real world that are understandable for the human user but also interpretable by machines due to the standardized data representation. The concepts can be linked together through relationships that express interactions and dependencies between the concepts.

Of course there are thousand of possible ontologies that could be used, but the context of the project is clear thus it has been easy to identify the ontologies that could exhaustively represent the needed data set. More important, after much considerations, we came to the conclusion that there are two fundamentals dimensions that need to be considered: a *structural* dimension, which semantically represent the data coming from the sensors, and the *domain* dimension which concerns the medical meaning of the data that is processed, but there are two distinct domain context in this scenario. As the main idea is to identify a series of symptoms in the data coming from the devices, one domain ontology necessarily has to describe the concepts of symptoms in a medical fashion, and moreover, these symptoms has to be associated to one or more possible diseases, and this is the other domain that has to be semantically described. Keeping this in mind, the knowledge base built for this framework is composed of three ontologies, the first represents the structural dimension and the two left represent the medical context:

- *Sensor Network*
- *Human Disease*
- *Symptoms*

### *Semantic Sensor Network Ontology*

The W3C Semantic Sensor Network Incubator Group has introduced the semantic sensor network (SSN) ontology [5] that provides a model to annotate sensors and their metadata and gathered data. The SSN ontology uses semantic concepts to model the physical attributes of sensor networks such as “sensor device”, “temperature sensor”, and “radio link”. Properties in the SSN model the relationship between concepts such as “occurredAt”, “observedBy” to relate sensor data annotations to domain models. We use the SSN ontology as a starting point for our method and correlate the data coming from the sensors to the actual medical concepts expressed in the domain ontology.

### *Disease Ontology*

Organising diseases in an ontology hierarchy is extremely useful as it forms a pathological classification of diseases for use in medical systems. Such an undertaking is massive given the number of known human diseases, let alone this ontology has to be updated as time passes and more diseases develop and are discovered. The most prominent disease ontology developed to date is the Human Disease Ontology (DOID). Started in 2003 as part of the NUGene project at Northwestern University, it has been published in several versions over several years and contains to this date over 8600 known human diseases and 14,600 terms. DOID is currently a standard ontology adopted by the OBO Foundry [14].

### *Symptoms Ontology*

Symptom Ontology (SYMP) was developed in 2005 by the Institute for Genome Sciences (IGS) at the University of Maryland. Today it contains more than 900 symptoms. SYMP’s hierarchy categorizes symptoms under certain headings for example categorizing all types of pain (arm, leg, headache, back pain, chest pain, etc.) under physical pain [14].

Currently, there is no ontology that defines disease class hierarchies, symptom class hierarchies, and establishes relations between disease and symptom classes. Such ontology would be very useful for diagnosis recommendation systems. There are in-progress attempts to modify the human disease ontology to include symptoms and relations between those symptoms to diseases. Also, there were models proposed for such undertaking. GHDO [6] proposes an ontology model that relates diseases to symptoms (phenotypes) and to the other three elements that uniquely identify a disease: disease type, causes, and treatment. However, no GHDO ontology has been published from the proposed model.

In order to obtain a common knowledge base where all the data can be semantically stored we have used the *Diseases and Symptoms Ontology (DSO)* [10], in which establishing relations between symptoms classes and diseases classes is done by defining a *has\_symptom* object property. The domain of the property is the set of diseases classes and the range is the set of symptoms classes. In the diagnosis process, each disease is known to have a number of symptoms. Correspondingly in DSO, each disease class needs to have a number of *has\_symptom* properties where each property links the disease class to one of its symptoms classes.



Once the knowledge base is built the next component is the core that handles the processing of the data; since this is the core component of the whole framework, the next section exhaustively explains how it has been developed and its main purpose.

## 4 The Processing

The processing phase, which is implemented and realized by the core component of the architecture presented in the previous section, is composed of three steps:

- Filtering phase
- CEP recognition phase
- Analysis phase

The first two phases have been implemented using the functionality provided by the Apache Flink® platform. The third using a probabilist inference engine developed in Prolog. Apache Flink® is an open-source stream processing framework for distributed, high-performing, always-available, and accurate data streaming applications. Thanks to Apache Flink® platform it has been possible to acquire different data streams, coming from the various sensors, and to perform a filtering in order to exclude non-relevant data to the next stages of the analysis. To perform this filtering for each sensor a value has been chosen, in a heuristic manner, which identifies a sort of threshold, if the measured value goes beyond the threshold value it indicates that there could be an anomaly in the patient's current health state. Once the different datasets have been limited, technically we have a series of anomalies that could very well be a clear evidence of an ongoing disease or they could be just some isolated events not due to a specific disease. Thus the next steps are about identifying specific event patterns that could lead to first an identification and categorization of symptoms and, later on, to the diagnose of a disease. The pattern defined in this scenario consists of two following events recognised during a time window of 10 seconds. The individual events were identified as the occurrence of the threshold crossing, as described above, the value of the sensor measurement. Once the pattern has been recognized, a corresponding symptom is instantiated in the DSO ontology. At this point the inference engine is started; this process retrieves all individuals corresponding to the ongoing symptoms and in a probabilistic manner makes possible diagnosis of ongoing diseases.

It is quite clear that system theoretic, analytic solutions to the problems of medical diagnosis are very hard to find. On the other hand, the intelligence of a human diagnostician is sufficient to achieve satisfactory results in the vast majority of diagnostic problems posed. Certainly, this performance cannot be explained by non-reproducible processes such as guessing or intuition. There must be some structure to diagnosis susceptible to formalization and automated reproduction. Generally there are two basic approaches to diagnosis. One, referred to as heuristic diagnosis, is associative in nature and relies on the formalized experience of experts in the field. The other, called model-based diagnosis, builds on a deeper

understanding of the matter of discourse and uses models to reproduce the diagnosed subject's behaviour. The former is an attempt to reverse the physiologic cause-effect relationships directly, while the latter tries to derive the observed symptoms from hypothesized diagnoses, simulating the known relationships and so determining the cause indirectly. It is not difficult to see how fuzzy set theory can help with heuristic diagnosis. Every trustworthy expert knows that his/her medical knowledge and the resulting diagnoses are pervaded by uncertainty. Uttered expert knowledge therefore abounds with imprecise formulations. This imprecision is not a consequence of rhetorical inability, but an intrinsic part of expert knowledge acquired through laborious experience. Any formalism disallowing uncertainty is therefore inapt to capture this knowledge stripping it of its uncertainty entails the danger of fallacies due to misplaced precision. Fuzzy set theory on the other hand was conceived with the formalization of vague knowledge in mind. Together with appropriate rules of inference it provides a powerful framework for the combination of evidence and deduction of consequences based on knowledge specified in syllogistic form.

The workflow of the diagnosis articulates as follows:

- Probabilistic assessment of symptoms with fuzzy techniques: for each symptom a *Truth Function* has been defined, starting from the value measured by the device. This *Truth Function* has been transformed in a *Prolog Fact* and it indicates the probability that a specific symptom has occurred. The truth value is obtained by the evaluation of the predicate *symptom\_value*, this is done for each possible symptom.
- Probabilistic assessment of diseases with Bayes' theorem: the inference and subsequent probabilistic assessment is realized through the Bayes's theorem, which describes the probability of an event, based on prior knowledge of conditions that might be related to the event.

Once the fuzzification step has been completed, we make the assumption that there isn't a correlation between the symptoms involved in a disease, and that each symptom is tied to every single disease by a *weight function*, using the Bayes' theorem, it is possible to state that:

$$P(D_i|R_k) = P(D_i|S_1) * P(D_i|S_2) * \dots * P(D_i|S_k) = W_{i1} * W_{i2} * \dots * W_{ik}$$

where  $P(D_i|R_i)$  is the probability of occurrence of the disease  $D_i$  given the set of symptoms  $R_k$ ,  $P(D_i|S_k)$  is the probability of occurrence of the disease  $D_i$  given the symptom  $S_k$  and  $W_{ik}$  is the weight associated between the symptom  $S_k$  and the disease  $D_i$ .

- Defuzzification: this is when the actual diagnosis is made; after each disease probabilistic value is calculated according to the Bayes' theorem, each and every one of this symptom is compared with a threshold value, heuristically defined. If the disease probabilistic values exceeds the threshold, then we can infer that a specific disease is occurring.

## 5 Conclusions

This paper has outlined a new approach to medical diagnosis based on fuzzy prolog techniques. This diagnosis is implemented and supported by an underlying framework that combines the most recent technologies that are changing the healthcare environment: IoT and Data Analytics. The framework here presented exploits the best features of wearable IoT devices to support real-time monitoring and tries to correlate every information and data coming from the devices in a semantic and context-aware manner through the use of an extensive knowledge base, built according to the most used de-facto standard in both IoT and medical field. Of course there are plenty of possibilities for improving the whole framework, e.g. using natural language processing to automatically instantiate the individuals in the DSO ontology, or extending the framework to new wearable devices.

## References

1. Mysignals. <http://www.my-signals.com/>
2. Burgun, A., Botti, G., Fieschi, M., Le Beux, P.: Sharing knowledge in medicine: semantic and ontologic facets of medical concepts. In: 1999 IEEE International Conference on Systems, Man, and Cybernetics, SMC 1999, vol. 6, pp. 300–305 (1999)
3. Castillejo, P., Martinez, J.F., Rodriguez-Molina, J., Cuerva, A.: Integration of wearable devices in a wireless sensor network for an e-health application. *IEEE Wirel. Commun.* **20**(4), 38–49 (2013)
4. Chan, M., Estève, D., Fourniols, J.-Y., Escriba, C., Campo, E.: Smart wearable systems: current status and future challenges. *Artif. Intell. Med.* **56**(3), 137–156 (2012)
5. Compton, M., Barnaghi, P., Bermudez, L., García-Castro, R.L., Corcho, O., Cox, S., Graybeal, J., Hauswirth, M., Henson, C., Herzog, A., et al.: The SSN ontology of the W3C semantic sensor network incubator group. *Web Seman. Sci. Serv. Agents World Wide Web* **17**, 25–32 (2012)
6. Hadzic, M., Chang, E.: Ontology-based multi-agent systems support human disease study and control. *SOAS* **135**, 129–141 (2005)
7. Jara, A.J., Belchi, F.J., Alcolea, A.F., Santa, J., Zamora-Izquierdo, M.A., Gmez-Skarmeta, A.F.: A pharmaceutical intelligent information system to detect allergies and adverse drugs reactions based on internet of things. In: 2010 8th IEEE International Conference on Pervasive Computing and Communications Workshops (PERCOM Workshops), pp. 809–812, March 2010
8. McGuinness, D.L., Van Harmelen, F.: Owl web ontology language overview. W3C recommendation 10.10 (2004)
9. Mezghani, E., Exposito, E., Drira, K., Da Silveira, M., Pruski, C.: A semantic big data platform for integrating heterogeneous wearable data in healthcare. *J. Med. Syst.* **39**(12), 185 (2015)
10. Mohammed, O., Benlamri, R., Fong, S.: Building a diseases symptoms ontology for medical diagnosis: an integrative approach. In: 2012 International Conference on Future Generation Communication Technology (FGCT), pp. 104–108. IEEE (2012)

11. Raskovic, D., Martin, T., Jovanov, E.: Medical monitoring applications for wearable computing. *Comput. J.* **47**(4), 495–504 (2004)
12. ABI Research: Wearable sports and fitness devices will hit 90 million shipments in 2017 (2012). <https://www.abiresearch.com/press/wearable-sports-and-fitness-devices-will-hit-90-mi/>
13. Saponas, T.S., Lester, J., Hartung, C., Kohno, T.: Devices that tell on you: the nike+ipod sport kit (2006)
14. Schriml, L.M., Arze, C., Nadendla, S., Chang, Y.-W., Mazaitis, M., Felix, V., Feng, G., Kibbe, W.A.: Disease ontology: a backbone for disease semantic integration. *Nucleic Acids Res.* **40**(D1), D940–D946 (2012)
15. Sebestyen, G., Hangan, A., Oniga, S., Gl, Z.: ehealth solutions in the context of internet of things. In: 2014 IEEE International Conference on Automation, Quality and Testing, Robotics, pp. 1–6, May 2014
16. Shahamabadi, M.S., Ali, B.B.M., Varahram, P., Jara, A.J.: A network mobility solution based on 6lowpan hospital wireless sensor network (NEMO-HWSN). In: 2013 Seventh International Conference on Innovative Mobile and Internet Services in Ubiquitous Computing, pp. 433–438, July 2013
17. Xu, B., Xu, L.D., Cai, H., Xie, C., Hu, J., Bu, F.: Ubiquitous data accessing method in iot-based information system for emergency medical services. *IEEE Trans. Industr. Inf.* **10**(2), 1578–1586 (2014)
18. Zhang, G., Li, C., Zhang, Y., Xing, C., Yang, J.: Semanmedical: a kind of semantic medical monitoring system model based on the IoT sensors. In: 2012 IEEE 14th International Conference on e-Health Networking, Applications and Services (Healthcom), pp. 238–243, October 2012

# Plug'n'play IoT Devices: An Approach for Dynamic Data Acquisition from Unknown Heterogeneous Devices

Argyro Mavrogiorgou<sup>(✉)</sup>, Athanasios Kiourtis,  
and Dimosthenis Kyriazis

Department of Digital Systems, University of Piraeus, Piraeus, Greece  
{margy, kiourtis, dimos}@unipi.gr

**Abstract.** The Internet of Things (IoT) is being hailed as the next industrial revolution and promises billion of IoT devices connected to the Internet in the near future. Emerging back-end support technologies not only have to anticipate this dramatic increase in connected devices, but also the heterogeneity of devices. This paper proposes a comprehensive approach for efficiently and rapidly integrating heterogeneous devices during runtime, in order to collect data. The proposed approach identifies both known and unknown devices' specifications and Application Programming Interfaces (APIs), classifies the specifications and illustrates the APIs into ontologies, while the latter are being mapped in combination with the classification's results to match the known with the unknown devices' APIs. All of these steps are being performed as preliminary steps for the proposed Dynamic Data Acquisition API, which is the final outcome of the mechanism that is responsible for translating the devices' APIs into a common format.

## 1 Introduction

Internet of Things (IoT) has multiple definitions [1, 2] by different organizations. However, all of them agree that IoT has emerged as a paradigm in which smart things actively collaborate among them, with other physical and virtual objects available in the Web in order to perform high-level tasks [3]. In other words, IoT mainly aims to interconnect everyday life items, by providing them with information processing capabilities in order to be able to sense, integrate, present, and react to all the aspects of the physical world [4]. It is an undeniable fact that IoT is nowadays growing exponentially together with the number of solutions and architectures proposed to handle it [5]. According to Machina Research [6], the total number of connected devices is expected to be 27 billions by 2024, while the total revenue opportunity is predicted to be up to \$1.6 trillions. Thus, it becomes clear that the number of devices is growing rapidly, resulting in a myriad of heterogeneous devices that will be connected to the IoT world in the near future.

More particularly, IoT devices such as mobile phones, wearable devices, monitoring sensors, actuators, etc., are typically characterized by a high degree of heterogeneity, in terms of having different capabilities, functionalities, and network protocols.

In such a scenario, it is necessary to provide abstractions for IoT devices and services to applications and end-users, as well as means to manage the interoperability between such heterogeneous elements [3]. To this end, the task of managing such an enormous number of heterogeneous devices that include their own software and hardware specifications and interfaces is very challenging [7]. In that case, the IoT promises to cope with this challenge by facilitating automatic interaction and access to all these devices [8]. This will enable the development of systems and applications that can explore and manage the diversity of these devices [9], regardless of each application's domain, such as home automation, intelligent energy management and smart grids, e-health management, traffic management, etc. [10, 11]. As a result, IoT developers should be able to build applications based on heterogeneous data independent of hardware and software capabilities, as well as dynamic mechanisms to rapidly integrate previously unknown devices during runtime [12]. However, existing integration technologies lack sufficient flexibility to adapt to these changes, as the techniques used for integration are both static and sensitive to new or changing device implementations and requirements [13]. Consequently, devices' integration is a very challenging research topic in the IoT area.

To address this challenge, in this paper a comprehensive approach is proposed that can be used to dynamically integrate both known and unknown devices during runtime, by providing a Dynamic Data Acquisition API, for efficiently supporting heterogeneous devices for being dynamically inherited into IoT environments and offer their data, without the need for application-level programming.

This paper is organized as follows. Section 2 describes the study of the state of the art regarding devices integration, while compares the existing approaches with our proposed approach. Section 3 describes the developed mechanism for integrating heterogeneous devices into an IoT platform, while Sect. 4 is addressing the future challenges, analyzing our conclusions and future plans.

## 2 Related Work

Regardless of the way in which devices are connected to the IoT, they should be uniformly discoverable and integrated with different platforms and systems, in order for the latter to have access to the devices' data and gain value out of it. To this concept, various IoT infrastructures have been proposed in the literature, putting their efforts on the integration of heterogeneous devices in order to be interoperable and pluggable to different IoT platforms and systems, while offering their data.

In this domain, SIGHTED [12] proposes a way to collect and provide uniform access to multiple heterogeneous devices' data, based on semantic web and linked data principles. In [14], the proposed framework converts sensor data into Resource Description Framework (RDF) and linked to existing data on Linked Open Data (LOD) cloud, whilst a sensor ontology schema based on O&M concepts is used with links to GeoNames [15] dataset for location properties. Trends of publishing sensor data on the LOD cloud are also discussed in [16], in order to improve accessibility without increasing complexity of solutions, while the authors in [17] support semantic sensor discovery without exploiting hierarchical and structured relations. Sense2Web [18] is

proposed as a platform that captures basic attributes of sensors in RDF using available linked data to create links to other resources, where sensor descriptions are manually submitted and stored in XML format to be transformed into RDF, and models these resources using ontologies linked to GeoNames and QU ontology [19]. SEMSENSE [20] is a system for collecting and publishing sensor data of just one single data source, by semantically enriching sensor data residing in MySQL database, based on manual mapping to SSN ontology concepts [21]. What is more, ContQuest [8] is a framework that among its functionalities, defines a development process for integrating new data sources including their data description and annotation, by using the Ontology Web Language (OWL) [22] to model and describe data sources. The proposed approaches in [23–26] cope with the frequent modification of data source's schemas, by providing homogeneous views of various data sources based on a domain ontology [13]. Furthermore, [27] presents an ontology based on data integration architecture within the context of the ACGT project, where emphasis is given to resolve syntactic and semantic heterogeneities when accessing integrated data sources. SPOT [28] proposes a smart-home platform built on a dynamic XML device driver abstraction model that tackles the aspects of data sources' heterogeneity, by offering an abstraction layer to realize an open, and unified API, while EcoDiF [3], in the same concept, proposes a Web-based platform for integrating heterogeneous devices with applications and users so as to provide services for real-time data control, visualization, processing, and storage. Furthermore, Xively [29] is a cloud based IoT platform for managing data derived from various devices, by providing a RESTful API for getting this data, visualizing it, and providing mechanisms to trigger events based on it, whilst S<sup>3</sup>OIA [30] is a service-oriented architecture for integrating various devices in the IoT context, by using a tuple space approach [31] to semantically express information about the devices integrated into the platform.

All of the aforementioned approaches have proposed several features regarding the integration and interoperability among heterogeneous data sources/devices, whilst most of them have identified ontologies as one of the basic technologies for the achievement of devices' integration. However, none of these implementations uses methods for efficiently and rapidly integrating heterogeneous devices during runtime, in order to gather data. As a result, all these approaches lack of sufficient flexibility and adaptability to solve challenges arisen from dynamically integrating both known and unknown devices during runtime. For that reason, in our approach an innovative mechanism is proposed, for integrating both known and unknown devices during runtime, by initially identifying the devices' software and hardware specifications and Application Programming Interfaces (APIs). In the next step, the classification of these specifications occurs, where according to the classification's results, mapping mechanisms are being applied to the APIs to match the known devices' and the unknown devices' data methods accordingly, that are responsible for gathering data. Based on these steps, a *Dynamic Data Acquisition API* is proposed, for efficiently supporting heterogeneous devices to be dynamically inherited into IoT environments and offer their data without the need for application-level programming.

### 3 Proposed Approach

In our approach, an innovative mechanism is proposed for easily and rapidly integrating heterogeneous devices during runtime, concerning both known and unknown devices, in order to be able to collect data out of them. More specifically, our approach consists of three (3) different stages. In the first stage the identification of both known and unknown *devices' specifications* (i.e. software and hardware specifications) and APIs takes place. Afterwards, in the second stage a classification mechanism is proposed, that is responsible for classifying devices' specifications based on "existing" (in terms of already defined APIs) devices' specifications. Finally, in the third stage, the devices' APIs are being illustrated into ontologies, which are being mapped in combination with the classification's results, so as to match the known with the unknown *devices' APIs data methods* (i.e. methods that are responsible for collecting data from each device). All of the aforementioned stages are being performed as preliminary steps for the proposed *Dynamic Data Acquisition API*, which is the final outcome of the mechanism, and responsible for translating the devices' APIs into a common format.

It should be noted that the proposed mechanism requires prior knowledge of the used devices, as for the (i) transmitted data format (e.g. csv/xml/xls files), (ii) APIs (i.e. source code), and (iii) specifications (i.e. hardware and software specifications) that will contain the same semantics in terms of specifications' descriptions and measurement units. What is more, it is assumed that the incoming devices that will be connected to the IoT platform are always reliable, whilst the network connection between the devices and the IoT platform is considered as out of scope concerning our approach. For that case, it is assumed that all the available devices allow remote control via HTTP over Wi-Fi, by exchanging JSON messages for this communication.

As depicted in Fig. 1, the architecture is composed of three (3) main stages:

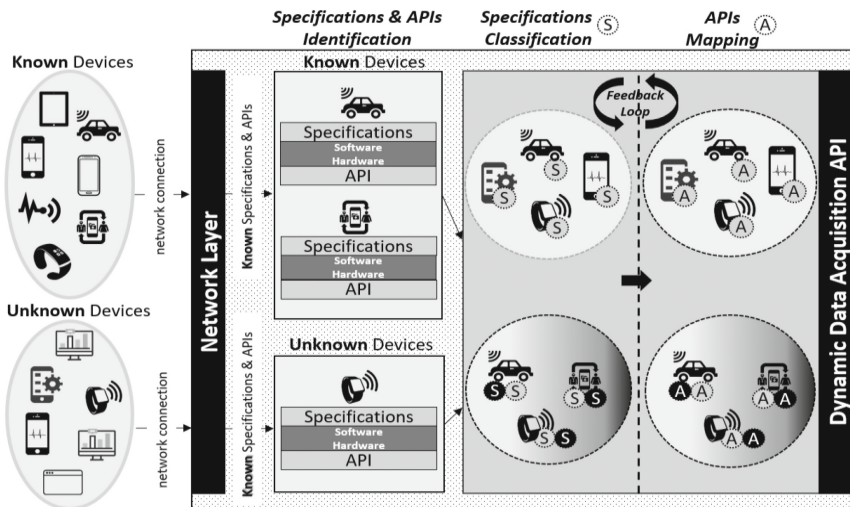


Fig. 1. Overall architecture of the developed mechanism



*Specifications & APIs Identification:* In the first stage of the developed mechanism, the identification of the various available devices (e.g. sensors, (mobile) applications, tablets, watches, etc.) that collect real-time data, takes place. Initially, the various devices are discovered and categorized into either known (in terms of predefined APIs methods) or previously unknown (in terms of undefined APIs methods) devices. Afterwards, all these devices are connected via the interface that is provided by the existing network layer to the IoT platform. It is assumed that this network layer is providing an interface to the various devices, thus being responsible for collecting general information from them, concerning both *devices' specifications* (i.e. hardware and software) and APIs (i.e. multiple methods). Therefore, information is gathered about (i) both known and unknown devices' specifications, (ii) known devices' APIs, not only in terms of source code, but also in terms of what exactly each method in the API represents, and (iii) unknown devices' APIs, only in terms of source code, as the representation of each method in the API is unknown.

*Specifications Classification:* In the second stage of the developed mechanism, the classification of the *devices' specifications* occurs. More particularly, knowing all the devices' (i.e. both known and unknown) specifications (e.g. brand, model, memory, etc.), these are classified according to the similar specifications they have, applying Multi-Class Linear Support Vector Machines (SVM) [32], along with the Bag of Words model [33], tuned properly. Such method was implemented, as it is a general technique that can be applied to a wide range of problems, providing accurate results. As a consequence, based on the classification's outcomes, it is possible to match the devices' APIs, assuming that the devices with the same specifications will have the same APIs. To this end, as depicted in Fig. 2, two (2) potential scenarios arise:

1<sup>st</sup> Scenario: The available known and unknown devices may have exactly the same specifications. After classifying them, it is observed that each device is classified into a single classification group (*one-to-one scenario*). For example, suppose that device A is a known device and device C is an unknown device, but they both have the same specifications. By applying the classification algorithm into their specifications, it is observed that these devices belong to the same classification group, as they have exactly the same specifications.

2<sup>nd</sup> Scenario: The available known and unknown devices may have partial specifications in common. After classifying them, it is observed that some devices may belong to one or more classification groups, having common specifications with one group of devices, while also having common specifications with a different group of devices (*one-to-many scenario*). For example, suppose that device A and device B are both known devices with different specifications, while device C is an unknown device, having some common specifications with device A and some other common specifications with device B. By applying the classification algorithm into these specifications, it is observed that device C belongs both to the same classification group with device A and to the same classification group with device B, as device C has some partial specifications of the same nature with the two devices (i.e. A and B).

*APIs Mapping:* The third stage of the developed mechanism is the pivotal stage of the mechanism, where the mapping of the APIs takes place. More particularly, according

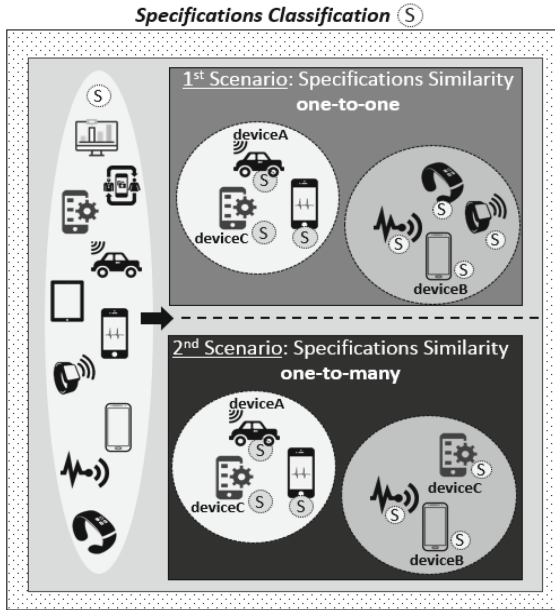


Fig. 2. Specifications classification stage

to the outcomes of the categorized devices' specifications into classification groups, the devices' APIs are mapped to match the different *APIs data methods* (i.e. methods that are responsible for collecting data from devices). In order to achieve this mapping, for each device's API, a Generic API Ontology is constructed, based on the approach proposed in [13], which is used to declaratively model the semantics of the devices' APIs and achieve the maximum level of their expressivity. Additionally, this approach is also based on [34–37], where ontologies are used for representing and processing the content of the data. In our case, each device's API methods are illustrated into a Generic API Ontology, adding semantic tags to the device's API in order to describe its methods in a meaningful standardized way, thus allowing to integrate and map diverse APIs. As a result, the known *APIs' data methods* will be able to be finally mapped with the unknown *APIs' data methods*. All of the aforementioned Generic API Ontologies are built through OWL, which is the current W3C recommendation for the exchange of semantic content on the Web, while their development and maintenance is implemented using the Protégé editor [38]. In more details, in the *Specifications & APIs Identification* stage, knowledge about known devices' APIs was acquired, not only in terms of source code, but also in terms of what exactly each method in the API represents. However, with regards to the unknown devices' APIs, the acquired knowledge referred only to the source code, as the representation of each method in the API was unknown. Consequently, by mapping all the devices' (i.e. both known and unknown) APIs through their illustration into different Generic API Ontologies, as well as by exploiting the classification's outcomes from the *Specifications Classification* stage, the developed mechanism concludes to the final APIs' mapping, where the

devices with the same specifications will result into having the same APIs. Thus, the data methods of the known devices' APIs source code (in terms of meaning) will result in the recognition of the data methods in the unknown devices' APIs source code, which were unknown before that step. To this end, as depicted in Fig. 3, two (2) potential scenarios arise, considering the two (2) different scenarios raised in the *Specifications Classification* stage:

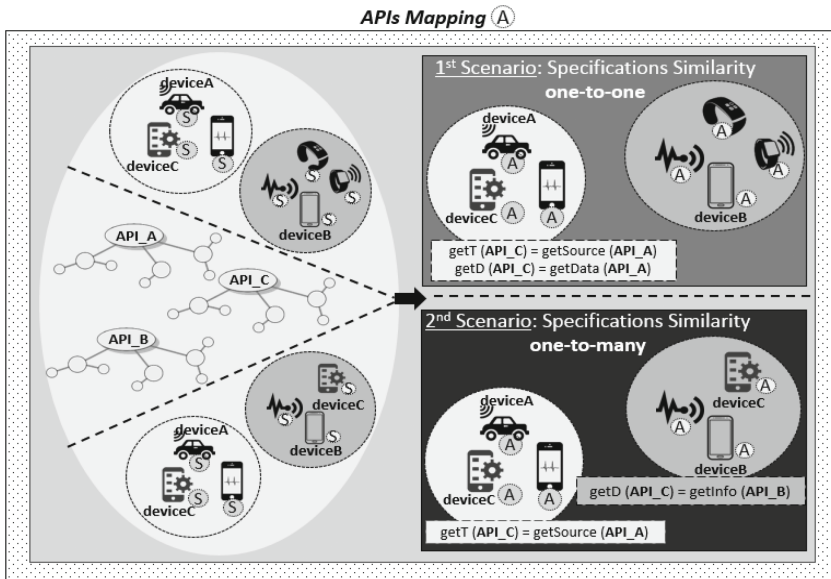


Fig. 3. APIs mapping stage

1<sup>st</sup> Scenario: According to the specifications classification's outcomes, each device belongs to a single classification group. Therefore, all the devices that are categorized into the same group will have the same APIs (*one-to-one scenario*). According to the example of the *Specifications Classification* stage, the known device A and the unknown device C were categorized into the same classification group, as they had the same specifications. Following this example, in this stage we conclude that these two devices have the same APIs, including the same data methods. More specifically, suppose that device A has an API\_A that includes a method called `getSource()` for getting the device's type and a method called `getData()` for collecting the devices' data, whose functionalities are known in advance, while device C has an API\_C that contains a method called `getT()` and a method called `getD()` whose functionalities are unknown. By illustrating both devices' (i.e. A and C) APIs into Generic API Ontologies and comparing them considering that device A has the same specifications with device C, we conclude that they have the same APIs, and as a result, their data methods will have the same functionalities as well. Therefore, we conclude that method `getT()` of device C is used for getting the device's type, while method `getD()` is used for collecting the devices' data.

2<sup>nd</sup> Scenario: According to the specifications classification's outcomes, some devices may belong to one or more classification groups. Hence, the devices that are categorized into many groups will have partially the same APIs with the other groups' devices (*one-to-many scenario*). On the example in the *Specifications Classification* stage, the unknown device C was categorized into both the same classification group with device A and the same classification group with device B, as device C has partial specifications in common with the two devices (i.e. A and B). Following this example, in this stage we conclude that device C has partially the same API with device A and device B, considering that they have a certain amount of specifications in common. More specifically, suppose that device A has an API\_A that contains a method called getSource() for getting the device's type and a method called getData() for collecting the devices' data, device B has an API\_B that contains a method called getType() for getting the device's type and a method called getInfo() for collecting the devices' data, whose functionalities are known in advance, while device C has an API\_C that contains a method called getT() and a method called getD() whose functionalities are unknown. By illustrating all the devices' APIs into Generic API Ontologies and comparing them considering that device C has partially the same API with device A and device B, we conclude that they have a partial common part with their APIs, while some of their methods have the same functionalities. Therefore, we conclude that method getT() of device C is used for getting the device's type (according to getSource() method of API\_A), whilst method getD() of device C is used for collecting the devices' data (according to getInfo() method of API\_B).

All of the aforementioned steps are being performed as preliminary steps for the proposed *Dynamic Data Acquisition API*, which is constructed in order to collect data from the existing devices' APIs, by translating these APIs into a common format (e.g. all the methods for acquiring data will be named as getDeviceData()). In more details, the proposed API's implementation is achieved using the Restlet Studio [39] that describes APIs with a set of visual tools, and auto-generates Java skeleton code for it, while the API's testing is accomplished using the Runscope [40]. To this end, if during the testing it is observed that the developed API does not meet the expected results, a feedback loop to the *Specifications Classification* stage will take place in order to cope with potential problematic, inefficient and incomplete results that may have occurred. Thus, the proposed API provides sufficient flexibility and adaptability regardless of the various underlying heterogeneous devices, which will be able to be dynamically inherited into IoT environments, avoiding their manual and ad-hoc integration into these environments.

## 4 Conclusions

In this paper, we have studied the challenging topic of data integration between heterogeneous devices for the IoT environments. We have considered data coming both from known and unknown reliable devices, and proposed an innovative approach to easily and rapidly integrate heterogeneous devices during runtime into an IoT platform, so as to collect data. In this approach, a classification mechanism was proposed based on the devices' specifications, accompanied with a mapping mechanism that was built

on top of the classification's outcomes and the devices' Generic API Ontologies, responsible for mapping the APIs that contain completely or partly similar data methods. All this information was used as an input for the proposed *Dynamic Data Acquisition API*, which was implemented in order to transform the devices' APIs methods into a common format.

Currently, we are working on the evaluation of the developed mechanism, by testing it with multiple heterogeneous devices. Our future work includes the development of a mechanism that does not require prior knowledge of the used devices' transmitted data formats and APIs, as well as prior knowledge of the devices' specifications. Moreover, this mechanism will be able to translate the devices individual specifications into a common format, thus not being necessary for the devices' specifications to contain the same semantics in terms of specifications descriptions and measurement units. Furthermore, one of our main goals is to develop a machine learning technique for the adaptive selection of the available devices, either known or unknown, ensuring that the criteria of reliability and predicting origination of the data are met. Finally, we are willing to implement a visualization module providing abstractions over the available devices, through a Web interface that will enable users to observe and manage the connected devices. With such an interface, users will be able to monitor the state and the location of their devices, while visualizing historical data stored in the platform.

**Acknowledgments.** The CrowdHEALTH project has received funding from the European Union's Horizon 2020 research and innovation programme under grant agreement No 727560. Athanasios Kiourtis would also like to acknowledge the financial support from the "Foundation for Education and European Culture (IPEP)".

## References

1. Overview of Internet of Things. ITU-T Y.2060 (2012)
2. Smith, I.: The Internet of Things 2012 - New Horizons-Cluster Book (2012)
3. Pires, F., et al.: A platform for integrating physical devices in the Internet of Things. In: Embedded and Ubiquitous Computing (EUC), pp. 234–241. IEEE (2014)
4. Chaqfeh, A., Nader, M.: Challenges in middleware solutions for the internet of things. In: Collaboration Technologies and Systems (CTS). IEEE (2012)
5. Montori, F., Bedogni, L., Bononi, L.: On the integration of heterogeneous data sources for the collaborative Internet of Things. In: Research and Technologies for Society and Industry Leveraging a Better Tomorrow (RTSI), pp. 1–6. IEEE (2016)
6. Global M2M market. <https://machinaresearch.com/news/global-m2m-market-to-grow-to-27-billion-devices-generating-usd16-trillion-revenue-in-2024/>. Accessed Mar 2017
7. Pham, C., Lim, Y., Tan, Y.: Management architecture for heterogeneous IoT devices in home network. In: Consumer Electronics, pp. 1–5. IEEE (2016)
8. Pötter, B., Sztajnberg, A.: Adapting heterogeneous devices into an IoT context-aware infrastructure. In: 11th International Symposium on Software Engineering for Adaptive and Self-managing Systems, pp. 64–74. ACM (2016)

9. Zanella, A., Bui, N., Castellani, A., Vangelista, L.: Internet of Things for smart cities. *IEEE Internet Things J.* **1**(1), 22–32 (2014)
10. Bellavista, P., Cardone, G., Corradi, A., Foschini, F.: Convergence of MANET and WSN in IoT urban scenarios. *IEEE Sens. J.* **13**(10), 3558–3567 (2013)
11. Zhou, G., Fan, P.: Analysis of the business model innovation of the technology of internet of things in postal logistics. In: *Industrial Engineering and Engineering Management*, pp. 532–536. IEEE (2011)
12. Nagib, A.M., Hamza, H.S.: SIGHTED: a framework for semantic integration of heterogeneous sensor data on the Internet of Things. *Procedia CS* **83**, 529–536 (2016)
13. Gong, P.: Dynamic integration of biological data sources using the data concierge. *Health Inf. Sci. Syst.* **1**, 7 (2013)
14. Patni, H., Henson, C., Sheth, A.: Linked sensor data. In: *International Symposium on Collaborative Technologies and Systems (CTS)*, pp. 362–370. IEEE (2010)
15. Shelby, Z., Hartke, K., Bormann, C.: The constrained application protocol (2014)
16. Keiler, C., Janowicz, K.: Linking sensor data-why, to what, and how? In: *SSN* (2010)
17. Pschorr, J., Henson, C.A., Patni, H.K., Sheth, A.: Sensor discovery on linked data (2010)
18. De, S., Elsaleh, T., Barnaghi, P., Meissner, S.: An internet of things platform for real-world and digital objects. *Scalable Comput. Pract. Exp.* **13**, 45–58 (2012)
19. Botts, M., Percivall, G., Reed, C., Davidson, J.: Sensor web enablement: overview and high level architecture. *Open Geospatial Consortium*, pp. 175–190. Springer (2008)
20. Moraru, A., et al.: Exposing real world information for the web of things. In: *Proceedings of the 8th International Workshop on Information Integration on the Web*, p. 6. ACM (2011)
21. Compton, M., et al.: The SSN ontology of the W3C semantic sensor network incubator group. *Web Seman. Sci. Serv. Agents. World Wide Web* **17**, 25–32 (2012)
22. OWL. <https://www.w3.org/TR/owl-guide/>. Accessed Mar 2017
23. Globle, C., et al.: Transparent access to multiple bioinformatics information sources. *IBM Syst. J.* **6**, 534–551 (2001)
24. Donelson, L., et al.: The BioMediator system as a data integration tool to answer diverse biologic queries. In: *Proceedings of MedInfo*, pp. 768–772 (2004)
25. Philippi, S.: Light-weight integration of molecular biological databases. *Bioinformatics* **1**, 51–57 (2004)
26. Eckman, B.A., Lacroix, Z., Raschid, L.: Optimized seamless integration of biomolecular data. In: *IEEE International Conference on Bioinformatics and Biomedical Engineering*, pp. 23–32 (2001)
27. Martín, L., et al.: Ontology based integration of distributed and heterogeneous data sources in ACGT. In: *HEALTHINF*, pp. 301–306 (2008)
28. Moazzami, M., et al.: SPOT: a smartphone-based platform to tackle heterogeneity in smart-home IoT systems. In: *Internet of Things (WF-IoT)*, pp. 514–519. IEEE (2016)
29. Xively: public cloud for the Internet of Things. <http://xively.com/>. Accessed Mar 2017
30. Vega-Barbas, M., et al.: Smart spaces and smart objects interoperability architecture (S<sup>3</sup>OIA). In: *6th International Conference on Innovative Mobile and Internet Services in Ubiquitous Computing*, pp. 725–730. IEEE (2012)
31. Nixon, L.J.B., Simperl, E., Krummenacher, R., Martin-Recuerda, F.: Tuplespace-based computing for the Semantic Web: a survey of the state-of-the-art. *Knowl. Eng. Rev.* **23**(2), 181–212 (2008)
32. SVMs. <http://www.support-vector-machines.org/>. Accessed Mar 2017
33. Bag of Words. <https://deeplearning4j.org/bagofwords-tf-idf>. Accessed 10 Mar 2017
34. Costa, A., et al.: CORES: Context-aware ontology-based recommender system for service recommendation. In: *19th International Conference on Advanced Information Systems Engineering* (2007)

35. Martino, B.D., et al.: An OWL ontology to support cloud portability and interoperability. *Int. J. Web Grid Serv.* **11**, 303–326 (2015)
36. Stefan, S.: Part-whole representation and reasoning in formal biomedical ontologies. *Artif. Intell. Med.* **34**, 179–200 (2005)
37. Smith, B.: From concepts to clinical reality: an essay on the benchmarking of biomedical terminologies. *J. Biomed. Inform.* **39**, 288–298 (2006)
38. Protégé. <http://protege.stanford.edu>. Accessed Mar 2017
39. Restlet. <https://studio.restlet.com/apis/local/info>. Accessed Mar 2017
40. Runscope. <https://www.runscope.com/>. Accessed Mar 2017

# Automatising Mashup of Cloud Services with QoS Requirements

Claudia Di Napoli<sup>1</sup>(✉), Luca Sabatucci<sup>2</sup>, and Massimo Cossentino<sup>2</sup>

<sup>1</sup> C.N.R., Istituto di Calcolo e Reti ad Alte Prestazioni,  
Via Pietro Castellino 111, 80131 Napoli, Italy  
`claudia.dinapoli@cnr.it`

<sup>2</sup> C.N.R., Istituto di Calcolo e Reti ad Alte Prestazioni,  
Viale Delle Scienze, Ed. 11, 90128 Palermo, Italy  
`{luca.sabatucci,massimo.cossentino}@cnr.it`

**Abstract.** Service mashups represent an appealing business opportunity for companies since value added applications can be provided to fulfill clients' needs by integrating their services with the ones available on the Internet accessible according to standard Web Services technologies. Clients' needs are usually expressed in terms of a required functionality that can be obtained as a mashup application, together with specified QoS requirements referring to non-functional characteristics of the application, such as price, time, reliability. In order to make this opportunity a reality, mechanisms allowing for automatic selection and composition of services are necessary to avoid human intervention in the composition process. Here, a framework for automatic mashup of Cloud services taking into account QoS users' preferences, is presented. It relies on both AI planning techniques for automatic service composition, and software agent negotiation to select a composition that meets the specified QoS preferences. It allows for a dynamic QoS-based mashup of services since the QoS values provided for the single services in the composition are not fixed, but they could vary according to the providers' strategy. The proposed approach can be applied when services are provided in the context of a competitive market of service providers.

## 1 Introduction

Despite Cloud computing is a model for enabling ubiquitous, convenient, on-demand network access, Cloud applications are currently developed as single units tethered to a single stack architecture [15]. This approach may represent a barrier for their efficient scalability, continuous delivery and distributed maintenance [11].

The objective of *Cloud Application Mashup* is to build a cloud application as a suite of integrated services. The first advantage is that services are independently deployable and replaceable. Services may be provided by several providers and be developed with different programming languages. Moreover, running on different nodes, services can be more efficiently scalable.



So far, the mashup technology is mainly intended as an instrument for web developers for integrating services and contents from more than one source in a new single graphical interface. This task involves the definition of a centralized control module that manages one or more HTTP protocols for data and process integration, and preserves the global application consistency.

This paper presents an approach for automatically generating Cloud Application Mashups based on user's goals and QoS requirements specification. The idea is that mashups are created for the consuming user, often directly by the users themselves. Therefore users will establish or modify situational collaborations for integrating services from a variety of cloud providers.

The approach pushes for the vision that Cloud services will be available on public Cloud marketplaces in which providers may store their offerings. Therefore, a mashup self-composition engine should act as a run-time mediator between user's goals and atomic Cloud services in order to realize the desired application with the required QoS values.

In the present work, a middleware for the automatic composition of services that satisfies a required user's goal is used, adopting a negotiation module to select services according to the QoS values they provide to meet the QoS user's preferences/requirements. The middleware, presented in [6], is applied to a real use case based on a Fashion Firm application to test its suitability to automatically generate Cloud services mashups with required QoS values.

The paper is organized as follows: Sect. 2 introduces the middleware used for automatic service composition and selection. Section 3 provides an example extracted from a research project to illustrate the proposed approach. Section 4 discusses some alternative approaches to service composition and selection. Finally some conclusions are drawn in Sect. 5.

## 2 Abstract Workflow Composition and Service Selection

The middleware adopted in the present work is the integration of MUSA (Middleware for User-driven Service Adaptation), a middleware for composing and orchestrating distributed services according to unanticipated and dynamic user's needs, and a Negotiation module providing a heuristic mechanism to select services whose providers are able to deliver QoS values that meet the global QoS requirements specified by the user [6].

The core aspect of MUSA [17] is the separation of 'what the system has to address' and 'how it will operate for addressing it'. MUSA's main abstractions are the *goal* and the *capability*. The former represents the result the system is delegated to address and it is expressed using the GoalSPEC language [19] based on structured English and adopting a core grammar to which domain-specific terms can be added. Conversely, the capability represents an atomic functionality the system knows to own for achieving a partial result to reach the specified goal. The concept of capability comes from AI (planning actions [7]) and service-oriented architecture (micro-services [13]). Indeed, this double nature is well represented by the separation of Abstract Capability – a description of

the effect of an action that can be performed – and Concrete Capability – a small, independent, composable unit of computation that produce some concrete output.

This approach has a number of benefits: 1. each capability is relatively small, and therefore easier for a developer to implement, 2. it can be deployed independently of other capabilities, 3. it makes it easier to organize the overall development effort around multiple teams, 4. it supports self-adaptation because of improved fault isolation.

In MUSA, the proactive means-end reasoning [16] aggregates system capabilities in order to generate a set of Abstract Workflows, each one able to address the user goals. The algorithm strategy is that of incrementally building a *solution space graph* by exploring different combinations of capabilities. To reduce temporal and spatial complexity, the algorithm adopts a symbolic representation of the states [14]: by ignoring a number of distinctions –that are irrelevant for the solution– it allows working with a smaller space. The resulting Abstract Workflows are produced by visiting the graph and by identifying three types of workflow patterns: sequences, exclusive-choices and structured-loops [18].

An *Abstract Workflow* produced by MUSA by processing a user's goal, is represented by a directed acyclic graph  $AW = (AS, P)$  where  $AS = AS_1, \dots, AS_n$  is a set of nodes, and  $P$  is a set of directed arcs. Each node represents an *Abstract Service* ( $AS$ ), i.e. a generic service description that specifies a basic required functionality, and that corresponds to an *Abstract Capability* in the MUSA terminology. Each directed arc that connects two nodes represents a precedence relation among the corresponding Abstract Services,  $p = (AS_i, AS_j)$  of  $P$ , i.e. it specifies the control and data flow between them implying that an instance of the Abstract Service  $AS_j$  cannot start its execution until an instance of the Abstract Service  $AS_i$  finishes its execution due to a dependence relation between  $AS_i$  and  $AS_j$  [4]. For each Abstract Service in the Abstract Workflow, MUSA retrieves a set of corresponding *Concrete Services* named *Concrete Capabilities* in the MUSA terminology.

When dealing with mashup of services, it is very likely the Concrete Services are either services available on the Internet provided by third parties, or proprietary services under the full control of the end user. We refer to the first ones as *External* services, and it is assumed that more services providing the same required functionality, as specified by the corresponding Abstract Service, are available in a service marketplace. The second ones are *Internal* services, and it is assumed that just one service providing the functionality required by the corresponding Abstract Service is available, so no selection is necessary.

For External services, a service selection is necessary to instantiate the corresponding Abstract Service. This selection is driven by the QoS attribute values specified by the end user when declaring its goals. In QoS-aware service composition the selection is based on the Quality of Service (QoS) properties, i.e. a measure of how well a service satisfies the customer's needs [22], in terms of non-functional aspects of the composition (e.g. performance, reliability, availability, cost). In fact, service implementations having similar functional capabilities are

distinguishable for their QoS values that determine whether a service is reliable, trustworthy, or efficient, since it may be functionally capable of performing a given task, but it might not be reliable or efficient enough in performing the task up to the user's satisfaction [20].

Here, negotiation is used as a dynamic service selection mechanism, aiming at selecting the services that match the non-functional requirements (QoS requirements), allowing to manage the dynamic nature of QoS values. In fact, while a service functionality is static, and it is a characterizing intrinsic feature of the service itself, its non-functional features may vary, as well as users' QoS requirements/preferences. This is even truer when services are provided in an open market of services, as it is the case for Cloud services provided by different Cloud providers at different market conditions, where services are considered digital goods to be purchased.

Two types of QoS attributes can be specified by the user:

- *QoS\_global* attributes that refer to requirements concerning a set of Abstract Services in the Abstract Workflow, specified as end-to-end requirements, and so they are obtained by composing the QoS values of the corresponding External services for each involved Abstract Service, according to a defined aggregation function depending on the type of the QoS.
- *QoS\_local* attributes that refer to requirements concerning a single Abstract Service in the Abstract Workflow, and so their value is directly provided by a single Service Provider.

For *QoS\_global* values, a coordinated negotiation approach among the providers of the potential component Concrete Services (whose functionality match the ones required by the Abstract Services in the Abstract Workflow) is adopted as proposed in [5]. The negotiation is composed of  $n$  concurrent negotiations occurring among a Service Negotiator, acting on behalf of the end user, and all Service Providers of Concrete Services matching the functionality required by each Abstract Service, where  $n$  is the number of Abstract Services for which the *QoS\_global* values were specified. Since they are end-to-end QoS values, a coordination step is required during negotiation allowing to evaluate if there is a composition of Concrete Services whose aggregated QoS values meet the end user's requirements. If a combination is found, the negotiation is successful, and the Concrete Services belonging to the combination are selected to instantiate the Abstract Workflow in a Concrete Workflow ready to be executed. If a combination is not found, another negotiation iteration (*round*) takes place, and the process continues until either a combination is found or a deadline (i.e., the maximum number of allowed negotiation rounds) is reached.

For *QoS\_local* values, the negotiation mechanism is the same as the one occurring for a single Abstract Service of the *QoS\_global* case without the coordination step since no QoS global evaluation is required.

### 3 A Mashup Application Example

To evaluate the applicability of the adopted approach for automatic generation of instantiated workflows with specified QoS values to real scenarios, it was applied to a real use case in the fashion domain. More specifically, the use case was provided within the OCCP project by a world known fashion enterprise, here named FashionFirm for privacy reason. The FashionFirm's B2B processes includes a set of internal services running on a proprietary cloud stack. This is a set of scalable backend services able to interact with the SaaS eCommerce platform (OrderPortal).

The objective of the project was to deliver a cloud architecture for the mashup of distributed applications, but without considering QoS user requirements. The architecture has been adopted to enrich the FashionFirm business process by adding new services, for the customer management, conceived as a mashup of cloud applications. This allowed to fast prototype the solution reusing already existing cloud application provided by third parts. The resulting mashup application, that we use as running example in this paper, is designed for supporting customers during the order management process.

When a retail-store requests for a product stock, the system merges the internal services with some external cloud services, such as: a Cloud Storage system for storing and delivering receipts, Voicemail for the async convey of recorded audio messages, and, a Cloud Calendar service for tracking delivery status. In addition, FashionFirm may specify some QoS parameters with the values required for the mashup application. For simplicity two QoS parameters are considered: *the cost* of a particular goal, usually intended as a QoS\_global parameters since it is the result of the costs of the services necessary to reach the goal; *the reliability*, in this example, referred to a specific functionality (i.e., Abstract Service) and as such it is provided by a single service and not by a composition of services QoS values.

#### 3.1 Abstract Workflow Generation

In MUSA, a designer describes the desired functionality with goals, specified via the goal-oriented language [19] GoalSpec, that represent conditions to be addressed by the final composed service. Below, there is a pair of business goals, reported as example.

```

GOAL to_notify_invoice:
  WHEN accepted(X) AND order(X) AND registered(Client) AND user(Client)
  THE SYSTEM SHALL ADDRESS
  MESSAGE Z SENT TO THE Client ROLE AND user(Client) AND invoice(Z)
  [COST MUST BE LOWER THAN 5]

GOAL to_deliver_order:
  WHEN MESSAGE X SENT TO THE Client ROLE AND invoice(X) AND user(Client)
  THE SYSTEM SHALL ADDRESS
  MESSAGE Z SENT TO THE SM ROLE AND delivery_order(Z) AND
  storehouse_manager(SM)
  [RELIABILITY MUST BE AS HIGH AS POSSIBLE]

```

It is worth noting that goal expressions are annotated (by using square brackets) with the quality requirements, i.e. expressions that define non-functional requirements in terms of the expected quality of the final service.

The capability language provides additional information about the available services to enable automatic reasoning: service selecting, service composition, check of conflicts and check of goal satisfaction. For instance, the availability of products in the FashionFirm storehouse is checked via the *CheckStoreHouse* capability. *CheckStoreHouse* produces two possible states where the order has been either accepted or refused according to the storehouse status.

```

CAPABILITY CheckStorehouse:
  Pre-Condition: available(X) & order(X) & registered(X) & user(X)
  Post-Condition: ( accepted(X) | refused(X) ) & order(X)
  EvolutionSet:
    AcceptableOrder: [add(accepted(an_order)), remove(available(an_order))
                      ],
    UnacceptableOrder: [add(refused(an_order)), remove(available(an_order))
                       ]
    
```

The *UploadOnCloudStorage* is a capability that gets the user’s credential for uploading a file in the user’s Cloud space.

```

CAPABILITY UploadOnCloudStorage:
  Pre-Condition: available(X) & invoice(X) & has_cloud_space(Y) & user(Y) &
                !uploaded_on_cloud(X)
  Post-Condition: upload_on_cloud(X) & invoice(X)
  Evolution: [add(uploaded_on_cloud(the_invoice))]
    
```

According to the available services, MUSA is able of producing more solutions for a set of goals. The *proactive means-end reasoning* works with the abstract capabilities, and it adopts a symbolic approach to satisfy the goal from a functional point of view.

Figure 1 reports an example of Abstract Workflow for the FashionFirm invoice management.

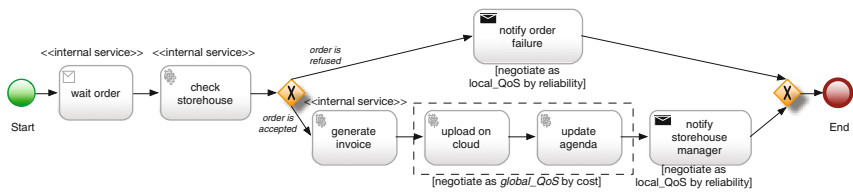


Fig. 1. An example of a generated Abstract Workflow.

Given that an Abstract Capability is an abstract description of a class of services, the Abstract Workflow cannot be executed as it is. For instance, in the case of *UploadOnCloudStorage*, many alternative Concrete Services are available in the market: Dropbox, Google Drive and Amazon Space are just a few examples. Each of these services may address the same result, but providing different QoS values (for example, regarding cost, reliability, time-to-complete, ...).

In order to become operative, it is necessary to select the concrete service for each category of services, according to the specified quality assets.

### 3.2 Negotiation for Service Selection

When the user declares the goals, also the QoS requirements (specified according to their typology), are provided. In the specific example of the FashionFirm application, the user specifies as QoS requirements its required **cost** for some sub-goals that are accomplished by more than one Concrete Service, and **reliability** for some others accomplished by just one Concrete Service. In both cases the Concrete Services are External services available on the market at given conditions. Nevertheless, these conditions cannot be fixed at design time, since they may change according to market demands and supply mechanisms.

For the considered generated workflow reported in Fig. 1, the cost requirements is specified as a QoS\_global value, resulting from the provision of **upload on cloud** and **update agenda** services (in most cases Cloud providers will provide the update agenda as a free of charge service in case a certain amount of Cloud resources are rented). Instead, the reliability requirement is specified as a QoS\_local value, since it is assumed that for each notification service a given trustability of the service provider is required depending on the nature of the service itself. Of course, assuming that reliability is a QoS\_local requirements is only to show the duplice nature of QoS parameters, since also this parameter could be specified at global level for the two notification services.

As described earlier, for the satisfaction of the QoS\_global requirement, a coordinated negotiation between the Service Negotiator and all available Service Providers takes place concurrently for each Abstract Service in the Abstract Workflow. If an agreement is reached upon composing QoS service values, the corresponding component Concrete Services are selected and bound to the Abstract Services, so generating an Instantiated Workflow ready to be enacted at the agreed QoS conditions. If the deadline is reached without an agreement, no result is provided, and a negotiation failure ends the process. The deadline, i.e., the number of allowed negotiation rounds, can be used to shorten the negotiation length in scenarios where time performances are a crucial requirement. In the considered scenario of a service marketplace, Service Providers adopt concession strategies modeled as Gaussian based functions representing the probability distribution of their offer during negotiation (refer to [5] for a detailed description of the strategies). On the contrary, the Service Negotiator does not provide counterproposals during negotiation since it cannot negotiate on the values of the QoS costs of the single components services independently from each other, so it can only accept or reject the proposals it receives once evaluating their possible combinations against the required QoS\_global value. The same strategies are adopted also in the case of the reliability QoS parameter, with the difference that no global evaluation is required in this case.

## 4 Related Works

This section provides an overview of the state of the art in two related research fields: service composition and service selection. This has been the base for the authors to set the background for the present work.

Several approaches deal with the problem to automatically build and execute a composition of services [9, 12, 26]. Colombo [3] is a framework for automatic composition of web-services that employs planning techniques. The idea is to synthesize a choreography of services by creating a mediator agent which can only send, receive and read messages. This approach gives great emphasis on syntactic aspects (ports, messages, queues, transitions) when linking the services, but it totally does not consider their QoS. Symbolic planning and model checking techniques are blended in [23] for creating executable processes as compositions of services. This approach improves general performance of automating the composition at the semantic level, but it offers a limited supports to real environmental data, and therefore it is not directly extendable for dealing with QoS. Goma and Hashimoto [8], in the context of the SASSY research project, propose dynamic reconfiguration to be executed by assembling architectural patterns. They use a connector adaptation state-machine with the objective to allow dynamic adaptation of distributed transactions. In SASSY the optimization of QoS is an architectural problem, consisting in searching for the pattern that best serves user-defined QoS goals.

When QoS values are expressed as end-to-end values, the problem to find a combination of services whose QoS values, once aggregated, meet the QoS requirements is known to be NP-hard. Optimizing algorithms relying on fixed QoS values and on prior knowledge of the component service QoS values are proposed as in [1, 2, 25], but they are not suitable in an open market of services where QoS values may change over time. Heuristics approaches have been investigated to find near-optimal combinations in dynamic environments. In this research line, negotiation mechanisms were shown to be a suitable approach to deal with QoS-aware SBAs [5, 10, 24]. Some approaches rely on bilateral one-to-one negotiation mechanisms such as in [21, 24], not allowing competition among providers. In other approaches negotiation occurs after an optimization phase, but only among the providers that do not provide the expected QoS local values [2].

The approach adopted in the present work relies on a coordinated negotiation mechanism taking place between the Service Negotiator and the Service Providers for each Abstract Service in the Abstract Workflow, taking into account their contribution to the global QoS values, as proposed in [5]. A coordination point to synchronize the concurrent negotiations is necessary for QoS global evaluation. This approach allows to properly exploit the competition among service providers.

## 5 Conclusions

The integration of the MUSA middleware for automatic composition services with the Negotiation module for service selection, allows for the automatic

generation of mashups of services characterized by QoS requirements. The different nature of services usually involved in a mashup application (External and Internal), and the different types of QoS requirements (global or local) are managed by the middleware that is able to clearly separate the functionality provided by a mashup application from its QoS. A real use case scenario based on a Fashion Firm application is used to preliminary test the middleware operational aspects.

We plan to setup an experimental evaluation of the system by considering the generation of more abstract workflows for a required application and to adopt different negotiation strategies with increasing number of service providers to test system scalability. Our objective is to prove that selecting services through negotiation helps to discharge service combinations that do not meet end user QoS requirements, so improving system performance. Of course, in order to reach this objective, the cost of negotiation should be also taken into account.

## References

1. Alrifai, M., Risse, T.: Combining global optimization with local selection for efficient QoS-aware service composition. In: Proceedings of the 18th International Conference on World Wide Web, WWW 2009, pp. 881–890. ACM, New York (2009)
2. Ardagna, D., Pernici, B.: Adaptive service composition in flexible processes. *IEEE Trans. Softw. Eng.* **33**(6), 369–384 (2007)
3. Berardi, D., Calvanese, D., De Giacomo, G., Hull, R., Mecella, M.: Automatic composition of transition-based semantic web services with messaging. In: Proceedings of the 31st International Conference on Very Large Data Bases, pp. 613–624. VLDB Endowment (2005)
4. Di Napoli, C.: Software agents to enable service composition through negotiation. In: Knowledge Processing and Decision Making in Agent-Based Systems, pp. 275–296. Springer, Heidelberg (2009)
5. Di Napoli, C., Pisa, P., Rossi, S.: Towards a dynamic negotiation mechanism for QoS-aware service markets. In: Pérez, J.B., et al. (eds.), Trends in Practical Applications of Agents and Multiagent Systems, Advances in Intelligent Systems and Computing, vol. 221, pp. 9–16. Springer (2013)
6. Di Napoli, C., Sabatucci, L., Cossentino, M., Rossi, S.: Generating and instantiating abstract workflows with QoS user requirements. In: Proceedings of the 9th International Conference on Agents and Artificial Intelligence, vol. 1, pp. 276–283 (2017)
7. Gelfond, M., Lifschitz, V.: Action languages. *Comput. Inf. Sci.* **3**(16), 1–16 (1998)
8. Goma, H., Hashimoto, K.: Dynamic self-adaptation for distributed service-oriented transactions. In: 2012 ICSE Workshop on Software Engineering for Adaptive and Self-Managing Systems (SEAMS), pp. 11–20 (2012)
9. Hashmi, K., Malik, Z., Najmi, E., Alhosban, A., Medjahed, B.: A web service negotiation management and QoS dependency modeling framework. *ACM Trans. Manage. Inf. Syst.* **7**(2), 1–33 (2016)
10. Lau, R.Y.K.: Towards a web services and intelligent agents-based negotiation system for B2b ecommerce. *Electron. Commer. Res. Appl.* **6**(3), 260–273 (2007)



11. Lewis, J., Fowler, M.: Microservices: a definition of this new architectural term. *Mars* (2014)
12. Moghaddam, M., Davis, J.G.: Service Selection in Web Service Composition: A Comparative Review of Existing Approaches, pp. 321–346. Springer, New York (2014)
13. Namiot, D., Sneps-Sneppé, M.: On micro-services architecture. *Int. J. Open Inf. Technol.* **2**(9), 24–27 (2014)
14. Newell, A.: The knowledge level. *Artif. Intell.* **18**(1), 87–127 (1982)
15. Papazoglou, M.P., van den Heuvel, W.-J.: Blueprinting the cloud. *IEEE Int. Comput.* **15**(6), 74–79 (2011)
16. Sabatucci, L., Cossentino, M.: From means-end analysis to proactive means-end reasoning. In: Proceedings of 10th International Symposium on Software Engineering for Adaptive and Self-Managing Systems, Florence, Italy, 18–19 May 2015
17. Sabatucci, L., Lodato, C., Lopes, S., Cossentino, M.: Highly customizable service composition and orchestration. In: Dustdar, S., Leymann, F., Villari, M. (eds.), *Service Oriented and Cloud Computing*. LNCS, vol. 9306, pp. 156–170. Springer (2015)
18. Sabatucci, L., Lopes, S., Cossentino, M.: Self-configuring cloud application mashup with goals and capabilities. In: *Cluster Computing* (2017 to appear)
19. Sabatucci, L., Ribino, P., Lodato, C., Lopes, S., Cossentino, M.: GoalSPEC: a goal specification language supporting adaptivity and evolution. In: *Engineering Multi-Agent Systems*, pp. 235–254. Springer (2013)
20. Shehu, U., Epiphaniou, G., Safdar, G.A.: A survey of QoS-aware web service composition techniques. *Int. J. Comput. Appl.* **89**(12), 10–17 (2014)
21. Siala, F., Ghedira, K.: A multi-agent selection of web service providers driven by composite QoS. In: Proceedings of 2011 IEEE Symposium on Computers and Communications (ISCC), pp. 55–60. IEEE (2011)
22. Strunk, A.: QoS-aware service composition: a survey. In: 2010 IEEE 8th European Conference on Web Services (ECOWS), pp. 67–74 (2010)
23. Traverso, P., Pistore, M.: Automated composition of semantic web services into executable processes. In: *International Semantic Web Conference*, pp. 380–394. Springer (2004)
24. Yan, J., Kowalczyk, R., Lin, J., Chhetri, M.B., Goh, S.K., Zhang, J.: Autonomous service level agreement negotiation for service composition provision. *Future Gener. Comput. Syst.* **23**(6), 748–759 (2007)
25. Yu, T., Zhang, Y., Lin, K.-J.: Efficient algorithms for web services selection with end-to-end QoS constraints. *ACM Trans. Web* **1**(1), 1–26 (2007)
26. Zeng, L., Boualem, B., Ngu, A.H.H., Dumas, M., Kalagnanam, J., Chang, H.: QoS-aware middleware for web services composition. *IEEE Trans. Softw. Eng.* **30**(5), 311–327 (2004)

# Towards Osmotic Computing: Looking at Basic Principles and Technologies

Massimo Villari, Antonio Celesti<sup>(✉)</sup>, and Maria Fazio

Dep. Ingegneria, University of Messina, Messina, Italy  
{mvillari,acelesti,mfazio}@unime.it

**Abstract.** Osmotic Computing is becoming the new paradigm in the area of Computing. This paper shows how it can represent the glue of recent topics including Cloud, Edge and Fog Computing, and Internet of Things (IoT). Osmotic Computing introduces elements allowing to treat computation, networking, storage, data transfer and management among Cloud and IoT devices in Edge computing layers in a more harmonized fashion. In particular, we discuss how it can enable an abstraction of services that could bring into a new Software Defined of Everything era.

## 1 Introduction

In recent years, several architectural models have been proposed from Cloud computing on. Cloud Federation [1] was the first meaningful step forward introducing the concept of collaboration between different providers. After that, with the advent of Internet of Thing (IoT), pervasive smart devices have become part of IoT Clouds promoting the rising of a new class of services named IoT as a Service (IoTaaS). In the end, as a consequence of the need to move resources and services near the edge of the network in order to optimize them, Fog and Edge computing paradigms have emerged as new trends. Osmotic Computing (OC) [2] is an emerging paradigm that aims at representing the glue among Federated Cloud, Fog [3], Edge [4] Computing (i.e., CC, FC, EC) and IoT [5] environments in order to optimize the deployment of future Internet services. Moreover, OC represents the capability to delivery new multiple microservices in both CC and EC sides.

The paper hereby provides a step forward OC. Specifically we discuss of the delivery of services follows an advanced approach in which sub-micro-services are deployed in containers [6], opportunely adjusting their landing in CC or EC accordingly to multiple constrains and needs: users requirements, devices constrains on the edge, as well network needs. The approach adopted here goes beyond the simple elastic behaviour of resources deployment, due to a continuous and dynamic bidirectional flow of adapted micro-services. OC follows the concept of osmosis. Considering two liquid solutions in a hermetic container separated from a membrane, these reach the equilibrium when a physical balancing formula is respected according to a physical/chemical principle. Figure 1 mimes this concept where Micro-services can move from Cloud to Edge and Vice-versa.

Seems to be rather clear that CC is representing the fulfilment of the vision of Internet pioneer Leonard Kleinrock who said in 1969: *Computer networks are still in their infancy, but as they grow up and become sophisticated, we will probably see the spread of computer utilities which, like present electric and telephone utilities, will service individual homes and offices across the country.* Moreover, it is quite trivial, that in future the IoT device explosion will create a key new challenge for the Cloud due to the high cumulative data rate of incoming data streams from many devices. As noted in recent paper, such unprecedented data flows from IoT devices deployed in Smart Cities can flood metropolitan area networks (MANs) and seriously congest Internet paths leading to centralized Cloud datacenters, such as Amazons Elastic Compute Cloud and Googles datacenter. Recently a new initiative in Networking area is appearing in IT market, dealing with new network functionalities, focused from world-wide Telco companies that want to differentiate their businesses become obsolete due to the introduction of Cloud and Softwarizations of many services, like the VoIP, that has reduce the total margin for usual phonecalls. To this, telco operators are looking at differentiating their incomes, hence they are sponsoring the FOG Computing paradigm, in particular the OpenFOG initiative, that is opening up new possibilities in the are of Network Virtualisation and Network Slicing.

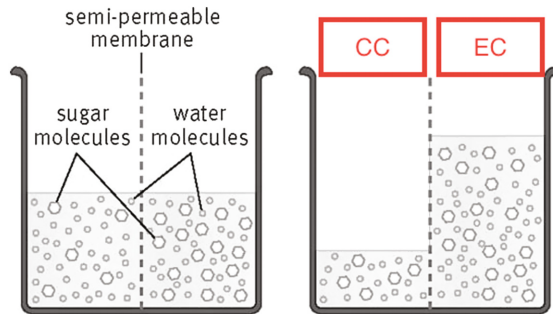


**Fig. 1.** Osmotic Computing as reported in [2].

Looking at the above reported trends and consolidated technologies, the Osmotic Computing introduces elements allowing to treat computations, storage, networking, data transfer and data management, among Cloud and devices in the Edge, like IoT, in a much more useful and harmonized way. The paper we present here below highlights these aspects, and provides insight on how all computations are going towards a common point of interest. Systems are going towards an abstraction of services and network facilities, since to Software Defined Everything (SDX).

The rest of the paper is organized as follows. Section 2 motivates why it is necessary to define an extra paradigm able to make a relevant clearness in this space. Section 3 motivates why Osmotic Computing fits the current industrial

scenario. Section 4 describes how Osmotic Computign can support the development of Future Internet services. Section 5 concludes the paper.

## 2 Osmotic Computing at a Glance

Osmotic Computing is introduced to harmonize the different named software functionalities that aim at the same capabilities but they are described a different way in different sub contexts. The sub contexts we are referring here, are reported as follows:

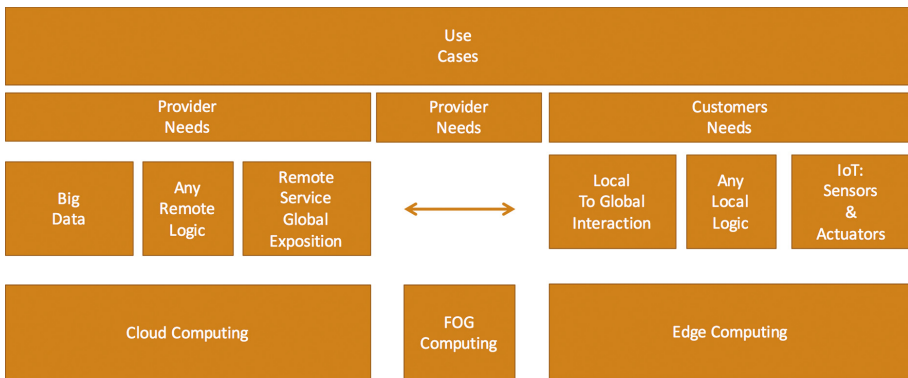


**Fig. 2.** Usual Subdivision of paradigms of Computation and collocation respect to End-to-End Services aimed at IT Customers.

1. Cloud Computing
2. Fog Computing
3. Edge Computing
4. IoT
5. Big Data
6. ..

Example if we consider the new seven pillars introduced in Fog Computing, reported here below, it is possible to see how these pillars might be assimilated in cloud, in edge, etc., computing. The question is why should they only belong to Networking, when Fog computing is an enabler in the networking for IoT, Cloud Edge, and Big Data functionalities? Why don't see them in a End to End approach?

- Security;
- Scalability;
- Open; Autonomy;
- Programmability;
- RAS (Reliability, Availability, and Serviceability);

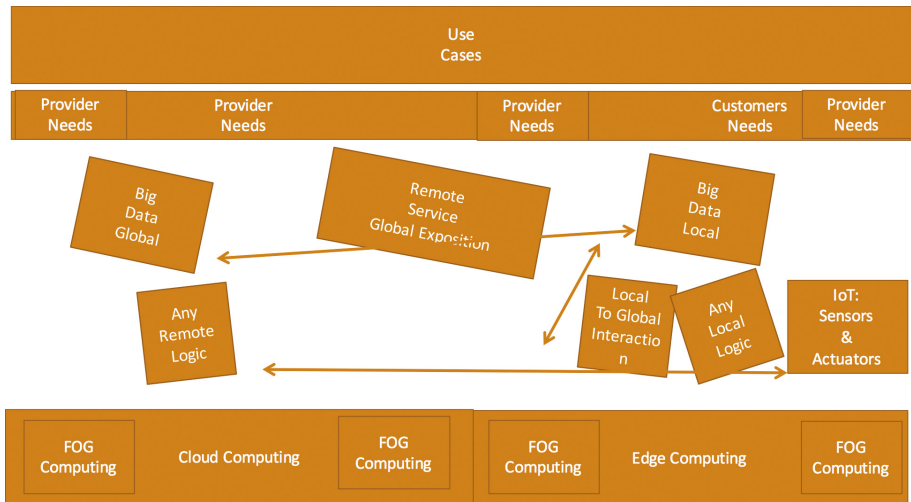


**Fig. 3.** Real Organization of paradigms of Computation and collocation respect to End-to-End Services aimed at IT Customers.

- Agility; and
- Hierarchy

In our thinking there is not an evident separation of functionalities in each context of 5 reported above. Looking at Figs. 2 and 3. The early one shows the common picture where for satisfying Customers (see Use-Cases), more providers rely on functionalities in a isolated way in each context. In the reality functionalities is not only part of one context, but the same characteristic can be found on the Edge, on the Cloud and in the Fog. Example see Big Data Analytics in Fig. 3, that can have a local approach with limited computation resources and even in a remote one with massive resources (as well remote services but even local services).

### 3 How Osmotic Computing Fits the Current Scenario

In the industrial environment, as in the consumer electronics space, embedded designers need to deliver more for less: more performance, functionality, and flexibility for less cost, lower power consumption, and smaller footprints. At the same time, industrial components must meet stringent requirements for reliability, robustness, and lifetime, even in the face of punishing operating conditions and they need to do it year after year.

The first step to meeting all these conflicting demands is to choose the appropriate central processing unit (CPU). Microprocessors (MPUs) deliver sophisticated, purpose-built performance, but at the cost of greater complexity, larger size, and bigger bills of materials (BOMs). Microcontrollers (MCUs) cant do it

all, but for the types of clearly constrained problems frequently found in industrial applications, the right MCU can deliver significant capabilities for a very reasonable price. Lets take a closer look at the performance characteristics and the design trade-offs involved in each to help you choose the right component for your product.

**Key differences** From a high level, we can classify the differences between an MCU and MPU in following ways: MCUs have internal flash memory and are intended to operate with a minimum amount of external support ICs. They commonly are a self-contained, system-on-chip (SoC) designs. MPUs rely on external memory and sophisticated power supplies to provide higher processing ability with much greater flash and RAM capacity.

Also known as application processors or media processors, MPUs are normally very high performance compared to MCUs produced at the same time. All that speed and digital functionality comes at the expense of reducing analog functionality and cutting out nonvolatile memory entirely, though. As a result, MPUs typically perform many system-level functions off-chip using external ICs such as NOR flash, dual data rate (DDR) RAM, power management ICs, analog-to-digital converters (ADCs), codecs, and touch-sense controllers.

MPUs generally use open-source operating systems such as Linux and Android, although high-reliability applications may require proprietary operating systems like those from Green Hills Software and Wind River. These operating systems include a library of drivers, for example for codecs, Ethernet, USB, etc. Most MPU providers create and maintain both Linux and Android releases for their evaluation boards, often supporting them with large software teams. Full-fledged operating systems make the development of software much more simple and lend themselves to plug and play hardware.

These levels of functionality require significantly more memory. The Linux kernel alone, without application code, can be 1 to 5 MB, for example. Although it can be stored in non-volatile flash, it must be transferred to DDR memory for high-speed execution. This approach results in faster execution of the code, but requires longer boot time, consumes board space, and adds to the BOM. Because of the sophistication of the applications, OSs, and hardware involved, MPUs require file and memory management functionality like structural partitioning, wear leveling, error correction code (ECC), and bad block management (for NAND). All of these capabilities add complexity and cost.

**MPU trade-offs** Although the performance of MPUs makes them effective for demanding applications like touch-screen HMIs, they are not necessarily the best solution for every problem, particularly in the industrial sphere. MPUs commonly use cores with extended pipelines, caches, speculative branching, and out-of-order execution. Although these features can greatly improve overall code execution performance, they also introduce some problems, like interrupt latency. Interrupt latency is defined as the time between when an interrupt event occurs and when code to service that interrupt starts to execute. Multi-stage pipelines can require several clock cycles to store the current pipeline information before beginning to service the interrupt, so that the process can be restarted coherently afterward.

For time-sensitive applications like motor control, consistent latency is critical for safe operation. Unfortunately, variability in user configurations prevents vendors from specifying interrupt latency for an MPU; as a result, the devices are not suitable for most motor control applications.

Variability introduces other problems. Although relying on the number of cycles for an instruction to complete is considered bad programming practice, many real-time embedded control systems are based on exactly that the assumption that the CPU will execute code in the exact number of cycles every time. This is known as deterministic code execution. When caches and speculative execution are enabled, as is frequently the case for MPUs, the number of cycles for a subroutine can vary. For real time applications like robotics and pick-and-place, this can be a problem.

The external PMICs required to create and monitor the supply voltage for an MPU range from switched-mode power supplies to simple, low dropout (LDO) linear devices. Switched-mode power supplies (SMPSS) have a higher conversion efficiency, but they can add 2to3 to the BOM per board. Some MPUs support low-power operating modes, but the leakage current of the high performance transistors and large amounts of memory makes these options less useful than in an MCU.

Many MPUs developed in the past five years have multi-core derivatives. This boosts the processing power several-fold without significantly increasing product costs, since the cores can share external resources. In most cases, the same CPU is used for all the cores, which is referred to as symmetrical multi-core processing. Some new MPUs, which border on being called MCUs, have asymmetrical, multi-core designs that combine an applications processor with a much smaller, less powerful embedded processor.

Today, the line between industrial and consumer electronics has blurred. Manufacturers use PCs to control machines, while meter readers and maintenance technicians use tablets to record readings. Meanwhile, users have come to expect the same level of convenience in their industrial tools as they find in their personal electronics, with high-level functionality and graphics-intensive interfaces. As a result, MPUs increasingly show up in industrial applications like networked industrial controls, relay controls in electric utility substations, and GPS units used to locate survey and construction equipment.

## 4 Development of Future Internet Services

A typical scenario where the Osmotic paradigm can be applied is depicted in Fig. 4. It shows possible IT resources (here defined Osmotic Resources) spread among Cloud and Edge interconnected by the Internet. The concept of Osmotic raises by the fact that any IT service is not confined in a specific area of the Internet, but it can find collocation among Cloud, Edge and Fog. Like a Solution in a chemical process of Osmosis that is able to flow from one bucket to another one through membranes and tubes.

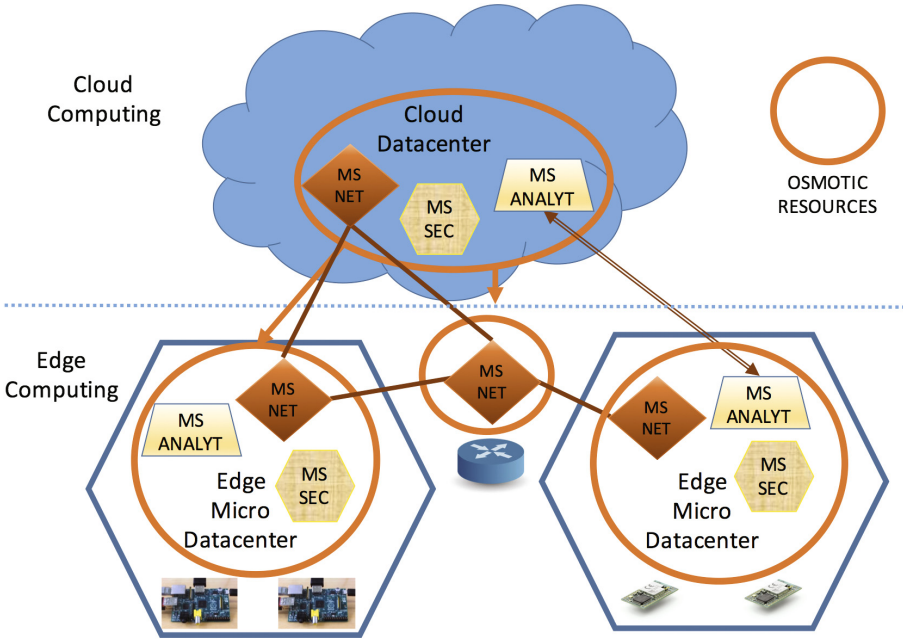


Fig. 4. Osmotic Scenario

#### 4.1 Mime the Chemical Solution: Osmotic MELS

In this section, looking at Fig. 5 we move on a step further respect to the basis concept of Osmotic Computing. Here we introduce the concept of MicroElementS (MELS), that are split into two main abstracted components: MS (MicroServices) and MD (MicroData). As it is possible to see in the Figure, the main root of the hierarchy is represented from MicroElementS, whereas underneath there are MSs and MDs. The leaf of hierarchy is represented by MUS & MOS along with MUD & MOD, that is User and Operational. MicroOperationalService (like an Operating System) and MicroUserService (like a user application on OS). MicroOperationalData (MS configuration) & MicroUserData (User Data). MD and MS are mobile, portable and cross-platform. In the real world scenario, an example of MS is a Docker [7] container. MD is a new entity, self-explicative, wrapped in JSON. MD can be passive data (can be read and write on SOs and devices). MD can be active (can be queried). E.g., MD stored in MongoDB on SOs and Devices. In Osmotic Computing, a Software Defined Membranes (SDMem) (Fig. 6) is able to filter MELS among Buckets, Chambers and Tubes. I/O in Buckets, Chambers and Tubes are governed by SDMem. In Osmotic Computing, the SDMem is a “Special” MEL. Let’s assume a MS-Web interface and its MOD: In cloud is a Restful API, moving to IoT (e.g., at a HOME) migrating and exiting from the Cloud (Bucket), the SDMem transforms it in CoAP and transit in Pipe(Network). The Bucket and the SDMem at



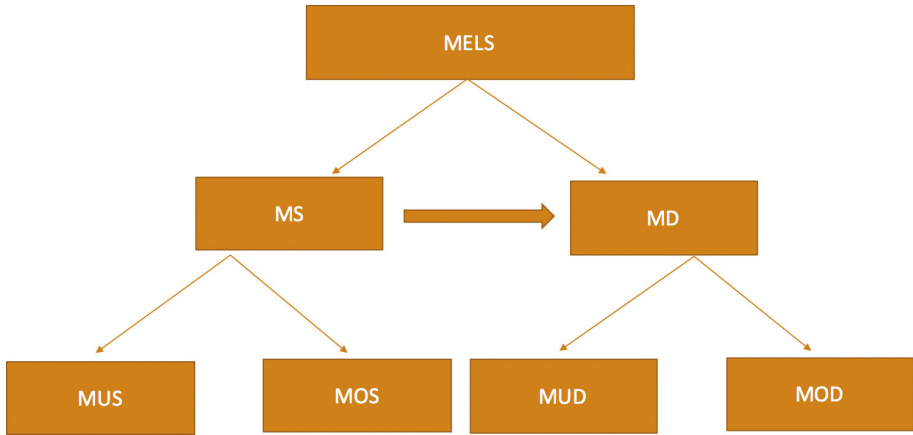


Fig. 5. Osmotic MELS

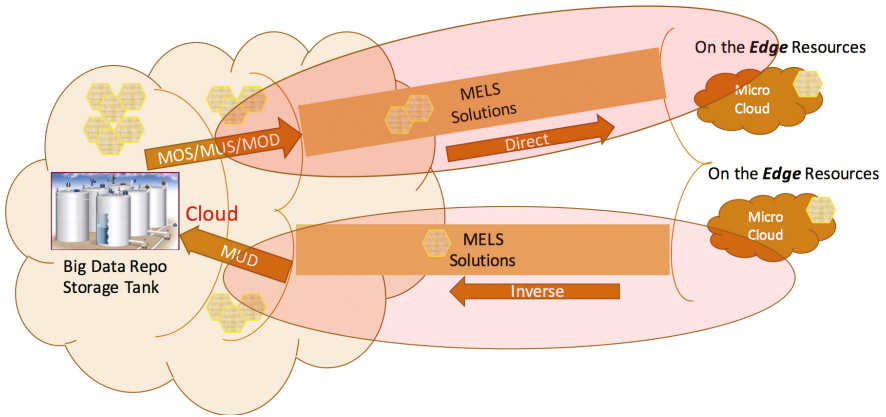


Fig. 6. SDMem: Isolated Mels.

destination (Gateway at Home) filter the MS and MDs to be deployed in IoTs (i.e., RPI - ESP32) at home(service injection with JSON configuration).

### 4.2 Infrastructures for Hosting MELS

In our considerations we split the infrastructures in two main domains Cloud and Edge resources. In the Cloud, there is the server side part of services, where massive and quasi-central resources are allocated. In the Edge less powerful resources are considered, where there is the higher level of distribution and scalability of services. Users have a major control on devices in the Edge where IoT (Sensors and Actuators) and Networking Gateways (I.e., routers for VDSL or Fibre Optics at Home.) are deployed. The concept of quasi-central derives from the fact that

current configurations of clouds rely on not so many cloud providers, hence a limited number of big players. Thanks to current level of resources abstraction **MELS** find their applicability on more infrastructures. We can have MELS in the Cloud, like the virtual appliances, the simple abstraction of Virtual Machines and Containers. Whereas the Containers are recently also confined into IoT with MPU (Raspberry, C.H.I.P, BeagleBlack, etc.) Vice versa, Javascript engines were born for web browser clients (see Node.js, Angular.js, Meteor.js, etc.) are moving into two directions: Serverless in the Cloud and APP development environments for Smart Devices. Moreover, there is the consolidated trend of porting a minimal version of the node.js (see Duktape) over arduino-like platforms (MCU). Finally, we can identify Cloud with Big Datacenters whereas Edge with micro-datacenters deployed over MPU and MCU.

## 5 Conclusion and Future Work

Osmotic Computing is becoming the new paradigm in the area of Computing. In this paper, we discussed how it can become the glue between Cloud, Edge and Fog Computing, and Internet of Things (IoT). In particular, after motivating why Osmotic Computing can fit new emerging industrial scenarios, we discuss how it, by the concept of MicroElementS (MELS) can concretely support the design and development future Internet services.

Recently Industry 4.0 [8] has emerged as the current trend of automation and data exchange in manufacturing technologies including cyber-physical systems, IoT and Cloud computing. In future works, we plan to define a piece of framework allowing to develop future Internet services in the context of Industry 4.0 according to the Osmotic Computing paradigm.

**Acknowledgment.** This work has been supported by the BEACON project, grant agreement number 644048, funded by the European Unions Horizon 2020 Programme under topic ICT-07-2014.

## References

1. Fazio, M., Celesti, A., Villari, M., Puliafito, A.: How to enhance cloud architectures to enable cross-federation: towards interoperable storage providers. In: 2015 IEEE International Conference on Cloud Engineering, pp. 480–486 (2015)
2. Villari, M., Fazio, M., Dustdar, S., Rana, O., Ranjan, R.: Osmotic computing: a new paradigm for edge/cloud integration. *IEEE Cloud Comput.* **3**, 76–83 (2016)
3. Chiang, M., Ha, S., Chih-Lin, I., Risso, F., Zhang, T.: Clarifying fog computing and networking: 10 questions and answers. *IEEE Commun. Mag.* **55**, 18–20 (2017)
4. Fan, C.T., Wu, Z.Y., Chang, C.P., Yuan, S.M.: Web resource cacheable edge device in fog computing. In: 2016 15th International Symposium on Parallel and Distributed Computing (ISPDC), pp. 432–439 (2016)
5. Celesti, A., Fazio, M., Giacobbe, M., Puliafito, A., Villari, M.: Characterizing cloud federation in iot. In: 2016 30th International Conference on Advanced Information Networking and Applications Workshops (WAINA), pp. 93–98 (2016)

6. Qasha, R., Cala, J., Watson, P.: Dynamic deployment of scientific workflows in the cloud using container virtualization. In: 2016 IEEE International Conference on Cloud Computing Technology and Science (CloudCom), pp. 269–276 (2016)
7. Cito, J., Gall, H.C.: Using docker containers to improve reproducibility in software engineering research. In: 2016 IEEE/ACM 38th International Conference on Software Engineering Companion (ICSE-C), pp. 906–907 (2016)
8. Wollschlaeger, M., Sauter, T., Jasperneite, J.: The future of industrial communication: automation networks in the era of the internet of things and industry 4.0. *IEEE Ind. Electron. Mag.* **11**, 17–27 (2017)

# Towards the Integration of a HPC Build System in the Cloud Ecosystem

Ioan Drăgan<sup>1,2</sup>, Teodora Selea<sup>1</sup>, and Teodor-Florin Fortiș<sup>1,3</sup>(✉)

<sup>1</sup> Institute e-Austria Timișoara, Timișoara, Romania  
{idragan,teodora.selea}@ieat.ro

<sup>2</sup> “Victor Babeș” University of Medicine and Pharmacy, Timișoara, Romania

<sup>3</sup> West University of Timișoara, Timișoara, Romania  
fortis@info.uvt.ro

**Abstract.** Once the Cloud computing matures, and the diversification of resources and levels at which they can be accessed, there is a growing need to identify specialized languages and technologies that can provide a high level of flexibility and transparency in accessing, managing, and utilizing these resources. In this context, the alignment of these capabilities with current developments, especially at topology, orchestration and management level, becomes a necessity. Such an implementation is usually based on a self-\* approach, which is also suitable for supporting the migration of selected HPC applications to the cloud. Our research is based on a self-organizing, self-management approach and investigates the option of self-configuration, supported by the **easybuild** toolchain.

**Keywords:** Cloud computing · Easybuild · Cloud orchestration

## 1 Introduction

While discussing the context of cloud computing evolution, Dave Geada asserted “the cloud will be heterogeneous.” [1] This heterogeneity, as predicted in Geada’s article, was merely based on an increase in the complexity of cloud environments, and closely related with the cloud deployment models. Thus, heterogeneity was closely related with the hybrid cloud deployment model, as an aggregation of public and private clouds, and in contrast with homogeneous cloud environments, where vendor lock-in was identified as a major blocking issue. Important research efforts were made in the direction of heterogeneous cloud environments, like those realized in a series of FP7/H2020 projects (e.g., mOSAIC – <http://mosaic-cloud.eu/>, modaClouds – <http://www.modaclouds.eu/>, HARNESS – <http://www.harness-project.eu/>, and others).

Though the heterogeneity of cloud environments was at the core of these research efforts, specific attention was paid for the specification, representation and annotation of cloud resources. For example, a cloud resource ontology was developed in the context of the mOSAIC project [2], the modacLOUD modeling language was developed in relation with the modaClouds projects [3], the OASIS

TOSCA specification was adopted in a series of approaches [4]. This was however an important step towards the definition of new cloud service models, more close to the physical machine than the initial Hardware-as-a-Service model was (e.g., bare-metal clouds, Metal as a Service).

With a plethora of novel resources becoming available in the context of cloud computing, new computing capabilities can be exposed for the use of cloud-based applications. Cloud resource management must now be solved both at the level of virtual and physical cloud resources, as new approaches are now available on top of cloud environments: mobile cloud computing [5], HPC in the cloud [6–8].

The evolving complexity of heterogeneity, exposed both at the level of deployment and service models, can be handled by using principles inspired from autonomic computing (namely self-management & self-organization of cloud resources) coupled with a dedicated service description language (SDL), which can thus offer a new method of provisioning heterogeneous cloud resources to deliver services.

By offering transparent access to a fully new range of resources, the cloud environment may become more appealing for a series of high performance computing (HPC) approaches, as it was demonstrated by the recent hybrid burst-out HPC approach, where the highly compute-intensive tasks are processed in a cloud HPC instance, while carrying out all other compute and data handling tasks locally [9].

A self-management & self-organization approach coupled with the transparent access to resources imply that the number, type or availability of underlying resources may not be known in advance to the cloud consumer. This is contrasting the classical approach where services are constructed in close relation with resource availability on providers' premises. In turn, a layered declarative approach is required, allowing the cloud consumer to rather declare what service(s) are requested, without any information about how that service(s) are to be provided.

The remainder of this paper is organized as follows: Sect. 2 offer a series of background information related with the heterogeneity of resources and HPC build tools; Sect. 3 motivates the choice for a specific service description language; while Sect. 4 discusses about the mechanisms which are specific to the CloudLightning approach, offering details related with the `easybuild` extension and the CloudLightning approach for automatic build of ad-hoc HPC applications.

## 2 Background Information and Related Work

Though the migration of HPC applications in cloud environments is not an easy task, due to various issues, ranging from performance bottlenecks to expensive cost models, various approaches were identified in order to ease this migration. In [6] the authors some optimization techniques of cloud virtualization for HPC. The vision of the CloudLightning project [10] is to offer a novel approach in cloud infrastructure management and delivery – based on the self-organizing and self-management principles – in order to efficiently use heterogeneous cloud resources, approach which will be demonstrated by the three HPC-inspired use-cases.

The heterogeneity of resources that may be available in the case of HPC applications, and which are being included in various cloud offerings (like in the case of IBM Spectrum computing, or Penguin computing on demand), transforms the compilation phase of HPC applications into a difficult and time consuming task. This task is even more demanding due to the variety of packages and libraries involved in the process and their dependencies and resource restrictions. In order to ease such a task, different HPC package managers and build tools are currently available. The **EasyBuild** framework offers an automated approach of the HPC compilation phase, targeting specific architectures and distributions [11]. Another approach is offered by **Spack**<sup>1</sup>, which supports multiple versions, configurations, platforms, and compilers, and **lmod**, a “Lua based module system that easily handles the MODULEPATH Hierarchical problem”<sup>2</sup> [11].

One approach, also considered in the context of the CloudLightning project, is to provide a customized cloud-based environment for supporting some HPC applications by abstracting the components and offering an automated way of compiling them. The system presented in [12] targets this idea, but still does not provide the same level of abstraction and flexibility aimed in our research. By contrast, our current approach enables an abstraction of services, allowing the system to choose between various hardware implementation of the same service. Still, Unruh *et al.* introduce the need of automated compilation using customizable pre-defined modules that can be linked together as the end-user designed the application topology.

Description of cloud services, by using specialized languages, is being offered in various frameworks, such as OpenStack Solum<sup>3</sup> or Apache Brooklyn<sup>4</sup>. They offer a specialized solution for the interaction between end-user and the cloud environment, where the end-user have the ability to describe the application in a TOSCA or CAMP blueprint, together with its dependencies, deployment artifacts and others. The blueprint is further decomposed into appropriate API calls for interacting with the underlying cloud infrastructure. One drawback of these approaches is the concern of the end-user regarding two issues: (1) what are the services and (2) how are they provided, together with the lack of ability to perform global deployment optimizations, as each component request is treated independently.

### 3 Requirements for a Cloud Service Description Language

One of the driving principles in designing a service description framework is the *separation of concerns*. This concept is based on the assumption that users (cloud consumers) concentrate on what are the service they require, while providing minimal (and preferably none) information about how the service is to be

<sup>1</sup> <https://spack.io/>.

<sup>2</sup> <http://lmod.readthedocs.io/en/latest/>.

<sup>3</sup> <https://wiki.openstack.org/wiki/Solum>.

<sup>4</sup> <https://brooklyn.apache.org>.

provided. In order to achieve this, a clear services interface between the service consumer and provider must be specified [13]. The cloud later, service provider, should be concerned only on the problem of how services are to be provided.

By using such an approach, the cloud consumer gets more flexibility in the description and characterization of the requested services, while the cloud service provider gets the ability to develop a variety of offerings, eventually adapted to diverse hardware configurations.

### 3.1 The CloudLightning Approach

CloudLightning<sup>5</sup> is a H2020 project that aims at offering solutions for providing cloud tailored computing and data processing capabilities on top of self-organising & self-managing infrastructures. The targeted beneficiaries are rather interested in deploying applications on CloudLightning-enabled computing resources. The project builds on top of existing software components and complements them with the autonomic (self-\*) capabilities.

In order to implement these capabilities, the project defines new means of provisioning heterogeneous resources to deliver services specified by using a bespoke service description language (CL-SDL). The self-organising behavior of the platform exploits these service specifications in different ways, providing mechanisms able to trigger the necessary management tasks for service commissioning, deployment, execution and monitoring [14]. A specific adaptation exposed by the system is inspired by requirements of high performance computing applications, and is represented by the formation and selection of several resource coalitions capable to support individual requirements for each of the target service. Typically, coalitions will be composed of tightly coupled groups of heterogeneous components.

### 3.2 CL-SDL Requirements

The CloudLightning approach identifies domains of concern at different layers, corresponding to the three categories of actors: end-users, as service consumers, enterprise application developers and operators or cloud service providers. Although different categories of actors can share concerns, a separation should appear if possible between these identified domains.

While concerns of the end-user are high-level, rather functional (e.g., service availability, continuity, security, etc.), the concerns of cloud service providers are low-level, highly resource oriented, and those of the enterprise application developer and operator are covering mappings and adaptations from the high-level concerns to the low-level ones.

Even if more flexibility can be attained at the level of each actor category, an important drawback can be identified at lower levels: the heterogeneous characteristic of the underlying infrastructure require more complex management

---

<sup>5</sup> <https://www.cloudlightning.eu>.

efforts from the cloud service provider. Services have to adapt to various constraints and QoS parameters that may have been received from upper layers. In fact, behind this complexity the cloud service provider receives more control and flexibility on their operations, and will respond with pre-configured collections of resources which are capable to meet the identified requirements.

The separation of concerns will consequently manifest on cloud application lifecycle management level and resource lifecycle management level, with full support from the service description language. In order to achieve this, the service description framework will use existing inputs in order to generate resource templates which are consequently submitted to specialized discovery and selection components of the self-organising & self-management system. Once the collection of relevant resources was identified, the service description framework will use the existing inputs together with the response for building a resourced version of the initial (abstract) specification (as detailed in Sect. 4).

### 3.3 The CloudLightning use-cases

**Genomics Sequence Alignment.** Genomics is the discipline of genetics that studies DNA information by applying various string sequencing algorithms on the DNA strings. By doing so it can predict and analyze the structure and functions of individual genes. The use of these techniques advanced medical field further towards a patient centered treatment and prevention mechanisms rather than the use of generic medicine. In order to achieve these goals one has to follow a series of labor intensive steps like (i) DNA sequencing (ii) sequence alignment (iii) sequence annotation (iv) various genetic analysis types. In the context of the CloudLightning project the sequence alignment algorithm is fine tuned in order to be computationally efficient on Maxeler's data flow engines (DFE), obtaining significant increase in overall performance.

**Oil and Gas Exploration.** Similar to the case of genomics and sequence alignment in the case of oil and gas exploration the algorithms deployed in order to determine whether there are resources under the surface extensively use high performance computers for image generation. The data used in order to generate the models of Earth's subsurface are collected from various seismic surveys and from simulations of multi-phase flow in porous media like rock formations. In this type of industry finding an 1% improvement in accuracy of prediction results in revenues of billions of Euro/USD. Current work is usually performed in-house on large dedicated servers or clusters without leveraging on accelerators as GPUs or even DFE's. The CloudLightning approach is to migrate such applications in such a way that the use of cloud resources is viable.

**Ray-Tracing.** The application comes under a broader category of image rendering that uses the laws of physics to generate more photo-realistic graphics from 2D or 3D models by means of computer programs like Monte Carlo methods. Usually the input to a ray-tracer engine will have a well defined data structures



as inputs like geometry or the structure of the object, viewpoint of the camera, texture of the object, lighting of the environment etc. The ray-tracing engine then renders by solving the rendering equations to produce the graphical image as output. In computer graphics, rendering is basically used by architects to conceptualize their ideas, gamers to display graphics, animation artists to create movies and many more areas where visual effects has a major role.

**Weather Research Forecasting (WRF).** The Weather Research & Forecasting (WRF) Model is a widely used system for obtaining weather forecasting or meteorological information, developed using parallel, computation-efficient and extensible algorithms, with a complex architecture [15]. Each of the building blocks of the WRF platform can be built individually, considering that different building mechanism and external dependencies for different types of architecture exist. Additionally, one must make sure that some of the modules are build in a certain order, due to the existing dependencies. Consequently, the building process is quite complex for the ordinary user of the system.

### 3.4 Transition to Self Compiling

Several problems can arise from the set of use-cases when using specialized architectures: the high cost of the infrastructure; additional skills and effort for compiling the desired code; code compatibility with the target architecture. Additional issues that have to be addressed are related with the way software can be compiled in order to deploy on the miscellaneous architectures that constitute the infrastructure.

For approaching some of these problems one has to adapt some of the mechanisms enabling on-the-fly compilation of software for various target architectures and library dependencies. The approach of on-demand (on-the-fly) compilation is a well studied field and various solutions can be used for achieving the goal on personal computers. For the case of cloud infrastructures it is a bit more complex to adapt such a solution due to the heterogeneous nature of cloud environments.

The solution that was considered for our current research is based on Easy-Build [11], a set of tools that enable users to compile applications on demand. The mixture of such mechanisms with the proposed solution from CloudLightning for self-managing clouds results into a system that can be configured to automatically adapt and compile software for newly added types of hardware to the cloud ecosystem.

## 4 The CloudLightning mechanisms

The CloudLightning mechanisms for implementing the separation of concerns is based on the CL-SDL, as detailed in Fig. 1. The service description language is basically used to describe relevant documents for the blueprint lifecycle management: an *abstract blueprint*, an *resource template* and the *resourced blueprint*.

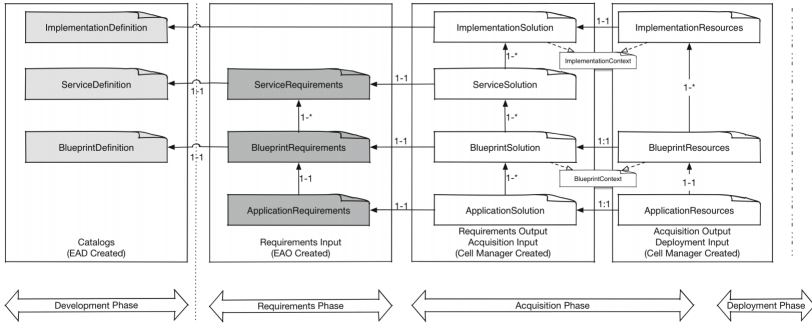


Fig. 1. API message flows

While first document is used to represent specific application requirements, constraints and metrics, the last one is filled after invoking the CloudLightning self-organising & self-management subsystem by a *service decomposition engine* (SDE). Once an *abstract blueprint* is presented at the gateway service, it will be decomposed into individual services, which will be further processed on demand. For each individual service, the SDE will check if a direct instantiation is possible, otherwise the CL-SOSM subsystem will be interrogated to support the selection of a proper implementation for the particular service. As an outcome of this step, the initial *abstract blueprint* will be updated with the resource information coming from the underlying subsystem. Next, the SDE and CL-SOSM will collaborate in order to construct the *resource templates* offering information about specific requirements for each service implementation, and the *resourced blueprint*, filled with the necessary resource information for further operation.

#### 4.1 Enabling HPC Applications with EasyBuild

In the CloudLightning context, lifecycle of an application can be defined as a sequence of five major steps (as presented in Fig. 2).

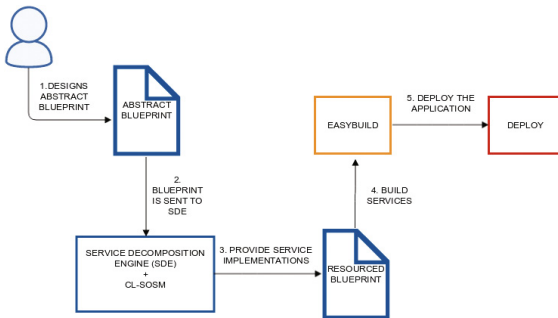
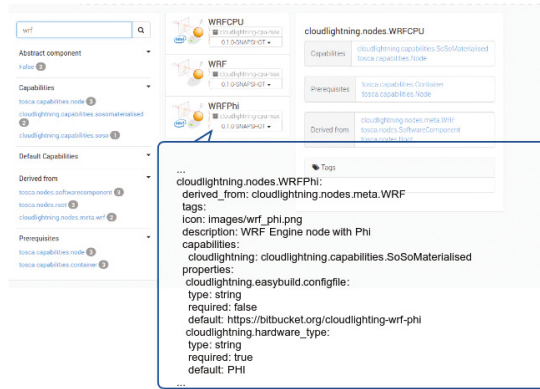


Fig. 2. Application lifecycle in the CloudLightning environment



**Fig. 3.** Sample of available services for the WRF usecase

**Step 1.** By using the CL-SDL, users design the application topology, representing components of the application and their relationships. Available services and their implementations are provided by the service developers and can be added to the CloudLightning environment using a CSAR (Cloud Service ARchive). Each CSAR will contain the description and functionality of individual services. For example, Fig. 3 presents a snippet from the OASIS TOSCA document describing a WRFPHI node, its abstract implementation, and the configuration in order to run on XEON-PHI architecture. Users select the desired abstract services, composes a topology and configures the requirements. After performing these steps an *Abstract Blueprint* results. The document is TOSCA compliant and contains the abstract definition of individual services required by the application.

**Step 2.** The *Abstract Blueprint* is sent to the Service Decomposition Engine (SDE), which extracts abstract services and their special user-customizations properties. Next, a requirement for their implementation is sent to the CL-SOSM system.

**Step 3.** Next, the response from CL-SOSM is used to replace each abstract service from the initial topology with its proper implementation. For WRF case presented, the user created a topology with two abstract WRF services, depending on each other. The outcome of the entire process is depicted in Fig. 4, where one abstract service was replaced with a WRFPHI implementation and the other one with a WRFCPU. The newly created topology, as described in the *Resourced Blueprint*, contains only concrete services, optimized by CloudLightning for a proper architecture.

**Step 4.** Build the application, from new topology description. The building process needs to take into consideration the architecture requirements and dependencies between services. *EasyBuild* enables us to fully automate the building process of a service by using a proper *EasyConfig* file. Gateway service decomposes the topology again and extracts services that incorporate *EasyConfig* files. Next step the gateway service sends requests to build the services, also handling

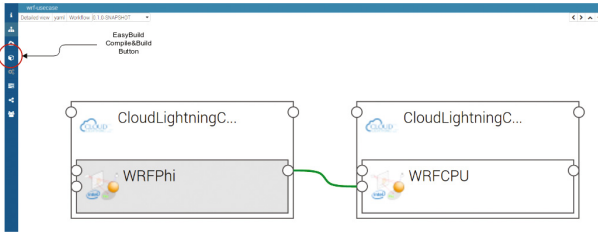


**Fig. 4.** Sample of a concrete topology for the WRF usecase

dependencies between them. As in our example if in the application topology ServiceB is in a *dependsOn* relationship with ServiceA, ServiceB is going to be build after ServiceA. Using building scripts for each service implementation increases the flexibility in designing application topology. Pre-build service implementations are not considering individual user customizations of services and the relationship between them.

**Step 5.** The deployment process: the CloudLightning system instantiates the proper containers and deploy the built sources generated in the previous step.

## 5 Conclusions

We presented the background of CloudLightning approach for an extensible service description language, capable to describe HPC workloads and with the capability to automatically build HPC applications provided that `easybuild/easyconfig` artifacts are available for such an application. The CloudLightning approach, coupled with the expression capabilities of the CLSDL, offer the ability to build tailored cloud environments based on the outstanding application's requirements and the exposed self-organising & self-management capabilities. By using HPC-inspired use-cases, one can emphasize the functionalities of CloudLightning solution on top of heterogeneous cloud resources, and the new means of accessing those resources. At the same time, these characteristics define the core capabilities for accessing heterogeneous resources which may be interesting while migrating HPC applications to cloud computing. When these capabilities are complemented by the ability to automatically build HPC applications based on the `easybuild`, it becomes possible both to fully describe the execution environment and to efficiently access the full range of resources that were made available via the CloudLightning coalition.

**Acknowledgment.** This work was partially funded by the European Union's Horizon 2020 Research and Innovation Programme through the CloudLightning project (<http://www.cloudlightning.eu>) under Grant Agreement Number 643946.

## References

1. Geada, D.: The case for the heterogeneous cloud. *Cloud Comput. J.* **11**(3), 521–525 (2011)
2. Moscato, F., Aversa, R., Di Martino, B., Fortiș, T.F., Munteanu, V.: An analysis of mOSAIC ontology for cloud resources annotation. In: 2011 Federated Conference on Computer Science and Information Systems (FedCSIS), pp. 973–980. IEEE (2011)
3. Ferry, N., Almeida, M., Solberg, A.: The MODAClouds model-driven development. In: *Model-Driven Development and Operation of Multi-Cloud Applications*, pp. 23–33. Springer Nature, December 2016
4. Soldani, J., Binz, T., Breitenbcher, U., Leymann, F., Brogi, A.: ToscaMart: a method for adapting and reusing cloud applications. *J. Syst. Softw.* **113**, 395–406 (2016)
5. Sanaei, Z., Abolfazli, S., Gani, A., Buyya, R.: Heterogeneity in mobile cloud computing: taxonomy and open challenges. *IEEE Commun. Surv. Tutorials* **16**(1), 369–392 (2014)
6. Gupta, A., Kale, L.V., Gioachin, F., March, V., Suen, C.H., Lee, B.S., Faraboschi, P., Kaufmann, R., Milojevic, D.: The who, what, why, and how of high performance computing in the cloud. In: 2013 IEEE 5th International Conference on Cloud Computing Technology and Science. IEEE, December 2013
7. Somasundaram, T.S., Govindarajan, K.: CLOUDRB: a framework for scheduling and managing high-performance computing (HPC) applications in science cloud. *Future Gener. Comput. Syst.* **34**, 47–65 (2014)
8. Mauch, V., Kunze, M., Hillenbrand, M.: High performance cloud computing. *Future Gener. Comput. Syst.* **29**(6), 1408–1416 (2013)
9. Payne, W.: Modular HPC goes mainstream, October 2016. <https://www.scientific-computing.com/feature/modular-hpc-goes-mainstream>
10. Lynn, T., Xiong, H., Dong, D., Momani, B., Gravvanis, G., Filelis-Papadopoulos, C., Elster, A., Khan, M., Tzovaras, D., Giannoutakis, K., Petcu, D., Neagul, M., Drăgan, I., Kuppudayar, P., Natarajan, S., McGrath, M., Gaydadjiev, G., Becker, T., Gourinovitch, A., Kenny, D., Morrison, J.: CLOUDLIGHTNING: a framework for a self-organising and self-managing heterogeneous cloud. In: *Proceedings of the 6th International Conference on Cloud Computing and Services Science. SCITEPRESS - Science and Technology Publications* (2016)
11. Geimer, M., Hoste, K., McLay, R.: Modern scientific software management using EasyBuild and Lmod. In: 2014 First International Workshop on HPC User Support Tools, pp. 41–51. HUST 2014. IEEE, Piscataway, November 2014
12. Unruh, I., Bardas, A.G., Zhuang, R., Ou, X., DeLoach, S.A.: Compiling abstract specifications into concrete systems—bringing order to the cloud. In: 28th Large Installation System Administration Conference (LISA 2014), pp. 26–42. USENIX Association, Seattle, WA (2014)
13. Morrison, J., Xiong, H., Dong, D., Momani, B.: D3.1.2 report on state of the art and draft architecture. Project deliverable, CloudLightning Project Consortium. <http://cloudlightning.eu/work-packages/public-deliverables/>
14. Marinescu, D.C., Morrison, J.P., Paya, A.: Is cloud self-organization feasible? In: *Adaptive Resource Management and Scheduling for Cloud Computing Workshop, ARMS-CC 2015*, pp. 119–127. Springer International Publishing (2015)
15. User’s guide for the advanced research WRF (ARW) modeling system version 3.8 (2016). [http://www2.mmm.ucar.edu/wrf/users/docs/user\\_guide.V3.8/contents.html](http://www2.mmm.ucar.edu/wrf/users/docs/user_guide.V3.8/contents.html)

**The 7th International Workshop  
on Intelligent Computing  
In Large-Scale Systems (ICLS-2017)**

# On Context-Aware Evidence-Based Data Driven Development of Diagnostic Scales for Depression

Philip Moore<sup>1</sup>(✉) and Hai Van Pham<sup>2</sup>

<sup>1</sup> School of Information Science and Engineering,  
Lanzhou University, Lanzhou, China  
ptmbcu@gmail.com

<sup>2</sup> School of Information Technology and Communication,  
Hanoi University of Science and Technology, Hanoi, Vietnam  
haipv@soict.hust.edu.vn

**Abstract.** There is a growing interest in health information technology using evidence-based approaches in clinical decision-support systems, the goal for such systems is ‘precision medicine’ using ‘interventional informatics’. However, the impact has been less than positive and it has been argued that interventional informatics using data-driven interventions is required to achieve evidence-based clinical decision-support. In this paper we discuss context-Aware, evidence-based, data driven development of diagnostic scales created using multi-disciplinary collaborative development. The goal is the development of novel dynamic scales for decision-support in healthcare provision and, while clinicians may derive benefit from such systems, there are potentially greater benefits for all stakeholders in medical triage systems using both face-to-face and remote consultations. While our focus lies in depression, the proposed approach will generalise to a diverse range of domains, systems, and technologies.

## 1 Background

Health Information Technology (HIT) has gained significant traction with the aim of achieving “precision medicine” (PM) using “interventional informatics” (InIs) [42]. While there have been positive benefits [on a clinical level] the impact of HIT “has been less than positive” in terms of computational tools to enable data-driven precision in the provision of clinical decision-support [42]. Embi & Payne [16] argue for a new clinical paradigm which leverages ‘point-of-care’ (PoC) activities, data, and resources to generate evidence through routine practice. Payne *et al.* [42] argue that InIs, using data-driven intervention at the PoC, is required to generate evidence-based clinical decision-support systems. While the need for such an approach in the provision of clinical decision-support is required to address the exponential growth in the demand for healthcare services, we may conclude that the development of effective PoC clinical decision-support systems has not been achieved.

InIs [in providing an effective basis for decision-support in clinical practice] essentially relates to the provision of novel scales which define the domain specific parameters including specific psychophysiological [54] metrics (see Sect. 3)

including cognitive features [33]. We consider the creation of such scales using a multi-disciplinary collaborative approach between domain experts and computer scientists, the ultimate goal being the creation of dynamic scales capable of providing an effective basis for decision-support in patient diagnostics and monitoring. In this paper we propose a context-aware InIs evidence-based data driven approach to enable the development of diagnostic scales and, while the focus of this paper lies in depression, we argue that the posited approach will generalise to other medical conditions and other domains, systems, and technologies.

The remainder of this paper is structured as follows: collaborative design is introduced in Sect. 2 with an overview of context-awareness in Sect. 3. Data-driven informatics and data processing are addressed in Sect. 4. Diagnostic scales are discussed in Sect. 5 with a brief overview of depressive states provided in Sect. 6. Collaborative systems development is considered in Sect. 7. A discussion is provided in Section 8 with concluding observations in Sect. 9.

## 2 Collaborative Design and Development

PM [42] has a correlation with *Targeted Personalised Service Provision* (TPSP) in *Context-Aware Systems* (CAS) applied in a broad range of domains, systems, and technologies [35]. CAS are domain specific [in both design and implementation] and require domain specific skills including a high level of domain knowledge and expertise combined with similar high levels of computational skills in programming and data structures [43]. In practice, in the creation of a CAS, individuals and organisations who possess the required domain knowledge generally lack the required computational skills. Similarly, those with the required computational skills may be barred from building a CAS due to the lack of domain knowledge.

If effective CAS systems [capable of delivering PM] are to be realised, the problem lies in the need to create a multi-disciplinary research and development structures capable of merging the domain knowledge [of clinicians and healthcare professionals] with the required computational skills [of computer scientists]. Such a collaborative approach will be also be required in translational research [2] where the research conducted in a laboratory environment is translated into ‘real-world’ clinical trials and ultimately clinical practice.

## 3 Context-Aware Systems

CAS are essentially *Decision-Support Systems* (DSS) designed to implement TPSP along with the identification of *appropriate* decisions [35]. Context is a concept which describes and defines the current prevailing *state* of an *entity*, an entity being defined as a *person, place or physical or computational* object [1]. CAS are highly domain specific, the domain-specific nature of context required the identification of specific function(s) and properties that identify an entities dynamically changing context, in this paper an individual patient’s context refers to the generality of their medical condition.



Context may be viewed a set of changing relationships to address short term and long term context(s). Context is inherently dynamic however, as context(s) evolve [over time], not all *Contextual Information* (CI) is changed. Consider a changing context from time [t1] to time [t2] (see Sect. 4). There are clearly data which will not change (a *static* context) and there are elements of a context which will change (a *dynamic* context). In practice almost any information available at the time of an individuals interaction [with a CAS] can be viewed as CI, such information may include: *physical* and *spatio-temporal* information with the *social* situation [35]. Research is however addressing an increasing range and scope of CI which includes:

1. *audio-visual* sensory information
2. *computational haptics*: senses which respond to motions and forces exerted by the interaction of the body with the external environment (sensations such as touch, temperature, pressure, etc. mediated by skin, muscle, tendon, or joint) and motor activities.
3. *computational psychophysiology* including: *electromyography* (EMG), *electrocardiography* (ECG), *electroencephalography* (EEG), and *galvanic skin response* (GSR).
4. *semantic* and *linguistic* information implemented using: *kansei* engineering with hedge algebras [43] and *semiotics* [20].
5. *abstract information*: such as an individuals emotional responses (to a range of stimuli).
6. Current research is investigating *dopamine*, *serotonin*, and *noradrenaline* as bio-markers for depressive states [51].

In considering the healthcare domain, the potential range of CI [see points 1–6] is fundamental in the development of PM and the related novel scales capable of modelling mental disorders including depression. In future CAS the use of cognitive features and metrics, such as abstract information, offers interesting potential opportunities in the diagnosis and monitoring of depression and depressive states.

There are significant data contained within social networks, also in the healthcare domain there are legacy systems, for example consider manuscript patient records. Such data has relevance in the diagnosis and management of depression, however retrieving such data requires the use of linguistics and semantics. We may also consider the developing field of ‘sentiment analysis’ [60] and how such an analysis identifies emotion (more accurately emotional response) [33].

## 4 Data-Driven Interventional Informatics

CI processed into information useful for use in *Context Processing* (CP) is central in CAS. Research into *Information Systems* (IS) has investigated the use of development frameworks and models, for example see [21]. While the proposed approaches differ the research concurs in identifying the need for a comprehensive framework or model. Wiederhold [57] argues for smart software to improve access

to the type and quality of information needed for ‘decision-making’. Going further, Wiederhold [57] has observed that the development of the concepts required in future IS requires the modelling of information processing which integrates data and knowledge.

The traditional view of IS is one where data is processed into information. Checkland & Holwell [8] have extended this view by introducing an intermediate stage termed CAPTA, which is defined as “data selected, created, or to which attention is paid” and involves the selection of data for processing into information useful to users or computational systems. We may view CAS as an extension of IS incorporating the capability to implement CAPTA and realise TPSP with decision-support with *Constraint Satisfaction and Preference Compliance* (CS) [35]. Moreover, we may further extend CAPTA to incorporate the concepts of *knowledge* and *wisdom*, wisdom being defined as ‘the ability to use knowledge and experience to make good decisions and judgements.

A discussion on the concept of knowledge and wisdom is beyond the scope of this paper, however we may observe that incorporating such concepts into CAS represents a paradigm shift in data management and usage which induces existential change in the way we view data. However, there are significant issues in the creation of cognitive models as discussed in [33]. In considering *data-driven interventional informatics* (DDII) data processing involves ‘real-time’ data processing (RTDP) and data analytics in big-data analytic solutions (BDAS), these approaches to data processing are considered in the following sections.

#### 4.1 Data Processing

The goal of RTDP, in a health-monitoring scenario, is to measure a patient’s current prevailing context. The objective in ‘real-time’ patient monitoring is to compare a patient’s context at time  $[t_0]$  and the changed (new) context [35] at time  $[t_1]$ . In a healthcare scenario a context measures the patient’s dynamically changing symptoms which characterise a patient’s medical condition, the time intervals between  $[t_0]$  and  $[t_1]$  will be defined by clinicians dependent on the patient’s medical condition and prescribed treatment plan following diagnosis.

The approach proposed to enable RTDP is detailed in [35]. As the proposed approach applies to patient monitoring the volume of data stored locally will be restricted to the existing context  $[t_0]$  and the new updated context at time  $[t_1]$  [35], thus the data storage requirements will be relatively small. Turning to BDAS the total volume of data, from multiple patients, is potentially huge [58]. For many reasons (including logging and further analysis) [52] the data may be sent at periodic intervals to BDAS using either: (1) a continuous data stream, or (2) bulk uploading at predefined intervals.

Data processing in BDAS is designed to implement: data cleansing to detect potential missing data and identify errors, ensure governance, and bring it to a format suitable for later analysis. There is therefore a data cycle from data capturing to final data persistence and analysis [15]. BDAS demand potentially massive data storage and computing power as compared to the demands of RTDP. Additionally, many current [often cloud-based] systems may use unstructured

data [a feature of many Internet-based systems] using horizontal and vertical scaling. Accommodating unstructured data stores is challenging for traditional relational database management systems (RDMS) resulting in the rise of solutions capable of managing unstructured data, for a discussion on traditional database systems and unstructured data systems see [36].

BDAS have differing goals as compared to RTDP. Big-data science [15] relates to a scenario in which very large volumes of data are gathered and processed to identify [in the case of health monitoring systems] trends in the data and potential prognoses predicated on multiple patient prognoses and outcomes over time. Clearly, the potential volume of data and outcomes [from multiple patients] presents unlimited opportunities for data mining along with significant challenges in terms of the management of the volume of data and the diversity in the sources of such data.

## 5 Diagnostic Scales and Depression

The traditional approach to the diagnosis and management of depression uses psychometrics which is a field of study concerned with the theory and techniques for psychological measurement.

Boyle [7] has questioned the reliability of psychometric scales observing that: “the term ‘internal consistency’ has been used extensively in classical psychometrics to refer to the reliability of a scale based on the degree of ‘withinscale’ item ‘intercorrelation’ as measured by the ‘split-half method’, or more adequately by Cronbach’s ‘alpha’, ‘KR20’, and ‘KR21’ coefficients as discussed in [11]”. The term *internal consistency* is however “arguably a misnomer” [7] as high estimates of internal item consistency/homogeneity may also suggest high levels of item redundancy, i.e., the same item may be expressed in a number of ways - this has a correlation with issues in the merging and matching of semantic ontologies [19]. In summary Boyle concludes that the general psychometric scales in use are limited and relatively dated.

An inventory for the measurement of clinical anxiety based on psychometric properties is proposed by Beck *et al.* [4], Beck *et al.* consider differentiating anxiety and depression where the cognitive “content-specificity hypothesis” is tested. Watson *et al.* [56] address the development and validation of brief measures of positive and negative affect (the *PANAS* scales). Poznanski *et al.* [45] propose a depression scale for children.

Lovibond & Lovibond [30] consider the structure of negative emotional states and perform a comparative analysis of depressive anxiety stress scales with the Beck depression and anxiety inventories. Yesavage [59] present a study [in a preliminary report] which addressed the development and validation of geriatric depression screening scales. Short screening scales to monitor population prevalences and trends in non-specific psychological distress was studied by Kessler *et al.* in [26].

The data used in the assessment of mental disorders is generally very subjective and is frequently based on self reporting by patients and observation

by healthcare professionals. For example, in the assessment of aggression and agitation in Alzheimer’s disease and dementias [17], the monitoring of the development of the condition frequently uses scales such as the well known and recognised ‘Cohen Mansfield Agitation Index’ to assess the Behavioural and Psychological Symptoms of Dementia (BPSD) [17]. Current research, for example see [25], is attempting to address the provision of objective data usable in the diagnosis and management of mental disorders in ‘real-world’ conditions.

It is clear that the quality of health monitoring and the related scales is generally uneven [32]. While in recent years there have been promising developments which are replacing the: “enthusiastic proliferation of hastily constructed measures that typified the 1970’s” [31], there remains an urgent need for new multi-modal scales incorporating both subjective and objective sensor data [derived from sensor networks] in both a machine and human readable formalism [34].

In this paper our focus lies in the realisation of effective diagnosis and management of depression which requires an “integrated approach” [53] using both face-to-face (F2F) and remote consultations to: (1) diagnose and prescribe treatments, and (2) implement post-discharge monitoring to check for relapse. As discussed in Sect. 1, to address these requirements we propose the development of novel scales which may be viewed in terms of a set of parameters (symptom metrics) against which a patient’s dynamic context may be measured. Such scales must incorporate: (1) psychological factors, (2) physiological factors, (3) cognitive features, (4) environmental conditions, and (5) social factors (see Sect. 3). Such scales may be considered to be context definitions which define and describe a patient’s current prevailing dynamic state as discussed in [35] and will be developed using a DDII with evidence-based medicine (EBM) approach.

The parameters and metrics used in the scales used in ‘real-time’ diagnostics and patient monitoring may be derived from BDAS (see Sect. 4) using data obtained in ‘real-time’ from multiple patients. The application of BDAS enables the identification of trends in the data related to actual prognoses and provide a basis upon which multi-modal diagnostic scales may be developed and updated over time.

## 6 Depressive States

Depression is a highly variable condition that impacts individuals across demographics and gender and is also a feature of a number of mental disorders [53]. Depression and depressive states reflect an individual’s low mood and aversion to activity resulting in significant *affects* in an individual’s thoughts, behaviour, feelings and sense of well-being [3]. In serious cases (clinical depression) patients may contemplate (or even commit) suicide [40]. Greenberg introduces the emotional component into the treatment of depression, recent evidence suggesting that recurrent episodes of severe depression are associated with changes in brain function that further heighten vulnerability and functional impairment [22]. It has been suggested that for individuals, memory(s) are pre-existing ‘brain state(s)’, such a conjecture may also apply to depression and depressive states [14].

An important component in the diagnosis and management of depression is cognition and related cognitive factors. A well understood and respected technique to measure brain activity is *electroencephalography* (EEG) with *magnetic resonance imaging* (MRI). These techniques have been central to research conducted in the Ubiquitous Awareness and Intelligent Solutions Lab (UAIS) in the School of Information Science and Engineering at Lanzhou University (LZU) where significant results have been reported in studies addressing depression with related emotion and Affective Computing (AC), reported research includes: [12, 24, 25, 28].

Space restricts a detailed discussion on the research conducted in UAIS at LZU however, in summary, the research conducted in has approached the study of depression on both conceptual and practical levels. Collaborative multi-disciplinary research has utilised EEG with MRI to enable the identification and selection of cognitive features relating to depressive states. A range of potential AI solutions have been investigated and tested including hybrid approaches with ontology-based data structures [9, 50]. The results are encouraging, there remain however challenges in collecting cognitive data in ‘real-world’ conditions.

From the foregoing discussion is clear that we may view depression on a spectrum as, while it may be clinical depression, it may also be a normal reaction to life events, dysthymia [18], or side effects resulting from drugs and medical treatments. There is also a clear synergy between the symptoms of depression and the emotive responses identified by behavioural biologists such as Plutchik in [44] where similar negative and positive reactions are discussed.

## 7 Collaborative Systems Development

We have considered Collaborative design and development in Sect. 2 where we posit that a multi-disciplinary collaborative approach is essential. Consider a design and development scenario for dynamic diagnostic scales for use in the management of depression. The stakeholders involved in the development process will be: (1) domain experts, (2) computer scientists, (3) patients diagnosed with depression, and (4) a healthy control group. In considering the identification of healthy individuals there is clearly an issue given that depression may be viewed on a spectrum (see Sect. 6), this must be addressed in the research design methodology with depressive states being classified using, for example, Gaussian distribution [48] or alternatively valence modelling [13, 39].

There follows a brief overview of the research and development process in which scales will be developed using an iterative process such as the recognised *spiral model* [5] used in software engineering. The process will require two stages: (1) design and development, and (2) translational research. In practice, the research process will involve a number of stages with incremental steps which is briefly outlined in the following sections.

## 7.1 Stage One: Research Design and Development

Currently, a presenting patient will be diagnosed by a clinician in a F2F consultation followed by [where required] referral to specialist psychiatric services. Diagnoses are generally made by clinicians based on observation of a patient's symptoms, and similarly, the majority of patient's are monitored in F2F consultations at intervals set by the clinician. Diagnostic scales may be useful in such consultations, moreover scales will provide a basis for autonomic diagnostic systems. A research plan will involve the following phases:

1. Team building: recruit the research team including (see Sect. 2).
2. Research phase: identify and collect the data (see Sect. 3 to identify the current 'state-of-the-art').
3. Create prototype scales: in a human and machine readable formalism.
4. Recruit research population: unbiased with respect to demographics, socio-economic status, racial profile, and gender.
5. Evaluation phase: test and evaluate the prototype scales.
6. Create new (updated) scales: implemented based on the results from the evaluation phase.
7. Recruit a new research population: unbiased evaluation study population (patients presenting with depression).
8. Evaluation phase: test and evaluate the new scales for their efficacy using the new unbiased population.

## 7.2 Stage Two: Translational Research

Translational research [2] is the stage in which laboratory research is translated into 'real-world' clinical practice. We postulate that the new diagnostic scales may be used in clinical practice with dynamic updating of electronic patient records as discussed in Sect. 4. It is recognised that the *operation and maintenance* is normally the longest phase in the software life cycle [49], in this stage collaboration is essential to develop a maintenance program to manage the dynamic updating process for the scales.

## 7.3 Experimental Examples

The collaborative development approach as discussed in Sect. 2 has been applied in research conducted by *Hanoi University of Science and Technology* (HUST) and *Lanzhou University* (LZU). The research conducted at LZU is introduced in Sect. 6. The research carried out by HUST is an experimental case study in the healthcare domain carried out in Vietnamese and Japanese hospitals during the period February to August 2016. Three medical conditions form the basis for the study, the conditions are: (1) influenza, (2) cough, and (3) sore throat.

Space restricts a detailed discussion on the HUST implementation which utilised the *Context Processing Algorithm* (CPA) [35] however in summary, to evaluate the CPA the multi-disciplinary approach was used to evaluate the performance of the CPA under 'real-world' conditions. In a comparative analysis

the CPA utilised the ‘rule-based’ approach (based on approximately 50 rules in the knowledge-base). The results achieved positive correct responses in the range 92% to 96% between context matches and expert diagnoses. Following updating of the new rules in our ‘knowledge-base’ our proposed system demonstrated significant improvement [in ‘rule-based’ system generated diagnoses] as compared to the results derived from expert diagnoses. For both the research projects conducted by LZU and HUST the multi-disciplinary approach proved effective in achieving significant results in ‘real-world’ conditions.

## 8 Discussion

Healthcare systems face many socio-economic and geo-political challenges which include meeting the exponential demand growth for healthcare services in both human and resource management terms. The growth is driven by many factors which include demographic change, the provision of technologically enhanced treatment options, and the desire to improve the quality of life for patients and carers alike [47].

Mental disorders make a growing contribution to the demand for medical and related social services [55]. To attempt to meet this demand, future clinical practice will employ HIT used in both F2F consultations and remote (possibly on-line) triage conducted by both qualified clinicians and trained healthcare professionals (such as psychiatric nurses). We have presented an overview of depression and have considered collaborative multi-disciplinary development of novel scales in both a machine and human readable formalism. To provide a basis upon which such scales may be developed we have presented an HIT approach employing EBM and DDII to enable RTDA and BDAS.

As discussed in Sects. 2 and 3, context is highly domain specific and may address a broad and diverse range of CI which may include: the *physical* conditions, *spatio-temporal* information, and the *social* situation. Research is however addressing an increasing range and scope of data and information including: cognitive features and the emotional component which is fundamental in the diagnosis and management of depressive states [33,38]. There are interesting developments in the field of machine cognition and the integration of emotional response, there is also developing interest in the use of bio-markers however there remain significant challenges and their use represents an open research question.

While much of the CI may be obtained using existing sensor technologies a principal challenge lies in capturing cognitive data using non-invasive sensors, this remains an open research question. Notwithstanding the limitations in current sensor technologies, wearable sensors have demonstrated the capability to measure a broad range of physiological and environmental data. Sensors can also monitor sleep patterns using newly developed user interfaces (including mobile devices) that are able to remotely control other computer devices through brain electrical activity. Nusser *et al.* [41] consider newly emerging measurement technologies [for intensive monitoring of individual behaviours and physiological responses] in a wide range of settings, space restricts a detailed discussion on sensor technologies however in summary:

- Emerging evidence suggests that commercial EEG headsets are capable of detecting emotional response [such as excitement or frustration] in a non-clinical : population.
- The creation of devices to record and transmit a diverse range of chronologically stamped data (see Sect. 3) usable in both RTDP and BDAS (see Sects. 4 and 8).

Wearable computing, with data and information integrated into electronic patient records will provide access for clinicians to monitor dynamic change in a patient's state (or context) to inform treatment options. Future 'real-time' diagnostic and monitoring systems [implemented in a range of settings] may use local data processing. For example, mobile devices may access and process data captured from sensor networks with sensors located both in the home and on the person, this may be viewed in terms of a *Body Area Network* (BAN) [10] (alternatively termed *Body Sensor Networks* (BSN) [29]). Such local processing may implemented using the *Web-of-Things* (WoT) using *Fog Computing* (FC) as discussed in [6] where FC and it's role in the *Internet of Things* (IoT) is introduced.

However, a significant challenge lies in 'open data' [23,46,58]. Additionally, patient data [used to store, query, and update patient data in continuous patient monitoring and diagnostics] can be variable, imprecise, and unreliable [37]. Additionally such data may gathered from different sources which include traditional RDMS, legacy systems, and systems which use unstructured data (or 'NoSQL') [often cloud-based systems] [36]. Addressing these challenges and developing future HIT systems forms the basis for future research.

## 9 Concluding Observations

In this paper, we have introduced a context-aware data driven approach using EBM based DDII with RTDA and related BDAS to enable the development and maintenance of novel scales to provide an effective basis for the diagnosis, management, and treatment of depression using autonomic decision-support systems. While clinicians may derive benefit from such systems, there are potentially greater benefits when decision-support systems are implemented in triage systems [in both F2F and *remote* consultations] for all stakeholders in healthcare provision.

We have identified both opportunities and challenges which present open research questions, additionally there are issues relating to visualisation and adaptation [27] with role-specific access rights and permissions. Addressing the open research questions is very challenging and the issues are not underestimated, however, a concerted and focused effort to implement the posited approach holds the potential to achieve significant improvements in the management of depression for all stakeholders where context-aware HIT assumes an important role in delivering high quality, safe, and cost effective clinical care with increased levels of precision.



## References

1. Abowd, G.D., Dey, A.K., Brown, P.J., Davies, N., Smith, M., Steggle, P.: Towards a better understanding of context and context-awareness. In: *Handheld and ubiquitous computing. Track 13: e-Health Technologies for Patient Monitoring (ETPM)*, pp. 304–307. Springer, Karlsruhe (1999)
2. Ashford, R., Moore, P., Hu, B., Jackson, M., Wan, J.: Translational research and context in health monitoring systems. In: *Proceedings of the Fourth International Conference on Complex, Intelligent and Software Intensive Systems (CISIS 2010)*, pp. 81–86. IEEE, Krakow (2010). doi:[10.1109/CISIS.2010.44](https://doi.org/10.1109/CISIS.2010.44)
3. Association, D.A.P., et al.: *Diagnostic and Statistical Manual of Mental Disorders*. American Psychiatric Publishing, Arlington (2013)
4. Beck, A.T., Epstein, N., Brown, G., Steer, R.A.: An inventory for measuring clinical anxiety: psychometric properties. *J. Consult. Clin. Psychol.* **56**(6), 893 (1988)
5. Boehm, B.W.: A spiral model of software development and enhancement. *IEEE Comput.* **21**(5, Chs 2–3), 61–72 (1988)
6. Bonomi, F., Milito, R., Zhu, J., Addepalli, S.: Fog computing and its role in the internet of things. In: *Proceedings of the First Edition of the MCC Workshop on Mobile Cloud Computing, MCC 2012*, pp. 13–16. ACM, New York (2012). doi:[10.1145/2342509.2342513](https://doi.org/10.1145/2342509.2342513)
7. Boyle, G.J.: Does item homogeneity indicate internal consistency or item redundancy in psychometric scales? *Pers Individ. Differ.* **12**(3), 291–294 (1991)
8. Checkland, P., Holwell, F.: *Information, Systems and Information Systems: Making Sense of the Field*. Wiley, UK (1997)
9. Chen, J., Hu, B., Moore, P., Zhang, X., Ma, X.: Electroencephalogram-based emotion assessment system using ontology and data mining techniques. *Appl. Soft Comput.* **30**, 663–674 (2015). <http://dx.doi.org/10.1016/j.asoc.2015.01.007>
10. Chen, M., Gonzalez, S., Vasilakos, A., Cao, H., Leung, V.C.M.: Body area networks: a survey. *Mobile Netw. Appl.* **16**(2), 171–193 (2011). doi:[10.1007/s11036-010-0260-8](https://doi.org/10.1007/s11036-010-0260-8)
11. Cronbach, L.J.: Coefficient alpha and the internal structure of tests. *Psychometrika* **16**(3), 297–334 (1951)
12. Dai, Y., Hu, B., Su, Y., Mao, C., Chen, J., Zhang, X., Moore, P., Xu, L., Cai, H.: Feature selection of high-dimensional biomedical data using improved SFLA for disease diagnosis. In: *The 2015 IEEE International Conference on Bioinformatics and Biomedicine (BIBM)*, pp. 458–463. IEEE, Washington D.C. (2015). doi:[10.1109/BIBM.2015.7359728](https://doi.org/10.1109/BIBM.2015.7359728)
13. Delplanque, S., Lavoie, M.E., Hot, P., Silvert, L., Sequeira, H.: Modulation of cognitive processing by emotional valence studied through event-related potentials in humans. *Neurosci. Lett.* **356**(1), 1–4 (2004)
14. Diekelmann, S., Born, J.: The memory function of sleep. *Nat. Rev. Neurosci.* **11**(2), 114–126 (2010). <http://dx.doi.org/10.1038/nrn2762>
15. Dobre, C., Xhafa, F.: Intelligent services for big data science. *Future Gener. Comput. Syst.* **37**, 267–281 (2014)
16. Embi, P.J., Payne, P.R.: Evidence generating medicine: redefining the research-practice relationship to complete the evidence cycle. *Med. Care* **51**, S87–S91 (2013)
17. Finkel, S., Burns, A.: Behavioral and psychological symptoms of dementia (BPSD): a clinical and research update. *Int. Psychogeriatr.* **12**, 9–12 (2000)
18. Fiske, S.T., Gilbert, D.T., Lindzey, G.: *Handbook of Social Psychology*, vol. 2. Wiley, Hoboken (2010)

19. Flouris, G., Manakanatas, D., Kondylakis, H., Plexousakis, D., Antoniou, G.: Ontology change: classification and survey. *Knowl. Eng. Rev.* **23**(02), 117–152 (2008)
20. Gilmore, R.: Introduction: The Search for Wisdom, pp. 1–12. Springer International Publishing, Cham (2017). doi:[10.1007/978-3-319-39895-2\\_1](https://doi.org/10.1007/978-3-319-39895-2_1)
21. Gorry, G.A., Scott Morton, M.S.: A framework for management information systems. Working Paper frameworkformana00gorr, MIT (1971)
22. Greenberg, L.S., Watson, J.C.: *Emotion-Focused Therapy for Depression*. American Psychological Association, Washington, DC (2006)
23. Grimson, J., Grimson, W., Hasselbring, W.: The SI challenge in health care. *Commun. ACM* **43**(6), 48–55 (2000)
24. Hu, B., Liu, Q., Zhao, Q., Qi, Y., Peng, H.: A real-time electroencephalogram (EEG) based individual identification interface for mobile security in ubiquitous environment (APSCC 2011). In: The 2011 IEEE Asia-Pacific Services Computing Conference (APSCC), pp. 436–441. IEEE, Jeju (2011). doi:[10.1109/APSCC.2011.87](https://doi.org/10.1109/APSCC.2011.87)
25. Hu, B., Majoe, D., Ratcliffe, M., Qi, Y., Zhao, Q., Peng, H., Fan, D., Zheng, F., Jackson, M., Moore, P.: EEG-based cognitive interfaces for ubiquitous applications: developments and challenges. *IEEE Intell. Syst.* **26**(5), 46–53 (2011). doi:[10.1109/MIS.2011.58](https://doi.org/10.1109/MIS.2011.58)
26. Kessler, R.C., Andrews, G., Colpe, L.J., Hiripi, E., Mroczek, D.K., Normand, S.L., Walters, E.E., Zaslavsky, A.M.: Short screening scales to monitor population prevalences and trends in non-specific psychological distress. *Psychol. Med.* **32**(06), 959–976 (2002)
27. Lam, F., Lalansingh, C.M., Babaran, H.E., Wang, Z., Prokopec, S.D., Fox, N.S., Boutros, P.C.: VennDiagramWeb: a web application for the generation of highly customizable Venn and Euler diagrams. *BMC Bioinform.* **17**(1), 401 (2016). doi:[10.1186/s12859-016-1281-5](https://doi.org/10.1186/s12859-016-1281-5)
28. Li, X., Hu, B., Shen, J., Xu, T., Retcliffe, M.: Mild depression detection of college students: an EEG-based solution with free viewing tasks. *J. Med. Syst.* **39**(12), 1–6 (2015)
29. Lo, B.P., Thiemjarus, S., King, R., Yang, G.Z.: Body sensor network—a wireless sensor platform for pervasive healthcare monitoring. Technical report, Imperial College, London, UK (2005)
30. Lovibond, P.F., Lovibond, S.H.: The structure of negative emotional states: comparison of the depression anxiety stress scales (DASS) with the beck depression and anxiety inventories. *Behav. Res. Ther.* **33**(3), 335–343 (1995)
31. McDowell, I.: *Measuring Health: A Guide to Rating Scales and Questionnaires*. Oxford University Press, New York (2006)
32. McHorney, C.A., Ware Jr., J.E., Raczek, A.E.: The MOS 36-item short-form health survey (sf-36): II. Psychometric and clinical tests of validity in measuring physical and mental health constructs. *Med. care* **31**, 247–263 (1993)
33. Moore, P.: Do we understand the relationship between affective computing, emotion, and context-awareness? *Int. J. Adapt. Innov. Syst.* (2016, in print)
34. Moore, P., Liu, H.: Modelling Uncertainty in Health Care Systems. In: Guo, Y., Friston, K., Aldo, F., Hill, S., Peng, H. (eds.) *BIH 2015. LNCS (LNAI)*, vol. 9250, pp. 410–419. Springer, Cham (2015). doi:[10.1007/978-3-319-23344-4\\_40](https://doi.org/10.1007/978-3-319-23344-4_40)
35. Moore, P., Pham, H.V.: Personalization and rule strategies in human-centric data intensive intelligent context-aware systems. *Knowl. Eng. Rev.* **30**(2), 140–156 (2015). doi:[10.1017/S0269888914000265](https://doi.org/10.1017/S0269888914000265). (Intelligent Computing in Large-Scale Systems)

36. Moore, P., Qassem, T., Xhafa, F.: NoSQL and electronic patient records: Opportunities and challenges. In: Proceedings of the 9th International Conference on P2P, Parallel, Grid, Cloud, and Internet Computing (3PGCIC 2014), pp. 300–307. IEEE, Guangzhou (2014). doi:[10.1109/3PGCIC.2014.81](https://doi.org/10.1109/3PGCIC.2014.81)
37. Moore, P., Thomas, A., Qassem, T., Bessis, N., Bin, H.: Monitoring patients with mental disorders. In: 9th International Conference on Innovative Mobile and Internet Services in Ubiquitous Computing (IMIS 2015), pp. 65–70. IEEE, Blumenau (2015). doi:[10.1109/IMIS.2015.15](https://doi.org/10.1109/IMIS.2015.15)
38. Moore, P., Van Pham, H., Hu, B., Liu, H., Qaseem, T.: Machine cognition and the integration of emotional response in the monitoring of mental disorders. In: The 2015 10th International Conference on P2P, Parallel, Grid, Cloud and Internet Computing (3PGCIC), pp. 372–379. IEEE, Krakow (2015). doi:[10.1109/3PGCIC.2015.38](https://doi.org/10.1109/3PGCIC.2015.38)
39. Moore, P., Xhafa, F., Barolli, L.: Semantic valence modeling: emotion recognition and affective states in context-aware systems. In: 28th International Conference on Advanced Information Networking and Applications Workshops (WAINA 2014), pp. 536–541. IEEE, Victoria (2014). doi:[10.1109/WAINA.2014.88](https://doi.org/10.1109/WAINA.2014.88)
40. NIMH: What is depression? (2015). <http://www.nimh.nih.gov/health/publications/depression/index.shtml>
41. Nusser, S.M., Intille, S.S., Maitra, R.: Emerging technologies and next-generation intensive longitudinal data collection. In: Models for Intensive Longitudinal Data, pp. 254–277 (2006)
42. Payne, P.R.O., Lussier, Y., Foraker, R.E., Embi, P.J.: Rethinking the role and impact of health information technology: informatics as an interventional discipline. *BMC Med. Inform. Decis. Making* **16**(1), 1–7 (2016). doi:[10.1186/s12911-016-0278-3](https://doi.org/10.1186/s12911-016-0278-3)
43. Pham, H.V., Moore, P., Tran, K.D.: Context matching with reasoning and decision support using hedge algebra with kansei evaluation. In: Proceedings of the Fifth Symposium on Information and Communication Technology (SoICT 2014), pp. 202–210. ACM, New York (2014). doi:[10.1145/2676585.2676598](https://doi.org/10.1145/2676585.2676598)
44. Plutchik, R.: *Emotion: A Psychoevolutionary Analysis*. Harper and Row, Nueva York (1980)
45. Poznanski, E.O., Cook, S.C., Carroll, B.J.: A depression rating scale for children. *Pediatrics* **64**(4), 442–450 (1979)
46. Raghupathi, W., Raghupathi, V.: Big data analytics in healthcare: promise and potential. *Health Inf. Sci. Syst.* **2**(1), 3 (2014). doi:[10.1186/2047-2501-2-3](https://doi.org/10.1186/2047-2501-2-3)
47. Scott, J.: Depression should be managed like a chronic disease: clinicians need to move beyond ad hoc approaches to isolated acute episodes. *BMJ Br. Med. J.* **332**(7548), 985 (2006)
48. Shah, P.J., Ebmeier, K.P., Glabus, M.F., Goodwin, G.M.: Cortical grey matter reductions associated with treatment-resistant chronic unipolar depression. Controlled magnetic resonance imaging study. *Br. J. Psychiatry* **172**(6), 527–532 (1998)
49. Sommerville, I.: *Software Engineering*. Pearson Education Limited, Harlow (2001)
50. Su, Y., Hu, B., Xu, L., Cai, H., Moore, P., Zhang, X., Chen, J.: Emotion+: physiological signals knowledge representation and emotion reasoning model for mental health monitoring. In: The 2014 IEEE International Conference on Bioinformatics and Biomedicine (BIBM), pp. 529–535. IEEE, Belfast (2014). doi:[10.1109/BIBM.2014.6999215](https://doi.org/10.1109/BIBM.2014.6999215)

51. Talanov, M., Vallverdú, J., Hu, B., Moore, P., Toshev, A., Shatunova, D., Maganova, A., Sedlenko, D., Leukhin, A.: Emotional simulations and depression diagnostics. *Biol. Inspired Cogn. Archit.* **18**, 41–50 (2016). <http://dx.doi.org/10.1016/j.bica.2016.09.002>
52. Terzo, O., Ruiu, P., Xhafa, F.: Data as a service (DaaS) for sharing and processing of large data collections in the cloud. In: *Proceedings of The 7th International Conference on Complex, Intelligent, and Software Intensive Systems (CISIS 2012)*, pp. 475–480. IEEE, Taichung (2013)
53. Thase, M.E.: Long-term nature of depression. *J. Clin. Psychiatry* **14**, 3–9 (1999)
54. Van Dam, N.T., Mallela, T., Eilam-Stock, T., Gu, X.: The embodied mind: Using psychophysiological signals to inform brain activity and connectivity during rest. In: *Advances in Computational Psychophysiology*, pp. 16–18 (2015)
55. Wang, P.S., Simon, G., Kessler, R.C.: The economic burden of depression and the cost-effectiveness of treatment. *Int. J. Methods Psychiatr. Res.* **12**(1), 22–33 (2003)
56. Watson, D., Clark, L.A., Tellegen, A.: Development and validation of brief measures of positive and negative affect: the PANAS scales. *J. Personal. Soc. Psychol.* **54**(6), 1063 (1988)
57. Wiederhold, G.: Mediators in the architecture of future information systems. *Computer* **25**(3), 38–49 (1992)
58. Xhafa, F., Qassem, T., Moore, P.: Collaboration through patient data access and sharing in the cloud. In: *The 6th International Conference on Intelligent Networking and Collaborative Systems (INCoS 2014)*, pp. 205–212. IEEE, Salerno (2014). doi:[10.1109/INCoS.2014.109](https://doi.org/10.1109/INCoS.2014.109)
59. Yesavage, J.A., Brink, T., Rose, T.L., Lum, O., Huang, V., Adey, M., Leirer, V.O.: Development and validation of a geriatric depression screening scale: a preliminary report. *J. Psychiatr. Res.* **17**(1), 37–49 (1983)
60. Zeb, S., Qamar, U., Hussain, F.: Sentiment analysis on user reviews through lexicon and rule-based approach. In: Morishima, A., Chang, L., Fu, T.Z.J., Liu, K., Yang, X., Zhu, J., Zhang, R., Zhang, W., Zhang, Z. (eds.) *APWeb 2016. LNCS*, vol. 9865, pp. 55–63. Springer, Cham (2016). doi:[10.1007/978-3-319-45835-9\\_5](https://doi.org/10.1007/978-3-319-45835-9_5)

# Simulation of Upward Underwater Image Distortion Correction

Chengtao Cai<sup>1</sup>(✉), Jia Zheng<sup>1</sup>, and Yanhua Liang<sup>2</sup>

<sup>1</sup> College of Automation, Harbin Engineering University, Harbin 150001, China  
caichengtao@hrbeu.edu.cn

<sup>2</sup> College of Electrical and Control Engineering,  
Heilongjiang University of Science and Technology, Harbin 150022, China

**Abstract.** Due to the effect of sea wave, the image captured by the camera underwater is not clear and the distortion. In order to pave the way for image correction and take corresponding measures to reconstruct the sea surface on the whole hemisphere image. This paper introduces the principle of Snell cone, analysis the principle of underwater imaging and proposes a method that along the Snell cone boundary element wave scattering calculation, obtain satisfies the linearized dynamic equations of wave height estimation, light path vector and fitting the whole image sequence, to estimate the wave ray tracing based on reverse. Furthermore, optical system model is built, and the light path through the air wave image generation is simulated by MATLAB. The simulation results show that, it can be used as a reference for the image distortion reduction of underwater imaging system.

**Keywords:** Image distortion · Snell cone · Reverse ray tracing

## 1 Introduction

Upward underwater imaging is a special form of underwater vision system for space imaging, usually the underwater vision is a visual image acquisition device located in the water, because the image light path through the seawater, resulting in images distortion and lower resolution imaging and so on. According to the observed target position, underwater visual system can be divided into water - water imaging system and water - air imaging system. Water - water imaging system refers to the visual image acquisition device and the target are both in the water; water - air imaging system refers to the visual image acquisition device in the water, the observed target at the surface or over the ocean in the air. Because of there are two kinds of medium (water and air) in the water - air imaging system, the method of imaging and processing has its particularity.

Upward underwater imaging is also known as virtual periscope. Virtual Periscope can help submarines assess activities above water, without using physical periscopes which flag their presence [1]. Virtual Periscope is an optical sensor completely submerged in the underwater platform to target sea observation, greatly enhancing the secret of the submarine. Upward underwater imaging technology in underwater floating channel security monitoring underwater submarine to sea and airspace warning, has been widely applied to marine environmental monitoring and forecasting of

hydrological wave fields. In many underwater conditions, often need to know the water environment and target information, underwater visual system can ensure safety at a reasonable deployment of floating channel based on the operation, reduce the probability of collision with the surface ship.

However, a major disadvantage of airborne imaging is due to the negative influence of surface waves on image quality. Images taken this way suffer severe refractive distortions, even if the water - air interface is flat [1, 2]. For distant objects, distortions attributed to flat-water can be countered by optical and computational methods [3, 4]. Surface waves introduce additional noise due to fluctuations of radiation seen by an imaging system [5]. The camera and the scene of interest are immersed in different media (water and air) with an interface in between complex reflection, refraction effects and caustics can make image real imaging hard (Fig. 1). Besides, the sea surface waves produce strong distortions in the image. Light reflected from a submerged object is distorted by refraction through the random slopes of the rippled sea surface.

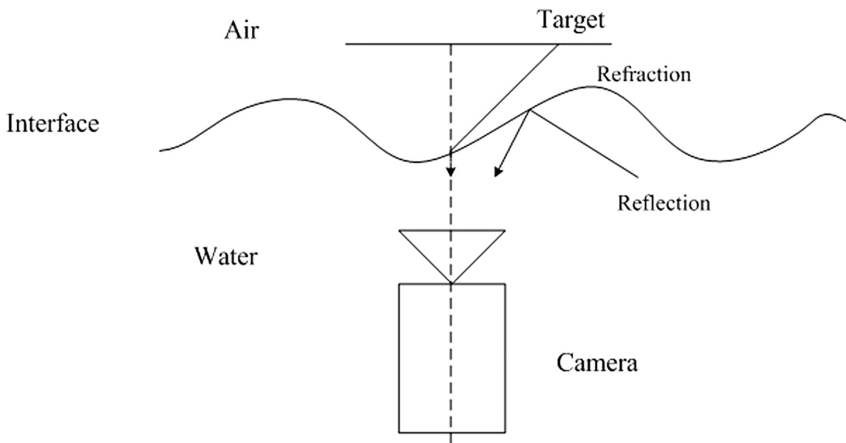


**Fig. 1.** Water - air interface image acquisition model

In this paper, in order to study the process and law of upward underwater imaging, we established the simulation models of sea waves and the normal vector of the optical path of sea surface based on reverse ray tracing. The key idea is to build a spatial distortion model of the water surface using the wave equation. In particular, we build a simulator for image distortion due to fluctuations of the water surface [6].

## 2 Research Status

The research and development of Areté Associate company in the US state of California Sherman, AUX began working on underwater imaging technology from the last century in 90s, in 1996 the company has made breakthrough progress in the technical field of underwater imaging, and applied to air permeable underwater imaging technology

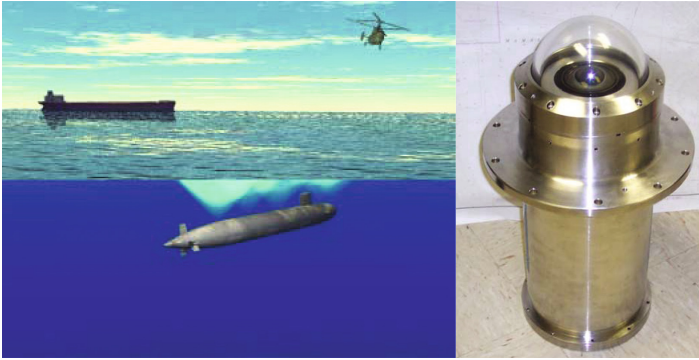


**Fig. 2.** Virtual Periscope based on the technology of upward underwater imaging developed by Areté Associate

patent based on Virtual Periscope at the same time, the application of this technology system was developed first applied to the submarine (Fig. 2).

In April 2001, the American Areté Associate company carried out the experiment of water - air imaging system for the first time in California's San Clemente Island, in the water 10 to 40 feet depth. the test results are close to being able to detect objects of 1 mile away, 100 feet high, and 50 feet above sea level, at the same time, Hubbard, a leader of Areté Associate, pointed out that the key algorithm is accurate mapping out of ocean surface topology and dynamic characteristics, and better understanding of the changing scene.

In August 2005, the United States Navy tested the water - air imaging system in Chicago, which is based on the principle that the ocean surface is an original lens actually, it absorbs the light from the surface of the water and reflects them into the water. The water - air imaging system captures the refracted light, and reduces them by the high-speed signal processing software which can put together an image of the sea, although this system got the image was not clear enough, but at least it can capture suspicious targets on the sea. The submarine warning at a distance of 60 m in the sea depth, it can find the target 1600 m away, and then early warning, for the study of underwater optical imaging technology provides a certain amount of information. Therefore, it is of great military value and practical significance to carry out underwater imaging technology to enhance the ability of environmental awareness and enhance the level of marine environmental monitoring technology [7-14].

### 3 Principle of Upward Underwater Imaging

The principle of refraction and reflection of light on the wavy sea surface is the same as that of the calm sea surface. So this paper we mainly analyzes the principle of refraction of the wavy sea surface. Since the formation of the Snell window is determined by the refraction of light, so the principle of the Snell cone is the same under the condition of waves as that of without waves. There are two elements can be defined in an

underwater image of the rough sea surface, a light path formed due to the refraction of direct sunlight at the surface and a Snell's circle representing an image of the sky distorted by the surface [15].

### 3.1 The Refraction Issue of Wavy Sea Surface

When there is a wavy water surface, light from the target point  $\vec{r}_1$  along the beam 1 arriving at the receiver (Fig. 3) [16]. The light falls upon the camera where in the presence of waves, appeared at the back of the target point  $\vec{r}_0$ . So we can say that the image distortion is due to that the observation system doesn't know the real path of the beam under the water surface. Receiver receives the light refraction as the light of target point  $\vec{r}_0$  instead of the target point  $\vec{r}_1$ . In order to avoid this kind of distortion, the image formation of the beam 1 should actually be replaced the beam 2 position, i.e. Simply to say, we should call the arrival direction as the light path correction process.

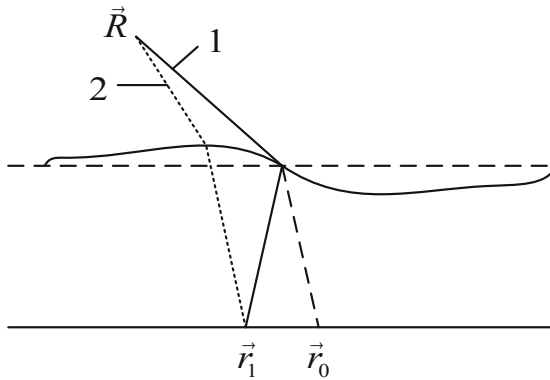


Fig. 3. Actual light path and virtual light path received by the receiver

For a receiver with limited resolution an exact correction is impossible. Therefore, generally, an actual image retrieved through a rough sea surface will differ from the real image that would have arrived through a flat plane surface [16].

### 3.2 Snell Window of Underwater Imaging

Observing the sea and air targets from the calm water, light in the water due to refraction will form a light cone, as shown in Fig. 4, finally converging to the optical system. The transmission of light on the water - air interface follows the Snell's law, that is, the law of refraction. The light cone is called the Snell cone, and the corresponding sea surface circle is called the Snell window. The Snell window has a decisive influence on the underwater imaging performance.



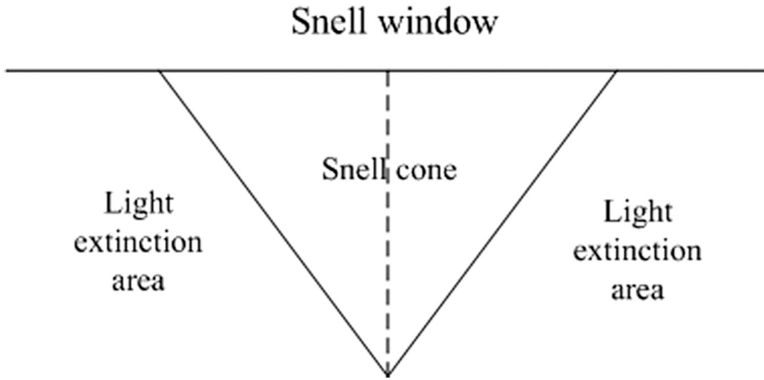


Fig. 4. The principle diagram of Snell window

On a flat plane surface, according to the Snell Law: all the light on the surface are refracted to the water, forming a cone of light, the horizontal line in Fig. 5 forming a circle with a radius of  $|u| = \rho^{-1}$  (Snell cone). The interior of the Snell cone can receive the internal total reflected light in the image. The bright and dark points of these two parts are separated by the light vanishing boundary. For the fluctuating surface, the light vanishing condition depends on the boundary position in the image. The location

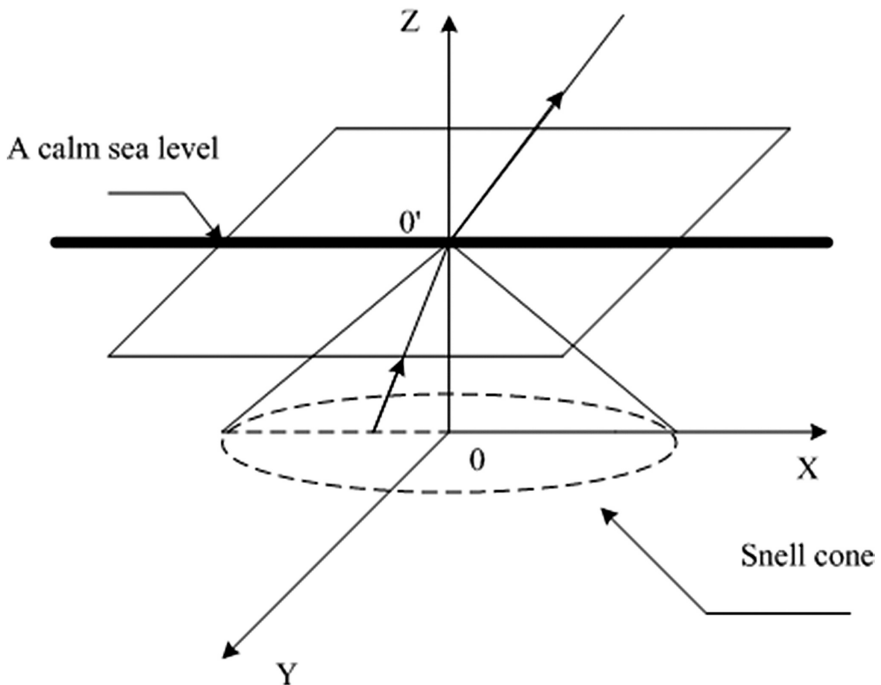


Fig. 5. The Snell cone formed by the light of a calm sea surface

of the light vanishing boundary determines the wave slope value. These bounds provide slope information only on one-dimensional subset of the image. In the linear dynamics of the ocean, the wave height distribution of the ocean surface can be expressed by a set of two-dimensional invariant Fourier coefficients, and each multiplied by a known frequency phase factor. The sea surface estimation issue can be considered to estimate these coefficients under given two-dimensional spatial data.

## 4 Simulation and Analysis

### 4.1 Simulation of Sea Surface Wave

The wave motion is a complicated stochastic process, using the spectral description of waves is one of the main ways of the research. The height of sea wave can be expressed as follows:

$$\eta(x, y, t) = \sum_{i=1}^M \sum_{j=1}^N a_{ij} \cos(k_i x \cos \theta_j + k_i y \sin \theta_j - \omega_i t + \varphi_{ij}) \tag{1}$$

Among them,  $\eta$  is the height of sea wave,  $a_{ij}$  is the amplitude of each harmonic,  $k_i$  is the wave number,  $\theta_i$  is the azimuth of harmonic direction,  $w_i$  is the wave frequency, and  $\varphi_{ij}$  is the phase of each harmonic wave number and azimuth. By random sampling,  $M$  and  $N$  distribution is the total number of sampling interval number  $k_i$  and azimuth  $\theta_j$ .

The amplitude of wave  $a_{ij}$  can be expressed by wave number spectrum  $\Psi(k, \theta)$ :

$$a_{ij} = \sqrt{\Psi(k_i, \theta_j) k_i \Delta \theta_j} \tag{2}$$

Each wave number  $k_i$  corresponds to a certain harmonic frequency  $w_i$ ,  $\Delta k_i$ ,  $\Delta \theta_j$  represents for the sampling interval,  $k_i$  and  $\omega_i$  satisfy the dispersion equation:

$$\omega^2 = gk \tag{3}$$

Among them,  $g$  is the acceleration of gravity.

The expression of wave number spectrum has many choices. In this paper, the widely used PM (Pierson-Moscowitz) spectrum is chosen.

$$\Psi(k, \theta) = \phi(k)D(\theta) \tag{4}$$

$$\phi(k) = \frac{0.0081}{\sqrt{gk^5}} \exp \left| -0.74 \frac{g^2}{k^2 v^4} \right| \tag{5}$$

$$D(\theta) = \frac{2}{\pi} \cos^2(\theta) \tag{6}$$

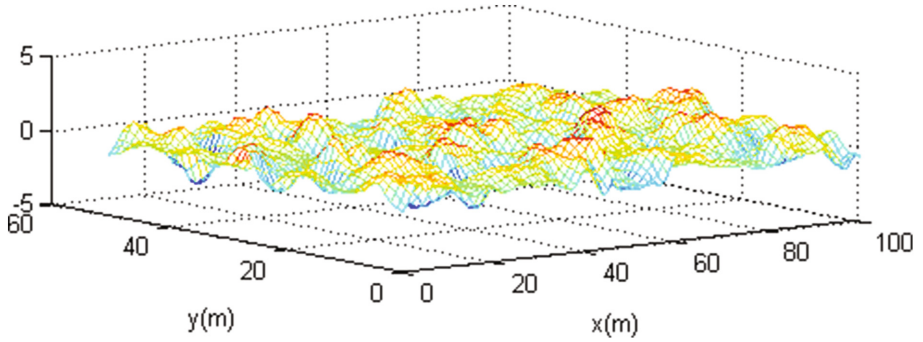


**Fig. 6.** Simulated sea wave (sea surface wind speed 5 m/s)

In the formula,  $v$  represents the average wind speed at the height of 10 m on the sea surface. The simulation results show that the sea surface wave velocity is about 5 m/s (Fig. 6).

#### 4.2 Simulation of Reverse Ray Tracing

Figure 7 is the normal vector of external light path simulated by MATLAB. The light through the sea surface may be reflected or may also occur refraction. If total reflection occurs, the pixel will be extinction; If refraction occurs, the Snell's law of refraction, shown in Eq. (7), can be used to calculate the optical path below the water surface and above the water surface. In this way, the path of the pixel receiving light radiation can be determined, which is the reverse ray tracing. The absorption and scattering effects of

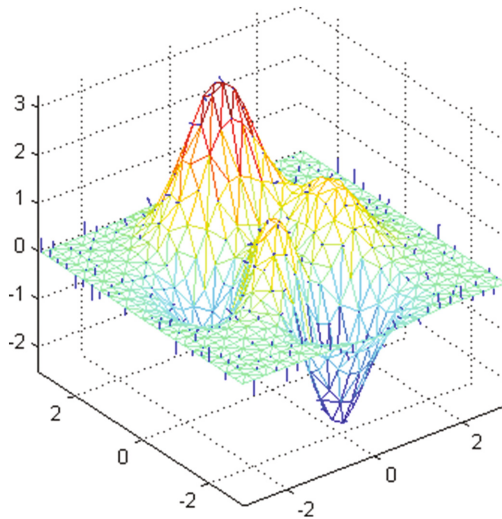


**Fig. 7.** External light path normal

light in seawater are not discussed. According to the sea wave height distribution, it can be obtained arbitrary diagram of the external light path by reverse ray tracing.

$$n_1 \sin \theta_1 = n_2 \sin \theta_2 \tag{7}$$

Where  $n_1$  and  $n_2$  are respectively the two medium refraction rate.  $\theta_1$  is the angle between the incident light and the interface normal,  $\theta_2$  is the angle between the refracted light and the interface normal.

### 4.3 A Simulator for Image Distortion Due to the Fluctuating Water Surface

Consider a stationary and planar scene  $I_g(x)$  settled at the bottom of the water pool, and a camera below the water, taking images downward. Due to the fluctuating water surface, each video frame  $I(x, t)$  is a distorted version of  $I_g(x)$  with the following relationship:

$$I(x, t) = I_g(x + w(x, t)) \tag{8}$$

where  $w(x, t)$  is the unknown distortion that varies over time. The water fluctuation model is illustrated in Fig. 8. The goal is to build a simulator for image distortion due to the fluctuating water surface [6].

According to the Snell's law, The distorted wave function  $w(x, t)$  is related to the height  $h(x, t)$ , we can express the wave equation as:

$$w(x, t) = \alpha \nabla h(x, t) \tag{9}$$

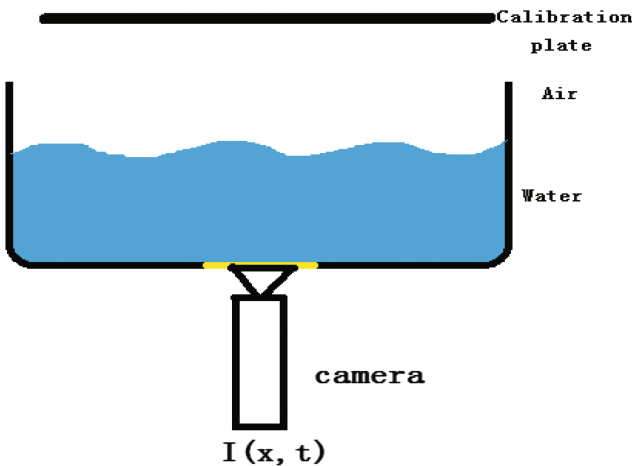
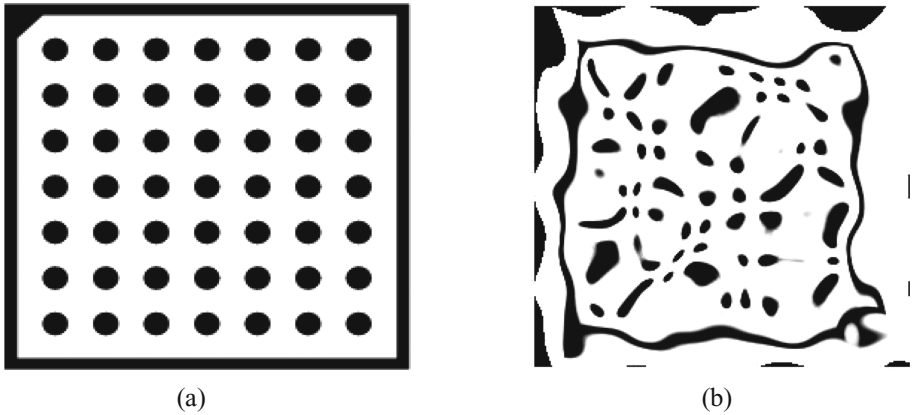


Fig. 8. The experimental model of the fluctuating water surface



**Fig. 9.** (a) The original image, (b) The distorted image

where  $\alpha$  is a constant related to the original water height  $h_0$  when the water surface is calm and relative refraction index between water and air [6].

According to Eqs. (8) and (9), a simulator for image distortion due to fluctuations of the water surface is built by MATLAB. Figure 9(a) is the original image and Fig. 9 (b) is the distorted image simulated by the simulator.

#### 4.4 Analysis of Simulation Result

The results from the simulation can be seen that using the models of sea waves and the normal vector of light path on the sea surface based on reverse ray tracing to simulate underwater imaging process is feasible, and it can effectively simulate the real sea surface scene. In addition, due to the influence of many factors, such as wind speed and the illumination conditions, but in the process of research are calibration to constant value, and so on, the ripples on the surface of sea water are transient and variability. Simulation of the water - air interface by analysis the radiance near the edge of Snell's window [17] or polarization light in the sky [18] was theorized, but it still has very important significance for the research. It paves the way for image correction and takes corresponding measures to reconstruct the sea surface on the whole hemisphere image.

## 5 Conclusion

In this paper, on the basis of reverse ray tracing, firstly, we mainly introduce the principle of upward underwater imaging. And then we simulate the wavy sea surface and the normal vector of light path on the sea surface. Finally, a simulator for image distortion due to fluctuations of the water surface is built. The advantage of the simulations is the highly real-time performance and we can study the process and the law

of upward underwater imaging by the vivid models. The next works are to make further research on underwater image distortion correction and compile program to achieve image distortion correction function. The results show that the simulations are effective and helpful in the range of error and they can be used as references for the image distortion reduction of underwater imaging system.

**Acknowledgement.** This work was supported in part by the National Natural Science Foundation of China (No. 61673129, 51674109) and the Harbin Application Research Funds (2016RQQXJ096).

## References

1. Alterman, M., Schechner, Y.Y., Swirski, Y.: Triangulation in random refractive distortions. In: IEEE International Conference on Computational Photography, pp. 1–10. IEEE (2013)
2. Suiter, H., Flacco, N., Carter, P., et al.: Optics near the snell angle in a water-to-air change of medium. In: Oceans, pp. 1–12. IEEE (2007)
3. Alterman, M., Swirski, Y., Schechner, Y.Y.: STELLA MARIS: Stellar marine refractive imaging sensor. In: IEEE International Conference on Computational Photography, pp. 1–10. IEEE (2014)
4. Schultz, H., Corrada-Emmanuel, A.: System and method for imaging through an irregular water surface: US, US7630077 (2009)
5. Levin, I.M., Savchenko, V.V., Osadchy, V.J.: Correction of an image distorted by a wavy water surface: laboratory experiment. *Appl. Opt.* **47**(35), 6650–6655 (2008)
6. Tian, Y., Narasimhan, S.G.: Seeing through water: Image restoration using model-based tracking. In: IEEE International Conference on Computer Vision, pp. 2303–2310. IEEE (2009)
7. Swirski, Y., Schechner, Y.Y., Herzberg, B., et al.: Stereo from flickering caustics. In: IEEE International Conference on Computer Vision, pp. 205–212. IEEE (2009)
8. Swirski, Y., Schechner, Y.Y., Herzberg, B., et al.: CauStereo: range from light in nature. *Appl. Opt.* **50**(28), F89 (2011)
9. Swirski, Y., Schechner, Y.Y., Nir, T.: Variational stereo in dynamic illumination. In: IEEE International Conference on Computer Vision, pp. 1124–1131. IEEE (2011)
10. Gracias, N., Negahdaripour, S., Neumann, L., et al.: A motion compensated filtering approach to remove sunlight flicker in shallow water images. In: Oceans 2008, pp. 1–7. IEEE
11. Liu, Y., Su, M., Yan, X., Liu, W.: The mean-square slope of ocean waves and its effects on radar backscatter. *J. Atmos. Oceanic Technol.* **17**, 1092–1105 (2000)
12. Kocak, D.M., Dalglish, F.R., Caimi, F.M., et al.: A focus on recent developments and trends in underwater imaging. *Mar. Technol. Soc. J.* **42**(1), 52–67 (2008)
13. Schechner, Y.Y., Karpel, N.: Recovery of underwater visibility and structure by polarization analysis. *IEEE J. Oceanic Eng.* **30**(3), 570–587 (2005)
14. Brox, T., Bruhn, A., Papenberger, N., et al.: High accuracy optical flow estimation based on a theory for warping, vol. 3024, pp. 25–36 (2004)
15. Molkov, A.A., Dolin, L.S.: Determination of wind roughness characteristics based on an underwater image of the sea surface. *Izv. Atmos. Oceanic Phys.* **48**(5), 552–564 (2012)

16. Dolin, L.S., Luchinin, A.G., Titov, V.I., et al.: Correcting images of underwater objects distorted by sea surface roughness. In: *Current Research on Remote Sensing, Laser Probing, and Imagery in Natural Waters*, p. 66150K. International Society for Optics and Photonics (2007)
17. Carter, P.W.: Reconstruction of through-surface underwater imagery. *Waves Random Complex Media* **16**(4), 521–530 (2006)
18. Schechner, Y.Y.: A view through the waves. *Mar. Technol. Soc. J.* **47**(5), 148–150 (2013)

# Survey of Big Data Platform Based on Cloud Computing Container Technology

Wei Liu<sup>1</sup>, Weibei Fan<sup>2</sup>, Peng Li<sup>1,3(✉)</sup>, and Liangde Li<sup>4</sup>

<sup>1</sup> School of Computer Science, Nanjing University of Posts and Telecommunications,  
Nanjing 210003, China

lipeng@njupt.edu.cn

<sup>2</sup> School of Computer Science and Technology, Soochow University,  
Suzhou 215006, Jiangsu, China

<sup>3</sup> Jiangsu High Technology Research Key Laboratory for WSN, Nanjing 210003, Jiangsu, China

<sup>4</sup> School of Electronic Science and Engineering,  
Nanjing University of Posts and Telecommunications, Nanjing 210023, China

**Abstract.** Big data, Internet of Things (IoT) and Cloud computing are the most profound changes in the development of new information technologies. With IoT, thousands of network sensors are embedded in the real world, and cloud computing provides the storage space and on-line processing service for the mass data generated by IoT, while big data contributes to value in the mass data. In this paper, it firstly introduces Cloud computing related knowledge and technology, followed by the description of big data and its general processing flow, then the relationship between container technology and cloud computing is described, and construction programs for big data platform based on cloud computing container technology is proposed. Finally, it proposes the optimization scheme of the platform, as well as the technical challenges faced by high-performance computing with respect to big data.

**Keywords:** Cloud computing · Container · Big data · Load balance

## 1 Introduction

With the growth of massive data, traditional IT (Information Technology) architecture is faced with the limitation of horizontally expanding, despite of its capacity of expanding. And traditional IT architecture and data processing cannot deal with big data environment effectively. Appropriate programs that can meet the requirements of big data and the expansion of the performance are necessary to resolve the problems of data storage, computing, management, analysis and other nodes. Cloud center is a perfect combination of new business demands and resource utilization mode with the data center under the cloud computing background. Cloud model has become an important way for enterprises to deal with challenges of big data by using data center platform [1]. Advantages by using cloud computing as the bearing platform of big data are listed as below.



- (1) Cloud Computing helps to reduce the complexity of big data platform, simplifying its operation and maintenance (O&M), improving resource and utilization efficiency. Through network-based service dispatched by cloud computing, hardware and other infrastructure can be integrated into intangible IT resources, and with the help of technologies including load balance, distributed computing, parallel computing, virtualization, network storage and unified management etc., seamless, customized and scalable IT services will be available.
- (2) Cloud computing provides flexible and efficient IT services based on big data, to suit a variety of individual needs. For cloud computing, there are applications based on distributed computing as big data. However, big data needs high-performance computing and storage expansion (horizontal and vertical) through clusters. With the help of the distributed system and virtualization flexible deployment of resources by cloud computing, analysis, processing and mining of big data can be carried out supported by efficient and flexible IT service, to meet the requirements of users' personalized customized mining & analysis on big data. As a bearing platform for big data, cloud computing has been widely applied and the IT infrastructure based on data center has been transformed from the traditional data center to the cloud data center [2].

Through the core technology of cloud computing - operating system virtualization technology, a computer will become multiple logical computers. Virtualization and partitioning technology has been developed, and gone through the development process from "hardware partition", "virtual machine", "quasi-virtual machine" to "virtual operating system" [3–6]. As a bearing layer for big data, this model is faced with some problems and challenges: (1) Complexed implementation and configuration. More price shall be paid due to the mass processing of the generation, destruction, operation, maintenance and management, as well as corresponding complex configuration. (2) Complicate updating and upgrading. Virtual host clusters are connected to multiple systems, while there are a lot of complex interactions between components, and upgrading to newer versions of products and hardware components may also cause difficulties. (3) Costs for cluster management are higher [7].

In this paper, we introduces and analyzes relevant works on cloud computing and big data, and the big data platform based on cloud computing container technology is proposed and designed. The rest of the paper is organized as follows: In Sect. 2, the development status and relationship (overview) of big data and cloud computing is introduced. In Sect. 3, the big data acquisition and preprocessing technologies based on the cloud platform is described. In Sect. 4, the adaptive processing of the big data platform is introduced, and detailed analysis of the flow processing and batch processing modes are carried out, in addition to the introduction of virtualization technology of container. In Sect. 5, the optimization of the platform is discussed, followed by two programs for optimization.

## 2 Relationship Between Big Data and Cloud Computing

Cloud computing is a technology promoted by different enterprises and research institutions synchronously, there are many definitions of cloud computing, and so far there is no recognized definition and standard. According to Ian Foster, cloud computing was defined as a large-scale distributed computing model driven by economies of scale, from which the abstract, virtualized, dynamically scalable and manageable computing resources, storage resources, platforms, and service form a shared pool [8]. And resources from the shared pool will be provided to the users outside the pool according to their requirements over the Internet.

Various data can be obtained by using new tools for collecting, searching, discovering and analyzing data. There is no formal definition about big data, of which the most common definition is “the data that cannot be handled or analyzed with traditional methods or tools”. And big data have five main technical characteristics, which are summarized as 5 V characteristics: Volume, Variety, Velocity, Veracity and Value [9].

Similarities exist between big data and cloud computing. Both of them serve for data storage and processing, a lot of storage and computing resources are necessary, and parallel processing technologies used for big data including massive data storage technology, mass data management technology and MapReduce are also the key technologies of cloud computing [10].

Combine big data with cloud computing, it will be an excellent match to each other, and both of them will be fully optimized.

## 3 Data Collection and Preprocessing of Container-Based Cloud Platform

### 3.1 Container Technology

The container technology represented by Docker have provided a matching implementation mechanism for micro-service concept, contributing to a substantial change in the new methods of application development and publishing. Docker was named as an open source project as well as a start-up company specializing in Linux containers [11]. A container refers to that multiple applications run on a single host, which is similar to computing virtualization. However, it does not mean that multiple operating systems are created through a virtualization server. It provides a more lightweight alternative, allowing multiple workloads to run on one host by virtualizing the operating system.

### 3.2 Collection Technology for Big Data and Big Data Preprocessing

At present, big data is collected in two ways: first, system log collection [12]. Second, network data collection: collection of unstructured data

In the real world, the data is generally incomplete and inconsistent, which cannot be directly used for data mining, or of which the mining results are unsatisfactory [13]. There are inconsistent and repeated data in the original data, some of which containing

noise. Such data with errors or anomalies (deviating from the expected value), not only take up storage space, but also greatly affect the data processing speed. In order to enhance the quality of data mining, a data preprocessing technique is developed. There are various methods for data preprocessing, such as data cleaning, integration, transformation, reduction and so on. These data processing technologies are used before data mining, which greatly enhances the quality of data mining model and reduces the time needed for actual mining [14–16]. For the traditional data preprocessing, more emphasis is put on the database cleaning, and data such as mysql and oracle has a fixed pattern. However, data preprocessing in the context of big data tends to put more emphasis on data warehouses cleaning. Firstly, the data are heterogeneous (all kinds of data sources), and thus greater efforts shall be made for unity. Secondly, the data may not have a fixed structure, which is called unstructured data, such as text files. Thirdly, the so-called data are so larger that a single program or a small distributed cluster can not be completed within a given time. Finally, such larger data has resulted in numerous useful information being overwhelmed by noise, confusing us with the role of these data. Therefore, for big data, the data preprocessing has become a critical part.

## 4 Adaptive Processing of Big Data Platform

### 4.1 Big Data Analysis and Processing Technology

Big data analysis is a process of the analysis algorithm running on the powerful support platform to find potential values in big data, such as hidden pattern and unknown relevance. According to the requirements of processing time, analysis & processing of big data can be divided into two categories.

**Stream processing:** Stream processing assumes that the potential value of the data is the freshness [17]. The data shall be processed as quickly as possible to get the results. In this way, the data will be arriving in streams. And in the process of continuous data streams arrived, only a small part of the data streams are stored in the limited memory because there are lots of data in the streams. Researches on stream processing theory and technology has been carried out for some years, with the representatives of the open source system include Storm, S4 [18] and Kafka [19]. Stream mode is used for online applications.

**Batch processing:** For batch processing, data is firstly stored and then analyzed. MapReduce is a very important batch model. The core idea of MapReduce is that the data is firstly divided into small chunks, which are parallel processed, and then intermediate results are obtained by the way of distributed model and allocated to get the final results. MapReduce allocates computational resources that are closer to the data storage location to avoid the communication expenditure of the data transfer. Because of its simplicity and efficiency, MapReduce is widely used in bioinformatics, web mining and machine learning.

The differences between these two approaches is shown in Table 1. In general, stream processing is appropriate for the data generated by streams and requiring rapid processing to obtain general results, so it would prefer batch processing to stream processing. Some researches attempted to integrate the advantages of both approaches.

**Table 1.** Comparison between batch processing and stream processing

	Stream processing	Batch processing
Input	Stream of new data updates	Data chunks
Data size	Infinite or unknown in advance	Known and finite
Storage	Not store or store non-trial portion in memory	Store
Hardware	Typical single limited amount of memory	Multiple CPUs and memory
Processing	A single or few pass over data	Multiple rounds
Time	A few seconds or even milliseconds	Much longer
Applications	Web mining, sensor networks, traffic monitoring	Widely adopted in almost every domain

## 4.2 Virtualization Technology of Big Data Platform Container

As one element must be achieved for virtualization technology, isolation is essential. Docker isolation must depend on the associated isolation characteristics supported by the host. At present, there are numerous related projects, and a Docker ecosystem has been gradually formed. Since its release in 2013, Docker has become a hot-pocket PaaS project. Redhat, Google, IBM, Baidu, Alibaba have started to use Docker [20]. The isolation of Docker container is mainly achieved through the namespace in Linux kernel. With the help of pid, net, mnt, uts and others, the network space file system and users are separated by namespace, respectively, and the process of users in the container is a sub-process of lxc-start, and different user processes are separated by pid namespace, but it is possible that different namespaces have the same process number. Processes in each namespace can only affect the process in the same space, and thus the processes in different containers do not affect each other [21].

In this paper, the big data platform taking virtualization as the core builds up big data application service and develops an environment architecture. In addition, based on the packaging and isolation of container virtualization, the scalable and transparent O&M (operation and maintenance) of the overall containerized micro-service platform is achieved, along with all types of PaaS and SaaS interfaces being open, to achieve the integration of development, commissioning, testing and O&M, and hardware and software separation and loosely coupled development and operation mode [22]. Platform virtualization for the main container has the following four aspects:

- (1) Image generation: The overall image building and continuous integration services can help users to pack up independent and reusable micro-service, and transform them into a container image.
- (2) Integration: The platform not only collects a large number of high-quality images from official Docker and its community in the image warehouse of this platform, but also supports any image source outside the platform. Micro-services containers can contribute to free combination and multiplying for users, which can easily integrate applications as building blocks. For example, users need a common

MySQL database service, and appropriate database service image shall be directly chosen from the images and connected to its micro-services without building an image.

- (3) Deployment: With respect to micro-services, due to the large number of components, cloud deployment has become a practical difficulty. The container is used as a supporter for application release, and only the container image and as long as a simple container configuration is prepared, the entire deployment process will be automatized, enabling one-click deployments for the complete application of multiple micro-service containers.
- (4) O&M: Due to the large number of independent processes with respect to micro-services, O&M and management of post-deployment has become another difficulty in practice. Shielding O&M of the cloud host and infrastructure, and through the container scheduling, automatic repair, automatic expansion, log monitoring and other advanced application life cycle services, intelligent hosting of containerized micro services can be achieved, and the cost of O&M can be further reduced.

Container virtualization and cloud computing provides a more flexible and scalable, efficient use of technical support for value mining of big data, simplifying the mining process of big data values and service delivery, enabling faster deployment of big data and application services, so as to bring benefits for more areas as well as provide application and service for industries and users.

### 4.3 Stream Computing Based on Container Virtualization

IoT collects the monitoring information from cold chain vehicles, and these data belong to the spatial and temporal information. For the processing of big data, taking Hadoop and Spark open source processing platform as the objects, the service interface and stream computing are analyzed, focusing on the stream computing technology. Based on Docker container, YARN and Mesos are clustered to deploy computing clusters including Hadoop and Spark, to build data as a service, and to carry out topology management, task assignment for computing cluster, in addition to various performance monitoring and warning [23].

As shown in Fig. 1, Spark is used for operational analysis, and the overall environment is OpenStack cloud [24]. A group application based on micro-services runs on different tenant networks, and there is a small Spark cluster as well. The software network tap installed on each Nova compute host captures network packets through the tenants' network. Wire-data captured from the tenant network are put into the Kafka bus. Meanwhile, connector is being written in Spark application to access to Kafka packet for the purpose of conducting a real-time analysis. In addition, research on system scalability will be carried out. By increasing the host linear, the data extraction speed may be increased.

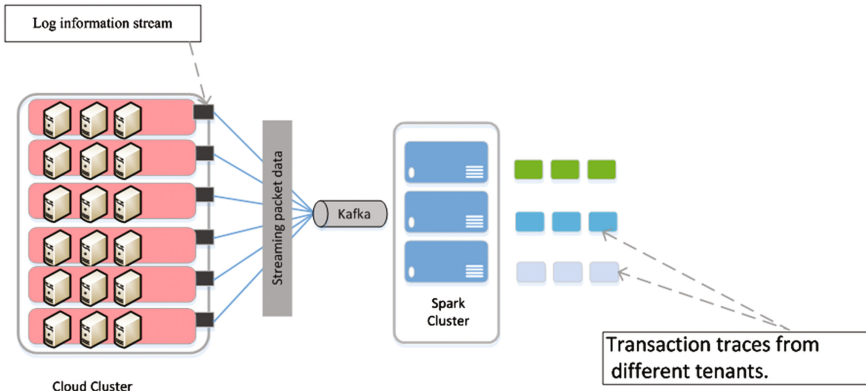


Fig. 1. Spark platform based on Docker

In this section, we propose and design a cloud computing distributed processing scheme for the big data platform which supports all kinds of heterogeneous data storage, transmission, processing, IO input and output. However, the existing distributed processing platform and parallel computing architecture are inadequate. Based on the requirements of real-time computing and batch processing, the containerized real-time processing and batch processing platform are proposed, so as to achieve horizontal expansion and vertical expansion of big data computing, and to further improve the degree of parallelism and energy efficiency.

## 5 Optimization of the Platform

Through the containerized Spark platform, various types of analysis applications can be operated simultaneously, and a unified big data platform can support batch processing, streaming and graphics processing and other different types of computing operations, which has a wide range of applications and prospects. The speed of Spark operations can be slow without proper tuning of the Spark operations, which completely excludes the advantages of Spark as a fast big data computing engine. Therefore, in order to make good use of Spark, a reasonable performance optimization is necessary.

### 5.1 Reduce the Execution Time for Batch Data

There are several optimizations in Spark that reduce batch processing time.

#### 5.1.1 Parallelism of Data Reception

When receiving data over a network, such as kafka, flume, socket, etc., it requires that the data should be deserialized and saved in the Spark. Thus the data connection becomes the bottleneck of system and the parallel reception of data must be taken into account. Note that each input DStream creates a receiver (running on the worker machine). It creates multiple input DStreams to receive data streams from different partitions from

the source for multi-stream reception [25, 26]. For example, a single input DStream receives two topic data could be split into double kafka input streams. This will run two receivers on two workers, thus allowing data to be received in parallel, improving overall throughput. Multiple DStreams can be merged to produce a single DStream, so that a single Dstream's transformation can be applied to the merged DStream.

### 5.1.2 Parallelism of Data Processing

If the number of concurrent tasks running on the computing stage is not large enough, the degree of parallelism in the data processing will not make full use of the sources of the cluster [27]. For example, distributed reduce operations, such as `reduceByKey` and `reduceByKeyAndWindow`, the default number of concurrent tasks is determined by configuration properties (configuration.html#spark-properties) - `spark.default.parallelism`. The degree of parallelism can be passed by the parameter (`PairDStreamFunctions(api/scala/index.html#org.apache.spark.streaming.dstream.PairDStreamFunctions)`), or the default value can be modified by setting the value of `spark.default.parallelism`.

## 5.2 Set the Correct Batch Size

For the purpose that a Spark Streaming application can run stably in a cluster, the system should be able to process the received data at a sufficient speed (i.e. processing speed should be greater than or equal to the received data) [28]. This can be observed through the stream of the network UI, and batch processing time should be less than the batch interval.

Depending on the property of the stream computing, the batch interval may significantly affect the data processing rate, which can be maintained by the application. Consider the example of `WordCountNetwork` where the system may print a word count every 2 s (batch interval is 2 s) for a particular data processing rate, but cannot print a word count every 500 ms. Therefore, in order to maintain the desired data processing rate in a production environment, an appropriate batch interval (i.e., the capacity of the batch data) should be set.

A good way to find out the correct batch capacity is to test the application with a conservative batch interval (5–10 s) and at a low data rate. To verify whether your system is capable of processing data or not, you can check the end-to-end delay (you can see the "Total delay" in the Spark driver's log4j log or use the `StreamingListener` interface). If the delay remains stable, then the system is stable. If the delay continues to grow, then the system cannot keep up with the data processing rate, which is unstable. Then you can attempt to increase the data processing rate or reduce the batch capacity for further testing. Because that the instantaneous increase in data processing speed may lead to an instantaneous growth of delay is normal, as long as the delay can return to a low value or less than the batch capacity.

## 6 Conclusion

Traditional big data processing architecture couldn't deal with the growing big data quickly and effectively, while now the format of big data is no longer a single, static, but streaming, with a variety of structures. This paper analyses the development and characteristics of cloud computing and big data, then proposes a big data platform based on cloud container technology, and puts forward an efficient data processing platform inspired by the idea of the parallel processing of cloud computing, then carries out a rapid analysis of food safety supply chain data, and summarizes the whole process of big data processing, including data collection and pretreatment, platform adaptive processing, statistical analysis process, followed by some platform optimization programs, in order to provide a theoretical and reference basis for further research.

**Acknowledgments.** The subject is sponsored by the National Natural Science Foundation of P. R. China (No. 61373017, No. 61572260, No. 61572261, No. 61672296, No. 61602261), the Natural Science Foundation of Jiangsu Province (No. BK20140886, No. BK20140888, No. BK20160089), Scientific & Technological Support Project of Jiangsu Province (No. BE2015702, No. BE2016777, BE2016185), China Postdoctoral Science Foundation (No. 2014M551636, No. 2014M561696), Jiangsu Planned Projects for Postdoctoral Research Funds (No. 1302090B, No. 1401005B), Jiangsu High Technology Research Key Laboratory for Wireless Sensor Networks Foundation (No. WSNLBZY201508).

## References

1. Cloud model-the new business model for the future of the Internet. [http://datacenter.chinabyte.com/178/9137678\\_2.shtml](http://datacenter.chinabyte.com/178/9137678_2.shtml)
2. Peng, L.I.U.: Cloud Computing. Publishing House of Electronics Industry, Beijing (2011)
3. Raekow, Y., Simmendinger, C., Jenz, D., et al.: On-demand software licence provisioning in grid and cloud computing. *Int. J. Grid Utility Comput.* **1**, 10–20 (2013)
4. Xinhuanet. China telecommunications and EMC release cloud information services of e cloud in Shanghai (2009). [http://news.xinhuanet.com/newmedia/2009-09/23/content\\_12099554.Htm](http://news.xinhuanet.com/newmedia/2009-09/23/content_12099554.Htm)
5. Kopetzky, R., Nther, M., Kryvinska, N., et al.: Strategic management of disruptive technologies: a practical framework in the context of voice services and of computing towards the cloud. *Int. J. Grid Util. Comput.* **1**, 47–59 (2013)
6. Zhang, J., Gu, Z., Zheng, C.: Survey of research progress on cloud computing. *Appl. Res. Comput.* **27**, 429–433 (2010)
7. Bashar, A.: Graphical modelling approach for monitoring and management of telecommunication networks. *Int. J. Space-Based Situated Comput.* **5**, 65–75 (2015)
8. Meng, X., Li, Y., Zhu, J.: Social computing in the era of big data: opportunities and challenges. *J. Comput. Res. Dev.* **12**, 2483–2491 (2013)
9. Gu, C.: An improved multilinear map and its applications. *Int. J. Inf. Technol. Web. Eng.* **3**, 64–81 (2015)
10. Mezghani, K., Ayadi, F.: Factors explaining IS managers attitudes toward cloud computing adoption. *Int. J. Technol. Hum. Interact.* **1**, 1–20 (2016)
11. Boettiger, C.: An introduction to Docker for reproducible research. *ACM SIGOPS Oper. Syst. Rev.* **1**, 71–79 (2015)
12. Chen, M.: CAP theory of distributed system design. *Comput. Educ.* **15**, 109–112 (2013)



13. Ben Seghir, N., Kazar, O., Rezeg, K.: A decentralized framework for semantic web services discovery using mobile agent. *Int. J. Inf. Technol. Web. Eng.* **10**, 20–43 (2015)
14. Lichy, J., Kachour, M.: Understanding how students interact with technology for knowledge-sharing: the emergence of a new ‘social’ divide in France. *Int. J. Technol. Hum. Interact.* **12**, 85–104 (2016)
15. Noy, N.F.: Semantic integration: a survey of ontology-based approaches, vol. 4, pp. 65–70. ACM, *Sigmod Rec.* (2004)
16. Han, J., Kamber, M.: *Data Mining: Concepts and Techniques*, Morgan Kaufmann, vol. 4, pp. 394–395. Machine Press (2006). (2001 in Chinese)
17. Tatbul, N.: Streaming data integration: challenges and opportunities. In: *Workshops Proceedings of the International Conference on Data Engineering, ICDE 2010*, 1–6 March 2010, Long Beach, California, USA, pp. 155–158 (2010)
18. Neumeyer, L., Robbins, B., Nair, A., et al.: S4: distributed stream computing platform. In: *IEEE International Conference on Data Mining Workshops, ICDMW 2010*, Sydney, Australia, 14 December 2010
19. Qiao, L., Surlaker, K., Das, S., et al.: On brewing fresh espresso: LinkedIn’s distributed data serving platform. In: *ACM SIGMOD International Conference on Management of Data*. ACM, pp. 135–1146 (2013)
20. Zhang, J., Xie, T.: Research of platform as a service architecture based on the Docker. *Inf. Technol. Inform.* **10**, 131–134 (2014)
21. Zhang, H., Kong, L., Huang, X., et al.: Design of a high speed XAUI based on dynamic reconfigurable transceiver IP core. *Int. J. Soft Comput. Softw. Eng.* **2**, 42–51 (2014)
22. Salih, N.K., Zang, T.: Survey and comparison for open and closed sources in cloud computing. *Int. J. Comput. Sci. Issues* **3**, 1280–1291 (2012)
23. Liu, Z., Wang, Y., Cai, L., et al.: Design and manufacturing model of customized hydrostatic bearing system based on cloud and big data technology. *Int. J. Adv. Manufact. Technol.* **1**, 261–273 (2016)
24. Sefraoui, O., Aissaoui, M., Eleuldj, M.: OpenStack: toward an open-source solution for cloud computing. *Int. J. Comput. Appl.* **3**, 38–42 (2012)
25. Gao, L., Yu, J., Ding, J.: Analysis and application of serIALIZATION and deserialization in the.NET framework. *Microcomput. Appl.* **11**, 1178–1182 (2007)
26. Zhang, P., Li, P., Ren, Y., et al.: Distributed stream processing and technologies for big data: a review. *J. Comput. Res. Dev.* **S2**, 1–9 (2014)
27. Wu, J., Yuen, C., Cheng, B., et al.: Streaming high-quality mobile video with multipath TCP in heterogeneous wireless networks. *IEEE Trans. Mobile Comput.* **9**, 1 (2016)
28. Chellappan, S., Snyder, M.E., Thakur, M.: Distributed exploratory coverage with limited mobility. *Int. J. Space-Based Situated Comput.* **2**, 114–124 (2014)

# A Planner for Supporting Countermeasures in Large Scale Cyber Attacks

Flora Amato<sup>1</sup>(✉) and Francesco Moscato<sup>2</sup>

<sup>1</sup> DIETI, University of Naples Federico II, Naples, Italy  
flora.amato@unina.it

<sup>2</sup> DiSciPol, University of Campania Luigi Vanvitelli, Caserta, Italy  
francesco.moscato@unicampania.it

**Abstract.** We are in a period where Computer Science leads lots of activities in many fields and the number of *Cyber* activities is growing up every day. Safety and security issues are going to be considered the most important properties in computer systems. But in the age of *Cyber* lives, *Cyber Crimes* are an everyday increasing problem. Thinking in large-scale, enacting Cyber attacks, or even countermeasures to attacks involving different Countries, may be compared to war declaration. In this scenario it is clear the problem of scheduling large-scale countermeasures to Cyber attacks. We propose here an automatic way to plan countermeasures to Cyber Attacks, that takes into account International laws and treaties as enabling condition to actions. The planning is based on a formal, multi-agent based, model of Actors in a Cyber scenario and on formal reasoning by counterexamples.

## 1 Introduction and Related Works

Current events saw a greater and greater interest in Cyber activities in everyday life. In case of Cyber attacks, prevention is a must to assure people in trusting Computer based system that are now going to worm our everyday lives. Anyway, it is a matter of fact that malicious cyber activities exist and that they lead to bad situations. Recent analyses shows how many and many Cyber attacks are successful in National and International enterprises as well as in private sector, whatever the goals of attacks are (and they range from blackmails, ransom or personal benefits of attackers, social analyses etc.) [6]. Many times, when attacks reach their goals, it is a problem to understand if taking countermeasures to attacks is allowed. Of course it is clear how to take countermeasures in the Computer Science field (i.e.: how to identify and trace attacks, how to defend systems from penetration and even how to respond with other attacks to attackers), but it is not clear if taking some actions in countermeasures is *legal* or not. This depend on laws in each Country when (a) the Cyber Crime is perpetrated in a single Counter, (b) the Country has a clear Law on Cyber Crimes.

The first point is clear: if a clear Law exists, depending on Country, Law punish Crimes with different punishments. For example, Italian Law punishes a man killing burglar in his own house in a heavier manner than USA Law.

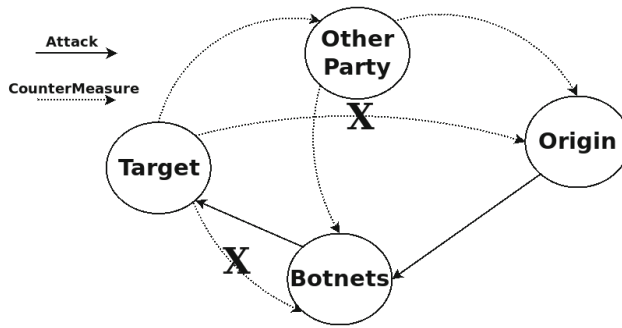


Fig. 1. Attacking scenario

The second point is anyway the main problem: it is really rare for a country to have some Laws that address specifically Cyber Crimes.

Let us imagine what happens on Large Scale, International scenarios. When a large-scale attack happens it usually involve a large number of nodes. In addition attacks evolve in many steps.

In addition, international laws and agreements depend on contracting parties. If the attacking scenario is the one depicted in Fig. 1, it is clear that, if *Origin* Country start the attack that is perpetrated through *Botnets* country with nodes in *Target* Country as victim, it is clear that if there are not available actions to enact countermeasures directly from Target to Botnets or Origin (because of existing laws or of lack of agreements), the countermeasures can be exploited by using agreements with Other parties that are allowed to interact with other countries.

Scheduling the sequence of actions for countermeasures is a problem due to the lack of clear laws and agreements on cyber crimes. In addition, Laws and Agreements from other field can be used at least for attributing cyber attacks evidences [19]. Anyway, despite the huge literature about analysis, defense and counter-attack measures [1, 10, 13, 15].

In particular, at the best of our knowledge, existing scientific literature do not refer at all to existing Laws and Agreements as enabling condition to enact any kind of reaction to attacks. On the other hand, existing laws and agreements do not take into account of taxonomies, models and dynamics of (continuously evolving) Cyber attacks and crimes. The only exception is the tentative of Tallinn Manual [20] to explicit address Cyber crimes from a perspective of an abstract interpretation of existing International Law.

In this paper we show a formal model able to describe interactions of some actors involved in large-scale, Cyber security threats. Actors include both attackers, victims and counter-attackers behaviors. While considering all possible measure to reply to attacks, we consider existing Laws and agreement as enabling condition. We do not limit only to Laws about Cyber Crimes, but we follow the example of Tallinn Manual in order to make abstract reasoning on laws belonging to other fields that can be applied in Cyber contexts.

The model we propose is based on a Multi-Agent [11] formal models. Possible goals of actors, enabling conditions and Laws and agreements contents are modeled by using a formal Ontology, on which we perform reasoning in order to identify if a given Law is applicable to a Cyber crime context.

## 2 Multi Agent Based Planning

This section describes the methodology used for generating new contents in games by PCG planning.

In brief, it enables to describe agents involved in a cyber-attack scenario and it allows for definition of actions implementing countermeasures, as well as for definition of rules and enabling conditions of countermeasures. We call *Agents* the pro-active elements. Agents in cyber-attack scenario belong to three different sets: *Victims* are the targets of attacks, *Attackers* and *Counter-Attackers*. Notice that a victim may act as attacker (or counter-attacker) in different stages of attacks (like it happens for botnets). In large scale cyber-attacks, as we introduced before, counter measures that agents are able to enact may be constrained by national and international law: hence, actions available to Agents are subject to some rules and enabling events.

In addition since international law on cyber crimes is not well defined, many rules depend on law in other juridical fields. We discuss the way we address this problem in the next section.

In this section we address only Agents, the state space they *sense* (i.e. the state of a running attack or the effects of a finished one) and the enabling rules for the actions they can enact.

In our methodology, formal models here enable formal planning: Fig. 2 describes (an abstract version of) the metamodel used for intelligent definition in games. More details can be found in [17].

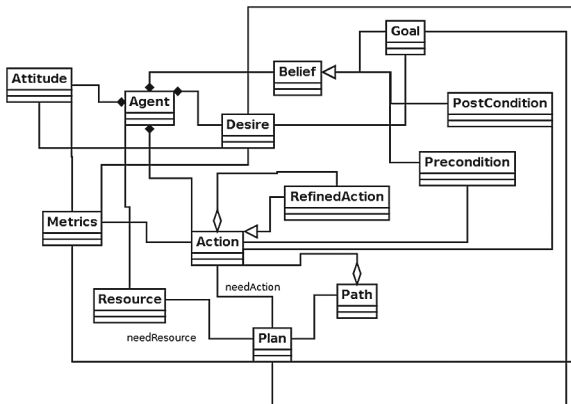


Fig. 2. Multi-agent meta-model

The metamodel extends the “Beliefs, Desires, Intentions” (BDI [22]) logics and in figures it is sketched by using a basic UML diagram.

Main elements for **Agents** description are **Beliefs**, **Actions**, **Plans** and **Desires**. *Beliefs* contains data representing information the agents know about their state in the environment, about the environment itself and about the beliefs they have about other agent. Particular types of Beliefs are the *Goals* they want to reach: a goal is represented hence by a particular assignment of variables in the beliefs of the agents. *Desires* represent combination of goals the agents want to reach depending on their *Attitudes*. *Actions* describe the steps the agents are able to perform in the environment. Abstract Actions can be refined by using lists of refined sub-actions. Beside their functional descriptions, actions are related to two particular types of beliefs: *Preconditions* and *Postconditions* are beliefs combined by logical formulas that respectively indicated what must be verified to enable action execution, and what are its effects. *Attitudes* describe preferences of agents about their available actions, goals, desires etc. Preferences evaluation involve definition and use of proper *Metrics*. *Resources* define all the non pro-active elements in the game. Finally, *Plans* are proper lists of actions that lead to a Goal.

For what the planning methodology concerns, one of the most used approach in classical planning is to find a sequence of actions achieving a goal state, is the State Space Informed Search. In the last years many works tried to develop new strategies to optimize the planning problem proposing different approaches [4,12,14]. Anyway, planning literature usually neglects a common problem in planning: the control of the existence of a plan. Approaches based on State Space Search are not efficient in detecting if a Goal is not reachable in any way and they result in excessive time and resources consumes. This problem is very important in Multi-Agent Systems, where concurrent execution of multiple agents complicate the state search problem because of resource sharing and of agents interactions. In our work we propose a Framework composed by a Modeling Tool, that provides the means to model Multi Agents Systems, and a Planner based on Counter Example of a Model Checking procedure.

The extended BDI metamodel also exploits First Order Logic (FOL) STRIPS [7,9] for pre and post condition definition of actions. The Counter Example search is performed by the UPPAAL [5] Model Checker. This need the application of proper model translation techniques in order to produce a timed automata representation of the multi-agent system. Counter examples are returned in form of UPPAAL traces and then translated in sequence of actions.

If the number of beliefs is large, generation of the whole automaton in a single run could be infeasible; for this reason, automata generation follows an iterative refinement approach: each time an agent finds a new feasible plan, refined actions and beliefs are used in the next step of the methodology.

Action refinement is a complex problem and it is out of the scope of this work. Anyway, similar refinement and composition techniques are in: [3,8,16,18].

### 2.1 Agent Based Planning Problem

In this section we provide a simplified version of the model we use to define our planning problem. The model is based on a Multi-Agent system representation of systems. We consider a variant of Beliefs, Desires, Intentions (BDI) logics [22] for our Multi-Agent System model that is a quadruple:

$$(Agents, World, \mathcal{T}\mathcal{S}, \mathcal{F})$$

where *Agents* is the set of all agents in the system; *World* represent the environment where agents executes;  $\mathcal{T}\mathcal{S}$  is a Transition System that resumes possible state transitions of agents in the environment and, finally,  $\mathcal{F}$  is a set of formulas expressed in first order logics that characterize each state in *World*.

We use a triple  $\langle n, d, v \rangle$  to define variables evaluations that describes states in the World, where  $n$  is the name of a variable,  $d$  represents its domain and  $v$  a value assigned to the variable. A State  $s \in World$  is a set of variable evaluation.

In addition, we call *State Conditions* of a state, the set of all formulas in  $\mathcal{F}$  that holds in a state  $s$ :

$$StateCondition(s) = \{ \phi \in \mathcal{F}, s \in World : s \models \phi \}$$

In addition,  $\phi$  cannot be a subformula of other formulas holding in  $s$ .

In this work we consider  $\mathcal{T}\mathcal{S}$ s and States with only one State Condition per state. If  $s \models \psi$ ;  $s \models \phi$  and  $s \models \psi \wedge \phi$ ; then we consider only the last formula as State Condition in  $s$ .

An Agent is in turn a triple:

$$(Actions, Beliefs, Goals)$$

*Actions* is a set of possible actions an agent is able to perform. Actions modify the environment changing *World* representation. They can also require the intervention of other agents in order to achieve common goals and in general, they include *communication* and *execution* actions. In addition, an action can be *reactive* if its execution depends on external events or messages; or *proactive* if its execution is decided directly by the agent. We call *Proactive Agent* an agent with at least one proactive action; an agent with no proactive actions and with at least one reactive action is a *Resource Agent*; an agent with no reactive or proactive actions is classified simply as a *Resource*.

*Beliefs* include the knowledges the agents have about: the *World*; the Agent itself; other Agents.

Notice that an agent may have a belief about the *World* which in turn is *not* true in the environment: in general, beliefs of each agents may not be exact. *Goals* is a set of states in  $\mathcal{T}\mathcal{S}$  that represent goals an agent want to reach. Since  $\mathcal{T}\mathcal{S}$  is not available when agents are defined, abusing notation we identify Goals with formulas in  $\mathcal{F}$  that are satisfied in goal states. We call these formulas: *Goal Conditions*. Notice that a goal condition is a State Condition for a goal state.

Beliefs are managed as World variables and states (they are practically local World representation in each agent). Agents define the  $\mathcal{T}\mathcal{S}$  Transition System on *World* states by means of *Actions*. An action  $\alpha \in \text{Actions}$  is a triple:

$$(\text{name}, \text{Precondition}, \text{Postconditions})$$

where *name* is trivially the name of the action; *Postconditions* is a set of formulas that hold in the new state; *Precondition* is a formula that *evaluates* true in a state  $s$  in order to *apply* (execute) the action and to produce a state transition:

$$s \xrightarrow{\alpha} s'$$

produces a transition from the state  $s$  to  $s'$ . If Precondition of  $\alpha$  evaluates true in  $s$ ,  $s'$  will be the same of  $s$ , except for variables involved in Postconditions evaluation. The values of these variables have to change in order to satisfy *all* effects in  $s'$ :

$$\forall \phi \in \text{Postconditions } s' \models \phi$$

In addition we must consider that an agent executing an action can access only to its local representation of *World*, i.e. to its beliefs. Hence, if agent's beliefs and World State are not synchronized (i.e., if the agents has a wrong belief about the world), it is possible that Precondition is evaluated true on beliefs, but *not* on *World* state.

In order to apply an action, we must execute the following two steps: (1) an agent tries to apply Postconditions in a state  $s$  producing a transition from  $s$  to  $s'$  if precondition is evaluated true on its *beliefs*; (2) if Precondition evaluates true in *World too*, then  $s \xrightarrow{\alpha} s'$  both in agent's Beliefs and in *World* too.

$\mathcal{T}\mathcal{S}$  is then the Transition System defined by the application of all actions in any state of *World*, performed by *all* Agents in the model. The execution of an action to build  $\mathcal{T}\mathcal{S}$  must follow the two steps previously defined. State transitions apply both to agents *Belief* and to *World*. Anyway Precondition control is enacted on Beliefs first. If evaluation fails on Beliefs, the action is not applied even if Precondition would evaluate true on *World*. In this model, a **Plan** to reach a Goal  $\mathcal{G}$  with given Goal Condition is a *path* from a starting state to a state where the Goal Condition holds. Notice that in a Multi Agent System, actions in a transition System can be executed by different agents, even concurrently. We consider here a path as a linear scheduling of concurrent applications of actions.

A Planning problem hence, is the problem of finding such a path or to state that the requested goal is unreachable in the current environment.

### 3 Attack and Countermeasures Modeling

In order to model actors involved in a Cyber Attack, we extended existing taxonomies in [21] for classification of actors and attacks. We classified attacks on the base of:

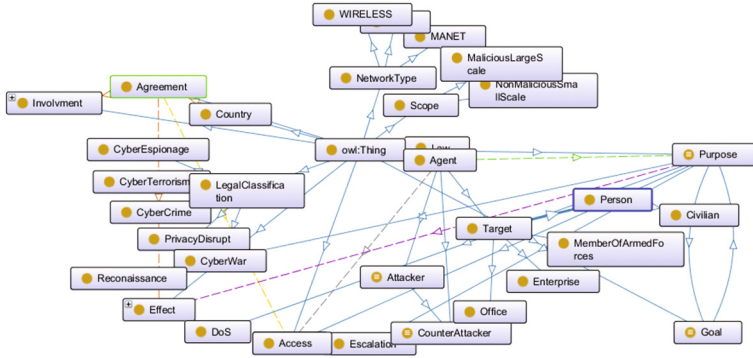


**Fig. 3.** A sketch of cyber crimes ontology

- their purposes (i.e. about Goals attackers want to reach)
- their legal classification
- severity of involvements (passive and active attacks)
- their Scope (malicious or not, large-scale or not etc.)
- based on the Network Types

In addition, we define an Agent both from Multi-Agent (i.e. of an actor having goals and performing actions to reach its goals) and from a Cyber Attack (i.e. as a target or an attacker or a counter-attacker) perspectives.

We further describe connections in agreements and laws, both considering abstract condition of Cyber Crimes (i.e. conditions that can be associated to other juridical fields) and Cyber effects of attacks.

In this way we define a complex ontology where we formalize connection among crimes, allowed punishments, and actions enabled by international agreements.

A part of this ontology (with some of the elements discussed before), is sketched in Fig. 3.

What we finally need is a way to translate ontology-based definition of a Cyber Crime scenario, into formal, analyzable model we can exploit in order to enact our planning methodology.

Next session describes the way we create this model.

## 4 Plan Generation

The methodology we are going to illustrate is based on the model presented in the previous section. The environment (*World*) is modelled in terms of states defined by means of  $\langle n, d, v \rangle$  triples. In addition, Agents are modelled in terms of Beliefs and Actions. Actions requires the definition of  $\langle name, Precondition, Effects \rangle$  triples, but we introduce in this phase an extension of the model since we need



some additional information during planning. Hence we extend Actions definition to the quadruple:

$$(name, Precondition, Effects, VarInfo)$$

where *VarInfo* set is necessary to specify variable domains, quantification (universal or existential), and eventually other properties.

During *Model Translation and Planning Phase*, a *Planner Engine* processes the model of the system. This produces a scheduling of actions representing the plan to achieve the requested goal. In the last phase, Agents perform plans action by action at run time. The *Execution Environment* monitors correct behaviours of agents: if for any reason the current goal is no longer reachable, or if scheduled actions cannot be executed, (because preconditions no longer meet or because Beliefs were different from *World* real configuration), the Execution Environment enacts a *Replanning* action that tries to retrieve new plans for the same goals (if they exist).

A planning actions execute with the following steps: (1) A Proactive Agents finds a plan in an environment with one ore more Resource Agents and resources. Actions in the plan are related to Resource Agents actions which in turn may use simple Resources. (2) The proactive Agent with the new plan, assigns sub-goals to Resource Agents that, in turn, executes planning actions at a different layer of abstraction to reach sub-goals. (3) Resource Agents executes their sub-plans to reach sub-goals assigned by proactive agents. This usually involves the use of simple Resources.

Proactive Agents are grouped into *clusters*. A Cluster is the set of Resource Agents that are serving the proactive agent at the moment. Proactive Agents are able to *ask* for a service only to Resource Agents in their clusters. Communication between agents is guaranteed by a very simple messages exchange protocol. It uses four kinds of messages: *Join*, used by Proactive Agents to ask for a Resource to join its cluster; *Leave* used by a Proactive to notify a Resource that it is no longer in its cluster; *SendGoal* to ask for a service; *OKJoin* an acknowledgement message.

The framework uses the UPPAAL Reasoning Engine to perform counter-example searching and it allows for smart accelerator as discussed in [2]. Two kinds of planners are implemented: a *Classical Planner* that is a simple implementation of the Breadth First and A\* state space search algorithms, and *Counter Example Planner*. The Plan search algorithm in the Counter Example Planner works in four steps: (1) The TA (Timed Automata) translator implements an algorithm for Agent models translation; (2) The TA is passed to the UPPAAL Reasoning Engine in order to produce a counter example (if any) to the following formula: “**A [] ;GoalCondition**” that is “*is it true that from initial state, only states where the goal condition is not satisfied are reachable?*”; (3) If the previous property is satisfied, then no plan exists for the current goal; otherwise, UPPAAL returns a *counter example* that is a path from the initial state to a state where the goal condition is satisfied, in form of an *Upaal trace*; (4) The Uppaal trace translator perform the translation from trace to a sequence of actions that is the agent plan.

**Data:**  $A$  a set of agents instances;  $E$  a set of Enabling conditions  $Act$  set of Actions

**Result:**  $Syn$ , Lists of Synchronization for Product Timed Automata,  $States$ , List of States od PTA

Init  $A$ ,  $E$  and  $Act$  with instances in the Ontology;

**forall** *Condition in the Ontology* **do**

    | Create a Set of Enabling Condition for each Action, depending on Country Agreements;

**end**

Create Goal States depending on Goal Effects

**forall**  $Act$  **do**

    | **if** *an enabling condition in  $E$  exists for an action* **then**

        | Create a State Starting from an Effect in the ontology, Ending in another Effect ;

    | **end**

**end**

Create Goal States depending on Goal Effects;

**Algorithm 1.** Model Transformation Algorithm

In order to generate an analyzable model for generating counterexample, we apply the following model transformation algorithm in Algorithm 1.

## 5 Conclusions

In this paper we described a methodology for enabling automatic planning of countermeasures to Cyber Crimes enabled by International Laws and Agreement. Planning exploits formal methods. It is based on multi-agent models and on counter-example guided planning procedure. Planning and generation of new contents depends on the definition of a formal Ontology. We presented a framework able to enact the methodology. Future works include the improvement of the counter-example planner algorithm and the extension of the methodology to conflicting interactions among agents and different types of International Agreements.

## References

1. Al-Musawi, B., Branch, P., Armitage, G.: Bgp anomaly detection techniques: a survey. *IEEE Commun. Surv. Tutorials* **PP**, 1 (2016)
2. Amato, F., Barbareschi, M., Casola, V., Mazzeo, A.: An fpga-based smart classifier for decision support systems. In: *Intelligent Distributed Computing VII*, pp. 289–299. Springer (2014)
3. Amato, F., Moscato, F.: Exploiting cloud and workflow patterns for the analysis of composite cloud services. *Future Gener. Comput. Syst.* **67**, 255–265 (2017)
4. Baier, J.A., Bacchus, F., McIlraith, S.A.: A heuristic search approach to planning with temporally extended preferences. *Artif. Intell.* **173**(5), 593–618 (2009)

5. Behrmann, G., David, A., Larsen, K.G., Pettersson, P., Yi, W.: Developing uppaal over 15 years. *Softw. Pract. Exp.* **41**(2), 133–142 (2011)
6. Biancotti, C.: Cyber attacks: preliminary evidence from the bank of Italy’s business surveys (2017)
7. Burfoot, D., Pineau, J., Dudek, G.: Rrt-plan: a randomized algorithm for strips planning. In: ICAPS, pp. 362–365 (2006)
8. Di Lorenzo, G., Moscato, F., Mazzocca, N., Vittorini, V.: Automatic analysis of control flow in web services composition processes. In: Proceedings - 15th EUROMICRO International Conference on Parallel, Distributed and Network-Based Processing, PDP 2007, pp. 299–306 (2007)
9. Fikes, R.E., Nilsson, N.J.: Strips: a new approach to the application of theorem proving to problem solving. *Artif. Intell.* **2**(3), 189–208 (1972)
10. Gandotra, E., Bansal, D., Sofat, S.: Malware analysis and classification: a survey. *J. Inf. Secur.* **5**, 56–64 (2014)
11. Gascueña, J.M., Navarro, E., Fernandez-Caballero, A.: Model-driven engineering techniques for the development of multi-agent systems. *Eng. Appl. Artif. Intell.* **25**(1), 159–173 (2012)
12. Haslum, P., Geffner, H.: Heuristic planning with time and resources. In: Sixth European Conference on Planning (2014)
13. Heartfield, R., Loukas, G.: A taxonomy of attacks and a survey of defence mechanisms for semantic social engineering attacks. *ACM Comput. Surv. (CSUR)* **48**(3), 37 (2016)
14. Hoffmann, J., Nebel, B.: The FF planning system: fast plan generation through heuristic search. *J. Artif. Intell. Res.* **14**, 253–302 (2001)
15. Mitchell, R., Chen, I.R.: A survey of intrusion detection techniques for cyber-physical systems. *ACM Comput. Surv. (CSUR)* **46**(4), 55 (2014)
16. Moscato, F.: Exploiting model profiles in requirements verification of cloud systems. *Int. J. High Perform. Comput. Networking* **8**(3), 259–274 (2015)
17. Moscato, F., Amato, F.: Thermal-aware verification and monitoring of service providers in metamorp(h)osy. In: Proceedings - 2014 International Conference on Intelligent Networking and Collaborative Systems, IEEE INCoS 2014, pp. 551–556 (2014)
18. Moscato, F., Amato, F.: Automatic cloud services composition for big data management. In: Proceedings - IEEE 30th International Conference on Advanced Information Networking and Applications Workshops, WAINA 2016, pp. 46–51 (2016)
19. Rid, T., Buchanan, B.: Attributing cyber attacks. *J. Strateg. Stud.* **38**(1–2), 4–37 (2015)
20. Schmitt, M.N.: Tallinn Manual on the International Law Applicable to Cyber Warfare. Cambridge University Press, New York (2013)
21. Uma, M., Padmavathi, G.: A survey on various cyber attacks and their classification. *IJ Netw. Secur.* **15**(5), 390–396 (2013)
22. Wooldridge, M.: Agent-based software engineering. In: IEE Proceedings on Software Engineering, pp. 26–37 (1997)

# Randomizing Greedy Ensemble Outlier Detection with GRASP

Lediona Nishani<sup>(✉)</sup> and Marenglen Biba

University of New York in Tirana, Kodra e Diellit, Tirana, Albania  
{ledionanishani, marenglenbiba}@uny.edu.al

**Abstract.** Ensemble methods have been recently used in many applications of machine learning in different areas. In this context, outlier detection is an area where recently these methods have received increasing attention. This paper deals with randomization in ensemble methods for outlier detection. We have developed a novel algorithm exploiting stochastic local search heuristics to induce diversity in an ensemble outlier detection algorithm. We exploit the capability of the GRASP heuristic to induce diversity into the search process and to maintain a good balance of exploitation and diversification in building the ensemble. The conducted experiments show interesting improvements over the greedy ensemble method and open the path for novel research in this direction.

**Keywords:** Outlier detection · Ensemble methods · Machine learning · Stochastic local search · GRASP

## 1 Introduction

The exponential growth of large databases has led to the need for monitoring and predicting economical flow, weather forecast or other various procedures in the whole real world data. Rare events distinguished from the daily basis processes are called outliers or anomalies. Even though outliers apparently are rare events, they pose a crucial importance for the system, thereby, making outlier detection a field, which demands a lot of attention in order to be expanded.

The most popular definition of outlier is “*an observation, which deviates so much from other observations as to arouse suspicions that it was generated by a different mechanism*” [1]. This definition was refined by Grubs [2] who has pointed out: “an outlying observation is one that appears to deviate markedly from other members of the sample in which it occurs”. Barnett and Lewis [3] have conceptualized the term of outlier as: “*An observation (or subset of observations) which appears to be inconsistent with the remainder of that set of data.*”

Data mining and machine learning algorithms have emerged in order to solve the outlier detection tasks. These methods are classified in three major directions: supervised, semi-supervised and unsupervised learning. Supervised methods consist of making their prediction for outliers through labeled data (known data), semi-supervised methods provide a normal class to be learned just like the supervised ones and capture some properties of the unsupervised approaches because the algorithm begin to learn by self developing itself. On the other hand, unsupervised methods consists of

regarding as outliers data members with different profile compared to the normal profile of the majority of data. The unsupervised methods are called interchangeably as anomaly detection or outlier detection methods. It happens that outliers may be a significant point of change that can show us the way to an activity that is not occurring in the right direction. In addition, where a person can deem a noise, another one can regard it as information [4]. Therefore, we cannot draw a strong line whether a data point is considered an outlier or not because it depends on the circumstances that the judgment is made [5].

Density-based cluster analysis is based on the notion of the cluster in a point density [6], where the number of the data points inside the bounds of a given area estimates density. One crucial characteristic of complex datasets in the real world is that they cannot specify density with global factors [7]. The local factor indicates outliers in different regions of the set of data. In this context, we have decided to investigate the line of research that tackles the local outlier algorithms LOF [8]. Our motivation relies in the fact that we have spotted some flaws in the greedy ensemble algorithm. While searching for the best candidate, the greedy ensemble algorithm can be isolated in the local maxima. Consequently, it can lose and not capture some outliers, which may be of great benefit in the global perspective of the dataset. We have come up and designed a novel algorithm upon the existing greedy ensemble approach by combining it with GRASP randomization procedure.

## 2 Outlier Detection

Outlier detection is the field, which handles the problems of capturing the outliers in a set of data. In the data-mining domain, this field concerns the disclosing of the exceptional activity behavior of particular data [9]. The traditional schemes that have been published and worked on this subject, have addressed the task of detecting outlier based on statistical framework LOF [8], Simplified-LOF [12], LOOP [11], LDOF [19], etc. Data mining communities have categorized outlier detection methods by four different groups [12]:

- statistical reasoning [13]. The data points are represented as a stochastic distribution where outliers are identified based on the relationship they have with the stochastic distribution of the data points.
- distance-based approaches proposed in [14–19] are intended to mitigate the shortcomings of statistical approaches. Their key idea is based on estimating distances between data points and assigning scores to data. The event, which has the larger score, is pronounced as outlier.
- density-based approaches [8, 11, 20, 21]. They rely on computing the densities of local neighborhoods. When the density of a data point is small, it appears that this data is far away from the normal behavior, therefore, it is considered as an outlier.
- model-based techniques determine the normal behavior by making use of predictive models just like neural networks or unsupervised support vector machines. Outliers are discerned as deviations from the learned model.

## 2.1 Ensemble-Based Outlier Detection

Making use of just one algorithm such as density-based or distance-based does not summarize entire kinds of outliers. Therefore, in order to provide the whole truth, it is appropriate to integrate various outlier detection outcomes by means of an ensemble-based approach, which will come up with a consensus finding.

Ensembles for outlier detection have inherited from ensemble-based classification approaches two major properties: accuracy (to be better than random) and diversity (to perform different errors in different algorithms). The main idea of combining various results is not only important in the ensemble clustering, but also even in related approaches such as subspace clustering and alternative clustering [22]. By transferring the idea of clustering in the outlier detection model, we yield in a reasonably improvement compared to individual models.

Diversity can be significantly induced by choosing different algorithms. Mixing different outcomes into a single outlier detection result can lead to disclosing many kinds of different outliers. Another intrinsic source for increasing diversity is parameterization (adjusting various parameters such as number of neighbors and distance functions). Data preprocessing and projection are specifically used in [23]. Additionally, the employment of sub sampling in a dataset is proposed in [24]. However, combining families of algorithms, local and global methods can potentially discover different kinds of outliers by obtaining an effective ensemble algorithm.

## 2.2 Greedy Ensemble

In order to make sense of what our approach consist of, it is crucial to explore in depth the greedy ensemble algorithm presented in [25].

First, it is selected a union  $K$  of data points from a set of individual outlier detectors. Moreover, it is created a target vector that assigns 1 for an object, which is in the  $K$  union of objects and 0 whether it does not belong to the union  $K$  of the top- $k$  outliers. Afterward, the ensemble is initialized with the algorithm, which has the most similar results with the target vector. Once it has found out the best outlier detector for providing a good accuracy of the ensemble approach, it is time for incorporating diversity. Diversity is induced by sorting remained outlier detectors in the decreasing order of being less similar to the target vector. When the new algorithm is included in the list of the detectors, testing and execution is performed in order to compare the results. If the greedy ensemble together with the new added algorithm performs better, let's say closer to the target vector, then this algorithm is kept and the list is updated. Otherwise, the algorithm is discarded and this decision will never be reconsidered. At each step of the algorithm, detectors are selected and then evaluated. This greediness characteristic is not beneficial for the algorithm because it can lead the algorithm to fall into local optima.

## 3 Stochastic Local Search and GRASP

Stochastic Local Search (SLS) are methods carried out to find solutions for combinatorial optimization problems [26]. They are regarded as the most thriving approaches particularly in the artificial intelligence area. That is the reason we have conceptualized

to combine concepts of Stochastic Local Search with greedy ensemble approaches in a novel ensemble algorithm.

Greedy Randomized Adaptive Search Procedure (GRASP) [27] is a SLS iterative procedure made of two major steps namely, the greedy construction and the local search step. It initiates from an empty candidate solution, and after every step adds the best solution based on the heuristic selection function. Moreover, the local search step performs the investigation of the neighborhood until the algorithm finds a local good solution. The two phases are iterated until a stopping factor appears to be accomplished.

Evaluating the elements leads to establishing of restricted candidate list (RCL), which is composed of the best solution candidates. The greedy aspect in this phase occurs when implementing the element in the solution by resulting in the smallest incremental cost. After creating the RCL, one element from RCL is selected randomly in order to be incorporated into the partial solution. Subsequently, the candidate list is updated and incremental costs are evaluated. The construction phase obtains candidate solutions that cannot be optimal. Therefore, it is performed the local search to enhance the solutions. The local search phase consists of an iterative procedure, which substitutes the actual solution with a better solution that can be found in the neighborhood of the current solution. It reaches the termination point when it has not discovered any better solution from the neighbors. The two crucial parameters that have to be set before executing the procedure are: the stopping criterion represented by the Max-Iteration and the quality of elements making up the RCL.

## 4 Randomized Greedy Ensemble with GRASP

This research paper aimed to combine the GRASP procedure by implementing it in the heuristic greedy ensemble approach. Our strategy consists on modifying the heuristic greedy approach in order to optimize and to increase its level of diversity and ROC AUC. We had this idea based on the logic that the best outlier results sometimes do not lead to the best outcomes. It happens that while searching for the best result, the algorithm may find out just the local maximum data point, but not the global maximum of the whole dataset. Therefore, in order to escape the local maxima, we need to employ randomization techniques into the greedy ensemble approach, which exhibits greediness properties. We have conceptualized that this kind of methodology can lead to a substantial increase of diversity. Randomization in practice is induced by modifying the pseudo code and incorporating the GRASP procedure into the greedy ensemble algorithm. At the same time, this adjustment is implemented in the class `GreedyEnsembleExperiment.java` in the ELKI Data Mining Framework. In java, the class of `GraspEnsemble` represents the randomization.

The logic and the design our novel algorithm are illustrated below through the pseudo code of the Randomized Greedy Ensemble Construction Algorithm. One parameter added from the GRASP perspective is the parameter  $\alpha$ , which is a value determining the probability that outlier detectors can be chosen. The restricted candidate list (RCL) is built upon  $\alpha$  parameter. RCL contains the best outlier detector results, and it can be updated over and over from the randomized GRASP procedure. Once the list is created; our algorithm can call the results of the GRASP procedure, which

underlie the outlier results of chosen detectors. Below in the Algorithm 4.1, our strategy is described step by step by highlighting the part of pseudo code added and altered from the previous algorithm of greedy ensemble algorithm.

```

Data:  $I$  individual outlier detection results
Data:  $n$  data set size
Data:  $\varphi$  expected / desired outlier rate
Data:  $\alpha \in [0,1]$ 
Data: seed
/* Compute preliminary outlier set:
 $K := \cup i \in I \text{ top-}k(i)$  with  $k$  minimal such that  $|K| \geq \varphi n$ ;
/* Compute target and weight vectors:
 $t := \{t_x := 1 \text{ if } x \in K\}$ ;
 $\omega := \{\omega_x := \frac{1}{2|K|} \text{ if } x \in K \text{ otherwise } \frac{1}{2(n-|K|)}\}$ ;
/* Initial ensemble - choose most similar result:
 $E := \emptyset$ ;
for  $i \in I$  do
  | if  $\text{dist}\omega(i, t) < \text{dist}\omega(E, t)$  then  $E := \{i\}$ ;
end
 $I := I \setminus E$ ;
/* Greedy ensemble construction:
 $pE :=$  current prediction of  $E$ ;
sort  $I$  by decreasing diversity to  $p$ ;
 $i :=$  remove first from  $I$ ;
 $pi :=$  prediction of  $E \cup \{i\}$ ;
if  $\text{dist}\omega(pi, t) < \text{dist}\omega(pE, t)$  then
   $E := E \cup \{i\}$ ;
   $pE := pi$ ;
  /* Optional: update  $t, K$ 
  sort  $I$  by decreasing diversity to  $p$ ;
end
while  $I \neq \emptyset$  do
   $I \leftarrow$  Greedy_Randomized_Construction( $\alpha$ , Seed, $I$ );
   $i :=$  remove first from  $I$ ;
   $pi :=$  prediction of  $E \cup \{i\}$ ;
  if  $\text{dist}\omega(pi, t) < \text{dist}\omega(pE, t)$  then
     $E := E \cup \{i\}$ ;
     $pE := pi$ ;
    /* Optional: update  $t, K$ 
    sort  $I$  by decreasing diversity to  $p$ ;
  end
end
return  $E$ 
procedure Greedy_Randomized_Construction( $\alpha$ , Seed, $I$ )
  Solution  $\leftarrow \emptyset$ ;
  Initialize the candidate set:  $C \leftarrow I$ ;
  Evaluate the incremental cost  $c(i)$  for all  $i \in C$ ;
  while  $C \neq \emptyset$  do
     $c^{\min} \leftarrow \min\{c(i) \mid i \in C\}$ ;
     $c^{\max} \leftarrow \max\{c(i) \mid i \in C\}$ ;
    RCL  $\leftarrow \{i \in C \mid c(i) \leq c^{\min} + \alpha(c^{\max} - c^{\min})\}$ ;
    Select an element  $s$  from the RCL at random;
    Solution  $\leftarrow$  Solution  $\cup \{s\}$ ;
    Update the candidate set  $C$ ;
    Reevaluate the incremental costs  $c(i)$  for all  $i \in C$ ;
  end;
  return Solution;
end Greedy_Randomized_Construction

```



## 5 Experiments and Results

### 5.1 Combining Various Scores and Algorithms

The first experiment is composed of two major phases namely: computing the ensemble members with various algorithms with different neighborhood size of  $k$  and building the ensemble by combining the results of individual algorithms into one output file. We have invoked the greedy ensemble through the command line, as various parameters are easier to be configured through batch files.

The first phase of our experiment consists of computing of ensemble members. This part will build a mixed matrix by making use of the class `ComputeKNNOutlierScores` provided from ELKI java code. The output file of the first part is composed of algorithms output per line for respectively parameters of  $k = 3, 5, 7, 9, 11, 13, 15, 17, 19, 21, 23, 25, 27, 29$ . This phase puts a score 0 or 1 for each of the data points, and in the end a unified score for all the data points placed in the input file of the dataset. The purpose of experiment's first part is to calculate and make use of various outlier detection algorithms that are based on the  $k$ -Nearest Neighbor such as  $k$ -NN,  $k$ -NN-Weighted, LOF, Simplified-LOF, LOOP, LDOF. This step is expected to take a lot of time, since it is determined to have a time complexity of  $O(n \log n)$ .

In the second phase, we have utilized the output of the first part as an input dataset and similarity evaluation are carried out into it. The evaluation process is undertaken from the main class `GreedyEnsembleExperiment.java`. In this class, we have modified the ELKI previous code by adding the `GraspEnsemble.java` designed accordingly for this experiment. Subsequently, we have compared the results of greedy ensemble of [25] with the results of our novel approach. In this step, an additional filter is added, which removes some attributes from the previous output (Table 1).

**Table 1.** The results of the second step obtained from the command line.

Type of ensemble	ROC AUC
Best individual	0.84 (LOF-09)
Naïve	0.5
Greedy	0.44
Random	0.5
Greedy to best	-2.5
Random Gain to Naïve	0
Greedy Gain to Random	<b>-0.10</b>

Our approach calculates for every outlier detector the true ROC AUC based on the outlier estimation. Subsequently, it compares all values by generating the best single algorithm that in our case is the LOF-09. All types of ensemble are created from 11 algorithms, each of them is used 14 times because we have started with  $k = 3$  and moved with a step of 2 till  $k = 30$ . Therefore, each of the algorithms is estimated 14 times in respect to the values of  $k$ ; hence, 11 algorithms fold 14  $k$  values consist of 154 methods overall investigated. When comparing the random ensemble with greedy

approach resulted that, our random ensemble has slightly improved over the greedy ensemble in terms of ROC AUC with 0.1. Greedy ensemble performs poorer than the naïve and random ensemble.

### 5.2 Combining Various Algorithms with the Same Neighborhood K

In the second experiment, we have built the ensemble with various algorithms, but with the same size of neighborhood for  $k = 30$ . This experiment is designed in the same way as the previous ones (Table 2).

**Table 2.** The results of building the ensemble with parameter  $k = 30$

Type of ensemble	ROC AUC
Best individual	0.97 (LOF-30)
Naïve	0.5
Greedy	0.44
Random	0.5
Greedy to best	-17.03
Random Gain to Naive	0
Greedy Gain to Random	<b>-0.1</b>

The best individual algorithm is found to be the LOF-30 based on the ROC AUC = 0.97. Regarding the random ensemble, this scenario yielded a random ensemble with a respective AUC = 0.5 and we can significantly discern that random ensemble performs slightly better than greedy ensemble with a value of gain = 0.1.

### 5.3 Combing LOOP Algorithms with Varying Neighborhood Size K with the Same Distance Function Manhattan (L1 Metric)

In the third experiment, we have managed to build a randomized ensemble from LOOP algorithms adjusted with various sizes of  $k = 2, 3, 4, \dots, 30$  with the same Manhattan distance function (Table 3).

**Table 3.** The results of building the ensemble with the same LOOP algorithm executed with varying  $k$  and the same distance function Manhattan metric

Type of ensemble	ROC AUC
Best individual	1 (LOOP-20)
Naïve	0.9981
Greedy	0.9965
Random	0.9981
Greedy to best	-0.01
Random Gain to Naive	0
Greedy Gain to Random	<b>-0.66</b>

When executed individually, the best algorithm that has exhibited the higher ROC AUC score is the LOOP-20. Our random ensemble appears to have a better ROC AUC = 0.9981 than the greedy heuristic approach.

Below, we have summarized our findings in the Table 4 in which is emphasized that our random ensemble appears to perform better than greedy ensemble when conducting experiments with various neighborhood size  $k$ .

**Table 4.** Summarization of the experiments results

Title of experiments	Greedy Gain to Random ROC AUC
1. Varying $k$ and various algorithms	-0.10
2. Combining various algorithms with $k = 30$	-0.1
3. Combining LOOP algorithms with varying $k$ with the same (L1 metric)	-0.66

## 6 Conclusions

This research paper has attempted to incorporate a stochastic local procedure as GRASP in the greedy heuristic scenario for optimization purposes of diversity. We added a novel class `GraspEnsemble` to the ELKI source code and expect that our effort to be included in the upcoming ELKI release version. However, ELKI is an open source code platform that can be further upgraded and enhanced. This paper made an effort to build a randomized ensemble mechanism, which combines various algorithms and at the same time has confirmed positive results in enhancing the greedy ensemble performance. We hope this novel research work will constitute a significant step towards the outlier detection domain in capturing meaningful outliers.

## References

1. Hawkins, D.: Identification of outliers. Monographs on Applied Probability and Statistics (1980)
2. Grubbs, F.E.: Procedures for Detecting outlying observations in samples. In: *Technometrics* 11.1 (1969), pp. 1–21 (1969)
3. Barnett, V., Lewis, T.: *Outliers in Statistical Data*, 3rd edn. Wiley, Hoboken (1994)
4. Ng, R., Subrahmanian, V.: *Stable for Semantics for Probabilistic Deductive Database*. University of Maryland (1990)
5. Blakeslee, S.: *Lost on Earth: Wealth of Data Found in Space*. The New York Times (1990)
6. Ester, M., Kriegel, H-P., Sander, J., Xu, X.: A Density-based algorithm for discovering clusters in large spatial databases with noise. In: *KDD 1996 Proceedings of AAAI (1996)*. Copyright © 1996. [www.aaai.org](http://www.aaai.org)
7. Ankerst, M., Breunig, M., Kriegel, H.-P., Sander, J.: OPTICS: ordering points to identify the clustering structure. In: *SIGMOD 1999 Proceedings of the 1999 ACM SIGMOD International Conference on Management of Data, Philadelphia, Pennsylvania, USA, 31 May–03 June 1999*, pp. 49–60. ACM, New York (1999). ©1999

8. Breunig, M.M., Kriegel, H.-P., Ng, R.T., Sander, J.: Lof: identifying density-based local outliers. In: Chen, W., Naughton, J.F., Bernstein, P.A. (eds.) *Proceedings of the 2000 ACM SIGMOD International Conference on Management of Data, Dallas, Texas, USA, 16–18 May 2000*, pp. 93–104. ACM (2000)
9. Tang, J., Chen, Z., Fu, A.W.-C., Cheung, D.W.: Enhancing effectiveness of outlier detections for low density patterns. In: *Proceedings of Pacific-Asia Conference on Knowledge Discovery and Data Mining (PAKDD)*, Taipei, Taiwan (2002)
10. Papadimitriou, S., Kitagawa, H., Gibbons, P.B.: LOCI: fast outlier detection using the local correlation integral. In: *IEEE 19th International Conference on Data Engineering (ICDE 2003)* (2003)
11. Kriegel, H.-P., Kroger, P., Schubert, E., Zimek, A.: LoOP: local outlier probabilities. In: *Proceedings of CIKM*, pp. 1649–1652 (2009)
12. Schubert, E., Zimek, A., Kriegel, H.-P.: Local outlier detection reconsidered: a generalized view on locality with applications to spatial, video, and network outlier detection. *Data Min. Knowl. Disc.* (2012). doi:[10.1007/s10618-012-0300-z](https://doi.org/10.1007/s10618-012-0300-z)
13. Hadi, A.S., Imon, A.H.M.R., Werner, M.: Detection of outliers. *Wiley Interdisc. Rev.: Comput. Stat.* **1**(1), 57–70 (2009)
14. Angiulli, F., Pizzuti, C.: Fast outlier detection in high dimensional spaces. In: *Proceedings of European Conference on Principles of Knowledge Discovery and Data Mining, Helsinki, Finland* (2002)
15. Knorr, E.M., Ng, R.T.: Algorithms for mining distance-based outliers in large datasets, pp. 392–403 (1998)
16. Orair, G.H., Teixeira, C.H.C., Meira Jr., W., Wang, Y., Parthasarathy, S.: Distance-based outlier detection: consolidation
17. Ramaswamy, S., Rastogi, R., Shim, K.: Efficient algorithms for mining outliers from large data sets. In: *SIGMOD Record*, vol. 29, pp. 427–438. ACM (2000)
18. Vu, N.H., Gopalkrishnan, V.: Efficient Pruning Schemes for Distance-Based Outlier Detection. In: *Machine Learning and Knowledge Discovery in Databases. Lecture Notes in Computer Science*, vol. 5782, pp. 160–175
19. Zhang, K., Hutter, M., Jin, H.: A New Local Distance-Based Outlier Detection (2009)
20. Approach for scattered real-world data. In: *Proceedings of 13th Pacific-Asia Conference on Knowledge and Discovery and Data Mining (PAKDD 2000)*, pp. 813–822
21. de Vries, T., Chawla, S., Houle, M.E.: Finding local anomalies in very high dimensional space. In: *Proceedings of the 10th IEEE International Conference on Data Mining (ICDM)*, Sydney, Australia, pp. 128–137 (2010). doi:[10.1109/ICDM.2010.151](https://doi.org/10.1109/ICDM.2010.151)
22. Keller, F., Müller, E., Böhm, K.: HiCS: high contrast subspaces for density-based outlier ranking. In: *Proceedings of the 28th International Conference on Data Engineering (ICDE)*, Washington, DC (2012)
23. Zimek, A., Gaudet, R.J.G., Campello, B., Sander, J.: Subsampling for efficient and effective unsupervised outlier detection ensembles. In: *Proceedings of the 19th ACM International Conference on Knowledge Discovery and Data Mining (SIGKDD)*, Chicago, IL, pp. 428–436 (2013). doi:[10.1145/2487575.2487676](https://doi.org/10.1145/2487575.2487676)
24. Breiman, L.: Bagging predictors. *Mach. Learn.* **24**, 123–140 (1996). © 1996 Kluwer Academic Publishers, Boston. Manufactured in The Netherlands
25. Schubert, E., Wojdanowski, R., Zimek, A., Kriegel, H.: On evaluation of outlier rankings and outlier scores. In: *Proceedings of the SIAM International Conference on Data Mining, (SIAM 2012)*, Anaheim, CA, pp. 1047–1058 (2012)

26. Schubert, E.: Generalized and Efficient Outlier Detection for Spatial, Temporal, and High-Dimensional Data Mining. Munchen, Germany (2013)
27. Hoos, H.H., Stützle, T.: Stochastic Local Search Foundations and Applications. Elsevier Inc., San Francisco (2005)
28. Resende, M., Ribeiro, C.: Greedy randomized adaptive search procedures. *J. Glob. Optim.* **6**, 109–133 (1995). Kluwer Academic Publisher, Netherlands

**The 4th International WorkShop  
on Energy-Aware Systems,  
Communications and Security  
(EASyCoSe-2017)**

# Energy Efficient System for Environment Observation

Giorgio Giordanengo<sup>1</sup>(✉), Luca Pilosu<sup>1</sup>, Lorenzo Mossuca<sup>1</sup>, Flavio Renga<sup>1</sup>,  
Simone Ciccia<sup>2</sup>, Olivier Terzo<sup>1</sup>, Giuseppe Vecchi<sup>2</sup>, Vincenzo Romano<sup>3,4</sup>,  
and Ingrid Hunstad<sup>3</sup>

<sup>1</sup> Istituto Superiore Mario Boella, Torino, Italy

{giordanengo,pilosu,mossuca,renga,terzo}@ismb.it

<sup>2</sup> Department of Electronics and Telecommunication,  
Politecnico di Torino, Torino, Italy

{simone.ciccia,giuseppe.vecchi}@polito.it

<sup>3</sup> Istituto Nazionale di Geofisica e Vulcanologia, Rome, Italy

{vincenzo.romano,ingrid.hunstad}@ingv.it

<sup>4</sup> SpacEarth Technology, Rome, Italy

**Abstract.** Environment observations provide a unique source of consistent information about the natural environment and they provide resource managers the information to assess the current state of the environment, weight the requirements of different uses by multiple stakeholders, and manage the natural resources and ecosystems in a sustainable manner. Most of the observations are based on satellites, but remote-sensing technologies alone cannot guarantee observations at the spatio-temporal resolution and with the accuracy requested for monitoring and modeling applications targeting, like weather and climate extremes and the complex feedback processes between the natural environment and human activities. Dense networks of standard and in-situ weather related sensors are present in EU and US, but it may happen that their data are not always available in real-time or updated with the required scale for various weather and climate applications. Then, high-resolution, (near) real-time on field monitoring systems are needed to satisfy the demand to sample environmental data, both in dense populated regions and in less developed and getting more populated regions, where essential in-situ observational capabilities can be lacking or deteriorating. The paper would demonstrate the possibility to have energy efficient computing and communication systems that can be employed for environment observation and that can enrich traditional in-situ and remote sensing environmental data, to enable a significant step forward in the environment monitoring of a wide range of weather and climate data. The paper will present an approach going in this direction (computing/communication everywhere with low-power constrains), tested in a harsh environment, by exploiting low-power boards to perform data pre-processing and reconfigurable antennas to send data in a more energetically convenient way applied to a real case as it may be the monitoring of ionospheric scintillation in Antarctica.

## 1 Introduction

Since 2003 a specially modified GPS receiver has been used by INGV, Upper Atmosphere Research Unit, for recording the phase and amplitude of the L1 signals during events of ionospheric scintillation at high latitude [1]. In Antarctica the first Global Navigation Satellite Systems (GNSS) receiver, for ionospheric purposes, was installed in 2006 at the Italian station “Mario Zucchelli”, Terra Nova Bay (74.7° S, 164.1° E), in the frame of the Italian National Program for Antarctic Research (PNRA). This site became part of the wider Ionospheric Scintillations Arctic Campaign Coordinated Observation (ISACCO), the Italian project for monitoring ionospheric scintillations and total electron content (TEC) in polar regions with modified GNSS receivers. Since then, three more installations have been done in Antarctica in the Italian-French station of Concordia (75.1° S, 123.4° E) on the Antarctic plateau, at 1200 Km from Mario Zucchelli base.

GNSS receivers constitute a very useful tool to investigate the Earth’s ionosphere. A radio wave, such as GNSS radio signals, that travels through the ionosphere is affected by a rapid amplitude and phase fluctuations called ionospheric scintillations [2]. Amplitude scintillation can create deep signal fades while phase scintillation are characterized by rapid carrier-phase changes that can produce cycle slips. Both effects can prevent a GNSS receiver from locking on to the signal and make it impossible to estimate a position [3]. Following the success of the first ionospheric scintillation event on Galileo, recorded in Antarctica in the frame of the DemoGRAPE Project [4], a multi-constellation GNSS receiver has been installed in the Mario Zucchelli station during the last summer campaign, in December 2016. The Italian Antarctic Ionospheric Observatory is nowadays covering almost one solar cycle of continuous GNSS data. The new facility to record also Galileo and GLONASS data make the observing facility unique and relevant to investigate the solar-earth physics and the ionosphere dynamics. Maintaining a continuous and unmanned observatory, needs an appropriate infrastructure in terms of computing, power, and connectivity. To fulfill this need the receiver has been integrated by an ad-hoc energy-efficient and self-sufficient GreenLab system realised by Istituto Superiore Mario Boella (ISMB) in the frame of “Upper Atmosphere Observations and Space Weather” PNRA Project. Data management system is also crucial to make data available and useful to scientific and application community. For this reason in the last years a lot of efforts have been devoted to develop data management platforms [5] and ICT infrastructures [6].

In this paper, the authors present a system able to satisfy the demand of more energetically efficient systems able to perform processing and (wireless) communications, with high quality link. To reach this result, the properties of reconfigurable antenna coupled to a software defined radio controller able to perform a real-time control of the antenna itself (e.g. to steer the main beam in the direction of the main station, or to vary the RF power needed to perform the communication), will be exploited with low power processing boards in order



to ensure a global energy consumption sustainable with a system powered by (limited) renewable energies [7,8].

The paper is organized as follows: Sect. 2 introduces the scientific and technological background and the chosen approach and architecture, Sect. 3 presents the experimental results of the tests performed in Antarctic Region, while Sect. 4 draws conclusions and perspectives.

## 2 System Design and Architecture

The system, formed by low power computing and communication technologies and powered by renewable sources, is sketched in Fig. 2. This system has been installed in the Italian Antarctic station *Mario Zucchelli* [9]. As shown in Fig. 2, the system is composed by four blocks:

1. energy supply unit, formed by solar panel and batteries to ensure energy in case of bad weather;
2. data acquisition, by the GNSS antenna and receiver for this specific application;
3. computing section, where collected data are pre-processed;
4. communication part, where pre-processed data are sent to the base-station (Fig. 1).



**Fig. 1.** Panoramic view of the test site in which the Tx and Rx are highlighted.

Solar energy is commonly employed in this Region because the sun, during the Antarctic summer, is always present and this is the season selected for the on-field experiments. The power supply module exploits this type of energy source through an optimized power management, and orchestrating the duty cycles of all other modules by switching off modules as soon as they finish their tasks. During winter periods, when the sun never rises for several months, other renewable sources can be exploited (e.g. wind), but this is out of the scope of this demonstrator.

The core of the system is formed by the computing and communication parts which allow, together, to exchange data between the observation point and the base station, where all data are collected, keeping low the overall power consumption. The computing mini-cluster performs raw-data pre-processing from

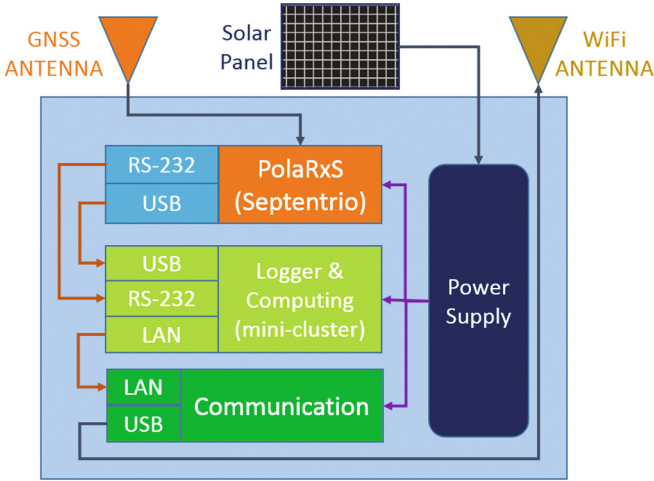


**Fig. 2.** Pictorial representation of the designed system.

the GNSS receiver (in the specific case a Septentrio PolaRxS [10]), to extract only a resume of all information collected to be sent in (near) real-time to the base-station. The communication module reads the reduced set of information coming from the computing part and, through a reconfigurable antenna coupled to Software Defined Radio (SDR) algorithms controlling the antenna itself, sends the data to the base-station. This solution allows to automatically discover the receiver’s position without the need of an accurate pointing and, in the meantime, to reduce the transmitted power since the Signal to Noise Ratio (SNR) is reduced with this technology.

All components have been selected and developed taking into account the harsh environmental conditions of the deployment Region; in the installation area, the temperature ranges are between  $-35^{\circ}\text{C}$  to  $8^{\circ}\text{C}$ . This means that all the materials employed need to be able to operate in these climate conditions and then components working in extended temperature range have to be used (since commercial equipment usually works in a range from  $0^{\circ}\text{C}$  to  $40^{\circ}\text{C}$ ). Finally, the whole system has also a receiver-side part located in the base station, which includes a receiver board and a network storage server. Even if important, this part is out of the scope of this work since it does not have constraints regarding power supply and temperature and then it will not be treated in the rest part of the paper.

### 2.1 Power Management

In order to implement a completely autonomous device, the system described in this paper is powered by renewable sources (i.e. solar energy). Depending on where the system is installed, solar energy is not always available in site. This is determined by many factors: weather conditions, latitude of the installation,

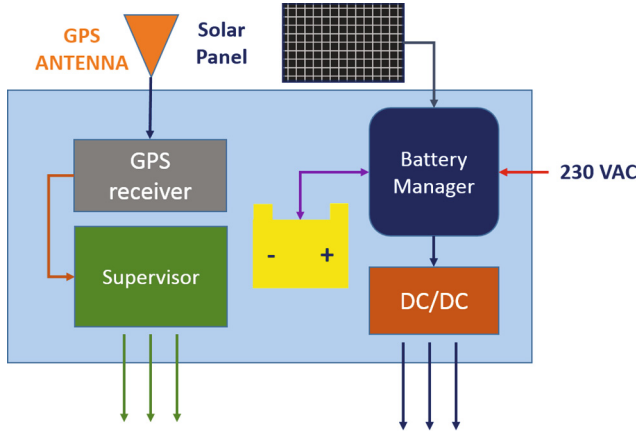


**Fig. 3.** Architecture of the power management unit.

yearly seasons and time of the day. Therefore, care should be taken in order to optimize the overall power efficiency of the entire system. In this paragraph, the adopted power management architecture and behavior is described in detail. Figure 3 shows the power management architecture. The Battery Manager (BM) is in charge to extract all available electrical energy generated by photovoltaic panels (see Fig. 4) and to store it into the battery module. The BM integrates also a Maximum Power Point Tracking (MPPT) algorithm, which is able to maximize the extracted power, as the external conditions change (e.g., panel temperature, solar radiation, presence of shades on a subset of photovoltaic cells), etc.). The DC/DC converter module, directly connected to the battery manager, is in charge to extract the available power from the battery, by generating all voltage needed to power the entire system. A GPS module is also included in the power management unit, with the main function to provide the absolute timing information to every component of the system architecture. An additional input power supply at 230 VAC is also included in the system architecture, to allow testing of the device without the need of photovoltaic modules.

In order to further optimize the power consumptions of the whole system, the power management unit integrates also a system supervisor. Such module feeds the electrical power to all other subcomponents of the system (i.e. computation, receiver, storage and antenna unit) using energy saving policies. Indeed, according to a series of preset operating profiles, the modules that are not used are safely switched off to save power. Various operating profiles (duty cycles) can be adopted on each power line, in order to implement specific energy saving behavior (e.g. the TX module can be temporarily powered on only once the acquisition and computation of new data is available). These profiles can be changed and stored on the fly using remote commands.



Fig. 4. Solar panels used by the system as primary source of energy.

## 2.2 Data Management

To acquire and process data from a multi-constellation GNSS Receiver (i.e. Septentrio PolaRxS), as well as to enhance data analysis by allowing pre-processing and providing it to users in near real time, data collection from Low Energy Boards has been exploited. The Data Management System, depicted in Fig. 5, consists of three main modules:

1. Data Acquisition
2. Data Analysis
3. Data Storage

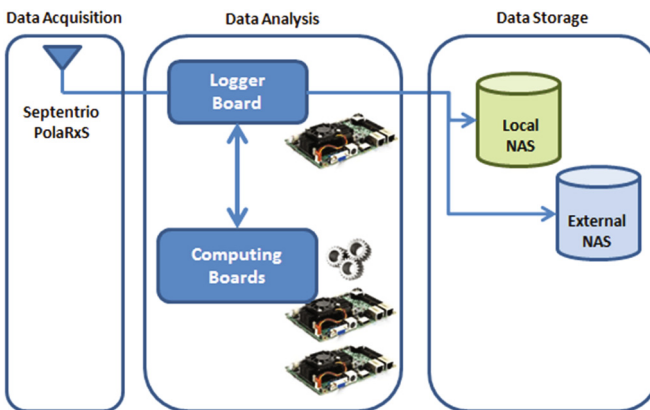


Fig. 5. Data Management System.

Data acquisition is based on the Septentrio PolaRxS receiver which runs over multiple frequencies and constellations for ionospheric monitoring and space weather observations. It is equipped with low noise control, and its features are high-quality, simultaneous Galileo, GLONASS and GPS signal tracking. This kind of receiver is particularly valuable for tracking rapid signal dynamics like those found in scintillation events. Thanks to its technology for analyzing interference and notch filtering for mitigation, it can be installed in crucial environments for radio broadcasting. GNSS receiver and logger board work together and are always active, 24 h a day. They are fitted out of automatic procedures for auto-configuration in case of unexpected reboot.

The Data Analysis module is composed of two boards, i.e. logger and computing. It is devoted to data acquisition from the receiver and its pre-processing. The logger is a Single Board Computer (SBC) which integrates all the components of a traditional desktop computer (e.g., CPU, main memory, I/O interconnections, storage, etc.) in a compact board. The Computing stage is formed by several SBCs that have been devoted to process data coming from the logger board. Periodically, the computing boards are switched on as soon as a given amount of raw data are received and they allow to execute several analysis based on the type of data retrieved. One of these analysis is related to the ionosphere which is the single largest contributor to the GNSS error budget, and ionospheric scintillation in particular is one of its most harmful effects. The Ground Based Scintillation Climatology can ingest data from high sampling rate GNSS receivers for scintillation monitoring like the widely used GPS for Ionospheric Scintillation and PolaRxS (GISTM). As mention before, the logger board is always active, 24h a day, while, in a energy-saving perspective, the computing boards can be activated only when they are really necessary, based on actual workloads.

Finally, data storage allows to manage and store data and associated meta-data. It consists of two NAS servers: the first one, namely Local NAS, is used for saving raw data; the second one, namely External NAS, stores elaborated data and makes them available for external users outside the base. In particular, the Septentrio PolaRxS receiver generates about 2 GB of raw data each day, that are reduced to about 100 MB a day after the pre-elaboration. The data storage module maintains data provenance and provides the necessary tools and interfaces to allow scientists to quickly identify outdated simulations using chronological traces. Data stored in Local NAS server allow to rerun simulations at any time, such as when a algorithm is updated.

### 2.3 Communications

The communication system is composed mainly by three parts:

1. Antenna;
2. Front-End;
3. Low Power PC with communication protocol fully software-defined.

The system is configured, by default, in “bidirectional” mode, i.e. radio nodes are able to both transmit and receive data. Nevertheless, the communication system

can also be set up in unidirectional mode. For instance, the typical one-way data-flow situation from the observatory point (where the data are acquired) to the base-station (where the data are stored). For brevity, the description of the communication system building blocks is addressed from the receiving point of view. However, the transmission side is identical.

The antenna is constituted by a classical phased-array, as depicted in Fig. 6, and it is formed by 4 patch antenna (Fig. 6a), coupled with a Beam-Forming Network based on phase-shifter (Fig. 6b) able to steer the beam of the antenna itself of about  $\pm 50^\circ$  in the horizontal plane [11, 12]. This configuration allows a raw pointing since the receiver position is automatically discovered.

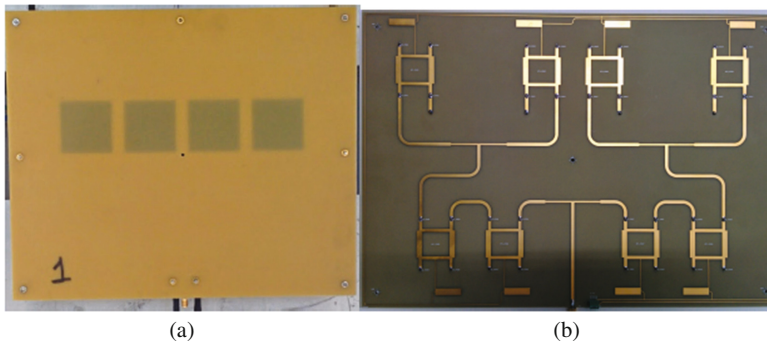


**Fig. 6.** Antenna used: phase-array formed by 4 patches (a) coupled with a Beam-Forming Network based on phase-shifter (b).

The Radio Frequency (RF) signal received by the antenna it is down-converted to base-band and digitized by exploiting a Universal Software Radio Peripheral (USRP) B200mini-i [13]. This is the front-end that, through an Analog to Digital (ADC) converter with 56 MHz of instantaneous bandwidth allows the interface between the RF and the digital world. It is a transceiver with the dimensions of a card (see Fig. 7), which can be employed in a frequency range from 70 MHz to 6 GHz. Furthermore, it is provided by a user-programmable Xilinx Spartan-6 Field Programmable Gate Array (FPGA). Such devices, coupled with the reconfigurable antenna, constitute the RF part and it is coupled to the board, through a high-speed USB 3.0 connection. Now, downstream of this device, the signal is digitized and it can be elaborate by the communication board, which is in charge to transmit/receive data coming from the computing part. For this purpose it has been exploited a Pico-ITX SBC board (see Fig. 8); this embedded board mount the latest generation of Ultra-Low Power Intel Core (i.e. 6th generation 14nm) processors and it is equipped with one DDR4 SO-DIMM with 4 GB memory capacity [14]. Finally, the PICO500 is built to withstand wide temperature conditions, ranging from  $-20$  to  $+70$  Celsius.

The board elaborates and treats the digital stream with a fully software implementation of a standard WiFi 802.11 receiver. The software algorithm

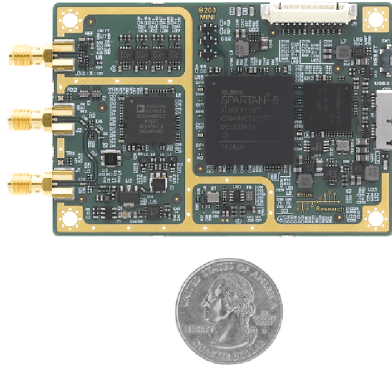


**Fig. 7.** USRP B200mini-i SDR/cognitive radio.

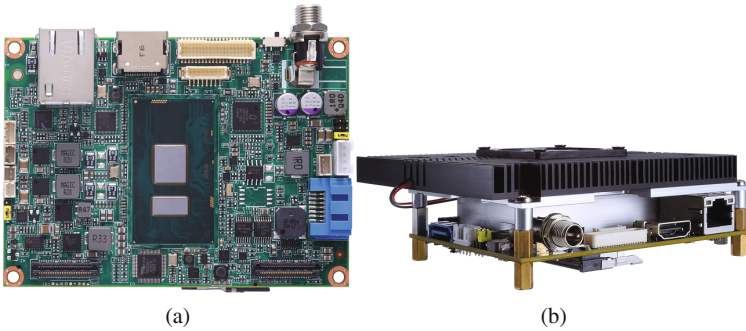


**Fig. 8.** Pico-ITX SBC embedded board: top view (a) and coupled with an active thermal solution (b).

exploits the signal information to control the antenna and to optimize the direction and the power of the signal to be transmitted/received. The IEEE802.11a/g/p wireless communication protocol has been implemented by exploiting GNURadio [15], a free and open-source software development toolkit that provides signal processing blocks to implement software radios. GnuRadio itself provides a baseline open-source version of the communication standard in question. Unfortunately, its computational complexity impedes operation in low power General Purpose Processors; thus, starting from this version, we developed a faster and lighter implementation of the transmitter and receiver, customized for Low-Power General Purpose Processor. The last link in the chain is the control of the antenna starting from the software; to do this an interface between the board and the antenna has been developed. This interface it is in charge to convert the digital signal coming from the software to a voltage that, applied to the beam-forming network of the designed antenna, it is able to steer the main beam, allowing to focus towards the base-station, where the receiver is waiting for the data.

The implemented test case is a point-to-point communication between the acquisition and the base-station; to perform the communication in a low-power perspective, the data collected and processed by the computing board are sent to the main station once an hour. This allows to reduce the power consumption, since the board and all stuffs connected to that board (i.e. antenna controller and USRP) are switched-on only to perform the data transmission, allowing to reduce the power consumption of the entire system.

### 3 Experimental Results

In this Section the results obtained on field will be depicted to demonstrate the validity of this type of system to perform low power processing and wireless communication, integrated together to be deployed in a critical environment like the Antarctic region.

#### 3.1 Communication Performance

Prior showing the tabulated results of the wireless communication tests, it is essential to illustrate the working principle of the realized communication link. The link implemented for this application is a point-to-point topology composed by two radio nodes:

- The Observatory Point Radio (OPR), i.e. the radio in charge to transmit data, in this case the node presenting the highest consuming. Thus, the energy minimization process has been applied on this side;
- The Base Station Radio (BSR), i.e. the radio in charge to receive the data and to identify the radio process.

These nodes employ the following high level ad-hoc protocol in order to communicate efficiently:

1. Observatory Point side, the energy supply unit turn on, with a programmable timer, the OPR board to load and transmit the stored information;
2. OPR board disseminates a request of transmission and poses to listening mode later;
3. BSR, at the reception of the request, sends a training sequence with the aim of revealing its spatial position;
4. OPR elaborates the training sequence by means of a spatial scan, i.e. electronically moves the antenna main beam. For each discovered position, the optimization algorithm keeps track about the training sequence power. At the end of the spatial scan, the processor directs the antenna main beam toward the direction of maximum received power. This configuration is maintained for all the permanence of the data transmission;
5. After data transfer success, OPR advices the energy supply unit that shut-down. The energy supply unit cut off power supply to the radio.



The reconfigurable antenna approach in a wireless communication link establishes two important advancement: first, by focusing all radiated energy toward the base station, it reduce in considerable manner the amount of power emitted by the transmitter. The latter is directly proportional to the radio instantaneous power consumption. In other words, the reduction in the transmitted power results in a decreased consumption of the radio. Second, since the antenna main beam is strongly focused toward the intended direction, noise and interferer are attenuated accordingly. This allows the transmitter to employ the highest communication rates to transfer the information. The greater is the communication rate the faster is the data transfer. Consequently, less time the radio is in active mode. These two factors critically affect the daily energy consumption of the proposed link Fig. 9 reports the outcomes of one-day transmissions. Each data transfer consists in a merge of 4 files of variable size, collected from the observatory system in one hour of monitoring. An example is reported in Table 1. The information about the total size of the data to be transmitted is included in the merged file. This way, the BSR system knows in advance how much data expects from the OPR system. At the end of the data transfer, BSR counts the amounts of received data. Then, the comparison of this number with the one retrieved from the header of the merged file it gives an estimation on the amounts of loosen bytes.

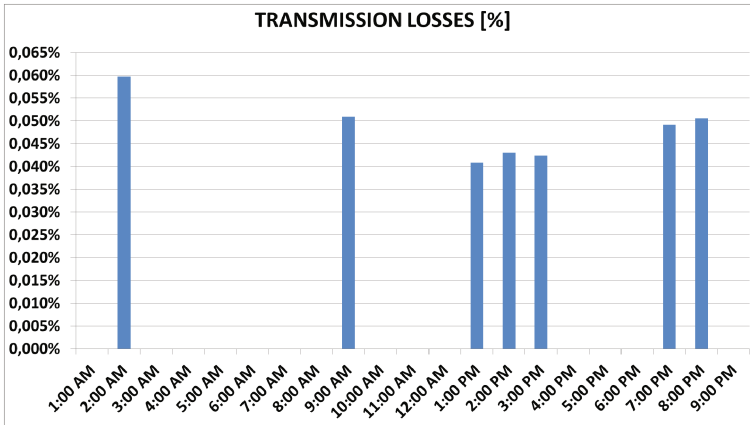


Fig. 9. Automatic transmission outcomes.

Table 1. Example of one hour data collection

Merged Files	Transmitted [Bytes]	Received [Bytes]	Losses [%]
<i>BTN0P_352o00.16_.ismr</i>	152.765	152.465	0,20
<i>BTN0P_352o15.16_.ismr</i>	148.123	148.123	0,00
<i>BTN0P_352o30.16_.ismr</i>	145.168	145.168	0,00
<i>BTN0P_352o45.16_.ismr</i>	143.902	143.902	0,00

## 4 Conclusions and Perspectives

An advanced prototype of a low power computing and communication system, self-sustained by means of renewable energy and advancements in communication, has been designed, realized and tested in Antarctica, allowing to test an autonomous system able to manage, pre-process and send data for a real test-case. All components, designed to allow the collection and transmission of scientific data in field, have been selected to be able to work in really harsh conditions; this allows to overcome unscathed the Antarctic summer campaign. Communication between measurement station and base station has been successfully tested and compared with data collected and sent in more standard way (i.e. wired transmission).

Future development of this systems include a fine tuning of its single building blocks, as well as possible improvements in terms of energy consumption and transmission extension by exploiting other low-power small-form-factor boards.

**Acknowledgements.** The authors are grateful to the Programma Nazionale di Ricerche in Antartide (PNRA) for supporting the project “Upper atmosphere observations and Space Weather” within PNRA D.C.D. 393 del 17/02/2015 PNRA14.00110 - Linea A1. The authors would like also to acknowledge the invaluable help of CLEAR elettronica srl, which provide the control board for the scheduling and power management and SOLBIAN energie alternative srl, which provide the solar panels. Finally we are grateful to ENEA for the logistic and the support during the campaign.

## References

1. De Franceschi, G., Alfonsi, L., Romano, V.: Isacco: an Italian project to monitor the high latitudes ionosphere by means of GPS receivers. *GPS Solutions* **10**(4), 263–267 (2006)
2. Mitchell, C.N., Alfonsi, L., De Franceschi, G., Lester, M., Romano, V., Wernik, A.W.: GPS TEC and scintillation measurements from the polar ionosphere during the October 2003 storm. *Geophys. Res. Lett.* **32**(12) (2005)
3. Aquino, M., Moore, T., Dodson, A., Waugh, S., Souter, J., Rodrigues, F.S.: Implications of ionospheric scintillation for gnss users in northern europe. *J. Navig.* **58**(2), 241–256 (2005)
4. Alfonsi, L., Cilliers, P.J., Romano, V., Hunstad, I., Correia, E., Linty, N., Dovis, F., Terzo, O., Ruiu, P., Ward, J., Riley, P.: First observations of gnss ionospheric scintillations from demogrape project. *Space Weather* **14**(10), 704–709 (2016)
5. Romano, V., Pau, S., Pezzopane, M., Spogli, L., Zuccheretti, E., Aquino, M., Hancock, C.M.: eSWua: a tool to manage and access GNSS ionospheric data from mid-to-high latitudes. *Ann. Geophys.* **56**(2) (2013)
6. Scionti, A., Ruiu, P., Terzo, O., Spogli, L., Alfonsi, L., Romano, V.: Demogrape: managing scientific applications in a cloud-federated environment. In: 2016 10th International Conference on Complex, Intelligent, and Software Intensive Systems (CISIS), pp. 426–431, July 2016
7. Ciccia, S., Giordanengo, G., Arianos, S., Renga, F., Ruiu, P., Scionti, A., Mossucca, L., Terzo, O., Vecchi, G.: Reconfigurable antenna system for wireless applications. In: 2015 IEEE 1st International Forum on Research and Technologies for Society and Industry Leveraging a Better Tomorrow (RTSI), pp. 111–116, September 2015

8. Ciccia, S., Vecchi, G., Giordanengo, G., Renga, F.: Software-defined reconfigurable antenna for energy efficient wireless links. In: 2016 IEEE International Symposium on Antennas and Propagation (APSURSI), pp. 1241–1242, June 2016
9. The mario zucchelli station. <http://www.italiantartide.it/stazione-mario-zucchelli>
10. Polarxs. <http://www.navtechgps.com/septentrio-polarxs-packaged-receivers/>
11. Orefice, M., Dassano, G.L., Matekovits, L., Pirinoli, P., Vecchi, G., Shurvinton, B.: A wide coverage scanning array for smart antennas applications. In: 2001 31st European Microwave Conference, pp. 1–4, September 2001
12. Dassano, G., Orefice, M.: Voltage controlled steerable array for wireless sensors networks. In: The Second European Conference on Antennas and Propagation, EuCAP 2007, pp. 1–4 (2007)
13. Usrc b200mini-i. <https://www.ettus.com/product/details/USRP-B200mini-i>
14. Pico-itx sbc. <http://www.axiomtek.it/>
15. Gnu radio, free and open-source software development toolkit. <http://gnuradio.org/>

# Balancing Demand and Supply of Energy for Smart Homes

Saqib Kazmi<sup>1</sup>, Hafiz Majid Hussain<sup>1</sup>, Asif Khan<sup>1</sup>, Manzoor Ahmad<sup>1</sup>, Umar Qasim<sup>2</sup>, Zahoor Ali Khan<sup>3</sup>, and Nadeem Javaid<sup>1</sup>(✉)

<sup>1</sup> COMSATS Institute of Information Technology, Islamabad 44000, Pakistan  
nadeemjavaidqau@gmail.com

<http://www.njavaid.com>

<sup>2</sup> Cameron Library, University of Alberta, Edmonton, AB T6G 2J8, Canada

<sup>3</sup> Computer Information Science, Higher Colleges of Technology,  
Fujairah 4114, United Arab Emirates

**Abstract.** Smart grid (SG) is one of the most advanced technologies, which plays a key role in maintaining balance between demand and supply by implementing demand response (DR). In SG the main focus of the researchers is on home energy management (HEM) system, that is also called demand side management (DSM). DSM includes all responses, which adjust the consumer's electricity consumption pattern, and make it match with the supply. If the main grid cannot provide the users with sufficient energy, then the smart scheduler (SS) integrates renewable energy source (RES) with the HEM system. This alters the peak formation as well as minimizes the cost. Residential users basically effect the overall performance of traditional grid due to maximum requirement of their energy demand. HEM benefits the end users by monitoring, managing and controlling their energy consumption. Appliance scheduling is integral part of HEM system as it manages energy demand according to supply, by automatically controlling the appliances or shifting the load from peak to off peak hours. Recently different techniques based on artificial intelligence (AI) are being used to meet aforementioned objectives. In this paper, three different types of heuristic algorithms are evaluated on the basis of their performance against cost saving, user comfort and peak to average ratio (PAR) reduction. Two techniques are already existing heuristic techniques i.e. harmony search (HS) algorithm and enhanced differential evolution (EDE) algorithm. On the basis of aforementioned two algorithms a hybrid approach is developed i.e. harmony search differential evolution (HSDE). We have done our problem formulation through multiple knapsack problem (MKP), that the maximum consumption of electricity of consumer must be in the range which is bearable for utility and also for consumer in sense of electricity bill. Finally simulation of the proposed techniques will be conducted in MATLAB to validate the performance of proposed scheduling algorithms in terms of minimum cost, reduced peak to average ratio (PAR), waiting time and equally distributed energy consumption pattern in each hour of a day to benefit both utility and end users.

## 1 Introduction

With the rapid increase in the world's population, electricity demand also increases. It is estimated that total energy demand at the end of 2020 will increase by 75% as compared to 2000. This increase may force utilities to reshape electricity generation and distribution in order to avoid demanding energy challenges. For this purpose, new technologies are integrating with the traditional electric grids to make them SG. In SG, advanced information and communication technologies provide customers the ability to interact with utility. To address these challenges, this paper presents energy management algorithms to schedule household appliances while meeting the constraints. The algorithms used in this synopsis are HSA, EDE and hybrid of HSA and EDE named as hybrid search differential evolution (HSDE). The behavior of the system embedded with these algorithms will be smarter and user satisfactory with respect to billing and PAR.

The rest of the paper is organized as: Related work is presented in Sect. 2. In Sect. 3, Proposed system model is introduced. Section 4 discuss proposed schemes and Sect. 5 include simulation and discussion, Sect. 6 conclude the paper.

## 2 Related Work

Researchers around the world work to optimally schedule appliances to benefit the consumers. The major focus of most of the researchers is on demand side management. Following are some papers which discuss the appliances scheduling.

PAR, daily energy consumption, electricity cost and the hourly energy consumption of shiftable and throttleable appliances of the consumers are the constraints of the objective function in [1], all of which are to be minimized. High energy consuming appliances are shifted to off peak hours to minimize the energy consumption and electricity bill in peak hours. The authors use the distributed algorithms that find the near-optimal schedule with minimal information exchange between the residential scheduler and consumers. The smart appliances present in smart homes work in automated fashion that provide consumers high comfort at less expense. In order to make home energy consumption more efficient, to control the power supply and demand numerous researches has been presented.

In [2] the authors present a review of different research works on a wide range of energy management controllers for smart homes which reduce energy consumption, PAR and energy wastage. The various HEM schemes, pricing schemes like real time pricing (RTP), critical peak pricing (CPP), time of use (TOU) and day ahead pricing (DAP) and energy consumption are discussed in detail.

In [3] the authors present a new optimization algorithm that is hybrid of wind driven and differential evolution (WDO and DE). Fifteen benchmark functions are tested which contain unimodal, multimodal, low dimensional and high dimensional to check the performance of proposed algorithm. The experimental results show that the proposed algorithm can be feasible in both low-dimensional and high-dimensional cases. The simulation results show that the performance

of WDO-DE algorithm is better than GA, BPSO, WDO, DE, and PSO to reach the optimal solution. The combined pricing schemes of TOU and inclined block rate (IBR) is used for bill calculation in [4]. In this paper, the authors present an efficient DSM model for residential energy management system to avoid peak formation while decreasing electricity bill and preserving user comfort level in acceptable limit. For this three heuristic algorithms; genetic algorithm (GA) binary particle swarm optimization (BPSO) and ant colony optimization (ACO) are used to evaluate the objective function. They suggest the GA based EMC better in term of electricity bill reduction and PAR minimization and maximization of user satisfaction than BPSO and ACO. The computational time of the algorithm is longer due to complexity in the program.

The authors in [5] study a society based load scheduling problem with different classes of appliances in the grid. While designing the optimization algorithm the overall society's satisfaction is kept under consideration. They design the smart grid with various constraints like minimize energy consumption, alter peak formation and limit the budget. The overall society's electricity usage pattern is observed keenly and sum of net consumption of all homes and their electricity cost are compared which give near-optimal scheduling. On the base of collected data the lower and upper bounds of the objective function are formulated. The simulation results show that the algorithm is effective in treating heterogeneous residences.

In [6] the negligence of user comfort in the previous papers is given consideration along with electricity cost saving and PAR reduction. They propose GA based algorithm for demand side management. Five types of appliances (tc, ua, el, iel, and r) are taken for scheduling and their mathematical models are formulated by considering thermal and comfort constraints. The pricing scheme used in this paper is real time pricing but when there is peak hours they integrate micro grid with the traditional grid so that the bill can be reduced and also user comfort can be increased.

The algorithms enable the consumers to pursue the best consumption benefits with in the consumption range. To improve the financial benefits of the electricity consumers a novel concept of cost efficient load scheduling framework is introduced in [7]. The authors merge the two pricing techniques RTP and DAP by using fractional programming approach. They have explained the effect of simple power shifting of specific appliances on the consumption cost, to show the direct relationship between consumption load pattern and cost. Further proposed algorithm allows the consumers fully utilize the electricity with remarkable savings of bill. Another contribution of the paper for the cost saving and minimization of  $CO_2$  emission in environment is integration of distributed energy resources (DERs) into the grid. This DER along with the fractional programming reduce the electricity cost efficiently. The PAR minimization and user comfort are not discussed in the paper.

A new population based meta-heuristic algorithm named harmony search algorithm (HSA) mimicking the improvisation process of musicians was developed by Geem [8] in 2000. It is simple concept based, less parameterized and

easily implementable algorithm. It has been successfully applied to various engineering and non engineering optimization problem. Author has suggested harmony in the music analogous to optimal solution vector and musician's improvisation process as analogy to local and global search in optimization technique. There are four steps in HSA; initialization of parameters, harmony memory generation, improvisation of new harmony from harmony memory (HM) and updating HM. Unlike GA, HSA generates a new optimal vectors considering all the available vectors in the search space whereas in GA only two parent vectors are selected to produce one better offspring. Therefore the flexibility and accuracy of HSA is better than other algorithm.

The fixed value of PAR and bw improvisation step of the traditional HSA cause poor performance and increase the number of iterations needed to find the optimum solution. The authors in [9] have introduced a variable PAR and bw values in the improvisation step to overcome the drawback. Moreover to check the affectivity of improved HS, they have applied this to different constraint and unconstraint benchmark functions. In [10] unit commitment problem is solved using HSA. The total electricity production cost is minimized by optimizing the controllable parameters within the limits. The HSA has fast convergence time and economical than conventional and improved GA.

### 3 Proposed System Model

DSM in a smart grid makes operation of the grid more reliable and stable. In smart home it manages and controls the energy usage by scheduling the appliances according to the scheduler embedded in the HEM system. The information is sent to the energy management controller (EMC) by smart meter and EMC accordingly schedules the appliances. Simple architecture of HEM system is shown in Fig. 1.

#### 3.1 Load Categorization

We classify appliances into three categories; fixed, flexible and uninterruptible appliances according to consumer usage behavior. Details of these categories are give below.

##### 3.1.1 Fixed Appliances

These are called fixed appliances because their operation length cannot be modified. The scheduler has to schedule it between user defined first timeslot and last timeslot. These appliances are light AC refrigerator and oven.

$$U(t) = \sum_{f_a \in F_{ap}} \sum_{t=1}^{24} \rho f_a \times \gamma f_a(t) \quad (1)$$

where  $a = 1, 2, \dots, n$  and  $t = [0 \ 1]$

$\gamma f_a(t)$  is *ON/OFF* state of the appliance in that timeslot.

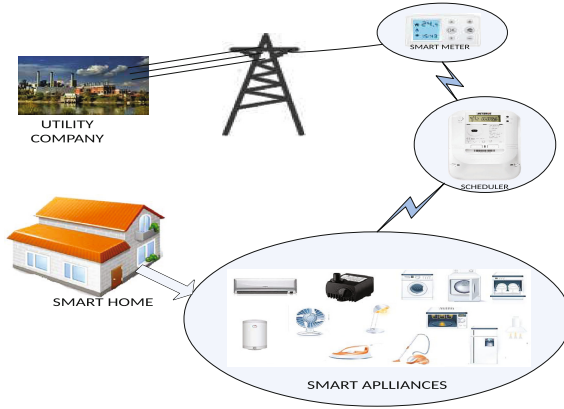


Fig. 1. Proposed system model

### 3.1.2 Flexible Appliances

Flexible appliances are those which operations can be shifted to any timeslot and when required can be interrupted during operation. These appliances are vacuum cleaner, water pump, water heater, and fans. As the AC and fans are both used for cooling purpose, the scheduler will schedule them accordingly so that user can get maximum comfort.

$$V(t) = \sum_{f_{ia} \in F_{iap}} \sum_{t=1}^{24} \rho f_{ia} \times f_{ia}(t) \tag{2}$$

where  $\gamma f_{ia}(t)$  is the *ON/OFF* state of the appliance in that hours. Our focus is to minimize the per hour cost of each appliance, as a result the overall cost will be reduced.

### 3.1.3 Un-interruptible Appliances

These appliances can be delayed or schedule earlier but once started operation cannot be interrupted until the operation completes. Washing machine, cloth dryer and dishwasher are included in this category.

$$W(t) = \sum_{u_a \in U_{ap}} \sum_{t=1}^{24} \rho u_a \times \gamma u_a(t) \tag{3}$$

## 4 Proposed Scheme

### 4.1 Hybrid HSDE Algorithm

The hybrid HSDE has the common features of EDE and HSA in it. The random selection step of HS algorithm is replaced by the fitness check step of EDE



which give a good result in term of user comfort and PAR reduction. The steps of HSDE are same as HS algorithm except in the improvisation of harmony the random selection is replaced by fitness evaluation of the new harmony vector and randomly selected target vector. The fittest is stored in the harmony memory and then search for the next fittest starts until some stopping criterion is reached.

$$H_{r1} = V_{r1} + F \times (V_{r2} - V_{r3}) \quad (4)$$

where  $H_{r1}$  is mutant vector,  $V_{r1}$  is target vector,  $F$  is mutant factor,  $V_{r2}$  and  $V_{r3}$  are other two randomly selected vectors from HM. After mutation crossover step follows same as in EDE. Here only three trial vectors are generated for evaluation so that the computational time does not prolong.

## 5 Simulation and Discussion

In this section we discuss the simulation results and analyze the performance of the scheduling algorithms in term of electricity cost savings, user comfort and PAR. Figure 1 shows the energy consumption in each hour before and after scheduling. By using scheduling algorithms most of the load has been shifted to off-peak hours to reduce electricity cost and PAR. It can be seen from the figure that maximum energy consumption is in unscheduled scenario i.e. 15.8 KWh in 16–17 timeslot which is reduced to 12.1, 12.5 and 13.2 KWh in case of HSDE, HSA and EDE respectively.

Figure 2 shows cost per hour profile. It shows that every algorithm is capable of maintaining cost per hour in the affordable range of the consumers. The cost in each hour of the algorithm is always less than the unscheduled cost. It shows that the maximum bill is charged in unscheduled model i.e. 465.6 cents in 9–10 h while it is reduced to 352.14, 320.90, 175.7 cents in 9–11, 12–14, and 22–24 timeslots by EDE, HSA and HSDE algorithms respectively.

The regular peak formation can cause the utility operation unstable and unreliable. So the scheduling algorithms help in reducing PAR as in Fig. 4. The PAR

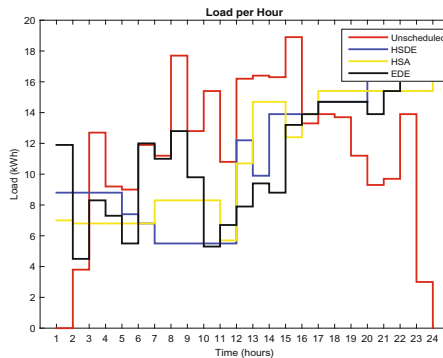


**Fig. 2.** Energy consumption per hour

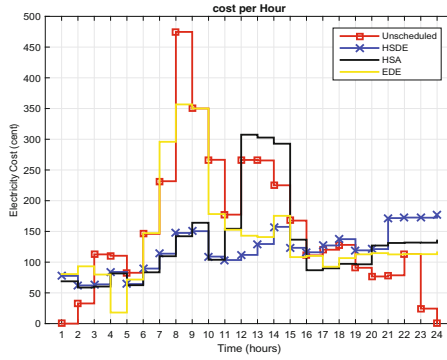


Fig. 3. Energy cost per hour

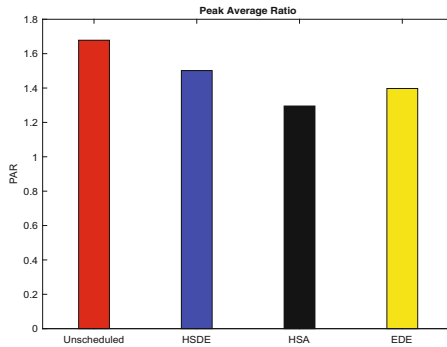
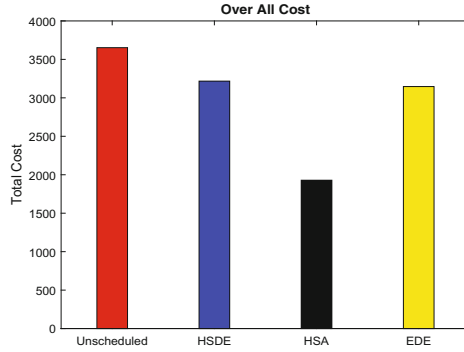


Fig. 4. PAR

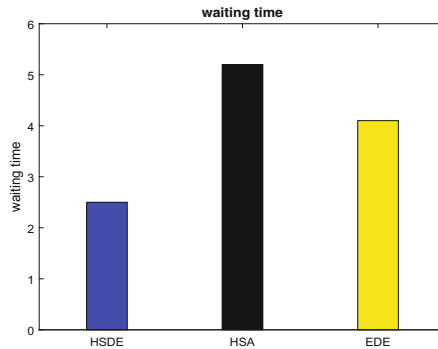
of unscheduled scenario is highest and the scheduling algorithms have reduced it significantly. These small peaks are bearable for the utility. HSA has very good nature against PAR i.e. it has smallest PAR value.

Figure 4 shows the difference in total cost between unscheduled and different scheduling schemes. It is clear that HSA has the lowest cost i.e. 1928.8 cents. On the other hand the most expensive bar is of unscheduled one i.e. 3043.4 cents. The HSDE and EDE has this range between unscheduled and HSA schemes i.e.2749.2 and 2435.6 cents respectively. The percentage reduction in electricity bill is 8.2 %, 36.6 % and 19.97 % in HSDE, HSA and EDE respectively. As the cost has inverse relationship with waiting time, the highest waiting time value of HSA as in Fig. 5 i.e. 5.2 h has the lowest cost i.e. 1928.8 cents and lowest waiting time in HSDE i.e. 2.5 h has highest electricity cost among the three algorithms.

A trade-off exists between user comfort and electricity cost in HEM system which can be seen from Figs. 4 and 5. As the waiting time is minimum in HSDE algorithm in Fig. 5 the cost of HSDE is maximum in Fig. 4. The EDE has slightly more waiting time than HSDE, its bar is slightly smaller than HSDE in Fig. 4. The bars of HSA in Figs. 4 and 5 is also reciprocal of each other (Fig. 6).



**Fig. 5.** Daily cost



**Fig. 6.** Waiting time

## 6 Conclusion

In this paper, the proposed HEM controller, by using HSA, EDE and HSDE has shown good reduction in PAR and cost. The hybrid HSDE has minimum waiting time and reduced cost than unscheduled scenario. However there always exists trade-off between waiting time and electricity bill as can be seen from Figs. 3 and 5.

## References

1. Liu, Y., Yuen, C., Huang, S., Ul Hassan, N., Wang, X., Xie, S.: Peak-to-coverage ratio constrained demand-side management with consumer's preference in residential smart grid. *IEEE J. Sel. Top. Signal Process.* **8**(6), 1084–1097 (2014)
2. Patel, K., Khosla, A.: Home energy management systems in future smart grid networks: a systematic review. In: 2015 1st International Conference on Next Generation Computing Technologies, pp. 479–483, September 2015

3. Bao, Z., Zhou, Y., Li, L., Ma, M.: A hybrid global optimization algorithm based on wind driven optimization and differential evolution. *Math. Probl. Eng.* **2015**, 1–20 (2015)
4. Rahim, S., Javaid, N., Ahmed, A., Aljerah, N.: Exploiting heuristic algorithms to efficiently utilize energy management controllers with renewable energy sources. *Energ. Build.* **129**, 452–470 (2016)
5. Moon, S., Lee, J.-W.: Multi-residential demand response scheduling with multi-class appliances in smart grid. *IEEE Trans. Smart Grid* **3053**, 1 (2016)
6. Homes, S., Qasim, U., Alrajeh, N., Iqbal, Z., Javaid, Q.: Real time information based energy management using customer preferences and dynamic pricing in smart homes. *Energies*, 1–31 (2016)
7. Ma, J., Chen, H., Song, L., Li, Y.: Residential load scheduling in smart grid: a cost efficiency perspective. *IEEE Trans. Smart Grid* **7**(2), 771–784 (2015)
8. Geem, Z.W., Kim, J.H., Loganathan, G.V.: A new heuristic optimization algorithm: harmony search. *Simulation* **76**(2), 60–68 (2001)
9. Mahdavi, M., Fesanghary, M., Damangir, E.: An improved harmony search algorithm for solving optimization problems. *Appl. Math. Comput.* **188**(2), 1567–1579 (2007)
10. Effatnejad, R., Hosseini, H., Ramezani, H.: Solving unit commitment problem in microgrids by harmony search algorithm in comparison with genetic algorithm and improved genetic algorithm. *Int. J. Tech. Phys. Probl. Eng. (IJTPE)* **21**, 61–65 (2014)

# EENET: Energy Efficient Detection of NETWORK Changes Using a Wireless Sensor Network

Walter Balzano<sup>(✉)</sup>, Aniello Murano, and Fabio Vitale

Dipartimento di Ingegneria Elettrica e Tecnologie dell'Informazione,  
Università degli Studi di Napoli Federico II, Naples, Italy  
wbalzano@unina.it

**Abstract.** Contextual services are having increasing importance in nowadays literature due to current availability of always-connected personal devices like smartphones and tablets. It is therefore increasingly important to have an affordable and accurate way for user localization in both indoor and outdoor environments. In outdoor GPS or GLONASS are reliable, but indoor a valid and ubiquitous localization system is still under research. One of the most promising methodology is wireless fingerprinting, which exploits available access points infrastructure. It is composed of two distinct phases: one *training* phase during which the interesting area is monitored and recorded and a *usage* phase in which the recorded data is used for localization purposes. The usage phase is reliable and accurate, but the training phase is often time consuming (in particular for large areas) as it must be performed manually and may also need to be repeated in case of structural and environmental changes. In this paper we propose a novel framework which uses an appropriate Wireless Sensors Network allowing continuous training over time in order to achieve real-time updating of the fingerprinting database without any human interaction, while also aiming to reduce power consumption needed for training phase, determining a minimal set of *sentinel*, which are sensors able to detect network alterations and able to trigger RadioMap rescanning.

**Keywords:** WSN · Wireless fingerprinting · Indoor localization

## 1 Introduction

Localization systems are nowadays an interesting research subject due to the possibilities of contextual services and their applications, allowed by personal devices like smartphones and tablets and their always-on network connection capabilities [1–6].

While in outdoor environments it is possible and affordable to use satellite based systems like GPS and GLONASS (which are Global Navigation Satellite Systems or GNSS), these systems are not available indoor due to their requirement of direct sky visibility for satellite connection. Many solutions have been

proposed in the latest years but most have low accuracy and reliability and are often limited to room-level positioning.

Some of these technologies leverage body mounted sensors to detect user movement in space [7], or wireless/GSM networks for coarse localization [8,9], or even hybrid solutions of both systems [10].

In indoor localization systems two aspects are often considered: system accuracy and energy consumption. Often it is necessary to find an opportune trade-off between these two values in order to achieve the desired accuracy while keeping energy consumption optimal.

One of the most common system for indoor localization exploits available wireless network infrastructures via Wireless Fingerprinting, which makes use of received signal strengths (RSS) evaluation and do not use geometrical solutions (i.e. based on angles or pure distances from fixed spots) [8,11]. In each place, the set of all visible access points and their RSS form an unique fingerprint which can be stored in a database for subsequent pattern matching, allowing user localization in space.

In this paper we present EENET, a framework which aims to improve currently available wireless fingerprinting methodologies using a network of wireless-enabled sensors, in order to improve localization reliability and accuracy while also reducing training efforts and energy consumption using a smart algorithm for network rescanning in case of structural changes and environmental alterations.

## 2 Related Works

Indoor localization methodologies are having a great deal of attention in the current literature, further stimulated by the widespread availability of small personal devices like smartphones.

Several projects have been presented in the latest years with a particular focus on Wireless Fingerprinting methodologies and several solutions have been proposed [12]. The very same technology has been also used successfully in outdoor environments [10,13,14].

Here we report some works which are closely related with our project.

In [15], authors developed a system which generates a radio model using sniffers and transmitters modules. It allows signal analysis and relies on the existing network infrastructure.

In *SMARTPOS* [16] authors analyze an interesting method for reducing body interferences in a Wireless Fingerprinting environment exploiting device digital compass. During training phase, compass is used to record four different fingerprints, which are then used during tracking phase to constrain the database search to a fourth of the total fingerprints in the RadioMap.

## Outline

The rest of the paper is organized as follows: in Sect. 3 we introduce current state-of-the-art regarding wifi fingerprinting methodologies. In Sect. 4 we describe the

layout and functioning of the proposed model. In Sect. 5 we report a short model validity analysis about system energetic efficiency with regards to existing similar solutions. In Sect. 6 we consider some conclusions and hints for future work directions.

### 3 Wireless Fingerprinting Based Systems

In this section we describe the current state-of-the-art of wireless fingerprinting systems for indoor localization. WiFi fingerprinting systems exploit wireless networks available in the area in order to determine, for each location, an unique *fingerprint* based on received signal strength (RSS) from nearby access points (AP). All fingerprints are associated to their physical location and stored in a database, named RadioMap, which allows subsequent pattern matching for position determination.

**Table 1.** Two different fingerprints stored in a RadioMap.

Location	BSSID	RSS
A	ca:7d:74:cc:4d:2d	-41 dBm
A	24:11:12:28:40:ea	-71 dBm
A	9c:d6:da:ff:04:3c	-60 dBm
B	ca:7d:74:cc:4d:2d	-78 dBm
B	24:11:12:28:40:ea	-54 dBm

WiFi fingerprinting systems normally have two distinct phases: a *training phase* and a *usage phase*.

During the first phase, an operator covers the interesting area using a device able to detect and store wireless fingerprints linked to map positions over time. All the gathered data are stored in the RadioMap (see Table 1).

During the usage phase, user devices read nearby networks signals and relays data to the localization server which uses a pattern matching algorithm against the RadioMap in order to find the most probable user position, which is then relayed back to the device for localization and to allow position-based services.

The training phase is totally manual, and may require several minutes or hours to be properly performed. The quality of the fingerprint depends on several factors: the number of the fingerprint recorded in each location (used for averaging the values thus allowing higher precision), the density of fingerprint locations recorded (which reduces number of interpolation needed when determining user position, increasing system precision), and the operator ability to choose the correct spot when placing the recorded fingerprint on the map (reducing positional drift). Improving each of these values lengthen the time needed for a proper training phase.

Over time, interferences, environmental changes (like humidity and temperature) and network structural changes may reduce positional reliability, making a new training phase mandatory in order to restore system functionality.

With regards to user segment, it's possible to use a generic *closest match* algorithm like

$$\min_{i=1 \rightarrow m} \left| \sqrt{\sum_{i=1}^m [S_R(i, j) - S_U(i)]^2} \right| \quad j = 1 \rightarrow n \tag{1}$$

where  $S_R$  is the signal of  $i$ -th access point as seen from  $j$ -th fingerprint (stored in RadioMap) and  $S_U$  is the signal of the same access point as seen by the user. The record  $j$  with the minimum norm is the most probable user position in space. This is true in particular for a dense RadioMap, while for a sparser one it may be needed to find a matching algorithm which uses interpolation to allow proper user positioning.

### 3.1 Wireless Fingerprinting Quality Evaluation

In order to determine fingerprinting systems quality, we considered three characteristics: *density* of the RadioMap, *precision* and *accuracy* for each fingerprint recorded.

**Density** is a property of the RadioMap as a whole, and is directly related to the number of fingerprints recorded in the interesting area. As aforementioned, having a higher density RadioMap allows usage of simple algorithms for localization and reduces the need of interpolation. Increasing the number of fingerprints recorded lengthen the training phase as the operator must stop in more places (see Fig. 1, first column).

**Precision** is a property of the single fingerprint, and is related to the number of raw samples gathered in each place. Increasing the number of samples requires the operator to stop in a single place for longer, thus increasing the time needed for training (see Fig. 1, second column).

	Density	Precision	Accuracy
Low	•	○	• *
High	•••••	•	• *

Fig. 1. Quality evaluation for wireless fingerprinting methodologies.



Lastly, **accuracy** is again a property of the single fingerprint, and is related to the distance between the selected spot and the true place of recording. It only depends on operator ability of choosing the correct place on the map during the training phase (see Fig. 1, third column).

## 4 Model Description

Here we present EENET model, composed of a user segment similar to other fingerprinting-based systems and a network of WSN modules used for real-time tracking of network conditions and performing automatic RadioMap updates. Moreover, classic training phases may be energy intensive for large areas, and therefore our project is also focused on keeping energy consumption needed to a minimum.

### 4.1 Sensors Network

For the WSN part we decided to use low powered XBee transmitters [14] based on the ZigBee protocol (IEEE 802.15.4) managed by a microcontroller which can be an *Arduino*, a *Raspberry Pi* or similar devices compatible with XBee transmitters. For our scope, we decided to use *Arduino* microcontrollers as they use very little power.

We identified three different kind of nodes:

- Coordinator. There is only one coordinator per WSN network. It assigns network addresses to the whole network and guarantees that the network is working;
- Routers. Can receive and reroute packages from adjacent nodes. These kind of node are mandatory for bigger networks, as they allow communication between distant zones. Routers are also used to broadcast scanning requests as ordered by the network coordinator;
- End devices. Can only send informations to nearby routers and/or coordinator, but is unable to reroute informations.

Network topologies can be very simple or complex depending on the area to be covered. In small areas a *star* topology with a network coordinator connected to several end devices may be enough, while in larger areas it is possible to use *cluster trees* (coordinator connected to routers, routers only connected to end devices with no connection between routers) or *mesh networks* (like cluster trees, but routers can also be interconnected).

### 4.2 EENET Deployment

The implementation of EENET system comes in two phases: one initial *distribution phase* and a *training phase*. During the distribution phase, the sensor network is deployed in the interesting area. For brevity's sake, we will only consider a large and dense mesh network, since all considerations also apply to

smaller and sparser WSNs. A proper distribution phase allows higher accuracy and precision, while also keeping energy consumption low.

Our model main goal is the determination of an appropriate fraction of WSN nodes known as *sentinel nodes* which are the minimum set able to recognise and rapidly detect any network structural changes. Sentinel nodes perform constant network scanning over time in order to detect network alterations for the whole WSN. Other nodes are *dormant* and wait until sentinels request a full rescan via WSN message broadcasting mechanic.

Tracking phase is composed of several steps:

1. WSN reads all the AP signals and builds a first RadioMap with the base network condition;
2. Each sensor reads nearby AP RSSs and discards weak signals;
3. For each AP, we select a group of sensors which have the strongest signal, and then we further choose only two of these sensors based on their relative distance (opting for the two which are most far apart), determining the subset of sentinel nodes;
4. Sentinel nodes poll the network for modifications every 15 s, using a two-threshold system for detection of slow, continuous changes;
5. When a change is detected, a rescan request is broadcasted via WSN;
6. All nodes, sentinel and dormant ones, perform several network scans over the next 3 min, sending all the data to the database server via WSN;
7. The server filters and integrates the data in order to determine a new RadioMap;
8. A new sentinel nodes determination step is performed and the cycle is repeated (from step 2).

Determining the best sentinel set is what allows the system energy consumption optimization: a small set running in realtime uses less current but may not notice a network alteration, while a bigger set will have a larger impact on battery duration but will be able notice even smaller signal updates.

It's important to notice that smaller effects on RSSs over time, like for instance atmospheric changes and interferences, may not be noticed by the sentinels a long sequence of tiny changes may not trigger the lower threshold), and is therefore fundamental to perform a full scan every  $\sim 1-2$  h in order to keep the RadioMap fresh and reliable. After each full scan, even scheduled ones, sentinel set must also be reconsidered.

### 4.3 Sentinels Choice

Sentinels choice is fundamental to achieve good system reliability while maintaining low energy impact. In Algorithm 2 we described a valid algorithm for sentinels determination. First of all we considered DISTANCESARRAY, a simple function which finds the distance matrix between several selected sensors. For each sensor we only consider its distance in relation with the next ones in the array. The result is an array of structures which contain the two sensors and

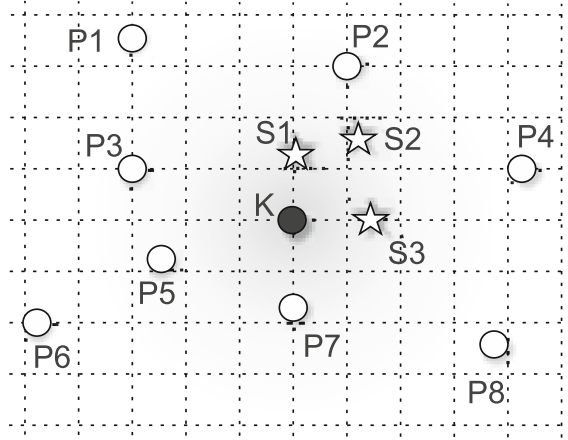


**Fig. 2.** Sentinel detection algorithm works in two phases: for each access point  $K$ , we select the subset of sensors which receive the strongest signals using a simple threshold (in figure indicated as stars,  $S_1, S_2, S_3$ ), then we choose the two which are most distant one to another (in this case we therefore select  $S_1$  and  $S_3$ ).

their distance. Obviously, we have that for each couple of nodes  $d(i, j) = d(j, i)$  and  $d(i, i) = 0$ , and therefore we only need to calculate  $n^2/2 - n$  distances.

As per sentinels determination, our logic works as follows. For each access point in the area:

1. we select the sensors which have the strongest signal for the selected AP, using a limit-based selection: we start with a strength limit of  $-30 \text{ dBm}$ , decreasing the limit by  $10 \text{ dBm}$  until we get at least 2 sensors;
2. we run the DISTANCESARRAY function on the selected sensors in order to find the distances between each element couple (Algorithm 1);

---

**Algorithm 1.** Function for distances array calculation

---

**Input:** sensors

**Output:** distances

```

1: function DISTANCESARRAY(sensors)
2:    $distances \leftarrow []$ 
3:   for  $i \leftarrow 0; i < \text{count}(\text{sensors}); i = i + 1$  do
4:     for  $j \leftarrow i + 1; j < \text{count}(\text{sensors}); j = j + 1$  do
5:        $from \leftarrow \text{sensors}[i]$ 
6:        $to \leftarrow \text{sensors}[j]$ 
7:        $distance \leftarrow \text{distance}(from, to)$ 
8:        $distances \leftarrow \{from, to, distance\}$ 
9:     end for
10:  end for
11:  return distances
12: end function

```

---

---

**Algorithm 2.** Sentinels set evaluation algorithm

---

**Input:** accessPoints, wsn**Output:** sentinels

```

1: function CALCULATESENTINELS(accessPoints, wsn)
2:   sentinels ← []
3:   for ap ∈ accessPoints do
4:     strongSensors ← [], limit ← -30
5:     while count(strongSensors) < 2 do
6:       strongSensors ← []
7:       for sensor ∈ wsn when sensor.signal > limit do
8:         strongSensors ← sensor
9:       end for
10:    end while
11:    ds ← distancesArray(strongSensors)
12:    // decrescent sorting on distances
13:    sort(ds)
14:    result ← ds[0]
15:    sentinels ← ds.from, ds.to
16:  end for
17:  return unique(sentinels)
18: end function

```

---

3. we sort the array by distances (highest to lowest);
4. we select the two sensors from the first result as sentinels.

The selected sentinels will be the ones with the strongest readings while also being as distant as possible.

After the sentinels for each access point have been selected, duplicates are removed. The whole algorithm is executed each time a network rescan request is issued on the WSN.

Limit step and starting values may be calibrated in order to get the best result on each rescan, but higher values may lead to increasing complexity due to the DISTANCESARRAY function which has complexity  $O(n^2)$  where  $n$  is the number of sensors selected.

## 5 System Performances Evaluation

As already mentioned in the outline, for brevity's sake we are only going to analyze system energetic behavior with regards to other similar systems. For system performance analysis, we suggest reading related works considerations as they also apply to this project too without any modification [12].

Let's consider an area with 5 access points and 100 sensors evenly distributed. We select 2 sensors for each AP as sentinels, and therefore we have up to 10 sentinels total (may be less if some duplicates are detected, i.e. a single sentinel is valid for more than one AP). Energy consumption is therefore reduced up to ~90% only due to the fact that a tenth of the sensors are actively scanning the area.

Let's now consider some possible scenarios:

- **Stable condition.** Sentinels are able to detect small changes of the network conditions over time: power consumption reduction is at its maximum, as full network rescan only happen in scheduled situations (every 1–2 h). Power consumption reduction is estimated in  $\sim 85\%$  of needed power without sentinel determination.
- **Worst case.** Sentinels detect great network alterations all the time. In this case, the whole WSN is constantly rescanning the area, and system is unable to optimize the power reduction. Even in this case, however, power consumption will never be higher than a system without sentinel determination. It is also important to notice that using our model in such an uncommon situation raises the computation complexity due to the sentinels determination algorithm which is executed each time a rescan is issued.
- **Average condition.** Sentinels normally detect small changes and scheduled rescan happen as normal (every 1–2 h). Drastic network changes may happen at irregular intervals, forcing full rescans other than scheduled ones. Power consumption reduction is estimated in  $\sim 50\%$  to  $\sim 80\%$  of the power needed without sentinel determination.

## 6 Conclusions and Future Work

In this paper we presented EENET, a model which allows energy-efficient network conditions tracking using a wireless sensor network. We considered selecting only a subset of nodes, sentinels, which perform constant scanning in order to reduce power consumption by  $\sim 70\%$  to  $\sim 90\%$  in average conditions.




Future work may include determination of more appropriate algorithms for sentinels selection and development of other methods for reliable and energy-efficient network alterations detection.

## References

1. Amato, F., Mazzeo, A., Moscato, V., Picariello, A.: A system for semantic retrieval and long-term preservation of multimedia documents in the e-government domain. *Int. J. Web Grid Serv.* **5**(4), 323–338 (2009)
2. Amato, F., Chianese, A., Moscato, V., Picariello, A., Sperli, G.: Snops: a smart environment for cultural heritage applications, pp. 49–56 (2012)
3. Amato, F., Mazzeo, A., Moscato, V., Picariello, A.: Exploiting cloud technologies and context information for recommending touristic paths. *Stud. Comput. Intell.* **511**, 281–287 (2014)
4. Palmieri, F.: Scalable service discovery in ubiquitous and pervasive computing architectures: a percolation-driven approach. *Future Gener. Comput. Syst.* **29**(3), 693–703 (2013)
5. Palmieri, F.: Bayesian resource discovery in infrastructure-less networks. *Inf. Sci.* **376**, 95–109 (2017)

6. Balzano, W., Del Sorbo, M.R., Murano, A., Stranieri, S.: A logic-based clustering approach for cooperative traffic control systems. In: International Conference on P2P, Parallel, Grid, Cloud and Internet Computing, pp. 737–746. Springer (2016)
7. Woodman, O., Harle, R.: Pedestrian localisation for indoor environments. In 10th UbiComp. ACM (2008)
8. Moghtadaiee, V., Dempster, A.G.: Wifi fingerprinting signal strength error modeling for short distances. In: IPIN 2012, pp. 13–15 (2012)
9. Balzano, W., Murano, A., Vitale, F.: V2v-en-vehicle-2-vehicle elastic network. *Procedia Comput. Sci.* **98**, 497–502 (2016)
10. Dao, T.-K., Nguyen, H.-L., Pham, T.-T., Castelli, E., Nguyen, V.-T., Nguyen, D.-V.: User localization in complex environments by multimodal combination of GPS, WiFi, RFID, and pedometer technologies. *Sci. World J.* **2014**, 7 (2014)
11. Mok, E., Retscher, G.: Location determination using wifi-fingerprinting versus wifi-trilateration. *J. Locat. Serv.* **1**(2), 145–159 (2007)
12. Balzano, W., Murano, A., Vitale, F.: Wifact-wireless fingerprinting automated continuous training. In: 2016 30th International Conference on Advanced Information Networking and Applications Workshops (WAINA), pp. 75–80. IEEE (2016)
13. Lu, B., Niu, J., Juny, J., Cheng, L., Guy, Y.: Wifi fingerprint localization in open space. State Key Laboratory of Software Development Environment, Beihang University, Beijing, 100191 (2013)
14. Niu, J., Lu, B., Cheng, L., Gu, Y., Shu, L.: Ziloc: energy efficient wifi fingerprint-based localization with low-power radio. In: WCNC, pp. 4558–4563. IEEE (2013)
15. Krishnan, P., Krishnakumar, A.S., Ju, W.-H., Mallows, C., Gamt, S.N.: A system for lease: location estimation assisted by stationary emitters for indoor RF wireless networks. In: INFOCOM 2004, vol. 2, pp. 1001–1011. IEEE (2004)
16. Kessel, M., Werner, M.: Smartpos: accurate and precise indoor positioning on mobile phones. In: MOBILITY (2011)

# Reducing the Impact of Traffic Sanitization on Latency Sensitive Applications

Mauro Migliardi<sup>1,2</sup> , Alessio Merlo<sup>3</sup> , and Sherenaz Al-Haj Baddar<sup>4</sup> 

<sup>1</sup> DEI – Università di Padova, Via G. Gradenigo 6, 35131 Padova, Italy  
mauro.migliardi@unipd.it

<sup>2</sup> CIPI – Università di Padova, Via G. Gradenigo 6b, 35131 Padova, Italy

<sup>3</sup> DIBRIS – Università di Genova, Viale F. Causa 13, 16145 Genova, Italy

<sup>4</sup> KASIT – The University of Jordan, Amman 11942, Jordan

**Abstract.** In our modern society the reliance on fast and reliable delivery of large amounts of data is steadily growing as more and more companies and public bodies use data analytics to support their decision processes. At the same time, the rise of the Internet of Things introduces into the public cyberspace a multitude of devices that are often ill-suited to implement strong security measures. For this reason, it is of paramount importance that the whole Internet traffic is fully sanitized from any malicious packet before it is delivered to the destination. Past work has proved that this compelling security requirement may be leveraged to implement an aggressive intrusion detection that may lead to energy savings in the network; however it may also negatively impact latency sensitive applications as the need to scrutinize all the packets may cause latency sensitive traffic to incur unwanted delays beyond the time needed to analyze it for security sake. In this paper, we describe a methodology that, while guaranteeing a full sanitization of the Internet traffic, allows reducing its impact on the delay introduced in latency sensitive traffic.

**Keywords:** Traffic sanitization · Latency sensitive applications · Timely delivery

## 1 Introduction

The reliance on digital information is now pervasive in our daily routine and this, together with the prospective of *everything connected* makes the thorough sanitization of Internet traffic a compelling need. At present, network attacks and cyber-security breaches have turned from the major nuisance that used to be in the past, into a full-fledged source of monetary damage. According to the Ponemon study [1], the cost of data breaches may ramp up to 158 dollars per stolen record and, in the average, each breach costed the target company 4 million dollars. These facts, together with the fact that data breaches have increased in size over the last 5 years [2], and the fact that the number of data breaches per year is increasing [3, 4], show that the need for aggressive analysis of Internet traffic to hunt down and eliminate all the packets whose sole goal is some sort of cyber-encroachment is a very urgent need. Furthermore, from a security perspective, IoT devices are often not ready for exposition to the public Internet as the

growing size and number of botnets comprising or solely constituted by such devices demonstrate [5, 6]. This is particularly dangerous for two main reasons: first, the size and resource limited nature of IoT devices often prevents them from being equipped with strong security mechanisms, second, intrusion into IoT devices will escalate from an economic problem to a full life-threatening situation as soon as remote control of physical devices will become a widespread reality.

All of these reasons call for a new approach to the problem of malicious and unwanted traffic. While in the past a best-effort approach where the burden to decide if a packet had legitimate reasons to reach its destination could be delegated to the destination itself, the current scenarios require the thorough sanitization of all traffic as it is not guaranteed that the final destination has the resources to cope with malicious intents. Consider as an example, the case of cars and legacy technologies such as Controller Area Network bus [7].

An aggressive approach to identification and removal of malicious traffic, however, is not necessarily bound to represent just a cost; as a matter of fact, past work has proved that it is possible to leverage malicious packets removal from the traffic streams to obtain a greening effect into networking [8] as the amount of unwanted traffic poisoning the streams is significant [6, 9, 10].

However, burdening the intermediate network nodes with the task of analyzing every packet for security purposes may introduce unwanted delays and delivery latency may become incompatible with real-time applications [11] such, as an example, VoIP based audio and video conferencing. Hence, in this paper we describe a methodology that allows mitigating the impact of aggressive intrusion detection on latency sensitive traffic offloading it to latency insensitive traffic.

The paper is structured as follows in Sect. 2 we provide some background material and we describe our methodology; in Sect. 3 we discuss some simulation results; finally in Sect. 4 we provide our concluding remarks.

## 2 Background and Our Methodology

Past work shows that unwanted traffic represents a significant part of the Internet Traffic [6, 9, 10], thus its early removal from the streams may generate significant energy savings. However, other work [11] also showed that there is a significant risk of introducing undesired delays into some flows because of congestion generated by inaccurate prediction of the incoming traffic. We argue that only a portion of the Internet traffic can be damaged by the introduction of these delays and we call it *Latency Sensitive Traffic* (LST). On the other side, a significant portion of the Internet traffic is not very sensitive at all to delays or it is sensitive to variation in delays (jitter) but not to delays that stay almost constant over all the packets in a flow, we call this *Latency Insensitive Traffic* (LIT). While traffic pertaining to the first category of LIT (e.g., peer-to-peer file transfer) has greatly diminished in the last years and, according to recent studies [12], now represents less than 10% of the global Internet traffic, all the streaming media services can be considered in the second category of LIT. In fact, it is not important for a video to start immediately when the play button is pressed, what is vital is that the video will not stop



or stutter during the playing time. Recent measurements showed that streaming video represented 64% of the global Internet traffic and the same study forecasts a growth to 85% of the whole Internet traffic by year 2020 [13].

In our methodology we assume that each packet is tagged as LIT or LST before it enters our system, how this is done, through use of QoS fields in the IP header or through dynamic traffic classification is beyond the scope of this paper.

Our methodology can be described as follows. First, the router routes all the incoming packets that are already tagged as good, puts all the packets tagged as LST in a queue and the packets tagged LIT into a second queue. Once this phase is completed, the router computes if it still has enough resources to route all the LST packets. If not enough resources are available, the router will proceed to route all the LST packets it can and it will delay the processing of the remaining LST packets and all the LIT packets to the next time slice. Obviously, this situation will cause internal queues of the router to grow; however, dimensioning the router capability to avoid exhaustion of buffer space is beyond the scope of this paper.

If resources are just enough to route all the LST packets, then no LST packet will be delayed, but the all the LIT packets will and we will be in a situation quite similar to the previous one. If, on the contrary, the resources available exceed the bare LST routing needs, our methodology will proceed to decide which portion of the traffic may be sent to security analysis (Figs. 1 and 2).

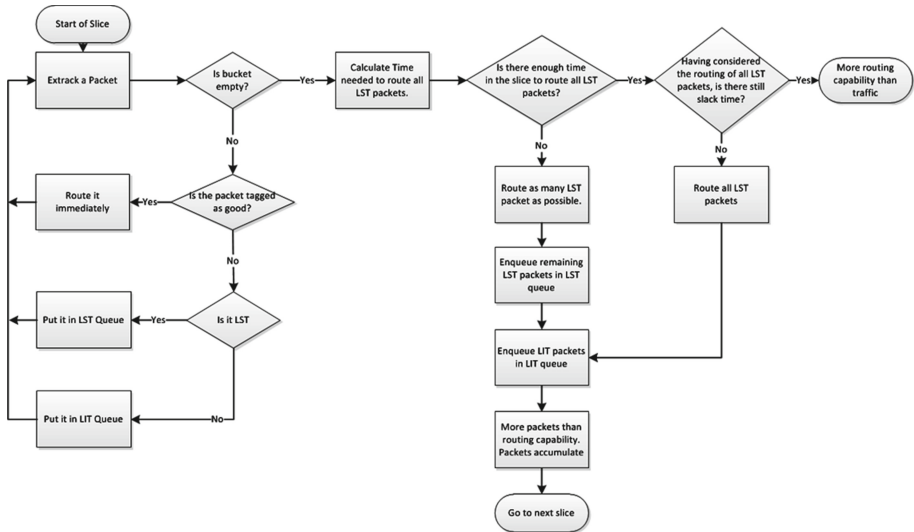


**Fig. 1.** The flow for the first phase of the algorithm in each time slice. Here the algorithm assesses the feasibility of security analysis in the current time slice.

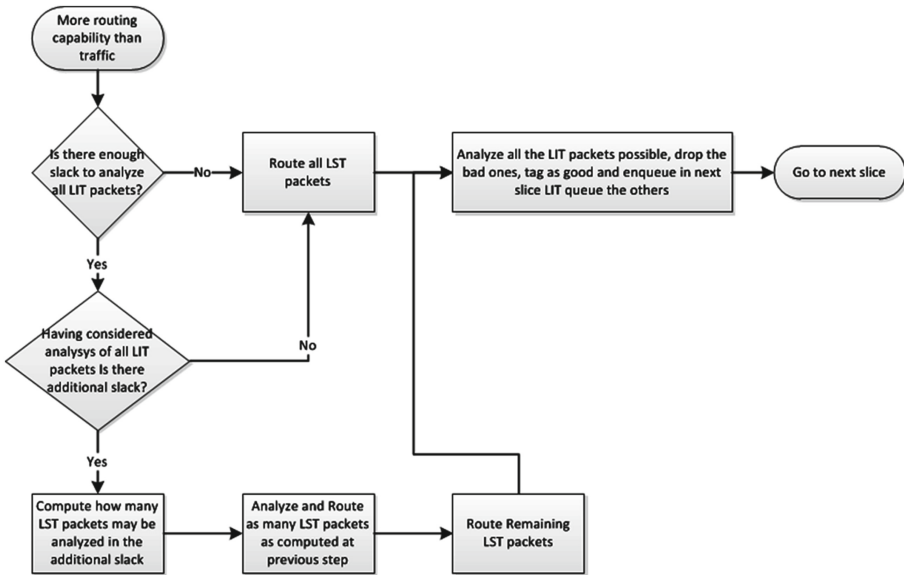


**Fig. 2.** The flow for the second phase of the algorithm in each time slice. The actual security analysis takes place in this phase.

In the second part of the flow our methodology is based on the fact that we start analyzing LST traffic, thus running the risk to delay it if the incoming traffic is larger than predicted, only if we have calculated that there are enough resources to both route all the LST packets and to analyze all the LIT packets.

If it turns out that incoming traffic is less than the router’s maximum routing capacity at a given time slice, the router checks to see if its remaining capacity is sufficient to analyze all unexamined incoming LIT packets. If it turns out that the router has enough room to accommodate these packets, it checks if it has further capacity to analyze unexamined LST packets, and analyzes then routes as many LST packets as it can. Next, it routes remaining LST packets it could not analyze. After that, the router analyzes as many LIT packets as it can, given its remaining capacity. Yet, it may turn out that the router has no slack to process LST packets altogether. In this case, it routes all LST packets it received, then analyzes and routes as many LIT packets as it can. Even if there is slack to handle only a subset of incoming unexamined LIT packets, the router would still route all LST packets first, then, would analyze and route as many LIT packets as it can handle. Thus, even if the prediction is wrong, as long as the size of the misprediction is smaller than the amount of LIT packets available, we can always avoid delaying LST packets by offloading the problems onto the LIT packets.

Analyzing a packet, whether it is LIT or LST, comprises figuring out if the packet is good or bad using a given intrusion detection tool. If the packet is found bad, it gets dropped immediately, while, if it turns out to be good, it gets labeled accordingly so that routers downstream will just route it without further concern.

### 3 Discussion and Simulation Results

In order to perform a preliminary evaluation of our methodology we have simulated the behavior of a single node in different load situations, with different traffic mixes in terms of LIT vs. LST and with different levels of error in the prediction of the incoming traffic. We have kept the percentage of malicious traffic present in the streams fixed at a 5% level as the focus of our study is the capability to prevent unwanted delays. Furthermore, the actual precision and reliability of the security analysis is out of the scope of this paper.

First of all, it is important to notice that in the case in which the amount of LST packets exceeds the router capability, there is no possible solution and LST packets will incur unwanted delay. Hence, we will disregard this case entirely and we will consider only the scenarios where the amount of LST packets is below the nominal routing capacity of the router.

In this case, if the prediction of the traffic incoming in the next time slice is correct, our methodology is always capable of preventing LST packets from being delayed offloading the problem onto LIT packets.

We first consider the scenario of a router working close or over its nominal capacity, with LST packets representing about 10% of the whole traffic.

In Fig. 3 we show how, as the amount of traffic grows, LIT packets are delayed and the percentage of analyzed traffic gets smaller, but no LST packet incurs into any delay.

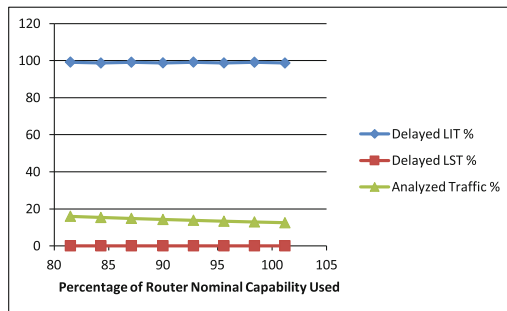


**Fig. 3.** The system offloads the burden of delay onto LIT packets. At different levels of load, different amounts of packets are analyzed but no LST packet is delayed.

Furthermore, it is important to notice that the amount of analyzed traffic would reduce the load of router downstream both in terms of further security analysis required and directly in terms of traffic to be routed because of the malicious packets already dropped.

We now introduce in the previous scenario a misprediction, that is the actual amount of traffic entering the router is larger than the one that was expected and used to compute the resource availability according to our methodology. More in details, we will evaluate a misprediction of 20% (Fig. 4).

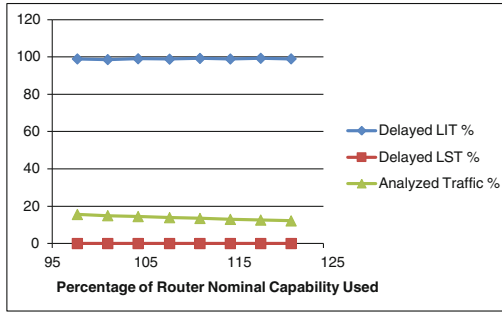


**Fig. 4.** The incoming traffic is 20% more than expected.

Even with a 20% misprediction of the actual router load, our methodology leverages the presence of LIT packets to avoid delaying LST packets. Actually, as long as the amount of unchecked LIT packets is sufficient to saturate the expected excess capacity of the router, the router does not engage in any analysis of the LST packets, hence all the LST packets are just routed and cannot incur any delay as long as their number does not exceed the total capability of the router.

Let’s now consider the case in which the amount of unchecked LIT packets is small and, according to our methodology, the router starts using its excess capacity to analyze LST packets. It is important to notice that having excess capacity in a router is a common situation as core networks are usually over-provisioned [14]. We simulate a scenario in which 95% of the traffic is Latency Sensitive and only 5% is Latency Insensitive, we then apply first a misprediction of 20% and then a misprediction of 40% of the total incoming traffic.

In Fig. 5 we can see that even with just 5% of LIT packets and a 20% misprediction our methodology allows avoiding any delay of LST packets at the cost of delaying all the LIT packets and analyzing a smaller portion of the incoming traffic.

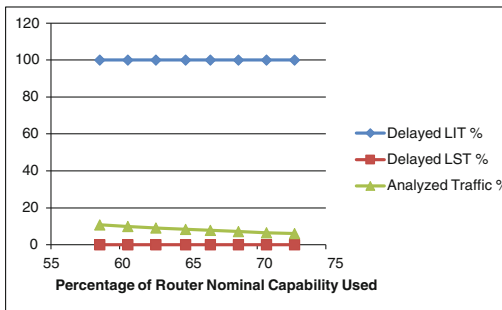


**Fig. 5.** The incoming traffic is 20% larger than expected and LIT packets are only 5% of the whole traffic.

Finally, in Fig. 6 we can see that when the size of the misprediction grows to 40% of the expected value, our methodology cannot avoid burdening a portion of the LST packets with an unwanted delay.

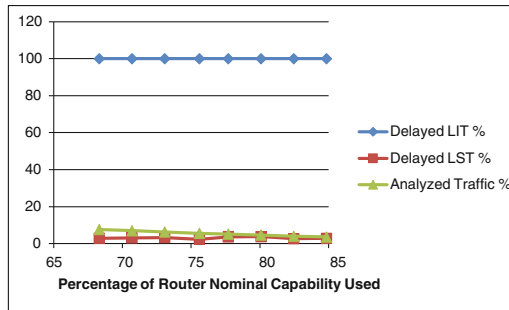


**Fig. 6.** The incoming traffic is 40% larger than expected and LIT packets are only 5% of the whole traffic.

It is however important to notice that a situation in which 95% of the traffic is constituted by LST packets is currently very far from the common Internet traffic.

## 4 Conclusions and Future Work

In this paper we have described a methodology targeted at mitigating the effects of the aggressive intrusion detection that, according to past work, allows reducing the energy cost of networking on latency sensitive applications. More in details, our aim is to avoid introducing unwanted delays in the flow of Latency Sensitive Traffic by offloading problems deriving from eventual unexpected traffic variations onto the Latency Insensitive portion of the traffic.

Our preliminary results show that our technique is promising and can cope with significant variations of the traffic from the expected level even with a high network load. However, our simulations have dealt only with a single node, thus a campaign of large scale simulations where a whole network is taken into account is required to fully validate the approach and to calculate the actual amount of energy savings with different traffic mixes.

## References

1. Ponemon Cost of Data Breach Study (2016). <https://www-03.ibm.com/security/data-breach/>. Last accessed 12 Apr 2017
2. Yahoo's data breach is one of the biggest in history. <http://www.businessinsider.com/yahoo-hack-data-breach-how-big-chart-2016-9?IR=T>. Last accessed 13 Apr 2017
3. Lord, N.: The History of Data Breaches. <https://digitalguardian.com/blog/history-data-breaches>. Last accessed 12 Apr 2017

4. Findings from the 2016 breach level index. <http://breachlevelindex.com/assets/Breach-Level-Index-Report-2016-Gemalto.pdf>. Last accessed 12 Apr 2017
5. Jerkins, J.A.: Motivating a market or regulatory solution to IoT insecurity with the Mirai botnet code. In: 2017 IEEE 7th Annual Computing and Communication Workshop and Conference (CCWC), Las Vegas, NV, pp. 1–5 (2017). doi:10.1109/CCWC.2017.7868464
6. Q4 2016 State of the Internet/Security Report. <https://www.akamai.com/us/en/about/our-thinking/state-of-the-Internet-report/global-state-of-the-Internet-security-ddos-attack-reports.jsp>. Last accessed 13 Apr 2017
7. Ring, M., Dürrwang, J., Sommer, F., Kriesten, R.: Survey on vehicular attacks - building a vulnerability database. In: 2015 IEEE International Conference on Vehicular Electronics and Safety (ICVES), Yokohama, pp. 208–212 (2015). doi:10.1109/ICVES.2015.7396919
8. Merlo, A., Migliardi, M., Caviglione, L.: A survey on energy-aware security mechanisms. *Pervasive Mob. Comput.* **24**, 77–90 (2015). doi:10.1016/j.pmcj.2015.05.005
9. Lan, K.C., Hussain, A., Dutta, D.: Effect of malicious traffic on the network. In: Proceedings of PAM 2003, San Diego, California, April 2003
10. Mallikarjunan, K.N., Muthupriya, K., Shalinie, S.M.: A survey of distributed denial of service attack. In: 2016 10th International Conference on Intelligent Systems and Control (ISCO), pp. 1–6, January 2016
11. Merlo, A., Migliardi, M., Spadacini, E.: IPS-based reduction of network energy consumption. *Logic J. IGPL* (in press). doi:10.1093/jigpal/jzw053
12. Netflix and Youtube grab 50% of peak Internet traffic, p2p fades into the sunset. <http://www.digitaltrends.com/home-theater/netflix-youtube-grab-50-peak-Internet-traffic-peer-peer-fades-sunset/>. Last accessed 13 Apr 2017
13. White paper: Cisco VNI Forecast and Methodology, 2015–2020. <https://www.cisco.com/c/en/us/solutions/collateral/service-provider/visual-networking-index-vni/complete-white-paper-c11-481360.html>. Last accessed 13 Apr 2017
14. Das, S., Parulkar, G., McKeown, N.: Rethinking IP core networks. *IEEE/OSA J. Opt. Commun. Networking* **5**(12), 1431–1442 (2013). doi:10.1364/JOCN.5.001431

# Design and Deployment of Identity Recognition Systems

Carlo Ferrari<sup>(✉)</sup> and Michele Moro

Department of Information Engineering, University of Padova,  
Via Gradenigo 6a, 35131 Padova, PD, Italy  
{carlo.ferrari,michele.moro}@unipd.it

**Abstract.** Modern Identity Recognition Systems (IRSs) can benefit from the simultaneous use of different biometric parameters but their activity cannot be modeled using a rigid sequential path because they have to take into account outcomes from different data as well as from different algorithms at different times. This paper is about the representation of an ad hoc composition of elementary recognition service in order to form an integrated recognition facilities, to be deployed within the scope of energy-aware systems. We aim to investigate the types of useful collaboration among IRSs components and to present a tool to assist designers both in the design process and in the system deployment phase. The tool define a catalogue of elementary recognition services that are typically associated with single trait recognition modules. They are considered as prototypical services that can be differentiated by proper parameter settings. Those basic building blocks can form compound collaborative patterns: composition rules are expressed both as logical association and causal relation (what-if rules). The recognition activity can be organized through different levels and feedback is allowed. Partition let to evaluate the overall QoS from performance figures that are associated with the elementary blocks, in order to certify expected Service Level Agreements (SLA)s. Deployment represents an important step before system release. The proposed approach is an interactive one: system administrators are asked to allocate all the components on actual machines and secure communication channels are automatically established. Scalability, redundancy and fault tolerance and energy issues can be addressed at this level.

## 1 Introduction

Although Biometric Systems are mainly for identity recognition Ratha and Govindaraju (eds.) (2008), Identity Recognition Systems (IRSs) effective design goes far beyond the classical issues related to pattern matching. Designers, systems developers and operators must cope with those questions (at the system level) that are related to robustness, scalability and security, in order to obtain systems that work properly without violating previous established Service Level Agreements (SLAs) with the final customers Coulouris et al. (2005). Historically, the most part of biometrics-based user authentication and recognition

systems are based upon the use of a single biometric trait that it is analyzed and processed according to the following general sequential schema Jain et al. (2000): involving raw data acquisition, feature extraction, matching against a template representations of users and final evaluation and decision. These activities can be further detailed at various levels to take into account noisy data, ambiguity in feature classification, automatic parameter set up and learning Kim et al. (2010), and they result in algorithms for recognition that fully employ the use of single parameters Ross and Jain (2004). Measured FRR and FAR can be used for performance evaluation and security level assessment. The sequential scheme appears to be too rigid and systems can usefully take into account the outcomes from different biometric parameters, that are concurrently analyzed. Moreover, different algorithm (in accuracy and speed) can be applied at different time whenever security requirements change. Hence the design becomes an ad hoc composition of simultaneous acquisition and evaluation phases.

Single trait Biometrics-based algorithms and models still remain at the core of IRS but true systems must be tailored according to the idea that QoS requirements can imply different choices at the design level with different effects on global performances. For instance, a low invasiveness requirement can bring to a weak classification and recognition, due to more unreliable data, resulting in a too high FAR, thus affecting a strong security requirement. Complexity is even higher when more than one biometric trait is used. The composition of elementary recognition service will form an integrated recognition facility and the way composition is made do influence QoS evaluation according to some overall rules and metrics Singh and Huhns (2005).

Elementary recognition services can differ with respect to sensor hardware and organization, matching algorithm implementation, matching algorithm parameterization, data acquisition time. The development of new and more robust integrated sensors with better resolution and accuracy, results in novel data acquisition equipments that can either replace or simply couple already existing one. Because of the quality of raw data is an important point in the recognition process, elementary service can be classified according to the hardware they are tighten to: they differ with respect to either the sensors in use or the auxiliary equipment that can operate for better data acquisition, (for instance, supplementary lights or automatic cleaning equipment). The quality of the measure of a given biometric parameter can vary because of differences in sensors and its evaluation is part of the QoS evaluation for the elementary recognition service. Systems that uses more than one sensor of a given kind employ a *Multisensor modality*. In single trait biometrics, feature extraction and matching can be organized in different ways. At this level, performances are mainly related to the computational issues of implemented algorithms and methods. In this case elementary services are tied to a given feature representation method or a matching algorithm. Systems that double the single trait recognition using different matching methods employ a *Multialgorithm modality*. Related to the previous modality there is the *Multi-instance modality*. The differences are in the algorithm parameterization (like the choice of thresholds or the weights in



the evaluation criteria). Appropriate parameterization can make the difference between good and bad recognition. Unfortunately good parameterization are not absolute but they may depend on the families of the object under recognition as well as on the quality of input data. Elementary services that just differ for the internal set up of some (well defined) parameters, implement specific instances of template recognition procedures. Sometimes, the acquisition of a biometric parameter can be repeated, in order to compare data at different time. We call this situation *Multisample modality*. Elementary recognition services are then linked to a reading of the same data source at a given time. This modality is not about flow of information (like video): the sampling produces a single and well defined reading that serves for the recognition step. Finally, multibiometrics relies on the simultaneous use of different biometric parameters. Elementary recognition services are naturally mapped to the various parameters in use (*Multimodal modality*).

The previous classification of the types of elementary recognition services defines a general catalogue of services the system designer can compose according to the design requirement from the actual application. A key point is about the availability of an increasing number of biometric parameters that can be measured at the same time, with different accuracies and processing speed. This approach enable a higher degree of flexibility that can better meet different and sometimes conflicting requirements from applications. This paper investigates the types of useful collaboration among IRSs components and presents a tool to assist designers both in the design process and in the system deployment phase. The elementary recognition services, that are typically associated to single trait recognition modules, are considered as prototypical services that can be used according to one or more the previously described modalities. An important issue is about the formation of compound collaborative patterns: In the next paragraph we will details the design pattern the system composition refers to and the composition rules that are expressed both as logical association and causal relation (what-if rules). Moreover we will describe the level organization of the systems and we introduce the way repetitions (loop in the process) can be managed to get a higher QoS. Deployment represents an important step. The proposed approach is an interactive one: system administrators are asked to allocate all the components on actual machines and secure communication channels are automatically established. Scalability, redundancy and fault tolerant issues can be addressed at this level. In the third paragraph the criteria that help in the deployment phase are presented. Partition let to evaluate the overall QoS from performance figures that are associated with the elementary blocks, in order to certify expected Service Level Agreements (SLA)s.

## 2 Identity Recognition Systems Design

Multibiometrics deals with the concurrent use of different biometric parameters, like fingerprints Cappelli et al. (2010), face Phillips et al. (2000), iris Daugman (2007), gait Goffredo et al. (2010) and so on. Their use is usually organized as

parallel threads (one for each trait) that singularly and separately work and bring evidence towards an identity statement. Data acquisition, feature extraction, and matching are repeated for each parameter, while evaluation is at least a two stage process made up of a preliminary (local) decision based on each single information and a final decision that is obtained considering the various local measures. Because there is no evidence that different types of biometric parameters are really related to each other, it is not possible to use quantitative measures from a given parameter, to either enforce or relax the quantitative evaluation of another parameter. It means that different biometric parameters are semantically disjoint and their composition is useful because impostors are obliged to forge more parameters at the same time. After fixing both the FAR and FRR, the design should minimize the time both for data acquisition and processing. Multibiometrics can be interpreted according to several modalities and designers have quite a lot of degree of freedom in setting up a system. First of all, they have to decide which biometric traits are useful with respect to the actual application (multimodality). Then they must pick up the correct parameterization or, even better, they prepare different algorithms with different parameterizations (multialgorithm and multi-instance). The recognition process can be enriched by considering the availability of different sensors (multisensor) and the possibility of adding (or repeating) data acquisition (multidata).

Multibiometrics is then a powerful tool for designing IRSs with a reasonable trade off between efficiency and accuracy. There is no doubt that a good data acquisition phase can make the difference between good and weak recognition but data acquisition should be as less invasive as possible. These two requirements are conflicting: environmental condition (like lighting conditions) can affect acquisition quality but improving the environment can imply a higher degree of invasiveness Wong et al. (2010). Parameterization plays an important role in the tuning of the recognition process. As another example of the need of balancing a tradeoff, we can consider the feature extraction step. It can be optimized according to the analysis of the expected population under exam: eyes location and shape is different for eastern peoples, with respect to western people and hair shaping can vary in time according to current trends in fashion. Finely tuned feature extraction and pattern matching algorithms work well for an expected population but can become completely useless in more general cases. Coverage and precision are then conflicting requirements. Finally, it must be considered that the expected security levels ask for different approaches. Severe algorithms can overconstrain the recognition process that becomes slow and computationally expensive; at the same time a weaker approach can give fast but unreliable responses. Modern Identity Recognition Systems can benefit from the simultaneous use of different biometric parameters in order to form an integrated recognition facility that results from an ad hoc composition of elementary recognition services. Their computational activity does not follow a strict sequential path because of the concurrent analysis of a single traits and the possibility of ad-hoc re-executions of those parts of the systems that do not meet some minimal quality levels.

The designers should refer at a general organizational model that can capture the relations of precedence and importance among the various elementary services. The model we propose is a level-based architecture where the recognition activity is organized through different levels and feedback is allowed. Levels host all the elementary services that work in parallel and whose results have to be directly combined to form a compound evaluation. In this way designers can put in proper evidence first level services, i.e. those basic elementary services that are considered compulsory coarse grain services, At higher level (and usually triggered by proper preconditions) there are more fine services that participate in the recognition process, when needed. The proposed tool organize the composition of services in levels that are separated by decision boxes. Decision boxes represent the composition rules, that are described in the next subsection. Both a single service and a composition service can be reactivated when the systems cannot reach a decision, or a decision has a too poor quality. Reactivation can use information from the previous processing. The mechanism for repetition is kept very simple: the services that are selected for redoing their computation are reactivated no more that three times in multidata modality and just two times in multisensor modality. Each elementary recognition service can participate in one repetition group (alone or together with other services in its level) and repetition cannot span two or more levels. System partition lets evaluate the overall QoS from quality figures that are associated with the elementary blocks, in order to certify expected Service Level Agreements (SLAs). QoS is generally associated with a user evaluation of non-functional properties like reliability, security, performance, availability, and dependability. Reliability can be mainly considered as a synonym of correctness. Performance is generally associated to responsiveness and speed while security is related to privacy and integrity both of data and code. Availability refers to redundancy and scalability and dependability is associated with robustness, adaptability and fault tolerance. A IRS is good if it identifies people quickly and correctly and it is completely transparent with respect to any kind of fault of its components. FAR e FRR measures for single trait biometrics well describe reliability of an elementary recognition service but composition asks for a more sophisticated schema. QoS specification can be organized as a tuple: each element in it is associated with a specific aspect of QoS: in the actual implementation we limit to a 4-tuple  $\langle R, P, S, A \rangle$ .  $R$  is related to reliability (FAR and FRR),  $P$  described average speed in term of the computational class cost of the recognition algorithm.  $S$  can be actually computed after deployment and at the design level is forced to be 1 (in the range  $[0, 1]$ ). The last component  $A$  measures the number of service in the unit time together with the fault probability.

System composition is based on a catalogue of Elementary Recognition Services (ERSs) that are typically associated with single trait recognition modules. They are considered as prototypical services that can be differentiated by proper parameter settings. ERSs are primarily grouped with respect to their basic modality to form the ERS families. Irix, Face, Voice, Fingerprint are some of these primary families. Inside each family there are all modules that

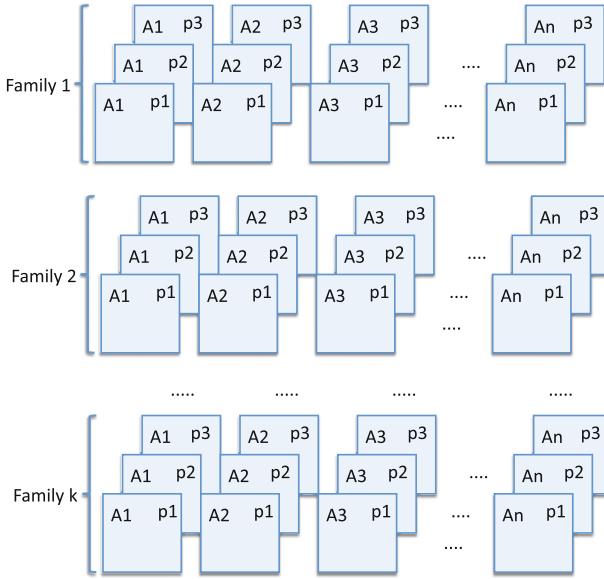


**Fig. 1.** The organization of Elementary Recognition Services.

implement different algorithms for recognition. Each subfamily can be further detailed when different parameterizations are available (see Fig. 1). The ERSs are linked by default to a given sensor hardware and to a single data reading. Whenever more sensors are in use the related ERS is duplicated in the design layout while further data reading implies the dynamic creation of a new ERS (an ERS clone). Finally, each ERS is tagged with its own QoS specification that will be used in assessing QoS of compound services.

### 2.1 Composition of Elementary Recognition Services

An identity statement can be easily confirmed/rejected if the analysis of the different parameters are congruent ones. But what can be done if the single evaluations are contradictory ones? How it is possible to take into account outcomes from different data as well as from different algorithms at different times? In the literature there are various approaches that correlate all the biometric readings in a final fusion step (see for instance, Nandakumar et al. (2008); Maurer and Baker (2007)). Our approach tend to use different reading at various stages: the ERSs are the basic building blocks that can form compound collaborative patterns: composition rules capture both logical association and causal relation (what-if rules). Logical propositions use five level truth values, namely *true*, *maybe-true*, *maybe*, *maybe-false*, *false*, in order to get a more gracefully transition between the true and false statements. Causal relation are modelled as couples  $\langle \textit{precondition}, \textit{action} \rangle$ , and precondition are sharply evaluated on a two truth values. By composing ERSs,

the designer can form Compound Recognition Services (CRSs), that can be grouped to form a library of recognition services.

Composition rules are considered as operators from a given number of inputs to a single output. Each input represents the outcome from a previous elementary or compound block. The output goes to another composition rule unless it represents the final evaluation. At present, four composition rule have been defined, namely, *AND*, *OR*, *Priority*, *Voting*. The AND rule, as well as the OR rule, consider the evidence from all their inputs, while the Priority rule and the Voting rule use some of their inputs, while discarding less meaningful evidences. The AND rule expresses the idea that evidence against a given hypothesis must count more than evidence in favour of it. On the opposite side, the OR rule means that evidence against a given hypothesis must count less than evidence in favour of it. Due to the choice of a five level truth values, both a single AND and OR rule are completely specified when the designer either fill completely the truth values table or it explicitly decide to use a default table (see, for instance, Table 1). The Priority rule is applied to completely filter one or more input, letting just one parameter to completely overcome the other. In this case the truth value of the winner input, becomes the output truth value. Voting rule means the final evidence is the one that get the major part of consensus from the inputs. Causal relation uses their inputs to trigger (or to block) the activity associated with their output. The boolean output have to be associated to all the proper combination of the truth values of inputs. They comprise the evaluation of QoS figures by proper thresholding.

**Table 1.** A truth table of a user specified AND rule (partial)

Input1	Input 2	Output
true	true	true
true	maybe-true	maybe-true
true	maybe	maybe
true	maybe-false	maybe-false
true	false	false
maybe-true	true	maybe-true
...	...	...

The application of a composition rule requires to compute the QoS evaluation of the compound recognition service starting from the QoS associated to its input according to the semantic of the rule itself. The QoS of the outcome after applying the Priority rule is exactly the QoS of the winner input. When a Voting rule is involved, the QoS of its outcome is computed considering the worse (component by component) value in the input QoSs that form the majority, except for the *P* component that will be the worse overall the inputs. The QoS computation after an OR rule causes the following effects: the *R* component

value becomes the better value among all inputs whose truth value is either true or maybe-true, the  $P$  component value is the worse value among all inputs, the  $S$  component value component remains 1 and the  $A$  component value is the worse value among all inputs. Similarly, after an AND rule, the  $R$  component value is the better value among all inputs whose truth value is either false or maybe-false, the  $P$  component value is the worse value among all inputs, the  $S$  component value component remains 1 and the  $A$  component value is the worse value among all inputs. As causal rules work as services switches, their effects on QoS are negligible.

### 3 Identity Recognition Systems Deployment

Deployment is usually referred to the efficient and reliable distribution of software components that is performed with automatic mechanisms that relieves the user from being forced to follow and check the correct installation and updating of such components. In deeper details software deployment can be seen as a process that consists of a number of different activities:

- Release: it is represented by the interface between developers and other actors in the software life cycle. At release time the software is packaged and accompanied by some metadata to describe a set of requirements such as resources on which it depends;
- Installation: this is the process of transferring the software to the user;
- Configuration: it can be seen as the customizing process of the software;
- Activation: the process including a possible final set-up of the system environment and the actual execution of the software. It is done through suitable graphical interfaces or activating scripts or daemons;
- Switching off: it is the opposite of the activation process;
- Monitoring: the process of observing the state of the running software in order to intervene in case of malfunctions, errors or exceptions, system crash included;
- Updating: the distribution and re-installation of newer versions of the software components; sometimes it requires a switching off of the previous version and the final activation of the new one;
- Adaptation: the process of modification of the installed software to positively react to possible changes in its running environment;
- Undeployment: it means the uninstalling of the software.

Some relevant examples of organized deployment systems are Enterprise JavaBeans and Linux modules. The EJB system exploits the convenient JAR file format to package all the components and add a metadata manifest, and promotes the isolation of the active components (beans) in containers with documented interfaces in order to improve security, persistence and transaction properties. Actually it represents a fine-grain and language-dependent mechanism. “Red Hat Package Manager” (RPM) is a Linux deployment system based on a manager that accesses remote databases describing all the details of the

downloadable packages and facilitates the installation and updating of a certain Linux distribution. RPM packages may contain scripts to support some phases of the deployment, including compilation of source files. Some high-level tools have been developed to make deployment even easier and safe. The RPM approach is a coarse-grain one and language independent. Its main weakness is that not all dependencies are explicitly modelled and those which are modelled are not modelled in terms of packages but referring to their content.

An IRS is usually being executed in a distributed environment onto heterogeneous machines. The tool for deployment has to facilitate and to automate the system set up that come from the design tool. It has to enable a fast configuration of the proposed architecture, while ensuring data security. Moreover it has to handle all the details related to connections and internetworking (like IP addresses, port, secure login to remote machines, and so on) and, finally, it should be as easy as possible to use. The approach we followed is an interactive one, being the system administrator asked to detail the involved machines. The IRS description is in the form of an XML file that is produced by the design tool. In a first implementation the overall architectures follows the client-server paradigm: the client machines get the data and the server execute the matchings according to the composition rules. Scripting is heavily used for controlling the system deployment and execution.

The interaction between the deployment tool (DT) and the system administrator (SA) can be described as it follows:

- DT get the XML file and asks the SA to specify the IP address of all the involved nodes;
- DT asks the SA to set a user (with root privileges) foreach selected machine;
- DT create and install (in each machine) both the script(s) for the deployment and the script for the start up;
- the scripts are then activated: they download automatically the code and make it ready for execution.

At this point the system is ready. The server starts listening any recognition request. Anytime a recognition process is started (by a client machine) the server automatically activates the ERSs in the system layout, get the data from the clients and executes the composition rules when all their input is available. Communications between the server and client is realized through a secure channel in order to protect the data in transit.

## 4 Conclusions

In this paper we presented a tool to assist both in the design of an Identification Recognition System and in its deployment onto a networked infrastructure. The system uses and integrates different biometric parameters. As Multibiometrics can be declined according to different paradigms (multisensor, multialgorithm, multi-instance, multidata and multimodality), a classification and a catalogue of elementary recognition services has been presented together with the rules for

their composition. A graphic interface for an easier interaction, has been defined. Composition do affect the overall QoS of the recognition system. Starting from the definition of QoS for the elementary recognition services, the composition rules define how to evaluate the QoS for compound services and for the overall system as a whole. The proposed tool is under validation through an extensive experimentation. Further works is about a more flexible deployment that uses intermediate servers that will be in charge of some compound service and about enhancing reliability through replication. At the design level we plan to add some automatic checks that will be applied to the user definition of the truth tables and new composition rules for a proper weighted averaging of inputs.

**Acknowledgements.** This work has been partially supported by the University of Padova Research Project CPDA157799 “Fostering Independent Living in the Aging Population through Proactive Paging and Cognitive Support”.

## References

- Cappelli, R., Ferrara, M., Maltoni, D.: Minutia cylinder-code: a new representation and matching technique for fingerprint recognition. *IEEE Trans. Pattern Anal. Mach. Intell.* **32**(12), 2128–2141 (2010)
- Coulouris, G., Dollimore, J., Kindberg, T.: *Concepts and Design*. Addison Wesley, Boston (2005)
- Daugman, J.: New methods in iris recognition. *IEEE Trans. Syst. Man Cybern. Part B Cybern.* **37**(5), 1167–1175 (2007)
- Goffredo, M., Bouchrika, I., Carter, J., Nixon, M.: Self-calibrating view-invariant gait biometrics. *IEEE Trans. Syst. Man Cybern. Part B Cybern.* **40**(4), 997–1008 (2010)
- Jain, A.K., Hong, L., Pankanti, S.: Biometrics: promising frontiers for emerging identification market. *Commun. ACM* **43**(2), 91–98 (2000)
- Kim, Y., Toh, K., Teoh, A.B.J.: An online learning algorithm for biometric scores fusion. In: *Proceedings of the Fourth IEEE International Conference on Biometrics: Theory, Applications and Systems (BTAS 2010)*, Washington DC, USA, pp. 1–6 (2010)
- Maurer, D.E., Baker, J.P.: Fusing multimodal biometrics with quality estimated via a Bayesian belief network. *Pattern Recogn.* **41**(3), 821–832 (2007)
- Nandakumar, K., Chen, Y., Dass, S.C., Jain, A.K.: Likelihood ratio-based biometric score fusion. *IEEE Trans. Pattern Anal. Mach. Intell.* **30**(2), 342–347 (2008)
- Phillips, P.J., Moon, H., Rizvi, S.A., Rauss, P.J.: The feret evaluation methodology for face-recognition algorithms. *IEEE Trans. Pattern Anal. Mach. Intell.* **22**(10), 1090–1104 (2000)
- Ratha, N.K., Govindaraju, V. (eds.): *Advances in Biometrics: Sensors, Algorithms and Systems*. Springer, Heidelberg (2008)
- Ross, A., Jain, A.K.: Multibiometric systems. *Commun. ACM* **47**(1), 34–40 (2004)
- Singh, M.P., Huhns, M.N.: *Service-Oriented Computing: Semantics, Processes, Agents*. Wiley, Hoboken (2005)
- Wong, R., Poh, N., Kittler, J., Frohlic, D.: Interactive quality-driven feedback for biometric systems. In: *Proceedings of the Fourth IEEE International Conference on Biometrics: Theory, Applications and Systems (BTAS 2010)*, Washington DC, USA, pp. 1–6 (2010)



# The Safety of Your Own App with App Inventor

Paolo Musmarra<sup>(✉)</sup>

Dipartimento di Informatica, Università degli Studi di Salerno,  
Via Giovanni Paolo II, 84084 Fisciano, SA, Italy  
pmusmarra@unisa.it

**Abstract.** Our society is a digital society, it needs to be a safer place and to be provided with tools to offer students the appropriate knowledge to create a security context because Networking, Web Systems, Database are vulnerable and can be a viable attack vector. The relationship between teenagers and new technologies is very complex and it is the focus of attention in today's school system. The Network plays a very important role in the life of teenagers born in the era of the web, of the social networks and of the social media. Everyone is connected all the time. Some searches show that Italian teenagers are online about ten hours a day and are often connected 24 h a day with mobile devices, thanks to free wi-fi widely available everywhere. The digital security is one of the digital citizenship's key: it is in the area 4 of the framework DigCompOrg (European Reference Framework for Digitally-Competent Educational Organization) and in the PNSD (Action#14) for the school system [1]. It is hugely important the role of schools in bringing teenagers to get to a conscious and responsible use of the Net because the school system can ensure basic ITC skills as part of digital competence. In my experience as a high school teacher, I have seen teenagers interested in ITC but with no skills in the use of it with responsibility and awareness. Therefore, we need to dedicate a module for information Assurance and Security as thread of an IT education. There is a methodological question about how the theoretical principles can be put into practice. In this paper an adaptable framework will be explained to build an App called "Security" with App Inventor for beginners. This framework will be rationalized and discussed along with teaching methods that have proven to be useful in helping students to maximize their programming and security experience. By this path, the didactic value of App Inventor will be showed as a performing tool for mobile app design activities, and, especially, the great possibilities for a class with beginners in computing science to gain knowledge about security and help teenagers to be active users of ITC devices.

## 1 Introduction

Today the services given by the Net are increased in number and there are very different ways to access to the Network, especially with mobile devices, such as tablets and smartphones. The digital security is one of the digital citizenship's key; it is in the area 4 of the framework DigCompOrg (European Reference Framework for Digitally-Competent Educational Organization). The vulnerability of ICT and the defence against attack from outside are the great questions and the vulnerabilities can be further

attributed to the lack of sufficient security knowledge and skills. Examining the computer science curricula of many universities still gravely fall short in improving security education for many reasons: one reason is that many computer science courses such as software engineering and programming or mobile programming do not include security or cybersecurity topics. For example, software engineers can design, develop and deploy their software project, but not frequently include security components into the software. Again, students frequently do not understand the strong correlation between security and other fields of computer science. Our society is the Digital Information's society: Digital Information is intangible, independently of tangible medium and it can easily be intercepted, copied, changed, deleted, forged. Since the approach to New Technologies is more and more early, the education path for security in ICT needs to be set out since the school years. Teaching ICT security means:

- to raise awareness among students of the risks that they take foolishly using information tools
- to give some functional tools to avoid to be vulnerable.

The last framework is the European record about the key skills: the digital competence is one of them and it is “confident and critical usage of information and communication technology for work, leisure and communication. It is underpinned by basic skills in ICT: the use of computers to retrieve, assess, store, produce, present and exchange information, and to communicate and participate in collaborative networks via the Internet. Digital competence requires a sound understanding and knowledge of the nature, role and opportunities of IST in everyday contexts: in personal and social life as well as at work. This includes main computer applications such as word processing, spreadsheets, databases, information storage and management, and an understanding of the opportunities and potential risks of the Internet and communication via electronic media (e-mail, network tools) for work, leisure, information sharing and collaborative networking, learning and research. Individuals should also understand how IST can support creativity and innovation, and be aware of issues around the validity and reliability of information available and of the legal and ethical principles involved in the interactive use of IST. Use of IST requires a critical and reflective attitude towards available information and a responsible use of the interactive media. An interest in engaging in communities and networks for cultural, social and/or professional purposes also supports this competence” [2]. Therefore, it is a priority to work on security culture since the school years, employing appropriate teaching strategies and technologies, developing projects and programs for a better knowledge of the digital world with which the teenagers interact.

This paper will discuss the possibility for High School's students to create an security App with App Inventor, using the method of learning by doing; the steps of the project and the features of this App will be fully described. Building the App called “Security”, the students will use the principles of security in a critical and conscious way. The App realised by the students will be fully secure because it will be created by them personally. The mobile learning can be a good tool to achieve the objectives of the educational system [3].

## 2 The Building of App Security: Steps and Methods

App Inventor has been successfully used to teach introductory programming concepts to beginners in both secondary and higher education courses [4]. O' Malley et other describe the mobile learning "Any sort of learning that happens when the learner is not at a fixed, predetermined location, or learning that happens when the learner takes advantage of the learning opportunities offered by mobile technologies" [5]. The use of mobile technology can improve the learners' motivation and the quality of their work as some projects show [6]. With learning mobile, active learning strategies are used and the learners learn in their own context, which will result in higher-level learning. This project can be carried out in a High School's course with beginners too. The beginners are students that have not teaching of Computer Science in their curriculum.

This section shows that a app can be built to create a user interface for a password like login screen and store the personal data and information so that they are reliable and persistent.

The main steps to the creation of your own mobile app with App Inventor are described below:

- First of all you need to decide what you want your app to do, chose the needed components and the non-visible components, and set the properties for each component using Component Designer.
- Secondly, learn to work with the Blocks Editor, using blocks of codes as a visual code and connected like puzzle pieces, to make the components work just drag-and-drop it into the Blocks Editor.
- Finally, test the app with tablets, smartphone or cell phone, or an emulator. In this case, we prefer to use cell phones, because it's more funnier this way, and it's easier to test mobile phone-specific functionalities.

### 2.1 Designing the Components

The user interface for the app is relatively simple: we create a first screen; it has a password TextBox in which we write a password and a button to verify password, as shown in Fig. 1.

In the second Screen we need to drag in a label that displays the word "Service", a text box to write the name of the text that we will store, a second label that displays the word "Password", a second text box to write the password. Three more buttons are needed: the first to find a Service; another to add a new Service, and the last to close the application. We will also need to drag in a TinyDB component to store personal information in the database, and a Notifier component, all of which will appear in the "Non-visible components" area. You can see how this should look in the snapshot of the Component Designer in Fig. 2.

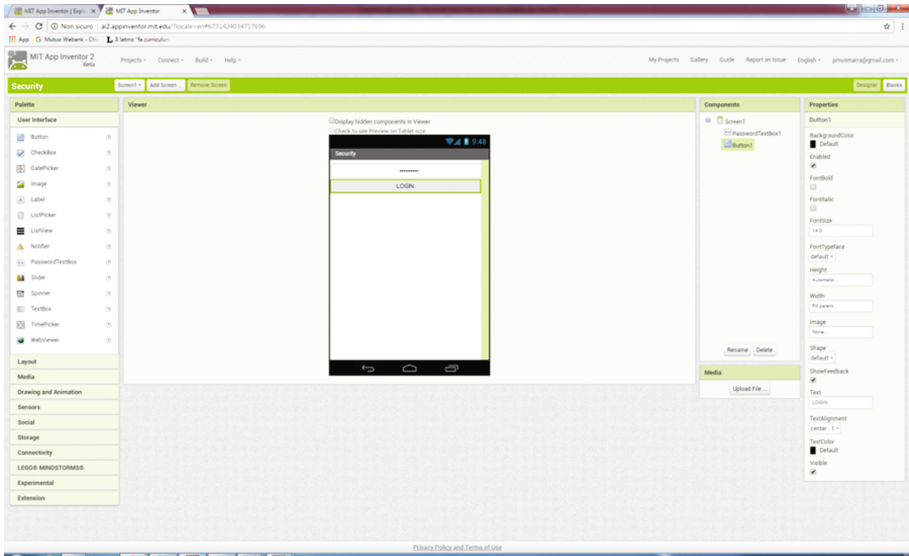


Fig. 1. Screen 1 in the component designer

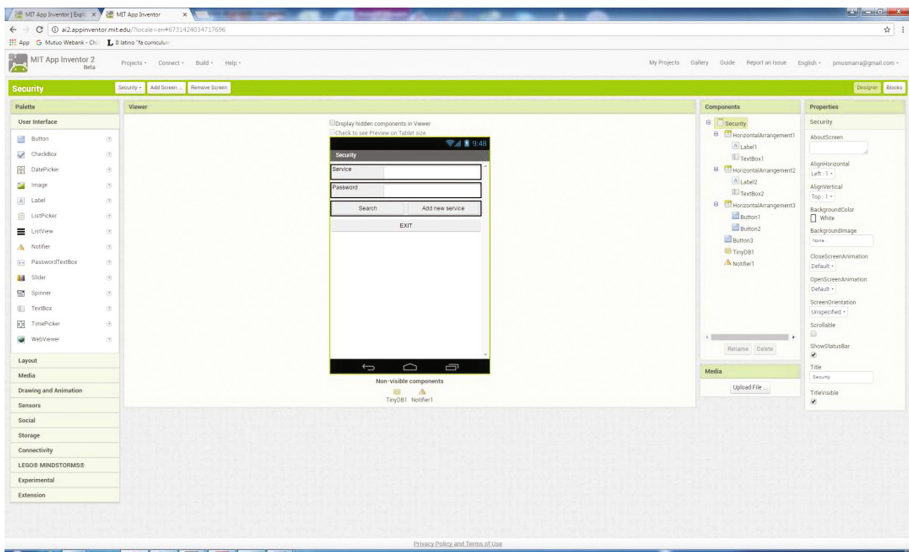


Fig. 2. Screen 2 in the component designer

## 2.2 Adding Behaviors to the Components. Screen 1

We will start programming the behavior when the button LOGIN is clicked and PasswordTextBox is triggered. Only if the password is equal to the value saved before, open another screen. Finally, it is possible to add and connect blocks as shown in Fig. 3.

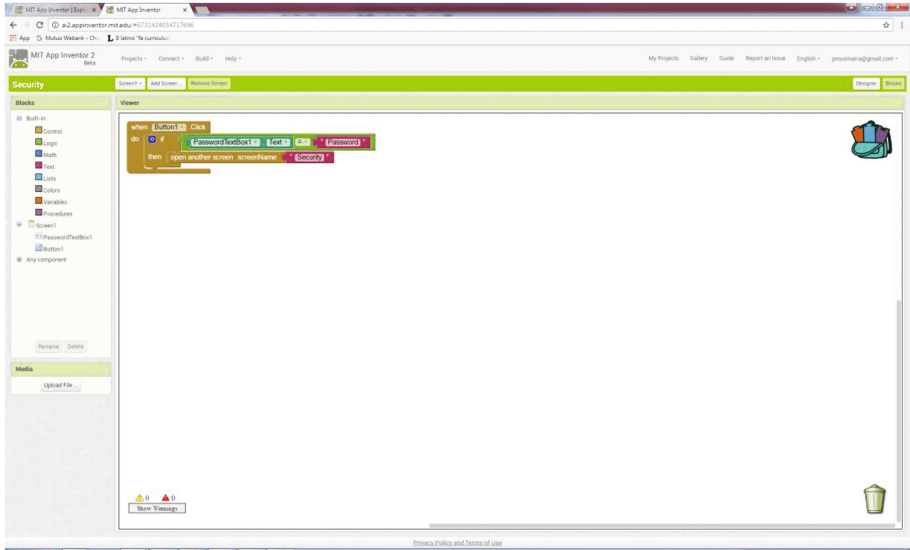


Fig. 3. Check password

### 2.3 TinyDB Components

TinyDB Component helps to store data persistently in App Inventor. Data are stored in a file on the Android device. StoreValue and GetValue are the two main TinyDB's functions. In this way, "the app can store information in the device's database, whereas with the latter, the app can retrieve information that has already been stored" [7].

To correctly use TinyDB component in many apps, the following scheme can be useful:

1. Store data to the database each time the user submits a new value.
2. When the app launches, load the data from the database into a variable or property.

Clicking the button "Add new item", the student calls a TinyDB component with the function StoreValue (the tag value equals to label of the service) to store new items and the Notifier Component is useful to indicate that operation is ok. When the Button "Search" is clicked, the students calls a TinyDB component with the function GetValue to retrieve information that has already been storage with the function StoreValue. When the button "Exit" is clicked, the screen is close (Fig. 4).

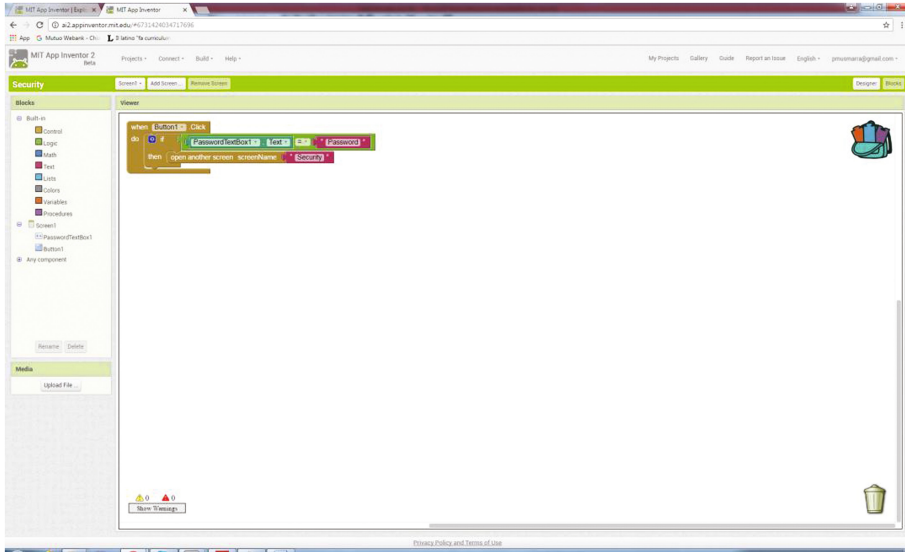


Fig. 4. Search and insert

## 2.4 Variations

Even if the students close the App and turn off the cell phone, they can retrieve the stored data on the cell phone. For this reason, this App is more secure than the Apps we can find in the play store: it has been created by us; the data are on the device and we know how it works. We can modify the login screen with two or more passwords to enter in the App; we can create many security systems because we know them. There is not a more secure system than the one that we create ourself.

## 3 Conclusions

In this paper we have presented a summary of security and of the actual issues in the High School's context. The need of security education is an essential element in computing and programming sciences and is recognized as being an excellent method of improving awareness in all students. A high level framework for the teaching aspects of security has been proposed, together with elements of mobile programming with App Inventor, a visual programming tools that enables students to see and test their own app. In our experience, we want to build an app to be secure and protect our personal information. This project helped the students to improve their ICT skills through the Computational Thinking that, as J. Wing wrote, "is a fundamental skill for everyone, not just for computer scientists. To reading, writing, and arithmetic, we should add computational thinking to every child's analytical ability" [8] and "Informally, computational thinking describes the mental activity in formulating a problem to admit a computational solution. The solution can be carried out by a human or machine, or more generally, by

combinations of humans and machines” [9]. With this project, the students have been introduced to security principles through the concepts of Access Control, the Login Screen creation with manage of username and password and OTP too. The students realised the App on Security, making an object by themselves.

We advocated to further explore for security education and for an integrated approach to promote and improve security education. We contributed to this approach by concretely exploring the possibility that a mobile development with App Inventor can be “easy” and “fun” to beginners. Actually, one of the great advantages of introducing programming to beginners with App Inventor is that it can help them avoid common syntax errors. We will continue to discuss with teachers and obtain opportunities to integrate important security topics into other non-security courses. We hope that our experiences will be helpful to other teachers who want to improve the integration of the security approach in other courses.

## References

1. PNSD: National Plan of Digital School in Italian Schools. [www.istruzione.it/scuola\\_digitale/](http://www.istruzione.it/scuola_digitale/)
2. Recommendation of the European Parliament and of the Council of 18 December 2006 on Key Competences for Lifelong Learning (2006/962/EC)
3. Raineri, M., Pieri, M.: Mobile learning. Dimensioni teoriche, modelli didattici, scenari applicativi, Milano, Unicopli. In: Pellerery, M. (ed.) *La valorizzazione delle tecnologie mobili nella pratica gestionale e didattica dell'istruzione e formazione a livello di secondo ciclo - Indagine teorico empirica; rapporto finale*. CNOS- FAP 2015 (2014)
4. Soares, A., Martin, N.L.: Teaching non-beginner programmers with app inventor: survey results and implications. In: *Proceedings of the Information Systems Educators Conference* ISSN, vol. 2167. Citeseer, 1435 (2014)
5. O'Malley, C., Vavoula, G., Glew, J.P., Taylor, J., Sharples, M., Lefrere, P.: Guidelines for learning/teaching/tutoring in a mobile environment. MOBIlearn project report, D4.1 (2003). <http://www.mobilelearn.org/download/results/guidelines.pdf>
6. Swan, K., van't Hoof, M., Kratcoski, A., Unger, D.: Teaching and learning with mobile computing devices: closing the gap. In: van der Merwe, H., Brown, T. (eds.) *Mobile Technology: The Future of Learning in Your Hands*, Learn 2005 Book of Abstracts, 4th World Conference on mLearning, Cape Town, 25–28 October 2005, pp. 157–161 (2005)
7. Wolber, D., Abelson, H., Spertus, E., Looney, L.: *App Inventor: Create Your Own Android Apps* (2014)
8. Wing, J.: Computational thinking. *Commun. ACM* **49**(3), 33–35 (2006)
9. Wing, J.: Research Notebook: Computational Thinking - What and Why? *The Link*. Carnegie Mellon, Pittsburgh (2011)

# Author Index

## A

Abid, Samia, [164](#), [189](#)  
Ahmad, Manzoor, [1000](#)  
Ahmad, Zaheer, [197](#)  
Ahmed, Adnan, [181](#)  
Ahmed, Farwa, [197](#)  
Amato, Alba, [844](#)  
Amato, Flora, [825](#), [964](#)  
Amendola, Danilo, [349](#)  
Aoki, Eiji, [795](#)  
Arif, S., [617](#)  
Ashby, Thomas J., [397](#)  
Aversa, Rocco, [834](#), [844](#)  
Aziz, A., [617](#)

## B

Baddar, Sherenaz Al-Haj, [1019](#)  
Balzano, Walter, [1009](#)  
Bañeres, David, [274](#)  
Barolli, Admir, [14](#)  
Barolli, Leonard, [3](#), [14](#), [24](#), [43](#), [56](#)  
Biba, Marenglen, [974](#)  
Bica, Mihai, [557](#)  
Böhm, Stanislav, [397](#)  
Borges, Altamir Rosani, [371](#)  
Bucci, Michelangelo, [299](#)

## C

Cai, Chengtao, [647](#), [943](#)  
Camarata, G., [577](#)  
Casola, Valentina, [854](#)  
Celesti, Antonio, [906](#)  
Cha, ByungRae, [762](#)  
Cha, YoonSeok, [762](#)  
Chella, Antonio, [249](#), [336](#)  
Chen, Fangzhou, [537](#)  
Chen, JianXia, [567](#)  
Chen, WuYan, [567](#)  
Chen, Xu, [667](#)

Cheng, Lu, [639](#)  
Choo, Kim-Kwang Raymond, [677](#)  
Chui, Stephen, [547](#)  
Chupakhin, Vladimir, [397](#)  
Ciccia, Simone, [987](#)  
Cima, Vojtech, [397](#)  
Comelli, Albert, [262](#)  
Cossentino, Massimo, [896](#)  
Cui, Yujia, [647](#)  
Cuka, Miralda, [3](#), [43](#)  
Cuzzocrea, Alfredo, [349](#), [361](#)

## D

Damiano, Rossana, [287](#)  
Dario, Bruneo, [864](#)  
De Benedictis, Alessandra, [854](#)  
Deng, Na, [667](#)  
Di Martino, Beniamino, [825](#), [834](#), [844](#), [875](#)  
Di Napoli, Claudia, [896](#)  
Di Stefano, A., [577](#)  
Ding, Jie, [657](#)  
Dissanayake, D.M.M.A.I.B., [152](#)  
Drăgan, Ioan, [916](#)  
Duolikun, Dilawaer, [31](#), [70](#), [94](#)  
Dvorský, Jiří, [397](#)

## E

Elmazi, Donald, [3](#), [43](#)  
Enokido, Tomoya, [31](#), [70](#), [82](#), [94](#)  
Esposito, Antonio, [875](#)  
Eto, Haruhi, [439](#)

## F

Fan, Weibei, [954](#)  
Fang, Wan, [499](#)  
Fazio, Maria, [906](#)  
Feng, YuMin, [508](#)  
Ferrari, Carlo, [1027](#)  
Ferri, Fernando, [361](#)



Fiandrino, Claudio, 475  
 Fortiş, Teodor-Florin, 916  
 Francesco, Longo, 864  
 Fujimori, Kiko, 778  
 Funabiki, Nobuo, 701

**G**

Gentile, Antonio, 216  
 Gentile, Vito, 216, 249  
 Giaccone, Paolo, 475  
 Giardina, Marcello, 249, 336  
 Giordanengo, Giorgio, 987  
 Gkioulos, Vasileios, 310  
 Goga, Klodiana, 384  
 Gorgan, Dorian, 557  
 Grasso, Giorgio Mario, 349  
 Grifoni, Patrizia, 361  
 GuangBo, Lei, 499  
 Gull, Saba, 197  
 Guo, Jiabao, 627

**H**

HaiNing, Li, 499  
 Hallsteinsen, Svein, 834  
 Haramaki, Toshiyuki, 743  
 Hayashida, Yoshiki, 451  
 He, Fan, 689  
 He, Xu, 589  
 Higuchi, Makoto, 323  
 Honda, Junichi, 128  
 Horiuchi, Takuma, 732  
 Horn, Geir, 834  
 HuaZhong, Jin, 499  
 Hunstad, Ingrid, 987  
 Huqing, Nie, 589  
 Hussain, Hafiz Majid, 1000  
 Hussain, Sardar Mehboob, 164  
 Hussain, Shahid, 205

**I**

Iguchi, Nobukazu, 711  
 Ikeda, Makoto, 3, 14, 24, 43, 56  
 Ilyas, N., 617

**J**

Javaid, Nadeem, 164, 181, 189, 197, 617, 1000  
 Javaid, Sakeena, 189  
 Jiang, Lingyun, 689  
 Jiang, Shanshan, 834

**K**

Kadavy, Tomas, 225  
 Kagawa, Tsuneo, 785  
 Kao, Wen-Chung, 701

Kawase, Hiroaki, 323  
 Kazmi, Saqib, 1000  
 Keung, Jacky, 205  
 Khalid, Rabiya, 164, 189  
 Khan, Arif Ali, 205  
 Khan, Asif, 181, 1000  
 Khan, Gul N., 547  
 Khan, Zahoor Ali, 164, 181, 189, 197, 617, 1000  
 Kim, JongWon, 762, 817  
 Kinoshita, Tetsuo, 526  
 Kintzel, William Richard, 371  
 Kiourtis, Athanasios, 885  
 Kiran, H., 617  
 Kishi, Kyohei, 117  
 Klarman, Szymon, 299  
 Koshizen, Takamasa, 323  
 Koyama, Akio, 117  
 Kulla, Elis, 3, 43  
 Kurokawa, Fujio, 439  
 Kushwaha, Nidhi, 864  
 Kwon, Yong-Moo, 805  
 Kyriazis, Dimosthenis, 885

**L**

Lai, Cristian, 106  
 Li, Chao, 567  
 Li, Liangde, 537, 954  
 Li, Maolin, 639  
 Li, Peng, 537, 599, 657, 954  
 Li, Xuan, 627  
 Liang, Yanhua, 647, 943  
 Liang, Yuan, 609  
 Liguori, Salvatore, 875  
 Liu, Gang, 627  
 Liu, Wei, 954  
 Liu, Yi, 56  
 Lo Re, Giuseppe, 262  
 Lombardo, Vincenzo, 287  
 Lwin, Kyaw Soe, 701

**M**

Madni, Hussain Ahmad, 181  
 Mahmood, Ahsan, 475  
 Maioli, Luca, 475  
 Maisto, Salvatore Augusto, 875  
 Maki, Naoto, 768  
 Manzoor, Awais, 181  
 Martinovič, Jan, 397, 407  
 Marulli, Fiammetta, 825  
 Matsubara, Satoshi, 432  
 Matsui, Nobumasa, 439  
 Matsumoto, Takanari, 323  
 Matsuo, Keita, 14, 56

Matsuura, Horacio, 421  
 Mattos, Mauro Marcelo, 371, 421  
 Mavrogiorgou, Argyro, 885  
 Mazumdar, Somnath, 407  
 Mazzeo, Antonino, 825  
 Merlino, Giovanni, 864  
 Merlo, Alessio, 1019  
 Messina, Antonio, 299  
 Meyer, Luiz Henrique, 421  
 Miao, Jingcheng, 609  
 Midiri, Federico, 262  
 Migliardi, Mauro, 1019  
 Milazzo, Fabrizio, 216  
 Miura, Satoru, 752  
 Miyamoto, Shugo, 323  
 Miyazawa, Toshiyuki, 432  
 Moore, Philip, 929  
 Morana, G., 577  
 Moro, Michele, 1027  
 Moscato, Francesco, 825, 964  
 Mossucca, Lorenzo, 987  
 Mumolo, Enzo, 349  
 Murano, Aniello, 1009  
 Musmarra, Paolo, 1037

**N**

Nacchia, Stefania, 875  
 Nagatomo, Takehiro, 721  
 Nakamura, Shigenari, 82  
 Nakamura, Shohei, 768  
 Nakashima, Makoto, 721  
 Nishani, Lediona, 974  
 Nishino, Hiroaki, 743, 752, 785

**O**

Oba, Zenjiro, 795  
 Oda, Tetsuya, 3, 14, 24, 43  
 Ogiela, Lidia, 82, 174  
 Ogiela, Marek R., 174  
 Oguri, Kiyoshi, 451, 463  
 Okada, Yoshihiro, 768  
 Ospedale, Francesco, 875  
 Ou, Ruan, 499  
 Ozera, Kosuke, 56

**P**

Pan, Bofeng, 677  
 Park, Meeree, 805  
 Park, Sun, 762  
 Parodi, Antonio, 384  
 Peng, Li, 589  
 Petrucci, Giovanni, 262  
 Pilato, Giovanni, 236  
 Pilosu, Luca, 987

Pintus, Antonio, 106  
 Pizzo, Antonio, 287  
 Pluhacek, Michal, 225  
 Portero, Antoni, 407  
 Prabodha, L.H.C., 152  
 Pribadi, Haikal, 299  
 Puliafito, Antonio, 864

**Q**

Qasim, Umar, 164, 181, 189, 197, 617, 1000  
 Qian, Cong, 599

**R**

Rak, Massimiliano, 854  
 Ranathunga, S., 152  
 Ranaweera, L.T., 152  
 Renga, Flavio, 987  
 Romano, Vincenzo, 987  
 Ruan, Ou, 667  
 Ruiu, Pietro, 384

**S**

Sabatucci, Luca, 896  
 Sakai, Yuki, 24  
 Salerno, Sergio, 262  
 Sato, Fumiaki, 323  
 Sato, Goshi, 139  
 Sato, Keizo, 721  
 Schicchi, Daniele, 236  
 Scialdone, Marco, 844  
 Scionti, Alberto, 407  
 Scopelliti, Laura, 262  
 Selea, Teodora, 916  
 Senkerik, Roman, 225  
 Serra, Alberto, 106  
 Serra, Montse, 274  
 Sheikholeslami, Ali, 432  
 Sher, Arshad, 197  
 Shiabat, Yoshitaka, 139  
 Shibata, Yuichiro, 451, 463  
 Shiratori, Norio, 139  
 Siddiqi, M.Z., 617  
 Soejima, Rie, 463  
 Song, Xiao Ou, 489  
 Song, XiaoHui, 508  
 Sorbello, Rosario, 249, 336  
 Sorce, Salvatore, 216, 249  
 Stichbury, Jo, 299  
 Sugawara, Shinji, 732  
 Sugie, Ryuta, 516  
 Sun, Lijuan, 689  
 Suzuki, Hiroyuki, 117  
 Syeda, Masooma Zehra, 805

**T**

Tachibana, Takahiro, 721  
 Tahara, Akane, 451  
 Tahir, J., 617  
 Tajima, Hirohisa, 128  
 Takano, Shigeru, 768  
 Takatsu, Motomu, 432  
 Takemoto, Kazuya, 432  
 Takizawa, Makoto, 14, 31, 70, 82, 94  
 Takumi, Ichi, 516, 526  
 Tamura, Hirotaka, 432  
 Tanaka, Masaharu, 439  
 Taniguchi, Chihiro, 701  
 Tanoue, Shuichi, 785  
 Terranova, Maria Chiara, 262  
 Terzo, Olivier, 384, 407, 987  
 Tessarotto, Marco, 349  
 Thu, Theint Theint, 451  
 Tian, Jingbai, 667  
 Torimoto, Yasuo, 323  
 Tramonte, Salvatore, 249, 336  
 Tsukamoto, Sanroku, 432

**U**

Uchida, Noriki, 139  
 Uchiya, Takahiro, 516, 526  
 Uno, Koji, 323  
 Urso, Alfonso, 299

**V**

Van Pham, Hai, 929  
 Vatankhahghadim, Behraz, 432  
 Vecchi, Giuseppe, 987  
 Venticinque, Salvatore, 834, 844  
 Viktorin, Adam, 225  
 Villano, Umberto, 854  
 Villari, Massimo, 906  
 Vinanzi, Samuele, 249  
 Vitabile, Salvatore, 262  
 Vitale, Fabio, 1009

Vithanage, W.R.R., 152  
 Vyas, O.P., 864

**W**

Wang, Chunzhi, 667  
 Wang, Yizhuo, 599  
 Wang, Zhengyuan, 689  
 Wanyuan, Jiang, 589  
 Watanabe, Kento, 526  
 Watanabe, Kenzi, 778  
 Watanabe, Ritsuko, 795  
 Watanabe, Ryo, 70, 94  
 Watanabe, Yasuhiro, 432  
 Wolthusen, Stephen D., 310

**X**

Xie, Runyu, 657  
 Xiong, Caiquan, 627  
 Xu, He, 537, 599, 657

**Y**

Yamasaki, Hironobu, 432  
 Yang, Hang, 609  
 Yang, Zhi, 567  
 Ye, Zhiwei, 667  
 Yokoyama, Hisashi, 128  
 Yoo, Danny, 432  
 Yoshihara, Kazuaki, 778

**Z**

Zafar, Ayesha, 164, 189  
 Zaw, Khin Khin, 701  
 Zeb, Adnan, 181  
 Zeng, Peng, 677  
 Zhang, Xian, 508  
 Zhao, Dongmei, 609  
 Zheng, Jia, 943  
 Zito, D., 577  
 Zou, Zhiqiang, 689